GEOLOGICAL SURVEY OF CANADA
COMMISSION GÉOLOGIQUE DU CANADA

PAPER 78-1A

CURRENT RESEARCH
PART A

Energy, Mines and Resources Canada
Énergie, Mines et Ressources Canada

1978

Notice to Librarians and Indexers

The Geological Survey's thrice-yearly "Current Research" series contains many reports comparable in scope and subject matter to those appearing in scientific journals and other serials. All contributions to the Scientific and Technical Report section of "Current Research" include an abstract and bibliographic citation. It is hoped that these will assist you in cataloguing and indexing these reports and that this will result in a still wider dissemination of the results of the Geological Survey's research activities.

Technical editing and compilation
R.G. Blackadar
P.J. Griffin
H. Dumych
E.J.W. Irish

Production editing and layout
Leona R. Mahoney
Lorna A. Firth
Michael J. Kiel

Typed and checked by
Debby Busby
Janet Gilliland
Suzanne Lalonde
Janet Legere
Sharon Parnham

GEOLOGICAL SURVEY
PAPER 78-1A

CURRENT RESEARCH
PART A

1978

Printing and Publishing
Supply and Services Canada,
Ottawa, Canada K1A 0S9,

from the Geological Survey of Canada
601 Booth St., Ottawa, K1A 0E8

or through your bookseller.

Catalogue No. M44/78-1A
ISBN - 0-660-01506-4

Price: Canada: $6.00
Other Countries: $7.20

Price subject to change without notice

I: SCIENTIFIC AND TECHNICAL REPORTS

ECONOMIC GEOLOGY

GEOPHYSICS

MARINE GEOSCIENCE

Page

REGIONAL GEOLOGY

Appalachian Region

Arctic Islands

Cordilleran Region

II: SCIENTIFIC AND TECHNICAL NOTES

III: DISCUSSIONS AND COMMUNICATIONS

INTRODUCTION

When the Geological Survey of Canada was formed in 1842 its objective was made clear in the enabling Act – to undertake a geological survey in order to ascertain the mineral resources of the country. Today the objective cannot be expressed quite so succinctly but in essence it is to provide a comprehensive inventory and understanding of Canada's geological framework so that activities that depend on geology can be supplied with the requisite data. This information enables the Survey to identify and to facilitate the discovery of non-renewable mineral and energy resources and to evaluate the effects that man's activities have on the landmass and thereby to assist in conserving our natural environment. Thus the principal objectives of the Geological Survey are:

- *To provide the geoscientific information needed to facilitate the discovery of non-renewable resources.*
- *To evaluate the energy and mineral resources available to Canada.*
- *To determine the capability of the landmass to withstand various types of use particularly in response to resource development and the disposal of waste.*

Information on bedrock and surficial geology is obtained through systematic surveys, regional studies, and national compilations and, as the 'Contents' page of this publication shows, these activities constitute a major part of the Survey's work. At present much of the information required to aid in the discovery and evaluation of our uranium and other metallic mineral resources is obtained from geophysical and geochemical surveys. Many of these are carried out under contract to private industry and the Survey has developed procedures to monitor this work. It has also become a national centre for research and development into new methodology. Many papers published in this series (although not in this volume) reflect this aspect of our work.

In 1978 'Energy' will continue to be a major issue facing Canadians. The Geological Survey can contribute to solving some aspects of this problem through joint federal-provincial programs designed to assess our coal resources, especially in the Maritimes where the current high cost of imported oil creates a serious drain on the economy. It will also contribute significantly to the annual update of our oil and natural gas, and uranium resources. Adequate data on which to base export decisions become increasingly important if Canada's trade deficit worsens and are also important in determining long-term internal distribution and pricing policies. Although the route of the Alcan Pipeline is now fairly well decided, the possibility remains of another pipeline to bring arctic gas to central Canada by way of a route to the west of Hudson Bay. The Geological Survey's expertise in terrain evaluation will undoubtedly be in demand as proposals reach the detailed planning stage.

The 82 reports and 27 notes that comprise this publication cover studies that were carried out to meet a wide range of objectives although as will be seen most are concerned with some aspect of expanding the geoscience base.

In order to assist in making uranium and thorium resource estimates, studies are being made of the nature and distribution of uranium deposits and their relationships to their geological environments. This information will permit better understanding of the metallogenic processes that determine the uranium potential of each region of Canada. Reports 25, 52, 53, 59 and 77 to 79 present preliminary results of studies carried out last summer in various parts of Canada in order to provide new information to improve the Survey's capability in this field.

Reports 40, 50, 51 and 54 to 57 cover studies done on other aspects of commodity metallogeny which, as in the case of uranium, are required to support metallic mineral resource evaluation. Evaluation depends on a mix of detailed mineral deposit studies and regional geology studies and these reports reflect this blend.

The Geological Survey's expanding activities in Marine Geoscience reflect the growing awareness that Canada's offshore areas may prove of great importance to our future development and that to exercise sovereignty we must make our presence obvious. Previous "Reports of Activities" (the forerunner of this publication) have included many reports dealing with the East Coast. In this publication four reports (61, and 64 to 66) describe marine geoscience studies on the West Coast. These provide regional understanding of the physical processes and engineering attributes that control the character of the coastline, seafloor, and sediments. Such studies are useful in planning offshore exploration for hydrocarbons and in assessing sources of building aggregates.

Less than one fifth of Canada is covered by surficial geological maps at a scale of 1:250 000 and the Geological Survey has as one of its long-term goals the completion of coverage at this scale. Reports 38 and 75 contribute to this. Report 37 presents the results of a study designed to provide information for an area along Skeena River in western British Columbia in order to assist in land use planning, urban and industrial development, and to assess engineering problems.

Systematic bedrock mapping is one of the Geological Survey's core programs and the 44 reports which have been grouped together in the Table of Contents under the heading "Regional Geology" present results from many parts of Canada.

The 22 papers devoted to the Cordilleran region attest to its importance as a source of metallic minerals. The updating of the reconnaissance phase of mapping in this region should soon be completed and this will provide a broad geological and tectonic framework which will be used to support detailed studies to advance our understanding of the formation and localization of mineral deposits. Reports 1 to 8 give the first results from 'Operation Dease', a three-year mapping program in northern British Columbia that will fill one of the largest remaining gaps in the 1:250 000 scale map coverage. The remaining Cordilleran reports describe a variety of observations including regional mapping (13 to 15) and structural studies (10, 20).

Studies of the Canadian Shield (22 to 24, 25 to 33, 35 and 76) are to a large degree directed towards completion of the 1:250 000 coverage of this area. Particular attention is being given to areas where supracrustal rocks have been preserved because such areas appear to have the greatest mineral potential. Report 24, in which the Aphebian sedimentary rocks in the northern Richmond Gulf area are described, and report 25 in which the uranium potential of the same area is assessed, illustrate this emphasis.

Although this volume is the first to appear under the title "Current Research", it continues a series initiated in 1962 under the title "Report of Activities". The change in title was made to reflect better the nature of the papers that are now included. However it was felt that the Geological Survey staff also need an outlet for technical notes and even in some cases for brief communications outlining field activities of particular general interest. The report has therefore been divided into Scientific and Technical Reports and Scientific and Technical Notes. In addition a Discussion and Communications section has been added. This will enable the staff and the public to comment briefly on current Geological Survey publications and also to present new data to supplement the results already published in our reports. A note to contributors to this section will be found following the Discussion section in this volume.

Geological Survey of Canada publications already reach a large and diverse audience. It is hoped that this new approach will enable us to meet the needs of an even larger constituency.

Ottawa, December 1, 1977

R.G. Blackadar
Chief Scientific Editor

Separates

A limited number of separates of the papers that appear in this volume are available by direct request to the individual authors. The addresses of the Geological Survey of Canada offices follow:

601 Booth Street,
OTTAWA, Ontario
K1A 0E8

Institute of Sedimentary and Petroleum Geology,
3303-33rd St. N.W.,
CALGARY, Alberta
T2L 2A7

British Columbia Office,
100 West Pender Street,
VANCOUVER, B.C.
V6B 1R8

Atlantic Geoscience Centre,
Bedford Institute of Oceanography,
P.O. Box 1006,
DARTMOUTH, N.S.
B2Y 4A2

When no location accompanies an author's name in the title of a paper, the Ottawa address should be used.

I: SCIENTIFIC AND TECHNICAL REPORTS

1. OPERATION DEASE

Project 770016

H. Gabrielse
Regional and Economic Geology Division, Vancouver

Abstract

Gabrielse, H., Operation Dease; Current Research, Part A, Geol. Surv. Can., Paper 78-1A, p. 1-4, 1978.

Cry Lake map-area (104I) in the Cassiar Mountains of north-central British Columbia is underlain by rocks ranging in age from Proterozoic to Cenozoic. All systems of the Paleozoic and Mesozoic are represented by fossiliferous strata. Pre-Mississippian rocks are exposed to the northeast of Kutcho Fault and are mainly of miogeoclinal aspect. Younger rocks include abundant volcanic strata. Those of late Paleozoic age are associated with alpine-type ultramafic bodies and are of oceanic affinity. Volcanic rocks of Mesozoic age are closely associated with granodioritic plutons and are probably in part of island-arc affinity. Southwesterly to southerly directed structures are regionally developed northeast of King Salmon Fault. In the northeast these structures are cut by northeasterly directed thrust faults. The latter are cut by mid-Cretaceous granitic rocks of the Cassiar Batholith and related stocks. Kutcho and Rapid River-Kechika Faults are the loci of probable significant transcurrent movements and separate markedly contrasting terranes.

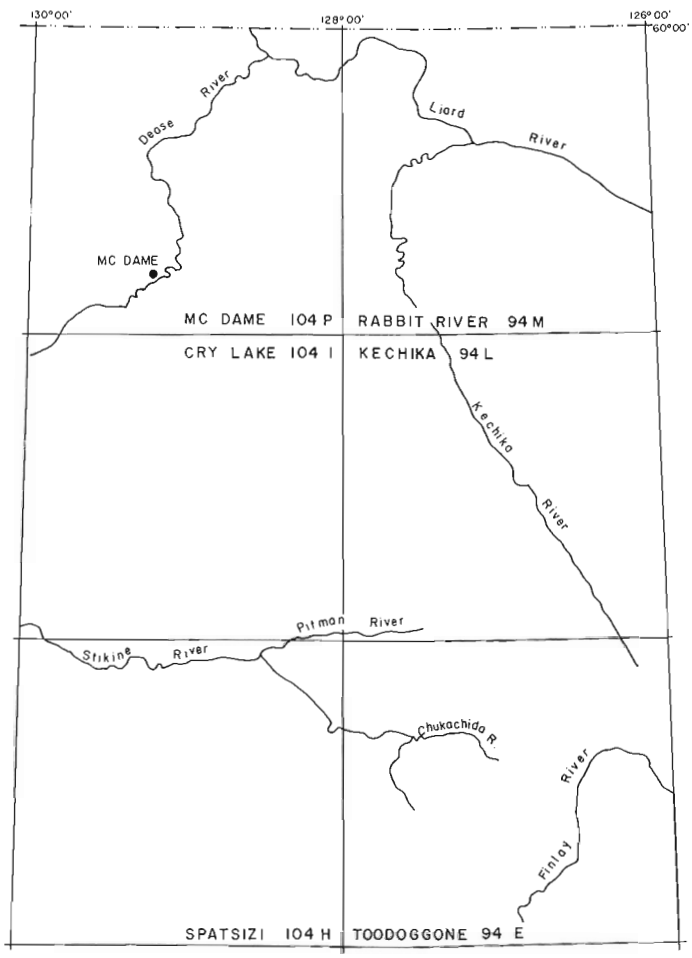

Figure 1.1. Index map, north-central British Columbia.

Introduction

Operation Dease was planned as a three-year project designed to: (a) facilitate the updating of regional mapping in Cry Lake (104I), Spatsizi (104H) and Dease Lake (104J) map-areas; (b) provide a framework for detailed studies of late Proterozoic sedimentary strata and late Paleozoic and Mesozoic volcanic and sedimentary rocks; (c) study the nature, age and contact relationships of the Hotailuh Batholith; (d) study the distribution of the various phases in the ultramafic complexes and examine the mode of occurrence of jade deposits; (e) investigate the structural style of the several stratigraphic assemblages, and (f) provide logistic support for a detailed biostratigraphic study of Lower Cambrian strata in Cassiar Mountains. During the 1977 field season most of the work was done in Cry Lake map-area. Accounts presenting the results of the various investigations are contained in the following 7 reports.

Stratigraphy

Figure 1.2 shows the distribution of the main stratigraphic assemblages in Cry Lake map-area. Each assemblage has distinctive lithological and structural characteristics. Upper Proterozoic to Middle or Upper Devonian strata are similar to those in McDame map-area to the north (Gabrielse, 1963). Probable correlative rocks, but including only minor carbonate, comprise a metamorphic assemblage flanking the southwest side of the Cassiar Batholith near Turnagain River and a gneissic terrane near Eagle River. Paleocurrent data indicate an easterly source for Lower Cambrian sandstone and a southeasterly source for Silurian and/or Devonian dolomitic sandstone.

The two Upper Paleozoic assemblages (Sylvester and Cache Creek groups) are intensely deformed and their relationship with adjacent strata are still not resolved. The Upper Mississippian Nizi Formation clearly overlies a thick sequence of mafic volcanic rocks assigned to the Sylvester Group. At least locally the Nizi carbonate is faulted against Pennsylvanian carbonate strata which are overlain by a thick

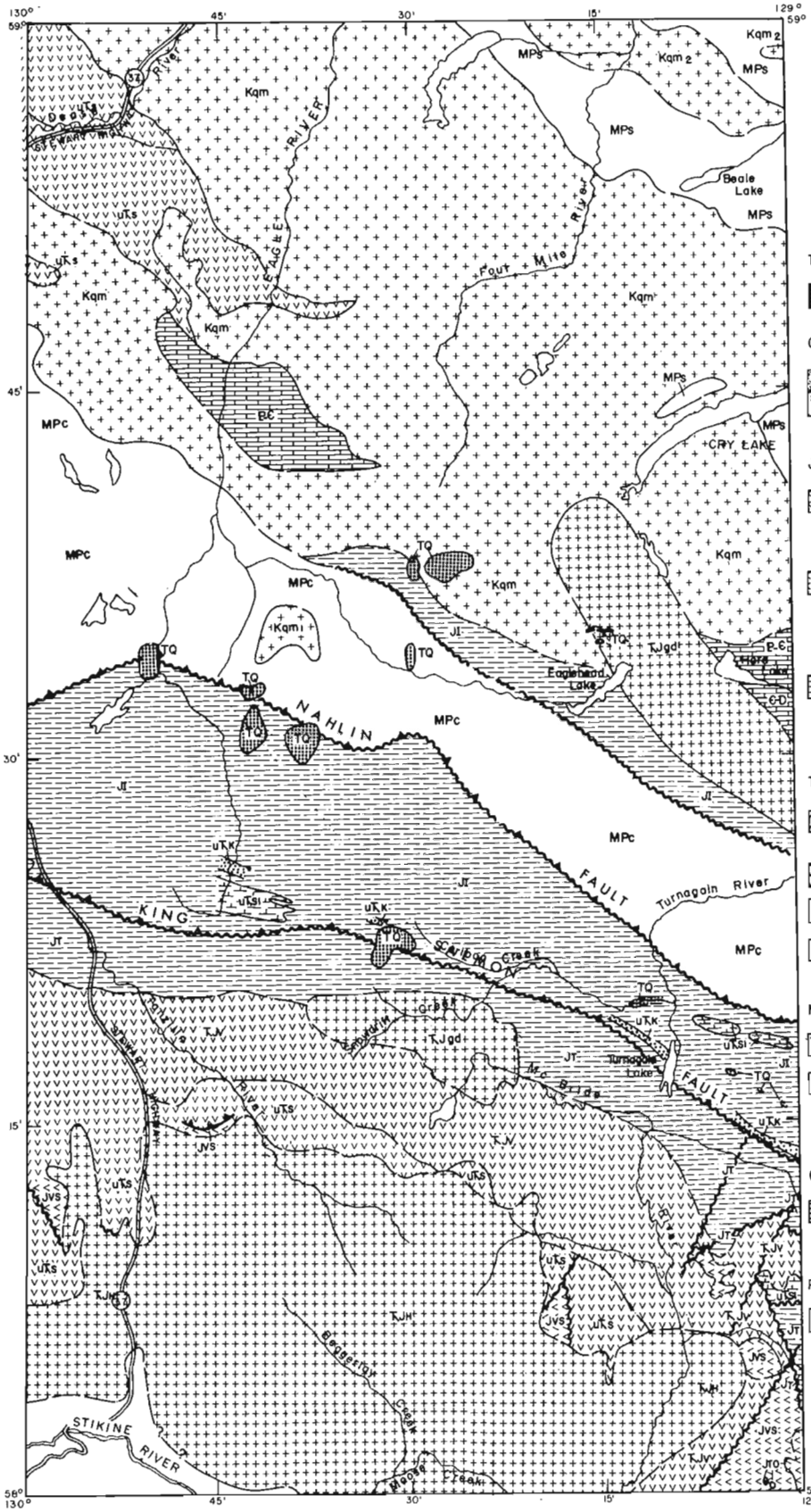

Legend for Figure 1.2

Stratified Rocks

TERTIARY AND QUATERNARY

TQ: Basalt; lava, tuff, agglomerate

CRETACEOUS(?) AND TERTIARY
UPPER CRETACEOUS(?) TO EOCENE(?)

KEs: Conglomerate, sandstone, shale

KEv: Rhyolite, pisolitic siliceous tuff, chalcedonic rhyolite breccia

JURASSIC
MIDDLE JURASSIC (mainly?)

JTO: "TOODOGGONE VOLCANICS": Mauve and green andesitic and dicitic volcanics; conglomerate, siltstone, shale

LOWER JURASSIC (mainly Toarcian)

JvS: "TOODOGGONE VOLCANICS": Andesite, dacite, rhyolite, green and maroon feldspar porphyry, tuff, breccia; calcareous siltstone, silty limestone

LOWER JURASSIC (mainly Pliensbachian)

JI,JT: INKLIN FORMATION: Greywacke, slate conglomerate (age range uncertain), locally includes

TAKWAHONI FORMATION: Greywacke, siltstone, argillite, conglomerate

TRIASSIC AND JURASSIC
UPPER TRIASSIC AND LOWER JURASSIC

TJv: Andesitic green and maroon weathering volcanics

UPPER TRIASSIC

uTs: STUHINI FORMATION: Augite porphyry, coarse-bladed feldspar porphyry; minor sedimentary rocks

uTsf: SINWA FORMATION: Felid limestone; minor calcareous shale

uTk: "KUTCHO FORMATION": Quartz-eye sericite schist, chlorite schist, breccia, conglomerate

MISSISSIPPIAN TO PERMIAN

MPc: CACHE CREEK GROUP: Chert, shale, limestone, ultramafics, gabbro, diorite, basic volcanics

MPs: SYLVESTER GROUP: Chert, slate, limestone, ultramafics, gabbro, diorite, basic volcanics; lower part includes chert arenite and chert-pebble conglomerate

CAMBRIAN TO DEVONIAN

€-D: Limestone, dolomite, sandstone, siltstone, shale; €-D$_l$, mainly black, carbonaceous phyllite, probably includes lower

PROTEROZOIC AND LOWER CAMBRIAN

P-€: Limestone, sandstone, shale, grit and metamorphosed equivalents: P$_L$-€$_l$ mainly metamorphosed clastic rocks

Legend (cont.).

Intrusive Granitic Rocks

MID-CRETACEOUS (mainly)

Kqm: CASSIAR BATHOLITH: Quartz monzonite, minor granodiorite and diorite; locally foliated or megacrystic near contact; abundant metasedimentary inclusions near Eagle River; age uncertain;
Kqm_1: Kqm_2 in part dioritic

MID-JURASSIC(?)

MJgd: Granodiorite, leucocratic, pink; fine to medium grained

UPPER TRIASSIC AND LOWER JURASSIC (may include younger rocks in part)

TJH: HOTAILUH Batholith: Granodiorite, syenodiorite, gabbro

TJgd: Hornblende diorite, quartz monzonite, in part foliated

Ultrabasic Rocks - Alaskan Type

UPPER TRIASSIC(?)

uTu: Dunite, peridotite, pyroxenite

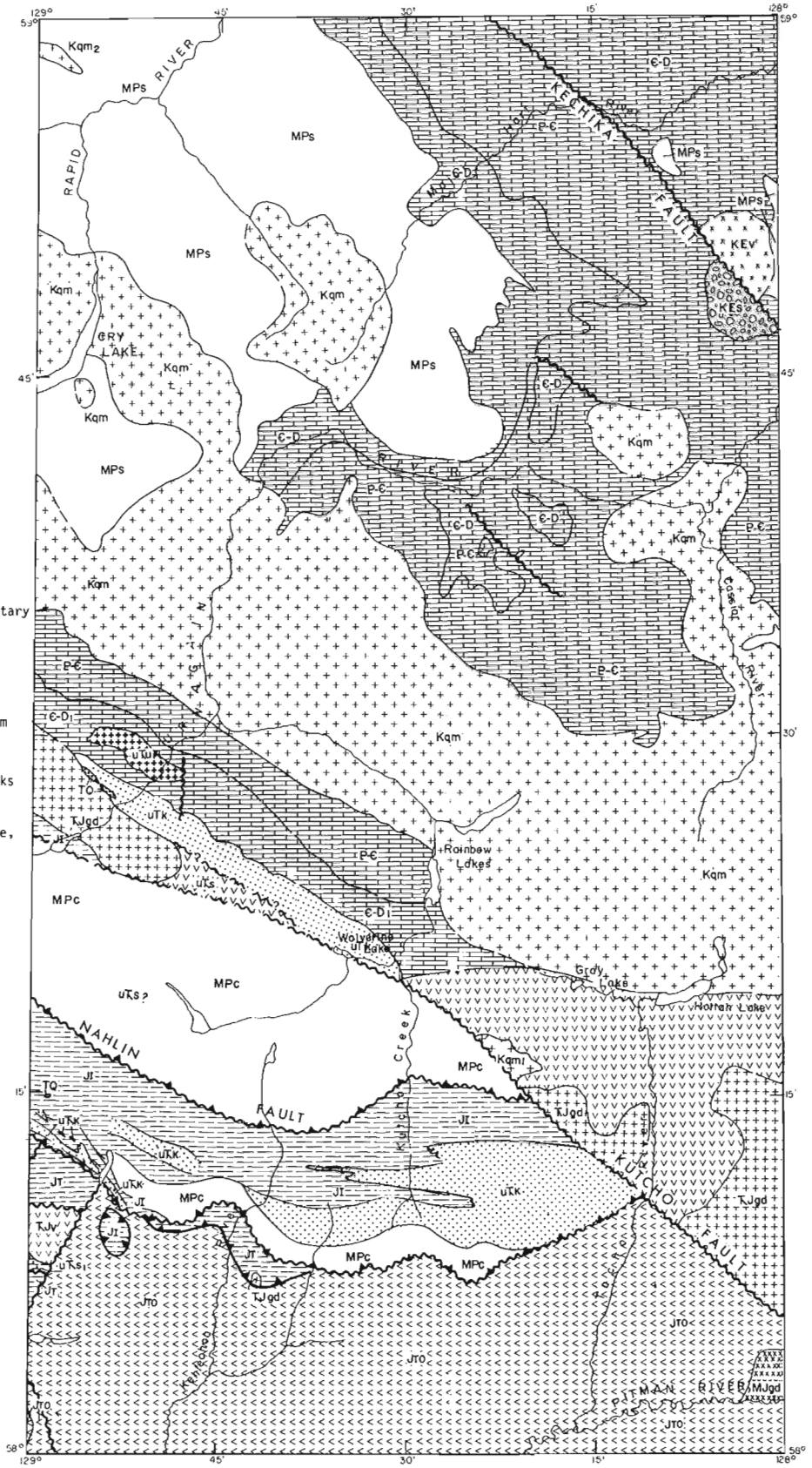

sequence of well layered volcanic and sedimentary rocks. Therefore, rocks mapped as Sylvester Group in McDame and Cry Lake map-areas are now known to include strata ranging in age from Mississippian to Permian.

Mesozoic assemblages are described elsewhere in this report. The following comments deal mainly with regional considerations. On the basis of mapping in southeastern Cry Lake map-area and north-central Spatsizi map-area it seems probable that volcanic rocks informally named the 'Toodoggone Volcanics' in Toodoggone map-area (see Fig. 1.1) (Carter, 1971; Gabrielse et al., 1977) almost completely flank the northern part of the Sustut Basin (Eisbacher, 1974). Locally, southeast of Pitman River to near the confluence of Chukachida and Stikine rivers in Toodoggone map-area, the volcanics have been removed beneath the unconformity at the base of the Sustut Group. In Toodoggone, Spatsizi and Cry Lake map-areas the volcanics are characterized by maroon weathering units in the lower part and mauve weathering rocks in the upper part. Free quartz is common and lens-shaped bodies of spherulitic rhyolite and flow banded rhyolite have been noted in the lower units in all three map-areas. Associated with the volcanics in Toodoggone map-area are pink weathering, even-grained, granodioritic rocks similar to the body north of Pitman River in Cry Lake map-area. A single K-Ar determination of 163 ± 6 m.y. (R.K. Wanless, pers. comm. 1977) was obtained on biotite from a pluton of this type north-northeast of the confluence of Chukachida and Stikine rivers.

Potassium-argon ages on hornblende from three localities in "Toodoggone Volcanics" near Finlay River are 186 ± 6 m.y. (Carter, 1971), and 178 ± 8 m.y. and 186 ± 8 m.y. (R.K. Wanless, pers. comm. 1975, 1977). Toarcian(?) fossils (H.W. Tipper, pers. comm. 1977) occur below rhyolitic members in north-central Spatsizi map-area and Bajocian fossils (H.W. Tipper, pers. comm. 1975) were found at one locality in Toodoggone map-area and are locally abundant in south-central Cry Lake map-area. Abundant nonmarine conglomerate intercalated with the volcanics in southeastern Cry Lake map-area contains clasts of fusulinid-bearing limestone that must have been derived from Cache Creek limestone to the north (J.W.H. Monger, pers. comm. 1977). Channels in the conglomerate also indicate a northerly source.

Anderson (1978) has described the granitic rocks of the Hotailuh Batholith. The granitic body near the headwaters of Snowdrift Creek cuts Lower Jurassic greywacke of the Takwahoni Formation and may be of the same age (mid-Jurassic) as the younger phases of the Hotailuh Batholith. A granodiorite to diorite body southwest of Hard Lake has given a K-Ar age on biotite of 182 ± 7 m.y. (R. Oddy, pers. comm. 1977). The northern boundary of the body has not been determined. The granitic rocks east of Tucho River are part of the Pitman Batholith which probably comprises a number of phases undifferentiated in regional mapping. Quartz monzonite of the mid-Cretaceous Cassiar Batholith is commonly megacrystic, particularly along its northeast margin where potash feldspar megacrysts are abundant.

Regional Structure

Four regional faults transect Cry Lake map-area (see Fig. 1.2). The southerly directed King Salmon Fault forms the southern boundary of the King Salmon assemblage comprising strongly foliated and imbricately thrust strata of Cache Creek, 'Kutcho', Sinwa and Inklin rocks. Nahlin Fault, also southerly directed, forms the southern boundary of the Cache Creek terrane, an area underlain by intensely deformed rocks. Both faults are truncated to the east by Kutcho Fault along which there may have been considerable transcurrent movement. The northwesterly continuation of Kutcho Fault has not been mapped. It probably follows the northern boundary of the Cache Creek Terrane. The Kechika Fault trends northwesterly across the northeasterly part of Cry Lake map-area and separates a terrane with strongly developed westerly directed structures to the southwest from northeasterly directed structures to the northeast. It, too, is believed to have been the locus of significant transcurrent movement. Between Kutcho and Kechika faults early southwesterly thrust and overturned structures are cut by later easterly directed faults (Gabrielse and Mansy, 1978).

References

Anderson, R.G.
1978: Preliminary report on the Hotailuh Batholith: It is distribution, age and contact relationships in the Cry Lake, Spatsizi and Dease Lake map-areas, north-central British Columbia; in Current Research, Part A, Geol. Surv. Can., Paper 78-1A, rep. 7.

Carter, N.C.
1971: Toodoggone River Area; p. 63-64 in Geology, Exploration and Mining in British Columbia, 1971; B.C. Dep. Mines Petrol. Resour.

Eisbacher, G.H.
1974: Sedimentary history and tectonic evolution of the Sustut and Sifton Basins, north-central British Columbia; Geol. Surv. Can., Paper 73-31.

Gabrielse, H.
1963: McDame map-area, Cassiar District, British Columbia; Geol. Surv. Can., Mem. 319.

Gabrielse, H., Dodds, C.J., Mansy, J.L., and Eisbacher, G.H.
1977: Geology of Toodoggone and Ware west-half map-areas, British Columbia; Geol. Surv. Can., Open File 483.

Gabrielse, H. and Mansy, J.L.
1978: Structure style in northeast Cry Lake map-area, north-central British Columbia; in Current Research, Part A, Geol. Surv. Can., Paper 78-1A, rep. 8.

2. STRATIGRAPHY AND STRUCTURE OF PROTEROZOIC ROCKS NEAR GOOD HOPE LAKE, McDAME MAP-AREA, BRITISH COLUMBIA

Project 770016

J.L. Mansy[1]
Regional and Economic Geology Division, Vancouver

Abstract

Mansy, J.L., Stratigraphy and structure of Proterozoic rocks near Good Hope Lake, McDame map-area, British Columbia; Current Research, Part A, Geol. Surv. Can., Paper 78-1A, p. 5-6, 1978.

Proterozoic strata near Good Hope Lake in McDame map-area are assigned to the Espee and Stelkuz formations of the Ingenika Group. They are overlain by rocks of the Lower Cambrian Atan Group. The strata are exposed in an anticlinorium the west limb of which is cut by several easterly directed, high-angle reverse faults. Westerly directed structures, important in Omineca and southern Cassiar mountains, are represented only by an asymmetrical anticline north of Good Hope Lake.

Stratigraphy

A section of the upper Proterozoic Ingenika Group was measured on the ridge south of Good Hope Lake (see Figs. 2.2, 2.3). The lowest exposed strata are part of the Espee Formation (see Mansy and Gabrielse, in press) comprising a sequence of buff, red and pink weathering dolostone, locally medium to coarse grained, and limestone and argillaceous limestone, commonly thinly laminated. Ferrodolomite or ankerite specks are typical of the limestone and oolites, pisolites, and oncolites are abundant in some beds. In the area the Espee Formation is probably more than 500 m thick but only 280 m are exposed in the measured section.

The Stelkuz Formation includes a great variety of lithologies that, in part, can be grouped into minor and major cycles. The lower part includes brown slates, buff lenses of channelled limestone and minor oolitic limestone. A conspicuous red-bed unit, about 80 m thick, is recognizable throughout the region. It occurs in the middle part of the formation and comprises a lower unit of calcareous red breccia with chips of red limestone, dolostone and slate; a middle unit of slaty and shaly red, green and purple cross-bedded siltstone, locally channelled; and an upper unit of red slate with lenses of limestone. The red beds are overlain by blue grey weathering, well-bedded limestone and dolostone, at least partly cross-bedded and of detrital origin. The upper part of the Stelkuz Formation includes abundant, locally micaceous sandstone, siltstone and shale, generally brown weathering. In parts of the McDame map-area these beds may be included in the Atan Group as mapped by Gabrielse (1963). The Stelkuz Formation south of Good Hope Lake is about 1000 m thick.

The base of the Atan Group is the base of a cross-bedded, white and pink quartzite unit containing clasts of quartz to 1 cm in diameter. The quartzite, about 200 m thick, has a central recessive part consisting of siltstone, shale and impure quartzite containing worm burrows. Overlying the quartzite are recessive weathering brown quartzites, micaceous shales and black shales, slates and siltstones about 80 m thick. The clastic sequence is overlain by archeocyathid-bearing limestone.

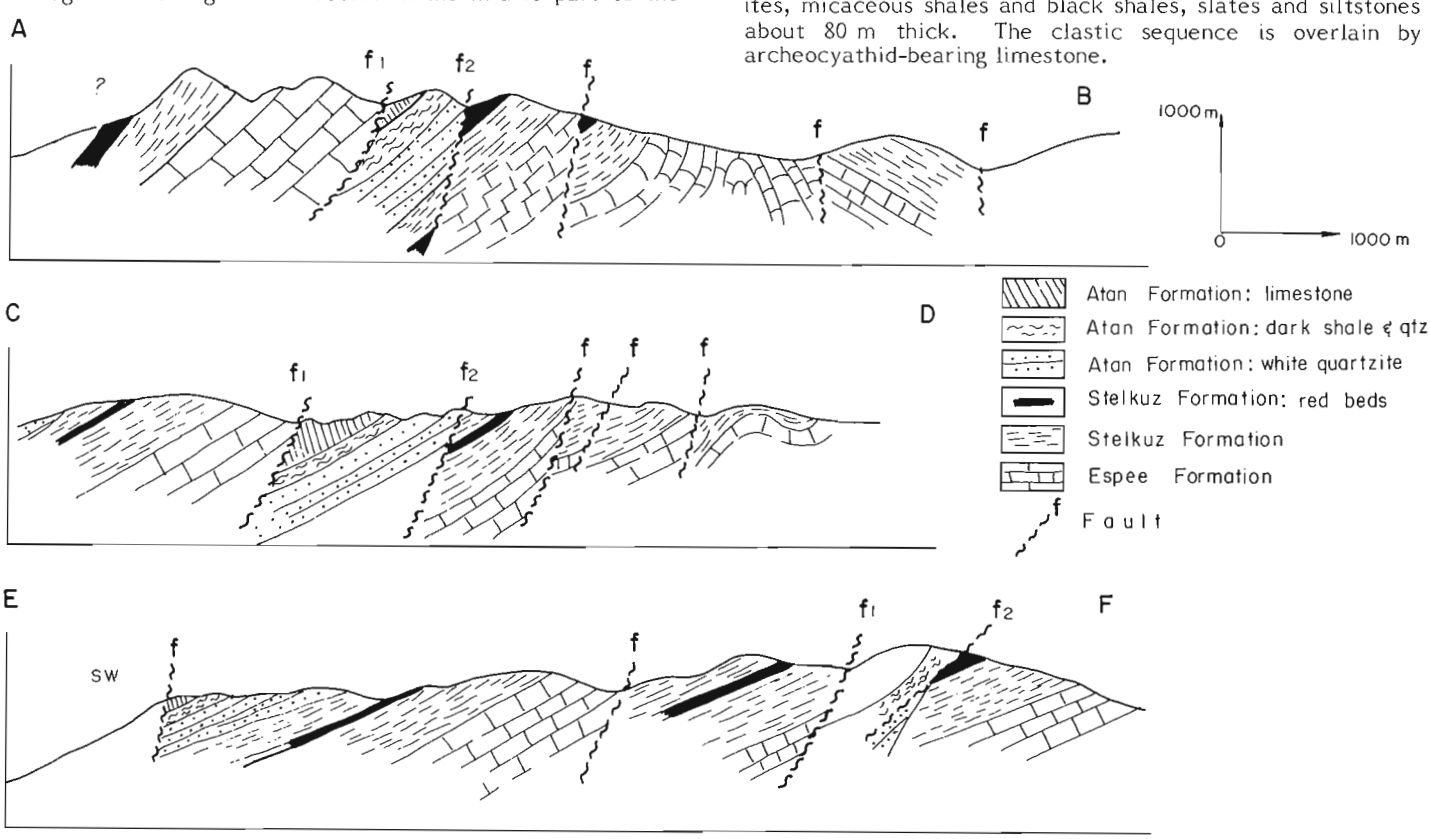

Figure 2.1. Diagrammatic cross-sections near Good Hope Lake, McDame map-area. See Fig. 2.3 for locations.

[1] University of Lille, France

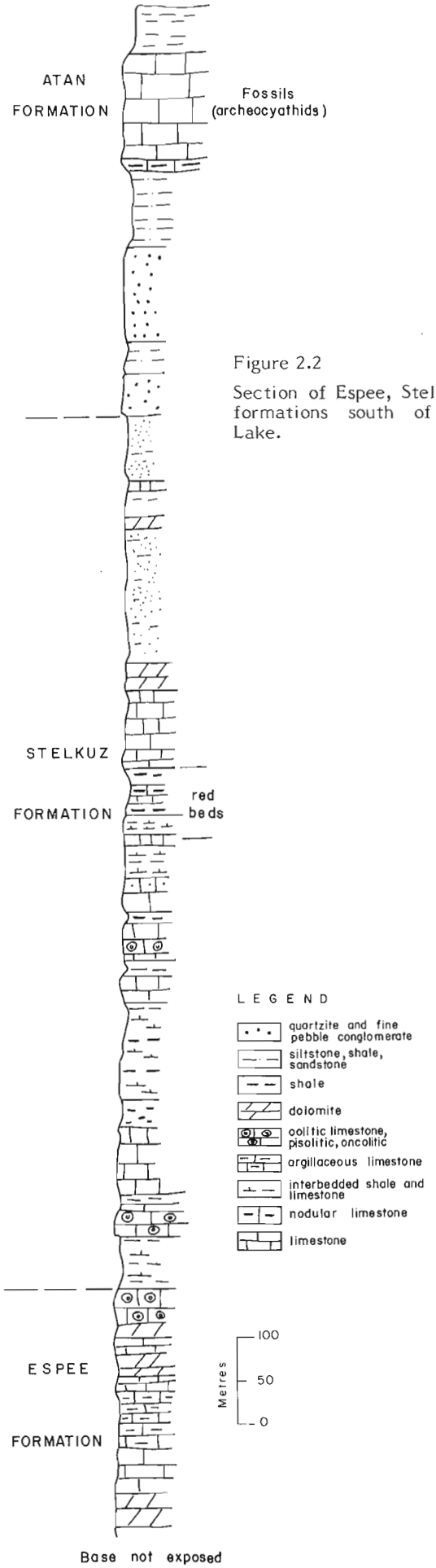

Figure 2.2

Section of Espee, Stelkuz and Atan formations south of Good Hope Lake.

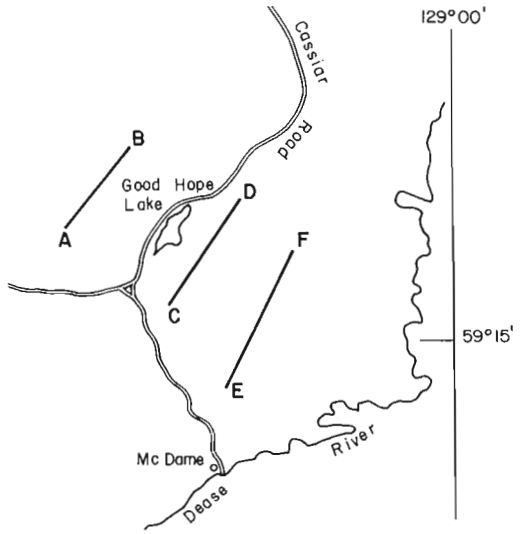

Figure 2.3. Index map, showing locations of cross-sections, Good Hope Lake area.

Structure

The structural style in the Good Hope Lake area is depicted in Figures 2.1 and 2.2. The only hint of westerly directed structures so prominent in southern Cassiar and Omineca mountains is the asymmetrical anticline north of Good Hope Lake. Dominant structures are clearly high angle, west-dipping reverse faults which repeat the section on the west limb of the major anticline. In general the major lithological units are relatively competent so that tight, similar folding is unimportant.

References

Gabrielse, H.
1963: McDame map-area, Cassiar District, British Columbia; Geol. Surv. Can., Mem. 319.

Mansy, J.L. and Gabrielse, H.
Stratigraphy, terminology and correlation of upper Proterozoic rocks in Omineca and Cassiar mountains, north-central British Columbia; Geol. Surv. Can., Paper 77-19. (in press)

3.

UPPER (CARBONATE) PART OF ATAN GROUP, LOWER CAMBRIAN, NORTH-CENTRAL BRITISH COLUMBIA

Project 650024

W.H. Fritz
Regional and Economic Geology Division

Abstract

Fritz, W.H., Upper (carbonate) part of Atan Group, Lower Cambrian, north-central British Columbia; Current Research, Part A, Geol. Surv. Can., Paper 78-1A, p. 7-16, 1978.

Preliminary results from the first detailed study of the upper Atan are presented and a type section is designated. Five upper Atan sections were measured in the Cassiar Mountains, and one Lower Cambrian section was measured in the nearby Kechika Ranges. Deposition of the upper Atan started in the middle carbonate belt during latest ***Fallotaspis****(?) Zone time and continued throughout most, if not all, of* ***Bonnia-Olenellus*** *Zone time. The age of uppermost Atan beds remains uncertain. Three grand cycles (clastic-carbonate pairs) can be recognized in the Atan Group. Correlation of the Atan Group is discussed.*

Introduction

In 1977 the upper (carbonate) part of the Atan Group was studied in conjunction with Operation Dease in order to provide needed biostratigraphic data on the map-unit. Five stratigraphic sections were measured in the Cassiar Mountains (see Fig. 3.1a, 3.1b for index map and sections) and one section was measured in the Kechika Ranges. Since a type area rather than a type section was designated in the description of the Atan (Gabrielse, 1963), time was allotted to finding a suitable section within the prescribed area. Section 1 of this report was located there, and is here designated as the type section for the upper part of the Atan Group. It is suggested that consideration be given to establishing a type section for the lower (clastic) part of the Atan Group by starting at the base of the lower segment of section 1 (base of unit 1) and measuring downsection in a northeasterly direction to the base of the Atan Group.

As shown on Figure 3.1b, only 1175 feet of the carbonate part of the Atan at section 1 is exposed and the remaining part is covered by talus. Thicker sections of the carbonate succession are exposed at section 4 (1870 feet) and section 5 (2928 feet). These sections, however, are not in the type area, they are less accessible, and section 5 has undergone moderate pervasive shearing and is extensively dolomitized. Section 5 is the only section known to the writer in which all of the carbonate portion of the Atan is exposed, and the thickness taken from this section is believed to represent the true thickness of the upper (carbonate) part of the Atan.

Strata measured in the Kechika Ranges (section 6) differs from the Atan in the Cassiar Mountains in that carbonate belonging to the **Nevadella** Zone, and probably part of the underlying clastic succession as well, is missing. Strata in the Kechika section will be referred to as the "upper Atan Group" to indicate that problems in matching the Lower Cambrian strata between the two areas still exist.

Previous Work

Gabrielse (1954) first described the Atan Group in the McDame map-area (104P) in north-central British Columbia as "comprising over 14,000 feet of sedimentary rocks..." consisting of "White and pink quartzite, limestone, dolomite, slate, red shale, argillite", all of which was assigned to the Lower and Middle Cambrian. In a second paper (1963, p. 26) the thickness was given as "more than 3,000 feet", while the gross lithologic description was repeated without much change. Although no type section was named, it is stated in the second paper (op. cit., p. 27) that "Excellent exposures occur in the mountains north and south of French River and near Atan Lake, after which the group is named.", and the age was restricted to the Lower Cambrian (p. 13). In a joint and most recent paper (Mansy and Gabrielse, in press) the base of the Atan was placed at the top of the Ingenika Group (top of Stelkuz Formation). After reading the latter paper, and after a discussion with J.L. Mansy, it is the writer's understanding that the Atan Group in the vicinity of sections 1-5 of this paper starts with a basal,white quartzite that is overlain by a thicker succession of brown to rust weathering, very fine grained sandstone and siltstone. The writer estimates that this clastic succession, here referred to as the lower Atan, is approximately 1500 feet thick near section 5 (northeast of point "a", Pl. 3.2, fig. 3).

The upper part of the Atan Group, here called the upper Atan, was described by Gabrielse (1963, p. 27, 29) as being composed of "relatively pure, thick-bedded to massive, blue-grey, buff, and reddish buff, grey, and black limestone and dolomite and very minor slate." The thickness for the upper Atan at a "generalized section northwest of Atan Lake" was given as 1500 feet.

Gabrielse (1963, p. 30, 31) has listed the faunal determinations and age assignments given various collections from the Atan Group and concludes that "all the fossils are of late Early Cambrian age." Descriptions of some of the upper Atan fossils have been given by Okulitch (1955), Okulitch and Greggs (1958) and Handfield (1969, 1971). Handfield's (1971, p. 17) finds of **Nevadella** in the upper Atan at the approximate location of the present section 1 and at One Ace Mountain, 41 miles to the north-northwest, proves that at least part of the upper Atan belongs to the medial part of the Lower Cambrian.

It is doubtful that any of the fossil collections mentioned are from strata at or near the top of the Atan Group. A single locality (GSC loc. 22757) in the lower part of the overlying Kechika Group is therefore important, in that it provides a minimum age for the Atan. This locality (Gabrielse, 1963, p. 39) is 7.3 miles west-southwest of the south end of Deadwood Lake and it has produced a trilobite that was identified by R.D. Hutchinson as cf. **Chancia** Walcott. Hutchinson assigned the trilobite to the late Lower or Middle Cambrian. The same trilobite was later inspected by A.R. Palmer, who recognized it (and the writer agrees) as belonging to the genus **Hedinaspis**, a genus that is restricted to the Upper Cambrian.

The Atan Group has been mapped or recognized over a considerable region outside the type area. In the Jennings River area immediately to the west, Gabrielse (1969) has mapped an undivided Good Hope (Ingenika) and Atan Group. To the east, in the Tuchodi Lakes area, the group has been recognized by Taylor (1969) and mapped by Taylor and Stott (1973). To the southeast, Rutter and Taylor (1968, p. 8) have recognized the group in the Pine Pass, Halfway River and Ware map-areas. North (1971, p. 309) extended the Atan-Kechika succession all the way from Peace River to the northwestern end of the Pelly Mountains.

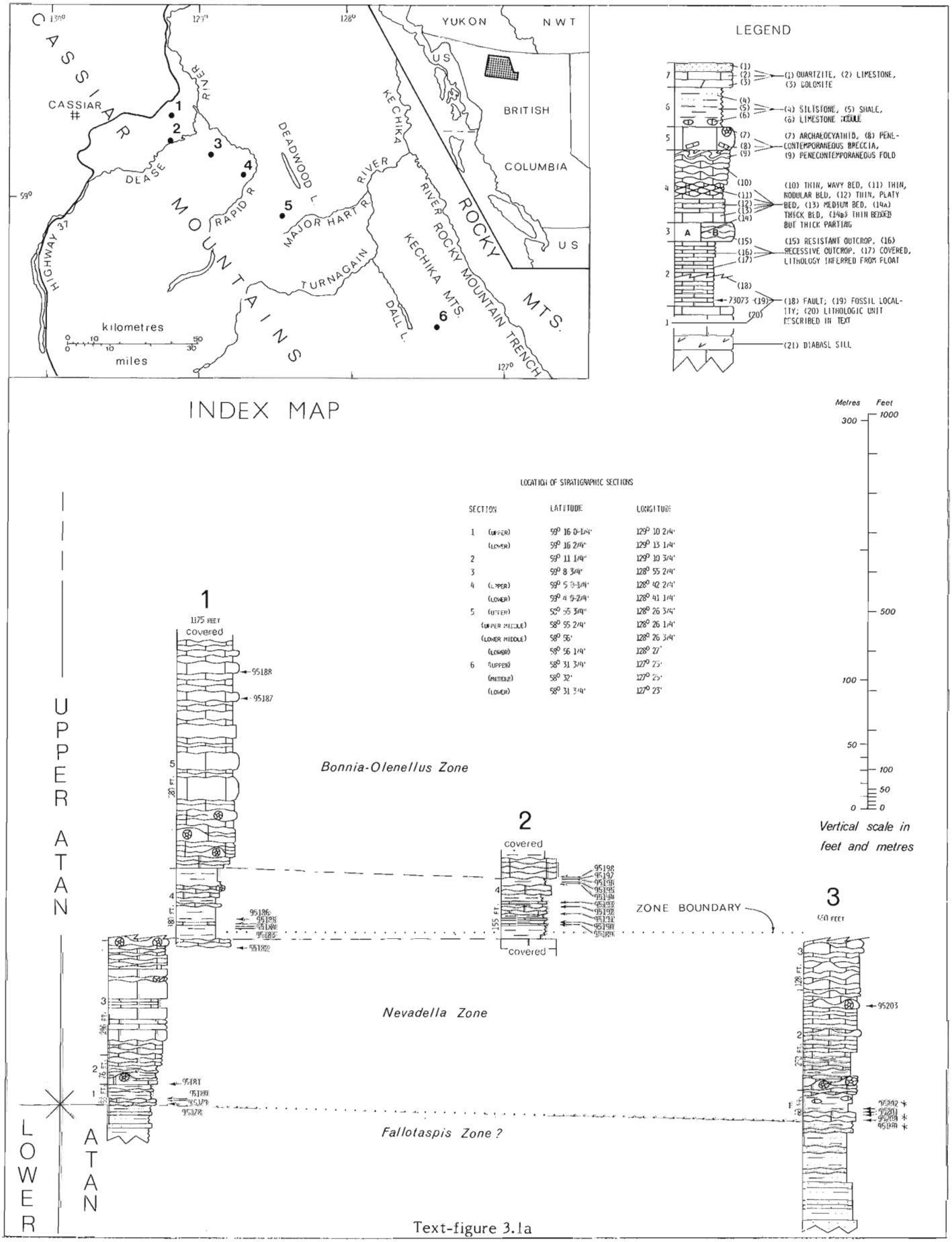

Text-figure 3.1a

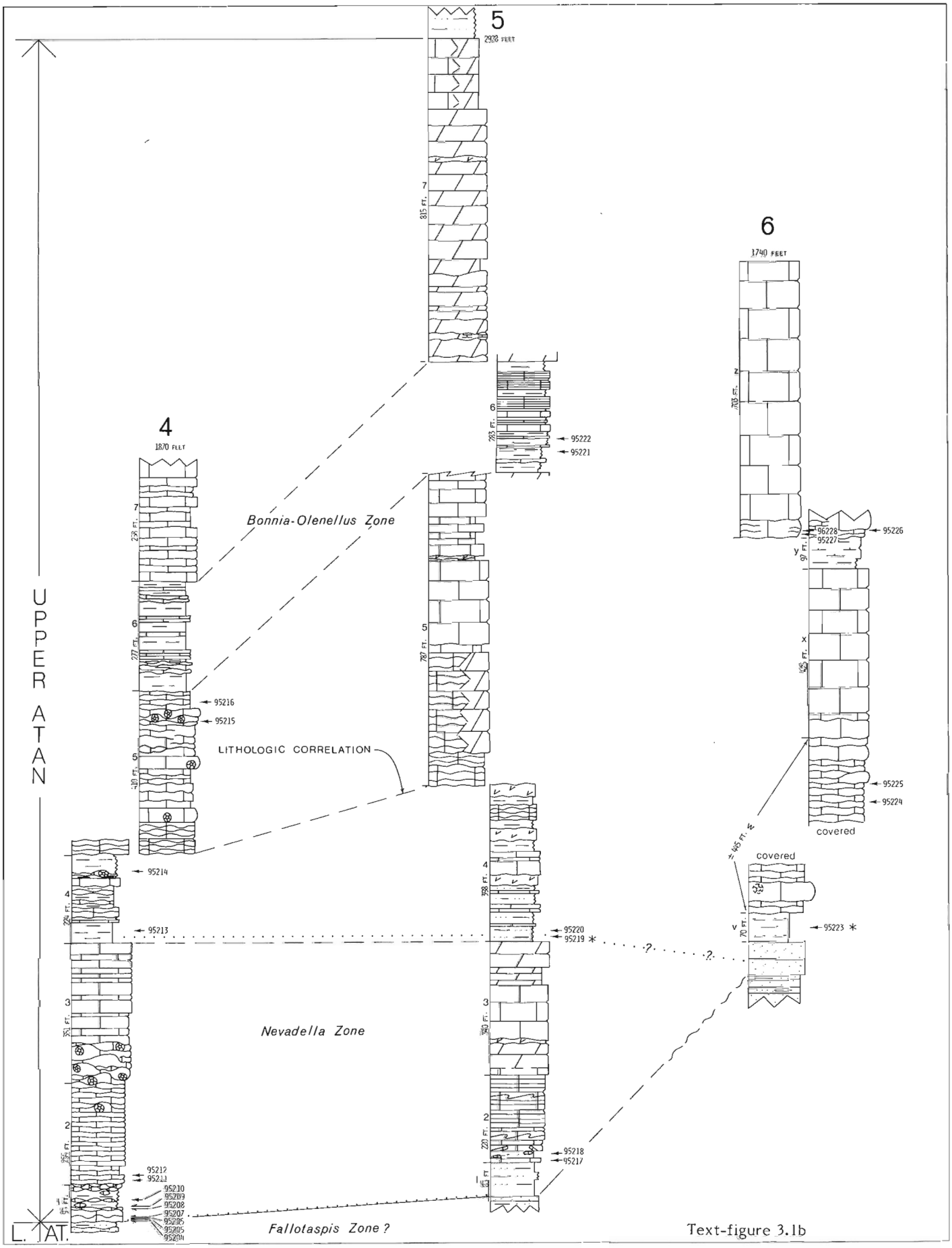

Text-figure 3.1b

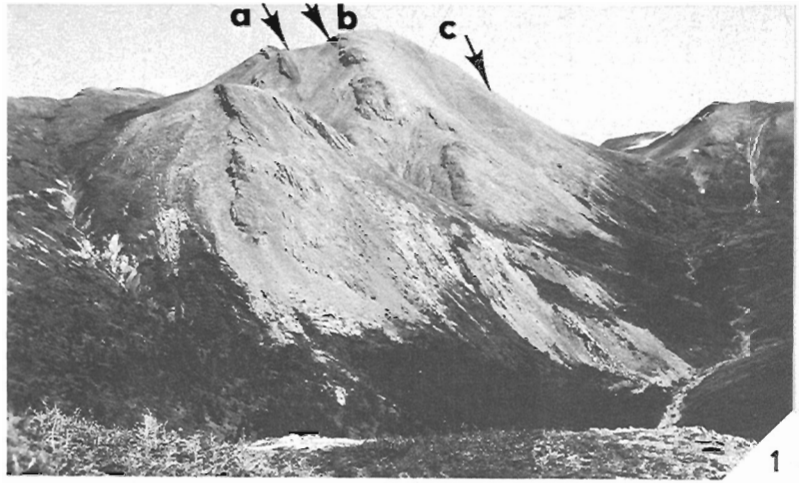

1

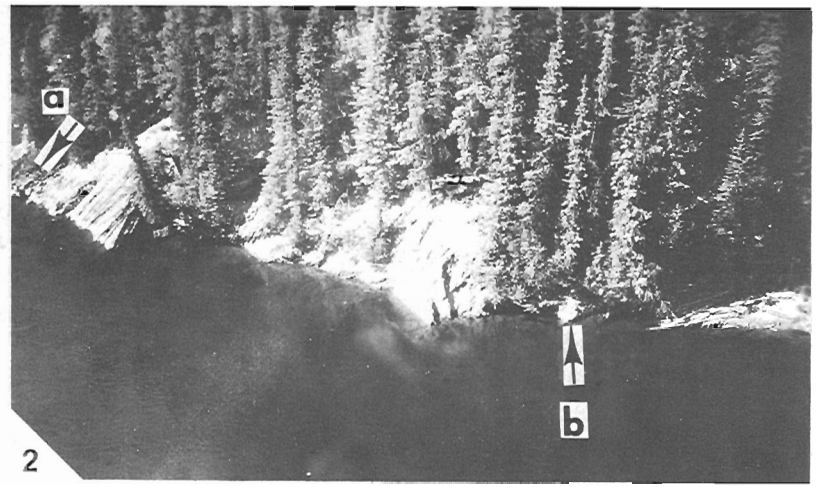

2

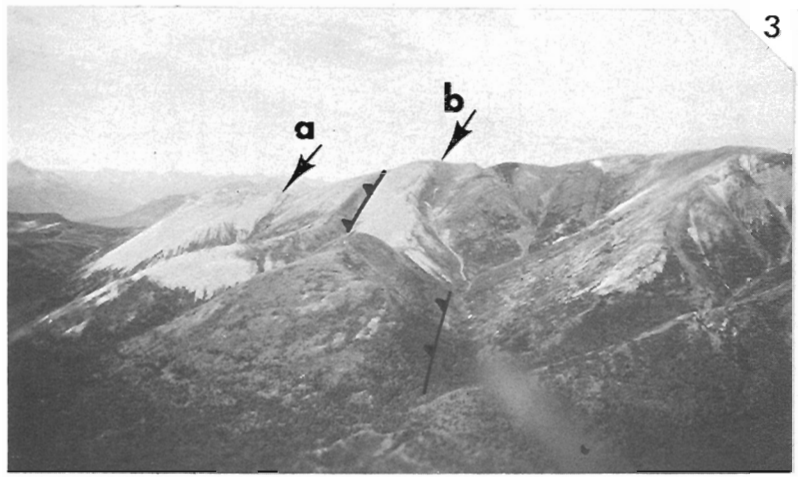

3

4

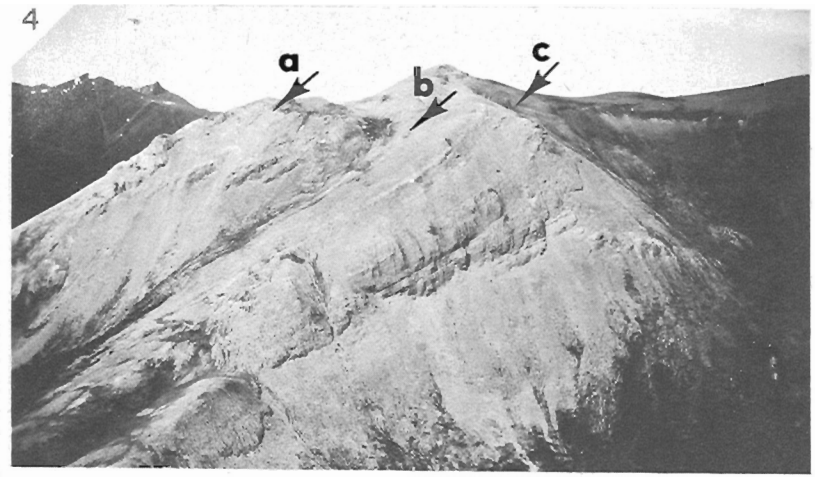

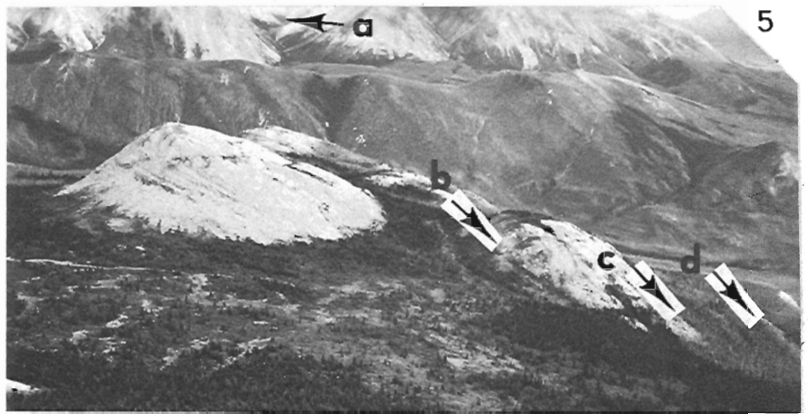

5

6

PLATE 3.1

Figure 1. View from near lower segment of section 1 looking east at upper segment of section 1. Base of unit 4 is at "a" and top is at "b". Youngest strata measured in unit 5 are at "c". Talus on dip slope to right of "c" probably covers younger Atan strata. GSC photo 203167.

Figure 2. View from helicopter looking at unit 4 in section 2 exposed on north bank of Dease River. Lowest outcrop of unit 4 is at "b" and top of same unit is at "a". GSC photo 203166-X.

Figure 3. View looking northwest at section 3. Units 1-3 were measured near ridge crest between "b" and thrust fault. Base of unit 1 in overlying thrust plate is at "a". GSC photo 203167-D.

Figure 4. View looking west at lower segment of section 4. Segment was measured from base of unit 1 at "c" to top of unit 4 at "a". Base of unit 4 is located at "b". GSC photo 203167-B.

Figure 5. View looking east at upper segment of section 4. Base and top of unit 5 is at "b" and "c", respectively. Top of unit 6 is at "d"; section continues to right and down dip slope from this point. Medium brown weathering siltstone at base of Kechika Formation is exposed on north slope of valley located at "a". GSC photo 203167-G.

Figure 6. View looking south at lower segment shown in Figure 4. Base of unit 1 is at "b", and base of thick-bedded, white weathering limestone rib located 97 feet above base of unit 3 is at "a". GSC photo 203167-H.

General Statements and Acknowledgments

Because the upper Atan in the Cassiar Mountains (sections 1-5) differs from the "upper Atan" in the Kechika Ranges (section 6), lithologic units in the former area have been assigned numbers while letters of the alphabet have been used to represent units from the latter area. This convention is adopted so that no direct correlation is implied in the text descriptions or in Figure 3.1a, 3.1b. Thicknesses for the units in both areas are given on the figures under the appropriate number or letter. Fossil identifications given in the text and ages implied in the figures are based on field and cursory laboratory observations. Detailed studies must await a thorough preparation of the material. Locality numbers marked by an asterisk on Figure 3.1a, 3.1b represent strata at horizons in nearby outcrops that have been projected into the measured section at approximatley the same stratigraphic level.

Assistance in measuring section 1 was provided by C.M. Henderson, and assistance with sections 1, 2, 4 to 6 was given to P.W. Fritz.

Upper Atan in the Cassiar Mountains

Unit 1

This unit is present at sections 1, 3 to 5 where it consists of light brown to light silvery brown weathering, slightly limy shale with a subordinate amount of limestone in scattered nodules and in thin, wavy beds. At the base of the unit in sections 1, 3 and 4 it is distinctive rose to brick red weathering limestone sub-unit. The limestone changes colour laterally to light grey or to light greenish grey and does not exceed 35 feet in thickness at any given section. Near section 3, GSC locality 95199 contains fossils that probably belong to the **Fallotaspis** Zone at a horizon one-half foot above the base of the rose coloured sub-unit. The locality is at point "a" (Pl. 3.1, fig. 3) and has yielded two trilobite cheeks that are questionably assigned to **Parafallotaspis**. Collections made at 8, 9, and 12 feet above the base of the sub-unit in section 4 and various other collections from the sub-unit elsewhere all belong to the overlying **Nevadella** Zone.

Unit 2

Medium to dark grey weathering limestone in broadly wavy, thin beds (Pl. 3.2, fig. 1) predominate in this interval. Some small penecontemporaneous folds (Pl. 3.2, fig. 2) are present, but folds exceeding one foot in height are rare. Penecontemporaneous slump breccia was noted in intervals 20 to 24 feet and 35 to 36 feet above the base of the unit in section 5. Large, hook-shaped genal spines belonging to the trilobite **Holmiella** are locally common on bedding planes of the thin bedded limestone. Sparse mounds of light to medium grey limestone are present at various horizons within the unit. These mounds contain archaeocyathids and they rarely exceed one foot in thickness.

Unit 3

Medium and thick bedded limestone of unit 3 produces resistant outcrops relative to thinner bedded strata in units 1, 2 and 4. The limestone weathers medium light to medium grey and the thicker beds are often irregular and contain sparse archaeocyathids. Between and also grading laterally into the thicker beds are beds containing fine to coarse grained limestone clasts. At section 1 there is a considerable thickness of thin and medium beds containing limestone clasts set in a sparry matrix.

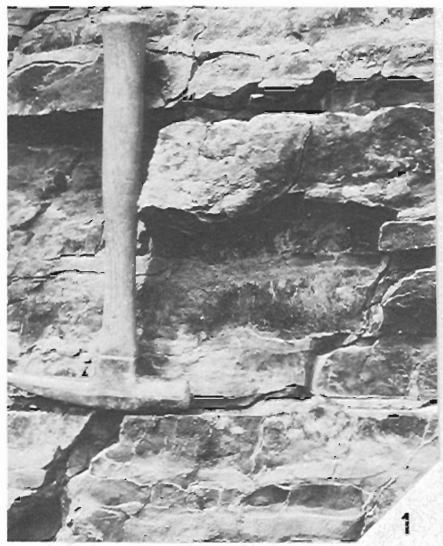

1

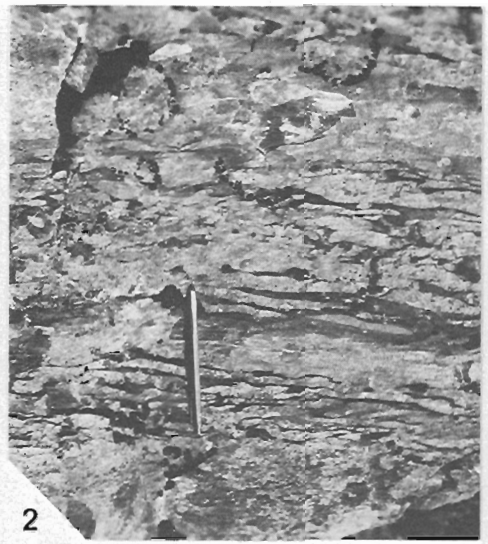

2

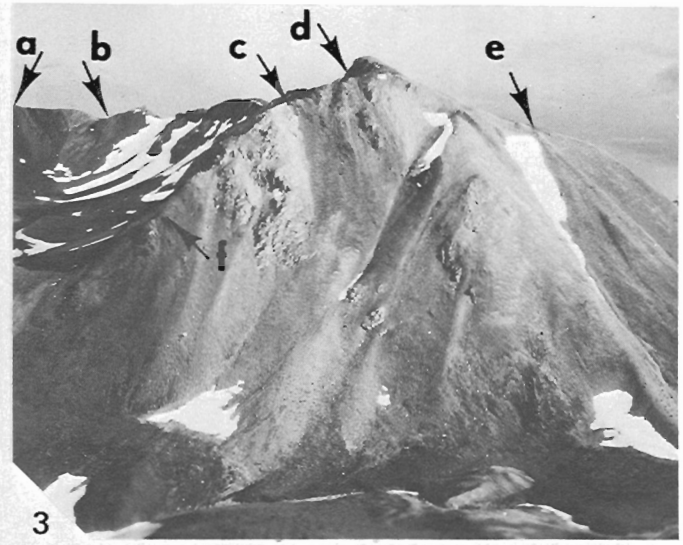

3

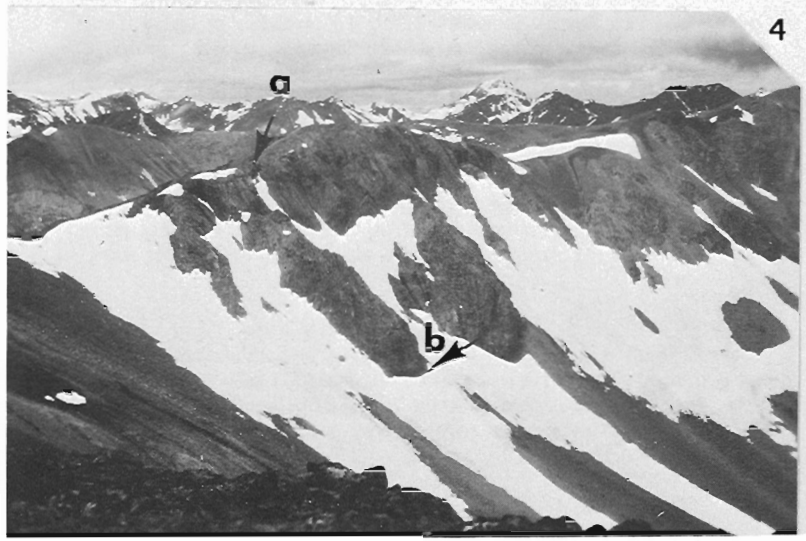

4

5

PLATE 3.2

Figure 1. Thin bedded, broadly wavy limestone 90 feet above base of unit 2 in section 4. Locality is approximately midway between points "a" and "b" in Figure 6 on Plate 3.1.GSC photo 203166-Y

Figure 2. Small, penecontemporaneous slump structures in thin bedded limestone in section 5. Surface shown is on local float block located 170 feet above base of unit 2. Medium light and medium dark grey weathering limestone is partially covered by black lichen. GSC photo 203167-C.

Figure 3. View looking southeast at lower segment of section 5. Base of unit 1 is at "f", and base and top of unit 4 is at "c" and "d", respectively. Exposure of unit 6 is at "e", but this unit was measured 1 mile farther southeast where outcrops are better. Units 1-4 are also exposed between points "a" and "b" at undescribed auxiliary section on far skyline. GSC locality 95219 was collected 10 feet above base of unit 4 in auxiliary section and is projected into main section shown in Figure 3.1b. GSC photo 203166-Z.

Figure 4. View looking west of cliff-forming limestone and dolomite in unit 5 of section 5. Base of unit is at "b" and point 480 feet stratigraphically above base is at "a". GSC photo 203166-W.

Figure 5. View looking northwest at upper segment of section 6. Base of segment at "b" is 215 feet below contact of units w and x. Base of shale unit y is at "a". Units v and the lower part of w are exposed on skyline immediately to the left of "c". Lower segment of section 6 shown in Figure 3.1b was measured on mountainside behind camera. GSC photo 203167-F.

Unit 4

Bright orange weathering shale plates covering a recessive interval mark this unit at sections 1, 2, 4 and 5 (Pl. 3.1, figs. 1, 2, 4; Pl. 3.2, fig. 3). At closer range a considerable amount of light greenish grey shale is conspicuous. Near the base of the upper third of the unit are limestone beds that contain archaeocyathids. The boundary between the **Nevadella** Zone and the **Bonnia-Olenellus** Zone at section 1 lies between GSC loc. 95182, located 21 feet below the base of unit 4 and **Olenellus**-bearing float collections 95183, 95184 and 95185 from 28, 33, and 38 feet, respectively above the base of the unit. At section 4 **Olenellus** was found in float 32 feet above the base of unit 4, and at section 5 the boundary is between a **Nevadella**-bearing collection (GSC loc. 95219) 10 feet above the base of unit 4 in a nearby auxiliary section (Pl. 3.2, fig. 3) and a **Olenellus**-bearing collection (GSC loc. 952220) found in local float 24 feet above the base of the unit. These observations, together with the finding of the lower **Bonnia-Olenellus** Zone index fossil **Laudonia** in the lower part of unit 4 at sections 1 and 2, indicate that the boundary between the **Nevadella** Zone and the **Bonnia-Olenellus** Zone lies within the lower part of unit 4.

Unit 5

Resistant medium to thick bedded limestone in unit 5 closely resembles strata in unit 3, even to the extent that thick, irregular beds containing archaeocyathids are present. As in unit 3 the thicker, lighter beds contain fine to coarse limestone clasts. **Proliostracus** found high in the unit (GSC loc. 95188) in section 1 indicates that strata at that level belong to the medial part of the **Bonnia-Olenellus** Zone.

Unit 6

At section 5 this unit is composed of light brown weathering shale and approximately one-third medium grey weathering, thin bedded limestone. Strata correlated with this unit in section 4 are mainly covered with vegetation except for outcrops of thin bedded, medium blue grey weathering limestone which is in part finely crystalline and in part fine to coarse grained. Two fossil localities in section 5 contain **Olenellus**, which dates the unit as belonging to the **Bonnia-Olenellus** Zone.

Unit 7

An incomplete but relatively undisturbed section in this unit was measured at section 4. The lower 184 feet consists of medium blue grey and medium light grey mottled limestone in medium and thin beds. Half of the strata above this level up to a talus and vegetation cover at the 258-foot level, and possibly 50 feet higher, resemble that below, and half consists of medium light grey limestone in thick to massive beds. At section 5, where many features are obscured by tectonic deformation, the lower 639 feet is composed of medium and thick bedded dolomite that weathers light pink, cream, and light brownish grey. The top 176 feet is composed of medium blue grey weathering limestone in thick beds that change laterally to cream weathering dolomite. No fossils were found in this unit at either of the two sections.

Basal strata in overlying Kechika Formation

Gabrielse (1963, p. 37) has observed that strata at the contact between the relatively competent Atan Group and the incompetent Kechika Group are either intensely deformed or covered at many places. Where exposed in the Cassiar Mountains, thick bedded carbonate of the Atan is typically overlain by silvery grey Kechika shale. However, at section 5, where a normal contact may exist, a hundred feet or more of medium brown Kechika siltstone immediately overlies the Atan. Here the siltstone is cleaved, and exposures are

limited to narrow stream cuts that are unsuitable for fossil collecting. Better siltstone outcrops were found three and three-quarters miles southeast of the upper segment of section 4 (see "a", Pl. 3.1, fig. 5). Fossils here are at best rare, as none were found during a two hour search, but this is still thought to be a likely area in which it may yet be possible to find the fossils necessary to date the base of the Kechika.

"Upper Atan" in the Kechika Ranges

Underlying quartzite

Immediately below the "upper Atan" in section 6 is approximately 85 feet of quartzite that is white on both weathered and fresh surfaces, and is fine to coarse grained. Since trilobites belonging to the **Bonnia-Olenellus** Zone are present a short distance above the quartzite (GSC loc. 95223), the quartzite must either belong to that zone or be older. It is tentatively thought that the quartzite is a basal sand overlying an erosion surface on the Ingenika Group. Time was not available to study the Ingenika outcrops in the area to see how much, if any, of the Ingenika strata is missing.

Unit v

The basal unit of the "upper Atan" in the Kechika Ranges is composed of shale that is in part light orange on weathered and fresh surfaces and in part light greenish grey on weathered and fresh surfaces. Although no fossils were found in the unit in the measured section, **Olenellus** sp. was located at two outcrops that lie along strike and are four and six miles northwest of the lower segment of section 6. The former and best locality (GSC loc. 95223) is at latitude 58° 33.5' and longitude 127° 29.5'.

Unit w

A covered valley separates the lower part of this unit in the lower segment of section 6 from the upper part in the upper segment of the section. No continuous outcrop of the unit was found elsewhere in the area, and the thickness given in Figure 3.1b is only a rough estimate. Medium grey limestone in thin and medium beds is the predominant lithology in both the lower and upper parts of the unit. This limestone is both finely crystalline and fine to coarse grained. A second, common, type of limestone present is in thick beds and thick (up to 22 feet) mounds that weather medium light grey and are finely crystalline to dense. Archaeocyathids were seen in outcrops of unit w in the lower segment of section 6 but not in the upper. Trilobites from the upper segment are **Olenellus** sp., **Bonnia** sp. and cf. Nelson, 1966, Plate 6, figures 6-9, 12, 13, all of which belong to the **Bonnia-Olenellus** Zone.

Unit x

This is a cliff-forming unit composed of medium light grey to white weathering limestone in thick beds. The limestone is dense to finely crystalline with some grains (pelletoids?) faintly outlined on fresh surfaces.

Unit y

Section 6 contains a rare exposure of this unit which is either talus covered or tectonically removed from the Lower Cambrian succession seen elsewhere in the area. The unit is composed of light rust to greenish grey weathering shale that is medium greenish grey on fresh surface. The lower 23 feet weathers to small plates while the remaining portion is blocky in outcrop and is more silty than that below. The presence of **Salterella** sp. in float from this unit testifies to this Lower Cambrian age.

Unit z

Most of the limestone in unit z is light grey to white weathering, thick bedded, and is almost identical to the limestone in unit x. The basal 48 feet contains medium light grey limestone in thin to thick beds that are medium dark grey on fresh surface and are both finely crystalline and fine to coarse grained. Strata younger than those included in this unit are not exposed on the mountain where the upper segment of section 6 is located, and younger strata could not be identified with certainty on the adjoining mountains where Lower Cambrian carbonate is more highly deformed.

Grand Cycles in the Atan Group

The upper Atan in the Cassiar Mountains is within a middle carbonate belt that fringed the North American craton in Lower Cambrian time. Clean carbonate in light coloured, archaeocyathid-bearing beds and mounds, and associated beds filled with carbonate intraclasts in sections 1 to 5, indicate a depositional site within but near the outer edge of the carbonate belt. The writer (Fritz, 1975, Fig. 1) has recognized three grand cycles (large clastic-carbonate pairs) in widely separated areas within the Cordilleran part of the belt, and it is not surprising, therefore, that the cycles are developed in the Cassiar Mountains.

The lower Atan and unit 1 combine to represent the lower (clastic) half-cycle of grand cycle A. The upper half-cycle is represented by units 2 and 3. The probable position of the **Fallotaspis-Nevadella** Zone boundary in the Cassiar Mountains is near the top of the lower half-cycle, as is the case in the Mackenzie Mountains (Fritz, 1976). Unit 4 and unit 5 of the upper Atan are correlated with the lower half-cycle and upper half-cycle of grand cycle B, respectively. The boundary between the **Nevadella** Zone and the **Bonnia-Olenellus** Zone lies within the lower half-cycle of grand cycle B. This boundary retains its position within the same half-cycle over a wide area, and has been documented in the middle shale member of the Poleta Formation of California and Nevada, the middle shale member of the Mural Formation in the Mount Robson and Cariboo Mountains areas, and in siltstone member B1 in the Mackenzie Mountains (Fritz, 1975, 1976). Unit 6 is tentatively assigned to the lower half-cycle of grand cycle C and unit 7 is tentatively assigned to the upper half-cycle. As mentioned earlier, no fossils have yet been collected from unit 7 and therefore the correlation to grand cycle C must be questioned.

In the Kechika Ranges at section 6 the "upper Atan" contains clean carbonate similar to that described in the Cassiar Mountains, and section 6 carbonate is also believed to have been deposited within the middle carbonate belt near its seaward margin. However, in section 6 older carbonate in the upper half-cycle of grand cycle A was either not deposited, or it was eroded before deposition of the white quartzite directly underlying unit v of the "upper Atan". All of the "upper Atan" units measured belong to the **Bonnia-Olenellus** Zone, but the fossil material available at the present time does not provide an accurate positioning of the units within the zone. The assignment of the various units in section 6 to grand cycles is therefore tentative at best. The writer presently favours placing the white quartzite and unit v in the lower half-cycle of grand cycle B, and units w and x in the upper half-cycle; units y and z are tentatively placed in the lower and upper half-cycles of grand cycle C, respectively.

Atan Group (?) in the Pelly Mountains

Although some questions remain to be resolved, the writer favours a tentative correlation of the Atan Group in the Cassiar Mountains with the Lower Cambrian succession near the Ketza River in the Pelly Mountains. Wheeler et al. (1960) divided the Ketza succession into a lower quartzite unit 1a, a medial phyllite and slate unit 1b, and an upper

archaeocyathid-bearing limestone unit 1c. Later, Tempelman-Kluit et al. (1975) placed an unconformity between units 1b and 1c, and removed units 1a and 1b from the Lower Cambrian by correlating them with the Proterozoic "grit unit" in the Selwyn Basin. They also show (1975, Fig. 2) several hundred feet of greenish grey shale overlying unit 1c, and a second unconformity separating this shale from an overlying Cambro-Ordovician phyllite.

The writer (1975) favours the original Lower Cambrian designation for units 1a and 1b, which he placed in the lower half-cycle of grand cycle A. The archaeocyathid-bearing limestone in unit 1c was placed in the upper half-cycle because of its position, lithology, and location within the **Nevadella** Zone. The first two reasons were used for placing the greenish grey shale overlying unit 1c in the lower half of grand cycle B, and it is probable that the boundary between the **Nevadella** Zone and the **Bonnia-Olenellus** Zone lies within this shale as it does within the half-cycle elsewhere. No local faunal evidence could be found to either confirm or deny the existence of an unconformity between the greenish grey shale and an overlying succession of dark shale and silty limestone. If the unconformity does indeed exist, these dark strata may be in part or completely younger than Atan. If it does not exist, they may represent a basinal, starved equivalent of part of the upper Atan. In either case, these dark strata do not contain Atan lithologies and should be excluded from the Atan Group.

In a recent and detailed study of the Ketza River succession, Read (1976, Fig. 7, p. 63, Pl. 9, figs. c, d) has shown evidence of strong bioturbation within unit 1a and he has not placed an unconformity between units 1b and 1c. Read's observations and the general lithology of units 1a and 1b suggest a direct correlation between these two units and the lower Atan plus unit 1 in the Cassiar Mountains. The basal white quartzite of the type Atan was not seen in the Ketza River succession, and it is not known from the limited outcrop in the latter area whether this quartzite is missing or if it lies a short distance below the surface.

Other Correlations

It has been mentioned earlier that the Atan Group has been recognized in the Pine Pass, Halfway and Ware map-areas. A comparison of data in the present paper with stratigraphic sections from these map-areas (Gabrielse, 1975; Street, 1967) does not substantiate this recognition. Sandstone and siltstone predominate throughout the Lower Cambrian in the three map-areas making it impossible to differentiate the lower (clastic) and upper (carbonate) lithologies that are the basic subdivisions within the Atan Group.

Reasons have been given under the description of section 6 for suggesting at least a delay in the full recognition of the Atan east of the Kechika River. This brings into question the mentioned use of the Atan Group in the Tuchodi map-area, which lies even farther to the east. The described Lower Cambrian succession (Taylor and Stott, 1973) there is unlike sections known to the writer from elsewhere in the Cordillera. It contains conglomerates that seem to be unique, and a thick succession of archaeocyathid-bearing, light coloured carbonates at a surprisingly high position. It is hoped that field work now being planned in this area will provide a basis for a refined correlation of these strata.

References

Fritz, W.H.

1975: Broad correlations of some Lower and Middle Cambrian strata in the North American Cordillera; in Report of Activities, Pt. A, Geol. Surv. Can., Paper 75-1A, p. 533-540.

Fritz, W.H. (cont.)

1976: Ten stratigraphic sections from the Lower Cambrian Sekwi Formation, Mackenzie Mountains, northwestern Canada; Geol. Surv. Can., Paper 76-22.

Gabrielse, H.

1954: McDame, British Columbia; Geol. Surv. Can., Paper 54-10.

1963: McDame map-area, Cassiar District, British Columbia; Geol. Surv. Can., Mem. 319.

1969: Geology of Jennings River map-area, British Columbia (104-0); Geol. Surv. Can., Paper 68-55.

1975: Geology of Fort Grahame E 1/2 map-area, British Columbia; Geol. Surv. Can., Paper 75-33.

Handfield, R.C.

1969: Early Cambrian coral-like fossils from the northern Cordillera of western Canada; Can. J. Earth Sci., v. 6, no. 4, p. 782-785.

1971: Archaeocyatha from the Mackenzie and Cassiar Mountains, Northwest Territories, Yukon Territory and British Columbia; Geol. Surv. Can., Bull. 201.

Mansy, J.L. and Gabrielse, H.

in press: Stratigraphy, terminology and correlation of Upper Proterozoic rocks in Omineca and Cassiar Mountains, north-central British Columbia; Geol. Surv. Can., Paper 77-19.

Nelson, C.A. and Durham, J.W.

1966: Guidebook for field trip to Precambrian-Cambrian succession, White-Inyo Mountains, California; Geol. Soc. Amer., Guidebook for Ann. Meeting.

North, F.K.

1971: The Cambrian of Canada and Alaska in Cambrian of the New World (Holland, C.H., ed.), Wiley-Interscience, New York, 456 p.

Okulitch, V.J.

1955: Archaeocyatha from the McDame area of northern British Columbia; R. Soc. Can., Trans., ser. 3, sec. IV, v. 49, p. 47-64.

Okulitch, V.J. and Greggs, R.G.

1958: Archaeocyathid localities in Washington, British Columbia, and the Yukon Territory; J. Paleontol., v. 32, p. 617-623.

Read, B.C.

1976: Lower Cambrian stratigraphy of Pelly Mountains, central Yukon Territory; unpubl. M.Sc. thesis, Univ. Calgary, Dept. Geol.

Rutter, N.W. and Taylor, G.C.

1968: Bedrock geology along Ingenika and Finlay Rivers, Peace River Reservoir area, British Columbia; Geol. Surv. Can., Paper 68-10.

Street, P.J.

1967: Trilobite zones in the Murray Range, Pine Pass map-area, British Columbia; unpubl. M.Sc. thesis Univ. British Columbia, Dept. Geol.

Taylor, G.C.

1969: Regional geology adjacent to the Alaska Highway between Fort Nelson and Muncho Lake, British Columbia; Edmonton Geol. Soc., Guidebook, 1969 field conference, p. 16-29.

Taylor, G.C. and Stott, D.F.

1973: Tuchodi Lakes map-area, British Columbia; Geol. Surv. Can., Mem. 373.

Tempelman-Kluit, D.J., Abott, G., Gordey, S., and Read, B.

1975: Stratigraphic and structural studies in the Pelly Mountains, Yukon Territory; in Report of Activities, Pt. A, Geol. Surv. Can., Paper 75-1A, p. 45-48.

Wheeler, J.O., Green, L.H., and Roddick, J.A.

1960: Quiet Lake, Yukon Territory; Geol. Surv. Can., Map 7-1960.

4. ULTRAMAFIC ROCKS IN CRY LAKE MAP-AREA (104 I), BRITISH COLUMBIA.

Project 490038

S. Leaming
Regional and Economic Geology Division, Vancouver

Abstract

Leaming, S., Ultramafic rocks in Cry Lake map-area (104 I), British Columbia; Current Research, Part A, Geol. Surv. Can., Paper 78-1A, p. 17-19, 1978.

Several large and many small ultramafic bodies occur in rocks of the Sylvester Group and particularly in rocks of the Cache Creek Group in Cry Lake map-area of north-central British Columbia. Numerous contacts between serpentinite and other rocks are reaction zones that are currently being exploited for jade (nephrite).

During the 1977 field season ultramafic bodies in the Cry Lake map-area (Fig. 4.1) were examined with the object of determining

1. the distribution of ultramafic and related gabbroic and volcanic rocks
2. variations in serpentinization of the ultramafic rocks
3. contact relationships with the enclosing rocks
4. the nature of contact reaction zones containing talc, listwanite, rodingite and nephrite
5. the geological setting of the ultramafic rocks.

Distribution

Except for the Alaskan-type ultramafic body north of Turnagain River and southwest of Hard Lake, the alpine-type ultramafic rocks in Cry Lake map-area occur entirely within areas underlain by the Cache Creek and Sylvester groups.

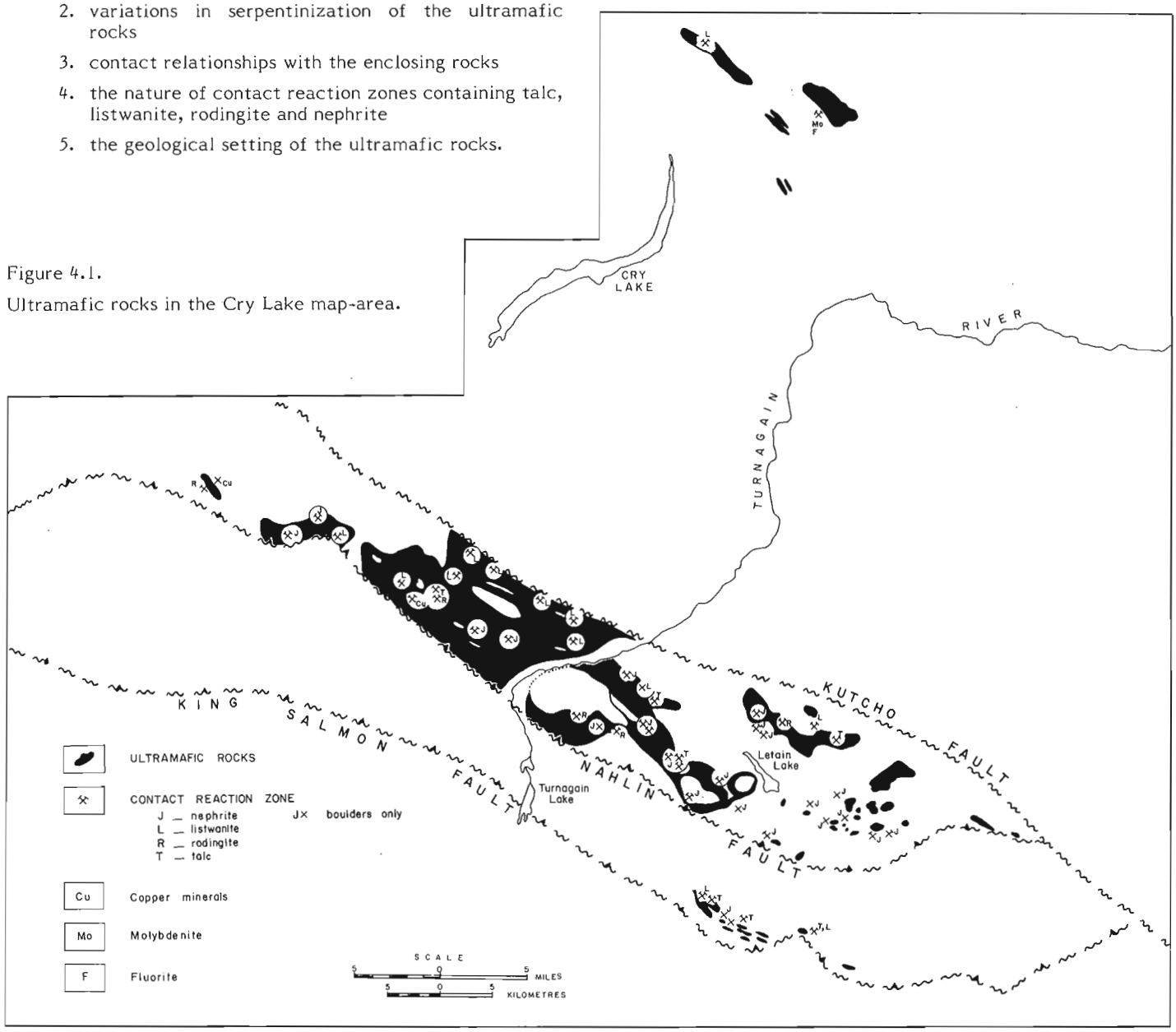

Figure 4.1.
Ultramafic rocks in the Cry Lake map-area.

This is shown in a diagrammatic cross-section in Figure 4.2. The ultramafic rocks are intimately associated with massive basaltic volcanics and irregular bodies of gabbro. No consistent relationships between the ultramafic, volcanic and gabbroic rocks is apparent. Many contacts are clearly tectonic but amounts of displacement are unknown. If these complexes are ophiolites, many of the criteria diagnostic of classic ophiolite complexes remain to be found.

Variations in Serpentinization

The ultramafic rocks in the Cry Lake map-area have been serpentinized to varying degrees. Some are completely altered, some partly altered, and others, comprising several large bodies, appear to be relatively fresh. The least affected rocks in some complexes appear to be dunites. These light brown, spheroidal weathering, dark green to black rocks appear massive and unserpentinizated in many hand specimens.

Serpentinization is most complete in the lower parts of ultramafic bodies and along wide shear zones, with the development of blackish green rocks with greasy luster and innumerable slickensided surfaces.

In places highly sheared serpentinite weathers light green and forms talus or felsenmeer of "fish-scale" serpentinite. This seems to be a weathering phenomenon because dark green serpentinite forms the cores of the scales. Most of the mountain saddles in the ultramafic terrain are underlain by sheared serpentinites. Less serpentinized ultramafics are commonly found at higher elevations and peaks not covered by greenstone. In places where serpentinization is not accompanied by deformation the rocks appear fresh and massive in the outcrop. Some of these rocks nevertheless are partly or extensively serpentinized.

An interesting phenomenon noted in several places is the development of peridotite nodules in the sheared serpentinite. These are roughly spherical or elliptical masses up to one metre in diameter but more commonly 5 to 10 cm in diameter occurring in clusters restricted to a few square metres lying in the regional foliation. The nodules are evidently formed by shearing stresses which rotate blocks of peridotite in a serpentine matrix. That movement was involved is evident from the slickensided surfaces in several directions commonly found on some of the nodules. Further evidence of the dynamic environment are the curving surfaces in the serpentinite which wrap around the massive nodules.

Serpentinization of gabbro and pyroxenite is generally minor.

Contact Relationships

Within the Sylvester Group a number of relatively small, narrow northwesterly trending bodies of ultramafic rocks contain a few tectonic inclusions, principally limestone.

Where the contacts are seen they are marked by shearing and in a few places by the development of listwanite (a rock comprising magnesite and quartz with minor mariposite).

The most easterly occurrence of ultramafic rock has been intruded by an apophysis of the Cassiar Batholith. Elsewhere it is in contact with greenstones of the Sylvester Group.

The southern belt of ultramafic rocks is a tectonic mélange of Cache Creek Group which include greenstone, schist, cherty limestone and ultramafic rocks. The southern margin of the mélange is bounded by the Nahlin Fault, a major thrust fault traceable westerly to the Atlin area. The northern margin is the Kutcho Fault. Northwest of Turnagain River, ultramafics occupy the full width between these two major faults but south of the river the ultramafic rocks are disposed in narrow bodies and small lenses within the Cache Creek Group.

Inclusions of greenstone, limestone and chert within the serpentinite exhibit sheared or faulted contacts. In two places serpentinites appear to be in intrusive contact with limestone, possibly a result of solid flow of incompetent serpentine during deformation.

Lack of any contact effect directly attributable to heat precludes the possibility of intrusion of ultramafic magma. The initial intrusion is considered to have been by solid flow of a crystal mush of ultramafic or partly serpentinized ultramafic rocks. The contacts are invariably tectonic.

Contact Reaction Zones

Contact reaction zones (metasomatites) include bodies of talc, rodingite, nephrite and listwanite formed by metasomatic changes at the contact of serpentinite with other rocks. The reaction is due to chemical differences in the adjacent rocks aided by ion exchange in a fluid medium pervading the rocks. Presumably the development of the metasomatites forms an effective barrier to further ion exchange because the bodies are invariably narrow. The widest zone noted in the Cry Lake map-area was a nephrite body about 10 m wide. Most are one or two metres wide. Many of the metasomatites range from 15 to 150 m long. In most cases the third dimension is probably similar to the length.

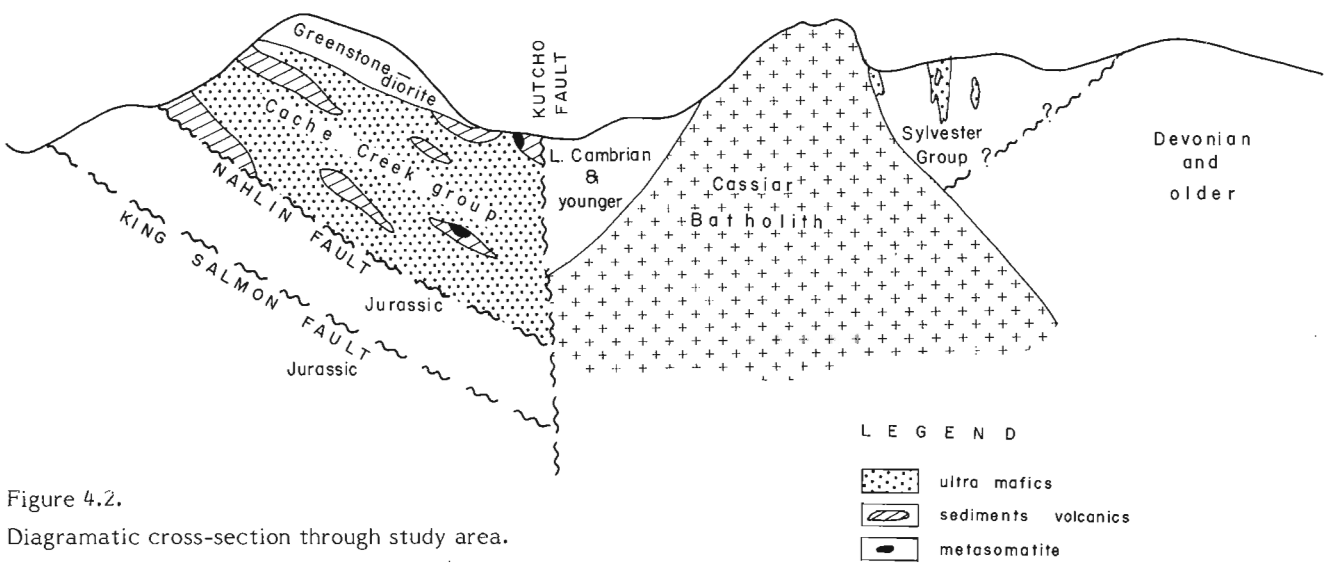

Figure 4.2.

Diagramatic cross-section through study area.

Of economic importance are the contact reaction zones consisting of nephrite. Initial production of nephrite in the map-area came from alluvial deposits. Currently production is coming mainly from talus blocks and their parent lodes.

During the course of field work a number of nephrite occurrences were seen. Some of these may have been previously undiscovered or at least unreported (see Fig. 4.1).

In a few places boulders of nephrite have no obvious in situ source. One of the best examples is the locality 20 km south of King Mountain where about 60 tonnes occur as boulders weighing up to 10 tonnes. Some of these are probably noncommercial because of schistose structure, but several appear very sound and hard. An occurrence about 14 km north-northwest of Turnagain Lake, and one near the head of Greenrock Creek merit further investigation. In situ and talus blocks occur in both localities but the in situ deposit in the Green rock locality is highly schistose and probably noncommercial.

Most of the other occurrences plotted on Figure 4.1 are either held as mineral claims and leases or are noncommerical because of small size or strong foliation. They may help however to focus further prospecting.

The serpentinites in the Cry Lake map-area are so extensive that much of the area has not been thoroughly investigated. The outcrops east of Kutcho Creek at the southeast end of the belt were not examined nor were all the serpentinite occurrences west of Kehlechoa River. The most important deposits in the map-area are those on the property of Cry Lake Jade Mines Ltd. At the time of a visit to the property about 200 tonnes of various grades were being processed for shipment. Initial production came from a deposit up to 10 m wide. The finest quality nephrite constitutes a small part of the lode.

A number of talc bodies in contact reaction zones were seen during the field season (see Fig. 4.1). All are sheared to varying degrees. Sound blocks for carving or other uses could not be obtained from any deposit examined because of innumerable shear planes. The individual deposits are not large and because of the remote location it is unlikely that the deposits could be commercially exploited in the foreseeable future.

Listwanite (-quartz-carbonate bodies) is a common alteration product of serpentinite along contact zones and many were seen in the map-area. The quartz occurs as veins and stringers in the carbonate, presumably magnesite. Elsewhere, notably in Russia, gold is found in listwanites and these rocks should be examined carefully. Many of the major placer gold fields are in ultramafic areas, although the source has not been identified. Interestingly, several listwanite zones feed into the drainage of Alice Shea and Wheaton creeks where placer gold has been recovered.

Several occurrences of chalcocite and/or tetrahedrite were noted in ultramafic rocks in the area. All are small pods probably only of mineralogical interest.

Disseminated chromite occurs in the ultramafic rocks in many places. Nodules up to 20 cm in diameter have been found along Wheaton Creek but no bands or layers of this thickness were seen in any of the rocks examined during 1977.

Fluorite occurs in granite near the granite-serpentinite contact northeast of the lower end of Cry Lake. The fluorite occupies flat fractures aggregating about one metre in thickness and can be traced for about 20 m along strike. A single rosette of molybdenite was found in the granite above the fluorite zone close to the serpentinite contact.

Geological Setting of Ultramafic Rocks in the Cry Lake map-area

Ultramafic rocks in the Cry Lake map-area are disposed in two tectonic mélanges:

1. Sylvester Group of late Paleozoic age and
2. Cache Creek Group, also of late Paleozoic age. Relationships between the groups are unknown.

Opinion on the origin of ultramafic rocks of the alpine-type is divided between two theories: (1) the oceanic crust concept and (2) direct intrusion from the mantle.

Oceanic crust is currently equated by many geologists with the ophiolite sequence of peridotite-gabbro-pillow lava with associated chert, limestone and pelite so common in orogenic belts around the world. The implication is that oceanic crust has been overthrust (obducted) onto the continental margins. Plate tectonics is currently favoured by many geologists as the mechanism for this emplacement.

Cache Creek rocks in the Cry Lake map-area may represent an ophiolite suite although recognition requires considerable imagination as several of the features characteristic of ophiolites are missing. Gabbro for instance is a very minor, even insignificant rock type. Pillow lavas are rare or nonexistent and the succession from peridotite through gabbro, diabase, to pillow lava with overlying marine sediments, particularly chert, is nowhere recognizable.

A case might be made for direct intrusion of an already differentiated crystal mush of relatively cold peridotite lubricated by interstitial liquid along fractures extending to the mantle. Later serpentinization and deformation associated with thrusting along the Nahlin Fault may explain the present distribution of the rocks.

5. LOWER MESOZOIC STRATIGRAPHY, CRY LAKE AND SPATSIZI MAP-AREAS, BRITISH COLUMBIA

Project 750015

J.W.H. Monger and Linda Thorstad[1]
Regional and Economic Geology Division, Vancouver

Abstract

Monger, J.W.H. and Thorstad, Linda, Lower Mesozoic Stratigraphy, Cry Lake and Spatsizi map-areas, British Columbia; Current Research, Part A, Geol. Surv. Can., Paper 78-1A, p. 21-24, 1978.

Lower Mesozoic strata in Cry Lake and Spatsizi map-areas, north-central British Columbia, comprise thick assemblages of dominantly andesitic volcanic rocks. A lower assemblage, possibly entirely of Late Triassic age, consists of volcaniclastic rocks characterized by augite porphyry and coarse bladed feldspar porphyry. These rocks grade upward into maroon feldspar porphyry breccias and flows of possibly Late Triassic and Early Jurassic age. The volcanic sequence is similar in lithology and general evolution to Late Triassic and Early Jurassic strata in Toodoggone and McConnell Creek map-areas along strike to the southeast. Northeast of the volcanic assemblage and separated from it by the King Salmon Fault, is a distinctive, commonly schistose terrane, designated the King Salmon assemblage, that consists of, lowermost, andesitic and dacitic pyroclastic rocks, gradationally overlain by probable Late Triassic carbonate and Early Jurassic fine grained clastic strata. In southeastern Cry Lake map-area the lower unit hosts massive sulphide mineralization.

Introduction

This study, part of a continuing investigation of stratigraphy, structure, and regional setting of the economically important lower Mesozoic volcanogenic assemblages of northern British Columbia, was carried out in conjunction with regional mapping of the Cry Lake and Spatsizi map-areas (104I, 104H) by H. Gabrielse, studies of Jurassic biostratigraphy by H.W. Tipper and of the Hotailuh batholith by R.G. Anderson. Monger is largely responsible for descriptions of strata in Spatsizi map-area and around the Hotailuh batholith in southwestern Cry Lake map-area. Thorstad is mainly responsible for the study of lower Mesozoic rocks to the northeast in Cry Lake map-area, north of the King Salmon Fault.

Cry Lake map-area spans three major structural subdivisions; the Omineca Crystalline Belt, the Hinterland Belt and the Intermontane Belt, separated from one another by major faults (Fig. 5.1). Lower Mesozoic successions, differing in both stratigraphy and structural style, are known from all three structural belts (Gabrielse, 1978). Southwesterly, in the Intermontane Belt, a thick, faulted and only locally metamorphosed, probable pre-Sinemurian (Lower Jurassic) volcanic succession is overlain by Sinemurian to Callovian sedimentary and volcanic rocks described by Tipper (1978). In the Hinterland Belt, between the Kutcho and the King Salmon faults, a highly deformed Mesozoic volcanic and sedimentary sequence, herein designated the King Salmon assemblage, is probably stratigraphically equivalent to both the pre-Sinemurian volcanics and the lower part of the sedimentary succession to the southwest. North of the Kutcho Fault, in the Omineca Crystalline Belt, variably deformed and metamorphosed lower Mesozoic volcanic and sedimentary rocks are probable equivalents to the strata in the Hinterland Belt. These successions are described below from south to north.

Intermontane Belt: Spatsizi map-area

Preliminary work shows that Triassic strata underlie the terrane 5 miles north of Cartmel Mountain, northwestern Spatsizi map-area, and probably extend discontinuously north-northwesterly to the Klastline Plateau on the western margin of the map-area. The Triassic succession comprises two units. The lower part consists of fine grained, banded tuff and massive, locally pillowed, augite porphyry in places containing carbonate blocks. The upper part comprises interbedded, laminated, tuffaceous siltstone and argillite, tuff and breccia with characteristic pink feldspar crystals, local basalt flows, and rare carbonate pods overlain by argillite and siltstone containing uppermost Triassic fossils.

These rocks are bounded by faults on the north and south bringing them into contact with a succession of red to brown, intermediate to acidic volcanics that contain Lower and Middle Jurassic fossils. Chlorite schist and marble exposed on the Klastline Plateau to the west, of probable late Paleozoic age, may form the basement to these rocks.

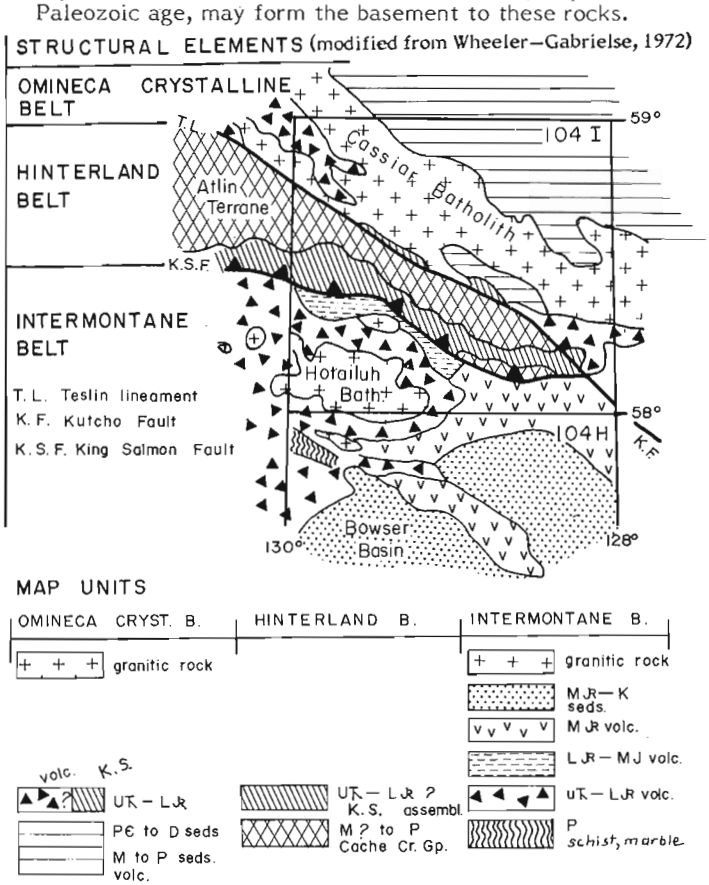

Figure 5.1. Index map showing general distribution of lithological assemblages and major structural elements in Cry Lake (104I) and northern Spatzizi (104H) map-areas.

[1] Department of Geological Sciences, University of British Columbia

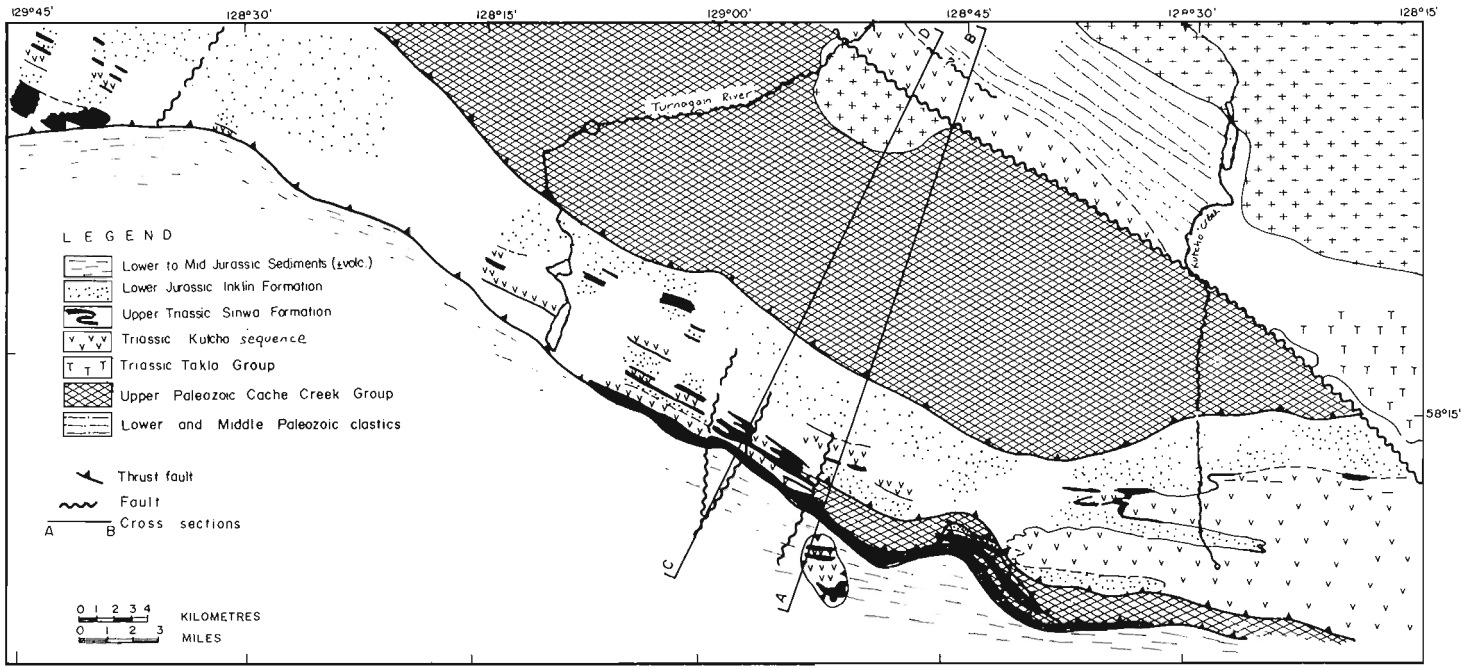

Figure 5.2. Distribution of lower Mesozoic rocks of the King Salmon assemblage.

Intermontane Belt: volcanic rocks around the Hotailuh batholith

The Hotailuh batholith largely intrudes the lower Mesozoic volcanic sequence but locally an early phase is overlain nonconformably by the volcanics (Anderson, 1978). The volcanic rocks dip radially away from the pluton and consist of two parts.

The lower sequence, exposed west, north and northeast of the pluton, consists of green, grey and locally red volcaniclastics, in places interbedded with argillite, and siltstone. The volcaniclastics are characterized by large crystals of augite porphyry and clasts of augite feldspar porphyry and locally, very prominent coarse "bladed" feldspar porphyry. Maximum thickness is probably less than 1000 m. Similar rocks outcrop almost continuously for 30 km west of the batholith, and apparently lie on schistose but fossiliferous Permian carbonate, tuff and argillite exposed near the confluence of Tuya and Stikine rivers.

The upper part of the lower succession is locally maroon, with a gradational contact between it and the overlying red and green succession of flows and volcaniclastics that predominate on the northeast, east and south sides of the Hotailuh batholith. The dominant lithology of the overlying succession is fine grained feldspar porphyry of intermediate composition that occurs as both breccias and flows. In places there are well bedded, red and green, variably epidotized crystal lithic tuffs, and elsewhere, minor acidic flows with rare quartz phenocrysts and ignimbritic members. Thickness of the sequence is approximately 700 m.

The age of this volcanic assemblage is in doubt. The lower unit is lithologically similar to the Upper Triassic, Takla Group, and the upper unit to the Lower Jurassic (Sinemurian) Telkwa Formation of the Hazelton Group exposed 250 km to the south-southeast in McConnell Creek map-area (Monger, 1977a). The paleontological evidence is equivocal. Probable Triassic fossils occur close to the contact on the northwest side of the Hotailuh batholith and, east of McBride River, Sinemurian strata overlie the succession. These data suggest that the above correlation with units to the south-southeast is correct. However, fossils, tentatively identified as Toarcian (late Lower Jurassic), occur seemingly interbedded with argillites of the lower succession on the northwest side of the Hotailuh batholith; further work is clearly necessary in this area.

Hinterland Belt: King Salmon assemblage

Stratigraphy: The King Salmon assemblage is economically important as it hosts massive copper zinc mineralization. The geology and deposits in the mineralized area were recently described by Pearson and Panteleyev (1975). In addition, the assemblage is geologically significant as it is closely associated with the Mississippian to Triassic Cache Creek Group; pre-late Mesozoic rocks rarely are known to be in this relationship.

The King Salmon assemblage, so named because it forms the thrust plate above the King Salmon Fault, consists of three lithological divisions that grade into one another (Figs. 5.2, 5.3). The lowest division is acidic to (locally) basic volcaniclastic rock, the middle division is carbonate and the upper division is largely phyllite. All three divisions are typically highly deformed, with a strong penetrative cleavage in most places, but the metamorphic grade is low, generally subgreenschist to greenschist facies.

The lowest division, herein called the "Kutcho sequence" from the extensive exposures near Kutcho Creek (Fig. 5.2), consists of intermediate and dacitic tuff and breccia, that in many places contains prominent β-quartz and altered feldspar crystals, the abundant metamorphic equivalents of these rocks, sericite schist, "quartz-eye" sericite schist and semischist and, uppermost, schistose conglomerate and sericitic argillite. Carbonate, as layers and lenses, is present throughout. Chlorite schist layers and lenses, with local chloritized pyroxene porphyry members, together with rocks reported by Pearson and Panteleyev (1975) as metagabbro, are considered to be metamorphic equivalents of "Takla-like" basic volcanics (Fig. 5.3). Copper-zinc sulphide horizons are in the sericite schist member. Apparent thickness of the Kutcho sequence is 3300 m, but the base is not exposed.

The middle division consists largely of foliated marble that is generally finely crystalline where dolomitized. It is believed to be equivalent to the Sinwa Formation. It contains

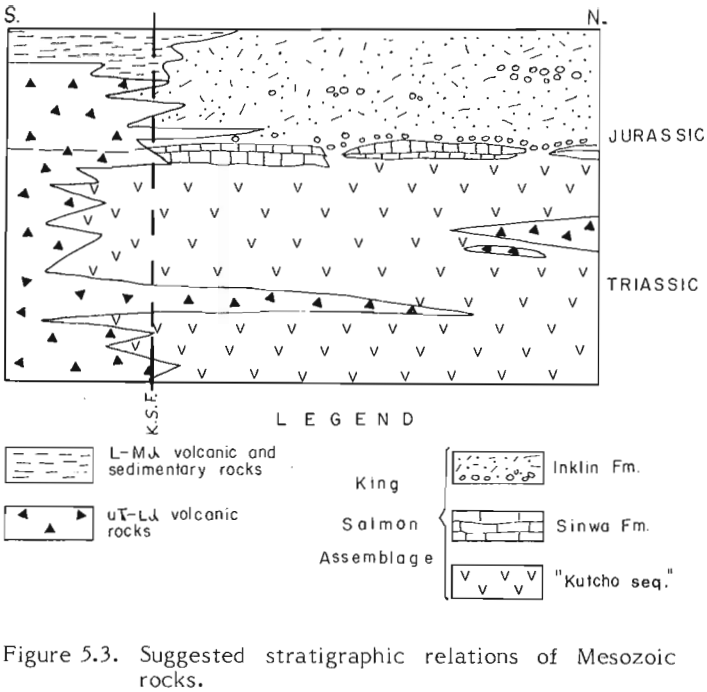

Figure 5.3. Suggested stratigraphic relations of Mesozoic rocks.

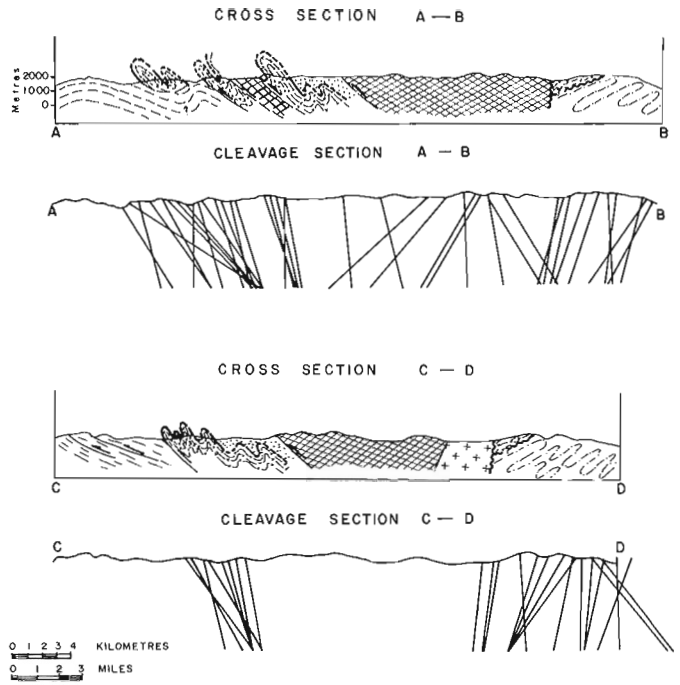

Figure 5.4. Cross-sections of the Hinterland Belt, between Turnagain River and Kutcho Creek (see Fig. 5.2). "Cleavage sections" show cleavage attitudes along the lines of the cross-sections.

a sparse fauna of crinoids, corals, bryozoa and pelecypods. Thickness of this division ranges from 0 to 150 m with much of the variation probably due to tectonism. In places, as on the divide west of Cariboo Creek, the carbonate is completely absent and a succession of thin, acidic tuff beds interlayered with carbonate grades upwards through conglomerate with carbonate clasts that in turn is overlain by phyllite of the uppermost division.

The upper division, correlated with the Inklin Formation, consists of phyllite and phyllitic siltstone with local greywacke and conglomerate beds. Conglomerate members are most common near the base of the division and consist mainly of acidic volcanic, carbonate and minor granitic clasts. The upper division rests apparently conformably on Sinwa carbonate or grades into the Kutcho sequence.

Age and correlation: The King Salmon assemblage is probably entirely of lower Mesozoic age. The upper division has long been correlated with the Inklin Formation of the Lower Jurassic Laberge Group on the bases of lithology and regional relationships, but no fossils are known from it in Cry Lake map-area (Gabrielse et al., 1962). The Sinwa Formation is uppermost Triassic in age in the type-area 150 km west of Cry Lake map-area, probably Upper Triassic age at Dease Lake immediately west of the map-area, and contains scleractinian corals and other fossils of definitely "post-Paleozoic", probably Triassic age, in the map-area (Monger, 1977b; H.W. Tipper, pers. comm.). No fossils are known from the Kutcho sequence, although earlier Monger (1977b) correlated it with the Lower Permian Asitka Group, largely because both units contain acidic volcanics. However, the gradational contacts with the overlying Sinwa and Inklin formations suggest that it is more probably of Triassic age.

Rocks lithologically and structurally similar to the Kutcho sequence outcrop in Toodoggone map-area, where they were correlated with the Asitka Group (Gabrielse et al., 1976). On the west side of the Omineca Mountains, 300 km to the southeast, the Sitlika assemblage closely resembles the Kutcho sequence (Paterson, 1974; Monger et al., in press). Locally, Kutcho rocks lie north of the Teslin lineament (see below). On strike to the northwest of these, in northeastern Dease Lake map-area, volcaniclastic rocks, flows, limestone pebble conglomerate, limestone and acidic volcanic dykes of the Nazcha and Shonektaw formations (Watson and Mathews, 1944; Monger, 1969) are possibly little metamorphosed equivalents of the King Salmon assemblage. Finally, probable Triassic acidic volcanics occur in the upper part of the Pavilion Group, southwestern British Columbia (Trettin, 1961), in a regional setting in many ways comparable with that in the north.

Structure: The King Salmon assemblage occurs mainly between the King Salmon Fault and Teslin lineament and is structurally isolated from all other rocks in Cry Lake map-area, with the exception of the Cache Creek Group. It appears to have been thrust in a southwesterly direction onto unfoliated strata as young as Middle Jurassic. Time of thrusting was as old as Toarcian (latest Early Jurassic; Tipper, 1978) or as young as earliest Cretaceous (Monger et al., in press).

The assemblage has undergone a single episode of penetrative deformation that has produced the characteristically well developed foliation, as recognized by Pearson and Panteleyev (1975). Locally this foliation is cross-cut by kink bands and is crenulated. Trend of the foliation is west-northwesterly, generally parallel with the King Salmon Fault and Teslin lineament. Dips of the foliation planes outline an asymmetric fan (Fig. 5.4). The foliation is parallel with the axial surfaces of major folds that are up to 2500 m in amplitude and 2000 m in wavelength and whose axes plunge gently westwards. Near the King Salmon Fault these are overturned to the southwest (Fig. 5.3). Folds in the King Salmon assemblage appear to be compatible with the King Samon Fault and presumably were produced at the same time.

The King Salmon assemblage occurs in the same structural belt as the Cache Creek Group. The latter unit has been affected by two deformations; a later one congruent with the deformation of the King Salmon assemblage and an earlier one shown by isoclinal folds, disruption of lithological units and local mylonitization. Most Cache Creek rocks are thrust over the King Salmon assemblage along a major, north-dipping fault, but a small, isolated body of Cache Creek strata, largely surrounded by and intimately associated with

the King Salmon assemblage, lies near the southern margin of the belt. This body appears to be an imbricate thrust slice that may have been emplaced in one of two ways. It is either a klippe of Cache Creek strata, infolded during deformation of the King Salmon assemblage, or else is a largely fault-bounded, anticlinal core with the King Salmon assemblage exposed on both flanks. If the latter, it has become completely detached; no depositional contacts remain, for the Cache Creek strata are in contact with all three units of the King Salmon assemblage.

Omineca Crystalline Belt

Small areas of augite porphyry flows and volcaniclastic rocks, very similar to Upper Triassic volcanogenic strata in the region, occur north of the Teslin lineament, in fault and intrusive contact with the Cassiar batholith. Rocks that are probably part of the Kutcho sequence also are known north of the lineament. These rocks include quartz-crystal-bearing tuffs and are far less deformed than those in the King Salmon assemblage and have only a weak to moderately developed cleavage. They lie in either stratigraphic or structural contact on highly deformed middle and lower Paleozoic strata.

References

Anderson, R.G.
1978: Preliminary report on the Hotailuh batholith: its distribution, age, and contact relationships in the Cry Lake, Spatsizi and Dease Lake map-areas, north-central British Columbia; in Current Research, Pt. A, Geol. Surv. Can., Paper 78-1A, rep. 7.

Gabrielse, H.
1962: Cry Lake, British Columbia; Geol. Surv. Can., Map 29-1962.

1978: Operation Dease; in Current Research, Pt. A, Geol. Surv. Can., Paper 78-1A, rep. 1.

Gabrielse, H., Dodds, C.J., and Mansy, J.L.
1976: Operation Finlay; in Report of Activities, Pt. A., Geol. Surv. Can., Paper 76-1A, p. 87-90.

Monger, J.W.H.
1969: Stratigraphy and structure of upper Paleozoic rocks, northeast Dease Lake map-area, British Columbia; Geol. Surv. Can., Paper 68-48.

1977a: The Triassic Takla Group in McConnell Creek map-area, north-central British Columbia; Geol. Surv. Can., Paper 76-29.

1977b: Upper Paleozoic rocks of northwestern British Columbia; in Report of Activities, Pt. A, Geol. Surv. Can., Paper 77-1A, p. 255-262.

Monger, J.W.H., Paterson, I.A., and Richards, T.A.
The Hinterland Belt of the Canadian Cordillera: new data from northern and central British Columbia; Can. J. Earth Sci., (in press).

Paterson, I.A.
1974: Geology of the Cache Creek Group and Mesozoic rocks at the northern end of the Stuart Lake belt, central British Columbia; in Report of Activities, Pt. B, Geol. Surv. Can., Paper 74-1B, p. 31-42.

Pearson, D.E. and Panteleyev, A.
1975: Cupriferous iron sulphide deposits, Kutcho Creek map-area. Geological field work; Brit. Columbia Dep. Mines Pet. Resour.

Tipper, H.W.
1978: Jurassic biostratigraphy, Cry Lake map-area, British Columbia; in Current Research, Pt. A, Geol. Surv. Can., Paper 78-1A, rep. 6.

Trettin, H.
1961: Geology of the Fraser River valley between Lillooet and Big Bar Creek; Brit. Columbia Dep. Mines Pet. Resour., Bull. 44.

Watson, K. deP. and Mathews, W.H.
1944: The Tuya-Teslin area, northern British Columbia; Brit. Columbia Dep. Mines, Bull. 19.

6. JURASSIC BIOSTRATIGRAPHY, CRY LAKE MAP-AREA, BRITISH COLUMBIA

Project 750035

H.W. Tipper
Regional and Economic Geology Division, Vancouver

Abstract

Tipper, H.W., Jurassic biostratigraphy, Cry Lake map-area, British Columbia; Current Research, Part A, Geol. Surv. Can., Paper 78-1A, p. 25-27, 1978.

Jurassic rocks of the Cry Lake map-area are mainly sedimentary and volcanic and of Sinemurian, Pleinsbachian, Toarcian, and Bajocian ages. The Lower Jurassic rocks are apparently affected by the King Salmon thrust fault and disrupted by a series of southwesterly directed imbricate thrust faults.

In the southern half of the Cry Lake map-area (104I) Lower and Middle Jurassic volcanics and sediments are poorly exposed in rounded hills and mountains that to the south merge into the Spatsizi Plateau. No well-exposed, unfaulted sections are known and information is available only from short sections exposed in thin imbricate fault slices. Although the several map units are lithologically fairly distinct, the many fossil collections have provided sufficient control to work out the structural style of these strata.

In the southwest part (Fig. 6.1), a section of Triassic and Jurassic volcanics (Monger and Thorstad, 1978) probably includes the oldest rocks in the study area. The Triassic rocks are, for the most part, augite porphyry basalts and feldspar porphyry basalts characteristic of the Upper Triassic Stuhini Group and these pass gradationally upward into red, maroon, green and grey subaerial breccias and tuffs lithologically similar to the Telkwa Formation of the Hazelton Group (Tipper and Richards, 1976). In several areas massive grey limestone of the Sinwa Formation is exposed unconformably below the Upper Sinemurian conglomerate but the base of the unit is not seen and its relation to the Triassic-Jurassic volcanics described above is unknown. It is a massively bedded sequence of grey limestone with local abundant fossil pelecypods and brachiopods. Generally it is fine grained and uniform, and in places contains minor chert.

The Upper Sinemurian strata are wholly correlative with the Telkwa Formation (Tipper and Richards, 1976, p. 11) and, although the section is volumetrically more sedimentary than the Telkwa Formation, the lithologic similarity is sufficient to justify inclusion as a nearshore marine facies of the Telkwa Formation. The conglomerate is generally coarse on the northeast side of the basin with clasts of fine grained limestone of the Sinwa Formation up to one metre in diameter, volcanic feldspar porphyry, coarse grained, low-mafic granitic rocks of unknown source, and chert, argillite and other rock fragments of probable Triassic or upper Paleozoic derivation. The conglomerate wedges out abruptly southwestward and is replaced, in part, by a thick shale-tuff sequence that is black to dark grey, massive, brittle and in part, finely laminated. Above the conglomerate is a second shale sequence with minor greywacke and few, if any, tuffaceous lenses. Overlying the shale is a sequence of feldspathic, green, andesitic to basaltic coarse breccia, minor tuff, and rare pebble conglomerate at the base. The shales in places contain a rich fauna and a few shale lenses in the conglomerates yielded diagnostic fossils indicating that the entire Upper Sinemurian and possibly part of the Lower Sinemurian are represented. Diagnostic ammonites recognized in the field are, in ascending order, as follows: **Arnioceras, Asteroceras, Gleviceras,** and **Paltechioceras.** Several other genera, as yet unidentified, are present, as well as abundant pelecypods, such as **Trigonia, Weyla,** and probably **Cardinia,** brachiopods, and corals. In the eastern part the Sinemurian beds rest unconformably on limestone of the Sinwa Formation but to the west the base is not seen. Because the conglomerates include clasts similar to the Triassic-Jurassic volcanics to the southwest, it is probable that the subaerial red volcanics are either correlative with or older than the Sinemurian section, in whole or in part, and this dominantly sedimentary Upper Sinemurian facies represents the northeast margin of the Whitehorse Trough, somewhat removed from the contemporaneous volcanism to the southwest.

The Takwahoni facies of the Laberge Group is a monotonous succession of interbedded greywacke and shale and rare lenses of pebble conglomerate that outcrops in southwestern parts of the area. The rocks are remarkably even-bedded, are dominantly greywacke, lack cross-bedding, exhibit some slump features and bioturbation marks, and show little channelling. Ammonite faunas are rare but Lower Pliensbachian **Uptonia** and **Protogrammoceras** were collected in a few localities and Upper Pliensbachian **Amaltheus, Arieticeras, Fuciniceras,** and **Prodactylioceras** were well-preserved in several collections. Some pelecypods, such as **Weyla** and **Trigonia,** occur in the Upper Pliensbachian beds. Contacts with older and younger strata are invariably faulted. Source of the sediment is not known but rare conglomerate and somewhat coarser and thicker greywacke beds on the southwest margin may suggest a southwesterly provenance. In places thin laminae of probable fine tuffaceous material indicate volcanic activity but the fineness of the material suggests it was distant.

The "Toodoggone Volcanics" is the informal name of a lithologic assemblage that is readily included in the Hazelton Group. It comprises interbedded marine and nonmarine sediments and volcanics of Toarcian to Bajocian age that underlie the southern part of the Cry Lake map-area (104I) and extend easterly into the type area, Toodoggone River map-area (94E) (Gabrielse et al., 1976) and into the Spatsizi map-area (104H) (studied mainly by Gabrielse). In this study area the assemblage is divisible into an upper and lower division. The lower division comprises mainly or entirely, rhyolitic flows, breccias and tuffs, red and maroon ignimbritic tuffs, breccias and volcanogenic sediments that apparently formed many centres, mainly to the south and west. In the northeast the section comprises mainly sediments with interbedded tuff and breccia. Coarse conglomerate with large limestone clasts and rock fragments predominate on the northeast flank and these wedge out rapidly to the west into thin pebble conglomerates that rest with erosional unconformity on Triassic and Jurassic volcanics. Interbedded are grey tuffaceous shale beds that in places include cream-coloured rhyolitic tuff that ranges from thin laminae in the northeast to dominant beds to the southwest beyond the study area. Lower Toarcian ammonites, belemnites, and pelecypods are locally abundant. **Harpoceras exaratum** Young and Bird, **Hildaites, Dactylioceras,** and **Weyla** were collected at several localities. The upper division was not seen in unfaulted contact except in the Spatsizi map-area to the south where the relationship is thought to be unconformable. In this area the lowest beds are interbedded marine shale and greenish breccia, siltstone, and

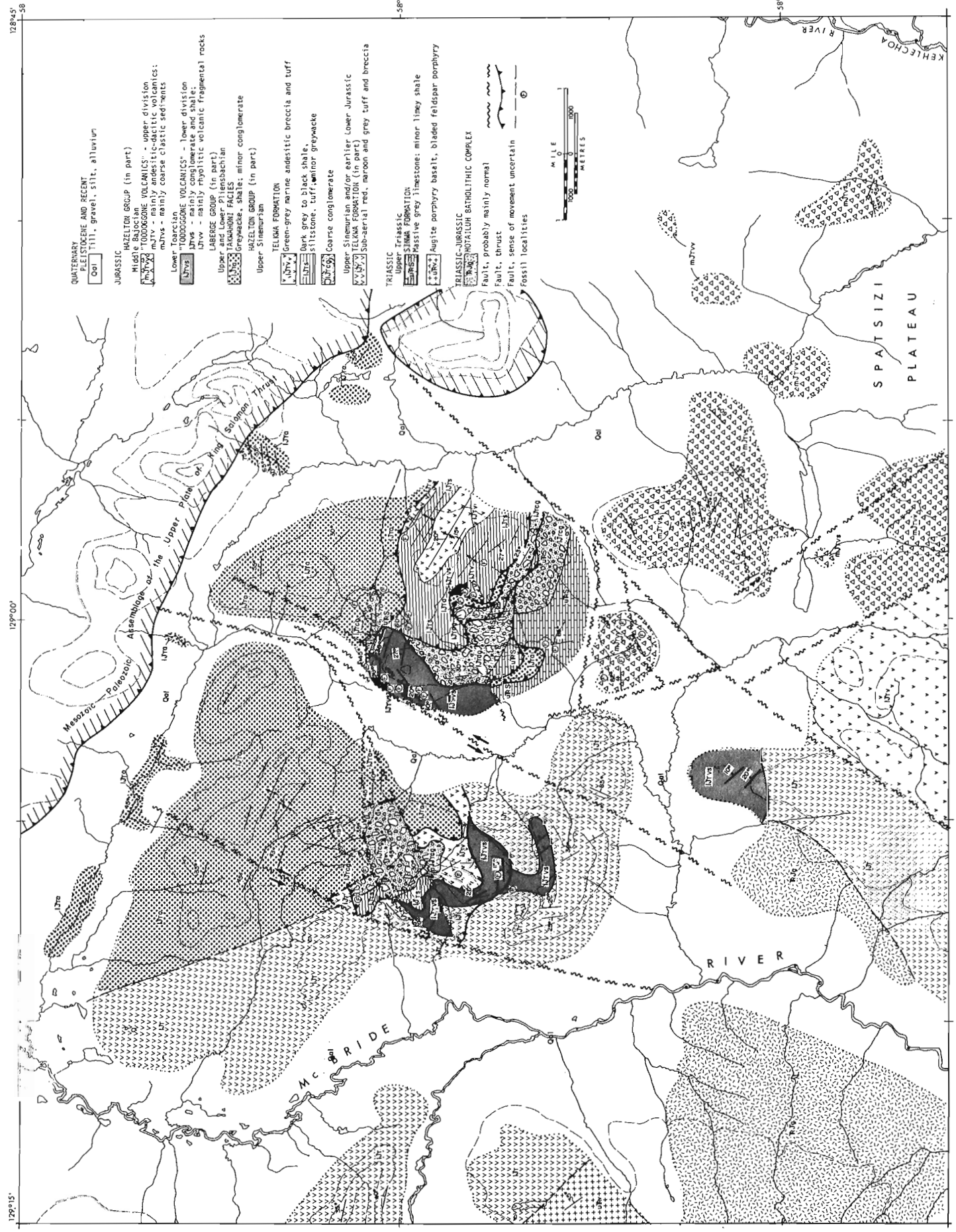

Figure 6.1. Jurassic strata in southern Cry Lake map-area.

tuffaceous shale; this is the only marine section of the division. These yielded several collections of Middle Bajocian ammonites with **Sonnia** sp. and with **Chondroceras** sp. Overlying this section are thick beds of chert-pebble conglomerate and interbedded shale and greywacke. Higher in the section drab grey to green, volcanic breccias and tuffs and reddish tuffs are interbedded with two or more conglomerate, shale, greywacke sequences.

The Jurassic sequences lie to the south of the King Salmon thrust fault and the deformation of the Lower Jurassic strata is thought to be directly related to this thrust. In the upper plate of the thrust fault massive limestone of the Sinwa Formation is thought to be the source of limestone clasts in Sinemurian, Toarcian, and Bajocian conglomerate. The Lower Jurassic beds are all involved in complex imbricate thrusting with transport to the southwest. Several faults roughly at right angles to the trend of the King Salmon Fault have some left-lateral strike slip movement but on a few the movement is mainly normal. The trend of the Lower Jurassic beds is generally northwest. The Middle Bajocian sediments and volcanics trend northeasterly, are block faulted, and are not involved in the thrusting that affected the Lower Jurassic strata. If this thrusting is related to the King Salmon Fault, then it is reasonable to suggest the time of movement of that fault is between Early Toarcian and Middle Bajocian time. Significantly, all the Sinwa limestone clasts in the Lower Jurassic conglomerates (pre-thrusting), are uniformly fine grained, massive limestone, whereas the limestone clasts in the Bajocian conglomerate (post-thrusting) are coarsely crystalline, veined, and sheared, as the Sinwa limestone in the thrust sheet is at present.

References

Gabrielse, H., Dodds, C.J., and Mansy, J.L.
1976: Operation Finlay; in Report of Activities, Pt. A, Geol. Surv. Can., Paper 76-1A, p. 87-90.

Monger, J.W.H. and Thorstad, L.
1978: Lower Mesozoic stratigraphy, Cry Lake (104I) and Spatsizi (104H) map-areas, British Columbia; in Current Research, Pt. A, Geol. Surv. Can., Paper 78-1A, rep. 5.

Tipper, H.W. and Richards, T.A.
1976: Jurassic stratigraphy and history of north-central British Columbia; Geol. Surv. Can., Bull. 270.

7. PRELIMINARY REPORT ON THE HOTAILUH BATHOLITH: ITS DISTRIBUTION, AGE, AND CONTACT RELATIONSHIPS IN THE CRY LAKE, SPATSIZI AND DEASE LAKE MAP-AREAS, NORTH-CENTRAL BRITISH COLUMBIA

Project 770016

R.G. Anderson[1]
Regional and Economic Geology Division, Vancouver

Abstract

Anderson, R.G., Preliminary report on the Hotailuh Batholith: Its distribution, age, and contact relationships in the Cry Lake, Spatsizi and Dease Lake map-areas, north-central British Columbia; Current Research, Part A, Geol. Surv. Can., Paper 78-1A, p. 29-31, 1978.

Preliminary data suggest that the Hotailuh Batholith in the Cassiar Mountains of north-central British Columbia consists of several distinct phases, including granodiorite, syenodiorite and gabbro, emplaced between late Triassic and mid-Jurassic time.

Introduction

During the 1977 field season field work began on the Hotailuh Batholith in Cry Lake (104I) and Spatsizi (104H) and Dease Lake (104J) map-areas with the object of establishing the distribution of the main granitic phases within the body and determining the relationship of the various phases to each other and to the surrounding country rock. Field work was carried out with the aid of helicopter support provided by the Operation Dease base at Turnagain Lake. Tentative identification of fossils was made by H.W. Tipper.

Geology

The Hotailuh Batholith, first named by Hanson and McNaughton (1936), underlies an area of 1140 km^2 in the Cry Lake, Spatsizi and Dease Lake map-areas (Fig. 7.1). Detailed mapping reveals the batholith to be much more complex than the relatively uniform biotite hornblende granodiorite or hornblende granodiorite as previously reported (Gabrielse **in** Leech et al., 1963, p. 46 and **in** Wanless et al., 1972, p. 20-21). At least five major phases may be recognized in the area studied.

Cake Hill Phase

Most of the western half of the Hotailuh Batholith is underlain by the Cake Hill phase which outcrops as far east as the headwaters of the Tanzilla River in the north, and Beggerlay Creek in the south. Mottled pink and white weathering, massive hypidiomorphic granodiorite with fresh prismatic hornblende is the predominant lithology although it grades into an outer margin of moderately foliated or lineated syenodiorite north of the Stikine River. Near the Cassiar-Stewart Highway, the granodiorite appears to grade into a well foliated (sheared?) hornblende diorite. South of Gnat Lakes, the well foliated hornblende diorite is associated with highly sheared augite porphyry at the contact. Variable amounts of sphene and magnetite are characteristic. All lithologies are cut by uncommon to rare augite and bladed plagioclase porphyry dykes and, south of Glacial Mountain, syenitic dykes.

The Cake Hill phase is nonconformably overlain by volcanics of probable Triassic age south of Glacial Mountain. The basal flow contains abundant rounded hornblende granodiorite pebbles and boulders identical in lithology to the underlying granitic rock. Within the overlying volcanic pile are thick, bladed plagioclase porphyry flows which are locally pillowed. South of peak 2473 m, thick, well bedded, siltstones and minor flows, tuff and carbonate (the latter containing Lower Jurassic fauna) apparently also nonconformably overlies the Cake Hill granodiorite. K-Ar age dates from the Cake Hill phase (Wanless et al., 1972) of 213 ± 11 m.y. (hornblende; GSC 70-34) support the paleontological evidence described above. Younger K-Ar ages determined from Cake Hill Lithologies, 157 ± 11 m.y. and 168 ± 8 m.y. (hornblende; GSC 70-29, Wanless et al., 1972), 147 ± 8 m.y. (hornblende; GSC 70-27, Wanless et al., 1972) and 139 ± 6 m.y. (biotite; GSC 70-28, Wanless et al., 1972) probably result from resetting of the system by the intrusion of the nearby granite of the potassic marginal phase. The contact of the Hotailuh Batholith and country rocks between peak 2473 m and Horn Mountain was not examined but its position on Figure 7.1. is taken from previous reconnaissance mapping in the area (Gabrielse, pers. comm., 1977). The rocks of the Hotailuh Batholith in the Dease Lake map-area were not examined during the field season but their distribution is also known from earlier work (Gabrielse, pers. comm., 1977). The southern contact of the Hotailuh Batholith, north of the Stikine River between Stewart-Cassiar Highway and Beggerlay Creek, remains poorly defined.

Potassic Marginal Phase

The potassic marginal phase is a moderately heterogeneous phase of pink weathering, massive, granite, syenite, quartz monzonite, monzonite and granodiorite. It intrudes the Triassic augite porphyry and Toarcian acidic tuffs, siltstones and feldspar porphyries along the northeastern and eastern margins of the batholith and forms the irregular apophysis east of Tsenaglode Lake. The mafic minerals are commonly chloritized and hornblende is more abundant than biotite. The characteristic feature of the potassic marginal phase is the presence of bluish grey megacrysts of plagioclase.

Locally a gradation from syenite and/or granite to quartz monzonite and/or monzonite away from the contact can be observed. At the contact the augite porphyry has an amphibolitic groundmass and augite phenocrysts are commonly uralitized. Clots of remobilized (?) pyrite and rare chalcopyrite are uncommonly seen in the metamorphosed augite porphyry. South of peak 2247 m screens of augite porphyry and bladed and medium grained plagioclase porphyry with associated cuspate inclusions in the granite suggest that some stoping of the country rocks occurred during the intrusion of at least part of the potassic marginal phase.

Syenodiorite Phase

An irregular body of massive to rarely foliated hornblende-biotite syenodiorite outcrops in the central part of the eastern half of the Hotailuh Batholith. The syenodiorite grades into a very heterogeneous dioritic core which consists of a number of minor dioritic phases, the most interesting of which is a massive, medium grained, rarely miarolitic acicular hornblende diorite. Irregular dykes of identical lithology cut quartz monzonite of the potassic marginal phase east of the main body of syenodiorite. Characteristic of the syenodiorite phase are: 2-5 per cent small rounded dioritic inclusions; uncommon to common poikilitic (?) plagioclase;

[1] Department of Geology, Carleton University, Ottawa, Ontario

fresh, euhedral biotite; and very common, well developed slabby vertical and horizontal jointing which give the cliffs a step-like appearance.

The syenodiorite examined during the 1977 field season is nowhere in contact with country rocks. Aplite and mottled, medium grained, pink and white minor granodiorite to quartz monzonite dykes intrude the syenodiorite. Potassium-argon ages (Wanless et al., 1972) of 155 ± 8 m.y. (hornblende; GSC 70-30), 163 ± 9 m.y. (hornblende; GSC 70-31, 1972), 163 ± 7 m.y. (biotite; GSC 70-32) have been determined from rocks within the syenodiorite phase.

McBride Granodiorite Phase

Fresh, homogeneous and massive hornblende-biotite granodiorite of the McBride granodiorite phase underlies the lower part of McBride River and forms a lobe of the Hotailuh Batholith east of longitude 129°15'W. Characteristic of this phase are abundant quartz, and equigranular textures. Along its western contact with a thin re-entrant of augite porphyry volcanics, the granodiorite is clearly intrusive. Augite porphyry has been metamorphosed to amphibolite and at the contact thin veinlets and dykes of the granodiorite are common. The nature of the eastern contact is not as clear because it is not exposed and the composition of the proximal volcanics may not record the effects of the intrusion of this phase. Uncommon silicification of the light grey chert breccia near the contact might imply that the contact is intrusive. Locally, a small massive, fine- to medium-grained diabase intrudes the granodiorite and contains small rounded granodiorite xenoliths near the contact. The contacts of the McBride granodiorite with the country rocks south of peak 2258 m and northwest of Mount Sister Mary were not examined.

Beggerlay Creek Gabbro Phase

A slightly heterogeneous, predominantly massive hornblende gabbro outcrops along the southern margin of the Hotailuh Batholith. It underlies most of the area south of Moose Creek, east of Moose Lake and as far west as the

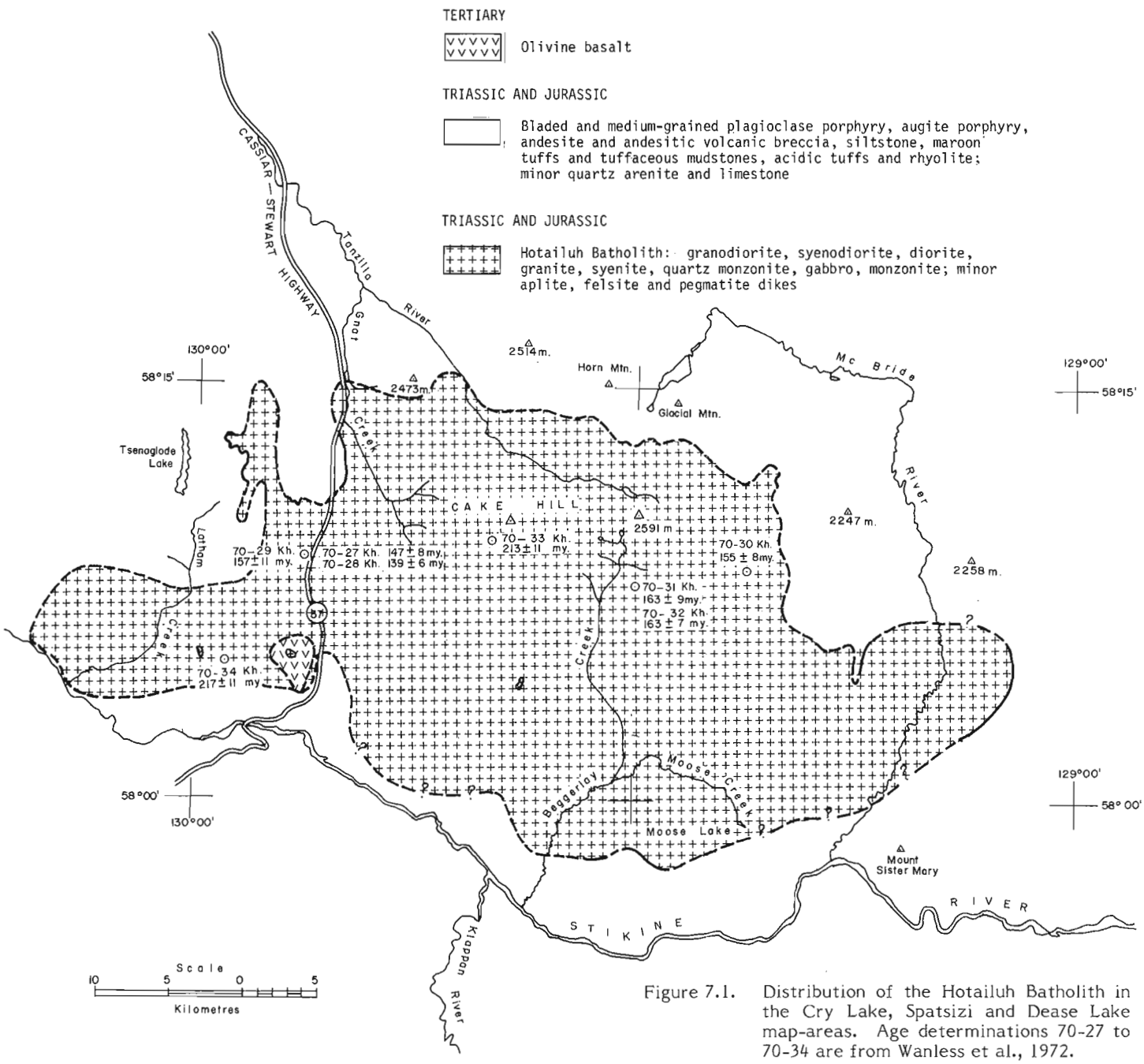

Figure 7.1. Distribution of the Hotailuh Batholith in the Cry Lake, Spatsizi and Dease Lake map-areas. Age determinations 70-27 to 70-34 are from Wanless et al., 1972.

confluence of the Klappan and Stikine rivers. Although hornblende gabbro is the predominant lithology, a gradation from pyroxenite through hornblende gabbro to hornblende diorite is seen. Locally the gabbro appears to be more felsic near the contact with the volcanics. When stained, thin potassic rims around the hornblende in the gabbro are commonly observed. Characteristic of this phase are coarse poikiloblastic(?) biotite megacrysts found in both the gabbro and the diorite.

The Beggerlay Creek gabbro clearly intrudes the Cake Hill phase, augite porphyry volcanics west of Beggerlay Creek and feldspar porphyry volcanics (of possible Jurassic age?) north of the Stikine River. Apophyses of gabbro intrude the Cake Hill syenodiorite near the contact. At the contact cataclastic zone of sheared gabbro, augen gneiss and gneiss one km wide is developed in the gabbro. The volcanics in contact with the gabbro are commonly metamorphosed to amphibolite. A metamorphosed feldspar porphyry screen in the gabbro outcrops southwest of Moose Lake.

Tertiary Volcanics

In the southwestern part of the Hotailuh Batholith, thin light grey to black, massive to diktytaxitic to scoriaceous olivine basalt flows cap the Cake Hill phase. These flows are up to 50 m thick but are commonly less than 20 m thick. The Tertiary cap west of the Stewart-Cassiar Highway may be more extensive than shown on Figure 7.1.

Mineralization having possible economic value is rare in the phases of the Hotailuh Batholith. Pyrite is the most abundant sulphide and uncommonly occurs in the hornblende diorite of the Cake Hill phase and in the hornblende-biotite diorite of the syenodiorite phase. Rare chalcopyrite and molybdenite occur in the miarolitic acicular hornblende diorite intrusions of the syenodiorite phase.

References

Gabrielse, H.
1962: Cry Lake map-area; Geol. Surv. Can., Map 29-1962.

Hanson, G. and McNaughton, D.A.
1936: Eagle-McDame area, Cassiar District, British Columbia; Geol. Surv. Can., Mem. 194, 16 p.

Leech, G.B., Lowdon, J.A., Stockwell, C.H., and Wanless, R.K.
1963: Age determinations and geological studies; Geol. Surv. Can., Paper 63-17, p. 45-46.

Monger, J.W.H. and Thorstad, L.E.
1978: Lower Mesozoic stratigraphy, Cry Lake (104I) and Spatsizi (104H) map-areas, British Columbia; in Current Research, Part A, Geol. Surv. Can., Paper 78-1A, rep. 5.

Wanless, R.K., Stevens, R.D., Lachance, G.R., and Delabio, R.N.
1972: Age determinations and geological studies; Geol. Surv. Can., Paper 71-2, p. 17-21.

8.

STRUCTURE STYLE IN NORTHEAST CRY LAKE MAP-AREA, NORTH-CENTRAL BRITISH COLUMBIA

Project 770016

H. Gabrielse and J.L. Mansy[1]
Regional and Economic Geology Division, Vancouver

Abstract

Gabrielse, H. and Mansy, J.L., Structure style in northeast Cry Lake map-area, north-central British Columbia; Current Research, Part A, Geol. Surv. Can., Paper 78-1A, p. 33-34, 1978.

Two important, distinct phases of folding are recorded in structures between Kutcho and Kechika faults in northeast Cry Lake map-area. The early phase is represented by asymmetrical folds with northeast dipping axial planes and in some places by recumbent, nappe-like structures overturned to the southwest. The second phase is evidenced by thrust faults, high-angle reverse faults and related folds directed northeasterly. Structures of both phases are truncated by granitic rocks of mid-Cretaceous age.

Structural Style

The main structures are shown in the cross-sections (see Figs. 8.1, 8.2). One of the best defined structures is the westerly overturned anticline in Four Brothers Range. The axis of the anticline dips gently to the east and in the southern part of the range only the lower, overturned limb is preserved. Farther north the axial planes dip more steeply. Because of the recumbent structure the oldest rocks in Four Brothers Range are exposed along the east flanks of the range, particularly in the deeply incised canyons (not shown in the cross-sections). They are probably correlative with the Tsaydiz and Swannell formations exposed in the Cassiar and Omineca mountains to the southeast. As is the case farther south, the rocks are regionally metamorphosed with the grade of metamorphism increasing with stratigraphic (not structural) depth.

North of Major Hart River early phase folds with easterly dipping axial planes are well developed in strata of the McDame Group. The folds are cut by steep northeasterly directed thrust faults. Similar thrust faults also involve volcanics and chert of the Sylvester Group. East of the main belt of Kechika Group strata the lower phase of deformation is only weakly developed or is absent.

Near Major Hart River the two most incompetent units are the lower part of the Sylvester Group consisting of shale and chert and the Kechika Group with a thick lower unit of thin bedded argillaceous limestone and calcareous shale and an upper unit of graptolitic shale and siltstone. These incompetent units are generally intensely deformed. Spectacular examples of recumbent folds in bedded chert can be observed in the north-facing cliffs just south of Major Hart River. These folds appear to be related to easterly directed thrust faults.

Structures along and south of Turnagain River are not completely mapped but it is apparent that recumbent, westerly overturned folds of regional extent are present. The best example of the fold style is shown in cross-section G-H, Figure 8.2, in which limestone of the Atan Group defines the structure. The early folds are cut by southwest dipping, high angle reverse faults which are associated with late folds and related cleavage.

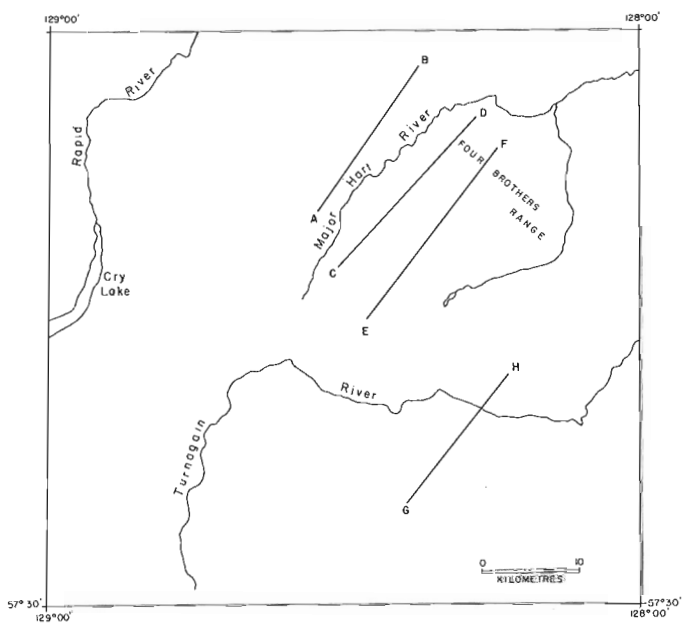

Figure 8.1. Locations of cross-sections in Figure 8.2.

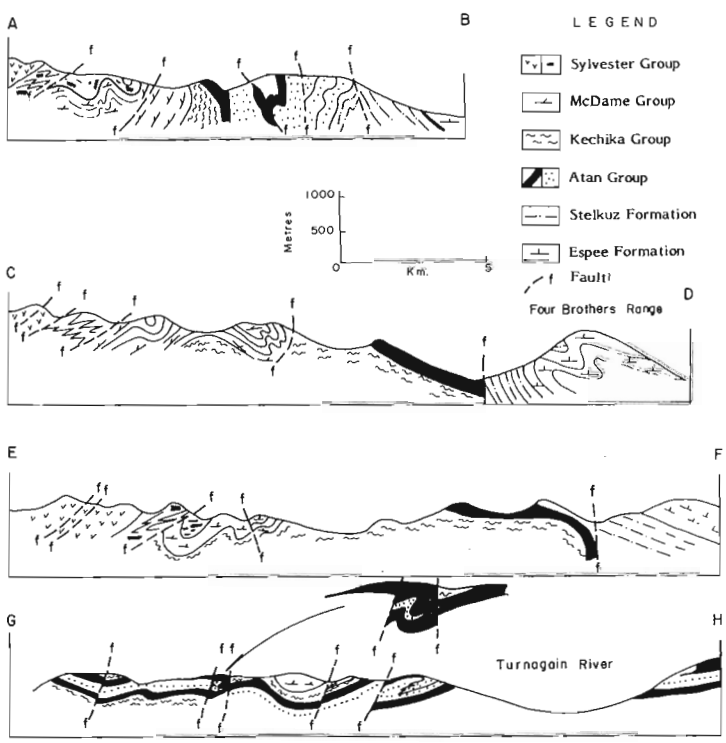

Figure 8.2. Diagrammatic cross-sections, northeast Cry Lake map-area. See Figure 8.1 for locations.

[1] University of Lille, France.

Northeast of Kutcho Fault and southwest of Cassiar Batholith two phases of deformation with the same temporal relationships as those northeast of the batholith are present in presumed lower Paleozoic rocks. The pendant of Sylvester Group in the Cassiar Batholith southeast of Cry Lake comprises highly deformed strata with local isoclinal and recumbent folds.

Regional Structure

Studies of the structural style in northeastern Cry Lake map-area are important in that they facilitate comparison between structures in Omineca and southern Cassiar mountains with those in northern Cassiar Mountains. In general, southwesterly directed structures are dominant in the region southeast of Rapid River in McDame map-area and southwest of Kechika Fault. Along a structural trend extending northwest into Yukon Territory, high-angle reverse faults dipping to the southwest are important elements in controlling the distribution of map-units. The transitional zone between the two regions of contrasting structural style lies between Major Hart and Rapid rivers in northeastern Cry Lake and southeastern McDame map-areas. There, the earlier formed structures appear to be progressively less well developed to the northwest rather than simply being overwhelmed by later northeasterly directed faults and related folds.

The distribution of regional structural domains in McDame, Cry Lake and Kechika map-areas strongly suggests that cumulative right-lateral displacements on Kechika and Thudaka faults (Gabrielse et al., 1977) probably total more than 150 km. Restorations of this order of magnitude are required to juxtapose terranes of similar structural style southwest of Kechika Fault in southwestern McDame map-area with those northeast of the fault in southwestern Kechika map-area.

Reference

Gabrielse, H., Dodds, C.J., Mansy, J.L., and Eisbacher, G.H. 1977: Geology of Toodoggone and Ware west-half map-areas, British Columbia; Geol. Surv. Can., Open file 483.

9. OPERATION SAINT ELIAS, YUKON TERRITORY

Project 730035

R.B. Campbell and C.J. Dodds
Regional and Economic Geology Division, Vancouver

Abstract

Campbell, R.B. and Dodds, C.J., Operation Saint Elias, Yukon Territory; Current Research, Part A, Geol. Surv. Can., Paper 78-1A, p. 35-41, 1978.

The Saint Elias Mountains are divisible into five distinct geological terranes separated by major faults. The Border Ranges and Walsh faults may be an old subduction zone and an ancient continental suture, respectively, whereas the Duke River and Denali faults are believed to be intra-continental strike-slip faults of mid to late Tertiary age.

Detailed study of part of the Kaskawulsh Group shows that the low grade metamorphic Paleozoic strata were first deformed on northeasterly trending folds and then refolded on northwesterly trends. A third deformation is related to major fault movements.

Introduction

Field work in 1977 continued that began in 1974 in the Saint Elias Mountains in Yukon Territory (Campbell and Dodds, 1975; Read and Monger, 1975; Eisbacher, 1975, 1976; Eisbacher and Hopkins, 1977; and Souther and Stanciu, 1975). Additional field work on the so-called Mush Lake Group was conducted by P.B. Read in 1975 (Read and Monger, 1976) who concluded his study during one month in 1977.

George Plafker and E.M. MacKevett Jr. of the United States Geological Survey provided valuable unpublished information from adjacent regions and contributed greatly to our understanding of the geology during visits in the field. During a brief visit J.A. Roddick of the Geological Survey of Canada examined some of the granitic rocks. Following a short field tour Warren Hamilton of the United States Geological Survey provided many provocative ideas and comments.

The principal objectives of the authors were to complete the mapping of the geology of the mountains within the Yukon (Campbell) and to study in detail the structure and stratigraphy of the Devonian and related rocks southwest of the Duke River Fault in the more accessible part of the region near Kaskawulsh Glacier (Dodds). The following report deals mainly with new data and the accompanying map is much simplified in those areas where information has been published previously (see references above). This applies particularly to late Paleozoic and Triassic, Jura-Cretaceous and Tertiary rocks along the northeastern margin of the mountains. Details of these rocks are not discussed herein.

Our knowledge of the western, rugged, ice-laden part of the mountains is necessarily based on helicopter fly-by and landing-site observations and this, coupled with the extensive ice cover, forces a degree of interpretation that commonly cannot be reinforced by extensive ground observations. Nonetheless the main elements of the geology comprising the distinctive geological terranes bounded by major faults, plutonic masses, and other major features can be mapped with confidence. Within individual terranes details of stratigraphy and structure could be mapped only where they are prominent and obvious. Much detail is omitted from the accompanying map in newly studied areas and considerable uncertainty remains in the interpretation of the geology south of the Seward Glacier and of Mount Vancouver where more work is required.

Geological Terranes of the Saint Elias Mountains

The Saint Elias Mountains are divisible into five geological terranes separated by major faults (Fig. 9.1):

1. Southwest of the Border Ranges Fault in the southwestern part of the region an extensive area of Cretaceous sedimentary and volcanic rocks is commonly metamorphosed, highly deformed, and intruded by early Tertiary plutons. In the extreme southwest the Cretaceous rocks are thrust over folded Tertiary marine sedimentary strata.

2. Along the Logan and Walsh glaciers a relatively small area of Pennsylvanian, Permian and Triassic sedimentary and volcanic rocks, extensively intruded by Jura-Cretaceous and possibly Tertiary plutons, lies between the Border Ranges and Walsh faults. The plutonic rocks form the Mount Logan massif.

3. A vast terrane of Paleozoic sedimentary and volcanic rocks informally named the Kaskawulsh Group is cut by plutons that range in age from Pennsylvanian to Tertiary and is bounded on the southwest partly by Walsh Fault and partly by Border Ranges Fault and on the northeast by Duke River Fault.

4. Between Duke River Fault and the Denali Fault System is a second belt of Pennsylvanian, Permian, and Triassic, with some Jura-Cretaceous, sedimentary and volcanic rocks cut by Cretaceous and Tertiary plutons.

5. Finally, northeast of Denali Fault System are Jura-Cretaceous sedimentary and related volcanic rocks of the Dezadeash Group cut by Cretaceous and Tertiary intrusions. The volcanic rocks may be entirely older than the sedimentary strata.

Rocks correlative with the Dezadeash Group (terrane 5) occur also above the late Paleozoic and Triassic rocks of terrane 4 immediately to the southwest, thus the Dezadeash Group may have a basement of late Paleozoic and early Mesozoic rocks, but this has not been conclusively demonstrated. In no other case is there evidence that adjacent terranes share common stratigraphic units except for plutonic masses and for Late Cretaceous and Tertiary sedimentary and volcanic rocks that postdate the age of some of the bounding faults. Thus the Kaskawulsh Group (terrane 3) is not known to underlie the rocks of terranes 1, 2 or 4, nor do rocks of the latter overlie strata of the Kaskawulsh Group. Similarly the Cretaceous rocks of terrane 1 were not deposited upon late Paleozoic and Mesozoic strata of terrane 2, nor are the latter known to be the basement of the former. The bounding faults thus appear to represent subduction zones, sutures or strike-slip faults of large displacement that separate terranes that have little common geological history.

Southwest of the Border Ranges Fault (Terrane 1)

The Border Ranges Fault (MacKevett and Plafker, 1974) is well exposed from the western border of the map-area eastward across the southern face of Mount Logan where it is

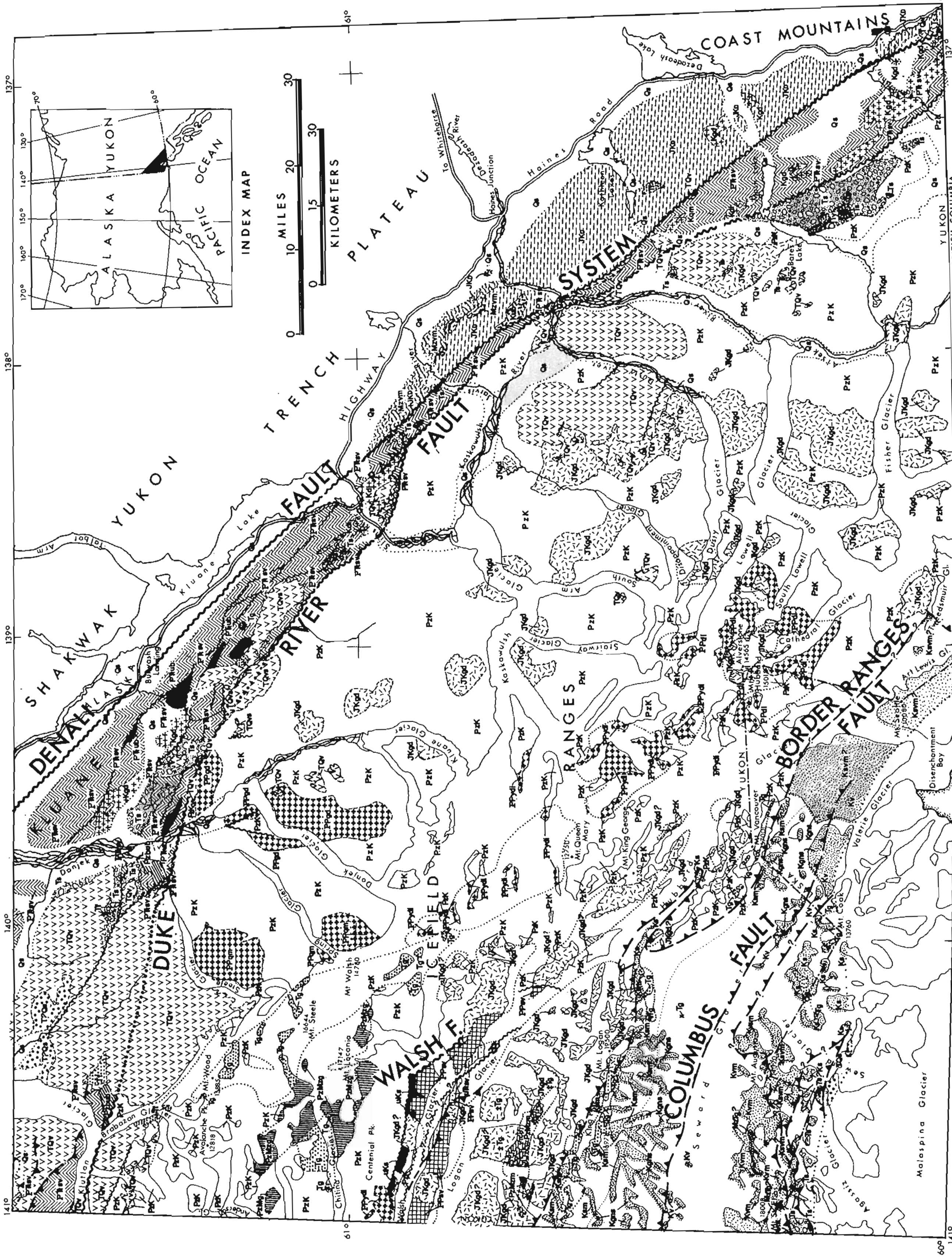

COAST MOUNTAINS
YUKON PLATEAU
SHAKWAK TRENCH
HIGHWAY
DENALI FAULT
DUKE RIVER FAULT SYSTEM
KLUANE
ICEFIELD RANGES
BORDER RANGES FAULT
COLUMBUS FAULT
WALSH F.
INDEX MAP
ALASKA
YUKON
PACIFIC OCEAN
MILES
KILOMETERS
Haines Road
Haines Junction
Kluane Lake
Seward Glacier
Malaspina Glacier
YUKON
BRITISH COLUMBIA

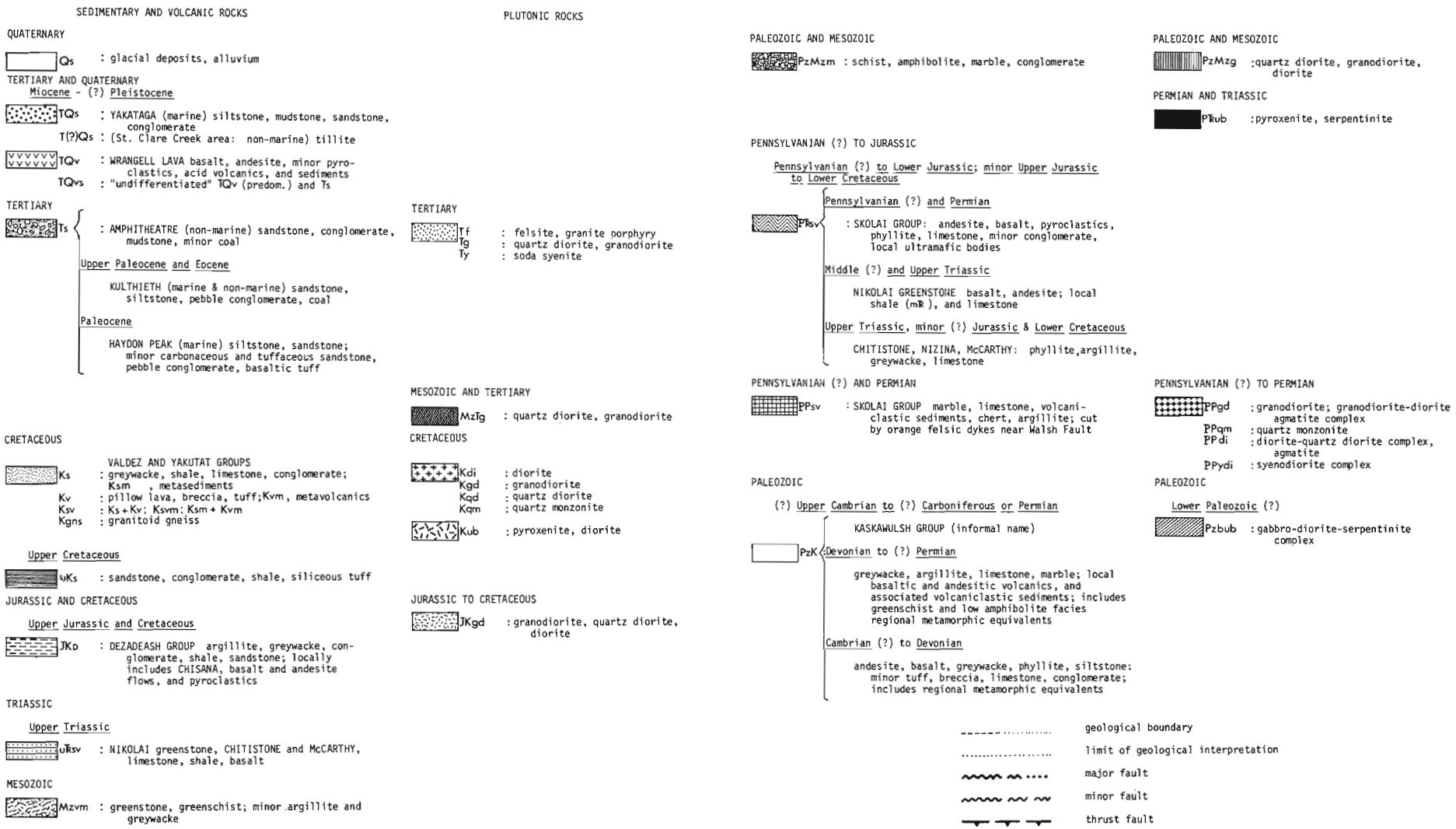

Figure 9.1. Geological map, St. Elias Mountains, Yukon.

a sharp, nearly vertical contact between black, Cretaceous metasedimentary rocks on the south, and grey, granitic rocks of the Mount Logan massif on the north. Locally the fault is cut by Tertiary plutons which may be more extensive, north of the fault, than has been recognized. Most of the granitic rocks immediately north of the fault are believed to be about 140 m.y. old based on isotopic ages obtained in Alaska to the west (MacKevett, 1976). If the plutonic rocks are Tertiary then the contact may be intrusive rather than a fault, an interpretation suggested by Warren Hamilton. South of Mount Vancouver and near the southern boundary of the map-area the location of the fault is less certain. Between Mount Logan and Mount Vancouver the fault is apparently folded or is offset by younger faults so that a thin band of fossiliferous Cretaceous rocks outcrops in Hubbard Glacier to the northeast of older(?) plutonic rocks and much more highly metamorphosed, older sedimentary and volcanic rocks (PzK). The band of metamorphic rocks (PzMzm) within the Mount Logan granitic mass northwest of the peak could be meta-Cretaceous strata exposed in a folded "window" of the Border Ranges Fault but they are just as likely late Paleozoic and Triassic.

The Cretaceous rocks south of Border Ranges Fault are equivalent and co-extensive with the Valdez Group to the west (MacKevett and Plafker, 1974) and with the Yakutat Group to the south and southeast (George Plafker, pers. comm., 1977). The rocks are believed to be mainly Early to Late Cretaceous in age and may include some Upper Jurassic strata. Within the map-area they contain early Lower Cretaceous fossils on the southeastern end of the Mount Logan massif on Seward Glacier (Sharp and Rigsby, 1956) and on Hubbard Glacier north-northwest of Mount Vancouver (a previously unreported locality). Fossils generally are extremely rare.

The rocks are variably metamorphosed sediments and volcanics. Along Seward Glacier between Border Ranges and Columbus faults the grade of metamorphism in a shale-greywacke sequence grades from weakly metamorphosed fossiliferous rocks through andalusite-bearing schist to biotitic granitoid gneiss. The gneiss is apparently thrust southward over low grade and unmetamorphosed volcanic rocks, including pillowed flows, tuff, and breccia along Columbus Fault which is exposed in many nunataks. The metavolcanic rocks are thrust over metasedimentary strata on the Saint Elias Fault and these metasedimentary rocks, in turn, are thrust over Tertiary marine sediments that range in age from Paleocene to Pleistocene. The Tertiary rocks contain thrust faults (George Plafker, pers. comm., 1977). Within the metavolcanic rocks a small granitic body on Mount Saint Elias has yielded an isotopic age which suggests it is late Triassic or early Jurassic (Hudson et al., 1977) implying that the enclosing rocks are still older or that the granitic body is an allochthonous "knocker". This problem requires additional isotopic dating and study.

The Cretaceous rocks, where metamorphosed, are intensely folded and pervasively foliated. The foliation mainly strikes east-west or slightly south of east and dips moderately to steeply northward near Mount Saint Elias and is very steep near Mount Logan. To the southeast the strike is more southeasterly and the metavolcanic and metasedimentary rocks seem to be interfolded giving a complex outcrop pattern.

The Tertiary rocks in the southwestern part of the map-area are nearly isoclinally folded but are unmetamorphosed and are not pervasively cleaved.

Tertiary plutons (probably 40-50 m.y. old) are mainly uniform grey unfoliated hornblende-biotite quartz diorite to granodiorite.

Between the Border Ranges and Walsh Faults (Terrane 2)

The Late Paleozoic and early Mesozoic sedimentary and volcanic rocks of terrane 2 are known only near Logan and Walsh glaciers. They are intruded by foliated hornblende-biotite quartz diorite and granodiorite believed to be late Jurassic or early Cretaceous in age (MacKevett, 1976) and are unconformably overlain by undeformed, fossiliferous, late Cretaceous, shallow-marine sediments. The Paleozoic and Mesozoic rocks extend westward directly into the McCarthy region where they were studied in detail by MacKevett (1976). They include parts of the Skolai Group, Nikolai greenstone, and the Chitistone and McCarthy formations. Thrust faults and fold axial planes dip southward. The Skolai Group in the narrow ridge between Logan and Walsh glaciers is metamorphosed and is predominantly carbonate. The Chitistone (limestone) and McCarthy (shale) formations are unmetamorphosed as is some of the remainder of the Skolai which contains chert, volcaniclastics, and minor limestone.

The Walsh Fault is not easily delineated. The contact between the Skolai and Kaskawulsh groups is a wide rusty weathering zone containing a vast number of felsic (including pink syenitic) dykes and small plutons, mainly in the Skolai, which obscure any obvious fault relationship. In addition, the fault is intruded by late Jurassic or younger quartz diorite plutons and locally is overlain by Upper Cretaceous strata. To the southeast the fault is believed to be cut by the younger Border Ranges Fault thus limiting the extent of the late Paleozoic and early Mesozoic rocks and permitting the juxtaposition of the Kaskawulsh Group (terrane 3) against Cretaceous rocks (terrane 1).

Between the Walsh-Border Ranges Faults and the Duke River Fault (Terrane 3)

Regional Aspects. Paleozoic rocks ranging in age from Late Cambrian or Early Ordovician to Carboniferous or Permian, including extensive Devonian carbonate (terrane 3), are informally named the Kaskawulsh Group (modified from Kindle, 1953). In the area beyond the region mapped in 1974 (Campbell and Dodds, 1975) carbonate is the predominant lithology but amphibolite, silicious schist, pelitic schist, and greenstone are abundant. Metamorphism varies from greenschist to low amphibolite facies and most of the rocks are foliated and/or recrystallized.

Plutons range from late Paleozoic (270 to 290 m.y.) diorite, quartz diorite and syeno-diorite masses through late Jurassic and Tertiary quartz diorite-granodiorite. All of the plutons seem to cut or warp the foliation thus at least one major deformation may be Paleozoic.

The Walsh Fault, apparently pre-Late Cretaceous in age, may represent a suture between terranes 2 and 3 that were joined in late Early Cretaceous or earlier whereas the Border Ranges Fault may be the trace of an early Tertiary subduction zone whereby Cretaceous greywacke and volcanic rocks were thrust under the two older terranes. The lack of deformation in the shallow-water Upper Cretaceous marine fossiliferous sandstone, shale, and conglomerate near Walsh Glacier suggests that the upper plate was not deformed during the underthrusting. The thrust faults involving Tertiary and Quaternary marine rocks near Mount Saint Elias indicate that underthrusting at the continental margin continued until recently and is likely still continuing. In contrast to the deformed Tertiary and Recent rocks near the Gulf of Alaska, Tertiary continental sedimentary and volcanic rocks farther inland are not highly deformed except in narrow zones near major faults. They are flat lying or gently tilted over broad areas.

Detailed Study. A detailed study of "Kaskawulsh Group" rocks was undertaken by Dodds in the region lying east of that briefly discussed above, that is within the limits of mapping of 1974 (Campbell and Dodds, 1975). The study, carried out in an area roughly outlined by Duke River Fault (the segment between upper Duke and Jarvis rivers), Donjek Glacier, upper reaches of Kluane and Kaskawulsh glaciers, and Kaskawulsh Glacier, lower Disappointment and Jarvis rivers, revealed a complex geological history. Exposure is remarkable, and the rock exceedingly fresh. However, limited colour variation together with relative monotony and subtlety of lithology (particularly southwest of a "line" approximately joining the snouts of Donjek and Kaskawulsh glaciers), make the choice of mappable units, interpretation, and extrapolation of geology (especially structural and stratigraphical aspects) difficult. Nowhere in the area does there appear to exist complete, representative stratigraphic sections. Sparsity of fossils and "facing" criteria, complexity and locally, intensity of deformation, and subtlety of lithology inhibit a complete comprehension of stratigraphy and stratigraphic relationships.

The "Kaskawulsh Group" rocks of the area outlined, however, are broadly divisible into three belts:

1. A northeastern belt (A) dominated by "greenstone", limestone, and quartz-rich coarse clastic rocks.

2. A central belt (B) dominated by micaceous quartzite, greywacke-argillite, and laminated silty limestone and limy siltstone.

3. A southwestern belt (C) dominated by limestone.

Units within these belts, although commonly not easily recognized extend for considerable distances, and reconnaissance work indicates that they are traceable both northwest and southeast, well beyond the region mapped in detail. The stratigraphy of belt (A) in Kluane Ranges, between the bend in Duke River and Jarvis River is comprehensible despite the structural havoc wrought by polyphase folding and the superimposed deformation resulting from displacements on Duke River Fault and fault strands related to Denali Fault System. Relationships between the three belts, however, are poorly understood.

The "greenstones" of belt (A) consist mainly of poorly sorted, variably sized, augite-bearing volcaniclastic sediments. Locally they contain minor basic volcanics and intercalations of siltstone, sandstone, and argillite. No fossils have been found in this unit. The volcaniclastic sediments locally grade laterally into augite ± plagioclase porphyritic volcanics, best observed in Kluane Ranges between Slims and Jarvis rivers. The "greenstones" are resistant cliff-formers, and almost without exception underlie the highest peaks of the belt. Purplish, and rusty weathering greywacke, siltstone, and sandstone, acid(?) volcanics and black argillite occur beneath, and in minor amounts within the volcaniclastics "greenstone" unit. This unit grades upwards into a sequence of rusty and purplish weathering greywacke siltstone, sandstone, and black argillite with minor basaltic(?) flows and augite-bearing volcaniclastic horizons. Probably overlying the "greenstone" and finer grained clastic units is a massively to moderately well bedded bluish grey limestone. The maximum (areal) exposure of limestone in this belt occurs northwest and southeast of the upper bend of Duke River. Due to both extensive faulting and folding complications the exact number of limestone members present is uncertain. Probably there are at least two; one the above, and the other a coral-bearing, faintly lilac-bluish grey, bioclastic limestone. Fossils from the former, collected in 1974 are of middle Devonian age. Locally, northwest of the upper bend in Duke River and within Kluane Ranges between Slims and Jarvis rivers, amygdaloidal andesitic and basaltic flows occur above the massive blue grey limestone. In the latter region these volcanics are intruded by dykes, sills, and small bodies of gabbro. Of very uncertain stratigraphic position, but structurally above the blue grey limestone, is a sequence of medium to coarse grained quartz-rich clastics which include conglomerate, pebble conglomerate, grits, and sandstones. Clasts are well rounded. These sediments are best exposed between Mount Hoge and Grizzly Creek, southwest of the upper bend of Duke River (associated with the limestones), and high in the Kluane Ranges between Slims and Jarvis rivers. Megafossils (many of them very poorly preserved) were collected from the limestones and samples were taken for microfossil (conodont) study.

The wide central belt (B) lies southwest and northeast of approximate lines joining, respectively, the snouts of Donjek and Kaskawulsh glaciers, and the upper reaches of Donjek, Kluane, and Kaskawulsh glaciers. This belt contains a sequence of moderately well sorted, generally fine to medium grained sediments. These include micaceous quartzite, calcareous quartz-rich arenite, greywacke-argillite (with poorly preserved sedimentary structures), black carbonaceous argillite and quartzite, thinly laminated silty limestone and limy siltstone and locally thin bedded (flaggy) blue grey limestone and thin bedded (laminated) very dark bluish grey limestone and limy siltstone. No fossils were found in this structurally complex belt, and consequently stratigraphic relationships are poorly understood and the age of rocks remains enigmatic. Although the stratigraphy is subtle, units can be mapped over surprisingly long distances. For example the dark bluish grey laminated limestone unit has been traced about 80 km, from northwest of the head of Kluane Glacier to Dusty Glacier. Limestones have been sampled for conodonts.

The limestone belt (C) southwest of the upper reaches of Donjek, Kluane,and Kaskawulsh glaciers has had little detailed work. Reconnaissance mapping indicates that it consists predominantly of both massive light bluish grey, and well bedded darker bluish grey limestones. The limestones are very resistant, producing a sharp rise in the relief within Icefield Ranges. Ridges are spectacularly rugged and not easily traversable. The belt is fairly narrow in the region described. However, it has been traced far beyond these limits and is much more extensive elsewhere. Both to the northwest and southeast (the latter in particular), the map pattern of the limestones is exceedingly sinuous due almost entirely to structural complexity. The ages of fossils collected by the writers from this belt have not been determined. Fossils obtained by Wheeler (1963) indicate a probable Devonian age.

The relationships between the three belts are not clearly understood. This is due largely to poor fossil control (particularly in central belt (B)) and to polyphase deformation. No definite facies equivalents of the "greenstones" were found at the southwestern margin of belt (A) where the belt terminates rather abruptly, apparently due largely to faulting and complexity of folding. The massive and moderately well bedded limestones (middle Devonian in part at least) of the northeastern belt (A), are traceable into the central belt (B) in the Donjek River valley south-southeast of the terminus of Donjek Glacier. Although fossils are rare, these limestones are probably equivalent to those of belt (C).

Several small plutons of Late Jurassic to Early Cretaceous age occur within the area of detailed mapping. All but one are of uniform hornblende-biotite granodiorite composition. The exception, just east of the headwaters of Donjek River, contains quartz diorite(?) and hornblendite phases, together with the common granodiorite phase. Similar plutons of varied composition are known elsewhere in the region. All plutons are discordant, contain fairly narrow, rusty contact aureoles, and are without exception, peripherally deformed by post intrusion tectonic event(s). A narrow belt containing gabbro bodies, some very coarse grained and remarkably fresh, occurs close to the trace of Duke River Fault between the upper bend of Duke River and south of Jarvis River. Dykes varying in composition from felsite to gabbro are abundantly present throughout the region;

andesite, basalt and gabbro dykes are the most common. Locii of many of the swarms appears to correspond to fault zones. In Kluane Ranges numerous basalt-gabbro and quartz-K spar.-biotite porphyry and felsite dykes delineate subsidiary faults undoubtedly related to Denali Fault System. There are several episodes of dyking, and the writers feel that the chronology of these is one of the keys to unravelling the nature and timing of at least some of the major structural events of the area.

Regional metamorphism, undergone by "Kaskawulsh Group" rocks within the limits of detailed mapping, does not appear to exceed biotite grade. Metamorphic prograding, as a generality, is from northeast to southwest. Much of the area of belt (A) is of chlorite or subchlorite grade, and only rarely and locally reaches biotite grade. In the central belt (B), however, there is an overall increase in regional metamorphic grade, and fine grained biotite is common in metamorphic assemblages. Reconnaissance work in belt (C) indicates that rocks were affected by low greenschist metamorphism only. The timing of regional metamorphism is not clear. However, it is pre Late Jurassic as the granodiorite plutons discordantly intrude and superimpose contact aureoles on the earlier regional metamorphic fabric. Randomly oriented biotite porphyroblasts locally with amphibole and cordierite are developed in the aureoles.

Deformation within the region mapped in detail is complex and polyphase, reaching maximum intensity adjacent to Duke River Fault, and fault strands related to, but southwest of the main trace of Denali Fault System. At least three deformational events affected the "Kaskawulsh Group" rocks, the timing of which are still not completely understood.

The earliest phase recognized (F_1) locally produced north to northeasterly trending isoclinal folds of probable southeasterly vergence. These folds are poorly displayed, due largely to the pervasive nature of (F_2) and to complications wrought by displacement along Duke River Fault and splays of Denali Fault System. Best examples occur on the ridges adjacent (both to northwest and southwest) to the terminus of Kaskawulsh Glacier, and on the southwest flanks of Kluane Ranges southeast of Slims River.

The second phase of folding (F_2) gives rise to medium and large scale northwesterly trending anticlines and synclines, generally slightly to moderately overturned to the northeast and similar in style. This is the dominant style of folding particularly in belts (A) and (C), and less obviously in belt (B). F_2 folds F_1, producing highly variable but often very steep plunges to the axes of F_1. The intensity of F_2, with associated fine spaced axial plane cleavage, has erased much of the evidence of F_1. High angle, southwesterly dipping, reverse faults dislocate F_2 structures. These faults are related to F_2 deformation and the frequency and magnitude of occurrence, increase markedly close to Duke River Fault in belt (A).

The third deformational event involves faulting, and locally both shattering of rocks and development of west-southwest through west-northwest fold trends. It occurs most obviously in the narrow belt close to Duke River Fault, where it is related to displacement on fault strands associated to Denali Fault System. Faults are dominantly strike-slip in character. However, minor thrust and high-angle reverse faults are also present. The curving trace of Duke River Fault just south of Slims River is a direct result of right lateral shift along these faults. The folds are usually minor in scale, and vary in style from open warps to moderately tight, steep limbed, assymmetrical (rarely overturned) forms. Vergence is generally northerly. Fold axes are as a rule, steep in strike-slip fault zones, and shallow in thrust segments. The affects of this deformational phase are more widespread than within the confines of the narrow belt described above, and in some areas to the west are more than just subtlely apparent.

The deformational history involving "Kaskawulsh Group" rocks is unquestionably complex, and much uncertainty still shrouds the timing of these events, particularly F_1 and F_2. The earliest recognizable phase (F_1 isoclinal) is poorly displayed, due both to the pervasive nature of F_2 and to strike-slip fault related effects of the third episode. F_1 is folded by the dominant, northwesterly trending F_2 phase. F_1 and F_2 fold episodes are post mid-Paleozoic and pre-Cenozoic. A middle to late Paleozoic age has been suggested for much of the pervasive deformation of "Kaskawulsh Group" rocks by Read and Monger (1976). However, it is interesting to note that Eisbacher (1975, 1976) reports surprisingly similar fold styles and trends in the Jura-Cretaceous Dezadeash Group rocks and substantiates a Late Cretaceous – earliest Tertiary phase of regional folding in the eastern St. Elias Mountains. Late Jurassic-Early Cretaceous granodiorite plutons discordantly intrude deformed "Kaskawulsh Group" rocks. These bodies are, however, peripherally affected by later deformational event(s) which are at least in part due to the third episode of deformation. The last (third) phase of deformation is almost certainly post Miocene (Eisbacher and Hopkins, 1977) and is related to the dramatic rise of the St. Elias Mountains.

The Duke River Fault and Denali Fault System

In contrast to the more westerly faults which may be sutures and subduction zones the Duke River Fault and the Denali Fault System seem to be major transcurrent breaks that intersect and dislocate other structures. They separate distinct terranes only insofar as they may have major horizontal displacements and not because they are necessarily related in any way to continental boundaries. The faults are believed to be intra-continental rather than inter-continental structures.

Right-lateral displacements on the Duke River and Denali faults may thus offset the Walsh Fault (the suture between terranes 2 and 3) from eastern Alaska west of the map-area to some as yet unknown location southeast of the map-area. If so the offset part of the Walsh Fault would lie east of the Denali Fault System. Data are not at hand to show if such is the case.

The Duke River Fault locally cuts the basal part of the Wrangell lava (TQv) which is no older than Miocene but it does not cut the youngest flows (see Campbell and Dodds, 1975 and Souther and Stanciu, 1975). Possible related faults cut the entire pile of lava hence movement on them is Pliocene or younger. The age of the major displacement is post Late Triassic and is probably post late Early Cretaceous or early Late Cretaceous (the age of the youngest rocks of terrane 4) and is pre-Miocene. The Duke River Fault is believed to branch from the Denali Fault System southeast of the map-area.

The Denali Fault System within the map-area (Shakwak and Dalton faults, Campbell and Dodds, 1975) cuts Wrangell lava (TQv) and the age of the major displacement is Late Cretaceous or younger; it is likely mainly Tertiary. Southeast of Kluane Lake a variety of features recognized by George Plafker indicate that right-lateral movement occurred on the Denali Fault System in the Pleistocene or Recent; some movement was possibly post glacial. Shorelines of Recent Lake Alsek, 3000 years old, apparently are not offset (V.N. Rampton, pers. comm., 1977) hence if any movement was postglacial it occurred between about 10 000 years and 3000 years ago. More study is required on these features. Northwest of the south end of Kluane Lake Bostock (1952) described linear features near Donjek River that might reflect Recent fault movements. These features could, however, be glacial in origin. Nothing else has been recognized that might indicate Pleistocene or Recent movements on this segment of the fault.

References

Bostock, H.S.
1952: Geology of northwest Shakwak Valley, Yukon Territory; Geol. Surv. Can., Mem. 267.

Campbell, R.B. and Dodds, C.J.
1975: Operation Saint Elias, Yukon Territory; in Report of Activities, Part A, Geol. Surv. Can., Paper 75-1A, p. 51-53.

Eisbacher, G.H.
1975: Operation Saint Elias, Yukon Territory; in Report of Activities, Part A, Geol. Surv. Can., Paper 75-1A, p. 61-62.

1976: Sedimentology of the Dezadeash flysch and its implication for strike-slip faulting along the Denali Fault, Yukon Territory and Alaska; Can. J. Earth Sci., v. 13, p. 1495-1513.

Eisbacher, G.H. and Hopkins, S.L.
1977: Mid-Cenozoic paleogeomorphology and tectonic setting of the St. Elias Mountains, Yukon Territory; in Report of Activities, Part B, Geol. Surv. Can., Paper 77-1B, p. 319-335.

Hudson, T., Plafker, G., and Lanphere, M.A.
1977: Intrusive rocks of the Yakutat-St. Elias area, south-central Alaska; U.S. Geol. Surv., J. Research, v. 5, p. 155-172.

Kindle, E.D.
1953: Dezadeash map-area, Yukon Territory; Geol. Surv. Can., Mem. 268.

MacKevett, E.M., Jr.
1976: Folio of the McCarthy Quadrangle, Alaska; U.S. Geol. Surv., Map MF-773A.

MacKevett, E.M., Jr. and Plafker, George
1974: The Border Ranges Fault in south-central Alaska; U.S. Geol. Surv., J. Research, v. 2, p. 323-329.

Read, P.B. and Monger, J.W.H.
1975: Operation Saint Elias, Yukon Territory: the Mush Lake Group and Permo-Triassic rocks in the Kluane Ranges; in Report of Activities, Part A, Geol. Surv. Can., Paper 75-1A, p. 55-59.

1976: Pre-Cenozoic volcanic assemblages of the Kluane and Alsek Ranges, southwestern Yukon Territory; unedited report to accompany Geol. Surv. Can., Open File 381.

Sharp, R.P. and Rigsby, G.P.
1956: Some rocks of the central Saint Elias Mountains, Yukon Territory, Canada; Am. J. Sci., v. 254, p. 110-122.

Souther, J.G. and Stanciu, C.
1975: Operation Saint Elias, Yukon Territory: Tertiary volcanic rocks; in Report of Activities, Part A, Geol. Surv. Can., Paper 75-1A, p. 63-70.

Wheeler, J.O.
1963: Kaskawulsh (Mt. St. Elias, east-half); Geol. Surv. Can., Map 1134A.

10.

STRATIGRAPHY AND STRUCTURE OF THE SUMMIT LAKE AREA, YUKON AND NORTHWEST TERRITORIES

Project 730069

S.P. Gordey
Regional and Economic Geology Division, Vancouver

Abstract

Gordey, S.P., Stratigraphy and structure of the Summit Lake area, Yukon and Northwest Territories; Current Research, Part A, Geol. Surv. Can., Paper 78-1A, p. 43-48, 1978.

Geologic mapping at a scale of 1:50 000 has permitted the subdivision of unmetamorphosed folded and faulted Hadrynian to Mississippian clastic and carbonate succession of the Summit Lake area, about 3750 m thick, into ten mappable stratigraphic units. Major and minor folds trend and plunge to the northwest, and pervasive axial-plane cleavage dips steeply northeast. The following phenomena appear to be of regional significance: (1) the unconformity beneath Cambro-Ordovician strata, (2) mappable subdivisions of the Hadrynian and (?) Lower Cambrian 'Grit Unit', and the Ordovician to Devonian Road River Formation, (3) derivation of the Devono-Mississippian 'Black Clastic Unit', at least in part, from 'Grit Unit' lithologies, and (4) Devono-Mississippian block-faulting.

Introduction

The Summit Lake area, in Nahanni map-area (105I) about 260 km north-northwest of Watson Lake, Yukon Territory, has been of considerable economic interest since the Canex-Placer Ltd. discovery, in 1972, of the Howard's Pass zinc-lead deposit. Reconnaissance geologic mapping by Blusson et al. (1968) outlined the distribution of major rock units. The purpose of this project is to refine the previous work and to investigate in relative detail the stratigraphy and structure of the Summit Lake area.

During the 1977 field season six weeks were spent mapping an area of 600 km^2 at a scale of 1:50 000. The results are summarized in Figures 10.1 to 10.3. Structural complications, facies changes, and the poor quality of exposure preclude accurate determinations of stratigraphic thickness.

Stratigraphy

The oldest exposed strata are thin to thick bedded, fine to very coarse grained gritty quartz sandstone, pale brown slate, and minor limestone of Hadrynian age (Hq). The sandstone, generally poorly sorted and characterized by large well-rounded 'floating' bluish opalescent quartz grains up to granule size, is commonly calcareous, and locally has thin to very thick interbeds of orange weathering finely crystalline sandy limestone. Poorly bedded finely crystalline black limestone, about 10 m thick, occurs at the top of the unit. In the sandstone large mud chips, ripple marks, cross-bedding, and scour and fill structures attest to a high energy shallow water depositional environment.

The above strata are overlain with sharp contact by a distinctive unit, about 650 m thick, of purple, maroon, and green slate (HI€p), which is thin bedded in its lower part, but thick to very thick bedded in its upper part. Within this slate pale green fine grained quartz arenite with interbedded pale brown and green slate (HI€ s) forms discontinuous lensoid units, locally at least several hundred metres thick. The sandstone occurs in thin beds that are typically massive but at some localities show planar and small scale cross-lamination. Locally occurring groove and flute casts are not abundant enough for meaningful paleocurrent determination.

The Hadrynian clastic rocks (Hq, HI€s, HI€p) are similar to strata which underlie extensive areas of central and southeastern Yukon and which have been referred to informally as the 'Grit Unit' (Gabrielse et al., 1973, p. 30).

Brown to buff weathering blue-grey slate of Early Cambrian age (1€p), locally at least 1000 m thick, overlies the maroon and green slate unit (H1€p). Bedding is defined by faint thin colour banding in shades of blue and grey. To the northeast, a similar slate intertongues with Lower Cambrian carbonate strata. The contact with the underlying maroon slate is marked by a discontinuous unit, up to 60 m thick, of limestone conglomerate (Fig. 10.4), massive blue-grey finely crystalline limestone, and orange weathering oolitic limestone. The conglomerate locally contains archaeocyathid clasts. The dark Lower Cambrian slate corresponds to the 'Phyllite Unit' as mapped by Gabrielse et al. (1973) in Flat River map-area to the southeast.

Conformably overlying the slate is a lithologically varied succession of overall buff and orange weathering limestone, and lesser amounts of siltstone, tuff, dolomite, and quartz arenite (€c). Due to facies changes and erosional bevelling beneath Upper Cambrian strata, its thickness ranges from 0 to possibly more than 1300 m. The limestone is laminated to thin bedded, the bedding commonly defined by blue and orange banding on weathered surfaces that is commonly not visible on fresh surfaces. Nodular to banded silty grey weathering limestone, which closely resembles the Upper Cambrian limestone unit (u€0c), and massive blue-grey weathering limestone are also abundant. All limestones are finely crystalline and blue-grey to black on fresh surfaces. The siltstone weathers pink to orange, is laminated to thin bedded, and is commonly thinly interbedded with blue-grey limestone. The tuff, which is dark weathering, is composed of aphanitic pale green angular fragments up to 2 cm in diameter. Although the tuff is usually massive, local lamination and graded bedding in the fine grained varieties (Fig. 10.5) indicate it is waterlain. Ochre weathering fine to coarsely crystalline grey dolomite and associated coarse grained cross-laminated quartz arenite form a minor yet distinctive component of the unit. The unit is similar to and likely correlative with the Sekwi Formation of Mackenzie Mountains (Gabrielse et al., 1973; Fritz, 1976). The laminated and bioturbated blue grey mudstone unit (€ p) is a presumed equivalent of some of the Lower Cambrian carbonate strata (€c).

Upper Cambrian and Ordovician grey to white weathering carbonate strata (u€0c) which overlie older units with marked unconformity (Fig. 10.2) form a homogeneous unit about 300 m thick of laminated to thin bedded finely crystalline blue-grey limestone. Northeast of Howard's Pass the bedding is thicker, commonly nodular, and the limestone siltier than to the southwest. The weathered surfaces of nodular varieties are distinctively pock-marked. The unconformity at the base of the unit corresponds to an important regional unconformity that separates Franconian from older strata over much of the northern Cordillera (Gabrielse et al., 1973, p. 51). The unit is equivalent and lithologically similar

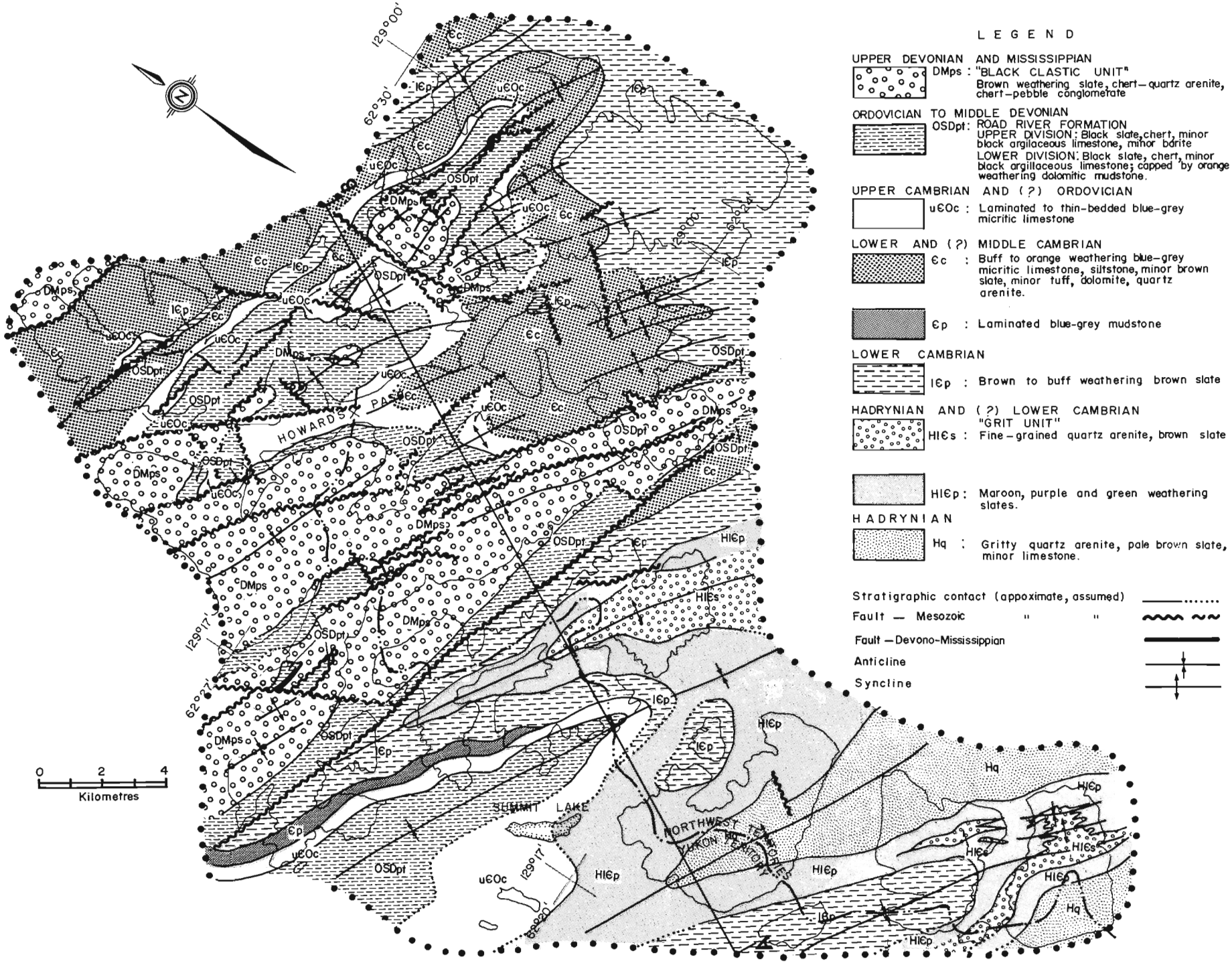

Figure 10.1. Geologic map of the Summit Lake area, Yukon and Northwest Territories.

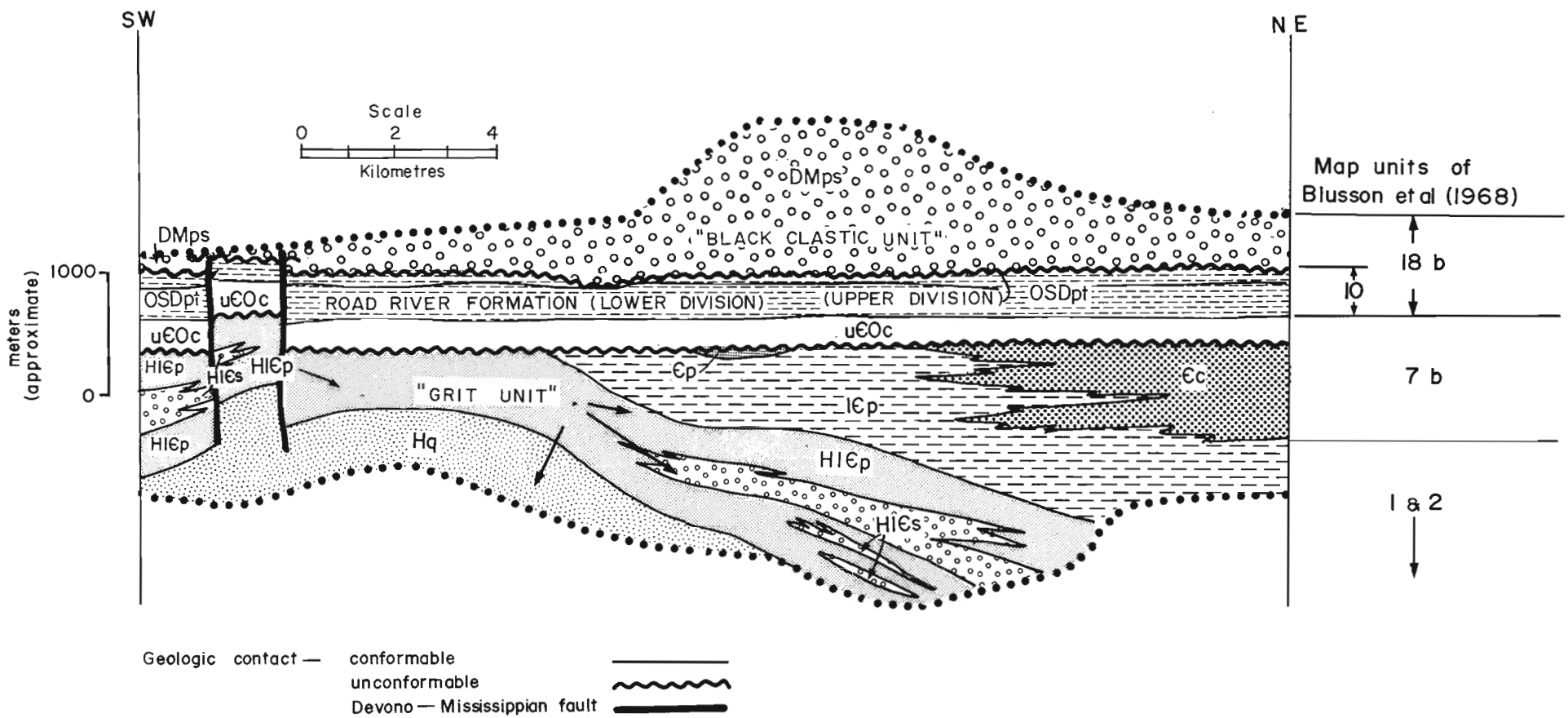

Figure 10.2. Diagrammatic stratigraphic cross-section, Summit Lake area.

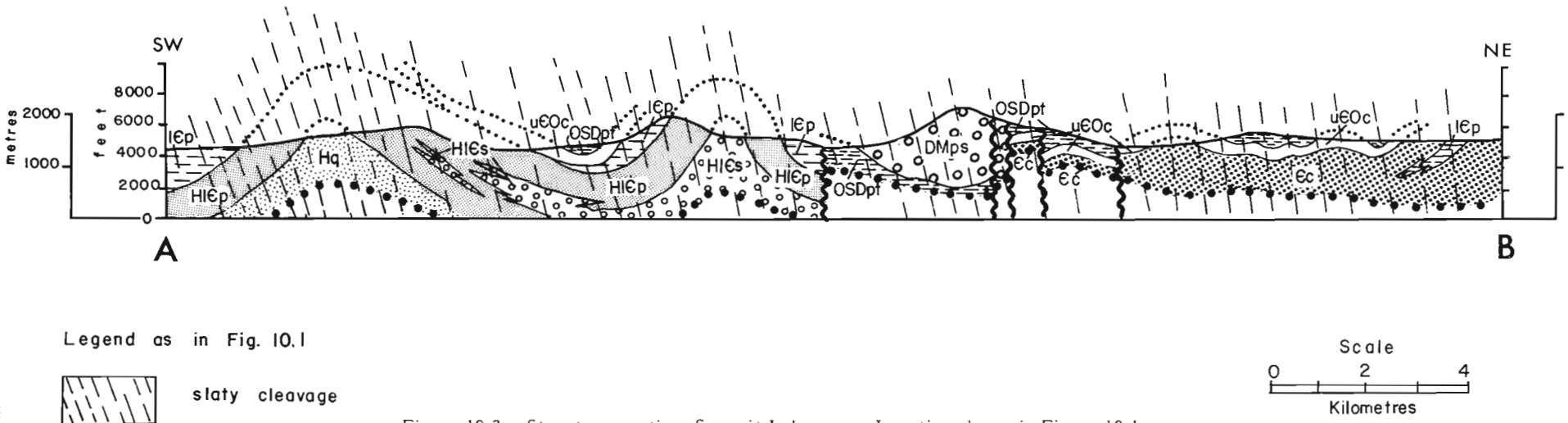

Figure 10.3. Structure-section, Summit Lake area. Location shown in Figure 10.1.

Figure 10.4

Limestone conglomerate at the contact between the maroon and green slates (H1Ꞓp) of the 'Grit Unit' and brown Lower Cambrian slates (1Ꞓp). Limestone clasts vary from platy and angular, as here, to well rounded. The matrix is fine grained commonly oolitic calcarenite.

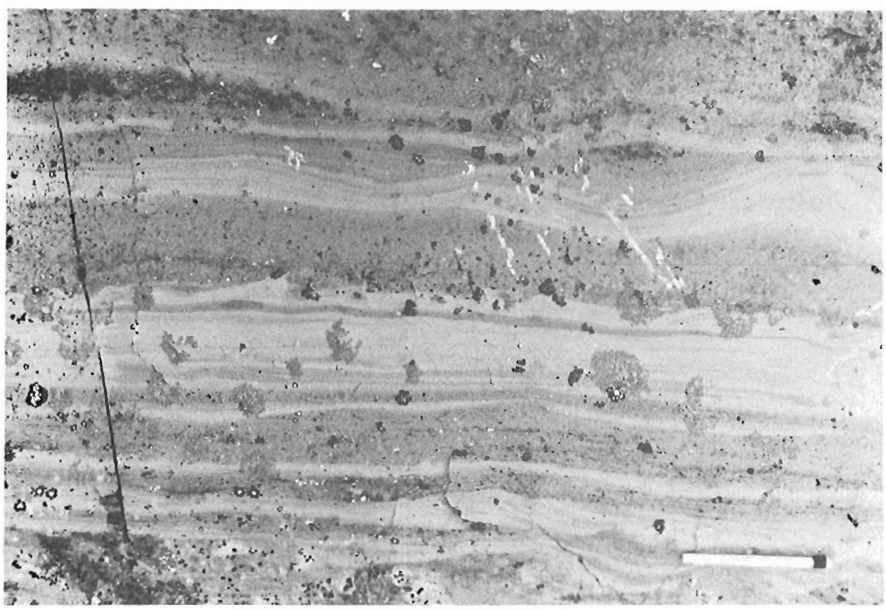

Figure 10.5

Pale to dark green laminated tuff. Along with relatively coarser grained massive tuffs they are a minor but distinctive rock type in the Lower Cambrian, predominantly carbonate unit (Ꞓc).

to the Rabbitkettle Formation (Gabrielse et al., 1973) of Mackenzie Mountains.

Black to brown slate and black chert of the Road River Formation (OSDpt) can be subdivided into two divisions, the mutual contact being defined by an excellent marker unit, 0 to 60 m thick, of orange weathering pyritic and dolomitic mudstone. The lower division, approximately 240 m thick, is of Ordovician, Silurian and(?) Early Devonian age, and the upper division, which varies from 0 to about 120 m in thickness, is of probable mid-Devonian age. Near Howard's Pass the formation weathers light bluish grey in contrast to its black weathering colour to the southwest.

The basal few tens of metres of the formation which are gradational and conformable with Cambro-Ordovician limestone (uꞒ 0c), is well laminated dark brown slate containing lenses, nodules, laminae and thin beds of grey finely crystalline limestone. Thin to thick beds of black finely crystalline limestone occur sporadically elsewhere in the formation. Near Howard's Pass poorly bedded thin bedded black chert and siliceous slate occurs near the top of the lower division. Thin bedded black chert is abundant within the lower division at other localities, but its stratigraphic position is not well known. The upper division, which is lithologically similar to the lower, contains minor graphitic sandstone and barite, the latter found locally in talus. In the absence of the orange mudstone, particularly in structurally complex or poorly exposed areas, the two divisions are difficult to separate.

Black slate of the lower division is host to the zinc-lead deposits at Howard's Pass which reportedly occur 200 feet above the contact with Cambro-Ordovician limestone (Sinclair and Gilbert, 1975, p. 89). The barite-bearing upper division may correspond to a barite-bearing sequence at Macmillan Pass 115 km to the north-northwest which is thought by Blusson and Dawson (Dawson, 1977, p. 1) to correspond to the Canol Formation of northern Mackenzie and Richardson mountains.

Brown weathering slate, quartz-chert arenite, and chert-pebble conglomerate of the 'Black Clastic Unit' (DMPs), at least 1500 m thick, overlie the Road River Formation unconformably, as indicated by the thickness variations of the upper division of the Road River strata. The lower 800 m of

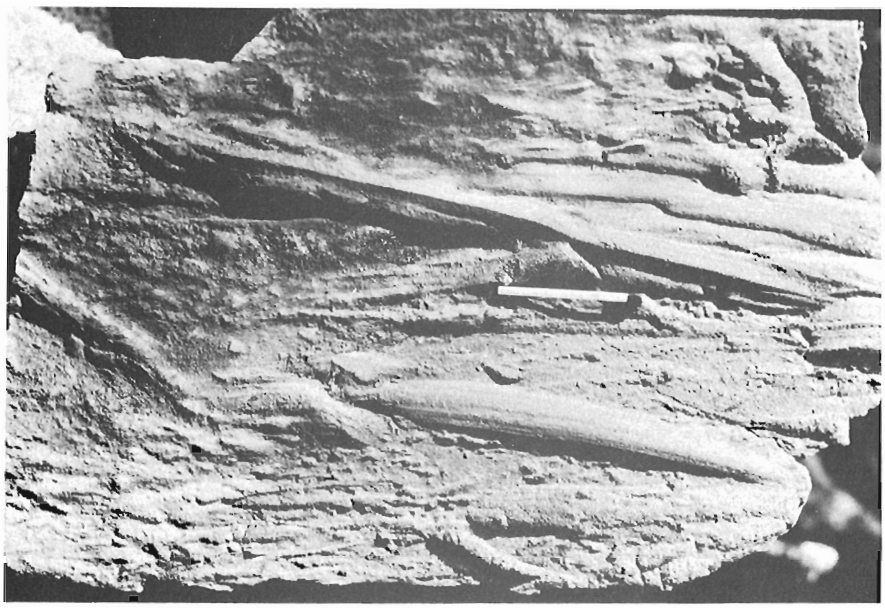

Figure 10.6

Groove casts on the base of a thin bed (talus block) of medium grained quartz-chert arenite of the 'Black Clastic Unit'. The rarity of sole marks and generally 'felsenmeer' exposures of the unit prohibit paleocurrent determinations.

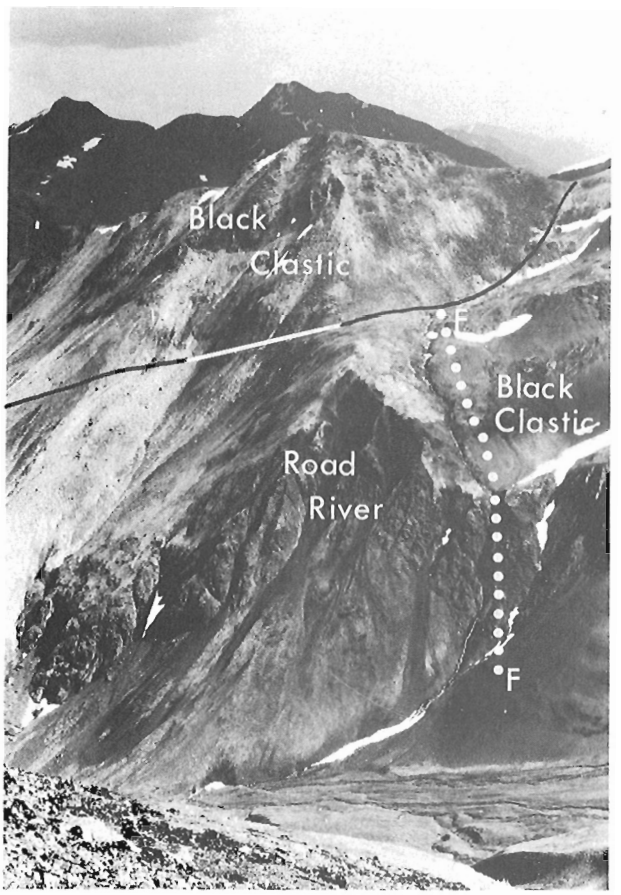

Figure 10.7. Fault of Devono-Mississippian age 5.5 km north of Summit Lake. The fault juxtaposes black weathering slate and chert of the Road River Formation (OSDpt) and brown weathering slate of the 'Black Clastic Unit' (DMps) and is overlain by 'Black Clastic Unit' chert-pebble conglomerate (DMps).

the unit is predominantly slate with minor coarse clastic interbeds, but higher in the unit coarse clastics predominate. Most of the conglomerate, which forms a minor part of the unit, is of pebble to cobble size. Boulder conglomerate is rare, with maximum observed clast size of 0.5 m. Both angular and rounded clasts are common, although large clasts are always well rounded. Individual sandstone and conglomerate beds range from a few millimetres to tens of metres in thickness. Chert forms most of the clastic detritus but non-chert quartz detritus is very abundant and quartz arenite is common. Conglomerate clasts are predominantly grey, black, and green chert but locally as much as 25 per cent are fine to coarse grained gritty quartz sandstone. The latter type have distinctive 'floating' blue quartz grains and are strikingly similar to (and derived from(?)) sandstones of the 'Grit Unit'.

Rhythmic interbedding and knife-sharp contacts of coarse clastics and slate, the sheet-like form, continuity and uniform thickness of some conglomerate units, and local graded bedding and sole marks (Fig. 10.6) indicate the coarse clastics were deposited as turbidite flows.

Structure

The strata are folded about west-northwest trending axes that plunge consistently to the northwest. Cleavage-bedding intersection lineations indicate the plunges vary from 0 to 40°. Although the major folds are relatively open (Fig. 10.3), the units are internally tightly folded, and slaty cleavage, dipping moderately to steeply to the northeast, is pervasive. Only relatively competent sandstone and conglomerate beds consistently lack cleavage. Steep probable dip-slip faults of late Mesozoic age disrupt the major fold structures. Devono-Mississippian faulting is documented at one locality (Fig. 10.7), and some of the presumed Mesozoic faults may be of similar age. The Devono-Mississippian block-faulting was likely related to the uplift of the source areas of the 'Black Clastic Unit', which lay to the west and southwest (Gabrielse, 1976, p. 496).

Acknowledgments

Appreciation is expressed to Canex-Placer Ltd. for logistical assistance. L. Unrau provided able assistance in the field.

References

Blusson, S.L., Green, L.H., and Roddick, J.A.
1968: Nahanni map-area, District of Mackenzie and Yukon Territory; Geol. Surv. Can., Map 8-1967.

Dawson, K.M.
1977: Regional metallogeny of the northern Cordillera; in Report of Activities, Part A, Geol. Surv. Can., Paper 77-1A, p. 1-4.

Fritz, W.H.
1976: Ten stratigraphic sections from the Lower Cambrian Sekwi Formation, Mackenzie Mountains, northwestern Canada; Geol. Surv. Can., Paper 76-22.

Gabrielse, H.
1976: Environments of Canadian Cordillera depositional basins; in Circum-Pacific Energy and Mineral resources; Am. Assoc. Pet. Geol., Mem. 25, p. 492-502.

Gabrielse, H., Blusson, S.L., and Roddick, J.A.
1973: Geology of Flat River, Glacier Lake, and Wrigley Lake map-areas, District of Mackenzie and Yukon Territory; Geol. Surv. Can., Mem. 366.

Sinclair, W.D. and Gilbert, G.W.
1975: Mineral industry report, 1973, Yukon Territory; Can. Dept. Indian and Northern Affairs, Publication EGS 1975-7, p. 89.

11. OBSERVATIONS ON THE STREAMING MECHANISM OF LARGE ROCK SLIDES, NORTHERN CORDILLERA

Project 760059

G.H. Eisbacher
Regional and Economic Geology Division, Vancouver

Abstract

Eisbacher, G.H., Observations On the Streaming Mechanism of Large Rock Slides, northern Cordillera; Current Research, Part A, Geol. Surv. Can., Paper 78-1A, p. 49-52, 1978.

Features exposed on postglacial rock slide deposits in the Mackenzie Mountains suggest that kinematic waves may be an important form of momentum transfer in the streaming behaviour of 'confined' and 'unconfined' dry debris streams.

Introduction

Debris streams (Hsu, 1975), originating from the collapse of high cliffs of carbonate strata, are common geomorphological features in the Mackenzie and Wernecke mountains. Due to sparse vegetation in this region many details possibly significant for understanding the streaming mechanism can still be recognized on postglacial debris lobes of different ages. Some observations were reported previously (Eisbacher, 1977). A comprehensive study of rock slides in the northern Cordillera, including mechanical and geological aspects, is in progress. This report describes two fundamental mechanical features of debris lobes in the Mackenzie Mountains. The examples are used to illustrate that height of fall during collapse and momentum transfer in the collapsing mass are significant parameters in both 'unconfined' and 'confined' debris streams.

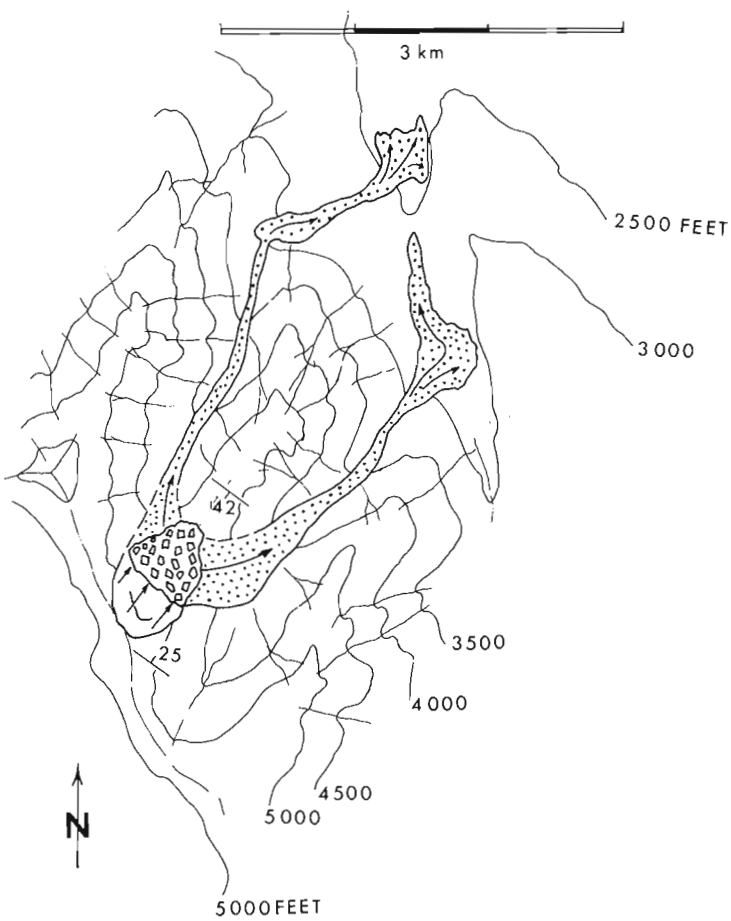

Figure 11.1. Sketch map showing the extent of the debris in the two lobes of the Twin Slides, Snake River map-area.

Corner Slide, an example of an unconfined debris stream
(64°52'N, 129°43'W)

This debris stream is situated in the northwest corner of Mt. Eduni map-area. Its lobe is covered with vegetation but debris deposits can be clearly outlined in the field (Fig. 11.2). The debris stream resulted from the collapse of about 100 x 10^6 m^3 of carbonate rocks of lower Paleozoic Mount Kindle and Franklin Mountain Formations (Aitken and Cook, 1974). Throughout the region these are by far the most collapse-prone lithological units. As far as can be reconstructed from the debris filled scar at Corner Slide, failure occurred on a steepened, shovel-shaped surface. Bedding on the mountain dips 10 to 15 degrees in the direction of the debris stream.

After collapse the material spread relatively unconfined onto the valley floor covering an area of about 4 km^2. One of the most distinct features of unconfined debris streams is the 'ramp'. It is well displayed on the Corner Slide (Fig. 11.2). The 'ramp' is relativley close to the scar of the collapsed cliff and material behind its frontal step makes up more than half of the debris stream. In other slides the volume of broken rock contained in the mass behind the ramp with respect to the total volume is even greater. Material in front of the ramp thins gradually and displays weak lineations in the direction of sliding. The ramp gives the impression of a frozen-in wave and consists of hugh blocks. It is certainly possible to imagine that during movement momentum was transferred from the material in the ramp onto loose debris in front, thus adding velocity and distance to the overall stream. Photos of immense unconfined debris streams on Mars, conveyed to me by Dr. K. Blasius, Planetary Science Institute, Pasadena, also show well defined ramps and lineated lobes radiating outward, in some cases for more than 30 km!

Twin Slides, an example of narrow confined debris streams
(65°16'N, 133°14'W)

The Twin Slides, located near Snake River, originated by the collapse of a narrow ridge following a rotational bedding plane slide (Fig. 11.3). The bedrock structure in the slide area is dominated by a northwesterly trending syncline of Proterozoic Rapitan Group and lower Paleozoic Franklin Mountain Formation (Norris, 1975). Erosion has created long narrow ridges perpendicular to the trend of the fold. Along one of these the carbonate rocks along the southwestern limb of the syncline underwent rotational failure and the front of the rockmass lost its footing on both sides of the ridge. Broken rock tumbled some 200 m into two parallel valleys (Fig. 11.1). The ridge behind the failed mass on Figure 11.3 probably gives a fairly good idea of the topography prior to failure. In the two valleys the debris streamed in relatively confined channels for two km until both streams opened into small fans and came to a halt.

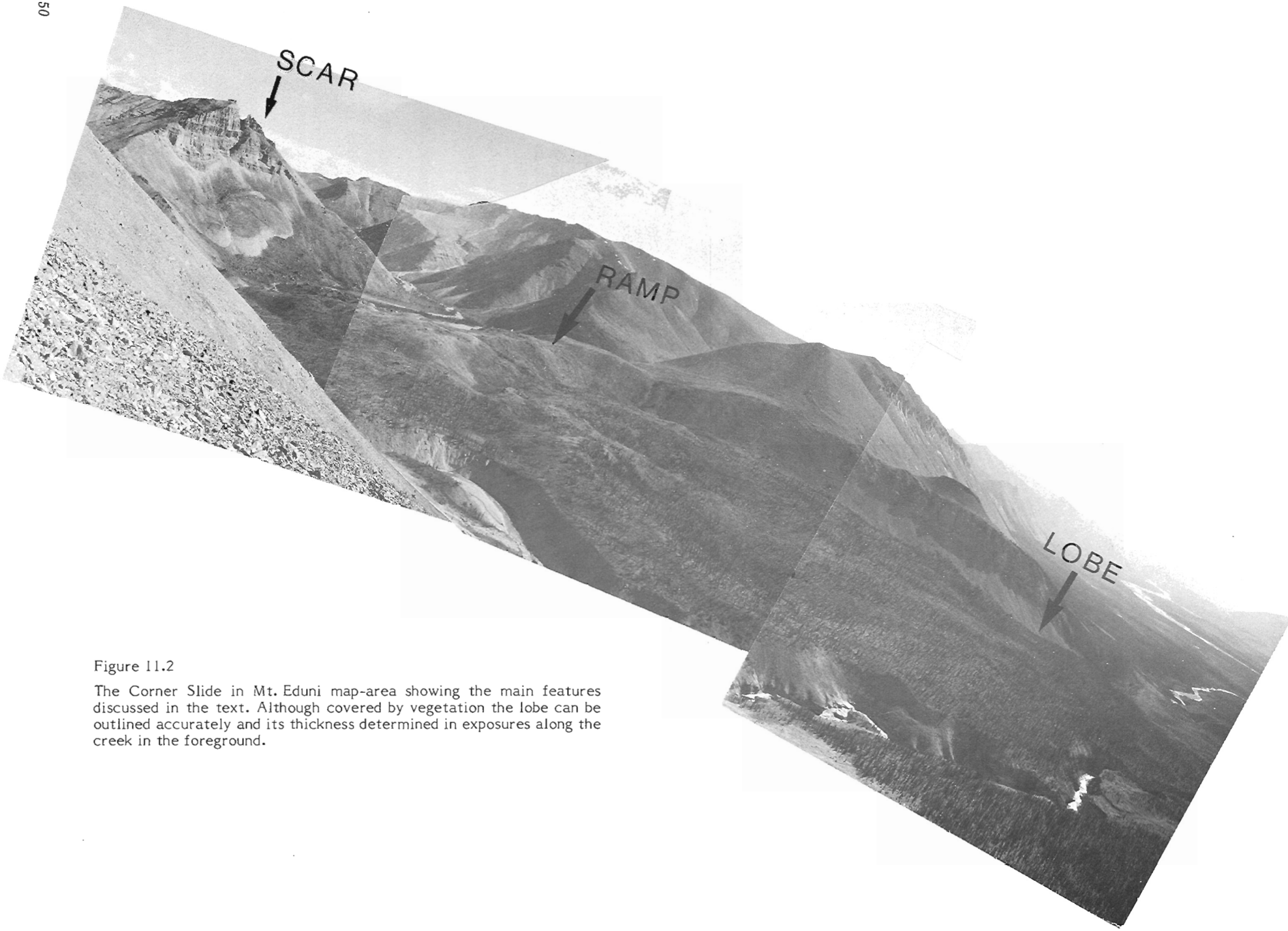

Figure 11.2

The Corner Slide in Mt. Eduni map-area showing the main features discussed in the text. Although covered by vegetation the lobe can be outlined accurately and its thickness determined in exposures along the creek in the foreground.

Ra = Rapitan Group

FM = Franklin Mountain Formation

Figure 11.3

The rotational failure of a transverse ridge of carbonate rock which led to the collapse and streaming of the debris on both sides of the ridge (Twin Slides).

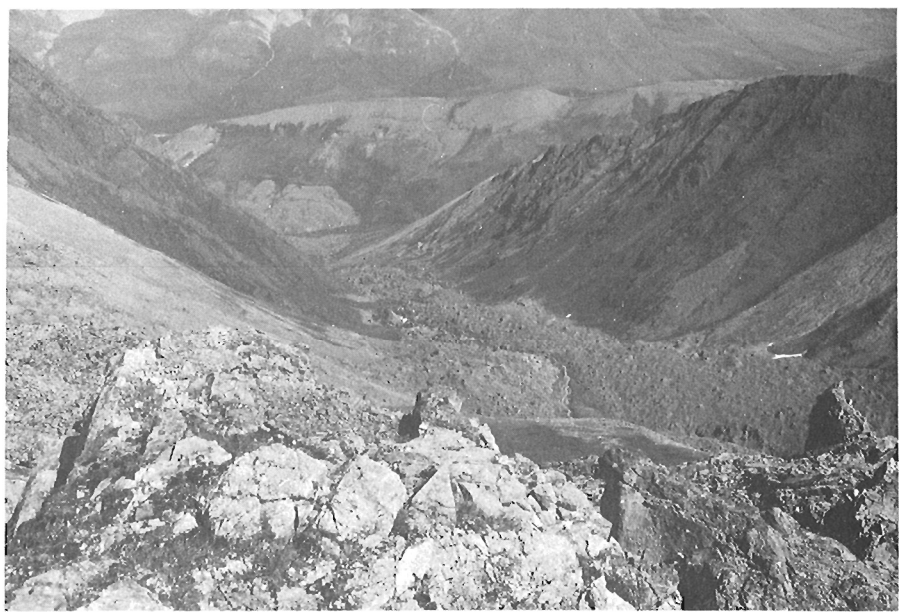

Figure 11.4

The right arm of the Twin Slides. Photo illustrates the narrow debris stream and its blockage towards the far distance.

Figure 11.5

Jet-like frontal lobes of the Twin Slides.

The right stream travelled a shorter distance than the left after having been impeded by a slope across its path (Fig. 11.4). On this slope part of the debris climbed about 50 m, suggesting that after two km of streaming the velocity of the mass still exceeded 30 m per second. The principal energy source for the streaming must have been the initial 200-m drop during collapse and momentum transfer as kinematic waves towards the frontal part of the debris. In places the debris deposits on the Twin Slides are not wider than a few tens of metres and it is difficult to imagine that such a narrow 'stream profile' was maintained throughout the time interval of movement. Both frontal lobes give the impression of debris jets issuing from a nozzle (Fig. 11.5). It is therefore concluded that kinematic waves propagating through the moving debris caused the jet-like effect near the front. The size of the largest blocks generally does not change from the back to the front of the lobes.

Conclusions

The unusual state of preservation of debris streams in the Mackenzie Mountains permits certain conclusions as to the driving mechanism of debris streams. The author suggests that the principal source of energy is kinetic energy transferred from the initial collapse by means of kinematic waves to the frontal portion of debris streams. Kinematic waves are well known in water-saturated debris flows (e.g. Johnson, 1970, p. 433-459) and there is no reason to believe that they are not significant in dry confined and unconfined debris streams as well.

References

Aitken, J.D. and Cook, D.G.
1974: Geological maps, northern parts of Mount Eduni and Bonnet Plume Lake map-areas, District of Mackenzie; Geol. Surv. Can., Open File 221.

Eisbacher, G.H.
1977: Rockslides in the Mackenzie Mountains, District of Mackenzie; in Report of Activities, Pt. A, Geol. Surv. Can., Paper 77-1A, p. 235-241.

Hsu, K.J.
1975: Catastrophic debris streams (Sturzstroms) generated by rockfalls; Geol. Soc. Am. Bull., v. 86, p. 129-140.

Johnson, A.M.
1970: Physical processes in geology; Freeman, Cooper & Co., 577 p.

Norris, D.K.
1975: Geological maps, Hart River, Wind River and Snakes River, Yukon and Northwest Territories; Geol. Surv. Can., Open File 279.

12. TWO MAJOR PROTEROZOIC UNCONFORMITIES, NORTHERN CORDILLERA

Project 750014

G.H. Eisbacher
Regional and Economic Geology Division, Vancouver

Abstract

Eisbacher, G.H., Two major Proterozoic unconformities, northern Cordillera; Current Research, Part A, Geol. Surv. Can., Paper 78-1A, p.53-58, 1978.

The youngest Proterozoic succession in the Mackenzie and Wernecke mountains contains two regional unconformities or disconformities. Locally, truncation of tectonic structures and considerable erosion is indicated beneath the unconformities. The lower unconformity underlies Redstone River Formation to the east, and Pinguicula Group to the west. The upper unconformity was probably created by a structural event which took place during deposition of the Sayunei Formation of the Rapitan Group. Facies relationships and paleocurrents suggest that the youngest Proterozoic depositional basin created during these structural events did not extend far to the northeast of the present outcrop margin. Possibly, two glaciations influenced the sedimentary sequence: one directly (Sayunei - Shezal formations), the other indirectly (upper part of Keele Formation).

Introduction

During the 1977 field season a wide ranging regional reconnaissance and local detailed studies of younger Proterozoic rocks were carried out in the Mackenzie Mountains and eastern Wernecke Mountains. This work was done with logistic support by J.D. Aitken. A major part of the field work was directed towards tracing the stratigraphic position and continuity of two regionally significant unconformities within the younger Proterozoic succession. In addition to the maps and reports by Wheeler (1954), Gabrielse et al. (1973), Aitken et al. (1973), and Blusson (1971), open file maps by Aitken and Cook (1974), Norris (1975), and Blusson (1974) were used during the field investigations.

Because the region studied is large and nomenclature of Proterozoic sedimentary and volcanic rocks is presently being established, the accompanying stratigraphic table must be considered preliminary and will be subject to revision as work continues. Nonetheless, Figure 12.1 outlines the principal units as they are presently conceived. The two stratigraphic intervals discussed in this report concern the succession which is generally shown as youngest Helikian or Hadrynian on geological maps of the region. The units display rapid facies variations, thickness changes, and depict the influence of deformation and volcanism. Older Proterozoic units such as those of the Katherine and Little Dal Groups (including map-units H_5 of Aitken and Cook, 1974, and H_{2a}, H_{2b} of Norris, 1975) seem to be characterized by formations and members which can be followed over large distances with only minor changes in stratigraphic detail (D. Long and J.D. Aitken, pers. comm. 1977). In contrast, the two younger sequences seem to reflect a more active tectonic setting within the opening Cordilleran miogeosyncline (Eisbacher, 1977).

The stratigraphy of the two successions and the nature of the unconformities and disconformities at their base are discussed separately for the Mackenzie Mountains and eastern Wernecke Mountains, and a possible correlation of the tectonic events in those mountain ranges is proposed (Figs. 12.1, 12.2).

Mackenzie Mountains

In the Mackenzie Mountains a thick, older succession of carbonate, quartzite, and shale reflects tectonic stability over a large area during much of Helikian time. However, towards the top of the Little Dal Group, basic lavas are intercalated within the shallow-water dolomite deposits. Basic dykes and sills possibly related to this magmatic event are found in all stratigraphic units below. The Little Dal Group is overlain by conglomerate, siltstone and gypsum of the Redstone River Formation, and mafic breccias are known to intrude these rocks as well (Gabrielse et al., 1973, and confirmed during the present studies). The contact between the Little Dal Group and the Redstone River Formation is generally abrupt, and locally as much as 150 m of fluviatile conglomerate constitutes the base of the Redstone River Formation. Contemporaneous faulting and regional arching along northerly to northeasterly trends probably account for most of the rapid facies changes and suggest a pronounced change in the tectonic setting of the region during deposition of the Redstone River Formation (Eisbacher, 1977, and in prep.). The composition of the coarse fluvial and alluvial fan deposits of the Redstone River Formation reflect almost totally the local lithologies of the underlying Little Dal Group dolomite and dolomitic siltstones. Paleocurrents are strongly influenced by local tectonic gradients but the general paleoslope as indicated by fluvial paleocurrents and gross facies changes was to the southwest (Fig. 12.5a). The subsequent transgression and deposition of laminated and turbiditic limestone and cherty dolomite of the Coppercap Formation was characterized by relative tectonic tranquility. Stratigraphic details of the Coppercap Formation can be carried across hinge lines which were the focus of faulting during Redstone River time (Eisbacher, in prep). Over wide areas the Coppercap Formation consists of two shoaling carbonate cycles which are thicker and better developed towards the southwestern, central part of the basin.

Towards the southern, northern and eastern outcrop margin limestone of Coppercap Formation oversteps the depositional edge of the Redstone River Formation and rests disconformably on Little Dal Group dolomites.

A second major unconformity occurs at the base or slightly above the base of the Rapitan Group. It must be stressed that, in one place or another, all of the formations of the Rapitan Group lie unconformably on older formations. However, most of the unconformable or disconformable contacts change into conformable boundaries in a down-basin direction (Eisbacher, in prep). The unconformity within or below the Sayunei Formation is the most pronounced and regionally significant break. In most of the easterly sections a considerable amount of pre-Sayunei erosion of older units can be demonstrated. The Sayunei Formation of the Rapitan Group is defined as a monotonous argillite-siltstone sequence interlayered with lenticular bodies of sharpclast siltstones (Eisbacher, in prep). It displays very rapid thickness changes and its base is disconformable, unconformable, or onlapping on older formations. The precise stratigraphic age of the deformation which created this hiatus is difficult to

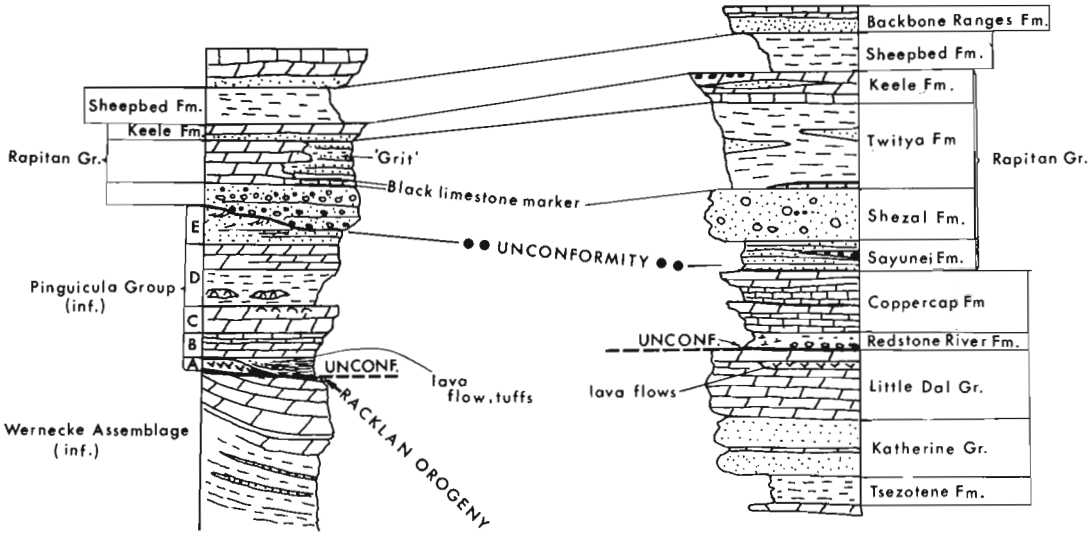

Figure 12.1

Stratigraphic chart of the youngest Proterozoic, Mackenzie Mountains (right) and eastern Wernecke Mountains (left), and suggested correlation between the two areas.

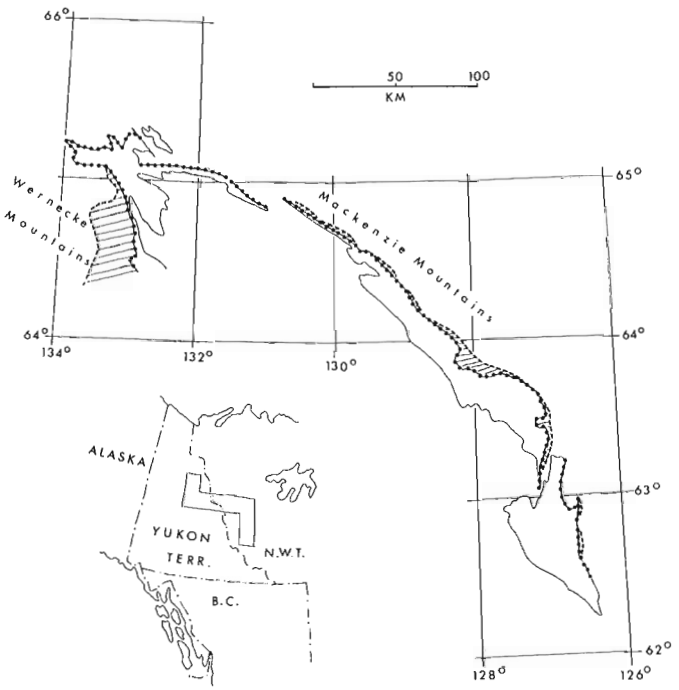

Figure 12.2 Outcrop area of the youngest Proterozoic rocks and the two major unconformities and disconformities in the Mackenzie and Wernecke mountains. Broken line - pre-Pinguicula and pre-Redstone River unconformity; Dotted line - pre- or intra- Sayunei unconformity.

determine but can be inferred from relationships exposed west of Keele River in the Sekwi Mountain map-area. There, carbonate strata of Coppercap Formation and basal buff-maroon siltstones of Sayunei Formation are deformed into large folds and broken by faults; these were brought to the attention of the author by H. Helmstaedt (pers. comm. 1976). The style of deformation is probably controlled by gypsiferous strata of the underlying Redstone River Formation. Fold axes and faults in the Coppercap and lower Sayunei Formation trend northerly. The folds are truncated and overlain with angular unconformity by sharpstone conglomerate which contains clasts derived from the underlying carbonates of the Coppercap Formation and fragments of the buff, maroon, and grey siltstone of the basal Sayunei Formation. This coarse unit, the iron-formation marker beds, and the glacial-marine deposits of the overlying Shezal Formation have not been displaced greatly prior to the late Mesozoic deformation of the Mackenzie Mountains.

Wernecke Mountains

The structural and stratigraphic relationships between the major Proterozoic successions were studied in Nadaleen and Snake River map-areas. The stratigraphy is summarized in Figure 12.1. The three Proterozoic packets are referred to informally as Wernecke Assemblage, Pinguicula Group, and Rapitan Group. Each will be discussed briefly.

1. Wernecke Assemblage (informal name)

Large regions of the Wernecke and Ogilvie Mountains are underlain by these rocks. Green (1972), and Bell and Delaney (1977) recognized a twofold subdivision with a lower clastic succession of phyllite, slate, siltstone and sandstone, and an upper, mainly dolomitic carbonate unit. Both units are intensely deformed, and intruded by heterolithic breccias and mafic dykes. Structural trends below the contact with the Pinguicula Group are predominantly north-northeasterly (Wheeler, 1954). Detailed examination of several areas near the unconformity between the Wernecke Assemblage and the Pinguicula Group suggests that some of the north-north-easterly trending folds formed prior to the deposition of the Pinguicula Group (Fig. 12.3). This deformation is the type Racklan Orogeny (Gabrielse, 1967). From the data gathered during this study it is evident that the Racklan Orogeny cannot be equated with the sub-Rapitan unconformity elsewhere and that it is older.

2. Pinguicula Group (informal name)

This unit overlies unconformably the older Wernecke Assemblage and throughout the Nadaleen map-area can be divided into five distinct formations, here referred to as A, B, C, D, E. These will be formally named in forthcoming reports.

A. The basal unit consists of basaltic flows, various types of tuffs, and grey argillite in the south grading into red silty laminites towards the north.

B. This unit consists of buff, thinly bedded platy dolomitic siltstones and grades upwards into thin bedded limestones.

C. This unit is defined by massive light grey limestone and recrystallized dolomite. It grades commonly into stromatolitic biostromes towards the top.

D. This unit consists of black shale and orange weathering stromatolitic biostromes and bioherms near the base, and grey to buff weathering particulate dolomite members near the top.

E. The highest unit throughout the area is a brown weathering quartzose sandstone with numerous bands of shale and dolomite near the base. The crossbedded quartzites at the top of the unit are ferruginous and include the rocks at the Hematite Creek locality described in detail by Wheeler (1954). All units of the Pinguicula Group increase in thickness towards the south. Between the angular unconformity at the base and the unconformity at the top of the group the formations are repeated by four major, westward directed, thrust faults.

3. Rapitan Group

The Rapitan Group was traced from its type area in the Snake River - Rapitan Creek region southward into the Nadaleen River map-area by detailed mapping (Fig. 12.2). In Snake River map-area the Rapitan Group consists of the four formations recognized in the Mackenzie Mountains (Sayunei, Shezal, Twitya, and Keele Formations). However, both the sharpstone channels of the Sayunei Formation and the glacial-marine deposits of the Shezal Formation are considerably thicker than in the Mackenzie Mountains.

Towards the south the Rapitan Group displays pronounced facies changes which can only be appreciated by walking out individual lithologic members. Basal conglomeratic channels of the Rapitan Group increase in thickness and glacial-marine diamictites thin rapidly to zero above the basal conglomerates. Above the diamictite a distinct marker composed of black turbiditic limestone and carbonate debris flows can be traced southward into a massive complex of shallow-water dolomite which rests directly on the basal boulder conglomerate. The conglomerate comprises densely packed dolomite and quartzite boulders, and could stratigraphically correspond to either the Sayunei or Shezal Formations farther north. The conglomerate rests with profound angular unconformity on Pinguicula Group rocks (Fig. 12.4) and the variety of Pinguicula units underlying the unconformity suggests that a phase of deformation preceded deposition of the Rapitan conglomerate. The conglomerate consists of channellized and internally imbricated layers of clasts with well bedded stringers of sandy material. The deposits could represent environments of braided rivers and the fill of submarine channels. The black limestone marker in the north and the massive dolomite farther south are overlain and laterally replaced by a thick succession of turbiditic grits stratigraphically equivalent to the Twitya Formation.

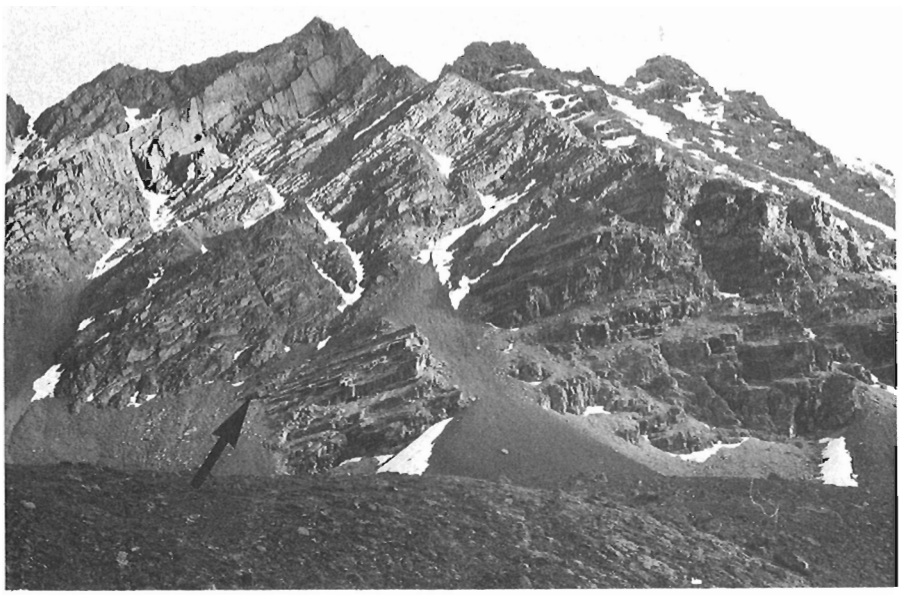

Figure 12.3

Angular unconformity between massive dolomite of the Wernecke Assemblage and red silty laminites of the basal Pinguicula Group (exposure in the southern-most part of the Snake River map-area).

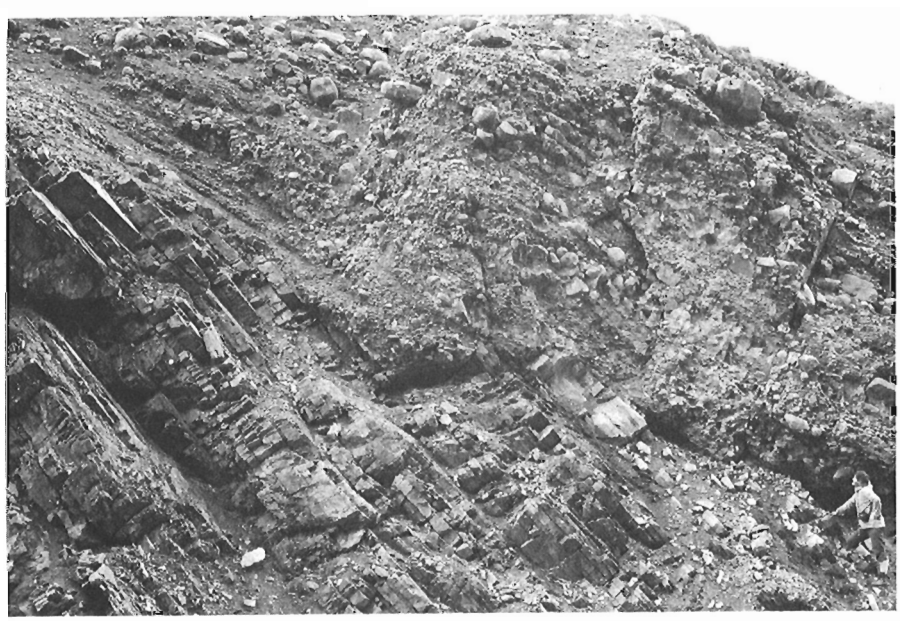

Figure 12.4

Boulder conglomerate of the Rapitan Group overlying unconformably unit D of the Pinguicula Group. Note man in lower right for scale.

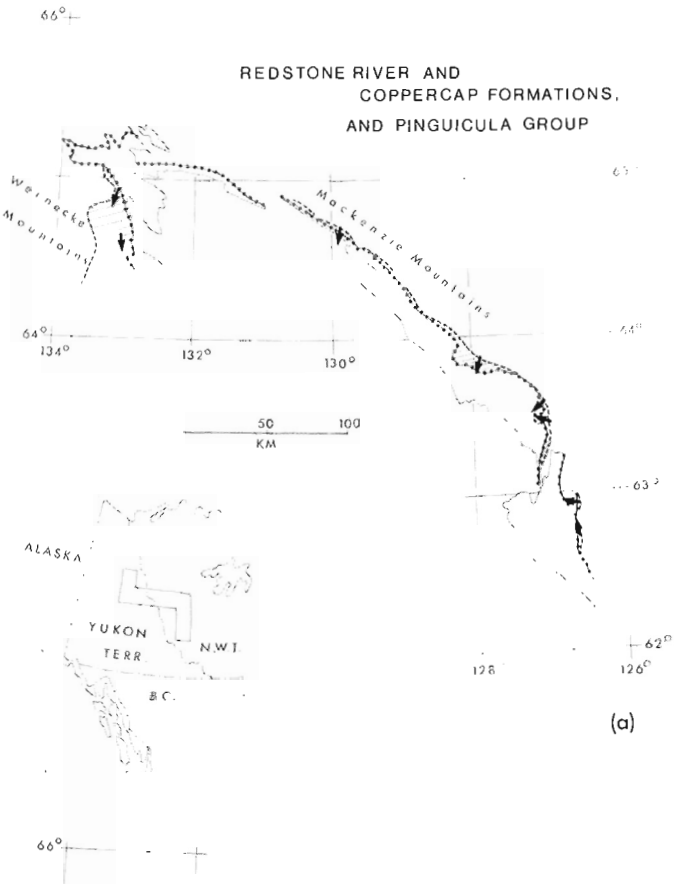

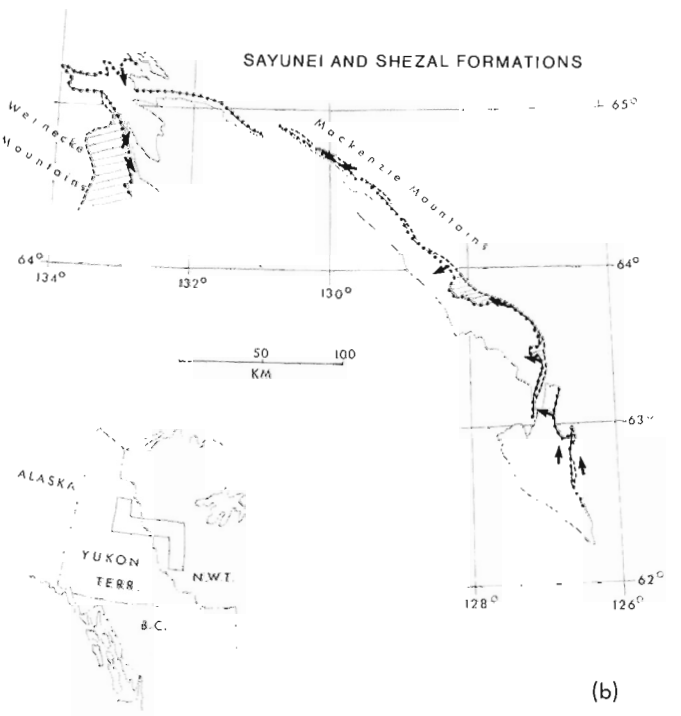

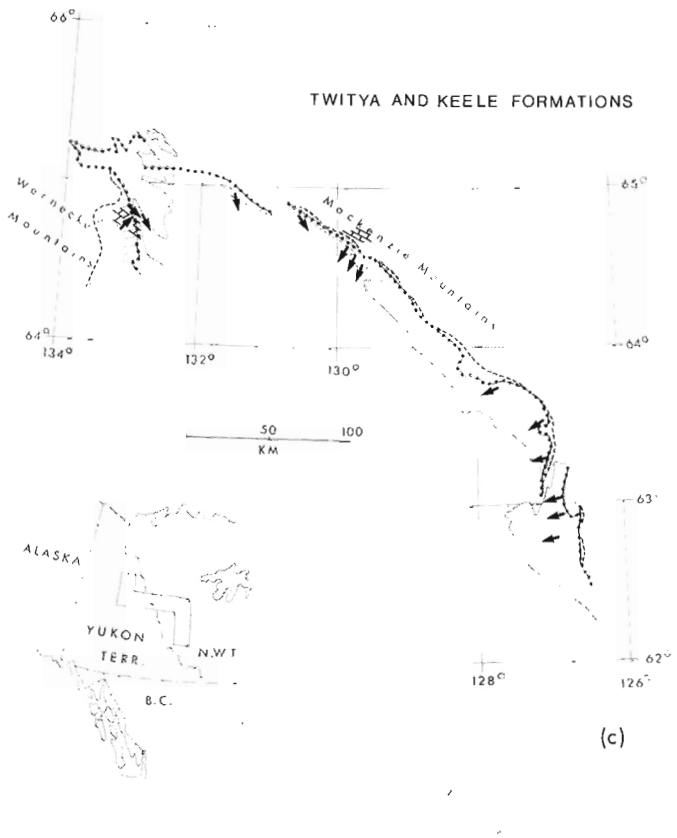

Figure 12.5 Paleoslopes as derived from paleocurrents and slump-folds of

a) Pinguicula Group and Redstone River - Coppercap Formations,
b) Sayunei and Shezal formations,
c) Twitya and Keele formations (grid pattern indicates carbonate platforms during deposition of Twitya Formation).

Paleocurrents in these grits are to the southeast and suggest that the massive dolomite complex formed the southwestern margin of the clastic Twitya basin (Fig. 12.5c). The Keele Formation (shallow-water carbonates and clastics) overlies both the massive dolomite and the basinal siliciclastic turbidites. Paleocurrents indicate south-southeastward progradation of this highly varied complex.

Regional Correlation

In many localities in the Mackenzie Mountains and the eastern Wernecke Mountains Rapitan Group rocks rest with profound angular unconformity on older carbonate strata. Local structural relationships suggest an intra-Sayunei tectonic event. Elsewhere the record of tectonism is limited to subaqueous flows of coarse angular material (Eisbacher, 1977). The Rapitan unconformity can be traced from the Mackenzie Mountains into the Wernecke Mountains where conglomerate overlies deformed Pinguicula Group (Fig. 12.2). Since both Pinguicula Group and Redstone River - Coppercap formations unconformably overlie older Helikian rocks it is conceivable that these two complexes were laid down roughly within the same time interval. This suggested correlation is shown as such in Figure 12.1 and is favoured by three points:

1. Two major shoaling cycles are recorded by the Coppercap Formation and by the units B, C, D, E of the Pinguicula Group.

2. Volcanic units directly below the base of the Redstone River - Coppercap couplet and at the base of the Pinguicula Group are unique within the otherwise nonvolcanic setting of the basin. Mafic dykes and sills are more common below these units than within them. A program of radiometric dating is being initiated in collaboration with Dr. R.L. Armstrong, University of British Columbia, to establish a radiometric time marker for the volcanic events.

3. Traces of copper, possibly derived from the volcanics and dykes occur in the lower units of the Pinguicula Group. Mineralization of a similar source has been actively explored in recent years in the Mackenzie Mountains.

Basin Geometry, Regional Paleoslope, and Sea Level

Paleoslopes determined from paleocurrent data and slump folds in the youngest Proterozoic formations of the Mackenzie and eastern Wernecke Mountains are shown in Figure 12.5a, b, c. It appears that the regional basin configuration was initiated by the deformation that produced the lower of the two unconformities. However, local paleoslopes varied markedly from place to place during deposition of the Redstone River and Coppercap Formations along the eastern basin margin. Varied local paleotopography also characterized the setting of the Sayunei Formation which was laid down during a second phase of deformation. Paleoslopes became more uniform on a regional scale during deposition of the Twitya and Keele Formations of the Rapitan Group. Both were deposited after a phase of regional glaciation (Shezal Formation). The Twitya Formation contains abundant evidence that carbonate platforms rimmed parts of the clastic basin immediately after the deposition of the last glacial diamictite. Coarse siliceous grits were transported centripetally into deeper water across both carbonate platforms and shallow clastic shelves. The Keele Formation represents the record of rapid basinward progradation of shallow water carbonate banks and siliceous clastics. Towards the outer prograding margin debris flow deposits characterize the Keele Formation. It is possible that eustatic sea level changes related to a second glaciation occurred during Keele time. A lowering of sea level might have produced exposed relief at the platform edge and debris flows issued near its front. Subsequent rise in sea level probably caused submergence under an extensive blanket of shale (Sheepbed Formation).

The youngest Proterozoic basin was therefore shaped by at least two major deformations and possibly two eustatic sea level changes.

Economic Significance

In the Mackenzie Mountains various types of copper mineralization have been prospected within Proterozoic strata. Although much of the mineralization occurs in dolomitic rocks near the top of the Redstone River Formation, other types of showings are known in formations above and below the Redstone River Formation. There, mineralization is encountered in diagenetic and tectonic pore space. The author has seen copper mineralization in Little Dal Group, Coppercap Formation, Sayunei Formation, and Keele Formation along the northwest trending Redstone Copper Belt. The Redstone River copper showings are therefore veiled by a "fuzzy" fringe and are stratabound only in a very broad sense. Paleocurrents in coarse fluvial and alluvial fan deposits of the Redstone River Formation indicate a south-southwesterly regional paleoslope with uplands to the northeast of the present erosional scarp. Detailed mapping in areas directly east of the main Redstone River outcrop also demonstrates that Coppercap Formation oversteps the depositional margin of the Redstone River Formation. Therefore, the depositional basin of the Redstone River Formation probably never extended far to the east of its present outcrop. On the basis of lithologic similarity and stromatolites Jefferson and Young (1977) concluded that "...copper mineralization, presently known at the Redstone River - Coppercap transition zone of the Mackenzie Mountains, probably occurs on Victoria Island at the very recessive Minto Inlet - Wynniatt transition zone." As indicated above, however, it does not seem probable that the Redstone River Formation ever extended across the 500 km that separate the two regions and the extrapolation of relative mineral potential over this distance is not supported by field evidence.

References

Aitken, J.D. and Cook, D.G.

1974: Geological maps, northern parts of Mount Eduni and Bonnet Plume Lake map-areas, District of Mackenzie; Geol. Surv. Can., Open File 221.

Aitken, J.D., Macqueen, R.W., and Usher, J.L.

1973: Reconnaissance studies of Proterozoic and Cambrian stratigraphy, lower Mackenzie River area (Operation Norman), District of Mackenzie; Geol. Surv. Can., Paper 73-9, 178 p.

Bell, R.T. and Delaney G.D.

1977: Geology of some uranium occurrences in Yukon Territory; in Report of Activities, Pt. A, Geol. Surv. Can., Paper 77-1A, p. 33-37.

Blusson, S.L.

1971: Sekwi Mountain map-area, Yukon Territory and District of Mackenzie; Geol. Surv. Can., Paper 71-22, 17 p.

1974: Five geological maps, northern Selwyn Basin, Yukon Territory and District of Mackenzie; Geol. Surv. Can., Open File 205.

Eisbacher, G.H.

1977: Tectono-stratigraphic framework of the Redstone Copper Belt, District of Mackenzie; in Report of Activities, Pt. A, Geol. Surv. Can., Paper 77-1A, p. 229-234.

in prep: Re-definition and subdivision of the Rapitan Group, Mackenzie Mountains; Geol. Surv. Can., Paper 77-25.

Gabrielse, H.

1967: Tectonic evolution of the northern Canadian Cordillera; Can. J. Earth Sci., v. 4, p. 271-298.

Gabrielse, H., Blusson, S.L., and Roddick, J.A.

1973: Geology of Flat River, Glacier Lake, and Wrigley map-area, District of Mackenzie and Yukon Territories; Geol. Surv. Can., Mem. 366, 153 p.

Green, L.H.

1972: Geology of Nash Creek, Larsen Creek, and Dawson map-area, Yukon Territory; Geol. Surv. Can., Mem. 364, 157 p.

Jefferson, C.W. and Young, G.M.

1977: Use of stromatolites in regional lithological correlations of upper Proterozoic successions of the Amundsen Basin and Mackenzie Mountains, Canada; Geol. Assoc. Can., Abstr. v. 2, 1977, p. 26.

Norris, D.K.

1975: Geological maps, Hart River, Wind River and Snake River, Yukon and Northwest Territories; Geol. Surv. Can., Open File 279.

Wheeler, J.O.

1954: A geological reconnaissance of the northern Selwyn Mountains region, Yukon and Northwest Territories; Geol. Surv. Can., Paper 53-7.

13. GEOLOGY OF HAZELTON (WEST-HALF) MAP-AREA, BRITISH COLUMBIA

Project 720038

T.A. Richards
Regional and Economic Geology Division, Vancouver

Abstract

Richards, T.A., Geology of Hazelton (west-half) map-area, British Columbia; Current Research, Part A, Geol. Surv. Can., Paper 78-1A, p. 59-60, 1978.

The area is underlain by Late Jurassic to Early Tertiary successor basin assemblages of the Bowser Lake, Skeena, and Sustut groups, containing locally significant thickness of volcanic rocks. Granodioritic intrusions, from large stocks to abundant dykes, are assigned to the Late Cretaceous Bulkley Intrusions. They are closely related to most of the mineral occurrences in the area. Mapping in the area was mainly completed in 1977.

Stratigraphy

Bowser Lake Group

The oldest rocks in Hazelton west-half (93M west-half) map-area are part of the Upper Jurassic Lower Cretaceous Bowser Lake Group. Contacts with the underlying Hazelton Group are not exposed in the map-area, but elsewhere it lies conformably on the Hazelton Group (Tipper and Richards, 1977). The Bowser has been arbitrarily divided into two informal units – lower and upper (Fig. 13.1). Contacts between the two are gradational, and the term "intermediate Bowser" was coined to classify outcrops where a decision between upper and lower could not be reached. The lower Bowser occupies the largest area. It appears to represent a northerly prograding deltaic assemblage with a gentle north to northwest dipping paleoslope (Richards and Jeletzky, 1975). The upper Bowser generally underlies many of the major valley bottoms. It is a shallow marine-lagoonal alluvial suite deposited on a gentle, west to southwest dipping paleoslope. The upper unit is generally finer grained than the lower, contains a much greater amount of carbonaceous material and is much less indurated. Megascopic clasts of red volcanics, biotite, quartz and rare chert and muscovite are present in the upper and absent in the lower. The two units represent end-members in the evolution of the southeastern part of the Bowser basin. Sedimentary rocks of the lower units reflect deposition controlled by tectonism along the Skeena Arch. The upper unit reflects tectonism in what eventually became the Omineca Crystalline Belt.

Skeena Group

The Skeena Group is of Early to Late Cretaceous age. It contains a wide variety of sedimentary and volcanic rocks and is generally poorly exposed. Its contact with the underlying upper Bowser Group is marked by laterally persistent chert-vein quartz-pebble conglomerate 10 to 30 m thick in the northeast, but is less well defined in the south. As mapped, sedimentary rocks of the Skeena Group contain common to abundant visible detrital muscovite; the conglomerates contain abundant chert and quartz. Paleocurrent data suggest an east to northeast source for the detritus. The lower members of the Skeena Group are interbedded sandstone, conglomerate, siltstone, and a distinctive pyritic black shale. These are nonmarine to shallow marine sediments of probably modest thickness (300 m ± ?). Overlying rocks in the south are pyroclastic and volcaniclastic alkali basalts of the Rocky Ridge Volcanics which are as much as 700 m thick. These are overlain by a suite of alluvial clastics comprising the Red Rose Formation.

Tentatively included in the Skeena Group are the Brian Boru volcanics (Sutherland Brown, 1960). They outcrop in the Rocher Deboule Range and the upper Suskwa River and each location is a distinctive assemblage. On Rocher Deboule Range they include abundant acidic pyroclastics that range from cherty rhyolite to hornblende porphyry. Near Suskwa River they are mainly andesitic. In the Rocher Deboule Range south of Brian Boru Peak, they appear to rest with angular discordance on the aforementioned units of the Skeena Group and are thus probably tectonically distinct. The Brian Boru volcanics have tectonic and lithologic similarities to the basalt volcanics (MacIntyre, 1976) in the Whitesail Lake map-area. The latter are probably correlative with the Ootsa Lake Group.

Sustut Group

The Sustut Group occupies a small sliver in the Bulkley Valley at the south edge of the map-area. The rocks are dated as Paleocene (Armstrong, 1944). They are a loosely indurated assemblage of rapidly deposited conglomerate, sandstone, siltstone and minor coal clasts and are mainly locally derived with all earlier mentioned rock units, particularly the Brian Boru volcanics, being present.

Bulkley Intrusions

Stocks of granodiorite, tonalite and diorite form the core of most of the mountain massifs. These are high-level intrusions, many with roofs preserved. They have, in general, domed the adjacent strata and superposed on them rusty hornfels haloes up to 1000 m wide. Small plugs and dykes, although not shown on Figure 13.1, abound, particularly in the vicinity of Hazelton. These bodies appear to be directly related to the mineral occurrences in the district.

Deformation

Deformation style is related to block faults. Each of the major mountain massifs appears to represent an uplifted block underlain by granitic rocks and older facies of the Bowser Lake Group. Younger rock assemblages occupy adjacent major valleys. Maximum displacement appears to be along the Bulkley Valley where the youngest strata are preserved. The block pattern is less evident to the northwest, where the oldest strata occupy the valley bottoms. Youngest rocks affected by the fault system are of Paleocene age in the map-area, but to the south, in the Smithers map-area, the Miocene Endako Group basalts are block faulted.

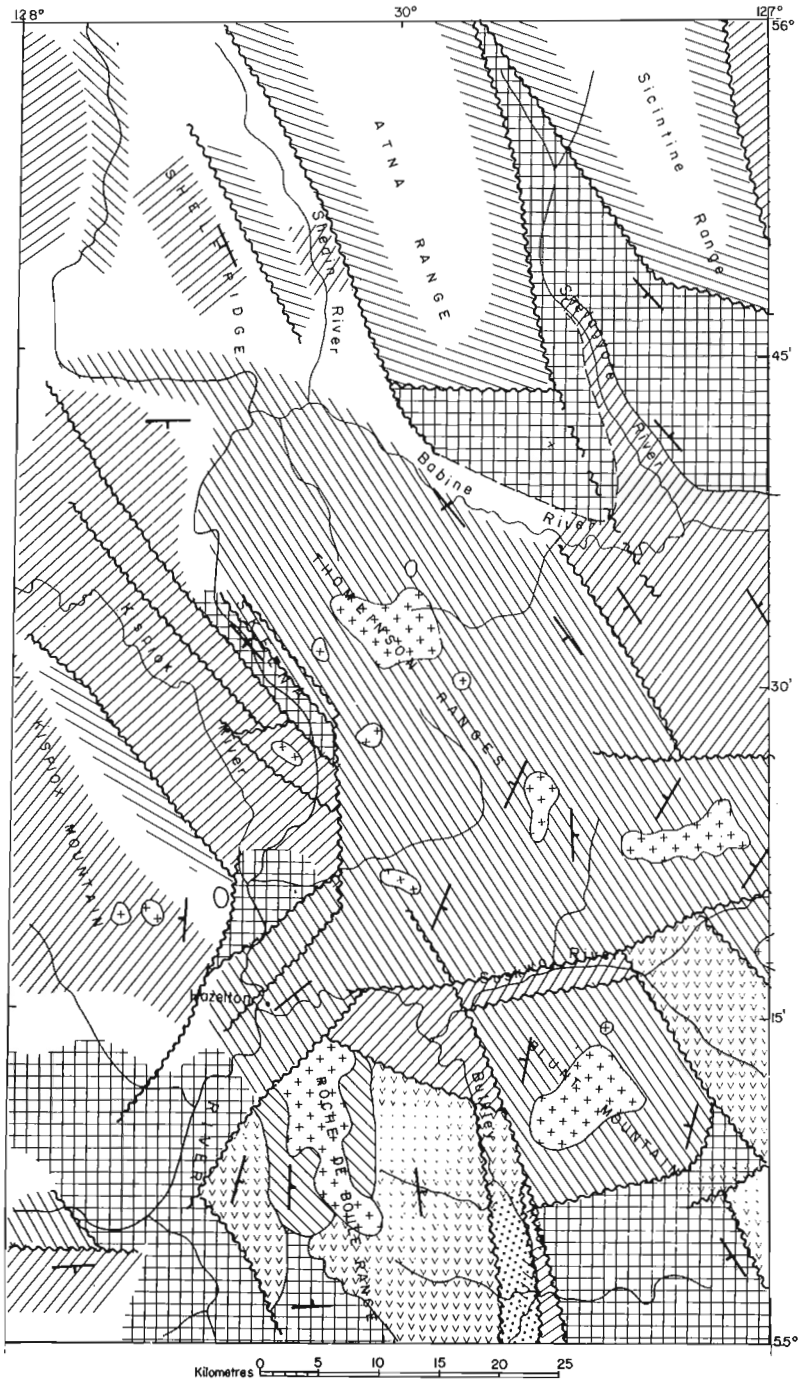

Figure 13.1

Legend

TERTIARY

Paleocene to Eocene

Sustut Group: sandstone, conglomerate, siltstone, minor coal; andesite and basalt.

CRETACEOUS

Upper Cretaceous

Bulkley Intrusions: granodiorite, tonalite, diorite, quartz monzonite. Brian Boru Volcanics: rhyolite, dacite, andesite and basalt; pyroclastic, flow and volcaniclastics.

Lower and Mid — Cretaceous

Skeena Group: black shale, conglomerate, sandstone, siltstone, minor coal; alkali basalt.

Upper Jurassic to Lower Cretaceous

Bowser Lake Group, upper part: sandstone, conglomerate siltstone, minor coal.

Bowser Lake Group, lower part: sandstone, conglomerate, siltstone.

fault : known, probable

generalized strike and dip of bedding

References

Armstrong, J.E.
1944: Preliminary map, Hazelton, British Columbia; Geol. Surv. Can., Paper 44-24.

MacIntyre, D.G.
1976: Evolution of Upper Cretaceous volcanic and plutonic centres and associated porphyry copper occurrences, Tahtsa Lake area, British Columbia; unpubl. Ph.D. thesis, Univ. Western Ontario, 149 p.

Richards, T.A. and Jeletzky, O.L.
1975: A preliminary study of the Upper Jurassic Bowser assemblage in the Hazelton west half map-area, British Columbia (93M-W1/2); in Report of Activities, Part A, Geol. Surv. Can., Paper 75-1A, p. 31-36.

Sutherland Brown, A.
1960: Geology of the Rocher Deboule Range; B.C. Dep. Mines Pet. Resour., Bull. 43, 78 p.

Tipper, H.W. and Richards, T.A.
1976: Jurassic stratigraphy and history of north-central British Columbia; Geol. Surv. Can., Bull. 270; 73 p.

RECONNAISSANCE GEOLOGY, LABERGE MAP-AREA, YUKON

Project 770017

D.J. Tempelman-Kluit
Regional and Economic Geology Division, Vancouver

Abstract

Tempelman-Kluit, D.J., Reconnaissance Geology, Laberge map-area, Yukon; Current Research, Part A, Geol. Surv. Can., Paper 78-1A, p. 61-66, 1978.

Laberge map-area includes parts of the Omineca Crystalline Belt and the Intermontane Belt and straddles Teslin lineament, the suture separating them. Mesozoic rocks have been separated into the Lewes River and Laberge groups but they are a single sequence of fanglomerates, turbidites and related rocks punctuated by carbonate reefs and distinction between the two groups of rocks is difficult. The carbonate reefs offer possibilities as hosts to concentrations of copper and contain bituminous material locally.

Introduction

Updating of geological mapping in Laberge map-area (105E) was begun during the summer of 1977. The area straddles Teslin lineament, the boundary between the Omineca Crystalline Belt and Intermontane Belt in Yukon Territory. It offers the opportunity to study these two disparate tectonic elements and the relations between them. Omineca Crystalline Belt is the Late Precambrian to mid-Paleozoic stable margin of the North American continent metamorphosed and granitized during the Cretaceous. By contrast the Intermontane Belt is a Mesozoic basin in which sediment accumulated, possibly at the edge of North America, but probably far from its present site. These two elements were juxtaposed about Cretaceous time.

Distribution of Rocks

Bostock and Lees (1938) provided an accurate map of the distribution of rock types in Laberge map-area, but their assignments to rock units were not consistent. For the following outline of the main reassignments the reader is referred to their map. Volcanic rocks mapped as Hutshi Group (their map-unit 9) include at least two different assemblages of volcanic rocks. In the Miner's Range they are a nearly flat lying sequence of intermediate to acid terrestrial tuff and breccia 2000 to 3000 m thick. These rocks are Eocene and are part of the Mount Nansen Group. Strata mapped as Hutshi Group on Teslin Mountain are also part of the same group. The porphyries (map-unit 12) and granitic bodies (map-unit 11) on Packers Mountain and nearby Claire Lake are subvolcanic equivalents of the Mount Nansen Group. The pluton (map-unit 11) 10 km east of Miller Lake is probably also related to the Mount Nansen and may be a Nisling Range alaskite equivalent. In contrast the 20-km-wide belt of rocks (map-unit 9) that extends from Boswell Mountain through the Semenof Hills and beyond includes massive basaltic volcaniclastic rocks and volcanic derived greywacke whose thickness and orientation are obscure. They are Mesozoic, possibly Triassic, and are correlatives of the Lewes River Group as used by Wheeler (1961). Two areas east of Lake Laberge mapped as Hutshi Group, one near Povoas Mountain, the other south of Laurier Creek, are underlain by volcanic-derived clastic rocks and are probably Mesozoic also.

Mesozoic Rocks of Whitehorse Trough

Mesozoic rocks of the Whitehorse Trough (the part of the Intermontane Belt in Yukon Territory) have been divided traditionally into the Lewes River and Laberge groups and Tantalus Formation. These units are Upper Triassic, Lower Jurassic and Upper Jurassic-Lower Cretaceous respectively. No type sections have been designated and no unequivocal boundaries are defined. In the most recent usage (Wheeler, 1961) the name Lewes River Group was applied to "Sedimentary and volcanic rocks containing Upper Triassic fossils and immediately underlying the Laberge Group." The "Laberge Group" was meant to include all clastic rocks above

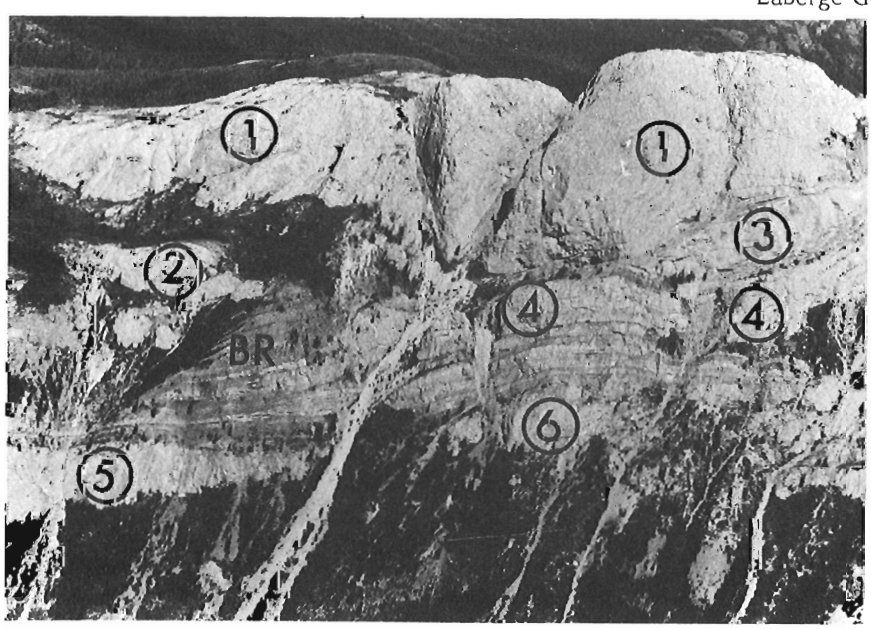

Figure 14.1

View north of Lime Peak in which six Upper Triassic reefs are arbitrarily numbered. About 500 m of section are shown. The width represented in the photograph is about 1 km. The massive white rocks are algal and coral bound pelleted lime muds of the main reefs, medium grey rocks are thin bedded bioclastic lime sands of back-reef facies (labelled BR) and black rocks are off-reef and sub-reef greywacke and shale. Note the asymmetry of the reefs. On the left they thin gradually (reefs 1 and 2) or merge with the back reef facies (reef 4). On the right they fall off abruptly (reefs 2 and 1 – partly off the picture) and abut clastic rocks that fringe and cover the reefs. Note the marked lateral thickness changes and how the reefs merge in the section so that at the right of the photograph reefs 1, 3, 4 and 6 form one essentially continuous long-lived reef. Reefs 5 and 6 pinch out toward each other in this view but they are probably the same reef.

the highest limestone in the Lewes River. Wheeler considered that a disconformity separates the two groups of rocks. Each unit was considered sufficiently lithologically distinctive to cause no confusion. Thus the Lewes River contains mainly volcanic-clast conglomerate and greywacke with limestone at the top, while the Laberge includes mainly granite-clast conglomerate and greywacke. In contrast the Tantalus Formation comprises chert-pebble conglomerate.

There is no problem recognizing the boundaries of the Tantalus Formation, because it is separated from the rocks below by an unconformity and because it is lithologically distinctive. However, the Lewes River and Laberge groups are a single sequence of fanglomerate, beach, reef and turbidite deposits which may be in part lateral equivalents of each other laid down from Late Triassic through Early Jurassic time with many local, but minor, hiatuses. Although this sequence changes lithologic character from bottom to top, it does so gradually and with alternations and no overall unequivocal boundary can be drawn. It is a sequence with many local unconformities, but none of these appear extensive enough to be used as the boundary of the two groups.

The limestone whose top has been used as the boundary between the Lewes River and the Laberge groups is reefoid (Fig. 14.1). It occurs as discontinuous lenticular bodies in a belt 30 km wide, but is best developed in a zone 10 km wide within this belt. Because the limestone lacks continuity even in the zone where it is commonest its top cannot be used to define a consistent boundary. As many as four reefs may be seen one above the other. Laterally two or more such reefs may merge so that dramatic changes in thickness over short lateral distances are common. Where determinable the reefs display a consistent asymmetry (Fig. 14.1). On their northeast side they grade abruptly into greywacke which contains limestone boulders to 5 m across (Fig. 14.5), presumably derived from the reefs during their growth. On their southwest sides the reefs tail out gradually into thin bedded impure bioclastic lime sands (Fig. 14.4) which merge, still farther behind the reefs with coarse quartzose sands (Fig. 14.3) that are texturally and compositionally much more mature than other sandstones in the region. The reefs lie directly on clastic rocks and their bases are parallel with the bedding of the greywacke and shale that is their substrate. Tozer (1958) studied the limestone where four reefs occur in a section 2000 m thick and considered the oldest limestone Karnian and the youngest Norian.

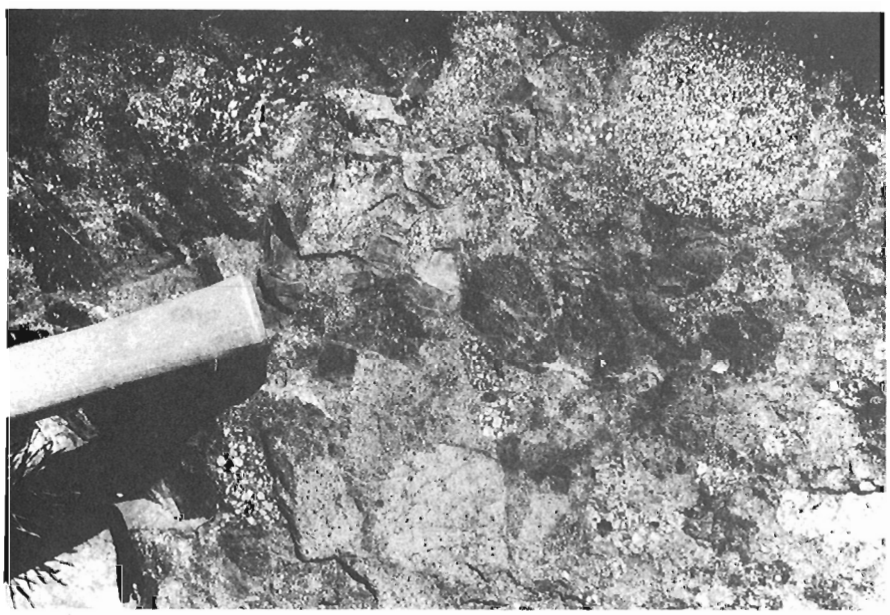

Figure 14.2

This conglomerate with numerous rounded granitic and subvolcanic boulders is typical of much of the Laberge Group although it also occurs in the Lewes River Group. It is found mainly southwest of Lake Laberge and is interpreted as fanglomerate. The conglomerate is interbedded with marine shale and turbidite, but some of the conglomerate is probably terrestrial.

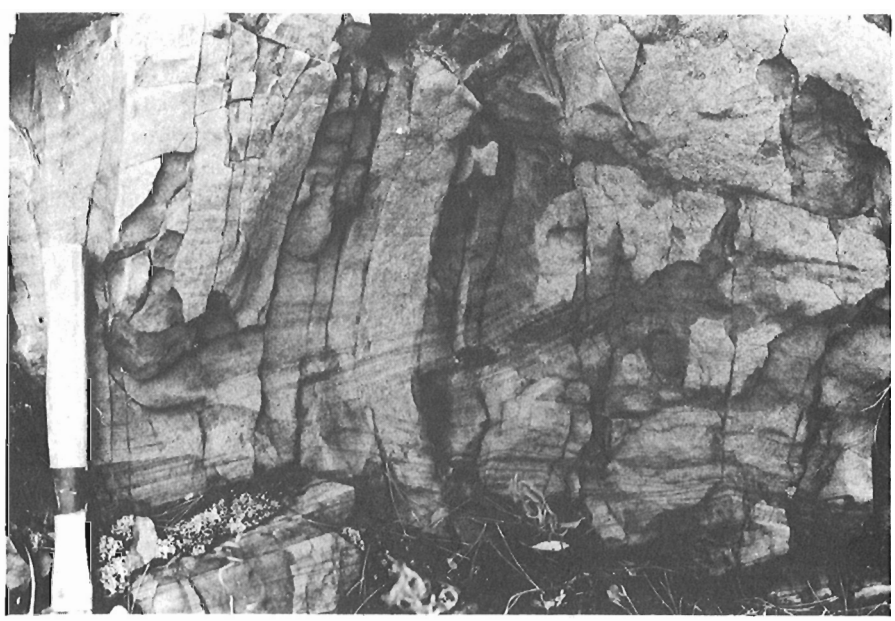

Figure 14.3

Cross-bedded quartzofeldspathic sandstone near Fox Lake. This rock is compositionally and texturally more mature than the greywacke in the Lewes River and Laberge groups and is interpreted as a beach deposit. Sands like this grade northeastward into the skeletal limestone of the back-reef facies (Fig. 14.4) and southwest into conglomerate of the Laberge type (Fig. 14.2).

Figure 14.4

Medium- to thin-bedded grey detrital skeletal limestone on Lime Peak. The location is at BR on Figure 14.1. This is an example of the back-reef facies that can be found on the western sides of many of the reefs. It is the transitional facies between the skeletal bound, pelleted lime muds of the reefs and the comparatively mature sands found behind the reefs (Fig. 14.3). Still farther back (southwest) is fanglomerate like that of Figure 14.2.

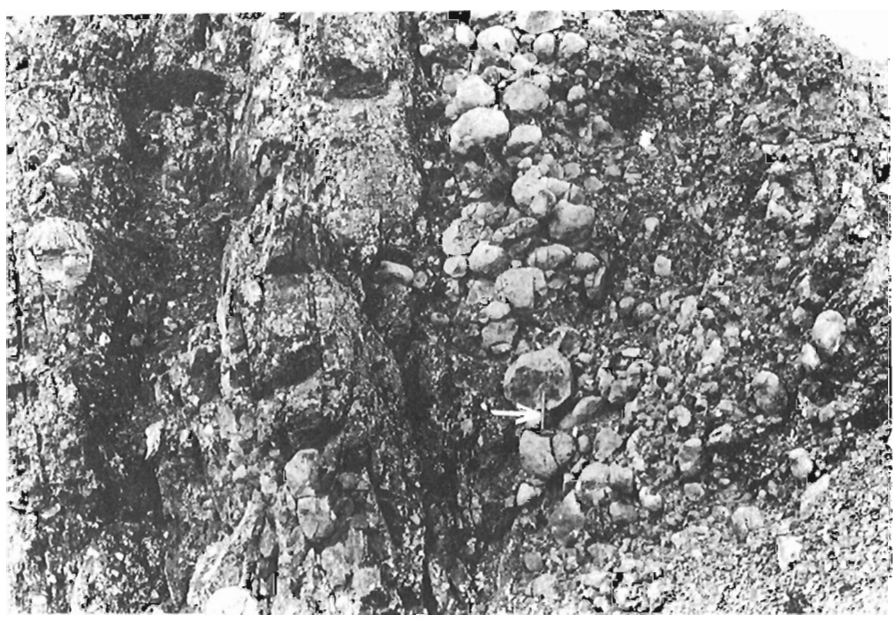

Figure 14.5

Vertical beds of conglomerate and greywacke a few kilometres east of Long Lake; tops are to the right. The large boulders (arrow points to hammer) in the right half of the picture and the few on the left are of the Upper Triassic reef limestone and this is an example of the coarse off-reef facies that can be found east of many of the reefs. In some beds limestone boulders predominate in a matrix of feldspathic quartz sand. Elsewhere limestone boulders are fewer and most clasts are of granitic and volcanic rocks.

Figure 14.6

This turbidite opposite the mouth of North Big Salmon River is typical of parts of the Laberge and Lewes River groups. Three incomplete Bouma sequences labelled BE, AE, ABE are shown. The pen (labelled) gives the scale. This turbidite represents some of the most outboard (i.e. northeastward) facies of Whitehorse Trough. Its age is unknown. It may be older, the same age as, or younger than the reefs.

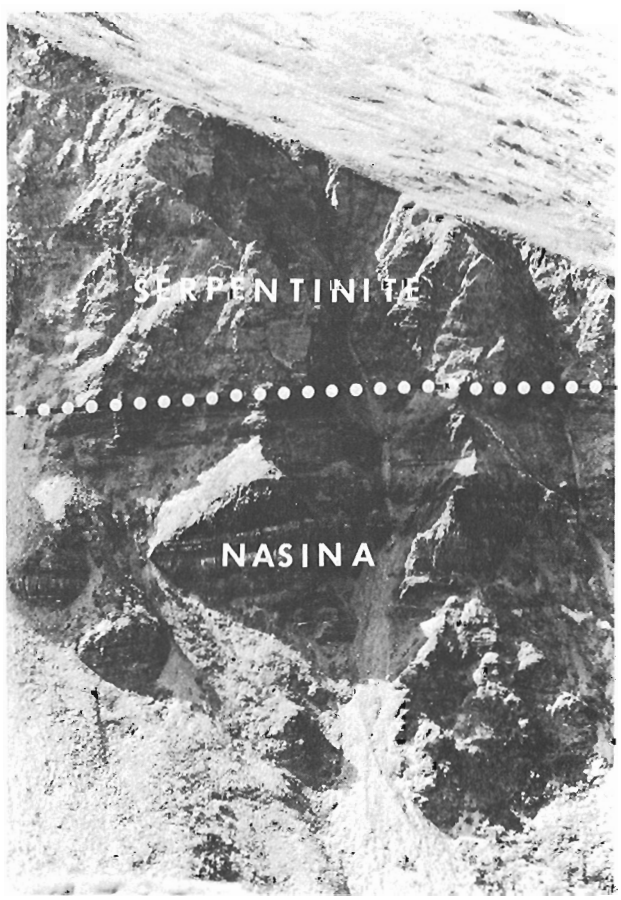

Figure 14.7

Serpentinized peridotite thrust above medium bedded, dark grey graphitic quartzite and graphitic black slate at the head of Teraktu Creek. The serpentinite is part of the Anvil allochthonous assemblage and is of late Paleozoic age. The quartzite is probably Silurian or Lower Devonian and an open marine facies (Nasina facies) of carbonate rocks on Pelly-Cassiar Platform.

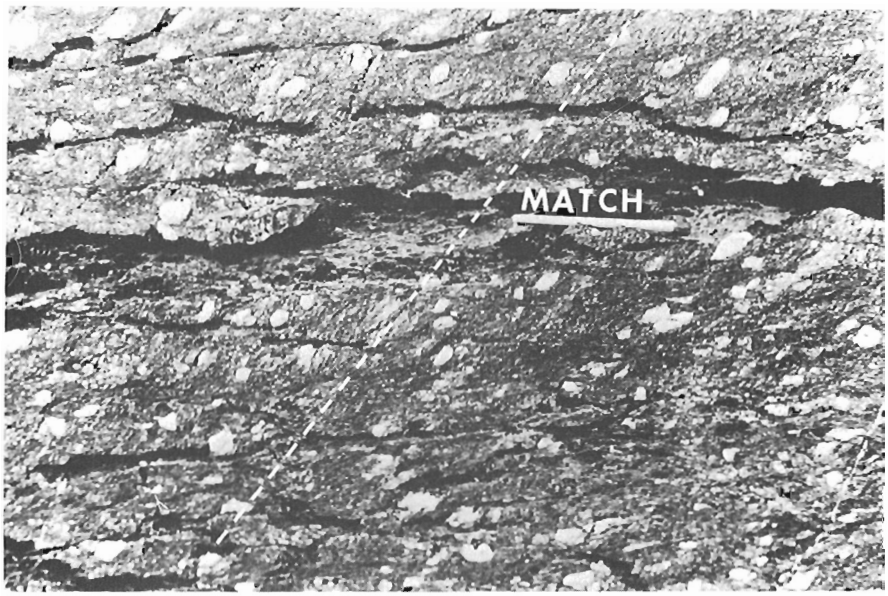

Figure 14.8

Augen blastomylonite 5 km east of Last Peak. This blastomylonite occurs in the zone locally as much as 5 km wide west of, and above, the Anvil allochthon which is itself thrust over the Nasina facies. It apparently marks the lower part of the highest and most southwestward allochthonous sheet in the Omineca Crystalline Belt. The Klondike Schist and related rocks are brought above the North American continental margin on this mylonite. Note that the blastomylonite fabric and the augen aligned with it are transposed by a new crenulation cleavage. In this photo the late crenulation cleavage is horizontal and the mylonite fabric slopes up to the right (its orientation is indicated by the dashed white line). The match gives the scale.

Practically there appears to be no clear boundary for distinguishing the Lewes River from the Laberge Group and in order to understand the relations between them it therefore seems realistic to map the individual conglomerate, sandstone, shale and limestone bodies by composition and texture. Only then can the Lewes River and Laberge groups be better defined.

Teslin Lineament

The Big Salmon River follows Teslin Lineament through much of Laberge map-area and because there is little outcrop in its valley the lineament is poorly exposed. Near Loon Lake and Fish Creek Teslin Lineament leaves the major valley and fair exposures are seen across it. There a moderately west dipping crenulation cleavage is developed in the Mesozoic rocks up to 3 km west of the lineament. This foliation increases in intensity toward the lineament and the rocks are metamorphosed to chlorite and locally biotite schist. Amphibolite and biotite gneiss similar to that found in much of Omineca Crystalline Belt abuts the lineament on the east. The foliation of these rocks also dips moderately to the west. The contact is sharp and well defined although the metamorphosed rocks on each side resemble each other. No structural mixing, whereby slices of one tectonic element are enclosed by rocks of the other, was noted. Teslin Lineament appears to be a west dipping fault that has brought the Intermontane Belt next to, and over the Omineca Crystalline Belt.

Metamorphic Rocks of Omineca Crystalline Belt

The metamorphic rocks of the Big Salmon Range (i.e. east of Teslin Lineament) can be readily subdivided as Bostock and Lees (1938) implied. The stratigraphic sequence and structural superposition are the same as seen in adjacent Quiet Lake map-area (Tempelman-Kluit, 1977). Metamorphosed rocks that are shelf-edge equivalents of Pelly-Cassiar Platform and which range from late Precambrian to Devonian, are overlain by ultramafic rocks presumably thrust above them (Fig. 14.7). Thrust above this sequence on a fault which dips steeply to the west is an assemblage of arkosic grit with associated intermediate to basic volcanic rocks (in part Klondike Schist). For the most part this upper allochthonous slice is now mylonite or blastomylonite (Fig. 14.8). The entire structural-stratigraphic sequence is metamorphosed and granitized, and the structually lowest slice has been most intensely affected. In places the quartz monzonite produced during this event has invaded its immediate cover. Especially intriguing is the western margin of the Quiet Lake batholith where a huge tongue or laccolith has invaded the mantling metamorphic rocks. Because the upper part of the tongue is eroded, granite now lies above its own metamorphic rocks on a gently dipping surface conformable with the foliation of the metamorphic rocks.

History of Whitehorse Trough

During the Late Triassic Whitehorse Trough was a back-arc basin in which the clastic debris from a volcanic arc that lay to the southwest accumulated. The southwestern margin of this basin was probably fault controlled. Near the southwestern edge of the basin debris collected in fans and river deltas whereas in deeper parts of the basin material was deposited as turbidite sheets. Early in the history of the basin volcanic detritus was the main debris supplied from the arc, but as it was eroded the clastic input contained progressively more granitic material. Karnian algae, corals and bivalves formed carbonate reefs in a wide belt along the southwestern margin of the basin, at about sea level. The reefs proliferated into the Norian and during their maximum development formed a discontinuous barrier behind which lay shallow lagoons fringed by sandy beaches. The reefs were individually killed by clastics that obliterated them; had it not been for this rapid input of debris a continuous barrier might have developed and survived.

During the Early Jurassic voluminous coarse debris, by now dominantly granitic, continued to be deposited in fans close to the southwestern margin of the basin, while in more central parts comparatively little material accumulated. About the early Middle Jurassic arkosic sand collected at the western and northern basin margin along and behind beaches but no sediment of this age is preserved in central parts of the basin. By the Late Jurassic or Early Cretaceous conglomerate interbedded with some shale and coal was deposited in restricted small basins or lakes across Whitehorse Trough. The chert and quartzite in this conglomerate can only have come from the northeast but not from the present Omineca Crystalline Belt. This mysterious source is now obliterated by the suture between Omineca Crystalline Belt and the Intermontane Belt. About the mid- or Late Cretaceous, Whitehorse Trough and the Omineca Crystalline Belt were juxtaposed.

Suggestions for Mineral Exploration

No new mineral occurrences were discovered, but three interesting exploration possibilities have been overlooked or ignored. Copper is known to be concentrated in carbonate reefs of the Whitehorse copper belt. Greg Morrison of the University of Western Ontario has recently studied these deposits and has suggested that their copper may have been concentrated in the reefs by fluids from the surrounding, arc-derived, high copper background clastic rocks. In his view the deposits do not owe their existence to the Coast Intrusions, which may have only metamorphosed the deposits and redistributed their metals. This interpretation implies that carbonate reefs elsewhere in Whitehorse Trough warrant exploration for concentrations of copper and that extensions of the copper belt should be sought not along the margin of the Coast Intrusions, but in the zone where reefs grew in Whitehorse Trough.

The carbonate reefs of Laberge map-area are locally bituminous particularly in the back-reef facies. These rocks and their flanking clastics offer possibilities as hosts for oil or gas concentrations if suitable reservoir and cap rocks can be found. This possibility appears to be untested.

Acid and intermediate volcanic and subvolcanic rocks of the Mount Nansen Group are host to several copper-molybdenum deposits in adjacent parts of Yukon (e.g. Casino, Mount Cockfield) and locally they enclose important gold-silver veins (e.g. Mount Nansen, Freegold Mountain). In Laberge map-area no mineral showings are known in these rocks, but as the Mount Nansen Group was not previously recognized in this map-area these targets have not been specifically explored.

References

Bostock, H.S. and Lees, E.J.
1938: Laberge map-area, Yukon; Geol. Surv. Can., Mem. 217.

Tempelman-Kluit, D.J.
1977: Quiet Lake and Finlayson Lake map-areas; Geol. Surv. Can., Open File 486.

Tozer, E.T.
1958: Stratigraphy of the Lewes River Group (Triassic), central Laberge area, Yukon Territory; Geol. Surv. Can., Bull. 43.

Wheeler, J.O.
1961: Whitehorse map-area, Yukon Territory; Geol. Surv. Can., Mem. 312.

15. NORTHEASTERN PART OF QUESNEL (93B) MAP-AREA, BRITISH COLUMBIA

Project 750035

H.W. Tipper
Regional and Economic Geology Division, Vancouver

Abstract

Tipper, H.W., Northeastern part of Quesnel (93B) map-area, British Columbia; Current Research, Part A, Geol. Surv. Can., Paper 78-1A. p. 67-68, 1978

The area is underlain mainly by Triassic to Jurassic volcanic and sedimentary rocks and by granitic rocks of Jurassic and Cretaceous age. Tertiary volcanic and sedimentary rocks underlie small areas. The region is transected by the Pinchi fault.

The published geological map of the Quesnel area (Tipper, 1959) is incomplete in the northeastern part. Additional work was carried out in this area in 1959 and in 1974. In response to many inquiries, the accompanying map and these brief notes are provided to fill this gap.

The oldest unit underlies a small area east of Dragon Lake and comprises shale, greywacke and limestone of Cambrian and (?) older age. This is a fault-bounded block, apparently exposed as a result of major movements along the extension of the Pinchi Fault. Fossils obtained from the limestone were identified by A.W. Norris as Lower Cambrian archaeocyathids.

The Cache Creek Group underlies an area of low relief in the southeastern part around Skelton Lake. The exposure is poor and stratigraphic relations are vague. Fossils from one locality were identified by C.A. Ross as **Boultonia** sp. and **Staffella**? sp. of Permian age (Leonardian to Wordian).

The lower part of the Quesnel River Group is separated from the older units by faults and stratigraphic relations are uncertain. In lithology it is similar to the Nicola Group of southern British Columbia and the Takla Group to the northwest. Fossils in the adjoining area to the east (Campbell, 1961) indicate a Late Triassic to Early Jurassic age.

The granodiorite and diorite pluton underlying Granite Mountain intrudes the Cache Creek Group and detritus from the pluton is included in Lower Jurassic (Pliensbachian) conglomerate on Dragon Mountain to the north. A radiometric age of 200 m.y. is reported (Sutherland Brown, 1973). The pluton near the east margin of the area is in part of similar lithology.

The upper part of the Quesnel River Group is entirely sedimentary. It is a mainly coarse clastic section on Dragon Mountain becoming dominantly shale along Quesnel River. The clasts of conglomerate include boulders from the Granite Mountain stock and pebbles and cobbles of the Cache Creek Group. Many fossil localities in this and adjoining areas were identified by Hans Frebold; **Amaltheus** sp., **Arieticeras** sp., and **Fuciniceras** sp. of Late Pliensbachian age. Near the summit of Dragon Mountain fragmentary remains of a marine reptile are associated with marine bivalves. In adjoining areas Early Pliensbachian, Toarcian?, and Bajocian faunas have also been found in the sedimentary unit.

The Cretaceous quartz monzonite and granodiorite pluton on the northeast side of Quesnel River is correlated with Cretaceous plutons to the southeast in Bonaparte Lake map-area (Campbell and Tipper, 1971) on the basis of similar lithology. In this area, rocks included in the unit intrude rocks as young as Pliensbachian. The small pluton in the north-central part (52°57'N Lat., 122°12'W Long.) is a coarse miarolitic quartz monzonite with large platy feldspar phenocrysts as much as 5 cm in diameter, unlike any plutons in this or adjoining areas. No radiometric ages are available on any of these plutons.

Along Victoria Creek a small area of Tertiary sediments is exposed. Age is thought to be mid-Tertiary but fossil evidence is lacking. West of these sediments, in a fault-bounded block, acid volcanics resemble mid-Tertiary volcanics of central British Columbia (Tipper, 1959).

Flat-lying olivine basalt similar to Late Miocene plateau lavas of central British Columbia lie unconformably on many older units. Their thickness is not great.

The area is heavily drift covered and was entirely glaciated by northerly to north-northwesterly moving ice. Along Quesnel River placer gold has been recovered from gravels probably derived from re-worked drift or from poorly consolidated late Tertiary gravels that have not been recognized as distinct from Quaternary deposits.

The area is intensely fractured and is transected by a major fault along Quesnel River and through Dragon Lake, possibly an extension of the Pinchi fault to the northwest (Armstrong, 1949; Tipper, 1961) and probably movement was transcurrent for the most part. All rocks older than the plateau lavas are cut by faults.

References

Armstrong, J.E.

1949: Fort St. James map-area, Cassiar and Coast Districts, British Columbia; Geol. Surv. Can., Mem. 252.

Campbell, R.B.

1961: Quesnel Lake, west half, British Columbia; Geol. Surv. Can., Map 3 - 1961.

Campbell, R.B. and Tipper H.W.

1971: Geology of Bonaparte Lake map-area; Geol. Surv. Can., Mem. 363.

Sutherland Brown, A.

1973: Gibraltar Mine in Geol. Exploration and Mining in British Columbia, 1973; B.C. Dep. Mines Pet. Resour.

Tipper, H.W.

1959: Quesnel, British Columbia; Geol. Surv. Can., Map 12-1959.

1961: Prince George, British Columbia; Geol. Surv. Can., Map 49-1960.

Figure 15.1 (over)

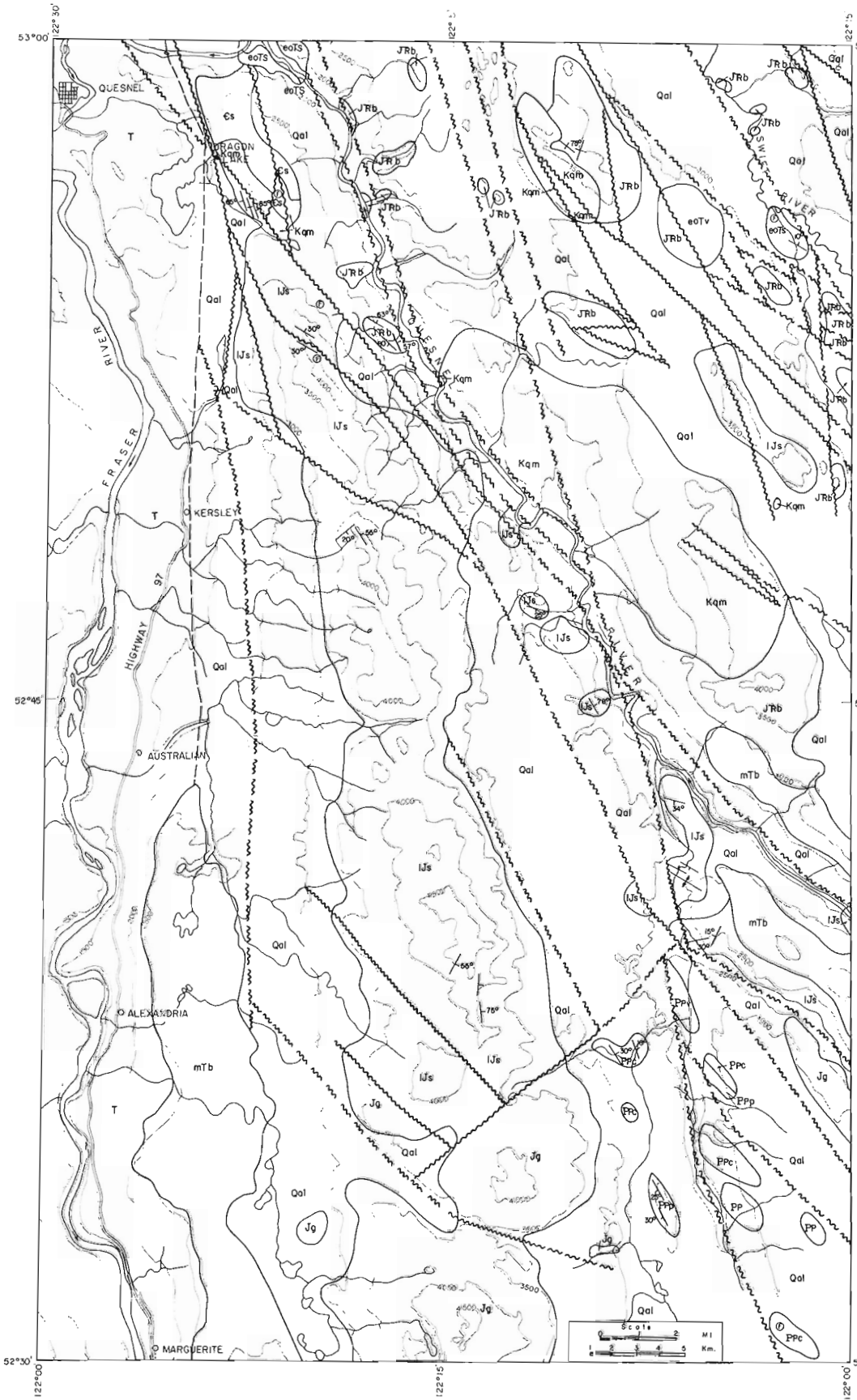

Figure 15.1

QUATERNARY
RECENT

Qal — alluvium, sand, silt, till

TERTIARY

T — undivided Tertiary sediments and volcanics (see G.S.C. map 12-1959)

mTb — olivine basalt flows, breccias, and tuffs; minor sediments at base

eoTv — dacite, rhyolite, andesite

eoTs — siltstone, sandstone

CRETACEOUS

Kqm — quartz monzonite, granodiorite

JURASSIC
LOWER AND (?) MIDDLE JURASSIC

IJs — QUESNEL RIVER GROUP (in part): shale, greywacke

JURASSIC AND/OR TRIASSIC

Jg — granodiorite, diorite

JURASSIC AND TRIASSIC

JTRb — QUESNEL RIVER GROUP (in part): augite porphyry basalt flows, breccia, and tuff; minor limestone shale, siltstone, greywacke

PENNSYLVANIAN AND PERMIAN

PPc — CACHE CREEK GROUP (in part): limestone

PPv — CACHE CREEK GROUP (In part): basic volcanics

PPp — CACHE CREEK GROUP (in part): shale and chert

CAMBRIAN AND (?) EARLIER

Cs — limestone, siltstone, greywacke

Fault (defined, approximate)

Geological contact (approximate)

Bedding (tops unknown) 25°

Fossil locality

16.

METAMORPHIC TERRANE, NORTHERN COAST MOUNTAINS WEST OF ATLIN LAKE, BRITISH COLUMBIA

Project 720041

L.J. Werner[1]
Regional and Economic Geology Division

Abstract

Werner, J.J., Metamorphic terrane, Northern Coast Mountains west of Atlin Lake, British Columbia; Current Research, Part A, Geol. Surv. Can., Paper 78-1A, p. 69-70, 1978.

Study of these metamorphic rocks has defined an upper-greenschist to lower-amphibolite grade metasedimentary and metavolcanic terrane of Paleozoic or earlier age. The rocks are isoclinally folded with general eastward vergence, and are in fault contact with fossiliferous Upper Triassic volcanic and sedimentary rocks to the east, bounded by Coast Intrusives to the west and south, and continue beyond the area studied to the north. Numerous granodiorite to quartz monzonite bodies intrude the metamorphic terrane, and near the eastern margin it is overlain by undeformed and unmetamorphosed Upper Triassic volcanic rocks. Relationships with these intrusive and volcanic rocks define a pre-Upper Triassic deformational and metamorphic event; preliminary geochronological studies indicate that this event is Permian or older.

This study was undertaken to determine lithology, structure, relationships and age of an extensive metamorphic terrane in the Coast Mountains west of Atlin, British Columbia. Mapping of the area, outlined in 1976 (Werner, 1977), was completed, and extended to west and south. The metamorphic rocks are in fault contact with fossiliferous Upper Triassic rocks to the east (Souther, 1971, p. 23), are bounded by Coast Intrusives to west and south, and were not mapped beyond Wann River to the north, although similar metamorphic rocks extend for 100 km to the northwest at least as far as Tutshi Lake (Christie, 1957).

Lithologies within the terrane include quartz-feldspar-muscovite to quartz-biotite schist (50 per cent of total area), marble (25 per cent), quartz-feldspar-hornblende gneiss (20 per cent) and hornblende amphibolite (Fig. 16.1). The easternmost area, east of Llewellyn Glacier, consists of slightly lower-grade quartz-chlorite-actinolite schist. The schists are consistently quartz-rich (commonly 60-70 per cent quartz) and locally retain the appearance of banded siltstones. Mafic minerals are uncommon and the general composition and appearance suggests that the schists are derived from quartz-rich marine sediments, mainly siltstones and fine grained sandstones. Interlayered with the schists are marble bands of varying thicknesses, from a few metres to as much as 150 m. The marbles vary from sparry, fetid coarsely crystalline calcite to layered, diopside-rich metadolomite. This variation is generally between beds, but some variation along strike of individual beds was seen, particularly near the toe of Willison Glacier. The marbles are derived from marine limestone and impure dolomite, which in at least one area, shows rapid variation in thickness along strike that cannot be accounted for by structural deformation and is probably original. In general the percentage of carbonate in the terrane diminishes east and west of a central, carbonate-rich band.

Gneissic rocks are found in some places close to intrusives, possibly as equivalents of the quartz-muscovite and quartz-biotite schists. Gneisses persist for little more than a few hundred metres from intrusive bodies, but the abundance of small stocks within the area accounts for the total percentage of gneiss.

Amphibolitic rocks occur as bands of hornblende-biotite amphibolite or hornblendite one to ten metres thick. They are interlayered with metasediments, commonly adjacent to carbonates, and are possibly derived from volcanics.

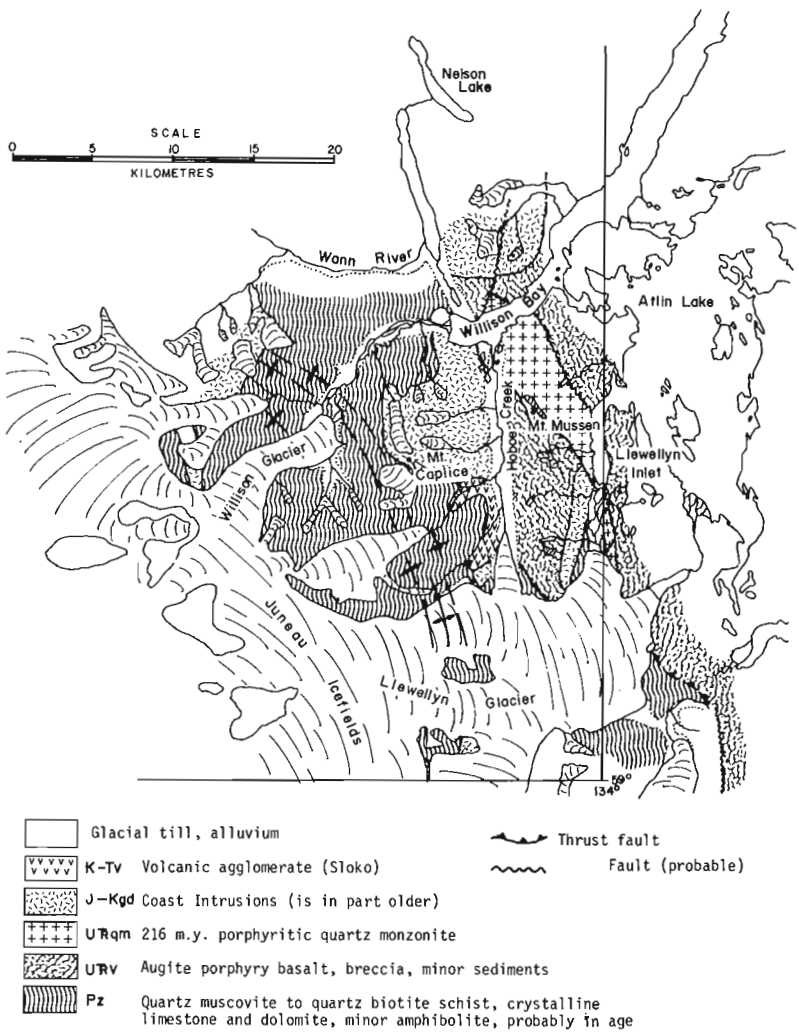

Figure 16.1 Generalized geology of metamorphic terrane, southwest of Atlin, B.C.

[1] Department of Geological Sciences, University of British Columbia.

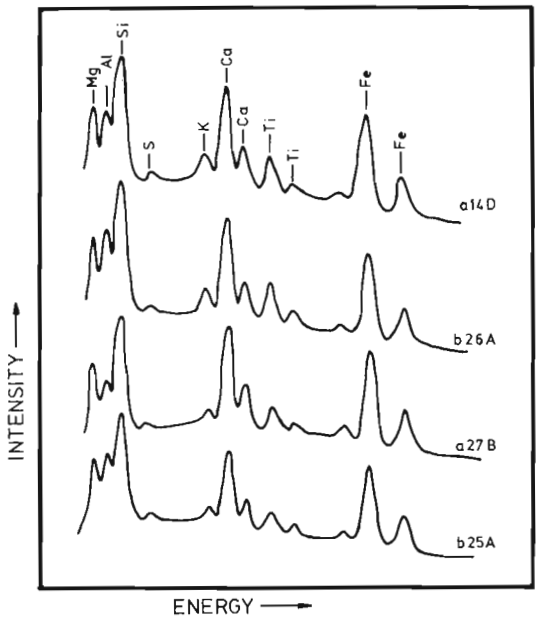

a14D, – Upper Triassic volcanics, dated with fossils, Torres Channel;
b26A, – float from outwash of Willison Glacier;
a27B, – pre-216 m.y. volcanics south of Mount Mussen.
b25A, – dyke intruding metasediments near Willison Glacier;

Figure 16.2. Relative intensity of X-ray spectrum from scanning electron microscope for four pyroxenes. Individual scans are vertically superimposed for comparison. Relative intensities of peaks indicate a similar composition for all four samples. The presence of aluminum and potassium due to feldspars, and sulphur reflects high pyrite content.

With the exception of some coarsely crystalline carbonates all metamorphic rocks show distinct compositional layering and well-developed foliation. The layering and foliation are always parallel, and everywhere tightly folded by northwest-southeast trending isoclinal folds with variable, gently plunging axes. Axial planes are nearly always west-dipping, and minor overthrusting to the northeast has occurred in places. Smooth, isoclinal folds are refolded by smaller scale wrinkles that are coaxial with the smooth folds; this suggests that there was progressive deformation with retrograde metamorphism. In some areas, in particular around the Mount Caplice intrusive body, there are also north to northeast trending minor folds. In general, the deformational style of the area is remarkably similar to that reported for similar rocks west of the Coast Intrusives (Forbes, 1959) but with an opposite direction of vergence.

Metamorphic grade is relatively constant in rocks north of Llewellyn Glacier. Wollastonite is generally developed in carbonate rocks, and garnet is locally common in quartz-muscovite schists around intrusive bodies. A garnet isograd can be defined around larger intrusives, but the pattern is complex because of the variation in composition of the host rocks and interference by folding and smaller intrusives. East of the toe of the Llewellyn Glacier, lower grade quartz-chlorite-actinolite schists may reflect their greater distance from the Coast Intrusives.

The metamorphic terrane appears to be pre-Late Triassic in age. The ridge extending south from Mount Mussen consists of green to purple augite porphyry breccia and basalt, lithologically similar to Upper Triassic volcanics farther east. The Mount Mussen volcanics are unfoliated except for thin bands along northwest-trending shear zones. Near Mount Mussen they are intruded by porphyritic granodiorite that has given an age of 216 m.y. (T.E. Bultman, pers. comm.). The volcanics are separated from metamorphic

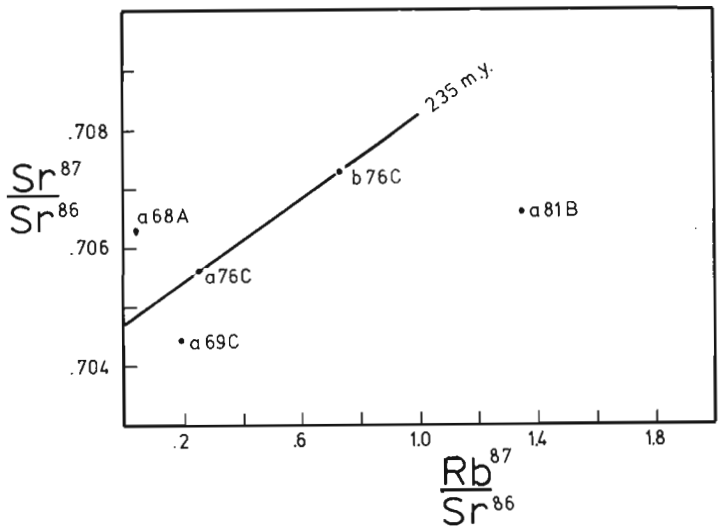

Figure 16.3 Whole-rock isotopic ratios for 5 samples from the metamorphic terrane west of Atlin. a69C-biotite-hornblende amphibolite; a68A-aplite dyke; a81B-quartz monzonite.

rocks on the southwest end of the ridge by a shear zone. On the east side of the ridge a hornblende diorite intrusive separates the Mount Mussen volcanics from metamorphic rocks. As the metamorphic terrane surrounds the volcanics on three sides, there may well be an unconformity between the two, although this cannot be proven. A similar relationship is found between probable Triassic volcanics and the metamorphic terrane, 12 km to the southwest on a nunatak in Llewellyn Glacier. Near the toe of Willison Glacier an undeformed, unmetamorphosed, augite porphyry basalt dyke intrudes the metamorphic terrane. Semiquantitative, energy dispersive electron microscope scanning indicated that the composition of augite phenocrysts in both the volcanic rocks and the dyke is very similar (Fig. 16.2). Preliminary isotopic dating by the writer has indicated that the metamorphic terrane may well be much older than Triassic. Two comagmatic phases of a granodiorite intrusion that cuts the metamorphic terrane 1 km northwest of Mount Caplice give an indicated Rb/Sr age of 235 m.y. (Fig. 16.3). A high $^{87}Sr\ ^{86}Sr$ ratio from one metamorphic sample is suggestive that the terrane is considerably older than the intrusion.

References

Aitken, J.D.

1959: Geology of Atlin map-area; Geol. Surv. Can., Mem. 307.

Christie, R.L.

1957: Geology of Bennett map-area; Geol. Surv. Can., Map 19-1957.

Forbes, R.B.

1959: The bedrock geology and petrology of the Juneau icefields area, S.E. Alaska; unpubl. Ph.D. thesis, Univ. of Washington.

Souther, J.G.

1971: Geology and mineral deposits of Tulsequah map-area, British Columbia; Geol. Surv. Can., Mem 362.

Werner, L.J.

1977: Metamorphic Terrane, northern Coast Mountains west of Atlin Lake, British Columbia; in Report of Activities, Pt. A, Geol. Surv. Can., Paper 77-1A, p. 267-269.

17. EASTERN MARGIN OF THE COAST PLUTONIC COMPLEX IN WHITESAIL LAKE MAP-AREA, BRITISH COLUMBIA

Project 770020

G.J. Woodsworth
Regional and Economic Geology Division, Vancouver

Abstract

Woodsworth, G.J., Eastern margin of the Coast Plutonic Complex in Whitesail Lake map-area, British Columbia; Current Research, Part A, Geol. Surv. Can., Paper 78-1A, p. 71-75, 1978.

Remapping began in 1977. Pre-Lower Jurassic volcanic and sedimentary strata near the east margin of the Coast Plutonic Complex have been penetratively deformed and metamorphosed to greenschist facies sometime between the Early Permian and Late Triassic. The high-grade Central Gneiss Complex may in part be correlative with these strata. The Early Jurassic and younger Hazelton Group has not been penetratively deformed on a large scale, has not been regionally metamorphosed, and is bounded on the west by a major high-angle fault.

Introduction

Remapping of Whitesail Lake (93E) map-area began during the 1977 field season. The project will focus on the structural and stratigraphic relations between the Coast Plutonic Complex and the flanking Intermontane Belt, on revision of the stratigraphy in light of recent work by Tipper and Richards (1976) to the north, and on correlation of the plutonic and metamorphic rocks of the area with units defined during the Coast Mountains Project to the west and south.

Previous mapping by Duffell (1959), Stuart (1960), Read unpubl. rep., 1963 and MacIntyre (1976) provides an excellent base for the present work. During the 1977 field season Woodsworth re-examined critical areas studied by Stuart (1960) and began subdivision of Duffell's (1959) Unit A along the east flank of the Coast Plutonic Complex. T.A. Richards spent several days examining Mesozoic strata just east of the Coast Plutonic Complex.

I thank S.J. Hills for excellent field assistance, Dave Newman and the staff of Okanagan Helicopters at Terrace for outstanding service, Y. Nishimura of Transwest Helicopters for excellent flying, and the people of Kemano, especially Doug Groves and Mrs. Jenny Gipps, for help in many ways.

Stratified Rocks

Central Gneiss Complex

The southwest part of the map-area (Fig. 17.2) is underlain by a broad belt of gneiss, migmatite and related plutonic rock that extends into Douglas Channel map-area to the west (Roddick, 1970). Banded hornblende-biotite gneiss, gneissic quartz diorite, migmatite and irregularly layered gneiss are the dominant lithologies. Bodies of relatively homogeneous plutonic rocks, not separated on Figure 17.2, in places grade into the gneiss and in other places cross-cut it. The Central Gneiss Complex was undoubtedly derived from sedimentary and volcanic strata that are probably, as is discussed below, pre-Jurassic in age.

Gamsby group[1]

The existence of Paleozoic strata in Whitesail Lake map-area was first established by Read (unpubl. rep., 1963) who collected Carboniferous or Permian fossils from a small area of limestone about 8 km southeast of Sandifer Lake. Details of these collections are given in Roddick (1970, p. 13). During the present work it was recognized that pre-Lower Jurassic (mostly Permian and older?) strata are much more widespread in the map-area than had previously been thought. These rocks, here informally called the Gamsby group, form a northwest-trending belt northeast of the Central Gneiss Complex.

The Gamsby group consists mainly of felsic and mafic tuffs and volcanogenic sandstone with lesser carbonate, argillite, and conglomerate. The most distinctive rocks are laminated mafic tuffs that alternate with laminated white-weathering rhyolitic tuffs and ignimbrites(?) (Figs. 17.1, 17.3). One or more members of dark grey argillaceous limestone locally grade into white, massive limestone. Intraformational conglomerate, breccia, and volcanic lenses are common in the limestone. Probable correlatives of at least part of the Gamsby group include the Lower Permian Asitka Group in McConnell Creek map-area, and upper Paleozoic rocks near Terrace, about 125 km northwest of Whitesail Lake map-area (Monger, 1977).

Hazelton Group

Strata correlated with the Hazelton Group are restricted to the eastern part of the area shown in Figure 17.2. The term "Hazelton Group" is used here in a general, rock-stratigraphic sense for strata lithologically

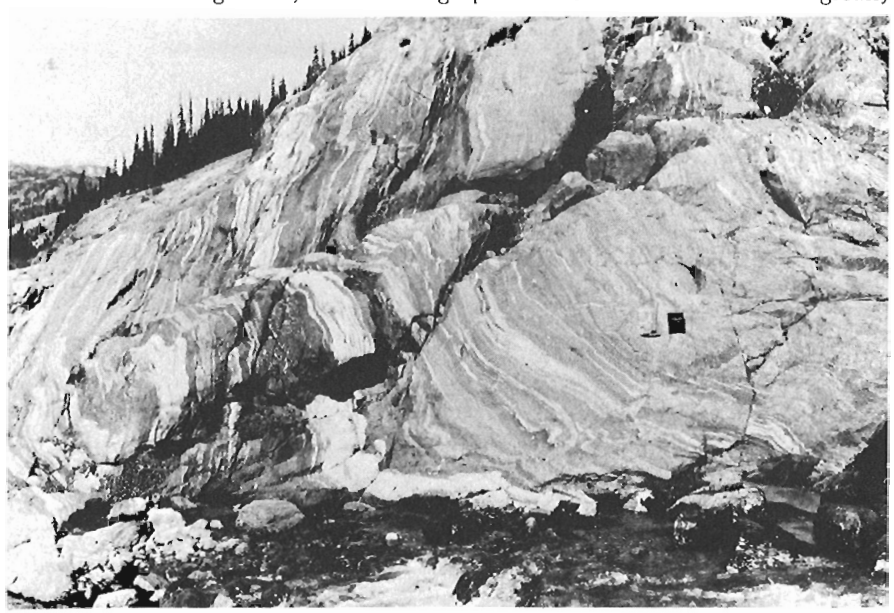

Figure 17.1. Typical strata of the Gamsby group: folded rhyolitic (white) and mafic tuffs about 8 km south-southeast of Sandifer Lake.

[1] Informal term.

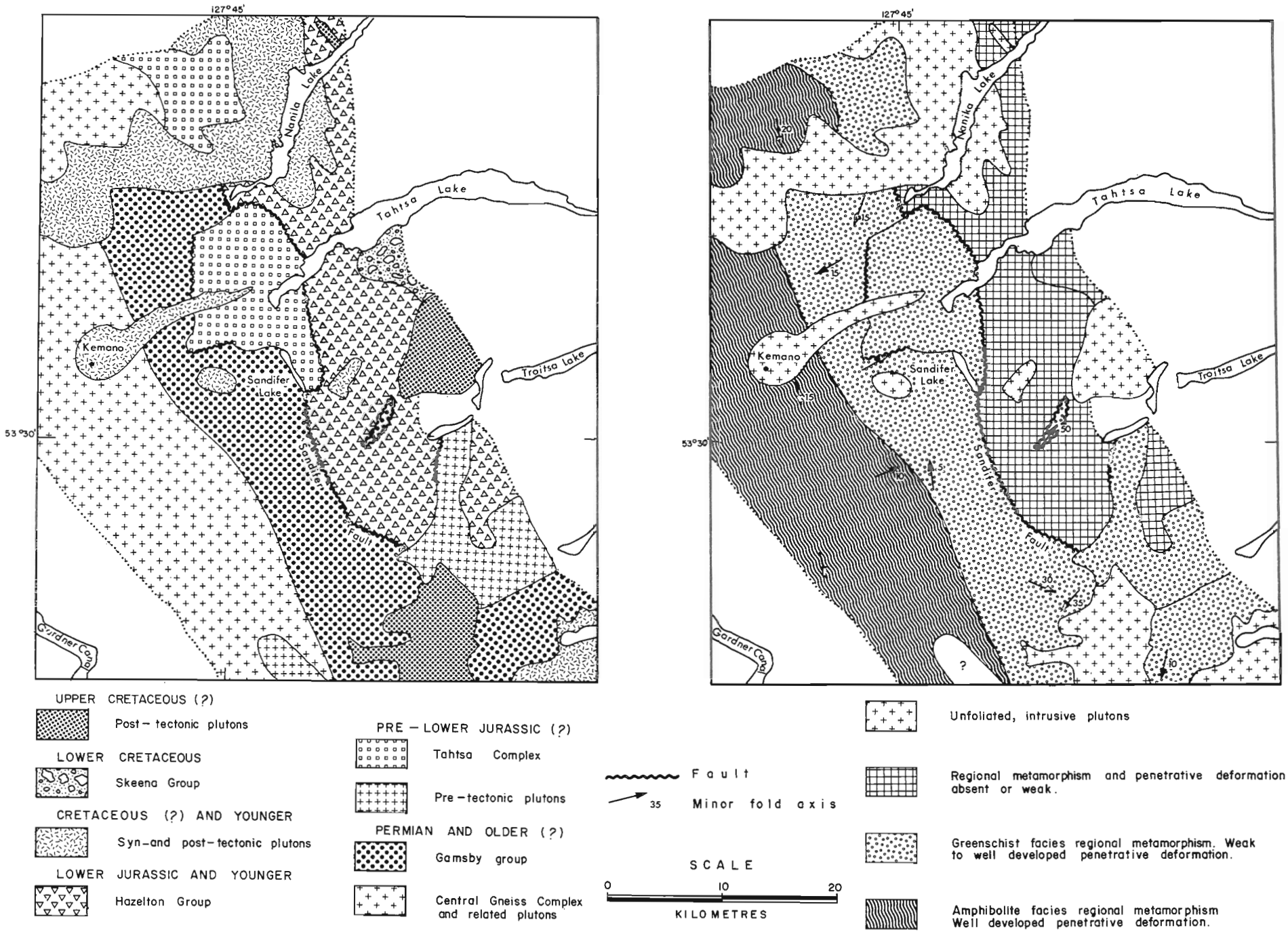

Figure 17.2. Sketch maps of geology (upper) and metamorphism (lower) in part of Whitesail Lake map-area.

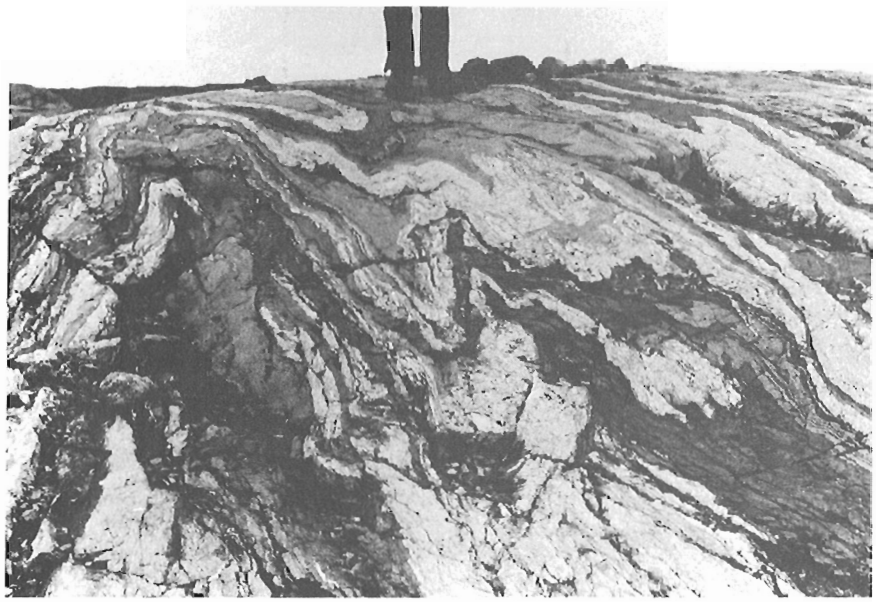

Figure 17.3.

Folded rhyolite and volcanogenic sandstone of Gamsby group 15 km northeast of Kemano.

Figure 17.4.

Near-horizontal roof (dashed line across middle of photo) of a miarolitic quartz monzonite pluton. The grey strata above the stock are Gamsby group. View to north from ridge 7.5 km northeast of Black Dome.

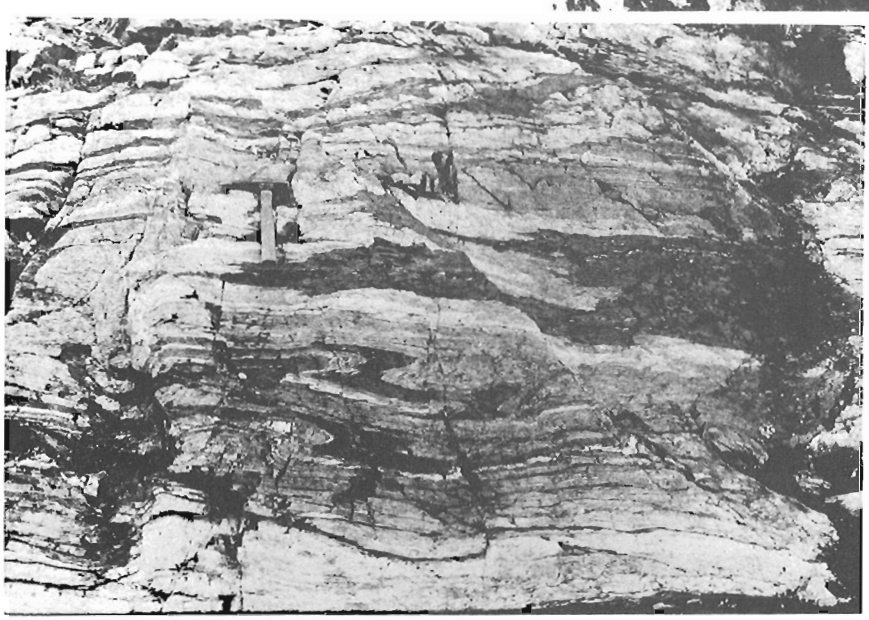

Figure 17.5.

Folded rhyolite and greenstone of Gamsby group 15 km northeast of Kemano.

similar to those described by Tipper and Richards (1976) in areas to the north. Because no fossils were found in this assemblage, rocks as old as Early Triassic and as young as Early Cretaceous may be included in the Hazelton Group shown on Figure 17.2.

Where examined, the Hazelton Group consists predominantly of rhyolitic to basaltic fragmental volcanic rocks, mainly lapilli tuff, tuff-breccia, and aquagene tuff. Greywacke, siltstone, immature sandstone and conglomerate are common in some areas. Fluvial conglomerate containing rare granitoid clasts outcrops 3 km southeast and 5 km south-southeast of the south end of Sandifer Lake. About 4 km southeast of Sandifer Lake a distinctive polymict conglomerate contains undeformed and unmetamorphosed volcanic clasts derived from the Hazelton Group and some phyllitic rhyolite and folded limestone clasts presumably derived from underlying Gamsby group strata. The matrix of the conglomerate is mainly red mudstone with rare mudcracks; the rock has a pronounced reddish colour. This conglomerate is similar to a polymict conglomerate forming the base of the Hazelton Group in other areas (Monger, 1977).

Skeena Group

Lower Cretaceous sandstone and shale south of Tahtsa Lake were not examined by the writer but are described by MacIntyre (1976) and Duffell (1959).

Tahtsa complex

Stuart (1960, p. 10) defined the Tahtsa complex as "an igneous complex of hornblende diorite and quartz diorite cut by quartz monzonite stocks, granodiorite dykes, and basic dykes". Re-examination of the type areas near the west end of Tahtsa Lake indicate that the complex may be interpreted better as a dioritized volcanic unit similar to many basic complexes found in the Coast Plutonic Complex. The complex consists largely of greenstone and lesser felsic rock (meta-rhyolite?). The greenstone has been feldspathized and dioritized to varying degrees and is cut by several generations of mafic and felsic dykes, many of which are also recrystallized and feldspathized. The entire complex, except for the youngest dykes, is cut by numerous shears and fractures that have been healed by epidote.

Greenschist-facies metamorphism has obliterated most primary sedimentary and volcanic structures. In places, the less dioritized parts of the complex resemble strata of the Gamsby group; in other places the Gamsby group seems to grade into the Tahtsa complex by increasing dioritization. It is tentatively suggested that the Tahtsa complex is, at least in part, correlative with the Gamsby group; in any event, a pre-Jurassic age is probable.

Plutonic Rocks

Plutonic rocks of many ages and varieties are exposed in the map-area. Probably the youngest are three stocks of miarolitic granite to granodiorite west and south-southwest of Troitsa Lake and north of Nanika Lake. These are high-level, unfoliated and slightly porphyritic plutons that cross-cut all other units and structures in the area. The gentle outward dips of the contacts of the southern of these bodies indicate that the stock is just beginning to be unroofed (Fig. 17.4). Numerous unfoliated to weakly foliated plutons are not miarolitic, are equigranular, and appear emplaced at greater depths than the miarolitic rocks. Most of these plutons are undeformed and unmetamorphosed and may have been emplaced during the Cretaceous and Tertiary.

An irregular body of pre-tectonic quartz diorite is exposed southeast of Troitsa Lake. The quartz diorite is cut by swarms of mafic dykes; plutonic rock and dykes have been sheared, fractured, and metamorphosed to greenschist facies.

Figure 17.6. Irregularly-layered gneiss of Central Gneiss Complex 17 km southeast of Kemano. Note similarity in layering and deformation between this and Gamsby group of Figure 17.5.

Structure, Metamorphism, and Age Relations

Pre-Jurassic deformation and metamorphism

The Gamsby group and the Hazelton Group show major differences in metamorphic and structural styles. The gross structure of the Gamsby group south of Sandifer Lake is approximately a gently dipping homocline, complicated perhaps by later thrusting (Fig. 17.4). Tight folds up to several metres in amplitude are superposed on this homocline; fold axes generally have gentle plunges (Fig. 17.2). A moderate schistosity, axial planar in some outcrops, is commonly present in the Gamsby group, particularly in the more mafic strata. Regional metamorphism to greenschist facies accompanied the penetrative deformation. In some localities metamorphic minerals such as actinolite have grown parallel with the axes of minor folds. Strata of the Hazelton Group have been neither penetratively deformed nor regionally metamorphosed, although a slight schistosity is commonly developed near shear zones. Clasts of folded and metamorphosed strata derived from the Gamsby group are found in the unmetamorphosed Hazelton polymict breccia, indicating that a major metamorphic and deformational event affected that area sometime between the Early Permian and Late Triassic.

The Tahtsa complex has also been metamorphosed to greenschist facies but recognizable minor folds are rare. Stuart (1960) thought that the Tahtsa complex was the basement on which the "Hazelton" rocks (Gamsby plus Hazelton) were deposited. Re-examination of all of Stuart's unconformities indicates that most are fault contacts and that none are unconformable.

The structural relations between the Gamsby group and the Central Gneiss Complex are not understood. Layering in the Central Gneiss Complex dips gently and is roughly parallel with bedding in the Gamsby group. In some places the Gamsby group seems to grade by increasing metamorphism into Central Gneiss Complex (Figs. 17.5, 17.6); in other places the contact may be a fault. Minor fold styles are much the same in both units, suggesting that strata forming the Central Gneiss Complex were involved in the folding event that affected the Gamsby group. If so, then the Central Gneiss Complex in this area contains no Hazelton or younger strata.

Western limit of the Hazelton Group

A major tectonic break, the Sandifer fault, forms the western limit of the Hazelton Group in the map-area. This break is a steep, west-dipping reverse fault that juxtaposes unmetamorphosed Hazelton strata against metamorphosed Gamsby rocks. The latest movement on this fault was probably pre-Late Cretaceous, as the extension of the fault south of the area shown in Figure 17.2 is cut by a high-level Upper Cretaceous(?) stock. Presumably the Hazelton Group once extended west across the fault into the area now occupied by the Coast Plutonic Complex but has been removed by uplift and erosion.

References

Duffell, S.
1959: Whitesail Lake map-area, British Columbia; Geol. Surv. Can., Mem. 299, 119 p.

MacIntyre, D.G.
1976: Evolution of Upper Cretaceous volcanic and plutonic centers and associated porphyry copper occurrences, Tahtsa Lake area,British Columbia; unpubl. Ph.D. Dissertation, Univ. Western Ontario, 149 p.

Monger, J.W.H.
1977: Upper Paleozoic rocks of northwestern British Columbia; in Report of Activities, Part A, Geol. Surv. Can., Paper 77-1A, p. 255-262.

Roddick, J.A.
1970: Douglas Channel-Hecate Strait map-area, British Columbia; Geol. Surv. Can., Paper 70-41, 56 p.

Stuart, R.A.
1960: Geology of the Kemano-Tahtsa area; B.C. Dep. Mines Pet. Resour., Bull. 42, 52 p.

Tipper, H.W. and Richards, T.A.
1967: Jurassic stratigraphy and history of north-central British Columbia; Geol. Surv. Can., Bull. 270, 73 p.

18. REGIONAL GEOLOGIC SETTING OF LEAD-ZINC DEPOSITS IN SELWYN BASIN, YUKON

Project 730069

S.L. Blusson
Regional and Economic Geology Division, Vancouver

Abstract

Blusson, S.L., Regional geologic setting of lead-zinc deposits in Selwyn Basin Yukon; Current Research, Part A, Geol. Surv. Can., Paper 78-1A, p. 77-80, 1978.

Further observations within the Mayo-Nadaleen River area suggest the possibility that the Keno Hill assemblage is Paleozoic not Mesozoic in age and all major silver-lead deposits in North Selwyn Basin are related to graphitic shales of general Canol Formation equivalent. Newly found shale-hosted zinc, lead, silver mineralization in Frances Lake area appears to be stratigraphically correlative and of similar type to large bedded deposits at Howard's Pass.

East Rackla River – Nadaleen River Area

During a brief visit to the recently discovered silver-lead-zinc deposits in the Rackla River area an attempt was made to refine the regional mapping within this and the immediately adjacent parts of Mayo and Nash Creek map-areas, in order to outline geologic controls to mineralization. Two principal findings indicate that not only is geologic refinement needed but possibly major age revision as well.

1. The newly discovered mineralization and related strata (Canol Formation) has marked similarities to that of the Keno Hill district
2. A thick section of Canol- and Imperial-like strata is traceable into, respectively, the "Lower Schist" and "Keno Hill Quartzite".

It seems possible that the enigmatic Keno Hill assemblage is of late Paleozoic age and that all the known high silver-lead deposits in Selwyn Basin may relate to the Canol Formation as the possible source rock. Included with the Canol Formation are the silver-bearing Pb-Zn deposits of MacMillan Pass, the very rich deposits of the Rogue River area (Plata, Inca) and the new finds at Rackla River.

Fossiliferous shale, limestone and quartzite of Triassic age, limited to a local area south of Kathleen Lakes, are no longer considered part of the Keno Hill section, although the relationship of the two sequences is still uncertain. The Mesozoic age assigned by Tempelman-Kluit (1970) to Keno Hill strata in Tombstone area depends on an apparent normal succession of "Lower Schist" (unit 11) over Triassic rocks (Unit 10), but another thrust fault (in an area of repeated thrusting) would reverse that relationship. The author believes that lithologically and structurally the Keno Hill section has more in common with the late Paleozoic than with the Mesozoic clastic sequences of northern Yukon and Alaska. Unlike the Keno Hill strata, the thick, post-Triassic piles of clastic rock occupy discontinuous successor basins and are nowhere intensely deformed and regionally metamorphosed. Nor are they intruded by diabase sills, a feature so characteristic of Keno and Tombstone areas and never adequately explained. The Mississippian or Permian Rampart Group (Mertie, 1937); Brosgé et al., (1969) and underlying beds of central Alaska, with their profusion of diabase sills and flows, and offset on Tintina fault some 500 km from Tombstone area, is considered the most likely Alaskan correlative of the Keno Hill assemblage.

Geologic Setting of Mineralization

Lead, zinc, silver mineralization found in several localities during 1976 was extensively explored by a number of companies with encouraging results. For the most part, mineralization occupies porous zones within a distinctive competent dolomite member ("Zebra dolomite") of the Proterozoic "Grit unit" where this succession is overthrust on dark shale and chert of the Road River and Canol formations. Similar silver-rich deposits, principally steely galena and quartz, are found locally within a geochemically-high silver zone of the Canol Formation in particular where cut by the thrust fault. The Canol Formation therefore appears to be a likely source of the metals – metals mobilized and emplaced in openings during or after thrusting. Based on intensive geochemical work a similar origin; i.e. that metals migrated from graphitic zones in the "Lower Schist", was proposed by Boyle (1965) for the rich silver veins of Keno Hill. Further enrichment of silver to values unique to the Keno district is attributed to supergene processes.

The "Grit unit" (Fig. 18.1) is overlain unconformably to the south by a thick sequence with black, pyritic, gossan-producing shales near the base grading up through shale and siltstone to predominately thin bedded siltstone and fine grained quartzite. This sequence, as much as 1500 m thick, contains numerous diabase sills and with increasing crystallization grades to the west into the "Lower Schist" and Keno Hill Quartzite. To the east and southeast this succession can be followed for many miles and although not continuously traceable is on trend with similar rocks of the Canol and Imperial formations in the MacMillan Pass area. North of Stewart River the Ordovician-Silurian Road River Formation, characterized by basinal chert, is progressively cut out below the thick clastic succession.

Whether or not the black shales above the "Grit unit" and the Canol Formation overthrust by the "Grit unit" are correlative, as proposed, it is clear that both are widespread and warrant careful prospecting particularly where high metal zones are in fault contact with competent rocks.

Frances Lake Area

Shale-hosted stratiform lead-zinc mineralization has recently been found within unit 10 of central Frances Lake map-area (Blusson, 1966). The area is mostly tree-covered and the geology is poorly known, but in view of the regional setting on the flank of Selwyn Basin, local stratigraphy, and mode of occurrence, this find must be considered significant, most readily comparable to mineralization at Howard's Pass.

Figure 18.2 showing part of central Frances Lake area, is a mainly speculative map, that fits the few known outcrops. Even though contacts are mostly inferred, except near the newly found mineralization at A, the map is useful in outlining the general succession and distribution of units and providing an exploration guide. In the area between Anderson Creek and Thomas River an attempt is made to illustrate the general structural style – close folding, mainly overturned to the south. The extensive area mapped as unit 2 south of Anderson Creek is predominately wavy banded limestone and shaly equivalents of late Cambrian-early Ordovician age but probably contains some infolded black shale of unit 3 especially in Anderson Valley. Northwest of Thomas River unit 3 probably includes the upper chert section and west of Tillei Lake it probably contains minor amounts of units 5 and 6.

Legend

uK | 6 — Black shale, limestone, quartzite

? uD-P | 5 — "Lower Schist" and "Keno Hill Quartzite": Black slate, phyllite, siltstone, quartzite; diabase sills

uD-M | 4 — Black pyritic shale, chert wacke and conglomerate, bedded barite

O-D | 2/3 — 2. Light grey dolomite. 3. Road River Formation: black shale and chert

H I | 1 — "Grit" Unit: varicoloured slate, feldspathic quartzite and conglomerate, micritic limestone. 1 a, vuggy dolomite 1 b, faulted and altered basic volcanics, zones of ankerite, serpentine and non-bedded chert.

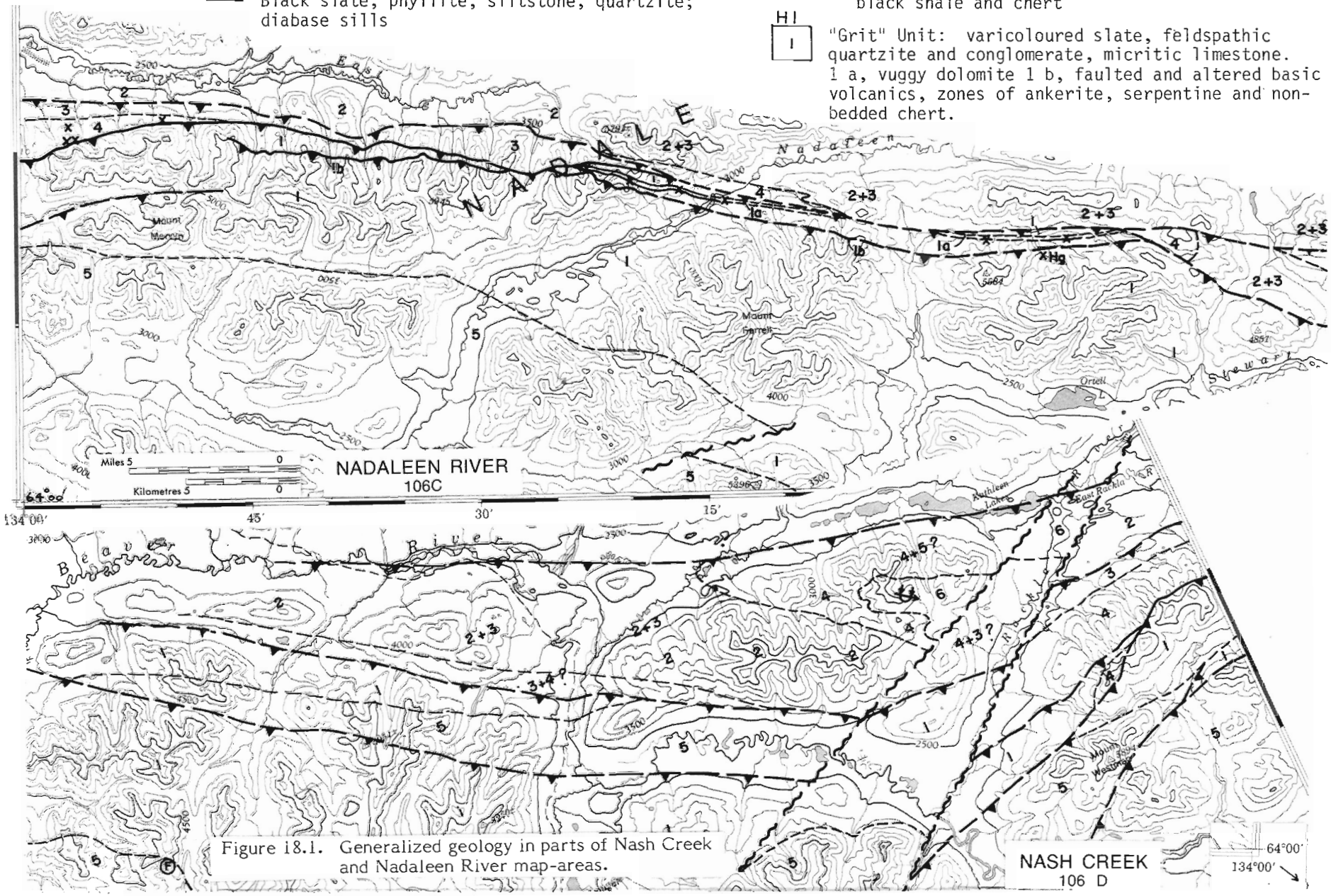

Figure 18.1. Generalized geology in parts of Nash Creek and Nadaleen River map-areas.

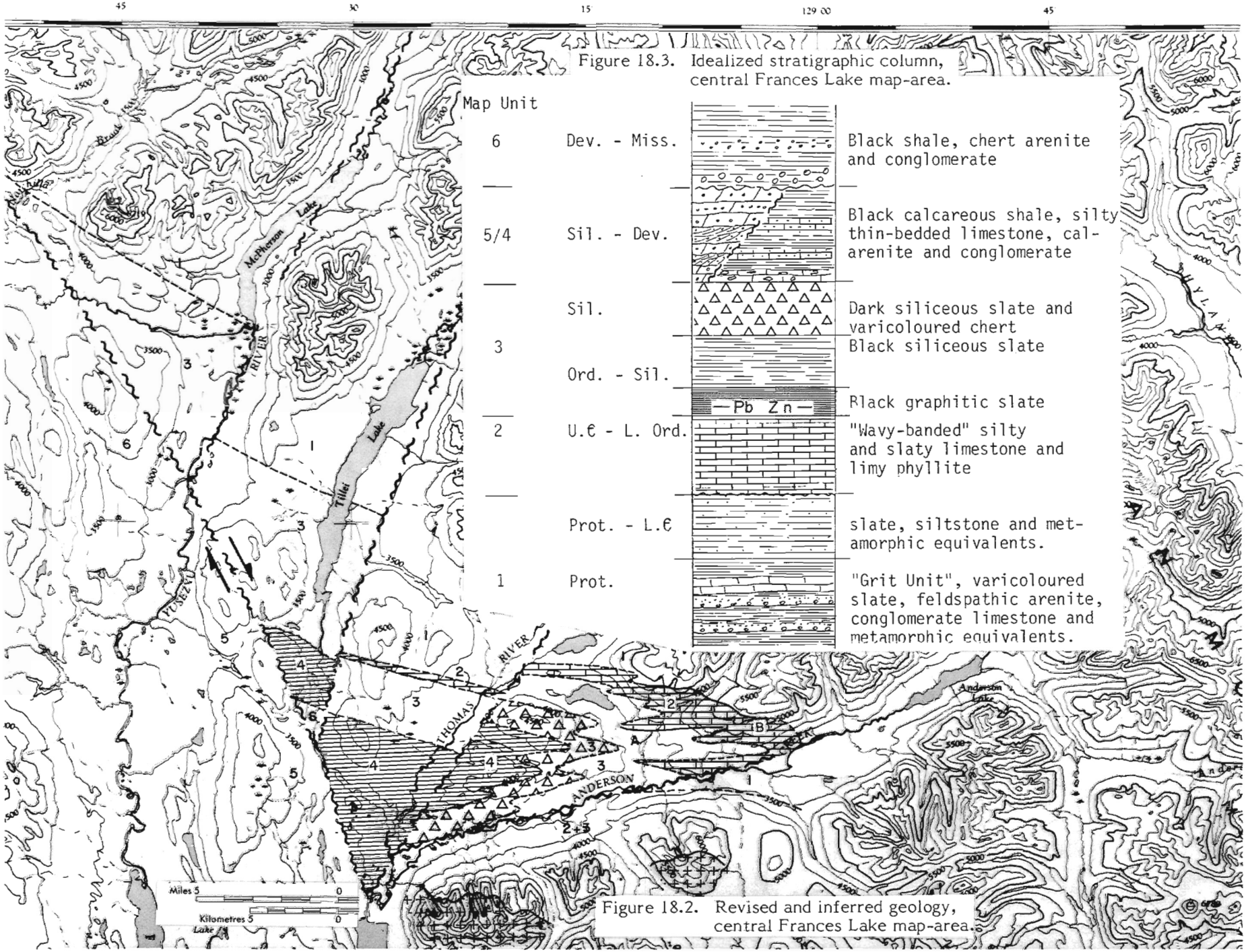

Figure 18.3. Idealized stratigraphic column, central Frances Lake map-area.

Figure 18.2. Revised and inferred geology, central Frances Lake map-area.

A regional metamorphic event, of probable pre-Late Devonian age, centred east and northeast of the area, has affected the northeastern part of the region between Anderson Creek and Thomas River, and produced up to sillimanite grade schists and gneisses in the "Grit" unit, calcareous phyllite in the 'wavy banded' limestone, and black phyllites with quartz lamellae, lenses and veins in the more siliceous graphitic shales.

The newly found lead-zinc mineralization is exposed only in the Anderson Creek tributary at point A (Fig. 18.2). Several bedded mineralized zones as much as a few metres thick cross the valley over a creek length of about 500 m, but appear to be fold repetitions of one or two main zones. As shown in Figure 18.3, this zone or zones, is within the lower part of the graphite-rich black shale, 30 m or more above the "wavy banded" limestone.

The lead and zinc occurs as galena and sphalerite in penetratively-transposed lamellae and bands, often with fine lens-shaped beads of quartz, in a host of black phyllite. In places sulphides are coarse grained and concentrated within minor fold hinges and micro-tectonic breaks, suggesting that along with quartz, the sulphides were mobilized locally by the regional metamorphic event.

Due to intense cleavage, it is doubtful that any direct paleontological dating of the mineralized zone is possible. However the zone immediately overlies the 'wavy banded' limestone, a generally reliable correlation marker of Cambro-Ordovician age, and underlies by a considerable interval fossiliferous shales and carbonates of apparent lower – middle Devonian age. The mineralized zone is therefore in the basal part of the Road River Formation and relates in general stratigraphic position to the extensive lead-zinc beds at Howards Pass, 90 km to the north. Dissimilar features of the Frances Lake mineralization, such as local coarse grain size and mobility of sulphides, abundance of quartz in lamallae, and relatively high silver content, are perhaps explained by its unique setting on the flank of a regionally metamorphosed terrain. Due to continuous overburden, strike length of mineralization is not known, but a second mineral occurrence at B, (Fig. 18.2) is a similar type, in an apparent infold of black shale in unit 2, suggesting mineralization may be continuous for at least 6 km.

The setting and potential size of this discovery sheds new light on similar shale terranes in this part of Selwyn Basin and in particular on nearby shale-hosted lead-zinc deposits such as Matt Berry, on the east arm of Frances Lake where type of mineralization and age of the host rock, black shale, have never been resolved.

References

Blusson, S.L.

1966: Frances Lake, Geology; Geol. Surv. Can., Map 6-1966.

1974: Nadaleen River, Geology; Geol. Surv. Can., Open File 205.

Boyle, R.W.

1965: Geology, geochemistry and origin of the lead-zinc-silver deposits of the Keno Hill-Galena Hill area, Yukon Territory; Geol. Surv. Can., Bull. 111.

Brosgé, W.P., Lanphere, M.A., Reiser, H.N., and Chapman, R.M.

1969: Probable Permian age of the Rampart Group, central Alaska: U.S. Geol. Surv. Bull. 1294-B, p. B1-B18.

Green, L.H.

1972: Geology of Nash Creek, Larsen Creek and Dawson map-areas, Yukon Territory; Geol. Surv. Can., Mem. 364.

Mertie, J.B., Jr.

1937: The Yukon-Tanana region, Alaska; U.S. Geol. Surv. Bull. 872.

Tempelman-Kluit, D.J.

1970: Stratigraphy and structure of the 'Keno Hill, quartzite' in Tombstone River – Upper Klondike River map-areas; Geol. Surv. Can., Bull 180.

19. METAMORPHISM OF THE NORTHERN SELKIRK MOUNTAINS, BRITISH COLUMBIA

E.M.R. Research Agreement 2239-4-182/77

R.W. Leatherbarrow[1] and R.L. Brown[1]
Regional and Economic Geology Division

Abstract

Leatherbarrow, R.W. and Brown, R.L., Metamorphism of the Northern Selkirk Mountains, British Columbia; Current Research, Part A, Geol. Surv. Can., Paper 78-1A, p. 81-82, 1978.

The Northern Selkirk Mountains have undergone Barrovian type regional metamorphism. Northwest trending mineral zones indicate progressively higher metamorphic grades towards a centrally located K-feldspar-sillimanite zone in which partial melting has occurred. The Selkirk fan structure is located within the metamorphic culmination. Pressure and temperature conditions prevailing during the peak of metamorphism will be determined by analysis of mineral assemblages.

Field mapping of Selkirk terrane within the Big Bend of the Columbia River, and subsequent laboratory studies, were initiated by Brown in 1973. Mapping by Franzen (1974); Van der Leeden (1976); Perkins (field seasons 1974 to 1976); Shaw (field seasons 1974 to 1977) and Leatherbarrow (field season 1975) outlined metamorphic mineral zones which were used as a basis for detailed sampling by Leatherbarrow (field season 1977). The object of this season's work was to map more exact locations for metamorphic boundaries, and to sample pelitic and calc-silicate assemblages for chemical analysis and subsequent quantification of pressure and temperature conditions during metamorphism.

Wheeler (1965) mapped the following northwest trending mineral zones (from southwest to northeast): garnet; sillimanite; and kyanite. The centrally located sillimanite grade area represents a metamorphic culmination and coincides with the Selkirk fan structure (Brown et al., 1977; Brown and Tippett, in press). Petrographic studies by Franzen (1974); Van der Leeden (1976) and Leatherbarrow (unpublished results) show that porphyroblast growth peaked syn- to post-D_2 followed by annealing of textures and limited new mineral growth during D_3 (summarized in Brown and Tippet, in press).

Before outlining current progress, two terms used in this paper warrant definition. An isograd is defined as the first appearance or disappearance of a metamorphic index mineral. An assemblage is a group of minerals generally found together in hand specimen but with stability relationships amongst phases not fully studied.

The mapped isograds trend northwest and are somewhat symmetrically arranged on both sides of a metamorphic culmination (Fig. 19.1) with mineral zones being narrower on the southwest side of the culmination. Attempts to trace isogradic surfaces into the third dimension were hampered by extensive vegetation and inadequate distribution of outcrops below the treeline.

Assemblages observed indicate that medium pressure Barrovian-type metamorphism has occurred. Metamorphic zones, proceeding from southwest to northeast across the culmination, are described as follows.

The lowest grade, greenschist facies chlorite-biotite zone rocks are characterized by chlorite-biotite porphyroblasts set in chlorite-muscovite-quartz matrix. Pyrite cubes are common.

Garnet porphyroblasts in a matrix assemblage of biotite-muscovite-quartz and feldspar define a garnet zone up to 4 km wide. Detailed examination suggests that locally the garnet isograd lies along the contact between pelitic schist and a 10-m-thick pure marble band. This suggests that some isogradic surfaces may be controlled by stratigraphy or fluid phase composition.

A staurolite zone, present as rare occurrences of the assemblage staurolite-garnet-biotite-muscovite-quartz and feldspar is up to 3 km wide.

Kyanite, staurolite and garnet porphyrobasts in a matrix of muscovite-biotite-quartz and feldspar typify the approximately 4-km-wide kyanite-staurolite zone. Staurolite becomes rare toward the northeast. The isograd defined by "kyanite-out" overlaps the isograd defined by "sillimanite-in" on the southeast side of the culmination.

Rare occurrences of the assemblage sillimanite-staurolite-garnet-feldspar-biotite and muscovite mark the sillimanite-staurolite zone. A more common assemblage, which also defines the higher grade sillimanite zone, is sillimanite-garnet-biotite-muscovite-quartz and feldspar. Garnet porphyroblasts rimmed by fibrolitic selvages give these rocks a distinctive "birdseye" texture. Thin section examination shows that sillimanite grows as fibrolite in biotite, muscovite or quartz. The total width of the sillimanite and sillimanite-staurolite zones is about 10 km. The Selkirk fan structure lies along the centre of the sillimanite zone.

The centre of the metamorphic culmination is defined by the co-existence of sillimanite and K-feldspar. The potassium feldspar is most commonly found within quartz-feldspar-mica segregations which constitute up to 5 per cent of some pelitic units; in addition the K-feldspar occasionally occurs within the matrix material. Sillimanite is found within some segregations as fibrolite mats 10 cm long. Muscovite is present; however in thin section it is observed to have a vermicular or "wormy" habit. This zone of partial melting is about 2 km wide but further work on samples collected this summer may extend the boundaries. Work on the petrogenetic significance of this assemblage is in progress.

Another sillimanite zone, about 5 km wide, occurs northeast of the culmination. Continuing northeast, kyanite reappears along a well defined isograd across which there is no band of coexistence of Al_2SiO_5 polymorphs. This suggests that equilibrium was achieved in this region during metamorphism.

The kyanite zone, which is about 8 km wide, is characterized by the assemblage kyanite-garnet-biotite-muscovite-quartz and feldspar. Commonly garnet porphyroblasts are enclosed by kyanite. Occasionally kyanite is found in quartz pods.

Farther to the northeast, near McNaughton Lake, a zone of staurolite-kyanite-garnet-biotite-muscovite-quartz and feldspar is encountered above treeline on some ridge tops. This zone is extrapolated northeast to McNaughton Lake, a distance of 2.5 km.

[1]Department of Geology, Carleton University, Ottawa, Ontario

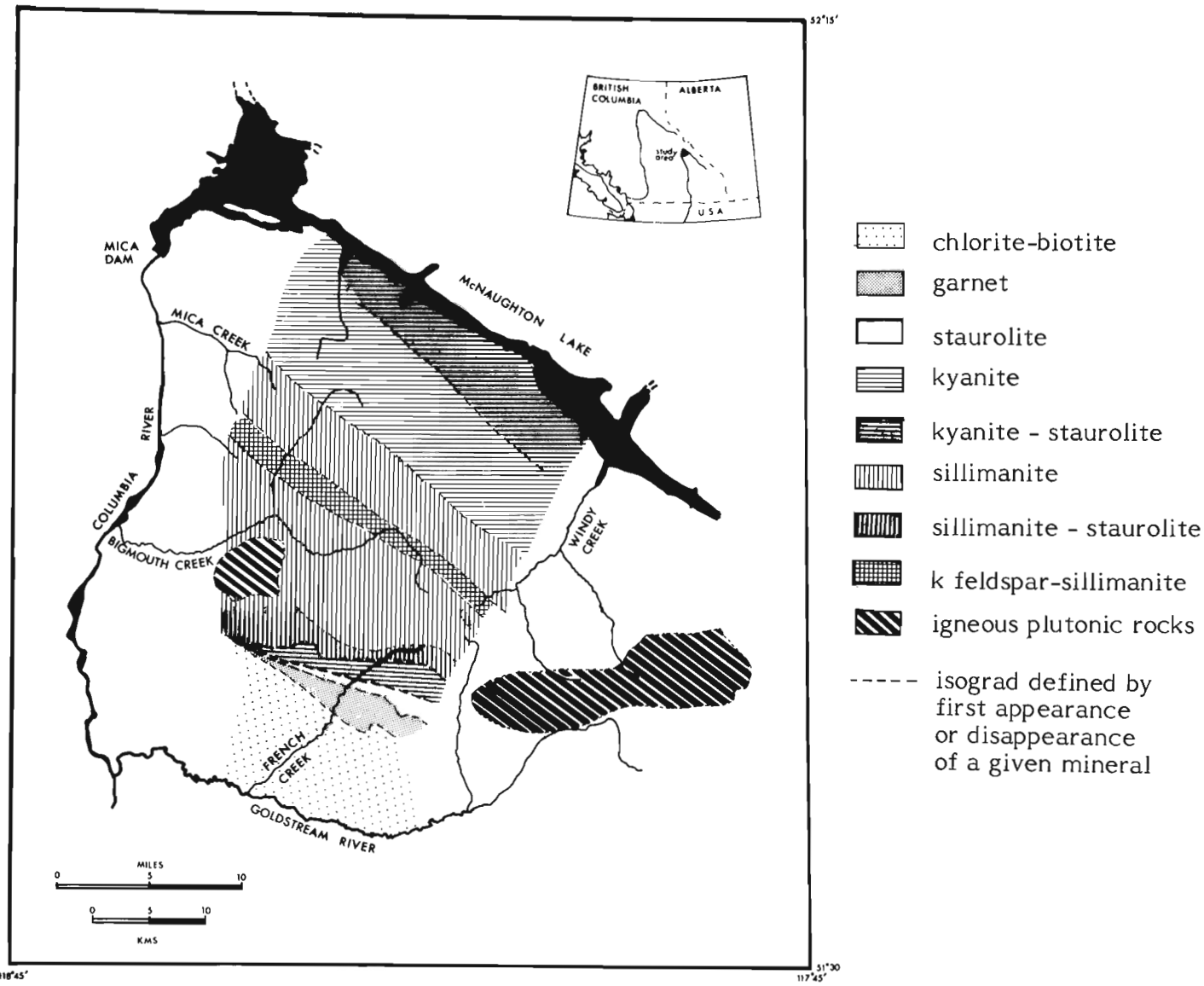

Figure 19.1. Metamorphic mineral zones within the northern Selkirk Mountains.

Compilation of assemblage data for rocks around the Adamant Pluton (southeast corner of Fig. 19.1) is not yet complete, however a few generalizations can be made. Preliminary work indicates that the assemblage kyanite-staurolite-garnet-muscovite-biotite-quartz and feldspar is common south of the pluton. A small area of sillimanite-bearing pelitic schist is located at the central part of the southern contact of the pluton. North of the pluton kyanite zone assemblages are found. Continuations of the sillimanite, and sillimanite-K-feldspar zones towards the pluton have not yet been determined.

Impure carbonates occur throughout the area; the assemblage dolomite-quartz reacts to form tremolite-calcite near the garnet isograd; diopside first appears southwest of the culmination midway through the kyanite-staurolite zone. Near the centre of the culmination diopside-hornblende-garnet-biotite-quartz-calcite and feldspar are found. Assemblages in the extreme northern part of the area contain diopside-hornblende-garnet-calcite and plagioclase. Petrographic studies are in progress to better define calc-silicate mineral zones, and to compare their distribution with zones observed in pelitic rocks.

References

Brown, R.L., Perkins, M.J., and Tippett, C.R.
1977: Structure and stratigraphy of the Big Bend area, British Columbia; in Report of Activities, Pt. A, Geol. Surv. Can., Paper 77-1A, p. 273-275.

Brown, R.L. and Tippett, C.R.
The Selkirk fan structure of the southeast Canadian Cordillera; Bull. Geol. Soc. Am. (in press).

Franzen, J.P.
1974: Structural analysis in the Selkirk fan axis near Argonaut Mountain, southeastern British Columbia; Carleton Univ., Ottawa, Ontario, unpubl. M.Sc. thesis, 55 p.

Van der Leeden, J.
1976: Stratigraphy, structure and metamorphism in the northern Selkirk Mountains southwest of Argonaut Mountain, southeastern British Columbia; Carleton Univ., Ottawa, Ontario, unpubl. M.Sc. thesis, 105 p.

Wheeler, J.O.
1965: Big Bend map-area, British Columbia (82 M east half); Geol. Surv. Can., Paper 64-32, 37 p.

20. STRUCTURAL SETTING OF THE ADAMANT PLUTON, NORTHERN SELKIRK MOUNTAINS, BRITISH COLUMBIA

E.M.R. Research Agreement: 2239-4-182/77

David Shaw[1]
Regional and Economic Geology Division

Abstract

Shaw, David, Structural setting of the Adamant Pluton, Northern Selkirk Mountains, British Columbia; Current Research, Part A, Geol. Surv. Can., Paper 78-1A, p.83-85, 1978.

The Adamant Pluton intrudes Proterozoic rocks of the Horsethief Creek Group which is subdivided into Lower Pelitic, Middle Marble and Upper Pelitic members. The pluton has an elongated ellipsoidal map outline, the long axis of which is aligned east-west. Rock types within the concentrically zoned mass range from hypersthene-augite monzonite in the core to biotite-hornblende granodiorite and quartz diorite in the outer zone. The region has undergone three main phases of deformation and these are described. Available evidence indicates that the pluton was emplaced before the Middle Jurassic phase II deformation. Hence the pluton is at least of Middle Jurassic age, but it could be considerably older.

Introduction

The area peripheral to the Adamant Pluton was mapped in detail during the field seasons of 1975, 1976 and 1977. The purpose of the study was to determine the relative timing of emplacement of the pluton with respect to the main regional phases of deformation, and its effect upon the geometry of regional fold patterns.

The Adamant Pluton is a zoned, igneous body with an elongated, ellipsoidal map outline. The long axis, in plan view, is aligned east-west and is 25.6 km in length. The maximum width of the pluton is 6.4 km. The core of hypersthene-augite monzonite is successively enclosed by a mixed zone of hornblende-quartz monzonite and granodiorite, a zone of biotite-hornblende granodiorite and a zone of quartz diorite (Fox, 1969).

The pluton has intruded Proterozoic metasediments of the Horsethief Creek Group. The stratigraphy of this group within the vicinity of the pluton has been subdivided into Upper Pelitic, Middle Marble and Lower Pelitic members (Brown et al., 1977). The trace of the Middle Marble member about the Adamant Pluton is shown in Figure 20.1.

Previous Work

The only previous work reported on the Adamant Pluton is that by Wheeler (1963, 1965) and Fox (1969). Fox concluded that the history of the pluton involved early intrusion of a hypersthene monzonite body, with later deformation and reintrusion, and associated metamorphism of the early monzonite to a mafic granodiorite. Regional deformation was believed by Fox to have caused upward emplacement of the mass as a crystalline diapir which pushed aside the country rocks along its roof and flanks. Hence he visualizes the pluton's latest stage of intrusion as being a disruptive syn- or post-tectonic event.

Adamant Pluton Structural Aureole

From Fox's data it is apparent that there is a structural aureole associated with the pluton's emplacement. The areas lying within and immediately outside of this aureole were examined in order to make comparisons.

The structural aureole extends approximately 6 km from the northern and southern margins of the pluton but is faulted out within a few hundred metres of the pluton in the west, and extends to the Rocky Mountain Trench in the east (Fig. 20.1).

Fabric Analysis

The Northern Selkirk Mountains region has undergone three main phases of deformation.

During the first phase of deformation at least one large scale nappe was formed which inverted the stratigraphy to the west of the study area. A planar fabric was produced during phase I, this fabric (S_1) is generally parallel to primary bedding (S_0) throughout the Northern Selkirks (Brown et al., 1977).

The second phase of deformation formed tight to isoclinal folds; outside of the structural aureole, in areas not affected by phase III deformation (Brown and Tippett, in press), axial surfaces are northwest-southeast trending and dip to the northeast.

The form of the phase III deformation varies from strong crenulation to large scale, tight folds, with a similar axial surface trend to that of the phase II structures. Phase III structures are primarily developed on the northeastern flank of the Selkirk Mountains where they dip to the southwest. Since the phase II and phase III structures are not isoclinal, the axial planar fabrics (S_2 and S_3 respectively) make a significant angle with primary bedding (S_0). These planar fabrics generally have similar attitudes but diverge sufficiently to allow phase II hinge lines to be deformed about phase III structures.

The relationships and attitudes change as both phase II and phase III axial surfaces are traced towards the pluton.

Phase III axial surfaces when traced towards the pluton are strongly deflected around it. The deflection is best seen in the area to the immediate south of Azimuth Mountain (Fig. 20.1). The axial surfaces that lie within the eastern part of this area have been deflected clockwise approximately ninety degrees to assume a northeasterly trend. The dip direction of these axial surfaces changes in the zone of deflection. Those axial surfaces which lie in the western part of the Azimuth Mountain area are deflected counterclockwise from a northwest to a westerly strike. The dip direction changes from southwest to northerly, and the axial surface passes through the vertical. In both the eastern and western parts the final orientation of the axial surfaces reflects the outline and steeply inward dipping nature of the pluton's southern margin.

The phase III fold axes (L_3), immediately outside of the pluton's structural aureole, pitch in S_3 predominantly towards the northwest. As the pluton is approached and the axial

[1] Department of Geology, Carleton University, Ottawa.

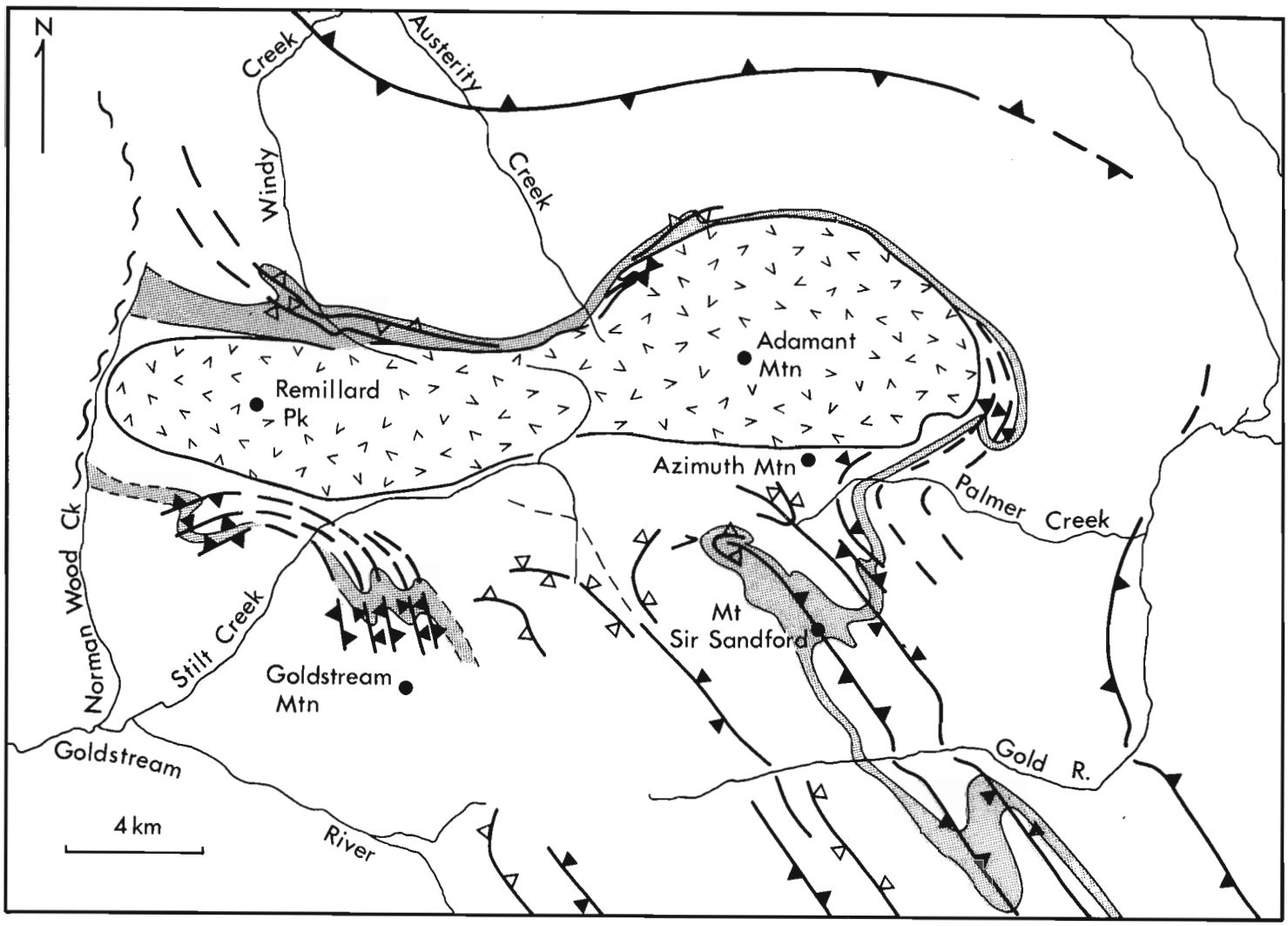

Figure 20.1

surfaces are deflected to the east, adjacent to Azimuth Mountain, the pitch direction of L_3 is reversed. This is reversed again as the axial surfaces go around the extreme southeast corner of the pluton (Fig. 20.1). The magnitude of pitch, of L_3 in S_3 in both the eastern and western parts, increases as the pluton is approached. Those L_3 lineations in the western part do not undergo a reverse in pitch when the axial surfaces containing them are deflected to the west.

In the region adjacent to the northwest corner of the pluton a deflection to the east of phase III axial surfaces is also observed (Fig. 20.1). However, the corresponding westerly deflection in the southwest corner of the pluton is obscured by poor outcrop and complex strain effects present along Norman Wood Creek. The phase III axial surfaces in this northwest region approach the pluton's structural aureole with a southeast strike and a southwest dip direction. Once within the structural aureole the axial surfaces (S_3) undergo a counter-clockwise deflection to an easterly strike and the surfaces dip steeply to the south. Once again the axial surfaces are drawn into a conformable orientation with the pluton's inward dipping perimeter. As the axial surfaces (S_3) approach the "hinge" zone of maximum curvature of the easterly deflection, the pitch direction of the phase III fold axes (L_3) in S_3 is reversed.

The eastern portions of the deflection zones, located adjacent to Azimuth Mountain and at the pluton's northwest margin, are connected by the trace of the Middle Marble member. This unit is on the upper limb of a major phase III antiform and it reflects the orientation of phase III axial surfaces as they go around the pluton's east end. The Middle Marble member is conformable to the outline of the pluton's perimeter and is steeply inward dipping below it. In order to go around the eastern end of the pluton, and connect with both "deflection zones", the Middle Marble goes around a

number of major "bends". At each "bend" the pitch trend of phase III fold axes is reversed and remains steep relative to the attitudes outside of the structural aureole.

The conformable "wrap around" seen at the eastern end of the pluton is not repeated at the western end. Going west from the Azimuth deflection zone, successive major phase III axial surfaces approach the pluton. Once within the structural aureole they show varied degrees of counter-clockwise deflection as they assume an orientation conformable with the inward dipping pluton margin. The Middle Marble member, adjacent to the pluton's southwest corner, is on the lower limb of a major phase III antiform, the axial surface of which lies to the west of Goldstream Mountain (Fig. 20.1). When traced northwards the axial surface dip direction changes from westerly to northerly to dip towards the pluton. The axial surface is then deflected to a southwesterly strike and it dips to the northwest. In doing so the axial surface passes through the vertical.

Phase II axial surfaces, within the structural aureole, where they are not folded by phase III structures, are conformable with the inward dipping pluton margin.

Contact Relationships

Within the pluton's outer zones there are tight folds which deform a foliation defined by planar preferred orientation of minerals and a weak compositional layering. Biotite and hornblende also locally lie in the axial surfaces of the folds. Although S_3 tends to conform to the trend of the pluton boundaries, local discordant relations have been observed. One instance on the map scale is illustrated in Figure 20.1. Here the axial planar fabric, and the associated tight folds, can be traced out of the pluton and into the country rock where they are correlated with S_3 and phase III folds respectively.

The deformed mineral planar fabric within the pluton has a similar orientation to that of S_2 in the adjacent country rock.

The metasediments, within the structural aureole, are generally concordant with the pluton's map outline. There are local discordant relationships but these are mainly limited to the two deflection zones.

Experimental Investigations

Finite Element Analysis

Although not reported in this report the author has used a two dimensional finite element analysis method that assumes a pre-phase III presence of the pluton as a rigid mass, and has observed that the geometry of the phase III axial surface deflection is reproduced.

Isotopic Dating

The pluton was sampled by the author from core to perimeter in order to carry out ^{87}Rb-^{86}Sr whole rock and Pb-zircon dating.

The ^{87}Rb-^{86}Sr ratio changes by .08 from core to perimeter. This ratio change is insufficient to derive an isochron.

The presence of zircon within the pluton appears to be limited to the outer zones. The hypersthene monzonite core samples were devoid of zircon. This may be explained by the zircon being of a metamorphic origin. Zircon may be absent from the nonmetamorphosed core because the zirconium is still "locked" within certain core minerals, probably within the feldspars. Hence a Pb-Pb date using the perimeter zone zircons may only yield the date of the metamorphism associated with the zircon formation.

Conclusions

The manner of the phase III axial surface deflection around the pluton is consistent with the pluton being present as a rigid body before the onset of deformation. The axial surface deflection and the "wrap around" effect, outlined by the Middle Marble, is analogous to the geometry of the fabric around a microscopic, pretectonic porphyroblast with an approximately ellipsoidal outline.

The phase III folds within the pluton's outer zones deform a fabric which the author believes to be S_2. This means that the pluton's emplacement is not just pre-phase III but at least as early as syn-phase II. However the highly discordant trend of the pluton, with respect to the regional strike of phase II axial surfaces, makes a pre-phase II emplacement more probable.

Since the surrounding metasediments were initially metamorphosed to upper amphibolite facies during the final stages of the phase II deformation, it appears that the Adamant Pluton was emplaced before the peak of regional metamorphism.

The phase II structures probably formed in Middle Jurassic (Wheeler, 1963, 1965; Brown and Tippett, in press). On available evidence the Adamant Pluton could be as young as Middle Jurassic, but an older age is equally possible.

References

Brown, R.L., Perkins, M.J., and Tippett, C.R.
1977: Structure and stratigraphy of the Big Bend area, British Columbia; in Report of Activities, Part A, Geol. Surv. Can., Paper 77-1A, p. 273-275.

Brown, R.L. and Tippett, C.R.
The Selkirk Fan structure of the southeastern Canadian Cordillera; Geol. Soc. Am. Bull. (in press)

Fox, P.E.
1969: Petrology of the Adamant Pluton, British Columbia; Geol. Surv. Can., Paper 67-61, 101 p.

Wheeler, J.O.
1963: Rogers Pass map-area, British Columbia and Alberta (82N west half); Geol. Surv. Can., Paper 62-63, 32 p.

1965: Big Bend map-area, British Columbia (82M east half); Geol. Surv. Can., Paper 64-32, 37 p.

21. GEOLOGY OF THE HEART PEAKS VOLCANIC CENTRE, NORTHWESTERN BRITISH COLUMBIA

E.M.R. Research Agreement 2239-4-51/77

J.J. Casey[1] and C.M. Scarfe[1]
Regional and Economic Geology Division

Abstract

Casey, J.J. and Scarfe, C.M., Geology of the Heart Peaks Volcanic Centre, northwestern British Columbia; Current Research, Part A, Geol. Surv. Can., Paper 78-1A, p. 87-89, 1978.

The Heart Peaks Plateau, one of several late Cenozoic volcanic centres, is broadly subdivided into flat-lying basalts and trachybasalts of the Level Mountain Group and rhyolite domes of the Heart Peaks Formation. Preliminary field and petrographic observations are discussed in the light of this bimodal distribution of rock types.

Introduction

The Heart Peaks Plateau of northwestern British Columbia rises roughly 900 m above the local topography between the Sheslay and Dudidontu rivers. The twin Heart Peaks at the centre of the flat-topped succession of volcanic rocks rise to 2013 m and the plateau covers an area of about 330 km^2. The plateau is sharply dissected on all sides by fast flowing streams which empty into the drainage system of the Inklin River to the north.

The volcanic rocks rest unconformably on a local basement of deformed Jurassic and Triassic sediments and calc-alkaline volcanics (Souther, 1971). These Mesozoic rocks occur in a northwesterly trending belt bounded on the south by the Coast Crystalline Complex and on the north by the Cassiar Crystalline Belt.

Previous mapping of the area has been by Gabrielse and Souther (1962) and Souther (1971). Heart Peaks is one of several late Cenozoic volcanic centres in northern British Columbia which show bimodal distribution of basaltic and felsic lavas. The volcanics of the Level Mountain Range 16 km to the east (Hamilton and Scarfe, 1977) and a series of late Miocene acid tuffs and basalts 26 km to the south (Panteleyev, 1964; Souther, 1971) are considered to be contemporaneous with the Heart Peaks.

This report, which covers work completed during the 1977 field season, represents a continuation of a program to study the Cenozoic volcanic rocks of northwestern British Columbia. Correlation of the Heart Peaks volcanic succession with larger centres such as Edziza (Souther, 1970; Souther and Symons, 1974) and the Level Mountain Range will contribute to a more complete understanding of this episode of volcanism in northern British Columbia. Souther (1970) has related the volcanism in this region to deep crustal rifting.

Mappable Units

The sketch map shows the distribution of the two distinct volcanic units, along with the locations of vents and dykes. The formation names, which have been taken from Souther (1971), emphasize a compositional distinction rather than a time-stratigraphic one.

The Level Mountain Group outcrops as generally flat-lying flows and pyroclastics. The southern end of the plateau shows a virtually uninterrupted vertical sequence of 600 m of basalt and trachybasalt. The textural and compositional variations among individual flow units are very subtle in any particular section; however, individual flows are easily distinguished by a weathered scoriaceous layer at the top of each flow. The basaltic flows average 4 to 6 m in thickness and frequently exhibit prominent columnar jointing. Textures range from fine grained to sparsely porphyritic. Pillow lavas are found at several places in the southern section, but neither these nor any other marker horizon could be correlated for any great distance across the plateau. A cliff on the southwestern edge of the plateau exposes a good 200 m succession of 22 basaltic flows. The cliff is the result of the Sheslay Slide (Souther, 1971) which flowed down to Sheslay valley to the west. The central and northern parts of the plateau, on the other hand, show a more complex section with thicker cooling units (10-15 m), an increasing abundance of pyroclastics, and evidence for at least one glacial erosional event.

Two contrasting eruptive styles are represented by the Level Mountain Group basaltic rocks: explosive activity represented by coarse vent agglomerates, and fluid fissure-type eruptions represented by linear dykes. Well exposed vents discordantly intrude the flat-lying flows in numerous locations. A typical vent agglomerate is composed of unsorted blocks of subrounded and angular material from sand size to 2-m sized boulders. Sulphurous material and striated blocks of debris are characteristically present and the pyroclastics always consist of fragments of basalt and trachybasalt similar to the surrounding lava flows. Mud flows composed of basaltic debris are exposed in several stream valleys. The numerous north-south striking linear dykes reflect a less violent fissure-type eruptive style. The basaltic dykes often show well developed lateral joints and in many cases contain large crystals of feldspar and hornblende. In most cases the dykes are similar in composition to the host lavas.

A distinct change, marked by an erosional event, occurs near the top of the volcanic succession. U-shaped glacial valleys in plagioclase-phyric basalts are filled with localized deposits of sand-sized glacial outwash sediments and with grey-weathered basalts or trachybasalts with well developed flow textures that commonly contain large black phenocrysts or xenocrysts of hornblende. Just below the highest flows, southeast of Heart Peaks, easterly striking glacial striae, and a layer of unconsolidated till with many granitic boulders indicate that the latest volcanic activity was synglacial.

The flows of the Heart Peaks Formation and the Level Mountain Group do not appear to be distinct time-stratigraphic units. A fine grained basaltic dyke, which could be traced for several miles, was observed to have intruded the uppermost basaltic flows of the Level Mountain Group as well as the acid rocks of the Heart Peaks Formation. Elsewhere there are vertical contacts between the two units and sill-like bodies of rhyolite suggest an intrusive relationship between the acid Heart Peaks rocks and the basic lavas of the Level Mountain Group.

The bright coloured domes of the Heart Peaks Formation are composed predominantly of porphyritic rhyolite with minor trachyte. The highly viscous nature of the acid lava has resulted in the formation of steep-sided domes in which extensive hydrothermal alteration has made individual flow units unrecognizable. On the western side of the plateau, several individual domes occur on a ridge, each easily distinguished by the variety of bright green and pink

[1] Department of Geology, University of Alberta, Edmonton, T6G 2E3

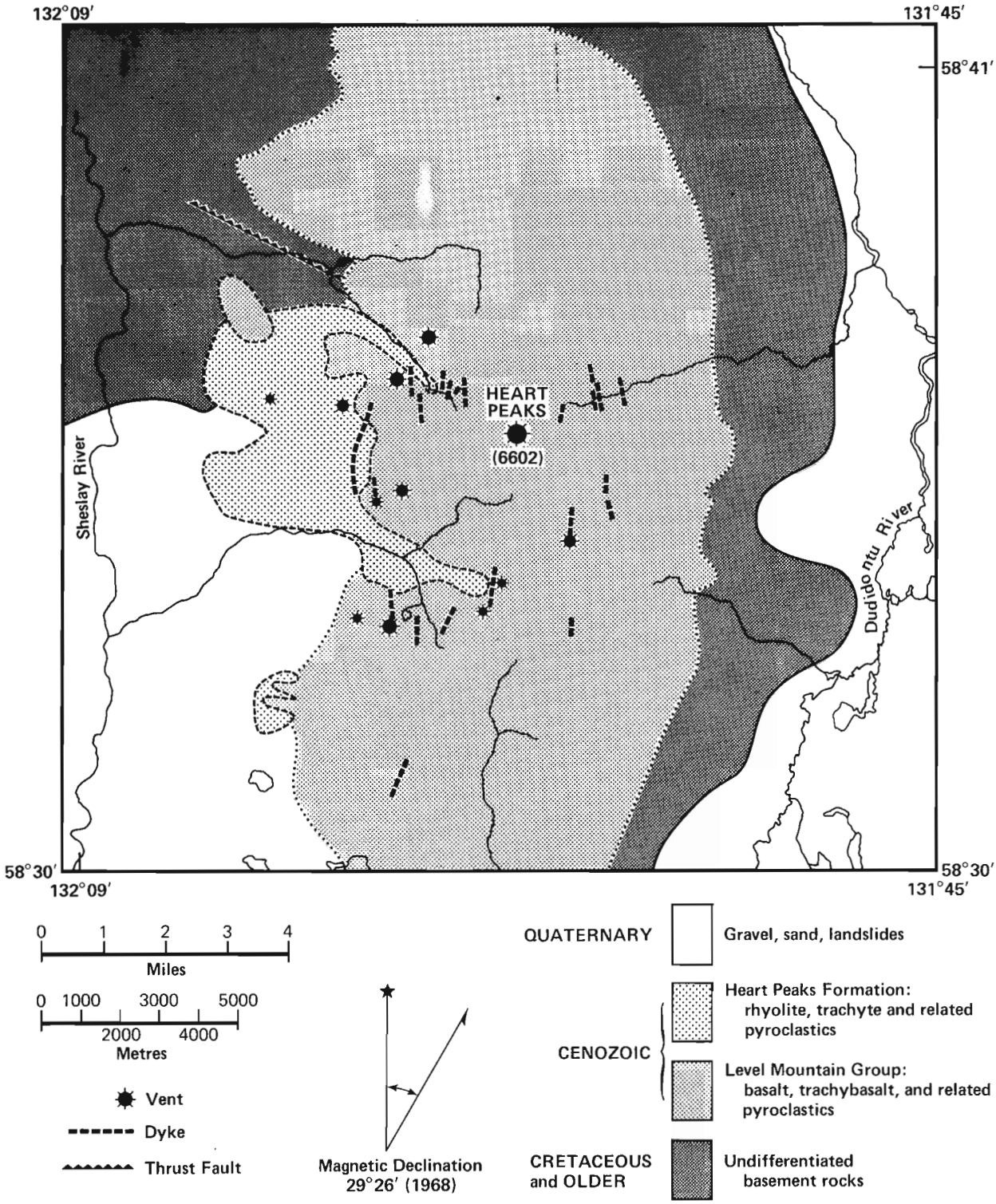

Figure 21.1. Heart Peaks Plateau, British Columbia.

colours exhibited by the weathering. The highest domes contain fresh glassy rhyolite with sparse phenocrysts, while the flows lower in the formation are often clogged with large anorthoclase and sanidine phenocrysts and are commonly autobrecciated. Fine grained ash fall and welded ash flow tuffs are frequently found and agglomeratic pyroclastics are not as extensive in this unit as in the Level Mountain Group.

Petrography

At this point a limited number of petrographic observations have been made on specimens collected in the summer of 1977. These details are far from complete and any firm conclusions regarding petrogenetic models or generalized petrologic details are unwarranted at this time.

Basalt, trachybasalt and rhyolite are the predominant rock types present in the Heart Peaks plateau. A typical fresh alkaline olivine basalt has an ophitic groundmass texture, with labradorite laths, pink titanaugite, corroded olivines and ubiquitous opaque oxides. Labradorite, olivine and augite occur as phenocrysts which comprise about 10 per cent of the rock. The trachybasalts show a large variation in mineralogy. Two feldspar phenocryst phases are usually present in varying proportions. Anorthoclase or sanidine coexist with plagioclase ($\sim An_{50}$). Commonly the alkali feldspar phenocrysts occur as cumulophyric and interpenetrant crystals. Augite occurs as phenocrysts, sometimes as glomeroporphyritic aggregates. Olivine is usually absent. Quartz sometimes occurs as corroded crystals. The groundmass displays a well developed eutaxitic texture of oriented plagioclase laths and minor granular augitic pyroxene and opaques. Apatite is present as inclusions in plagioclase.

The rhyolites of the Heart Peaks Formation are quite uniform in texture. Sanidine phenocrysts set in a very fine-grained to glassy matrix of quartz and feldspar occur in the rhyolite domes. The pink weathered rhyolites lower in the succession appear to contain alkali feldspar phenocrysts of varying composition. One phase of highly weathered phenocrysts (up to 2 cm) coexists with a less weathered phase. Unlike the peralkaline salic rocks of the adjacent Level Mountain Range, the acidic rocks of the Heart Peaks Formation do not appear to contain any alkali-rich ferromagnesian minerals.

Many features of the Heart Peaks volcanics have yet to be investigated. Detailed investigations of feldspar compositions, mineralogical trends, and major and trace element analyses are presently being undertaken as part of this study. This data will allow evaluation of petrogenetic models which must account for the bimodal distribution of magma compositions.

Acknowledgments

The Department of Energy, Mines and Resources (agreement 2239-4-51-77), the National Research Council (Grant A8394), and the Boreal Institute for Northern Studies, the University of Alberta, are thanked for financial support. J.G. Souther suggested the topic and J. Andersen ably assisted in the field. T. Hamilton reviewed the manuscript.

References

Gabrielse, H. and Souther, J.G.
1962: Dease Lake, British Columbia; Geol. Surv. Can., Map 21-1962.

Hamilton, T.S. and Scarfe, C.M.
1977: Preliminary report on the petrology of the Level Mountain Volcanic Centre, northwest British Columbia; in Report of Activities, Part A, Geol. Surv. Can., Paper 77-1A, p. 429-433.

Panteleyev, A.
1964: A Late Tertiary sequence in the Sheslay River vicinity; unpubl. B.A. thesis, Univ. British Columbia.

Souther, J.G.
1970: Volcanism and its relationship to Recent crustal movements in the Canadian Cordillera; Can. J. Earth Sci., v. 7, p. 553-568.

1971: Geology and mineral deposits of the Tulsequah map-area, British Columbia; Geol. Surv. Can., Mem. 362, p. 1-84.

Souther, J.G. and Symons, D.T.A.
1974: Stratigraphy and paleomagnetism of Mount Edziza volcanic complex, northwestern British Columbia; Geol. Surv. Can., Paper 73-32, p. 1-48.

22.

GEOLOGY OF THE EAST BULL LAKE LAYERED GABBRO ANORTHOSITE INTRUSION, DISTRICT OF ALGOMA, ONTARIO

E.M.R. Research Agreement 2239-4-175/77

P. Born[1] and R.S. James[1]
Regional and Economic Geology Division

Abstract

Born, P. and James, R.S., Geology of the East Bull Lake, layered gabbro anorthosite intrusion, District of Algoma, Ontario; Current Research, Part A, Geol. Surv. Can., Paper 78-1A, p.91-95, 1978.

The intrusion is elliptical in shape (13 km by 4 km) and consists of rock compositions which vary between gabbro and anorthosite, recrystallized to greenschist facies mineralogy. A few specimens show primary olivine, plagioclase and clinopyroxene in that order of crystallization. Nine zones are recognized within the intrusion. Their distribution, and the measured orientations of shallow-dipping, metre scale, isomodal and graded layers of cumulate origin, outline a basin morphology for the complex. Minor Cu-Ni mineralization has been observed adjacent to a west-northwest striking fault zone which transects the intrusion. A massive porphyritic syenite body is in abrupt (fault?) contact with this intrusion along its southeast margin. The spatial relationship between the two is not unlike that described from Grenville-type anorthosites.

Introduction

The East Bull Lake gabbro-anorthosite complex is an elliptically-shaped body (13 km by 4 km) which underlies an area of approximately 36 km^2. It is located 30 km north of Massey, Ontario and approximately 32 km east of Elliot Lake (NTS 41 J/8). Although it is smaller in size, the geology of this complex is very similar to that exhibited by the Shakespeare-Dunlop gabbro-anorthosite (James and Harris, 1977, Card and Palonen, 1976) which outcrops 16 km to the east on the west side of Agnew Lake. Together with a smaller intervening intrusion of the same type, these complexes occur over a distance of 40 km along a west-northwest direction from Agnew to Whiskey lakes. These layered gabbro-anorthosite bodies lie north of the basal Proterozoic-Archean unconformity and are in fault contact with older(?) Archean granite, gneiss and mafic volcanic rocks, and younger(?) Nipissing diabase. In both the Shakespeare-Dunlop and East Bull Lake complexes, gently dipping (5-30°) layers of cumulate origin outline basin-type structures which are apparently little deformed from their original orientation. Fault contacts characterize the relationship between the complexes and adjacent rock units. Chilled marginal facies and intrusive relationships are singularly absent. These data suggest to us that these bodies are layered igneous complexes which have been emplaced, subsequent to crystallization (early Proterozoic?), into their present crustal position by major tectonic movements.

General Geology

Previous geological mapping in this area was done by Douglas (1925) and Moore and Armstrong (1943). The latter authors outlined the boundaries of the East Bull Lake intrusion. In Figure 22.1, the geology of this intrusion is presented. Nipissing diabase, Archean granites, and mafic metavolcanic rocks are in contact with the gabbro-anorthosite complex along its northern, western, and southern boundaries. Diabase dykes, which intrude all rock-types in the complex, are common at anorthosite-granite contacts in the few places it has been observed and suggest that a faulted relationship exists between the two. A large lensoid mass of coarse grained syenite is in contact with the complex along its southern and southeastern boundary. Abrupt contacts showing no intrusive relationships and/or prominent photo-linears characterize both syenite-anorthosite and mafic volcanic-anorthosite boundaries suggesting to us that these latter units are in faulted contact with the complex.

The rock-types found within the gabbro-anorthosite intrusion range from meta-anorthosite to meta-pyroxenite using the classification of Windley et al. (1973). For ease of description rock names are used without the prefix "meta". Based on the examination of a few thin sections and in order of crystallization, olivine, calcic plagioclase (near An_{60}) and augite are the original major silicate phases. Mineral textures and crystal layering structures indicate that many of the rock-types originated as igneous cumulates. Alteration of the primary minerals to talc, iron oxides, epidote, actinolite and blue-green hornblende appears to be widespread in the intrusion and probably reflects one or more episodes of low to medium grade regional metamorphism.

In Figure 22.1 the intrusion is divided into nine zones (Jackson, 1967) based on recognizable field criteria such as rock-types, and type of layering (or lack of it). In Table 22.1 detailed information for each of these zones is presented. Some zones consist of many layers of two or more rock types; others are composed of a single thick layer. Isomodal layers and/or mineral graded layers 0.5 to 5 m thick are common and even abundant in some zones. Cross-bedding has been observed in a few metre-thick quasi-isomodal layers.

The two stratigraphic columns (Fig. 22.2) illustrate the succession of zones observed north and south of a major shear zone which strikes at 290° and transects the intrusion (Fig. 22.1). That part of the complex north of the shear zone best illustrates the original shape of the igneous body. In Figure 22.1 the outcrop pattern of each zone in this portion of the complex and the orientation of layering (particularly abundant in the Metre-scale Layered Zone) indicate that the intrusion is an ovoid basin that consists of a sequence of zones which dip inwards at an average angle of 20°. Section A-A[1] (Fig. 22.2) best illustrates the succession of zones on this part of the complex. Section B-B[1] (Fig. 22.2) illustrates the succession of zones for that part of the complex south of the major transecting shear zone in Figure 22.1. The stratigraphic sequence is noticeably different in this part of the intrusion. Also layers within zones and zone boundaries strike uniformly at near 060° and dip at 10-20° to the northwest. This part of the intrusion consists of four fault blocks; the relationships between each other as well as to the northern portion of the intrusion are unclear.

[1] Department of Geology, Laurentian University, Sudbury, Ontario P3E 2C6.

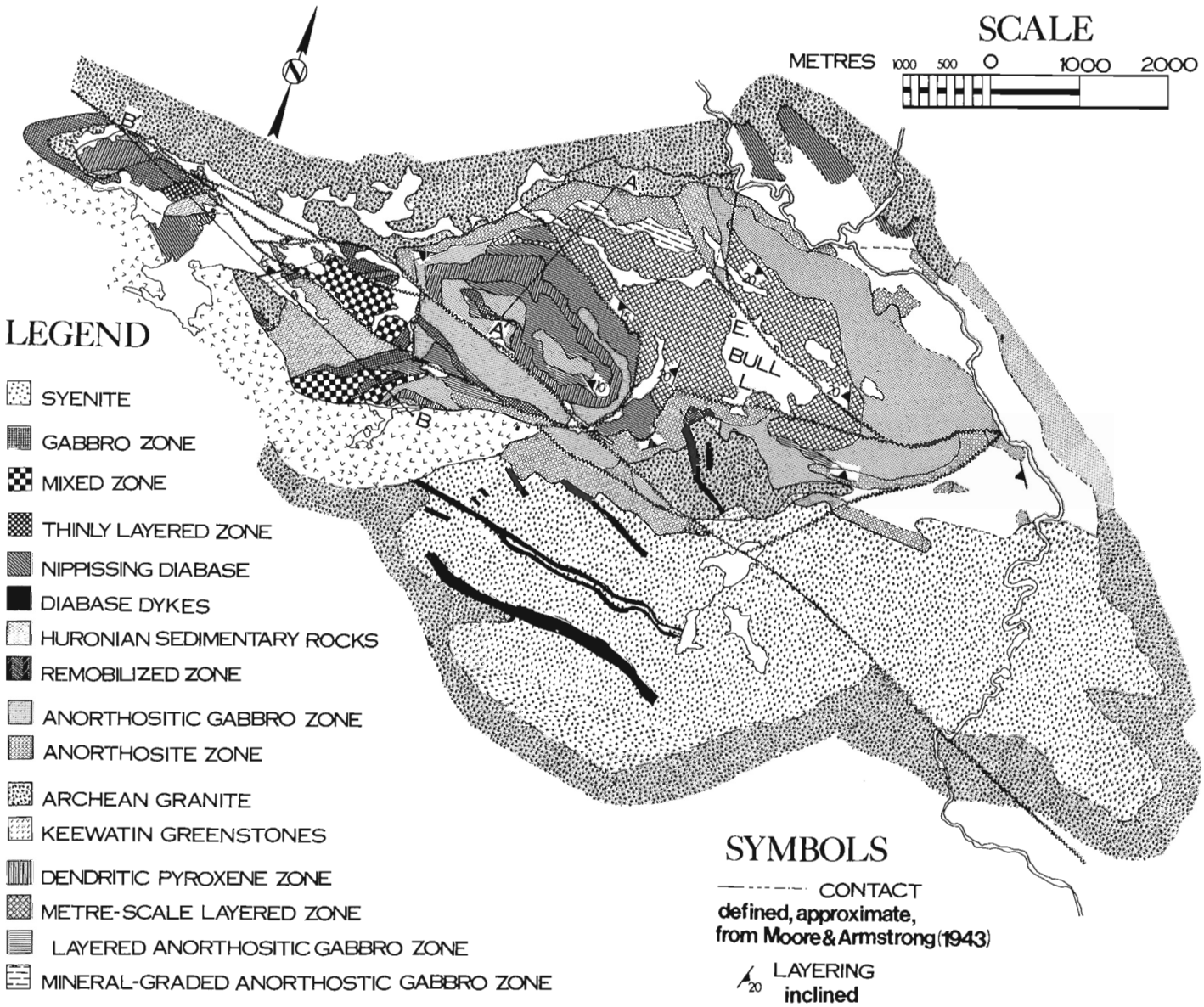

Figure 22.1 Geology of the East Bull Lake gabbro-anorthosite intrusion.

Stratigraphy

Section A-A^1 is representative of the stratigraphy in the northern portion of the complex. The upper half of this section (from the base of the Layered Gabbro-Anorthosite Zone) forms an elevated plateau and is separated from the underlying zones by a 30 to 40 m fault scarp. Type 1 Anorthosite Zone (Table 22.1) forms the base of the section in this area. Discontinuous isomodal layering and pyroxenitic xenoliths are features which distinguish this zone from the massive unlayered rock unit of the immediately overlying Anorthositic Gabbro Zone (not illustrated in section). Thin and often sparsely distributed mineral graded layers in the Mineral Graded Zone contrast sharply with the abundant isomodal layering in the overlying Metre-scale Layered Zone. Anorthosite, anorthositic gabbro, and gabbro form continuous isomodal layers throughout this zone although gabbro is common only near the top of the section. Where layers of all three rock-types are present, a cyclical repetition of layers upwards in the section is observed i.e. gabbro-anorthosite-anorthositic gabbro. The upper part of this section forms a continuous sequence uninterrupted by faults. The Layered Gabbro Anorthosite Zone, in which isomodal layers of gabbro are diagnostic, occurs at three stratigraphic levels (see Fig. 22.1) in association with the Metre-scale Layered Zone and two overlying zones. The major fault at the base of this unit appears to have considerably reduced the distribution of this unit. The Dendritic Pyroxene Gabbro Zone forms an almost continuous elliptical outcrop pattern in the upper portion of this stratigraphic section. Diagnostic of this zone are isomodal layers and ovoid patches of coarse grained gabbro containing pyroxene crystals 1-6 cm long in rosette-type arrangements. Similar zones are recognized in the Shakespeare-Dunlop intrusion (James and Harris, 1977) and a gabbro-anorthosite sill in May Township (Cape, 1973).

Section B-B^1 (Fig. 22.2) illustrates the stratigraphy within the largest fault block from the southern portion of the intrusion. Although most of the zones in this section are identical to those already described from the northern part of the complex, their vertical distribution is sufficiently different to make reasonable correlations impossible. As in section A-A^1, a type 1 Anorthosite Zone lies at the base of this section. However, the type 2 Anorthosite Zone occurs at four stratigraphic levels in this section for which there are no equivalents in the northern portion of the complex. In section B-B^1, a Gabbro Zone is found at four different stratigraphic positions; the major rock-type in this zone ranges from

massive to porphyritic varities and also contains some mineral-graded layers. In section A-A[1] the Gabbro Zone is very thin and occurs only at the top of the stratigraphic column.

Certain zones occur exclusively within one stratigraphic section. The Metre-scale Layered and Mineral-graded Anorthositic Gabbro zones occur only in section A. The lithologies in the Mixed Zone and Thinly Layered Zone, are gabbro and very coarse grained anorthositic gabbro; both zones occur only in Section B. In the Thinly Layered Zone, the lithologies are interlayered while in the Mixed Zone irregularly shaped blocks of both rock-types, together with very minor interlayered sections, predominate. We believe this latter zone formed at least in part as an interlayered sequence which was subsequently disrupted by tectonic-induced instability in the magma chamber.

Zones Associated with Main Intrusion Syenite Zone

The southeastern boundary of the gabbro-anorthosite complex is against a large elliptically-shaped body of massive coarse grained porphyritic syenite. Neither rock-type has been observed to intrude the other, nor have xenoliths of one been found in the other. In the vicinity of contacts, diabase dykes, which elsewhere cut both the gabbro-anorthosite rocks and syenites, are common and suggest to us that fault contacts characterize the present relationship between these two igneous bodies. Fine grained syenite dykes (0.2-0.3 m in width) intrude the gabbro-anorthosite rocks particularly along its southeastern margin, as well as the syenites and diabase dykes. To our knowledge this syenite intrusion(?) is unique in the region and together with the syenitic segregations reported by Card et al. (1977) in a sill of gabbro-anorthosite

Table 22.1

Description of rock units

Zone	Thickness (metres)	Major Rock Types	Layering	Characteristic Features
Anorthosite Zone Type I	40-120	very coarse grained anorthosite and anorthositic gabbro	Discontinuous isomodal layers (1-5 m thick) of gabbro, and anorthositic gabbro. Also minor mineral grading and size grading in layers.	1) coarse grained habit of anorthosite 2) Discontinuous layering 3) Pyroxenite xenoliths (10-20 cm in diameter)
Anorthosite Type II	30-300	very coarse grained anorthositic gabbro	None	massive and coarse grained habit
Massive Anorthositic Gabbro Zone	40-550	medium to coarse grained anorthositic gabbro	Minor cross-bedded mineral graded layers near western edge of northern portion of intrusion.	1) lack of layering 2) subophitic texture
Mineral graded Anorthositic Gabbro Zone	50-80	medium to coarse grained anorthositic gabbro	Mineral graded layers 0.5 - 4 m in thickness; sharp layer contacts.	1) Mineral graded layers
Metre-scale Layered Zone	200-800	medium to coarse grained anorthositic gabbro and anorthosite	Alternating isomodal layers of 0.2-3 m thick of anorthositic gabbro and anorthosite. Anorthosite as thinner layers compared to anorthositic gabbro. Layer contacts sharp. Isomodal gabbro layers in upper quarter of this zone.	1) Isomodal layering 2) when gabbro layers are present the cycle of layers is gb- anorth-anorth.gb.
Layered Anorthositic Gabbro Zone	30-110	medium to coarse grained anorthositic gabbro and coarse grained gabbro	Isomodal gabbro layers 0.5-5 m thick interlayered with much thicker (massive) anorthositic gabbro. Mineral grading common in anorthositic gabbro.	1) Isomodal gabbro layers in mineral graded anorthositic gabbro.
Dendritic Pyroxene Gabbro Zone	30-120	medium to coarse grained anorthositic gabbro and very coarse grained dendritic gabbro	Layers of isodomal dendritic pyroxene gabbro, 0.2-3 m thick (also as ovoid patches) within massive anorthositic gabbro.	Layers and ovoid patches of dendritic pyroxene gabbro. Pyroxenes crystal 1.6 cm in length often in feathery patterns; rarely plagioclase exhibits a similar pattern.
Massive Gabbro Zone	10-90	medium grained gabbro	A few mineral graded layers in western part of intrusion which exhibit variable plagioclase phenocryst content.	Massive except in western portion of intrusion where locally it contains mineral (plagioclase) graded layering.
Thinly Layered Zone	50	subequal proportions of medium grained gabbro and very coarse grained anorthositic gabbro	Isomodal layers 0.3-3 m thick of the two major lithologies.	Interlayered medium grained gabbro and coarse grained anorthositic gabbro.
Mixed Zone	20-300	approximately equal amounts of medium grained gabbro and very coarse grained anorthositic gabbro	Very rarely 5-7 m thick isomodal layers of anorthositic gabbro with thinner layers of gabbro.	Blocks and irregular shaped zones of variable size consisting of gabbro in sharp contact with anorthositic gabbro and vice-versa.

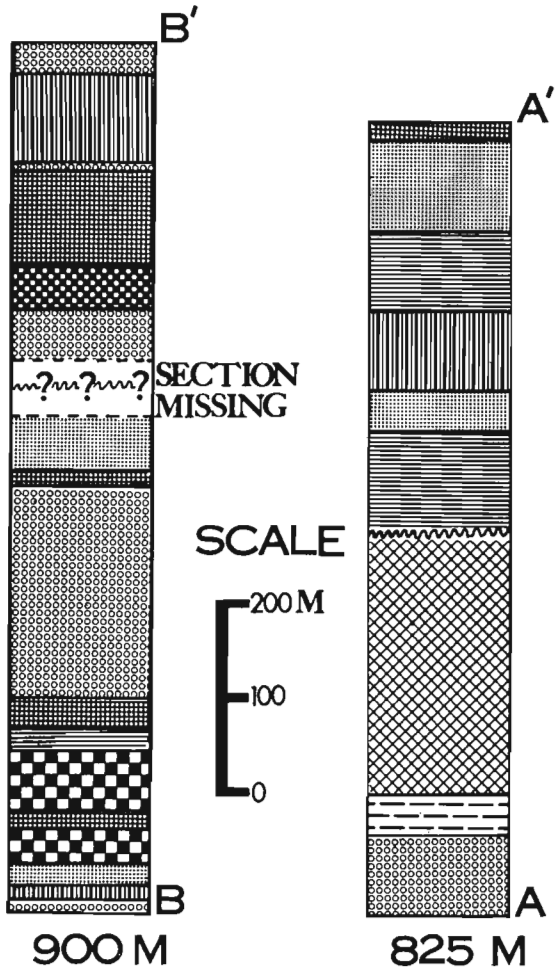

Figure 22.2 Stratigraphic sections A-A^1, B-B^1.

immediately south of the Shakespeare-Dunlop intrusion, suggests that there may be a genetic link between these two major rock-types. Further research on this topic is in progress.

Remobilized Zone

Massive medium grained gabbro together with minor lenses and patches of anorthosite (<5 per cent mafic minerals) constitute the major lithologies in this zone. Structures in a few outcrops suggest that the anorthosite originally may have formed as isomodal layers up to 5 m thick. However, intense shearing throughout this zone which we believe is directly related to the major fault immediately south of this zone, has largely destroyed original structures. Linear zones occupied by late diabase dykes and fragments of basement granitic rocks (which outcrop immediately south of this zone) parallel the aforementioned fault zone and intrude the gabbro and anorthosite. Clearly, this zone has been produced by events associated with late faulting of the gabbro-anorthosite and syenite intrusions.

Sulphide Occurrence

Pyrrhotite and minor chalcopyrite are disseminated in narrow zones of intensely sheared anorthositic gabbro and anorthosite. Diabase dykes and quartz veins have been emplaced along these shear horizons which strike west-northwest in a similar orientation to the major shear zone which transects the intrusion. The two major localities where this mineralization has been observed are located 1.2 km southeast of the east end of East Bull Lake within the Anorthositic Gabbro Zone, and 0.8 km south of East Bull Lake in the Remobilized Zone. At both localities intensive drilling by various exploration companies over the past 25 years has failed to detect any major sulphide concentration. The geology suggests that the mineralization is a late phenomena analogous to that reported by James and Harris (1977) in the Shakespeare-Dunlop intrusion and unrelated to the igneous processes which formed the anorthositic intrusion.

Summary

1) Gabbro, anorthositic gabbro, and anorthosite are the predominant rock-types in the intrusive complex. The anorthosites probably represent plagioclase cumulates. The gabbro and anorthositic gabbros are found interlayered with anorthosite in the Metre-scale Layered Zone. This suggests to us that at least in this zone they represent pyroxene and/or plagioclase cumulates (Wager and Brown, 1968). Sedimentary structures such as cross-beds, bifurcating layers, and mineral-graded layers suggest the presence of some minor local current action during the crystallization of the intrusion.

2) Faulted contacts characterize the association of other rock-types with the gabbro-anorthosite intrusion. Internally the intrusion can be divided into two parts separated by a major east-west striking shear zone. The stratigraphy exhibited in each part is different, and correlation between them is not presently possible. This suggests that the two main parts of the intrusion probably represent two different structural levels. The northern part of the intrusion forms a basin-type structure, which best illustrates what we believe to be the original morphology of the complex.

3) The spatial relationship which exists between the gabbro-anorthosite intrusion and the syenite is similar to that found in Grenville-type anorthosites where felsic intrusions are associated with massive to weakly layered anorthositic rocks.

References

Cape, D.F.

1973: A petrologic and geochemical study of a gabbro, anorthositic gabbro intrusion and neighbouring volcanics, northwest corners of May Township; Unpubl. B.Sc. thesis; Univ. of Windsor, Ont., 62 p.

Card, K.D., Innes, D.F., and Debecki, R.L.

1977: Stratigraphy, sedimentology and petrology of the Huronian Supergroup in the Sudbury-Espanola area; Ont. Div. Mines, GS16, 99 p.

Card, K.D. and Palonen, P.A.

1976: Geology of the Dunlop-Shakespeare area, District of Sudbury; Ont. Div. Mines; GR139, Div. Mines; 52 p., Map 2313.

Douglas, V.G.

1925: The Whiskey Lake area, District of Algoma; Ont. Dept. Mines, v. XXXIV, pt. 4, p. 34-49.

Jackson, E.D.

1967: Ultramafic cumulates in the Stillwater, Great Dyke, and Bushveld intrusions; in Ultramafic and Related Rocks, Wyllie, P.J., ed., New York; John Wiley, p. 20-38.

James, R.S. and Harris, B.J.

1977: Geology of Shakespeare-Dunlop layered gabbro-anorthosite intrusion, Ontario; in Report of Activities, Part A, Geol. Surv. Can., Paper 77-1A, p. 411-414.

Moore, E.S. and Armstrong, H.S.

1943: Geology of the East Bull Lake area; Ont. Dept. Mines, v. LII, pt. 6, 19 p., Map 52d.

Wager, L.R. and Brown, G.M.

1968: Layered igneous rocks; Oliver and Boyd, London, 588 p.

Windley, B.F., Herd, R.K., and Bowden, A.A.

1973: The Fiskenaesset complex, West Greenland, Part I, A preliminary study of the stratigraphy, petrology and whole rock chemistry from QeQertarssuatsiaq; Groenlands Geol. Unders., Bull., 106, 80 p.

23.

GEOLOGY OF THE HELIKIAN ROCKS OF THE BATHURST INLET AREA, CORONATION GULF, NORTHWEST TERRITORIES

Project 770012

F.H.A. Campbell
Regional and Economic Geology Division

Abstract

Campbell, F.H.A., Geology of the Helikian rocks of the Bathurst Inlet area, Coronation Gulf; Current Research, Part A, Geol. Surv. Can., Paper 78-1A, p. 97-106, 1978.

The Tinney Cove Formation fault-derived fanglomerates, conglomerobreccias, fluvial sandstones and conglomerates were deposited in narrow elongate(?) troughs as Helikian sedimentation commenced in the Bathurst Inlet area. Following uplift and erosion, fluvial conglomerates and trough cross-bedded conglomerates of the Ellice River Formation were deposited in elongate basins formed by reactivation of earlier faults. Intertidal red mudstones and shales of the uppermost Ellice River were deposited as a precursor of the subtidal to intertidal stromatolitic Parry Bay Formation. The Parry Bay carbonates were deposited on a stable platform, increasingly complex to the northwest, with little accompanying terrigenous sedimentation.

Regional uplift, erosion, and formation of solution collapse breccias occurred prior to deposition of the unconformably overlying, discontinuous, intertidal to supratidal mudstones and stromatolitic carbonates of the Kanuyak Formation. Basalt flows of the Ekalulia Formation, extruded onto the unconsolidated Kanuyak sediments, temporarily interrupted sedimentation, which resumed as volcanism ended, with deposition of the conformably overlying terrigenous clastics of the Algak Formation. Quartz-pebble conglomerates and orthoquartzites on the Jameson Islands at the north end of Bathurst Inlet may be the proximal facies equivalents of the Rae Group in the Coppermine area to the west.

Introduction

This study was designed to determine the stratigraphic affinity between the Helikian sediments and volcanics of the Bathurst Inlet and Coppermine areas (Fig. 23.1). During the 1977 field season the rocks of the Bathurst Inlet area from the Western River Falls to Kent Peninsula were investigated (Fig. 23.2). Two new formations have been defined (Algak and Ekalulia) and are correlated with strata in the Coppermine area (Fig. 23.8), based on the work by Campbell and Cecile (1975, 1976), and Baragar and Donaldson (1973).

The depositional history of the Helikian rocks of the Bathurst Inlet area is summarized in ascending stratigraphic order below, and in Table 23.1.

Stratigraphy

Tinney Cove Formation

Following early folding and faulting of the Aphebian Goulburn Group (Campbell and Cecile, 1975, 1976), north-northwest and north-northeast trending faulted basins were the loci of deposition of the clastic conglomerobreccias of the T_1 member of the Tinney Cove. The linear(?), fault-delineated troughs are best exposed in the Tinney Cove-Young Island area, where the minimum apparent displacement on exposed syndepositional faults is at least 75 m (Fig. 23.3).

The base of the T_2 member rests with marked erosional angular unconformity on the Brown Sound Formation of the Goulburn Group (all stratigraphic terminology of the Goulburn Group after Campbell and Cecile, 1976). Steep-sided channels are filled with angular blocks of Brown Sound and possibly Amagok formations up to 1.5 m in maximum dimension. In addition, boulders of calcite (up to 12 cm) are also present. The blocks and boulders are set in crudely trough cross-bedded, coarse grained arkose and arkosic grit.

Paleocurrent data from T_2 trough cross-beds are shown in Figure 23.4. The dispersal pattern of the T_2 member appears to be intricately related to active movement on the earlier, T_1-associated, syndepositional faults. However, due to the poor quality of the exposure, and thus the apparently limited lateral extent of the T_1, the presence of fault-related troughs could not everywhere be confirmed. The regional dispersal pattern of the T_2 appears to be a continuation of the north-west to north-northwest-paleoslope first established during deposition of the Goulburn Group (Campbell and Cecile, 1976) with local fault-controlled modification.

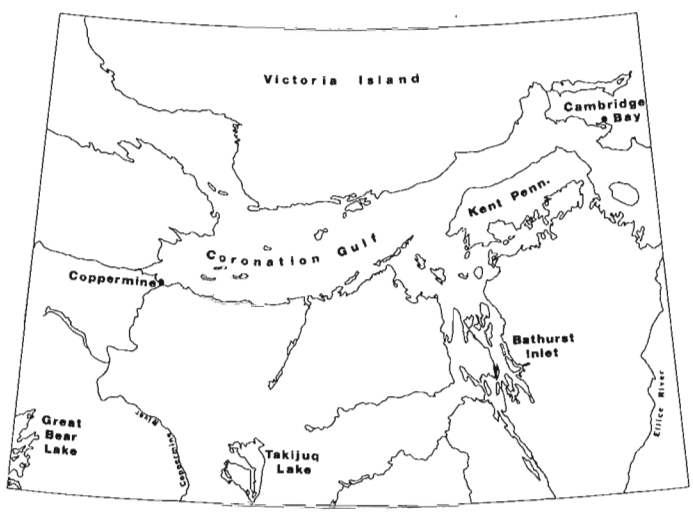

Figure 23.1. Location map.

The upper contact of the T_2 is exposed at only one known location, where it is unconformably overlain by the basal conglomerate of the Ellice River Formation. The thickness of the T_2 member is unknown, but is believed to be of the order of 250 m.

Ellice River Formation

The Ellice River Formation, first defined by Tremblay (1971), was identified in the Bathurst Inlet area by Fraser (1964) and Campbell and Cecile (1975). The formation consists of quartzites and feldspathic quartzites that are texturally and mineralogically more mature than the Tinney Cove.

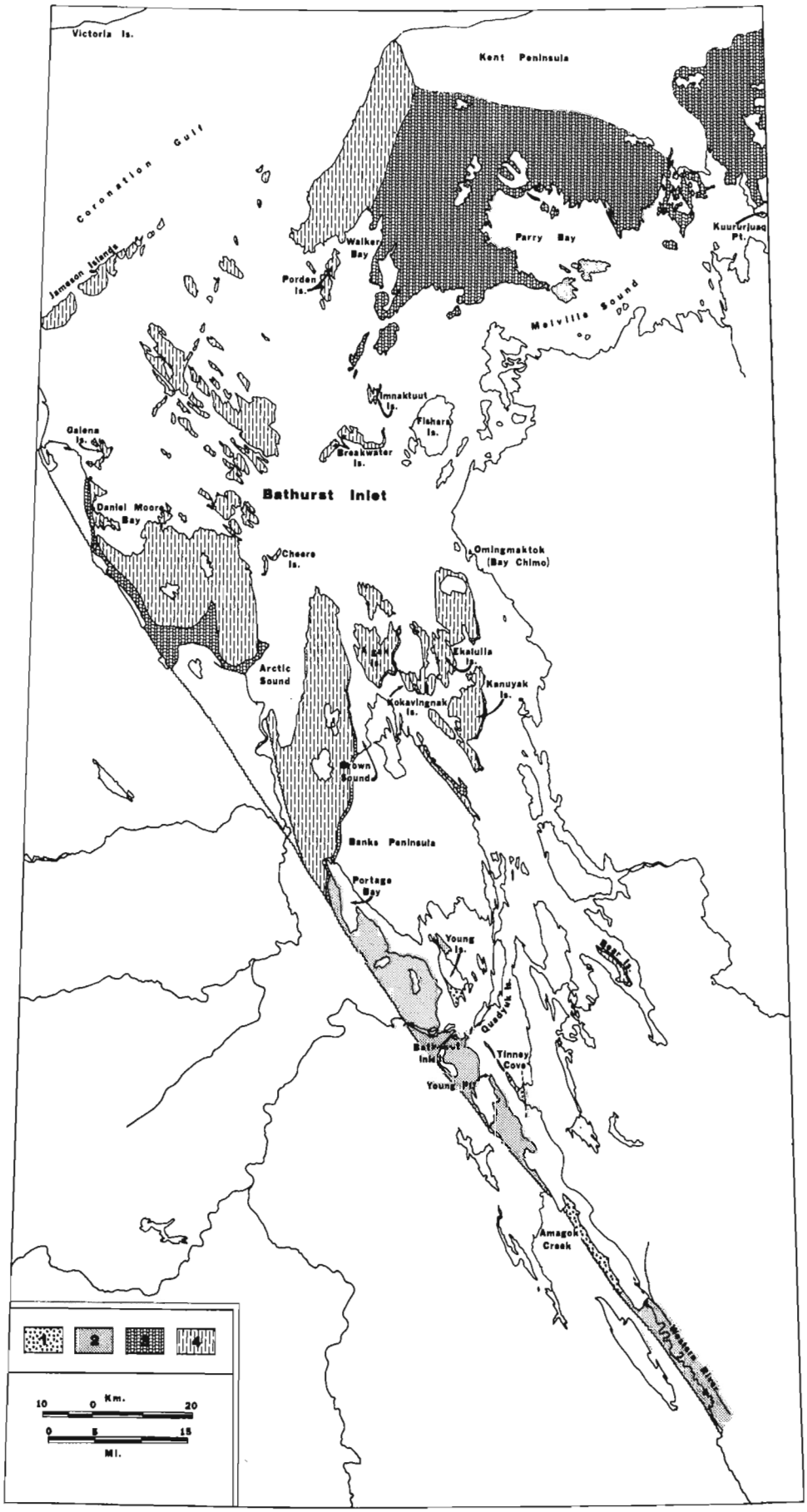

Campbell and Cecile (1975, 1976) subdivided the formation into two members – a conglomeratic phase (E_1) and a sandy phase (E_2). Detailed examination in 1977 showed that the conglomeratic phases in the upper part of the formation are the basal portions of mega-scale, fining-upward cycles, and are probably not caused by repetition of the section due to faulting. The formation is here redefined as containing two members – the basal conglomerate member (E_1) and an upper member (redefined as E_2), composed of sand-dominated, very large-scale, conglomerate-based, fining-upward cycles.

The base of the E_1 member rests unconformably on both the folded Goulburn Group and also on the arkoses of the T_2 member of the Tinney Cove succession. At Amagok Creek, the E_1 rests with angular unconformity on the Amagok Formation, and at Young Point it rests on red mudstones of the Brown Sound Formation. West of Young Island, the E_1 rests directly, with a slight angular unconformity, on T_2 sandstones. The conglomerate varies in thickness up to 40 m, and is characterized by large (10-30 cm), well rounded quartz boulders in a matrix of quartz pebbles and grit. There are no recognizable clasts of Tinney Cove in the E_1. There is an abrupt decrease in the clast sizes upwards in the member, but no lateral variation was noted, possibly due to poor exposure.

Large-scale (0.5-3 m) trough cross-bedding is locally abundant in the E_1 member, as at Amagok Creek. However, the paleocurrent data are derived mostly from the E_2 member (Fig. 23.4).

At Elliot Point, near the mouth of Burnside River, the basal E_1 member contains a thin (15 m) unit of massive vesicular basalt (E_{1B}). The sub-member is associated with ferruginous, volcaniclastic sandstones unlike the sandstones in the remainder of the formation. Vesicles in the flows, up to 1.0 cm, are filled with calcite. There is very little contact metamorphism at the base of the E_{1B} basalt, and the top of the flow is blocky, but not appreciably scoured or eroded. The sub-member was identified only at this locality and its lateral extent is unknown.

Figure 23.2.

Distribution of Helikian rocks in the Bathurst Inlet area. Locations on the map are those referred to in the text.

1 – Tinney Cove Formation;

2 – Ellice River Formation;

3 – Parry Bay Formation;

4 – Undifferentiated Kanuyak, Ekalulia and Algak formations

Adapted in part from Fraser (1964) and Campbell and Cecile (1975, 1976).

Table 23.1

Undifferentiated Paleozoic rocks

AGE		
		Unconformity
HELIKIAN		Jameson Island sediments (stratigraphic affinity uncertain): quartz-pebble conglomerate; pink and white quartzite and grit; minor siltstone (35 m).
		Algak Formation: Reddish to purple arkose and siltstone; minor mudstone and shale (35 m).
		Ekalulia Formation: Massive olive-green basalt; minor pillowed basalt; rare doloarenite (300-500 m).
		Kanuyak Formation: Dolomite block megabreccia; chert-pebble conglomerate; minor quartzite; coarse grained doloarenite; oolitic and pisolitic dolomite; stromatolitic dolomite; red arkose, siltstone, and mudstone; (0-60 m).
		Unconformity
		Parry Bay Formation: Thin- to thick-bedded doloarenite, dolosiltite, rare dololutite; minor grey-black shale and mudstone; stromatolitic dolomite; oolitic and pisolitic intraclast-bearing dolomite; rare chert-pebble conglomerate and concretionary dolomite; (220 m).
		Ellice River Formation: E_{2M} submember: Red mudstone and siltstone with minor red arkose and rare fine grained quartz-pebble conglomerate; minor beds of fine grained doloarenite; (100 m).
		E_2 member: Reddish, pink, and white quartzite with interbedded quartz-pebble conglomerate; quartz grit; minor siltstone and rare mudstone; (500 m).
		E_{1B} submember: Reddish, vesicular, massive basalt; (10-20 m).
		E_1 member: Quartz-pebble and boulder conglomerate; minor white quartzite; (2-10 m).
		Unconformity
		Tinney Cove Formation: T_2 member: Reddish, pink, and locally mottled, poorly-sorted arkose and arkosic grit; minor quartz-pebble-bearing arkose and siltstone; (200 m). T_2 member: Red, very coarse grained fanglomerate; sedimentary megabreccia; coarse grained polymictic conglomerate.
		Unconformity
APHEBIAN	GOULBURN GROUP	Amagok Formation Brown Sound Formation Kuuvik Formation Peacock Hills Formation Quadyuk Formation Burnside River Formation Western River Formation
		Unconformity
ARCHEAN		Undifferentiated gneissic and granitic rocks

The E_2 member comprises trough- and large-scale planar cross-bedded (possibly sand waves), buff, reddish or white quartzite. These sediments extend from the valley of Western River in the Beechey Lake area in the south, to the Portage Bay area in the north. Trough cross-beds vary in size up to 2 m across, and their size appears to have little relation to the paleocurrent direction.

Paleocurrent patterns in the E_2 member appear in part to be controlled by periods of reactivation along earlier syndepositional faults (Fig. 23.4). Paleocurrents south of Young Point are predominantly directed southwestwards, whereas farther north, at Young Point, they are directed mainly to the northeast, along the Quadyuk Island syndepositional faults which shed the T_1 fanglomerates. In the Portage Bay area, very large (6 m) curviplanar cross-beds are arranged in cross-cutting arrays. The dominant paleocurrent direction indicated by these cross-beds is to the southwest.

Red mudstones, siltstones, and thin, fine grained doloarenites (E_{2M} sub-member), which for the uppermost unit in the Ellice River are exposed only in the northern part of the area, outcrop on Imnaktuut and Hurd Islands (Fig. 23.2). E_{2M} strata rest directly on the orthoquartzites of the E_2 member, with little or no interbedding of the mudstone-dominated sub-member with the quartzite-dominated member. The total thickness of the E_{2M} sub-member is estimated to be about 30 m.

Mudstone and siltstone dominate the lower part of the sub-member, with doloarenites increasing in abundance and thickness towards the top of the unit. Mud flake and chip conglomerates are locally abundant in the uppermost part of the sub-member. Salt casts, mudcracks, and possible rainprints, together with abundant small-scale ripple marks, indicate the shallow marine depositional environment of the sub-member. The top of the sub-member is defined as the first appearance of fine grained dark grey doloarenite and interbedded black mudstones and siltstones of the overlying Parry Bay Formation. The contact is sharp and there is no interbedding of the red and black mudstones.

The E_{2M} sub-member also outcrops on the Hurd Islands, where it is coarser grained, and locally contains thin quartz-pebble conglomerate units with small pebbles generally less than 0.5 cm in a fine grained arkosic matrix. Planar cross-bedding is locally abundant, and hopper-shaped salt casts are common on the tops of many of the beds. The contact with the overlying rocks of the Parry Bay Formation was not observed in this area.

Thin units of red mudstone interbedded with the lowermost Parry Bay in the Portage Bay area may be the uppermost part of the E_{2M} sub-member.

Parry Bay Formation

The term Parry Bay Formation was introduced by Fraser (1964) to define those carbonate rocks which apparently conformably overlie the Ellice River Formation. Fraser (op. cit.) did not locate the contact between the two formations, but was correct in his interpretation that the two are conformable.

The Parry Bay Formation outcrops from Bear Island in the south-central part of Bathurst Inlet, to the eastern end of Kent Peninsula (Fig. 23.2). The formation is dominated by clastic, shallowing-upward cycles and laterally-linked and isolated stromatolites in the southern part of the inlet, with a marked facies change to the north (terminology after James, 1977).

The basal part of the Parry Bay Formation is exposed only in the northern part of the area on Imnaktuut Island (Fig. 23.2). There, the formation is in conformable contact

with the E_{2M} sub-member of the underlying Ellice River Formation. The lowermost part of the Parry Bay Formation consists of interbedded dark grey, fine grained doloarenite and mudstone or siltstone. Minor, thin beds of laterally-linked low-amplitude hemispherical stromatolites are also present. The total thickness of the terrigenous clastic-dominated part of the formation is approximately 25 m, and is transitional upwards into the "normal" carbonate sequence.

Many detailed sections were measured through the Parry Bay Formation, in an attempt to delineate sub-units within the formation, but with little success. However, criteria defined by James (1977) for recognition of shallowing and deepening-upward cycles were identified in all sections. The Parry Bay in the southern part of the basin appears to be dominated by repetitive shallowing-upward cycles, many capped by sheets of laterally-linked domal stromatolites, which are locally mud-cracked. These in turn are overlain by coarse or fine grained clastic dolomite, oolites, or pisolites with or without intraclasts. In the northern part of the basin the formation is dominated by stromatolitic dolomite, with minor clastic-dominated sequences.

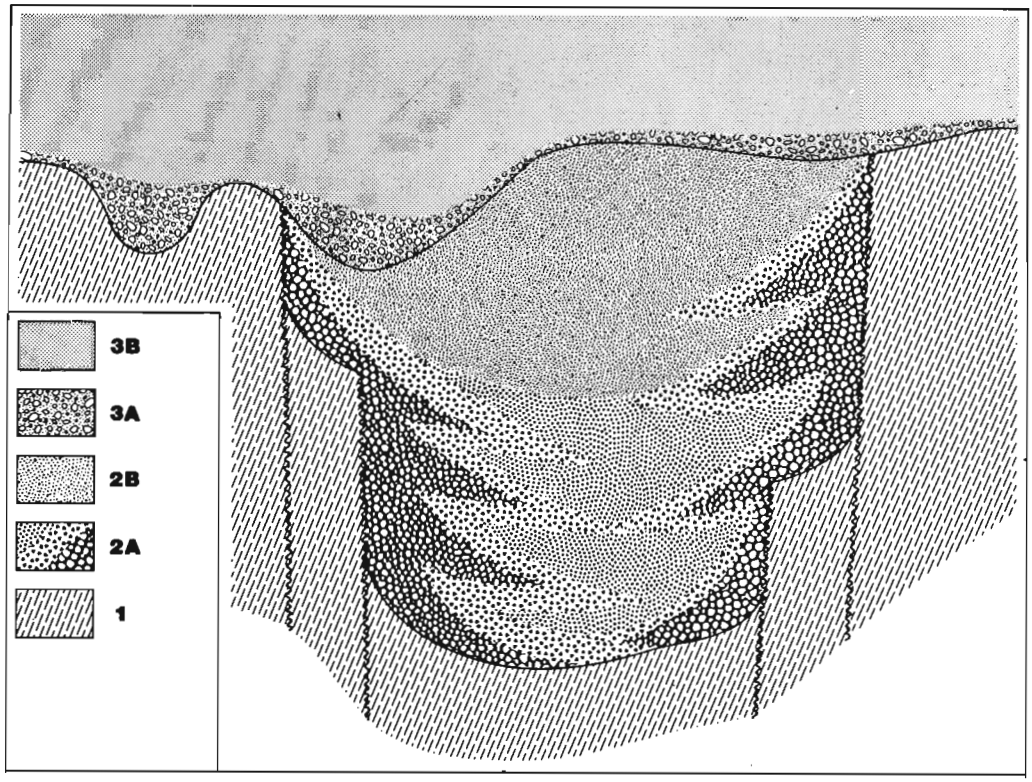

1 – Undifferentiated Goulburn Group rocks;
2A – Fanglomerates and other rocks of the T_1 member;
2B – Coarse arkose and arkosic grit of the T_2 member;
3A – Basal quartz-pebble and polymictic conglomerates of the E_1 member of the Ellice River Formation;
3B – Orthoquartzite and protoquartzites of the E_2 member of the Ellice River Formation.

Figure 23.3. Diagrammatic representation of fault-related deposition of the fanglomerates and conglomerobreccias of the T_1 member of the Tinney Cove Formation, and their relationships to the overlying rocks. The maximum known relief on the syn-depositional faults is of the order of 100 m.

Stromatolites occur in both the coarse and fine grained divisions but appear to be slightly more common in the finer grained uppermost divisions. Intraclasts of laminated stromatolite fragments occur in various sizes up to 15 cm in all divisions, but are most common in the basal division. Thin beds of oolites and pisolites, with or without intraclasts, occur predominantly in the lowermost parts of the cycles.

The laterally-linked (hemispherical) stromatolites are slightly elongate in all parts of the formation, but the elongation direction is only locally very well defined, presumably due to the coalescing nature of adjacent stromatolites. Where possible, the elongation directions of the individuals were measured to provide data on paleoslope and depositional environment (Figs. 23.5A, 23.5B). While divergent elongations were obtained in the south-central part of the area, elongations become more pronounced and tighter grouped in the northwest and northeast.

Stromatolite facies in the Parry Bay Formation

Stromatolite facies are well developed throughout the Parry Bay Formation, from Bear Island in the south to Walker Bay in the northwest (Fig. 23.2). The stromatolites increase in diversity to the north, coincident with the thickening of the entire formation. The facies changes are vertical as well as lateral, with the variations shown in Figure 23.6. The southern part of the basin is dominated by LLH, **Collenia**-type stromatolites throughout the formation. The first change in stromatolite morphology occurs on the west shore of Arctic Sound, where anastomosing branching stromatolites and well-developed "tuning-fork" branching types occur in the upper part of the section.

The contact between the LLH, **Collenia**-type stromatolites and branching varieties is abrupt. The anastomosing stromatolites show subcircular outlines of individual columns on all exposed surfaces. These are interpreted as **Tungussia**-type stromatolites in that the branching is tree-like. These are overlain in turn by large columns of conical stromatolites up to 40 cm in diameter and 1.5-2.0 m high. These are interpreted as a **Conophyton**-type. However, the columns are strongly laterally linked and individual laminae can be traced for several columns. The synoptic relief on the individual columns was at least 0.5 m in some locations, as individual laminae can be traced from the intercolumn space across the top of the column and into the next space.

The **Conophyton**-type stromatolites are in turn overlain in the northern part of the basin by steep-sided, high-relief bioherms composed of branching upright to horizontal columns. These bioherms are up to 5 m high and are separated from each other by debris-filled intermound channels. The columns themselves are slightly elongate, but most are circular. In general, the branching is of the "tuning fork" type, with little or no upward increase in the diameter of the stromatolite columns.

Overlying the bioherms is a thin sequence of small isolated and laterally-linked bioherms composed of branching and non-branching columnar stromatolites. The bioherms

vary in size up to 1.5-2.0 m high and the individual columns commonly range from the base of the bioherm to the top. Near the base they are frequently horizontal, and in one case actually grew downwards. The columns appear to originate from a central part of the small bioherm, and branch outward and gradually turn upwards at the margin of the structure. This type of bioherm with its contained anastomosing subhorizontal stromatolites is termed a "Menorah-type", after the seven-branched Hebrew candelabra. These bioherms appear to be restricted to the northernmost upper part of the Parry Bay Formation, but the area in the eastern part of Kent Peninsula was not examined, and they may be abundant there.

The top of the Parry Bay Formation is an eroded, solution-pitted, channelled surface throughout the Bathurst Inlet area, with local sharp relief up to 25 m, and gently-sloping valleys (up to 20 m) filled with either the Kanuyak or Ekalulia formations. As the top of the Parry Bay is an eroded surface and the base is not exposed, the only thickness estimates are minima; the thickest section measured was 217.4 m (west of Arctic Sound).

In summary, repetitive shallowing-upward cycles, vertical and lateral facies distribution, and elongation orientations of the contained stromatolites, together define a part of the major Paleohelikian carbonate-dominated basin in the Bathurst Inlet area. The basin is subdivided about a northeast-southwest trending slope-break into a stromatolite-dominated subtidal platform in the northern part of the basin, and a subtidal to intertidal clastic carbonate-dominated regime in the south.

Stability was maintained in the northern part of the basin throughout its depositional history while periodic fluctuations of sea level occurred in the southern part and are recorded in the clastic sequence.

Kanuyak Formation

The term Kanuyak Formation was coined by Fraser (1964) for those sediments which unconformably and discontinuously overlie the Parry Bay Formation (his unit 17a). The formation everywhere unconformably overlies the Parry Bay from Bear Island in the southeast to Kent Peninsula in the north. However, it is very thin, discontinuous, and occupies only the depressions in the Parry Bay, and never covers the entire surface of the underlying formation.

It is apparently in conformable contact with the basalts of the overlying Ekalulia Formation (unit 18 of Fraser, 1964). The thickness of the formation locally varies markedly from 0 to 118 m at a maximum. However, the latter figure includes some 35 m of breccia, which should probably not be included in the total. While the entire formation is rarely more than 30 m thick at any given location, and commonly is absent, the sequential development of the various sediments in the sections is identical at all locations, as summarized in Table 23.2.

Salt casts, mudcracks, and very small-scale ripple marks characterize the red muddy part of the formation in some parts of the basin, indicating a supratidal to intertidal environment. The stromatolites at the top of the formation in the uppermost subdivision are different from all those in the underlying Parry Bay Formation in that they form isolated hemispheres, with characteristically rippled internal laminations. Oolites, pisolites and associated intraclast breccias are commonly associated with these stromatolites, and the oolites are particularly well developed within the uppermost two metres of the formation at almost all locations.

The entire formation becomes finer grained to the north and northeast, until on Kent Peninsula (Fig. 23.2) the sediments of the formation consist almost entirely of fine grained red arkose, and laminated stromatolitic dolomite and minor doloarenite. Quartzite was noted at only one location, in the

Table 23.2

	Ekalulia Formation

KANUYAK FORMATION	Oolitic, pisolitic, and stromatolitic dolomite
	Laminated doloarenite, dolosiltite; minor quartzose dolomite and quartzite
	Red mudstone with interbedded dolosiltite
	Dolomitic arkose, chert-pebble conglomerate, arkose, minor fine grained breccia
	Coarse grained arkose, minor coarse grained doloarenite
	Dolomite-block megabreccia, minor chert-pebble arkosic conglomerate
	----------Unconformity----------

south-central part of the basin, on the mainland southwest of Kanuyak Island, where it occurs near the basal part of the formation, and was probably derived from the same source area as the underlying Ellice River Formation, which is not exposed in the area.

Paleocurrent data from trough cross-bedded, coarse grained, red arkose exposed at the north end of Portage Bay indicates dispersal from the northeast to the southwest.

The top of the formation is exposed at almost all localities. It is conformably overlain by the basalts of the Ekalulia Formation, which have flowed onto the unconsolidated and uncemented Kanuyak laminated dolomites and oolitic sediments, locally producing spectacular soft-sediment deformation structures. In the northern part of the basin at the western end of Kent Peninsula, the basalts have incorporated large blocks of Kanuyak sediments into the lowermost flows. Some possible tuffaceous sediments are also present in the uppermost 1 m of the Kanuyak, perhaps indicative of the first stages of the eruptive activity in the Bathurst Inlet area.

Pre-Kanuyak Breccias

Very coarse grained, large-scale oligomictic breccias of Parry Bay Formation fill deep depressions in the uppermost part of the Parry Bay in the Kanuyak Island-Ekalulia Island area. The flanks of these deposits, where exposed in section, are vertical to overhanging, and upwards of 25 m deep (Fig. 23.7). The lateral contacts are locally overhanging, irregular, and show no signs of movement or tectonic brecciation. In plan view, this breccia filling is apparently irregular. Likewise, the basal contact is also irregular, with numerous steep-sided scarps arranged apparently at random beneath the breccia. One very narrow (less than 2 m) breccia zone extends more than 75 m below the base of the Kanuyak Formation, but as it was only seen in cross-section, its lateral extent could not be determined.

The irregular depressions are chaotically filled with huge, angular, irregular, blocks of the adjacent Parry Bay Formation. These are completely unsorted and lack any internal vertical or lateral arrangement.

The large blocks are set in a matrix of smaller dolomite and chert fragments from concretions, also derived entirely from the Parry Bay. The tops of the breccias have been reworked and incorporated into the basal part of the overlying Kanuyak Formation. Nowhere were the Ekalulia basalts seen to rest directly on the breccias, and thus their depositional relationships are unknown.

The sub-Kanuyak breccias are interpreted as solution breccias produced during a prolonged period of pre-Kanuyak uplift and erosion. There is no indication of pre- or syn-

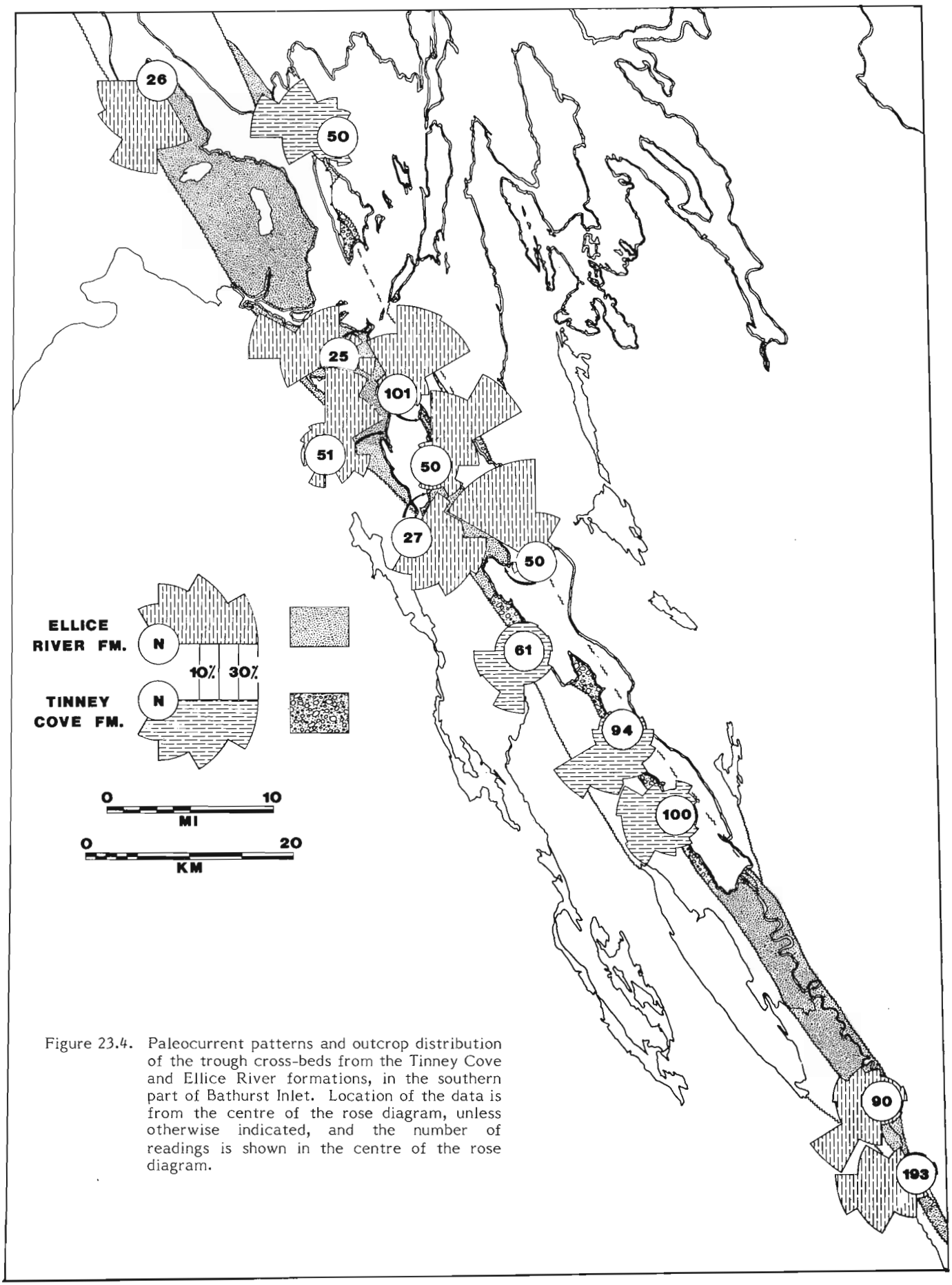

Figure 23.4. Paleocurrent patterns and outcrop distribution of the trough cross-beds from the Tinney Cove and Ellice River formations, in the southern part of Bathurst Inlet. Location of the data is from the centre of the rose diagram, unless otherwise indicated, and the number of readings is shown in the centre of the rose diagram.

depositional tectonic movement, which could have produced the breccias, as they contain no detritus of Kanuyak origin. There is evidence of minor evaporite deposition in the Parry Bay Formation, although much of the formation is shallow water, and evaporite solution collapse is a possible hypothesis.

Ekalulia Formation

The term Ekalulia Formation is here proposed for the lavas which conformably overlie the Kanuyak Formation, and locally unconformably overlie the Parry Bay Formation. Previously, these lavas had been termed the Coppermine flows (Fraser, 1964), but the use of the term Coppermine Group (Baragar and Donaldson, 1973) in the Coppermine area leads to some confusion, and the new name has thus been proposed.

The flows are named for the large island in the east-central part of Bathurst Inlet, immediately west of Bay Chimo (since re-named Umingmaktok). Although the spelling of the official name means nothing in Inuktituut the correct spelling and meaning is given in O'Neill (1924) as Ekallulialuk (translated meaning – "plenty of fish"). The formation is well exposed on this island and, in addition, both the base and the top of the formation are also present.

For the most part the flows are massive, but pillowed flows are randomly disseminated throughout. The basal massive flows rest conformably on the underlying sediments of the Kanuyak Formation. However, at one location in the basin, a 0.75-m unit of laminated doloarenite occurs some 5 m above the base, indicating a temporary return to

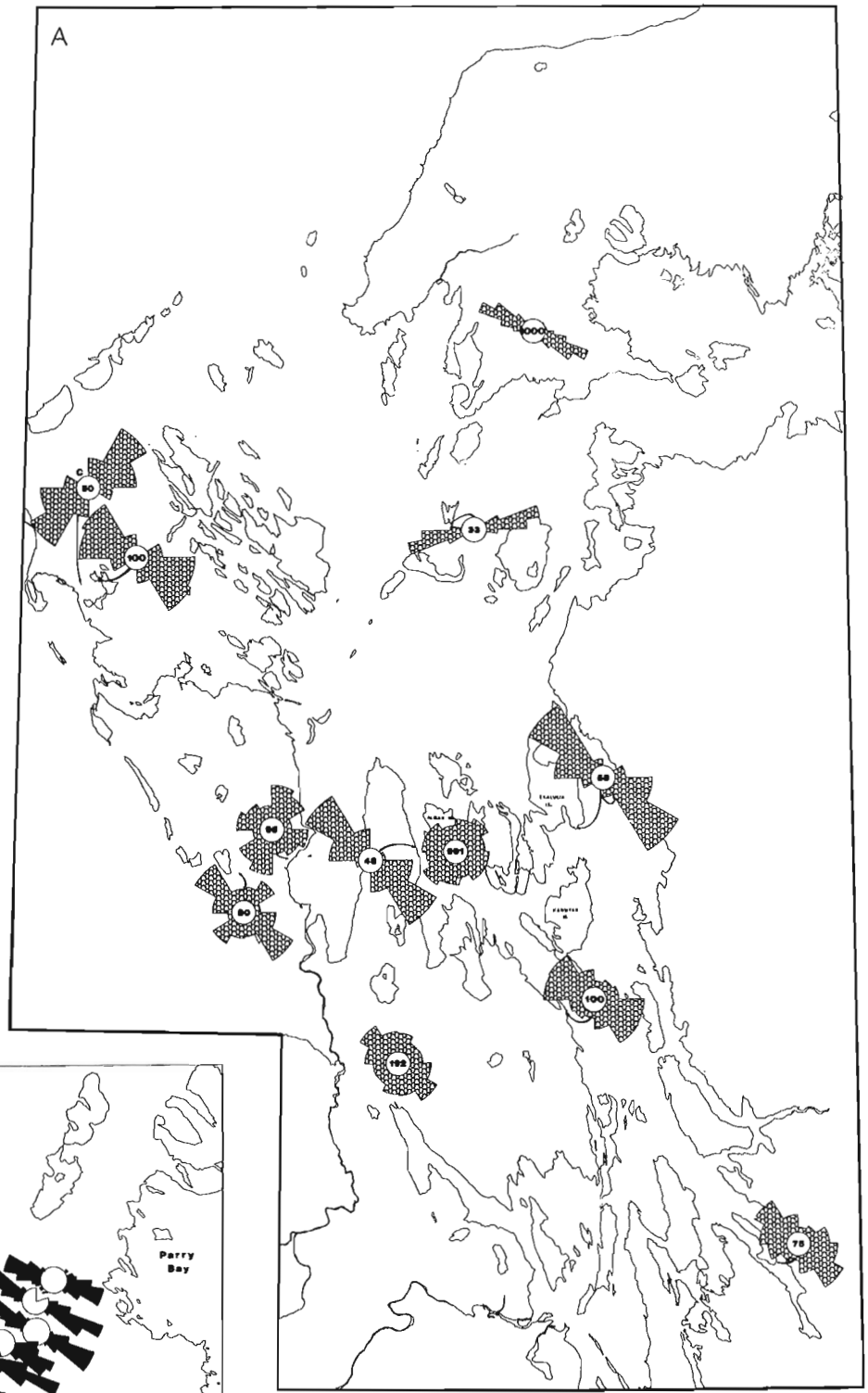

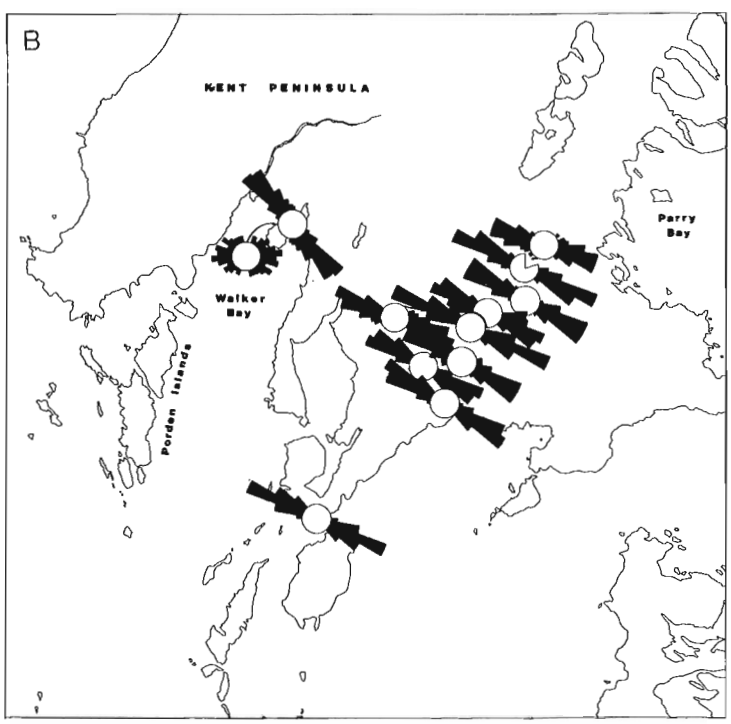

Figure 23.5

A – Stromatolite elongation orientations in the Parry Bay Formation in the Bathurst Inlet area. The diameter of the centre of the roses is 20 per cent, and the number of readings is as shown for each. The "C" designation is a slightly elongated **Conophyton** type.

B – Detailed stromatolite elongation orientations in the Parry Bay Formation, from the western end of Kent Peninsula. Data are plotted in 10° segments. The diameter of the circle is 20 per cent, and the number of readings at each location is 50. All data from the centre of the rose, unless otherwise indicated.

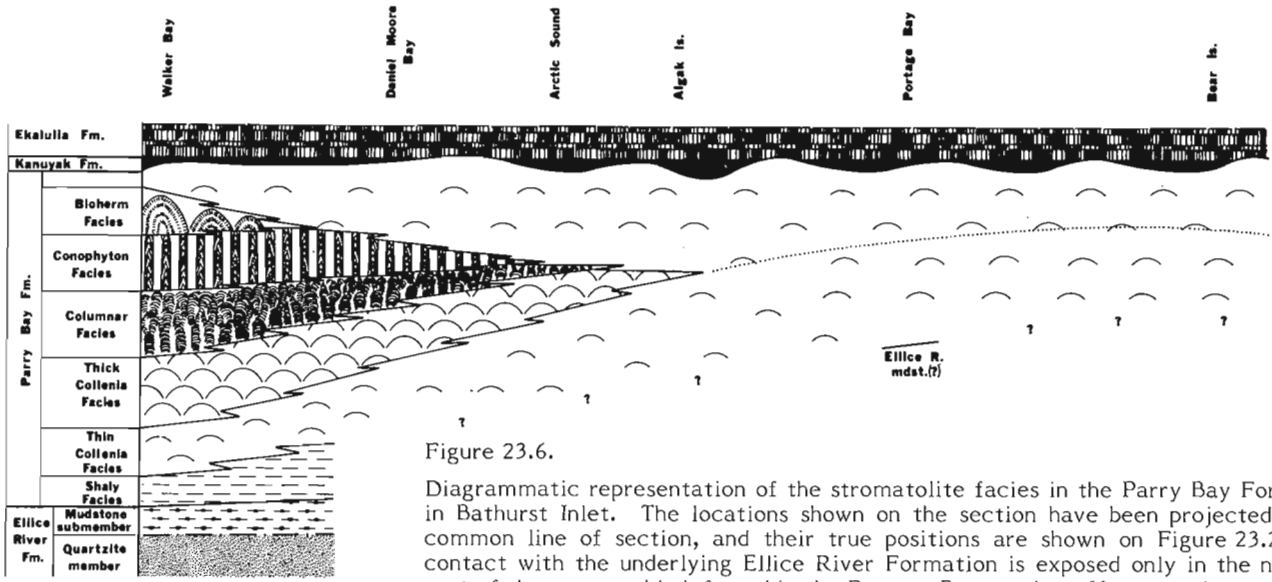

Figure 23.6.

Diagrammatic representation of the stromatolite facies in the Parry Bay Formation in Bathurst Inlet. The locations shown on the section have been projected onto a common line of section, and their true positions are shown on Figure 23.2. The contact with the underlying Ellice River Formation is exposed only in the northern part of the area, and is inferred in the Portage Bay section. Not to scale.

marine conditions. Elsewhere, pillowed flows also occur at approximately the same stratigraphic position, showing that the submergence was not a local phenomenon. Individual flows vary in thickness from 2 to 6 m, and characteristically have an olive-green massive base and a reddish brown blocky top. Vesicles filled with quartz and carbonate are locally abundant.

The top of the formation is defined as the first appearance of the thin to thick bedded, red, fine grained trough and planar cross-bedded arkose and siltstone. While the top and the base of the formation are exposed on Ekalulia Island, the thickness of the formation is unknown, due in part to the nature of the exposure, the shallow dips, and the repeated diabase sills which intrude the entire formation. The base and the top of the formation are also exposed on the southeast side of Kokavingnak Island (Fig. 23.2); there the thickness of the formation is estimated at approximately 300-500 m, but the possibility of removal of part of the formation due to faulting cannot be ruled out. Fraser (1964) estimated the total thickness to be approximately 2000 feet, but this appears to be high.

Algak Formation

The Algak Formation consists of arkose and reddish siltstone which conformably overlie the Ekalulia Formation at all localities. They are well exposed on Ekalulia and Kokavingnak islands, but the name "Algak" was chosen for the formation for phonetic reasons. Algak Island (Inuktituut for hand) is immediately adjacent to both well-exposed sections of the formation on the other islands. Fraser (1964) did not name these sediments, but they obviously form a part of the Coppermine Group of Baragar and Donaldson (1973).

The entire formation consists of thin- to thick-bedded, locally trough and planar cross-bedded reddish arkose and siltstone, with minor red mudstone and shale. These sediments occur in thin (usually less than 1 m) fining-upwards cycles with an arkosic base and a silty or muddy top. Rarely, mudcracks are present in the uppermost parts of the cycles, and mud chips and flakes are locally abundant in the basal parts. Limited, inconclusive, paleocurrent data indicates that the sediments were transported from the east to the northwest or southwest. There is no apparent variation in the sediments from the base to the top of the formation, as the proportions of the sediments remains relatively constant throughout. However, the top of the formation is not exposed in the area, and there may be finer grained sediments to the west or north which are the distal equivalents of the coarser grained sediments in the south-central part of the inlet. The maximum exposed thickness of the Algak Formation is less than 50 m.

Jameson Islands sediments

The sediments on the Jameson Islands (Fig. 23.2) are an enigma in that they bear no resemblance to the sediments in the remainder of the inlet. They consist of a basal sequence of coarse grained, trough cross-bedded, quartz-pebble conglomerate and grit, overlain by progressively finer grained pink to white-weathering quartzites, with minor finer grained sandstones and siltstones near the top of the section. Neither the base nor the top of these sediments is exposed at the sections examined, and thus their relationships to the other units in the area are uncertain. Fraser (1964) assigned these sediments to the Algak Formation (see above), but they are totally unlike the other sediments of the remainder of the formation. In addition to the abundant quartz pebbles in the lower part of the section, fragments of possible Archean rocks are also present. To the west, equivalent sediments rest unconformably on the Archean basement, and these fragments may have been derived from the west.

These sediments may also form the proximal facies of the Rae Group sediments which outcrop to the west, in the Coppermine area, and unconformably overlie the Coppermine Group (Baragar and Donaldson, 1973). However, more detailed examination of the Jameson Islands-Coppermine area is required before any interpretation of their stratigraphic affinity can be made.

Correlation

The stratigraphic succession present in Bathurst Inlet can be correlated with the sequence in the Coppermine area, but many of the units present in the latter are thinner or missing completely in the Bathurst Inlet area. For example, the Dismal Lakes Group in the Coppermine area is equivalent to the Kanuyak Formation in the Bathurst area, and the latter has a maximum thickness of only some 60 m.

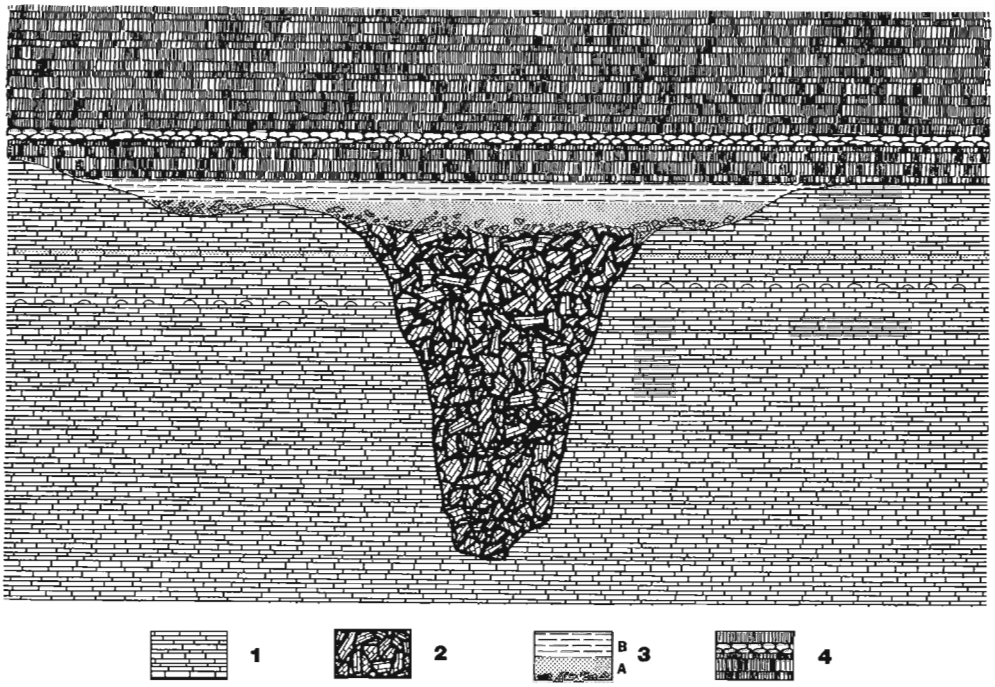

1 - Parry Bay Formation;
2 - Collapse breccia formed of blocks of the Parry Bay;
3A - Basal part of the Kanuyak Formation composed of reworked blocks of the Parry Bay breccia, set in a coarse-grained arkosic matrix;
3B - Mudstone, shale, and stromatolitic dolomite from the upper part of the Kanuyak Formation;
4 - Massive and pillowed basalt of the Ekalulia Formation.

Figure 23.7.

Diagrammatic representation of the development of solution collapse breccias in the uppermost part of the Parry Bay Formation, and their relationships to the overlying rocks. The breccia-filled structure is at least 15 m deep.

Age	Bathurst Inlet Area	Coppermine & East Arm, Great Slave Lake Areas
Helikian	RAE GROUP (?)	RAE GROUP[1]
	UNCONFORMITY	UNCONFORMITY
	ALGAK FM.	HUSKY CREEK FM.[1]
	EKALULIA FM.	COPPER CREEK FM.[1]
	KANUYAK FM.	DISMAL LAKES GP.[1]
	UNCONFORMITY	UNCONFORMITY
	PARRY BAY FM.	HORNBY BAY GP.[1]
	ELLICE RIVER FM.	
	UNCONFORMITY	UNCONFORMITY
	TINNEY COVE FM.	ET THEN GP.[2]
	UNCONFORMITY	UNCONFORMITY
Aphebian	GOULBURN GROUP	GREAT SLAVE SUP'GP.[2] & EPWORTH GP.[3]

Figure 23.8.

Proposed correlation of Helekian strata from the Bathurst Inlet area with those elsewhere in the Bear-Slave Province. Lithologic and stratigraphic data from outside Bathurst Inlet are from: 1) Baragar and Donaldson (1973); 2,3) Hoffman (1973).

The proposed correlation of the formations and the groups examined during the course of the field work in 1977 are shown in Figure 23.8. Although the Tinney Cove Formation has no equivalent in the Coppermine area, it is interpreted as correlative with the Et Then Group in the East Arm of Great Slave Lake (Hoffman, 1973).

The correlation is based on the presence or absence of unconformities, and the lithologies of the sediments and volcanics in the various formations. No correlation based on stromatolite morphologies is attempted or implied.

Structural Geology

Syndepositional north-northwest and north-northeast-trending high-angle transcurrent faults were active during the deposition of the Tinney Cove Formation. Locally, as on Young Island (Fig. 23.2), these faults become shallow angle along strike, and thrust deformed sediments of the Brown Sound Formation of the Goulburn Group over the basal conglomerobreccias of the Tinney Cove, in a manner similar to that described by Crowell (1974).

The transcurrent faults controlled the sites of maximum accumulation of the Tinney Cove, but also apparently controlled the dispersal patterns of the overlying Ellice River Formation, as shown from the rapid change in the paleocurrent patterns within the formation (Fig. 23.4).

The remainder of the formations in the Bathurst Inlet area are undeformed for the most part, except for the Parry Bay and uppermost Ellice River formations on Imnaktuut Island (see Fig. 23.2), where they are steeply dipping to the south (60°-75°), and are repeatedly faulted. This appears related to an inferred major east-west trending fault.

Elsewhere in the basin, the sediments and volcanics have been vertically displaced along the reactivated transcurrent faults. On the western side of Bathurst Inlet the entire Proterozoic succession has been stripped from the Archean basement and the Parry Bay Formation is in fault contact with the Archean gneisses. The total amount of vertical displacement cannot be estimated. The remainder of the sediments and volcanics in the basin are near-horizontal, unmetamorphosed, and apparently undisturbed.

Economic Geology

Little of economic significance was noted during the course of the season. Native copper was noted at some localities in the Ekalulia Formation, but this had been previously described by O'Neill (1924) and Fraser (1969). Some disseminated sulphides were noted locally in the dolomites of the Parry Bay Formation, but these appear directly related to the ubiquitous diabase dykes and sills in the area. On Kent Peninsula, a black mudstone and shale beneath the **Conophyton** facies of the Parry Bay Formation contains disseminated sulphides, primarily pyrite, but also some chalcopyrite, and in addition also gives a radiometric response about 10 times background on the scintillometer. This unit appears to be continuous beneath the **Conophyton** facies in the formation, but pinches out to the southwest, coincident with the thinning of the overlying stromatolitic unit.

Metamorphic "soapstone" occurs in the uppermost part of the Parry Bay Formation wherever the formation is in contact with the numerous diabase sills and dykes. It has long been utilized by the local inhabitants for carving, and most of the accessible locations show abundant evidence of long use.

References

Baragar, W.R.A. and Donaldson, J.A.
1973: Coppermine and Dismal Lakes map-areas Geol. Surv. Can., Paper 71-39, 2 maps, 20 p.

Campbell, F.H.A. and Cecile, M.P.
1975: Report on the geology of the Kilohigok Basin, Goulburn Group, Bathurst Inlet, N.W.T.; in Report of Activities, Part A, Geol. Surv. Can., Paper 74-1A, p. 297-306.

1976: Geology of the Kilohigok Basin, Goulburn Group, Bathurst Inlet, District of Mackenzie; in Report of Activities, Part A, Geol. Surv. Can., Paper 76-1A, p. 369-377.

Crowell, J.C.
1974: Origin of late Cenozoic basins in southern California; **in** Tectonics and Sedimentation, Soc. Econ. Pal. and Mineral. Spec. Pub. No. 22, Ed. by W.R. Dickenson, p. 190-204.

Fraser, J.A.
1964: Geological notes on the northeastern District of Mackenzie; Geol. Surv. Can., Paper 63-40, 1 map, 20 p.

James, N.P.
1977: Facies Models – 8. Shallowing-Upward Sequences in Carbonates; Geoscience Canada, Vol. 4, No. 3, p. 126-136.

Hoffman, P.F.
1973: Evolution of an early Proterozoic continental margin: the Coronation Geosyncline and associated aulcogens of the northwestern Canadian Shield; **in** A Discussion on the evolution of the Precambrian Crust, Eds. J. Sutton and B.F. Windley, Phil. Trans. Soc. Roy. Soc. London, Vol. 273, p. 547-581.

O'Neill, J.J.
1924: The geology of the Arctic coast of Canada, west of Kent Peninsula; **in** Report of the Canadian Arctic Expedition, 1913-1918; Southern Party – 1913-1916; Vol. XI, Geology and Geography, Part A, 107 p., 1 map.

Tremblay, L.P.
1971: Geology of the Beechey Lake map-area, District of MacKenzie – a part of the western Canadian Precambrian Shield; Geol. Surv. Can., Mem. 365, 56 p., 1 map.

24.

GEOLOGICAL ENVIRONMENT OF APHEBIAN RED BEDS OF THE NORTH HALF OF RICHMOND GULF, NEW QUEBEC

Project 770027

F.W. Chandler
Regional and Economic Geology Division

Abstract

Chandler, F.W., Geological environment of Aphebian red beds of the north half of Richmond Gulf, New Quebec; Current Research, Part A, Geol. Surv. Can., Paper 78-1A, p. 107-110, 1978.

Aphebian geological history of the north half of the east-trending graben at Richmond Gulf consists of a phase of braided fluviatile sedimentation followed by one of shallow marine deposition.

Westward transport of initial fluviatile sediments ceased on effusion of terrestrial basalt. Succeeding red beds were transported eastward. Subsequent pink and overlying grey pyritic sandstone were transported southeast to southwest. Following block faulting and marine transgression terrigenous arenites and stromatolitic dolomite were deposited and overlain by basaltic volcanics. Sedimentary units thin northward onto the margin of the graben.

Introduction

This study is part of a project which aims at an integrated knowledge of Canadian red beds and their associated mineralization. The Richmond Gulf area (Fig. 24.1) was chosen because of the known sedimentary copper mineralization and the possibility of uranium mineralization. Also the regional geology of the area has features similar to some attributed elsewhere (Burke and Dewey, 1973) to triple junction tectonics. The area was included in reconnaissance mapping of Eade (1966) and Stevenson (1968). The shore of the gulf was mapped by Woodcock (1960) who also mapped inland areas by means of aerial observations and interpretation of aerial photographs.

Geological studies in 1977 were carried out mainly by F.W. Chandler. A. Miller helped with these as well as assessing the uranium potential of the area. Red beds of the Richmond Gulf Formation were sampled by K. Clark for paleomagnetic studies. Fine grained clastics from this unit as well as from the Pachi Formation were collected for Rb/Sr isochron analysis. The lack of zircons in the Pachi volcanic unit prevented use of this mineral in radiometric dating by the U/Pb method.

New data arising from the summer's work include reassignment of the stratigraphic position of some outcrop areas, refinement of the structural geology, reinterpretation of the geological history, an account of the sedimentary environments, and information on the sedimentary copper mineralization at the base of the Nastapoka Group and on uranium in the Pachi sediments and the Richmond Gulf Formation (A. Miller, 1978).

General Geology

The stratigraphic nomenclature followed in this report is that of Woodcock (1960), except that his unconformity between the Pachi Group and the overlying Richmond Gulf Formation is considered to be a disconformity of no great significance.

The map-area lies across the northern half of a post-Archean east-trending graben that has been filled by Aphebian unmetamorphosed terrestrial feldspathic sandstone (Pachi Formation and overlying Richmond Gulf Formation). The Pachi volcanics, of similar attitude, separate the two sedimentary units. These units were block-faulted, eroded and then overlain with slight angular unconformity by the transgressive marine Nastapoka Group consisting mainly of terrigenous arenites and dolomite succeeded by a volcanic unit.

The Archean basement consists of locally hematite-stained granitic gneiss which is compositionally varied and massive to nebulitic. Minor mafic agmatite is also present. The basement is exposed as a fault-bounded 200 m high cliff overlooking the northern shore of the gulf at the edge of the graben. It is also exposed in the form of east-trending partially fault-bounded horsts that form high rounded hills in the central and southern parts of the map-area.

Sedimentary rocks of the Pachi Group nonconformably overlie the basement over much of the area. They are extensive around Persillon Lake, more so than as shown by Woodcock (1960). Three kilometres west of the lake they are over 500 m thick but are considerably thinner over horsts and pinch out at the northern edge of the graben. In various localities the basal beds of the Pachi sediments vary from fine grained sandstone to boulder ortho- and paraconglomerate. They range through grey-green to pink or may be hematite-stained. They are predominantly quartzofeldspathic in composition and white quartz pebbles are generally present.

West of Persillon Lake the overlying strata consist of waxy green grit with scattered white quartz pebbles. The bulk of the overlying remainder of the unit consists mainly of trough cross-bedded pink feldspathic sandstone and pebbly grit. The pebbles consist of white quartz and angular fragments of pink granite and feldspar. Minor red or green mud-cracked siltstone and white quartz pebble layers a few centimetres thick are also present. The upper 100 m of the unit, generally exposed in cliff sections, is of similar lithology to the bulk of the unit but is distinguished by an unusually high concentration of ilmenitic(?) black sand laminae and by several units of red and green laminated siltstone-mudstone up to 4 m thick. The most continuous of these fine grained units was traced over a kilometre.

A coarser facies is restricted to that part of the formation north of the North River. It consists of quartz-pebble conglomerate and arkose with quartz pebbles. The conglomerate is hematite stained and at least 10 m thick. The arkose contains abundant, probably ilmenitic black sand laminae.

The Pachi volcanic unit of basaltic composition (Hews, 1976) conformably overlies the Pachi sediments and overlaps them north of Richmond Gulf. It forms the cap rock of prominent cuestas and its thickness varies from 20 to at least 50 m. The fresh rock is maroon-grey. Soft sediment deformation of the Pachi sediments is widespread at its lower contact and evidence of lithified clasts of this underlying unit is absent. The sandstone has been baked at least a metre

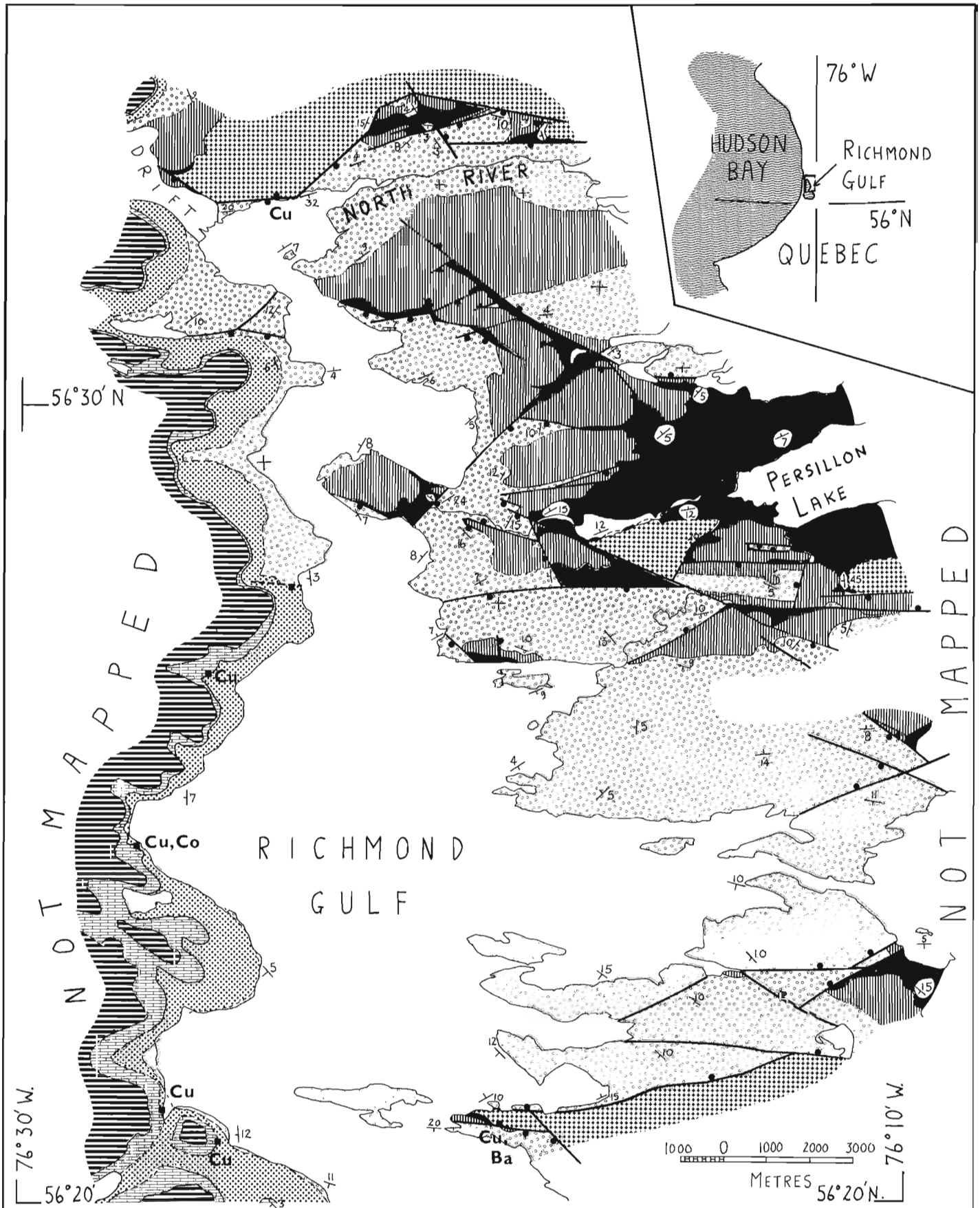
HUDSON BAY
76°W
RICHMOND GULF
56°N
QUEBEC
NORTH RIVER
DRIFT
PERSILLON LAKE
56°30'N
NOT MAPPED
NOT MAPPED
RICHMOND GULF
Cu
Cu
Cu,Co
Cu
Cu
Cu, Ba
76°30'W.
56°20'
76°10'W.
56°20'N.
1000 0 1000 2000 3000
METRES

Figure 24.1

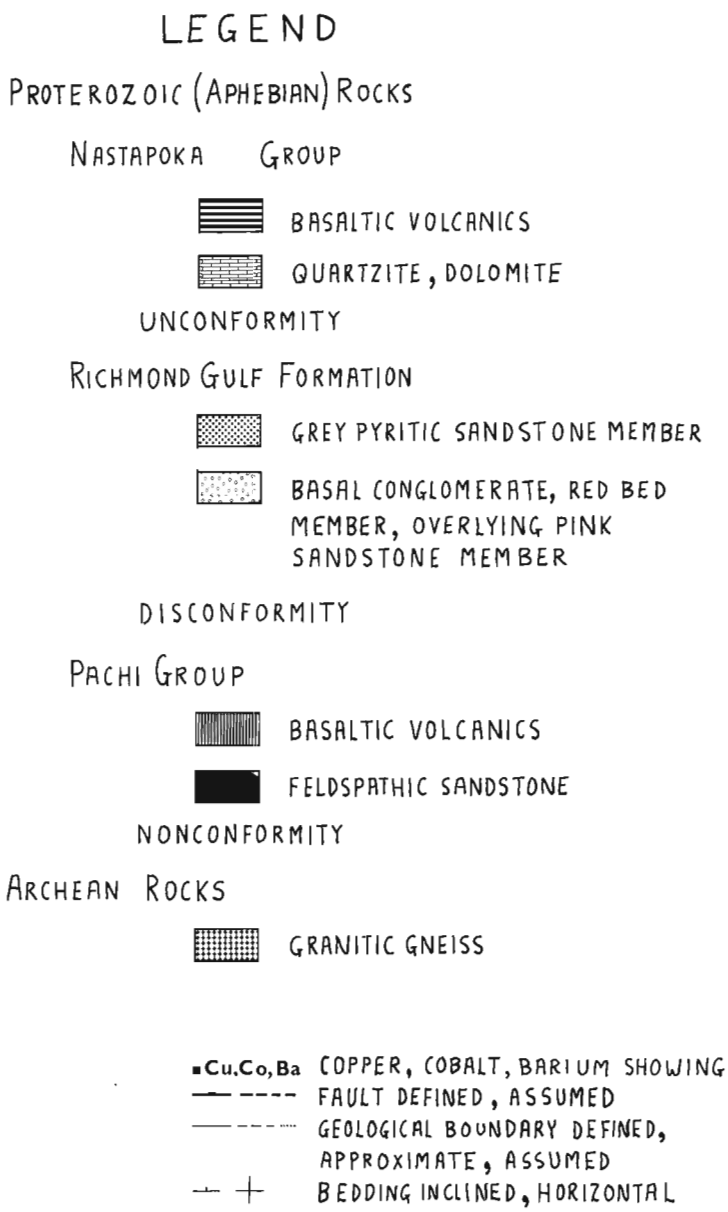

Figure 24.1 Geological map of the north part of Richmond Gulf, New Quebec.

below the contact. In the volcanic unit vesicles, small agates and columnar joints (Woodcock's (1960) ellipsoidal structures) are widespread. Except for one example 1.5 km northwest of Richmond Gulf interflow sediments are absent. Pahoehoe lava toes in the middle of the unit suggest that it may comprise more than one flow closely spaced in time. The upper few metres of the unit are red and aphanitic, and the upper surface bears ropy flow structures.

The Richmond Gulf Formation disconformably succeeds the Pachi volcanic unit. The basal member of the formation is a cobble to boulder conglomerate composed entirely of fragments of the underlying volcanic unit. It is generally no more than 1 m thick and is absent in places. It is set in a red fine grained sand to grit or rarely carbonate matrix. The conglomerate is overlain by three successive members, a red bed, a pink feldspathic sandstone and a grey feldspathic sandstone member. Since the boundary between the red bed member and the pink member is not clearly defined the two units have not been separated on the accompanying map (Fig. 24.1). Woodcock (1960) pointed out the influence of granitic source rock in determining the colours of the different rock-types of the Richmond Gulf Formation. This writer would rather stress the presence of iron oxide minerals or of pyrite in the heavy mineral fraction of he sedimentary rocks.

The red bed member, at least 80 m thick south of the mouth of the North River, consists of pink to red cross-bedded sandstone, fine grained red flaggy sandstone and rippled, mud-cracked dark red siltstone. Ilmenitic(?) black sand laminae are prominent in the red bed unit. The pink feldspathic sandstone member, probably more than 100 m thick consists of alternating pink and grey-green coarse grained sandstone and grit with scattered white quartz, pink granite, pink feldspar and rare volcanic pebbles, the last probably derived from the Pachi volcanic unit. Black heavy minerals are less prominent than in the red bed member. The pink feldspathic member passes gradationally upward into a unit not dissimilar in its sedimentary structures, texture, and the composition of its clastic grains. This grey member, up to 180 m thick, is distinguished from the underlying unit by its pure white, light grey or buff weathering colour, by the grey colour of the fresh rock, and by the presence of disseminated pyrite rather than black heavy minerals.

The Richmond Gulf formation is overlain with gentle angular unconformity by the Nastapoka Group. The sediments of this group are about 100 m thick in the southwest corner of the map-area and thin to about 6 m in the northwest corner. In the south the sediments consist mainly of laminated and stromatolitic dolomite and of quartz and feldspathic arenites and in the north of fine grained red and buff sandstone and siltstone and minor mud-cracked shale.

The unconformity beneath the Nastapoka Group has a sharp local topography upon the Richmond Gulf Formation that includes cliffs and hills with a relief up to 25 m. These features are flanked by pebble to cobble conglomerate composed of carbonate fragments and fragments from the underlying Richmond Gulf Formation as well as by carbonate-cemented cross-bedded feldspathic sandstone. Where the relief on the unconformity is not marked, the basal unit is a brittle laminated silty dolomite. The sediments of the Nastapoka Group are overlain by a basaltic (Woodcock, 1960) volcanic unit which contains columnar joints and abundant agates.

Structure

East of Richmond Gulf the pink feldspathic member of the Richmond Gulf Formation and older units are strongly block-faulted. The throw of the faults is normal and stepped southward away from the margin of the graben, or near horsts

the throw is away from the horsts. Individual faults have throws up to 50 m. West of Richmond Gulf more or less east-striking fractures transect the grey sandstone member of the Richmond Gulf Formation and the overlying Nastapoka Group, but these units are little displaced. Bedding in the block-faulted rocks dips less than 20° except near faults where dips of 45° are not uncommon. Dip azimuths are varied. West of Richmond Gulf the younger rocks which are not block-faulted dip more gently to the west.

Geological History

Woodcock (1960) suggested that Richmond Gulf lies upon the site of an east-trending graben. Northward thinning, overlap and facies changes in the sequence indicate that the graben had relief during deposition of most of the sediments.

Though most prominent in the red bed member of the Richmond Gulf Formation mud-cracked sediments occur throughout the Pachi Group and the Richmond Gulf Formation. Unimodal paleocurrents measured mainly from trough cross-beds and ripple marks suggest terrestrial instead of intertidal environments of deposition during exposure, especially since no marine sediments are suspected in the Pachi Group and the Richmond Gulf Formation. Transport of the Pachi sediments was south-westward from a granitic source area. A very low content of fine-grained material suggests a braided rather than a meandering fluvial regime.

The presence of widespread laminated and rippled siltstone units, in the upper part of the Pachi sediments one of which is mud-cracked throughout is suggestive of sometimes ephemeral lacustrine conditions.

Evidence already considered suggests that subaerial extrusion of the Pachi volcanics interrupted this regime. Abundance of mud-cracked fine grained sediments as well as small scale of fining-upward cycles and eastward directed paleocurrents measured from trough cross-beds and ripple marks in the red bed member of the Richmond Gulf Formation suggest that the extrusion of the underlying volcanic unit may have reduced and reversed the paleoslope of the north half of the graben. Paleocurrents measured from the pink member in the south part of the map-area and a few from the grey member changed from southward to south-westward. It is possible that the barrier to paleoflow caused by the Pachi volcanic episode was now less significant.

Following deposition of the red bed member of the Richmond Gulf Formation but before deposition of the Nastapoka Group the sediments were tilted by extensive block-faulting. The raised blocks formed cuestas composed of the Pachi sediments and capped by the Pachi volcanics, and the red beds of the Richmond Gulf Formation underlie many depressed blocks. Woodcock's (1960) observation that the red beds were deposited in valleys formed as a result of the block faulting appears incorrect.

Lithification and erosion of the grey member of the Richmond Gulf Formation into a landscape of some relief preceded a marine transgression and deposition of the shallow marine sediments of the Nastapoka Group. Northward thinning and facies change in the group are evidence that the graben had relief during the transgression.

Economic Geology

Mineralization in the area includes copper and uranium. The former is present in both the sediments and in the Archean gneiss. Uranium is present in the sediments of the Pachi Group and the Richmond Gulf Formation (A. Miller, 1978).

Copper in the sediments is present as chalcopyrite, bornite and green secondary minerals in sandstone at the top of the Richmond Gulf Formation and in carbonate at the base of the Nastapoka Group. Erythrite (cobalt bloom) accompanies chalcopyrite and pyrite in the carbonate at one locality (Fig. 24.1). As far as the writer knows cobalt has not previously been reported from the area. The middle two of the four copper occurrences shown on the west side of Richmond Gulf (Fig. 24.1) are already known (Stevenson, 1968). It may be significant that the mineralization was found where a red bed sequence with an upper grey pyritic part is overlain by biogenic marine carbonates. In the vicinity of the northern three examples of copper mineralization mentioned above the upper 10 m or so of the grey member of the Richmond Gulf Formation is exceedingly rust stained. Some grab samples from the rusty sandstone would deserve the name pyritite.

Traces of chalcopyrite are also present in a fracture in the basement at the northern end of the Gulf and in a 2 m square barite-rich pod in the basement at the southern boundary of the area.

Geochemical uranium anomalies were found by A. Miller in hematitic quartz-pebble conglomerate and in arkose with quartz pebbles in the Pachi Formation as well as associated with black sand layers in red beds in the Richmond Gulf Formation. Values of several times background were detected by neutron activation analysis. A more comprehensive discussion of the uranium anomalies is given by Miller (1977).

References

Burke, Kevin and Dewey, J.F.

1973: Plume-generated triple junctions: Key indicators in applying plate tectonics to old rocks; J. Geol., v. 81, p. 406-463.

Eade, K.E.

1966: Fort George River and Kaniapiskau River (west half) map-areas, New Quebec; Geol. Surv.Can., Mem. 339, 84 p.

Hews, P.C.

1976: A Rb-Sr whole-rock study of some Proterozoic rocks, Richmond Gulf, Nouveau Quebec; M.Sc. thesis, unpubl., Carleton Univ., Ottawa, 64 p.

Miller, A.

1978: Uranium reconnaissance of the northern Richmond Gulf area, New Quebec; in Current Research, Part A, Geol. Surv. Can., Paper 78-1A, report 25.

Stevenson, I.M.

1968: A geological reconnaissance of Leaf River map-area, New Quebec and Northwest Territories; Geol. Surv. Can., Mem. 356, 112 p.

Woodcock, J.R.

1960: Geology of the Richmond Gulf area, New Quebec; Geol. Assoc. Can., Proc., v. 12, p. 21-40.

25. URANIUM RECONNAISSANCE OF THE NORTHERN RICHMOND GULF AREA, NEW QUEBEC

Project 750058

A.R. Miller
Regional and Economic Geology Division

Abstract

Miller, A.R., Uranium reconnaissance of the northern Richmond Gulf area, New Quebec; Current Research, Part A, Geol. Surv. Can., Paper 78-1A, p.111-117, 1978.

Ground radiometric and geochemical anomalies were located within the Proterozoic red bed sequence, Richmond Gulf area, New Quebec. Uranium and/or thorium anomalies occur at the Archean-Proterozoic unconformity, in pebbly lenses and beds of the Pachi arkose and within coarse pink arkoses of the Richmond Gulf Formation.

Introduction

This project was conducted during the 1977 field season within portions of NTS zone 34C/8,9, Richmond Gulf area, New Quebec. The purpose was to examine and evaluate the geological favourability for uranium mineralization within the Proterozoic red bed sequence and underlying basement complex. The uranium evaluation was conducted in conjunction with stratigraphic and sedimentological studies of the red bed sequence under the direction of F.W. Chandler.

This report discusses

1) the types of radioactive anomalies and their stratigraphic position;

2) petrography and mineralogy of the anomalies;

3) uranium and thorium contents of the various stratigraphic units and anomalous zones within the study area.

General Geology

The rocks of the Richmond Gulf area have been divided into two groups: the upper Nastapoka Group and lower Richmond Gulf Group. The uranium investigation was restricted to the lithologies of the Richmond Gulf Group and underlying basement complex. Woodcock (1960) divided the lower Proterozoic strata of the Richmond Gulf area into two unconformable rock sequences: the lower Pachi Group consisting of a lower arkose overlain by an extrusive unit of andesitic composition, and the upper Richmond Gulf Formation consisting of conglomerate, red and maroon mudstone-arkose sequences grading into grey arkose.

The basement complex consists of massive to weakly foliated leucocratic granitic and granodioritic gneisses. Quartz-potassic feldspar pegmatites and white quartz stringers conform with the regional foliation and remnant infolds of biotite paragneiss. The basement rocks exposed immediately below the unconformity southwest of lac Persillon and beneath the outlier north of Richmond Gulf exhibit an intense reddening of the potassic feldspar, light apple green saussuritization of the plagioclase, and chloritization of the mafic minerals. These features suggest a relict portion of a deeply weathered regolith.

The Pachi Group rests with angular unconformity upon the basement complex. Briefly the Pachi arkose consists of a basal white quartz and granite cobble to boulder conglomerate overlain by a thin, light green sericitic arkose which grades upwards into coarse pink to red cross-bedded arkose. The latter is overlain conformably by a highly hematitized and propylitized andesitic unit.

The basal volcanic boulder conglomerate of the Richmond Gulf Formation lies with angular unconformity upon the Pachi volcanic unit. The remainder of the Richmond Gulf Formation consists of a thick sequence of cross-bedded red and maroon mudstone-arkose units grading up section into grey and white cross-bedded arkoses. Sedimentary structures in the Pachi arkose and Richmond Gulf arkoses indicate a braided fluvial environment (Chandler, 1978).

The Pachi arkose and Richmond Gulf Formation are relatively flat lying with bedding attitudes to 20 degrees. The area is intensely block faulted about east-west and northwest-southeast directions. The resulting topographic expression is one of long linear to curved cuestas. The dip slopes expose the Pachi andesite and the volcanic boulder conglomerate – red to maroon mudstone-arkose of the Richmond Gulf Formation whereas the precipitous to steep scarp slope allows excellent exposure of the Pachi arkose. The scarp slope permits examination of between 50 and 175 m of the Pachi arkosic section. The intense faulting of the supercrustal rocks is manifested by zones of closely spaced joint sets. Fracture fillings, consisting of quartz, calcite and chlorite are rare; no radioactive fracture zones in the supercrustal rocks were recognized during ground traverses.

Radioactive Anomalies

Field radiometric readings were conducted with a McPhar TV-1A scintillometer. Radioactive anomalies were detected within the underlying basement complex, Pachi arkose and Richmond Gulf arkose. The radioactive anomalies were divided into:

1) hematite-filled fractures within the basement complex adjacent to the unconformity and;

2) black heavy mineral concentrates within the Pachi and Richmond Gulf arkoses.

1. Hematite-filled fracture zones

Anomalous radioactive fracture zones were found within the basement complex immediately below the unconformity northeast of the North River and southwest of lac Persillon (Fig. 25.1). The red, biotite-rich granitic rocks near the unconformity northeast of the North River contain narrow hematite-cemented brecciated fracture zones. Fractures consist of angular granite fragments cemented by very fine grained hematite and specularite. Individual fractures were traced up to 20 m along strike with widths to 3 cm. Scintillation readings are sporadic along strike but are consistently three to four times background levels compared to the hosting biotite granite. Scintillation responses indicate a significant thorium content and little, if any, uranium. No secondary uranium minerals were recognized.

The leucocratic saussuritized gneiss southwest of lac Persillon contains fine fracture zones parallel to the regional foliation. These fracture zones commonly associated with quartz-potassic feldspar pegmatitic stringers contain hematite-specularite knots to 5 mm in size. These hairline fracture zones exhibit a similar radiometric signature as the brecciated fractures northeast of the North River.

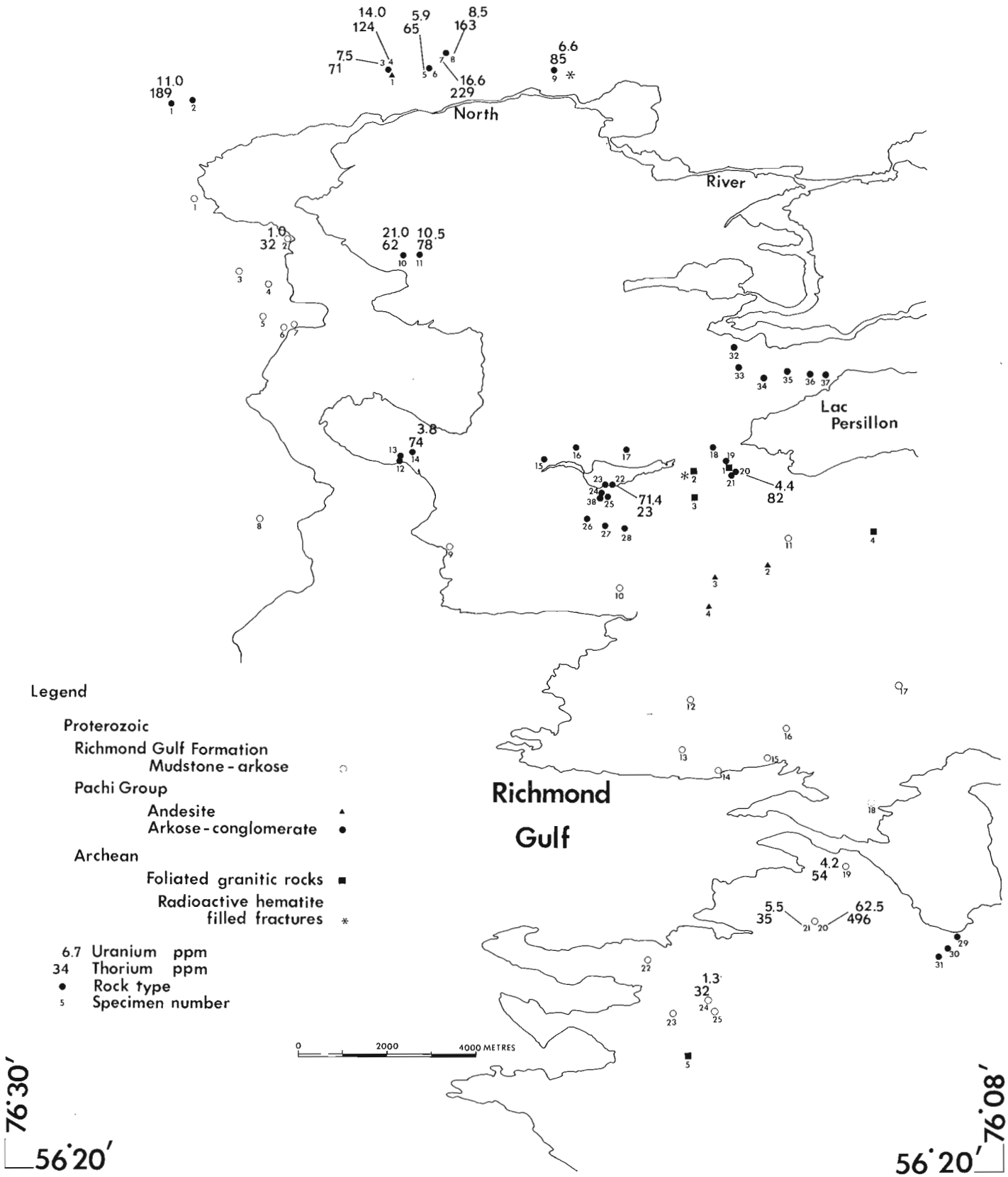

Figure 25.1. Sample locations and anomalous uranium and/or thorium contents for rocks from the Richmond Gulf area, New Quebec.

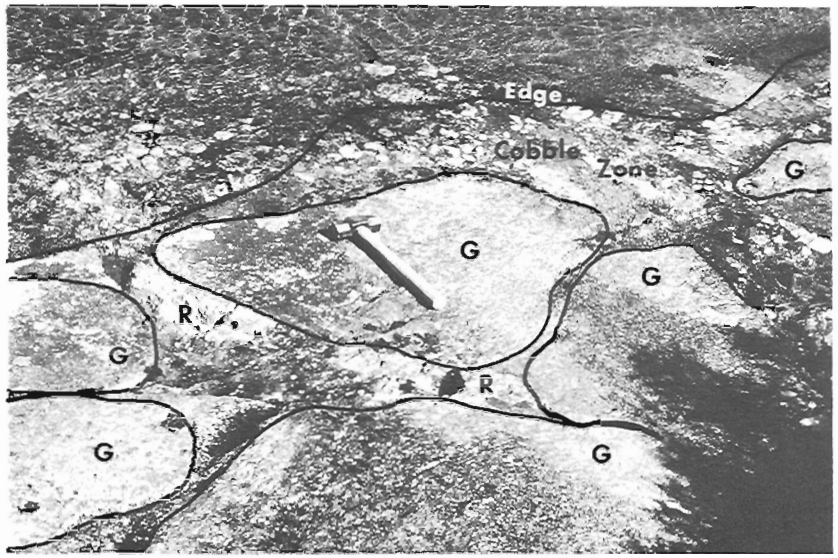

Figure 25.2. Photograph of the Archean-Proterozoic unconformity located immediately west of lac Persillon, site of anomalous Pachi specimen 22. The Pachi conglomerate consists of quartz cobbles, granitic boulders (G) with radioactive interstitial poorly sorted arkose (R).

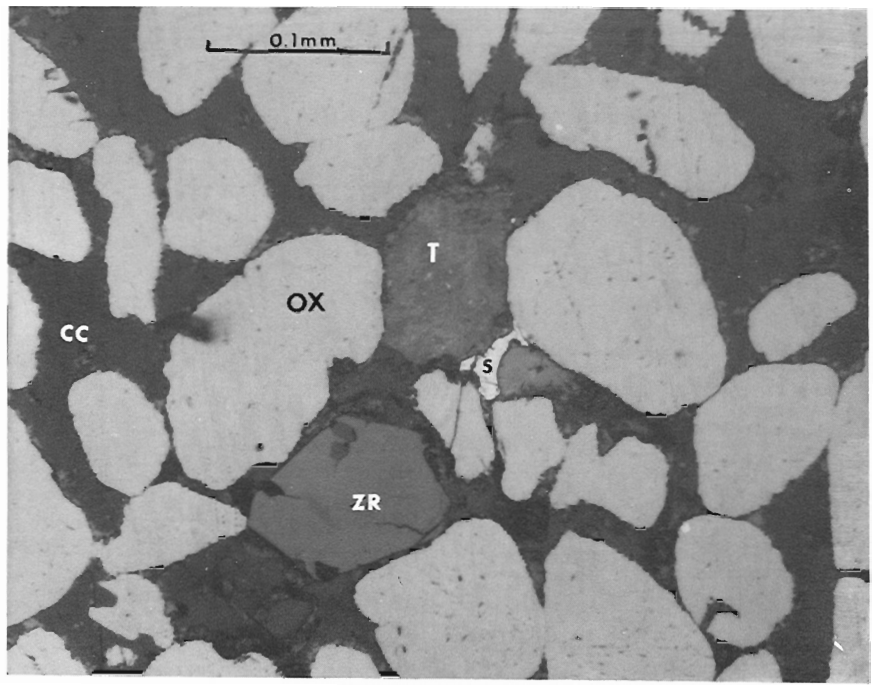

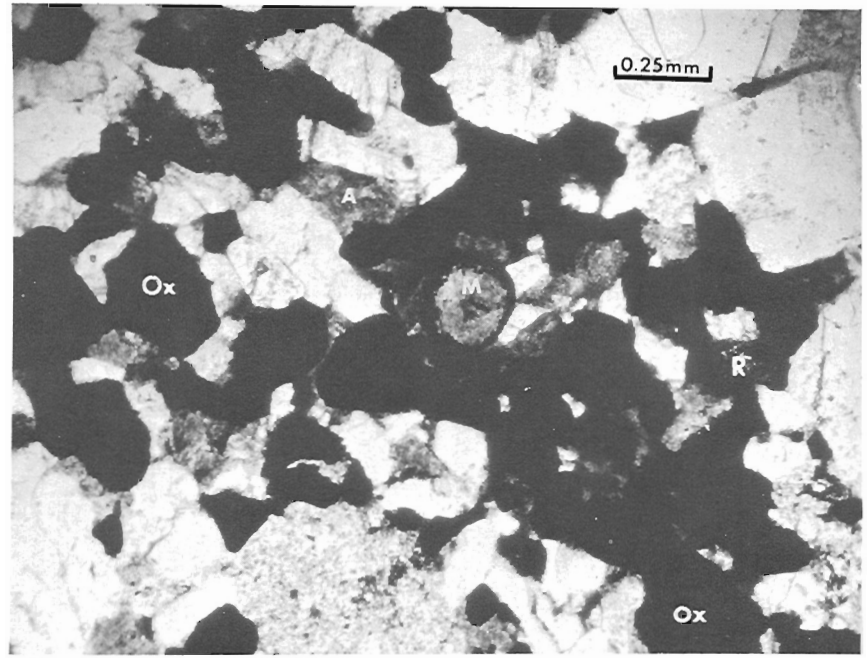

Figure 25.3. Photomicrograph of tourmalinized quartz pebbly arkose with interstitial detrital heavy minerals: thorium-rich monazite (M), black magnetite and titanomagnetite (Ox) and secondary rutile/anatase aggregates (R). Clear areas are quartz, feldspar and quartz-feldspar granitic clasts. Interstitial areas (A) consist of very fine grained sericite, hematite and tourmaline. Pachi specimen 11, Table 25.1. Transmitted light.

Figure 25.4 (left)

Photomicrograph of black heavy mineral rich cross-bed, Richmond Gulf Formation, specimen 20, Table 25.1. Cross-bed consists of magnetite and titanomagnetite (Ox), zircon (ZR), mottled thorite (T) cemented by calcite (CC) and iron sulphide (S). Reflected light.

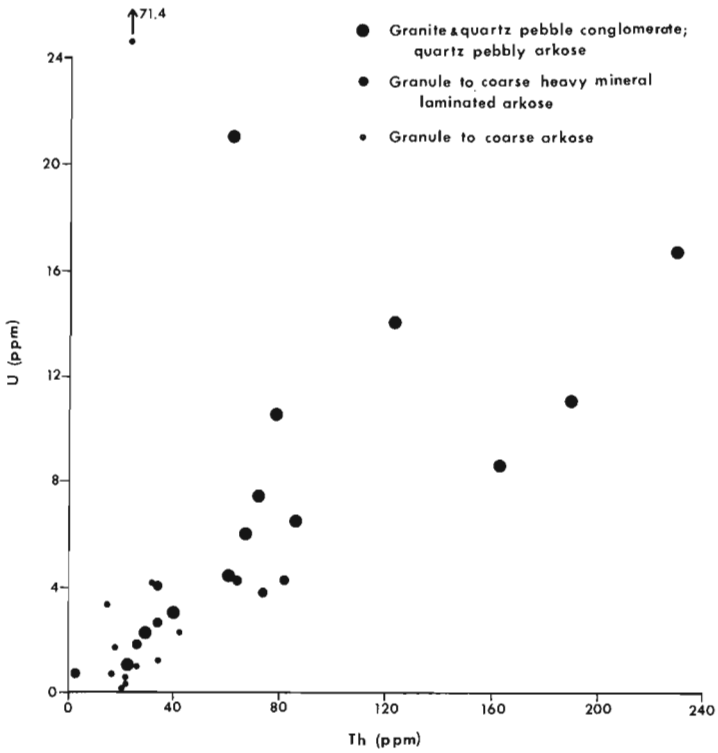

Figure 25.5. Uranium vs thorium plot for various lithologies of the Pachi arkose.

2. Radioactive heavy mineral concentrations

Radioactive, black, heavy mineral sands were recognized within the Pachi arkose and red, maroon and pink arkoses of the Richmond Gulf Formation. The radioactive anomalous sands occur at three stratigraphic levels:

1) the conglomerate at the Archean-Proterozoic unconformity;

2) pebbly arkose and granite-quartz pebble conglomerate zones within the Pachi arkose and;

3) coarse pink arkose of the Richmond Gulf Formation.

The Archean-Proterozoic unconformity is characterized by a granite cobble to boulder conglomerate. This basal unit was recognized at several localities by F.W. Chandler and the writer and several small pods were seen in fault contact with the basement complex. All faulted conglomeratic pods are nonradioactive. The unfaulted radioactive unconformity southwest of lac Persillon was examined along a strike length of approximately 3000 m (Fig. 25.1, Pachi specimens 19, 22, 23) and give anomalous and above background uranium and/or thorium contents. The basement complex at this location is interpreted as a topographic high during Pachi sedimentation.

Radioactive lenses and beds of Pachi quartz pebbly arkose occur between greenish sericitic arkose near the base of the Pachi arkose to within 15-25 m of the top of it, a stratigraphic interval of approximately 225 m. Lenses are up to 60 m in strike length and up to 2 m in thickness. The pebbly arkose lenses are interpreted as gravel bars within the braided fluvial system.

Radioactive beds were examined for strike lengths up to 1.5 km because of the excellent exposure along scarp slopes. Individual beds or series of beds vary up to 3 m in thickness and are maroon, pebbly, with interstitial black heavy mineral concentrations or characterized by zones of numerous

Table 25.1

Partial Analyses of Thorium Minerals

	Pachi Arkose		Richmond Gulf Arkose			
	Specimen 11		Specimen 20			
	Grain 1	Grain 2	Grain 1	Grain 2	Grain 3	Grain 4
SiO_2	15.3	16.0	10.6	14.9	13.9	13.2
ThO_2	56.8	57.0	46.1	53.6	52.1	50.9
UO_2	1.6	1.3	0.6	3.6	3.4	1.2
PbO	0.0	0.0	2.4	0.1	0.1	0.1
FeO	3.4	1.4	10.7	3.7	6.2	16.0
CaO	1.4	2.1	1.9	1.6	1.6	1.2
P_2O_5	1.7	1.8	4.4	2.4	2.4	1.8
Y_2O_3	1.4	1.4	0.8	1.4	1.9	0.8
Nd_2O_3	2.1	1.9	2.1	1.4	1.4	1.4
Ce_2O_3	2.8	2.7	2.6	2.2	1.8	2.0
La_2O_3	N.A.	N.A.	1.2	0.6	0.6	0.7
S	0.1	0.2	9.8	1.2	2.4	0.6

N.A. = Not Analyzed

discontinuous heavy mineral foreset beds. The lateral continuity of the radioactive, pebbly, cross-bedded arkose, the fining upward character of the radioactive beds, variation in heavy mineral accumulation within beds and light pink, coarse, heavy mineral deficient beds underlying the anomalous beds suggest that the radioactive beds represent flood deposits in a fluvial system.

The Richmond Gulf mudstone-arkose sequence contains anomalously radioactive heavy mineral foreset beds within light pink, coarse grained, hematite-mottled, trough cross-bedded arkose. Black heavy mineral beds occur generally as wispy 1-2 mm foreset beds and rarely as discontinuous ripple laminated planar beds and foreset bed accumulations up to 8 cm thick.

Petrography of the Radioactive Arkosic Units

1. Basal Archean-Proterozoic unconformity

The unconformity is exposed along the southern shore of the small lake immediately west of lac Persillon. The unconformity is marked by a cobble to boulder conglomerate with clasts of granitic potassic feldspar augen gneiss, foliated granite, white quartz, quartz-potassic feldspar pegmatoids and rare jasper (Fig. 25.2). The radioactive sand beds and the detritus that is interstitial to the pebbles and boulders, consist of poorly sorted (0.07-2 mm) quartz, feldspar and composite quartz-feldspar grains set in a sericitic matrix. Very fine, heavy minerals, to 0.04 mm occur within the sericitic matrix. Hematite coats all clasts and quartz cement replaces interstitial sericite.

2. Coarse lenses and beds within the Pachi arkosic unit

Radioactive pebbly arkose and polymictic pebble conglomerate lenses and beds occur throughout the Pachi arkose. The Pachi arkose is typified by a coarse to granule grain size, pink to light pinkish grey coloration and trough cross-bed stratification with thin streaks and laminations of black heavy minerals. Radioactive Pachi lenses and beds are characterized by:

i) an increase in the size and abundance of the clasts and in particular quartz pebbles to 6 cm in size;

ii) a deep red to maroon coloration compared to the pink to whitish pink bounding arkosic units and;

iii) an increase either in the abundance of black heavy minerals as interstitial fine sand sized detritus or in the thickness and number of foreset bed accumulations.

The conglomeratic unit, north of North River, is polymictic, generally matrix supported, pink to light pink in colour with tabular and trough cross-stratification. Clasts include round to subrounded greyish white to white quartz, granite and mylonitic granitic gneiss, rare jasper and subrounded to subangular red to pink alkali feldspar. Quartz, granite and gneiss clasts range up to 6 cm in size. Matrix material consists of granule to fine sand sized quartz, alkali feldspar, composite feldspar-quartz grains and altered biotite plates set in a very fine sericitic matte. Hematite is the dominant cement with minor quartz and feldspar. The angularity of feldspar clasts, possibly derived from augen gneisses, altered biotite plates, and abundance of fine sericitic matrix material indicates the immaturity of this rock unit. Alteration is represented by opaque biotite plates, hematite, quartz and feldspar cements, very fine grained clusters of rutile/anatase and abundant tourmaline in zones of black, heavy mineral concentrations. Tourmaline, variety schorl, occurs as anhedral interstitial grains and occasionally as subhedral radiating clusters between heavy mineral concentrations (Fig. 25.3). Texturally, the heavy minerals occur either as round to subrounded grains to 0.5 mm in size irregularly distributed in the sericitic matrix amongst the granule to pebble sized clasts, or as thin, 2-3 mm thick laminations, defining trough cross-bed stratification.

Black sand pods and laminations occur within the mottled pink, coarse grained trough cross-beds of the Richmond Gulf Formation. Black sand laminations to 5 mm in thickness occur in hematite mottled arkose. The arkose contains fine, 1-2 mm, brick red hematite flecks in a mottled pink to grey pink arkose. Finely bedded to massive black sand pods, up to 10 cm in length and up to 8 cm in thickness consist of iron-titanium oxides, refractory heavy minerals, quartz and feldspar cemented by calcite, quartz, hydrous iron oxide, minor chlorite and very fine grained iron sulphide, pyrite or marcasite (Fig. 25.4).

Mineralogy of the Radioactive Zones

The mineralogy of the heavy mineral sands in the Pachi and Richmond Gulf arkoses is similar. The nonradioactive minerals are: abundant magnetite and two-phase titanomagnetite, zircon and apatite. Radioactive minerals were identified using a Materials Analysis Company electron microprobe equipped with a Kevex energy dispersive spectrometer for spectra identification followed by quantitative analyses. Radioactive minerals include opaque and translucent thorite and translucent thorium-rich monazite with trace rare-earth contents. The variation in iron content of the analyzed thorite grains corresponds with the degree of opacity. The thorite grains contain up to 3.6 UO_2 (wt%), Table 25.1. The identity of a thorite-like mineral containing 9.8 wt %S (Table 25.1, specimen 20, grain 1) remains unexplained.

Uranium and Thorium Geochemistry

Uranium contents were determined by neutron activation-delayed neutron counting at Atomic Energy of Canada Ltd. Thorium contents were determined by X-ray fluorescence at the Geological Survey of Canada using CANMET standard DL-1 containing 0.0083% Th. The results are listed in Table 25.2 and those uranium and/or thorium values that are one standard deviation above the mean for any one stratigraphic unit are recorded on Figure 25.1.

The uranium and thorium contents of the basement rocks compare to crustal abundances for granitic rocks. However the Th/U ratios are higher compared to crustal ratios (Handbook of Geochemistry).

Uranium values of pink to red, medium to coarse grained Pachi arkose without significant heavy mineral laminations are very low ranging from 0.2-1.2 ppm. With an increase in the grain size and accompanying heavy mineral accumulations, the uranium values increase up to six times background. Anomalous uranium values,greater than 8.8 ppm occur within the granite-quartz pebble conglomerate, pebbly arkose and fine to coarse sands of the basal unconformity. Thorium contents in the Pachi arkose vary directly with uranium (Fig. 25.5) except for the basal sands on the unconformity where no apparent correlation exists between uranium and thorium (Table 25.1, Pachi specimens 22, 23). The Th/U ratios for the Pachi arkosic units are higher than crustal averages and may reflect the high ratios of the basement rocks. Limited sampling of the Pachi andesitic unit shows no significant uranium or thorium content.

Uranium analyses throughout the Richmond Gulf Formation and from the various lithologies within it are very low ranging from 0.4 to 1.5 ppm excluding the anomalous specimens. The four anomalous uranium and/or thorium samples represent heavy mineral accumulations in sedimentary structures that are smaller and less continuous than the anomalous beds and lenses in the Pachi arkose. Richmond Gulf arkoses contain higher Th/U values than the Pachi arkosic rocks due to generally lower uranium values.

Table 25.2

Uranium and Thorium Abundances, Richmond Gulf Area

Stratigraphic unit	Specimen number	U(ppm)	Th(ppm)	Rock type
Basement complex	1	5.9	50	Hematitic chloritic granite
	2	2.7	39	Leucocratic granite
	3	2.1	21	Hematitic leucocratic granite
	4	4.2	25	Foliated hematitic granite
	5	2.0	21	Augen granitic gneiss
Pachi arkose	1	11.0	189	Quartz pebbly arkose
	2	4.1	33	Fine grained gray arkose
	3	7.5	71	Granite-quartz pebble conglomerate
	4	14.0	124	Granite-quartz pebble conglomerate
	5	5.9	65	Granite-quartz pebble conglomerate
	6	3.0	39	Granite-quartz pebble conglomerate
	7	16.6	229	Granite-quartz pebble conglomerate
	8	8.5	163	Granite-quartz pebble conglomerate
	9	6.6	85	Quartz pebbly arkose
	10	21.0	62	Quartz pebbly arkose
	11	10.5	78	Quartz pebbly arkose
	12	0.7	16	Pink coarse arkose
	13	0.2	20	Pink coarse arkose
	14	3.8	74	Maroon heavy mineral laminated arkose
	15	1.8	26	Maroon heavy mineral laminated arkose
	16	4.2	52	Maroon heavy mineral laminated arkose
	17	2.6	35	Pink heavy mineral laminated arkose
	18	1.6	N.D.	Sericitic granular arkose
	19	3.4	14	Sericitic pebbly arkose
	20	4.4	82	Granular heavy mineral laminated arkose
	21	4.0	35	Granular heavy mineral laminated arkose
	22	71.4	23	Maroon coarse grained arkose
	23	6.6	N.D.	Gray coarse grained arkose
	24	4.2	52	Quartz pebbly arkose
	25	1.0	23	Mottled pink granular arkose
	26	0.3	N.D.	Pink medium grained arkose
	27	0.6	N.D.	Pink medium grained arkose
	28	1.2	33	Pink medium grained arkose
	29	0.3	21	Pink medium grained arkose
	30	0.7	3	Granular heavy mineral laminated arkose
	31	1.7	17	Maroon laminated mudstone
	32	0.8	N.D.	Granular pink arkose
	33	0.6	21	Granular light pink sericitic arkose
	34	0.3	7	Coarse pink arkose
	35	4.4	N.D.	Granular sericitic heavy mineral laminated arkose
	36	2.3	42	Coarse pink arkose
	37	1.0	25	Coarse pink arkose
	38	2.3	29	Quartz pebbly arkose
Pachi andesite	1	0.1	N.D.	Amygdaloidal aphanitic
	2	0.3	N.D.	Amygdaloidal aphanitic porphyritic
	3	0.1	N.D.	Aphanitic porphyritic
	4	0.2	N.D.	Amygdaloidal aphanitic
Richmond Gulf Formation	1	0.5	19	Medium grained pink arkose
	2	1.0	32	Maroon siltstone-arkose
	3	1.2	N.D.	Light pink arkose
	4	0.5	N.D.	Coarse whitish gray arkose
	5	0.8	N.D.	Coarse greenish gray arkose
	6	0.4	N.D.	Coarse white arkose
	7	1.0	N.D.	Coarse pink arkose
	8	0.4	14	Coarse gray arkose
	9	1.0	N.D.	Maroon laminated siltstone
	10	0.8	N.D.	Coarse hematite mottled arkose
	11	0.6	28	Maroon heavy mineral laminated arkose
	12	1.3	18	Coarse hematite mottled arkose
	13	1.3	N.D.	Granular hematite mottled arkose
	14	0.7	7	Coarse heavy mineral laminated arkose
	15	0.8	N.D.	Coarse heavy mineral laminated arkose
	16	0.9	N.D.	Medium grained heavy mineral laminated arkose
	17	0.8	N.D.	Coarse hematite mottled arkose
	18	1.5	N.D.	Medium grained pinkish gray arkose
	19	4.2	54	Medium grained pink heavy mineral lamianted arkose
	20	62.5	496	Black heavy mineral crossbed from specimen 21
	21	5.5	35	Coarse hematite mottled heavy mineral laminated arkose
	22	1.2	23	Coarse pink arkose
	23	0.4	N.D.	Medium grained maroon arkose
	24	1.3	32	Coarse pink heavy mineral laminated arkose
	25	1.3	N.D.	Coarse red heavy mineral laminated arkose

Conclusion

The Pachi arkose contains anomalous uranium but primarily thorium abundances concentrated in pebbly horizons and a particularly noteworthy uranium anomaly at the basal unconformity. The hematite-rich character of these clastic sediments indicates that the sediments were deposited after the oxy-atmoversion and limits the potential for the preservation of uraninite-quartz pebble conglomerate type occurrences. The presence of thorium-bearing detrital minerals and high Th/U ratios for the arkosic and basement rocks may suggest a thorium-rich source region. However the uranium content of the basal unconformity, 71.4 ppm, represents the most favourable horizon for exploration in the Richmond Gulf area. It should be emphasized that the unconformity examined in the study area represents a local inlier and that the major unconformity of basal Pachi arkose is exposed to the east of the study area for a north-south distance of approximately 65 km (Eade, 1966; Stevenson, 1968).

Acknowledgments

The author acknowledges G. Plant for the energy dispersive and quantitative analyses of the thorium minerals, G. Lachance for the X-ray fluorescence scans for thorium and J. Kerswill for statistical analysis of the data.

References

Chandler, F.W.
1978: Geological environment of Aphebian red beds of the north half of Richmond Gulf, New Quebec; in Current Research, Part A; Geol. Surv. Can., Paper 78-1A, rep. 24.

Eade, K.E.
1966: Fort George River and Kaniapiskau River (west half) map-areas, New Quebec; Geol. Surv. Can., Mem. 339.

Handbook of Geochemistry
1974: Editor: Wedepohl, K.H.; chapters on thorium, uranium.

Roscoe, S.M.
1969: Huronian rocks and uraniferous conglomerates in the Canadian Shield; Geol. Surv. Can., Paper 68-40.

Stevenson, I.M.
1968: A Geological Reconnaissance of Leaf River map-area, New Quebec and Northwest Territories; Geol. Surv. Can., Mem. 356.

Woodcock, J.R.
1960: Geology of the Richmond Gulf area, New Quebec; Proc. Geol. Assoc. Can., v. 12, p. 21-39.

26. THE BLACHFORD LAKE INTRUSIVE SUITE: AN APHEBIAN ALKALINE PLUTONIC COMPLEX IN THE SLAVE PROVINCE, NORTHWEST TERRITORIES

Project 710023

A. Davidson
Regional and Economic Geology Division

Abstract

Davidson, A., The Blachford Lake Intrusive Suite: An Aphebian alkaline plutonic complex in the Slave Province, Northwest Territories; Current Research, Part A, Geol. Surv. Can., Paper 78-1A, p. 119-127, 1978.

The Blachford Lake Intrusive Suite is defined to include all the plutonic rocks of alkaline affinity that form a coherent complex in the vicinity of Blachford Lake, located at the south margin of the Slave Province. It is subdivided into major named and minor unnamed units, each of which is described and characterized. The Suite displays a differentiation trend from mafic to felsic with time, ending with altered and mineralized rocks that contain concentrations of U, Th, Nb, Y and rare-earth metals, possibly of economic importance. All available evidence supports its age as post-Archean, but as predating deposition of the mid-Aphebian Great Slave Supergroup in the east arm of Great Slave Lake.

Introduction

The granitic rocks between Blachford Lake and Hearne Channel in the East Arm of Great Slave Lake (Henderson, 1941) at the southern edge of the Slave Province were recognized during field studies in 1971 to be in large part a multi-phase intrusion of alkaline character (Davidson, 1972). Subsequent petrographic studies cast some doubts on the validity of certain conclusions drawn at that time, namely that the gabbro body in the vicinity of Caribou Lake is older than the granite to the west and therefore not part of the alkaline complex (Davidson, 1972, p. 109), and that a small mass of diorite is apparently included in the main body of alkaline granite (Davidson, 1972, p. 110). In addition, a K-Ar radiometric age of 2057 ± 56 m.y. (Wanless, pers. comm., 1973) has been obtained on amphibole from the alkaline granite, an age much younger than was expected from Slave Province plutonic rocks. Also, airborne γ-ray spectroscopy, undertaken by the Geological Survey, and prospecting have revealed that radioactive mineralization (Davidson, 1972, p. 112) is more widespread than previously suspected. To date, 316 mineral claims have been staked by Highwood Resources Ltd., of Calgary, and drilling and trenching are being undertaken in zones that have returned interesting assays for U, Th, Nb, Y, and rare earth elements.

As a consequence of the above, three weeks' field work aimed at resolving the controversial age relationships and

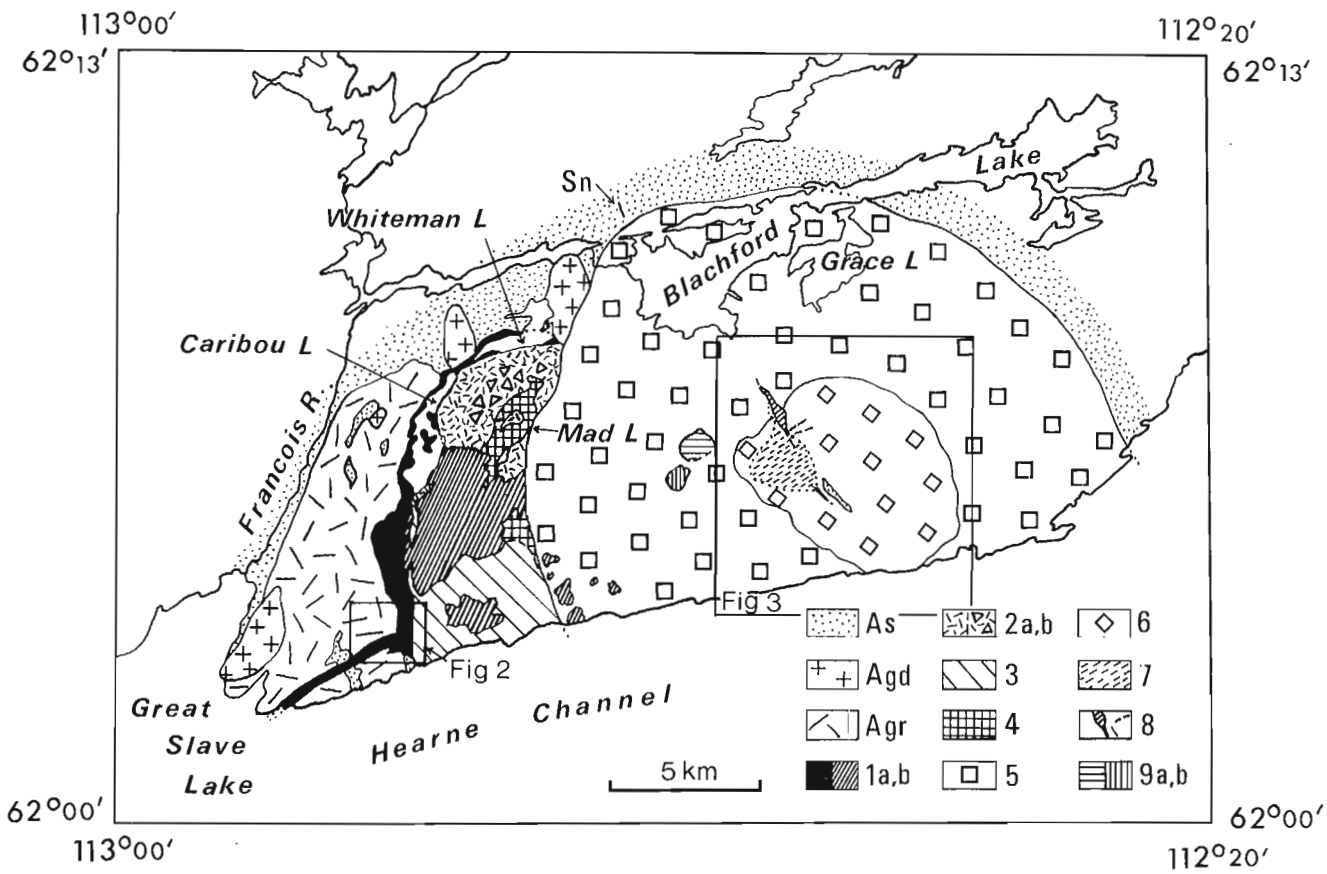

Figure 26.1. Revised geology of the plutonic rocks in the Blachford Lake area. See text for legend.

Table 26.1

Correlation between rock units in the East Arm of Great Slave Lake and the Blachford Lake area

East Arm, Great Slave Lake[1]		Blachford Lake area	map-units (Fig. 26.1)
Mackenzie diabase dykes	=	Mackenzie diabase dykes	–
Basic sills, Christie Bay		not present	
Et-then Group		not present	
Diorite, monzonite laccoliths	=	Diorite, granodiorite	9a,b
Great Slave Supergroup		not present	
east-northeast diabase dykes	=	east-northeast diabase dykes	–
'Easter Island dyke'	=	Blachford Lake Intrusive Suite	1-8
Wilson Island Group		not present	
Archean metamorphic complex	=	two-mica granite	Agr
		biotite granodiorite	Agd
		Yellowknife Supergroup	As

[1] After Hoffman et al. (1977, p. 121).

evaluating the extent and nature of the mineralization was undertaken in July 1977. This paper reports a revised evaluation of the age relationships, defines the Blachford Lake Intrusive Suite and its component units, and relates the mineralization to the latest stage of magmatic differentiation of the alkaline complex. Figure 26.1, a map of the geology of the Blachford Lake area, supersedes a similar map by Davidson (1972, Fig. 1). Table 26.1 lists the rock units found in the Blachford Lake area and equates them with the chief elements of the stratigraphic succession established in the East Arm of Great Slave Lake immediately to the south (Hoffman, 1968; Hoffman et al., 1977). Naming of the Blachford Lake Intrusive Suite and its component units follows the recommendations of Sohl (1977). Throughout this report, the terminology used for the intrusive plutonic rocks is the one recommended by the IUGS Subcommission on the Systematics of Igneous Rocks (Streckeisen, 1976).

The Blachford Lake Intrusive Suite

Blachford Lake Intrusive Suite is the name given to all the contiguous rock units forming the plutonic complex of alkaline character north of Hearne Channel and east of Francois River, District of Mackenzie (Fig. 26.1, units 1-8). The alkaline rocks intrude metasedimentary schists of the Yellowknife Supergroup (unit As) and calc-alkaline granodiorite (unit Agd) and granite (unit Agr) plutons whose rocks are petrogenetically identical to radiometrically dated Archean plutonic rocks in the neighbouring parts of the southern Slave Structural Province. The alkaline complex is intruded in turn by east-northeast-trending diabase dykes, small plutons of diorite and granodiorite (subunits 9a,b), and northwest-trending diabase dykes of the Mackenzie swarm, dated between 1100 and 1200 m.y. (Leech, 1966). Although not in exposed contact with the Great Slave Supergroup (Aphebian in age) which occupies much of the east arm of Great Slave Lake immediately to the south, the alkaline rocks are considered to be the older on the basis that the unconformity at the base of the Great Slave Supergroup truncates a similar east-northeast-trending diabase dyke swarm in the basement exposed on the Simpson Islands, 35 km south of Hearne Channel (Table 26.1).

Alkaline intrusive rocks underlie an area close to 235 km^2 north of Hearne Channel. If the subcircular outline continues and closes southwards, a total area approaching 375 km^2 would be enclosed. Such a projected outer contact would transect the north shore of Blanchet Island, 5 km south across Hearne Channel. Here, however, only sediments of the Great Slave Supergroup intruded by diorite laccoliths are found. Thus the Blachford Lake Intrusive Suite either has been eroded to below the present exposed level south of Hearne Channel, or Hearne Channel itself is the locus of a major fault, down-dropped to the south. Subsidiary faults on the mainland show no evidence of lateral displacement.

The Blachford Lake Intrusive Suite shows a remarkable range in composition. The rocks that crystallized during a sequence of intrusive events, whose order has been established from exposed cross-cutting relationships of both dykes and main contacts, illustrate a change with time from mildly alkaline gabbro, through increasingly alkaline diorite, syenite, and granite, to highly peralkaline granite and syenite. Five distinct and volumetrically important intrusive events have been recognized. The rocks emplaced during each of these events have correspondingly distinctive compositional and textural characteristics, and are localized within the confines of the whole alkaline complex. These characteristics are utilized in naming the individual units of the intrusive suite. In addition, the rocks of the last of the five main intrusive events have been subdivided on compositional and spatial grounds, even though the two do not display any structural relationships that would serve to separate them significantly with respect to time. The six named plutonic units, equivalent in status to formations in stratiform rocks, are included in Table 26.2 which in addition lists unnamed rocks related to four other events, all in time sequence. Three of these four other events are represented by intrusive rocks whose areal extent is too small to show in Figure 26.1; the fourth is the last event in the sequence and is manifest as late-stage alteration, veining and mineralization.

Caribou Lake Gabbro (subunits 1a, b)

Gabbroic rocks and related anorthosite and diorite were first reported from the vicinity of Caribou Lake by Stockwell (1932) who, along with Henderson (1938, p. 10), interpreted them as older than the surrounding granitic rocks. Based on the relationships of dykes observed in 1971 Davidson (1972, p. 109) considered this interpretation to be correct. Subsequent petrographic study of specimens collected at that time, however, raised the suspicion that the gabbroic rocks are in fact younger than those granitic rocks (Davidson, 1972, Fig. 1, map-units 2 and 3) lying to the north and west. The evidence is:

a) both the granitic and sedimentary rocks immediately adjacent to the outer contact of the gabbro body contain high temperature metamorphic minerals (hypersthene, spinel);

b) gabbro immediately adjacent to these granitic rocks is fresh, not hydrated or metamorphosed;

c) granitic dykes within the gabbro are of alkaline character and related to the younger granitic intrusions to the east, not to the calc-alkaline granitic rocks to the north and west.

This past summer, the contact between gabbro (subunit 1a) and all three country rock units (As, Agd, Agr) was found exposed at several localities. Fine granophyre-like intergrowths both in the matrix of the granitic rocks and in thin veinlets that penetrate a few centimetres into chilled gabbro is taken as evidence for local country rock melting.

Table 26.2

Subdivision of the Blachford Lake Intrusive Suite, listed in time sequence

unit (Fig. 26.1)	Rock units
7,8	alteration, veining and mineralization
–	trachyte dykes
6	Thor Lake Syenite
5	Grace Lake Granite
4	Mad Lake Granite
–	leucocratic perthite granite
3	Hearne Channel Granite
2a,b	Whiteman Lake Quartz Syenite
1a,b	Caribou Lake Gabbro
–	anorthosite, anorthositic gabbro

The Caribou Lake Gabbro is exposed only on the western side of the alkaline complex, where it underlies an area of approximately 20 km^2. It is intruded by younger units of the Blachford Lake Intrusive Suite to the east, whose emplacement has removed much of what must have been a considerably larger pluton. That which remains illustrates progressive change from the chilled margin inwards as follows:

a) massive olivine gabbro of irregular grain size and characterized by pegmatitic patches, particularly along the west and north shores of Caribou and Whiteman lakes respectively;

b) massive to faintly layered, equigranular, medium grained noritic gabbro, in places with plagioclase crystals aligned to give a primary foliation parallel to compositional layering; this planar fabric is subparallel to the outer contact and dips steeply inwards;

c) interlayered pegmatitic gabbro with coarse magnetite lenses, medium grained gabbro with thin magnetite-rich layers, and fine to medium grained sulphide-bearing gabbro, the latter weathering readily to rusty brown rubbly soil; this zone gives rise to a pronounced aeromagnetic anomaly (Geol. Surv. Can., Map 3023G, 1962);

d) pegmatitic hornblende gabbro and leucogabbro, grading eastwards to coarse, uniform, massive augite-hornblende-biotite leucodiorite.

The extent of this last category is shown separately (subunit 1b) in Figure 26.1, but is included with the Caribou Lake Gabbro because it is completely gradational with the gabbroic units to the west.

Thin sections reveal that all types of the Caribou Lake Gabbro contain, in addition to minor brown hornblende as overgrowths on pyroxene, small amounts of primary deep red-brown biotite, an indication of alkaline character. Forsteritic olivine is apparently restricted to the contact region and is commonly surrounded by vermiform coronas of hypersthene and plagioclase, attesting to the gabbro's saturated nature with respect to SiO_2. Orthopyroxene and clinopyroxene are intergrown in the noritic gabbros, and fayalitic olivine is present in the leucogabbro and leucodiorite. Plagioclase composition changes from An_{55-40} in the gabbros to An_{40-25} in the leucodiorite, in which it is commonly antiperthitic. Apatite is a common accessory mineral.

Rounded to angular xenoliths of coarse anorthosite and anorthositic gabbro, ranging in size from less than a metre to several tens of metres, occur within all phases of the Caribou Lake Gabbro south and southeast of Caribou Lake, and particularly within the western part of the leucodiorite unit. Many xenoliths display pronounced planar alignment of tabular plagioclase crystals; orientation varies from block to block. These anorthositic rocks contain calcic plagioclase (An_{75-60}), and must be the product of an earlier crystallization event that has been broken up by and carried along with the Caribou Lake Gabbro magma during its emplacement.

The 300 m wide gabbro dyke that extends southwest through the two-mica granite (Fig. 26.2) was examined in detail especially at its juncture with the main mass of the Caribou Lake Gabbro. The following observations were made:

a) although its contacts with the adjacent granite are not exposed, it is fine grained at its outer margin, coarsening inwards to even, medium-grained;

b) near the northeast end the dyke has a granular texture indistinguishable from that of the main gabbro mass, but to the southwest it gradually assumes a diabasic texture and contains traces of free quartz;

c) it is cut in at least five places by narrow, northwest-trending dykes with moderate southwest dip composed of hornblende alkaline granite, likely related to the nearby Hearne Channel Granite (unit 3), and quite unlike the adjacent two-mica granite;

d) it and the alkaline granite dykes are cut by an east-northeast-trending diabase dyke of the same swarm that cuts all units of the Blachford Lake Intrusive Suite.

It seems fairly certain, therefore, that this large dyke is directly connected to the main mass of the Caribou Lake Gabbro. It is younger than the two-mica granite and not, as previously stated (Davidson, 1972, p. 109), a septum within it.

Whiteman Lake Quartz Syenite (subunits 2a,b)

This unit of the Blachford Lake Intrusive Suite intrudes the Caribou Lake Gabbro and is well exposed along the south shore of Whiteman Lake. Its contact with gabbro is essentially vertical. It does not penetrate the outer contact of the Caribou Lake Gabbro except at its northeasternmost part, where it is in contact with biotite granodiorite (see Fig. 26.1). It underlies an area of about 8 km^2, and its central part (subunit 2b) is full of xenoliths, some of them hundreds of metres across, composed of metasediment (As), granodiorite (Agd) and various phases of the Caribou Lake Gabbro (subunits 1a, 1b). The distribution of the different types of gabbro in this xenolithic core more or less reflects a continuation of the zonation found in the gabbro to the southwest, suggesting that the gabbro inclusions are not much removed from their original positions. Around the xenolithic core the quartz syenite is relatively free of xenoliths except for scattered, small, rounded inclusions of metasediment and locally of gabbro near its outer contact. Bedding is well preserved in many of the metasediment xenoliths and illustrates that the xenoliths have been insensibly rotated with respect one to another, just like the anorthosite blocks in the Caribou Lake Gabbro.

Although quartz syenite is the predominant rock type, it varies systematically in composition and appearance. Along the north and west sides this intrusion is light greenish to pinkish grey, brown and crumbly weathering, massive, uniform, medium grained hornblende-perthite quartz syenite. In addition to hornblende, it contains variable amounts of biotite, pale green clinopyroxene, and partly altered fayalite. In places its quartz content is high enough for the rock to be termed granite. Towards the southeast the quartz content decreases as it grades to dark green (where fresh) syenite

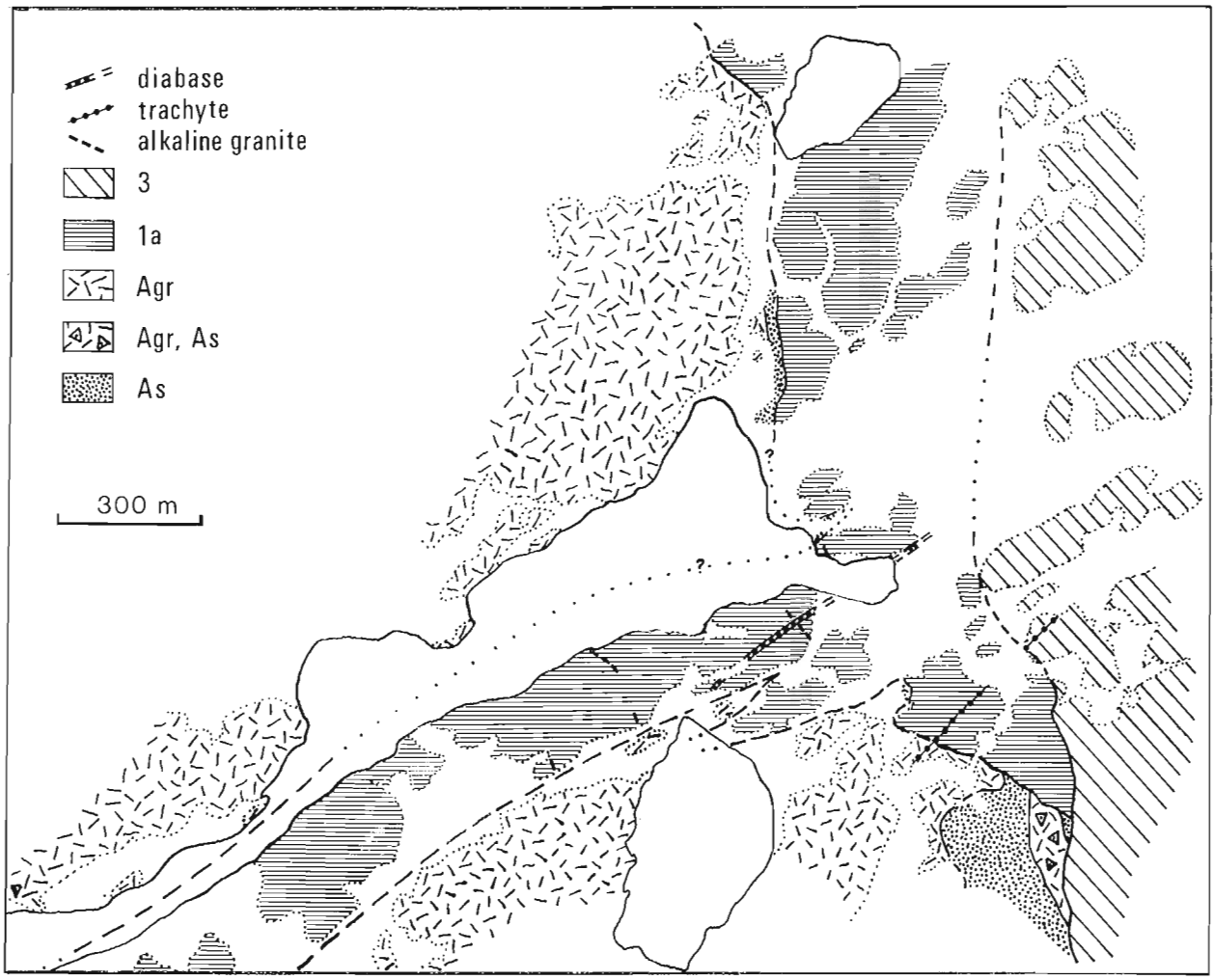

Figure 26.2. Detailed outcrop map illustrating the geological relationships in the region of the juncture between the main mass and the southwest dyke extension of the Caribou Lake Gabbro. The area of this map is outlined in Figure 26.1, and the same legend is used.

almost entirely devoid of quartz and containing fayalite and green clinopyroxene as the principal mafic silicates. In these syenites the larger perthite grains have antiperthitic oligoclase cores. Zircon is a common accessory mineral, apatite is virtually absent. In the vicinity of Mad Lake, two phases of this unit are present, the coarse, green, fayalite-pyroxene syenite occurring sparingly as xenoliths, along with much more abundant metasediment xenoliths, in medium grained quartz syenite, indicating that the Whiteman Lake Quartz Syenite is not a single phase intrusion and that the quartz-poor variety is earlier. The green quartz-poor phase is not unlike the leucodiorite (subunit 1b) in appearance; south of Mad Lake the two occur together and are hard to distinguish in the field, where both are cut by dykes of xenolithic quartz syenite. Uniform quartz syenite dykes are common in the Caribou Lake Gabbro southwest of the main body of the Whiteman Lake Quartz Syenite.

Hearne Channel Granite (unit 3)

Massive, medium grained, subequigranular, and predominantly brownish pink in colour, the Hearne Channel Granite underlies some 9 km^2 in the southwest part of the alkaline complex, and presumably extends to the south beneath Hearne Channel. It intrudes the Caribou Lake Gabbro, cutting through its outer contact into metasediments (unit As) and two-mica granite (unit Agr) along its west side (Fig. 26.2). Here the contact is steep, but along the northern edge it is locally flat lying beneath leucodiorite (subunit 1b) that caps the hills; this contact likely steepens northwards. The mass of leucodiorite in the centre of the Hearne Channel Granite has gently to moderately inward dipping contacts, and is probably an in situ roof pendant. A large dyke of Hearne Channel Granite extends north from the western edge of the main pluton, intruding the Caribou Lake Gabbro close to the gradational contact between gabbro and leucodiorite. The Hearne Channel Granite is intruded by dykes of fine grained, sugary granite at its northeast side, apparently related to the Mad Lake Granite (unit 4). Both are clearly intruded by the Grace Lake Granite (unit 5).

This granite is characterized by two features: a) it contains scattered, large xenocrysts of dark plagioclase, readily identified in the field; and b) its matrix contain graphically intergrown quartz and feldspar, visible only in thin section. Hornblende with the optical properties of ferrohastingsite is the chief mafic mineral, but biotite occurs as well in most rocks. Neither fayalite nor pyroxene have been observed. Like the Whiteman Lake Quartz Syenite, larger feldspar grains have antiperthitic plagioclase cores and perthite rims; broad, alternating zones of perthite and antiperthite are present in some. The xenocrysts are andesine and are not antiperthitic; they may be overgrown by narrow rims of either perthite or antiperthitic sodic

oligoclase. They are likely derived from some phase of the adjacent Caribou Lake Gabbro, but are not noticeably concentrated near contacts. Unlike the Whiteman Lake Quartz Syenite, the Hearne Channel Granite is compositionally uniform and all but lacks xenoliths.

Mad Lake Granite (unit 4)

Two small bodies of this distinctive granite, 3 and 1 km^2 in area, intrude the Whiteman Lake Quartz Syenite and the Hearne Channel Granite respectively. Both intrude the leucodiorite subunit of the Caribou Lake Gabbro, and both are intruded by the Grace Lake Granite (5). Contact relationships are particularly well exposed around the shores of Mad Lake, whose water level has dropped more than 1 m in recent years. On the east side of the northern body north of Mad Lake, this granite was observed in two places to have intruded a leucocratic perthite granite similar in texture to but finer grained than the Grace Lake Granite. There is no doubt, however, that the main body of the Grace Lake Granite is younger. This leucocratic granite intrudes the Whiteman Lake Quartz Syenite, and must represent an intrusive event between the Whiteman Lake and Mad Lake intrusions. The Mad Lake Granite contacts dip gently to moderately outwards beneath the older rocks, and within the exposed area of the northern body several of the hills are capped by xenolithic Whiteman Lake Quartz Syenite. It seems therefore that this granite is only just unroofed and likely that its two exposed bodies are connected at depth.

The Mad Lake Granite is massive, uniform, and generally pink in colour. It is characterized by a subporphyritic texture, with feldspar phenocrysts set in a fine to medium grained granular matrix in which hornblende and biotite grains are regularly scattered, giving a 'salt-and-pepper' texture. Granitic dykes within the leucodiorite phase of the Caribou Lake Gabbro (subunit 1b) are distinguished from those related to the Whiteman Lake Quartz Syenite and to the Hearne Channel Granite by this texture. Thin sections show that the feldspar phenocrysts are perthitic, locally with antiperthite cores, but that the matrix contains two feldspars, microcline, and sodic oligoclase. Quartz is rarely present as small, partly resorbed phenocrysts, but is abundant throughout the matrix as small, equant grains and is not intergrown with feldspar. These features plus the lack of plagioclase xenocrysts distinguish the Mad Lake and Hearne Channel granites, although the mafic mineralogy is identical.

Grace Lake Granite (unit 5)

The remarkably uniform Grace Lake Granite is by far the largest unit of the Blachford Lake Intrusive Suite, underlying an area of 155 km^2 north of Hearne Channel. It intrudes all earlier units of the Suite along its west contact, biotite granodiorite west of Blachford Lake, and Yellowknife metasediments along the rest of its contact. This outer contact is essentially vertical in most places, but is locally steeply inward dipping. Near its southwest margin the Grace Lake Granite contains numerous rafts of coarse leucodiorite (subunit 1b) cut by syenite and granite dykes (subunit 2a, units 3, 4). Many of these rafts are exposed on hilltops and may either be roof pendants or have not sunk far below the now eroded roof. Dykes of Grace Lake Granite extending from the contact are rare, but enough of them were observed to substantiate the age relationships. The core of the Grace Lake Granite pluton is occupied by the Thor Lake Syenite. The contact between these two units is gradational over a very few metres, and relationships with dykes are absent.

The Grace Lake Granite is a massive, coarse grained, equigranular, amphibole-alkali feldspar granite. Its colour varies from reddish pink through buff to light grey or pale greenish grey, the latter showing the least amount of microscopic alteration. The freshest samples were collected from the northwest side of Grace Lake and along the north shore of Blachford Lake; elsewhere pink and buff varieties predominate. It is a hypersolvus granite with randomly oriented, euhedral perthite feldspars. Quartz content averages 25 per cent by volume, but has a tendency to decrease slightly towards the syenite core. Inversely, the amphibole content, averaging 7 per cent, increases slightly inwards, concomitant with a gradual change in texture caused by the amphibole's tendency to form larger poikilitic grains enclosing smaller feldspar euhedra. Thin sections show that most of the amphibole is riebeckite and that the feldspar is coarse mesoperthite. Fluorite is invariably present in amounts up to one per cent, and forms drop-like grains within the other minerals. Other accessories are zircon and monazite; apatite, sphene, and magnetite are absent. Some thin sections show small, rounded grains of green pyroxene or its alteration products enclosed by riebeckite. In some rocks close to the syenite core the amphibole is dark ferrohastingsite with riebeckite overgrowths. Acmite occurs in some rocks as overgrowths on riebeckite and is associated with astrophyllite locally. Biotite is very rarely present, and then only as a secondary mineral, occurring with albite and hematite in place of riebeckite. This mineralogy is typical of SiO_2-saturated agpaitic igneous rocks (Currie, 1976).

In a few places the Grace Lake Granite contains clusters of Yellowknife metasediment xenoliths, some of them individually many tens of metres in size. Between Blachford Lake and the syenite core, several apparently thin and flat-lying lenses of syenite were noted. This syenite, in addition to its lack of quartz, differs from the enclosing granite in that it contains pyroxene rather than amphibole, is brown rather than pink or buff, and is relatively more prone to weathering. Narrow, fine grained granite dykes with the same mineralogy as their coarse grained host occur here and there. So do lenses of pegmatite and of sugary-textured quartz-albite rock with acmite prisms.

Thor Lake Syenite (unit 6)

The Thor Lake Syenite occupies a roughly oval 30 km^2 area in the centre of the Grace Lake Granite pluton. Although more variable in composition and texture than the surrounding granite, these two rock units have much in common. The contact between them is gradational across a very few metres, less along the north and east sides than elsewhere, and is nothing more than an abrupt decrease in quartz content; there is no accompanying change in the coarse grain size, nor any evidence of syenite dykes in granite or vice versa.

Five varieties of syenite, based on textural and compositional differences recognizable in the field, are found to have coherent distribution (Fig. 26.3). The subunits are:

6a, coarse to medium grained, dark green, rusty-weathering fayalite-pyroxene syenite, locally containing enigmatite and hornblende, with colour index (CI) 15-50;

6b, coarse grained hornblende syenite (CI 5-15);

6c, inequigranular hornblende syenite characterized by very coarse, highly poikilitic hornblende (CI 15-35);

6d, subporphyritic hornblende syenite characterized by feldspar euhedra with purple cores and pink margins (CI 10-20);

6e, medium grained hornblende syenite with aligned hornblende crystals (CI 20-30).

Boundaries between these types are gradational over a few tens of metres, with the exception of the southwest contact between subunits 6b and 6c, where an abrupt change occurs across a line of metasedimentary screens. The mafic syenite (subunit 6a) is the most distinctive of these five types. In the field it forms a prominent ridge of dark, rusty, rubbly-weathering rock with a steep outer face and a more gentle inward slope. It is separated from the Grace Lake Granite by a narrow but ever-present gradational zone of hornblende

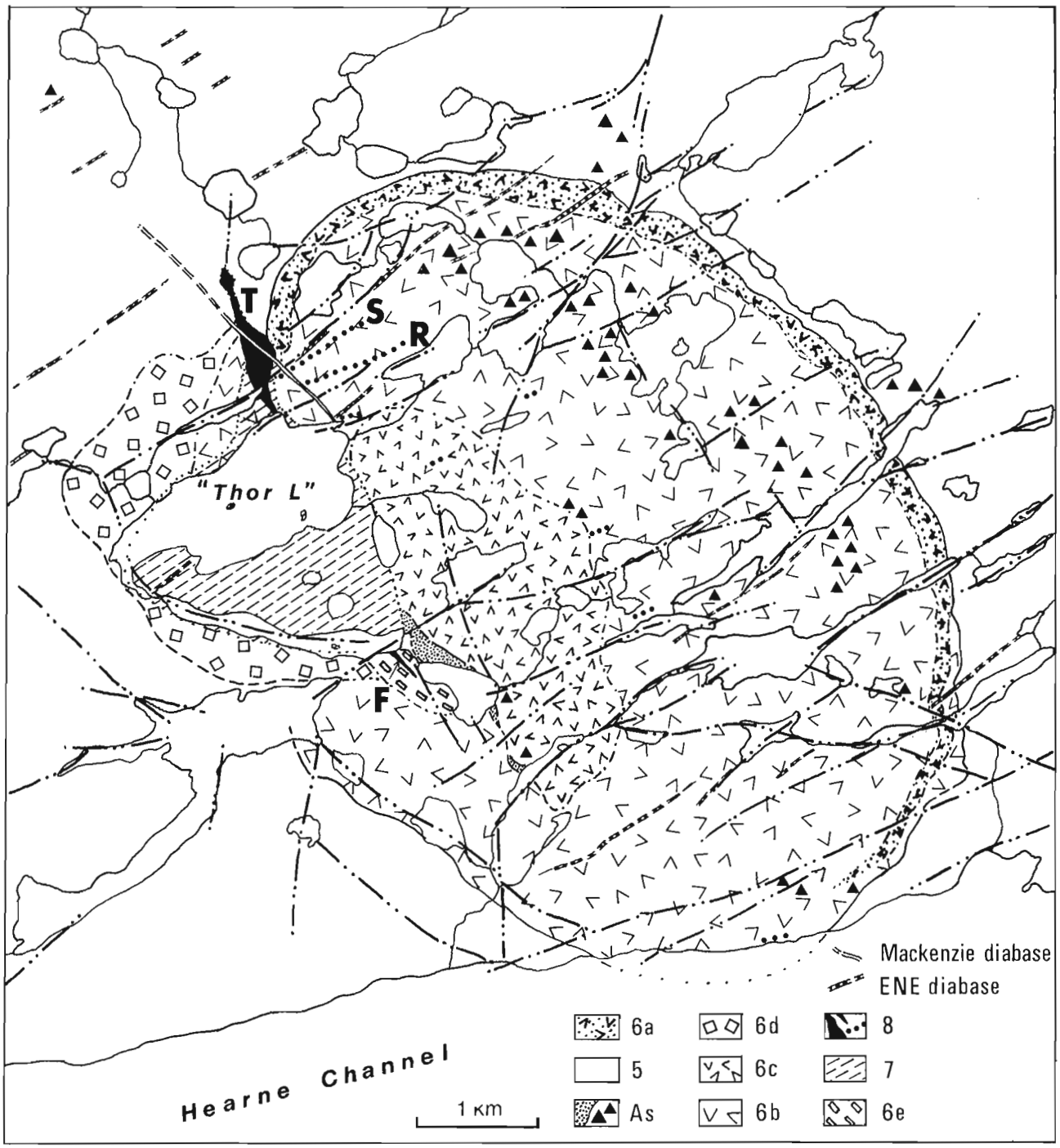

Figure 26.3. Detailed geology of the Thor Lake Syenite showing the R, S, T and Fluorite (F) zones of mineralization. See text for legend. The area of this map is outlined in Figure 26.1.

syenite (subunit 6b) which widens southwards along the east margin as the mafic syenite peters out within it. It was at first thought that the mafic syenite has the form of a layer dipping gently inwards between the Grace Lake Granite and the main mass of syenite, its resistance to erosion being responsible for its scarp-like topographic expression (Davidson, 1972, p. 110). Careful re-examination of the contact zone, however, has revealed a poorly developed, steeply inward plunging alignment of feldspar laths within the border syenite, likely indicative of a steep contact. The subporphyritic syenite (subunit 6d) north of Thor Lake[1] has a much less well defined contact with the Grace Lake Granite. It contains gradational patches of quartz syenite, locally rich enough in quartz to be termed granite, that are texturally similar to the Grace Lake Granite to the north. The southwest granite-syenite contact crosses topographic relief high enough to intimate that it too is very steep.

A significant internal feature of the Thor Lake Syenite is the abundance of metasediment xenoliths, a few of which exceed 100 m across, mainly concentrated in the hornblende syenite (subunit 6b) in a zone about 1 km from the Grace Lake Granite contact along the north and east sides (Fig. 26.3). Similar xenoliths also occur sporadically around the margins of the poikilitic syenite (subunit 6c), in addition to the large screen at its southwest margin. Thermal

[1] Thor Lake is an unofficial name in local use and is taken from the name applied to mineral claims staked in that area.

Table 26.3

Weight per cent rare element oxides, mineralized zones in the vicinity of Thor Lake

	1	2	3		4	
			av.	(range)	av.	(range)
U_3O_8	1.14	tr	0.035	(0.015-0.065)	0.051	(0.030-0.120)
Nb_2O_5	31.5	tr	1.49	(0.88 -2.18)	1.44	(0.58 -3.48)
CeO_2	3.27	2.79	0.21	(0.09 -0.41)	0.31	(0.14 -0.65)
Y_2O_3	0.01	8.45	0.012	(0.002-0.025)	0.125	(0.01 -0.38)
ThO_2	0.02	10.2	0.021	(0.007-0.040)	0.029	(0.005-0.110)

1 Highly radioactive high grade grab sample, S-zone.

2 Highly radioactive high grade grab sample, R-zone.

3 Average and range, 5 trenches, total 139', T-zone.

4 Average and range, 7 drill intersections, total 102.5', S-zone.

metamorphism of the included metasediments has produced dense hornfels containing the assemblage plagioclase-quartz-cordierite-biotite-hypersthene.

The Thor Lake Syenite, like the Grace Lake Granite, is cut by narrow dykes of similar composition to the enclosing syenite. In the same way, pegmatite lenses and dykes contain little or no quartz, and sugary-textured dykes contain albite and acmite, not quartz. The development of these late-stage rocks may be related to subsequent alteration and mineralization, and is discussed more fully below.

Very fine grained to aphanitic pink, red, or mauve felsite dykes, of trachyte or quartz trachyte composition and in places porphyritic, occur in various rock units outside as well as within the confines of the Thor Lake Syenite. In general these dykes are less than 5 m wide, are vertical, and strike northeasterly. Red colour is usually a sign of alteration. One such dyke cuts across the syenite-granite contact 1 km north of the northern bay of Thor Lake, but was not recognized within the adjacent intensely altered rocks. Another cuts cleanly across the contacts separating two-mica granite, Caribou Lake Gabbro and Hearne Channel Granite (Fig. 26.2). A 4 m wide dyke has been traced for several hundred metres in the two-mica granite 2 km west of Caribou Lake; it is truncated by a diabase dyke of the east-northeast-trending swarm. Yet another trachyte dyke cuts biotite granodiorite 8 km northwest of Caribou Lake, far outside the alkaline complex. It is possible that some of these dykes are related to salic volcanic rocks in the Great Slave Supergroup, although so far none has been found to cut east-northeast-trending diabase dykes.

Late-stage Veining, Alteration and Mineralization (units 7, 8)

Veins of alkaline pegmatite and related albite-rich rocks occur throughout the Thor Lake Syenite, but are most common in a broad, northwest-trending zone passing just east of Thor Lake. Pegmatites contain K-feldspar, albite, acmite and/or hornblende, and locally carry minor biotite, fluorite, and quartz; small amounts of chalcopyrite were noted at one place. Some large acmite crystals have amphibole cores. Intimately associated at some localities, but occurring separately at others, are veins or dykes of fine grained, pink to cream albite containing coarser prismatic acmite; a few contain amphibole needles. In some veins the albite is coarse and assumes a bladed habit. Most of the veins trend east-northeast and dip at various angles to the south, some quite shallowly.

The area inside the outer contact of the Thor Lake Syenite is everywhere well exposed, with the exception of a broad triangular region south of and including Thor Lake. This low-lying region contains few outcrops, widely scattered, and all of them small. The exposed rock types are varied and unusual, quite unlike any of the syenite units so far described, and are grouped together as unit 7 (Fig. 26.3). Some of these rocks are similar to the pegmatite and acmite-albite veins occurring within the syenites to the east. The rocks have highly variable grain sizes and are composed predominantly of albite and iron oxides, the latter being in part pseudomorphous after acmite. Fresh acmite-K-feldspar-albite rock outcrops in the southeast apex of this triangular area adjacent to altered syenite whose feldspars are reddened and whose hornblende is replaced by fine greenish micaceous aggregates. Outcrops on the peninsula in the southwest part of Thor Lake are composed of pale pink albite with lesser amounts of K-feldspar, deep purple fluorite, buff to pale brown carbonate and, in places, unidentified green, serpentine-like aggregates. Brown to purplish black rocks containing albite and fine grained opaque material including magnetite occur on the two small islands in Thor Lake and along the southern shore. These occurrences coincide with a broad, positive aeromagnetic anomaly centred over the alteration zone. Syenite outcrops along the northwest shore of Thor Lake and the southwest shore of the narrow lake to the south are altered to the extent that hornblende has been replaced by fine aggregates of hematite, albite, fluorite and pale biotite. The area underlain by unit 7 is therefore interpreted as a zone in which pre-existing syenites have been intensely altered, accompanied by much veining with albite-rich rocks. It is a plausible hypothesis that this zone developed under the influence of a late-stage magmatic vapour phase related to, though probably slightly later than, the emplacement of the pegmatites and acmite-albite veins to the east.

Extending north-northwest of Thor Lake for at least 1250 m is a zone of black rocks containing pink to buff coloured fluorite-albite veins and irregular masses (unit 8). This zone cuts through the outer syenite contact into the Grace Lake Granite. The black rocks contain various proportions of quartz, albite, deep purple fluorite, a silvery-white, non-elastic mica, minor biotite and carbonate, and are heavily dusted with fine opaque material. These black rocks are in sharp contact with partly altered syenite or granite. This zone is referred to by Highwood Resources Ltd., the holder of mineral claims surrounding this area, as the T-zone (Fig. 26.3). Similar rocks are associated with narrow systems of syenite pegmatite and acmite-albite veins extending east-northeast from the southern exposed part of the T-zone, and are referred to as the R- and S-zones. Two kilometres south-southeast of the southern exposed end of the T-zone, at the opposite extremity of the alteration zone (unit 7), a 3 m wide vein of similar black rocks associated with brown and pink carbonate-fluorite-albite rocks, locally containing pyrite and chalcopyrite, cuts hornblende syenite (subunit 6e). This vein can be traced to the southeast for nearly 300 m, but narrows to a few centimetres in width southeastwards. This vein is referred to as the Fluorite zone (F in Fig. 26.3). The T-zone and the Fluorite zone are essentially in line with one another, but drilling will be required to prove their continuity as no rock is exposed in the part of the alteration zone between them.

All these zones give above background scintillometer readings, and all contain patches giving very high radiation counts. High counts are also obtained in various places within the alteration zone. Ground-based γ-ray spectrometer

surveys indicate that both U and Th are present, and that in some particularly radioactive spots, either one occurs almost to the exclusion of the other (S.M. Roscoe and S.S. Gandhi, pers. comm.). This is borne out by analyses[1] of extremely high grade grab samples, given in columns 1 and 2 of Table 26.3. Column 3 of this Table gives the weighted average oxide contents of channel samples from each of five trenches in the T-zone, and the lowest and highest of the five analyses. The trenches are cut perpendicular to the strike of the T-zone, range from 5.5 to 13.5 m (18 to 44 feet) in length for a total of 42.5 m (139 feet), and are distributed along a strike length of 610 m (2000 feet). Column 4 gives the same information for seven intersections of mineralization, ranging from 2.1 to 11 m (7 to 36 feet) and totalling 31.25 m (102.5 feet), in five drillholes in the S-zone; two holes have two intersections each. Analyses from two trenches across the Fluorite zone are similar except that rare-earth oxide contents are greater. An interesting aspect of these analyses is the fact that there is a strong positive correlation between Nb and U. There is also a weak correlation between Y and Th. In the trench and drillhole analyses, U and Th do not show a consistent inverse relationship.

The ore mineralogy has not been determined to date, with the exception that ixiolite, uranothorite, xenotime and phenakite have been identified by X-ray methods. Thin sections of mineralized rock show the opaque material, that likely contains much or all of the analyzed elements, to be very fine grained.

Pegmatites and albite-rich veins containing rare minerals are not restricted to the region of the Thor Lake Syenite. Quartz-feldspar pegmatite containing acmite, fluorite, astrophyllite, zircon, and bastnaesite occurs in granite east of Grace Lake. Fine grained quartz-albite rock with large, poikilitic acmite prisms, minor fluorite, bastnaesite, and small euhedra of a metamict mineral occurs as narrow dykes in granite west of Blachford Lake. Related dykes and veins beyond the outer contact of the Grace Lake Granite are rare, but one occurs in the Yellowknife metasediments northwest of Blachford Lake (Sn in Fig. 26.1), and was a former tin prospect, the Stannum Group (Mulligan, 1975, p. 97). It is composed of quartz, K-feldspar, albite, alkali amphibole and/or acmite, minor fluorite, pyrite, traces of cassiterite, and a brick red, fine grained mineral that could be xenotime. This dyke averages 1 m in thickness, strikes northwesterly, dips 60° northeast, and can be traced for more than 400 m. At its southeast end it cuts Grace Lake Granite dykes within metasediments, but has not been traced into the main granite pluton. It is noted that this dyke lies close to the northwesterly strike projection of the T-zone.

Zones of partly to wholly altered syenite and granite occur close to Hearne Channel in the Thor Lake Syenite and the Grace Lake Granite to the west, but have not been delimited to date. An aerial radiometric anomaly (Roscoe, pers. comm., 1977) coincides with part of an unexplained aeromagnetic anomaly (Geol. Surv. Can., Map 3023G, 1962) between Hearne Channel and the small granodiorite pluton (subunit 9b, Fig. 26.1).

Summary and Comments

The Blachford Lake Intrusive Suite contains several plutonic rock units related to one another by their alkaline character, and displaying a differentiation trend from mafic to felsic with time. Late-stage alteration and mineralization has concentrated the rare elements U, Th, Nb, Y and rare-earths, possibly in economic quantity. The Suite represents a number of successive intrusive events that led to emplacement of a complex of mildly alkaline to peralkaline rocks at high crustal level at some time during the first half of Aphebian time. An exhaustive radiometric age determination program is currently underway.

The alkaline complex has much in common in shape, size, lithology and tectonic setting with ring complexes of alkaline granite and related syenites and mafic rocks elsewhere, notably those in northern Nigeria (Jacobsen et al., 1958). In view of the fact that several such alkaline intrusions usually occur together in the same region, it is suggested that others may be present in the area of the southern Slave Province, as yet undiscovered in terrane mapped only as undivided granitic rocks. If, as in Nigeria, most of the granite complexes are of biotite granite type, lacking obvious alkaline characteristics, similar complexes in the southern Slave Province could easily have been passed over as late Archean intrusions related to Kenoran orogeny. This possibility may have importance with respect to economic potential, as it is these biotite granites rather than the peralkaline ones, for instance, that have associated tin mineralization in Nigeria.

Only one other intrusion that may be related to the alkaline complex at Blachford Lake has so far been recognized. It is referred to as the Easter Island dyke (Table 26.1) because it is well exposed on Easter Island, some 30 km south of Hearne Channel in the east arm of Great Slave Lake. This predominantly mafic intrusion was visited briefly by the author in order to compare it with the Caribou Lake Gabbro. The relationships between the Easter Island dyke and its surrounding rocks as outlined by Hoffman et al. (1977, p. 119) were confirmed; in summary, this dyke is exposed for nearly 30 km, strikes east-northeast,has a maximum thickness of the order of 200 m, and shows a differentiation trend from mafic to felsic along its length from west to east. It intrudes Archean crystalline rocks and is cut by east-northeast-trending diabase dykes. It is in fault contact with the basal Hornby Channel Formation of the Great Slave Supergroup (Sosan Group) which elsewhere is known to truncate the east-northeast-trending diabase dyke swarm. The Easter Island dyke is alkaline (biotite-bearing) and its extreme differentiation product is syenitic. Although it does not have any textural correlatives among the Blachford Lake Intrusive Suite, it may none-the-less be related; certainly it is of similar relative age.

Concerning the two small plutons emplaced within the Grace Lake Granite just west of the Thor Lake Syenite (Fig. 26.1, subunits 9a and b), it is worth noting that both cut cleanly across east-northeast-trending diabase dykes in the surrounding granite. These plutons are correlated (Table 26.1) with the diorite laccoliths emplaced within the Great Slave Supergroup south of Hearne Channel on the basis that the characteristic rocks composing the diorite stock (subunit 9a) are texturally and compositionally indistinguishable from those of the diorite laccoliths on Blanchet Island, 10 km to the south.

References

Currie, K.L.
1976: The alkaline rocks of Canada; Geol. Surv. Can., Bull. 239, 228 p.

Davidson, A.
1972: Granite studies in the Slave Province; in Report of Activities, Part A, Geol. Surv. Can., Paper 72-1A, p. 109-115.

Henderson, J.F.
1938: Beaulieu River area, Northwest Territories; Geol. Surv. Can., Paper 38-1, 20 p.

1941: Beaulieu River map-area; Geol. Surv. Can., Map 581A.

Hoffman, P.F.
1968: Stratigraphy of the lower Proterozoic (Aphebian) Great Slave Supergroup, east arm of Great Slave Lake, District of Mackenzie; Geol. Surv. Can., Paper 68-42, 93 p.

[1] All analyses reported here are courtesy of Highwood Resources Ltd. (D.G. Thomas, pers. comm., 1977).

Hoffman, P.F., Bell, I.R., Hildebrand, R.S., and Thorstad, L.
1977: Geology of the Athapuscow Aulacogen, east arm of Great Slave Lake, District of Mackenzie; in Report of Activities, Part A, Geol. Surv. Can., Paper 77-1A, p. 117-129.

Jacobsen, R.R.E., MacLeod, W.N., and Black, R.
1958: Ring complexes in the younger granite province of northern Nigeria; Geol. Soc. London, Mem. 1, 72 p.

Leech, A.P.
1966: Potassium-argon dates of basic intrusive rocks of the District of Mackenzie, N.W.T.; Can. J. Earth Sci., v. 3, p. 389-412.

Mulligan, R.
1975: Geology of Canadian tin occurrences; Geol. Surv. Can., Econ. Geol. Rept. 28, 155 p.

Sohl, N.F.
1977: Note 45 – Application for amendment concerning terminology for igneous and high-grade metamorphic rocks; Am. Assoc. Pet. Geol., Bull., v. 61, p. 248-251.

Stockwell, C.H.
1932: Great Slave Lake – Coppermine River area, Northwest Territories; Geol. Surv. Can., Sum. Rept., pt. C, p. 37-64.

Streckeisen, A.
1976: To each plutonic rock its proper name; Earth-Sci. Rev., v. 12, p. 1-33.

27. GEOLOGY OF THE RED WINE MOUNTAINS, LABRADOR: THE PTARMIGAN COMPLEX

Project 750011

R.F. Emslie, L.J. Hulbert[1], C.P. Brett[2], and D.F. Garson[3]
Regional and Economic Geology Division

Abstract

Emslie, R.F., Hulbert, L.J., Brett, C.P., and Garson, D.F., Geology of the Red Wine Mountains, Labrador: The Ptarmigan Complex; Current Research, Part A, Geol. Surv. Can., Paper 78-1A, p. 129-134, 1978.

The Red Wine Mountains of southern Labrador are underlain by an interspersion of high grade metasedimentary and meta-igneous rocks, the Ptarmigan Complex. The metasedimentary rocks consist of two distinct lithologies, the Hope gneiss and the Beaver gneiss. The quartzofeldspathic to semipelitic Hope gneiss contains the regional metamorphic mineral assemblages, sapphirine + quartz and hypersthene + sillimanite + quartz. The relatively mafic Beaver gneiss predominantly comprises orthopyroxene-, clinopyroxene- and garnet-bearing layered amphibolites with quartzofeldspathic and quartzite interlayers. These paragneisses are intimately intruded by a group of basic and anorthositic rocks and a younger, pyroxene-bearing, monzodiorite, quartz monzonite, granite group.

The Ptarmigan Complex forms the core region of a gneiss salient thrust northward during folding of the Seal Lake synclinorium. The northern margins of the complex are defined by wide cataclastic zones. Penetrative deformation of the complex produced internal structures consistent with northward thrusting of the complex over lower grade rocks.

The Grenville Front in this region appears to be a complex zone of imbricate slices. Similar rocks and structural relationships may characterize the southern flank of the Grenville Front Low gravity anomaly over a distance of 600 km.

Introduction

The Red Wine Mountains form a prominent southwesterly-trending range of high hills lying south of the Nascaupi Fold Belt in south-central Labrador (Fig. 27.1) and are contained within the Grenville Structural Province. The name Ptarmigan Complex is proposed here for the complex of meta-igneous and metasedimentary rocks that underlies the range. Reconnaissance mapping by Stevenson (1969) has shown that similar metasedimentary rocks with lesser, or negligible, amounts of meta-igneous material are traceable to the south and west for more than 150 km. This belt, including the Ptarmigan Complex, is characterized by marked positive Bouguer anomalies as shown on the Gravity Map of Canada published by the Earth Physics Branch, Map 74-1.

Study of the Ptarmigan Complex was undertaken because reconnaissance investigations (Lee, 1953; Stevenson, 1967, 1969) indicated that it consisted of a suite of anorthositic and related gabbroic rocks; as such it comprises the largest mass of these rocks lying near the unmetamorphosed Michikamau and Harp Lake complexes on the opposite side of the Grenville Front. The Ptarmigan Complex is thus of interest for comparative purposes in terms of the original igneous assemblage and its age and also as a study of the effects of the Grenvillian Orogeny with respect to the metamorphic mineral assemblages developed and the intensity and style of deformation. The Mealy Mountains complex, about 160 km east-southeast of the Ptarmigan Complex, shows some effects of metamorphic overprint but is not penetratively deformed (Emslie, 1976).

The intrusive ages of anorthositic and related rocks in central Labrador north of the Grenville Front are well established as Paleohelikian. The ages of similar suites in the Grenville Province are still in dispute and detailed studies of occurrences relatively near to known Paleohelikian complexes should help to establish whether or not age correlation is reasonable.

Regional Setting

Major structural features in the region are shown in Figure 27.1. The part of the Nascaupi Fold Belt shown is underlain mainly by greenschist and lower grade rocks of the Seal Lake Group of Neohelikian age. These rocks comprise a major synclinorium whose southern limb is steeply overturned to the north. The fault zone bounding the southern flank of this structure consists in part of cataclastic zones and is generally recognized as a northward directed thrust or steep reverse fault marking the position of the Grenville Front in this region (Brummer and Mann, 1961; Stockwell, 1963).

A major gneiss salient adjoins the Nascaupi Fold Belt to the south and the core of this salient is occupied by the Ptarmigan Complex. Rocks underlying the northern part of the gneiss salient are mainly a heterogeneous assemblage of granitic gneisses, paragneisses and migmatite and contain amphibolite facies mineral assemblages along the northwestern margin (Currie et al., 1975). Observations made up to 10 km northwest and north of the Ptarmigan Complex during the present work show that coexisting muscovite-quartz in paragneisses is widespread so that these gneisses are also not above regional amphibolite facies. Granulite facies mineral assemblages characterize all rock types within the Ptarmigan Complex and muscovite is absent; the boundary of the complex is abrupt, marked by severe structural dislocation and not part of an isograde progression.

The Ptarmigan Complex lies at the northern apex and along the northwestern side of a broad triangular wedge bounded by intense shearing and cataclasis on low-angle to relatively steep southerly-dipping surfaces. The outline of the wedge roughly mimics the southern fault-bounded margin of the Nascaupi Fold Belt and the axis of the Seal Lake synclinorium.

[1] Department of Geological Sciences, University of Regina, Regina, Saskatchewan S4S 0A2.

[2] Department of Geological Sciences, Queen's University, Kingston, Ontario K7L 3N6.

[3] Department of Geology, University of Ottawa, Ottawa, Ontario K1N 6N5.

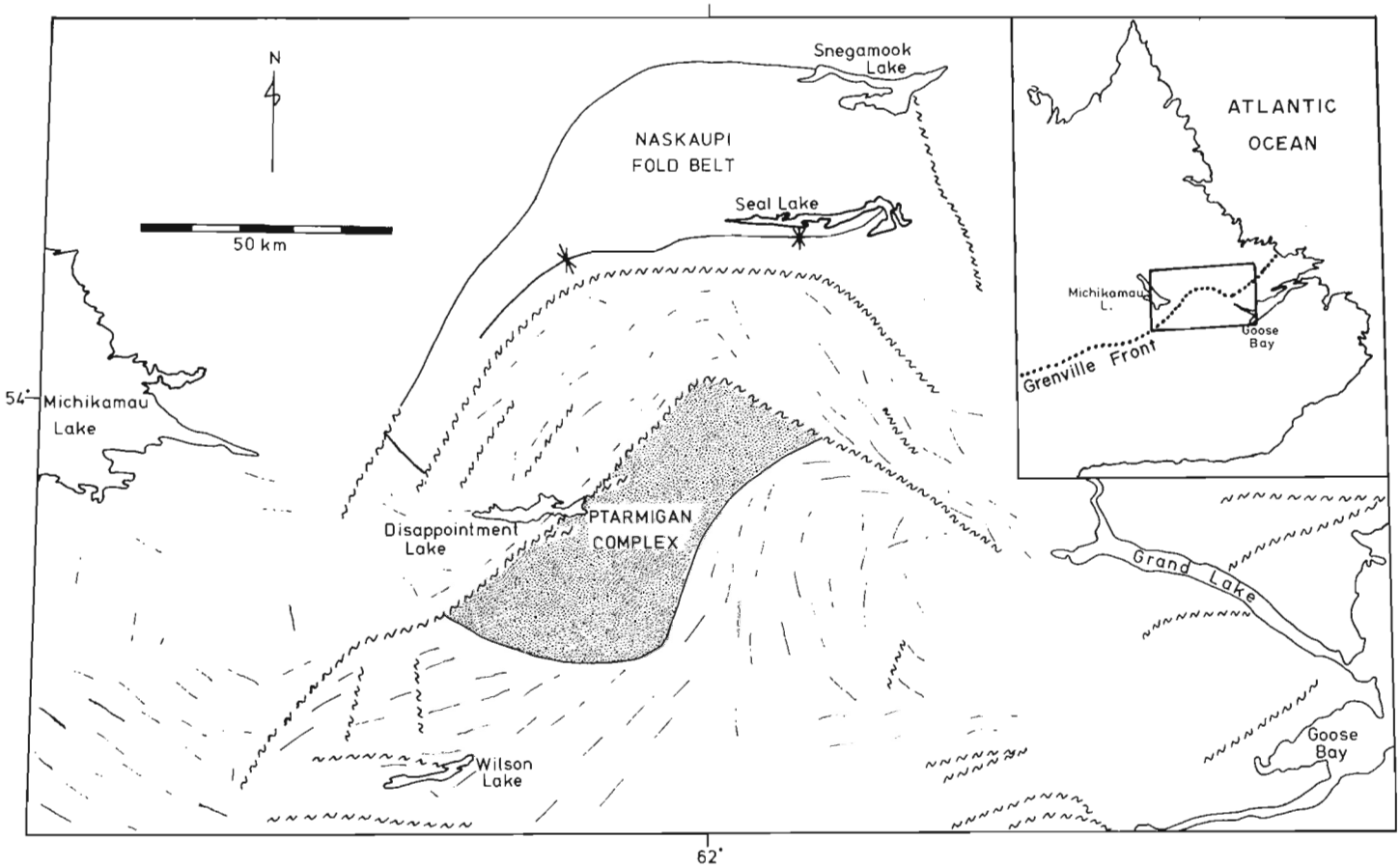

Figure 27.1 Regional structural setting of the Ptarmigan Complex. Structural trends in surrounding rocks shown by light lines.

Geology of the Ptarmigan Complex

A geological sketch map with the major units of the Ptarmigan Complex is shown in Figure 27.2. The metasedimentary rocks are divided into two main units, the Hope gneiss and the Beaver gneiss. The meta-igneous rocks consist of three units: 1) basic rocks including gabbro, norite, minor peridotite, leucogabbro, leuconorite and anorthosite; 2) chiefly monzonitic rocks ranging from monzodiorite to quartz monzonite; 3) pyroxene-bearing porphyritic granite.

Hope Gneiss

The Hope gneiss is most widespread of the two metasedimentary gneiss units. It is typically buff-weathering, rich in quartz and feldspars and for the most part leucocratic although darker layers and zones occur sporadically throughout the unit. Small scale layering is continuous locally but more commonly a discontinuous but marked foliation is caused by quartz and feldspar concentrations and wispy layers and streaks of mafic minerals. Hypersthene, biotite, garnet and sillimanite are visible in many hand specimens. Thin sections show that assemblages with coexisting hypersthene + sillimanite + quartz and sapphirine + quartz are widespread. Small scale folding is a common feature in outcrops and stages of deformation can be observed ranging from well defined folds with axial plane foliation through intermediate stages where fold hinges become disconnected from attenuated limbs to thoroughly sheared rocks in which fold hinges are rare or absent and only warps and crenulations in schistose layers persist.

Beaver Gneiss

The Beaver gneiss is characterized by a relatively mafic appearance but locally contains interbeds of quartzofeldspathic composition and thin quartzite layers. Many outcrops are well layered on a scale of a few millimetres to several metres. On the average much of the gneiss is medium grained although coarse grained hornblende and garnet are prominent in many outcrops. Additional common minerals are clinopyroxene, orthopyroxene, and plagioclase. Small scale folds are common and hornblende lineation subparallel to fold axes is widely present. Many outcrops have a slight to marked rusty appearance due to the common occurrence of disseminated sulphide accessory minerals.

Meta-igneous Rocks

a) Basic Group. Gabbros ranging from fine to medium grained with equigranular to ophitic and subophitic textures are the most abundant basic rocks in the complex. Subordinate in amount but widespread in occurrence are leucogabbros, leuconorites and anorthosites with medium to very coarse grain sizes. Internal relations among the basic rocks range from well developed regular layered sequences to highly complex intrusive relationships to gradational boundaries. Orthopyroxene is the predominant mafic mineral in the more leucocratic rocks but orthopyroxene and clinopyroxene are about equally abundant in many gabbros. Deep green spinel is prominent locally and euhedral grains poikilitically enclosed in pyroxene suggest that some is of primary igneous origin. Local ultramafic layers and lenses occur in the gabbroic rocks and some of these contain abundant olivine together with orthopyroxene and clinopyroxene and small amounts of plagioclase heavily charged with small euhedral spinel crystals; olivine does not occur in contact with

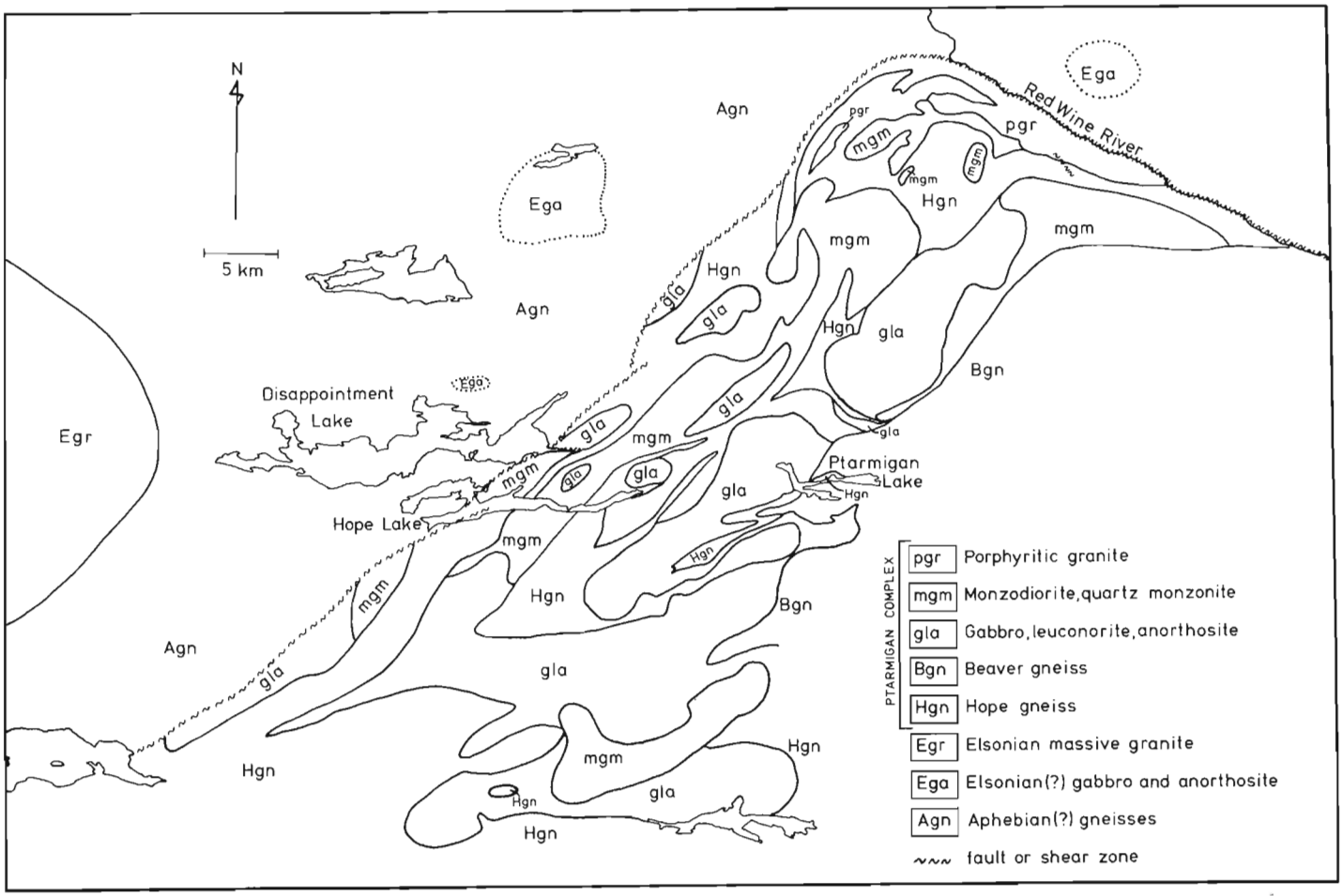

Figure 27.2. Sketch map of the main geological units of the Ptarmigan Complex and its surroundings.

plagioclase. Orthopyroxene megacrysts containing abundant plagioclase lamellae parallel to (100) of the pyroxene host occur in anorthosite and leuconorite and commonly have rounded outlines. Several examples of coarse orthopyroxene subophitically intergrown with tabular plagioclase were observed to contain plagioclase lamellae. Garnet occurs only sporadically in all of these metabasic rocks and is more common near contacts with, and inclusions of, paragneiss. Small gabbroic intrusive bodies, dykes, and sills occur in both of the metasedimentary gneiss units.

b) Intermediate and Silicic Group. These rocks have colour indexes ranging from about 40 to 15; quartz is more abundant in those with lower colour index. Alkali feldspar is visible even in rocks with high colour index; the compositional range is approximately from monzodiorite to quartz monzonite. Most of the rocks are medium grained but fine grained and coarse porphyritic varieties are also common. Pyroxenes occur in all of the rock compositions and are usually accompanied by variable amounts of hornblende and biotite. Some of the plutons are relatively homogeneous, others contain a considerable range of compositions and grain sizes, usually with gradational boundaries. Mineral layering occurs locally in these rocks, particularly the more mafic varieties, but is not persistent. Dykes of intermediate and silicic rocks cut the paragneisses and the basic group.

c) Granite. Porphyritic granite with prominent perthitic alkali feldspar phenocrysts occurs around the northern margin of the complex. The pale pink to purplish pink phenocrysts make it a highly distinctive rock. The colour index is about 15 to 20; the dark minerals consist of pyroxenes in part but these are normally subordinate to hornblende and biotite. The rock is increasingly sheared and schistose approaching the bounding cataclastic zone of the complex; perthite phenocrysts become augen of diminishing size with increasing degrees of cataclasis.

d) Diabase Dykes. Metadiabase dykes cut all of the other units of the Ptarmigan Complex. These, however, are typically deformed, boudinaged and metamorphosed. No examples of fresh, unmetamorphosed diabase dykes were discovered.

Rocks Bordering the Ptarmigan Complex

Detailed information on the rocks bordering the Ptarmigan Complex on the north and particularly on the northwest is scanty because of sparse outcrops in the low-lying muskeg-riddled terrain. Scattered outcrops in the surrounding area consist mainly of medium to coarse grained granitic gneisses containing large and small pods and lenses of pelitic and semi-pelitic schists and gneisses in which epidote and muscovite + quartz are common. Sillimanite (fibrolite) and garnet occur with muscovite + quartz at several localites.

The two bodies of gabbroic rocks lying northwest of the complex (Fig. 27.2) were sketched on the basis of their aeromagnetic anomaly patterns. Outcrops of fresh, unmetamorphosed gabbro and feldspathic gabbro occur within the anomalous areas. In places, these gabbros contain inclusions of pelitic schists similar to those found in the surrounding terrane.

Internal Deformation of the Complex

Lithologic trends and penetrative foliation in all units of the Ptarmigan Complex strike in a general southwesterly direction and dip toward the southeast at steep to moderate angles. Strained fabrics, cataclasis, and incipient cataclasis are widespread in all rock types and clearly appear to have largely postdated or outlasted metamorphism.

Striking lineations are developed as small scale fold axes, crenulation axes, mineral orientation and mineral streaking, elongated inclusions and augen. One or more of these features, though not present everywhere, are widely developed in all units of the complex. A plot of a sampling of these lineations is shown in Figure 27.3 in which a strong maximum plunging about 40° almost due south is readily apparent. Lineations with similar attitudes are also present in the main boundary cataclastic zone and in the wall rocks northwest of the complex. Narrow mylonite and ultramylonite zones occur in meta-igneous rocks in many places in the complex; these commonly have low (<40°) southerly dips and some are subhorizontal.

Economic Minerals

Local disseminations of pyrrhotite, chalcopyrite, and pyrite occur sporadically in the Beaver gneiss on the east side of the complex, particularly around Ptarmigan Lake. A little pyrrhotite and chalcopyrite are visible in many specimens of ultramafic composition. Small pods and irregular masses of opaque oxide minerals occur in rocks of the basic group and opaque oxide concentrations in lensy layers are present in some outcrops of Hope gneiss.

Discussion

Age Relationships

Pending the outcome of geochronologic studies on components of the Ptarmigan Complex the depositional or crystallization ages of the units and their metamorphic ages can only be speculated upon. However, some broad inferences can be drawn. The Hope gneiss and the Beaver gneiss represent relatively thick metasedimentary sequences and their character suggests that they may be as old as Aphebian but probably not older. If the meta-igneous suite that intrudes the gneisses is Paleohelikian like the Elsonian complexes to the north, an Aphebian age is indicated for the metasedimentary gneisses. On the other hand, if the meta-igneous suite is younger than Paleohelikian, the Hope and Beaver gneisses may, accordingly, be younger. Metamorphism and deformation that last affected the Ptarmigan Complex was almost certainly related to the Grenvillian Orogeny. The severity of this event largely obliterated any evidence of earlier metamorphism and deformation although folded stratiform foliation, evident on different scales in the paragneisses, may be relic from an earlier event.

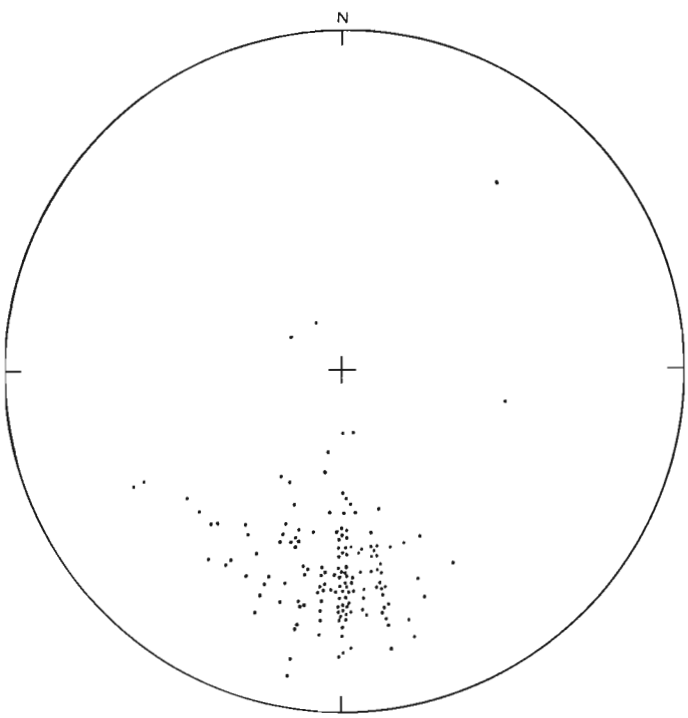

Figure 27.3 Equal-area projection of a variety of lineations occurring in all rock units of the Ptarmigan Complex.

Some potential clues to age relations exist in the terrane north and northwest of the Ptarmigan Complex. The unmetamorphosed gabbro and feldspathic gabbro bodies are likely to be examples of Paleohelikian Elsonian magmatism. Their richness in orthopyroxene and relatively feldspathic character is unlike basic rocks of the Neohelikian Seal Lake Group. The large granite on the west margin of Figure 27.2 is traceable into similar granite of known Paleohelikian age at the southeastern end of Lake Michikamau (Stevenson, 1969). The area of anorthosite northeast of the Ptarmigan Complex (Fig. 27.2) is also presumably Paleohelikian in age. There is, therefore, evidence for the existence of Paleohelikian Elsonian magmatism nearby in the surrounding terrane some, or most, of which may be relatively unaffected by the Grenvillian Orogeny.

Metamorphism

All rocks of the Ptarmigan Complex have been subjected to granulite facies metamorphism. The mineral associations sapphirine + quartz and hypersthene + sillimanite + quartz are widespread in the Hope gneiss. Preliminary examination has not revealed the presence of cordierite. Occurrences of sapphirine associated with these and similar assemblages have been described by Morse and Talley (1971) and Leong and Moore (1972) from the Wilson Lake area to the south (Fig. 27.1). Regional mapping by Stevenson (1969) showed that the Wilson Lake rocks are very likely equivalent to the Hope gneiss. Morse and Talley (1971) suggested, based on experimental results of Hensen and Green (1970), that the mineral assemblages reflected equilibration temperatures of 1100 to 1150°C and pressures of 11 to 13 kb. Subsequent studies have shown that high oxygen and low water fugacities probably play a significant role in reducing the P, T stability fields of the mineral assemblages to less extreme values (Leong and Moore, 1972; Chatterjee and Schreyer, 1972; Newton, 1972; Seifert, 1974). Notwithstanding these qualifications, it seems probable that some, or all, of the metasedimentary rocks of the complex display mineral assemblages consistent with relatively high temperature, high pressure metamorphism.

Metamorphic effects on the igneous components of the Ptarmigan Complex are less clear, although the rocks contain mineral assemblages compatible with granulite facies metamorphism. Garnet is not widespread in the basic rocks and its common occurrence in proximity to paragneiss contacts suggests contamination effects may be important. Garnet is perhaps slightly more common in the intermediate and silicic rocks although it is still by no means abundant or widespread. At this stage of investigation it is not clear that the meta-igneous rocks were metamorphosed to the same P, T conditions as the paragneisses, although it seems likely. The incompatibility of olivine and plagioclase in the ultramafic rocks suggests that they may be regarded as reconcilable with intermediate pressure granulites (Green and Ringwood, 1967).

Structural Relations

The gross relationships of the Ptarmigan Complex to the regional structural setting seem to be reasonably clear. Folding of the Seal Lake synclinorium was caused (or accompanied) by northward transport of rocks in the gneiss salient to the south. Some distance back from the leading edge of the salient, higher grade (of possibly deeper origin) rocks of the Ptarmigan Complex were thrust over medium grade gneisses. The occurrence of unmetamophosed, possibly Elsonian intrusive rocks in a zone north of the Ptarmigan Complex suggests that tectonic imbrication in this zone may be highly complex, incorporating wedges and slivers with differing metamorphic histories. Faults south of the Ptarmigan Complex (Fig. 27.1) have strikes consistent with northward tectonic transport on thrusts or steeper reverse faults but relative motions on them are largely unknown; they may indicate that northward directed transport influenced a broad region.

Internal structures in the Ptarmigan Complex are consistent with northward material transport. Linear structures in the various rock units plunge to the south and are therefore regarded as a lineations. They imply a penetrative bulk flowage mechanism operating while the rocks were at relatively high temperatures. Late, small, narrow, mylonite zones suggest that application of the stress field was protracted throughout the cooling period.

Gravity Expression

The positive Bouguer anomaly over the Ptarmigan Complex is consistent with the presence of basic rocks together with granulite facies mineral assemblages in all units. The anomaly is the easternmost of a group of such positive gravity "nodes" lying along and near the southern flank of the so-called "Grenville Front Low" negative Bouguer anomaly (Fig. 27.4).

In Figure 27.4, anomaly 1 is associated with the Ptarmigan Complex locality. Anomaly 2 is the southwesterly extension of granulitic gneisses similar to the Hope gneiss.

At the southern end of the Labrador Trough, anomaly 3 also contains granulite facies rocks and major cataclastic and mylonite zones indicate that progressively deeper rocks were brought up by northward thrusting (Wynne-Edwards, 1961).

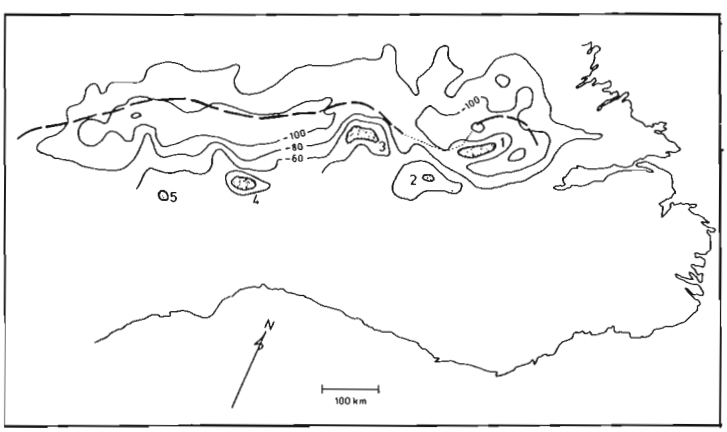

Figure 27.4 Relationships of the Ptarmigan Complex and other positive gravity "nodes" (shaded and numbered 1 through 5) to the Grenville Front Low. Contours are in milligals, adapted from the Gravity Map of Canada published by the Earth Physics Branch, Map 74-1. The heavy dashed line is the approximate position of the Grenville Front. See text for explanation.

Anomaly 4 is east of Manicouagan Lake. North-northwest directed thrusting is indicated by cataclastic zones and faults. Granulite facies gabbros and associated anorthositic rocks from the south have been brought into abrupt contact with amphibolite facies gneisses (Kish, 1968).

Anomaly 5 lies within a large complex of pyroxene granulites, anorthositic rocks and paragneisses along and west of the Rivière aux Outardes. These rocks are bounded on the north by amphibolite facies "grey gneisses" (Murtaugh, 1965; Franconi et al., 1975).

The physical significance of these positive gravity nodes relative to the Grenville Front Low is by no means clear but northerly directed thrusting of deep seated high grade metamorphic rocks over low grade rocks seems sufficiently consistent to suggest a relationship to a common origin. Thomas and Tanner (1975) suggested that the southern edge of the Grenville Front Low may be a suture zone marking the former site of a continental margin. Although severe tectonism, characterized by north to northwesterly directed thrusting of imbricated, nappe-like slices seems to be related to this zone, evidence to support the presence of a former ocean floor remains unestablished.

References

Brummer, J.J. and Mann, E.L.

1961: Geology of the Seal Lake area, Labrador; Bull. Geol. Soc. Am., v. 72, p. 1361-1382.

Chatterjee, N.D. and Schreyer, W.

1972: The reaction enstatite$_{ss}$ + sillimanite = sapphirine$_{ss}$ + quartz in the system MgO - Al_2O_3 - SiO_2; Contr. Mineral. Petrol., v. 36, p. 49-62.

Currie, K.L., Curtis, L.W., and Gittens, J.

1975: Petrology of the Red Wine alkaline complexes, central Labrador and a comparison with the Ilimaussaq complex, southwest Greenland; Report of Activities, Part A, Geol. Surv. Can., Paper 75-1A, p. 271-280.

Emslie, R.F.

1976: Mealy Mountains complex, Grenville Province, southern Labrador; in Report of Activities, Part A, Geol. Surv. Can., Paper 76-1A, p. 165-170.

Franconi, A., Sharma, K.N.M., and Laurin, A.F.

1975: Betsiamites (Bersimis) and Moisie Rivers area; Que. Minist. Rich. Nat., Geol. Rep. 162, 149 p.

Green, D.H. and Ringwood, A.E.

1967: An experimental investigation of the gabbro to eclogite transformation and its petrological application; Geochim. Cosmochim. Acta, v. 31, p. 767-833.

Hensen, B.J. and Green, D.H.

1970: Experimental data on coexisting cordierite and garnet under high grade metamorphic conditions; Phys. Earth Planet. Interiors, v. 3, p. 431-440.

Kish, L.

1968: Hart-Jaune River area, Saguenay County; Que. Dept. Nat. Resour., Geol. Rep. 132, 98 p.

Lee, B.W.

1953: The Red Wine Mountains map-area; a preliminary report on a portion of Labrador lying between latitudes 53°10' - 54°00'N and longitudes 61°40' - 62°17'W; Dep. Mines, Agric. Resour., Newfoundland (open file report).

Leong, K.M. and Moore, J.M. Jr.

1972: Sapphirine-bearing rocks from Wilson Lake, Labrador; Can. Mineral., v. 11, p. 777-790.

Morse, S.A. and Talley, J.H.

1971: Sapphirine reactions in deep-seated granulites near Wilson Lake, central Labrador, Canada; Earth Planet. Sci. Lett., v. 10, p. 325-328.

Murtaugh, J.C.

1965: Géologie de la Région du Lac Tétépisca; Que. Minist. Rich. Nat., Rep. Prelim. 536, 6 p.

Newton, R.C.

1972: An experimental determination of the high-pressure stability limits of magnesian cordierite under wet and dry conditions; J. Geol., v. 80, p. 398-420.

Seifert, F.

1974: Stability of sapphirine: a study of the aluminous part of the system $MgO - Al_2O_3 - SiO_2 - H_2O$; J. Geol., v. 82, p. 173-204.

Stevenson, I.M.

1967: Goose Bay map-area, Labrador; Geol. Surv. Can., Paper 67-33, 12 p.

1969: Lac Brûlé and Winokapau Lake map-areas, Newfoundland and Quebec; Geol. Surv. Can., Paper 67-69, 16 p.

Stockwell, C.H.

1963: Third report on structural provinces, orogenies, and time-classification of rocks of the Canadian Precambrian Shield; in Age Determinations and Geological Studies (Including Isotopic Ages - Report 4), Geol. Surv. Can., Paper 63-17, p. 125-131.

Thomas, M.D. and Tanner, J.C.

1975: Cryptic suture in the eastern Grenville Province; Nature, v. 256, p. 392-394.

Wynne-Edwards, H.R.

1961: Ossokmanuan Lake (west half), Newfoundland; Geol. Surv. Can., Map 17-1961.

28.

RECONNAISSANCE GEOLOGY OF THE PRECAMBRIAN SHIELD ON ELLESMERE AND COBURG ISLANDS, CANADIAN ARCTIC ARCHIPELAGO

Project 760023

T.Frisch, W.C. Morgan and G.R. Dunning[1]
Regional and Economic Geology Division

Abstract

Frisch, T., Morgan, W.C., and Dunning, G.R., Reconnaissance geology of the Precambrian Shield on Ellesmere and Coburg islands, Canadian Arctic Archipelago; Current Research, Part A, Geol. Surv. Can., Paper 78-1A, p. 135-138, 1978.

Reconnaissance geological mapping of the Precambrian Shield on Ellesmere and Coburg islands has been completed. The Shield area was metamorphosed entirely in the granulite facies. Detailed work on the unmetamorphosed Proterozoic sedimentary and igneous rocks of the Thule Basin has enabled correlations to be made both between the three main areas of outcrop and with the lower part of the Wolstenholme Formation on Greenland. Minor occurrences of Cu-Fe sulphides and malachite are common in metasedimentary basement rocks; malachite is also found in Thule Basin igneous rocks.

Introduction

The 1977 field season saw the initiation of airborne reconnaissance mapping of the northernmost part of the Canadian Shield. The Shield areas of eastern and southern Ellesmere Island and Coburg Island (Fig. 28.1) were mapped on a scale of 1:250 000 (NTS 39B, C and F, and parts of 39D, G and H; part of 48H; and parts of 49A, B, D, E and H). Mapping on Devon Island is planned for 1978 and that work should complete the geological reconnaissance of the Churchill Province of the Canadian Shield.

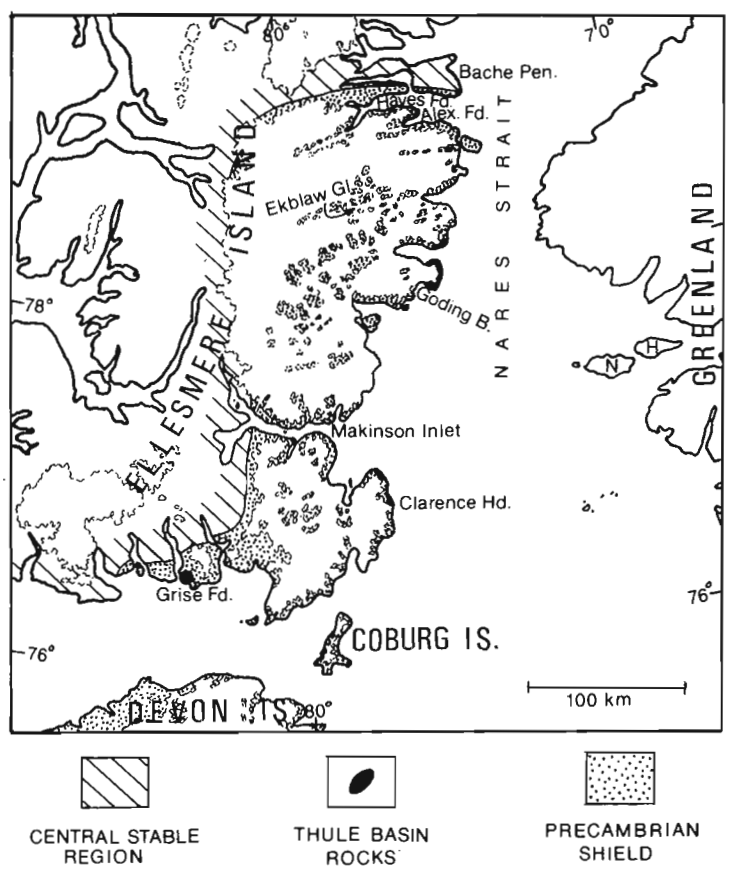

Figure 28.1 Locality map showing the extent of the Precambrian Shield on Ellesmere and Coburg islands. Only the major rock exposures in the area of heavy ice and snow cover are shown. Northumberland and Herbert islands in Greenland are marked "N" and "H".

Relief and permanent snow and ice cover in the map-area are considerable (Fig. 28.2). Coastal cliffs commonly rise to 500 m and nunataks to 1500 m a.s.l. The greatest relief - 2300 m - is found in the northwestern part of the area.

Prior knowledge of the Precambrian was based chiefly on the dog-sledge traverses of Christie (1962a,b), whose observations were of necessity confined largely to the coasts but included considerable detail on the Proterozoic Thule Basin rocks. A K-Ar date of 1760 m.y. on a gneiss from southeast Ellesmere Island is the only isotopic age available.

Crystalline Basement

The entire crystalline basement of Ellesmere and Coburg islands has been metamorphosed in the granulite facies. Rocks that in the field appear to be of amphibolite grade are interpreted as having been downgraded.

The basement rocks may be divided into the following broad groups:

(1) Massive to foliated quartzofeldspathic granulites. These rocks appear more or less homogeneous, are green on fresh, and brown or red on weathered surfaces, and commonly carry abundant feldspar porphyroblasts. They are the major rock-type in the Grise Fiord area.

(2) Metasediments. These include garnet-biotite gneisses, commonly with sillimanite and/or cordierite, well-banded hornblende ± pyroxene gneisses, diopside-bearing marble, and subordinate quartzite. Amphibolite is a common associate.

(3) Amphibolites, which generally carry at least one pyroxene.

(4) Granulite gneisses are distinct from the granulites of unit (1) in that they are heterogeneous and well banded pyroxene-bearing quartzofeldspathic rocks. Some have a metasedimentary aspect and indeed may be associated with, or even grade into, undoubted metasediments. Other varieties are of more uncertain origin. If an equilibrium one, the association hypersthene-sillimanite-quartz found in this unit suggests temperatures and pressures of metamorphism in the neighbourhood of 900°C and 10 kb.

(5) Granitic rocks. These are generally pink and weather red or brown, similar to the granulites, a fact which makes their distinction from the latter difficult at times, unless sampling is possible. The unit includes a diversity of types and, probably, ages of rock. In the Grise Fiord area and elsewhere, pink granite invaded and partly assimilated granulite. This major event was followed by severe

[1] Department of Geology, Carleton University, Ottawa.

Figure 28.2 Typical Shield terrain in gneisses and granulites north of Makinson Inlet. GSC 203055-Q

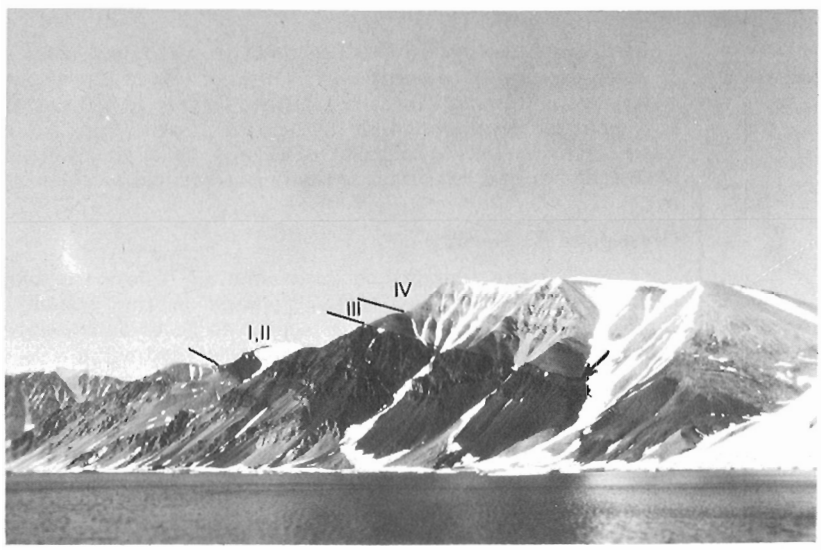

Figure 28.3 Unmetamorphosed Thule Basin rocks overlying steeply-dipping gneisses immediately south of Clarence Head. The Roman numerals refer to the units shown in Figure 28.4. At this locality, unit I is only 4 m thick. Arrow at right points to the thin, resistant stromatolitic carbonate bed at the base of unit III. GSC 203055-P

deformation, resulting locally in a granite-banded granulite gneiss. Garnet is common in both the granulite and granite. A medium- to coarse-grained, potassic granite outcrops extensively in the northwestern part of the area. While generally massive, this granite is foliated in places. In fact—discounting aplites and pegmatites — no undoubted post-tectonic granitic rocks were observed. A similar impression was gained by G.D. Jackson (pers. comm., 1977) in the spatially-related high-grade terrain of Bylot Island and northeastern Baffin Island.

Minor bodies of anorthosite were noted in the northern part of the area.

Relations between lithologic units of the basement have been largely obscured by intense deformation (or are frequently hidden under snow and ice). Generally, dips are steep to vertical and isoclinal folds are common. Recumbent folds were also recognized and, judging by frequent rapid changes in dip from shallow to steep, probably constitute a major fold type. A later phase of tectonism gave rise to broad, open folds. A northerly regional gneissic trend can be discerned but local variations are numerous and marked.

In lithology, grade of metamorphism and tectonic style, the crystalline basement of Ellesmere Island bears many similarities to that of northwestern Greenland (Dawes, 1976).

Proterozoic Thule Basin Rocks

Unmetamorphosed sedimentary and igneous rocks nonconformably overlie basement in several areas on the east coast of Ellesmere Island (Fig. 28.1). These beds belong to the Thule Basin sequence, the bulk of which is exposed on the Greenland side of Nares Strait (Christie, 1972). Figure 28.3 shows part of the southernmost outcrops, near Clarence Head; their variegated appearance and gentle dip are typical.

A schematic columnar section of the Thule Basin sequence on Ellesmere Island is presented in Figure 28.4. Nowhere is the entire section exposed nor are the successions in the various localities identical, yet the similarities suffice to permit correlations between them. Further analysis of the field data is necessary but the thickness of the entire section probably lies between 1000 and 1500 m, somewhat less than the 1800 m thickness estimated by Christie (1972).

The sediments clearly were deposited in a nearshore to subaerial environment. Orientations of cross-bedding commonly indicate westward-directed currents but bimodal transport patterns, strongly suggestive of tidal influence, predominate in many localities.

The Thule Basin sequence on Ellesmere Island can readily be correlated with the lower part of the Wolstenholme Formation of middle Proterozoic age (Dawes, 1976) in the Thule area of Greenland, in particular Herbert and Northumberland islands (Fig. 28.1).

Paleozoic Strata

The Precambrian Shield on Ellesmere Island is bordered on the west by Paleozoic rocks of the Central Stable Region (Christie, 1972). Evidence that the sedimentary cover once extended much farther over the Shield is provided by Paleozoic outliers in the interior of the Shield area.

The Paleozoic strata comprise carbonates and clastics ranging in age up to Devonian. Although structurally simple, the Paleozoic rocks form a succession that is unusually thick and complex, considering its proximity to the Precambrian Shield. Systematic mapping of these rocks has yet to be undertaken in much of the area.

The Precambrian-Paleozoic contact was mapped over the entire area and examined at a number of localities. The underlying granitic and granulitic basement rock is commonly a dusky red, a feature attributable to weathering, but no regolith was observed. The basal Paleozoic strata are quartz-pebble conglomerate, quartz sandstone and ripple-marked silty sandstone, some of which are ferruginous. No fossils have been found but these beds are probably lower Cambrian.

The striking contrast between the light-weathering Paleozoic and the darker basement greatly facilitates recognition of major block faulting. Faults with throws of several hundreds of metres are common.

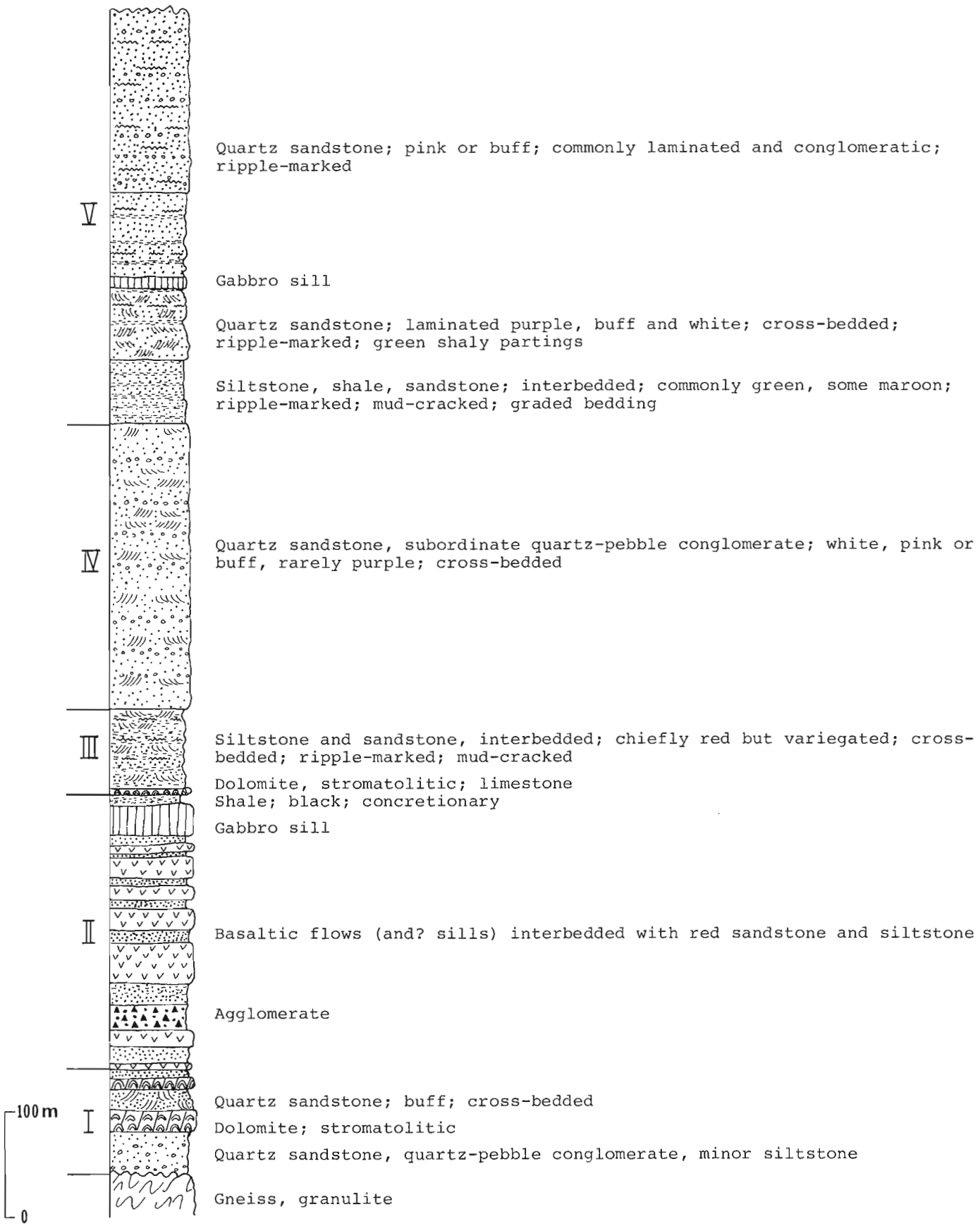

Figure 28.4 Composite, somewhat schematic columnar section of the Thule Basin sequence on Ellesmere Island. Compare this with section 8 (Herbert and Northumberland islands) of the sequence on Greenland in Dawes (1976, Fig. 232).

Diabase Dykes

Diabase dykes are distributed throughout the Precambrian terrane, generally trending northerly or northeasterly; they have not been seen cutting Paleozoic rocks. No major swarms were noted but dykes are numerous in the areas of Thule Basin strata, particularly Clarence Head and Goding Bay (Fig. 28.1).

Economic Geology

Minor occurrences of metallic minerals are common in the metasedimentary unit (2) of the crystalline basement. In the Alexandra Fiord area (Fig. 28.1), impressive gossans have developed over pyrrhotite ± chalcopyrite ± sphalerite-rich zones up to 8 m wide in the gneisses. Malachite staining was found in metasediments on the north shore of Makinson Inlet, along Ekblaw Glacier and on the south shores of Hayes Fiord and Bache Peninsula (Fig. 28.1); it was also seen on the cliffs formed by unit II of the Thule Basin sequence near Clarence Head (Fig. 28.3).

Seams of low-grade coal are abundant in sediments of the Eureka Sound Group of Cretaceous-Tertiary age, which outcrop in the Central Stable Region near the western edge of the ice cap.

Acknowledgments

We are grateful to the following persons and organizations. E.T. Lisle and D.I. Brisbin (field assistants); W.F. Christensen (camp manager/radio operator); D.A. MacDonald (cook); the helicopter crews of Liftair International, Ltd., Calgary, for their flying skill; the Polar Continental Shelf Project, for generous Twin Otter support and much other assistance; E. Zwick, for expediting at Resolute Bay; Cpl. J.E. Grant, RCMP, and Mrs. Grant, for many courtesies and hospitality at Grise Fiord; M. Vaydick, DINA settlement manager at Grise Fiord, for his help; the Captain and crew of CCGS Louis S. St. Laurent, for efficient caching of materiel in the field in 1976; and the Royal Canadian Mounted Police, for permission to use their buildings at Alexandra Fiord.

References

Christie, R.L.

1962a: Geology, Alexandra Fiord, Ellesmere Island, District of Franklin (map with marginal notes); Geol. Surv. Can., Map 9-1962.

1962b: Geology, southeast Ellesmere Island, District of Franklin (map with marginal notes); Geol. Surv. Can., Map 12-1962.

1972: Central Stable Region; in Guidebook to Excursion A66, The Canadian Arctic Islands and the Mackenzie Region, D.J. Glass, ed.,; XXIV Int. Geol. Congr., Montreal, p. 40-87.

Dawes, P.R.

1976: Precambrian to Tertiary of northern Greenland; in Geology of Greenland, A. Escher and W.S. Watt, eds.; Geol. Surv. Greenland, Copenhagen, p. 248-303.

29. A SUBDIVISION OF THE NORTHERN CHURCHILL STRUCTURAL PROVINCE

Project 770022

W.W. Heywood and Mikkel Schau
Regional and Economic Geology Division

Abstract

Heywood, W.W. and Schau, Mikkel, A Subdivision of the northern Churchill Structural Province; Current Research, Part A, Geol. Surv. Can., Paper 78-1A, p. 139-143, 1978.

Fault zones divide the northern Churchill Structural Province into three smaller blocks or subprovinces, each exposing a different level of crust. The deep-level Queen Maud Block is bounded on the west by the Thelon Front, and on the southeast by the Slave-Chantrey mylonite zone. The high to intermediate level Committee Bay Block, southeast of the mylonite zone, is bounded on the south by the McDonald-Amer-Meadowbank fault system. The intermediate to deep level Armit Lake Block lies south of the above system and is bounded on the south by the Chesterfield fault. All blocks have been cut by later northwest fault systems and dyke sets. The blocks pre-date the Hudsonian Orogeny. Aphebian and later sedimentary and volcanic rocks lie along the fault zones. The fault zones may be loci of ore deposits.

Faults and mylonite zones divide the northern Churchill Structural Province (Stockwell, 1964) into three blocks (or subprovinces), each exposing a different "level of crust". The proposed division is shown in Figure 29.1. The eastern boundaries of the blocks terminate beneath the Paleozoic cover of Foxe Basin and northern Hudson Bay and the western boundary is the Thelon Front. Movement of the blocks terminated before the upper division of the Dubawnt Group was deposited in Paleohelikian(?) time. Rocks in each block range in age from middle(?) Archean to Paleozoic. The relatively uniform K-Ar dates of "Hudsonian" age that are characteristic of the area (Heywood, 1967; Wright, 1967) may mark the cessation of argon diffusion in micas due to uplift of blocks above a critical crustal level or the end of widespread shearing rather than a widespread fold episode.

The three blocks are named, from northwest to southeast: the Queen Maud Block, Committee Bay Block, and the Armit Lake Block. Their similarities and differences are summarized in Table 29.1. The geological history, where known, is quite similar for each of the blocks. It is apparent that the main differences are mineralogical and structural and therefore are those that represent different levels of the crust. Granulite facies mineral assemblages characterize the deeper level crust, whereas greenschist and lower amphibolite assemblages occur in the higher level segments. The same rock type is also emplaced in different structures, depending on the level of crust exposed. The structural setting of anorthosite bodies, for example, differs in each block. In the deep level Queen Maud Block, anorthosite bodies form concordant sheets in high grade gneisses (Heywood, unpublished manuscript); in the medium level Armit Lake Block they form flattened and foliated stocks as much as 30 km long and more or less concordant with enclosing gneisses (Heywood, 1967; Schau and Hulbert, 1977; Gordon, 1971); whereas in the high level Committee Bay Block small anorthosite stocks and dykes clearly cross-cut the Prince Albert Group and basement gneisses. Also in this block, large gabbroic sills with anorthosite-rich layers intrude the late Archean Prince Albert Group.

The blocks are separated by fault systems which were formed at different times in different milieus (Table 29.2). The earliest system, the Slave-Chantrey mylonite belt, which formed at a deep crustal level, separates the Queen Maud Block from the Committee Bay Block. It is a wide mylonite belt (Reinhardt, 1969) typical of rocks which fall in the quasi-plastic regime (Sibson, 1977). The younger McDonald-Amer-Meadowbank fault system is in part a narrow mylonite zone and in part a well-defined fault trace (Heywood, 1977; Hoffman et al., 1977) of the elasto-frictional (Sibson, 1977) regime. This system separates the Queen Maud and Committee Bay blocks from the Armit Lake Block. The lesser-known Chesterfield fault system separates the Armit Lake Block from the central part of the Churchill Structural Province to the south.

The movement on these faults is not well known. The Chesterfield fault appears to be a reverse fault system with a vertical separation as much as 15 km(?) based on preliminary estimates of metamorphic contrast on either side of the system (greenschist vs. medium pressure granulite facies) (Reinhardt and Chandler, 1973; Schau and Hulbert, 1977; Geol. Surv. Can. Metamorphic Map 1975A, in prep.). The McDonald portion of the McDonald-Amer-Meadowbank system is a dextral strike-slip fault with about 75 km movement deduced from stratigraphic studies by Hoffman et al. (1977). A similar amount of movement has not yet been shown for the more easterly portion of this system. The amount of movement of the Slave-Chantrey mylonite zone is unknown. Thomas et al. (1976) postulated two possible offsets on that part of the zone contiguous with the later McDonald system. These are dextral offsets of 75 and 120 km. If the movement deduced for the later McDonald fault is removed, a horizontal separation of either 0 or 45 km may be attributed to the Slave-Chantrey zone. Reinhardt (1969) established a movement of 1.6 km on one branch of this zone. The vertical component of the main mylonite zone is unknown but high-grade rocks abut low-grade rocks north-northeast of Baker Lake, suggesting that the separation may locally be considerable. Although the main zones are thought to localize most fault movement, numerous splays are present. The western portion of the mylonite zone is the site of the Athapuscow Aulacogen (Hoffman et al., 1977) and has locally been involved in the complicated tectonics associated with this structure. To the east it appears that the mylonite zone has had a simpler history; however, a detailed sedimentological investigation of the Chantrey Group may prove otherwise.

Aphebian sediments such as quartzites, dolomites and minor graphitic mudstones, were deposited on the Archean basement during a quiescent period early(?) in the history of the faulting. Sediments were also deposited on or near the fault zones during or after the movements. These deposits, which include the East Arm sequence (Hoffman et al., 1977), Bathurst Inlet sequence (Campbell and Cecile, 1975, 1976; Campbell, 1978), Dubawnt Group (Donaldson, 1965; Blake and LeCheminant, 1977; Blake et al., 1977), all contain immature sediments and volcanic rocks.

Table 29.1
Summary of main features of the Queen Maud, Committee Bay and Armit Lake blocks

	QUEEN MAUD BLOCK	COMMITTEE BAY BLOCK	ARMIT LAKE BLOCK
Paleozoic cover	Extensive in northeastern sector	Extensive in eastern sector	Extension in eastern sector
Diabase dykes	Rare, few in southern area	Common, widely spaced, continuous for tens to hundreds of kilometres	Rare, widely spaced
Granite, porphyritic (Nueltin type)	On eastern and western margins	Most in northeast trending zone in central part	Most common on eastern margin
Paleohelikian cover	Southeastern margin	At extreme northeast and southwest?	Western margin
Granite and gneiss	Local granite plutons. Local development of gneiss in Chantrey group	Gneiss developed from Penrhyn Group and preceding rocks. Local plutons. Augen gneiss developed from preceding plutons	Possible late pluton
Aphebian metasediment	Not reported	Chantrey, Amer, Hurwitz, Penrhyn groups	Hurwitz Group northeast of Baker Lake
Archean gneisses?	Archean? granites, gneisses and agmatites	Gneisses developed from Prince Albert Group and underlying gneisses. Intruded by large batholiths	Gneisses, in part of metasedimentary origin, granitic plutons
Anorthosite	Layers associated with gneisses	Small pods, deformed but appear discordant to Prince Albert Group and basement gneisses Possibly related to some gabbros.	Small stocks, deformed but discordant, at Baker Lake, Daly Bay, Walrus Island, Coats Island
Gabbro	Stocks, sills, dykes; possibly several ages	Small pods of several ages. Large sill-like bodies with anorthosite layers in eastern part	Small stocks of several ages, some large bodies with ultramafic affinities
Archean metasediments	Archean paragneiss and associated lime silicate gneiss	Prince Albert Group	Possibly granulites near Baker Lake. Quartzite of probable Archean age
Peridotite	Hornblendite associated with gneisses	Komatiite flows, sills, dykes in Prince Albert Group and derived gneisses; intrude older gneisses	Segregations in granulite terrane near Baker Lake
Basement gneisses	Layered grey gneiss, charnokitic gneiss	Grey gneiss, granite gneiss	Possibly charnokitic gneiss in Baker Lake area
Structural complexity	Insufficient data	Hudsonian deformation (possibly two) in Foxe Fold Belt; Kenoran deformation preserved in Committee fold belt; Pre-Prince Albert Group preserved in small areas	Hudsonian deformation? Kenoran deformation? Pre-Kenoran deformation?
Metamorphism general grade	Granulite and upper amphibolite facies, less commonly lower amphibolite	Predominantly amphibolite facies, ranges from greenschist to granulite	Amphibolite to granulite facies, granulite especially near northern and southern boundaries
Average chemical composition	Insufficient data. Small area same as average composition for shield gneiss	Similar to average gneiss composition of the Shield	Insufficient data
Gravity regional	Generally negative with Perry River Low and Boothia Peninsula high	Generally negative. High on Melville Peninsula over granulites and low over northeast trending granite belt. Wager Bay low is over Nueltin type granite	Negative at north and positive at south boundaries. Highs at Coral Harbour, Baker Lake, Daly Bay and Boas River. First three with granulite and anorthosite
Aeromagnetics regional	Generally above average for region strong linear pattern 100 km wide near Thelon Front	Generally below average for region	Generally above average, especially near margins
Radiometric data range (λ=1.42)	K/A 1710-1880 m.y. mainly greater than 1710 m.y.	K/A 1500-2200 m.y. mainly 1600-1700 m.y. Rb/Sr 2280-2590 m.y.? Zr 2500-3000 m.y.	K/A 1600-1800 m.y. Rb/Sr 2070-3100 m.y.; 1780 m.y. on Dubawnt cover Zr 2000 m.y.
Topography	Back River Lowlands	Wager Plateau	Wager Plateau
LEVEL OF CRUST	"DEEP LEVEL CRUST"	"HIGH TO INTERMEDIATE LEVEL CRUST"	"INTERMEDIATE TO DEEP LEVEL CRUST"
Mapping	Reconnaissance scale only	Reconnaissance with detail in Hayes River-Kellett River, Mackar Inlet, Kingora River and the Penrhyn Group of Melville Peninsula	Reconnaissance with detail at Daly Bay, east end of Baker Lake, Amer Lake and Schultz Lake

Table 29.2
Summary of main features of faults and mylonite zones

	Slave-Chantrey Mylonite Zone	McDonald-Amer-Meadowbank Fault	Chesterfield Fault Zone	Late Faults Sherman Inlet Hayes River Rae Isthmus Roes Welcome Sound
Orientation	ENE to NE ± Vertical Rifting and/or Strike-slip	ENE - E - NE ± vertical Strike-slip?	E North dip Reverse	NW, some N to NE ± vertical
Width	50 km near East Arm, Garry Lake Chantrey Inlet	Generally less than 1 km	Less than 1 km? commonly few tens of metres	Narrow fault zones
Fault rocks	Mylonites, ultramylonite, cataclasite. Some large undeformed blocks	Mylonite, local ultramylonite Few undeformed blocks	Cataclasite, crush breccia, mylonite. Narrow fault zone	Cataclasite, crush breccia Narrow zone
Movement	Unknown, possibly as much as 45 km strike slip. Western end site of Athapuscow Aulacogen	Up to 75 km determined from sedimentary facies studies, magnetic anomaly displacement	~15 km dip slip (from preliminary petrographic P. estimates from both sides of fault).	Up to 1 km + determined from displacement of Paleozoic cover
Youngest rocks affected	Wilson Island Group Chantrey Group	Hurwitz Group Dubawnt "Amer Group" Group Et-Then Group	Hudsonian Granite at Cross Bay	Silurian
Oldest rocks affected	Unknown age: basement gneiss with anorthosite layers	Older Archean basement gneiss	Older Archean basement gneisses, anorthosites	Older gneisses
Oldest rocks not affected	Sosan Fm_1 in EastArm (Aphebian) Dubawnt Group (Paleohelikian)	Granite in Wager Bay area (Paleohelikian)	South Channel conglomerate (Paleohelikian) of Dubawnt Group	None
Associated faults	Possibly Murchison, Amer, Kellett	Probably Murchison, Kellett	Not known	Not known
Cut by younger faults (eg)	Bathurst strike-slip fault (Paleohelikian) Rae Isthmus Fault	Sherman Inlet Fault Hayes River Fault Vertical Rae Isthmus Fault displacement Roes Welcome Sound 1 + km Fault	Cross Bay Fault Roes Welcome Sound Fault Rae Isthmus Fault	
Dykes that cross the faults	Mackenzie dykes	Mackenzie Dykes	Mackenzie Dykes	Not known Dykes parallel fault trend
Post fault volcanism	Post Hornby Channel diatremes Basic and silicic volcanics of Sosan Kahochella groups. Central diabase swarm? of 2nd stage of Athapuscow Aulacogen	Minor basaltic volcanism in East Arm area	Diatremes and alkalic volcanics at Christopher Island Fm_1 of Dubawnt Group	Not known

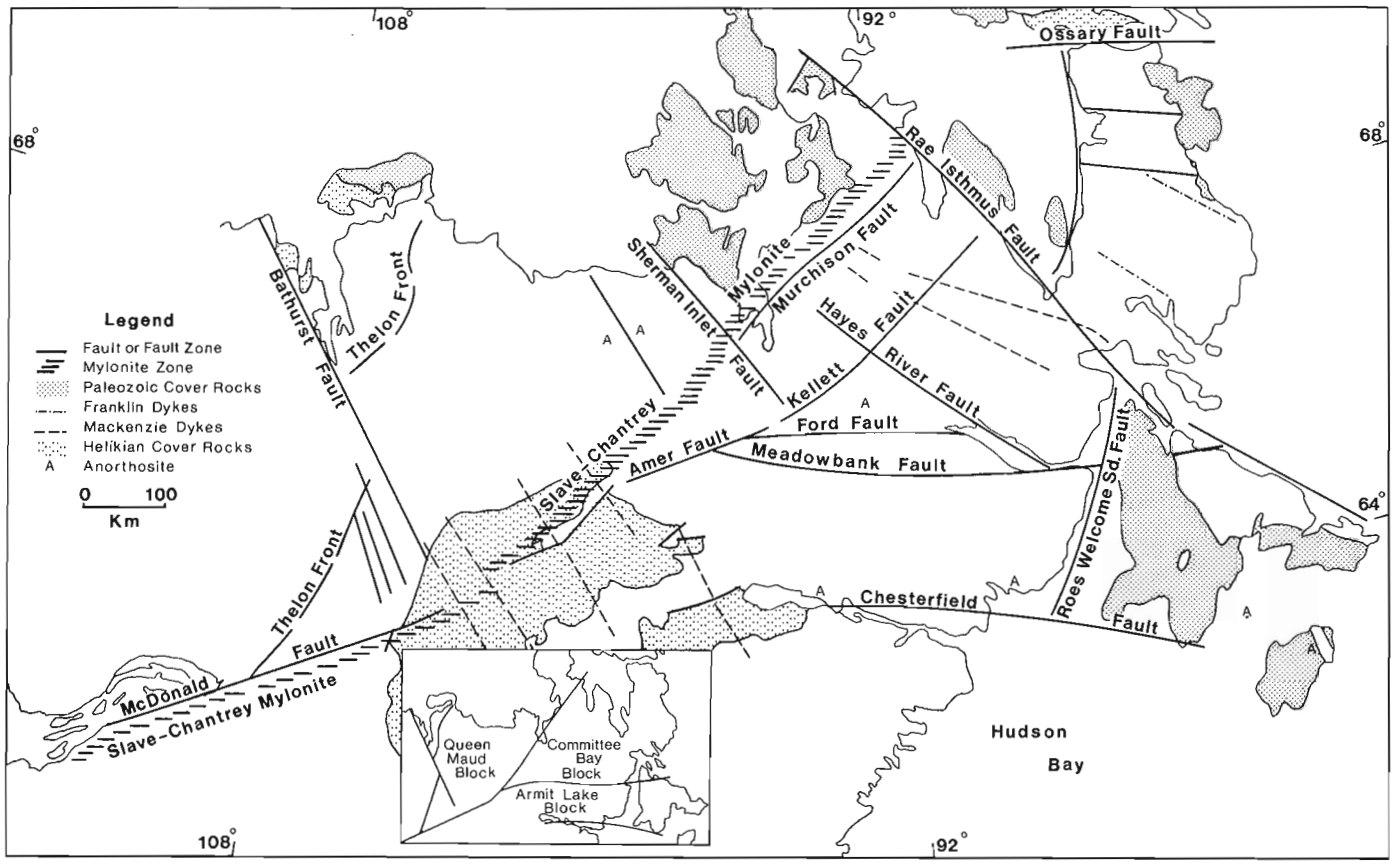

Figure 29.1 Subprovinces of the Northern Churchill Structural Province showing main faults and mylonite zones.

Later fracturing and faulting with a predominantly northwest direction transects the major tectonic blocks. Both Franklin and Mackenzie dykes parallel this trend. The latest faulting displaces Silurian sediments at least one kilometre with a mainly dip-slip component.

The three structural blocks or subprovinces have acted as a unit since the "Hudsonian Orogeny". Rearrangement of blocks seems to have characterized the Aphebian epoch and may represent the commonest manifestation of the Hudsonian Orogeny. The Foxe Fold Belt is the only well-defined Hudsonian fold belt within the region. It occurs in the east-central part of the Committee Bay Block and consists of a deformed and metamorphosed Aphebian sequence of quartzites, marbles and graphitic shales (Heywood, 1967; Reesor, 1972, 1974; Reesor et al., 1975; Okulitch et al., 1977; Jackson and Taylor, 1972). Late Aphebian to Paleohelikian plutons occur along a southwest extension of the Foxe Fold Belt axis.

This preliminary subdivision of the northern part of the Churchill Structural Province poses many interesting geological and metallogenic problems. The following are among those requiring further examination. A sedimentological study of the Chantrey Group may unravel the history of the eastern part of the Slave-Chantrey mylonite zone and the Murchison fault system. Diatremes and mineral showings that commonly occur along major fault zones and in fault related volcanic rocks warrant study (Reinhardt, 1972; Hoffman et al., 1977; Campbell, 1978; Blake et al., 1977; LaPorte, 1974). For example, concentrations of a rare U-Se noble metal assemblage occur at Christopher Island (Pringle and Miller, 1977) along the Chesterfield fault zone; similar minerals occur at Uranium City in a similar(?) fault zone. Anorthosite and related rocks that occur in granulite terrane at Baker Lake, Armit Lake, Daly Bay, Walrus and Coats islands on the north side of the Chesterfield fault, lie along the axis of a gravity anomaly. Do these mark a fundamental division of the Churchill Structural Province?

Acknowledgments

We would like to thank Peter Chernis for drafting and B. Cox for typing the manuscript and tables. F.C. Taylor and W.F. Fahrig read earlier versions of the manuscript.

References

Blake, D.H. and LeCheminant, A.N.

1977: Paleohelikian alkaline volcanic rocks of the Dubawnt Group, District of Keewatin, Northwest Territories; in Geol. Assoc. Can., Program with Abstracts, v. 2, p. 8.

Blake, D., Miller, A., and Schau, Mikkel

1977: Potassic volcanic rocks of the Paleohelikian Dubawnt Group and associated Cu, U, and Se mineralization, Christopher Island Region, District of Keewatin, N.W.T.; in Geol. Assoc. Can., Program with Abstracts, v. 2, p. 8.

Campbell, F.H.A.

1978: Geology of the Helikian rocks of the Bathurst Inlet area; in Current Research, Part A, Geol. Surv. Can., Paper 78-1A, rep. 23.

Campbell, F.H.A. and Cecile, M.P.

1975: Report on the geology of the Kilohigok Basin, Goulburn Group, Bathurst Inlet, N.W.T.; in Report of Activities, Part A, Geol. Surv. Can., Paper 75-1A, p. 297-306.

1976: Geology of the Kilohigok Basin, Goulburn Group, Bathurst Inlet, District of Mackenzie; in Report of Activities, Part A, Geol. Surv. Can., Paper 76-1A, p. 369-377.

Donaldson, J.A.

1965: The Dubawnt Group, Districts of Keewatin and Mackenzie; Geol. Surv. Can., Paper 64-20.

Gibb, R.A. and Halliday, D.W.

1974: Gravity measurement in southern District of Keewatin and southeastern District of Mackenzie; Can. Earth Physics Br., Gravity Map series 124-131.

1975: Gravity measurements in northern District of Keewatin and parts of District of Mackenzie and District of Franklin; Can. Earth Physics Br., Gravity Map series 139-148.

Gordon, T.M.

1971: Petrology and structure of the Daly Bay Complex, District of Keewatin; in Report of Activities, Part A, Geol. Surv. Can., Paper 71-1A, p. 111-112.

Heywood, W.W.

1967: Geological notes, northeastern District of Keewatin and southern Melville Peninsula, District of Franklin, Northwest Territories (Parts of 46, 47, 56, 57); Geol. Surv. Can., Paper 66-40.

1977: Geology of the Amer Lake map-area, District of Keewatin; in Report of Activities, Part A, Geol. Surv. Can., Paper 77-1A, p. 409-410.

Hoffman, P.F., Bell, I.R., Hildebrand, R.S., and Thorstad, L.

1977: Geology of the Athapuscow Aulacogen, East Arm of Great Slave Lake, District of Mackenzie; in Report of Activities, Part A, Geol. Surv. Can., Paper 77-1A, p. 117-129.

Jackson, G.D. and Taylor, F.C.

1972: Correlation of major Aphebian rock units in the northeastern Canadian Shield; Can. J. Earth Sci., v. 9, no. 12, p. 1650-1669.

LaPorte, P.J.

1974: Mineral Industry Report 1971 and 1972, vol. 2 of 3, Northwest Territories, east of 104°; Can. Dep. Indian and Northern Affairs.

McGrath, P.H., Hood, P.J., and Darnley, A.G.

1977: Magnetic anomaly map of Canada; Geol. Surv. Can., Map 1255A, 3rd ed.

Okulitch, A.V., Gordon, T., Henderson, J.R., Reesor, J.E., and Hutcheon, I.E.

1977: Geology of the Barrow River map-area, Melville Peninsula, District of Franklin; in Report of Activities, Part A, Geol. Surv. Can., Paper 77-1A, p. 213-215.

Pringle, G.J. and Miller, A.R.

1977: A study of Cu-S-Se minerals; electron microprobe analyses and X-ray powder; in Report of Activities, Part B, Geol. Surv. Can., Paper 77-1B, p. 113-116.

Reesor, J.E.

1972: Penrhyn Group metamorphic complex, Melville Peninsula, District of Franklin; in Report of Activities, Part A, Geol. Surv. Can., Paper 72-1A, p. 106-107.

1974: Penrhyn Group metamorphic complex, Melville Peninsula, District of Franklin; in Report of Activities, Part A, Geol. Surv. Can., Paper 74-1A, p. 153.

Reesor, J.E., LeCheminant, A.N., and Henderson, J.R.

1975: Geology of the Penrhyn Group metamorphic complex, Melville Peninsula, District of Franklin; in Report of Activities, Part A, Geol. Surv. Can. Paper 75-1A, p. 349-351.

Reinhardt, E.W.

1969: Geology of the Precambrian Rocks of Thubin Lakes map-area in relationship to the McDonald Fault System, District of Mackenzie; Geol. Surv. Can., Paper 69-21, p. 29.

1972: Occurrences of exotic breccias in the Petitot Islands and Wilson Island map-areas, East Arm of Great Slave Lake, District of Mackenzie; Geol. Surv. Can., Paper 72-25, p. 43.

Reinhardt, E.W. and Chandler, F.W.

1973: Gibson-MacQuoid Lakes map-area, District of Keewatin; in Report of Activities, Part A, Geol. Surv. Can., Paper 73-1A, p. 162-165.

Schau, Mikkel and Hulbert, L.

1977: Granulites, anorthosites and cover rocks northeast of Baker Lake, District of Keewatin; in Report of Activities, Part A, Geol. Surv. Can., Paper 77-1A, p. 399-407.

Sibson, R.H.

1977: Fault rocks and fault mechanisms; Geol. Soc. Lond., J. v. 133, p. 191-213.

Stockwell, C.H.

1964: Fourth report on structural provinces, orogenies and time-classification of rocks of the Canadian Precambrian Shield; Geol. Surv. Can., Paper 64-17, pt. II, p. 1-21.

Thomas, M.D., Gibb, R.A., and Quince, J.R.

1976: New evidence from offset aeromagnetic anomalies for transcurrent faulting associated with the Bathurst and McDonald faults, Northwest Territories; Can. J. Earth Sci., v. 13, p. 1244-1250.

Wright, G.M.

1967: Geology of the southeastern barren grounds, parts of the Districts of Mackenzie and Keewatin; Geol. Surv. Can., Mem 350.

30. AGE OF EXOTIC BLOCKS IN DIATREME DYKES OF THE ATHAPUSCOW AULACOGEN, SIMPSON ISLANDS AREA, EAST ARM OF GREAT SLAVE LAKE, DISTRICT OF MACKENZIE

Project 660009

P.F. Hoffman
Regional and Economic Geology Division

Abstract

Hoffman, P.F., Age of exotic blocks in diatreme dykes of the Athapuscow Aulacogen, Simpson Islands area, East Arm of Great Slave Lake, District of Mackenzie; Current Research, Part A, Geol. Surv. Can., Paper 78-1A, p. 145-146, 1978.

Blocks of dolomite and salt-casted siltstone, occurring in diatreme dykes of the Simpson Islands area, are positively identified as being derived from the Stark megabreccia (Christie Bay Group). The diatremes are therefore much younger than the uraniferous Sosan Group, which they intrude. This effectively rules out the suggested genetic link between the diatreme dykes and the 2200 m.y. "Easter Island" dyke, a minor differentiated alkaline complex, intruded at the inception of the aulacogen. The absence of blocks derived from formations between the Sosan and Stark suggests that, when the diatremes were intruded, the area had already been tectonically denuded by gravity slides (nappes) and, interestingly, that the Stark megabreccia, which covers the slide nappes, also remained behind at the source of the slides. The diatreme dykes may be the same age as recently described "intrusive sedimentary breccias" at Bathurst Inlet.

Irregular northeast-trending dyke-like intrusive bodies of exotic heterolithic breccia were described by Reinhardt (1972) in the Simpson Islands area, near the southwest end of the Athapuscow Aulacogen. The breccias intrude Archean granitic basement rocks and subfeldspathic arenites, locally uraniferous, of the overlying Sosan Group (Aphebian). The breccias consist of angular to rounded blocks, mostly granite and arenite, in a tuffisite matrix. Minor exotic blocks of dolomite and varicoloured siltstone have been a puzzle because they do not resemble any formations found in situ in the Simpson Islands area.

The best known of the diatremes, because of associated uranium mineralization, occurs in "Vestor Channel" (Fig. 30.1). It cuts Sosan arenites and is faulted against Archean granitic rocks intruded by the "Easter Island" dyke, a minor differentiated alkaline complex. Biotite from the alkaline dyke has been dated radiometrically by the K-Ar method at 2200 m.y. (Burwash and Baadsgaard, 1962, p. 28) and 2170 m.y. (Leech et al., 1963, p. 61). The "Easter Island" dyke is tentatively correlated with the Blachford Lake Intrusive Suite (Davidson, 1978), a major differentiated alkaline plutonic complex, 35 km to the north. Both alkaline complexes are cut by a regional swarm of northeast-trending diabase dykes, which pass beneath and do not cut the Sosan Group (or the Union Island Group).

Despite this evidence, certain geologists who worked for Vestor Explorations Ltd have suggested a genetic relationship between the "Easter Island" dyke and the "Vestor Channel" diatreme, and have concluded, therefore, that the dyke post-dates the Sosan Group. This issue has important regional implications. If the Vestor geologists are correct, it follows that the Sosan Group is older than 2200 m.y., that the alkaline complexes do not mark the inception of the aulacogen, and that 2200 m.y. is not the age of inception of the aulacogen or, by extension, the Coronation Geosyncline.

These suggestions are now ruled out thanks to positive identification of the exotic dolomite and siltstone blocks in two of the three major diatremes (the southern one, in Petitot Islands, was not examined). They are derived from the Stark megabreccia (Christie Bay Group), a formation much younger than the Sosan Group and younger also than the Seton Island volcanic complex, which has been dated radiometrically by the Rb-Sr method at 1870 m.y. (Baadsgaard et al., 1973). The dolomite blocks contain bipolar current ripples and stromatolites, typical of the Stark dolomites. The basal Sosan dolomite does not contain such ripples, the Union

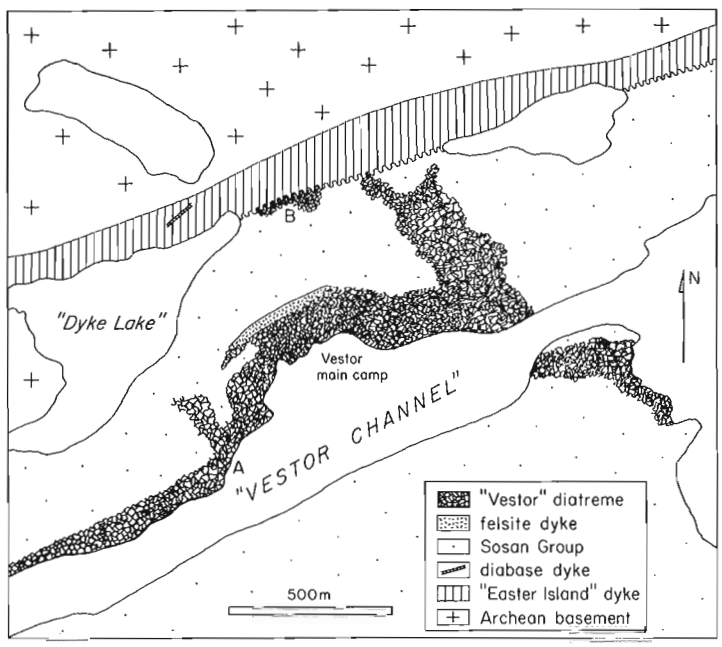

Figure 30.1. Geology around the Vestor Explorations Ltd main camp, located at 61°46'N, 122°38'20"W. Siltstone blocks with abundant halite casts are located at "A"; breccia containing Sosan and "Easter Island" dyke blocks at "B". Map is simplified from Reinhardt (1972) and Walker (1977).

Island and Wilson Island dolomites are not stromatolitic, and dolomites of the Duhamel Formation (Sosan Group) are characteristically arenaceous and cherty (Hoffman, 1968). Pethei Group nappes derived from this area are of a non-dolomitic basinal facies (Hoffman et al., 1977). The siltstones, especially those in "Vestor Channel" (Fig. 30.1), locally contain abundant and well formed halite casts. Such casts are very common in the Stark siltstones and the only other formation in which they occur, the Portage Inlet Formation (Christie Bay Group), is even younger than the Stark. Many of the siltstone blocks contain thin graded beds of feldspathic arenite, not found in the type Stark, east of Snowdrift, but entirely representative of its western facies, well exposed on nearby Blanchet and Caribou islands. A few

blocks contain angular dolomite fragments in a brecciated siltstone matrix, indicating that brecciation of the Stark itself, a regionally pervasive feature, had already taken place before diatreme emplacement. The abundance of greenish as well as reddish siltstone blocks is atypical of the Stark but is attributable to reduction of ferric pigment during diatreme activity. I conclude that the diatremes must be younger than the Stark megabreccia, much younger than the Sosan Group, and unrelated to the "Easter Island" dyke.

Only one exposure, northeast of "Dyke Lake" (Fig. 30.1), has been cited as providing direct evidence of the relative ages of the "Easter Island" dyke and Sosan Group (Walker, 1977, p. 42); elsewhere they are in fault contact. I found this exposure to be a diatreme breccia containing blocks of both Sosan and alkaline dyke rocks. No age relations are possible.

The Simpson Islands area is the source of the nappe complex, composed of Kahochella and Pethei Group rocks, that stretches from Keith Island to Snowdrift River (Hoffman et al., 1977). The absence of Kahochella and Pethei blocks in the diatremes suggests that tectonic denudation had already taken place before the diatremes were emplaced. The fact that the Stark megabreccia, which covers the nappes, was left behind in their source area supports the novel hypothesis that the nappes slid subcutaneously beneath the Stark (Hoffman, 1978a, 1978b).

The diatremes pre-date at least the last movement of the northeast-trending strike-slip faults and may be about the same age as the "intrusive sedimentary breccias" in the Goulburn Group (Aphebian) at Bathurst Inlet (Cecile and Campbell, 1977). The Goulburn breccias are ascribed to sedimentary volcanism whereas the fact that the Simpson Islands breccias intrude basement rocks supports Reinhardt's diatreme hypothesis; unless the basement rocks are themselves allochthonous and have Stark megabreccia beneath them, just itching to squirt up through any cracks!

Acknowledgments

Valuable discussions and unpublished information were generously provided by J.P.N. Badham, F.H.A. Campbell, M.P. Cecile, A. Davidson, M. Minnerat and R.R. Walker.

References

Baadsgaard, H., Morton, R.D., and Olade, M.A.D.
1973: Rb-Sr isotopic age for the Precambrian lavas of the Seton Formation, East Arm of Great Slave Lake, Northwest Territories; Can. J. Earth Sci., v. 10, p. 1579-1582.

Burwash, R.A. and Baadsgaard, H.
1962: Yellowknife-Nonacho age and structural relations; **in** Tectonics of the Canadian Shield, ed. J.S. Stevenson; R. Soc. Can., Spec. Publ. no. 4, p. 22-29.

Cecile, M.P. and Campbell, F.H.A.
1977: Large-scale stratiform and intrusive sedimentary breccias of the lower Proterozoic Goulburn Group, Bathurst Inlet, N.W.T.; Can. J. Earth Sci., v. 14, p. 2364-2387.

Davidson, A.
1978: The Blachford Lake Intrusive Suite: an Aphebian alkaline plutonic complex in the Slave Province, N.W.T.; in Current Research, Part A, Geol. Surv. Can., Paper 78-1A, rep. 26.

Hoffman, P.F.
1968: Stratigraphy of the lower Proterozoic (Aphebian), Great Slave Supergroup, East Arm of Great Slave Lake, District of Mackenzie; Geol. Surv. Can., Paper 68-42, 93 p.

1978a: Large-scale subcutaneous gravity slides (nappes) in the Athapuscow Aulacogen (middle Precambrian), Great Slave Lake, Northwest Territories; in Abstracts with Programs, 12th Annual Meeting (Tulsa), South-Central Section, Geo. Soc. Am., in press.

1978b: Tectonic history of the Athapuscow Aulacogen (middle Precambrian), Great Slave Lake, Northwest Territories; Abstracts for National Meeting (Oklahoma City), Bull. Am. Assoc. Pet. Geol., in press.

Hoffman, P.F., Bell, I.R., Hildebrand, R.S., and Thorstad, L.
1977: Geology of the Athapuscow Aulacogen, East Arm of Great Slave Lake, District of Mackenzie; in Report of Activities, Part A, Geol. Surv. Can., Paper 77-1A, p. 117-129.

Leech, G.B., Lowdon, J.A., Stockwell, C.H., and Wanless, R.K.
1963: Age determinations and geologic studies (including isotopic ages – Report 4); Geol. Surv. Can., Paper 63-17, 140 p.

Reinhardt, E.W.
1972: Occurrences of exotic breccias in the Pettitot Islands (85H/10) and Wilson Island (85H/15) map-areas, East Arm of Great Slave Lake, District of Mackenzie; Geol. Surv. Can., Paper 72-25, 43 p.

Walker, R.R.
1977: The geology and uranium deposits of Proterozoic rocks, Simpson Islands, Northwest Territories; unpubl. M.S. thesis, University of Alberta, Edmonton, 193 p.

31.

GEOLOGY OF THE CORONATION GEOSYNCLINE (APHEBIAN), HEPBURN LAKE SHEET (86J), BEAR PROVINCE, DISTRICT OF MACKENZIE

Project 770019

P.F. Hoffman, M. St-Onge[1], D.M. Carmichael[1], and I. de Bie[2]
Regional and Economic Geology Division

Abstract

Hoffman, P.F., St-Onge, M., Carmichael, D.M., and de Bie I., Geology of the Coronation Geosyncline (Aphebian), Hepburn Lake sheet (86J), Bear Province, District of Mackenzie; Current Research, Part A, Geol. Surv. Can., Paper 78-1A, p. 147-151, 1978.

This is the first interim report summarizing new 1:125 000 scale mapping and tectonic synthesis. Two orogenies are recognized in the geosyncline. The older involves folding and thrusting of the Epworth Group and was followed by emplacement of the Hepburn Batholith, a discordant intrusive complex not a remobilized basement diapir. There is no evidence of gravitational spreading in the batholith linking its emplacement mechanically with the older orogeny. The younger orogeny involves folding and bulk flattening of the batholith itself and metamorphic rocks as far west as the Wopmay Fault. Mixed basic and felsic submarine volcanic rocks along the west side of the batholith may be products of rifting at the beginning of the Wilson Cycle, and should be explored for base metals. The younger orogeny, previously unrecognized, suggests a collision event and the possibility that a complete Wilson Cycle may be recorded in the geosyncline.

Introduction

The Coronation Geosyncline (Aphebian) provides the oldest compelling geological evidence in the world for operation of the "Wilson Cycle" (Dewey and Burke, 1974), i.e. the opening and closing of ocean basins. Nevertheless, there remains uncertainty as to whether, during closure, the Coronation continental margin converged with an oceanic spreading ridge, a magmatic arc, or another continental margin (Burke et al., 1977).

The original conception of the Coronation Geosyncline (Hoffman, 1973) was based on a basin analysis of the Epworth Group (Fig. 31.1), which occurs mainly in the external zone of the geosyncline. Work in the internal zone followed with regional mapping of most of the Great Bear Batholith (McGlynn, 1975, 1976; Hoffman and Bell, 1975; Hoffman et al., 1976; Hoffman and McGlynn, 1977), a potassic volcano-plutonic depression, which makes up the western half of the internal zone. In the eastern half, comprising the Hepburn Batholith and the metamorphosed eugeosynclinal rocks it intrudes, there has been little regional mapping since the reconnaissance work of Fraser et al. (1960). No stratigraphy has been established and little is known of age relations between it and the external zone. Regional mapping has fallen far behind the requirements for tectonic synthesis.

The current project, begun in 1977, will involve 1:125 000 scale mapping of the Hepburn Lake sheet (Fig. 31.1), which straddles the type Hepburn Batholith and the internal-external boundary. It is hoped that this mapping will be extended in future to include the Redrock Lake sheet (86 G) to the south and parts of the Coppermine sheet (86 O) to the north. A special study of metamorphism related to the batholith will be undertaken by Marc St-Onge under the supervision of D.M. Carmichael.

Although it will be several years before a final synthesis of the Coronation Geosyncline can be made, some important and unanticipated observations have emerged from mapping along the Coppermine River, easily the most accessible and well-exposed traverse of the geosyncline.

(1) Formations of the Epworth Group are mappable, despite increasing metamorphic grade, as far west as the Hepburn Batholith. This is true even of migmatites, marginal to the batholith, the various types of which correlate directly with differences in premetamorphic lithology.

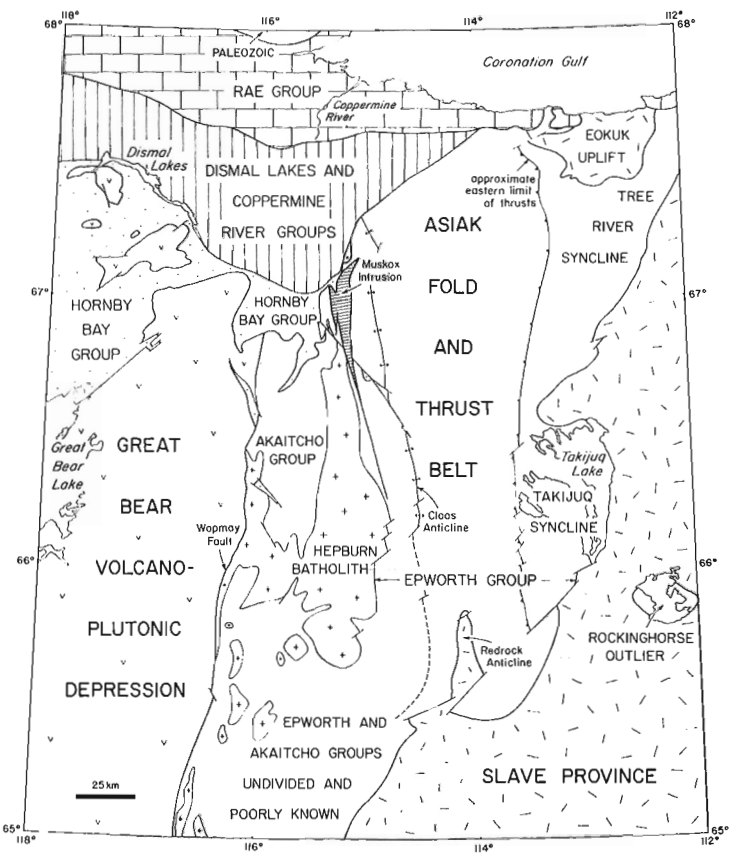

Figure 31.1 Regional tectonic setting of the Hepburn Lake sheet (dotted). Cloos Anticline and its conjectured southern extension (dashed) separate the internal and external zones of the geosyncline. The Asiak Fold and Thrust Belt extends from the Hepburn Batholith to the eastern limit of thrusting. Adapted from McGlynn (in press).

[1] Queen's University, Kingston.

[2] Carleton University, Ottawa.

(2) An important and unique regional structure, here named the Cloos Anticline (Fig. 31.1), forms the boundary between the internal and external zones. The structure is a facies boundary and has been the locus of transcurrent and possible thrust faulting. More important, however, is the tantalizing evidence that it might once have been an enormous and long-lived submarine fault scarp, perhaps the Coronation continental slope, a few kilometres west of the edge of the Rocknest shallow-water carbonate shelf (Fig. 31.2), known from previous work.

(3) The Hepburn Batholith appears to be a discordant magmatic intrusive complex that was subsequently deformed. It has neither the internal structure nor contact relations of a remobilized basement diapir or gneiss dome. There is no evidence of spreading in the batholith to link it mechanically with compression of the Asiak Fold and Thrust Belt (Fig. 31.1).

(4) Metamorphosed volcanic and sedimentary rocks west of the batholith are not correlative with the Epworth Group. Neither the age nor tectonic significance of this important group of rocks, here named Akaitcho Group (Fig. 31.1), is certain, but they may be products of initial rifting in the Wilson Cycle.

(5) There were two major periods of deformation (orogenies). One occurred before intrusion of the batholith, the other after. The two have similar trends but are not co-extensive. The older involves folding and thrusting of the Epworth Group. The younger affects the Akaitcho Group, the small part of the Epworth Group that lies adjacent to the batholith, and the batholith itself. The younger deformation was not previously recognized and suggests the possibility of a collision event in the Wilson Cycle.

Epworth Group of the External Zone

Three formations are exposed in the Asiak Fold and Thrust Belt (Fig. 31.1) east of Cloos Anticline. The Odjick Formation (Eo) consists of greenish argillites with thin (centimetre-scale) graded beds of white quartzite. A few quartz pebblestone beds occur at various horizons. The overall thickness of the formation is difficult to estimate because of pervasive minor folding but probably approaches 3 km. The Rocknest Formation (Er) contains an important facies change, across which thick bedded stromatolitic dolomite, 1 km thick, passes westward through thin bedded non-stromatolitic dolomite, containing slump breccias, into a red argillite, less than 100 m thick, that contains only minor concretionary and redeposited dolomite. Regardless of facies, the Rocknest Formation is overlain by about 80 m of black laminated pyritic and carbonaceous shale (Ef). The black shale, which is a tongue of the Fontano Formation (Fig. 31.2) of the internal zone, is overlain by at least 1400 m of thick bedded coarse grained greywacke turbidites (Eg), the Recluse Formation. A swarm of basic sills, concentrated both geographically and stratigraphically near the Rocknest facies change, was intruded before folding and thrusting. A few of the sills are more than 100 m thick and have pegmatitic zones near their tops.

There are two main classes of faults: (1) thrust faults,which trend north-northwest, dip west-southwest and are thought to be broadly coeval with the major folds; and (2) high-angle transcurrent faults, which are younger, trend northeast, and have major dextral strike-slip and minor dip-slip components. The major folds and thrusts have zero regional plunge and many had remarkable continuity before being segmented by transcurrent faults. The first major syncline east of Cloos Anticline (Fig. 31.2), for example, is cored by Recluse greywacke for more than 150 km. Thrust faults are variable in length, major ones exceeding 50 km, and in displacement, which diminishes to zero at both ends of each thrust trace. Most plunging structures reflect minor rotation of blocks bounded by transcurrent faults.

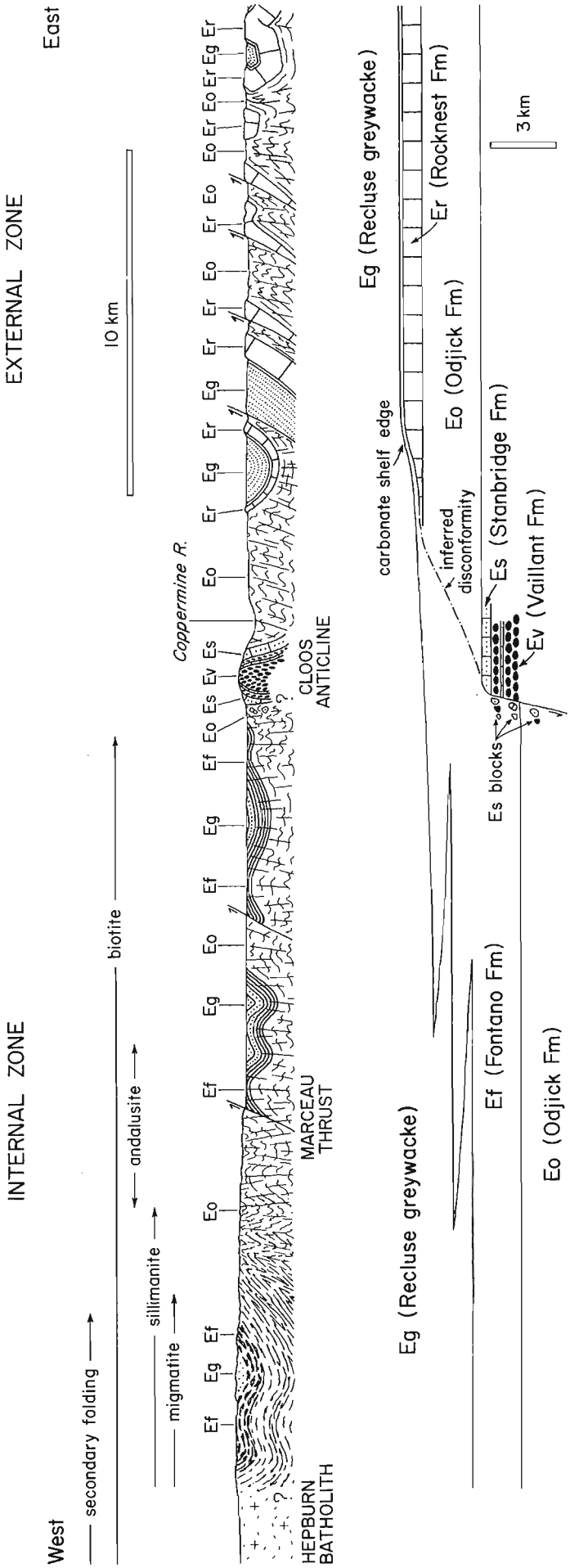

Figure 31.2 Structural cross-section and tentative correlation chart of the Epworth Group across Cloos Anticline at 66°30'N.

Minor structures are highly dependent on lithology. Tight upright chevron folds, with wavelengths of less than 1 km, are ubiquitous in the Odjick argillite and are locally developed in the other formations. The Rocknest dolomite commonly lacks minor folds but small-scale thrust wedges make measurement of stratigraphic sections a tricky business.

Cloos Anticline

Cloos Anticline is an important and unique structure, far from fully understood, that forms the boundary between the external and internal zones (Fig. 31.1). It has been mapped in detail between Vaillant and Stanbridge lakes, a distance of 75 km, and is known to widen northward from there (Baragar and Donaldson, 1973). Its southward extent is a matter of speculation. It is named after the late Prof. Ernst Cloos, who taught several generations of Canadian graduate students at The John Hopkins University and who will be remembered for his pioneering structural studies of the Blue Ridge-South Mountain Anticline in the central Appalachians, a structure in some ways analogous to Cloos Anticline.

The anticline is isoclinal (Fig. 31.2) and cored by chloritic metabasalt, here named Vaillant Formation (Ev). Fragmental and pillow structures are well preserved in places, although there is generally a strong cleavage (steeply-dipping), patches of massive epidote (pre-cleavage), and stretched strain indicators (southwest-plunging). The metabasalt is intercalated and overlain by cherty stromatolitic dolomite, here named Stanbridge Formation (Es). The dolomite is variable in thickness, in part because of truncation by faults that bound the anticline, and is characterized by beds and lenses of quartz gritstone, locally cross-bedded. Stratigraphic relations between the Stanbridge and Odjick formations are obscured by poor exposure along the east margin of the anticline but Fraser (1974) mapped basalts, similar to the Vaillant, conformably beneath the Odjick and not far above basement granitic rocks in Redrock Anticline (Fig. 31.1), at the south end of the fold and thrust belt. Dolomite similar to the Stanbridge Formation, but thinner, occurs above fragmental basalt and beneath Odjick quartzite near Eokuk Uplift, at the north end of the belt. As the Stanbridge dolomite does not closely resemble the Rocknest Formation and basalt occurs nowhere else in the Epworth stratigraphy, the two formations in Cloos Anticline are interpreted to underlie the Odjick Formation.

The anticline is bounded by faults on both margins. The east margin is very poorly exposed but the Stanbridge-Odjick contact is locally a north-trending high-angle fault into which northwest-trending transcurrent faults are deflected. The west margin is better exposed and there also the top of the Stanbridge Formation is a fault, but a fault that may have been active during sedimentation. Intensely brecciated and silicified Stanbridge dolomite is faulted against tightly folded green and black phyllite of the internal zone (see below). The phyllites are believed to be much younger than the dolomite, probably correlative with the interval between the upper Odjick and basal Recluse of the external zone (Fig. 31.2). Isolated blocks of Stanbridge dolomite, many containing the diagnostic quartz grit, are scattered in the phyllite as far as 1 km from the fault trace. Southeast of Stanbridge Lake, an enormous wedge of dolomite breccia, possibly a submarine talus cone, occurs within laminated black phyllite adjacent to the fault trace. A mass of Vaillant metabasalt, more than 1 km in length, occurs within this breccia and appears to have been detached from the anticline by slumping. These relations suggest that the fault had a syndepositional throw, west side down, equal to the thickness of the Odjick Formation and that it produced a major west-facing submarine escarpment. Was this the Coronation continental slope?

The entire anticline is presumably allochthonous, as many west-dipping thrust faults emerge to the east, and its bounding faults may also have had thrust movement. We hope the significance of this intriguing structure will be clarified as mapping continues along its length.

Epworth Group of the Internal Zone

West of Cloos Anticline, the Epworth Group can be recognized, despite increasing grades of metamorphism, as far west as the Hepburn Batholith (Fig. 31.1). The Recluse greywacke is lithologically similar to that east of the anticline, but its lower contact is much more gradational and the underlying black phyllite, here named Fontano Formation (Ef), is much thicker (Fig. 31.2). Thin tongues of greywacke pinch out into the black phyllite from a source area to the northwest. The black phyllite is pyritic, has distinct carbonaceous laminations and locally contains thin beds of grey dolomite. East of Marceau Thrust (Fig. 31.2), the black phyllite is underlain by unlaminated green phyllite, tentatively identified as upper Odjick, although quartzite beds are lacking. More firmly correlative with the Odjick Formation are the schists, paragneisses and migmatites, west of Marceau Thrust, which do contain thin beds and relics of white quartzite. Migmatite derived from Fontano phyllite is characterized by an intricately vermiform granitic component and contains rusty zones and abundant sillimanite. In contrast, migmatite derived from Recluse greywacke is coarsely agmatitic and does not contain an alumino-silicate.

This part of the Asiak Fold and Thrust Belt is dominated by simple upright folds, of 1-5 km wavelength, with strong axial-plane cleavage (Fig. 31.2). Marceau Thrust, which has been traced for 50 km, is the only major thrust fault. Adjacent to the batholith, bedding in the schists is transposed into the cleavage to form a secondary gneissic foliation. The foliation is itself thrown into large upright folds, called secondary folds hereafter, that are nearly coaxial with the primary folds to the east. The secondary folds and foliation are continuous with those in the batholith. Transcurrent faults of northwest trend and sinistral strike-slip cut the Marceau Thrust and both generations of folds. Subsequent dip-slip on the largest of these transcurrent faults is responsible for a previously unmapped outlier of Hornby Bay sandstone (Helikian), 6 km in length, located on the north side of the Coppermine River valley 8 km east of the Muskox Intrusion (Fig. 31.1).

Being predominantly pelitic, these rocks are well suited for metamorphic study. Mineral isograds are not deflected where they cross formational contacts and the alumino-silicates, andalusite and sillimanite only, are consistently if unspectacularly developed. Isograds, defined by the first appearance of each of the following, are being mapped regionally:

1) biotite, identified microscopically,
2) andalusite, megascopic knots,
3) sillimanite, microscopic and field identifications,
4) granite, pods developed in situ,
5) migmatite, defined as containing more than 30 per cent in situ granitic component, and
6) sillimanite in intimate association with K-feldspar.

The general metamorphic environment is one of low pressure (bathozone 2 of Carmichael, in press) and the isograds appear to be concentrically related to the batholith. The andalusite isograd crosses Marceau Thrust without deflection, and both it and the biotite isograd appear to swing across primary folds without undulation, although relations are complicated in places by transcurrent faults. Field relations north of Muskox Lakes suggest that the isograds are involved in the secondary folding, but this important observation requires more extensive mapping and petrographic corroboration.

Hepburn Batholith

Only the north end of the batholith (Fig. 31.1) has been mapped to date and, there, it is a discordant polyphase intrusive complex. It is in contact, in different places, with metasedimentary rocks of the Odjick and Fontano formations, and both metasedimentary and metavolcanic rocks of the Akaitcho Group. The intrusive contacts are sharp, in spite of subsequent deformation, both between various intrusive phases and with the migmatitic country rocks. The oldest intrusive phase is a medium grained biotite tonalite that is intruded and enclosed by the main phase, a medium grained biotite adamellite. Coarse K-feldspar porphyroblasts are typically developed in zones within the adamellite and, locally, extending a few metres into the surrounding country rocks. A partial ring dyke, composed of porphyroblastic adamellite similar to the main phase of the batholith, intrudes the Akaitcho Group (see below). The adamellites are intruded by fine grained leucocratic stocks and plutons, ranging in composition from granodiorite to granite, that cluster along the east margin of the batholith.

All of the intrusive rocks, possibly except certain late leucocratic stocks, bear a pervasive protomylonitic (Higgins, 1971) foliation. In the adamellite, for example, quartz is highly attenuated and considerable bulk flattening is indicated by the way the foliation is deflected around the K-feldspar porphyroblasts. The foliation is coplanar and continuous with that in the Akaitcho Group (see below) and the adjacent part of the Epworth Group; it cross-cuts the batholith and is not concentric with either the batholith as a whole or its individual intrusive components. In the west half of the batholith, the foliation dips east-northeast but, in the east half, it is thrown into upright folds that are continuous with secondary folds in the Epworth Group. Intrusive contacts are involved in this folding. The foliation contains a pervasive near-horizontal stretching lineation, which also cross-cuts the batholith and is co-axial with the stretching lineation of the Akaitcho Group and secondary folds. These features indicate that a general east-west flattening and north-south stretching occurred after intrusion of the batholith. Were they the result of ductile flow during emplacement, as would be the case if the batholith were simply a remobilized basement diapir, as envisaged by Frith et al. (1977) for the Rodriguez diapir, 200 km to the south but described by them as being of Hepburn type, the foliation would be concentric with respect to the batholith and the stretching lineations either radially-disposed or steeply-dipping. Neither do the observed relations support the view of Hoffman (1973), based on the gravity spreading model of Price (1973), that compression of the Asiak Fold and Thrust Belt is mechanically related to dilatant transverse spreading of the batholith.

Akaitcho Group

The metamorphic rocks west of the Hepburn Batholith, here named Akaitcho Group (Fig. 31.1), are not correlative with the Epworth Group. Neither their internal structure nor stratigraphy has been worked out, and they will be a major focus of mapping in 1978. The group is known from previous work (Hoffman, 1972) to extend at least as far south as Wentzel Lake, near the southwest corner of the Hepburn Lake sheet, and are lithologically favourable for base metals exploration.

Metabasalt, metafelsite and metasedimentary rocks occur intercalated in roughly equal proportions. The metabasalt is commonly pillowed, where not highly metamorphosed, and may be several kilometres thick. The felsic rocks include rhyolitic tuffs, rich in fragmented crystals of K-feldspar and quartz, and dacitic flows, sparsely porphyritic and locally spherulitic. The metasedimentary rocks are predominantly pelites, characteristically olive coloured, commonly tuffaceous and rarely containing thin beds of white quartzite. Metaconglomerate occurs at Wentzel Lake and pods of serpentinite are known in amphibolitic migmatite derived from the Akaitcho Group.

The pervasive foliation in the Akaitcho Group dips east-northeast along the Coppermine River but elsewhere the foliation is folded. The foliation is locally so intense as to convert the felsic volcanic rocks to phyllonites. Spherulites make ideal strain markers and indicate flattening across the foliation combined with horizontal stretching. This pattern of strain appears consistent throughout the Akaitcho Group, as well as the Hepburn Batholith.

Metamorphic studies are more difficult in the Akaitcho than the Epworth Group. Pelitic rocks are in the minority and they are not everywhere very aluminous. Metamorphic gradients are very steep on the west side of the batholith, the isograds of andalusite and sillimanite plus K-feldspar being less than 1.5 km apart in places, albeit somewhat forse-shortened by postmetamorphic strain. Metamorphic grade increases toward the Wopmay Fault (Fig. 31.1) from a low situated west of the batholith.

Attempts to establish the mutual relations of the Akaitcho and Epworth groups by mapping around the north end of the batholith have so far been thwarted by major transcurrent faults, down-dropped fault blocks of Hornby Bay sandstone and the Muskox Intrusion (Fig. 31.1). Although not in contact, it appears that the Epworth Group may be truncated by the Akaitcho Group and that the two may have been separated by a thrust before intrusion of the batholith. The lack of andesite in the Akaitcho Group suggests that it is not arc-related but perhaps the product of initial rifting in the Wilson Cycle. If so, the youngest metabasalts should be roughly correlative with the Vaillant Formation of Cloos Anticline. It should be possible to test that correlation with mapping around the south end of the Hepburn Batholith (Fig. 31.1).

Discussion

Perhaps the most significant, although as yet very tentative, observation is the younger orogeny. It opens up the possibility of a collision event and the idea, even more speculative, that a complete Wilson Cycle might be recorded in the geosyncline. This, in turn, casts new light on the origin of the Great Bear volcano-plutonic depression (Fig. 31.1). Its uniformly high-silica high-potash characteristics make it an uncomfortable candidate for either arc- or rift-related magmatism. Burke et al. (1977) suggest that it results from postcollision thickening and partial fusion of the crust, citing the Tibetan plateau as a modern example. They see similarities between the Wopmay Fault and the Himalayan back thrust of the Kailas Range (Gansser, 1964, p. 141), although the Wopmay Fault dips much more steeply and its associated conglomerates, miniscule when compared with those of the Kailas, were shed away from, not toward, the fault. The impression that Great Bear volcanism took place in a broad depression, not on a plateau, is troublesome for the Tibetan analogy. Nevertheless, there is great complexity in collision sutures (Dewey, 1977) and it is interesting that Molnar and Tapponnier (1975, 1977) have linked regional strike-slip fault systems, much like the vast system of northeast-dextral and northwest-sinistral strike-slip faults that permeates the Bear-Slave region, to the effects of continental collision. Note, however, that this fault system postdates the entire magmatic evolution of the Great Bear depression. We invite you to anticipate the radiometric age of the single exposure of basement rocks in the depression, discovered at Hottah Lake by McGlynn (1976), which, if it exceeds 2000 m.y., will strengthen the case for collision.

Acknowledgments

We were ably assisted in the field by Beniot Violette and Hardolph Wasteneys, and our operations were expedited in Yellowknife by Helen Mary Oliver of the Department of Indian Affairs and Northern Development.

References

Baragar, W.R.A. and Donaldson, J.A.

1971: Coppermine and Dismal Lakes map-areas (Report and Maps 1337A and 1338A); Geol. Surv. Can., Paper 71-39, 20 p.

Burke, Kevin, Dewey, J.F., and Kidd, W.S.F.

1977: World distribution of sutures – the sites of former oceans; Tectonophysics, v. 40, p. 69-99.

Carmichael, D.M.

Metamorphic bathozones and bathograds: a measure of postmetamorphic uplift and erosion on the regional scale; Am. J. Sci., in press.

Dewey, J.F.

1977: Suture zone complexities: a review; Tectonophysics, v. 40, p. 53-67.

Dewey, J.F. and Burke, K.

1974: Hot spots and continental breakup: some implications for collisional orogeny; Geology, v. 2, p. 57-60.

Fraser, J.A.

1974: The Epworth Group Rocknest Lake area, District of Mackenzie (Report and Map 1384A); Geol. Surv. Can., Paper 73-39, 23 p.

Fraser, J.A., Craig, B.G., Davison, W.L., Fulton, R.J., Heywood, W.W., and Irvine, T.N.

1960: North-central District of Mackenzie; Geol. Surv. Can., Map 18-1960 (with descriptive notes by J.A. Fraser).

Frith, Rosaline, Frith, R.A., and Doig, R.

1977: The geochronology of the granitic rocks along the Bear-Slave Structural Province boundary, northwest Canadian Shield; Can. J. Earth Sci., v. 14, p. 1356-1373.

Gansser, A.

1964: Geology of the Himalayas; Interscience (John Wiley and Sons), London, 289 p.

Higgins, M.W.

1971: Cataclastic rocks; United States Geol. Surv., Prof. Paper 687, 97 p.

Hoffman, P.F.

1972: Cross-section of the Coronation Geosyncline (Aphebian), Tree River to Great Bear Lake, District of Mackenzie; in Geol. Surv. Can., Paper 72-1, Part A, p. 119-125.

1973: Evolution of an early Proterozoic continental margin: the Coronation Geosyncline and associated aulacogen, northwest Canadian Shield; in Evolution of the Precambrian Crust, ed. J. Sutton and B.F. Windley; Philos. Trans. R. Soc. London, Ser. A, v. 273, p. 547-581.

Hoffman, P.F. and Bell, I.

1975: Volcanism and plutonism, Sloan River map-area, Great Bear Lake, District of Mackenzie; in Report of Activities, Part A, Geol. Surv. Can., Paper 75-1A, p. 331-338.

Hoffman, P.F., Bell, I., and Tirrul, R.

1976: Sloan River map-area (86K), Great Bear Lake, District of Mackenzie; in Report of Activities, Part A, Geol. Surv. Can., Paper 76-1A, p. 353-358.

Hoffman, P.F. and McGlynn, J.C.

1977: Great Bear Batholith: a volcano-plutonic depression; in Volcanic Regimes in Canada, ed. W.R.A. Baragar, L.C. Coleman and J.M. Hall; Geol. Assoc. Can., Spec. Paper 16, p. 169-192.

McGlynn, J.C.

1975: Geology of the Calder River map-area, District of Mackenzie; in Report of Activities, Part A, Geol. Surv. Can., Paper 75-1A, p. 339-342.

1976: Geology of the Calder River (86F) and Leith Peninsula (86E) map-areas, District of Mackenzie; in Report of Activities, Part A, Geol. Surv. Can., Paper 76-1A, p. 359-366.

Geological map of the Bear-Slave region, District of Mackenzie; Geol. Surv. Can., in press.

Molnar, Peter and Tapponnier, Paul

1975: Cenozoic tectonics of Asia: effects of a continental collision; Science, v. 189, p. 419-426.

1977: Relation of the tectonics of eastern China to the India-Euasia collision: application of slip-line field theory to large-scale continental tectonics; Geology, v. 5, p. 212-216.

Price, R.A.

1973: Large-scale gravitational flow of supracrustal rocks, southern Canadian Rockies; in Gravity and Tectonics, ed. K.A. de Jong and R. Scholten; Interscience (John Wiley and Sons), New York, p. 491-502.

32. THE BACK RIVER VOLCANIC COMPLEX – A CAULDRON SUBSIDENCE STRUCTURE OF ARCHEAN AGE

Project 740019

M.B. Lambert
Regional and Economic Geology Division

Abstract

Lambert, M.B., The Back River volcanic complex – A Cauldron subsidence structure of Archean age; Current Research, Part A, Geol. Surv. Can., Paper 78-1A, p. 153-157, 1978.

A volcanic pile exposed in plan view comprises dominantly felsic to intermediate volcanic rocks including tuffs, breccias, lavas and domes that erupted in both subaerial and subaqueous environments. Volcanism began in a shallow sea with eruption of andesitic and basaltic flows and breccias. The pile built up above sea level during explosive eruptions of voluminous pyroclastic flows. Eruptions culminated in cauldron subsidence in the southern part of the complex and rhyolite domes, flows and dykes rose along two concentric, ring-fracture systems. Some domes collapsed to produce extensive subaqueous lahars on the flanks of the volcanic complex. Carbonate, probably related to tufa deposits, impregnated porous breccias along ring-fracture systems bounding the caldera complex.

Introduction

The Back River volcanic complex lies between the Contwoyto River and the headwaters of the Back River about 480 km northeast of Yellowknife, Northwest Territories. It comprises dominantly felsic to intermediate volcanic rocks including tuffs, breccias and lavas, that erupted in both subaerial and subaqueous environments (Figs. 32.1, 32.4).

This report summarizes the stratigraphy (a general outline only is given here because stratigraphic descriptions of various parts of the complex are contained in previous reports (Lambert, 1976, 1977)), new data, and significant features derived from the most recent mapping, namely the nature of rhyolitic domes and a cauldron subsidence feature.

Mapping of this complex on a scale of 1:25 000 was completed during the 1977 field season. R.M. Easton, J. Percival, J.P. Sorbara and D.L. Beaumont, provided superb assistance and carried out three-quarters of the mapping during this season.

Stratigraphy

Sediments of the Yellowknife Supergroup of Archean age (Henderson, 1970) completely surround the volcanic pile (Fig. 32.1). They comprise dominantly greywacke and mudstone, but include minor coarse wacke, graphitic shale, iron-formation and carbonate at the top of the succession. In the northern parts of the map-area, the volcanic succession lies conformably on the sediments, whereas in some places along the eastern and western margins the sediments and volcanics interfinger.

In one locality on the east-central side of the complex, brown weathering, oolitic carbonate (Fig. 32.2) lies at the top of a succession of interbedded volcanics (massive to fragmental andesites and dacites) and sediments (greywackes and coarse grained wackes). This is the only known locality of oolite in Archean terranes of the Slave Province. The well sorted rock comprises about 75 per cent closely packed ooids, 10 per cent dacite and andesite fragments, and 15 per cent sparry calcite cement. Ooids, ranging from 1.4 to 2 cm across, form spheroids to ovoids, having cores of angular volcanic rock fragments and concentric shells of calcite. In thin section, arcuate streaks of mosaic-textured, microcrystalline quartz and zones rich in iron oxide define the concentric pattern. Irregular to bladed sparry calcite, however, has extinction patterns radial to the core of ooids. The generally accepted interpretation that oolites indicate chemical precipitation of $CaCO_3$ around nuclei in agitated shallow water, is reasonable for this deposit.

The volcanic rocks are divided into 6 units (units 3 to 8, Fig. 32.1) with a considerable overlap in composition. Basalts (unit 3) are dominantly pillow lavas and breccias with minor mafic volcanic clastic sediments in the northwestern corner of the map-area. Sills and possible flows of hornblende and pyroxene porphyry (unit 8) are probably closely related in time and space to eruption of the subaqueous basalts. Andesites (unit 4) are a very diverse unit varying from pillow lavas, breccias and massive flows in the northern part of the complex, to water-laid and air-fall tuffs, ash flows, and pyroclastic breccias in its central and southern parts. Some of the andesitic units in the south-central part contain abundant dacite. Dacite (unit 5) comprises air-fall and ash-flow tuffs, domes, lavas and associated breccias that erupted dominantly in a subaerial environment. Rhyolite (unit 6) forms dome and lava complexes, ring-fracture intrusions, and tuff units that were emplaced both in subaerial and subaqueous environments.

Plutons (unit 9) of tonalite, granodiorite and adamellite intrude volcanic and sedimentary rocks around the margins of the volcanic complex. These fine- to medium-grained rocks commonly have sharp, cross-cutting contacts with the sediments and volcanics. Larger granitic bodies commonly have fine grained chilled margins. Some of these highly differentiated bodies, contain phases that are 90 per cent hornblende. Within the southern margin of the volcanic complex six ovoid granitic bodies range from 100 to 500 m across. These bodies are commonly hornblende-rich granodiorite. Contact metamorphism around some larger plutons produced narrow hornfelsic zones and zones of biotite enrichment in the surrounding sediments. The granitic rocks are regarded as high level plutons and the many small bodies are probably apophyses of the larger masses.

Gabbroic dykes (unit 10) cut all rocks in the map-area. These steeply dipping intrusions are up to 1000 m wide. Some are continuous for up to 20 km, whereas others are short and stubby and end abruptly with blunt ends. Some large dykes along the western margin of the complex are highly differentiated. Chilled diabase margins grade inward into coarse grained, ophitic, quartz-bearing gabbro, then into pink weathering granophyre in the core. Granophyric cores contain up to 25 per cent quartz and graphitic granite and 50 per cent albite.

In general, the volcanic complex overlies sediments of the Yellowknife Supergroup. The transition from subaqueous to subaerial environments of deposition (Fig. 32.4) is marked by an iron-formation, oolitic carbonate, and a change over short distances from marine greywacke-mudstone succession through volcanics and sediments deposited in shallow water to subaerial domes, lavas and ash flows. There is no evidence that the volcanic pile was ever completely covered with marine sediments.

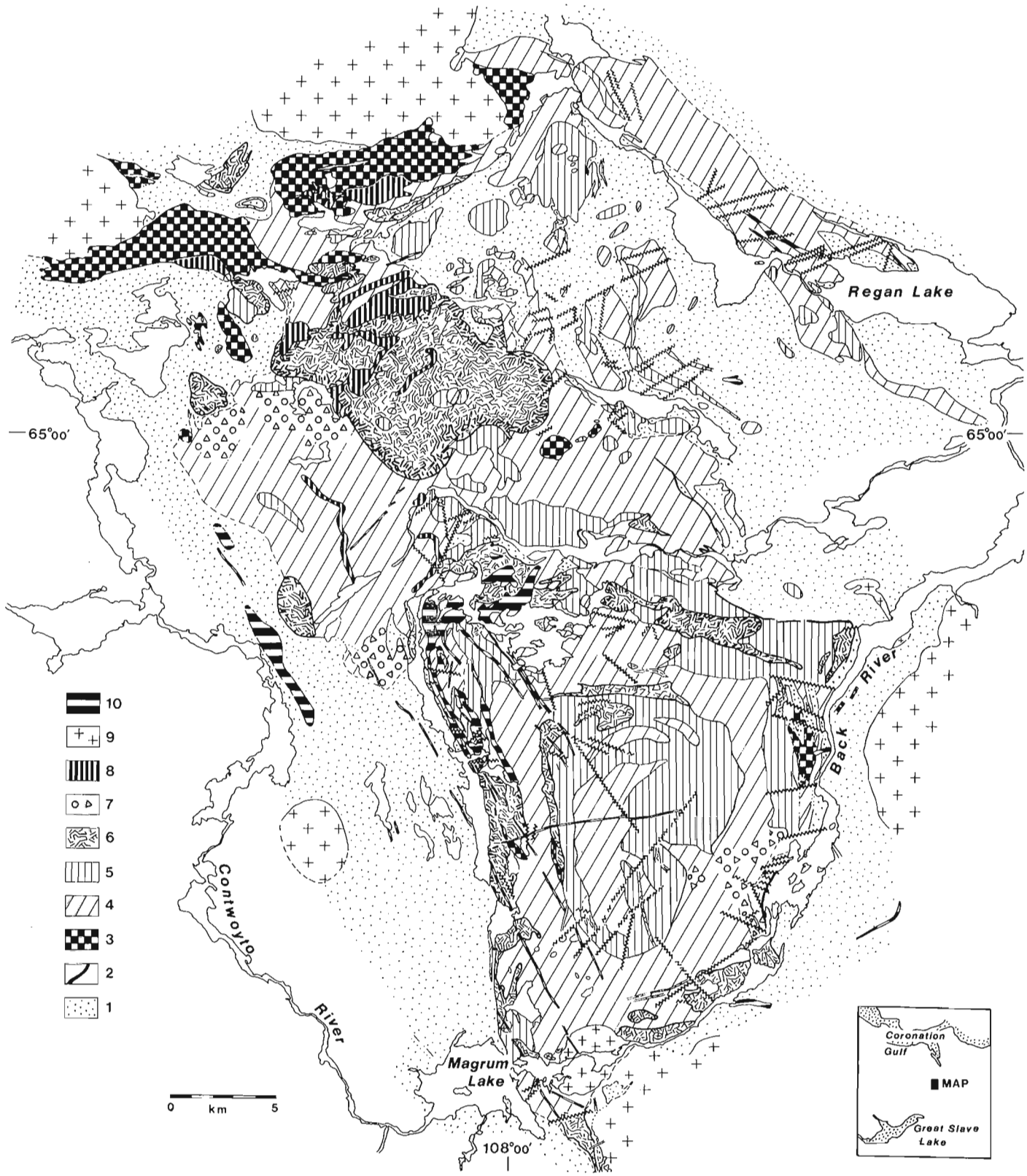

1 – greywacke, mudstone;
2 – iron-formation;
3 – basalt;
4 – andesite, dacite;
5 – dacite;
6 – rhyolite;
7 – laharic breccia;
8 – mafic porphyry;
9 – granodiorite, tonalite, adamellite, hornblendite;
10 – gabbro, granophyre.

Figure 32.1. Generalized geology of the Back River volcanic complex, Slave Province, N.W.T.

The bulk of the volcanic pile has suffered little regional deformation and is essentially exposed in plan view. Although the massive nature of most of the volcanic rocks makes it difficult to establish the attitude of the units, the following features support the undeformed state: (1) flat to gently undulating contact between volcanics and sediments in the northern part of the map-area; (2) circular to oval shapes of rhyolite domes; (3) steeply dipping to vertical concentric fracture systems outlining relict calderas; (4) undeformed pillow lavas; and (5) lack of penetrative deformation structures in the massive volcanic units. Layered volcanic rocks that are interbedded with sedimentary rocks along the flanks of the volcanic complex, however, are deformed. Steep dips in the water-laid tuffs along the northwestern side of the volcanic complex, an anticline that plunges gently southward at the southern tip of the complex, and a small, gently northward plunging syncline along the eastern side of the complex, testify to this deformation. Sediments surrounding the volcanic terrane exhibit several episodes of deformation. Shales display complex fold patterns that are contained between gently undulating beds of greywacke or against essentially undeformed massive volcanics. It appears that the massive core of the volcanic pile has behaved as a rigid block, whereas the flanking deposits and surrounding sediments have absorbed most of the strain during regional deformation.

Cauldron Subsidence Features

The concentric arrangement of units in the southern half of the complex crudely outlines a cauldron subsidence structure. Figure 32.3 summarizes the main features of this structure: two ring-fracture systems, and a subradial fracture system marked by a peripheral array of faults, fractures and dykes.

An outer ring-fracture system is inferred from the locus of elongate to equant domes and flows of rhyolite along the northern, western and southern sides, a swarm of large gabbro

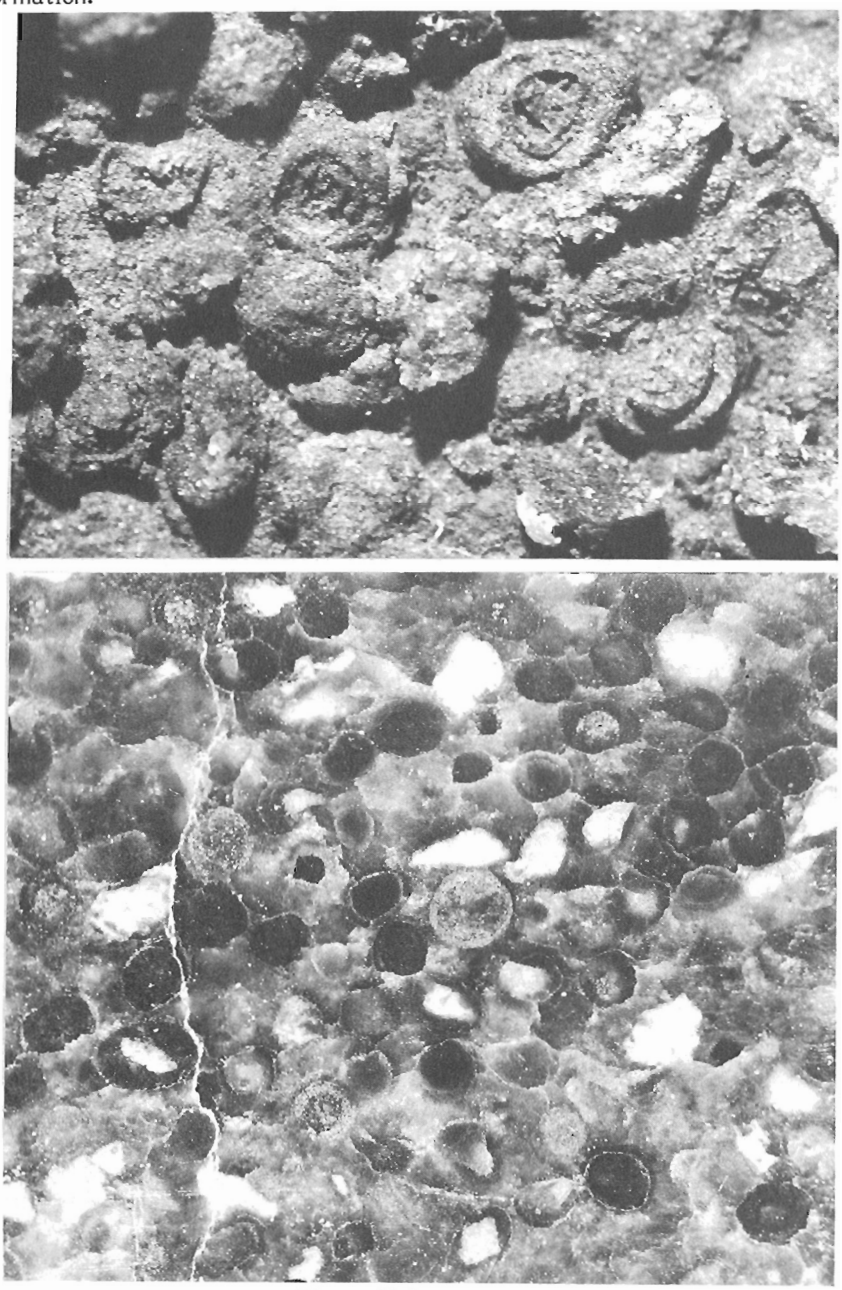

Figure 32.2.

Oolite from the Back River complex.

intrusions along the northwestern side, and a zone of intense shearing and brecciation along the southwestern side of the complex. Near-vertical arcuate zones of brecciation define a north-south trending, elliptical, inner ring-fracture system which outlines the rim of a caldera that was 12 km long and 8 km wide. Steep-sided, deep, arcuate valleys follow these ring-fractures along the northern and western sides. Lithology changes across this circular structure from dominantly andesite and minor basalt on the outside to dominantly dacite to felsic andesite tuff and breccia on the inner sides.

The arcuate zones of intense brecciation, ranging from 100 to 400 m wide, cut across lithologies. In these zones the breccia varies from masses of huge angular to subrounded blocks in an unsorted matrix of fine breccia and grit in the centre to closely packed, steeply dipping slivers of rock near the margins that grade outward progressively into intensely fractured and massive rock. Foliation in the breccia, defined by preferred orientation of slivers, is roughly parallel to the trend of the breccia zones. In some places a vertical layered effect is defined by zones of dominantly fine grit within the breccia.

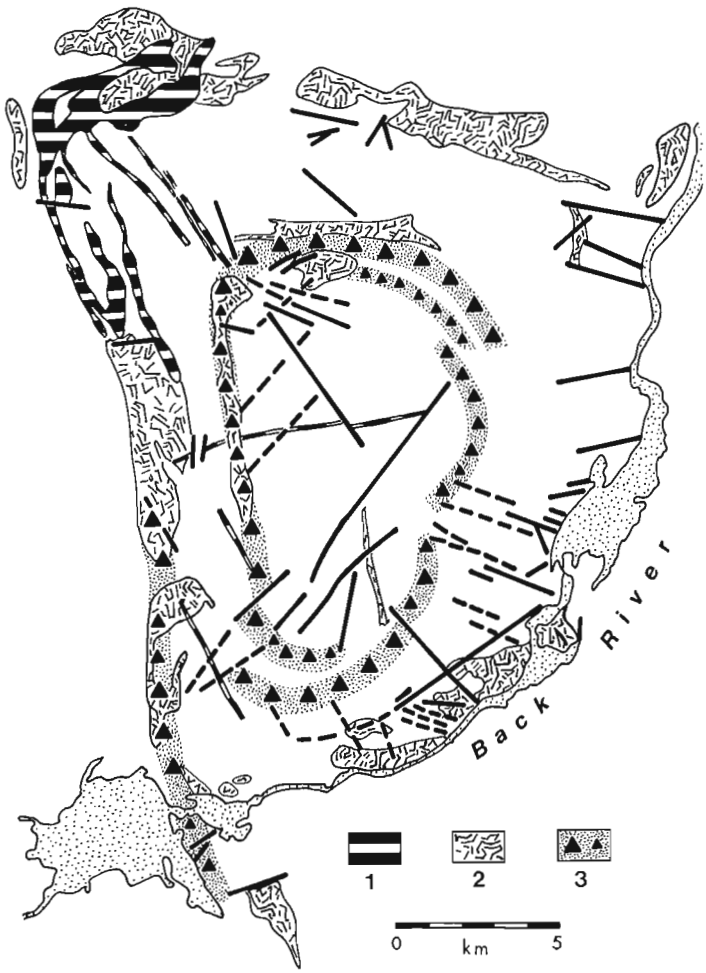

Figure 32.3. Features of the cauldron subsidence structure showing two concentric ring structures outlined by gabbroic intrusions(1), rhyolite domes and dykes(2) and arcuate zones of steeply-dipping tectonic breccia impregnated with carbonate(3). Solid and broken heavy lines are faults and fractures.

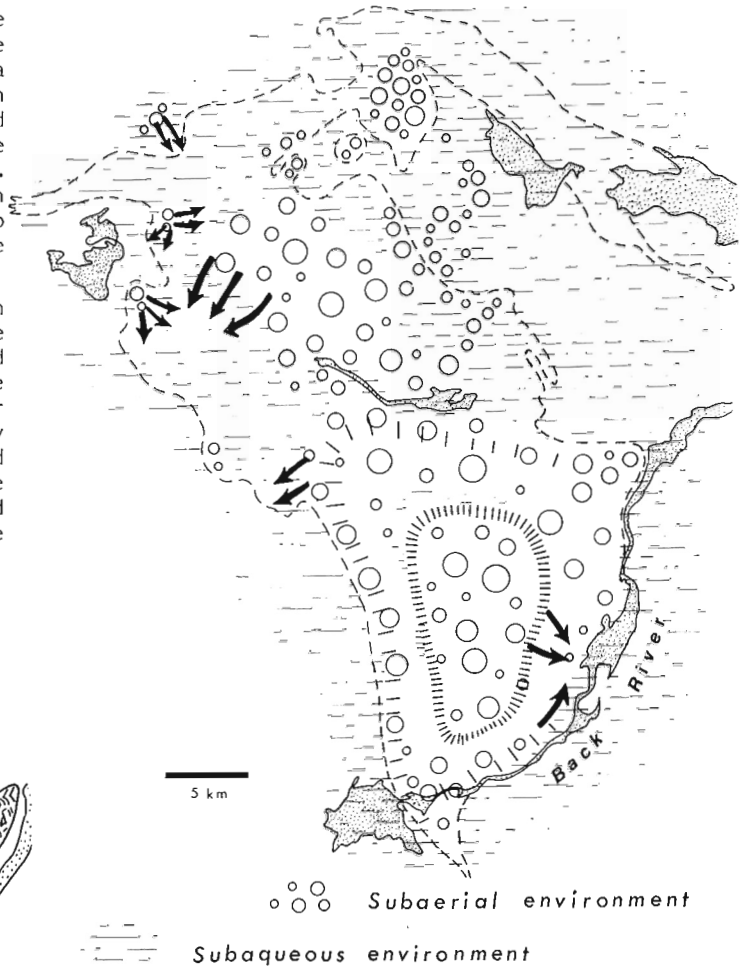

Figure 32.4. Environments of deposition in the Back River volcanic complex. Arrows indicate source and movement of laharic breccias, conglomerate and tuffs related to felsic domes. Radiating hatched pattern outlines ring-feature systems.

Associated with zones of brecciation along the southwestern side of the complex, and in several locations near the inner zone of brecciation, are rhyolite boulder conglomerates and layered breccia units with shallow dip. These units comprise blocks of intact rhyolite and rhyolite breccia up to 5 m across in a generally unsorted and non-layered matrix. Largest blocks tend to be near the base of the units. These units in some places are associated with grits and breccias showing well developed bedding. The succession is interpreted as avalanche and fluviatile debris that cascaded from unstable walls along the margin of the caldera.

In most places the gritty matrix of tectonic and avalanche breccias is impregnated with dark grey to dull brown weathering carbonate and siliceous carbonate. Locally blocky, carbonate-rich grit in zones of intense shearing has an alignment of clasts and contorted flow layering in the carbonate matrix that gives the rock a "pseudo-bedded" appearance. Carbonate also occurs as layered dykes, lenses or large equant pods within carbonate-impregnated breccias. These pods of carbonate or siliceous carbonate are massive to fine layered and laminated. In some places delicate layering is at an angle to bedding in tuffaceous rocks that enclose them. Carbonate also occurs as fracture filling in crumble breccias associated with some rhyolite domes. Carbonate that fills fractures and impregnates breccias yet forms massive to layered pods and lenses, may be related to tufa and sinter deposited by circulating groundwater in highly porous terrain during the waning stages of volcanism.

Rhyolite Domes and Flanking Deposits

Rhyolite domes and flows occur along the ring-fracture zones, form a dome and lava complex about 10 km across in the north-central part of the map-area, and several small domes along the northern and northwestern margins of the volcanic complex. In general, domes are recognized by circular to distorted oval forms, thick zones of crumble breccias on flanks and auto-brecciated to flow layered margins that grade into massive cores. Around some domes, crumble breccias grade outward into rhyolite boulder conglomerate. Domes that have risen in subaqueous environments (as indicated by interbedding of flanking deposits with water-laid tuffs and mudstones, and by sediments that completely surround the domes) commonly have deposits of rhyolite block, laharic (or mass flow) breccias that extend up to 3 km from the dome (Fig. 32.4). Laharic breccias characterize the subaqueous sides of large dome complexes, whereas crumble breccias characterize the subaerial sides. The laharic breccias are generally massive boulder breccia units with a mixture of rounded, subangular to angular clasts in unsorted and non- to crudely-bedded matrix of fine breccia and grit. Large boulders and blocks (ranging from 20 to 100 cm across) make up from 15 to 70 per cent of the rock and usually have random distribution within a unit. Elongate blocks, however, have preferred orientation. Although clasts are dominantly rhyolite and dacite, porphyritic andesite clasts are common. Layering characteristics in distal portions of some mass flows are similar to those in subaqueous ash flows, with the exception that clasts are generally subrounded lithic fragments, not pumiceous material. In some areas, however, subaqueous domes have proximal units interpreted as subaqueous ash flows.

In general, the abundance of large blocks and the proportion of massive laharic units decreases and the proportion of bedded units and volcaniclastic wackes increases away from the domes. These deposits are interpreted as subaqueous avalanches that originated when portions of the domes collapsed and spewed aprons of coarse, clastic debris into the sea.

Concluding Remarks

The Back River complex records a history of volcanism in Archean time that began with the effusion of basaltic and andesitic magma on the sea floor, producing submarine domal-ridges of breccia and pillow lavas. Volcanism may have occurred in an area where the sea was relatively shallow. The volcanic pile gradually emerged and explosive eruptions of voluminous felsic pyroclastics produced a subaerial ash-flow field. Water-laid tuffs, possibly subaqueous ash flows, landslide debris and volcaniclastic sands accumulated in shallow margins along the flanks of the volcano. The eruptions culminated in cauldron subsidence and rise of rhyolite domes along ring fractures and in shallow seas marginal to the emergent volcanic pile. At present we are viewing a block of Archean volcanics, preserved essentially in its original attitude, and for the main part undeformed, that behaved like a buttress in a sea of sediments that absorbed most of the strain during regional deformation.

References

Henderson, J.B.
1970: Stratigraphy of the Archean Yellowknife Supergroup, Yellowknife Bay-Prosperous Lake area, District of Mackenzie; Geol. Surv. Can., Paper 70-26.

Lambert, M.B.
1976: The Back River Volcanic Complex, District of Mackenzie; in Report of Activities, Part A, Geol. Surv. Can., Paper 76-1A, p. 363-365.

1977: The southwestern margin of the Back River Volcanic Complex, District of Mackenzie; in Report of Activities, Part A, Geol. Surv. Can., Paper 77-1A, p. 179-180.

33.

GEOLOGY OF THE BARROW RIVER AND HALL LAKE MAP-AREAS, MELVILLE PENINSULA, DISTRICT OF FRANKLIN

Project 760026

Andrew V. Okulitch, Terry Gordon, J.R. Henderson[1], I.E. Hutcheon, and M. Turay
Regional and Economic Geology Division

Abstract

Okulitch, Andrew V., Gordon, Terry, Henderson, J.R., Hutcheon, I.E., and Turay, M., Geology of the Barrow River and Hall Lake map-areas, Melville Peninsula, District of Franklin; Current Research, Part A, Geol. Surv. Can., Paper 78-1A, p. 159-161, 1978.

The Foxe Fold Belt on Melville Peninsula consists of an Archean basement complex unconformably overlain by metasediments of the Proterozoic Penrhyn Group. The basement complex includes granitoid gneiss intermingled with metasediments and metavolcanics correlated with the Prince Albert Group. The Penrhyn Group consists of thin basal orthoquartzite, conglomerate and meta-regolith overlain by a thick calcareous unit, a paragneissic unit and a heterogeneous marble-quartzite-paragneiss unit. No unconformities were detected within the Penrhyn Group.

Metamorphism of the Penrhyn Group was largely coeval with deformation and reached the sillimanite zone. Some evidence of retrograde metamorphism was observed. Orogenic events in the Foxe Fold Belt affected the basement complex 2500 m.y. ago prior to deposition of the Penrhyn Group and both the complex and the group 1700 m.y. ago.

In the Penrhyn Group, recumbent structures, some possibly of great extent, are deformed by upright folds that trend northeast. Earliest deformation may not have involved basement, but during later events basement was emplaced over and into the group. Plutons 1600 m.y. old, which are mostly post-tectonic, are related to northerly cross-folding in some areas.

No mineral occurrences of economic importance were found.

Field operations from 15 June to 15 August, 1977 concluded geologic mapping of the Foxe Fold Belt in Melville Peninsula. Eleven 1:50 000 scale map-areas in the north halves of areas 46O and P and along the southern border of 47A were examined. Petrographic studies were made before and after the field season. Results presented here are preliminary in nature and will be subject to revision when anlayses are complete. Additional information is available on 1:50 000 scale maps and marginal notes of areas 46O/9, 10, 11, 13, 15, 16; 46P/12, 13; 47A/3 and part of 46J/13 which have been placed on open file. Reference should also be made to previous reports on the area (Schau, 1973, 1975; Reesor, 1974; Reesor et al., 1975, 1976; Okulitch et al., 1977a, 1977b).

Figure 33.1 shows the distribution of major lithologic units. Within the Archean basement complex, layered granitoid gneiss, layered amphibolite, foliated granitoid gneiss and feldspar augen gneiss were identified but their mutual contacts are almost everywhere gradational and they are commonly intermingled. Orthoquartzite, layered amphibolite, anorthositic gabbro, as well as garnet-, biotite- and muscovite-bearing paragneiss and schist, small layers of iron-formation (oxide facies) and minor felsic rocks (possibly metarhyolite or felsic tuff) were mapped within the basement complex and are tentatively ascribed to the Archean Prince Albert Group found northwest of the Foxe Fold Belt (Heywood, 1967). Correlation is made on the basis of considerable lithologic similarity, although these rocks occur as discontinuous zones and lenses within granitoid gneiss units. Age relations between the Prince Albert Group and the gneiss units are varied; some units may be basement to the group, others appear to intrude it and still others may be derived from it by recrystallization and migmatitic processes. In area 46O/16 a body of anorthositic gabbro and amphibolite in the form of a folded lensoid sheet 30 km in lateral extent, lies within granitoid gneiss but structurally above the Prince Albert Group. It has foliated margins but a massive interior and may intrude or be genetically associated with the group, but being wholly within the basement complex, it is presumed to pre-date the Penrhyn Group. Similar but smaller gabbroic sills intruding the Prince Albert Group have been noted by Schau (1975).

The Penrhyn Group unconformably overlies the basement complex. A discontinuous but extensive basal unit of orthoquartzite with minor conglomerate containing rare hematite clasts, lies along most of the three main contact zones (Fig. 33.1). Associated biotite- and sillimanite-bearing pelite, with no free quartz and very rich in potassium and aluminum, may be a meta-regolith derived from weathering of granitic basement rocks. The discovery of rocks similar to the Prince Albert Group within the basement complex of the Foxe Fold Belt and the presence of hematite clasts in the basal unit of the Penrhyn Group provide strong evidence for the previously inferred pre-Penrhyn, possibly Archean age of the Prince Albert Group.

The generalized concepts of stratigraphy of the Penrhyn Group described previously (Okulitch et al., 1977a) were confirmed by this year's work. The basal sequence is overlain in succession by a predominantly calcareous unit and a thick unit comprising a variety of paragneissic rocks followed by a heterogeneous unit of interbedded marble, quartzite, calc-silicate gneiss and paragneiss. A previously proposed unconformity between the bulk of the group and the stratigraphically highest unit of quartz-biotite-muscovite psammite and greywacke, is no longer believed to be present. Laterally and in places throughout the section, psammite becomes coarsely crystalline and indistinguishable from paragneiss.

Examination of thin sections of pelitic and semi-pelitic rocks indicates that the reactions:

muscovite + quartz → k feldspar + sillimanite;
andalusite → sillimanite

can be mapped in areas 46O/6 and 11 and may extend into O/4. These isograds are poorly defined but trend approximately north-northeast. It is not clear whether these are prograde or retrograde isograds.

Petrographic study reveals that some inconsistency exists between field and compositional classifications of paragneiss, calc-silicate gneiss and grey biotite quartzite. This may be primarily because of the presence of units of intermediate lithologies and because of probable facies

[1]Department of Geology, Carleton University, Ottawa, Ontario K1S 5B6.

changes. In addition, detailed mapping in well-exposed areas indicates that although the lateral continuity of beds of these lithologies is commonly good, polyphase folding makes them appear to pass gradationally from one to another. Such cryptic gradations as well as small scale interbedding of these multi-lithologic successions hinder delineation of stratigraphy in most areas.

On conclusion of the regional mapping, detailed structural studies were carried out in areas 47A/3 (M. Mazurski and P. Chernis), 46P/12 and 13 (J.R. Henderson), 46P/13 (M.L. Hill), 46O/14 (C. Waythomas) and 46O/15 (T.M. Gordon) to better our understanding of the involved and prolonged structural evolution of the fold belt. Brief mention of hypotheses currently under consideration is made here. Considerable revision is expected as work proceeds and at present, no consensus has been achieved by the authors.

Deformation of the Archean basement complex prior to deposition of the Penrhyn Group is difficult to isolate from later events but appears to include at least one gneiss-forming event (apart from one inferred to have produced basement to the Prince Albert Group, for which no direct evidence was found). Remnants of metasedimentary and metavolcanic rocks within migmatitic gneiss may have been part of the Prince Albert Group. Studies to the northwest in the adjacent Committee Fold Belt (Schau, 1973, 1975) where later folding was less intense, shed more light on these events than the present work.

Geometry of structures within the Penrhyn Group in many, but not all, areas is more complex than that of the Penrhyn-basement interface, suggesting that early deformation of the group may not have involved basement. Alternately, the Penrhyn cover appears more deformed because of its layered nature, whereas the lack of mappable layers within the basement complex precludes recognition of

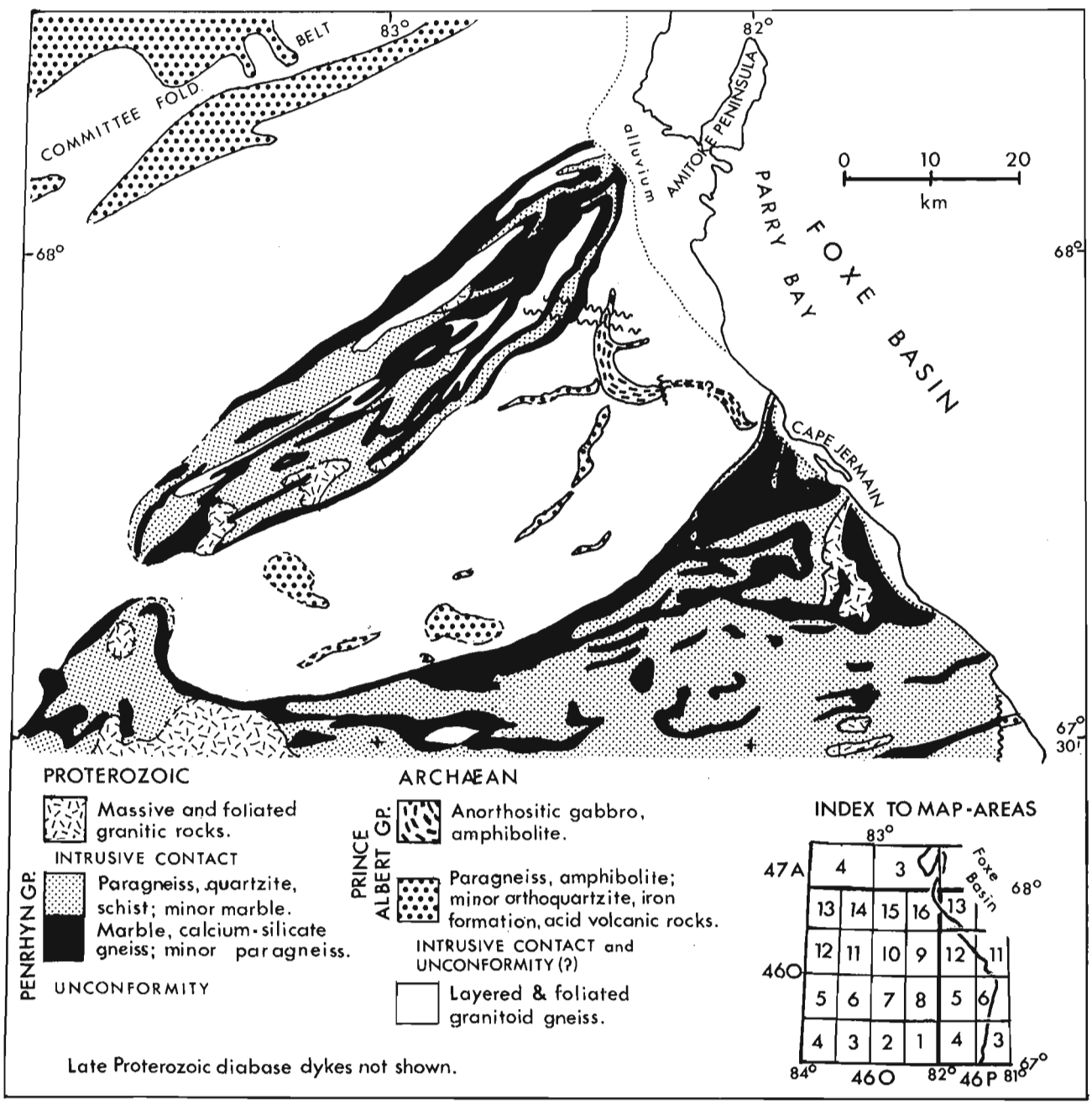

Figure 33.1. The distribution of major lithologic units.

all fold phases. At least two and possibly three phases of macroscopic folding affected both cover and basement. The basement lies above basal units of the Penrhyn Group along both sides of the large basement mass in areas 46O/9, 10,11, 15 and 16. Exposure of basement in a broad synform and Penrhyn cover in a broad antiform (a reversal of expected relationships) suggests the presence of an allochthonous basement nappe covering 3000 km^2, the under-limb of which is exposed at the present level of erosion. Alternatively, the observed overturning is a smaller scale, more local phenomenon, albeit of considerable lateral extent, and the basement is autochthonous. Smaller bodies of basement lie above the Penrhyn Group in areas 46O/15 and 47A/3 and these may have been thrust and folded into place. The widespread presence of the basal Penrhyn succession in contact with basement may mean that only limited movement took place along the basement-cover interface. Dislocations may exist within the cover and may extend down to or into the basement. The general uniformity of metamorphic grade over large areas of the fold belt indicates that either little tectonic thickening of the stratigraphic pile took place during metamorphism or that metamorphism was imposed about parallel to the present erosion surface on an already thickened or 'stacked' succession.

Later folding about axes trending generally east-northeast west-southwest deformed the pre-existing over-turned and recumbent structures described above. Mesoscopic structures associated with later folds vary considerably in tightness from place to place, in some areas being tight to isoclinal and in others, open warps. In many areas intense east-northeast, west-southwest elongation in the fold belt has transposed early fold axes and mineral lineation into parallelism with later structures. Mesoscopic fold style and orientation are of limited assistance in assigning a given structure to a particular fold phase.

Late northerly trending conical folds alter the regional plunge of earlier folds and are possibly related to syn- and post-tectonic granitic emplacement.

Limits to the timing of events in the Foxe Fold Belt that were presented previously (Okulitch et al., 1977a) remain unchanged. Some parts of the basement complex may be as old as 2900 m.y.[1]. Acid volcanic rocks of the Prince Albert Group on the west side of Melville Peninsula have yielded a preliminary date of about 2700 m.y.[1]; other dates from the basement complex suggest plutonic and metamorphic events circa 2500 m.y.[1]. Metamorphism of the Penrhyn Group ended about 1700 m.y. ago and post-tectonic plutons cutting the group cooled about 1600 m.y. ago (Heywood, 1967). The span of time therefore available for deposition and deformation of the Penrhyn Group is 800 m.y. Numerous facets of its evolution will doubtless remain enigmatic.

No mineral occurrences of economic importance were found. Scintillometer investigations for uranium proved unrewarding. A very small occurrence of asbestiform serpentine within ultramafic rock of the Prince Albert Group lies in area 46O/11. Several thin sulphide-bearing schist, paragneiss and calc-silicate layers were mapped but only iron sulphides were seen.

References

Heywood, W.W.
1967: Geological notes, northeastern District of Keewatin and southern Melville Peninsula, District of Franklin, Northwest Territories (parts of 46, 47, 56, 57); Geol. Surv. Can., Paper 66-40.

Okulitch, Andrew V., Gordon, Terry, Henderson, J.R., Reesor, J.E., and Hutcheon, I.E.
1977a: Geology of the Barrow River map-area, Melville Peninsula, District of Franklin; in Report of Activities, Part. A, Geol. Surv. Can., Paper 77-1A, p. 213-215.

Okulitch, Andrew V., Gordon, Terry, Henderson, J.R., Reesor, J.E., Hutcheon, I.E., and Turay, M.
1977b: 1:50 000 geological maps; Geol. Surv. Can., Open Files 433-443.

Reesor, J.E.
1974: Penrhyn Group metamorphic complex, Melville Peninsula, District of Franklin; in Report of Activities, Part. A, Geol. Surv. Can., Paper 74-1A, p. 153.

Reesor, J.E., LeCheminant, A.N., and Henderson, J.R.
1975: Geology of the Penrhyn Group metamorphic complex, Melville Peninsula, District of Franklin; in Report of Activities, Part. A, Geol. Surv. Can., Paper 75-1A, p. 349-351.

Reesor, J.E., LeCheminant, A.N., Henderson, J.R., Hutcheon, I.E., and Miller, A.
1976: 1:50 000 geological maps; Geol. Surv. Can., Open File 307.

Schau, M.P.
1973: Volcanic rocks of the Prince Albert Group; in Report of Activities, Part. A, Geol. Surv. Can., Paper 73-1A, p. 175-177.

1975: Volcanogenic rocks of the Prince Albert Group, Melville Peninsula (47A-D), District of Franklin; in Report of Activities, Part. A, Geol. Surv. Can., Paper 75-1A, p. 359-361.

[1] Radiometric data from R.K. Wanless, personal communications, 1976, 1977.

GEOLOGY OF THE ANORTHOSITIC SILL AT ST. CHARLES, ONTARIO

E.M.R. Research Agreement 1135-D13-4-30/76

D.H. Rousell[1]
Regional and Economic Geology Division

Abstract

Rousell, D.H., Geology of the anorthositic sill at St. Charles, Ontario; Current Research, Part A, Geol. Surv. Can., Paper 78-1A, p. 163-168, 1978.

The St. Charles Sill occurs within the Grenville province and is 11 km long, 0.8 km wide, dips steeply northeast, and trends N63°W. The rocks range from anorthosite to gabbro and consist essentially of plagioclase (An_{41}-An_{58}) and hornblende with lesser amounts of biotite and garnet. They are within the almandine amphibolite facies. The sill comprises interlayered massive and penetratively deformed rocks. The former are characterized by large plagioclase phenocrysts and the latter by mafic layers, boudinage structure, similar folds, flowage zones, and a hornblende lineation. Limited chemical data indicate Fe_2O_3 (total Fe reported as Fe_2O_3) and MgO enrichment at the margins of the sill, and a uniform chemical composition in the remainder. The sill may represent a synorogenic intrusion.

Introduction

The St. Charles body is situated approximately 40 km southeast of Sudbury within the Grenville Province (Fig. 34.1). The body is 11 km long and as much as 0.8 km wide with the long axis trending N63°W. The trend of this axis is parallel to structural trends within the surrounding gneisses. Accordingly, the body is considered to represent a sill on the basis of shape in plan view and conformable trends. Although the sill generally dips steeply to the northeast, there are local shallow dips, particularly at the southeastern end. Lumbers (1975) mapped and briefly described the St. Charles Sill. Present work indicates the sill extends 3 km more in a northwesterly direction than indicated by Lumbers (1975).

Rocks of the sill are part of the anorthosite suite, are mineralogically simple, and consist essentially of plagioclase and hornblende. They are shown on the geological map (Fig. 34.1) as either massive or foliated. A more detailed subdivision is not warranted because of the relatively small scale of the map. The surrounding granitic gneisses were

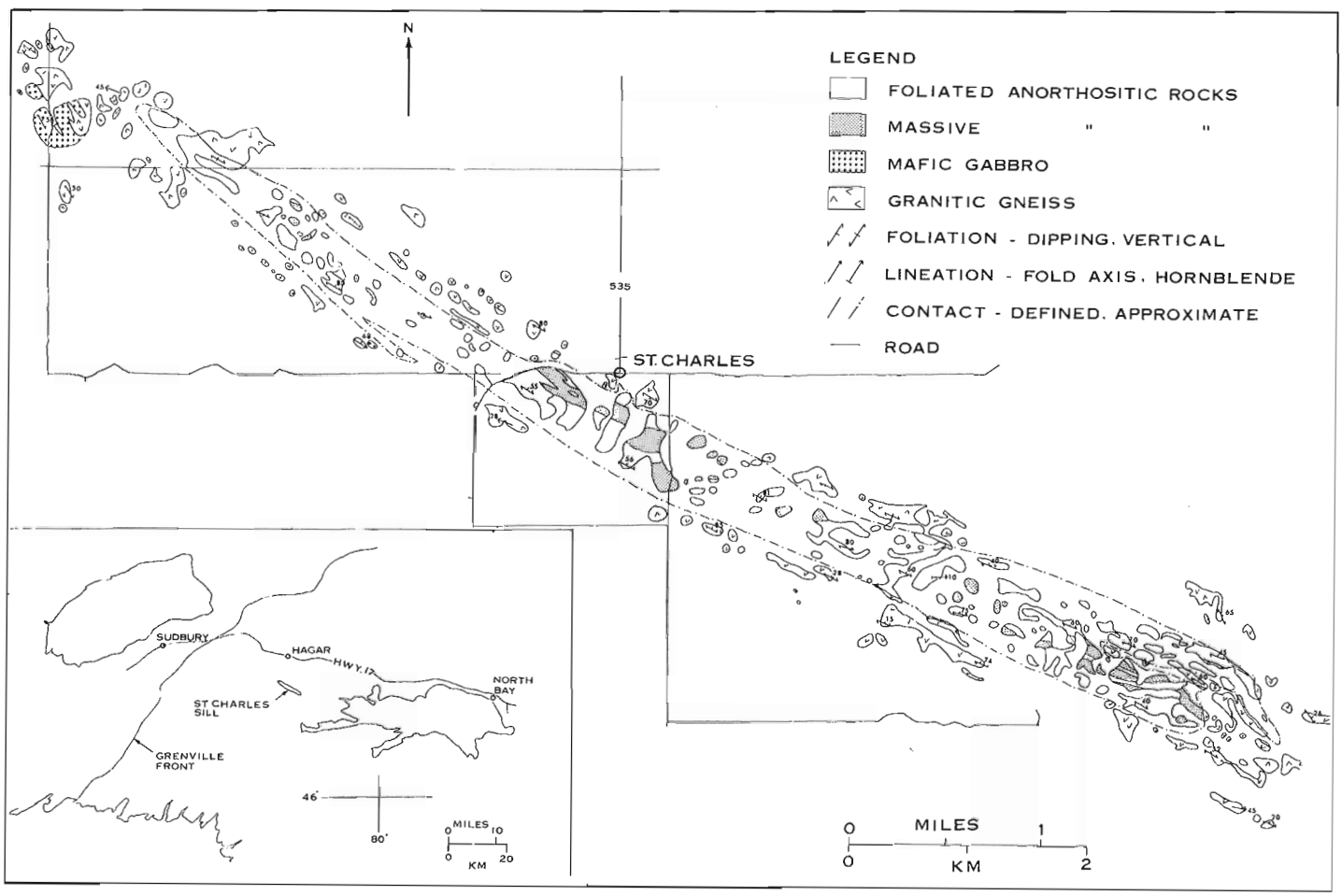

Figure 34.1. Geological map of the St. Charles Sill.

[1] Department of Geology, Laurentian University, Sudbury, Ontario, P3E 2C6.

Table 34.1

Modal data for selected specimens from the St. Charles Sill

Spec. no.	3-2	182	105	126	130	145	114	77-2
Plagioclase	92.0	83.8	75.0	79.4	65.4	66.4	49.0	16.6
Hornblende	6.0	11.8	17.4	16.6	26.8	11.2	-	62.6
Biotite	0.2	0.2	0.2	2.6	5.2	0.6	14.2	-
Garnet	0.8	1.2	0.4	-	-	9.6	28.4	-
Opaque	-	1.2	0.4	0.8	1.6	3.6	2.6	0.6
Sericite	0.2	1.2	-	-	0.6	0.2	1.6	-
Epidote	0.4	0.2	5.0	0.2	-	-	1.2	7.2
Chlorite	-	tr	-	-	tr	-	2.6	-
Allanite	-	-	-	-	0.2	-	-	0.8
Apatite	-	-	-	0.2	0.2	tr	-	-
Quartz	0.4	0.4	1.6	-	-	0.6	0.4	-
Sphene	-	-	-	0.2	-	-	-	-
Clinopyroxene	-	-	-	-	-	7.8	-	-
Scapolite	-	-	-	-	-	-	-	12.2
Per cent An	52	48	51	49	48	43	36	-

Notes:

1. 500 point counts per thin section.
2. Rock types: 3-2 anorthosite; 182 – gabbroic anorthosite; 105 – anorthositic gabbro; 126 – foliated gabbroic anorthosite; 130, 145 – foliated anorthositic gabbro; 114 – garnet-rich band; and 77-2 mafic gabbro (not part of the St. Charles Sill).

remobilized and intrude the margins of the sill in the form of sills and dykes. A small body of mafic gabbro, located near the northwestern end of the sill, is briefly described.

Mapping, at a scale of 1:15 840, began in the summer of 1976 and was completed in 1977. This report sets out preliminary results of petrographic, chemical and structural investigations. Plagioclase compositions were determined by measuring maximum extinction angles of albite twins on the universal stage. Values given are averages of at least four and as many as ten grains per thin section.

Petrography

Buddington (1939) classified anorthositic rocks in terms of per cent mafic minerals as follows: anorthosite (0 to 10 per cent), gabbroic anorthosite (10 to 22.5 per cent), anorthositic gabbro (22.5 to 35 per cent), gabbro (35 to 65 per cent), and mafic gabbro (65 to 77.5 per cent). This terminology is followed in this report. Table 34.1 sets out modes and plagioclase compositions of a representative suite of rocks from the St. Charles Sill. Similar data are given in Table 34.2 for a suite of chemically analyzed specimens. Figure 34.2 is a plot of 13 massive and 13 foliated sill rocks in terms of per cent mafic minerals and plagioclase composition. The term diorite should be substituted for gabbro for those rocks which have a plagioclase composition less calcic than An_{50}.

The rocks range from anorthosite to gabbro and the plagioclase composition ranges from calcic andesine to sodic labradorite.

Massive Anorthositic Rocks

According to Lumbers (1975), the massive rocks are confined to the interior of the body and the intensity of deformation increases toward the margins. In actual fact massive rocks locally occur at the margins as well as the interior of the sill. Massive and deformed rocks are interlayered, particularly at the southeastern end of the sill (Fig. 34.1). Other layers are too small to be shown on the geological map. Most massive rocks are gabbroic anorthosite. Mafic layers, present in the foliated anorthositic rocks, do not occur in the massive rocks.

Massive anorthositic rocks are light grey, coarse grained, and characterized by plagioclase phenocrysts as large as 30 cm by 20 cm (Fig. 34.3). Mafic minerals occur as interstitial blebs (Fig. 34.4).

In thin section, these rocks appear remarkably fresh. Plagioclase occurs as twinned euhedral to subhedral laths together with minor anhedral, untwinned grains. Zoning, both normal and reverse is present and local irregular zoning imparts a mottled appearance. Zoned crystals have a range in composition of as much as 10 per cent An. The average plagioclase composition of the rocks ranges from An_{48} to An_{55}.

Hornblende is green in colour and occurs as subophitic masses approximately 3 cm across. Individual grains are approximately 0.3 cm in diameter and commonly poikilitically enclose small plagioclase grains and locally, quartz grains. Biotite occurs as dark reddish brown grains, as much as 0.4 cm in length, and associated with hornblende. Garnet, in grains approximately 0.3 cm in diameter, is common but occurs in minor quantities. Hornblende and biotite are locally replaced by chlorite and epidote and plagioclase by sericite, but the amounts of these secondary minerals is minor. Accessory minerals include opaques (generally pyrite), allanite, apatite and spinel.

Foliated Anorthositic Rocks

The foliated rocks are medium to coarse grained and vary from thinly laminated gneisses (Fig. 34.5) to rocks in

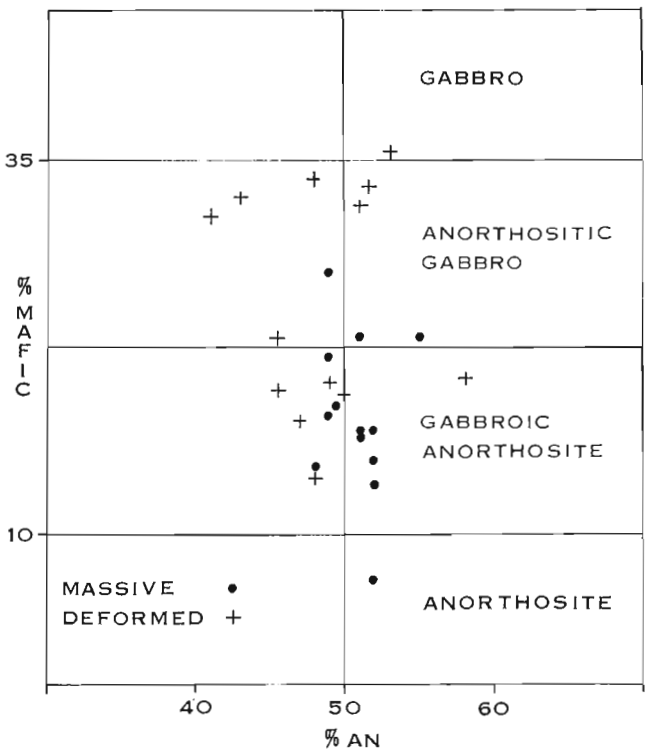

Figure 34.2. Plot of per cent mafic minerals versus plagioclase composition for anorthositic rocks of the St. Charles Sill.

which lineation dominates over a foliation (Fig. 34.6). Mafic layers are locally present (Fig. 34.7) some of which are garnet-rich (Table 34.1, specimen 114). Rock types range from gabbroic anorthosite (Table 34.1, specimen 126) to anorthositic gabbro (Table 34.1, specimens 130 and 145), and gabbro (Table 34.2, specimen 1). Essentially the same minerals are present in the deformed rocks as in the massive rocks. Large plagioclase crystals, characteristic of the massive rocks, are absent.

Thin section examination indicates there are two types of plagioclase. One type is euhedral to subhedral and strongly twinned and the other type is anhedral with poorly developed twinning. Both types display zoning, generally normal, but locally reverse, and the two types appear to have similar compositions. The anhedral plagioclase partially replaces the euhedral plagioclase. The plagioclase composition of the foliated rocks ranges from An_{41} to An_{58}. The plagioclase is calcic andesine in the majority of specimens.

Hornblende and biotite display a dimensional preferred orientation. The pleochroism of these minerals is the same in the massive rocks as in the deformed rocks. Clinopyroxene, partially replaced by hornblende, is present in one specimen (Table 34.1, specimen 145). Other minerals locally present in minor amounts are garnet, opaque, sericite, epidote, chlorite, allanite, apatite, quartz, spinel, and sphene.

Mafic Gabbro Body

A small body of foliated mafic gabbro occurs near the northeastern end of the St. Charles Sill. The body is separated from the sill by granitic gneiss. The mafic gabbro is characterized by a high hornblende content and the presence of scapolite (Table 34.1, specimen 77-2). These rocks are probably not part of the sill.

Granitic Gneiss

The country rocks surrounding the St. Charles Sill consist of fine to medium grained, pink to mauve weathering gneisses. Layers vary in width from a few centimetres to several metres. Rocks within some of the wider bands are massive. Minerals present are untwinned or weakly twinned plagioclase, microcline, biotite, hornblende, quartz, and epidote. Granitic pegmatite occurs locally.

Lumbers (1975) described the country rocks surrounding the sill as migmatitic biotite gneiss of sedimentary origin and migmatitic and gneissic quartz monzonite of intrusive origin. The conclusion that the biotite gneiss is derived from sedimentary rocks must be based on regional studies because evidence for such an origin for the local rocks is not readily apparent.

Chemical Analyses

Nine specimens were collected across the sill from an exposure located approximately 0.5 km southeast of St. Charles. Chemical analyses, modes, and plagioclase compositions of these specimens are presented in Table 34.2. Specimen 1 is from the southwestern edge and specimen 9 is from the northeastern edge of the sill.

The rocks are similar in terms of both major and trace elements. Specimens 1, 8 and 9 have a relatively high Fe_2O_3 (total Fe reported as Fe_2O_3) and MgO content which might suggest that the borders of the sill are more mafic than the central portion. However, present data are insufficient to define any obvious chemical variations across the sill. It is possible that metamorphism tended to homogenize the rocks.

Structure

Boudinage and similar folds, indicative of flow, occur in the deformed rocks. Figure 34.7 shows a fold in a mafic layer. The fold limbs are truncated and the layer displays tectonic thickening and thinning. What may be referred to as "flowage zones" commonly occur at or near the hinge of folds (Fig. 34.8). The foliation is apparently disrupted by flowage.

The foliated rocks are locally characterized by a hornblende lineation. The development of this lineation may be seen in numerous well exposed contacts which display the transformation of massive to deformed anorthositic rocks. This fabric change generally takes place over a distance of less than one metre. The hornblende blebs in the massive rocks become recrystallized and converted to lenses (Fig. 34.9) and with more intense deformation to thin streaks (Fig. 34.6). With still further deformation, the rocks assume a gneissic appearance (Fig. 34.5). In Figure 34.6 the hammer lies in the plane normal to the long axis of the lineation. That portion of the outcrop to the right of the hammer is curved through an angle of 90° and is parallel to the long axis of the lineation. These lineated rocks may be deceptive in outcrops where the exposure is limited to a single plane parallel to the lineation because the rocks appear to be dominated by a foliation rather than a lineation. They are tentatively placed in the L>S subdivision of Flinn's (1965) fabric system.

Lineations, consisting of both hornblende and fold axes, tend to trend parallel to the long axis of the sill and to have shallow plunges to the northwest or southeast.

Discussion

According to Lumbers (1975) the anorthositic rocks of the region were emplaced between 1200 and 1500 m.y. ago. Metasedimentary rocks were subjected to a complex history of deformation and plutonism followed by Late Precambrian high rank regional metamorphism which culminated between 1400 and 1200 m.y. ago.

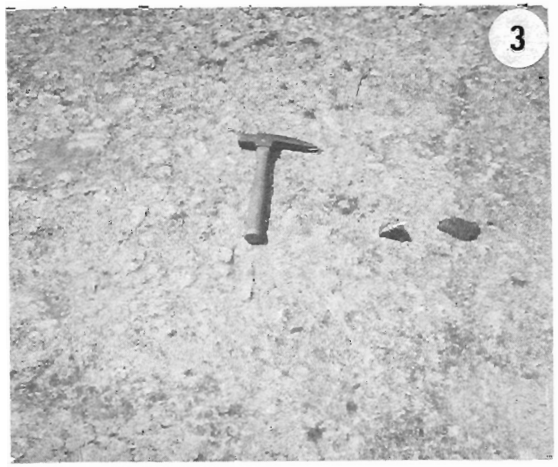

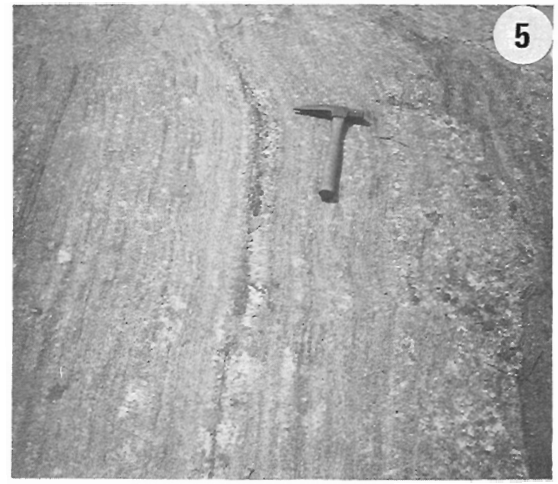

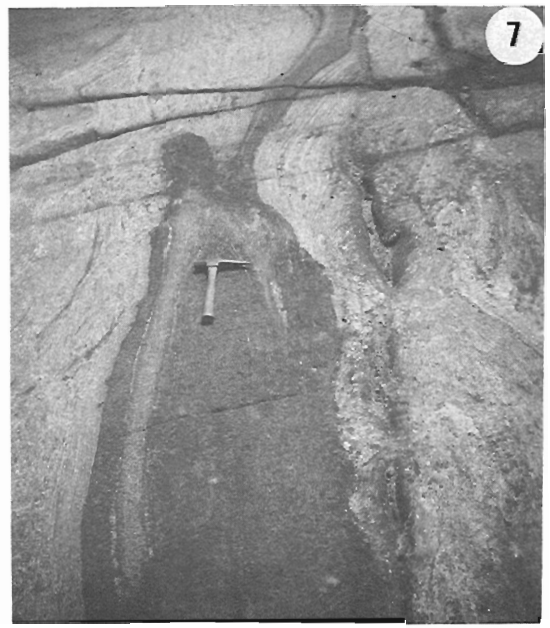

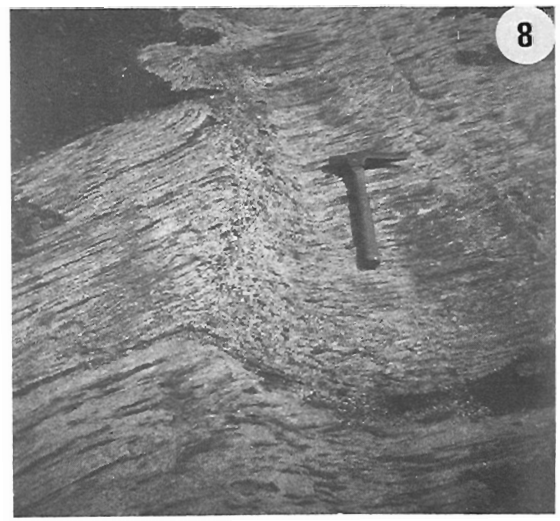

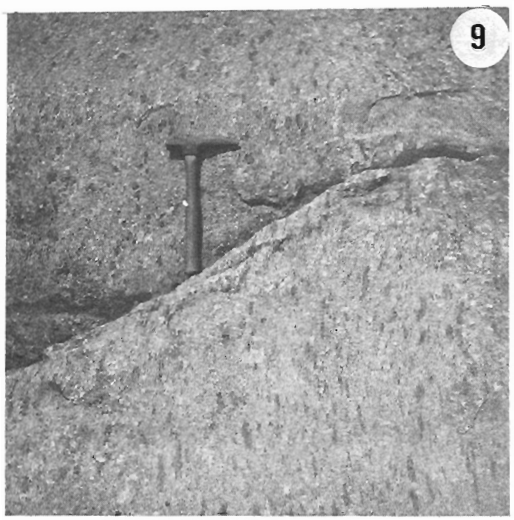

Figures 34.3 to 34.9

3. Massive anorthosite with large plagioclase phenocrysts.
4. Massive anorthositic gabbro.
5. Gneissic anorthositic rocks.
6. Lineated anorthositic rocks.
7. Fold in mafic band.
8. Flow structure near hinge of fold.
9. Lineated anorthositic rocks.

Table 34.2

Chemical analyses and modes of specimens from the St. Charles Sill

Spec. no.	1	2	3	4	5	6	7	8	9
				Chemical analyses (weight per cent)					
SiO_2	50.19	53.28	51.51	51.40	52.77	52.00	51.98	50.40	53.12
Al_2O_3	23.78	24.38	25.05	25.38	25.68	25.41	25.32	23.84	24.72
Fe_2O_3	6.78	3.85	4.31	4.15	3.32	3.13	3.56	6.39	5.43
MgO	2.98	1.46	1.81	1.96	1.53	1.31	1.75	2.37	2.07
CaO	10.23	10.05	10.33	10.79	10.68	10.61	10.34	10.38	7.14
Na_2O	3.66	4.10	4.00	3.84	4.39	4.13	4.36	3.79	4.38
K_2O	0.68	0.82	0.78	0.71	0.63	0.53	0.73	0.82	0.72
H_2O	0.70	0.75	0.96	0.64	0.87	0.64	0.75	0.64	0.75
TiO_2	0.90	0.55	0.68	0.57	0.49	0.44	0.34	0.85	0.79
P_2O_5	0.15	0.22	0.13	0.10	0.10	0.10	0.08	0.20	0.14
S	0.02	0.00	0.02	0.00	0.01	0.01	0.01	0.00	0.01
MnO	0.10	0.05	0.06	0.05	0.04	0.04	0.04	0.08	0.07
Total	100.17	99.51	99.64	99.59	100.51	98.35	99.26	99.76	99.24
				Trace elements (p.p.m.)					
Cu	19	7	22	9	9	14	10	10	20
Zn	40	27	35	29	22	20	28	47	40
Co	45	40	55	35	35	55	40	38	40
Ni	40	15	30	40	19	32	30	30	28
Cr	32	11	33	25	27	23	8.5	50	35
				Modes[1] (volume per cent)					
Plagioclase	62.6	78.4	82.4	82.6	81.2	86.4	80.2	80.6	79.2
Hornblende	27.8	19.2	10.2	14.8	16.0	10.6	10.8	15.6	15.8
Biotite	3.8	1.0	0.8	1.8	1.0	2.6	1.0	1.2	2.4
Garnet	1.6	0.2	-	-	0.8	-	tr	0.4	tr
Opaque	2.0	0.2	-	0.2	0.2	0.2	tr	tr	tr
Sericite	1.8	0.6	1.8	0.4	-	-	2.8	1.2	1.0
Epidote	0.2	tr	2.6	tr	tr	-	1.8	0.4	0.6
Chlorite	0.2	-	2.0	0.2	0.4	-	2.8	0.2	0.6
Allanite	-	-	tr	-	tr	-	0.4	-	-
Apatite	-	0.4	0.2	tr	0.4	0.2	0.2	0.4	tr
Quartz	-	-	-	-	tr	tr	tr	-	0.4
Spinel	-	-	-	-	-	-	-	-	tr
				% An					
Per cent An	53	58	48	51	50	52	51	47	46

Notes:

1. 500 point counts per thin section.
2. Specimens 4, 5, 6 and 7 are massive, the rest are foliated; specimen 1 is gabbro, the rest are gabbroic anorthosite.
3. Fe_2O_3 is total Fe as Fe_2O_3.

The St. Charles Sill may have been emplaced during a tectonic event. The fact that some of the rocks escaped deformation suggests that emplacement may have taken place during the waning stages of deformation. Because deformed and undeformed rocks are interlayered, it may be that all the rocks were at or near the threshold of the physical conditions necessary for flow. Hornblende and biotite display a prominent dimensional preferred orientation in the deformed rocks and this suggests syntectonic recrystallization rather than post tectonic annealing recrystallization. The country rocks must have been mobile after the emplacement of the sill because they intrude it in the form of sills and dykes.

All rocks of the sill are within the almandine-amphibolite facies of regional metamorphism. In the massive rocks the original igneous texture is preserved and the plagioclase has probably not undergone recrystallization. In the foliated rocks the plagioclase is partially and perhaps entirely recrystallized. Hornblende likely formed from original pyroxene.

Mafic layers within the foliated rocks may represent original layers or they may be the result of the tectonic elongation of mafic blebs.

The original disposition of the sill is uncertain. It seems likely that the body was initially less elongate than the present shape in plan view.

Massive anorthosite bodies have been divided into two groups – andesine type and labradorite type. Anderson and Morin (1969) review the attributes of each. In the andesine type the plagioclase is An_{48-23}, the predominant rock in anorthosite, and the shape domical. In the labradorite type the plagioclase is An_{63-45}, the predominant rock is gabbroic anorthosite, and the shape irregular. The plagioclase composition of the St. Charles Sill lies within the area of overlap of the two types. The body is sill-like in shape and is not domical and the major rock type is gabbroic anorthosite. Although some of the attributes are similar to the labradorite type, the sill cannot be positively related to either type.

The writer is presently studying the fabric changes which take place during the transformation from massive to deformed anorthositic rocks.

References

Anderson, A.T. and Morin, M.
1969: Two types of massif anorthosites and their implications regarding the thermal history of the crust; in Origin of anorthosite and related rocks, Y.W. Isachsen, ed., Mem. 18, N.Y. State Mus. Sci. Serv., p. 57-69.

Buddington, A.F.
1939: Adirondack igneous rocks and their metamorphism; Geol. Soc. Am., Mem. 7, 354 p.

Flinn, D.
1965: On the symmetry principle and the deformation ellipsoid; Geol. Mag., v. 102, p. 36-45.

Lumbers, S.B.
1975: Geology of the Burwash area, Districts of Nipissing, Parry Sound, and Sudbury; Ont. Div. Mines Geol. Rep. 116, 158 p.

35. A DETAILED CROSS-SECTION THROUGH THE SOUTHERN MARGIN OF THE FOXE FOLD BELT IN THE VICINITY OF DEWAR LAKES, BAFFIN ISLAND, DISTRICT OF FRANKLIN

Contract 93564

Clinton R. Tippett[1]
Regional and Economic Geology Division

Abstract

Tippett, Clinton R., A detailed cross-section through the southern margin of the Foxe Fold Belt in the Vicinity of Dewar Lakes, Baffin Island, District of Franklin; Current Research, Part A, Geol. Surv. Can., Paper 78-1A, p. 169-173, 1978.

The Aphebian Piling Group along the southern margin of the Baffin Island Foxe Fold Belt mantles an Archean basement terrane and consists of a basal quartzite and schist overlain by a thick metagreywacke-phyllite section which contains a variable assemblage of amphibolites and ultramafics near its base. Early isoclinal interfolding of basement and cover during the peak of metamorphism was followed by compressional folding which dominated deformation at upper levels while initiating and localizing along antiformal hinges the active gravitational gneiss remobilization which superceded it at depth. The present outcrop pattern is dominated by elongate domes surrounded by complex fabrics resulting from the superimposition of upright folding and gneiss doming on an older subhorizontal schistosity.

The 1977 field season involved two months 1:50 000 scale mapping of a detailed structural and stratigraphic cross-section through part of the southern margin of the Foxe Fold Belt near Dewar Lakes, Baffin Island (DEW line site FOX 3, Fig. 35.1). Foot traversing, aided by canova boat transportation, was undertaken chiefly within sheets 27B/5 and 27B/12 (Fig. 35.2). This work will form part of a doctoral thesis at Queen's University and is sponsored by the Geological Survey of Canada under the supervision of Dr. W.C. Morgan. It is part of a continuing study of the Baffin Island Foxe Fold Belt (Morgan et al., 1975, 1976).

Regional Geology

The extent of the metamorphosed supracrustal Piling Group on central Baffin Island was reported by Jackson (1969, 1971) who named the group and proposed a correlation with the Penrhyn Group on Melville Peninsula to form part of the Foxe Fold Belt (Jackson and Taylor, 1972). Subsequent detailed work has expanded our knowledge of the belt on Baffin Island (Chernis, 1976; Morgan et al., 1975, 1976).

Regional considerations and geochronological studies have indicated that the supracrustal rocks are Aphebian in age and overlie an Archean granitoid basement complex. These basement rocks outcrop in a series of domal culminations along the northern and southern margins of the east-west trending Piling belt. They are overlain by a miogeoclinal sequence that is predominantly carbonates to the north and impure quartzites to the south. Above the southern quartzites an assemblage of amphibolitic to ultramafic rocks occupies a restricted stratigraphic interval in the lower part of the overlying greywacke-siltstone unit and may be a facies equivalent of the extensive sulphide facies iron-formation and rusty schists which occupy the same interval to the north. A eugeoclinal flysch assemblage blankets the miogeoclinal sequence and dominates the central part of the synformal belt.

Stratigraphy

The Piling Group has a stratigraphy which, although complicated by metamorphic transformations and thickness variations, is constant throughout the study area. The granitoid basement complex is overlain sequentially by an impure basal quartzite with interlayered schists, an amphibolite to hornblendite interlayered with metasediments and calc-silicate gneisses and a thick sequence of greywacke-siltstone or its metamorphic equivalent – migmatitic paragneiss. The previously reported basal metaconglomerate (Morgan et al., 1976) is now interpreted as boudinaged quartz veins in a highly deformed schistose matrix. Carbonate-bearing rocks form only thin calcsilicate gneisses associated with some of the thicker amphibolites.

1. Basement Complex

Granitoid basement rocks ranging from granite to granodiorite averaging quartz monzonite in composition are exposed in a series of domes across the area. As named geographical features are rare, these domal culminations have been numbered to facilitate reference to them (Fig. 35.2). The presence of relict layering, amphibolite and biotite schist boudins and sheets, pods of ultramafic rocks (Dome 4) and augen suggesting a coarser parent, all support the concept that a heterogeneous gneiss terrane formed a basement to the supracrustals and was subsequently remobilized.

The gneisses are pink, orange or grey on fresh surfaces with a distinctive yellowish white weathered surface. They are generally mafic-poor and although minor muscovite or sillimanite may occur marginal to the metasediments, the actual basement-cover contact is usually sharp and distinctive. A penetrative biotite and local ribbon quartz

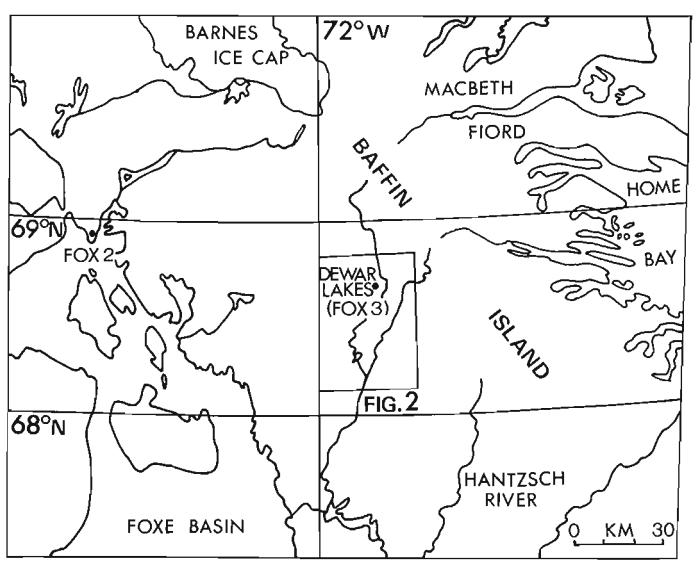

Figure 35.1. Location map.

[1]Department of Geological Sciences, Queen's University, Kingston, Ontario, K7L 3N6

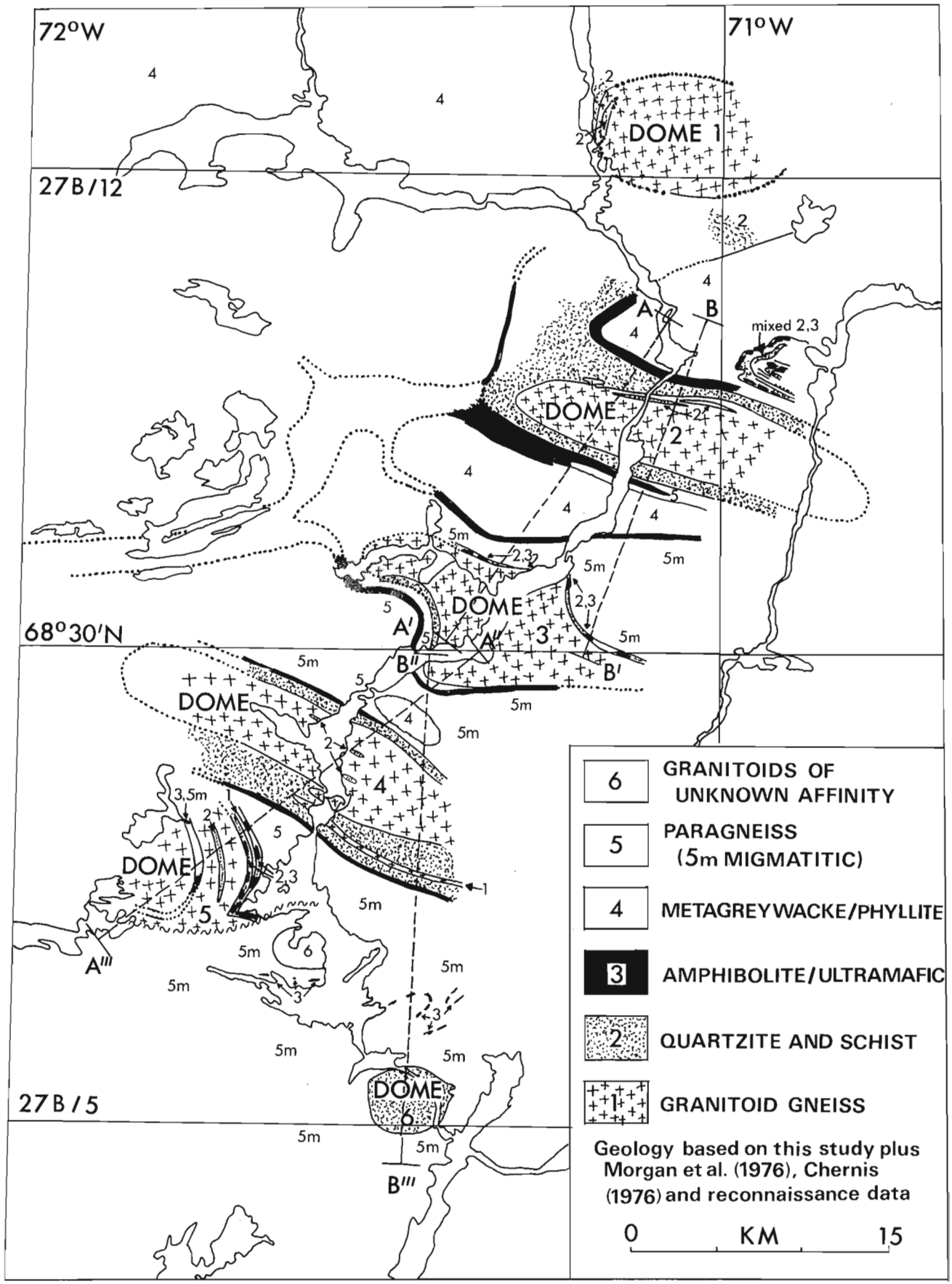

Figure 35.2. Geological map of the study area excluding diabase dykes.

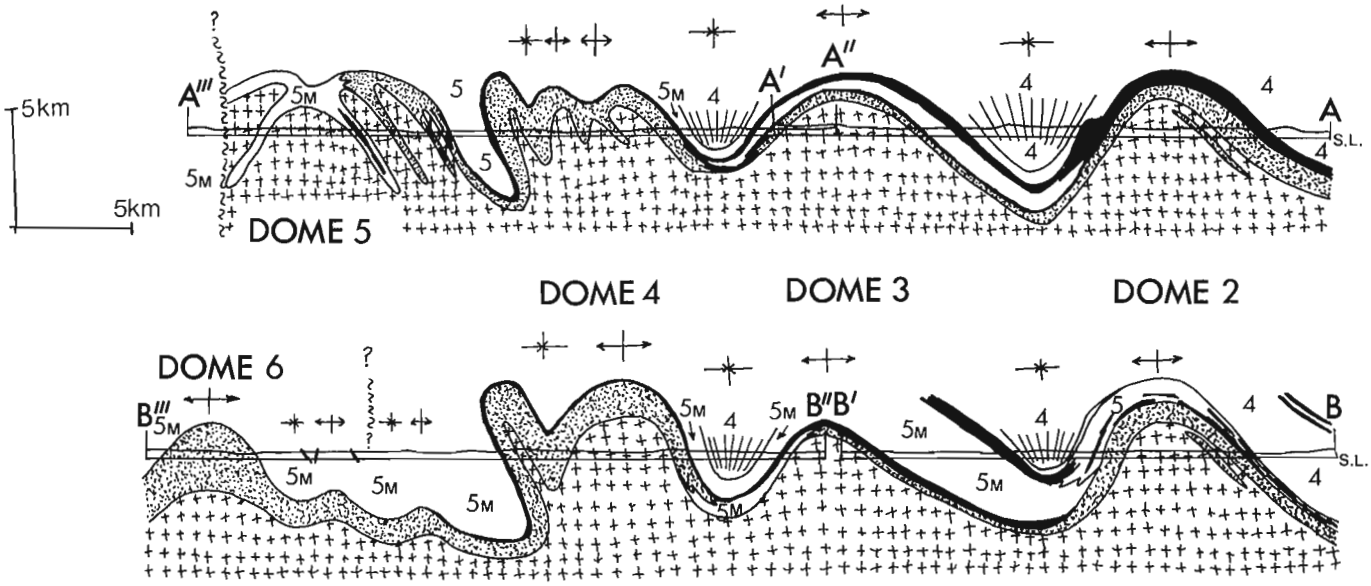

Figure 35.3. Schematic and interpretive cross-sections through the study area showing D3 closures only. See Figure 35.2 for legend.

schistosity arches across the domes and is concordant with the contacts. Only along the northern margin of Dome 2 is there a marked divergence between this schistosity and the older layering. Elsewhere all layering, as well as early pegmatites and quartz veins, has been isoclinally folded and transposed parallel to the schistosity. Nowhere is layering observed to be truncated by the basement-cover contact. The degree of heterogeneity and the strength of layering increase towards the margins of the domes although poorly developed laminations on various scales occur throughout.

Gneisses in the north are finer grained and contain elongate mm- to cm-sized augen of quartz and feldspar and a strong biotite mineral streaking, both parallel to the long axis of the domes. Cross-cutting pegmatites 1-15 m thick and up to 2 km long make up 5-20 per cent of Dome 2 and form distinctive sets whose orientations may be related to late stresses within the dome. They locally cross the basement-cover contact and spread out as sills in the overlying quartzite, producing an apparent truncation which was initially thought to identify the dykes as a presedimentary feature. Farther south the pegmatites are smaller and more evenly distributed. Weak to moderate folding and locally developed marginal schistosity characterize these late syntectonic intrusives.

2. Impure Quartzite and Schist unit

Flaggy to blocky, greyish white quartzites of the basal metasedimentary unit generally contain 90-95 per cent fine to medium grained quartz with various combinations of muscovite, biotite and feldspar. These impurities are concentrated in thin layers producing a pronounced colour lamination and fissility on the millimetre and centimetre scale. On the scale of metres, the quartzite is interlayered with more dominantly schistose rocks containing up to 80 per cent combined muscovite and biotite with some sillimanite and garnet. The high grade equivalent of the unit is a distinctive quartzofeldspathic rock with mm to cm sized pods of sillimanite, feldspar and quartz. Biotite schist and amphibolite sheets and boudins are locally present near the base of the quartzite but their relationship to amphibolites in the basement gneiss and in the overlying metasediments is not known. The quartzite-schist sequence does not seem to contain any internal markers such that although poorly preserved cross-beds marginal to Dome 2 are right way up, rare minor folds suggest at least limited transposition of sedimentary layering and the extent to which the original bedding has been disrupted or overturned remains unknown.

Whereas the lower contact with the basement is generally sharp, the upper contact may be gradational with interlayered quartzite and paragneiss over a transition zone of some tens of metres. Thicknesses vary without an apparent regular pattern with Domes 1, 2, 4 and 6 being flanked or cored by substantial thicknesses of quartzite while Domes 3 and 5 have very thin mantles.

3. Amphibolite and Ultramafic rock unit

Mafic-rich rocks which overlie the quartzite unit possess a complex, irregular, internal stratigraphy. Compositionally they range, both overall and along strike, from speckled amphibolites with subequal hornblende and plagioclase, through black to dark green hornblendites and into ultramafic rocks with partially serpentinized porphyroblasts of olivine. Although locally massive, they are predominantly strongly foliated and internally well layered on the scale of mm to cm. South of Dome 2, highly deformed, possibly metavolcanic pillow-like shapes were observed whereas north of Dome 2, cm-thick bands of amphibolite in siltstone suggest a metasedimentary origin. The close association with banded calcsilicate gneisses supports the latter suggestion while the presence of massive sulphides (see Economic Geology) seems to favour the former. Possibly both metasedimentary and metavolcanic amphibolites are present.

A variable thickness of paragneiss commonly separates the mafic rocks from the quartzite while north of both Domes 2 and 3 there appears to be upper and lower amphibolite sequences within the metagreywacke. As a general rule, however, there is simply a single amphibolite or hornblendite, usually along the upper contact of the quartzite. These distinctive units pinch out to the east and south with the hornblendite north of Dome 4 passing gradationally into a finely laminated transitional metasediment and Dome 6 lacking a mantling amphibolite.

4. Metagreywacke-Metasiltstone unit

The metamorphosed flysch of the central eugeoclinal zone extends out over the quartzite and contains the amphibolite-ultramafic unit in its lower levels, in which association it is locally sulphide-bearing and rusty. A series of transitions occur from north to south and similarily from high to low stratigraphic levels changing a fine grained, recognizably sedimentary rock into a strongly deformed and highly metamorphosed migmatitic paragneiss. In neither state are internal marker horizons recognizable.

At low grade sedimentary bedding and laminations are preserved. Other sedimentary features, with the exception of concordant, compositionally zoned calcsilicate nodules, were not recognized. The flysch is composed of 0.1-3 m layers of metagreywacke, rarely containing monocrystalline grains of quartz and feldspar several mm in diameter, alternating with 1-20 cm layers of siltstone or phyllite. Both are poor in K-feldspar. Lateral facies changes do not appear to be present while more massive, thickly bedded units seem to become dominant higher in the section.

At higher grades the metagreywacke-phyllite is transformed through the intermediate step of nonmigmatitic paragneiss into a rusty to medium brown migmatitic paragneiss. Original sedimentary layering is transposed parallel to a strong schistosity and, where disrupted, blocks containing relict layering in a more schistose matrix may be observed. Where folding and boudinage have not been severe, the paragneiss is made up of blocky biotite-quartz-feldspar horizons alternating with schistose biotite-garnet-sillimanite-quartz-feldspar horizons. Both this alternation and regular variations in the content of sillimanite pods are probably partly equivalent, respectively, to original sedimentary layering and grading. Boudins of hornblende-plagioclase amphibolite and more rarely hornblendite are scattered throughout while the high-grade equivalents of calcsilicate pods are not as abundant as at lower grade.

Abundant white pegmatite in the form of veins, sheets and boudins makes up from 10 to 90 per cent of the pegmatite paragneiss but shows no systematic regional variation with the alternation of pegmatitic and paragneiss occurring on the scales of centimetres to tens of metres. The boundary across which pegmatite appears is very marked and is accompanied by the recrystallization of the metagreywacke into a paragneiss.

Metamorphism

The single most important metamorphic reaction to have affected the rocks in the study area is the breakdown of muscovite in the presence of quartz to produce sillimanite and K-feldspar. This reaction occurred at progressively higher stratigraphic levels to the south suggesting some sort of metamorphic culmination in that direction. Distinctive pods of sillimanite, feldspar and quartz characterize the altered basal quartzite as well as some horizons in the migmatitic paragneiss. Reactions which produced garnet and sillimanite have not yet been defined. The restricted chemical compositions of the gneisses, quartzites and metagreywackes prevented the development of index minerals which might have detailed the metamorphic conditions more exactly.

It should be noted that the bulk of the white pegmatite which cross-cuts the paragneiss sequence is trondjemitic in composition. This probably relates to the K-feldspar deficient nature of the original metasediments such that although the first increment of melting would have produced a "normal" granite-quartz monzonite, the rapid loss of all K-feldspar in the restite would have permitted the composition of the melt to progressively approach that of the plagioclase-rich paleosome. Both the lack of in situ anatectic textures in the zone of first appearance of melt and some space problems north of Dome 3 indicate that considerable mobilization of melt from deeper regions has occurred. As well, the abrupt termination of a high degree of anatexis at the basement-cover contact indicates that although the basement was of a more favourable composition for a high degree of anatexis, it was relatively anhydrous during the peak of metamorphism and could not produce the same percentage of melt as did the water-saturated metasediments.

Textural data indicate that the metamorphic peak preceded the last regionally penetrative deformation whose associated schistosity is axial planar to folded pegmatites probably generated during anatexis. Late annealing recrystallization has been pervasive with the exception of plagioclase which is often fractured and shows evidence of retrograde metamorphism. Although the schistosity is bent around porphyroblasts, it is difficult to determine the actual timing of metamorphism since the latest phase is often coplanar with earlier phases in critical areas. Evidence from the southern migmatites suggests, however, that the peak was syndeformational with the major earlier phase.

Structural Interpretation

The structures observed in the area are interpreted in terms of three phases of deformation.

1. D1

As mentioned above, compositional layering in the basement gneisses is oblique to schistosity along the northern margin of Dome 2 and is transposed parallel to it elsewhere. This, combined with the presence of amphibolites, ultramafics and possible early dehydration, suggests one or more presedimentary phases of deformation which have been collectively referred to as D1. The shape and orientation of D1 folds are not known.

2. D

At low stratigraphic levels to the north and at progressively higher ones to the south, a subhorizontal schistosity exists which is axial-planar to isoclinal folds of the basement-cover contact. Mesoscopic folds associated with this deformation are present in several locations in both gneiss and metasediments and have hinges generally colinear with or at a small angle to the present domal trend. The size of major D2 structures is unknown but, with the exception of tongues of gneiss and quartzite up to 0.1 km in thickness and 10-15 km in length which are closely confined to the vicinity of the domes (Figs. 35.2, 35.3), major structures involving inversion of the stratigraphic sequence have not been outlined. Mineral lineations of biotite, sillimanite and hornblende have been correlated with this phase although their mechanical significance is unclear. Metamorphism is tenatively interpreted as being synchronous with this phase of deformation

3. D3

The regional expression of the third phase of deformation is a refolding of the early basement-cover isoclines (D2) and their related subhorizontal schistosity by folds with steeply dipping axial planes and gently plunging hinges (D3). In addition, however, some of the observed fabric relationships require further explanation. These fabric relationships are summarized below:

- A strong fabric gently arches across the domes without being folded by recognizable compressional structures.
- Extensive chocolate-tablet boudinage of quartz veins and pegmatites occurs along both the ends and flanks of the domes.
- Zones next to the basement-cover contact contain folds of reversed or "cascading" vergence which deform the dominant schistosity.

- In zones farther from the domes, the dominant schistosity is a crenulation of the schistosity which passes over the domes.
- In zones still farther from the domes, this crenulation cleavage passes into a new schistosity which defines intersection lineations in the low grade metasedimentary rocks which they contain. The pocket between Domes 3 and 4 is a doubly plunging synform while the one between Domes 2 and 3 has not been observed to close to either east or west. Lineations plunge at up to 70 degrees to the east in the latter area.

Gneiss doming of a terrane previously possessing a subhorizontal schistosity would account for the above features, however, another set of observations requiring explanation also exists.

- The domes posses a pronounced linear form with Dome 3 probably being a composite of two closely-spaced en echelon domes.
- The broad flysch basin to the north is folded about upright, shallowly plunging folds showing no spatial relationship to gneiss doming.
- Upright D3 closures at 1-2 km intervals fold S2 in the southern migmatites as well as over the crest of Domes 4 and 6.
- Folds away from the basement-cover contact have the vergence expected for compressional deformation.

As a result, a combination of lateral compression and gneiss doming is required to explain the observed fabrics and geometry. Compressional folding localized the position and shape of the incipient domes with the gneiss being remobilized along the antiformal hinges and subsequently dominating the deformation at lower levels. Higher in the section and to the south, as well as in the central part of the belt and the pockets of upright D3 schistosity between Domes 2 and 3 and Domes 3 and 4, compressional deformation was prevalent producing strong folding of both the migmatitic paragneiss and the metagreywacke-phyllite. The relative contributions of lateral compression and of pinching between the rising domes in the deformation of the above-mentioned pockets is unclear.

There are very few areas in which S2 has been preserved from D3. On the top and margins of the domes the two phases were roughly coplanar producing minor rotation and further flattening of the earlier fabrics, such that there the penetrative schistosity is properly called S2/S3. The increasing divergence of S2 and S3 off the margins of the domes is responsible for the zones in which S3 is a crenulation of S2. Above the zone in which S2 was originally developed, S3 is the first schistosity to have developed in the rocks. Compressional folding was responsible for much more of the D3 deformation to the south as compared to the north. Quartzite is folded into the crest of Dome 4 about upright axial planes and cascading folds are rare.

Several differences exist between this sequence and that of Morgan et al. (1976) although D1 and D2 are similar. Gravity-driven doming during D3 was not considered earlier as an active force in the formation of the basement culminations which were interpreted as solely the result of compressional folding. Variable plunges along the domal trend were thought to be the result of D4 cross-folding and although some sporadic crenulations at high angles to that trend were observed during the present study, they are neither persistent nor strong enough to be related to such a regional cross-folding. The variation in hinge lines is considered here to be a natural part of compressional folding and gneiss doming.

The age of the structural and stratigraphic break south of Dome 5 is unknown but as it truncates part of a dome south of the main dome, it is presumably post-D3. Stratigraphically it is south side down and possesses considerable offset in both vertical and horizontal directions as no trace of the truncated dome is present south of the break.

Unit 6 is of unknown origin and may be either remobilized basement which has pierced the quartzite-amphibolite cover sequence during its ascent, or a plutonic intrusive. The unit is at least pre-D3 and D3 folds wrap around it and it appears to contain an even earlier fabric (S2?).

Economic Geology

The major amphibolite north of Dome 3 is associated with an extensive gossan made up predominantly of rusty schists. Just west of the lake system (68°33'N, 71°14'W) blocks of massive pyrrhotite with 2-3 per cent disseminated chalcopyrite and bornite are derived from a layer in the gossan estimated to be 40-50 cm in thickness. Along strike to the west a small amount of malachite stain occurs in a calcsilicate associated with the same amphibolite (68°33'N, 71°19'30"W). Farther south, a 1 cm pod of molybdenite was observed in a granitoid vein which cross-cuts Dome 5 (68°22'N, 71°41'30"W).

References

Chernis, P.J.
1976: Stratigraphy, Structure and Metamorphism of the Piling Group at Dewar Lakes, Baffin Island, N.W.T.; Unpubl. B.Sc. thesis, Carleton University, Ottawa, Ontario, 64 p.

Jackson, G.D.
1969: Reconnaissance of north-central Baffin Island; in Report of Activities, Part. A, Geol. Surv. Can., Paper 69-1A, p. 171-176.

1971: Operation Penny Highlands, south-central Baffin Island; in Report of Activities, Part. A, Geol. Surv. Can., Paper 71-1A, p. 138-140.

Jackson, G.D. and Taylor, F.C.
1972: Correlation of major aphebian rock units in the northeastern Canadian Shield; Can. J. Earth Sci., v. 8, p. 1650-1669.

Morgan, W.C., Bourne, J., Herd, R.K., Pickett, J.W., and Tippett, C.R.
1975: Geology of the Foxe Fold Belt, Baffin Island, District of Franklin; in Report of Activities, Part. A, Geol. Surv. Can., Paper 75-1A, p. 343-347.

Morgan, W.C., Okulitch, A.V., and Thompson, P.H.
1976: Stratigraphy, Structure and Metamorphism of the West Half of the Foxe Fold Belt, Baffin Island; in Report of Activites, Part. A, Geol. Surv. Can., Paper 76-1A, p. 387-391.

36. ASPECTS OF GLACIAL HISTORY, SOUTHEASTERN ELLESMERE ISLAND, DISTRICT OF FRANKLIN

Project 750063

W. Blake, Jr.
Terrain Sciences Division

Abstract

Blake, W., Jr., Aspects of glacial history, Southeastern Ellesmere Island, District of Franklin; Current Research, Part A, Geol. Surv. Can., Paper 78-1A, p. 175-182, 1978.

Field work around Makinson Inlet, Ellesmere Island, has revealed that erratics, striated rock surfaces, and marginal drainage channels are widespread. These features, plus the glacial sculpture on Bowman Island, show that a major outlet glacier formerly flowed eastward in Makinson Inlet, draining a significant mass of ice that lay to the west of the present-day ice caps. A fossil peat deposit indicates an ice-free interval >44 000 years (GSC-140-2) ago with a climate more favourable than that of today. During Holocene time the sea penetrated to the head of the west arm of Makinson Inlet by 8930 ± 100 years B.P. (GSC-2519) and to the head of the north arm by 7330 ± 80 years B.P. (GSC-1972).

Introduction

During the summer of 1977 (June 23 to August 21) work on the project entitled "Quaternary Geochronology, Arctic Islands" was concentrated around Makinson Inlet, Ellesmere Island (Fig. 36.1). In addition, a three-day trip was made to the southeastern coast of the island and to Coburg Island, and four days were devoted to a re-examination of marine deposits at Cape Storm, southwestern Ellesmere Island. The second half of July was spent studying glacial deposits and landforms in the vicinity of Cape Herschel, north of the 78th parallel, and highlights of the work carried out there have been described previously (Blake, 1977). The present article will deal with various aspects of the investigations around Makinson Inlet.

As a complement to the writer's investigations of glacial history, R.A. Souchez and R.D. Lorrain of Université Libre de Bruxelles, Belgium, carried out a program of sampling basal ice from a number of outlet glaciers on the eastern side of the north arm of Makinson Inlet. Their work is intended to provide a better understanding of the chemical processes occurring at the ice/rock interface in polar glaciers as opposed to the temperate glaciers they have investigated previously in the Alps (Souchez and Lorrain, 1975).

Another component of the 1977 work involved coring of lake sediments from an ice platform. The lightweight nature of the coring equipment which was utilized (for ease of transport in the field) and an early thaw of the lakes, resulting from the exceptionally good weather throughout the early part of the summer, created problems in the coring program. R.J. Richardson is studying the short cores recovered from a lake to the west-southwest of the Swinnerton Peninsula base camp (Fig. 36.2).

A Hughes 500C turbine helicopter was used in the field, and the availability of this machine made it possible to visit a number of localities which otherwise would have been difficult to reach. In addition to helicopter support, two Honda ATC's (All-Terrain Cycles) were used for travel within a few kilometres of our base camp on Swinnerton Peninsula, near the head of the western arm of Makinson Inlet (Figs. 36.1, 36.2). These vehicles also were transported to more distant sites by Twin-Otter aircraft or were carried in a sling under the Hughes helicopter, and thus even greater mobility was achieved.

Geomorphology and Glaciation

Makinson Inlet is by far the largest fiord along the Ellesmere Island coast of northern Baffin Bay. The inlet extends for almost 100 km from its mouth in Smith Bay to the head of the north arm. The ice caps that dominate the east coast are localized over the Precambrian terrane – the Southeastern Highlands (Roots, 1963). In this part of Ellesmere Island nunataks and high domes on the ice caps attain elevations of more than 1100 m a.s.l., or, to the north of Makinson Inlet, more than 1500 m. Water depths in excess of 500 m are the rule in the middle reaches of the Inlet (Sadler, 1973). By contrast, elevations of the plateau surface developed on the Paleozoic rocks of Swinnerton Peninsula and elsewhere around inner Makinson Inlet rarely exceed 500 m a.s.l., and water depths are generally less than 200 m. Thus the total relief is significantly less in this region, which is part of the Southern Plateau as described by Roots (1963).

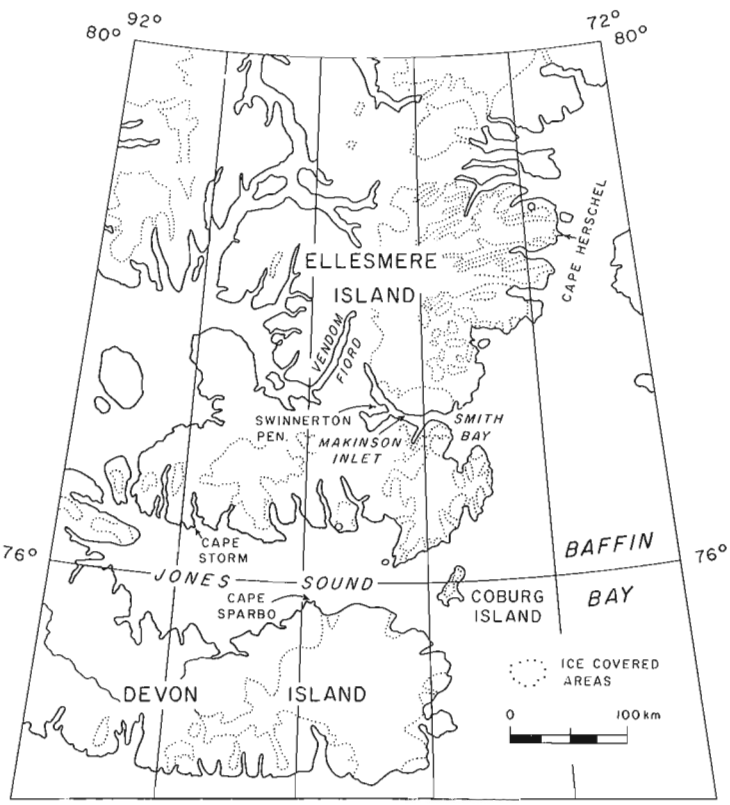

Figure 36.1. Location map, southeastern Ellesmere Island.

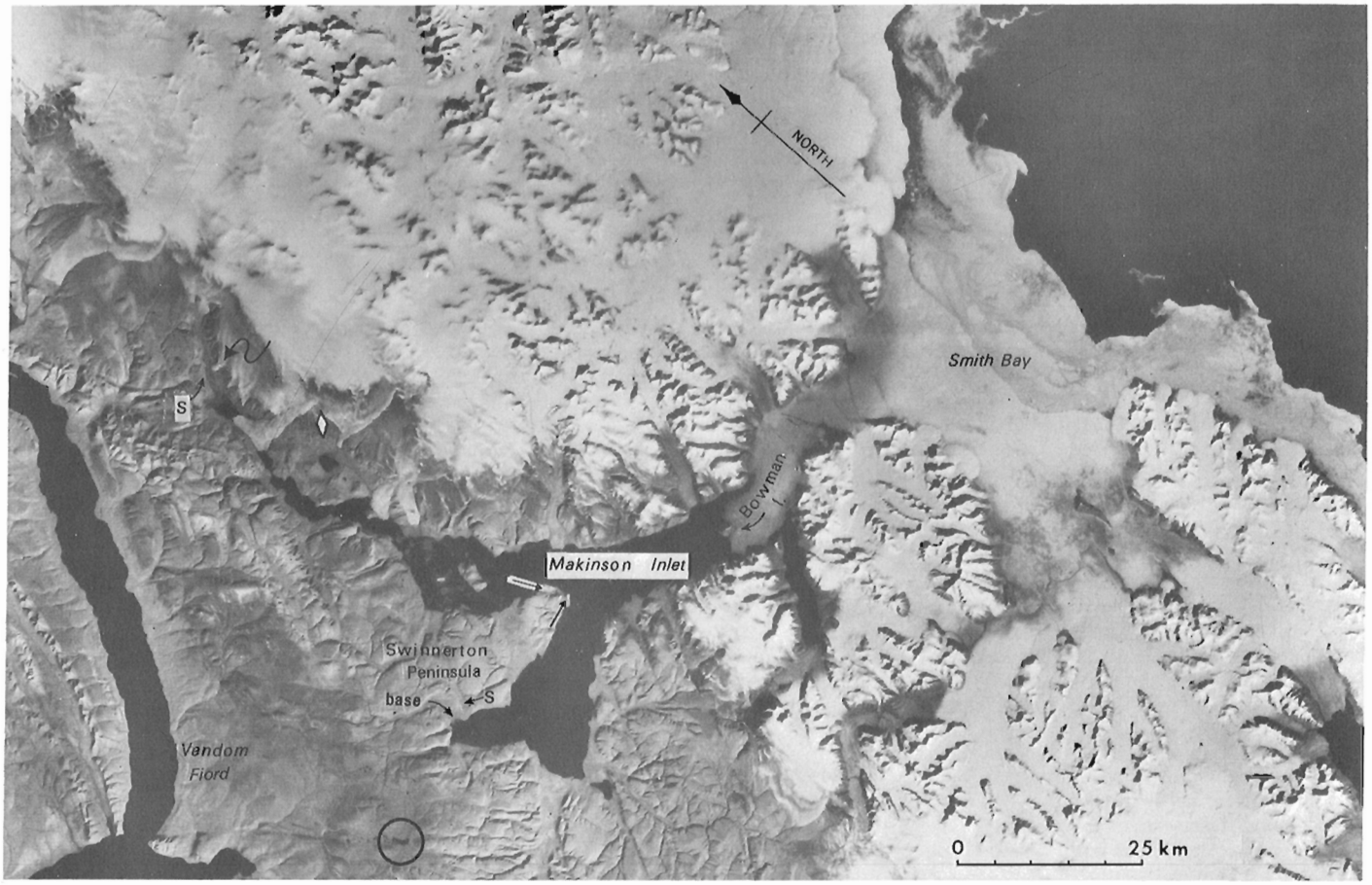

Figure 36.2. LANDSAT image of the Makinson Inlet area, Ellesmere Island. Arrows at the eastern end of Swinnerton Peninsula indicate the former direction of ice flow; the S-symbol refers to the two new sites with dated marine shells mentioned in the text; the diamond (south end) indicates where "old" peat occurs; the encircled lake is where coring was attempted; and the wavy arrow north of the head of the inlet indicates the glacier where in situ willows have been exposed by recent retreat of the ice (cf. Fig. 36.10). Image E-1758-17500, spectral band 7, August 20, 1974.

Evidence for much more extensive glacierization than at present is widespread in the form of innumerable erratic boulders, striated rock surfaces, and marginal drainage channels. Examination of the headlands at the eastern end of Swinnerton Peninsula revealed the presence of striated dolomite on the plateau surface at elevations between 300 and 345 m. These smoothed and polished surfaces indicate, as might be expected, converging flow within a significant mass of ice which was being channelled seaward via Makinson Inlet (Figs. 36.2, 36.3). Twenty-five kilometres east of Swinnerton Peninsula, the resistant Precambrian granitic and granulitic rocks of Bowman Island (Frisch, 1977), at approximately the same elevation (300 m), exhibit massive sculpturing and polishing by the outlet glacier that once filled Makinson Inlet. The amount of erosion that has taken place in order to carve Bowman Island into its present form provides additional evidence that the inner parts of this fiord system were buried deeply beneath ice during the last glaciation. This concept is in line with estimates of maximum ice thickness for the Innuitian Ice Sheet of 1900 m (Paterson, 1972), 2000 m (CLIMAP, 1976), and >2000 m (Sugden, 1977). Yet a marked contrast exists between the classic glacial landforms displayed on Bowman Island (Figs. 36.4 to 36.6) and certain parts of the plateau surface to the north, where incipient tors or tor-like landforms are present although erratics litter the surface (Figs. 36.7 to 36.9). Makinson Inlet and environs appear to represent an excellent example of what Sugden (1974) has described as a landscape of "selective linear erosion" (cf. also Sugden, 1968). This type of landscape is characterized by valleys in which tremendous amounts of scouring take place along pre-existing drainage lines or structural lineaments, whereas the adjacent "upland plateau remnants between the troughs generally show little or no sign of glacial erosion, and it is common to find the surface covered with regolith" (Sugden, 1974, p. 179-180).

Erratics of granite and other shield rocks were observed to be widespread on the plateau surfaces cut in Paleozoic rocks of Swinnerton Peninsula, and they also are abundant to the west around Vendom Fiord (R.F. Roblesky, pers. comm. 1977). It is evident, therefore, that at some time, and in all probability on repeated occasions, boulders were carried westward by more extensive ice than exists at present, for the Paleozoic/Precambrian boundary is close to the western margin of the ice caps, both to the north and south of Makinson Inlet (Christie, 1962; Frisch, 1977). However, the erratics also document the eastward flow of ice out Makinson Inlet. Erratic cobbles and boulders of Paleozoic rocks are ubiquitous along the rim of the plateau on the north side of the inlet, and they are present in far greater numbers on Bowman Island. In addition marine shell fragments are present in the thin till which overlies the striated bedrock on the northeast corner of Swinnerton Peninsula and on Bowman Island, in both cases at elevations up to 300 m or more. On Bowman Island this is the same till in which Paleozoic rock fragments are so abundant. One limestone cobble contained a

well preserved pygidium and an incomplete thorax of the Late Silurian trilobite Encrinurus (Frammia) arcticus (Haughton)[1] which is a characteristic faunal element of the Read Bay Formation (Bolton, 1965). The nearest locality to Bowman Island where rocks of the Allen Bay and Read Bay formations (undifferentiated) are known to occur is the north arm of Makinson Inlet, over 45 km distant (R.F. Roblesky, pers. comm., 1977; cf. also Kerr and Thorsteinsson, 1972; McGill, 1974; Kerr, 1976).

Marginal drainage channels occur throughout the inner Makinson Inlet region, and they provide valuable information as to the pattern of ice retreat. For the purposes of this preliminary report it is sufficient to note that they are particularly abundant and well developed to the west and northwest of Swinnerton Peninsula, and they are also abundant on either side of the north arm of Makinson Inlet.

Absolute Age Determinations

A long and complicated sequence of events is recorded in the deposits of the Makinson Inlet region, and more field and laboratory studies will be required before all the relationships between glacial, lacustrine, and marine environments are understood fully. Reconnaissance investigations in the early 1960's by J.G. Fyles and R.L. Christie provided the first materials on which radiocarbon age determinations could be carried out; thus some insight into chronology was gained at that time.

One of the most interesting discoveries made by Fyles in 1961 was a peat deposit exposed in a valley wall east of the north arm of Makinson Inlet (Fig. 36.2). This peat, at an elevation of approximately 365 m, was overlain by boulders on the floor of a large drainage channel. Its age was determined originally to be >36 400 years (GSC-140; Dyck and Fyles, 1964). A new determination on the remainder of the sample, however, gave a value of >44 000 years (GSC-140-2), and at the same time the predominant constituent was determined by M. Kuc to be the moss **Calliergon giganteum,** a species typical of moss bog tundra (Blake, 1974). The site was revisited in 1977, and new collections were made. Remains of beetles were found in the massive peat deposit, and a thorough study of them should provide valuable paleoenvironmental information. However, the very presence of beetles, including the ground beetle **Amara alpina** (Payk.)[2], indicates environmental conditions somewhat more favourable than those of today. At present **A. alpina** is not known to occur north of Cape Sparbo (Fig. 36.1) on the Jones Sound coast of Devon Island (Lindroth, 1963, 1968), approximately 240 km south of the Makinson Inlet site. It would appear that at least two episodes during which glacier ice occupied the north arm of Makinson Inlet are reflected in the peat bearing sequence here. One glacial episode is needed in order that the channel could be cut by meltwater, then an ice-free interval during which tundra bogs developed on the floor of the channel, followed in turn by another glacial episode during which the mass of boulders and finer materials overlying the peat were washed down the channel and deposited.

With regard to other "old" materials, a determination on fragments of **Hiatella arctica, Mya truncata,** and **Astarte** sp. collected by J.G. Fyles at 85 to 90 m a.s.l. in the south-central part of Swinnerton Peninsula gave values of 29 430 ± 680 years (GSC-134; standard preparation, with the outer 10% of shells removed by leaching) and 29 800 ± 220 years (GSC-134; second preparation, inner 37% of shells). Although Fyles (in Dyck and Fyles, 1964) suggested that, in view of the good agreement between the two determinations, they might represent the approximate absolute age rather than a minimum age, a case can also be made for the latter interpretation (cf. Olsson and Blake, 1962; Olsson, 1968; Blake, 1974).

Prior to the collections made this past summer the oldest Holocene materials that had been dated were pelecypod shell fragments collected at the head of the south arm of Makinson Inlet by R.L. Christie in 1960; the result on the inner fraction of shells was 8200 ± 220 years (GSC-146; Dyck and Fyles, 1964; Craig and Fyles, 1965). A new determination on aragonitic shells of **Hiatella arctica,** collected at approximately 40 m a.s.l. from the basal unit of a sequence of marine sediments 2 km east of the base camp on Swinnerton Peninsula (Fig. 36.2), has given a value of 8930 ± 100 years (GSC-2519). This date indicates the time by which marine waters had penetrated close to the innermost part of the west arm of Makinson Inlet. The date also indicates that the glaciated surfaces on Bowman Island, more than 40 km to the east, have been free of ice for more than 9000 radiocarbon years, yet they retain their high polish and fresh-appearing striae (cf. Figs. 36.5, 36.6).

North of the ice-dammed lake that now exists at the head of the north arm of Makinson Inlet an important collection of marine shells was made in 1973 by S.B. McCann. In a fresh exposure which had been undercut recently by the river, a silt/clay unit was exposed at approximately 36 m a.s.l. (Fig. 36.2); aragonitic shells of **Hiatella arctica** from this unit were determined to be 7330 ± 80 years old (GSC-1972), a value only marginally older than shells of the same species collected 3 km east of the head of Vendom Fiord by D.A. Hodgson in 1972 (7010 ± 80 years; GSC-1858)[3]. There is thus a difference of roughly 1400 to 1800 radiocarbon years in the age of the earliest marine fauna between the site on Swinnerton Peninsula and the site north of the head of Makinson Inlet. This is a crude measure of the time it took for the lobe of ice occupying the north arm to disappear, although the exact position of the ice front in this arm at 9000 to 8800 years B.P. is unknown.

Not only did a marine fauna formerly penetrate north of what is now the head of the north arm of Makinson Inlet, but coniferous driftwood (**Picea** sp., identified by R.J. Mott) also floated in. At some point in time an ice-dammed lake, far larger than the present lake, existed in the area, but details of the chronology must await radiocarbon dating of organic materials collected from the lacustrine deposits preserved on the flanks of the valley (cf. Fig. 36.10).

One other aspect of chronological studies is worthy of mention. Many of the outlet glaciers that descend towards, and reach, the north arm of Makinson Inlet from the ice cap to the east appear to have retreated recently following a slight advance. In the case of the largest of these lobes in the valley under discussion (Fig. 36.2), numerous intact arctic willows, still rooted in place, are exposed through the thin and discontinuous layer of gravelly boulder till laid down by the glacier (Fig. 36.10). The ice also advanced over peat deposits, so a good chance exists to pin-point the age of this Neoglacial advance more precisely.

Pumice and Driftwood on Raised Beaches

At a site 1.5 km west of the base camp on Swinnerton Peninsula an expanse of raised beaches was found to contain a number of imbedded driftwood logs. In addition two pieces of dark brown pumice were discovered, and instrumental levelling showed them to be at an average elevation of 21.5 m. This is close to the elevation postulated for the 5000 year-old shoreline in this area on the basis of dated driftwood (**Picea** sp., identified by L.D. Gill) logs collected in 1972 at the same site by D.A. Hodgson and a few kilometres to the east by R.B. Taylor (Blake, 1975). At the time of writing no new age determinations are available, but eventually it should be possible to construct an emergence curve for Swinnerton Peninsula and to determine whether the pumice, which appears identical to the material found along the south coast of Ellesmere Island, did in fact reach Swinnerton Peninsula at approximately the same time.

[1] Identified by T.E. Bolton

[2] Identified by J.V. Matthews, Jr. (Unpubl. GSC. Fossil Arthropod Rep. No. 77-11).

[3] The age of 6980 ± 80 years reported by Hodgson (1973) was prior to the $^{13}C/^{12}C$ ratio being determined, hence the slight change in age.

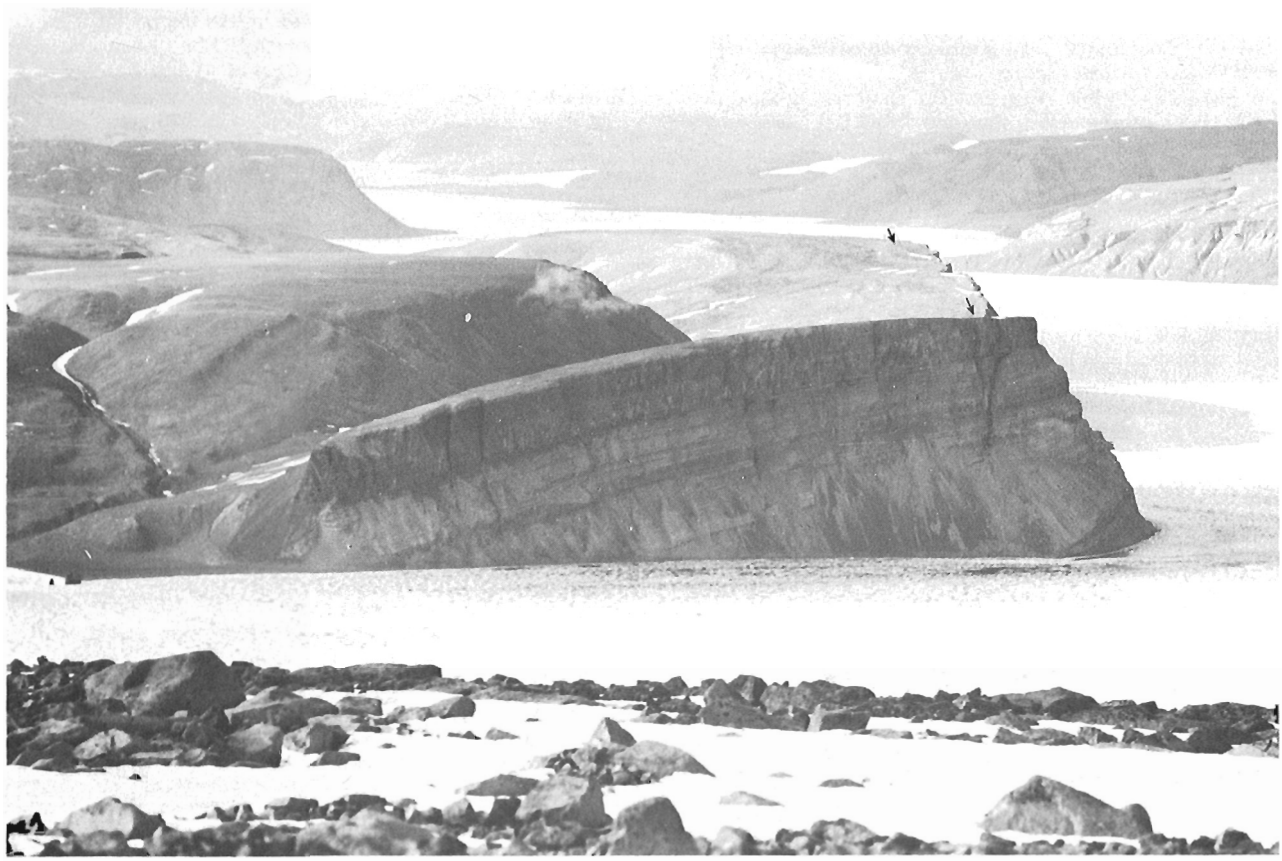

Figure 36.3. Telephoto view north at the eastern tip of Swinnerton Peninsula and the north arm of Makinson Inlet. Two sites with striated bedrock at elevations between 300 and 345 m are indicated by arrows; at the northern locality shell fragments were abundant in the till overlying the striated bedrock. July 7, 1977. (GSC-203262-B).

Figure 36.4. Telephoto view southeast at Bowman Island from the plateau on the north side of Makinson Inlet. The top of the island is approximately 570 m a.s.l., whereas the ice-capped mountains beyond, on the south side of the inlet, rise to over 1000 m. The shoulder of the island, where Figures 36.5 and 36.6 were taken, is indicated by the arrow. July 9, 1977 (GSC-203262-D).

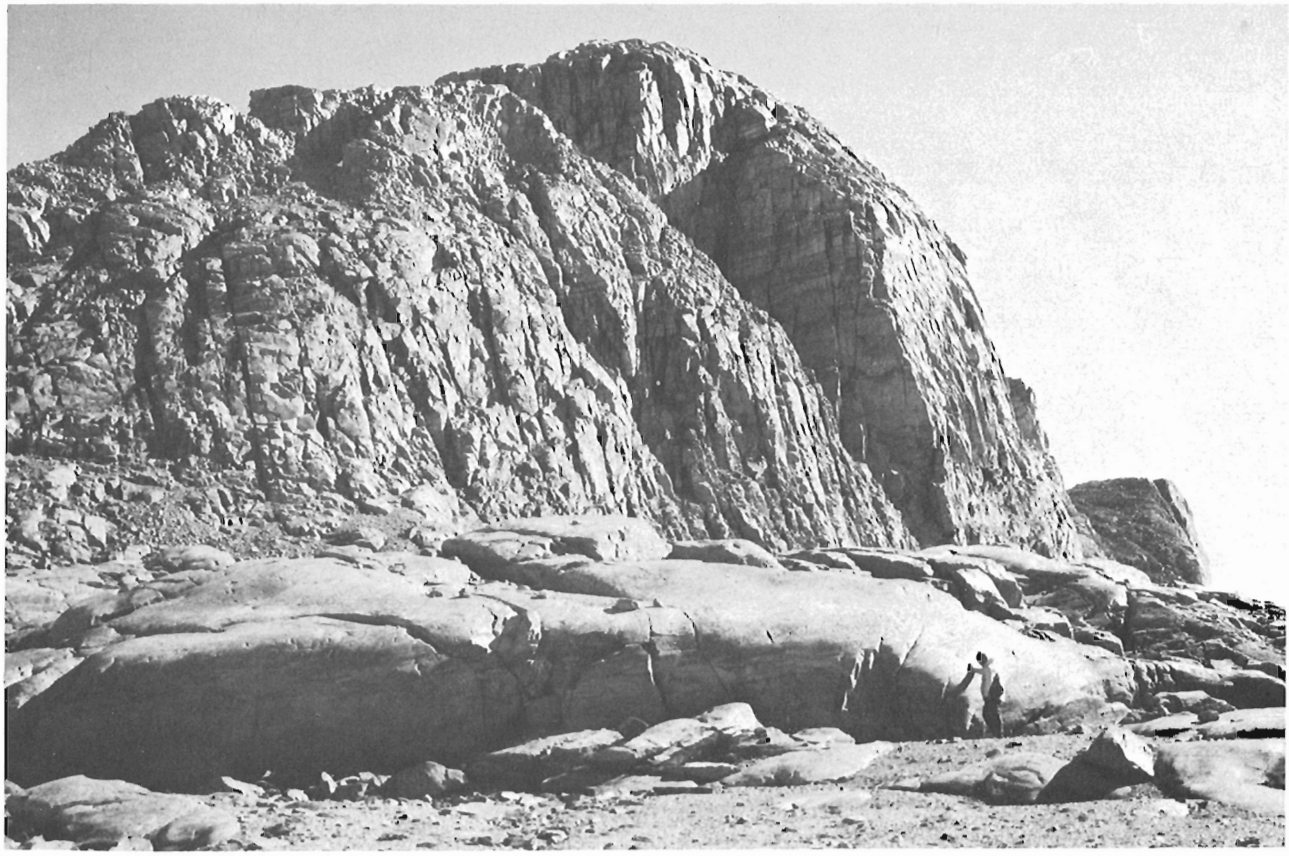

Figure 36.5. View eastward along the south side of Bowman Island, on shoulder at approximately 250 m a.s.l. Note the smoothed and polished granite in foreground. July 14, 1977 (GSC-203262-E).

Figure 36.6. View southward at shaped and plucked outcrop of granite on the shoulder of Bowman Island shown in Figure 36.5, at approximately 260 m a.s.l. Ice flowed from right to left in the photograph (west to east). The plateau (>600 m a.s.l.) in the distance is covered by a thin carapace of ice. July 14, 1977 (GSC-203262-F).

Figure 36.7. View eastward at a typical segment of the plateau along the north side of Makinson Inlet. The top of the small ice cap is more than 975 m a.s.l. The arrow indicates the point from which Figure 36.8 was taken. Numerous Paleozoic erratics are present on the Precambrian bedrock. July 9, 1977 (GSC-203262).

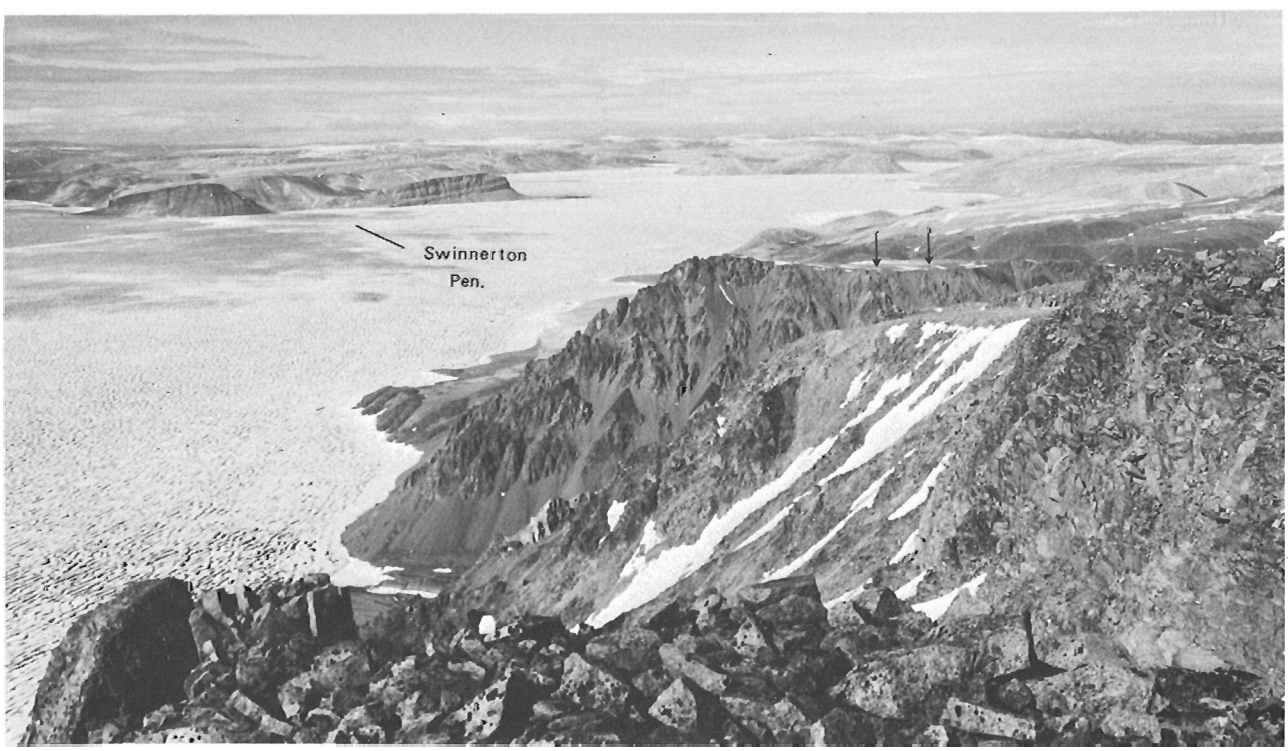

Figure 36.8. View northwest at the eastern tip of Swinnerton Peninsula and the north arm of Makinson Inlet from the point on the plateau indicated in Figure 36.7. The lower segment of the plateau in the foreground (arrows) is characterized by incipient tors or tor-like landforms (cf. Fig. 36.9). July 9, 1977 (GSC-203262-C).

Figure 36.9. View north-northwest at an incipient tor developed in garnetiferous metasediments on the plateau illustrated in Figure 36.8. The elevation of the top of the tor is approximately 525 m. Erratics of granite and Paleozoic rocks (limestone, dolomite, sandstone) are common on the plateau surface and on the tor itself. July 6, 1977 (GSC-203262-A)

Figure 36.10. Telephoto view eastward across the valley north of the head of Makinson Inlet (cf. Fig. 36.2) at terrain dissected by meltwater channels. The outer edge of the area covered by bouldery debris (circles) marks the limit of a Neoglacial advance of this outlet glacier. Between this limit and the ice, numerous in situ, rooted willows have been exposed by recent recession of the glacier. A former ice marginal position of a lobe flowing southward into Makinson Inlet is marked by a concentration of boulders along the hillside (black arrows); lacustrine silt deposits, in which large ice wedges have developed, are exposed lower on the slope (white arrow). August 15, 1977 (GSC-203262-G).

Acknowledgments

Again I acknowledge with thanks the logistical support provided by T. Frisch, Regional and Economic Geology Division, and by the Polar Continental Shelf Project (G.D. Hobson, Director) during the 1977 field season. R.J. Richardson provided capable assistance in the field. S.B. McCann, now at Atlantic Geoscience Centre but in 1973 at McMaster University, kindly allowed me to cite an unpublished radiocarbon age determination. The samples of driftwood have been examined by L.D. Gill and R.J. Mott; the beetles have been determined by J.V. Matthews, Jr. T.E. Bolton of the Director General's Office identified the trilobite specimen, and R.F. Roblesky, University of Calgary, supplied information on the distribution of Paleozoic bedrock units and erratics. The age determinations have been carried out by the staff of the Radiocarbon Dating Laboratory, under the supervision of W. Dyck, J.A. Lowdon and I.M. Robertson. B.G. Craig and R.N.W. DiLabio provided constructive comments on the manustript.

References

Blake, W., Jr.
1974: Studies of glacial history in Arctic Canada. II. Interglacial peat deposits on Bathurst Island; Can. J. Earth Sci., v. 11, p. 1025-1042.

1975: Radiocarbon age determinations and postglacial emergence at Cape Storm, southern Ellesmere Island, Arctic Canada; Geogr. Ann., Ser. A., v. 57, p. 1-71.

1977: Glacial sculpture along the east-central coast of Ellesmere Island, Arctic Archipelago; in Report of Activities, Part C, Geol. Surv. Can., Paper 77-1C, p. 107-115.

Bolton, T.E.
1965: Trilobites from Upper Silurian rocks of the Canadian Arctic Archipelago: **Encrinurus (Frammia)** and **Hemiarges;** in Contributions to Canadian Palaeontology; Geol. Surv. Can., Bull. 134, p. 1-14.

Christie, R.L.
1962: Geology, southeast Ellesmere Island, District of Franklin; Geol. Surv. Can., Map 12-1962.

CLIMAP Project Members
1976: The surface of the ice-age earth; Science, v. 191, p. 1131-1137.

Craig, B.G. and Fyles, J.G.
1965: Quaternary of Arctic Canada; in Antropogenovye period v Arktike i Subarktike; Naucho-Issl. Inst. Geol. Arktiki, Trudy 143, p. 5-33 (in Russian with English summary).

Dyck, W. and Fyles, J.G.
1964: Geological Survey of Canada radiocarbon dates III; Radiocarbon, v. 6, p. 167-181.

Frisch, T.
1977: Reconnaissance mapping of the Precambrian Shield on Ellesmere and Coburg Islands, Canadian Arctic Archipelago; Northern Miner (Annual Review Number), v. 63, p. C20.

Hodgson, D.A.
1973: Landscape and late-glacial history, head of Vendom Fiord, Ellesmere Island; in Report of Activities, Part B, Geol. Surv. Can., Paper 73-1B, p. 129-136.

Kerr, J. Wm.
1976: Stratigraphy of central and eastern Ellesmere Island, Arctic Canada. Part III. Upper Ordovician (Richmondian), Silurian and Devonian; Geol. Surv. Can., Bull. 260, 55 p.

Kerr, J. Wm. and Thorsteinsson, R.
1972: Geology, Bauman Fiord; Geol. Surv. Can., Map 1312A.

Lindroth, C.H.
1963: The fauna history of Newfoundland, illustrated by Carabid beetles; Opuscula Entomologica, Supp. 23, 112 p.

1968: The ground-beetles of Canada and Alaska, Part 5; Opuscula Entomologica, Supp. 33, p. 649-944.

McGill, P.
1974: The stratigraphy and structure of the Vendom Fiord area; Bull. Can. Pet. Geol., v. 22, p. 361-386.

Olsson, I.U.
1968: Modern aspects of radiocarbon datings; Earth-Sci. Rev., v. 4, p. 203-218.

Olsson, I.U. and Blake, W., Jr.
1962: Problems of radiocarbon dating of raised beaches, based on experience in Spitsbergen; Norsk Geogr. Tidsskr., v. 18, p. 47-64.

Paterson, W.S.B.
1972: Laurentide Ice Sheet: estimated volumes during late Wisconsin; Rev. Geophys. Space Phys., v. 10, p. 885-917.

Roots, E.F.
1963: Southern Ellesmere Island and some localities north of Bay Fiord and Graham Island — Physiography; in Fortier, Y.O. et al., Geology of the north central part of the Arctic Archipelago, Northwest Territories (Operation Franklin); Geol. Surv. Can., Mem. 320, p. 266-275.

Sadler, H.E.
1973: On the oceanography of Makinson Inlet; Arctic, v. 26, p. 76-77.

Souchez, R.A. and Lorrain, R.D.
1975: Chemical sorting effect at the base of an alpine glacier; J. Glaciol., v. 14, p. 261-265.

Sugden, D.E.
1968: The selectivity of glacial erosion in the Cairngorm Mountains, Scotland; Inst. Br. Geogr., Trans. and Papers, no. 45, p. 79-92.

1974: Landscapes of glacial erosion in Greenland and their relationship to ice, topographic and bedrock conditions; in Progress in geomorphology: papers in honour of David L. Linton, eds. E.H. Brown and R.S. Waters, Inst. Br. Geogr., Spec. Publ. 7, p. 177-195.

1977: Reconstruction of the morphology, dynamics and thermal characteristics of the Laurentide Ice Sheet at its maximum; Arct. Alp. Res., v. 9, p. 21-47.

TERRAIN HAZARDS IN THE SKEENA AND KITIMAT RIVER BASINS, BRITISH COLUMBIA

Project 750078

J.J. Clague
Terrain Sciences Division, Vancouver

Abstract

Clague, J.J., Terrain hazards in the Skeena and Kitimat River basins, British Columbia; Current Research, Part A, Geol. Surv. Can., Paper 78-1A, p. 183-188, 1978.

Terrain hazards in the Skeena and Kitimat River basins, British Columbia include floods, landslides, bank erosion, gullying, and snow avalanches. Alluvial plains, terraces, and fans are potential flood sites in the area. Ground transportation routes could be inundated locally during large floods. Localized undercutting of river banks is accompanied at some sites by slumping of unconsolidated bank sediments. Other slope stability hazards include slides and flows involving late Pleistocene marine silt and clay in the Terrace-Kitimat area and highly fluid, fast moving debris flows occurring on steep slopes underlain by foliated metamorphic rocks in the Prince Rupert-Port Edward area. Snow avalanches disrupt road and rail traffic and are a threat to life in the Skeena Valley between Terrace and Prince Rupert.

Introduction

Between 1975 and 1977 field investigations were conducted in the Skeena and Kitimat River basins, British Columbia in order to provide information on the character and distribution of Quaternary sediments and landforms in the area. An important objective of this program is the assessment of terrain hazards within those valleys that dissect the rugged Hazelton and Coast Mountains and that serve as transportational corridors and population centres. These valleys are drained by Bulkley, Skeena, Kispiox, Kitwanga, Kitsumkalum, and Kitimat Rivers, are floored by a variety of unconsolidated sediments, and are bordered by steep sediment-veneered rock slopes (Fig. 37.1). Terrain hazards include floods, landslides, bank erosion, gullying, and snow avalanches.

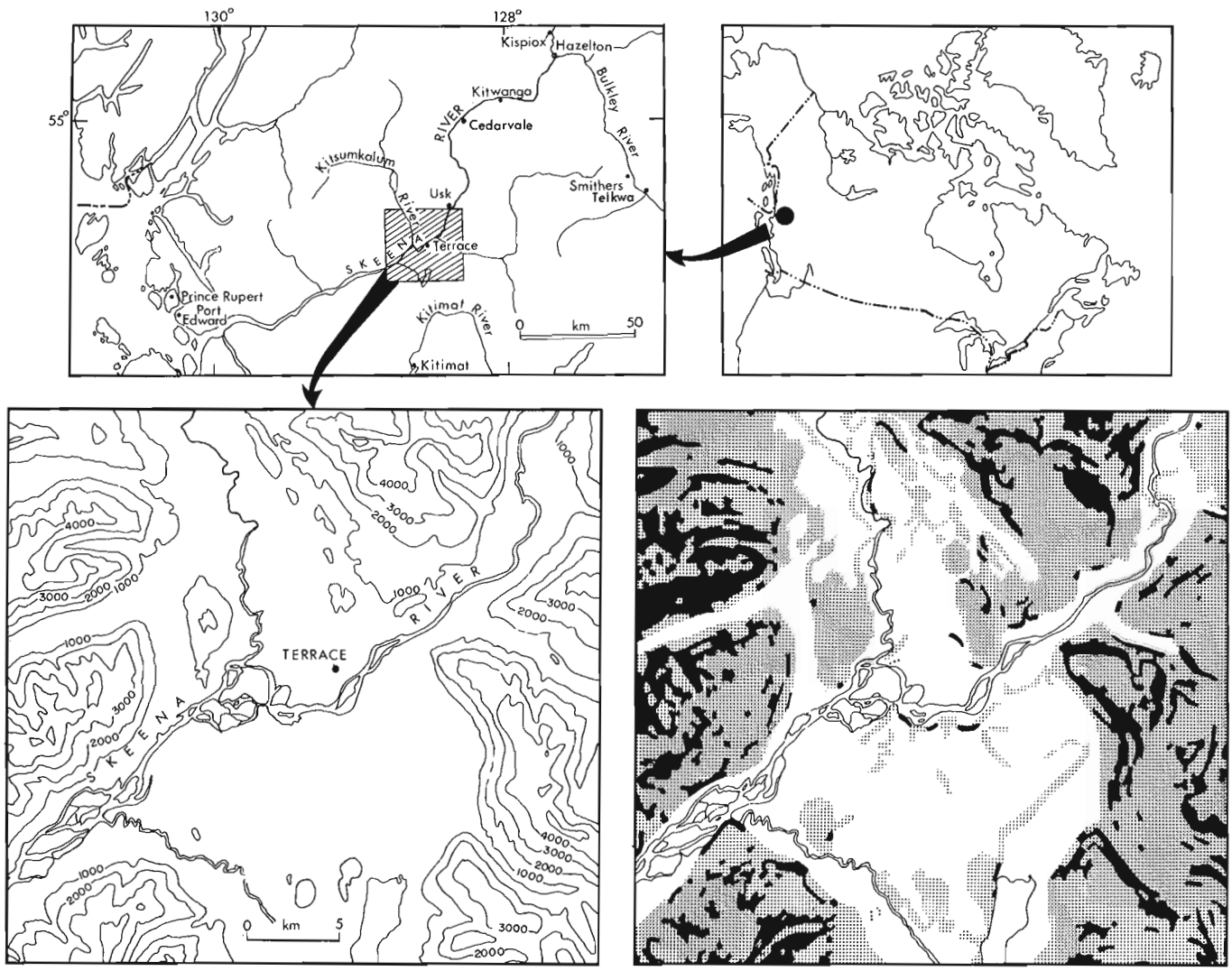

Figure 37.1. Index map of study region (top left). Inset maps (bottom) show the topography (left) and terrain gradients (right) of a representative area within this region. Topographic contour interval is 305 m (1000 feet). The following slope classes are depicted on the terrain gradient map: <10°, no pattern; 10-30°, stippled; >30°, black.

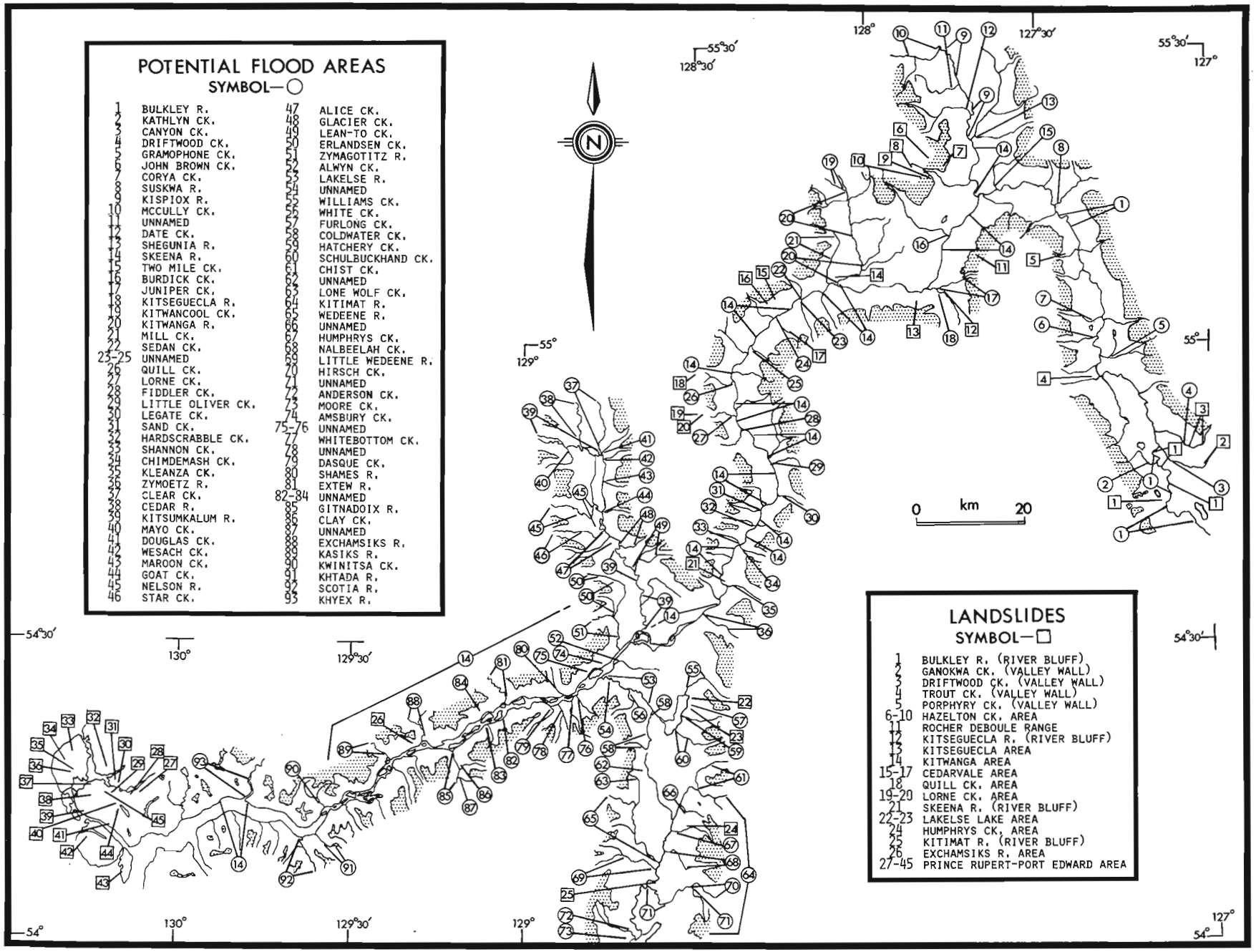

Figure 37.2. Landslides and potential flood areas in the major valleys of the study area. Landslides include both flows and slides and involve bedrock, unconsolidated sediments, or both. Landslides no. 27 through 45 in the Prince Rupert-Port Edward area are debris flows and/or avalanches. The stippled areas are higher than 915 m (3000 ft) in elevation.

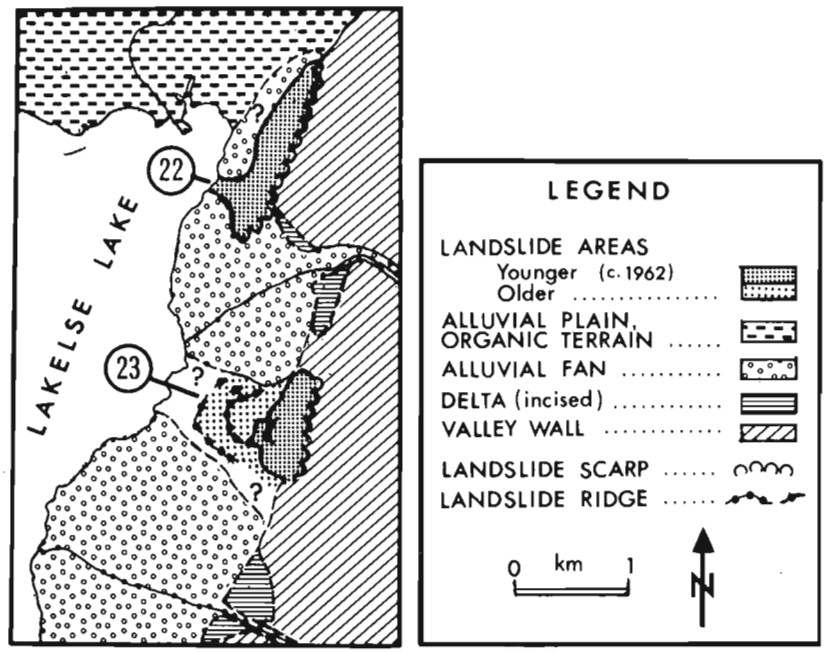

Figure 37.3. Two landslides at the northeast end of Lakelse Lake. The failures occurred in Pleistocene marine clay overlain in part by alluvial fan sediments. The numbers '22' and '23' identify the flows in Figure 37.2.

Floods

Potential flood areas include alluvial plains and low terraces of major rivers and streams, and alluvial fans located where tributary streams enter trunk valleys (Fig. 37.2).

The main criterion used to identify the potential flood areas shown in Figure 37.2 is vertical proximity of alluvial surfaces to bankfull levels of adjacent streams. Unfortunately, no quantitative estimate of the probability or magnitude of flooding can be made for these areas, in large part because pertinent streamflow records are either short in duration or nonexistent. Available records, however, do indicate that maximum instantaneous discharges of the major rivers for the period of measurement (<50 years) are 10 to 20 times greater than mean annual discharges (Water Survey of Canada, 1974). Rare flood events (e.g., those with recurrence intervals of 100 years or more) would exceed the largest flows of the streamflow records. The rivers and streams in the study area thus are subject to large variations in discharge, and it is probable that rare flood events would result in inundation of portions of flood plains, low terraces, and non-incised fans.

Many of the flood areas shown in Figure 37.2 are uninhabited and undeveloped, thus the flood hazard to life and property is minor. However, low alluvial terraces at Telkwa, Hazelton, Kispiox, Kitwanga, Cedarvale, Usk, Terrace, and Kitimat are inhabited and might be inundated during unusually large floods. In addition, Highway 16 and the Canadian National Railways line, the main ground transportation routes in the area, might be flooded in several places by Bulkley and Skeena Rivers.

Some flood prevention measures have been undertaken. For example, dyking of Kitimat River near its mouth has lessened the likelihood of flooding at Kitimat. Also, the British Columbia Department of Highways has modified several channels spanned by highway bridges in an attempt to minimize the impact of bank erosion and flooding on these structures.

Slope Stability

Because the Skeena and Kitimat River basins are areas of high local relief and have abundant precipitation and moderate to high seismic activity (Whitham and Hasegawa, 1975), the probability of landslides is relatively high. The susceptibility of an area to mass movement, however, is also a function of the physical properties of surface and near-surface materials. Thus, for example, certain types of sediments common on the valley floors of the study area, such as Pleistocene marine mud and clayey till, are susceptible to failure on gentle slopes, whereas most steep bedrock slopes appear to be stable.

Most landslides in the Skeena and Kitimat River basins are associated with (1) steep bluffs of unconsolidated sediments bordering the main rivers, (2) areas underlain by Pleistocene marine mud and clay rich till, and (3) steep slopes underlain by foliated metamorphic rocks.

Landslides of the first and second groups include both slides and flows. Examples are two comparatively large landslides at the northeast end of Lakelse Lake (Figs. 37.2 and 37.3) which were caused by the failure of Pleistocene marine clay overlain in part by permeable alluvial fan sediments. A provincial park campsite and part of the highway linking Terrace and Kitimat were destroyed by flowage at the northern site (Fig. 37.2, no. 22). In the future, landslide movements similar to those at Lakelse Lake may take place in other parts of the Terrace-Kitimat region, because fine grained marine sediments occur at the surface and beneath younger strata over much of the valley floor and low valley walls between Kitimat and Kitsumkalum Lake (Clague, 1977).

Several submarine landslides at the head of Kitimat Arm south of Kitimat also resulted from the failure of marine clay (Golder Associates, 1975; Bell and Kallman, 1976; Luternauer and Swan, 1978). Submarine landslide movement on the west side of Kitimat Arm in April 1975 generated a wave which caused approximately $600 000 damage to waterfront facilities in the area (Golder Associates, 1975, p. 1).

Highly fluid, fast moving debris flows caused by the failure of a thin surface layer of water saturated, weathered, and broken rock are associated with steep slopes underlain by foliated metamorphic rocks. The largest of these flows travelled for several hundred metres and produced tracks of devastation in mature forest similar in appearance to avalanche tracks (Fig. 37.4). One such flow temporarily blocked Highway 16 near Port Edward in 1977. These flows appear to be confined to areas of high precipitation (> 250 cm/y) and to slopes underlain by schistose and gneissic rocks in the vicinity of Prince Rupert and Port Edward (Fig. 37.2).

Similar to these debris flows are slushflows and mudflows, consisting of sediment, snow, and water, which move rapidly down high gradient stream courses and avalanche tracks during spring thaw. Upon reaching low gradient slopes, these flows terminate as fan- and ribbon-shaped bodies of debris.

Erosion

Rapid contemporary erosion in the Skeena and Kitimat River basins appears to be restricted to the concave banks of certain river bends. In many areas bank erosion is accompanied by slumping of unconsolidated sediments from oversteepened river banks. Although quantitative data on erosion rates in the area are rare, the Skeena River for a distance of several hundred metres at one site southwest of Terrace has cut back a 7 m high bank at an average rate of 9 m/y between 1963 and 1974. It is emphasized, however, that erosion of this magnitude is very limited in areal extent.

Figure 37.4. Avalanche tracks, Skeena Valley east of Prince Rupert (top), and landslide track and colluvium produced by debris flow near Port Edward (bottom). The debris flow originated on a steep slope (only partially visible in the background), cut a swath through dense forest, and buried the road in the foreground.

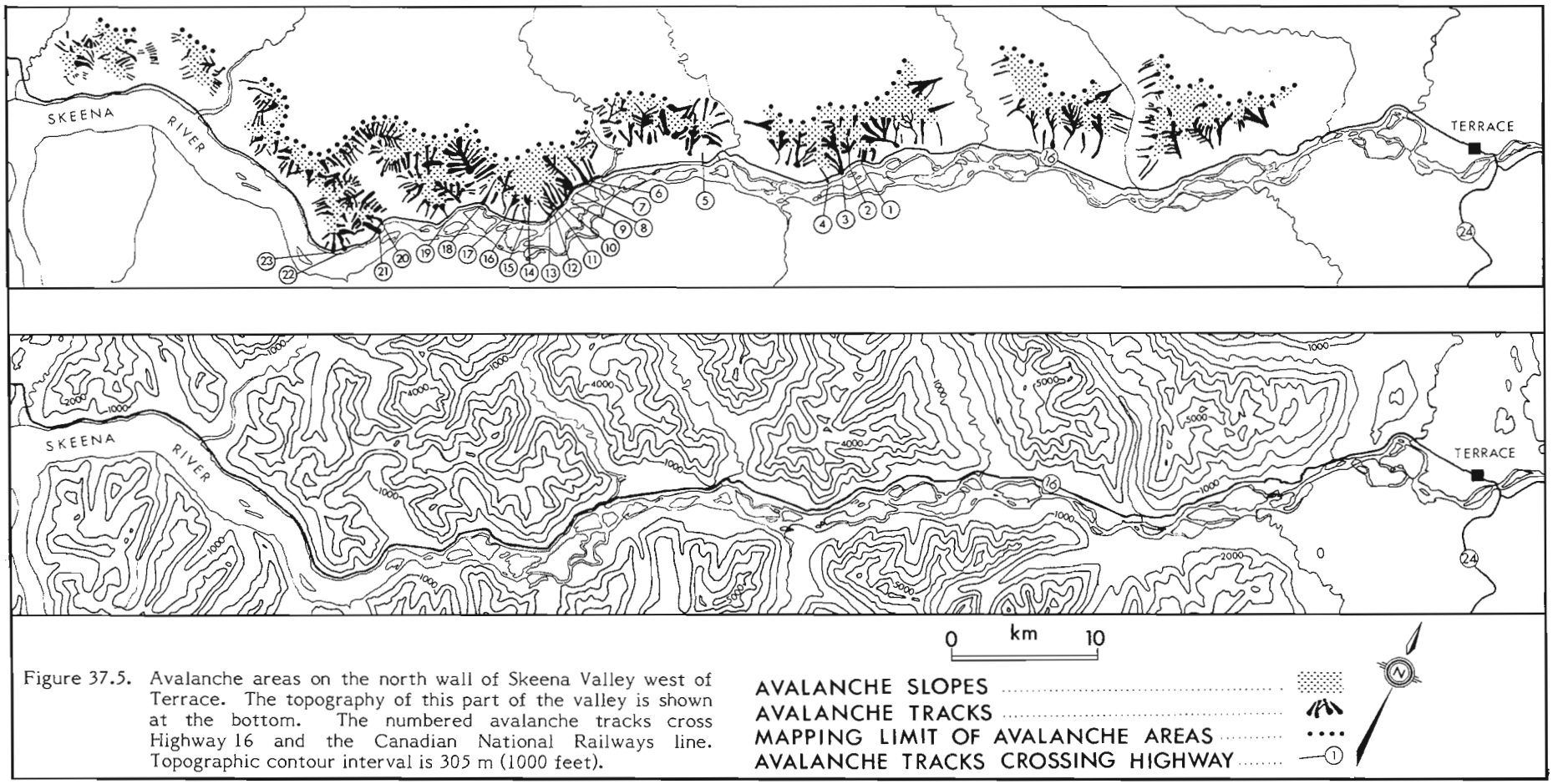

Figure 37.5. Avalanche areas on the north wall of Skeena Valley west of Terrace. The topography of this part of the valley is shown at the bottom. The numbered avalanche tracks cross Highway 16 and the Canadian National Railways line. Topographic contour interval is 305 m (1000 feet).

distance of several hundred metres at one site southwest of Terrace has cut back a 7 m high bank at an average rate of 9 m/y between 1963 and 1974. It is emphasized, however, that erosion of this magnitude is very limited in areal extent.

Much of the area underlain by Pleistocene marine silt and clay between Kitimat and Kitsumkalum Lake is dissected by steep-walled gullies heading in amphitheatre-shaped bowls. Erosion of these fine grained sediments is continuing, probably largely as a result of groundwater sapping at the heads of the gullies. Unfortunately, there are no data on erosion rates in these areas.

Gullying of limited magnitude and areal extent also is occurring on steep, sediment covered slopes, especially those which have been clear-cut logged.

Snow Avalanches

The Avalanche Task Force of the British Columbia Department of Highways has identified Skeena Valley between Terrace and Tyee (the latter is a Canadian National Railways station located approximately 25 km southeast of Prince Rupert) as one of three highway corridors in the province with high avalanche hazard ratings (Figs. 37.4 and 37.5). Highway 16, the only road connecting the coastal community of Prince Rupert with the remainder of the province, is located in this corridor and is closed for lengthy periods due to avalanches [average annual closure time is 13 days (Avalanche Task Force, 1974, Table 1)].

The seriousness of this problem is highlighted by an avalanche in January 1974 which killed seven persons and destroyed a service station, cafe, and small trailer park 45 km west of Terrace. This catastrophic avalanche was triggered by unusually heavy snowfall (200 cm in the 12 days preceding the snowslide) followed by warmer temperatures and heavy rainfall.

Although the avalanche hazard to life and property is greatest in Skeena Valley west of Terrace, largely because of the proximity of the highway and railway to steep valley walls, avalanches are common in almost all tributary valleys to Bulkley, Skeena, Kispiox, Kitwanga, Kitsumkalum, and Kitimat Rivers. The valley walls in the upper reaches of many of these tributaries lack forest cover and appear to be swept regularly by avalanches. Fortunately, these tributary valleys are uninhabited (although many are accessible by logging roads) so that snowslides pose a threat only to those individuals entering the valleys during the winter and spring.

References

Avalanche Task Force
1974: Report on findings and recommendations [of Avalanche Task Force] to the Honorable Graham R. Lea, Minister of Highways, September 30, 1974; mimeo rep., B.C. Dep. Highways, Victoria, 33 p.

Bell, L.M. and Kallman, R.J.
1976: The Kitimat River Estuary, status of environmental knowledge to 1976; Environ. Can., Reg. Bd., Pacific Reg., Estuary Working Group, Spec. Estuary Ser., no. 6, 296 p.

Clague, J.J.
1977: Generalized surficial geology, Kitimat, British Columbia; Geol. Surv. Can., Open File 470 (map, 1 sheet).

Golder Associates
1975: Report of B.C. Water Resources Service on investigation of seawave at Kitimat, B.C.; mimeo. rep., Golder Associates, Vancouver, 9 p., 6 figs., 1 appendix.

Luternauer, J.L. and Swan, D.
1978: Kitimat submarine slump deposit(s): a preliminary report; in Current Research, Part A, Geol. Surv. Can., Paper 78-1A, rep. 61.

Water Survey of Canada
1974: Historical streamflow summary, British Columbia, to 1973; Environ. Can., Inland Waters Dir., Water Resour. Br., Ottawa, 694 p.

Whitham, K. and Hasegawa, H.S.
1975: The estimation of seismic risk in Canada – a review; Energy, Mines Resour. Can., Earth Phys. Br. Publ., v. 45, no. 2, p. 137-162.

38. LITHOSTRATIGRAPHY OF THE QUATERNARY SEDIMENTS EAST OF JESSE BAY, BANKS ISLAND, DISTRICT OF FRANKLIN

Project 740065

Jean-Serge Vincent
Terrain Sciences Division

Abstract

Vincent, Jean-Serge, Lithostratigraphy of the quaternary sediments east of Jesse Bay, Banks Island, District of Franklin; Current Research, Part A, Geol. Surv. Can., Paper 78-1A, p.189-193, 1978

The detailed study of sediments in coastal sections east of Jesse Bay on Banks Island has revealed the existence of three or possibly four separate glacial events. Associated with each of these events, both before and after ice advance, are sequences of marine and terrestrial bone, peat, shell, and wood bearing sediments. The lithostratigraphic correlation of the sequences is presented and a brief description of the units is given.

Introduction

Within the Banks Island surficial geology inventory project, detailed investigation of the Quaternary stratigraphy of four selected coastal areas of southern and eastern Banks Island was conducted (Fig. 38.1).

As an illustration of the abundance of information provided by the sequence of Quaternary materials on Banks Island, this paper is a brief preliminary interpretation of the lithostratigraphy of coastal sections located east of Jesse Bay (site 3 of Fig. 38.1). Final correlations as well as definitive statements on the genesis of certain units and the establishment of a chronostratigraphy will have to await the results of various laboratory investigations of samples.

Lithostratigraphy and Description of Units

Twelve sections situated between 72°13'40"N — 119°51'W and 72°14'40"N —119°44'W at varying intervals along the coast were studied and their lithostratigraphy was established (Fig. 38.2). The sections are labelled A to L and are presented in succession from west to east. The various lithological units identified in the sections are correlated and labelled 1 to 10. In order to avoid a multiplicity of units, the different textural facies resulting from a single major event were grouped as one unit. Locations of points where algae, bone, peat, shells and wood were found also are indicated in Figure 38.2.

Unit 1

The oldest unit, observed in sections F, H, K, and L, comprises rhythmically bedded or massive sediments that vary in texture from clay to fine sands. Among other evidence, the presence of marine shells and algae (organic matter tentatively identified as such by R.J. Mott of the Paleoecology Laboratory) indicates that the unit is marine in origin. Massive ice bodies in these sediments were noted in sections cut in a deep gorge (Figs. 38.3 and 38.4).

Unit 2

Unit 2, found in sections F, G, H, and L, is a moderately stony, calcareous, very dark greyish brown (10 YR 3/2), sandy silt till (Figs. 38.3 and 38.6). Foreign and striated stones are common in this till as well as dispersed thin bands of light coloured fine sands.

Unit 3

Unit 3, composed mainly of fine sands with some medium sand and small gravel, was noted only in section H. This unit, surmised to be of marine origin, separates the tills of units 2 and 4 that, in the other sections, are in contact with each other (Fig. 38.6).

Unit 4

Unit 4, observed in sections F, G, H, and L, is a moderately stony, calcareous, light yellowish brown (orange appearance) (10 YR 6/4), sandy silt till (Figs. 38.3 and 38.6). Apart from its distinctive colour, this till, based on field observations, is similar to till of unit 3. Detailed laboratory investigations are needed in order to ascertain the degree of similarity and hence the possible relationship of these two tills.

Unit 5

This lithological unit, which coarsens upwards, generally consists of marine, shell bearing, rhythmically bedded sediments which grade to peat and wood bearing fluvial-deltaic sands and gravels (Figs. 38.5 and 38.7). The entire sequence clearly indicates sedimentation in a progressively shallowing water body. At the end of the cycle the sequence was terrestrial.

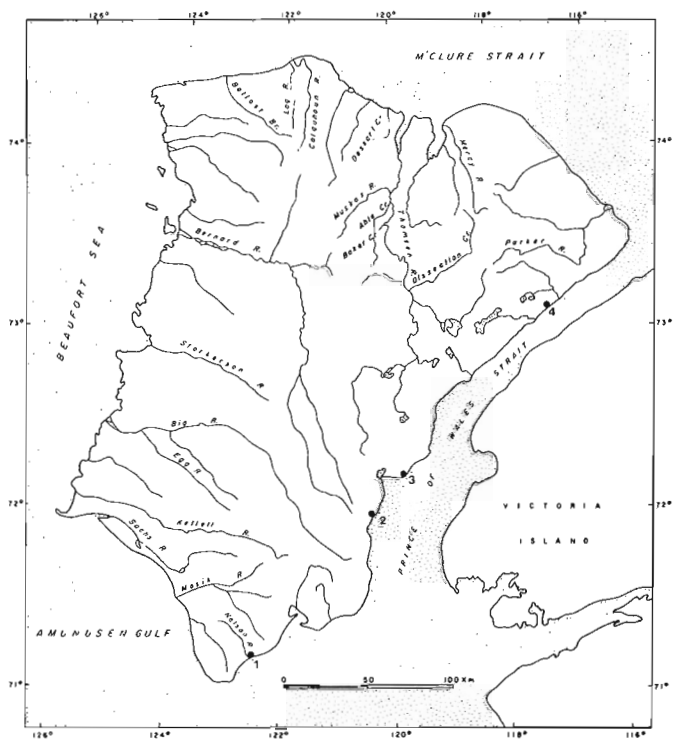

Figure 38.1. Location map of Banks Island showing the sites studied during summer 1977.

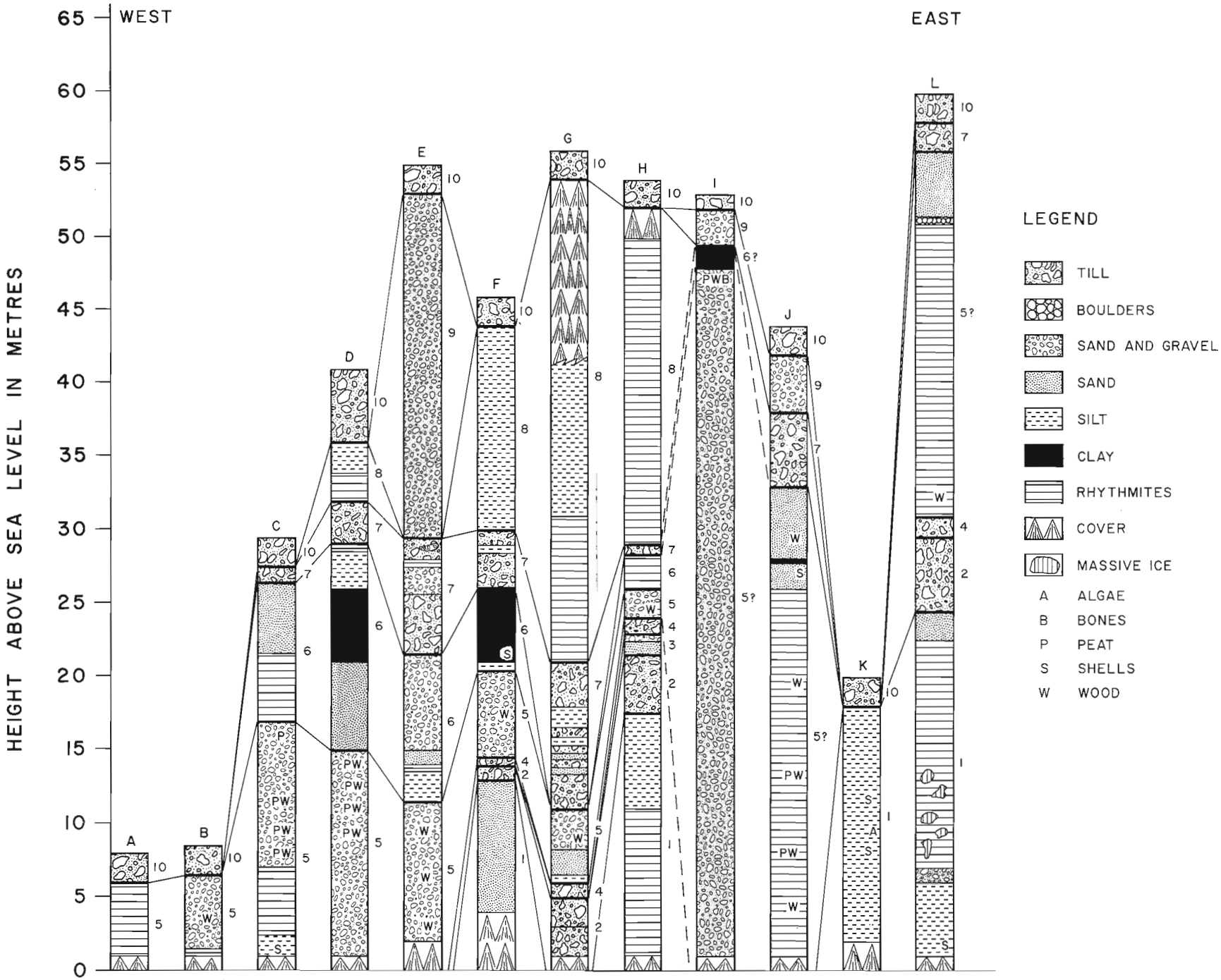

Figure 38.2. Lithostratigraphy of the Quaternary sediments east of Jesse Bay, Banks Island.

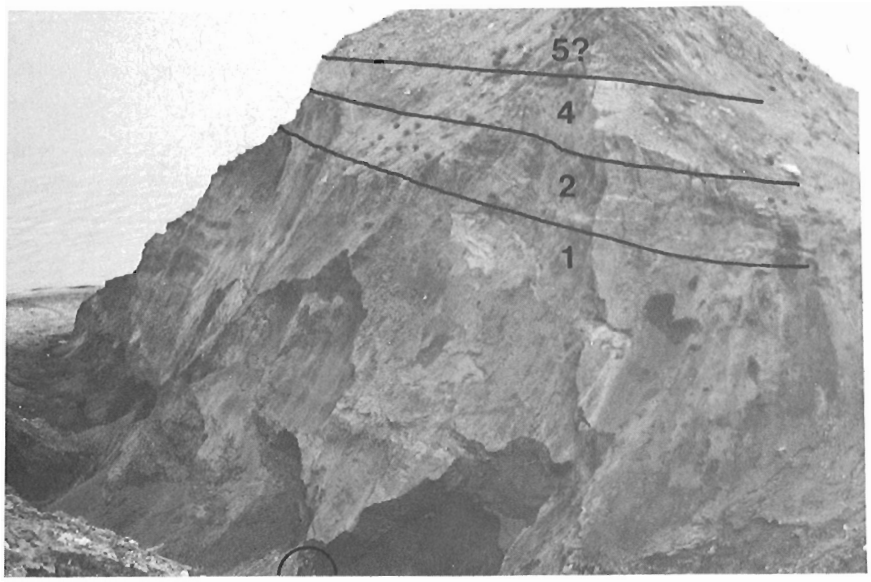

Figure 38.3

General view of the lower part of section L. Numbers on the units refer to those used in Figure 38.2; scale is given by the person standing at the bottom left centre of the photograph.

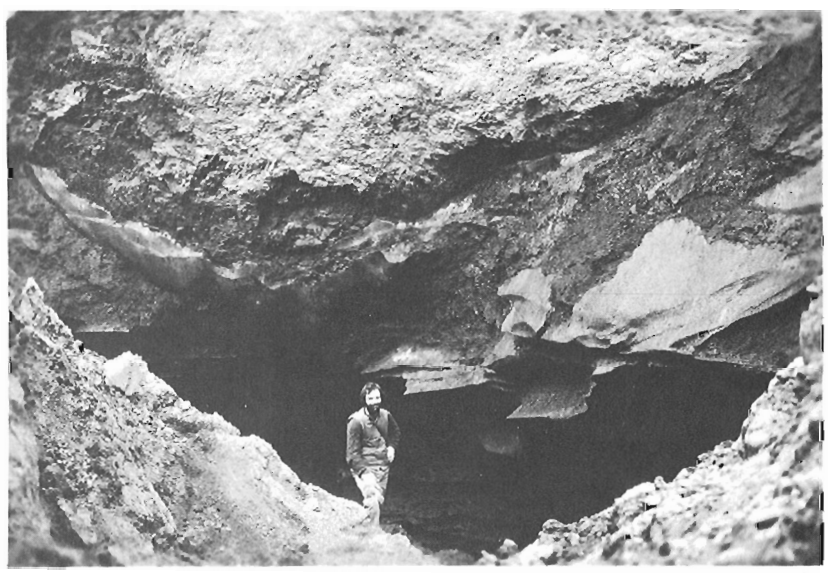

Figure 38.4

View of massive ice bodies in rhythmically bedded marine sediments of unit 1 in section L.

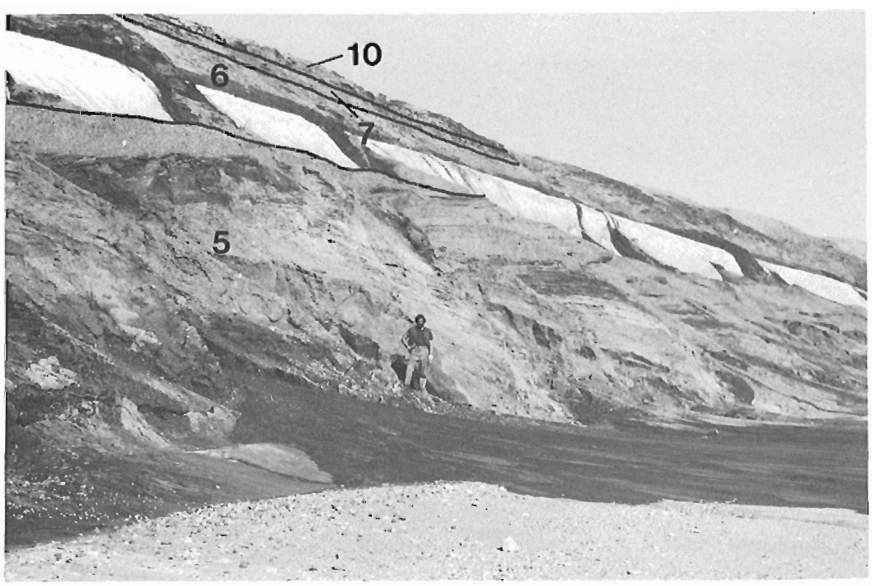

Figure 38.5

General view of section C. Units are labelled as shown in Figure 38.2. Note the nivation hollows that have developed in the easily erodible fine sediments of unit 6 and the deep gully incision that has resulted from the melting of snow.

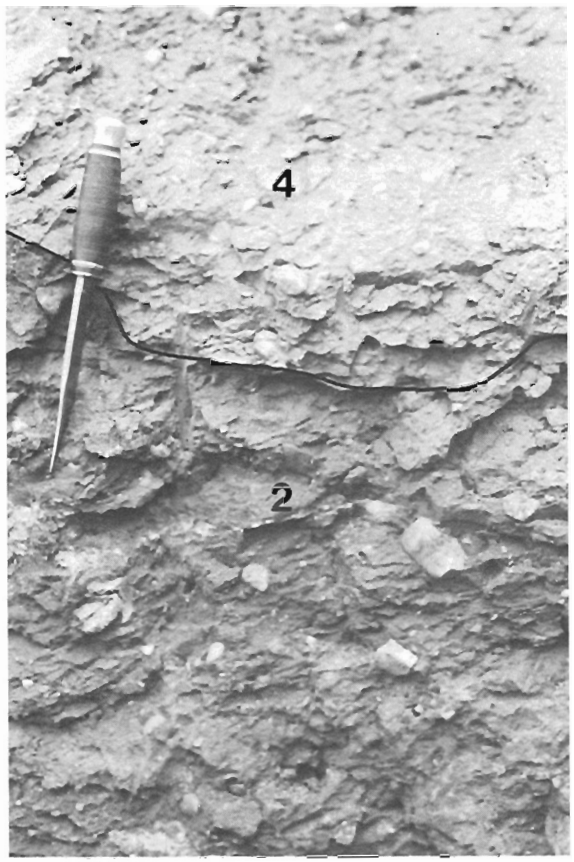

Figure 38.6. View of the contact between tills of units 2 and 4 in section F.

Figure 38.7. Detailed view of rhythmically bedded marine sediments of the lower part of unit 5 in section C.

Figure 38.8. Contact between the silty rhythmically bedded silts of unit 8 and till of unit 7 in section D.

Unit 6

Unit 6 generally comprises rhythmically bedded or massive sediments that vary in texture from clay to medium grained sands. In section E stratified sands and gravels also are present. No clear gradational trend was observed in the sequence, but it is evident that this unit, compared to the underlying sediments of unit 5, indicates a return to deeper water. The presence of shells in section F likely indicates a marine origin for the sediments.

Unit 7

This unit is a moderately stony, noncalcareous, very dark greyish brown (10 YR 3/2), sandy silt till (Fig. 38.8). In sections E, F, and G this till is clearly interstratified with the water-laid sediments of unit 6, indicating the presence of a water body at the ice front.

Unit 8

Unit 8 is a sequence of rhythmically bedded greyish silts with some fine sand and clayey silt (Fig. 38.8); the sediments commonly are disturbed by faults of limited offset. This unit is thought to be of marine origin and is present in the same stratigraphic position from Nelson River in southern Banks Island to north of Parker River in northeastern Banks Island.

Unit 9

This unit is composed of stratified, well sorted sands and gravels of probable ice contact origin. It is not known at this time if the unit is related genetically to the retreat of the ice that deposited unit 7 or to the advance of the glacier that deposited unit 10.

Unit 10

Unit 10 is a moderately stony, generally thin, very calcareous, pinkish grey (7.5 YR 6/2), silty till. This till is on the surface in the interfluves in the area. It represents the last glacial advance on Banks Island.

Conclusion

Based on the lithostratigraphy of the coastal sections east of Jesse Bay, it is possible to identify three or possibly four main glacial events represented by the tills of units 2, 4, 7, and 10. Evidence for marine inundation of the area, associated with each ice advance both before and after each event, is clearly indicated by units 1, 5, 6, and 8. A return to a subaerial environment after glacial or marine episodes can be ascertained definitely, for the period between deposition of till units 4 and 7 because of the presence of terrestrial sediments in the uppermost part of unit 5.

It is hoped that the laboratory study of various samples collected in the intertill deposits will aid in the establishment of the chronostratigraphy of the deposits. Further work also will involve correlating tills found in the coastal stratigraphic succession with the various till sheets of known extent that have been mapped previously on Banks Island.

Acknowledgments

The author would like to acknowledge the able field assistance of A. Doiron and F. Auger, Université du Québec à Montréal and University of Ottawa, respectively. The author is also greatly indebted to the Polar Continental Shelf Project which provided logistical support.

39. GEOLOGY OF PUDDLE POND AREA, RED INDIAN LAKE MAP-SHEET, NEWFOUNDLAND

Project 770026

R.K. Herd
Regional and Economic Geology Division

Abstract

Herd, R.K., Geology of Puddle Pond area Red Indian Lake map-sheet, Newfoundland; Current Research, Part A, Geol. Surv. Can., Paper 78-1A, p. 195-197, 1978.

The northwestern part of the Puddle Pond map-area (12A/5) is underlain by a complex of igneous and metamorphic rocks of probable Grenvillian to Devonian age. Early migmatites and paragneisses are cut by granite, granodiorite, diorite and granodioritic orthogneiss. Hornblende gabbro, norite, and minor ultramafic rocks are present. An isolated outcrop of anorthosite found south of Puddle Pond, and highly metamorphosed marble-calcsilicate rock found in migmatite, suggest the presence of Grenville basement farther east than previously known in the southern Long Range.

Introduction

As the initial stage of a program to revise the geology of Red Indian Lake map-area (12A, west half) at 1:250 000 scale (Riley, 1957, 1962), mapping began at 1:50 000 scale in the Puddle Pond map-area (12A/5). Kean (1976, 1977) has been mapping at a scale of 1:50 000 in the Victoria Lake area to the east.

Puddle Pond map-area is in the southern Long Range Mountains of western Newfoundland east of St. George's Bay and 30 km east of the Trans-Canada Highway. The Southwest Brook – Burgeo road (Route 480) currently under construction, plus forest access and logging roads, provide access to the map-area. Fixed-wing and helicopter transport is available at Pasadena and elsewhere near Corner Brook. Work in 1977 was concentrated in the northwest corner of the map-area.

The southern Long Range in the map-area is a deeply dissected, glaciated plateau, with alpine vegetation in upland areas, ample outcrop, and hilltops which reach 500 to 700 m above sea level. Stream valleys and lower slopes are covered by glacial debris, fluvial deposits, and thick forest; outcrops are sparse but can be found along streams and roadcuts. Soil erosion exposes bedrock in logged areas. No waterways can be traversed by canoe, and animal trails must be followed through scrub spruce and tamarack on upper hill slopes.

Ground traverses throughout the area shown in Figure 39.1 comprised the field work in 1977; above-average rainfall curtailed work in July.

Geology

Figure 39.1 is a geological sketch-map of the northwestern part of Puddle Pond map-area and of parts of adjacent map-areas. All rocks are igneous and/or metamorphic; some are apparently of Helikian or earlier (Grenville) age, intimately associated with metamorphosed equivalents of younger cover rocks, and all intruded by several generations of granitoid rocks, both massive and foliated (orthogneisses) and minor intrusions.

The oldest rocks appear to be biotite-rich paragneiss (unit 1) which varies from sillimanite-bearing (aluminous) to calc-silicate – rich. One large area of calc-silicate and marble (unit 2) is an inclusion in migmatite (unit 3). Paragneiss (unit 1) and migmatite (unit 3) are complexly associated west and south of North Lake and south of Southwest Brook, and are intergradational. It seems probable that units 1 to 3 at least are Helikian or older (Grenvillian orogen). Gabbro, metagabbro, and coarse amphibolite (unit 4) are associated with the paragneiss and migmatite as xenoliths and as a mass next to the calc-silicate inclusion (unit 2). Hornblende norite (unit 5) and hornblende gabbro and anorthositic gabbro (unit 6) occur in the southwest part of the area mapped and may be co-genetic. Primary igneous layering locally exhibiting mineral grading appears in both units. Both have been deformed and their boundaries recrystallized and migmatized. Serpentinite (unit 7) in an isolated exposure is probably related to the gabbro-norite complex. Mylonitic gneiss (unit 8) forms a narrow zone along the northeastern border of the gabbro body (unit 6) and is partly developed from the gabbro.

Hornblende-biotite plutonic rocks (unit 9), ranging from diorite to granite are the most extensive rocks in the mapped area. Hornblendite (subunit 9e) probably represents a border phase. Inclusions of hornblendite and of porphyritic gabbro (subunit 6c) appear especially in diorite and granodiorite. The granitoid rocks are commonly massive, coarsely jointed and cut by pink aplite dykes.

The youngest gneiss is apparently an orthogneiss (unit 10) which cuts most rock units and contains inclusions of them. Distinctive massive pink biotite granite (unit 11) around North Lake cuts migmatite (unit 3), orthogneiss (unit 10), and diorite-granodiorite (unit 9), and appears to be the youngest rock in the mapped area and may be Devonian. Dykes of similar granite and perhaps offshoots from the North Lake body cut most rocks of the area. In addition to the mapped units 1 to 11, there are dykes of pegmatite, diorite, diabase, and aplite.

Structure

All rocks but the pink granite (unit 11) are foliated, at least locally. Earliest foliations, as seen in the migmatites and paragneisses, trend east and northeast to northwest. Some foliations may be parallel to axial surfaces of northeast-trending antiforms and synforms defined by minor folds in migmatite and paragneiss north of Southwest Brook, and by graded igneous layering in the hornblende gabbros and norites. Clearly the youngest major structures in the area occur in the zone of migmatization bordering the orthogneiss (unit 10). The zone extends northwesterly across the mapped area, and it is clear that older structures within this zone have been rotated into conformity.

Metamorphism

Mineral assemblages in the paragneisses and migmatites indicate lower to middle amphibolite facies conditions. No significant contact-metamorphic effects of granites or granodiorites/diorites (units 9, 11) have been found. Migmatization associated with the orthogneiss (unit 10) may be relatively high-temperature, high-pressure amphibolite facies, as diopside, hypersthene, garnet, and hornblende occur where hornblende norite (unit 5) adjoins the orthogneiss.

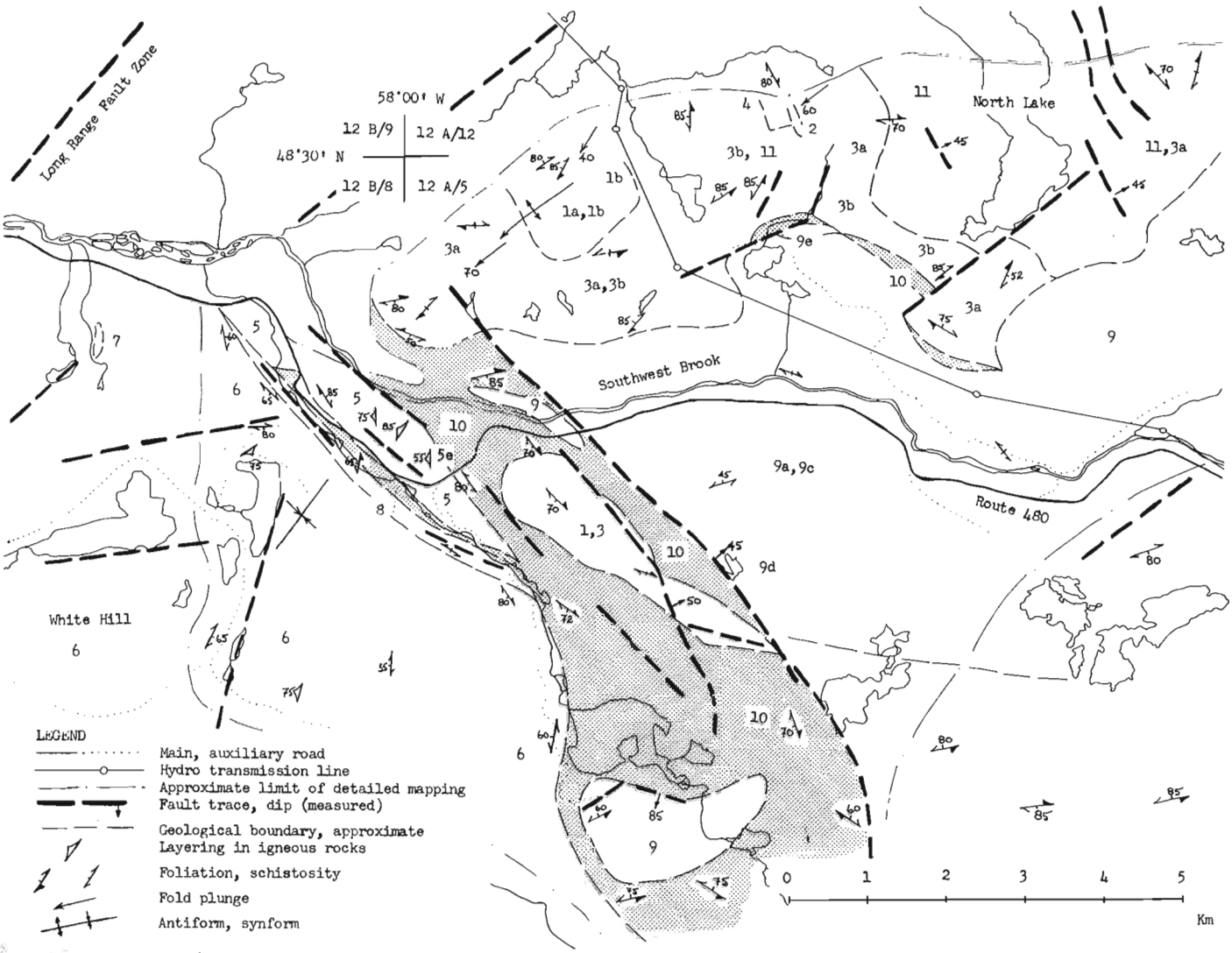

DEVONIAN (?)

11 Biotite granite, pink, massive

DEVONIAN AND/OR OLDER

10 Orthogneiss of granite-granodiorite composition: 10a, leucocratic augen gneiss; 10b, layered biotite gneiss; 10c, interlayered white orthogneiss and pink porphyritic granitoid gneiss

9 Hornblende-biotite granitoid rocks: 9a, diorite; 9b, quartz diorite; 9c, granodiorite; 9d, granite; 9e, hornblendite with biotite aggregates

8 Mylonitic gneiss, pink, with epidote

7 Serpentinite

6 Hornblende gabbro and anorthositic gabbro: 6a, noritic; 6b, ophitic; 6c, porphyritic with hornblende and plagioclase phenocrysts; 6d, leucocratic

5 Hornblende norite: 5a, medium grained, massive and coarsely jointed; 5b, layered; 5c, pegmatitic with inclusions; 5d, porphyritic with hornblende phenocrysts; 5e, agmatite of norite and white orthogneiss

4 Gabbro, metagabbro and coarse grained amphibolite

POSSIBLY HELIKIAN AND/OR OLDER

3 Migmatite composed of: paragneiss of unit 1 locally with (3a) sillimanite, cordierite and garnet; or (3b) calc-silicate minerals; and granodioritic gneiss, with inclusions of amphibolite, metagabbro, calc-silicate rock, sillimanite schist, rarely serpentinite, etc.

2 Marble and calc-silicate rock with garnet, diopside, quartz and sphene

1 Paragneiss, biotite-rich; 1a, contains sillimanite; 1b, contains tremolite

Figure 39.1. Geology of the northwestern part of Puddle Pond map-area.

Metallic Mineral Occurrences

Two flakes of molybdenite were noted in older granodioritic pegmatite (unit 9?) southwest of North Lake. Elsewhere minor pyrite and hematite occur in shear zones and associated with late pegmatites. The hornblende norite body (unit 5) contains abundant magnetite and the hornblende gabbro lesser amounts; chromite and nickel minerals were not observed.

Regional Correlations

It is too early in this project to make definite correlations of the Puddle Pond geology with other parts of western Newfoundland, but some of the rocks described here invite speculative correlations.

The migmatite and paragneiss are similar to the probable Grenvillian Long Range Gneiss near Port aux Basques (Brown, 1976a). Alternatively, they could represent metamorphosed Hadrynian-Cambrian Fleur de Lys rocks, and the abundant amphibolitic inclusions could be equivalent to the Birchy Schist (Williams and St-Julien, 1978). The Glover Formation occurring just north of the map-area, contains basic volcanics and ultramafic rocks, providing a possible source for gabbros and amphibolites seen in xenoliths and in larger masses. An anorthosite resembling that at Steel Mountain to the west, was found south of Puddle Pond in the northeastern part of the map-area during reconnaissance, and strongly suggests that Grenvillian rocks occur farther east than previously considered in this part of the Long Range.

The hornblende norite (unit 5) is similar to parts of the Bay of Islands complex, especially to the gabbros on the Lark Harbour road (Williams and Malpas, 1974). The hornblende norite (unit 5) and gabbro (unit 6) together might represent oceanic crust, obducted over Grenville basement (cf. Brown, 1976b) and migmatized along its margins. Significantly, the marginal agmatitic unit of hornblende norite (subunit 5e) contains a variety of disoriented mafic and ultramafic exotic inclusions and could represent a migmatized tectonic mélange.

Acknowledgments

Geological mapping assistance was provided by N.A.C. Rey, W.P. Carew, and G.S. Hayes. Logistical advice from D.R. Grant, B.A. Greene, B.F. Kean, and E.G. Rodgers is gratefully acknowledged, as is logistical support from Environment Canada through use of facilities at the Newfoundland Forest Research Centre, Pasadena. Staff of Labrador Linerboard Ltd., of Singleton, of Western Construction Co., and of the Newfoundland Department of Transport and Communications provided invaluable information on local road conditions. H. Williams provided stimulating discussions.

References

Brown, P.A.
1976a: Geology of the Rose Blanche map-area (11 O/10), Newfoundland; Mineral Devel. Div., Nfld. and Lab. Dept. Mines and Energy, Report 76-5, 16 p.

1976b: Ophiolites in south-western Newfoundland; Nature (London), v. 264, no. 5588, p. 712-715.

Kean, B.F.
1976: Geology of the Victoria Lake area; in Report of Activities, 1975, Mineral Devel. Div., Nfld. Dept. Mines and Energy, Report 76-1, p. 31-37.

1977: Geology of the Lake Ambrose sheet, west half; in Report of Activities, 1976, Mineral Devel. Div., Nfld. Dept. Mines and Energy, Report 77-1, p. 21-25.

Riley, G.C.
1957: Red Indian Lake (west half), Newfoundland; Geol. Surv. Can., Map 8-1957.

1962: Stephenville map-area, Newfoundland; Geol. Surv. Can., Mem. 323, 72 p., Maps 1117A and 1118A.

Williams, H. and Malpas, J.
1974: The regional setting and structure of the west Newfoundland ophiolites; Geol. Assoc. Can., Min. Assoc. Can., 74 Fieldtrip Manual A-2, 12 p.

Williams, H. and St-Julien, P.
1978: The Baie Verte – Brompton line in Newfoundland and regional correlations in the Canadian Appalachians; in Current Research, Part A, Geol. Surv. Can., Paper 78-1A, rep. 44.

THE GEOLOGY OF THE WEST MINE, PILLEYS ISLAND, NEWFOUNDLAND

E.M.R. Research Agreement 2239-4-32/77

E.C. Appleyard[1] and E.G. Bowles[1]
Regional and Economic Geology Division

Abstract

Appleyard, E.C. and Bowles, E.G., The geology of the West Mine, Pilleys Island, Newfoundland; Current Research, Part A, Geol. Surv. Can., Paper 78-1A, p. 199-203, 1978.

The West Mine orebody comprises a syngenetic, stratiform massive sulphide and associated vein stockwork deposit hosted by felsic volcanics of calc-alkaline affinities. Alteration facies and primary stratigraphic elements provide the best geological guides for exploration. The deposit possesses many common elements with the Kuroko deposits of Japan and with other orebodies within the host Roberts Arm Group of Upper Ordovician (?) volcanics.

Introduction

Mineralization has been known within the Roberts Arm volcanic rocks on Pilleys Island, Notre Dame Bay, Newfoundland for over 100 years, but no commercial production has occurred since 1908. Current levels of exploration for volcanogenic ore deposits are high throughout the Appalachian region and this occurrence has attracted considerable attention. Despite several tantalizing discoveries no mineralized zones of current economic interest have been discovered.

The objectives of this study are both to add to the inventory of knowledge of this interesting deposit and to contribute to the understanding of altered host rocks associated with mineralization.

The "Old" Mine is the only one of numerous occurrences of mineralization in the Pilleys Island area which has been exploited commercially (Fig. 40.1). This property was operated by several owners intermittently between 1889 and 1908 during which time about 500 000 tons of pyritic ore were mined as a source of sulphur with copper, silver and gold being recovered as a byproduct (Horsburgh, 1968). The mine manager at the time of closure estimated that about 27 per cent of the total production had been cupriferous pyrite ore running 3 to 3.5 per cent Cu (Walker, 1960). Production terminated because the orebody was truncated by a fault and the company was in financial difficulties.

The "South" Mine orebody (Fig. 40.2) was discovered in 1921 when eight holes were drilled in an attempt to find the faulted extension of the orebody. Extensive additional

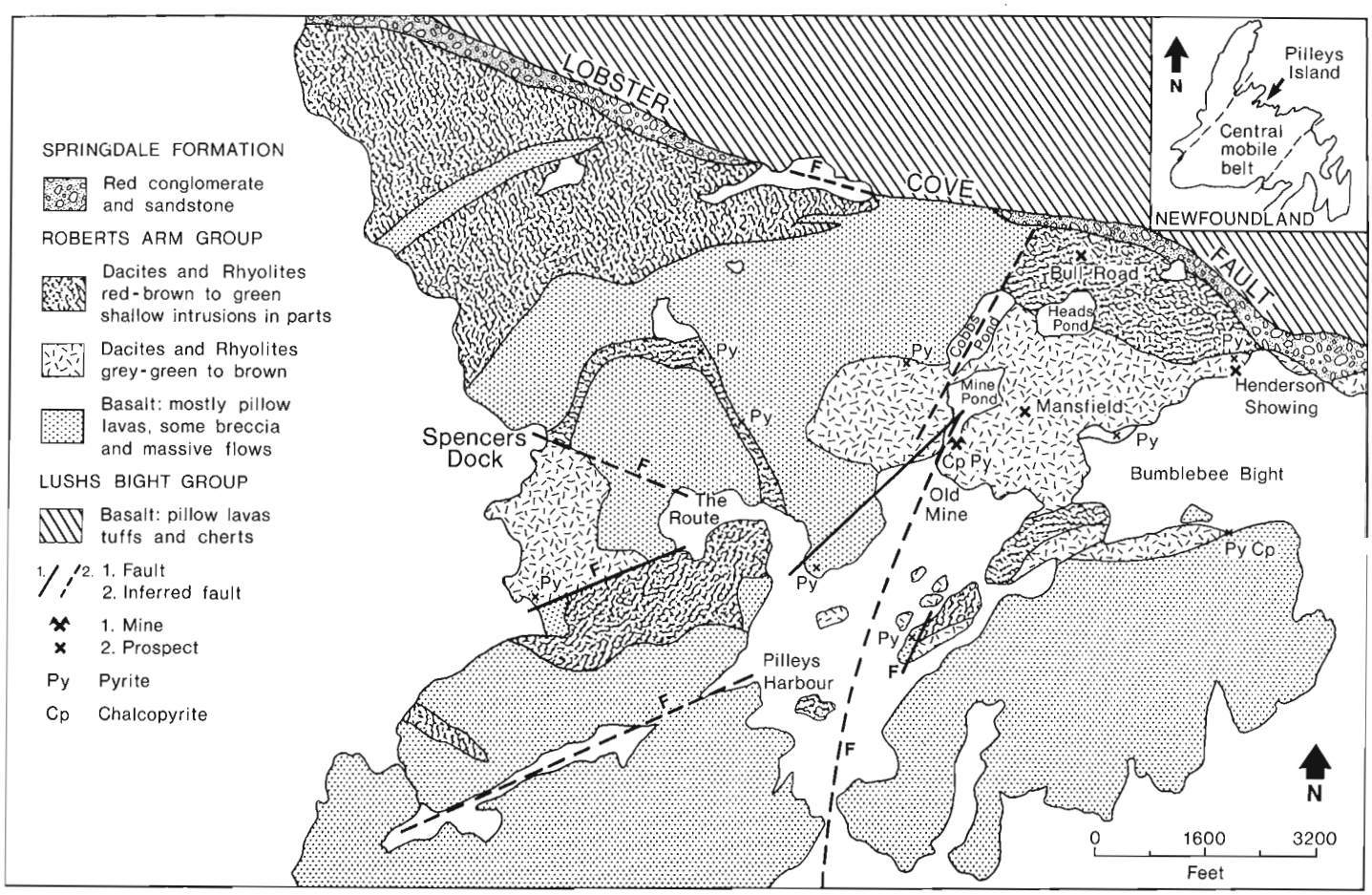

Figure 40.1. General geology of Pilleys Island showing the setting of the Old Mine (after Espenshade, 1937).

[1] Department of Earth Sciences, University of Waterloo, Waterloo, Ontario, N2L 3G1.

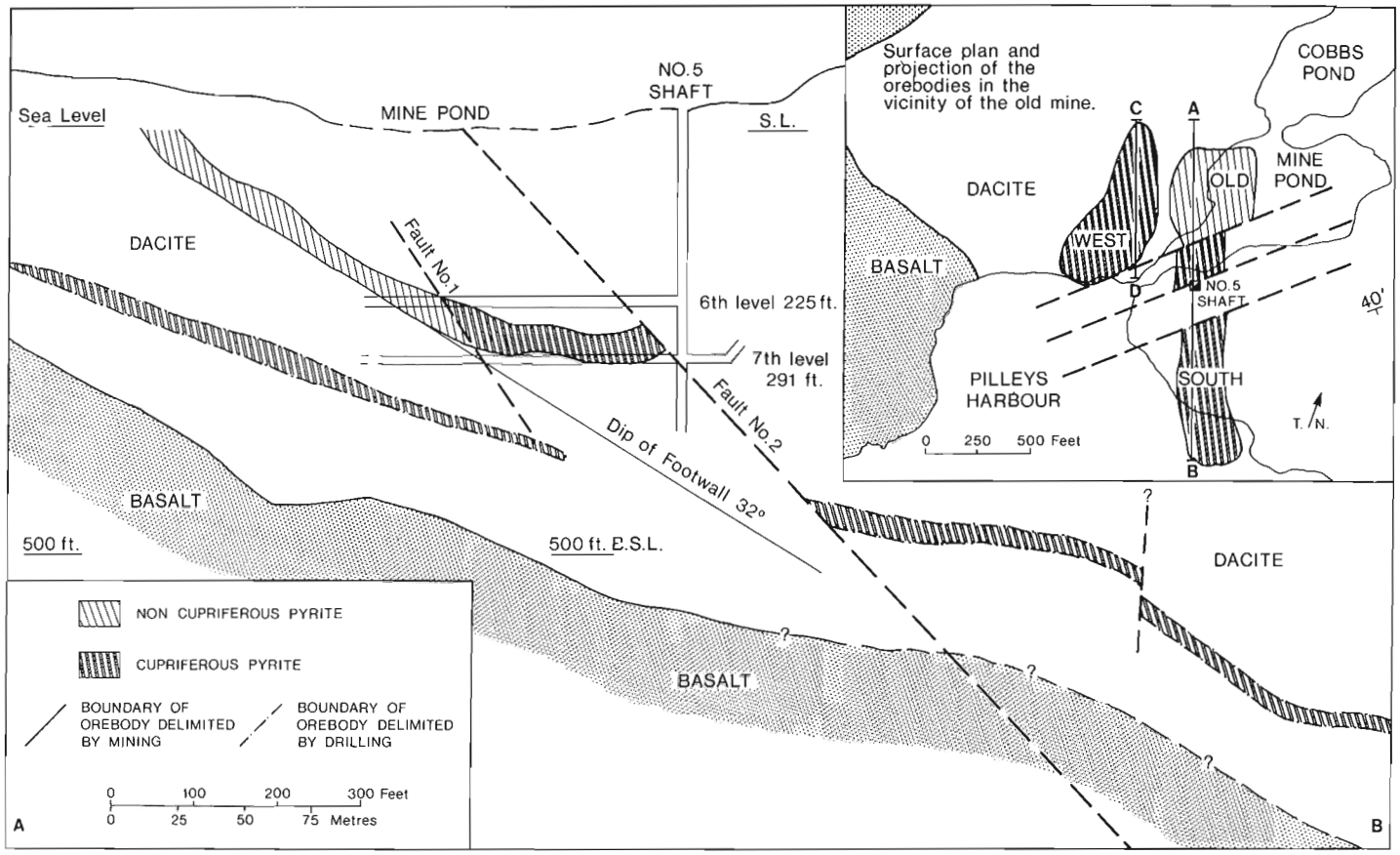

Figure 40.2. Detailed plan and cross-section of geology in the vicinity of the Old Mine showing projected outlines of orebodies (modified after Lawton, 1921).

exploratory drilling in 1951-52 and 1956-58 by the Pilleys Island Copper-Pyrite Co. resulted in the discovery of the "West" Mine orebody (Fig. 40.2) which was further delimited by drilling conducted by Brinex between 1967 and 1970.

The "Old", "South" and "West" orebodies form a physically contiguous group (Fig. 40.2) and are thus convenient to consider together.

Other sulphide occurrences in the Pilleys Island area are also associated with felsic volcanics and include the "42" orebody, the Bull Road, Henderson and Mansfield showings and numerous minor gossans (Fig. 40.1; see also Strong, 1974; Bichan, 1959; Harris et al., 1975).

The local volcanic sequence forms part of the Roberts Arm Group, a calc-alkaline suite (Strong, 1973) of possible Upper Ordovician age (Bostock, 1976). This Group hosts other important sulphide deposits at Gull Pond (Dean, 1974), Lake Bond, and Buchans (Thurlow et al., 1975).

Scope and Status of Study

During the present study some 3000 m (10 000 ft.) of drill core representing 15 holes contiguous to the West Mine orebody were re-examined, sampled, and studied using petrographical, mineralogical, and geochemical methods. This report provides a description of the volcanic setting of the mineralized facies along with petrographic descriptions of altered facies of host rocks.

Geology of the Occurrence

Primary Stratigraphic Relationships

The volcanic rocks in the mine area comprise a lower basaltic sequence overlain by an upper, variably massive to pyroclastic and autoclastic sequence of felsic volcanics with a thickness of about 150 m (500 ft.) (Figs. 40.2, 40.3).

The basalts have not been subdivided in this study as most of the drillholes did not penetrate very far into this unit. Except for one area of strong chloritization, the contact with the upper felsic rocks is sharply defined in core as is also the case in surface exposures. The basalts appear to comprise a series of massive and pillowed flows, individual members being distinguishable by differences in colour, vesicularity, porphyritic textures, etc. Thicknesses average about 2 m (range 1-6 m). The colours vary from dark grey to purplish brown, the latter caused by an extensive dissemination of finely-divided hematite. Flow margins are generally aphanitic and non-vesiculated. Pillows commonly contain frothy patches with more than 50 per cent amygdales now infilled with calcite and, less commonly, barite. Pillowed units appear more common at depth and towards the margins of the drilled block of ground. Interstices between pillows often contain jasper, quartz and disseminated pyrite. The majority of flows are non-porphyritic and consist of a fine grained groundmass of interlocking feathery laths of plagioclase with interstitial devitrified mesostasis, iron oxides, and relict clinopyroxenes. Porphyritic varieties are marked by small (< 1 mm) euhedral laths of albite and stubby crystals of bottle green augite. Some reddish orange idiomorphs may be iddingsite after olivine.

The major part of this sequence is fresh and unmineralized but locally is highly altered. The rocks have previously been described as andesites (Grimley, 1968; Strong, 1973) but Horsburgh (1968) referred to them as spilites.

The felsic unit comprises an interlayered pile of flows and pyroclastic units, including a distinctive lithic breccia (Fig. 40.3).

The unit mapped regionally as "grey dacite and rhyolite" comprises thin flows of distinctly flow-banded dacite (nomenclature follows chemical studies of Strong, 1973) which is

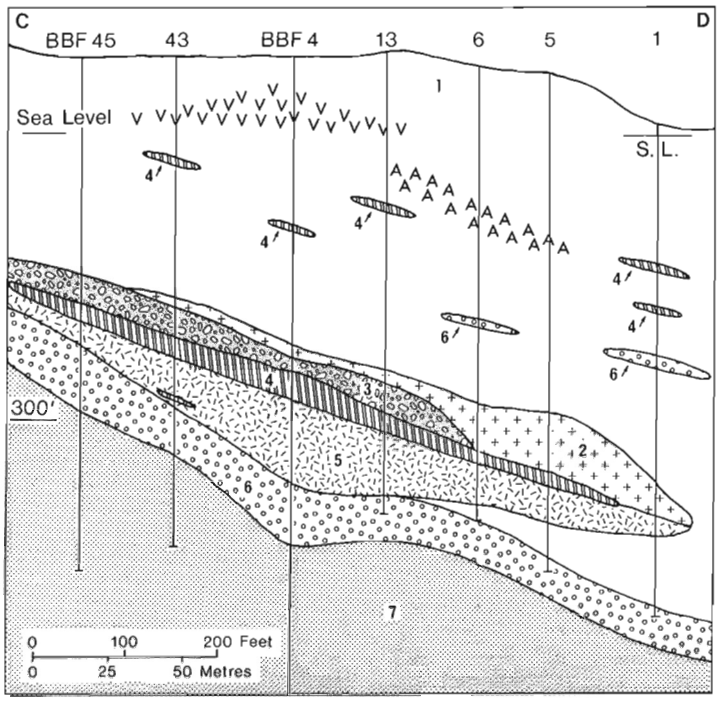

1 — grey dacite (V symbols = vitric lapilli tuff; A symbols = autobrecciation)
2 — sericite-quartz schist
3 — dacite lithic breccia
4 — massive sulphides
5 — vein stockwork
6 — chlorite-rich breccia
7 — basalt, mostly massive and pillowed flows

Figure 40.3. General geology along Section C-D through the West Mine orebody based on drillhole information.

light greenish grey, very fine grained to aphanitic, and commonly porphyritic. Vesicularity varies from 0 to 10 per cent with the predominantly circular to oval amygdales infilled with quartz. The groundmass comprises a mesostasis with abundant interlocking laths of albite and orthoclase. Subrounded phenocrysts of quartz (< 2 mm) and isolated euhedral phenocrysts of orthoclase and albite (< 2 mm) are generally common. Flow margins are marked by devitrified chilled zones possessing perlitic textures and prominent spherulites.

Interbedded with the flows are vitroclastic horizons. One of these is a distinctive vitric lapilli tuff comprising dark greenish devitrified clasts in a fine grained whitish, siliceous matrix. The clasts vary in shape from angular to curved and wispy and in size from 0.2 to 3.0 cm (av. 1.5 cm). The ratio of clasts to matrix is about 60:40. Individual horizons range from 15 to 75 cm (6-30 inches) in thickness and appear to be more prominent in the upper part of the felsic sequence. Only one horizon, at depths greater than 30 m (100 ft.) possesses sufficient continuity to be correlated from one hole to another.

In addition to the interflow pyroclastics a distinctive dacite lithic breccia overlies the main massive sulphide lens. This rock comprises a heterogenous assemblage of subrounded to angular clasts of pale cream coloured, variably altered dacite along with a small percentage of massive sulphide fragments in a fine grained siliceous groundmass with disseminated sulphides. Clasts range in size from 0.1-5 cm (av. 1.5 cm) and comprise up to 95 per cent of the rock. The deposit represents transported debris of local derivation. A similar dacite lithic breccia containing sulphide fragments occurs directly above the massive sulphide at the Bull Road showing (Harris, 1976). Such horizons may represent temporal breaks in the construction of the volcanic edifice or intermittent tectonic disruption of its form.

Alteration

Areas of alteration are strikingly associated with visible mineralization. These phenomena comprise a spectrum of types ranging from thin zones (0.1-3 cm) marginal to quartz-pyrite veinlets, to areas of pervasively altered rocks tens of metres in size (Fig. 40.4).

Zonation of the alteration is displayed by colour and mineralogical effects marginal to veinlets but the massive altered zones possess an equivalent set of mineral assemblage facies. Four facies have been distinguished in this study.

(a) Quartz-sericite ± feldspar facies. Dacite flows and pyroclastics both show this form of alteration. The groundmass is a mat of very fine grained sericite and minor quartz with relict laths of feldspar still evident. Large rounded aggregates of quartz probably represent amygdales but some are recrystallized quartz phenocrysts. Disseminated sulphides are present in quantities greater than 10 per cent and consist predominantly of pyrite.

(b) Sericite-quartz facies. The host for this alteration appears to have consisted principally of fine grained vitric tuffs although primary textures necessary for identification have largely been obliterated. It differs from the previous facies in having a much greater content of sericite, sulphides (up to 50 per cent), less quartz and is completely lacking in feldspar. This unit occupies a 30 m (100 ft.) thick conformable zone in the hangingwall of the main sulphide lens of the West mine (Fig. 40.4).

(c) Quartz ± sericite ± chlorite facies. This facies is coincident with a stockwork zone of quartz-pyrite veins found directly beneath the main sulphide lens (Fig. 40.4). Quartz and sulphides are abundant with minor sericite and chlorite. Feldspar is absent.

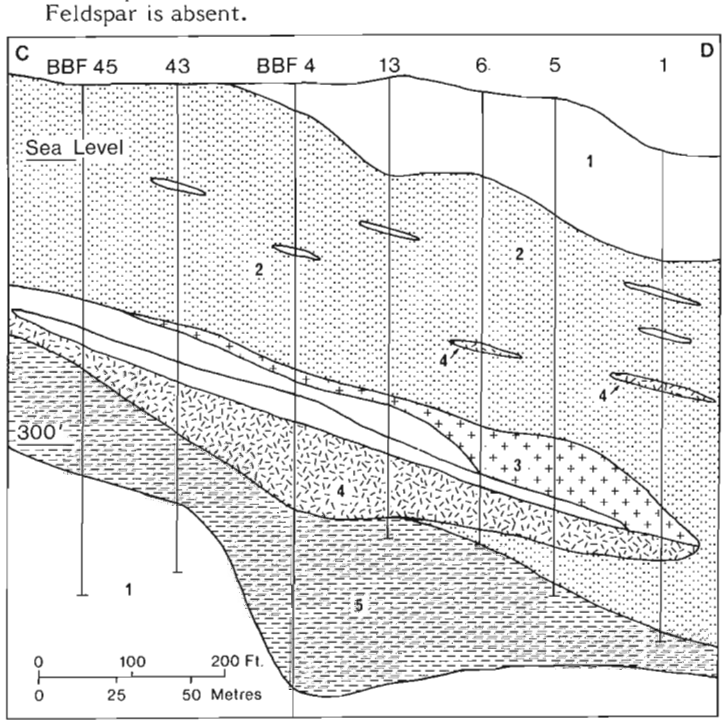

1 — unaltered rocks, dacites and basalts
2 — quartz-sericite ± feldspar facies
3 — sericite-quartz facies
4 — quartz ± sericite ± chlorite facies
5 — chlorite ± sericite facies

Figure 40.4. Alteration effects in the host rocks of the West Mine orebody along section C-D.

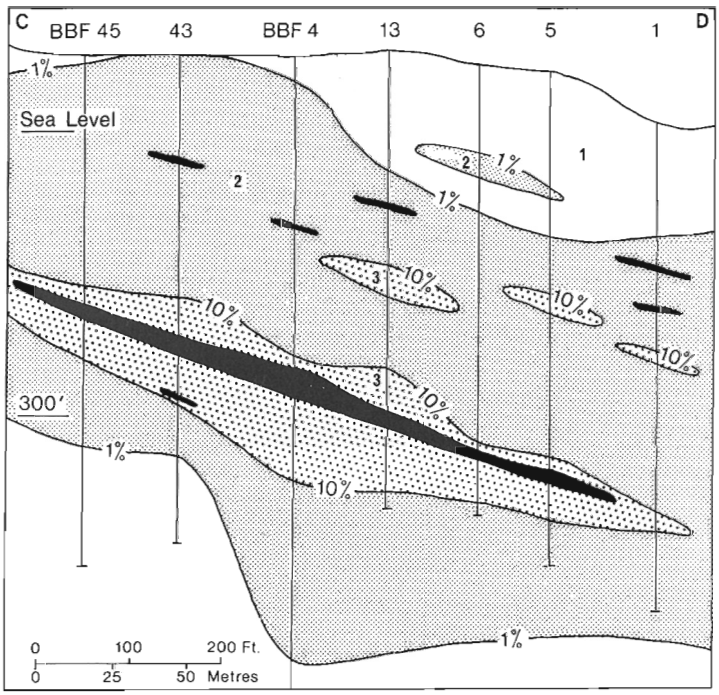

Figure 40.5. Distribution of sulphide mineralization along section C-D through the West Mine orebody. Legend: 1 – < 1 per cent sulphides; 2 – 1 to 10 per cent sulphides; 3 – 10 to 50 per cent sulphides; shaded - massive sulphides (> 50 per cent sulphides).

(d) Chlorite ± sericite facies. This chlorite-rich facies of alteration is restricted to a narrow, conformable zone beneath the main sulphide lens (Fig. 40.4). Chlorite is the predominant mineral and quartz is much less abundant than in the overlying quartz ± sericite ± chlorite facies. The host appears to have been a brecciated dacite. The rock is composed of 0.5-6 cm (av. 3 cm) rounded to subangular altered dacite fragments in a fine grained, very dark, chlorite-rich matrix. This type of chloritization associated with brecciation is not found in the subjacent altered basalts where chlorite has developed interstitially within normal mesostasis. Insufficient penetration by drilling prevents a complete description of the form of this unit but it is suggestive of the intense chloritic alteration associated with pipes beneath many other massive sulphide bodies (Sangster, 1972).

A condensed form of these facies borders the network of thin quartz-pyrite veinlets elsewhere in the sequence. These borders consist of bleached and sericite-enriched zones with, in some cases, a chlorite rind developed directly adjacent to sulphides.

Mineralization

Mineralization of two types (1) sulphide-bearing vein stockworks and (ii) massive sulphide lenses, occur above the basalt/dacite interface throughout this section of the mine. Figure 40.5 illustrates the distribution of sulphides with values > 50 per cent being considered massive sulphide bodies.

Two horizons with massive sulphide lenses occur within the section. All are conformable to the enclosing volcanics. The upper horizon comprises a series of thin, discontinuous sulphide lenses in an en echelon pattern at the 36 m (120 ft.) level. The mineralization comprises principally massive pyrite with very little copper (av. 0.19 per cent Cu). These lenses may be lateral equivalents of the Old Mine orebody.

The main ore lens is also a concordant body, dipping 20° south-southeast, about 12 m (40 ft.) thick in the centre, thinning gradually to its limits. It possesses a sharp hangingwall contact with the overlying dacite lithic breccia. In plan it is elongated in a north-northeast direction (Fig. 40.2). It appears to be emplaced within highly altered vitric tuffs. The mineralization within the lens is predominately pyrite, often with colloform texture. The silicate gangue consists of abundant quartz and minor sericite and chlorite. No evidence of layering was observed although ore in the Old Mine possesses this feature (Horsburgh, 1968); instead the massive ore resembles a highly altered tuff saturated with sulphides.

The main vein stockwork occurs beneath the main massive sulphide lens and increases in diameter upwards to embrace it. The host rocks were originally volcanoclastic dacites but are now very strongly altered to the quartz ± sericite ± chlorite facies. Quartz is a predominant component, comprising 40 to 90 per cent. Pyrite is the most common sulphide occurring in medium grained disseminations, aggregates, and stringers. Mineralization in this zone often contains higher copper values than the massive sulphide lens (av. 1-5 per cent Cu). Pyrite is often fractured and cemented by either chalcopyrite or quartz. Chalcopyrite and sphalerite also occur occasionally as blebs within pyrite or as separate grains. Galena is virtually absent.

Structural Geology

Although elsewhere in the Roberts Arm Group facing criteria are relatively common (Bostock, 1975) they are less so on Pilleys Island. Bostock (1976) shows southerly facing and dipping pillow structures north of the village but northward facing and variably north and south dipping pillows south of the mine. No direct evidence was found in the present study to indicate whether the gently (20°) southerly dipping sequence in the mine is in a normal or inverted attitude but the relationship of vein stockworks to massive sulphides and the distribution of alteration leads us to assume the sequence is not overturned. This interpretation contrasts with that of Espenshade (1937) who suggested these rocks were on the locally overturned western limb of a northeast striking anticline.

Two faults cut the rocks of the Old Mine and presumably continue to the south of the West Mine section (Fig. 40.2). The so-called Mine Fault (Fault No. 2, Fig. 40.2) appears to offset the orebody in a normal sense with a vertical displacement of about 60 m (200 ft.). The South Mine orebody can however be correlated with a horizon of sulphide concentration beneath the Old Mine orebody (Walker, 1960) which would involve little or no vertical displacement on the Mine Fault. Horsburgh (1968) suggested on the basis of a reassessment of core and surface geology that movement on the Mine Fault is predominately horizontal with only a moderate throw. Lawton (1921) had reached a similar conclusion with the movement supposedly having a dextral strike-slip sense. If this is so, the faulted extension of the South Mine orebody would be beneath the Mine Pond, northeast of the Old Mine orebody and the extension of the non-cupriferous Old Mine orebody would be expected to the southwest beneath Pilleys Harbour.

Metamorphism

Metamorphism throughout the area is of very low grade (sub-greenschist) levels. Insufficient studies have been made to characterize it further.

Discussion

Although glib comparisons with occurrences elsewhere can often distract attention from important unique characteristics, it is safe to note that the Pilleys Island mineralization has many of the characteristics associated with the Mesozoic Kuroko deposits of Japan, and are consistent with a syngenetic association with the host

volcanics. In this sense they are similar to the deposits at Buchans and Gull Pond. In terms of Kuroko-type mineral zoning (Lambert and Sato, 1974) Pilleys Island quartz-pyrite-chalcopyrite stockwork deposits with associated silicification are comparable to **keiko** (siliceous) ores. The West Mine and Old Mine stratiform massive orebodies appear to be principally of the **ryukako** (pyritic) ore type with transitions to facies with chalcopyrite and sphalerite termed **oko** (yellow ore). The South Mine may also be of **oko**-type. The sphalerite-galena-chalcopyrite-pyrite ores of the Bull Road showing appear to be the only **kuroko** (black ore) discovered to date in the district. No **sekkoko** (gypsum ore) bodies have yet been discovered although minor barite has been reported in amygdales in the dacite hosts and underlying basalts and has been reported as an ore gangue in the Old Mine (Horsburgh, 1968). Ferruginous cherts (**tetsusekiei** beds) are found elsewhere in the Roberts Arm Group associated with mineralization, e.g. Gull Pond, but presumably have been eroded from the Pilleys Island section.

All the mineralization at Pilleys Island in the Old-South-West mine area occurs within vitroclastic felsic volcanics and underlies distinctive dacite lithic breccias. Comparable breccias occur at both Buchans (Thurlow et al., 1975) and Bull Road (Harris, 1976) and are never far above the contact with underlying basalts. The volcanic paleotopography of these mafic/felsic accumulations may have been a controlling factor in localizing the deposition of the sulphides in a similar manner to that operative at Buchans (Thurlow et al., 1975).

Metal-rich polymetallic "black ores" are not presently found in the Old-South-West mine section. They were either not deposited during that episode of mineralization, were eroded and dispersed shortly after their deposition, or were transported locally in a pre-lithified condition to a more distal part of the area. The preservation of the small Bull Road deposit with average ore of 1.09% Cu, 2.87% Zn, 0.32% Pb and 0.50 oz./t Ag (Harris, 1976) makes this latter possibility an attractive model for further exploration.

The sericite-quartz alteration which is readily recognized in hand specimen is broadly indicative of mineralized zones but the centre of most intense mineralization is best located by re-constructing the form of the four facies of alteration outlined above. Zones of intense quartz-sericite-chlorite and chlorite ± sericite alteration which are coincident with horizons of felsic vitric tuffs and lithic breccias are particularly favoured sites for sulphide accumulation.

References

Bichan, W.J.
1959: Pilleys Island Copper-Pyrite Limited; Unpublished report for Frobisher Ltd.

Bostock, H.H.
1975: Volcanic rocks of the Appalachian province: Roberts Arm Group, Newfoundland (2E); in Report of Activities, Part A, Geol. Surv. Can., Paper 75-1A, p. 1-3.

1976: Volcanic rocks of the Appalachian province: Roberts Arm Group, Newfoundland (2E and 12H); in Report of Activities, Part A, Geol. Surv. Can., Paper 76-1A, p. 173-175.

Dean, P.L.
1974: The Gullbridge Copper Deposit; in Strong, D.F. (Ed.) Plate Tectonic Setting of Newfoundland Mineral Occurrences, NATO Advanced Studies Institute Guidebook, p. 80-86.

Espenshade, G.H.
1937: Geology and mineral deposits of the Pilleys Island area; Nfld. Dept. Nat. Res., Geol. Sect., Bull. 6.

Grimley, P.H.
1968: Résumé of field activities and proposed drilling programme 1967-68, Pilleys Island, Nfld.; Unpublished report on file with Mineral Resources Div., Nfld. Dept. Mines and Energy.

Harris, A.
1976: The Bull Road Showing, Pilleys Island, Newfoundland; Unpublished report to Consolidated Morrison Explorations Ltd.

Harris, A., Newman, P., and Harris, V.
1975: Geology and economic potential of Pilleys Island, Newfoundland; Unpublished report to Consolidated Morrison Explorations Ltd.

Horsburgh, J.R.
1968: The geology of the Pilleys Island prospect, Notre Dame Bay, Newfoundland; Unpublished B.Sc. thesis, Royal School of Mines, London, England.

Lambert, I.B. and Sato, T.
1974: The Kuroko and associated ore deposits of Japan: a review of their features and metallogenesis; Econ. Geol., v. 69, p. 1215-1236.

Lawton, N.O.
1921: Supplemental report on the Pilleys Island Mine property, Pilleys Island, Notre Dame Bay, Newfoundland; Unpublished report for Blast Furnace Products Ltd.

Sangster, D.F.
1972: Precambrian volcanogenic massive sulphide deposits in Canada: a review; Geol. Surv. Can., Paper 72-22.

Strong, D.F.
1973: Lushs Bight and Roberts Arm groups of central Newfoundland: possible juxtaposed oceanic and island-arc volcanic suites; Geol. Soc. Amer., Bull., v. 84, p. 3917-3928.

1974: Mineral occurrences of the Pilleys Island area; in Strong, D.F. (Ed.) Plate Tectonic Setting of Newfoundland Mineral Occurrences, NATO Advanced Studies Institute Guidebook, p. 87-94.

Thurlow, J.G., Swanson, E.A., and Strong, D.F.
1975: Geology and lithogeochemistry of the Buchans polymetallic sulphide deposits, Newfoundland; Econ. Geol., v. 70, p. 130-144.

Walker, W.B.G.
1960: Report on Pilleys Island Copper-Pyrite Ltd.; Unpublished report for Frobisher Limited.

41.

PALYNOLOGICAL INVESTIGATION OF THE WINDSOR GROUP (MISSISSIPPIAN) OF PORT HOOD ISLAND AND OTHER LOCALITIES ON CAPE BRETON ISLAND, NOVA SCOTIA

Project 740110

J. Utting[1]
Regional and Economic Geology Dvision

Abstract

Utting, J., Palynological investigation of the Windsor Group (Mississippian) of Port Hood Island and other localities on Cape Breton Island, Nova Scotia; Current Research, Part A, Geol. Surv. Can., Paper 78-1A, p. 205-207, 1978.

Two palynological assemblage zones are recognized from the Windsor Group on Cape Breton Island; Assemblage zone I occurs in subzone B and may extend downward or laterally into subzone 'A' and Assemblage zone II in subzones C, D and possibly E?

Tentative correlation with the British Visean suggests that the Lower Windsor assemblages are probably not older than the upper part of the Upper ***Caninia*** *(C_2S_1) zone and not younger than the Lower* ***Dibunophyllum*** *(D_1) zone whereas the Upper Windsor is not older than the Lower Dibunophyllum zone (D_1) and not younger than the Upper* ***Posidonia*** *(P_2) zone.*

A preliminary palynological investigation of the Windsor Group suggested that differences in the vertical distribution of miospores throughout the group might provide the basis for establishing assemblage zones (Utting, 1977). The preliminary study, and subsequent work summarized in the present report, were carried out under contract with the Geological Survey of Canada as support for H.H.J. Geldsetzer (Regional and Economic Geology Division, Project 740110). Field work was financed by National Research Council grant, No. A-4286 and by the Ministry of Intergovernmental Affairs of Québec.

This report is concerned mainly with a detailed investigation of Windsor rocks in the Port Hood Island section. Also studied were samples collected at other localities on Cape Breton Island from the lower part of the Lower Windsor and the upper part of the Upper Windsor (Fig. 41.1). The Port Hood Island section was selected for sampling because it is well exposed compared to most outcrops of the Windsor Group (including the type section), and is relatively complete; present there are rocks of subzones B, C, D, and E of Bell (1929). A further advantage of this section is that the macro- and microfauna have been studied by previous workers, thus providing useful stratigraphic control, e.g. Stacy, 1953; Globensky, 1967; Mamet, 1970 and von Bitter, 1976. Less favourable aspects of the section are that beds from the lower part of the Lower Windsor are not present, only part of subzone E of the Upper Windsor is exposed, and the lower part of subzone C may be missing due to faulting (P.S. Giles, pers. comm., 1976). Most of the 35 samples collected from subzones B, C, and D contained well preserved miospores. No ideal lithology suitable for palynological preparation was found within the E limestone, although the organic residues obtained in the course of the conodont study carried out by von Bitter, were processed for palynomorphs. Miospores are present occasionally in these residues, but preservation is generally poor and only non-diagnostic long ranging forms were found. Many of the miospore taxa in samples from subzones B, C, and D were found to occur from the bottom of the section to the top of subzone D. These include:

Rugospora minuta Neves and Ionnides 1974
Retusotriletes incohatus Sullivan 1964
Punctatisporites irrasus Hacquebard 1957
Punctatisporites planus Hacquebard 1957
Endosporites micromanifestus Hacquebard 1957
Cyclogranisporites palaeophytus Neves and Ioannides 1974
Crassispora trychera Neves and Ioannides 1974
Lycospora noctuina (Butterworth and Williams 1958) var **noctuina** Somers 1972
Schopfites claviger Sullivan 1968
Rugospora polyptycha Neves and Ioannides 1974
Auroraspora macra Sullivan 1968
Endosporites minutus Hoffmeister, Staplin & Malloy 1955.

However, certain forms, apparently lacking in subzone B, appear near the base of subzone C and continue upwards into subzone D. For example **Schopfipollenites ellipsoides** (Ibrahim) Potonié and Kremp 1954, **Acanthotriletes** sp. A, **Discernisporites** sp. A, **Spelaeotriletes** sp. D, **Knoxisporites triradiatus** Hoffmeister, Staplin and Malloy 1955. This limited vertical distribution allows an older and a younger assemblage zone to be recognized; the older (Assemblage zone I), occurs in the Lower Windsor subzone B and is identified mainly on negative evidence in that it lacks the "diagnostic" forms which characterize the younger assemblage (Assemblage zone II) of Upper Windsor subzones C and D.

In view of the lack of exposure of the lower part of the Lower Windsor in the Port Hood Island section, supplementary material was investigated from other localities in Cape Breton Island (see Fig. 41.1). Eight samples, all collected by H.H.J. Geldsetzer, were obtained from subzone A, that is, from above or within the basal Windsor laminite and below the massive evaporite. Unfortunately, although many of the samples contained abundant miospores, preservation was poor except for one sample (D 1370, 98-3); this poor preservation, which prevented confident identification of the specimens, appears to be the result of pyrite corrosion. Sample D 1370, 98-3, contained an assemblage generally similar to that of Assemblage I from subzone B of the Port Hood Island section. This indicates that similar miospore assemblages occur in both subzone B and certain beds of "subzone A", despite the fact that a massive evaporite separates the two units in many parts of Cape Breton Island and probably elsewhere in the Atlantic Provinces. Thus Assemblage Zone I may extend downward into older rocks of "subzone A", although if the latter is largely a lateral facies equivalent of the lower part of subzone B, as confirmed by Geldsetzer (1977), any difference in age between the assemblages may be slight.

Because no lithologies suitable for palynological study were found in subzone E on Port Hood Island an investigation was made of the youngest Windsor beds found elsewhere. One region where a number of boreholes have been drilled through the Windsor Group is the Lake Enon area near Loch Lomond (Fig. 41.1, loc. 3); cores from two boreholes (Noranda 4 and Noranda 12) were made available for sampling by Kaiser Celestite Mining Ltd. Only the approximate stratigraphic position of the material sampled is known, this being based on

[1] Institut National de la Recherche Scientifique, INRS-Pétrole, Université du Québec, Sainte-Foy, Québec G1V 4C7.

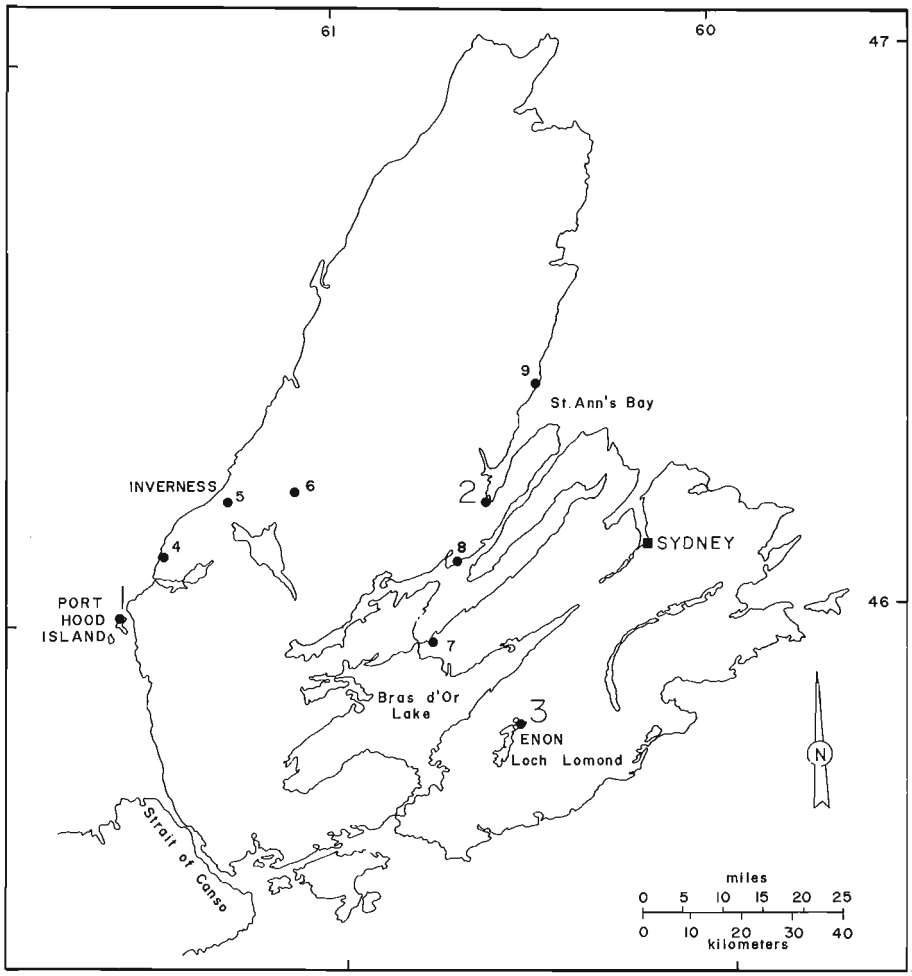

1. D1384, 35 samples, Port Hood Island (subzones B, C and D).
2. D1370, 98-3, 1 sample, North Gut St-Anns (subzone A).
3. D1325, K4, K5 and K60, 3 samples, Noranda 4; and D1332, K54, K55 and K57, 3 samples, Noranda 12, Lake Enon, Loch Lomond (subzone E?).
4. D1383, 126-8, 1 sample, Lake Ainslie, Mabou Mines (subzone A).
5. D1380, 116-3, 1 sample, Lake Ainslie, Broad Cover River (subzone A).
6. D1381, 118-6, 1 sample, Lake Ainslie, Gillisdale (subzone A).
7. D1365, 56-5, 1 sample, Grand Narrows, Christmas Island (subzone A).
8. D1371, 107-9, 1 sample, Baddeck, Red Point (subzone A).
9. D1373, 106-5 and 106-6, 2 samples, Bras d'Or, North Shore (subzone A).

Figure 41.1

Location of samples (with Geological Survey of Canada Sample Numbers) investigated on Cape Breton Island.

estimates made by Geldsetzer utilizing lithostratigraphic data (pers. comm.). Samples from beds thought possibly to be subzone E contained assemblages similar to Assemblage II of Port Hood Island, as well as two species not seen in the Port Hood Island samples. In Noranda 4 and 12 occur rare specimens of **Grandispora spinosa** Hoffmeister, Staplin & Malloy 1955, and in Noranda 4 occur a few specimens of **Schulzospora** cf. **S. elongata** Hoffmeister, Staplin and Malloy 1955. In view of the uncertainty concerning the precise age of these beds it is not yet possible to draw any definite conclusions concerning the occurrence of these forms, although it is interesting to note that Neves and Belt (1970) **G. spinosa** and **Schulzospora rara** Kosanke 1950 from the top of the Windsor Group in the Pomquet River Section of the Antigonish Basin. Thus, should further work prove these forms to be restricted to the youngest beds of the Windsor Group they may well be useful stratigraphic markers and enable further subdivision of Assemblage II.

Detailed work concerning the vertical ranges of the various taxa, illustrations of the forms found, and conclusions concerning biostratigraphic correlation continues. It was found that although the Windsor assemblages differ from those recorded from Viséan rocks of other areas, there are sufficient similarities with the Viséan assemblages of the British Isles to permit preliminary correlations. A general zonal scheme for the British Viséan was published by Neves et al. (1972, 1973), and comparison with this zonation suggests that the Lower Windsor is not older than the upper part of the **Lycospora pusilla** (Pu) zone. The material from the Upper Windsor subzone E? is not older than the **Tripartites vestustus-Rotaspora fracta** (VF) zone and none of the Upper Windsor samples so far studied would appear to be younger than the lower part of the **Bellispores nitidus/Reticulatisporites carnosus** (NC) zone. In terms of the new stage names proposed for the Dinantian in Britain by George et al. (1976), this implies that the Lower Windsor material studied from subzones A and B are not older than Arundian, and may be younger, for example Holkerian and/or Asbian. On the other hand the youngest Windsor samples investigated so far (subzone E?) are probably of Brigantian age although Assemblage II (subzone C and D) may be Asbian. In comparison with the macrofaunal zones, this suggests that the Lower Windsor assemblages are probably not older than the upper part of the Upper **Caninia** (C_2S_1) zone and not younger than the Lower **Dibunophyllum** (D_1) zone, whereas the Upper Windsor is not older than the Lower **Dibunophyllum** (D_1) zone and not younger than the Upper **Posidonia** (P_2) Zone.

References

Bell, W.A.
1929: Horton-Windsor District, Nova Scotia; Geol. Surv. Can., Mem. 155.

Geldsetzer, H.H.J.
1977: The Windsor Group of Cape Breton Island, Nova Scotia; in Report of Activities, Part A, Geol. Surv. Can., Paper 77-1A, p. 425-428.

George, T.N., Johnson, G.A.L., Mitchell, M., Prentice, J.E., Ramsbottom, W.H.C., Sevastopulo, G.D., and Wilson, R.B.
1976: A correlation of Dinantian rocks in the British Isles; Geol. Soc. London, Special Report No. 7, p. 1-87.

Globensky, Y.
1967: Middle and Upper Mississippian conodonts from the Windsor Group of the Atlantic Provinces of Canada; J. Paleontol., v. 41, no. 2, p. 432-448.

Mamet, B.L.
1970: Carbonate microfacies of the Windsor Group (Carboniferous), Nova Scotia and New Brunswick; Geol. Surv. Can., Paper 70-21, 121 p.

Neves, R. and Belt, E.S.
1970: Some observations of Namurian and Viséan spores from Nova Scotia, Britain and Northern Spain; in C.R. 6me Cong. Int. Strat. Géol. Carb., Sheffield 1967, v. 3, p. 1233-1249.

Neves, R., Gueinn, K.J., Clayton, G., Ioannides, N., and Neville, R.S.W.
1972: A scheme of miospore zones for the British Dinantian; in C.R. 7me Cong. Int. Strat. Géol. Carb., Krefeld 1971, v. 1, p. 347-353.

Neves, R., Gueinn, K.J., Clayton, G., Ioannides, N., Neville, R.S.W., and Kruszewska, K.
1973: Palynological correlations within the Lower Carboniferous of Scotland and northern England; Roy. Soc. Edinburgh, Trans., v. 69, p. 23-70.

Stacy, M.C.
1953: Stratigraphy and paleontology of the Windsor Group (Upper Mississippian) in parts of Cape Breton Island, Nova Scotia; N.S. Dep. Mines, Mem. 2, 143 p.

Utting, J.
1977: Preliminary palynological investigation of the Windsor Group (Mississippian) of Nova Scotia; in Report of Activities, Part A, Geol. Surv. Can., Paper 77-1A, p. 347-349.

von Bitter, P.H.
1976: Paleoecology and distribution of Windsor Group (Viséan -? Early Namurian) conodonts, Port Hood Island, Nova Scotia, Canada; in C.R. Barnes, ed., Conodont Paleoecology, Geol. Assoc. Can., Spec. Paper 15, p. 225-241.

42.

CARMANVILLE MAP-AREA, NEWFOUNDLAND; THE NORTHEASTERN END OF THE APPALACHIANS

Project 730044

R.K. Pickerill[1], G.E. Pajari Jr.[1], K.L. Currie, and A.R. Berger[2]
Regional and Economic Geology Division

Abstract

Pickerill, R.K., Pajari, Jr., G.E., Currie, K.L., and Berger, A.R., Carmanville map-area, Newfoundland; the northeastern end of the Appalachians; Current Research, Part A, Geol. Surv. Can., Paper 78-1A, p. 209-216, 1978.

Carmanville map-area (2E/8) straddles a major northeast-trending tectonic boundary. Northwest of the boundary an ocean floor sequence of ultramafics, mafic volcanics and Ordovician turbidites (Davidsville Group) were disturbed by olistostromes and tectonic slides commencing in Ordovician time. Southeast of the boundary the rocks are of continental aspect (Flinns Tickle complex, Gander Lake Group). The Flinns Tickle complex was metamorphosed prior to emplacement of the major granitoid plutons. The Gander Lake Group consists of three major subunits, one of which is a cataclasite. All major plutons appear to be of similar (Devonian?) age, although the petrography of the plutons differs markedly across the boundary. The latest peak of regional metamorphism, near 640°C, 4 kilobars, occurred coincident with, or slightly preceding, major emplacement of plutons. Complex histories of structural deformation and metamorphism, involving at least four periods of deformation, have been deduced on opposite sides of the tectonic boundary, but no direct way has been found to correlate them. There is no direct evidence for late Precambrian or early Paleozoic orogeny. The observed relations are compatible with obduction of oceanic material commencing in the Ordovician and terminating in the Devonian.

Introduction

Williams (1964a) observed that the Appalachian orogen in Newfoundland forms a two-sided symmetrical system, bounded on both sides by crystalline basement. The success of plate tectonic theory in modelling the western side of the orogen (Dewey and Bird, 1971; Williams et al., 1974) suggests that the eastern side can be explained in similar terms. However, even the exact location of the eastern margin of the orogen remains uncertain. The Carmanville map-area (2E/8) straddles a major north-northeast trending tectonic boundary separating ultramafic rocks of oceanic type with overlying mafic volcanic and sedimentary rocks of Early-Middle Ordovician (Arenig-Caradoc) age from a metamorphic assemblage consisting of a polydeformed and polymetamorphosed gneiss complex and a homogeneous fine grained mass of quartz-plagioclase-biotite schist. Both terranes were intruded by Devonian granitoid plutons whose character varies strongly between the two contrasting terranes. Geological considerations suggest that the tectonic boundary separates the central mobile belt of Newfoundland from continental material, including crystalline gneisses to the east. The stratigraphy, structure, intrusive history, and metamorphism of the Carmanville map-area elucidate the nature of the northeastern margin of the Appalachians. The Carmanville map-area was largely burned over in 1961. The visibility and rock exposure are therefore unusually good by Newfoundland standards, although large areas are covered by boulder fields. In many cases these fields are sufficiently angular and monomict that they indicate underlying bedrock. Access, by means of a net of deteriorating bush roads, is presently good.

Description of Formations

The rocks of the map-area are divided into seven major units, namely the Flinns Tickle complex (units 1-2), the Gander Lake Group (units 3-5), the Davidsville Group (units 7-11), with which we include the underlying ultramafic rocks (unit 6), the Rocky Bay and Frederickton plutons (unit 15), the Island Pond, Aspen Cove and White Point plutons (units 12-14), the Ragged Harbour and South Pond plutons (units 16-18), and the Deadmans Bay Pluton (unit 19).

The Flinns Tickle complex (units 1-2) outcrops in a narrow belt extending south-southwest from Musgrave Harbour to South Pond. The unmigmatized part of the complex (unit 1) consists of mesocratic quartz-plagioclase-biotite gneisses of fine to medium grain, with many pelitic interbeds, and rare garnet-amphibolite layers or boudins. Sillimanite is very commonly present, either as a fibrolitic breakdown product of biotite, or as stout euhedral prisms. South of the ponds of Ragged Harbour River, beds containing stout sillimanite prisms are intricately folded, while clumps of large pink andalusite crystals cut across the small folds. At Flinns Tickle, three generations of sillimanite can be recognized, including two generations of stout sillimanite prisms, and a late generation of fibrolite developed at the expense of biotite. Muscovite is common in some parts of the complex, and the univariant assemblage sillimanite-kspar-muscovite-quartz is widespread. Presumably the stable occurrence of both sillimanite alone and muscovite alone must result from varying water fugacity. Kspar-bearing parts of the complex grade into migmatized portions, in which thin sills and obliquely cross-cutting veins of muscovite-granite are abundant. An arbitrary boundary of 25 per cent by area of granitic material was used to delimit the boundary between units 1 and 2. Unit 2 in turn grades into unit 16, which contains more than 50 per cent of granitic material. Amphibolitic beds within the Flinns Tickle complex are rich in quartz, and lack plagioclase. Presumably they represent relics of calcareous beds. Such beds are commonly boudined, even where the surrounding rock displays little obvious evidence of deformation. More commonly the whole complex is intricately small-folded on sinuously curving planes which tend to dip and plunge away from the nearest major pluton. More competent beds, such as amphibolite, have been extensively boudined and rotated in the Flinns Tickle area to yield folded, rotated inclusions.

The Gander Lake Group (as defined by Kennedy and McGonigal, 1972) (units 3-5) forms a homogeneous mass of intensely deformed, fine grained, quartz-rich rocks. No exposed contact with the underlying Flinns Tickle complex has been found in this area, but Blackwood (1977) reported an unconformity. West of South Pond uniform, homogeneous Gander Lake Group occurs within 200 m of intricately folded

[1] University of New Brunswick, Fredericton, New Brunswick E3B 5A3.

[2] Memorial University of Newfoundland, St. John's, Newfoundland.

poly-metamorphosed Flinns Tickle complex. However, other exposures suggest that parts of the Flinns Tickle complex may be highly metamorphosed equivalents of the Gander Lake Group. The southeastern part of the Gander Lake Group is a very homogeneous, fine grained, gritty, pale grey quartz-plagioclase (An_{25-35})-biotite rock weathering to white or pale pink. Microscopically the rock contains significant tourmaline. The northwestern part of this unit contains small amounts of apparently prograde chlorite, thereby grading into the central part of the Group (unit 4) which consists of pale green, strongly schistose quartz-muscovite-chlorite-calcite rocks. The northwestern part of the Gander Lake Group consists of hard, platy-fracturing apple green rocks of cataclastic aspect. Microscopically these rocks (unit 5) can be seen to be considerably recrystallized (blastomylonitic), although the cataclastic character remains obvious. Structural information is obtained with difficulty from the Gander Lake Group because of its uniformity. No trace of relict sedimentary structure has been found, but three periods of tectonic deformation can be recognized. Older fabrics may have been obliterated, since the oldest observed fabric is commonly severely transposed. The earliest structures trend almost due north, while later generations trend progressively more to the northeast. All have produced tight small-folding, generally dipping moderately to steeply westward and plunging gently southward. Some or all of this deformation may be associated with the Ragged Harbour Fault, which truncates the Gander Lake Group, and roughly parallels the trend of structures within it. The ubiquitous presence of oligoclase within the Gander Lake Group suggests that metamorphism reached amphibolite facies, but the presence of broad areas of muscovite-chlorite rocks demonstrates either extensive retrograding, or possibly a drop in grade toward the southwest.

The Gander River ultramafic belt (Jenness, 1963) in this area forms a thin strip extending from the head of Ragged Harbour some 14 km southwest to beyond Shoal Pond. Displaced slivers of ultramafic rocks are found in both directions beyond the end of the belt, leaving little doubt that ultramafic rocks must be continuous at depth. Substantial amounts of ultramafic rocks are also found on the east side of Rocky Bay, in Aspen Cove, and within the "mobile" matrix of the olistostrome (unit 8). The ultramafic rocks consist mainly of antigorite, but rare, less altered, exposures suggest that originally websterite was the predominant rock-type with lesser amounts of lherzolite and peridotite. Malpas and Strong (1975) have remarked on the upper mantle character of the opaques (chrome spinels). Schistose parts of the belt are extremely rich in dolomite and ankerite-magnesite, which locally have reacted with the surroundings to produce chlorite and actinolite. Progressive tectonic deformation of the ultramafic rocks can be observed in the roadcut leading to the highway bridge over Ragged Harbour River. The western part is massive (but completely altered). The eastern parts of the cut show progressively stronger foliation, which in the final exposures is folded. This increasing deformation is thought to result from proximity to the Ragged Harbour Fault.

The Davidsville Group (units 7-11) was originally defined by Kennedy and McGonigal (1972), who believed that the Davidsville Group did not exhibit significant regional metamorphism. This impression is erroneous, and the rocks called by us "Gander sequence" (Currie and Pajari, 1977) are in fact metamorphosed equivalents of the Davidsville Group. We therefore describe the general characteristics of the Davidsville Group here, and will discuss the metamorphism subsequently. No contact between the ultramafic rocks and the Davidsville Group has been discovered, but on Shoal Pond, conglomerate beds containing ultramafic debris appear to lie close to the base of the Davidsville Group (unit 9), although a thin screen of mafic volcanic rocks (unit 6) appears to separate the ultramafics from the sedimentary rocks.

Volcanic rocks in the Carmanville area consist of a number of volcanic lithofacies, each distinguished on a descriptive and genetic basis. These lithofacies are present as huge "knockers" or rafts (up to 7 km wide). The lithofacies may be summarized as: (i) Volcanic conglomerates (unit 7d) of poorly sorted pebble to boulder sized fragments resting unsupported in a fine grained matrix (mud-sand). Fragments are rounded and consist of basaltic material with occasional ultrabasic blocks, and masses of pillow lavas. Hydroplastic deformation of the volcanoclastic blocks, inverse grading in an otherwise structureless deposit, and channelling of underlying units testifies to their origin as submarine debris flows. (ii) Volcanoclastic sandstones and conglomerates (unit 7b), which originated as turbidites or grain flows, with occasional thin limestone beds. Turbiditic units (2-20 cm) exhibit A, AB or B divisions of the Bouma sequence. Grain flow units are structureless, ungraded, contain occasional randomly oriented clasts and are 10-35 cm thick. (iii) Pillowed basaltic lavas (unit 7h). (iv) Massively bedded hyaloclastites (unit 7h) which may contain tongues of pillow lavas.

Unit 8 is a submarine gravity slide or olistostrome containing huge "knockers" of unit 7 at its base which themselves are separated by thin slivers of black shale. Stratigraphically upwards the volcanic blocks decrease in number and size and are accompanied by an increase in greywacke, siltstone, and sandstone flyschoid "knockers". Towards the top of the olistostrome the blocks are composed chiefly of flyschoid greywackes enclosed within a pelitic matrix which illustrates a cleavage produced under soft-rock conditions. Knockers within this part of the succession exhibit varying degrees of hydroplastic deformation.

Units 9-11 consist of grey-green, maroon and black, occasionally pyritiferous, shales, pebbly mudstones, siltstones, sandstones and conglomerates and their metamorphosed equivalents. They represent a resedimented sequence of submarine mass-transport flows, particularly turbidity and inertia flows. Turbidites are arbitrarily divided into three types: - i) Thinly bedded (0.5-5 cm) units of fine sand and silt that are commonly graded or laminated (A and B divisions) and overlain by darker silty mudstones. Basal contacts are sharp and non-erosional. These possibly represent outer fan or interchannel middle or inner fan deposits. ii) Coarser and thicker (5-200 cm) units of sandstone separated by silty mudstone. Individual units may be amalgamated or simple. Basal contacts are sharp and non-erosional. Many exhibit good A, AB or ABC Bouma divisions, and sand rolls, ball and pillow and detached load structures formed by loading and liquefaction under high rates of deposition are also conspicuous. These possibly represent inner or middle fan deposits. iii) Pebbly sandstones and conglomerates which cannot be described using the Bouma model. Units are graded and cross-stratified and are considered to represent inner or middle fan channel deposits.

Intimately associated with the turbidite deposits are inertia flows which consist of either ungraded structureless pebble conglomerates or massive (120 cm) structureless sandstones containing randomly oriented clasts and interpreted as grain flows and localized pebbly mudstones interpreted as slurry flows (see Carter, 1975). Other non-turbiditic horizons occur in places and consist of mudstones with gradational silty laminations; these are interpreted as material reworked by normal bottom currents during quiescence or, alternatively, may be outer fan or basin plain deposits.

Thus far, no body fossils have been recorded from the area proper. The age of the Davidsville Group (units 7-11) therefore remains uncertain and must be estimated by correlation with previously recorded data from localities within the Davidsville Group to the southwest. In this respect Jenness (1963) has recorded the brachiopod genera **Hesperothis, Chaetes, Valcourea** and **Horderleyella**(?) and the graptolites **Climacograptus** spp., **Dicranograptus,**

Diplograptus and **Nemagraptus** from the Gander Lake area. The genera are collectively indicative of a Middle Ordovician (Caradoc) age. More recently McKerrow and Cocks (1977) have recorded deformed brachiopods assignable to **Hesperothis** and an undescribed new orthid probably related to **Eostrophonema** from the Davidsville Group at Gander Lake and a single trilobite pygidium **Annamitella**(?) cf. **Annamitella**? **borealis**. This fauna clearly indicates an Arenig or Llanvirn age and in addition shows affinities with faunas from the southeast of the Iapetus Ocean in coastal New England and Wales (see Neuman, 1964; Bates, 1968). Thus, though based on rather sparse and isolated faunal evidence, it would appear that the Davidsville Group is at least Arenig to Caradoc in age and, as most of the fossil localities are well removed from the base of the sequence, may contain even older rocks.

Although the Davidsville Group within the Carmanville map-area has not yielded body fossils a number of previously unrecorded trace fossils were discovered. The most profitable locality in this respect is found on Green Island in unit 8. Here the olistostrome yielded an ichnofauna provisionally diagnosed as **Tomaculum, Planolites, Sinusites, Lockeia**?, **Phycodes**, bilobate repichnia, cf. **chondrites**, cf. **Bergauria** and horizontal bifurcating trails. Though no facies specific and depth related inchnofaunas are present the list does include useful chrono-stratigraphic indicators - viz. **Bergauria** which is Cambro-Ordovician and **Tomaculum** which is generally regarded as Ordovician (Hantzschel, 1975). Elsewhere in the region ichnofaunas are particularly sparse and poorly preserved. Where present they are found as hypichnial casts and are usually restricted to **Planolites** and **Sinusites**. An important exception is found within a turbiditic facies of unit 7 some 2000 m north of Mann Point where a single thin (5 cm) turbidite unit is thoroughly bioturbated by **Chondrites**.

Granitoid plutons of the Carmanville map-area fall into four major types which may be described as the Rocky Bay type, Aspen Cove type, Ragged Harbour type, and Deadmans Bay type. Two quartz diorite plutons (unit 15) intrude the central part of the Davidsville Group (Rocky Bay and Frederickton plutons). The Frederickton Pluton consists of two bodies separated by a screen of metamorphosed sediments and basalts. The northern and smaller body is cut by a 500 m wide east-west trending zone characterized by a more potassic composition (granodiorite) which has been intruded by numerous dykes. The granodiorite and most of the dykes have a well developed foliation roughly parallel to the foliation in the surrounding rocks. The central parts of both the Frederickton and Rocky Bay plutons are massive and dykes are uncommon. In the marginal facies of both plutons, amphibole is more abundant than biotite and exhibits a primary preferred dimensional orientation that is only poorly developed, if at all, in biotite. Both plutons exhibit a well developed contact aureole containing andalusite and cordierite and displaying widespread rheomorphic deformation.

Three similar bodies of quartz monzonite outcrop in the southeastern parts of the Davidsville Group (Aspen Cove and Island Pond plutons and White Point complex, units 12-14). These bodies all contain an essentially massive core of quartz monzonite (unit 14) consisting of about 20 per cent quartz, 30 per cent each of oligoclase (An_{25-30}) and faintly perthitic alkali feldspar, with 15-20 per cent of biotite and traces of muscovite. The margins of the intrusions are markedly enriched in muscovite and alkali feldspar, at the expense of plagioclase and biotite and pass gradationally into garnetiferous aplite, which is common in the dyke phases. Phases containing abundant fine grained biotite (unit 13) and approaching micro-granite occur commonly as dykes in the White Point complex, and sparsely as marginal phases in the Island Pond pluton.

The Island Pond pluton displays a well-defined contact aureole of andalusite-cordierite type. The Aspen Cove pluton displays a good aureole of the same type to the west and northwest, but to the east it passes gradationally into migmatite and lit-par-lit gneisses containing fibrolitic sillimanite (unit 12). The White Point complex consists essentially of such lit-par-lit and migmatitic material, with relatively small pods of homogeneous, massive to foliated granitoid rocks.

The Ragged Harbour and South Pond complexes (units 16-18) exhibit a characteristic core of trachytoid porphyritic quartz monzonite (unit 17) containing laths of faintly perthitic alkali feldspar about 2-3 cm long by 0.5-1.0 cm in the other directions. These crystals exhibit both planar and linear orientation. In some cases aligned inclusions occur, crossing the crystals at an angle, and continuous with faint foliation in the matrix, demonstrating postsolidification growth. In other cases the inclusions are concentric, and the crystals appear to be phenocrysts. Sharply defined dykes of porphyritic material cut the surrounding non-porphyritic granitoid rocks (unit 16). In other places the contact appears to be gradational. Typically the mafic minerals of the porphyritic phase consist of biotite, with traces of muscovite. In the case of the Ragged Harbour Pluton, an oval area of about 2 km in length is much more leucocratic. The rock consists essentially of quartz and perthitic potash feldspar, with accessory amounts of muscovite and reddish, pinhead garnet (unit 18). This unit appears to be the youngest phase of the Ragged Harbour Pluton, but it could be a separate intrusion, since no contacts have been found. The Ragged Harbour and South Pond plutons are joined by a belt of heterogeneous and migmatitic granitoid rocks, most commonly consisting of medium to coarse grained, faintly gneissic, pale grey biotite granodiorite. Nebulous screens and schlieren of Flinns Tickle complex (units 1-2) up to 100 m across occur irregularly within this matrix, and in a few places the rock approaches migmatite. Typically however it is fairly clean granitic gneiss.

Only the western extremity of the Deadmans Bay Pluton outcrops in the map-area. The contact with the Flinn's Tickle sequence is approximately conformable, but xenoliths of the latter are found within the pluton. The plutonic rocks vary slightly from place to place, but consist in general of massive, coarse biotite granodiorite containing 25-40 per cent of pink alkali feldspar megacrysts 2-6 cm in length. Megacrysts may exhibit plagioclase rims, and/or zones of inclusions. Alignment of euhedral megacrysts commonly defines an excellent foliation in the rocks, but no tectonic foliation is present.

Structural Geology

The map-area falls into two separate domains. We have therefore measured deformation separately in each domain.

Davidsville Group

Although the gross structure and hence the stratigraphy of the Davidsville Group is imperfectly understood, the rocks show clear evidence of repeated metamorphism and deformation. The Davidsville Group exhibits a dominant planar fabric commonly trending northeast-southwest with steep dips. Over most of the map-area the fabric is a slaty cleavage, but between Rocky Bay and Ragged Harbour it becomes a through-going schistosity. This main fabric is axial planar to close to isoclinal folds with similar styles and plunges that vary, often within a few metres, from steep to horizontal. Where bedding is thinly laminated, a prominent bedding-cleavage intersection is found.

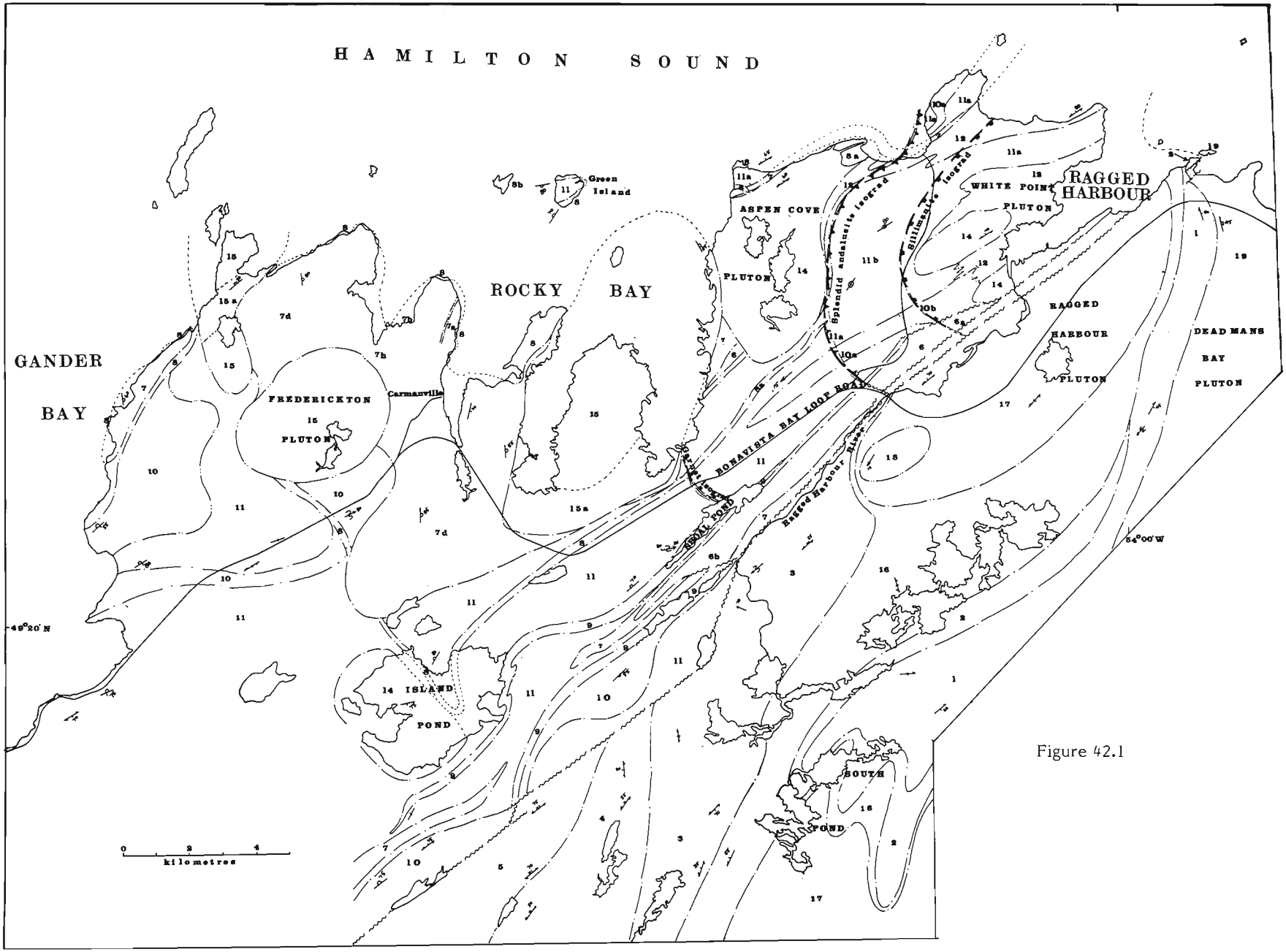
HAMILTON SOUND
GANDER BAY
ROCKY BAY
RAGGED HARBOUR
WHITE POINT PLUTON
ASPEN COVE PLUTON
Green Island
FREDERICKTON PLUTON
Carmanville
BONAVISTA BAY LOOP ROAD
CANAL POND
Ragged Harbour River
RAGGED HARBOUR PLUTON
DEAD MANS BAY PLUTON
14 ISLAND POND
SOUTH POND
49°20'N
54°00'W
0 2 4
kilometres

Figure 42.1

MAP LEGEND

DEVONIAN OR CARBONIFEROUS(?)

19 DEADMANS BAY PLUTON; Coarse grey biotite granodiorite with pink alkali feldspar megacrysts

LATE DEVONIAN

RAGGED HARBOUR AND SOUTH POND PLUTONS (units 16-18)

18 White muscovite leucogranite, commonly garnetiferous. Commonly aplitic with coarse grained to graphic schlieren and patches

17 Trachytoid, porphyritic (or porphyroblastic) pale grey biotite granodiorite

16 Heterogeneous granitoid gneiss and pegmatite with schlieren of units 1, 2

DEVONIAN

ROCKY BAY AND FREDERICTON PLUTONS

15 Homogeneous coarse grey tonalite with poikilitic biotite clots, commonly amphibole-bearing, marginal phases rich in lineated amphibole. 15a, foliated granodiorite rich in dykes

ISLAND POND AND ASPEN COVE PLUTONS AND WHITE POINT COMPLEX (units 13-15) (may be younger than 16-18)

14 Massive to foliated, coarse pink biotite-muscovite quartz monzonite, locally garnetiferous in leucocratic phases

13 Fine grained, equigranular biotite granodiorite and quartz monzonite

12 Sheeted complex of biotite-muscovite granodiorite, commonly garnetiferous, with sheets of units 9a, 10a and 11a, patches of coarse pegmatite, and dykes of unit 14

ORDOVICIAN

DAVIDSVILLE GROUP (units 7-11)

11 Finely interbedded black slate and grey greywacke and siltstone. 11a, metamorphosed equivalents, quartz-biotite-muscovite-garnet schist. 11b, rocks containing granitic pods and veins (anatectic melt)

10 Black, grey-green and maroon shale, including minor amounts of 10. 10a, metamorphosed equivalents, quartz-biotite-muscovite-andalusite-garnet (-cordierite) schist, 10b, sillimanite-bearing schists

9 Conglomerate of siltstone and greywacke pebbles, with minor ultramafic and plagiogranite debris in a chloritic matrix. Abundant interbeds of 10

8 Olistostrome breccia 6-7 and shale, siltstone and greywacke blocks with soft sediment deformation, all in a black pyritic, pelitic matrix. 8a, metamorphosed olistostrome breccia, 8b, indurated intensely deformed and fractured metapelite and chlorite-amphibolite schist

7 Massive to pillowed greenstone, agglomerate, tuff, minor black pelitic schist. 7a, shattered chloritized plagiogranite and porphyry, 7b, volcanoclastic fine-grained sediments and limestone, 7d, debris flows, 7h, hyaloclastites

6 GANDER RIVER ULTRAMAFIC BELT. Massive to schistose pyroxenite, peridotite and dunite. 6a, serpentinite, talc-chlorite-amphibole schist 6b, carbonate masses

ORDOVICIAN OR OLDER

GANDER LAKE GROUP (units 3-5) (age unknown relative to units 6-11)

5 Fine-grained, intensely cataclastic, pale green quartz-rich rocks and blastomylonite

4 Pale green, homogeneous quartz-muscovite-chlorite calcite schist, with rare amphibolite layers

3 Fine grained, homogeneous quartz-plagioclase-biotite schist

PRECAMBRIAN(?)

FLINNS TICKLE COMPLEX (units 1-2)

2 Heterogeneous gneisses containing more than 25 percent by area of granitoid component, usually as lits (lit par lit gneiss, migmatite, etc.)

1 Quartz-plagioclase-biotite gneisses, commonly containing garnet and sillimanite. Minor quartzite and garnet amphibolite

Primary fabric; tops unknown, tops known, overturned .....

Primary igneous fabric .....

Schistosity; inclined, vertical, second schistosity, third schistosity .....

Gneissosity; inclined, vertical .....

Rodding; pencil structure, mullions, mineral lineation .....

Minor folds with plunge and attitude of axial plane; sense of tectonic transport known, unknown .....

Fault of shear zone .....

Orientation of granitoid sweats and partial melts; inclined vertical .....

Geological contact; defined, approximate, deduced from airphotos, assumed .....

The main fabric is a composite of two deformation episodes, D1N and D2N, as can be seen in many thin sections where schistosity or slaty cleavage sweeps around porphyroblasts containing straight inclusion trails inclined to the external fabric. The evidence suggests that the main fabric resulted from two nearly co-planar deformations separated in time by a period of porphyroblastesis. In some localities D2N is represented by strong S2N crenulation cleavage at low angles to S1N. Rare separate macroscopic folds of D1N have been recognized.

On many outcrops this main fabric is kinked or crenulated, or both, by later structures. The earlier of these consists of a prominent crenulation cleavage, S3N, and associated minor F3N folds and crinkles. Some large folds, for example the open bend on the southwest side of Ladle Cove Head appear to be of D3N age. A generally shallow-dipping set of crenulations and minor folds with associated cleavage is widely developed in the Davidsville Group. At Ladle Cove Head and southeast of Island Pond these structures clearly postdate D3N. Analogy suggests that other shallow-dipping crenulations, minor folds, and cleavage may belong to this post D3N deformation.

Many outcrops throughout the area exhibit one or more sets of kink bands, mostly dipping steeply at high angles to S1N/S2N. They are best developed where the main fabric is strong slaty cleavage, and may occur singly, or in conjugate sets associated with small quartz and calcite veins. In places these kinks clearly postdate D3N crenulations. A small area east of Island Pond exhibits distinctive intense chevron-type small folding which may also postdate D3N. The significance of these small folds is not understood.

The Gneisses and Gander Lake Group

The structural evolution of gneisses and migmatites southeast of the Ragged Harbour Pluton appears similar to that of the higher grade parts of the Davidsville Group. Gneissic inclusions in the migmatites contain an intense crenulation cleavage (D2S) due to transposition of earlier gneissic banding (S1S). This S2S fabric is tightly folded about generally northeast-trending axial planes parallel to and continuous with the foliation in the migmatite matrix (units 2 and 13). Thus migmatization appears to have postdated D2S and occurred before or during a D3S deformation, as is the situation in the migmatitic terrane around Wesleyville (Jayasinghe and Berger, 1976).

The Gander Lake Group likewise exhibits three major periods of deformation, though it is not obvious that they are correlative to those in the gneisses. Identifiable S0 planes are extremely rare in the Gander Lake Group. An early north or north-northwest trending cleavage (S2S?) isoclinal to tight, minor folds (F2S?) occurs ubiquitously in the southern part of the group. The fabric is partially and locally transposed by a north-northeast trending cleavage (S3S?) locally associated with isoclinal, attenuated small folds (F2S?). Near the Ragged Harbour break, both of these structures are transposed and obliterated by intense northeast-trending, northwest-dipping cleavages, (S4S?) axial plane to rather rare, very attenuated isoclines (F4S). This S4S(?) cleavage normally intensifies to the northwest, but in a few areas this is reversed.

Granitoid Plutons

The Ragged Harbour Pluton postdates the structures in the migmatites, as pointed out by Kennedy and McGonigal (1972), but is itself foliated, especially in the west and north, thus providing evidence of a deformation later than D3 in the gneisses. The foliation parallels the most intense cleavage in the Gander Lake Group, and intensifies in the same direction.

All plutons northwest of the Ragged Harbour break exhibit, at least locally, a parallel cleavage (S3N). In the case of the Frederickton and Rocky Bay plutons this cleavage affects only the K-rich (older?) phases. The Island Pond Pluton exhibits a central foliated septum, while the Aspen Cove and White Point plutons are foliated on their margins. All exhibit a S to L-S fabric, generally vertical to steeply dipping. In many places foliation is cut at low angles by closely spaced microshears which constitute a crenulation cleavage. Around the Aspen Cove Pluton it can be demonstrated that fabric in the granite postdates S1N/S2N. Some of the thinner dykes and sheets in the country rocks can be seen to be folded by F3 crenulations and even post D3N kink bands. The evidence of the granitoid plutons suggests that D3N should be identified with D4S.

The Deadmans Bay megacrystic granite cuts the trend of both the Davidsville and the (D4S) foliation of the Ragged Harbour Pluton. It exhibits no tectonic fabric apart from some local shearing on east-west trending surfaces near Flinns Tickle. We conclude that it was emplaced after D4S.

Metamorphism

The Davidsville Group lies mainly in the chlorite-muscovite field, that is in low greenschist facies. Plutons intruded into this material contain andalusite-cordierite-garnet in their thermal aureole. Northeast of Carmanville, regional metamorphism of the Davidsville Group rises to amphibolite grade. We have been able to map successively the first appearance of garnet, chiastolite, coarsely crystalline pink andalusite-muscovite pods (splendid andalusite), and fibrolite. These data are shown on Figure 42.1. We have also obtained some incomplete data on the first appearance of biotite, which roughly parallels that of garnet, and of staurolite, which is rare. The lines marking the first appearance of minerals all display strong curvature about the White Point complex suggesting that this migmatite complex lies near the maximum of regional metamorphism. The P/T conditions of this maximum can be estimated from the continued stability of muscovite, the melting of compositionally favourable beds (Currie and Pajari, 1977, unit 11b) and the disappearance of andalusite, as being near 640°C and 4 kilobars (Fig. 42.2). The activity of water must have been close to 1.0 in order to stabilize muscovite on the solidus. Within the White Point complex, massive phases of the complex appear to intrude the migmatitic phases suggesting that intrusion slightly postdates peak metamorphism. Intrusions and melt pods exhibit two fabrics, postdating the main foliation, suggesting that intrusion occurred between D2N and D3N.

Megatectonic Considerations

The geophysical, geological, and sedimentological evidence suggests that the Davidsville terrane is an ocean floor sequence resting on ultramafic rocks thinly veneered by mafic volcanics. The thick east-facing succession of hyaloclastites and debris flows around Carmanville does not fit into this sequence, and its structure and facing are likewise anomalous. We conclude that this sequence represents remnants of an allochthonous sheet. This allochthonous sheet is spacially associated with olistostrome and mélange which form its base. The olistostrome in turn lies relatively low in the stratigraphy of the Davidsville Group. Therefore olistostrome formation and stacking of slices commenced early in the history of the Davidsville, possibly as early as Arenig. The original source of the volcanic slice is unknown at present but it presumably derived from a volcanic arc. The disposition of the oceanic terrane, with its southeastern boundary, extending southwest from Ragged Harbour is compatible with obduction from the northwest. Along the northeast part of this boundary, major faulting on this line is compatible with large displacement, but to the southwest large scale movement, if any, is less obvious.

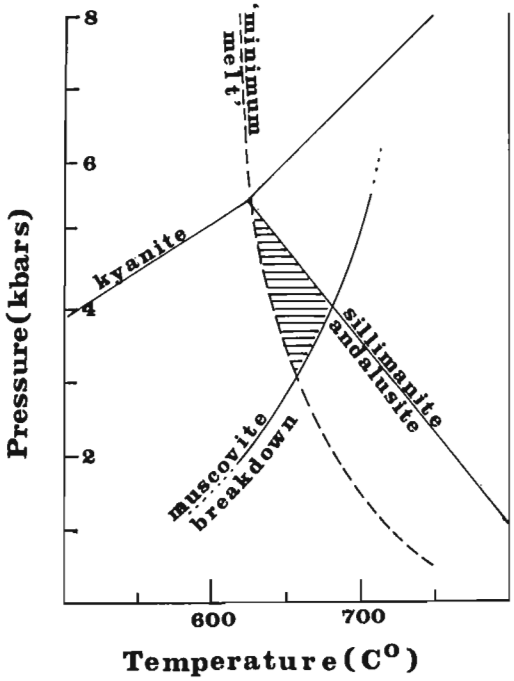

Figure 42.2

Estimate of peak metamorphic conditions in the Carmanville area. The most probable conditions of peak metamorphism lie in the hachured area. The aluminosilicate phase fields are taken from Richardson et al. (Am. J. Sci., v. 269, p. 259-272 (1969)). The alternate diagram of Holdaway (Am. J. Sci., v. 271, p. 97-131 (1971)) does not allow for the observed coexistence of andalusite and granitic melt. The 'minimum melt' curve is taken from Luth et al. (J. Geophys. Res., v. 69, p. 759-773 (1964)). The presence of plagioclase in the starting materials and/or activities of water less than 1.0 cause this curve to migrate to the right, so that the size of the hachured area would be reduced. Similarly the decrease in activity of water would cause the muscovite breakdown (after Kerrick, Am. J. Sci., v. 272, p. 946-958 (1972)) to migrate to the left, further reducing the hachured area. The activity of water must excede 0.9 to allow the coexistence of the observed phases.

To the southeast of this boundary, the polymetamorphic gneiss terrane exhibits the characteristics of continental basement. The lithologies of the Gander Lake Group correspond with a continental shelf or rise deposit. Hence, they could well be lateral correlatives of, or slightly older than, the Davidsville Group, as suggested by similar rocks of Cambro-Ordovician age in the comparable structural position elsewhere in the Appalachians and Caledonides (Rast et al., 1976). A corollary of this model requires large amounts of sediments to have been telescoped under, or ahead of, the ocean floor sequence as it was emplaced. We assume this material to be the ultimate source of both the thermal and magmatic activity during the Devonian.

In conclusion we note some things which we did not see:

1) There is no evidence of subduction, but only of obduction. This observation reinforces the symmetry of central Newfoundland noted by Williams (1964a).

2) There is no evidence of Precambrian orogeny, nor of Cambro-Ordovician metamorphism. The Ganderian orogeny of Kennedy (1975) appears to be fictitious.

3) There is no evidence of major granitoid pluton emplacement prior to Devonian. Thus the original interpretation of Williams (1964b) and Jenness (1963) has been vindicated, though in a vastly different setting.

References

Bates, D.E.B.

1968: The Lower Paleozoic brachiopod and trilobite fauna of Anglesey; Bull. Brit. Museum (Natural History), Geology, v. 16, p. 125-199.

Blackwood, R.F.

1977: Geology of the Hare Bay area, northwestern Bonavista Bay; in Report of Activities, Nfld. Dept. Mines and Energy, Mineral Development Division, Rep. 77-1, p. 7-14.

Carter, R.M.

1975: A discussion and classification of subaqueous mass-transport with particular application to grain-flow, slurry-flow and fluxoturbidites; Earth Science Reviews 11, p. 145-177.

Currie, K.L. and Pajari, G.E.

1977: Igneous and metamorphic rocks between Rocky Bay and Ragged Harbour, northeastern Newfoundland; in Report of Activities, Part A, Geol. Surv. Can., Paper 77-1A, p. 341-345.

Dewey, J.F. and Bird, J.M.

1971: Origin and emplacement of the ophiolite suite: Appalachian ophiolites of Newfoundland; J. Geophys. Res., v. 76, p. 3179-3206.

Hantzschel, W.

1975: Trace fossils and problematica; in Treatise on Invertebrate Paleontology (C. Teichert, editor), Part W. University of Kansas Press; Geol. Soc. Am., Lawrence, Kansas, p. W1-W269.

Jayasinghe, N.R. and Berger, A.R.

1976: On the plutonic evolution of the Wesleyville area, Bonavista Bay, Newfoundland; Can. J. Earth Sci., v. 13, p. 1560-1570.

Jenness, S.E.

1963: Terra Nova and Bonavista map-areas, Newfoundland; Geol. Surv. Can., Mem. 327, 184 p.

Kennedy, M.J.

1975: Repetitive orogeny in the northwestern Appalachians - new plate models based upon Newfoundland examples; Tectonophysics, v. 28, p. 39-87.

Kennedy, M.J. and McGonigal, M.H.

1972: The Gander Lake and Davidsville Groups of Northeastern Newfoundland. New data and geotectonic implications; Can. J. Earth Sci., v. 9, p. 453-459.

Malpas, J. and Strong, D.F.

1975: A comparison of chrome spinels in ophiolites and mantle diapirs of Newfoundland; Geochim. Cosmochim. Acta, v. 39, p. 1045-1060.

McKerrow, W.S. and Cocks, L.R.M.

1977: The location of the Iapetus Ocean suture in Newfoundland; Can. J. Earth Sci., v. 14, p. 488-495.

Neuman, R.B.

1964: Fossils in Ordovician tuffs, northeastern Maine; U.S. Geol. Surv., Bull. 1181-E, p. E1-E38.

Rast, N., Kennedy, M.J., and Blackwood, R.F.

1976: Comparison of some tectonostratigraphic zones in the Appalachians of Newfoundland and New Brunswick; Can. J. Earth Sci., v. 13, p. 868-875.

Williams, H.

1964a: The Appalachians in northeastern Newfoundland - a symmetrical two-sided system; Am. J. Sci., v. 262, p. 1137-1158.

1964b: Botwood, Newfoundland; Geol. Surv. Can., Map 60-1963.

Williams, H., Kennedy, M.J., and Neale, E.R.W.

1974: The northeastward termination of the Appalachians; in The Ocean Basins and Margins, v. 2 (F. Stehli, editor), Plenum Press, p. 79-123.

43. ST. GEORGE AND TABLE HEAD CEPHALOPOD ZONATION IN WESTERN NEWFOUNDLAND

Project 680130

Rousseau H. Flower[1]
Regional and Economic Geology Division

Abstract

Flower, R.H., St. George and Table Head Cephalopod Zonation in western Newfoundland; Current Research, Part A, Geol. Surv. Can., Paper 78-1A, p.217-224, 1978.

Faunal zones based mainly on cephalopods are proposed in the Ordovician Canadian St. George Group of western Newfoundland recognizing a sequence of Gasconadian, Demingian, Jeffersonian, and Cassinian, with some finer divisions in the Cassinian. Erosion of the St. George surface, most marked on Port au Port Peninsula, probably occurred in early Whiterock time (zone L of western Utah) which was a period of uplift, warping and erosion in western Newfoundland. The Table Head Formation represents deposition in zones M and N of Utah.

Introduction

Isolated occurrences of cephalopods have long been known from the Ordovician limestones of western Newfoundland (Billings, 1861-65; Barrande, 1867-1877; Hyatt, 1894, 1900), but not the detailed succession of such. Thanks to National Science Foundation grant GB 6809 it was possible for the writer to spend about a month in 1969 and nearly two months in 1971 collecting fauna mainly from the St. George Group and Table Head Formation. Although the grant was primarily for the systematic study of cephalopods, and large collections were made, it first became necessary to know the faunal succession; this is the subject of the present discussion.

The first great expansion of cephalopods is in the Gasconadian, Lower Canadian; the first time that the cephalopods became significant elements in shelly faunas of the Paleozoic. Ellesmeroceratidae dominate the faunas (Flower, 1964). The Middle-Upper Canadian development is marked by the expansion of two new orders, the Endoceratida and Tarphyceratida; the piloceroids are particularly characteristic among the endoceroids. The Table Head limestone contains a fauna of Whiterock aspect (Flower, 1968a, b, 1971, 1975, 1976a, b, c) marked by advances beyond Canadian faunas, but older and more primitive than those of the Chazy.

Previous Work

Early work (Logan, 1863) resulted in lettered divisions of the Lower Paleozoic beds of western Newfoundland. Schuchert and Dunbar (1934) presented a revision of these divisions; additional reinterpretations are to be found in Whittington and Kindle (1963, 1969) and Whittington (1968). These investigations propounded one great perplexity. Schuchert and Dunbar (1934) presented a succession based primarily on observations on the Port au Port Peninsula reporting the "**Diphragmoceras** beds" as lying above beds with piloceroids. The **Diphragmoceras** beds, sampled during the present investigation, have yielded a variety of genera, all Ellesmeroceratidae of Lower Canadian aspect. Finding such a fauna above a piloceroid fauna is an anomaly comparable to finding a dinosaur fauna above one with mastodons. This succession, however, was generally accepted. Riley (1962), citing unpublished work by Sullivan, indicated a zonation on the Port au Port Peninsula as shown by Table 43.1.

This succession involves the **Diphragmoceras** beds, 1 km southwest of The Gravels, to the Gravels (1 on Fig. 43.1b) and thence to the contact with the Table Head limestones, which can be found both to the northeast and the northwest (2 and 3 on Fig. 43.1b). Whittington and Kindle (1969) noted that this section is incompletely exposed, but essentially continuous. The stratigraphic position of beds 2 to 17 rest upon the assumption that there is a continuously ascending section from Lower Cove to the east.

Faunal Succession, Port au Port Peninsula

The following sequence was established on Port au Port Peninsula during the present investigation. Gross estimates only of the thicknesses of the various units are given. The resulting sequence of faunal units can be rather widely recognized in Newfoundland and can be correlated broadly with divisions of the Canadian throughout North America; these correlations are indicated in Figure 43.2.

I. The **Diphragmoceras** beds, at Green Head (Schuchert and Dunbar, 1934, p. 47), are 1.7 km southwest of the road across The Gravels, and consist of medium to dark grey limestones with some parts highly dolomitic, containing a prolific cephalopod fauna with minor gastropods (**Euconia** and some high-spired forms), **Finkelnburgia,** and stromatolites. Some of the stromatolites form small to medium sized columns with lamellae regular and close enough that they may be taken for straight cephalopods in the field. The cephalopods are exclusively Ellesmeroceratidae and include **Ellesmeroceras, Ectenolites, Dakeoceras, Levisoceras, Bridgeoceras** (which from this new material now can be assigned with certainty to the Ellesmeroceratidae), and three new genera. This is the source of Hyatt's (1900, p. 514) **Diphragmoceras.** This fauna is unquestionably Gasconadian (Flower, 1964, p. 23, 148, 149). Beds below were not examined; they are exposed in a vertical cliff that drops to the sea. Whittington and Kindle (1969) have shown that beds between this point and those farther west along the south shore contain some significant Cambrian beds. Marked changes in strike and dip occur and continuity of the beds downward to the west is broken by faults. The main cephalopod-bearing beds occupy a thickness of 7.5 m; 6.1 m higher occurs another algal bed at 3.0-4.6 m of predominantly columnar algae with apparently the same fauna, but fossils are scarcer.

II. Overlying dolomitic limestones, a 6 m interval, with gastropods — an **Ophileta**(?) and a large **Lystospira.**

III. Some distance higher (3-9 m) occur two thin bands 1 m apart containing pink limestone pebbles, suggesting a break in the section and implying elevation of a nearby surface to supply the pebbles. This marks a period of uplift and erosion which was probably universal throughout eastern North America. Succeeding beds are vermicular dolomites and dolomitic limestones with sparse fossils (**Lecanospira** and **Basslerocera**s). Higher beds were not examined in detail at this locality, but from here to The Gravels there are considerable covered intervals and changes in dip and strike suggesting faulting of the strata.

In Figure 43.1b, number 1 indicates the section from the **Diphragmoceras** beds to The Gravels; part of this section is covered. Numbers 2 and 3 indicate continuity of the section northwest to the base of the Table Head Formation near

[1] New Mexico Bureau of Mines and Mineral Resources, New Mexico Institute of Mining and Technology, Socorro, New Mexico 87801.

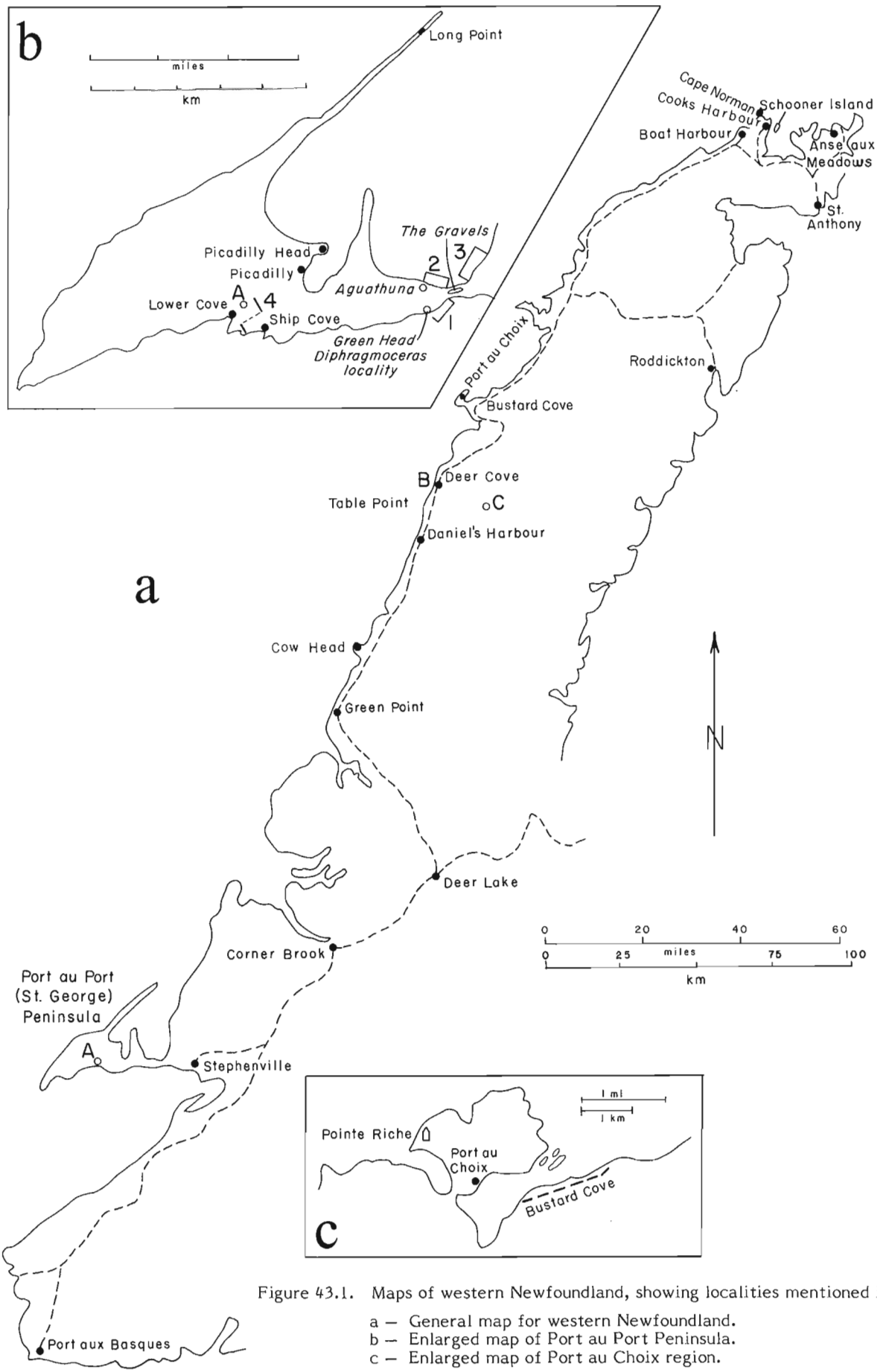

Figure 43.1. Maps of western Newfoundland, showing localities mentioned in the text.

a — General map for western Newfoundland.
b — Enlarged map of Port au Port Peninsula.
c — Enlarged map of Port au Choix region.

A, B and C represent the localities of faunas A, B and C in the upper St. George Group discussed in the text, and indicated in Figure 43.2.

Table 43.1

Succession on Port au Port Peninsula
(after Riley, 1962)

	feet below top	approximate thickness of interval in metres
(barren or unassigned)	0-40	12
Zone of **Ceratopea** (beds 44-52)	40-95	16.5
(barren or unassigned)	95-610	154.5
Zone of **Maclurites** (beds 36-38)	610-890	84
(barren or unassigned)	890-1431	162.3
Zone of **Diphragmoceras** (bed 17)	1431-1446	4.5
(barren or unassigned)	1446-2200	226.2
Zone of **Lecanospira** (bed 2)	2200-2220	6
(barren or unassigned)	2220-2430	64
Zone of **Piloceras** (bed 2 or 1)	2430-2500?	21

The last column is an addition by the writer; it should be noted that large intervals of the St. George Group yield no fossils or only unidentifiable fragments, most commonly poorly preserved gastropods.

Aguathuna, and northeast to the base of Table Head Formation on the mainland.

IV. At the south shore just east of Lower Cove, at the base of section 4 on Figure 43.1b, similar vermicular dolomitic limestones were found containing poorly preserved but unmistakable **Bassleroceras;** the beds exposed are 24-30 m thick. A fault at Lower Cove appears to eliminate more of the upper dolomites at the south shore than are present in the hillside to the northeast of Lower Cove. Horizon IV contains the fauna noted by Whittington and Kindle (1969, p. 658). This fauna is Demingian, and strongly resembles the more vermicular and more dolomitic phases of the lower half of the Fort Ann Formation in the Fort Ann region (Flower, 1964, p. 158). It overlaps unit III above.

V-VI. Across a distance of a hundred metres, interval V is covered or sporadically exposed, then, just before reaching a turn in a lane leading north from the main road, there is a conspicuous, white weathering 1.5 m **Cryptozoan** ledge and for 6 m above this occurs the **Pycnoceras apertum** fauna (VI), also in light grey, white weathering limestones. This horizon contains **Pycnoceras apertum** (by lithology the holotype came from these beds), endoceroids including **Proendoceras** and **Clitendoceras,** Baltoceratidae, Protocycloceratidae and a variety of smooth low-spired gastropods, certainly neither **Lecanospira** nor **Orospira.** It can be traced eastward to Ship Cove.

VII. There follows light to medium grey limestone, weathering light grey, barren (except for poorly preserved and generically undeterminable low-spired gastropods). This interval is 54 m thick.

VIII. The **Cassinoceras wortheni** zone consists of somewhat darker weathering limestones, with hues of blue and drab; fresh surfaces are light grey and fossil surfaces and stylolitic structures are commonly pink. This zone is subdivisible into three subzones as follows (in ascending order):

1. A thickness of 6-7.5 m of limestone, slightly lighter than the beds above, yielding silicified **Ceratopea unguis** and a **Teiichispira,** also occasional Tarphyceratidae, Endoceratida, and **Protocycloceras.**

2. An interval 12 to 18 m of massive limestones with sparse 0.3-0.6 m dolomite intervals, yielding the main **Cassinoceras wortheni** fauna. Several species of **Cassinoceras** and at least one of true **Piloceras** occur, associated with slender Endoceratidae, small Protocycloceratidae and Baltoceratidae, coiled shells including a large new **Eurystomites,** smaller **Tarphyceras, Centrotarphyceras** and possibly **Pionoceras** and **Curtoceras.** Gastropods include macluritid operculae similar to those illustrated by Billings (1861-1865, p. 243, figs. 228-230; fig. 229 is the commonest and the most conspicuous), **Maclurites, Murchisonia simulatrix, M. cicelia** and other much larger species. Sponges are sparse, trilobites are present but fragmentary. There is little silicification of these limestones, and their fossils are difficult to chop out or to prepare.

3. Above this are 6-9 m of slightly lighter weathering limestone in beds 0.3-0.9 m thick, alternating with frequent 0.6-1.2 m beds of tan weathering dolomite. These beds have a sparse cephalopod fauna mainly of endoceroids and piloceroids, which are quite different from those of the beds below. This interval was insufficiently collected but is marked by a long very slender **Ceratopea** operculum.

IX. There follows a thickness of 60-75 m of light grey white weathering dolomite; bedding is obscure, but evidently steepens toward the top of the section. A fault occupies the valley in which Lower Cove is found (the hills immediately to the west expose the barren interval between the **Pycnoceras apertum** fauna and the **Cassinoceras wortheni** fauna). Three to 5 m above the base of the dolomite are three to four thin bands of white weathering porcelaneous chert in discontinuous bands, none more than 10 cm thick, without fossils. Twelve metres up in the section some scattered siliceous material has yielded a small fauna of small **Tarphyceras** (probably only the inner whorls were silicified), a low-spired gastropod with the outer angle very sharp, and a small **Palliseria.** This is a late Canadian fauna, containing the oldest **Palliseria** certainly known. It is indicated by A on Figures 43.1a and b, and on Figure 43.2. In Nevada, **Palliseria** occurs in the **Palliseria-Maclurites-Girvanella** beds, rather high in the Whiterock Stage (Ross, 1964a, b).

In joining lower beds of the **Diphragmoceras** zone with a much better section east of Lower Cove, the result is a zonation in which Gasconadian, Demingian, Jeffersonian, and Cassinian beds can be recognized in a sequence comparable to that which occurs throughout North America from the Appalachians to Nevada. It is also possible to recognize many of these horizons farther north in western Newfoundland.

The section downward from the **Diphragmoceras** beds to the west is interrupted by faults. The section east of Lower Cove is continuous.

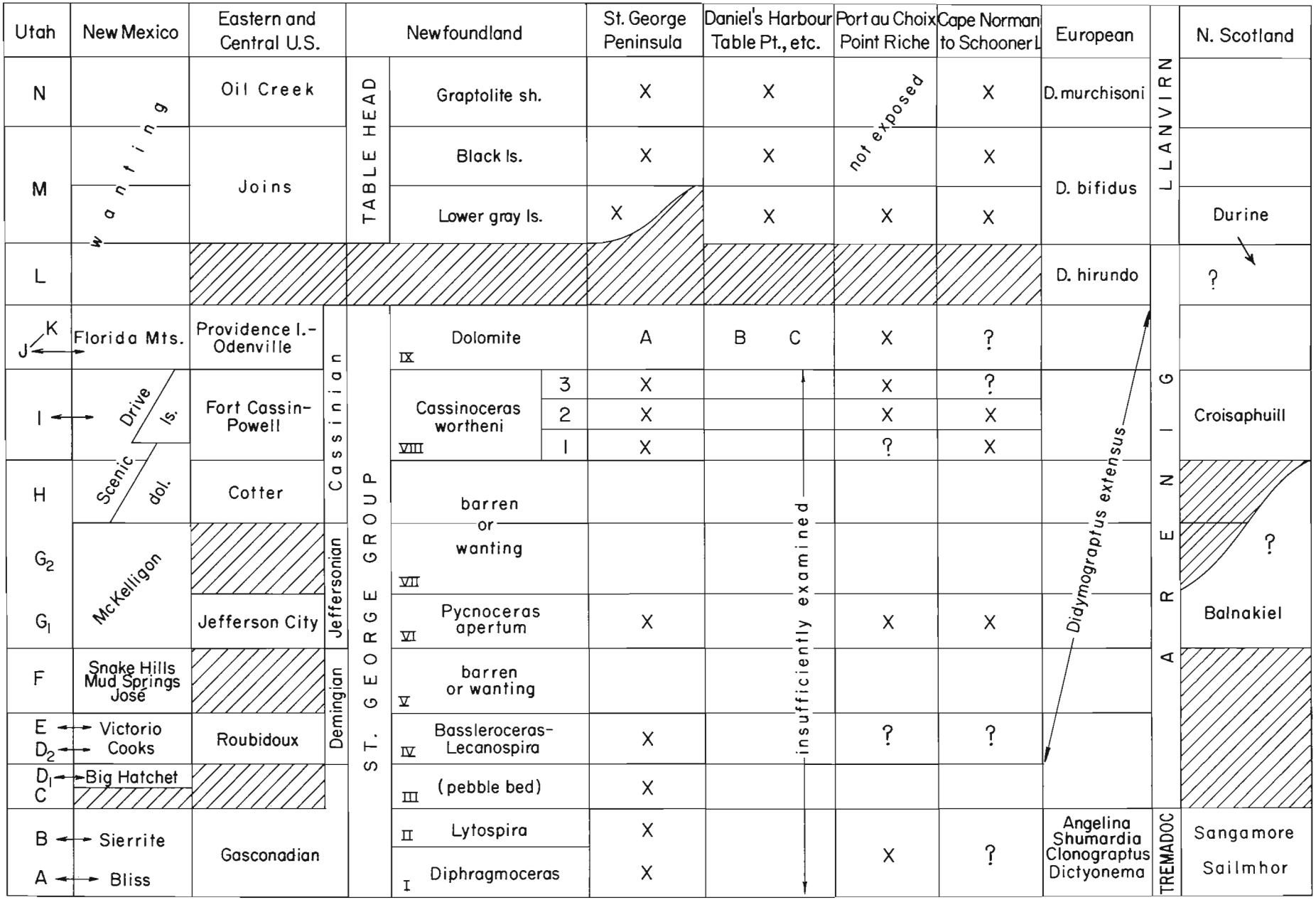

Figure 43.2

Correlation of St. George Group and Table Head Formation of western Newfoundland showing the main zones, their occurrence as observed in four main sections; on the left equivalent beds of eastern and central United States are indicated. It is held, for reasons discussed elsewhere, that eastern North America has gaps in deposition one representing zones C and lower D of Utah, another representing the high Demingian of New Mexico (the José, Mud springs and Snake Hills), a third representing the upper half of the McKelligon of New Mexico, and another representing zone L. Firm correlations between the classic Ibex section of western Utah and the El Paso Group of New Mexico occur only where arrows are present. Faunas A, B and C in the upper St. George Group are discussed in the text.

Table Point Region

To the north of Table Point (the type section of the Table Head Formation, Fig. 43.3) the section descends into upper dolomites of the St. George Group. At B on Figure 43.1a, known locally as Deer Cove, medium to light grey weathering dolomites have yielded a distinctive fauna, the most conspicuous elements of which are large piloceroid siphuncles of the shape of true **Piloceras**, but unlike it in their blade and tube arrangement, also a large **Eurystomites** and smaller coiled forms, with some Baltoceratidae and Protocycloceratidae. This is unlike the **Cassinoceras wortheni** fauna. A second isolated exposure (C on Figure 43.1a), exposed by a bulldozer, occurs along a gravel road to Hawke Bay which branches northerly from the Newfoundland Zinc mine road; the exposure is 19 road-km from the junction of the mine road and coastal highway 430. The fauna there has yielded a small but unmistakeable **Buttsoceras**, a true **Proterocameroceras**, a possible **Tarphyceras** or **Curtoceras** (weathered below the middle), and a small obese coiled shell with low but prominent closely-spaced costae, which is possibly an undescribed genus. It is known only from an impression of the exterior, so it is uncertain whether it belongs to the Tarphyceratidae or to the Trocholitidae.

Port au Choix Region

There is an erosional unconformity between the Table Head limestone and the underlying St. George Group (Cumming, 1968, p. 3, fig. 5). The uppermost St. George beds (Fig. 43.4) are light grey to light tan weathering dolomites, and are largely barren. This is division I of Logan; Schuchert and Dunbar give a thickness of 45 m for these beds. Below are medium to dark grey weathering limestones containing the **Cassinoceras wortheni** fauna, with the long slender **Ceratopea** of the uppermost zone, and the fauna of the second zone. Passing northward, descending in the section, a thickness of barren dolomitic limestones is encountered, but with the **Pycnoceras apertum** fauna in dark grey slightly dolomitic limestone. The thickness of the intervening barren interval was not measured, but is less than half that found on Port au Port Peninsula. Below this fauna is a **Cryptozoan** bed comparable to that of the Port au Port Peninsula. On the east side of Bustard Cove the **Cassinoceras wortheni** horizon is more fully exposed (Whittington and Kindle, 1963, 1969) in beds not belonging to a lower or higher horizon. Collections from this place, incomplete stratigraphically, have yielded a large fauna with **Deltoceras planum**, some new large **Aphetoceras**, piloceroids and smaller cephalopods.

Schuchert and Dunbar (1934) and Whittington and Kindle (1963) have noted, and Cumming (1968) has presented a map, showing the lower grey limestones of the Table Head Formation on the southern half of the peninsula, and extending south along the shore. Neither the upper black limestone nor overlying graptolite shale is exposed.

Cape Norman and Vicinity

Near the lighthouse on Cape Norman, beds of dark grey dolomitic limestone are exposed that yield the main **Cassinoceras wortheni** fauna. Several other exposures yield this same fauna between Cape Norman and Cooks Harbour, but there is rapid lateral gradation into dolomite in which the fossils are greatly obscured or obliterated. The upper light grey dolomites of previous sections have not been definitely recognized. From Boat Harbour east toward Cape Norman are (1) vermicular dolomites with traces of the **Basslerocerас** fauna, and (2) ledges of dark dolomitic limestones with the fauna of the **Pycnoceras apertum** horizon. Above are barren dolomites. This region is separated by a fault from the beds at Cape Norman.

Schooner Island was briefly examined in a section from Schooner Cove south to the peninsula just north of Savage Cove. The lowest beds seen are vermicular dolomites suggestive of the **Basslerocerас** horizon, but no fossils were seen. There follow some dolomites with light grey lenses full of cephalopods, suggestive of the **Pycnoceras apertum** fauna, but dolomitization is so advanced that proper identification of the fauna is not possible. Passing south, the **Cassinoceras wortheni** fauna is well developed. It occurs in a black, slightly dolomitic limestone containing abundant worm borings and irregular masses of chert. The first and second subzones could be readily recognized.

St. George Erosion

Cumming (1967, p. 12, 1968) recognized that St. George deposition was followed by a period of uplift and erosion, and pointed out the relevance of this phenomenon to the mineral deposits in the St. George Group. He reported a channel 9 m deep in buff dolomite of the St. George surface filled with a black limestone of the Table Head Formation, in the quarry at Aguathuna. Additional evidence exists. Northwest of The Gravels, light grey Table Head limestone lies on tan weathering limestone, which represents the lowest of the three subzones of the **Cassinoceras wortheni** beds, as it yielded **Teiichispira** and **Ceratopea** cf. **unquis.** This means that in contrast to the section east of Lower Cove the upper dolomites, comprising at least 75 m of dolomites and 18-24 m of the underlying limestones have been removed.

The overlying Table Head limestones are massive beds, a much lighter grey than at Table Point or Point Riche, and much less fossiliferous. Megafossils, particularly the cephalopods, so abundant at those northern localities, are scarce and are confined to only a few bedding planes.

At Picadilly, the highest beds exposed of the St. George are again the lowest of the three subzones of the **C. wortheni** faunas, and thus there is a removal of upper beds. However, at that locality, there is none of the lower grey limestone of the Table Head; there are 4.5-7.5 m representing the upper black limestones, though again lighter than at Table Point, followed by the upper graptolite-bearing shales, which are exposed for some distance farther to the northwest where the coast is nearly parallel to the strike of the beds. However, at the Picadilly Head provincial park there is a breccia of light grey limestone boulders to pebbles in a similar grey matrix; both have yielded a sparse fauna but one of lower Table Head age.

The period of uplift, warping, and then uneven erosion of the St. George surface can be reasonably dated. Of the three faunules so far recovered (A, B and C on Figure 43.1a) from the upper dolomites, division I (IX of Figure 43.2), one contains a distinctive fauna with **Buttsoceras**, true **Proterocameroceras**, and a small obese, closely costate coiled shell. The **Buttsoceras** indicates that this fauna is latest Canadian. L.M. Cumming has collected a similar fauna from the Roddickton region on the east side of the Great Northern Peninsula. If St. George deposition continued to the close of Canadian time, the period of uplift and erosion must have occurred in early Whiterock time. The graptolite, conodont and trilobite faunas suggest that the lower Table Head is equivalent to zone M of western Utah (Ross, 1951; Hintze, 1951, 1952). The cephalopod evidence supports this correlation. Wutinoceratidae, unknown in Utah below zone N and unknown in Nevada below the **Palliseria** zone, appear first in the lower beds of the Table Head limestone, as does **Aethiosolen**, which is also not known in Utah below lower zone N, although in Nevada it appears in the sponge beds. **Nolanoceras** and **Eogomphoceras** are found in the Sponge Beds of Nevada which may be low N or M, and both range through the lower Table Head limestones. In the middle of the lower grey limestones of the Table Head Formation **Holmiceras** appears, a genus formerly known only from the Kunda of the Balto-Scandinavian region, and the lower grey limestone is also the source of a true **Cyclolituites, C. americanus,** a genus known in Scandinavia only from the late Whiterock Lasnamägian (Flower, 1975).

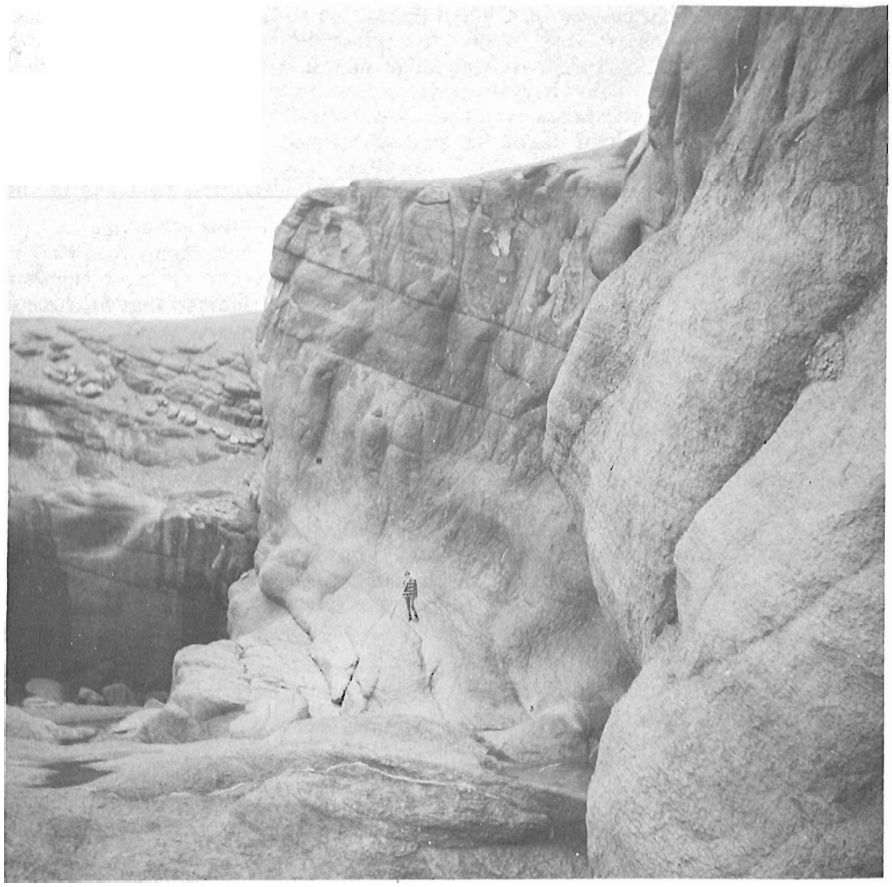

Figure 43.3

Massive grey limestone that is typical of the lower 810 feet of the Table Head Formation at its type section near Table Point. Note the rubble of limestone chips formed along the weathered upper surface of these limestones. GSC photo no. 123889 (L.M. Cumming).

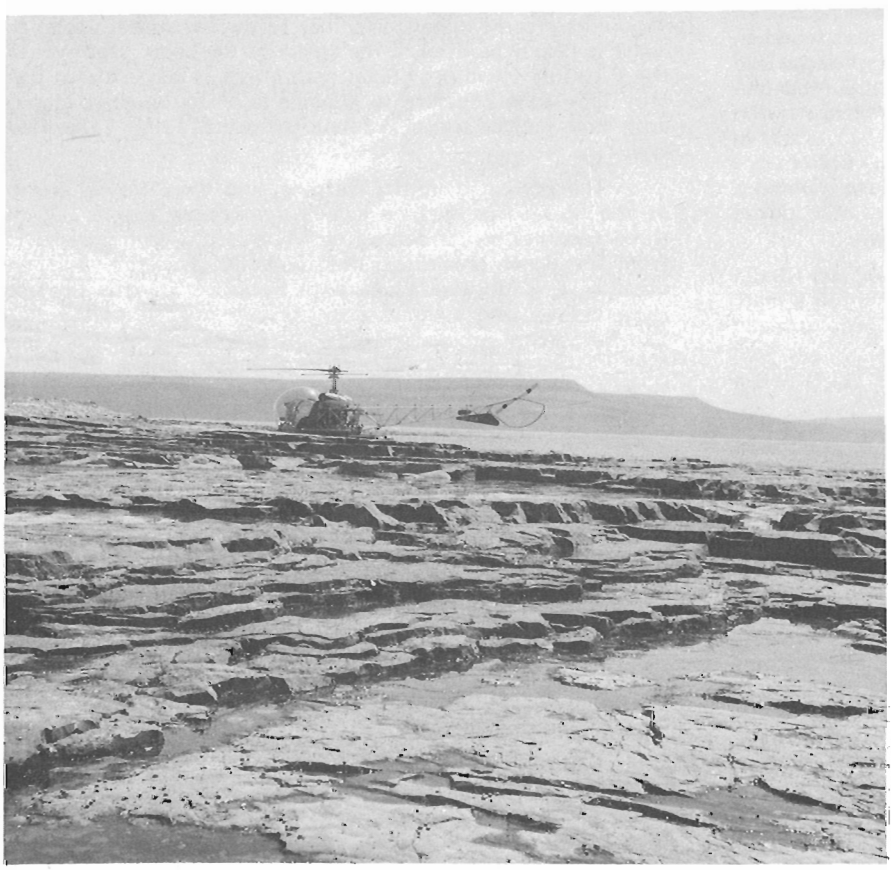

Figure 43.4

View from Turr Island (50°51'04"N, 57°06'38"W), near Port au Choix, toward the southeast and the summit of the Highlands of St. John. Turr Island is underlain by flat-lying, tan, dolomite of the St. George Group. GSC photo no. 1-7-71 (L.M. Cumming).

There is, then, considerable evidence indicating that the Table Head limestone represents zone M, the **D. bifidus** fauna of England and the Balto-Scandinavian region, but not zone L, which is basal Whiterock in western Utah, and reasonably continues through zone N. Bergström and Cooper (1973) have shown that in North America **D. bifidus** occurs at two discrete horizons, of which the Texas and Arkansas occurrences are Upper Canadian, while those of the Kanosh of Utah and the Joins of Oklahoma equate with the European zone.

It is also worthy of note that just as the lower limestones of the Table Head Formation are lighter in colour and more massive on Port au Port Peninsula than at Table Point or more northern localities, the same is true of the St. George Group. The **Pycnoceras apertum** faunas are in light grey-white-weathering limestones on Port au Port Peninsula; comparable faunas occur in dark grey slightly dolomitic limestones both at Port au Choix and at Cape Norman. Likewise, the **C. wortheni** faunas occur in light to medium grey limestones on Port au Port Peninsula.

At Port au Choix and Cape Norman these beds are very dark limestones, somewhat dolomitic, and are even darker on Schooner Island, where the lithology is reminiscent of the Croisaphuill limestone of northern Scotland. The faunas also are closely allied; both contain **Cassinoceras** and true **Piloceras**, similar Tarphyceratidae, Baltoceratidae and Protocycloceratidae, although some occurrences in the Croisaphuill fauna have not yet been published.

Maps showing localities discussed above can be found in Schuchert and Dunbar (1934, p. 2), Williams (1967), Cumming (1968), Kluyver (1975), Whittington and Kindle (1969) and Riley (1962). A map presented by Bird and Dewey (1970) differentiates the St. George Group and Table Head Formation, but they recognize Table Head only in a narrow belt extending south from Cooks Harbour with no Table Head at the type locality or several other significant occurrences, notably on Port au Port Peninsula.

Additional Faunal Notes

Barrande (1874, text part 3, p. 716-724; 1870, pls. 430-435 pars) described a number of fossils from Newfoundland collected by M. le Capitain de la fregate Cloué, commandant de la station francaise dans ces parages en 1859 et 1860. They are elsewhere indicated as "near fishing villages in Newfoundland". Ulrich et al. (1944) noted the illustrations of Barrande, but overlooked his later description of these fossils, and suggested that **Nautilus avus, Orthoceras recedens** and **Trochoceras incipiens** may have come from the Canadian, although neither the precise horizon or locality are known. It was possible for the writer to see most of this collection in the Musée d'Histoire Naturelle, Paris (which Barrande reported as the repository of this material). Of these **Orthoceras insulare** and **O. atlanticum** are Endoceratidae, the first is a synonym of **O. piscator** Billings, as Barrande had suggested. **O. clouei** includes a specimen of **Cyrtonybyoceras haesitans** and two or more species assignable to **Wutinoceras; Trochoceras incipiens** is a valid species assignable to **Plectolites** and **Nautilus avus** is a **Litoceras.** All are from the Table Head limestone in its northern range. A likely source is Point Riche which is near the harbor of Port au Choix and of easy access.

The lower Table Head is predominantly limestone, but may be dolomitic locally. L.M. Cumming collected Table Head actinoceroids from the northeastern part of St. John's Island where, from the dolomitic matrix, they were first thought to come from the St. George Group. There has been some confusion as to the stratigraphic origin of **Litoceras;** Ulrich et al. (1942) believed that **Litoceras versutum** (Billings), from dolomitic beds of the Bonne Bay area, came from St. George Group (see also Ulrich et al., 1944). After extensive collecting of coiled cephalopods, both in the St. George Group and in the Table Head limestone, it is clear that there is no true **Litoceras** in the St. George Group nor in any known Late Canadian faunas. Specimens very close to **L. versutum** have been obtained in the Table Head limestone, from which I have obtained at least 35 large coiled cephalopods; all but two belong to **Litoceras.**

Correlations

Current investigations by the writer and others lead to the conclusion that St. George Group embraces strata ranging in age from Gasconadian, Lower Canadian, through high and probably highest Canadian beds. The Gasconadian equates with the Tremadoc of Great Britain. Middle-Upper Canadian beds equate with the lower Arenig of Great Britain up to the base of the **Didymograptus hirundo** horizon, the Billingen and Hunneberg of the Baltic realm. The Whiterock Stage of North America includes as its lower unit the **Didymograptus hirundo** zone of Great Britain, the Volkhov of the Baltic region, and zone L, the Juab limestone of western Utah. It is in this interval that uplift and erosion of the St. George surface occurred. Evidence from several faunal groups supports the equivalence of the lower Table Head limestones with zone M of western Utah, the Joins of Oklahoma, the **Didymograptus bifidus** horizon of Great Britain, and most of the Kunda (excluding the lower Hunderum or Expansus Limestone).

Inclusion of northern Scotland on Figure 43.2 was influenced by current investigations of cephalopods. The Sailmhor Limestone is a dolomite which has yielded abundant Ellesmeroceratidae, confirming its Gasconade and Tremadoc equivalence. The Sangamore Formation is a barren dolomite. The Sangamore-Balnakiel contact has yielded Ellesmeroceratidae like those of the Sailmhor, and also some piloceroids, suggesting that collections from there represent two sides of a Gasconadian-Jeffersonian break. Higher Balnakiel beds yield faunas within the limits of Jeffersonian and early Casssinian. The Croisaphuill is a black dolomitic limestone with a fauna unquestionably allied to that of the **Cassinoceras wortheni** fauna of the St. George Group, the Fort Cassin of the Champlain valley, which is reasonably equated with zone I of western Utah. In placing the Durine, I have followed Higgins (1967) in equating it with the Joins of Oklahoma. A slightly earlier age assignment seems possible.

Acknowledgments

Additional material contributing to this summary was supplied by the collections and data of Charles Schuchert and C.O. Dunbar, loaned through the courtesy of Karl Waage from the Yale Peabody Museum collections. Other Newfoundland materials were loaned by the Geological Survey of Canada through the courtesy of T.E. Bolton. L.M. Cumming guided me to some localities, and aided in collecting, as did W.T. Dean. H.B. Whittington supplied valuable locality information and has read this paper and supplied some valuable suggestions, as have L.M. Cumming and T.E. Bolton.

It was due to the gracious hospitality and support of Le Vicompte et la Vicomptessa de Menorval (La Vicomptessa is Eliane Basse, Directeur de Récherches Paléontologiques de la Sorbonne) that I was introduced to those in charge of various collections in Paris, and my way there made smooth.

In addition to National Science Foundation support already noted, I wish to acknowledge the assistance of my wife, Francis Bacon, the family of Trevor Bennett and particularly his son Paul, who was not only of immense help in collecting, but managed to get my chisels sharpened almost nightly; a day of chopping in either the Table Head or much of the St. George can dull chisels to uselessness.

Additional help and courtesies were supplied by John Bennett of Lower Cove, Mr. and Mrs. Leo Brake of Stephenville, and Mr. and Mrs. Romeo Billard of Port au Choix.

References

Barrande, J.
1867-1877: Système Silurien du centre de la Bohême, Prague, Part 2, Cèphalopodes; Texte part 1, 1867, 712 p.; part 2, 1970, 263 p.; part 3, 1874, 804 p.; part 4, 1877, 297 p.; pls. 1-107, 1865; pls. 245-350, 1868; pls. 351-460, 1870; pls. 461-544, 1877.

Bergström, S.M. and Cooper, R.A.
1973: **Didymograptus bifidus** and the trans-atlantic correlation of the Lower Ordovician; Lethaea, v. 6, p. 313-340.

Billings, E.
1861-1865: Palaeozoic Fossils, Volume 1, containing descriptions of new or little known species of organic remains from the Silurian Rocks; Geol. Surv. Can., Separate Rep. 431.

Bird, J.M. and Dewey, J.F.
1970: Lithosphere plate, continental margin tectonics and the evolution of the Appalachian orogen; Geol. Soc. Am. Bull., v. 81, no. 4, p. 1031-1060.

Cumming, L.M.
1967: Platform and klippe tectonics of western Newfoundland; in Appalachian Tectonics, Clark, T.H., editor, p. 10-17.

1968: St. George-Table Head disconformity and zinc mineralization, western Newfoundland; Can. Mining Metal. Bull., p. 1-5.

Flower, R.H.
1964: The nautiloid order Ellesmeroceratida; N.M. Bur. Mines Miner. Resour., Mem. 12.

1968a: The first great expansion of the actinoceroids; N.M. Bur. Mines Miner. Resour., Mem. 19, pt. 1, p. 1-6.

1968b: Some additional Whiterock cephalopods; N.M. Bur. Mines Miner. Resour., Mem. 19, pt. 2, p. 17-55.

1971: Cephalopods of the Whiterock Stage; in Paleozoic Perspectives, a Paleontological Tribute to G. Arthur Cooper, Durtro, J.T., editor, Smithsonian Contrib. Paleobiol., no. 3, p. 101-111.

1975: American Lituitidae; Bull. Am. Paleontol., v. 67, p. 139-172.

1976a: New American Wutinoceratidae; N.M. Bur. Mines Miner. Resour., Mem. 28, pt. 1, p. i-iv, 5-12.

1976b: Some Whiterock and Chazy endoceroids; N.M. Bur. Mines Miner. Resour., Mem. 28, pt. 2, p. 13-39.

1976c: Ordovician cephalopod faunas and their role in correlation; in The Ordovician System, Bassett, M.G., editor, Univ. Wales Press — Nat. Mus. Wales, p. 523-552.

Higgins, A.C.
1967: The age of the Durine member of the Durness Limestone Formation at Durness; Scottish J. Geol., v. 3, no. 3, p. 382-388.

Hintze, L.F.
1951: Lower Ordovician detailed sections of western Utah; Utah Geol. Surv., Bull. 39.

1952: Lower Ordovician trilobites from western Utah and eastern Nevada; Utah Geol. Surv., Bull. 48.

Hyatt, A.
1894: Phylogeny of an acquired characteristic; Am. Phil. Soc., Proc., v. 32, no. 143, p. 349-647.

1900: Cephalopods; in Zittel-Eastman Textbook of Paleontology, v. 1, 1st ed., p. 536-592.

Kluyver, H.M.
1975: Stratigraphy of the Ordovician St. George Group in the Port-au-Choix area, western Newfoundland; Can. J. Earth Sci., v. 12, p. 589-594.

Logan, W.E.
1863: Report of the geology of Canada; Geol. Surv. Can., Rept. Prog. 1863.

Riley, G.C.
1962: Stephenville map-area, Newfoundland; Geol. Surv. Can., Mem. 323.

Ross, R.J.
1951: Stratigraphy of the Garden City Formation in northeastern Utah and its trilobite fauna; Yale Peabody Mus. Nat. Hist., Bull. 6.

1964a: Middle and Lower Ordovician formations in southwest Nevada and adjacent California; U.S. Geol. Surv., Bull. 1180C.

1964b: Relations of Middle Ordovician time and rock units in basin range, western United States; Am. Assoc. Pet. Geol. Bull., v. 48, no. 9, p. 1526-1554.

Schuchert, C. and Dunbar, C.O.
1934: Stratigraphy of western Newfoundland; Geol. Soc. Am., Mem. 1.

Ulrich, E.O., Foerste, A.F., Miller, A.F., and Furnish, W.A.
1942: Ozarkian and Canadian cephalopods: Part I, Nautilicones; Geol. Soc. Am., Sp. Paper 37.

Ulrich, E.O., Foerste, A.F., Miller, A.K., and Unklesbay, A.G.
1944: Ozarkian and Canadian cephalopods: Part III: Longicones and summary; Geol. Soc. Am., Sp. Paper 58.

Whittington, H.B.
1968: Zonation and correlation of Canadian and early Mohawkian Series; in Studies of Appalachian geology, Interscience Publ., John Wiley and Sons, p. 49-60.

Whittington, H.B. and Kindle, C.H.
1963: Middle Ordovician Table Head Formation, western Newfoundland; Geol. Soc. Am. Bull., v. 74, p. 745-758.

1969: Cambrian and Ordovician stratigraphy of western Newfoundland; Am. Assoc. Pet. Geol., Mem. 12, p. 655-664.

Williams, H.
1967: Geology, Island of Newfoundland; Geol. Surv. Can., Map 1231a.

THE BAIE VERTE-BROMPTON LINE IN NEWFOUNDLAND AND REGIONAL CORRELATIONS IN THE CANADIAN APPALACHIANS

E.M.R. Research Agreement 2239-4-128/77

Harold Williams[1] and Pierre St-Julien[2]
Regional and Economic Geology Division

Abstract

Williams, Harold and St-Julien, Pierre, The Baie Verte-Brompton Line in Newfoundland and regional correlations in the Canadian Appalachians; Current Research, Part A, Geol. Surv. Can., Paper 78-1A, p. 225-229, 1978

Mafic-ultramafic complexes along a narrow zone in the Quebec and Newfoundland Appalachians are host to the asbestos deposits that make Canada the world's largest producer of asbestos fibre. The narrow zone of mafic-ultramafic complexes is termed the Baie Verte-Brompton Line. Rocks and structures to the west of the line record the evolution and destruction of the ancient continental margin of eastern North America. Rocks to the east record the generation of oceanic crust and thick volcanic arc sequences. The Baie Verte-Brompton Line is interpreted therefore as the surface trace of an ancient continent-ocean interface. The present study is concerned with the correlation of rocks and structures that border the line along the full length of the Canadian Appalachians.

Definition

The Baie Verte-Brompton Line is a narrow structural zone marked by discontinuous mafic-ultramafic plutons (St-Julien et al., 1976). The zone is well-defined in northwest Newfoundland and throughout the Eastern Townships of Quebec, implying correlation of rocks and structures along the length of the Canadian Appalachians. Mafic-ultramafic plutons that define the Baie Verte-Brompton Line are bordered to the west by polydeformed metamorphic rocks: the Fleur de Lys Supergroup in Newfoundland, and the Sutton-Bennett Schists in Quebec. To the east, the mafic-ultramafic plutons are followed by megaconglomerates or olistostromal black-shale mélanges: basal parts of the Flatwater Group (Williams et al., 1977; Williams, in press) in Newfoundland, and the St-Daniel Formation (St-Julien and Hubert, 1975) in Quebec.

The Baie Verte-Brompton Line is an important structural junction in the Canadian Appalachians. Rocks and structures of the Humber Zone (Williams, 1976) to the west of the line record the evolution and destruction of the Early Paleozoic continental margin of eastern North America. To the east, the Dunnage Zone records the generation of oceanic crust and the construction of island arcs. The Baie Verte-Brompton Line therefore marks an ancient continent-ocean interface, which theoretically extends the full length of the Appalachian Orogen. Its mafic-ultramafic complexes are interpreted as remnants of oceanic crust and mantle, and these rocks are host to the asbestos deposits that make the Baie Verte-Brompton Line the world's richest asbestos belt.

Extent and Relationships in Insular Newfoundland

During the summer of 1977, the first author attempted to trace the rocks and structures that define the Baie Verte-Brompton Line across insular Newfoundland. In co-operation with the second author, reciprocal visits were made between Newfoundland and Quebec to compare more closely the rocks and structures at the distal extremities of the Baie Verte-Brompton Line in Canada.

Polydeformed and metamorphosed ophiolitic mélange of the Birchy Complex (Williams, 1977) along the west margin of the Baie Verte-Brompton Line, extends from its type area in Coachman's Harbour 100 km north to the south end of Groais Island. There, bright green lenses of actinolite-fuchsite schist and talc-fuchsite schist occur in association with black pelitic albite schist. The bright green schist lenses vary from 2 cm wide and 10 cm long to 1 m wide and up to 10 m long. They are interpreted as original ultramafic blocks in a black shale matrix, and as in the type area, the black pelitic schists are associated with green chloritic schists of Birchy type. Similar mélanges can be traced southward from Coachman's Harbour to Mic Mac Lake, indicating continuity of these rocks for at least 130 km in northwest Newfoundland.

East of the Baie Verte-Brampton Line in northwest Newfoundland, megaconglomerates at the base of the Flatwater Group (Williams et al., 1977; Williams, in press) can be traced 20 km north of Mic Mac Lake. The largest blocks within the conglomerate reach dimensions of several tens of metres across and the lithologies of the blocks and the type of matrix vary considerably from place to place. In the south at Mic Mac Lake, the largest blocks consist of a variety of internally brecciated to foliated gabbros, volcanic breccia, and altered green volcanic rocks set in a matrix of dark grey to black pebbly mudstone. Farther north at Kidney Pond, large blocks of altered ultramafic rocks and virginite occur in association with gabbro and mafic to silicic volcanic boulders in a matrix of black shale. At the north end of Flatwater Pond, the matrix of the megaconglomerates is tuffaceous and the blocks are mainly gabbros (including foliated varieties with green fuchsitic smears), mafic volcanics, quartz diorite or trondhjemite, and small pebbles of granodiorite. About 20 km farther north, the conglomerate matrix is sandy to chloritic and the commonest clasts are hard quartzose greywacke, quartz, serpentinite, and marble.

An occurrence of megaconglomerate at the former Terra Nova copper mine in Baie Verte may be a correlative of the Flatwater megaconglomerates. It has huge internally brecciated ultramafic blocks up to 10 m wide, set in a black shale matrix. An internally brecciated massive sulphide block nearby with exposed dimensions of 1 m by 3 m is also isolated in the black shale matrix. Conceivably, the Terra Nova orebody was confined to a huge isolated block, or series of blocks, immersed in shale.

Another occurrence of pebbly black shale on the south side of the Advocate asbestos mine may be a further Flatwater correlative. It has mostly grey-green tuffaceous clasts but also contains local carbonate clasts and possibly a huge raft of metagabbro more than 10 m across. This same megaconglomerate horizon may occur on the coast at the north side of Schooner Cove, suggesting greater continuity of the Flatwater conglomerates than was previously suspected.

[1] Department of Geology, Memorial University of Newfoundland, St. John's, Newfoundland A1C 5S7.

[2] Département de Géologie et Minéralogie, Université Laval, Québec, Québec G1K 7P4.

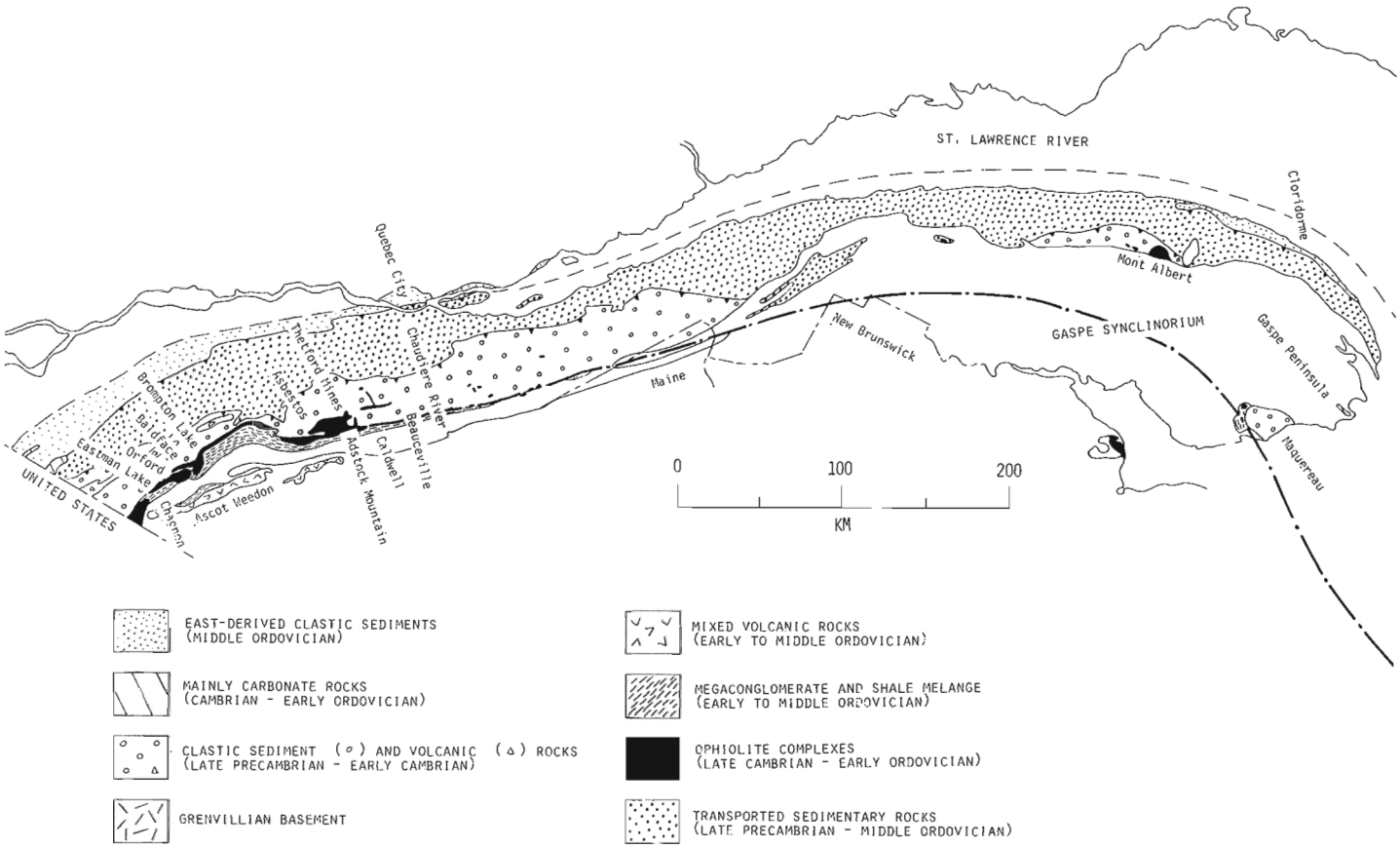

Figure 44.1. Regional Correlations along the western margin of the Canadian Appalachians.

Comparison between West Newfoundland and Québec Appalachians

Similarity of rocks and structures between west Newfoundland and Quebec supports the contention that the Baie Verte-Brompton Line is a continuous structural zone throughout the Canadian Appalachians, and that the line is the surface trace of an ancient continental margin-ocean interface. Correlation of the major structural features and lithofacies belts between west Newfoundland and Quebec is summarized in Figure 44.1 and comments on correlative belts from west to east follow.

The autochthonous sequence of western Newfoundland, i.e. Grenvillian basement and Cambrian-Ordovician carbonate terrane, is hidden throughout most of the Quebec Appalachians by an extensive structural cover of transported rocks. Basement rocks are brought to the surface only locally along thrust faults (e.g. 30 km south of Quebec City) and Cambrian carbonates (Corner of the Beach and Murphy Creek formations) occur at Gaspé Peninsula. The Tibbit Hill volcanics at the base of the Oak Hill sequence are an analogue of the Lighthouse Cove volcanics in Newfoundland, and all are interpreted as the products of rifting at the ancient continental margin of eastern North America. Oceanward derived clastic rocks that overlie the west Newfoundland carbonate terrane and precede the emplacement of Taconic allochthons (e.g. Goose Tickle, upper Table Head, and Taylors Pond formations) are represented in Quebec by the Cloridorme Formation at Gaspé and the Middle Ordovician flysch near Quebec City.

Transported sedimentary sequences of western Newfoundland (those of the Humber Arm and Hare Bay Allochthons) are the dominant structural feature of the Quebec Appalachians and analogues can be traced from the tip of Gaspé Peninsula southwestward to the Canada-United States border.

Ophiolite complexes of highly allochthonous nature in west Newfoundland, e.g. Bay of Islands Complex, are rare in the Quebec Appalachians, but the Mont Albert ultramafic pluton is thought to be a direct analogue.

A zone of polydeformed and metamorphosed psammitic to pelitic schists in Newfoundland (Fleur de Lys Supergroup), which lies immediately west of the Baie Verte-Brompton Line, appears to be a correlative of the Sutton-Bennett Schists (Rosaire, Caldwell, Oak Hill) of the Eastern Townships and of the Maquereau Group of Gaspé Peninsula. Small metamorphosed and deformed ultramafic bodies within the Fleur de Lys, now interpreted as structurally emplaced, are thought to be analogous to the Pennington Dyke, e.g. near St-Pierre de Broughton, and related mafic bodies throughout the Sutton-Bennett Schists of Quebec. Small mafic-ultramafic bodies like those mentioned above are common throughout the full length of the Appalachian Orogen in southerly continuations of the same belt of deformed and metamorphosed clastic rocks.

In Newfoundland, greenschist and ophiolitic mélanges of the Birchy Complex, which form a continuous narrow zone immediately west of the Baie Verte-Brompton Line, may be represented in Quebec by the banded volcanics southeast of Caldwell and northwest of the St-Daniel Formation (locally termed Brompton rocks) near Orford Mountain. In Quebec, these banded volcanics can be traced from east of Eastman Lake 30 km northeastward to east of Brompton Lake.

Feb 3/78
Author advised that text on these pages (226-227) has been interchanged.

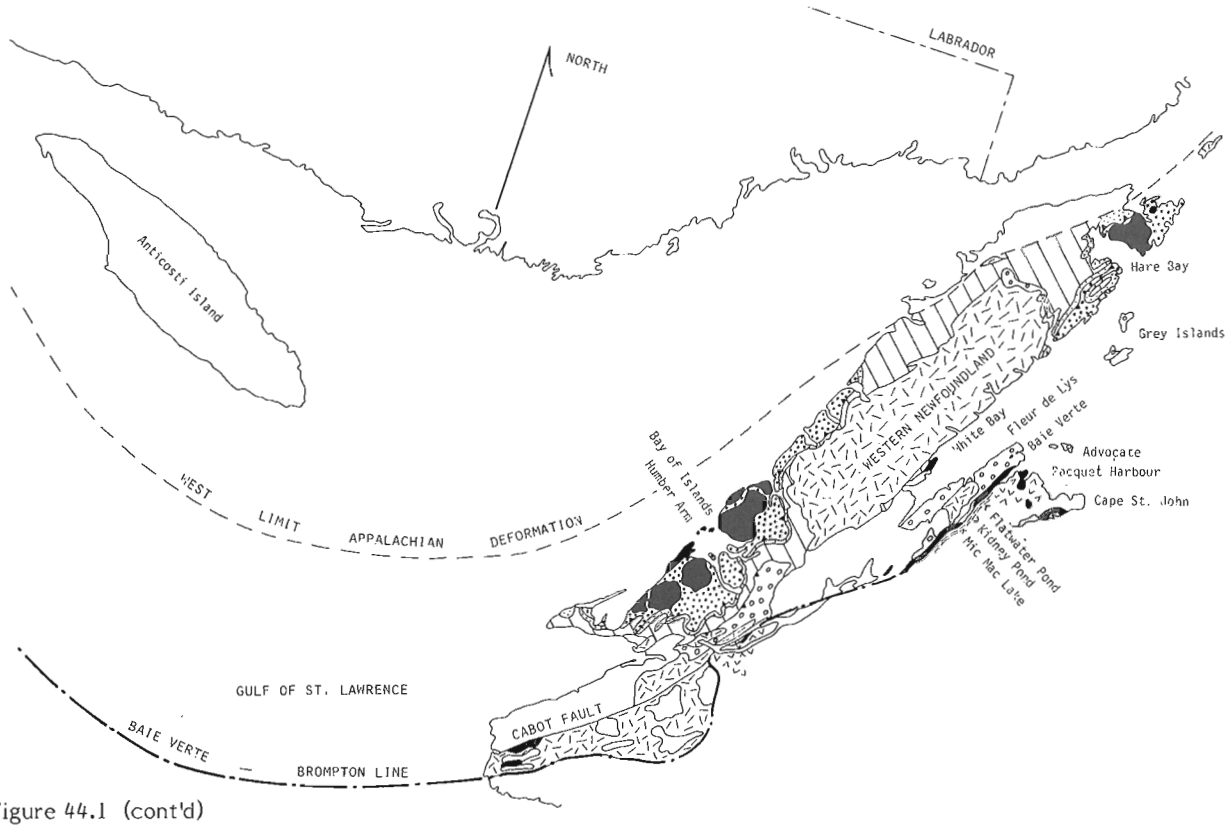

Figure 44.1 (cont'd)

Discontinuous mafic-ultramafic plutons that define the Baie Verte-Brompton Line can be traced 100 km southward from Baie Verte to Sandy Lake. Farther south, the lineament is hidden by Carboniferous strata or the waters of Grand Lake. At Glover Island of Grand Lake (Fig.44.2), psammitic to pelitic schists are followed eastward by mafic volcanic rocks (Glover Formation of Riley, 1957). Near Northern Harbour, an east-dipping east-facing pluton consisting of serpentinized peridotite overlain by layered gabbros occurs between the schists (west) and mafic volcanic rocks (east). This structural situation is similar to that found along the Baie Verte-Brompton Line to the north. Accordingly, the Baie Verte-Brompton Line is interpreted to pass through Glover Island and the mafic-ultramafic rocks there are interpreted as ophiolitic. Still farther south at Lewa-seech-jeech Brook, volcanic rocks of the Glover Formation (east) are separated from pink gneisses and foliated granites (west) by the Cabot Fault.

Black graphitic argillites and siliceous argillites at Corner Pond[1] (Fig.44.2), which are mapped as an intergral part of the Glover Formation (Riley, 1957), contain a rich graptolite fauna. Forms originally collected by P.M. Dimmell and identified by R.B. Richards indicate an Early Ordovician (Arenigian) age for these rocks (Dean, 1976). Material collected during the summer of 1977 contains **Phyllograptus anna** Hall and **Didymograptus protobifidus** Elles in addition to the forms reported by Richards (new identifications by D. Skevington), further confirming the original assignment of the graptolite assemblage to the Didymograptus Nitidus Zone (Middle Arenig). This age suggests correlation of the Glover Formation with the Snooks Arm Group of Notre Dame Bay, and in both widely separated areas the dated rocks are underlain by ophiolitic complexes.

West of the south end of Glover Island, zones of banded pink gneisses and foliated granites alternate with northeast-trending zones of pelitic to calc-silicate schists (Fig.44.2). The gneisses are correlated with the Grenville Long Range Complex, and the repetition of zones is interpreted as thrust imbrication of crystalline basement and a metamorphosed cover sequence. Farther west, at the extreme southwest corner of Grand Lake, the gneisses are separated from easternmost exposures of the western Newfoundland carbonate terrane by a deep northeast-trending depression. Again the relationship suggests structural juxtaposition of carbonates and gneisses, and thrusting of the gneisses westward against the carbonate rocks. The structural style and rock units of this area are analogous to the structures and rocks of the Blue Ridge Province of the southern Appalachians where westward thrusting of basement gneisses above cover rocks is commonplace.

South of Grand Lake, gneisses and schists that are probably in part Grenville extend well east of the Cabot Fault and the southward projection of the Baie Verte-Brompton Line. The relationship of the Glover Formation and mafic-ultramafic rocks at Little Grand Lake to gneisses farther south is unknown. Presumably the contact is a structural dislocation, now complicated by later metamorphism and granite intrusion. The structural setting of rock groups in this southern area implies that the Bai Verte-Brompton Line lies well east of the Cabot Fault, where it may be coincident with the Cape Ray Suture (Brown, 1973) farther south. The offset between Baie Verte-Brompton Line at Glover Island compared to the northward projection of the Cape Ray Suture, suggests that an ancient eastward salient in the former continental margin of eastern North America exists in this area to the south of Grand Lake, or that the more westerly position of this line at Glover Island merely reflects the surface expression of highly allochthonous rocks.

[1] Informal name, not approved by Canadian Permanent Committee on Geographical Names.

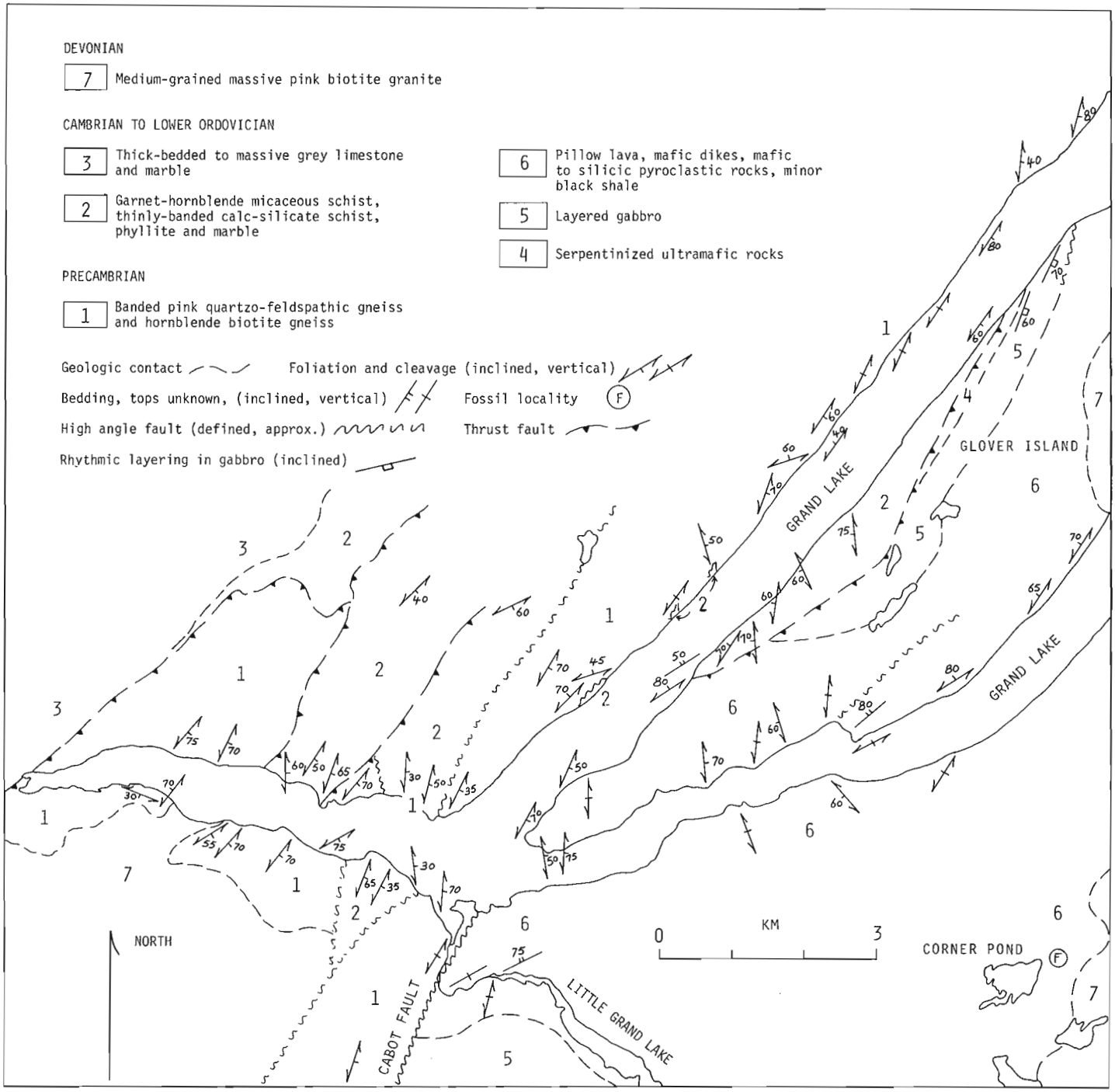

Figure 44.1 General Geology at the south end of Grand Lake.

Ophiolite complexes like those represented by the Advocate Complex in Newfoundland abound along the Baie Verte-Brompton Line throughout the Quebec Appalachians. Typical examples from south to north are the Chagnon, Orford and Baldface ophiolite complexes, and the Asbestos and Thetford Mines complexes.

East of the Baie Verte-Brompton Line, megaconglomerates and olistostromal mixtures like those of the Newfoundland Flatwater Group are found in the Quebec St-Daniel Formation. Examples with matrices that vary from pebbly to black shaly and tuffaceous at Mic Mac Lake, Kidney Pond and Flatwater Pond, respectively, in Newfoundland, can be matched with examples found 3 km west of Chaudière River near the town of Beauceville (northwest of town) and in Coldstream River southwest of Adstock Mountains and south of Thetford Mines. Peculiar Flatwater conglomerates with sandy matrix, unique to the locality 20 km north of Flatwater Pond in Newfoundland, form a marker horizon in the shaly St-Daniel Formation that can be traced 20 km from south of Adstock Mountain toward Beauceville. Other examples of megaconglomerates in Newfoundland at Terra Nova mine and south of Advocate mine have counterparts in the St-Daniel Formation.

Finally, the Pacquet Harbour and parts of the Cape St. John Groups of the northeast Burlington Peninsula in Newfoundland may correlate with Ascot-Weedon volcanics of Quebec.

All of the above mentioned rocks have been interpreted in a variety of contrasting local models; however, the continuity of rocks and structures is beyond question and the authors feel that a single model must suffice for the interpretation of all.

Silurian and Devonian rocks of the Gaspé Synclinorium unconformably overlie transported Ordovician and older rocks, and the depositional and structural trends of the younger cover sequence cross the Baie Verte-Brompton Line and earlier Ordovician structures. Similarly, Silurian rocks of western Newfoundland locally overlie transported rocks at western White Bay, and they overlie Ordovician ophiolitic and volcanic rocks to the east of the Baie Verte-Brompton Line. Clearly the Ordovician continental margin and at least westerly parts of the adjoining ocean were destroyed before Silurian depositon.

Acknowledgments

The first author acknowledges the field assistance of Alvin Crocker during the course of this study and the many hospitalities shown by the people of Coachman's Cove, Newfoundland. He acknowledges E.M.R. Research Agreement as well as further financial support for his work in the Appalachians through an Izaac Walton Killam Special Senior Research Scholarship and National Reserach Council of Canada Grant A 5548.

References

Brown, P.A.

1973: Possible cryptic suture in south-west Newfoundland; Nature (London) Phys. Sci., v. 245, p. 9-10.

Dean, W.T.

1976: Some aspects of Ordovician correlation and trilobite distribution in the Canadian Appalachians; in M.G. Bassett, (ed.); The Ordovician System, Cardiff University of Wales Press and National Museum of Wales, p. 227-250.

Riley, G.C.

1957: Red Indian Lake (west half) Newfoundland; Geol. Surv. Can., Map 8-1957.

St-Julien, P. and Hubert, C.

1975: Evolution of the Taconian Orogen in the Quebec Appalachians; Am. J. Sci., v. 275A, p. 337-362.

St-Julien, P., Hubert, C., and Williams, H.

1976: The Baie Verte-Brompton Line and its possible tectonic significance in the northern Appalachians; Geol. Soc. Am., Abstr. Progr., v. 8, no. 2, p. 259-260.

Williams, H.

1976: Tectonic-stratigraphic subdivisions of the Appalachian Orogen; Geol. Soc. Am., Abstr. Progr., v. 8, no. 2, p. 300.

1977: Ophiolitic Melange and its significance in the Fleur de Lys Supergroup, northern Appalachians; Can. J. Earth Sci., v. 14, p. 987-1003.

Geology Baie Verte Peninsula and western White Bay; Newfoundland Dep. Mines Energy, Min. Dev. Div., Map and accompanying notes. (in press)

Williams, H., Hibbard, J.P., and Bursnall, J.T.

1977: Geological setting of asbestos-bearing ultramafic rocks along the Baie Verte Lineament, Newfoundland; in Report of Activities, Part A, Geol. Surv. Can., Paper 77-1A, p. 351-360.

45.

VOLCANIC ROCKS OF THE APPALACHIAN PROVINCE: ROBERTS ARM GROUP, NEWFOUNDLAND

Project 730043

H.H. Bostock
Regional and Economic Geology Division

Abstract

Bostock, H.H., Volcanic rocks of the Appalachian Province: Roberts Arm Group, Newfoundland; Current Research, Part A, Geol. Surv. Can., Paper 78-1A, p. 231-233, 1978.

The Upper Ordovician Roberts Arm volcanic rocks on southern Triton Island display northward overturned folds and slickensides suggesting compression from the southeast. Minor folds in the Springdale Group along the Lobster Cove Fault plunge moderately to steeply implying transcurrent fault movements.

The Loon Pond granitic pluton and its discontinuous marginal felsitic facies appear to occupy an antiformal zone within the Roberts Arm volcanics. Metamorphism related to the pluton was recognized along a limited southeast sector of the contact. Trace contents of tin (0.025 wt. per cent) are present in some Loon Pond felsites.

Preliminary anlayses of Roberts Arm basalts from a single sample section show that the basalts southeast of Crescent Lake are enriched in titanium and may therefore have evolved in a tectonic setting distinct from those farther northwest. Basalts of the Roberts Arm Group proper, northwest of Crescent Lake, may be divided into phosphorus-rich and phosphorous-poor belts.

Field work on the Roberts Arm Group, Notre Dame Bay, Newfoundland (2E and 12H), was completed with 1:25 000 scale mapping of southern Triton Island, and parts of the Hall Hill complex and Roberts Arm Group near and south of Loon Pond. Petrochemical samples have been collected at 150 m intervals along a series of 5 sections representative of volcanic rocks in the area, and from 3 additional sections chosen to investigate problems arising from preliminary chemical data and to provide a basis for comparison of the Roberts Arm Group with adjacent volcanic suites. Brief descriptions of the Roberts Arm Group were given in Bostock (1975, 1976). The following notes describe the results of field work not covered in these reports and provide some preliminary observations based on petrochemistry.

Triton Island

The Upper Ordovician Roberts Arm Group, exposed along the southern shores of Triton Island, is separated from tholeiitic spilitic basalts of the Lower Ordovician Lushs Bight Group in the northern part of the island by the Lobster Cove Fault. Pillowed to massive spilitic basalts which predominate in the Roberts Arm Group, are accompanied by pillow breccia, some intercalated chert-siltstone-greywacke lenses, and minor keratophyre, the latter being much less abundant than on Pilley's Island on strike immediately to the west. Axes of tight, northward overturned folds intersect the south coast of Triton Island from the southwest and are tangent to the Lobster Cove Fault east of Cards Harbour. In the interior western part of the island and on the northwest coast the flows are northward facing and overturned; on the north coast of Big Island they are inverted and nearly flat lying. Slickensides are common, and in places on the coast form spectacularly polished surfaces. Slickensides trend mostly 140 to 160° and plunge south from 0 to 35°. Plucking along slickensided southeast-dipping surfaces suggests movement of the hanging wall northwestward.

The Lushs Bight Group consists predominantly of pillowed to massive flows for several 100 m north of the Lobster Cove Fault. In this region the flows face south and dip moderately (35 to 55°) south although dips steepen locally near the fault. Farther north pyroclastic rocks are more abundant, steeper dips are encountered, and structural discontinuities are likely present within the assemblage.

The Silurian Springdale Group unconformably overlies the Roberts Arm Group along and immediately south of the Lobster Cove Fault in the western part of Triton Island, but in the east it is preserved only as small isolated fault remnants. On Triton Island the group consists of about 30 m of red beds. Talus breccia at the base of the group, from a few tens of centimetres to 15 m in thickness, is gradational to altered spilite of the Roberts Arm Group below, and is intercalated at its upper contact with about 20 m of overlying red sandstone and siltstone. Fragments in the breccia are mostly up to 10 cm in diameter and angular, consisting of altered spilite like that on the surface of the Roberts Arm Group beneath. Many fragments are amygdular, a structure which is common in Roberts Arm spilite. A few fragments of red chert and rare red siltstone and gabbro were also found. The sandstone and siltstone at the west shore of the island contain graded beds in the lower part and mudcracks in the upper part of the sequence. Cross-beds suggest current flow predominantly from the west. Bedding in the Springdale Group dips steeply and is overturned to the north at both ends of the Triton Island. Minor folds are not common but three minor fold axes in coastal exposures plunge steeply at angles of 45 to 75°.

Structural observations on Triton Island suggest that the Roberts Arm Group, sandwiched between the Tommys Arm Fault offshore south of Triton Island and Lobster Cove Fault, has been deformed through compression from the southeast. Evidence that would suggest that the Lobster Cove Fault is a folded thrust with movement from the northwest (Dean and Strong, 1977) has not been found.

Loon Pond and Vicinity

The Roberts Arm Group east, south and west of Loon Pond consists primarily of spilitic basalt and pillow lava. Greywacke, siltstone, and chert are concentrated in large lenses southeast of the Crescent Lake – Tommys Arm Fault. Small bodies of keratophyre and felsitic tuffs are locally present.

Rocks within the fault block between Loon Pond and the Crescent Lake – Tommys Arm Fault are steeply dipping and face east. Rocks on either side of this block are also steeply dipping but face west to northwest. The Loon Pond pluton has been emplaced along the antiformal zone between these blocks and is therefore the same age or younger than

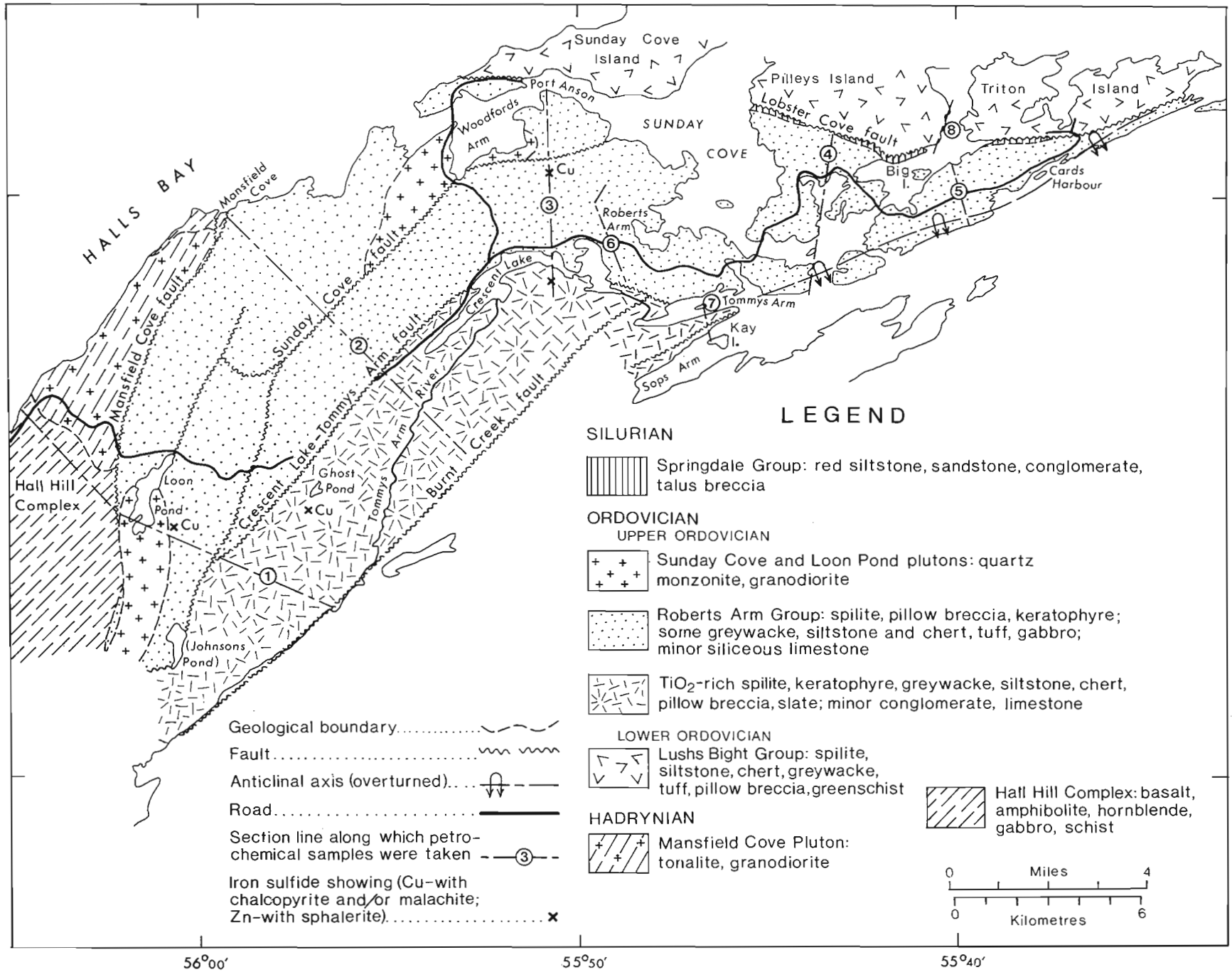

Figure 45.1. Geology of Notre Dame Bay area, Newfoundland.

faulting. In this respect it differs from the Sunday Cove pluton to the northeast which supplied magma for flows and sills in the upper part of the Roberts Arm Group along Halls Bay and has been truncated by the Sunday Cove Fault. West of a lake known locally as Johnsons Pond (Fig. 45.1), the Roberts Arm basalts have been converted to amphibolite but elsewhere metamorphism due to emplacement of the Loon Pond pluton appears slight.

The Hall Hill complex (Currie, 1976) to the west of Loon Pond, consists primarily of massive basalt and amphibolite with some hornblende gabbro, pillow lava and schist, intruded locally by granitic dykes and veins. North and west of Loon Pond it is separated from the Roberts Arm Group by the Mansfield Cove Fault, but farther south the Roberts Arm basalts pinch out and felsites, which form a discontinuous marginal facies about the Loon Pond pluton, directly intrude the Hall Hill complex. Basalt dykes of the Hall Hill complex intrude the late Hadrynian Mansfield Cove pluton but hornblende gabbro bodies within the complex resemble similar rocks within this pluton. The Hall Hill complex may therefore include rocks that are both younger and older than the Mansfield Cove pluton.

Preliminary Petrochemistry

Chemical analyses of the Roberts Arm basalts in a section (number 2, Fig. 45.1) indicate that two or possibly three types of basalt are represented:

1. titanium-rich basalts (wt. per cent TiO_2 mostly 1.50 to 2.20) southeast of Crescent Lake,
2. phosphorous-poor basalts (wt. per cent P_2O_5 mostly 0.11 to 0.22) in the fault block between the Crescent Lake – Tommys Arm and Sunday Cove faults, and
3. phosphorous-rich basalts (wt. per cent P_2O_5 mostly 0.20 to 0.40) northwest of the Sunday Cove Fault. These ranges are comparable to those found in ocean island basalts, island arc tholeiites, and island arc calc-alkaline basalts respectively.

Trace element analyses of some 100 samples of keratophyre from various centres within the Roberts Arm Group has shown that keratophyres associated with the Loon Pond pluton have low but significant tin contents (0.025 wt. per cent). Zinc in amounts about 0.013 wt. per cent is present in all of 13 basalt samples collected over an interval of 760 m along section 3 (Fig. 45.1) southeast of Woodfords Arm. Background zinc content for this section is about 0.009 wt. per cent. The consistency of this anomaly is in contrast to higher but erratic values present in rocks from other sections and suggests uniform slight concentration of zinc in one of the gangue minerals in this area.

Metallic Mineral Showings

Four mineral showings not previously referred to have been investigated during the current work (Fig. 45.1). These comprise one occurrence of chalcopyrite with sphalerite and extensive gossan (Rust Pond showing south of Ghost Pond), one gossan in which only disseminated pyrite was found (south of Crescent Lake) and two minor occurrences of chalcopyrite (on section 3, Fig. 45.1) and southeast of Loon Pond.

The Rust Pond showing occurs in association with a keratophyre lens as much as 60 to 90 m thick between spilitic basalts. Pillows in the vicinity suggest that the keratophyre is a steeply dipping flow or sill facing northwest. Gossan from disseminated pyrite is best developed along the northwest (upper) side of this body but shallow trenches totalling about 35 m in length suggest that disseminated to massive pyrite is common throughout. Gossan due to disseminated pyrite and some chalcopyrite is also well developed in a zone 2 m wide and about 15 m or more long within banded basic rocks immediately below the keratophyre. The keratophyre pinches out within a few tens of metres southwest of the showing but extends an unknown distance to the northeast beneath Rust Pond.

Pyrite with malachite occurs along fractures in a thin band of red chert within basalt where it is crossed by an abandoned logging road to the southeast of Loon Pond. This occurrence is about halfway between two minor chalcopyrite occurrences reported by Dean (1976) along the east margin of the Loon Pond pluton.

Traces of chalcopyrite were found in spilite on section 3 (Fig. 45.1) about 1.5 km southeast of Woodfords Arm. The spilites are cut by minor felsite dykes at this locality. Chalcopyrite occurs within rocks characterized by low anomalous zinc contents discussed above.

References

Bostock, H.H.

1975: Volcanic rocks of the Appalachian Province: Roberts Arm Group, Newfoundland (2E); in Report of Activities, Part A, Geol. Surv. Can., Paper 75-1A, p. 1-3.

1976: Volcanic rocks of the Appalachian Province: Roberts Arm Group, Newfoundland (2E and 12H); in Report of Activities, Part A, Geol. Surv. Can., Paper 76-1A, p. 173-175.

Currie, K.L.

1976: Studies of granitoid rocks in the Canadian Appalachians: Part 2; in Report of Activities, Part A, Geol. Surv. Can., Paper 76-1A, p. 155-163.

Dean, P.L. and Strong, D.F.

1976: Springdale, Newfoundland; Geol. Surv. Can., Open File 379, map with marginal notes.

1977: Folded thrust faults in central Notre Dame Bay; Am. J. Sci., v. 277, p. 97-108.

46. A GAMMA-RAY SPECTRAL LOGGING SYSTEM INCLUDING DIGITAL PLAYBACK, WITH RECOMMENDATIONS FOR A NEW GENERATION SYSTEM

Project 740085

P.G. Killeen, J.G. Conaway and Q. Bristow
Resource Geophysics and Geochemistry Division

Abstract

Killeen, P.G., Conaway, J.G. and Bristow, Q., A gamma-ray spectral logging system including digital playback, with recommendations for a new generation system; Current Research, Part A, Geol. Surv. Can., Paper 78-1A, p. 235-241, 1978.

The system is the result of improvements based on experience with two different analog chart recording borehole spectrometer systems. It includes a four-channel portable gamma-ray spectrometer interfaced with a digital cassette tape recorder, a single-pen analog chart recorder in a compact battery-operated package, and a manually operated winch (capacity > 300 m of cable). The winch includes a level wind and an electronic depth fiducial. Depth is recorded along with spectral data (total count, K, U, and Th channels) and a 5-digit thumbwheel-controlled identification number. Probes designed to fit boreholes of size AX (48 mm) or larger are currently available commercially. Auxiliary equipment includes a minicomputer which provides for complete flexibility in processing and presentation of the cassette-recorded data and allows spectral stripping corrections and ratio computations to be carried out, and multi-channel analog plots to be produced showing all pertinent information.

Properly calibrated, the system can provide grade-thickness information for uranium and thorium as well as lithologic information from potassium. The system is backpack portable and is easily operated on-site during a drilling program.

Introduction

In order to compute borehole radioelement assays from gamma-ray spectral logs it is necessary that the log data be in digital form. There are several advantages to recording the gamma-ray logs directly in digital form in the field rather than digitizing analog chart records at a later time in the office. Digital recording avoids the problem of lost data due to pen excursions off the chart paper. A direct digital recording is inherently more accurate than a digitized analog trace, and digital recording permits increasing the sampling time for slow detailed logging, in order to produce better counting statistics and a more reliable borehole assay. The additional cost of digitizing strip charts is avoided and in situ field data reduction is made possible if appropriate computation equipment is available.

Experience gained during the 1975 summer field season using leased, "off-the-shelf" instrumentation for borehole gamma-ray spectrometry (Killeen, 1976; Killeen and Bristow, 1976) has led to the development of the portable gamma-ray spectral logging system described in this report. This system utilizes both a high density digital cassette tape recorder to store quantitative data for later processing, and a single pen strip chart recorder for on-site qualitative analysis. The digital data are recorded in ASCII code, thus allowing playback into any EIA RS232C compatible terminal or computer port at baud rates from 150-1200, via an AC powered playback unit at the base camp.

The gamma-ray spectral logging system is designed to be backpack portable (Fig. 46.1) to permit logging of holes drilled in terrain which is not accessible even by a four-wheel drive vehicle. The length of cable on the winch is limited by the weight which an average person can carry. A cable length of 230 m was chosen for the system. The electronics of the spectral logger are entirely battery powered and the winch is manually operated. The main components of the gamma-ray spectral logger and the field playback system are shown in the block diagrams of Figures 46.2, 46.3. The portable gamma-ray spectrometer is a McPhar Spectra 44D, a standard model which can be connected to a 76 x 76 mm (3 x 3 in) NaI (Tl) detector for surface exploration work when not being utilized for borehole logging.

The spectrometer is interfaced with a Memodyne model 201 cassette tape recorder and a Rustrak model 2146 strip chart recorder as shown in Figure 46.4. The borehole probe, winch, cable, depth counter, pulley and tripod were purchased from Exploranium. Some modifications were necessary to interface the components of the various manufacturers.

Figure 46.1. Portable gamma-ray spectral logging system including backpack winch, borehole probe and tripod, and instrumentation case. GSC 202941-S.

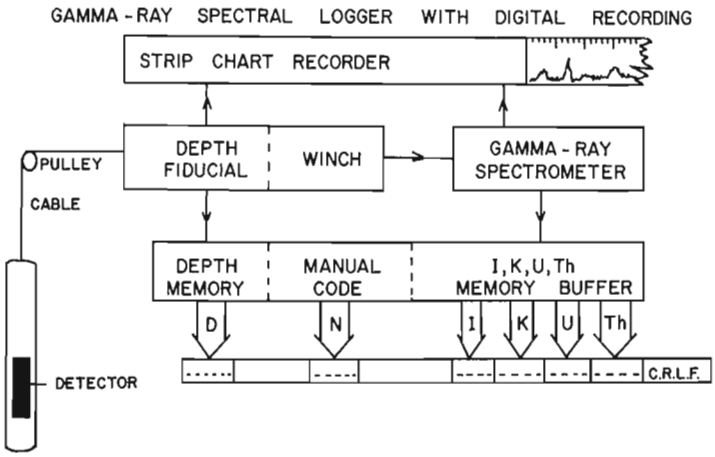

Figure 46.2. Block diagram illustrating interfacing of components of the gamma-ray spectral logging system and the transfer of data to the magnetic tape.

The assembly and debugging of the backpack portable gamma-ray spectral logging system took place in the first part of the summer of 1976, and the system was field tested in the Bancroft uranium mining area of Ontario later in the summer. The system was designed to eliminate many of the problems encountered in using existing gamma-ray spectral logging systems, and to incorporate the precision and versatility of digital field recording. The following is a more detailed description of the components and operation of the gamma-ray spectral logger. Only the main characteristics of each component have been described; for more information, the particular manufacturer should be consulted.

The Portable Gamma-Ray Spectrometer

The McPhar Spectra 44D is a four-channel analyzer. One channel records the integral or total count, while the other three channels are set to record gamma rays in selected energy bands related to potassium, uranium and thorium. The counting period is switch selected; intervals of 1, 2, 4, 6, 8, 10, 20 and 30 seconds or minutes are available.

In the borehole logging system, a counting period of 2 s is the minimum time possible since it requires about 1.4 s to record the data on the cassette tape. After each counting period the four channels of spectral data are transferred to a buffer memory in the cassette tape interface. There they are combined with the current depth reading from the depth memory, and the value of the manual thumbwheel code number. The spectrometer erases its memory and begins another counting period immediately. In the meantime, the contents of the buffer are recorded in ASCII code on the tape along with carriage return and line-feed characters which are used to control the field playback terminal.

The Spectra 44D also provides an analog output for recording any one of the four channels selected on a single pen strip chart recorder. Time constants of 1, 2, 5 and 10 seconds are available and eight amplitude ranges can be selected.

The Cassette Tape Recorder

The Memodyne model 201 is a high density digital incremental cassette recorder with low power requirements. The recording density is 615 BPI (bits per inch) with a storage capacity of over 2.2 million bits per 300 foot cassette. The data recorded per counting period include: integral channel (4 characters) K (4), U (4), Th (4), Depth (6), manual code (5), carriage return (1) and line feed (1).

Including inter-record gaps, about 8600 records can be recorded on one tape. Since the maximum data rate is 180 BPS (bits per second), about 1.4 s is required for recording data from one sample period. The fastest recording rate would be using the minimum counting time of 2 s, and it would therefore take about 300 min to fill the tape. At a logging speed of 3 m/min, data from a hole of about 900 m depth could be recorded on one cassette. Since the maximum cable available on the winch is 230 m, this represents nearly four maximum-depth holes per cassette. At 1 m/min 300 m of hole could be logged on one cassette. Of course, counting periods longer than 2 s would increase the data storage capacity in terms of length of hole logged and recorded per cassette.

The Strip Chart Recorder

The Rustrak model 2146 strip chart recorder is of the single pen pressure-type design with event marker. The chart paper is about 5 cm wide and moves at 1.25 cm/min. This was the most compact DC powered chart recorder available, and was small enough to fit in the aluminum carrying case along with the cassette tape, recorder and spectrometer. The chart recorder provides a qualitative record to aid in identifying anomalous zones while logging. These anomalous zones could then be logged at a slower speed for detailed analysis later. This strip chart recorder has not been synchronized to the motion of the winch, and does not have easily adjustable paper speeds. There is no small DC powered chart recorder known to the authors which has these features.

The spectrometer, cassette-recorder, and strip chart recorder are contained in a single carrying case (Fig. 46.4). External inputs to the case for battery power, depth fiducial, and signal from the borehole probe permit the cover of the case to be closed during operation in poor weather.

The Borehole Probe, Winch, Cable, Depth Indicator, Pulley and Tripod

All of the components described in this section were purchased from Exploranium. The borehole probe assembly consists of a 25 x 76 mm (1 x 3 in) NaI(Tl) detector, a high-voltage power supply, and a signal amplifier, all contained in a 38 mm diameter probe housing. Energy resolution of this detector with 230 m of cable is about 10.9%.

The four-conductor cable is free-flooding 4.8 mm O.D. steel-armour type weighing 9 kg/100 m. The cable is wound on a manually operated winch with 2 gear ratios, automatic level wind, hydraulic brake, electronic digital depth counter and back-up mechanical depth counter. The pulley and tripod

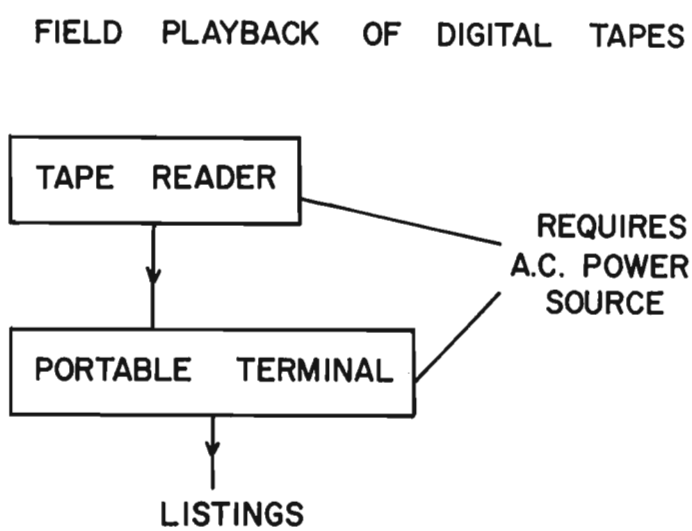

Figure 46.3. Main components of field playback system.

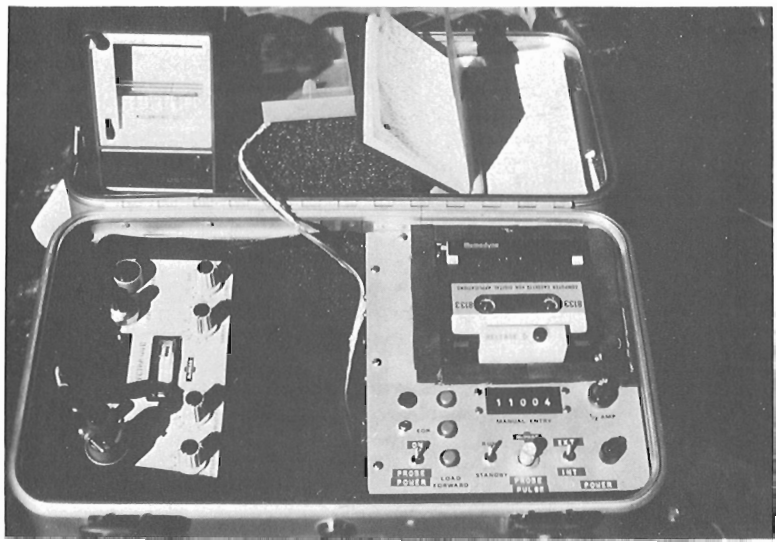

Figure 46.4

The Spectra 44D gamma-ray spectrometer, Memodyne digital cassette tape recorder, Rustrak strip chart recorder, and instrumentation carrying case. GSC 202941-R.

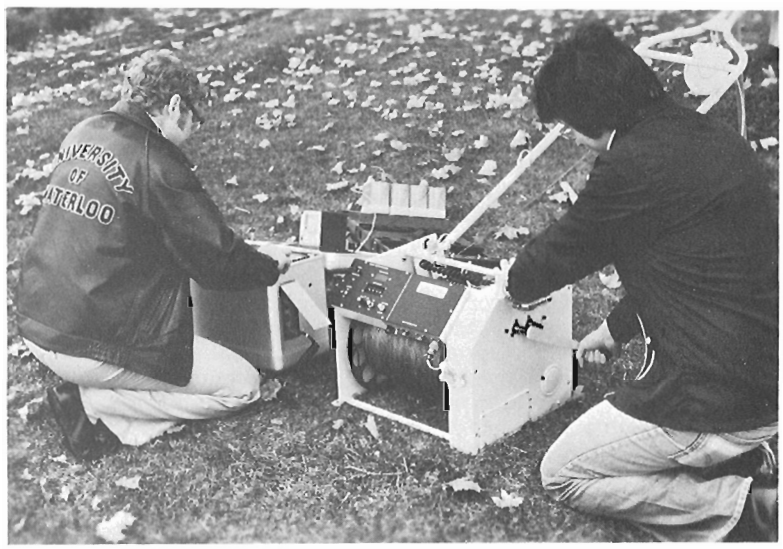

Figure 46.5

Operation of the spectral logging system; instrumentation (left) and winch with depth counting panel and attached tripod and pulley. GSC 202941-T.

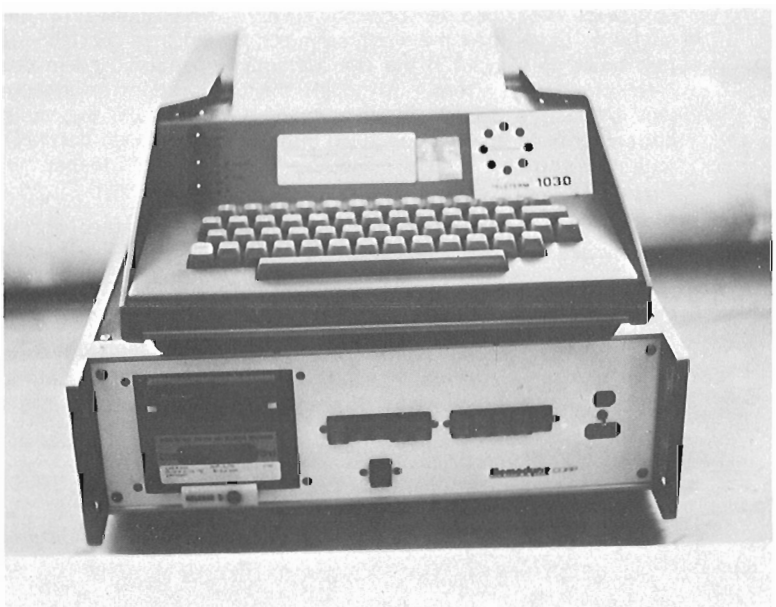

Figure 46.6

The Memodyne digital cassette tape recorder, and a standard data terminal used in the field as a playback system. The system yields listings of the raw data and verifies the field tapes. GSC 202941-L.

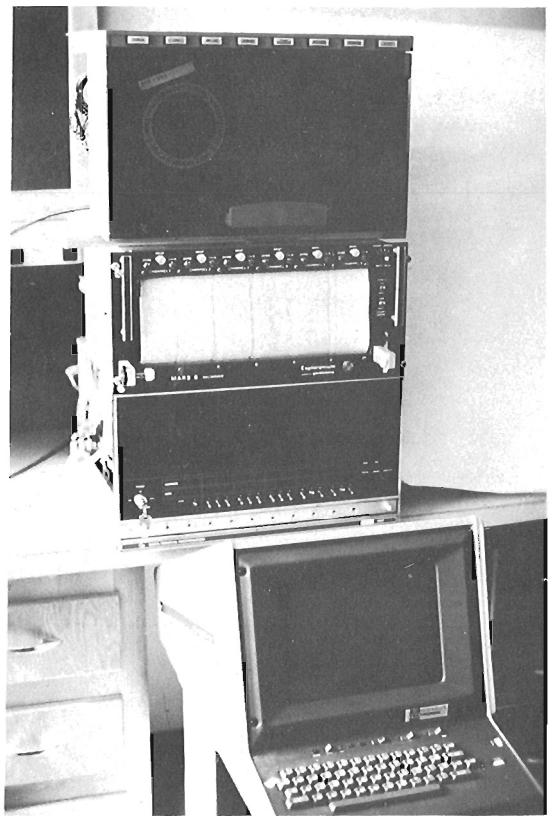

Figure 46.7. Data reduction system including from top to bottom, the 9-track tape drive, 6-pen chart recorder, NOVA minicomputer, and a display terminal. The system carries out computations on the raw data from the cassette tapes and outputs the corrected data as listings on the terminal and corrected logs on the chart recorder. GSC 203254-K.

DATA REDUCTION CAPABILITY
CHART RECORDER PLOTS BY MINICOMPUTER

1. REVERSE PLOTS (LOGGING UP OR DOWN)
2. DEPTH SCALE EXPANSION
3. COUNT SCALE EXPANSION
4. SMOOTHING
5. SPECTRAL STRIPPING
6. RATIO PLOTS
7. PEAK FINDING
8. PEAK AREA CALCULATIONS
9. EDIT DATA
10. LIST DATA BETWEEN SPECIFIED DEPTHS

Figure 46.8. Data reduction features of the minicomputer-based system including plotting capability on the chart recorder.

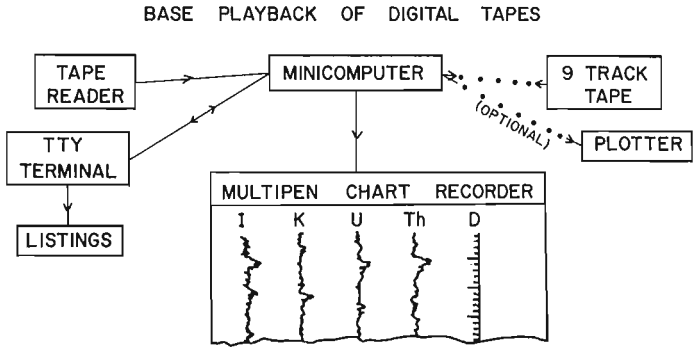

Figure 46.9. Block diagram illustrating the interfacing of components of the data reduction system.

are connected to the winch (Fig. 46.5) which must therefore be located near the borehole. A 4 digit LED depth-counter display is located on a panel on the winch. The counter is bi-directional and is operated from magnetic sensors on a roller located inside the level wind mechanism. The panel has an output for the depth fiducial, and also an output to control a stepping motor on a strip chart recorder for synchronizing the paper speed with the logging speed. Battery power for the depth indicator is provided by six D-cells located in the frame of the winch. Power for the other components of the system is provided by four 6-volt lantern batteries connected in series.

Playback and Data Reduction

The field playback system consists of a Memodyne model 3122 tape reader and a standard data terminal as shown in Figure 46.6. This provides a listing of the recorded data, in order to ensure that the field recording system has operated properly. Complete processing of the digital data is provided by a NOVA minicomputer.

The resulting processed logs are plotted under computer control via 8-bit digital-to-analog converters on a 6-pen MARS-6 strip chart recorder (Fig. 46.7). This system permits presentation of the data in a variety of ways: as logs of the data in raw form, stripped, smoothed, as ratios, expanded, compressed, or even reversed to present in the same form data recorded while moving either up or down the hole (Fig. 46.8). The software developed for use with this system has been described by Bristow (1977). The reading of the cassette tapes into the minicomputer memory is carried out (as shown in Fig. 46.9) via the Memodyne reader used in the field playback system. Although the data reduction system can be office based, in this case it comprises the main components of a truck-mounted minicomputer-based borehole logging system. (The G.S.C. 'DIGI-PROBE' logger in Fig. 46.10.)

The weights of the various components of the logging system are shown in Figure 46.11.

Quantitative In Situ Radiometric Assay Logging

If the digital gamma-ray spectral logging system described here is properly calibrated it is possible (assuming radioactive equilibrium) to do accurate in-situ assaying in the borehole. This log, which will be referred to as the

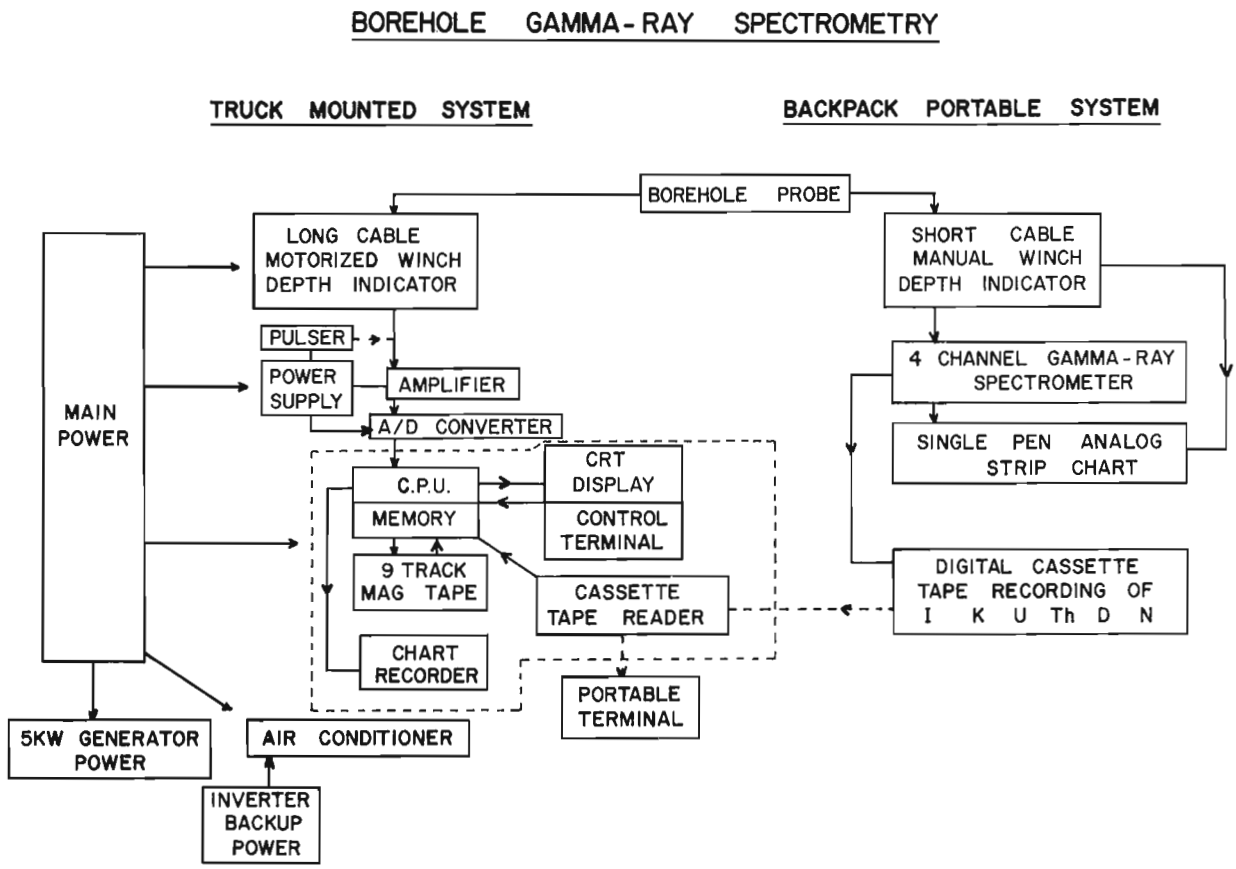

Figure 46.10. Block diagram of the new G.S.C. DIGI-PROBE logger illustrating the interplay of the backpack portable gamma-ray spectral loogger and the truck-mounted spectral logger. Cassette tapes recorded on the portable system are read by the DIGI-PROBE logger, which can also carry out the data reduction and multi-pen chart recording.

		COMPONENTS	WEIGHT kg.	WEIGHT (lbs)
1	A	SPECTROMETER		
	B	STRIPCHART	10.4	23.0
	C	CASSETTE TAPE RECORDER		
2	A	WINCH		
	B	CABLE (230m)	44.5	98.0
	C	DEPTH COUNTER		
3		1.5" BOREHOLE PROBE	4.8	10.5
		CASE	1.8	4.0
4		PULLEY + TRIPOD	5.2	11.5
5		EXTERNAL POWER (4 x 6 VOLT LANTERN BATTERIES)	6.4	14.0
			73.1	161.0

Figure 46.11. Weights of the components of the backpack portable gamma-ray spectral logging system.

radiometric assay log (R.A. log), would represent a significant saving of time and money and would provide assays of much larger sample volumes than the analysis of core samples. Quantitative radiometric assaying by total count gamma-ray logging has been used in uranium exploration and development in the United States for over 15 years. Until recently the method has not been utilized in Canada for several reasons:

(a) The probe electronics were not sufficiently compact to fit in typical small diameter Canadian mining exploration boreholes.

(b) Uranium ore deposits in Canada commonly contain significant quantities of thorium which interfere with uranium determinations by total count logging and

(c) There were no calibration facilities available in Canada.

Objection (a) is no longer valid because of advances in electronic miniaturization. Objection (b) can be overcome through the use of gamma-ray spectrometry in the borehole. Objection (c) has recently been eliminated by the construction of the new borehole calibration facilities at Bells Corners near Ottawa (Killeen, 1978), and at Fredericton, New Brunswick.

Discussion and Recommendations

It is beyond the scope of this paper to discuss calibration and quantitative radiometric assay logs, but recommendations for facilitating R.A. logging based on experience with the system described here are presented.

First, it should be stated that the digital logging system described above worked satisfactorily. Experience with this system has led to the conclusion that a motorized winch is highly desirable. Logging is a relatively slow operation, and the tedium involved in the monitoring and continuous attention necessary to maintain a constant speed with a manual winch, especially in deep holes, is liable at best to have a soporific effect on the logger, or at worst actually threaten his sanity. Having conceded the need for a motorized winch it follows that AC power (i.e. a small portable generator) will be required. This broadens the choice of most of the other components of the logging system, since the system is no longer restricted to the rather limited number of chart recorders, tape drives, etc. that operate on DC battery power.

Consider also the problem of producing the R.A. log in the field. Can one expect to have complete data reduction in terms of ore grades and thicknesses on the spot, without requiring a large computing system to provide it? The answer is yes, if instead of computing in-situ assays by the standard iterative process developed by Scott et al. (1961) and Scott (1963) the raw gamma-ray logs are deconvolved by a microprocessor as suggested for thermal gradient logs (Conaway, 1977; Conaway and Beck, 1977).

With all of the above considerations in mind it is suggested that an improved portable gamma-ray spectral logging system should consist of seven units or modules, five of which would have standard RS232C-E1A interfaces. These seven components are discussed below.

1. The Spectrometer

No great changes are required in the spectrometer except those necessary to interface with the other components. The raw data should be recorded on cassette tape, and simultaneously processed by a microprocessor with output on a chart or data terminal. Accumulating time of less than 1 s is desirable.

2. The Cassette Tape Recorder

The digital cassette tape recorder should be more versatile than the one described in this paper. The new unit should have the ability to record data at least once per second, and preferably faster. It should have the facility for file marks, and the ability to record more than one log on a tape, including the ability to search for a given log for playback. The cassette recorder should have playback (reader) capacity to enable reprocessing the data by the task module (microprocessor/controller assembly). Other features such as 'rewind' and 'fast forward' are desirable.

3. The Chart Recorder

A single channel strip chart is all that is necessary, preferably bi-directional, and with both axes of motion digitally controlled. This would enable the depth information to drive the depth axis of the chart.

4. Winch, Depth Counter

The winch and cable are selected for the user's particular requirements, but the depth counter or encoder should produce at least 200 pulses or fiducials per metre, providing a unique depth count for every spectrometric reading even at very slow logging speeds. The depth counter must be reversible, i.e. subtract counts while moving up the hole. This unit would not require a standard RS232C-EIA interface, but would be connected to the spectrometer by a simpler arrangement.

5. Electric Generator

The portable AC generator should be as lightweight as possible for the power requirements of the system. The generator may be selected from among the commercially available ones which are light enough to be considered portable; these range from 300 W (under 20 kg) to 1500 W (as light as 31 kg).

6. The Task Module

The microprocessor is the heart of the digital data reduction operation. It should perform the following functions:

1. Scale the data and transfer to the chart recorder if desired.
2. Apply spectral stripping and/or ratioing.
3. Deconvolve and smooth the raw log by application of suitable digital filters, to produce the in situ R.A. log (Conaway and Killeen, 1978).
4. Do (3) and integrate over specified distances to give grade-thicknesses.
5. Plot or print the processed data according to instructions.

The task module will carry out instructions given to it through the keyboard terminal. For example the digital filters may be changed by reading new values in from a program cassette tape or Read-Only Memory (ROM) under instructions from the terminal. New filters may be necessary for optimum results whenever the calibration parameters change, such as for changes in borehole diameter, casing type, logging speed, probe type, etc. These filters will have been precomputed from data obtained at a borehole calibration facility such as the new Geological Survey calibration facilities near Ottawa.

7. Terminal

Any compact, lightweight, rugged portable printing terminal equipped with the industry standard RS232C-EIA interface will suffice. The terminal will act as the communication input to the task module, to change values of parameters as described above and to modify the output.

Conclusions

The suggested new generation logging system described above would require no major new hardware development, since all of these components are currently available commercially. The system would, however, represent a significant advance in portable gamma-ray logging technology. Increased flexibility and reliability in both the logging and data recording aspects of the system have been stressed. In addition, incorporation of the latest microprocessor technology into the system would allow the production of in situ radiometric assay logs, quickly and inexpensively.

Acknowledgments

The authors wish to thank Jacques Parker of the Nuclear and Analytical Instrumentation Section, for help with the design and interfacing of the system components, and Bill Hyatt, Gordon Bernius and Tom Payne of the Radiation Methods Section for their help in the field testing program. Constructive criticism of the manuscript by K.A. Richardson is also greatly appreciated.

References

Bristow, Q.
1977: A system for the offline processing of borehole gamma-ray spectrometry data on a NOVA minicomputer; in Report of Activities, Part A, Geol. Surv. Can., Paper 77-1A, p. 87-89.

Conaway, J.G.
1977: Deconvolution of temperature gradient logs; Geophysics, v. 42, p. 823-837.

Conaway, J.G. and Beck, A.E.
1977: Continuous logging of temperature gradients; in A.M. Jessop (editor), Heat Flow and Geodynamics, Tectonophysics, v. 41, p. 1-7.

Conaway, J.G. and Killeen, P.G.
1978: Quantitative uranium determinations from gamma-ray logs by application of digital time series analysis; Geophysics, submitted for publication.

Killeen, P.G.
1976: Portable borehole gamma-ray spectrometer tests; in Report of Activities, Part A, Geol. Surv. Can., Paper 76-1A, p. 487-489.

Killeen, P.G. (cont.)
1978: Gamma-ray spectrometric calibration facilities - a preliminary report; in Current Research, Part A, Geol. Surv. Can., Paper 78-1A, rep. 47.

Killeen, P.G. and Bristow, Q.
1976: Uranium exploration by borehole gamma-ray spectrometry using off-the-shelf instrumentation; IAEA Proceedings of the International Symposium on Exploration of Uranium Ore Deposits, Vienna, April 1976, p. 393-414.

Scott, J.H.
1963: Computer analysis of gamma-ray logs; Geophysics, v. 28, p. 457-465.

Scott, J.H., Dodd, P.H., Droullard, R.F., and Mudra, P.J.
1961: Quantitative interpretation of gamma-ray logs; Geophysics, v. 26, p. 182-191.

47. GAMMA-RAY SPECTROMETRIC CALIBRATION FACILITIES – A PRELIMINARY REPORT

Project 720085

P.G. Killeen
Resource Geophysics and Geochemistry Division

Abstract

Killeen, P.G., Gamma-ray spectrometric calibration facilities – a preliminary report; Current Research, Part A, Geol. Surv. Can., Paper 78-1A, p. 243-247, 1978.

In order to make quantitative measurements of radioelement concentrations with a gamma-ray spectrometer the spectrometer must be calibrated using sources having (1) known radioelement contents, and (2) geometry similar to that in which the measurement will be made. In the case of portable gamma-ray spectrometers the measurement in the field will generally be made on relatively flat outcrop surfaces. This may be simulated using a flat concrete pad approximately flush with the ground surface. In the case of gamma-ray spectral logging, the measurement geometry is, of course, a borehole. In this case model boreholes including appropriate "ore" zones can be constructed in concrete.

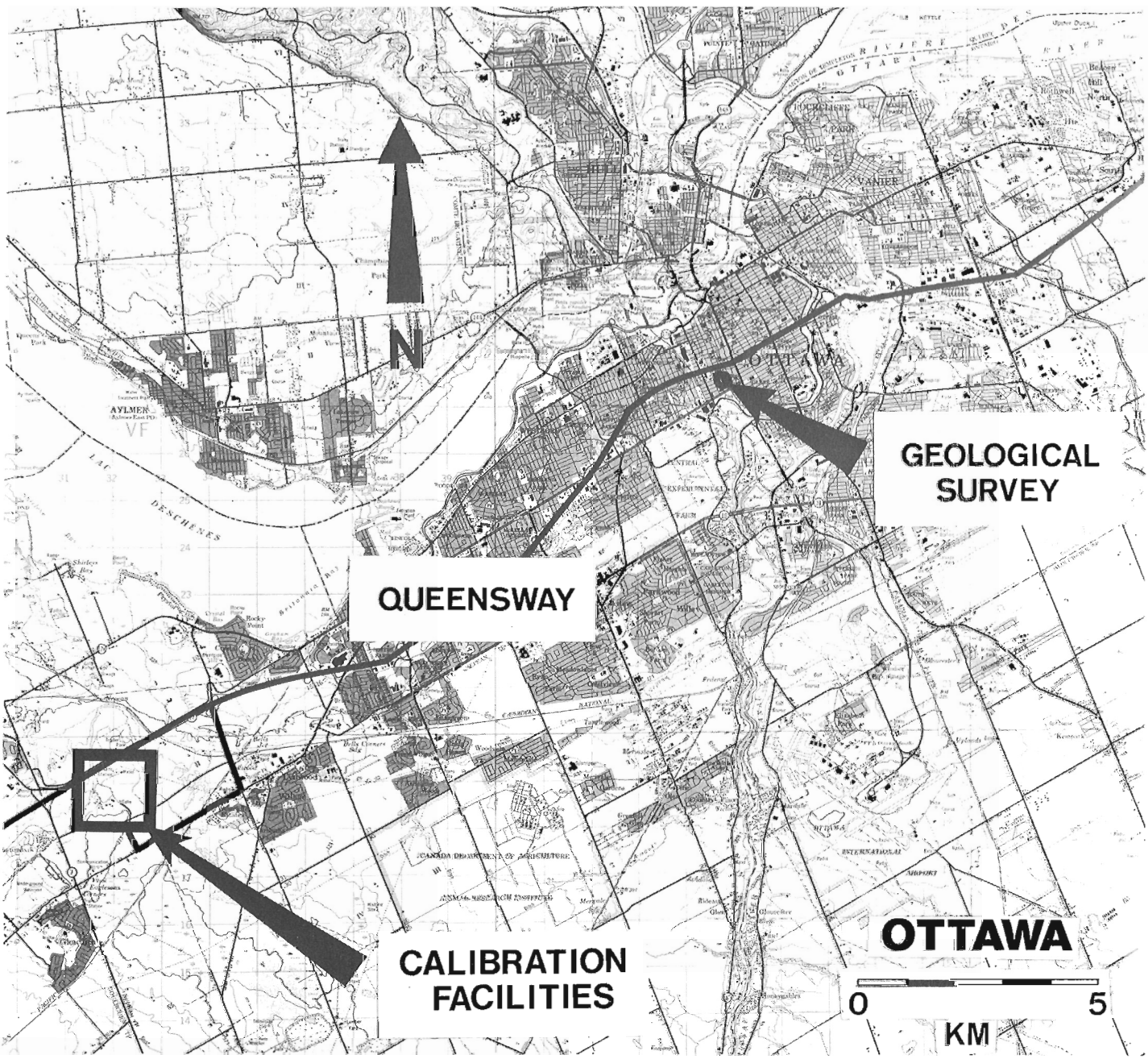

Figure 47.1. Location of the Geological Survey calibration facilities for portable gamma-ray spectrometers and gamma-ray spectral logging equipment.

Introduction

In October 1976, the Geological Survey of Canada completed the construction near Ottawa of extensive calibration facilities for gamma-ray spectrometry equipment as mentioned above. They meet or exceed the recommendations of the IAEA (1976). This paper comprises a preliminary report on the new facilities: their location, description, preliminary analyses of samples taken during construction, and the procedure for obtaining access to the calibration facilities, and preliminary recommended procedures for carrying out the calibration measurements.

Location of the Calibration Facilities

The new calibration facilities are located on the property of the CANMET (E.M.R.) laboratory complex at Bells Corners approximately 10 km west of Ottawa. Figure 47.1 shows the location. The calibration facilities consist of a set of 10 calibration pads for portable spectrometers, located along a gravel road leading to an abandoned quarry in which nine test columns containing the model boreholes are constructed (see Fig. 47.2).

Calibration Pads for Portable Gamma-Ray Spectrometers

The calibration pads are concrete cylinders, 60 cm thick and 3 m in diameter, making effectively infinite sources if the detector of the portable gamma-ray spectrometer is centrally located on and within a few inches of the surface of the pad. Three pads contain different potassium concentrations, three contain different uranium concentrations and three contain different thorium concentrations. The different radioelement concentrations were obtained by adding to the concrete appropriate amounts of uranium ore, thorium oxide, or nepheline syenite for U, Th, and K respectively. A tenth pad, referred to as the blank pad, was constructed with no radioelement additives. The preliminary mean values of the radioelement contents of some of the samples taken during construction are given in Table 47.1. At the time of this writing, not all of the samples have been analyzed. Thus, although subject to revision, these preliminary values indicate the range of concentrations available for calibration purposes. The five pads at Uplands Airport, which had previously been used for calibration of portable instruments, have a very limited range of radioelement concentrations since they were designed for calibrating airborne gamma-ray spectrometers (Grasty and Darnley, 1971) and will continue to be used for that purpose. The new calibration pads should greatly improve the accuracy and repeatibility of determinations of calibration factors.

The recommended procedure for carrying out calibration measurements is explained in greater detail on handout sheets provided to users of the calibration facilities. These include a detailed location map, a table of pad numbers with their radioelement concentrations, and information about obtaining clearance for access to the calibration site. This information may be obtained by contacting the Radiation Methods Section, Resource Geophysics and Geochemistry Division of the Geological Survey of Canada.

Basically the calibration procedure for portable gamma-ray spectrometers consists of taking several readings on each pad in order to obtain good counting statistics, with the detector at a slightly different location near the centre of the pad for each reading. Counting times will depend on detector size.

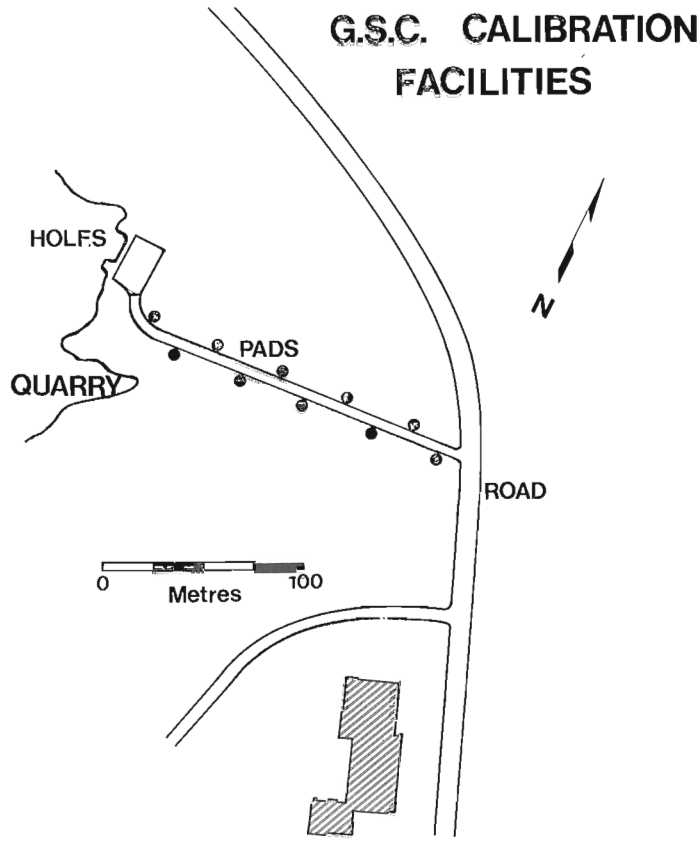

Figure 47.2. Detailed locations of the 10 calibration pads and the model holes on the property of the CANMET laboratory complex at Bells Corners.

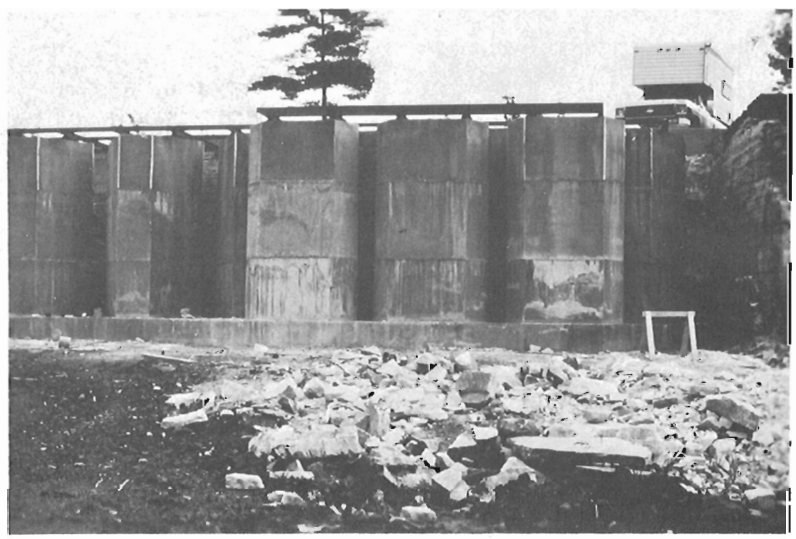

Figure 47.3. The nine concrete test columns viewed from inside the quarry showing the "ore zones" and a logging truck parked above in the working area for calibrating logging systems. (GSC photo 203254-0).

If these data, along with the types and serial numbers of the spectrometers and detectors are given to the Geological Survey, the calibration constants will be computed; there is no charge for this service. The use of the calibration constants for computing in situ assays was described by Killeen and Cameron (1977).

Table 47.1

Preliminary mean radioelement concentrations for calibration pads

Pad Number	K%	eU ppm	eTh ppm
PK-1-OT	0.88		
PK-2-OT	1.48		
PK-3-OT	2.87		
PU-4-OT		6.10	
PU-5-OT		42.49	
PU-6-OT		458.15	
PT-7-OT			8.10
PT-8-OT			62.00
PT-9-OT			310.07
PB-10-OT	0.24	0.16	1.39

Model Boreholes for Calibrating Gamma-Ray Logging Systems

For calibration of borehole gamma-ray spectrometers a set of nine models have been constructed along the wall of a rock quarry as shown in Figure 47.3. Each of the models consists of a concrete column 3.9 m in height with an "ore zone" 1.5 m thick sandwiched between an upper and lower barren zone as shown in Figure 47.4. Each test column contains 3 boreholes of diameters A (48 mm), B (60 mm) and N (75 mm) intersecting the ore zones as shown in Figure 47.5. Three of the test columns contain ore zones of different concentrations for potassium, three for thorium, and three for uranium. These ore zones were produced by mixing suitable additives with the concrete as described above for the calibration pads.

The preliminary mean values of the radioelement concentrations in samples taken during construction are given in Table 47.2. Revised radioelement concentration values will be determined and published at a later date when all of the samples have been analyzed. The radioelement concentrations in the barren zones are the same as for the blank pad (PB-10-OT) in Table 47.1.

The calibration procedure for gamma-ray spectral logging equipment consists of three parts: (1) the determination of the stripping factors, (2) the determination of the sensitivity i.e. the relation between count rates and ore grade, and (3) the determination of instrument response characteristics (if the logging data are to be computer processed to improve accuracy and resolution (e.g. Scott et al., 1961; Scott, 1963; Conaway and Killeen, 1978; Killeen et al., 1978).

The stripping factors can be determined relatively quickly by observing the count rates obtained in the uranium and potassium channels of the spectrometer, while the borehole probe is positioned inside a thorium ore zone, and then inside a uranium ore zone. (This would also give the upward stripping factor, i.e. uranium counts in the thorium window.) In practice the count rate should be determined at several positions near the centre of each ore zone in order to obtain an accurate average value. As in the case of the calibration pads, if these data are supplied to the Geological Survey, stripping factors will be computed.

Having determined the stripping factors, these can then be applied to logs recorded in the field. The stripping factors will enable the stripped gamma-ray log to be plotted as shown in the conceptual example of Figure 47.6. From top to bottom in this figure are shown the anomalies in the 4

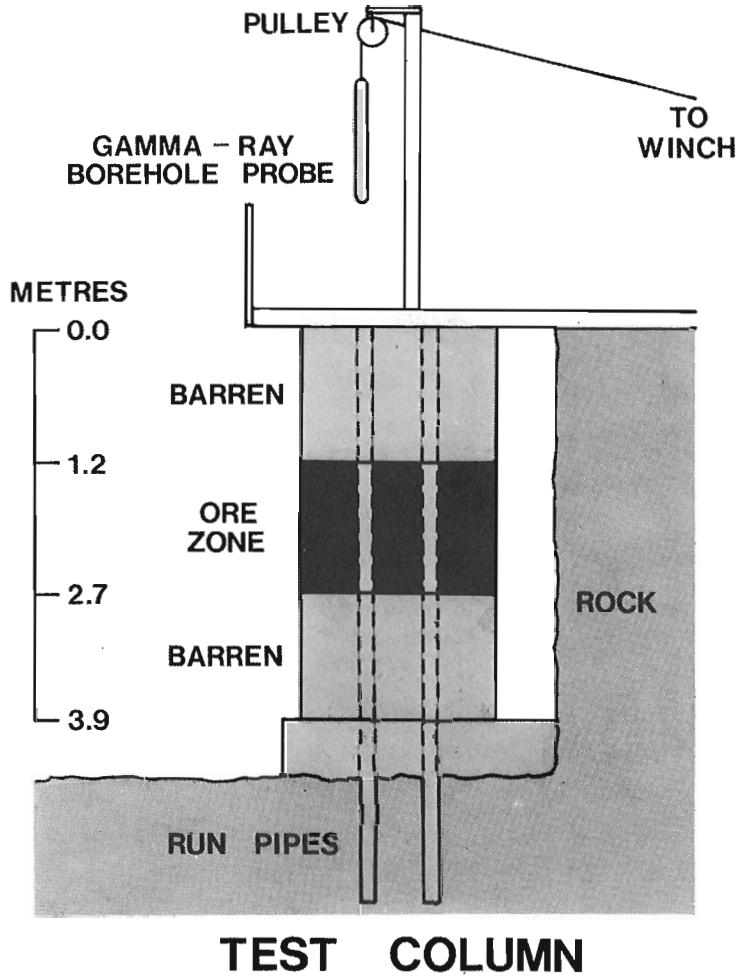

Figure 47.4. Cross-sectional view of a test column, showing two of the three holes in the column, the run pipes which extend 3.0 m below, and the hoist and pulley on top of the column.

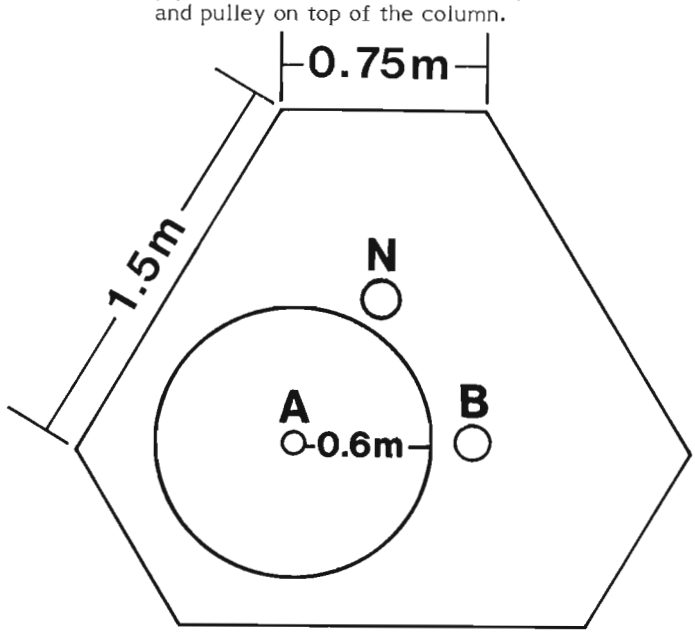

Figure 47.5. Plan view of a test column showing location and spacing of the three sizes of model boreholes.

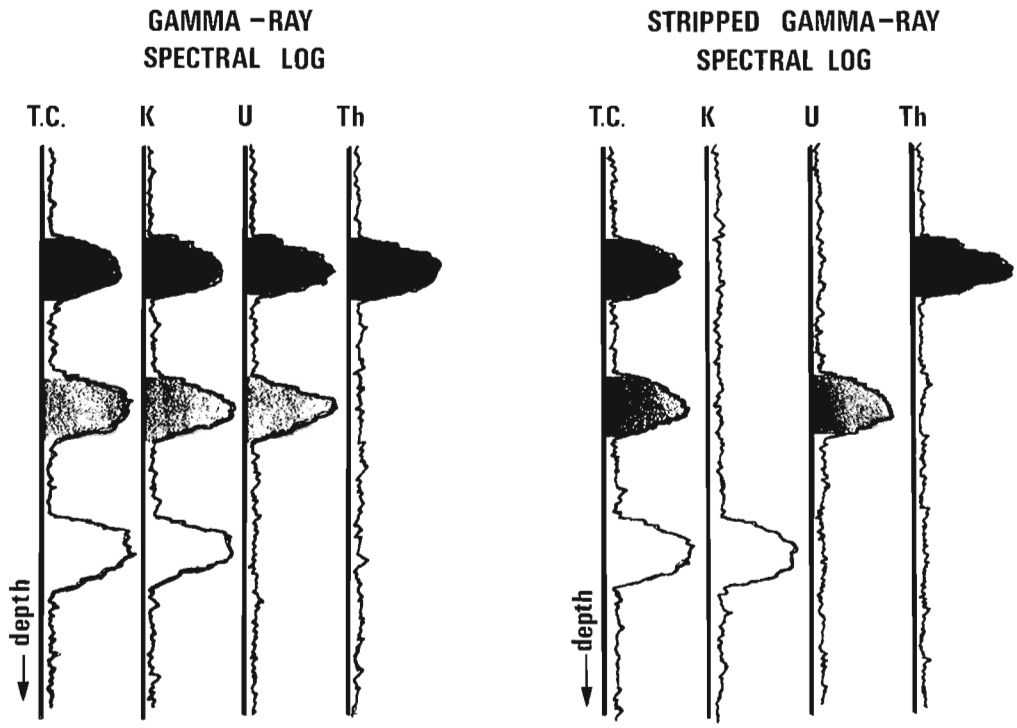

Figure 47.6.

Comparison of unstripped and stripped gamma-ray spectral logs showing anomalies caused by K, U, and Th respectively.

Table 47.2

Preliminary mean radioelement concentrations for test columns

Column Number	K%	eU ppm	eTh ppm
BK-1-OT	0.72		
BK-2-OT	1.14		
BK-3-OT	3.01		
BU-4-OT		14.32	
BU-5-OT		100.67	
BU-6-OT		948.58	
BT-7-OT			8.20
BT-8-OT			34.93
BT-9-OT			347.11

channels of the spectrometer (total count, K, U, and Th) caused by logging through a thorium zone, a uranium zone, and a potassium zone respectively. The left side of Figure 47.6 shows the unstripped log illustrating the ambiguous situation which arises when anomalies appear in the uranium and potassium channels even when no uranium or potassium is present. The right side of Figure 47.6 shows the stripped gamma-ray spectral log, which clearly indicates which of the radioelements caused each of the three anomalies shown in the total count channel.

The ultimate objective of gamma-ray spectral logging is quantitative downhole assaying, particularly of uranium, which is part (2) of the calibration procedure. In this case, the determination of the system calibration constant K is carried out using stripped data obtained as in step (1) above by means of the equation

$$K = \frac{G}{I}$$

Here G is the known radioelement concentration (grade) in parts per million (ppm) and I is the average measured gamma-ray intensity in counts/s near the centre of the ore zone; the units of K, then, are ppm s/count. The raw field log is then multiplied by K to give the ore grades in cases of uniform ore zones approximately 1 m or more in thickness (i.e. infinitely thick). The grade values obtained for thinner zones will be lower than the actual grade.

In order to enhance the accuracy and resolution of ore grade determinations in thin beds and complex sequences, it is necessary to carry out step (3), the determination of the system response characteristics. More information on this can be found in Conaway and Killeen (1978).

The logging equipment calibration facilities are designed to permit calibration of logging systems in both wet and dry holes of sizes A, B, and N, uncased or with various types of casing material.

As in the case of the calibration pads, handout sheets with further information and recommended procedures will be provided to those persons interested in calibrating gamma-ray logging equipment in the model boreholes. The Geological Survey will endeavour to compute the calibration factors for gamma-ray spectral logging systems when the recommended procedures are followed.

It should perhaps also be mentioned here that two model boreholes containing different uranium ore zones have been constructed in Fredericton, in co-operation with the New Brunswick Department of Natural Resources. These two model holes are approximately 125 mm in diameter and may be used in the calibration of total count gamma-ray logging equipment. Future additional calibration facilities are planned for other locations in Canada. These will probably consist of sets of seven calibration pads (2 for each radioelement and one blank), and model boreholes of a simpler design. It is hoped that calibration of gamma-ray spectrometric equipment will become a more common practice in Canada as these calibration facilities become more readily available.

References

Conaway, J.G. and Killeen, P.G.
1978: Quantitative uranium determinations from gamma-ray logs by application of digital time series analysis; Geophysics, submitted for publication.

Grasty, R.L. and Darnley, A.G.
1971: The calibration of gamma-ray spectrometers for ground and airborne use; Geol. Surv. Can. Paper 71-17.

IAEA
1976: Radiometric reporting methods and calibration in uranium exploration; IAEA Technical Report Series No. 174, 57 p.

Killeen, P.G. and Cameron, G.W.
1977: Computation of in situ potassium, uranium and thorium concentrations from portable gamma-ray spectrometer data; in Geol. Surv. Can., Paper 77-1A, p. 91.

Killeen, P.G., Conaway, J.G., and Bristow, Q.
1978: A gamma-ray spectral logging system including digital playback, with recommendations for a new generation system; in Current Research, Part A, Geol. Surv. Can., Paper 78-1A, rep. 46.

Scott, J.H.
1963: Computer analysis of gamma-ray logs; Geophysics, v. 28, p. 457-465.

Scott, J.H., Dodd, P.H., Droullard, R.F., and Mudra, P.J.
1961: Quantitative interpretation of gamma-ray logs; Geophysics, v. 26, p. 182-191.

MAGNETIC FABRIC OF ROCKS

Project 730160

E.J. Schwarz
Resource Geophysics and Geochemistry Division

Abstract

Schwarz, E.J., Magnetic fabric of rocks; Current Research, Part A, Geol. Surv. Can., Paper 78-1A, p. 249-252, 1978.

Determination of the anisotropy of magnetic susceptibility is an accurate and rapid tool in the investigation of rock fabric and should therefore be of interest to structural geologists, metamorphic petrologists and sedimentologists. Therefore, the basics of the method are briefly discussed in qualitative terms and some parameters to describe degree of anisotropy, lineation and foliation are listed. A few examples based on new data are analyzed.

Introduction

The arrangement of grains or crystals in a rock is called fabric. Fabric, crystallinity and granularity of a rock define its texture. There are various ways to determine fabric. When macroscopically visible, lineation and foliation can be rapidly measured in the field with a compass, otherwise, a microscope or special X-ray techniques must be used.

The orientation or alignment of magnetic grains or crystals defines a magnetic fabric. Even a weak magnetic fabric can be conveniently detected by the determination of the anisotropy of magnetic susceptibility which can be rapidly carried out. The limitations of this method are that no direct information on the silicate fabric is obtained and that in some cases the interpretation of the anisotropy of susceptibility is ambiguous. This is because the anisotropy is due either to shape of the magnetic grains (shape anisotropy) if these are composed of magnetite, or to orientation of magnetically strongly anisotropic crystals (magnetocrystalline anisotropy) if these grains are formed by hematite αFe_2O_3 or pyrrhotite Fe_7S_8. Hence, the magnetic constituents must be known, for instance, from thermomagnetic analysis.

Magnetic fabric can be determined rapidly and should therefore be considered first if fabric studies are required in geological interpretation (Graham, 1954). To provide a background for interested geologists, the method to determine magnetic fabric and its analysis are discussed in an

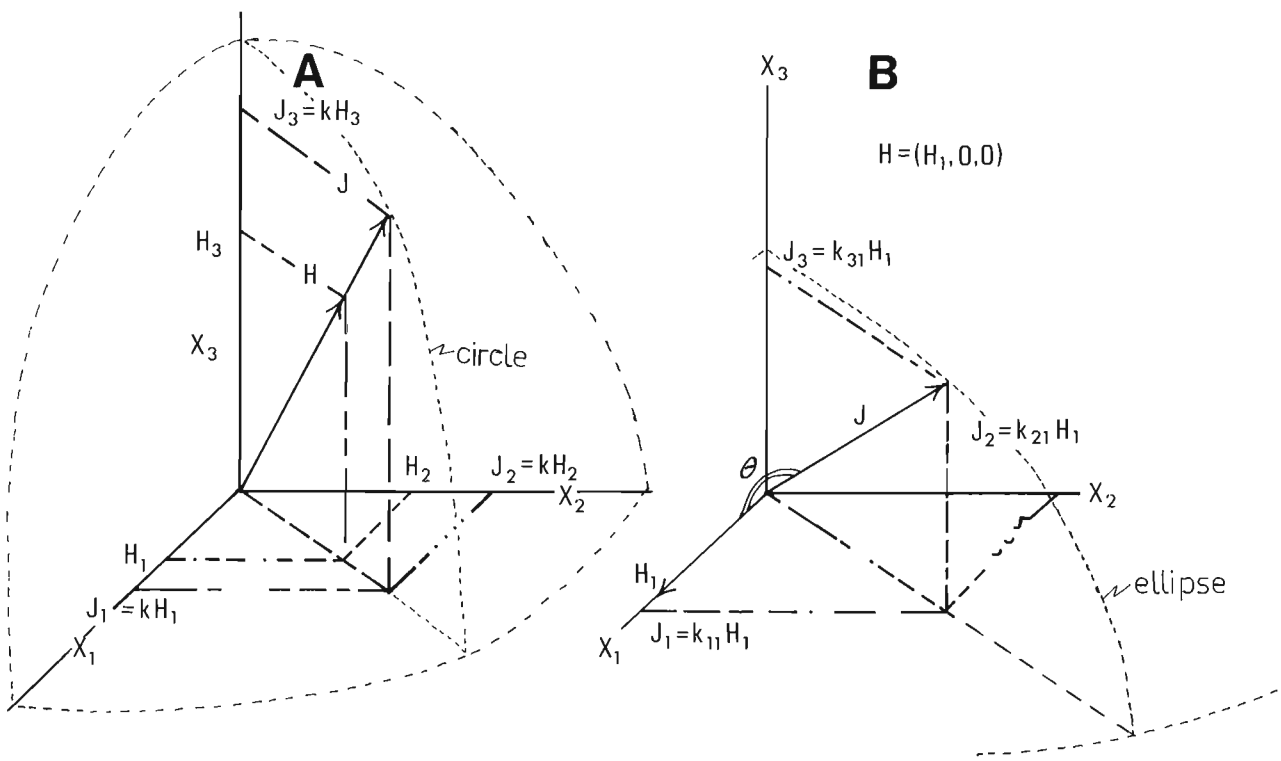

Figure 48.1. Parallel orientation of induced magnetization (J) and magnetic field (H) in isotropic sample (A) and general case of non-parallelism between J and H in an anisotropic case (B). Dashed lines on A indicate sphere with radius J formed by the end points of J during three-axial rotation. In case B an ellipsoid would be formed.

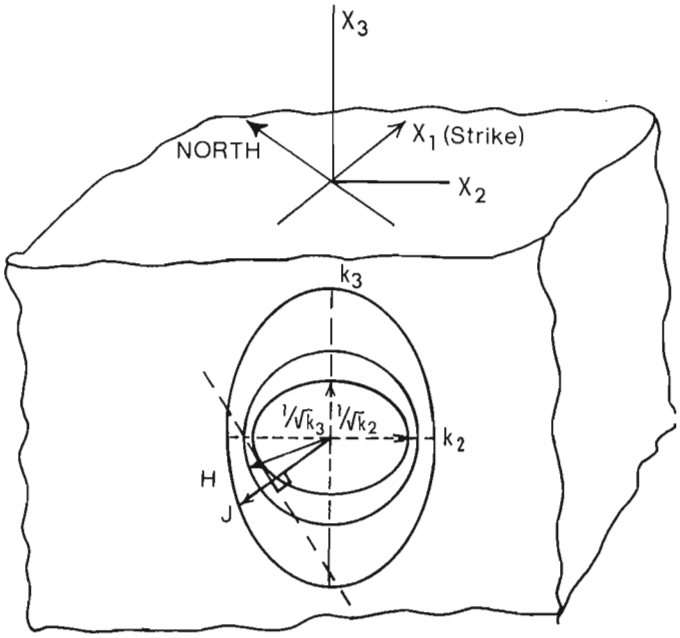

Figure 48.2. Three-dimensional views of sample with orientation markings and co-ordinate system. Front surface shows two-dimensional sections of two different but related ellipses as discussed in the text.

elementary manner. A few examples involving different rock types are given.

What is Anisotropy of Susceptibility

The magnetization (J) acquired by a rock sample in a weak applied field (H) is proportional to the field by a parameter called the susceptibility. In other words, the susceptibility is a measure of the capacity of acquiring magnetization in a magnetic field. Thus:

$$J = k\,H$$

Both J and H are vectors; they have as properties a certain magnitude and a certain direction. If J is parallel to H for all directions of the field, the susceptibility is just a simple number and the sample is called magnetically isotropic. Thus, if this sample is rotated around its centre as a ball-joint, the end-point of J will describe a sphere as indicated on Figure 48.1A (Field H is fixed in direction and magnitude as is the geomagnetic field). However, in general the magnetization will both vary in magnitude and make a smoothly varying angle (θ) with the applied field if the sample is rotated in the field (Fig. 48.1B). It is clear that the susceptibility cannot be given in the form of a simple number for magnetically anisotropic rocks.

Thus, for an isotropic material:

$$J_1 = k\,H_1$$
$$J_2 = k\,H_2$$
$$J_3 = k\,H_3,$$

if J_1, J_2, J_3 and H_1, H_2, H_3 indicate three orthogonal components of J and H respectively (Fig. 48.1A). However, in the case of an anisotropic material, magnetization components are generated along all three axes of the co-ordinate system even if the field is aligned parallel to one of these axes (Fig. 48.1B). Consequently, by summing all terms generated by aligning H along all three axes, the magnetization of an anisotropic material can be described by:

$$J_1 = k_{11}H_1 + k_{12}H_2 + k_{13}H_3$$
$$J_2 = k_{21}H_1 + k_{22}H_2 + k_{23}H_3$$
$$J_3 = k_{31}H_1 + k_{32}H_2 + k_{33}H_3$$

where the nine coefficients:

$$k_{11}\ k_{12}\ k_{13}$$
$$k_{21}\ k_{22}\ k_{23}$$
$$k_{31}\ k_{32}\ k_{33}$$

form a tensor of the second rank. These terms can be represented in short by $J_i = k_{ij}\,H_j$ where i, j = 1, 2, 3. The mathematics of tensor analysis are given in detail by, for instance, Nye (1957). The following describes in a qualitative way the basic concepts employed in the mathematics to compute the shape (and volume) of the ellipsoid representing the tensor k_{ij} from measurements of the susceptibility in at least 6 directions through the sample. This would provide a basic understanding of anisotropy.

The significance of the terms $J_i = k_{ij}\,H_j$ can be easily understood from Figure 48.2. Suppose we have a sample oriented with respect to the geographic co-ordinate system. The sample is kept in the same orientation while the constant and homogeneous field H of unit strength is rotated with respect to three orthogonal axes (X_1, X_2, X_3) joining in the centre of the specimen. The end points of H then describe a sphere indicated by a circle in Figure 48.2. The values J then lie on an ellipsoid around the specimen centre indicated by the large ellipse in Figure 48.2. Denoting the susceptibility along the axes by k_1, k_2, k_3, an ellipsoid with semi-axes $1/\sqrt{k_1}$, $1/\sqrt{k_2}$, $1/\sqrt{k_3}$ then represents the tensor k_{ij} (i, j = 1, 2, 3). To geologists, the similarity of the ellipsoid k_{ij} with the indicatrix, of which the radius is given by the refractive index or the square root of the dielectric constant in the radius directions, is clear. The angle between applied field H and the resulting magnetization J is also graphically expressed by Figure 48.2. For a given direction of H, which can be represented by a radius vector of the sphere around the centre of the sample, draw the tangent at the intersection of the vector H with the ellipse with semi-axis $1/\sqrt{k_2}$, $1/\sqrt{k_3}$. Then draw a line from the centre perpendicular to the tangent. This line represents the direction of the

Table 48.1

Some anisotropy parameters for orebodies in the Sudbury area, Proterozoic igneous rocks on the East Coast of Hudson Bay, and phenocrysts in the St. Jean anorthosite

Rock	No. of samples	k_{max}/k_{min}	k_{int}/k_{min}	k_{max}/k_{int}	E
Sulphides Strathcona M.	20	1.57	1.09	1.39	1.27
Sulphides Copper Cliff M.	16	2.08	1.24	1.70	1.40
Komatiite Smith Island (NWT)					
upper part	13	1.05	1.03	1.03	1.00
lower part	24	1.12	1.07	1.06	0.99
Basalt Richmond Gulf	16	1.011	1.010	1.003	1.003
Plagioclase Anorthosite	2	1.29	1.03	1.25	0.84
Pyroxene Anorthosite	2	1.09	1.07	1.01	1.05

magnetization vector J. The radius vector from the origin of the co-ordinate system to the ellipse representing the values J with semi-axes (J_2, J_3) then gives both direction and the magnitude of the magnetization vector J. This graphical representation relates direction and magnitude of H, J, and the corresponding value for k (from the radius $1/\sqrt{k}$). It is useful to note that J is parallel to H only if H is oriented along one of the principal axes of the ellipse. This property can be used in iterative processes to find the orientation of the principal axes from a set of measurements obtained by rotating the specimen with respect to H following a fixed sequence of orientations. Nye (1957) gives a detailed account of tensor analysis. The susceptibilities represented by the principal axes are called principal susceptibilities and they form the basis of magnetic fabric studies.

Magnetic Fabric Parameters

The ellipsoid of representation of the tensor k_{ij} is determined for individual samples in the manner indicated above. Now we wish to examine what information can be obtained from the characteristic properties of this ellipsoid. The volume of the ellipsoid is only related to the bulk or average susceptibility and is therefore only of interest in magnetic surveying. However, the shape of the ellipsoid is of great interest in fabric studies. Therefore, the maximal, intermediate, and minimal susceptibilities (respectively k_{max}, k_{int}, k_{min}) and their directions with respect to the co-ordinate system are computed.

1. Degree of anisotropy is defined as $P = k_{max}/k_{min}$. For a given type and concentration of a ferromagnetic mineral, this ratio varies in proportion with the degree of preferred orientation of crystals and/or grains assuming a constant average grain shape.

2. The total anisotropy can be expressed by:

$(k_{max}-k_{min})/(k_{max}+k_{int}+k_{min})/3)$ or $(k_{max}-k_{min})/k_{int}$.

3. The coefficient k_{max}/k_{int} describes the degree of linear orientation in the maximum susceptibility plane (or magnetic foliation plane) and is a measure of the magnetic lineation as expected for an assemblage of uniaxial particles showing directional preference of their long axes.

4. The coefficient k_{int}/k_{min} describes the degree of planar orientation or magnetic foliation. This arises, for instance, from an assemblage of uniaxial grains of which the long axes are distributed randomly in the maximum susceptibility plane.

5. The ratio of the coefficients for lineation and foliation yields the coefficient $E = (k_{int})^2/k_{max}.k_{min}$ indicating whether either the lineation (E<1, oblate ellipsoid or cigar-shaped) or the foliation is best developed (E>1, prolate ellipsoid or two long dimensions).

6. Another parameter describing the prolateness of the ellipsoid is $(k_{max}-k_{int})/(k_{int}-k_{min})$, while the oblateness can be represented by $(k_{int}-k_{min})/(k_{max}-k_{int})$. A combination of these is:

$q = (k_{max}-k_{int})/(k_{max}+k_{int} - k_{min})$.

If $k_{max}=k_{int}$: q = 0, and we have purely planar fabric. If $k_{int}=k_{min}$, q = 2 and we have purely linear fabric.

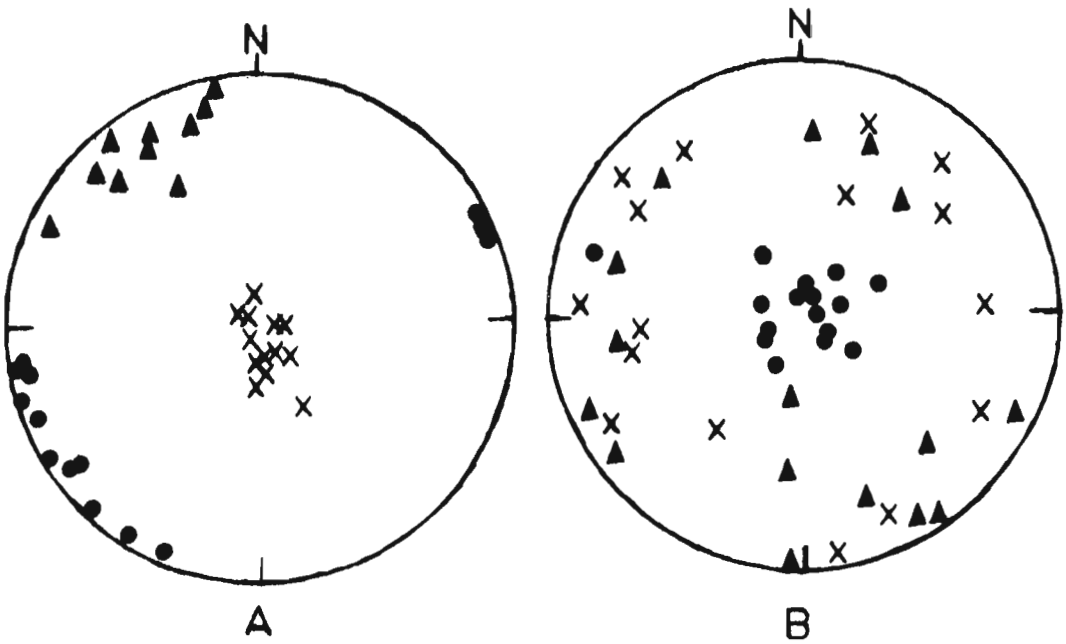

Figure 48.3. Directions of principal susceptibilities plotted in lower hemisphere of a stereographic diagram for Richmond Gulf basalt (A) and Copper Cliff deposit (B). Crosses, triangles and dots indicate respectively k_{min}, k_{int}, and k_{max}.

Examples showing differences in parameters indicating type of magnetic fabric are shown in Table 48.1. The sulphides from mines near Sudbury are strongly anisotropic (high k_{max}/k_{min}), their high E values indicate well-developed foliation, and in addition the Copper Cliff deposit shows marked lineation in the foliation plane. The significance of this is not entirely clear: magnetic pyrrhotite (Fe_7S_8) has high susceptibility in the basal plane and very low susceptibility at right angles to this plane (parallel to the crystallographic c-axis). Thus, the foliation indicates layering of the basal planes of Fe_7S_8 crystals. The cause of the lineation, however, is unknown. The lower part of the komatiitic basalts of Smith Island and adjacent New Quebec also contains Fe_7S_8. The degree of anisotropy is also fairly high as shown by their average k_{max}/k_{min}. The rest of the rocks listed contain only magnetite grains as the predominant magnetic constituent. A high degree of anisotropy – indicated by a high average k_{max}/k_{min} – is observed for the samples cut from a single plagioclase crystal from an anorthosite body in the Grenville province. In this case, lineation is relatively well developed as evidenced by both low k_{int}/k_{min} and E. The likely explanation is that magnetite needles (high shape anisotropy) tend to be aligned in one crystallographic direction. On the other hand, the pyroxene phenocryst from the same rock only shows some foliation (see k_{int}/k_{min} and E values).

In addition to the computation of anisotropy factors, the directions of the mutually perpendicular principal susceptibilities k_{max}, k_{int} and k_{min} may be plotted stereographically. This yields additional information. For instance, Table 48.1 shows that the Richmond Gulf basalts are very weakly anisotropic. This weak anisotropy may be due to either flow during emplacement or tectonic effects. A diagram of the directions (Fig. 48.3A) shows tight grouping with k_{max} and k_{int} in the flow plane. In other words, the maximum and intermediate dimensions of the magnetite crystals are in the flow plane which is consistent with a flow pattern. Lineation in the Copper Cliff deposit is borne out by the grouping of k_{max} directions and the zonal distribution of both k_{min} and k_{int} (Fig. 38.3B).

These few examples show that weak anisotropies due to a slight tendency of alignment of non-equidimensional magnetite grains can be detected. Various types of fabric can be described and analyzed by computing anisotropy factors and/or plotting the directions of the principal susceptibilities with respect to the geographic co-ordinate system. The use of the method should be considered wherever fabric studies are required for geological interpretation if there is no reason to expect that silicate fabric will differ from the magnetic fabric and if fabric cannot be determined in the field. The magnetic method is sensitive and rapid.

References

Graham, J.

1954: Magnetic susceptibility anisotropy, an unexploited petrofabric element; Geol. Soc. Am., Bull., v. 65, p. 1257.

Nye, J.F.

1957: Physical properties of crystals; Oxford University Press, 322 p.

SOME NEW MINERAL OCCURRENCES IN CANADA

Project 640048

Ann P. Sabina
Central Laboratories and Administrative Services Division

Abstract

Sabina, Ann P., Some new mineral occurrences in Canada; Current Research, Part A, Geol. Surv. Can., Paper 78-1A, p. 253-258, 1978.

New occurrences of twenty-three relatively uncommon minerals were recently discovered and are described briefly. Four of these minerals occur in British Columbia, one in Alberta and the remainder in Ontario and Quebec. For each occurrence, brief descriptions of the mineral, its mode of occurrence, the associated minerals and its location are given. Included are occurrences of: ancylite, aurichalcite, bakerite, brugnatellite, burbankite, catapleiite, gunningite, hydromagnesite, hydrotalcite, hydroxyl-bastnaesite, hydrozincite, kasolite, ludwigite, perovskite, perrierite, phillipsite, pseudocubic quartz crystals, pyroaurite, sepiolite, stilpnomelane, tochilinite, uranophane, woodruffite.

Several new localities of relatively rare mineral species were encountered in the course of field investigations in Ontario and Quebec during the summer of 1977. These occurrences along with some mineral occurrences in Alberta and British Columbia are described briefly in this report. The minerals were identified by X-ray powder diffraction (by A.C. Roberts) and supplemented, in some cases by microprobe analysis (by A.G. Plant). The specimens are now in the National Mineral Collection.

Descriptions of these minerals and their localities follow. The National Topographic Series index number referring to 1:50 000 map sheets is given for each locality.

Ancylite $SrCe(CO_3)_2(OH)\cdot H_2O$

Burbankite $(Na,Ca,Sr,Ba,Ce)_6(CO_3)_5$

Catapleiite $Na_2ZrSi_3O_9\cdot 2H_2O$

Phillipsite $(K_2,Na_2,Ca)(AJ_2Si_4)O_{12}\cdot 4\text{-}5H_2O$

These minerals occur sparingly in igneous dykes and sills which intrude Ordovician limestone at the Miron quarry, Jarry Street at Papineau Avenue, Montreal (31H/12). The igneous intrusions are believed to be satellite bodies related to the Monteregian intrusion. Ancylite was also found at the property of Desmont Mining Corporation, Limited near Wilberforce, Ontario (31E/1).

Figure 49.1. Pseudocubic quartz crystals on botryoidal quartz, Red Deer River valley, Alberta. The crystals average 1 mm along the edge (GSC 203246-A).

At the Miron quarry, ancylite occurs as vitreous to greasy, greenish brown to dark green, finely granular and platy aggregates (2 to 3 mm in diameter) in massive white analcime and in granular masses consisting of calcite and potash feldspar. Crystals of natrolite and, less commonly, of burbankite are associated with the ancylite.

The burbankite occupies small cavities measuring 3 to 4 mm in diameter in dolomite, analcime, natrolite, and in the igneous rock. It occurs as colourless, white or reddish hair-like to acicular aggregates in the cavities, and as bluish white finely flaky encrustations on natrolite.

Catapleiite forms light brown, greenish brown and orange lamellar and radiating platy aggregates (1 to 2 mm in diameter) in white massive potash feldspar which occupies fracture zones in the igneous rock. Its lustre varies from vitreous, pearly to greasy and is commonly characterized by a coppery tarnish.

Phillipsite occurs as snow white, sugary, spotty encrustations on the igneous rocks.

The dykes and sills at this quarry contain a number of other minerals which generally occupy vugs and fracture zones; these minerals are however, sparsely distributed. The following have been observed; dawsonite, fluorite, strontianite, harmotome, vesuvianite, titanite, acmite, chlorite, anatase, siderite, ilmenite, quartz, pyrite, sphalerite, magnetite and graphite. Ancylite at the Desmont property near Wilberforce, Ontario is intimately intergrown with stillwellite which was recently reported from the deposit (Sabina, 1977). The ancylite – stillwellite intergrowths form light brown vitreous masses in coarsely crystalline calcite.

Hydromagnesite $Mg_5(CO_3)_4(OH)_2 \cdot 4H_2O$

Hydromagnesite was identified in specimens collected from the Princess sodalite quarry near Bancroft, Ontario (31F/4), and from a road-cut on the west side of Highway 148 at a point 0.6 km south of Bryson, Quebec (31F/10). At the Princess quarry, it occurs as silky white fibrous aggregates in massive natrolite which is commonly associated with sodalite. In the locality near Bryson, hydromagnesite forms silky white flaky coatings on serpentine and on crystalline limestone which is exposed by a road-cut. Brucite, pyroaurite, szaibelyite, hydrotalcite, apatite, spinel, aragonite, mica, chlorite, magnetite, pyrrhotite and sphalerite are also present in the crystalline limestone.

Hydrotalcite $Mg_6Al_2(CO_3)(OH)_{16} \cdot 4H_2O$

Brugnatellite $Mg_6Fe^{+3}(CO_3)(OH)_{13} \cdot 4H_2O$

Hydrotalcite was noted in specimens from three localities: a road-cut on Highway 105 near Maniwaki (31J/5); rock exposures along the du lièvre River at the des Cèdres dam near Notre-Dame-du-Laus, Quebec (31J/4); and a railway-cut at Chaffeys Locks, Ontario (31 C/9). At each locality, it occurs sparingly in crystalline limestone. It occurs as charcoal-grey, greasy nodules associated with chondrodite, spinel, clinoamphibole, serpentine, amber mica, pyrite and graphite in the crystalline limestone exposed by a road-cut on the west side of Highway 105 at a point 10.4 km south of its junction with Highway 117. This is just north of the village of Maniwaki. In the exposures at des Cèdres dam, hydrotalcite occurs as white flaky aggregates and as waxy white nodules in association with clinohumite, spinel, olivine, serpentine, clinoamphibole, ilmenite and rutile. Brugnatellite forms white flaky coatings on clinohumite.

At the Chaffeys Locks occurrence, greasy, grey nodules of hydrotalcite are associated with clinohumite, spinel, serpentine, apatite, clinopyroxene, clinoamphibole, olivine and tourmaline.

Hydroxyl-bastnaesite $(Ce,La)CO_3(OH,F)$

This rare mineral was originally described in 1964 from carbonatites of a stock of alkalic and ultrabasic rocks, presumably in Russia (Kirillov, 1964). It was found during this investigation in specimens collected from the property of Desmont Mining Corporation, Limited near Wilberforce, Ontario (31/E/1).

At this locality it occurs as brownish yellow to dark brown, waxy to resinous finely granular aggregates in coarsely crystalline calcite. Associated with it are stillwellite, monazite, thorianite, uranothorite, clinopyroxene, ancylite, garnet, titanite, pyrite, potash feldspar and quartz. The calcite occurs in veins and lenses in sugary diopside-calcite rock enclosed in marble.

Kasolite $Pb(UO_2)SiO_4 \cdot H_2O$

Uranophane $Ca(UO_2)_2Si_2O_7 \cdot 6H_2O$

Kasolite and uranophane occur in tremolite-bearing diopside marble exposed by an open-cut on a ridge which parallels the Gibson Road at Tory Hill, Ontario (31D/16). The occurrence is north of McCue Lake and about 1100 m by road west of the junction of the Gibson Road and Highway 121.

Kasolite occurs as bright yellow, waxy, finely granular irregular masses in sugary diopside, uranophane as pale yellow to light brownish yellow, waxy, massive aggregates associated with thorianite. Coarse prismatic and bladed aggregates of white, grey and light green tremolite are common in the marble. Thorite, uraninite, apatite, talc, pyrite and quartz are also present in the marble.

Ludwigite $Mg_2Fe^{+3}BO_5$

Ludwigite occurs in serpentine marble at the Stephen Cross quarry near Wakefield, Quebec (31G/12). It occurs as black longitudinally striated slender prisms commonly measuring 0.5 cm long, as acicular aggregates, and as finely fibrous and granular masses. The lustre varies from adamantine to submetallic in the crystals, and from velvety, resinous to submetallic in the fibrous and granular massive varieties. The streak is dark green. Magnetite, pyrrhotite, brucite and pyroaurite are intimately associated with the massive variety. Clinohumite, spinel, olivine, pyrite and tochilinite occur sparingly in the marble.

Perrierite $(Ca,Ce,Th)_4(Mg,Fe)_2(Ti,Fe^{+3})_3Si_4O_{22}$

Perrierite occurs in crystalline limestone exposed by a shallow open-cut on the northern part of the property of Desmont Mining Corporation, Limited near Wilberforce, Ontario (31E/1). It occurs sparingly as reddish brown, striated plates forming small irregular masses in the limestone. It resembles titanite which is also present in the crystalline limestone; the resinous lustre, platy habit and striations distinguish perrierite from titanite. Associated minerals include chondrodite, amber mica, pyrite, clinoamphibole, clinopyroxene, tourmaline, pyrrhotite, sphalerite, graphite and molybdenite.

Perrierite also occurs in crystalline limestone which is exposed by a road-cut on Highway 60 at a point 2.3 km west of Golden Lake village, Ontario (31F/11). At this locality, perrierite is in the form of black, resinous to adamantine plates which are less than 1 mm long and are sparsely distributed in the limestone. Chondrodite, mica, clinoamphibole, serpentine, clinopyroxene, apatite, titanite, graphite, rutile, pyrrhotite, and tochilinite are associated with perrierite.

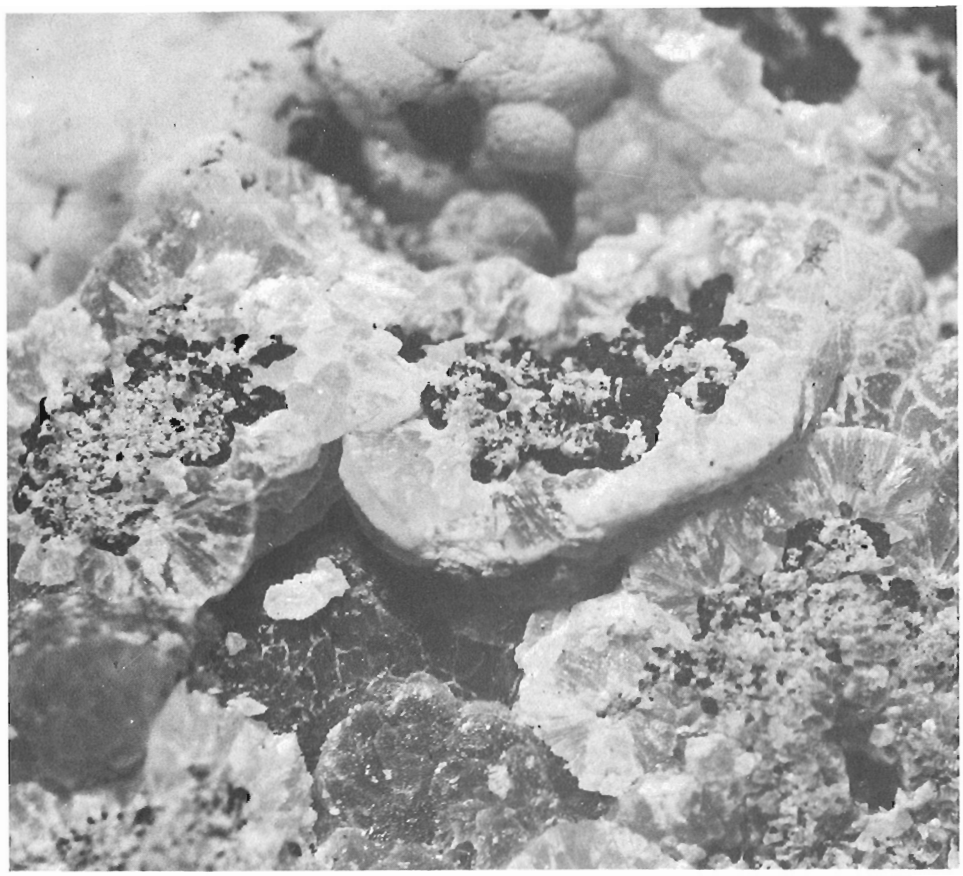

Figure 49.2

Woodruffite in botryoidal smithsonite, Willett Mines Limited property, Lardeau, British Columbia. X 10 (GSC 203094-R).

Pseudocubic Quartz SiO_2

An occurrence of pseudocubic quartz crystals was brought to the author's attention by Mr. Fred Dorwood, of Edmonton, Alberta, who submitted several specimens for identification. They were collected from a locality along the Red Deer River valley, about 4 miles northwest of Drumheller, Alberta (82P/7). The quartz crystals are associated with silicified wood which occurs in the Upper Cretaceous Edmonton Formation consisting of sandstone, siltstone, shale, coal, and ironstone (Irish, 1967). The formation is exposed extensively along the valley of the Red Deer River in the Drumheller area.

Rhombohedral crystals of quartz resembling cubes and referred to as pseudocubic quartz crystals occur on botryoidal quartz which forms masses around a core of goethite-bearing silicified wood, and occupies fissures in the silicified wood. These crystals result from the development of only one set of the rhombohedral faces of normal quartz crystals, the other rhombohedral faces and the prism faces being completely excluded in their development. The pseudocubes occur singly and as groups of crystals in random orientation and as interlocking "cubes" resembling the Greek key symbol. The individual crystals measure on the average, 1 mm along the edge. Their surfaces are smooth with a frosty appearance; the broken crystals reveal the interior to be colourless, transparent, vitreous with a conchoidal fracture. The rhombohedra are characterized by sharp edges and the corners are unmodified by other rhombohedral faces. They appear to have developed from the botryoidal quartz; some rhombohedra project only partially from the botryoidal quartz, and are characterized by rounded edges and finely botryoidal surfaces.

Other crystal forms of quartz occur on the botryoidal quartz. Included are (a) colourless transparent prisms (about 1 mm in diameter) terminated at one or both ends by rhombohedral faces but lacking transverse striations on the prism faces, and (b) rhombohedral plates stacked to form narrow columns measuring about 1 cm by 2 mm. These rhombohedral plates are commonly curved and have cloudy to frosty surfaces.

The botryoidal quartz is translucent, colourless, white or grey with some inky blue areas, the blue colour possibly due to iron; some of the globular forms resemble ammonites. The surface of the botryoidal quartz is generally smooth but in some areas, has a rough appearance due to a profusion of protruding rhombohedral faces resembling normal quartz crystal terminations but with edges that are generally rounded.

The X-ray powder pattern of each of these varieties of quartz is that of low-quartz. Occurrences of pseudocubic quartz crystals are rare. One notable occurrence is in Artesia, New Mexico where these crystals occur with prismatic crystals and with doubly terminated crystals resembling hexagonal pyramids. The New Mexican pseudocubic crystals differ from the Red Deer River crystals in that they are larger (up to 1 cm across) and are commonly modified by a rhombohedral face at the corners (Tarr and Lonsdale, 1929). Crystals averaging 0.5 mm along the edge have been reported from localities in Germany(Witteborg, 1933).

Pyroaurite $Mg_6Fe_2^{+3}(CO_3)(OH)_{16}\cdot 4H_2O$

Nodules of colourless to grey translucent pyroaurite are associated with greenish yellow serpentine in magnesite-dolomite ore at the Canadian Refractories Limited property in Kilmar, Quebec (31G/15). The nodules measure up to 0.5 cm in diameter. Associated with the pyroaurite are: brucite, clinopyroxene, talc, phlogopite, spinel, titanite, pyrite, graphite and sphalerite.

Sepiolite $Mg_4Si_6O_{15}(OH)_2 \cdot 6H_2O$

Bakerite $Ca_4B_4(BO_4)(SiO_4)_3(OH)_3$

Bakerite occurs sparingly with sepiolite in massive diopside-bearing calcite at the North Showing of Canadian All-Metals Explorations Limited property near Tory Hill, Ontario (31D/16). Bakerite is colourless, transparent, vitreous, massive, and forms irregular masses measuring 1 to 2 mm across on calcite; rare tabular and squat prismatic crystals have developed in some of the massive bakerite. These crystals measure up to 0.5 mm long. The bakerite generally occurs at the edges of sepiolite-filled pockets in calcite. Sepiolite is white, silky to waxy, and scaly, craggy or pulverulent. In some pockets, barite is admixed with sepiolite. Silky, finely flaky white talc is commonly associated with sepiolite, and clinoamphibole, amber mica and colourless quartz occur in the calcite.

The diopside-rich calcite occurs in a silicated marble zone enclosed in a complex of quartzite, paragneiss and granite gneiss. Other minerals occurring in the marble are: uraninite, thorianite, betafite, zircon, pyrite, magnetite, graphite and serpentine. The deposit was explored in 1955 for radioactive mineralization by an adit and open-cuts.

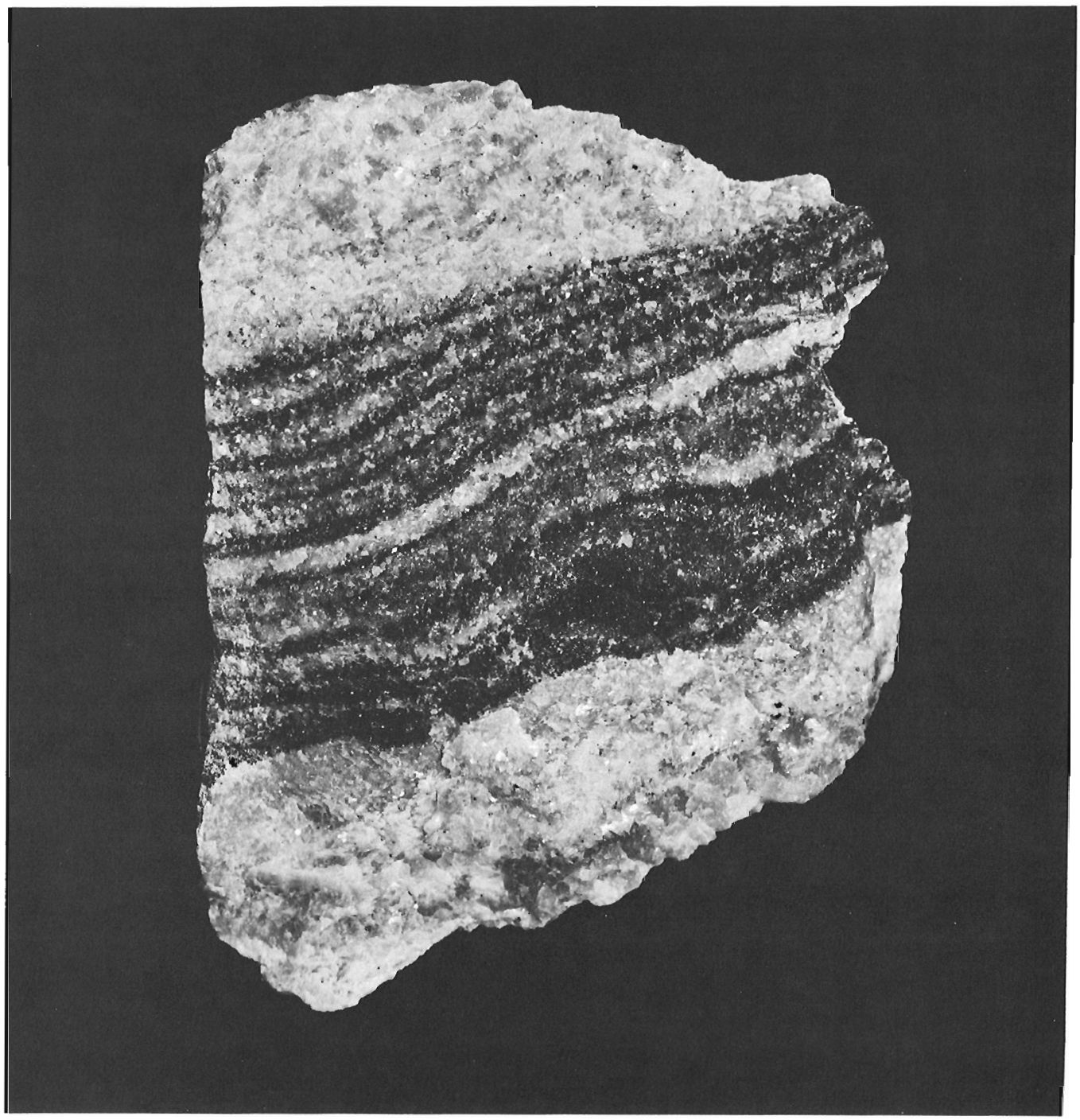

Figure 49.3. Tochilinite-bearing bands in serpentine marble, Stephen Cross quarry, Wakefield, Quebec. The bands are composed of disseminated and nodular tochilinite with minor pyrrhotite, pyrite, pyroaurite and perovskite, Actual width of banded zone is 7 to 7.5 cm (GSC 203247-A).

Stilpnomelane $K(Fe,^{+2},Fe,^{+3}Al)_{10}Si_{12}O_{30}(OH)_{12}$

Stilpnomelane was found in specimens collected from an inactive soapstone quarry located 1.6 km northwest of St-Pierre-de-Broughton, Quebec (31L/6). It occurs as dark green and dark brown radiating, foliated, and randomly oriented plates in coarsely granular quartz-plagioclase aggregates. The individual plates measure 2 to 3 mm in diameter. In some specimens, the plates form bands in the rock. Talc is commonly associated with the stilpnomelane. Other minerals present in the deposit are: magnesite, dolomite, chlorite, pyrite, galena, magnetite, chromite, goethite, and quartz crystals.

Tochilinite $6Fe_{0.9}S \cdot 5(Mg,Fe)(OH)_2$

Perovskite $CaTiO_3$

Tochilinite was originally reported as an unnamed mineral in 1969 from the Muskox Intrusion in the Northwest Territories and described as a new mineral species in 1971 from serpentinite in a copper-nickel deposit, Voronezh region, U.S.S.R.; it was also reported from Cornwall, England, from Morgantown, Pennsylvania, and from the Dumont Nickel Corporation property near Amos, Quebec (Jambor, 1976). This investigation has yielded four new occurrences: at the Maxwell quarry and the Stephen Cross quarry near Wakefield, Quebec (31G/12) and in road-cuts near Douglas, Ontario (31F/10) and near Golden Lake, Ontario (31F/11).

At the Maxwell and Stephen Cross quarries, which were formerly mined for brucite by the Aluminum Company of Canada, it occurs fairly abundantly in serpentine marble which is enclosed in syenite and monzonite. Perovskite is also found in the marble. Tochilinite occurs sparingly in crystalline limestone exposed by road-cuts on Highway 60 at points 2 km northwest of its junction with County Road 5 near Douglas, Ontario and 2.3 km west of Golden Lake village, Ontario.

At the Stephen Cross and Maxwell quarries, tochilinite is black and generally with a greasy lustre, but may also be sooty, velvety, submetallic or bronzy. It occurs as: coatings which partly or completely surround nodules of brucite, grey serpentine, and white, grey and pink pyroaurite; irregular veinlets in serpentine nodules; unevenly distributed fine disseminations in calcite and in serpentine; irregular finely granular masses replacing massive serpentine; nodules measuring up to 2 mm in diameter and composed of layers of fine flakes; fibrous aggregates replacing fibrous calcite; flaky aggregates in which the flakes are jagged and flexible. The granular and nodular tochilinite commonly form conspicuous bands in the serpentine marble. Perovskite, as black adamantine anhedral grains, is a relatively rare accessory mineral. More common minerals associated with tochilinite are pyrrhotite, pyrite, magnetite, apatite, spinel, vesuvianite, hydromagnesite, galena and graphite.

At the occurrence near Douglas, Ontario, tochilinite is intimately associated with serpentine producing greasy black, very finely granular smear-like patches in crystalline limestone. Magnetite is associated with the serpentine-tochilinite aggregates. Other minerals occurring in the crystalline limestone include pyrrhotite, ilmenite, amber mica, clinohumite, spinel, clinopyroxene, clinoamphibole, apatite, chlorite, and molybdenite. Hydrotalcite occurs as white coatings on spinel and on clinohumite.

At the Golden Lake locality, tochilinite forms microscopic dendritic coatings composed of thin black plates with the characteristic bronze lustre. It occurs sparingly in crystalline limestone with chondrodite, mica, clinoamphibole, serpentine, clinopyroxene, rutile, apatite, titanite, graphite, pyrrhotite, and perrierite.

Woodruffite $(Zn,Mn^{+2})Mn_3^{+4}O_7 \cdot 1\text{-}2H_2O$

Aurichalcite $(Zn,Cu)_5(CO_3)_2(OH)_6$

Gunningite $(Zn,Mn)SO_4 \cdot H_2O$

Hydrozincite $Zn_5(CO_3)_2(OH)_6$

These minerals are associated with smithsonite which occurs in the silver-lead zinc deposit (Moonshine claims) formerly (1954-1957) worked by Willett Mines Limited near Lardeau, British Columbia (82K/2). The ore mineralization consists of galena and sphalerite with minor chalcopyrite and quartz in fracture zones in Lower Cambrian crystalline limestone (Fyles, 1964). The workings consist of adits, a shaft and trenches. Specimens from the deposit were collected by Mr. Allan Ingleson of Calgary, Alberta.

The specimens examined consist of masses of crystalline smithsonite capped by radiating fibrous smithsonite producing botryoidal surfaces. The mineral is grey with a vitreous lustre. Woodruffite and aurichalcite occur in the smithsonite, and gunningite and hydrozincite form patchy encrustations on it. Gunningite occurs as white, earthy, crumbly aggregates, hydrozincite as white, compact, powdery, and finely botryoidal crusts. Gunningite also forms crusts on woodruffite. Aurichalcite, as light blue flaky aggregates, is associated with the fibrous smithsonite. Orange to brown pulverulent goethite occurs in smithsonite.

The woodruffite is black with a lustre that varies from sooty to velvety, greasy and submetallic. It occurs in smithsonite occupying spaces between the fibrous cap and the crystalline aggregates, and admixed with crystalline massive smithsonite. Beneath the fibrous cap, which is 1 to 2 mm thick, woodruffite occurs as paper-thin, concentric layers forming spheres and hemispheres conforming to the botryoidal cap of smithsonite. The layers are smooth, finely botryoidal or crinkly and friable, and commonly have open spaces between the layers. Woodruffite also occurs as randomly oriented thin plates and scales, and as finely granular aggregates admixed with and occupying pockets in crystalline aggregates of smithsonite.

References

Fleischer, Michael
1975: 1975 Glossary of Mineral Species; Mineralogical Record, Inc.

Frondel, Clifford
1953: New manganese oxides: hydrohausmannite and woodruffite; Am. Mineral., v. 38, p. 761-769.

1962: Dana's System of Mineralogy; v. 111, Silica Minerals, 7th edn.; John Wiley and Sons, Inc.

Fyles, James T.
1964: Geology of the Duncan Lake area, Lardeau district, British Columbia; B.C. Dept. Mines Pet. Resour., Bull. 49.

Hogarth, D.D., Moyd, L., Rose, E.R., and Steacy, H.R.
1972: Classic mineral collecting localities in Ontario and Quebec, Excursions A47-C47, XXIV Int. Geol. Cong., Montreal, 1972

Irish, E.J.W.
1967: Geology, Drumheller, Alberta; Geol. Surv. Can., Map 5-1967.

Jambor, J.L.
1976: New occurrences of the hybrid sulphide tochilinite; in Report of Activities, Part B, Geol. Surv. Can., Paper 76-1B, p. 65-69.

Kirillov, A.S.
1964: Hydroxyl-bastnäsite, a new variety of bastnäsite; Dokl. Akad. Nauk. S.S.S.R., v. 159, p. 1048-1050.

Palache, C., Berman, H., and Frondel, C.
1944: Dana's System of Mineralogy, 7th edn., v. I, II; John Wiley and Sons, Inc.

Sabina, Ann P.
1968: Rocks and minerals for the collector: Kingston, Ontario to Lac St-Jean, Quebec; Geol. Surv. Can., Paper 67-51.

1977: New occurrences of minerals in parts of Ontario; in Report of Activities, Part A, Geol. Surv. Can., Paper 77-1A, p. 335-339.

Satterly, J.
1957: Radioactive mineral occurrences in Bancroft area; Ont. Dep. Mines, Ann. Rep., v. 65, pt. 6, 1956.

Tarr, W.A. and Lonsdale, John T.
1929: Pseudo-cubic quartz crystals from Artesia, New Mexico; Am. Mineral., v. 14, p. 50-53.

Witteborg, Werner
1933: 'Pseudocubic' quartzes from the massive limestone of Westphalia; Central. Min. Geol. Paläon., 1933A.

50.

AGE AND ORIGIN OF THE GOLD-BEARING SHEAR ZONES AT YELLOWKNIFE, NORTHWEST TERRITORIES

Project 700015

John B. Henderson
Regional and Economic Geology Division

Abstract

Henderson, John B., Age and origin of the gold-bearing shear zones at Yellowknife, Northwest Territories; Current Research, Part A, Geol. Surv. Can., Paper 78-1A, p. 259-262, 1978.

Major gold deposits at Yellowknife occur in shear zones in a thick sequence of predominantly mafic volcanic flows at the western margin of an Archean basin in Slave Province. The shear zones are restricted to the lower mafic part of the volcanic pile, are earlier than an unconformity at the base of overlying sedimentary rocks, and are probably about the same age as dacite porphyry dykes that may be the subvolcanic conduit system to a felsic centre in the upper part of the volcanic pile.

Previous workers have concluded that the shear zones occur along thrust faults and were related to folding of supracrustal rocks associated with the intrusion of granodiorite plutons. It is suggested here that the shear zones resulted from movement along large gravitational slides during the accumulation of the volcanic pile. These zones were then folded along with the enclosing volcanic rocks. These synvolcanic structures could have provided zones for transport of fumarolic material and aqueous solutions. This probably accounts for extensive alteration along the zones and the localization of Au deposits within the zones.

The major gold deposits at Yellowknife are in shear zones in a thick sequence of predominantly mafic, massive and pillowed volcanic flows at the western margin of an Archean basin in the southern Slave Province.

At Yellowknife the Yellowknife Supergroup stratigraphy (Henderson, 1970) is displayed across a major north trending vertical isoclinal syncline which is offset by a series of sinistral faults (Fig. 50.1). The thick volcanic pile, the Kam Formation, is unconformably overlain by conglomerates and shallow water sandstones of the Jackson Lake Formation. The Banting Formation felsic volcanic tuffs, breccias, and minor folds have been shown by Baragar (1975) to conformably overlie the Jackson Lake sandstones. In the basin to the east the very much thinner mafic volcanic flows that are thought to be correlative with the Kam Formation are conformably overlain by a thick sequence of greywacke-mudstone turbidites, the Burwash Formation, which in turn is conformably overlain by similarly much thinner Banting felsic volcanics. The Banting is conformably overlain by more greywacke mudstone turbidites in the core of the syncline.

The geology and structure of the Kam volcanics have been described in detail by Henderson and Brown (1966) and that of the shear zones by Campbell (1949), Brown and Dadson (1953) and Brown et al. (1959). Boyle (1961) has described the geology and geochemistry of the gold deposits. The following description of the shear zones is based on their work.

The shear zones consist of two types. Simple, narrow zones parallel to the attitude of the flows occur in three distinct systems and are commonly associated with tuffaceous units within the volcanic pile. The much larger discordant structures occur in several separate systems and contain the economic gold deposits. Individual shear zones within the systems range from distinct breccias with well-preserved clasts up to 15 cm to schist zones in which the original nature of the rocks is lost. In some cases there is a gradation from breccia to schist. The contact between relatively undeformed country rock and the shear zone is commonly gradational. The shear zones, particularly the larger discordant zones, are very complex. They consist of an interlacing network of sheared material separated by blocks of only weakly deformed volcanics. The largest system, the Giant-Campbell, is up to 400 m wide, and consists of several shear zones separated by little deformed blocks. The ore-bodies occur as narrow discontinuous bodies within the shear zones and are localized near the noses of unsheared blocks where the deformation has been particularly intense and complex and dilatant zones are available for quartz vein accumulation.

The flows face southeasterly and are vertical or dip steeply to the southeast. The discordant shear zones intersect the strike of the flows at a moderate angle in the southern or stratigraphically higher part of the section, but are more parallel in the northern or lower part of the formation. In general the shear zones dip to the west between 40° and 60° although some parts of the system dip east and indeed appear to be folded into a complex syncline-anticline pair (Brown and Dadson, 1953; Brown et al., 1959). Shear planes within the shear zones have a similar strike but a generally steeper dip than the zones themselves. Movement on the zones, where it can be demonstrated, is west side up. This corresponds to the sense indicated by cleavage relations in most zones. Campbell (1949) determined a 350 m displacement on the Con system, Boyle (1961) measured a 200 m displacement on part of the Negus Rycon system, and Brown et al. (1959) report movement of over 450 m on part of the Giant Campbell system.

As far as the origin of these structures is concerned, most authors have concluded that the structures are the locus of a thrust fault system and that the faulting was related to the folding of the supracrustal rocks and intrusion of the granodiorite plutons that lie to the west (Campbell, 1949; Brown and Dadson, 1953; Boyle, 1961; Henderson and Brown, 1966). There seems to be little doubt that the shear systems involve some displacement. However, another possibility should be considered regarding the time and sense of displacement. It is suggested that initial movement took place during the accumulation of the Yellowknife supracrustal rocks, before they were folded into their present configuration, and that the displacement was normal rather than reverse, although there would have been later movement on these structurally weaker zones during the subsequent deformation and intrusive events.

Supporting this conclusion, the following should be considered. The shear zones occur only within the mafic volcanic pile. The apparent displacement of marker horizons in the volcanic sequence (Henderson and Brown, 1966) along the Giant-Campbell shear zone (Fig. 50.1B) does not extend

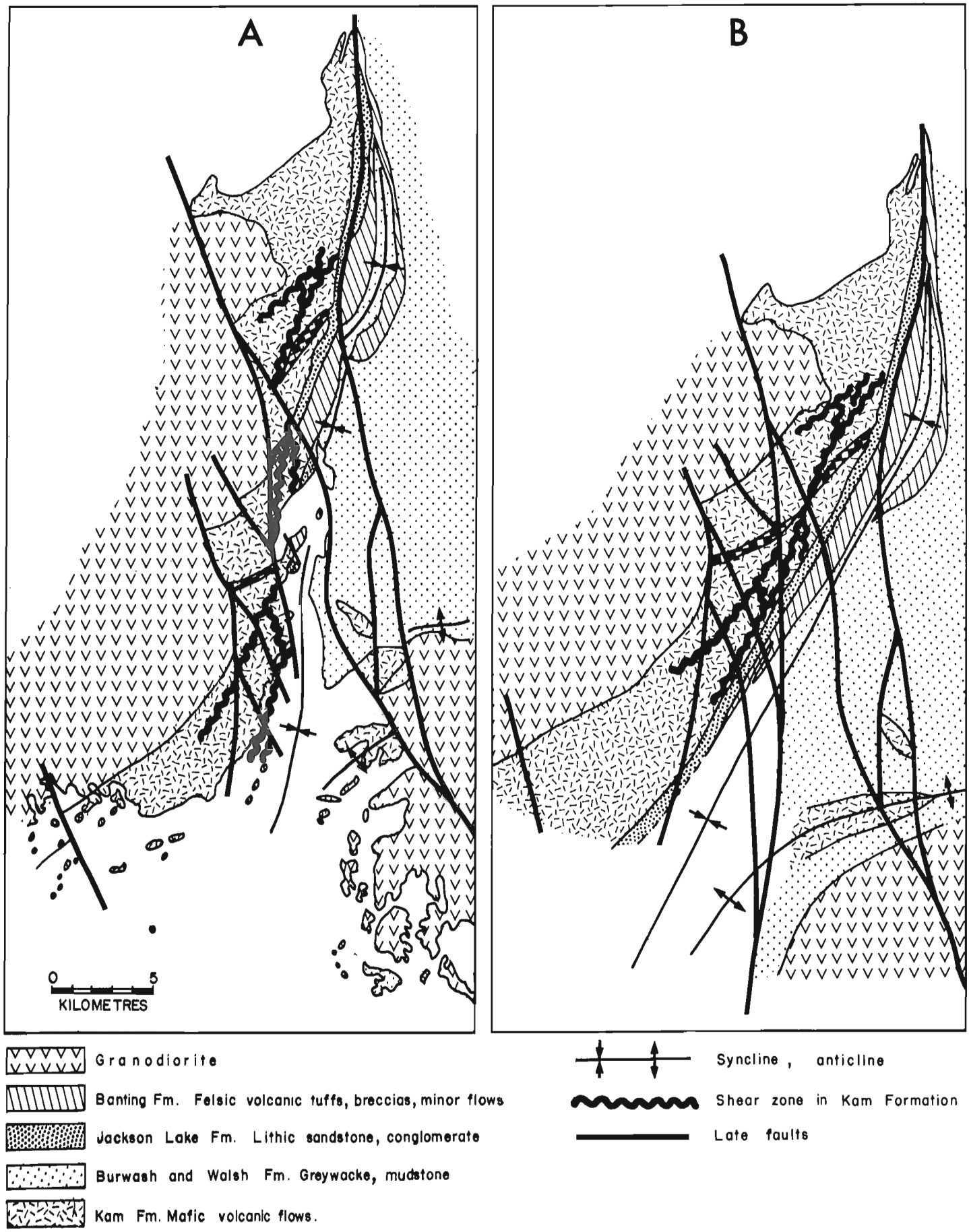

Figure 50.1 A- General geology of the Yellowknife area.

B- General geology of the Yellowknife area with displacement on the late faults replaced showing location of major shear zones.

Checkered unit in the Kam Formation is a felsic volcanic marker horizon that shows the apparent displacement on the Giant-Campbell shear zone. Note that the unconformable contact between the Kam and overlying Jackson Lake Formation is not displaced along the shear zone.

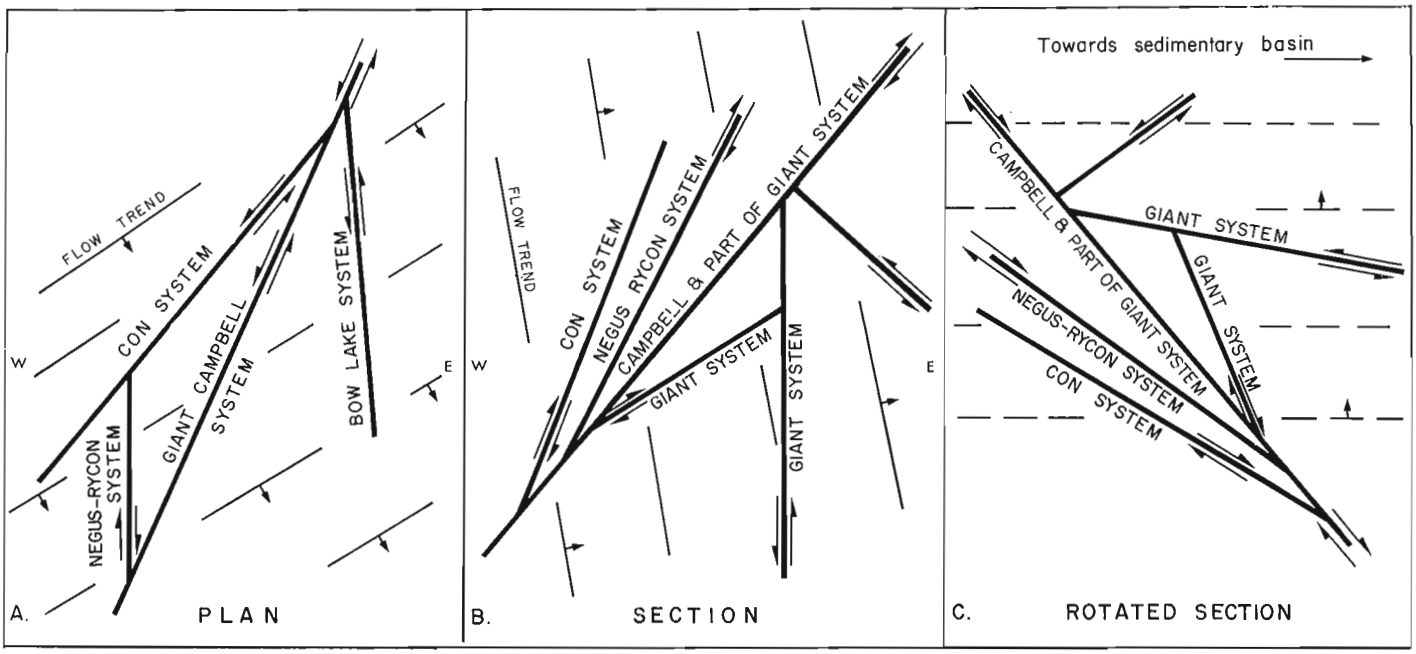

Figure 50.2 Diagrammatic plan and sections showing movement and relationship of shear zones (after Boyle (1961))
A Plan
B Section
C Rotated Section, flows rotated into horizontal position.

into the overlying sediments. On the Prosperous Lake map (scale 1 inch = 1 mile) of Jolliffe (1946) the contact between the Kam and Jackson Lake formations is not offset where the shear zones (not plotted on Jolliffe's map) would intersect the contact. Thus the movement on the shear zones is older than the unconformity. In this regard the relationship between the shear zones and a set of felsic porphyry dykes is of interest. In the north-central part of the mafic volcanic Kam Formation there is an extensive network of anastomosing cross-cutting dacite porphyry dykes that may represent the subvolcanic conduit system to a felsic centre. According to Henderson and Brown (1966), the porphyry bodies are also truncated at the unconformity between the Kam and the overlying Jackson Lake volcanic lithic sandstones. Thus the extrusive part of the centre, if it existed, was eroded prior to deposition of the Jackson Lake sandstones which are clearly derived from a felsic volcanic source (Henderson, 1975). The relationship between these porphyries and the major shear zones is equivocal as the porphyries both cut and are cut by the shear zones (Henderson and Brown, 1966). An interpretation of this is that initial shear zone movement was contemporaneous with the emplacement of the dyke complex (and possibly felsic volcanism?) with the shear zones cutting earlier dykes and being cut by later dykes, but with everything being truncated at the unconformity.

Since the Banting felsic volcanics, the Burwash greywackes and the equivalent of the Kam mafic volcanics on the east limb of the structure are all conformable (Henderson, 1970) and the Banting volcanics and Jackson Lake sandstones on the western limb are also conformable (Baragar, 1975), the first movement on the shear zone occurred possibly during the accumulation of the Kam mafic volcanics and certainly before the deposition of the Jackson Lake sandstones.

It is suggested that the movement was caused by gravitational slides due to the instability of the main volcanic pile. Earliest movement was on the concordant zones associated with tuff beds (Boyle, 1961; Henderson and Brown, 1966). The water-saturated tuff beds may have acted as planes of weakness along which the early movement would start. Later movement was generally on the discordant west-dipping slip surfaces (Fig. 50.2). Movement on the shear zones as presently oriented has been shown to be west side up (Campbell, 1949; Boyle, 1961). If the flows are rotated into a horizontal position about the more or less horizontal synclinal axis in Yellowknife Bay, the shear zones become a series of planes dipping moderately southeastward along which blocks of volcanics could have slipped downward towards the adjacent basin to the east (Fig. 50.2). An example of this sort of collapse was reported by van Bemmelen (1954) where part of the cone of the recent Merapi volcano in central Java, including the crater and part of the underlying conduit, an area 18 km long and up to 10 km wide made up of several sliding masses, slumped into an adjacent valley lowering the original 3300 m height of the volcano over 300 m, and initiating renewed eruption of the volcano. Similarly, Moore (1966) has interpreted the east rift zone of Kilauea volcano on the island of Hawaii as being due to gravity slides that are still moving.

The slip surfaces of these structures at Yellowknife would provide a conduit, certainly for meteoric waters downward into the volcanic pile and, if volcanism was still active as seems most likely, could have provided a site for the passage of fumarolic material upward. Both processes would greatly speed up the alteration and devitrification of the volcanic flows in the vicinity of the movement surfaces. This early alteration could explain the width of the present shear zones and the diffuse nature of their contact with the volcanics. The altered zones would be a zone of weakness along which later movement during folding of the supracrustal rocks could take place. If the orientation of the zone was at an angle to the direction of later movement the zone itself could have been folded due to shearing associated with this later movement. The folded aspect of the shear zones in the Giant Yellowknife mine is clearly illustrated by Brown et al. (1959) although they felt the formation and apparent deformation of the zones was concurrent.

Boyle (1961) has suggested that the gold and associated mineralization in the deposits in the shear zones were derived entirely from the altered volcanics in the shear zones during metamorphism of the volcanic rocks. The early formation of the shears and their alteration, together with the much greater volume of water available in the shear zones at that

time, would provide an easier mechanism for the mobilization of the relevant elements. In a recent study by Kerrich et al. (1977) it was suggested the deposits are hydrothermal in origin on the basis of the reduced nature of the iron in the shear zones. Like Boyle, they believe the shearing and mineralization took place during folding and metamorphism of the pile. Their model requires a large volume of water and a temperature gradient. If the process took place more or less contemporaneously with volcanism the former would be more readily available, and the latter, depending on the composition of the volcanic gases, unnecessary.

Acknowledgments

J.C. McGlynn and M. Schau in reviewing this note made several helpful suggestions for improvement. The author particularly wishes to thank Mikkel Schau for many useful discussions.

References

Baragar, W.R.A.

1975: Miscellaneous data from volcanic belts at Yellowknife, Wolverine Lake and James River, N.W.T.; in Report of Activities, Part A, Geol. Surv. Can., Paper 75-1A, p. 281-286.

Boyle, R.W.

1961: The geology, geochemistry and origin of the gold deposits of the Yellowknife district; Geol. Surv. Can., Mem. 310.

Brown, C.E.G. and Dadson, A.S.

1953: Geology of the Giant Yellowknife Mine; Can. Inst. Min. Metal., Trans., v. 56, p. 69-86.

Brown, C.E.G., Dadson, A.S., and Wriggelsworth, L.A.

1959: On the ore-bearing structures of the Giant Yellowknife gold mine; Can. Inst. Min. Met., Trans., v. 62, p. 107-116.

Campbell, N.

1949: The Con-Rycon Mine, Yellowknife, N.W.T.; Can. Inst. Min. Met., Bull., v. 42, no. 446, p. 288-292.

Henderson, J.B.

1970: Stratigraphy of the Archean Yellowknife Supergroup, Yellowknife Bay - Prosperous Lake Area, District of Mackenzie; Geol. Surv. Can., Paper 70-26.

1975: Sedimentology of the Archean Yellowknife Supergroup at Yellowknife, District of Mackenzie; Geol. Surv. Can., Bull. 246.

Henderson, J.F. and Brown, I.C.

1966: Geology and structure of the Yellowknife greenstone belt, District of Mackenzie; Geol. Surv. Can., Bull. 141.

Jolliffe, A.W.

1946: Prosperous Lake map-area; Geol. Surv. Can., Map 868A.

Kerrich, R., Fyfe, W.S., and Allison, I.

1977: Iron reduction around gold-quartz veins, Yellowknife District, Northwest Territories, Canada; Ec. Geol., v. 72, p. 657-663.

Moore, J.G.

1966: Gravity slide origin of rift zones of some Hawaiian Volcanoes; Bull. Volcanol., v. 29, p 719-720.

van Bemmelen, R.W.

1954: Mountain Building; Martinus Nyhoff, The Hague.

COPPER METALLOGENY, LAKE HURON AREA, ONTARIO

Project 700059

William N. Pearson[1]
Regional and Economic Geology Division

Abstract

Pearson, William N., Copper metallogeny, Lake Huron area, Ontario; Current Research, Part A, Geol. Surv. Can., Paper 78-1A, p. 263-268, 1978.

Copper deposits and occurrences in the north shore region of Lake Huron (41 I, J, K, N/1, 2) vary immensely in their types, regional settings, ages and lithologies of host rocks, size and form, associated metals, mineralogy, and degree, of deformation and metamorphism. Brief descriptions of some deposits and of the various deposit types are presented and preliminary explanations are offered for some of the metallogenic patterns.

Introduction

The north shore region of Lake Huron has a long and colourful mining history dating from prehistoric times. The discovery, in 1846, of copper at Bruce Mines and its subsequent development by the Montreal Mining Company, heralded the beginning of Ontario's immense mineral industry. W.E. Logan (quoted in Hornick, 1975), then Provincial Geologist, surveyed the area in 1849 and reported that "In no part of the country visited, from the vicinity of Sault Ste. Marie to Shebawenchning (190 km (120 mi) east) was any great area wholly destitute of cupriferous veins and it would appear singular if a region extending over a space between 1000 and 2000 square miles (2560 and 5120 km^2), and so marked by indication, did not in the course of time yield many valuable results". In 1864, the discovery of the Sudbury ores during building of the Canadian Pacific Railway, focussed prospecting attention on Sudbury and the area northeast of Lake Huron. By the early 1900's several copper occurrences were known in the Massey area, two of which became the Massey and Hermina Mines. Prospecting and mining activity has continued thoughout the region during this century although often sporadically. Since the 1950's most activity has been on uranium and exploration for copper has declined. The copper occurrences of the north shore region are nevertheless numerous and varied, and warrent further study as new sources of copper are sought.

The purpose of this study is to examine and document copper occurrences in a region defined geographically by National Topographic Sheets (N.T.S.) 41 I, J, K and N/1, 2 with the aim of elucidating the metallogenic history and to delimite areas that warrant further exploration. The important nickel-copper deposits of the Sudbury Nickel Irruptive will not be emphasized. Field work was initiated in the summer of 1977, during which time 104 deposits and occurrences were examined. A regional overview was obtained and samples were collected for petrographic, mineralogical and chemical analyses; these data will serve as a basis for followup work in the summer of 1978.

The author is grateful to R.V. Kirkham of the Geological Survey of Canada for suggesting and helping in the planning of this project and to D. Innes, Ontario Division of Mines, Resident Geologist, in Sudbury and P. Giblin, Regional Geologist, E.J. Leahy and G. Bennett of the Ontario Division of Mines in Sault Ste. Marie for their invaluable assistance during the summer's field work. Thanks are also extended to the many local residents, prospectors, and industry and government geologists, who freely gave information and services and much enjoyed hospitality. R.V. Kirkham reviewed the manuscript and offered many helpful suggestions.

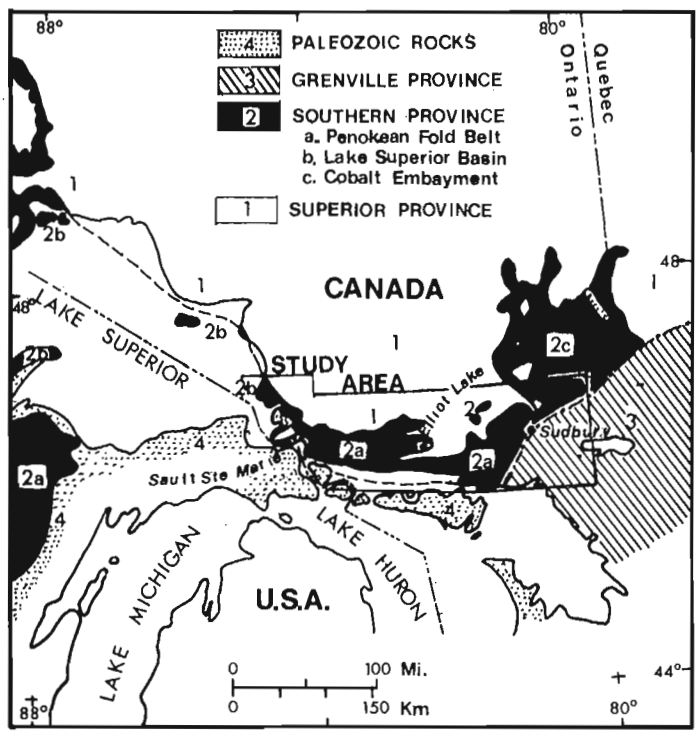

Figure 51.1 Location of study area and major tectonic elements therein (modified after Card et al., 1972).

Regional Geological Setting

The project area is underlain predominantly by Proterozoic supracrustal rocks of the Southern Province, in particular the Aphebian Huronian Supergroup of the Penokean Fold Belt and Cobalt Embayment and the Keweenawan volcanic and clastic sedimentary rocks of Helikian age of the Lake Superior Basin. To the north the Southern Province rocks unconformably overlie Archean granitic, metavolcanic, and metasedimentary rocks of the Superior Province whereas to the east, the Penokean Fold Belt and rocks of the Cobalt Embayment are truncated by the Grenville Front that marks the abrupt transition to the highly deformed and metamorphosed rocks of the Grenville Province. To the south the Huronian strata are unconformably overlain by lower Paleozoic rocks. In the Sault Ste. Marie area sedimentary strata of Hadrynian(?) age (Jacobsville Formation) unconformably overlie Helikian, Aphebian, and older rocks (Card et al., 1972, Fig. 51.1).

[1] Department of Geological Sciences, Queen's University, Kingston, Ontario K7L 3N6.

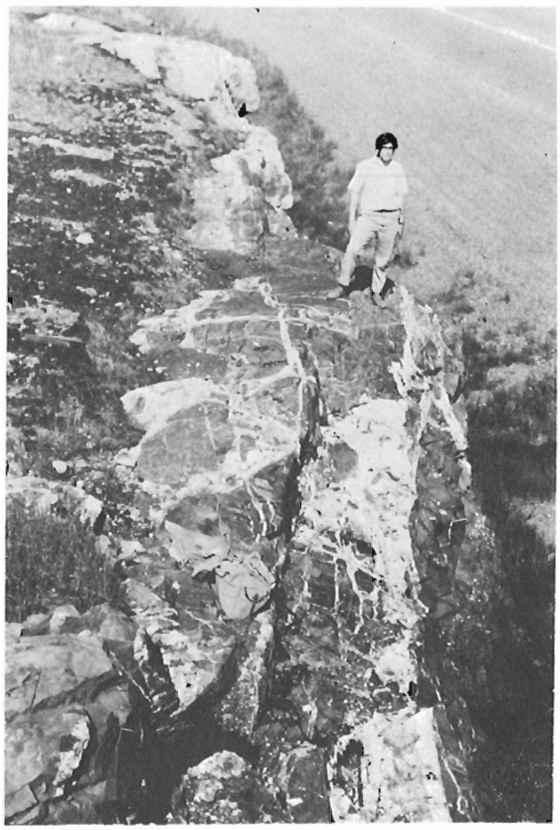

Figure 51.2 Typical anastomosing quartz-carbonate-chalcopyrite-pyrite-specularite vein. Highway 17 about 40 km west of Iron Bridge (GSC Photo 202516E by R.V. Kirkham).

Numerous mafic sills and dykes have been emplaced in the Southern Province and adjacent areas. The most extensive of these are the Nipissing Diabase intrusions that have been radiometrically dated at 2150 m.y. (Van Schmus, 1965). Granite forms much of the Superior Province and is exposed as inliers within the Southern Province; granite is considered to form much of the basement beneath the Proterozoic supracrustal rocks (Card et al., 1972). Proterozoic granitic plutons are present in the more strongly deformed and metamorphosed Sudbury-Espanola segment of the Penokean Fold Belt.

The major deformation within the Southern Province is younger than that of the Superior Province (2550 m.y.) but older than that of the Grenville Province (1000 m.y.) (Stockwell, 1972). Structural data indicates that major folding began prior to the intrusion of the Nipissing Diabase (2150 m.y.) (Card et al., 1972), but exact timing of orogenic events within the Southern Province remains a subject of controversy. The Huronian rocks of the Sault Ste. Marie-Elliot Lake segment of the Penokean Fold Belt are moderately to little deformed in contrast to the more strongly deformed rocks of the Sudbury-Espanola segment.

Geology of the Copper Deposits

Copper occurrences are highly varied in nature and are present within a wide spectrum of geological settings ranging from Archean granites to Paleozoic sediments. The deposits examined have been tentatively classified as follows:

1) veins,
2) contact metasomatic deposits,
3) copper-nickel deposits in mafic and ultramafic intrusions,
4) "sedimentary" copper deposits,
5) volcanogenic massive sulphides and stringer zones, and
6) porphyry deposits.

Table 51.1 lists representative examples of each deposit type.

Veins

Vein deposits are ubiquitous throughout the study area and these constitute the most common mode of copper occurrence, particularly in the Sault Ste. Marie-Elliot Lake area. The vein deposits are of two major morphological types: 1) simple veins that consist of one or more relatively large (of the order of 1-3 m (3-10 ft) wide) quartz or quartz-carbonate veins; and 2) vein swarms consisting of one or more zones of small, subparallel, highly vuggy quartz and quartz-carbonate veins (Fig. 51.2), many with quartz-carbonate cemented breccia containing silicified fragments. The former characteristically cut Nipissing Diabase whereas the latter typically occur in fault zones cutting Huronian sedimentary rocks, notably the Gowganda Formation, and Keweenawan volcanic and sedimentary rocks. Veins within the Gowganda Formation, at many localities, are close to or cut the hematitic arkose members.

Table 51.1: Representative examples of major deposit types

1. Veins

   a) Chalcopyrite-pyrite ± specularite: Bruce Mines, Hy-Tower Mines, Crownbridge, Destorada, Bilton Option, Glagoma Mine, Bi-Ore Mine; specularite-rich: Gould Copper Mine, Mickey Copper Mine;

   b) Polymetallic: i) Zn-Pb-Ag-Cu: Jardun Mines;
   ii) Pb-Ag-Cu: Prace Mine;
   iii) Bornite-chalcocite-native copper: Coppercorp Mine; Begley (?);
   iv) Cu-Co ± Bi ± U ± Ni: Burden Lake, Gimby;

   c) Au-bearing veins: McMillan Mine, Majestic Mine, Shakespeare Mine;

   d) Deformed and metamorphosed vein deposits: Alexander Mine, Spanish River Mine, Shakespeare Township (Noranda), Massey Mine; Springer Mine.

2. Contact Metasomatic

   a) Skarns: Two-Horse Lake, Cobden River, Hart Township, Foster Township, Emerald Lake (?);

   b) Non-skarns: Sudbury Ski area, Desbarats Lake.

3. Cu-Ni in mafic and ultramafic intrusions:

   a) In Nipissing Diabase: numerous in McKim Township, Shakespeare Township (Falconbridge).

   b) In mafic and ultramafic intrusions younger than Nipissing Diabase: East Bull Lake, Mongowin Pluton.

4. "Sedimentary copper deposits: Desbarats, Stag Lake, Birch Island.

5. Volcanogenic massive sulphides and stringer zones:

   a) In Archean volcanic rocks: Stralak, Lake Geneva Mine;

   b) In Huronian volcanic rocks: Denison and Graham Townships, Pater Mine (?);

   c) Sulphide facies iron formation: East Pecors, Highway 108.

6. Porphyry deposits: Jogran Porphyry, Tribag breccias (East and Breton Breccias) Nystedt (?).

On the basis of ore mineralogy and metal contents, the veins are of four major types:

1) Chalcopyrite-pyrite (or pyrrhotite) ± specularite-bearing veins with minor precious metals;

2) Polymetallic veins of three main types: Zn-Pb-Ag-Cu, Pb-Ag-Cu, and Cu-Co ± U ± Ni;

3) Bornite-chalcocite-native copper-bearing veins; and

4) Au-bearing arsenopyrite-pyrite-quartz veins with minor chalcopyrite.

The chalcopyrite-pyrite ± specularite-bearing veins are the most common type; specularite is particularly abundant in occurrences within Gould Township. Polymetallic veins, spatially associated with mafic intrusions, are most prevalent within the Superior Province near Sault Ste. Marie whereas auriferous veins are found mainly in the Espanola area and are rare to the west. Bornite-chalcocite-native copper-bearing veins are principally confined to fault zones cutting Keweenawan rocks.

The deposits of the Massey Copper Zone (Robertson, 1976), that typically consist of quartz ± carbonate-chalcopyrite-pyrrhotite ± pyrite, have undergone penetrative deformation and regional metamorphism. Several of the quartz-carbonate-chalcopyrite-pyrite ± specularite occurrences in the Iron Bridge area are possibly unmetamorphosed equivalents (e.g. Bilton Option and Bar-Fin). The abundance of pyrrhotite in the Massey Zone as compared to its rarity in the little deformed deposits to the west, suggests that this mineral is probably a product of metamorphism.

At Begley, located 42 km (26 miles) north of Sault Ste. Marie, a large quartz vein system cuts Archean granite and consists of many stages of quartz veining. The proportion of sulphide-bearing (bornite, chalcopyrite and chalcocite) veins is small in relation to the vein system as a whole, suggesting that only part of the vein system carried copper. The veins may be genetically related to a mafic dyke that cuts the granite near the vein system.

Contact Metasomatic Deposits

Contact metasomatic deposits are generally small and erratic, and are developed in Huronian sedimentary rocks thermally metamorphosed by Nipissing Diabase intrusions. Skarns have been formed within limesones of the Espanola Formation whereas occurrences formed within non-calcareous sedimentary rocks lack the calcsilicate assemblages typical of skarn deposits.

Skarns are typically magnetite-rich and several were explored primarily as iron prospects. At Cobden River, located 11 km (6.9 mi) north of Iron Bridge, chalcopyrite occurs preferentially in the coarse grained chlorite-rich portions of skarns rather than within the magnetite-rich layers. In Foster Township, an unusual tungsten-bearing idocrase-diopside-garnet skarn contains large stockworks of quartz veins and irregular bodies of pyrrhotite, pyrite, scheelite, and chalcopyrite that replace skarn approximately parallel to bedding (Card, 1968a). The distribution of skarn deposits is controlled by the extent of the Espanola Formation since it is the only significant limestone-bearing member of the Huronian Supergroup.

Contact metasomatic deposits in non-calcareous sediments occur throughout the study area. One kilometre (0.6 mi) northwest of Desbarats Lake chalcopyrite and pyrite occur as disseminations and in quartz veinlets in quartzite of the Lorrain Formation along its contact with a Nipissing Diabase dyke. Radioactivity, up to 500 times background, is present locally. One of the best exposed and most extensive deposits of this type is located in Sudbury immediately west of the Sudbury Ski area (D. Innes, pers. comm., 1977). There, contact metamorphosed Mississagi quartzite adjacent to Nipissing gabbro contains small lenses and disseminations of pyrrhotite and chalcopyrite over a strike length of several hundred metres. The width of the sulphide zone is highly variable but in places it is up to 5 m (16 ft) wide. The quartzite is strongly deformed near the contact. Sudbury-type breccia is widespread throughout the quartzite but there is no spatial relationship of mineralization to the breccias.

Copper-nickel Deposits in Mafic and Ultramafic Intrusions

Copper-nickel occurrences in gabbroic intrusions of Nipissing Diabase are abundant in the Sudbury area, notably McKim Township (D. Innes, pers. comm., 1977). The sulphide zones are typically pod- or lense-like and contain pyrrhotite, pentlandite, chalcopyrite, pyrite, and locally arsenopyrite and gersdorffite. Blue quartz of uncertain origin is commonly associated with the sulphides (D. Innes, pers. comm., 1977). The zones occur typically along the margins of gabbroic intrusions that contain fragments of wall rock, however, mineralization is not spatially-related to the xenoliths. The occurrences have commonly been deformed and the sulphides redistributed. The presence, however, of round and in places teardrop-shaped sulphide blebs (D. Innes, pers. comm., 1977) in less deformed deposits indicates a probable magmatic origin in the sulphides (Naldrett, 1969). One of the largest known deposits in Nipissing Diabase, the Shakespeare (Falconbridge) prospect located 1.2 km (0.75 mi) north of Agnew Lake, is estimated to contain 2.7-3.6 million tons (3-4 million tons) grading 0.34% Ni and 0.40% Cu (Shklanka, 1969, p. 264).

Copper-nickel deposits are also found within younger mafic and ultramafic intrusions. The Mongowin Pluton, a small composite plug dated at 1770 m.y. (Card, 1968b), contains patches and disseminations of pyrrhotite, chalcopyrite, pentlandite, and minor pyrite in the peridotite portion of the pluton, near the northeast and to a lesser extent, southern contacts with hornfelsic Gowganda sedimentary rocks (Card, 1968a, b). Card (1968b) suggested that the sulphides were possibly derived by alteration of silicate minerals containing copper and nickel in solid solution. Small occurrences have been reported (Shklanka, 1969, p. 86) in the East Bull Lake gabbro-anorthosite complex of probable Huronian age (D. Innes, pers. comm., 1977).

"Sedimentary" Copper Deposits

A "sedimentary" copper deposit is here defined as a concordant or peneconcordant deposit, hosted within sedimentary rocks, whose origin is probably related to sedimentary processes (cf. Kirkham, 1974).

Significant occurrences within the Huronian Supergroup appear to be restricted to the Lorrain Formation. At Desbarats, disseminations, blebs, and rare veins of chalcopyrite and pyrite occur within slightly radioactive, hematitic feldspathic quartzite that is overlain by green recessive argillite (Gower, 1956) and underlain by essentially barren, pink quartzite. All units are part of the Lorrain Formation. The rocks have been folded into an open anticline whose fold axis plunges at a low angle to the west. The mineralization is sporadic and generally of low grade and appears to be largely confined to the feldspathic quartzite immediately beneath the argillite. The best showings occur near the hinge of this anticline suggesting that the concentration of sulphides might have some structural control.

At Stag Lake, north of Elliot Lake, low grade disseminated chalcopyrite, pyrite, and minor chalcocite occur within pink Lorrain quartzite over a strike length of approximately 3.2 km (2 mi) (Sutherland, 1965). The quartzite is overlain by the predominantly argillaceous Gordon Lake

Figure 51.3 Proterozoic/Paleozoic unconformity with local, disseminated chalcopyrite and pyrite in sandy, dolomite-filled depressions in barren Lorrain quartzite. Highway 68, 0.8 km east of Lewis Lake (GSC Photo 202516F).

Formation that contains some gypsum and anhydrite nodules (Kirkham, 1974). Small amounts of chalcopyrite and pyrite are present within the argillite unit as disseminations in coarse grained tops of thin graded beds, in sandstone lenses, and in sandstone matrices of intraformational breccias.

Although lithologically the two deposits are somewhat similar, stratigraphically the Desbarats occurrence is in the lower part of the Lorrain Formation whereas that of Stag Lake is at the top. The deposits, therefore, represent two distinct sedimentary units.

Two field localities mentioned by D. Innes (pers. comm., 1977) and examined with R.V. Kirkham were found to contain probable sedimentary copper occurrences within Paleozoic rocks at or near the Proterozoic/Paleozoic unconformity. On Highway 68, 0.8 km (0.5 mi) east of Lewis Lake, disseminated chalcopyrite and pyrite occur within Ordovician(?) dolomite at this unconformity (Fig. 51.3). The sulphides are of limited extent and are confined to small, sandy, dolomite-filled depressions and in fractures in the uppermost Lorrain quartzite along the unconformity; negligible sulphides occur in the overlying strata or in the underlying quartzite.

Under the wharf at Moredolphton Warehouse and Landing in the community of Birch Island traces of chalcopyrite were found in a highly pyritic lower Paleozoic quartz sandstone just above the unconformity. No significant radioactivity was noted, however the beds outcrop along the shore of Lake Huron, thus any uranium that may have been present could have been readily leached out. Rusty quartz sandstone beds, within a red bed sequence, are exposed along the west shore of McGregor Bay, 0.8 km (0.5 mi) to the east. However, it is not known whether these beds are stratigraphically equivalent to the pyritic ones.

According to Kirkham (pers. comm., 1977) these two localities, the latter in particular, have many features in common with the stratiform uranium-copper occurrences in lower Paleozoic rocks of the Ottawa area (Charbonneau et al., 1975). This, coupled with the fact that lower Paleozoic rocks in the northern Manitoulin Island area are highly diachronous adjacent to old Lorrain quartzite hills having considerable paleotopographic relief, suggests that there could be significant facies changes that warrant exploration.

Volcanogenic Massive Sulphides and Stringer Zones

This category is very broad and includes copper occurrences within Archean greenstone belts, Archean sulphide facies iron formation, and those in Huronian volcanic rocks.

Stratabound volcanogenic massive sulphide deposits are common within Archean greenstone belts north of Sudbury, notably the Benny Belt (Card and Innes, 1976). There, deposits occur typically at mafic-felsic meta-volcanic contacts and contain massive lenses or disseminations of pyrrhotite, pyrite with subordinate chalcopyrite and sphalerite. Several localities also contain important lead and silver. At the Lake Geneva Mine an irregular, tabular, massive sulphide body containing sphalerite, galena, silver, pyrite, and minor pyrrhotite and chalcopyrite occurs in highly metamorphosed and deformed felsic and mafic pyroclastic and metasedimentary rocks cut by numerous granitic and mafic dykes (Card and Innes, 1976). The sulphide body is approximately 200 m (700 ft) long, up to 3 m (10 ft) wide and extends to a depth of about 300 m (1000 ft) (Ibid.). During the period 1941-1944, 73 108 tonnes (80 588 tons) of ore containing 9.21% Zn and 3.34% Pb and some silver were produced. Reserves of 103 400 tonnes (114 000 tons) averaging 10% Zn and 3% Pb, 21 800 tonnes (24 000 tons) averaging 8% combined metals, and 29 000 tonnes (32 000 tons) averaging 6% combined metals have been reported (Shklanka, 1969).

Copper-bearing sulphide facies iron formation occurs in Archean metasediments but is included here because of its suspected genetic relationship to volcanism (Goodwin, 1973). Pyrrhotite, pyrite, and minor chalcopyrite occur typically as disseminations and veins within carbonaceous quartz-rich metasediments. A well exposed and readily accessible but lean example that is considered to be iron formation (Giblin et al., 1977) is present on Highway 108 immediately south of the Elliot Lake Municipal Airport road.

In the Huronian Stobie Formation extensive sulphide-rich units occur within pelitic interflow metasediments. The zones are generally less than 3 m (10 ft) thick but these have been traced along strike for some 25 km (15 mi) from Denison to Graham Townships (Card et al., 1977; Innes, 1972). Pyrrhotite, pyrite, and chalcopyrite occur as disseminations, fracture-fillings, and stratiform layers with chalcopyrite most abundant in the "stirred" flow top portions of the metavolcanic-metasedimentary cycles (Card et al., 1977; Innes, 1972).

The Pater Mine, located 0.4 km (0.25 mi) east of Spragge, is hosted in mafic metavolcanic rocks of the Spragge Group that are considered correlative to Huronian volcanic rocks in the Sudbury-Espanola area (Robertson, 1970). The ore zone trends east-west, dips 80° to 85° south, and was mined to the 2900 foot (884 m) level with lateral workings extending to 1300 feet (396 m). Average width of the zone was 2.7 m (9 ft) (Robertson, 1970). The ore is strongly deformed and commonly resembles a "conglomerate" consisting of scattered round quartz blebs surrounded by pyrrhotite and lesser chalcopyrite (Robertson, 1970). The origin of the deposit is uncertain, but it may represent a strongly deformed and metamorphosed volcanic massive sulphide deposit with associated quartz stringer zones.

Porphyry Deposits

A porphyry deposit, as defined by Kirkham (1972) is a "large, low- to medium-grade deposit in which the hypogene sulphides are primarily structurally controlled and which is spatially and genetically related to felsic or intermediate porphyritic intrusions". The Batchawana area breccia pipes, the Jogran Porphyry, and possibly the Nystedt prospect satisfy this definition.

In the Batchawana area five breccia pipes have been identified, known as the Breton, East, West, South, and Palmer Breccias, that are of probable Keweenawan age (Blecha, 1974; Armbrust, 1969). The first four breccias occur in a cluster near the north contact of the Archean greenstone belt with Archean granite whereas the latter is present within the central part of this belt 4.8 km (3 mi) southwest of the Breton Breccia (Blecha, 1974). The breccias are composed of fragments of granite, diabase, mafic metavolcanics, and felsite set in a predominantly quartz-calcite matrix that contains pyrrhotite, pyrite, chalcopyrite, minor molybdenite, sphalerite, galena, and rare scheelite, wolframite, stibnite, and native copper (Blecha, 1974; Armbrust, 1969) (Fig. 51.4). Quartz, sericite, and kaolinite, considered to have formed by hydrothermal alteration of breccia fragments (Armbrust, 1969), are abundant near highly mineralized areas in the Breton Breccia. Blecha (1974) estimated that the East Breccia contains about 114 million tonnes (125 million tons) grading about 0.13% Cu and 0.03 to 0.05% MoS_2, and that the Breton Breccia, prior to production, contained about 36 million tonnes (40 million tons) averaging about 0.2% Cu.

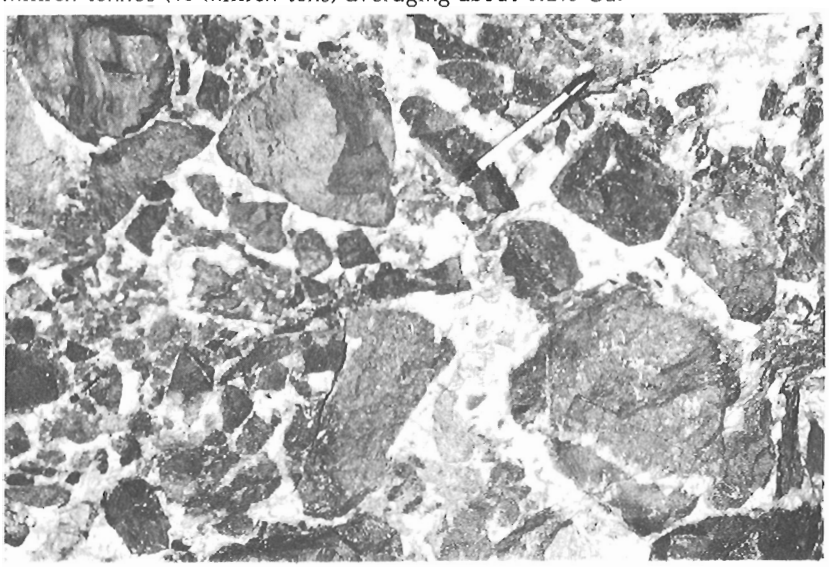

Figure 51.4 Typical breccia with quartz-carbonate-sulphide matrix. Underground, Breton pipe, Tribag Mine (GSC Photo 202516G by R.V. Kirkham).

Blecha (1974) considers that the pipes represent collapse breccias that formed as a result of withdrawal of a deep-seated pulsating magma of felsic composition.

The Jogran Porphyry is an altered quartz-feldspar porphyry plug, 180 m (600 ft) in diameter, of probable Keweenawan age (Giblin, 1966; Blecha, 1974) that intrudes Archean mafic metavolcanic rocks. The porphyry contains low-grade, uniformly disseminated grains and fracture-fillings of pyrite and chalcopyrite with minor molybdenite and rare galena. Parts of the porphyry are variably altered to sericite, chlorite, carbonate, and epidote. Veins of probable hydrothermal biotite occur in the surrounding metavolcanics. A porphyry similar to that of Jogran was intersected during deep diamond drilling of the Breton Breccia (Blecha, 1974).

At the Nystedt prospect, located 17 km (11 mi) north of Sault Ste. Marie, stockworks of quartz veins containing pyrite, chalcopyrite, and/or specularite cut highly deformed syenitic to monzonitic phases within the Gros Cap Batholith of Archean age. The specularite-bearing veins appear to occur peripherally to chalcopyrite-pyrite areas. A northwest trending diabase dyke swarm cuts these rocks, however there is no evidence to suggest that the mineralization is spatially related to diabase. Thus this occurrence may be an Archean porphyry copper deposit, although the abundant specularite, lack of molybdenite, and the very erratic nature of the mineralization would be unusual for this deposit type.

Copper Metallogeny

Preliminary observations and conclusions are as follows:

1) Nipissing Diabase intrusions afford an excellent opportunity to study metallogenic variations in rocks emplaced over a relatively restricted period of geological time. These rocks are well-dated, volumetrically important throughout the study area, and the copper occurrences related to them exhibit systematic regional variations. For example, Ni-Cu occurrences in Nipissing Diabase, so abundant in the Sudbury area, are rare to the west of Espanola. Chalcopyrite-pyrite-bearing quartz-carbonate veins, related to Nipissing Diabase, predominate in the Sault Ste. Marie-Elliot Lake area whereas polymetallic veins are common near Sault Ste. Marie, but minor elsewhere (Card and Patterson, 1973).

2) Volcanogenic massive sulphide deposits hosted in Archean metavolcanic rocks are commonly polymetallic Zn-Pb-Cu-Ag-Au, whereas those within Huronian volcanic rocks contain mainly iron-copper. This deposit type is unknown in Keweenawan rocks.

3) Known porphyry copper deposits, except one questionable occurrence, are related solely to the Keweenawan rift system and plutonism, an unusual environment for this deposit type (Kirkham, 1973);

4) "Sedimentary" copper deposits in the Huronian Supergroup are confined to rocks of the Lorrain Formation, which are the oldest host rocks in Canada known to contain this type of mineralization (Kirkham, 1974). The absence of such deposits in the underlying formations is probably real rather than apparent. The Lorrain Formation was deposited, at least in part, in a tropical, fluvial or littoral environment, in the presence of an oxygenated atmosphere in contrast to the anoxic atmosphere and vigorous, possibly glacial regime that probably prevailed prior to its deposition (Card et al., 1972; Roscoe, 1973).

Conclusions

Copper deposits in the study area vary greatly in their settings, ages, and lithologies of host rocks, size and form, associated metals, mineralogy, degree of deformation and metamorphism, and distribution in space. Further research will concentrate on better defining these metallogenic variations, on explaining why such variations exist, and to see if they can be utilized to define areas favourable for exploration.

References

Armbrust, G.A.

1969: Hydrothermal alteration of a breccia pipe deposit, Tribag Mine, Batchawana Bay, Ontario; Econ. Geol., v. 64, p. 551-563.

Blecha, M.

1974: Batchawana area - a possible Precambrian porphyry copper district; Can. Inst. Min. Met., Trans., v. 77, p. 393-398.

Card, K.D.

1968a: Economic geology of the Espanola-Whitefish Falls area, District of Sudbury; Ont. Dep. Mines, Open File Report 5017, 29 p.

1968b: The Mongowin Pluton; Ont. Dep. Mines, Misc. Paper 14, 27 p.

Card, K.D., Church, W.R., Franklin, J.M., Frarey, M.J., Robertson, J.A., West, G.F., and Young G.M.

1972: The Southern Province; **in** Price, R.A. and Douglas, R.J.W. (eds.): Variations in Tectonic Styles in Canada; Geol. Assoc. Canada, Spec. Paper 11, p. 335-379.

Card, K.D. and Innes, D.G.

1976: Benny area, Spanish-Johnson Lakes sheet, Sudbury; Ont. Div. Mines, Prelim. Map, P. 1110, Marginal Notes.

Card, K.D., Innes, D.G., and Debicki, R.L.

1977: Stratigraphy, sedimentology and petrology of the Huronian Supergroup in the Sudbury-Espanola area; Ont. Div. Mines, Geoscience Study 16, 99 p.

Card, K.D. and Patterson, E.F.

1973: Nipissing Diabase of the Southern Province, Ontario; **in** Young G.M. (ed.): Huronian stratigraphy and sedimentation; Geol. Assoc. Can., Spec. Paper 12, p. 7-30.

Charbonneau, B.W., Jonasson, I.R., and Ford, K.L.

1975: Cu-U mineralization in the March Formation Paleozoic rocks of the Ottawa - St. Lawrence Lowlands; in Report of Activities, Part A, Geol. Surv. Can., Paper 75-1A, p. 229-233.

Giblin, P.E.

1966: Recent exploration and mining development in the Batchawana area of Ontario; Can. Min. J., April, p. 77-80.

Giblin, P.E., Leahy, E.J., and Robertson, J.A.

1977: Geological compilation of the Blind River-Elliot Lake sheet, Districts of Algoma and Sudbury; Ont. Div. Mines, Prelim. Map P.304 (1977 Revision).

Goodwin, A.M.

1973: Archean iron-formations and tectonic basins of the Canadian Shield; Econ. Geol., v. 68, p. 915-933.

Gower, J.A.

1956: Geology of the Desbarats area; Ont. Div. Mines Resident Geologist Files, Sault Ste. Marie, SSM-3, geological map 1"=500'.

Hornick, G.L. (ed.)

1969: The Call of Copper; North Shore Printing, Bruce Mines, reprinted 1975.

Innes, D.G.

1972: Proterozoic volcanism and associated sulphide-bearing metasediments in the Sudbury area, Ontario; unpublished B.Sc. Thesis, Laurentian Univ., Sudbury.

Kirkham, R.V.

1972: Porphyry deposits; in Report of Activities, Part B, Geol. Surv. Can., Paper 72-1B, p. 62-64.

1973: Tectonism, volcanism and copper deposits; in Volcanism and Volcanic rocks, Geol. Surv, Can., Open File 164, p. 129-152.

1974: A synopsis of Canadian stratiform copper deposits in sedimentary sequences; Cenetare de la Société Géologique de Belgique, Gisements Stratifromes et Provinces Cuprifères, Liege, 1974, p. 367-382.

Naldrett, A.J.

1969: A portion of the system Fe-S-O between 900 and 1080°C and its application to sulphide ore magmas; J. Petrol., v. 10, Part 2, p. 171-201.

Robertson, J.A.

1970: Geology of the Spragge area; Ont. Dep. Mines Geol. Rep. 76, 109 p.

1976: Geology of the Massey area, Districts of Algoma, Manitoulin and Sudbury; Ont. Div. Mines, Geoscience Rep. 136, 130 p.

Roscoe, S.M.

1973: The Huronian Supergroup, a Paleoaphebian succession showing evidence of atmospheric evolution; **in** Young, G.M. (ed.): Huronian stratigraphy and sedimentation; Geol. Assoc. Can., Spec. Paper 12, p. 31-47.

Shklanka, R.

1969: Copper, nickel, lead and zinc deposits of Ontario; Ont. Div. Mines, Min. Resource. Circ. 12, 394 p.

Stockwell, C.H.

1972: Revised Precambrian time scale for the Canadian Shield; Geol. Surv. Can., Paper 72-52, 4 p.

Sutherland, W.D.

1965: Stag Lake copper prospect; Ont. Div. Mines, Resident Geologist Files, Sault Ste. Marie, SSM-708, 10 p.

Van Schmus, W.R.

1965: The geochronology of the Blind River-Bruce Mines area, Ontario, Canada; J. Geol., v. 73, p. 775-780.

52. EVALUATION OF SELECTED URANIUM-BEARING AREAS IN CANADA

Project 750010

V. Ruzicka
Regional and Economic Geology Division

Abstract

Ruzicka, V., Evaluation of selected uranium-bearing areas in Canada; Current Research, Part A, Geol. Surv. Can., Paper 78-1A, p. 269-274, 1978.

A number of different kinds of uranium mineralization, investigated during 1977 in British Columbia, Northwest Territories, Ontario and the Maritime Provinces, are described briefly. In the southern part of the Canadian Cordillera sandstone-type deposits in the Beaverdell area, exhibit geological features analogous to those of deposits being developed in the adjacent part of the United States Cordillera. Areas containing Proterozoic sediments in the Churchill Structural Province, the Yathkyed Lake Basin and Amer Lake area, District of Keewatin, are the subjects of intensive exploration. Among the areas with potential uranium resources in Ontario, in addition to the existing uranium mining districts, are those containing uranium mineralization in metamorphosed, Huronian(?), sediments; in the environments of carbonate-alkaline complexes; and, Archean sedimentary-volcanic assemblages, such as the Kirkland Lake – Larder Lake belt. The Appalachian orogenic belt contains geological environments favourable for orthomagmatic-anatectic, volcanogenic, sandstone and vein-type uranium deposits.

Introduction

During 1977 the Geological Survey of Canada participated in federal energy research and development activities through two major programs:

1. the Federal-Provincial Uranium Reconnaissance Program (U.R.P.); and

2. the Uranium Resource Evaluation Program (U.R.E.P.)

The tasks of the Federal-Provincial Uranium Reconnaissance Program were outlined by Darnley (1976). The Uranium Resource Evaluation Program continued in areas studied in the previous years (E.M.R., 1977) and in new areas favourable for uranium mineralization (Fig. 52.1). Several reports on these studies are included in this volume.

The author conducted field work in the following areas:

A. Southern Canadian Cordillera (with R.T. Bell and S.S. Gandhi);

B. Yathkyed Lake Basin and adjacent area of the Ennadai Fold Belt;

C. Churchill area of the Wollaston Lake Fold Belt;

D. Amer Lake;

E. Superior, Southern and Grenville structural provinces of Ontario; and,

F. Appalachian region (with H.E. Dunsmore).

This paper summarizes the results of field work in the areas noted above and reports on current laboratory and office work in uranium and thorium investigations.

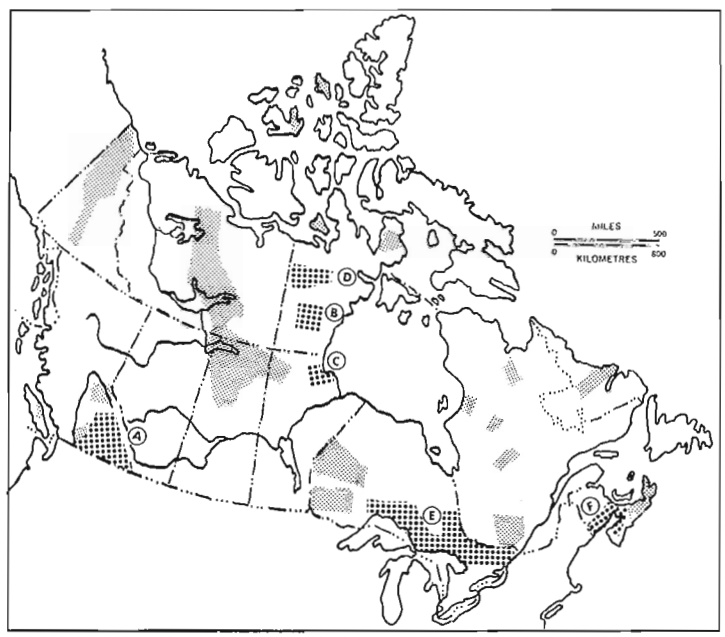

A= southern Canadian Cordillera;

B= Yathkyed Lake Basin and adjacent area of the Ennadai Fold Belt;

C= Churchill area of the Wollaston Lake Fold Belt;

D= Amer Lake area;

E= Parts of the Superior, Southern and Grenville Structural Provinces in Ontario;

F= Appalachian Region.

Figure 52.1. Areas studied by the Uranium Resource Evaluation Section in 1977. Areas reported on in this report are shown by coarse stippled pattern.

A. Southern Canadian Cordillera
(with R.T. Bell and S.S. Gandhi)

At present no uranium is produced in the Canadian Cordillera; however in the adjacent northern part of the Cordillera of the United States the Midnite Mine has produced about 8 million pounds of U_3O_8 in ores averaging 0.23 per cent U_3O_8 during 14 years of operation (Nash and Lehrman, 1975). Several other uranium occurrences are known in both the American and Canadian Cordillera (Fig. 52.2).

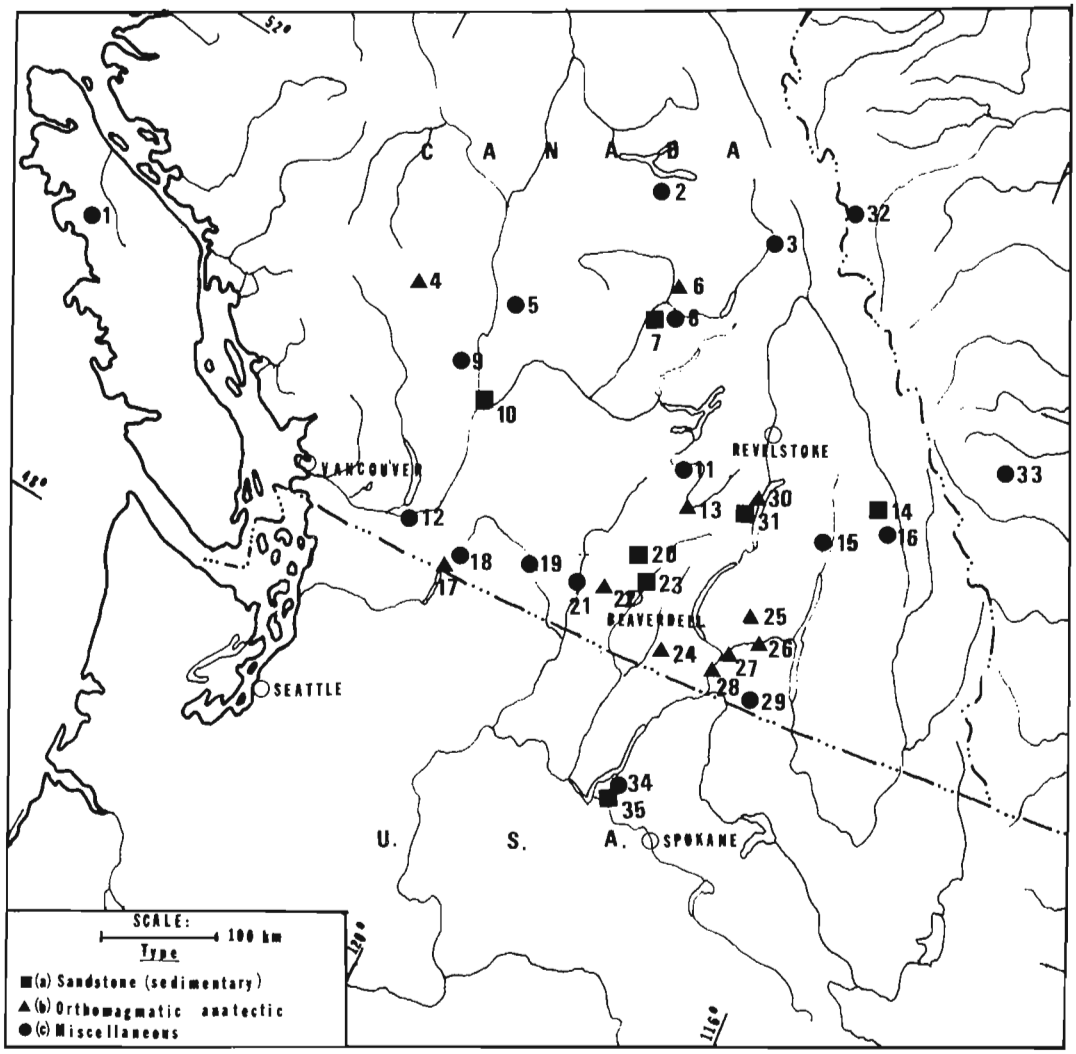

British Columbia

1 = Zeballos area;
2 = Horsefly River;
3 = Lempriere area;
4 = Bridge River area;
5 = Clinton;
6 = Raft Batholith;
7 = Joseph Creek;
8 = Birch Island area (Rexspar);
9 = Texas Creek (Index);
10 = Lytton area;
11 = Armstrong;
12 = Harrison Lake;
13 = Spar;
14 = Bugaboo Creek;
15 = Bullock Mine;
16 = Annette – Slide;
17 = Hope area;
18 = A.M. Claims;
19 = Hedley Lake;
20 = Kelowna area;
21 = White Lake Basin;
22 = Allandale Lake;
23 = Fuki – Donen;
24 = Boundary Exploration;
25 = Marmuph Claims;
26 = Lucky – Bill – Tag;
27 = Gibson Creek;
28 = Genell area;
29 = Lost Creek Area;
30 = Cameron – Jenkins 1;
31 = Cameron – Jenkins 2;

Alberta

32 = Jasper Park;
33 = Burnt Timber Creek area;

Washington

34 = Midnite Mine;
35 = Sherwood Mine.

Figure 52.2. Uranium occurrences in the southern part of the Canadian Cordillera and the northern part of the U.S. Cordillera.

Uranium occurrences that have been explored in the southern Canadian Cordillera can be classified into the following general types:

(a) sandstone;

(b) orthomagmatic-anatectic

Sandstone-type deposits

Sandstone-type deposits are presently being explored in the Beaverdell area, British Columbia (Christopher and Kalnins, 1977; Bell, 1977). Here, uranium mineralization, mainly autunite and/or meta-autunite (ibid.) occurs in Tertiary clastic sediments that unconformably overlie other metamorphic rocks of the Monachee Group and intrusive rocks of the Nelson, Valhalla and Coryell complexes. Here and there uranium-bearing sediments are, in turn, overlain by plateau lavas. A distinctive feature observed locally on the older rocks (e.g. Valhalla (?) intrusives) is a regolith up to several metres thick accompanied by extensive kaolinization. The granitic rocks show locally anomalous radioactivity[1].

The Early Tertiary volcanics and sedimentary rocks of the Marron and Kettle River formations in the same area are also anomalously radioactive, locally more than 10 times background (e.g. near Rock Creek TV1A readings were: T_1 = 600 cpm, T_3 = 80 cpm). Fragments of these volcanics are a common component of the uranium-bearing sediments.

The uranium-bearing sediments are unconsolidated or poorly consolidated conglomerates and sandstones with locally interbedded mudstones. The uranium mineralization is commonly associated with carbonaceous matter. The sediments fill scour channels and local depressions in the pre-Miocene surface. The major part of the uraniferous sediment unit is covered with plateau lavas.

Geological features of the Beaverdell uranium deposits resemble, in part, those observed in the Sherwood Mine near Spokane, Washington. This deposit occurs in locally coarse carbonaceous clastic sediments of the Gerome Formation of Oligocene age that were deposited in a channel at the contact of a deeply weathered (several tens of metres) granite body. The deposit is overlain by a thick clay bed. The principal uranium minerals are autunite with subordinate pitchblende and coffinite. The presently identified reserves of the Sherwood Mine are more than 5000 tonnes uranium metal in ores with an average grade of about 0.80 per cent U (J. Veelik, Sherwood Mine, pers. comm.).

A conceptual genetic model (Ruzicka, 1977a) that would correspond with features observed in the deposits noted above would postulate:

a) a source area of weathered intrusive and extrusive felsic and/or alkaline rocks that contain above background uranium; in this case rocks of the Nelson, Valhalla and Coryell intrusions, and the Kettle River and Marron volcanics or their equivalents;

[1] For example, a TV-1A (McPhar portable gamma-ray spectrometer) T-1 in situ reading on a syenite exposure of the Coryell intrusion near Rock Creek yielded 15 000 counts per minute or approximately 8 times background.

b) host rocks should be permeable to uranium-bearing solutions with this aquifer constrained and protected by impermeable mudstone layers and/or lava caps;

c) host rocks that contain reductants or precipitants; in this case carbonaceous matter or solutions derived from basaltic volcanism.

Environments favourable for this type of mineralization exist not only in the Beaverdell area, but also in the Omineca and Intermontane belts of British Columbia (Christopher and Kalnins, 1977).

Orthomagmatic-anatectic type deposits

Occurrences of the orthomagmatic-anatectic type were studied at the following localities:

1. At China Creek near Castlegar where white granite pegmatites containing autunite (?) along fractures in orthoclase-rich zones are being investigated by several companies.

2. In the Grand Forks area (explored by Consolidated Boundary Exploration Limited), where white pegmatites contain crystals or uraninite (up to 1 mm in diameter) with abundant biotite and almandine garnet.

3. In the Salmon Arm area where a granite body, approximately 10 km northwest of Salmon Arm, is intruded by several pegmatite and diabase dyke systems. In situ TV-1A readings on one of the pegmatite dykes within an area several m^2 were: T_1 = 22 000 cpm, T_2 = 600 cpm, T_3 = 50 cpm. No uranium minerals were observed but scattered grains of zircon are present.

4. In the Cranberry Creek area, south of Revelstoke, where locally radioactive pegmatites are exposed over a distance of several kilometres. Here, the highest radioactivity is concentrated along fractures, in areas with limonitic alteration. This area is presently being explored by prospectors W. Cameron and F. Jenkins of Revelstoke who have also found an additional interesting radioactive occurrence in the Cranberry Creek area. Here the radioactivity is confined to metamorphosed and sheared conglomerates of the Shuswap Metamorphic Complex. A grab sample, chemically assayed, contained 0.006 per cent U and a higher amount of thorium (F. Jenkins, pers. comm.). An autoradiograph of a sample collected by the author at this locality shows parallel arrangement of radioactive minerals in the host rock (Fig. 52.3). The sample is being further studied in the laboratories of the Geological Survey.

B. Yathkyed Lake Basin and Adjacent Areas of Ennadai Fold Belt, Northwest Territories

A number of companies, including Urangesellschaft Canada Limited, Pan Ocean Oil Limited, Essex Minerals Company and Noranda Mines Limited are engaged in exploration for uranium in sediments and volcanic rocks of the Dubawnt Group and in the pre-Dubawnt rocks of the Ennadai Fold Belt west of Yathkyed Lake and southeast of Tulemalu Lake, District of Keewatin. The geology of a part of this area was recently described by Eade (1976). In this area uranium mineralization occurs in several environments, as follows:

a) In the basement rocks of the Ennadai Fold Belt, within a short distance of the present pre-Dubawnt unconformity. The main uranium mineral is pitchblende (locally botryoidal) preferentially filling fractures and breccia zones in greenstones. Gangue material is calcite with some base metal sulphides (pyrite, chalcopyrite, galena) locally the basement rocks are capped by a regolith.

b) In sediments of the South Channel and Christopher Island formations. Uranium mineralization in these sediments is disseminated without obvious structural or lithological control or occurs in breccia or fracture zones. It also occurs in the sediments in zones near dykes consanguinous with Christopher Island volcanics.

c) As disseminations or as fracture fillings in igneous rocks (Christopher Island volcanics, syenite dykes).

The characteristics of mineralization in the Yathkyed Lake Basin and adjacent rocks resemble those of some occurrences in the Baker Lake area.

C. Churchill Area of the Wollaston Lake Fold Belt

Two radioactive fracture zones were investigated in Aphebian quartzite of the Wollaston Lake Fold Belt approximately 13 km east of Churchill, Manitoba. The quartzite is impure, locally cross-bedded and contains scattered pebbles or cobbles up to 5 cm in diameter. The fracture zones rarely exceed one metre in width and discontinuous radioactivity is traceable for a distance of up to 100 m. The in situ TV-1A reading in the most radioactive area was: T_1 = 32 000 cpm, T_2 = 1400 cpm, T_3 = 700 cpm. No uranium minerals were observed megascopically. The radioactive zones occur within a short distance (approximately 100 m) of the Precambrian/-Phanerozoic unconformity.

D. Amer Lake Area, Northwest Territories

Several companies, including Cominco Limited (Aquitaine option), Western Mines Limited and Uranerz Exploration and Mining Limited are exploring for uranium in the Aphebian (?) rocks of the Amer Group northeast of Thelon Basin, District of Keewatin. The geology of a part of the area was recently described by Heywood (1977). A generalized succession consists of a lowermost unit of white orthoquartzite interbedded with feldspathic quartzite and schist, overlain by dolomitic limestone which is in turn overlain by an arkose/siltstone unit. The uppermost part of the sequence consists of phyllite and black slate.

The uranium mineralization is dominantly confined to the arkose/siltstone unit and is either generally stratabound and relatively continuous with local redistribution along faults and fractures or occurs in scattered lenses. The main uranium minerals are apparently pitchblende and uranophane (megascopic determination). Magnetite is associated with uranium mineralization at several localities.

Mineragraphic studies are at present under way in order to establish a genetic model for the 'Amer Lake' type of uranium mineralization. The author's field observations support a model where the 'pre-Amer' intrusive and volcanic rocks containing magnetite iron-formation provided both the source of the clastic material that hosts the uranium mineralization, and the source of uranium that mainly accumulated syngenetically with the sediments and was further concentrated during their diagenesis.

The author briefly examined and sampled a uranium occurrence approximately 150 km west of Amer Lake. The uranium mineralization is confined to the basal portion of Thelon Formation unconformably overlying a granite body capped by a thick regolith.

The sequence starts with a strongly hematized conglomerate (TV-1A reading on T-1 in situ = 20 000 cpm); it is overlain by maroon sandstone (TV-1A reading on a boulder: T-1 = 60 000 cpm, T-2 = 4000 cpm, T-3 = 400 cpm) containing abundant uranium-bearing apatite. The upper part of the sequence consists of thinly laminated and cross-bedded white to cream sandstone (TV-1A reading in situ not exceeding 4000 cpm on T-1).

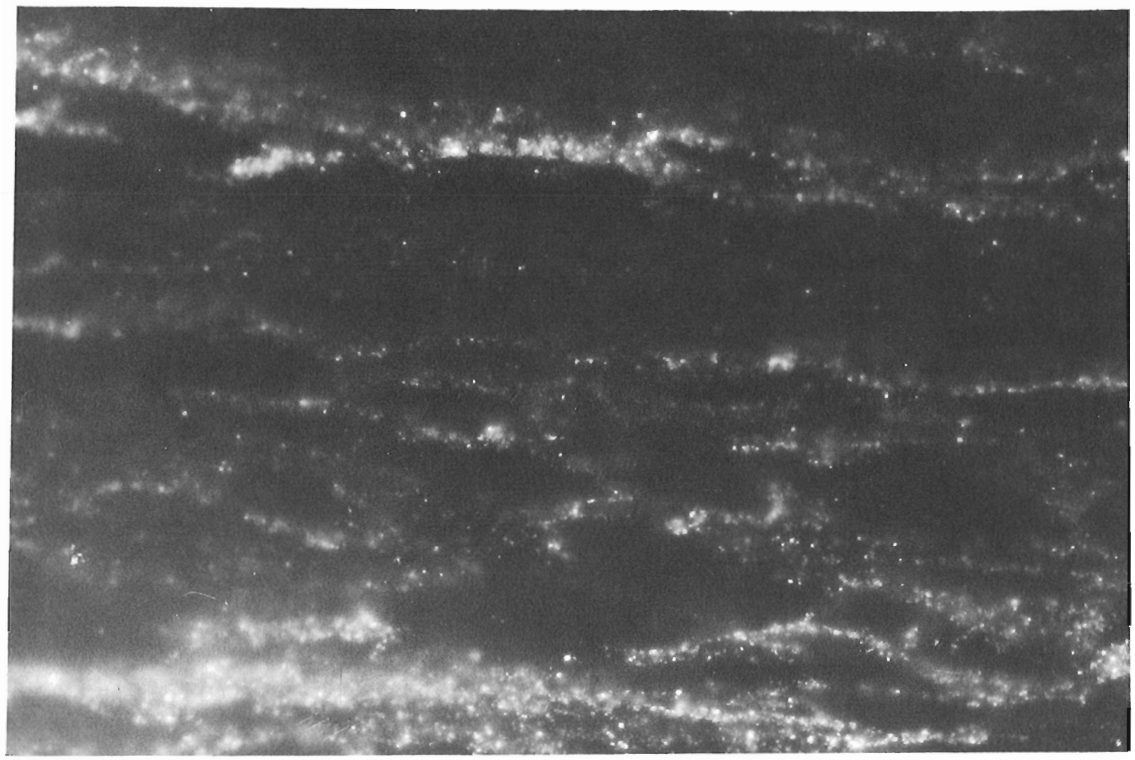

Figure 52.3. Autoradiograph of a portion of a sample collected from the Cameron – Jenkins 2 occurrence south of Revelstoke, British Columbia (Loc. 31, Fig. 52.2). White areas are result of radiation from mainly thorium-bearing minerals.

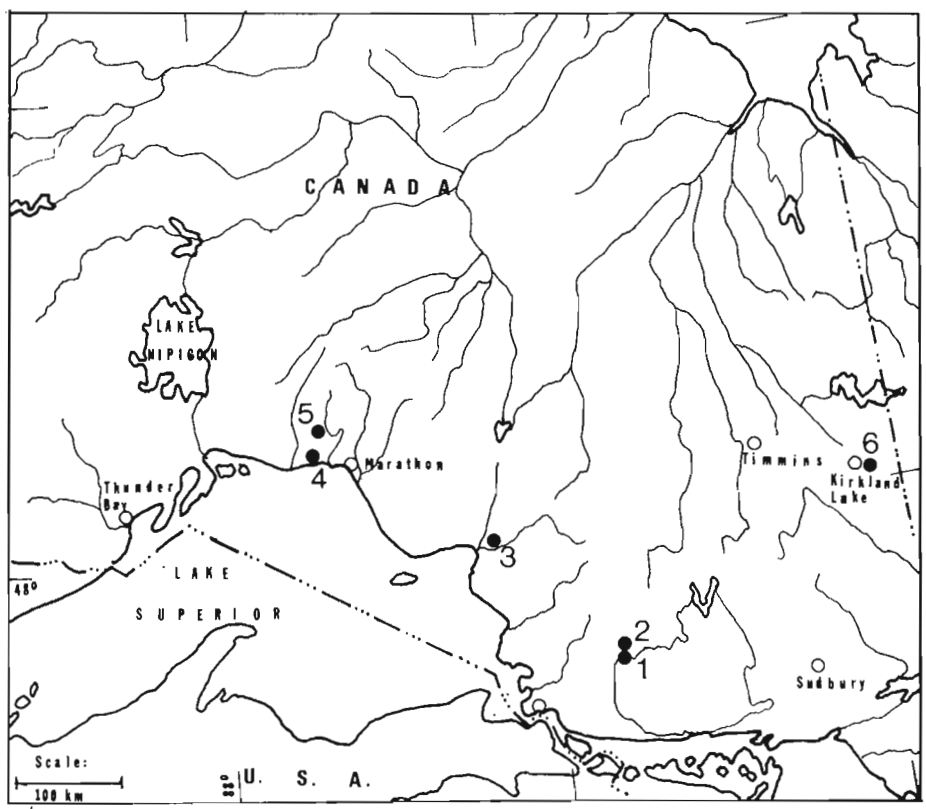

Figure 52.4

Index map showing locations of radioactive occurrences in Ontario reported in this paper.

1 = Seabrook Lake area "a";
2 = Seabrook Lake area "b";
3 = Wawa – Firesand area;
4 = McKellar Creek;
5 = Prairie Lake area;
6 = Kirkland Lake – Larder Lake area.

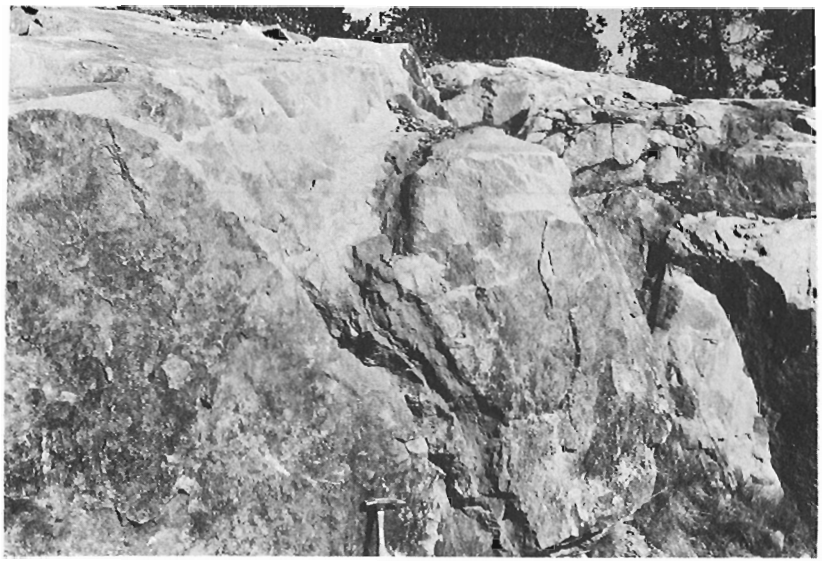

Figure 52.5.

Radioactive carbonate vein near the Seabrook Lake carbonatite, approximately 50 metres south of a bridge across the Mississagi River near Aubrey Falls, Ontario.

E. Superior, Southern and Grenville Structural Provinces in Ontario

In addition to assessment of target areas that are being investigated for uranium in Ontario by various organizations, including the Ontario Division of Mines, Imperial Oil Limited, Kerr Addison Mines Limited, Sherrit Gordon Mines Limited, Moncrieff Uranium Mines Limited and New Insco Mines Limited, studies were also conducted in other environments such as those of carbonate-alkaline complexes katazonally metamorphosed Huronian (?) sediments in the Grenville Structural Province and Timiskaming sediments and igneous rocks in the Kirkland Lake – Larder Lake area.

Carbonate veins in the vicinity of carbonate-alkaline complexes were identified in a number of localities (Fig. 52.4) including:

a) Near the Seabrook Lake carbonatite, approximately 50 m south of a bridge across the Mississagi River near Aubrey Falls in a road-cut of Highway 129 (Fig. 52.5). The vein is about 10 cm wide, strikes 360° and dips 70° east. A spectrochemical analysis of a sample taken from a radioactive portion of the vein detected among other elements: Ti - 4200 ppm, Ba = 3800 ppm, Sr = 890 ppm, Zr = 240 ppm and Y = 40 ppm and U (by neutron activation) = 142 ppm.

b) Near a diabase dyke in a road-cut on Highway 129 approximately 16 km north of the Mississagi River, a carbonate vein strikes 075° and dips 80° north. A grab sample (analyzed spectrochemically) contained: Ti = 6600 ppm and U (analyzed by neutron activation) = 284 ppm.

c) In the vicinity of the Firesand carbonatite diatreme the following carbonate thorium-bearing veins were identified by radiometric testing:

i) in a road-cut of Highway 101 approximately 1.6 km east of the northeast tip of Wawa Lake;

ii) approximately 2 km east of the outskirts of Wawa in a road-cut of Highway 101;

iii) approximately 2.4 km south of Highway 101 along the Firesand Road. TV-1A reading on this carbonate vein in an old trench was: T-1 = > 100 000 cpm, T-2 = 12 000 cpm and T-3 = 3000 cpm.

d) In the vicinity of the McKellar Creek diatreme, approximately 200 m west of McKellar Creek in a road-cut of Highway 17 near Marathon, Ontario. This vein is 10 cm wide.

It is felt that such carbonate veins in the vicinity of carbonatite complexes warrant more study.

Uranium mineralization related to the Prairie Lake carbonate-alkaline complex approximately 40 km northwest of Marathon, Ontario, is at present a target for exploration by New Insco Mines Limited. Here, relatively high grade uranium bodies occur in the ijolite phase of the complex.

A carborne radiometric survey in an area of metamorphosed sediments that are presumably Huronian was conducted by N. Prasad and J.E. Kerswill of the Uranium Resource Evaluation Section in the Grenville Structural Province north of North Bay, Ontario.

Samples of uranium occurrences in Timiskaming sedimentary and igneous rocks in the Kirkland Lake – Larder Lake area collected by the author in 1976 (Ruzicka, 1977b) were analyzed spectrochemically for selected nonradioactive elements and by neutron activation for uranium. Abnormally high uranium contents were detected in samples of trachytic rocks (Table 52.1). The results of investigation of other areas visited in Ontario during 1977 will be published after completion of laboratory studies.

F. Appalachian Region (with H.E. Dunsmore)

Exploration for uranium in Atlantic Canada is being conducted by several companies, including Inco Limited, Gulf Minerals Canada Limited, Imperial Oil Limited, Lacana Mining Corporation and others. The exploration targets are:

i) uranium mineralization in granitic rocks; certain granitic rocks of the Appalachian Orogen unusually high in uranium and are possible targets for uranium deposits similar to the deposits in Hercynian granites in Europe (Ruzicka, 1971);

ii) uranium mineralization in volcanic rocks; uranium occurrences of the volcanogenic type have been investigated in Canada in the past (Gross, 1957);

iii) Uranium mineralization in Carboniferous sediments; Dunsmore (1977) reported several localities containing uranium mineralization in sandstones that may be related to the formation of evaporites and subsequent diagenesis; alternatively the mineralization may be related in part to paleovolcanism and/or supergene processes (Prest et al., 1969);

iv) uranium mineralization of supergene or hypogene origin controlled by tectonic structures such as, for example, mineralization in the Lutes Mountains north of Moncton, New Brunswick.

Table 52.1

Spectrochemical analyses of radioactive grab samples
from Kirkland Lake – Larder Lake area, Ontario

Values in per cent***

Locality*	Si	Al	Fe	Ca	Na	Mg	Ti	Mn	Ag	B	Ba	Be	Cr	Mo	Ni
KL-2	25.	8.8	8.9	2.9	1.3	1.5	.56	.25	.0005	.012	.42	.00066	.0055	.005	.0038
KL-4	29.	5.8	5.8	6.0	1.9	3.0	.51	.13	.0005	.005	.075	.0003	.034	.005	.015
KL-5	25.	7.2	5.6	.74	72.0	1.9	.69	.086	.0005	.005	.12	.0003	.065	.005	.017
KL-7	28.	5.4	5.0	7.7	2.0	3.0	.49	.14	.0005	.005	.13	.0003	.019	.005	.012
KL-10	30.0	8.7	6.4	1.6	72.0	.62	.92	.18	.0005	.025	.61	.00084	.0022	.005	.015

Values in per cent***

Locality*	Sr	Yb	Zn	Zr	As	Ce	Co	Cu	La	Pb	V	Y	U**
KL-2	.14	.0004	.037	.049	.20	.025	.0036	.016	.019	.070	.041	.0069	105
KL-4	.047	.0004	.020	.022	.20	.020	.001	.15	.010	.070	.017	.004	241
KL-5	.016	.0004	.020	.026	.20	.020	.0098	.045	.010	.17	.025	.004	1170
KL-7	.10	.0004	.039	.025	.20	.020	.0049	.012	.010	.070	.030	.004	4250
KL-10	.088	.0004	.020	.087	.20	.045	.0026	.012	.029	.070	.040	.0087	39

*KL-2:	Latitude = 48°10'10"	Longitude = 79°56'12";	host rock:	trachyte tuff
KL-4:	48°10'00"	79°53'55"		conglomerate
KL-5:	48°09'58"	79°53'29"		greywacke
KL-7:	48°09'55"	79°53'43"		trachyte
KL-10:	48°09'00"	79°56'50"		trachyte

**Determined by neutron activation, values in ppm.

***Expected to be accurate within 5% of value reported.

References

Bell, R.T.
1977: Geology of some uranium occurrences in Western Canada; in Report of Activities, Part A, Geol. Surv. Can., Paper 77-1A, p. 31-32.

Christopher, P.A. and Kalnins, T.
1977: Exploration for basal type uranium deposits in B.C.; Western Miner, April 1977, p. 75-79.

Eade, K.E.
1976: Geology of the Tulemalu Lake map-area (65J), District of Keewatin; in Report of Activities, Part A, Geol. Surv. Can., Paper 76-1A, p. 379-381.

Energy, Mines and Resources, Canada
1977: 1976 Assessment of Canada's uranium supply and demand; Rep. EP 77-3, June 1977, 19 p.

Darnley, A.G.
1976: The Canadian uranium reconnaissance program; Am. Nuclear Soc., Washington, November 1976, 5 p.

Dunsmore, H.E.
1977: Uranium resources of the Permo-Carboniferous Basin, Atlantic Canada; in Report of Activities, Part B, Geol. Surv. Can., Paper 77-1B, p. 341-347.

Gross, G.A.
1957: Uranium deposits in Gaspé, New Brunswick and Nova Scotia; Geol. Surv. Can., Paper 56-5.

Heywood, W.W.
1977: Geology of the Amer Lake map-area, District of Keewatin; in Report of Activities, Part A, Geol. Surv. Can., Paper 77-1A, p. 409-410.

Nash, J.T. and Lehrman, N.J.
1975: Geology of the Midnite uranium mine, Stevens County, Washington; U.S. Geol. Surv., Open file Report 75-402, 36 p.

Prest, V.K. et al.
1969: Occurrences of uranium and vanadium in Prince Edward Island; Geol. Surv. Can., Paper 68-74, 14 p.

Ruzicka, V.
1971: Geological comparison between East European and Canadian uranium deposits; Geol. Surv. Can., Paper 70-48, 195 p.

1977a: Conceptual models for uranium deposits and areas favourable for uranium mineralization; in Report of Activities, Part A, Geol. Surv. Can., Paper 77-1A, p. 17-25.

1977b: Assessment of selected uranium occurrences and areas favourable for uranium mineralization in Canada; in Report of Activities, Part A, Geol. Surv. Can., Paper 77-1A, p. 27-29.

53. URANIUM MINERALIZATION IN THE NIPIGON AREA, THUNDER BAY DISTRICT, ONTARIO

Project 750098

J.M. Franklin
Regional and Economic Geology Division

Abstract

Franklin, J.M., Uranium mineralization in the Nipigon area, Thunder Bay District, Ontario; Current Research, Part A, Geol. Surv. Can., Paper 78-1A, p. 275-282, 1978.

Occurrences include high grade veins at Greenwich Lake, low grade uranium associated with sulphides at the Enterprise Mine lead-zinc-barite veins, hematized float near Innes Lake and the Prairie Lake carbonatite occurrence.

The two vein type occurrences are similar and formed within the Sibley basin. Metals for the veins were derived by leaching of basement rocks and the matrix of basal Sibley sandstone and were precipitated in structural and stratigraphic traps. Uranium-enriched albitic pegmatite with accessory apatite was the source of the metal at Greenwich Lake where metals were remobilized into Keweenawan-related faults. Any zone within the Sibley basin which (a) has uranium-enriched basement rocks, (b) may be near onlaps of basal Sibley sandstone against Archean paleotopographic high areas, and (c) is cut by major Keweenawan-related faults or fracture systems involving basement rocks, has some potential for supergene-type deposits. The absence of a well developed paleosol reduces, but does not eliminate the probability of finding more such occurrences.

Introduction

Discovery of very rich vein-type uranium deposits (e.g. Rabbit Lake, Key Lake) in the region of the Neohelikian Athabasca sandstone basin (1350 ± 50 m.y., Ramaekers and Dunn, 1976) in northern Saskatchewan has raised interest in assessing the uranium potential of other Helikian sedimentary basins. The Sibley Group is a superficially similar sequence of continental to shallow marine red-beds which overlie Aphebian and Archean rocks. It occupies an elongate basin extending from the Sibley Peninsula near Thunder Bay northwards to Armstrong, Ontario (Fig. 53.1). This paper reviews the geology of uranium occurrences in the Marathon-Thunder Bay region, including three occurrences in the Sibley basin, and gives a preliminary assessment of the uranium potential of the region. The preliminary nature of this study must be emphasized, as much additional data must be collected to further refine the model.

Acknowledgments

K.G. Fenwick, J.S. Scott and J. Mason, Ontario Division of Mines, Thunder Bay, assisted with preliminary field studies and provided useful background information. M.M. Kehlenbeck and K.H. Poulsen, Lakehead University outlined the major feature and aided in regional reconnaissance of the Quetico belt. R. Blair, R. Tanaka and R. Benkis, RiO Tinto Mines Ltd., conducted the author on a tour of the Greenwich Lake property and provided information on local geology. Dr. F. Joubin, M.W. Resources Ltd., allowed access to the property and drill core, and made many useful suggestions. W. MacRae collected some of the regional data, while employed as the author's senior assistant. T. Gilmour supplied drafting services.

Regional Geology

A maximum of 225 m of Helikian sedimentary rock overlies the Archean, and locally, the Aphebian basement in the Sibley Peninsula-Nipigon region. The uranium occurrences are in both Archean and Helikian rock.

Archean

The Quetico gneiss belt (Fig. 53.1) which underlies much of the area is, on a regional scale, a northeasterly trending, large anticlinal or domal structure. This belt has deformed, highly metamorphosed metasedimentary strata on the limbs and a core of trondhjemite, migmatite and pegmatite. The metasedimentary domains are highly folded (Kehlenbeck, 1976) and consist of arenaceous to argillaceous rocks, with turbidite-type structures. Sillimanite and cordierite attest to high metamorphic grade (Kehlenbeck, 1976) and much quartz-feldspar mobilizate occurs as irregular veins in the metasedimentary terranes. Albitic pegmatite bodies and massive, lensoid quartz monzonite bodies occur throughout the belt; the latter appear to be "late" intrusions.

The Shebandowan-Wawa belt to the south of the Quetico belt (Fig. 53.1) includes basalt, greywacke and granitic intrusions. Metamorphism of this belt is less intense than in the Quetico. Similar volcanic rocks, with minor sedimentary rock, including iron-formation, occur in the Wabigoon belt immediately north of the Quetico belt.

Most of the area has been mapped by McIlwaine and Tihor (1975), MacDonald (1939), Coates (1972), Carter (1975), Kaye (1966), and Pye (1965) and more detailed descriptions of the Quetico belt are available from these reports.

Aphebian

The Gunflint and Rove formations (Moorhouse, 1960) overlie the Shebandowan-Wawa belt near Pass Lake and at Dorion Landing (McIlwaine and Tihor, 1975). The Gunflint Formation is composed of taconite, the Rove Formation of black shale. These rocks are at least 1650 m.y. old (Faure and Kovach, 1969) and are not deformed or strongly metamorphosed. The Gunflint Formation was deposited in a paralic basin, whereas the Rove Formation was deposited in a starved basin.

Helikian

Helikian strata (Sibley Group, Osler Group) cover the basement rocks through much of the Nipigon area (Fig. 53.1), and form the lowermost part of the Keweenawan Supergroup. The Sibley Group is 1300 m.y. old, whereas the Osler Group is 1150-1200 m.y. old.

The Sibley Group is deposited in an elongate, northerly trending trough and also the Keweenawan basin which generally conforms to the present Lake Superior area. Details are given in Table 53.1.

The Osler Group is exposed on Black Bay Peninsula and numerous islands in Lake Superior, and consists primarily of subaerially deposited tholeiitic basalt with very minor rhyolite and minor intercalated fluvial clastic rocks. A large

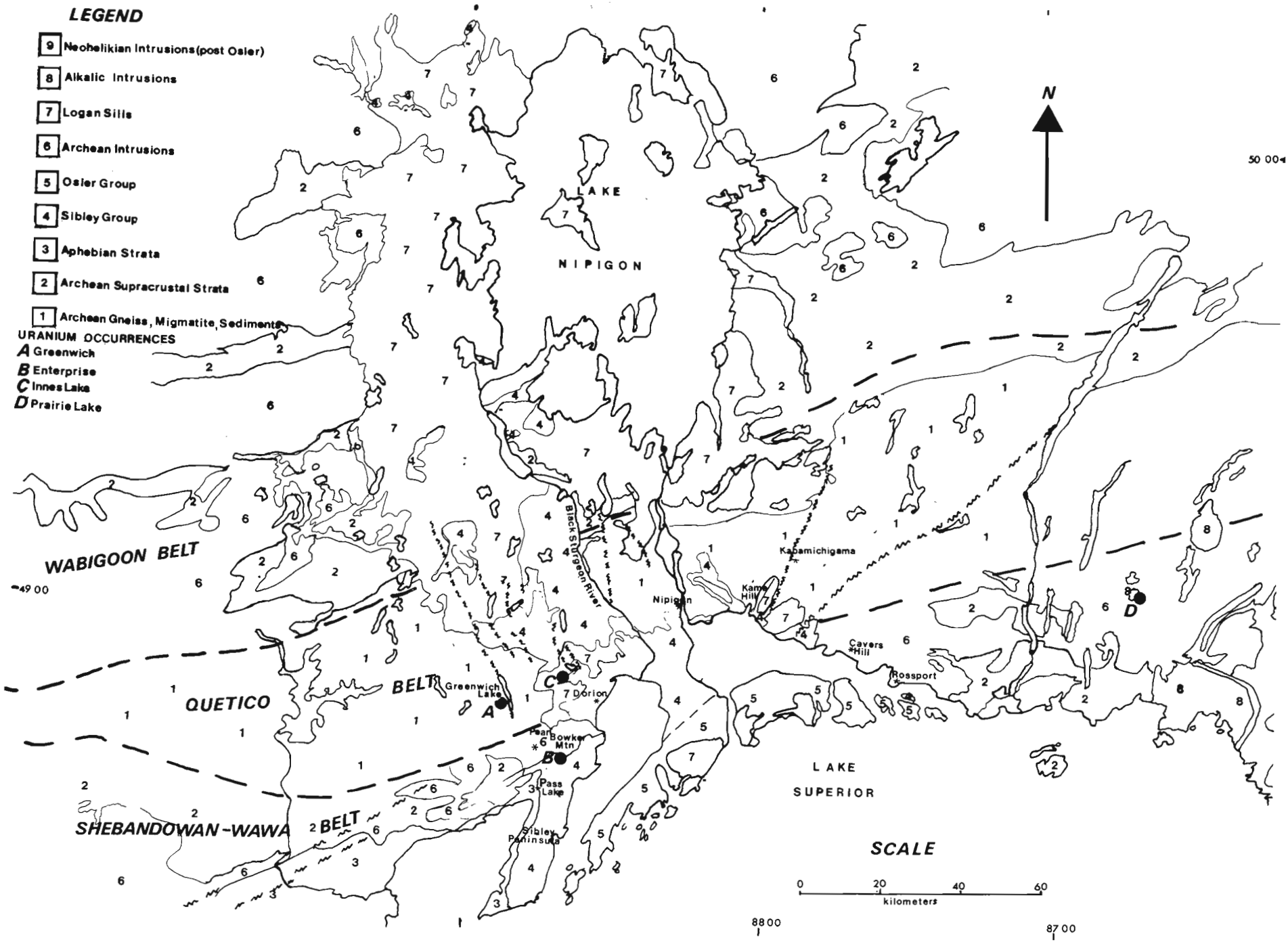

Figure 53.1. Geology and uranium occurrences in the Nipigon area, Thunder Bay District, Ontario. (Geology after Ontario Division of Mines Map 2199, Ontario Geological Map, West Central Sheet.)

Table 53.1

Stratigraphy of the Sibley Group[1]

Formation	Max. Strat. thickness metres	Description
Kama Hill	100	Most laterally extensive of the three formations; purple moderately fissile shale and siltstone; quartz, authigenic microcline, mixed layer smectite-type clay, illite are characteristic minerals; synaeresis cracks, ripple-marks, halite and gypsum casts, stromatolites, mudchip breccias are characteristic structures. Deposited in shallow water, periodically emergent, partially evaporitic, warm environment.
Rossport	150	Three members include upper and lower red dolomitic members, and an intermediate chert-carbonate and stromatolite member. Dolomitic members contain variable clastic content with less than 2% hematite, are aphanitic, and exhibit a spotted texture. Chert carbonate member is carbonaceous. This unit was deposited in shallow water, and the dolomite is probably primary.
Pass Lake	75	Thick to thin bedded pink to white quartz arenite, present dominantly in southern portion of basin; lenses of locally derived conglomerate at the base. Cement is dolomite, calcite, quartz and minor barite. Few sedimentary structures (ripples, cross-beds). Clast compositions indicate dominant derivation from immediate basement rock. Probably deposited in a beach to shallow marine environment.

[1] The formations described above are informally named.

variety of Helikian intrusions is present in the northern Lake Superior region, including Logan tholeiitic sills (Blackadar, 1956), gabbro intrusions (McIlwaine and Wallace, 1976; Giguere, 1975; and Guel, 1970) and alkaline intrusions (Mitchell and Platt, 1977) including the Port Coldwell and Killalla Lake syenitic bodies and the Prairie Lake carbonatite complex.

The Helikian rocks were deposited in a continental rift system (Card et al., 1972). The main rift follows closely the arcuate shape of the Lake Superior shoreline, is bounded by normal faults, and to the north contains both the Sibley and Osler groups. A secondary, at least partially fault-bounded, trough extends northward from the Dorion-Nipigon area at a high angle (120°) to the main rift zone, and represents a "failed arm". The Sibley Group and Logan sills occupy this secondary arm. The fault and fracture system bounding this secondary, north trending trough is well developed, as north trending lineaments are common (see maps accompanying McIlwaine and Tihor, 1975 and Coates, 1972). Facies relations in the Sibley Group sediments within the southern portion of the trough indicate that activation of these faults initiated sedimentation into the Sibley basin.

Uranium Occurrences

Economically significant concentrations of uranium have been found in at least four localities within the area north of Lake Superior. Of these four, the Innes Lake (Fig. 53.1) is a hematized breccia float with several thousand parts per million (ppm) uranium. The origin of this float is unknown.

A second occurrence is in the Prairie Lake carbonatite complex (Northern Miner, 1976) where uranium occurs primarily in pyrochlore (D. Watkinson, pers. comm.) and possibly betafite. The uraniferous zones include an area near the centre of the body at the contact between ijolite and carbonatite, and a second zone within the carbonatite unit. This body was not examined but additional data are available from Sage (1976) and Watkinson and Barnett (1971).

The remaining two occurrences, at Greenwich Lake and the Enterprise Mine, are described below.

Greenwich Lake

The Greenwich Lake area (Fig. 53.2) is underlain by arenaceous to argillaceous metasedimentary rocks, sill to lensoid quartz monzonite intrusions, and pegmatite dykes. The metasedimentary rocks are highly metamorphosed and deformed, are in the Quetico belt, and have up to 20 per cent quartz-feldspar "sweat" mobilizate dykes. At the south end of Greenwich Lake, excellent exposures of metasedimentary rocks exhibit many turbidite sedimentary structures, including graded beds, small scale cross-beds and rip-ups. Farther north, the metamorphic grade increases rapidly, and the sedimentary sequence is disrupted by numerous quartz monzonite lenses and pegmatite dykes.

The largest lens of quartz monzonite (Fig. 53.2) is approximately 2500 m wide, and is relatively homogeneous. These lenses appear to be similar to the late-syntectonic intrusions that occur throughout the Quetico belt, and possibly similar to those described by Kehlenbeck (1977) in the Shebandowan-Wawa belt.

Three types of pegmatite which cut the metasedimentary sequence are quartz-feldspar "sweat"-type mobilizate veins and dykes, pink microcline-bearing dykes, and white albite-muscovite-biotite-quartz bodies. The pink, syenitic pegmatites are possibly co-magmatic with the quartz-monzonite intrusions and cut all other pegmatite types as well as the metasedimentary rocks. They commonly contain irregular, narrow (5-10 cm) aplitic dykes. The albitic pegmatite bodies constitute one of the uranium hosts and are described below.

Uranium occurs in two very distinct geologic environments, in pegmatites and in quartz-pyrite-pitchblende veins. The latter cut both metasediments and pegmatites.

Pegmatites. The albitic pegmatites are characteristically uraniferous, typically containing 60-100 ppm uranium. At Greenwich Lake (Fig. 53.2) these bodies are typically lensoid to dyke-shaped, 5 to 30 m wide and unzoned. They consist of albite (70-80%), quartz (10-20%), biotite (1-10%), muscovite (1-5%) and apatite (0.1 to 0.5%). The distribution of quartz and apatite is irregular. Uranium occurs in uraninite (X-ray diffraction identification) in close association with biotite. It is important to note that virtually all

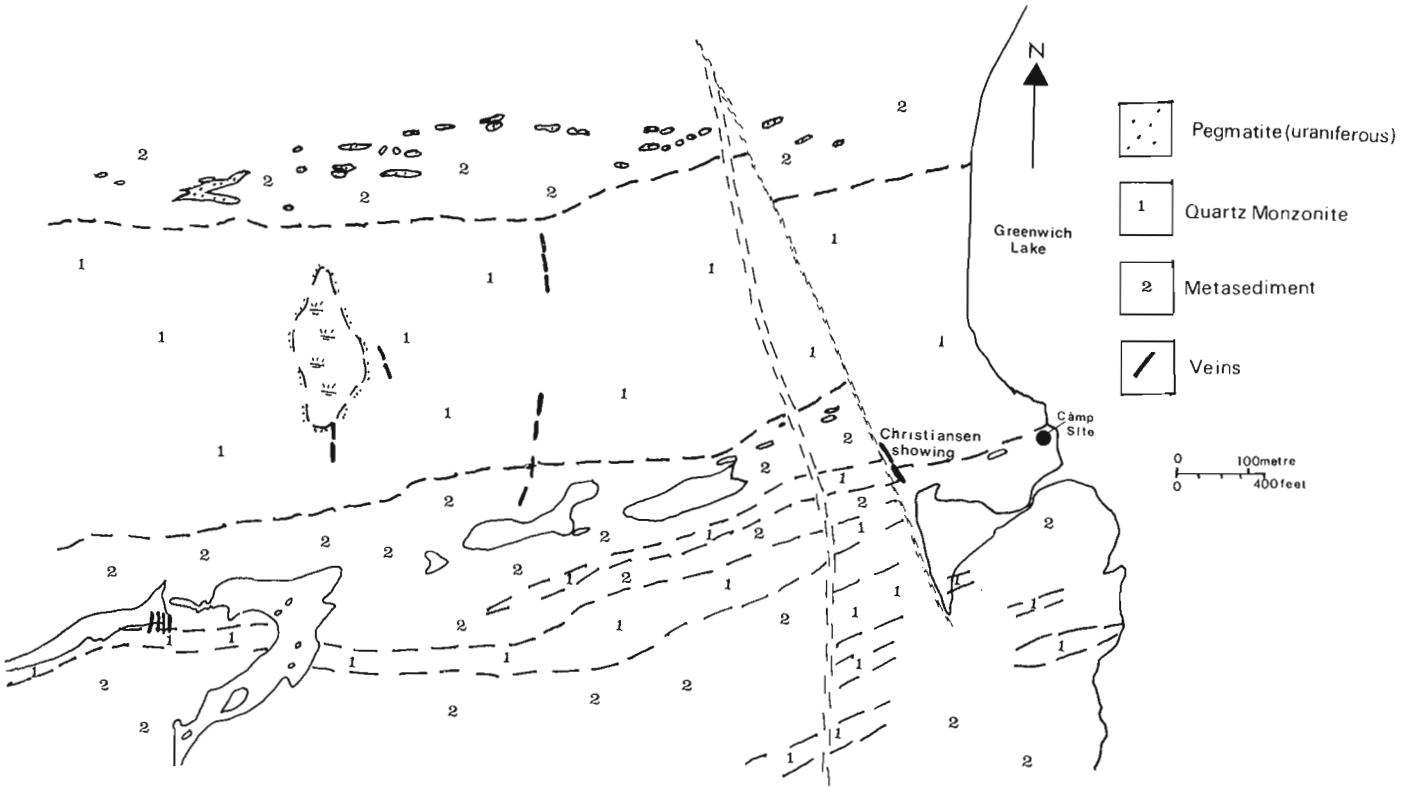

Figure 53.2. Geology of the Greenwich Lake uranium occurrences (after R. Blair, Rio Tinto Mines Ltd. company report, Ontario Division of Mines assessment files).

white pegmatite with accessory apatite is uraniferous. Major minerals in the pegmatite are commonly 1 to 5 cm in diameter, and thus are not particularly coarse grained when compared with classical zone pegmatites.

The uraniferous pegmatites are conformable with the easterly trend of the metasedimentary rocks (Fig. 53.2). They have sharp, regular boundaries and include a few stoped blocks of country rock. Blocks of massive to slightly foliated, medium grained, medium grey tonalitic gneiss are scattered through these pegmatites. A local source for the tonalitic gneiss blocks is not evident, but they resemble compositionally and texturally the oldest "grey gneiss" noted by Goldich (1972) in the Minnesota River valley.

The uraniferous pegmatites remain genetically obscure. They are texturally and mineralogically distinct from the mobilizate-type and appear distinctly magmatic, and not metamorphic in origin. More detailed study of their petrology is necessary before an origin can be proposed.

Vein type occurrences. At Greenwich Lake, uraniferous veins occupy a set of north trending faults and fractures (Fig. 53.2).

The largest vein, the Christiansen showing, is up to 1 m wide, at least 20 m long, occupies a fault zone, and is composed of red and white fine grained quartz, pyrite and pitchblende. A typical sample contains 0.5 to 2.0% uranium. The vein is vuggy, and the quartz-crystal terminations are zoned, indicating periodic precipitation of vein materials in an open space. A few fragments of red and buff cherty material in the vein are similar to those observed at the Thunder Bay amethyst mine as well as at several lead-zinc barite occurrences in the area (Franklin and Mitchell, 1977) and are altered Sibley (Rossport) dolomite.

The quartz monzonite wall rock is altered, with disseminated pyrite and secondary quartz present through approximately one metre of vein wall rock. The vein walls are slickensided, and small veins occupy fractures which lie at a high angle to the main vein. Veins formed in fractures in quartz monzonite rather than faults appear to be narrow (typically 5 to 20 cm in width) and discontinuous (rarely more than 2 m in length) and are similarly composed of pitchblende, pyrite and quartz.

In general, the Greenwich Lake veins are thought to have an origin similar to the lead-zinc barite veins described below.

Enterprise Mine

The Enterprise mine is the only uranium bearing vein of a group of lead-zinc-barite veins found throughout the southern part of Sibley basin. A detailed description and summary of their genesis may be found in Franklin and Mitchell (1977). Some of the features important to the uraniferous Enterprise occurrence are:

1) Vein metal content of the lead-zinc-barite group varies regionally, and reflects basement composition. These uranium-enriched veins at Enterprise probably formed proximal to a uraniferous basement "source" rock.

2) Veins occur in the Rossport dolomite immediately above the zone where the Pass Lake sandstone thins against an Archean paleo-positive area, now represented by Bowker Mountain. The latter is composed of quartz monzonite. Immediately below the unconformity between the Sibley Group and Archean rocks, some feldspar has decomposed to clay.

3) The veins contain as much as 540 ppm uranium (Ruzicka, 1976), in apparent spatial association with galena.

4) S and K-Ar isotopic studies indicate that depositional temperature was approximately 100°C.

Table 53.2

Uranium content of various lithologies

Unit	Range (ppm)	N	Mean	Median	Ref.
Aphebian Shale	1-19	30	6.8	5.0	
Sibley Dolostone*	1-21	56	2.7	1.5	
Quartz Monzonite	1-10	10	4.2	3.0	
Pegmatite	9-3550	15	470	60	
Sibley Sandstone	0.4-0.8	5	0.5	N/A	
Areas					
Sibley, Disraeli Lake	0.1-22	14	5.0	4.6	
Sibley, Dorion	1.6-3.6	10	2.1	2.0	
Sibley, Enterprise	0.4-7.1	27	2.4	2.1	
Enterprise and Pearl Q. Monzonite	0.5-8.9	8	4.3	4.6	
Greenwich Lake Q. Monzonite	2.6-10	2	6.3	N/A	
Quetico metasediments	1.8-4.7	3	2.9	N/A	
Archean metavolcanics**	0.2-3.2	21	1.4	1.5	
Greenwich vein material	63-6490	4	4130	N/A	
Comparative data					
Average Granite***	2.2-7.6	680	2.9		1
Average black shale			8		2
Average carbonate	0-7	54	2.2	1.4	
Average greywacke			2.1		3

*Includes Disraeli Lake
**From Sturgeon Lake, Ontario
***Non-alkaline granites only
N/A not applicable

[1]Swanson, 1961

[2]Rogers and Adams, 1969

[3]Rogers and Richardson, 1964

5) Pb isotope studies indicate that galena is formed from highly radiogenic lead, probably generated in a uranium-rich source.

6) Metals were derived by leaching of basement rocks and matrix of the locally derived Pass Lake sandstone, and were transported in chloride-rich solutions through the sandstone. Deposition occurred due to mixing of these metals with organic-derived H_2S in local gas traps.

Uranium Content of Various Lithologies

A reconnaissance survey of the uranium content of various lithologic units is underway, prompted by the studies of the Greenwich Lake and Enterprise Mine uranium occurrences which indicate that metal enrichment in basement rocks adjacent to high grade veins may be an indication of the presence of favourable source material for vein formation.

The uranium contents of various rock units are presented, along with some comparative data, in Table 53.2.

In sampling, widespread regional coverage of each lithotype or stratigraphic unit was attempted, in order to examine variations within units or lithotypes, as well as to establish the uranium levels for each rock type.

From the statistics in Table 53.2, as well as inspection of the data, some facts are of interest, although clearly many of the sample populations are too small to draw definite conclusions. The important points are:

a) the content of uranium in pegmatite is clearly one to two orders of magnitude higher than any other rock type;

b) the Aphebian shale has a single population with median and mean values very close to the average value for black shale;

c) the Sibley samples have two populations; the samples from the Disraeli Lake area have almost twice the U content of those from the other areas. The uranium content of the Sibley dolomite is close to the average value for dolomite (Rogers and Adams, 1969);

d) the veins at Greenwich Lake are locally very rich in uranium;

e) quartz monzonite has a higher uranium content than that of typical granite.

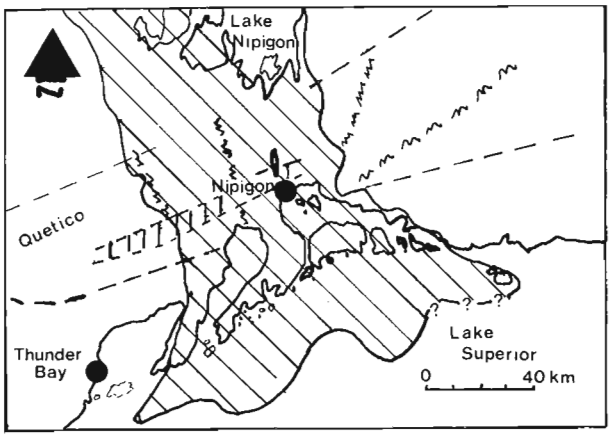

Sibley depositional basin

Uraniferous pegmatite zone

Keweenawan faults

Figure 53.3. Geological features controlling uranium deposition, Thunder Bay District, Ontario.

Genetic Model

The lead-zinc-barite veins at the Enterprise Mine and the Greenwich Lake veins have similar features and it is probable that the processes which operated to form both vein systems are similar as outlined by Franklin and Mitchell (1977). The critical factors are:

1. Suitable content of metal in the immediate basement rock and locally derived Pass Lake sandstone

2. Proximity to the Sibley-Archean unconformity and preferably proximity to an onlap of the Pass Lake sandstone against a basement "high" source rock; thus a stratigraphic "trap" was available.

3. Availability of a suitable structural trap, such as a well developed fracture or fault zone.

4. Presence during the time of vein formation of a sufficient hydraulic gradient to allow for groundwater movement, and consequent basement and sandstone leaching. Sufficient permeability was available in the sandstone.

From the regional zonation pattern of zinc and lead versus copper in the veins, it is evident that the vein metallic constituents reflect basement metal ratios, and the veins overlying a more uranium-rich basement may also be enriched in uranium. Thus the Enterprise Mine veins, which overlie quartz monzonite and are not laterally far removed from the Aphebian shale (both moderately rich in U relative to other basement rocks), have some uranium. The Greenwich Lake veins lie in an obvious uranium-rich environment, as the pegmatites are excellent proximal source rocks.

The unconformity control on lead-zinc-barite deposits is well established. Similar relationships exist for uranium deposits in the Athabasca region.

The most pervasive fractures and faults in the Sibley basinal area are associated with the Keweenawan rift system. The north trending faults prevalent at Greenwich Lake are also manifest elsewhere and provided an excellent fluid conduit and depositional location.

The greatest hydraulic gradients would probably have developed along the basin margins, particularly where the basin developed as a fault-bounded trough. The downward movement of water would be considerable on these margins, and downward leaching, particularly in highly oxidizing, relatively warm equatorial conditions that prevailed during Sibley deposition, would be most effective in these regions.

A genetic model for the uraniferous veins might include the following:

a) after deposition of the lower units of the Sibley Group in a "failed-arm" graben or half graben, downward percolating waters might leach metals from the basement; more waters circulating through the permeable, locally derived basal Pass Lake sandstone have altered much of its matrix, thus also releasing metal. As the matrix of the sandstone was also locally derived, the composition of the circulating fluid derived partially by matrix alteration would reflect local basement compositional variation and enrichment.

b) metals would move in solution in the relatively permeable Pass Lake sandstone perhaps only a short distance to depositional sites such as unconformity pinchouts and basement fractures;

c) deposition of sulphides appears to have been induced by mixing of metalliferous brines with local, organic-derived H_2S gas. This gas filled fractures and onlap traps.

Uranium Potential of the Region

The important parameters derived from the genetic model for the uranium-bearing veins of the Nipigon area may be applied to assess the uranium potential of the entire Sibley basin for additional deposits. In so doing it is important to compare these genetic parameters with those from similar, but better understood uraniferous areas. Sandstone-related deposits have been extensively studied and a comparison with the significant genetic parameters assigned to vein type deposits in sandstone basins, such as the Athabasca region, should be useful. Some interesting comparisons are as follows.

Source rocks

Darnley et al. (1977) have stated the empirical relationship that uranium deposits occur in areas where above average uranium contents are measured on a regional scale, and furthermore, as uranium deposits are commonly formed due to recycling and concentration of uranium by supergene processes, these anomalous regions represent areas of excellent potential. In the Thunder Bay region, the present reconnaissance survey has attempted to evaluate the magnitude and distribution of anomalously enriched strata or lithotypes. Two source rocks within the basement of the Sibley basin stand out, namely the quartz monzonites, which have higher uranium content than the average of granitic rocks, and pegmatites, which are highly enriched, but much less common. Furthermore, the granitic complexes, which may have been source rocks to the Gas Hills and Wind River basins of Wyoming (IATA 1977, p. 286), have uranium contents that are very similar to the quartz monzonites of the Enterprise area.

The quartz monzonite bodies are quite large (e.g. Bowker Mountain is 5-7 km in diameter) but an assessment of their distribution within the Sibley basin is difficult due to Proterozoic cover and lack of discrimination on pre-1970 maps.

The pegmatites represent by far the best uranium source and with their distinctive mineralogy (accessory apatite) they can be readily recognized. Reconnaissance traverses from the Dog Lake-Kivikoski area eastward to Nipigon-Orient Bay revealed that apatite-bearing pegmatites are distributed somewhat irregularly through a narrow (0.2 to 1 km wide) but laterally extensive zone (Fig. 53.3) near the southern margin of the Quetico belt, extending from

Hwy. 800 to near Nipigon. These pegmatites all have anomalously high γ-ray activity (recorded as uranium on a McPhar TV1 instrument). A parallel zone may exist near the northern edge of the Quetico belt as similar pegmatites occur along Hwy. 800 in this region. Where these zones extend under the Sibley basin, as, for example, in the Disraili Lake area, the potential for high grade secondary veins may be increased.

A somewhat analogous situation exists in the Athabasca region. There, where uranium-enriched metasedimentary calc-silicate and pelitic rocks pass under the Athabasca Sandstone, very rich secondary veins have been formed, possibly by a supergene process involving remobilization of lower grade uranium mineralization from the Wollaston rocks into a paleosol-vein type concentration (Langford, 1974; Beck, 1977).

The pegmatite zone in the southern Quetico belt is probably much less extensive than the uranium-enriched portion of the Wollaston, thus confining regionally the potential for high grade secondary veins.

Nature of the supracrustal secondary rocks

Based on studies of the better exposed southern half of the Sibley Group, the Pass Lake sandstone was deposited in a beach environment, the dolomitic Rossport formation[1] was deposited in a shallow marine environment, and the Kama Hill formation was deposited in a periodically emergent tidal-mud flat regime. The Athabasca Sandstone however, is predominantly of fluvial origin (Ramaekers and Dunn, 1976). Perhaps the amount of subsurface water movement in the fluvial sediments may have been greater than in the beach or shallow marine Pass Lake formation, and hence a large scale leaching in the latter may have been absent. This important difference in the sedimentary history of the Sibley sequence diminishes the potential of the basin for high grade uranium deposits. However, the possibility that a more fluvial regime existed in the northerly part of the basin cannot be discounted.

Nature of the unconformity

The unconformity between the Sibley Group and Archean rocks is generally sharp and well-washed. The Pass Lake sandstone generally contains a few boulders of locally derived basement rock and along its southwestern margin, a few local conglomerate lenses, probably formed in outwash fans along a fault scarp. No well developed paleosol is present, although feldspar breakdown is common in immediately subjacent quartz monzonite. The contact with Aphebian shale at Pass Lake is similarly sharp and lacking in a well developed paleosol, but five or more metres of pervasive alteration to red and green colour is present in the shale.

The basement rocks below the Athabasca, however, have a well-developed regolith (Ramaekers and Dunn, 1976). The weathering phenomena which produced this paleosol may have been responsible for releasing uranium to the hydrosphere and preservation of this paleosol allowed for eventual leaching, possibly by downward percolating groundwaters, of the uranium. The absence of this type of regolith under the Sibley Sandstone is a negative factor in establishing the uranium potential of the basin. Such a horizon may have been developed, then removed by subsequent shoreface wave action, as the deposition of the Sibley transgressed northwards onto the basement, within the fault-bounded basin.

Structural control on vein deposition

The veins occur either as unconformity onlap "traps" or in major basement fracture zones. The former are controlled by paleogeography, the latter by syn- or post-Sibley faults and fractures. Faults associated with both the main Keweenawan rift and the secondary Sibley basin are extensive and apparently have been active over a long period of time. The Greenwich Lake veins are in a north-trending fault which is part of a system that dominates that portion of the basin. Other such major faults are known along the Black Sturgeon River (at least 250 m of post-Sibley vertical movement), the Nipigon River, and northeasterly trending zones extending from near Kama Hill (Fig. 53.1). Any of these zones are suitable depositional sites. Copper mineralization in the Kabamichigama area (Oja, 1970) northeast of Nipigon (Fig. 53.1), galena-fluorite veins at Cavers Hill (Fig. 53.1) and ameythst north of Nipigon are all indications that the mineralizing process was operative. Critical to the uranium potential is the presence of uranium-rich source rock, such as the apatite-bearing albitic pegmatites in the region of a fracture system.

Summary

The important positive parameters in assessing the uranium potential of the Sibley basin are:

1) the presence of ore-grade uranium mineralization in lead-zinc-barite type veins;

2) the close spatial relationship of these veins to the Sibley Group and the basal unconformity with Archean basement rocks;

3) the evident local source of metal (basement rocks and sandstone matrix);

4) the warm, equitorial depositional environment of the Sibley Group, which promoted effective leaching of metals from the appropriate source material;

5) the relatively effective concentration of metals into suitable structural traps, producing high grade veins;

6) the significant enrichment of uranium in regionally developed pegmatites which form a distinct, laterally extensive zone within the basement to the Sibley Group, and therefore are an important source rock;

7) the extensively developed rift-related fault systems which act as loci for metal deposition.

The important negative factors are:

1) the confined zone within the Quetico belt (relative to the Wollaston belt) within which uraniferous source rocks (pegmatites) occur places narrow regional constraints on high priority areas for prospecting. The volume of uranium available for leaching and redeposition in high grade veins is probably much less than in the Wollaston-Athabasca system. Furthermore, the pegmatites themselves may be too small to develop economic grades and tonnages.

2) the absence of a regolith under the southern part of the Sibley basin may indicate that there was insufficient leaching of source material to provide large high grade veins.

3) the non-fluvial origin of the Sibley is distinctly different from the Athabasca in its depositional history. Although the exact genetic relation of this fluvial environment to the deposition of uranium is not understood, the hydraulic characteristics of subsurface waters may be affected by its presence.

Additional areas of possible uranium mineralization:

1) Any area underlain by uraniferous pegmatite, transected by major Keweenawan rift-related faults, or highly fractured rocks, and at one time overlain by the Sibley Group (Fig. 53.3) is worthy of further examination.

2) The immediate north shore of Lake Superior from Rossport to Nipigon may have been a basin margin to the Keweenawan depositional basin, and is worthy of examination.

[1] Pass Lake, Rossport and Kama Hill are informal terms.

3) The Pass Lake sandstone is well exposed on the islands off Rossport (Giguere, 1975) and has both oxidized (hematitic) and reduced (green-grey) portions. The possibility of disseminated sandstone-type uranium occurrences similar to that noted by Ramaekers and Dunn (1976) should be investigated.

References

Beck, L.S.
1977: History of uranium exploration in Saskatchewan with special reference to changing ideas on metallogenesis; Sask. Geol. Soc. Spec. Pub. no. 3, ed. C.E. Dunn, p. 1-10.

Blackadar, R.G.
1956: Differentiation and assimilation in the Logan Sills, Lake Superior District, Ontario; Am. J. Sci., v. 254, p. 623-645.

Card, K.D., Church, W.R., Franklin, J.M., Frarey, M.J., Robertson, J.A., West, G.F., and Young, C.M.
1972: The Southern Province, Chapt. in Variation in Tectonic styles in Canada (Price and Douglas, eds.); Geol. Assoc. Can., Spec. Pub. no. 11, p. 335-380.

Carter, M.W.
1975: Geology of the Dickison Lake area, Ontario, District of Thunder Bay; Ont. Div. Mines, Geol. Rep. 123, 82 p.

Coates, M.E.
1972: Geology of the Black Sturgeon River area, District of Thunder Bay; Ont. Dep. Mines and Northern Affairs, Geol. Rep. 98, 41 p.

Darnley, A.G., Charbonneau, B.W., and Richardson, K.A.
1977: Distribution of uranium in rocks as a guide to the recognition of uraniferous regions; in "Recognition and evaluation of uraniferous areas"; Int. Atomic Energy Agency, Vienna, 1977.

Faure, G. and Kovach, J.
1969: The age of the Gunflint Iron-formation of the Animikie Series in Ontario, Canada; Geol. Surv. Am. Bull., v. 80, p. 1725-1736.

Franklin, J.M. and Mitchell, R.H.
1977: Lead-zinc-barite veins of the Dorion Area, Thunder Bay District, Ontario; Can. J. Earth Sci., v. 14, no. 9, p. 1962-1978.

Giguere, J.F.
1975: Geology of St. Ignace Island and adjacent islands, District of Thunder Bay; Ont. Div. Mines; Geological rep. 118, 35 p.

Goldich, S.S.
1972: Geochronology in Minnesota; Chapter II in Geology of Minnesota, a Centennial volume; Minn. Geol. Surv., St. Paul, Minn.

Guel, J.J.C.
1970: Geology of Devon and Pardee Townships and the Stuart Location; Ont. Div. Mines, Geol. Rep. no. 87, 52 p.

International Atomic Energy Agency
1977: Recognition and evaluation of uraniferous areas; IAEA, Vienna, 1977.

Kaye, L.
1966: Eayrs Lake-Starnes Lake area; Ont. Dep. Mines, Map 2172.

Kehlenbeck, M.M.
1976: Nature of the Quetico-Wabigoon boundary in the De Courcey-Smiley Lakes area, northwestern Ontario; Can. J. Earth Sci., v. 13, p. 737-748.

Kehlenbeck, M.M. (cont'd.)
1977: The Barnum Lake Pluton, Thunder Bay, Ontario; Can. J. Earth Sci., v. 14, no. 9, p. 2137-2167.

Langford, F.F.
1974: Origin of Australian uranium deposits; a universal process that can be applied to deposits in Saskatchewan; in Fuels, a geological approach; Sask. Geol. Surv., Spec. Pub. no. 2, G.R. Parslow, ed., p. 229-244.

MacDonald, R.D.
1939: Geology of Gorham Township and vicinity; Ont. Dep. Mines, 48th Ann. Rep., v. 48, pt. 3, 18 p.

McIlwaine, W.H. and Tihor, L.A.
1975: Dorion-Wolf Lake area, District of Thunder Bay; Ont. Div. Mines, Prelim. Maps P 994, P 995.

McIlwaine, W.H. and Wallace, H.
1976: Geology of the Black Bay area, Thunder Bay District; Ont. Div. Mines, Geosci. Rep. no. 133.

Mitchell, R.H. and Platt, R.G.
1977: The Port Coldwell Complex Guidebook; Twenty-third annual meeting, Institute on Lake Superior Geology, Lakehead Univ., Thunder Bay, Ontario.

Moorhouse, W.W.
1960: Gunflint Iron Range in the vicinity of Port Arthur; Ont. Dep. Mines, Ann. Rep., v. 69, pt. 7, p. 1-40.

Northern Miner Press
1976: "New Insco Mines to drill unique uranium occurrence"; Northern Miner, Nov. 11, 1976, p. 1, 7.

Oja, R.V.
1970: Keweenawan copper deposits in the Archean of northwestern Ontario; Institute on Lake Superior Geology, 16th Annual Meeting, Thunder Bay, Ontario.

Pye, E.G.
1965: Georgia Lake area; Ont. Dep. Mines, Geol. Rep. no. 31, 113 p.

Ramaekers, P.P. and Dunn, C.E.
1976: Geology and geochemistry of the Eastern margin of the Athabasca basin; in Uranium in Saskatchewan, Sask. Geol. Soc., Spec. Pub. no. 3, C.E. Dunn, ed.

Rogers, J.J.W. and Adams, J.A.S.
1969: Uranium; Chap. 92 in Handbook of Geochemistry, Ed. K.H. Wedepohl, Springer Verlag, New York.

Rogers, J.J.W. and Richardson, K.A.
1964: Thorium and uranium contents of some sandstones; Geochem. Cosmochim. Acta, v. 28, p. 2005.

Ruzicka, V.
1976: Assessment of some Canadian uranium occurrences; in Report of Activities, Part A, Geol. Surv. Can., Paper 76-1A, p. 341-342.

Sage, R.P.
1976: Geology of the Prairie Lake carbonatite; Ont. Div. Mines, Map MP 1070, scale 200 feet = 1 inch.

Swanson, V.E.
1961: Geology and geochemistry of uranium in marine black shales, a review; U.S. Geol. Surv., Prof. Paper 356-C, 67 p.

Watkinson, D.H. and Barnett, R.L.
1971: Petrology and uranium-niobium mineralization of the alkali-rock-carbonatite complex at Prairie Lake, Ontario; abs.; Can. Mineral., v. 10, pt. 5, p. 921.

PORPHYRY OCCURRENCES OF SOUTHERN YUKON

Project 770071

W.D. Sinclair
Regional and Economic Geology Division

Abstract

Sinclair, W.D., Porphyry occurrences of southern Yukon; Current Research, Part A, Geol. Surv. Can., Paper 78-1A, p. 283-286, 1978.

Numerous porphyry copper and molybdenum occurrences have been found in southern Yukon in recent years although none are currently economic. However, the occurrences have many features in common with the economic deposits in British Columbia and the potential for economic deposits in southern Yukon is considered good. The most significant occurrences are discussed briefly.

Introduction

Most of the copper and virtually all of the molybdenum produced in the Canadian Cordillera comes from porphyry deposits in British Columbia. Comparable geological environments exist in southern Yukon and numerous porphyry occurrences have been found in recent years although only one, Casino, has significant reserves which approach an economic grade. A preliminary assessment of these occurrences was begun while the author was with the Regional Geologist's Office of the Department of Indian and Northern Affairs in Whitehorse and is continued as part of a study of copper and molybdenum deposits in Canada by the Geological Survey of Canada. In 1977, a number of occurrences in southern Yukon and northern British Columbia were examined and sampled for petrographic and geochemical studies. This paper summarizes the geology of known occurrences and presents some initial impressions.

The distribution of porphyry occurrences in southern Yukon is shown in Figure 54.1. In the following discussion, occurrences have been grouped according to their geographical distribution. The Tad, Granite Mountain, Cork, Trudy, Alligator, Skukum, and Mung occurrences have not been visited by the author and information on them has been taken from the literature.

Dawson Range

The Casino deposit in the Dawson Range is the most important occurrence in southern Yukon with published reserves of 162 million tonnes grading 0.37 per cent copper and 0.039 per cent molybdenite (Godwin, 1976). It occurs in subvolcanic rocks of the Upper Cretaceous Casino Complex which cuts Mesozoic granitic rocks of the Klotassin Batholith and Yukon Metamorphic Complex schist and gneiss of Paleozoic or older age. Disseminated and fracture-controlled pyrite, chalcopyrite, and molybdenite with traces of bornite and sphalerite occur in a large breccia pipe consisting mainly of tuff and tuff breccia although cobble breccia containing some boulder-sized fragments occurs in places along the margin of the breccia pipe. Large cavities are a conspicuous feature in the breccia and permeability was a significant factor in localizing mineralizing solutions. Hypogene mineralization is best developed within a central zone of potassic alteration characterized by hydrothermal biotite and potassium feldspar. Magnetite and tourmaline are also present. Quartz-sericite-pyrite alteration, which also contains tourmaline, surrounds the potassic zone. Supergene enrichment is an important feature of the Casino deposit. Godwin (1976) estimated that the grade of copper in the supergene-enriched zone has been increased by a factor of approximately 1.7. The age of the Casino mineralization has been dated at 69.5 ± 2.2 m.y. based on potassium-argon dating of hydrothermal biotite and is coeval with the formation of the Casino Complex , dated at 71.2 ± 2.6 m.y. by potassium-argon methods (Godwin, 1975).

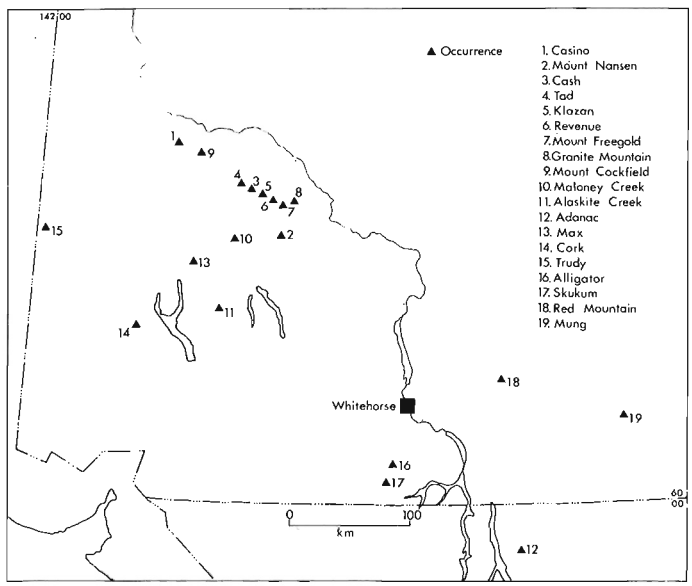

Figure 54.1 Location map.

The Mount Nansen deposit is approximately 50 km west of Carmacks in the southern part of the Dawson Range. This deposit is related to a Tertiary subvolcanic complex of porphyry dykes, plugs, and small breccia pipes which intrudes Mesozoic plutonic rocks. Pyrite and chalcopyrite occur along fractures and are disseminated in zones of sericitized porphyry surrounding tourmalinized, but unmineralized, breccia pipes. Molybdenite is generally associated with quartz veins. A zone of supergene enrichment is present but is erratic. Exploration by Cyprus Anvil Mining Corporation from 1971 to 1973 indicated variable, but generally low, grades averaging approximately 0.10 to 0.15 per cent copper and less than 0.01 per cent molybdenum (Sawyer and Dickinson, 1976). Finely disseminated molybdenite and minor amounts of chalcopyrite and pyrrhotite also occur locally in Mount Nansen Group volcanic rocks intruded by a small porphyry plug 3 km west of the main deposit. The porphyry complex is considered to be coeval with overlying Mount Nansen Group volcanic rocks for which a potassium-argon whole rock age of 58.4 ± 3.0 m.y. has been determined (Tempelman-Kluit and Wanless, 1975).

The Cash deposit is one of a number of occurrences situated along the valley of Big Creek, a distinct northwest-trending lineament in the northeast part of the Dawson Range. Other occurrences along this lineament include the Tad, Klazan and Revenue. At the Cash deposit, two small feldspar porphyry stocks of Tertiary age intrude schist and gneiss of the Yukon Metamorphic Complex and monzonite of Mesozoic age. Pyrite, chalcopyrite, and molybdenite occur

along fractures, in quartz veins and are disseminated in both the feldspar porphyry and the intruded metamorphic rocks. Potassic alteration consisting of hydrothermal potassium feldspar, biotite and/or magnetite occurs locally along fractures and is associated with higher grades of mineralization. Quartz-sericite alteration, also typically fracture-controlled, is more common. Diamond drilling by Western Mines Ltd. in 1975 and Archer, Cathro and Associates Ltd. in 1977 has indicated low grade mineralization averaging approximately 0.2 per cent combined copper and molybdenum over an area 2500 by 800 m. Although oxidation is present to 50 m below bedrock surface, supergene enrichment is negligible. The feldspar porphyry stocks are thought to be coeval with Eocene Mount Nansen Group volcanic rocks which outcrop to the west.

The Tad occurrence, 20 km northwest of the Cash deposit, was explored by International Mine Services Ltd. in 1969 and 1970. According to Craig and Milner (1975) two mineralized zones were found. One consists of traces of molybdenite in quartz veins cutting propylitically altered quartz monzonite and the second consists of disseminated galena and sphalerite in brecciated and argillically altered quartz monzonite porphyry.

The Klazan occurrence is 8 km southeast of the Cash deposit. Drilling by Atlas Explorations Ltd. in 1970 in the area of a distinct gossan zone intersected a quartz vein stockwork with associated quartz-sericite alteration in fine grained feldspar porphyry of Tertiary age. Pyrite and traces of chalcopyrite, molybdenite, sphalerite, and galena occur disseminated in the feldspar porphyry. Traces of molybdenite can be seen in the quartz vein stockwork. Two significant sections were encountered by the drilling, one 14 m averaging 0.17 per cent copper and the other 3 m averaging 0.16 per cent copper and 0.408 per cent molybdenum (Pilcher and McDougall, 1976).

At the Revenue property, 13 km southeast of the Klazan occurrence, Tertiary (Eocene?) feldspar porphyry and related zones of breccia intrude schist and gneiss of the Yukon Metamorphic Complex and monzonite of Mesozoic age. Chalcopyrite is sparsely disseminated in sericitized feldspar porphyry and breccia and traces of molybdenite occur in quartz veins. Drilling by Kaiser Resources Ltd. in 1970 located very low grade mineralization (0.02 to 0.05 per cent copper) with slightly higher grades centred near the western margin of a large breccia zone in the feldspar porphyry (Craig and Laporte, 1972). Supergene enrichment has been negligible.

On the southeast side of Mount Freegold, a Tertiary complex of quartz-feldspar porphyry, rhyolite porphyry, and rhyolite breccia intrudes Mesozoic granodiorite and hornblende syenite. Pyrite and arsenopyrite with traces of chalcopyrite occur along fractures and are disseminated in highly sericitized rhyolite breccia and associated wall rocks. Drilling by Rayrock Mines Ltd. in 1975 encountered minor gold and silver values (Sinclair et al., 1976).

At Granite Mountain, chalcopyrite, minor pyrite, and pyrrhotite and sparse molybdenite occur disseminated and along hairline fractures in weakly altered monzonite (Findlay, 1969). The mineralization is widespread, occurring over an area 330 by 330 m, but is relatively low grade, averaging approximately 0.1 per cent combined copper and molybdenum (Pilcher and McDougall, 1976).

At Mount Cockfield, a quartz-feldspar porphyry stock of probable Tertiary age is weakly altered and cut by quartz veinlets which carry sparse chalcopyrite and molybdenite (Craig and Laporte, 1972). Drilling by United Keno Hill Mines Ltd. in 1970 indicated very low grade mineralization averaging 0.03 per cent copper and 0.013 per cent molybdenum over more than 2 km^2 (Pilcher and McDougall, 1976).

The Maloney Creek property is situated in the southernmost part of the Dawson Range. Pyrite, chalcopyrite, and molybdenite are present along fractures, in quartz veins and disseminated in schist and gneiss of the Yukon Metamorphic Complex and in porphyritic intrusive rocks of Tertiary (Eocene?) age. Sericite alteration accompanies the mineralization. Minor potassic alteration occurs locally and consists mainly of potassium feldspar envelopes along quartz veins and magnetite in narrow veinlets. Western Mines Ltd. drilled the property in 1976 and found the mineralization to be very low grade, averaging less than 0.1 per cent combined copper and molybdenum (Morin et al., 1977). Supergene enrichment appears to have been negligible.

Ruby and Nisling Ranges

The Alaskite Creek occurrence is in the Ruby Range, 23 km east of Kluane Lake. The property is underlain mainly by Nisling Range alaskite which has been dated at 50 to 60 m.y. (Tempelman-Kluit and Wanless, 1975). The principal rock type is a medium to coarse grained leucogranite which is intruded by porphyritic phases of similar composition. Molybdenite occurs locally as coarse rosettes in thick (up to 2 cm) quartz veins and, to a lesser extent, on "dry" fractures cutting the leucogranite. This style of mineralization is similar to that found at the Adanac deposit near Atlin, British Columbia and the host rocks are identical. It is noteworthy that this type of mineralization – coarse molybdenite rosettes in quartz veins – was considered economically insignificant prior to the discovery of Adanac.

On the Max property in the Nisling Range, Nisling Range alaskite intrudes quartz monzonite of mid-Cretaceous age and Yukon Metamorphic Complex rocks. Mineralization consists of chalcopyrite and molybdenite in quartz veins and disseminated in quartz monzonite; chalcopyrite with pyrite and pyrrhotite in breccia zones in quartzite; and, locally, molybdenite rosettes in quartz veins in quartzite. Drilling by Imperial Oil Enterprises Ltd. in 1971 encountered sparse mineralization in the quartz monzonite (Craig and Milner, 1975; Pilcher and McDougall, 1976).

Saint Elias Mountains

The Cork occurrence, situated 20 km west of Burwash Creek in the Kluane Ranges southwest of the Shakwak Fault, has been described by Craig and Laporte (1972). It is centred on a stock or dyke of quartz latite porphyry which intrudes Permian sediments and Ordovician or younger volcanics. Pyrite and chalcopyrite occur disseminated and along fractures in weakly altered porphyry and in the adjacent skarn and hornfelsic sedimentary and volcanic rocks; molybdenite is present along fractures in the porphyry. The mineralization grades 0.23 per cent copper and 0.0054 per cent molybdenum over 66 by 100 m (Pilcher and McDougall, 1976). Alteration minerals in the porphyry are sericite, kaolinite and some hydrothermal biotite. The age of the Cork porphyry and related mineralization has been dated at 26 ± 0.3 m.y. (Christopher et al., 1972). The belt of Tertiary volcanic and intrusive rocks which contains the Cork occurrence extends through the St. Elias Mountains into adjacent Alaska (Muller, 1967) and other occurrences may be present along it.

The Trudy occurrence south of Beaver Creek consists of pyrite, chalcopyrite, and traces of molybdenite along fractures in a weakly altered stock ranging in composition from quartz monzonite to quartz diorite (Pilcher and McDougall, 1976). The age of the stock is probably Cretaceous; quartz monzonite hosting porphyry mineralization at Carl Creek and Horsfeld in nearby Alaska has been dated at 111 m.y. (Hollister et al., 1975).

Whitehorse Area

The Alligator occurrence, 45 km south of Whitehorse, consists of sparse pyrite, chalcopyrite, and molybdenite in quartz veins associated with fault and fracture zones in granodiorite of probable Cretaceous age (Craig and Milner, 1975; Pilcher and McDougall, 1976). The Skukum occurrence, 60 km south of Whitehorse, consists of pyrite and chalcopyrite disseminated in a weakly altered breccia at the contact between Cretaceous granodiorite and Skukum Group volcanic rocks of Tertiary age (Findlay, 1969; Pilcher and McDougall, 1976). Minor amounts of fracture-controlled copper and molybdenum sulphides occur along the Whitehorse Copper Belt west of Whitehorse, but these appear to be related to the skarn deposits of the Whitehorse Copper Belt and are not considered porphyry occurrences.

Big Salmon Range

The Red Mountain occurrence is 80 km east of Whitehorse in the Big Salmon Range of the Pelly Mountains. Pyrite, molybdenite and traces of chalcopyrite occur in a quartz vein stockwork cutting strongly sericitized quartz feldspar porphyry considered by Mulligan (1963) to be Tertiary in age. The occurrence is marked by a spectacular gossan 300 by 200 m developed over altered porphyry containing up to 5 per cent pyrite but only low grade molybdenum mineralization (less than 0.05 per cent molybdenite) was observed in diamond drill core from the property. The quartz feldspar porphyry appears to have a limited distribution and there are no other porphyry prospects in the area.

Nisutlin Plateau

The Mung occurrence is 180 km east of Whitehorse in the Nisutlin Plateau. It consists of chalcopyrite, molybdenite and pyrite in quartz veins and fractures in an intrusive breccia which has been partially altered to chlorite, epidote and undetermined clay minerals (Craig and Milner, 1975; Pilcher and McDougall, 1976). The breccia is part of a small stock or dyke of granodiorite probably related to granitic rocks of the Cassiar Batholith to the southeast mapped as Jurassic and/or Cretaceous by Poole et al. (1960).

Summary

Porphyry prospects occur throughout southern Yukon but are concentrated primarily within a northwest-trending belt in the Dawson Range. Other belts may be present in the Ruby and Nisling Ranges or in the Saint Elias Mountains, but there are too few occurrences known in these areas to define any such belts. Within the Dawson Range, the majority of occurrences are associated with small, epizonal intrusions considered to be subvolcanic feeders for the Mount Nansen Group or Casino volcanic rocks (Tempelman-Kluit, 1974). Mineralization is usually present in the altered intrusive rocks but may also be present in the intruded country rocks, either older, unrelated intrusive or metamorphic rocks, or coeval volcanic rocks. Quartz-sericite alteration is common to many of the occurrences, but potassic alteration appears to occur only in the higher grade deposits. The age of the Dawson Range deposits is probably Eocene although only Mount Nansen (Eocene) and Casino (latest Cretaceous) have been dated radiometrically. Other porphyry occurrences in the southern Yukon range in age from late Oligocene (Cork) to as old as Jurassic (Mung).

Although exploration to date has resulted in the discovery of only one deposit of near-economic proportions (Casino), porphyry occurrences in southern Yukon have many features in common with economic porphyry deposits in British Columbia. However, many of the known occurrences are poorly documented and cannot be properly assessed at the present time. The relatively recent discovery of the Cash deposit suggests that the full potential for porphyry copper and molybdenum deposits in southern Yukon has not yet been realized and that much exploration remains to be done.

References

Christopher, P.A., White, W.H., and Harakal, J.E.

1972: K-Ar dating of the 'Cork' (Burwash Creek) Cu-Mo prospect, Burwash Landing area, Yukon Territory; Can. J. Earth Sci., v. 9, p. 918-921.

Craig, D.B. and Laporte, P.

1972: Mineral Industry Report, 1969 and 1970, Yukon Territory and Southwestern Sector, District of Mackenzie; Dep. Indian and Northern Affairs.

Craig, D.B. and Milner, M.

1975: Mineral Industry Report, 1971 and 1972, Yukon Territory; Dep. Indian and Northern Affairs, EGS 1975-6.

Findlay, D.C.

1969: The mineral industry of Yukon Territory and southwestern District of Mackenzie, 1967; Geol. Surv. Can., Paper 68-68.

Godwin, C.I.

1975: Alternative interpretations for the Casino Complex and Klotassin Batholith in the Yukon Crystalline Terrane; Can. J. Earth Sci., v. 12, p. 1910-1916.

1976: Casino; **in** Porphyry Deposits of the Canadian Cordillera; Can. Inst. Min. Metal., Spec. Vol. 15, p. 344-354.

Hollister, V.F., Anzalone, S.A., and Richter, D.H.

1975: Porphyry copper deposits of southern Alaska and contiguous Yukon Territory; Can. Inst. Min. Metal., Bull., v. 68, p. 104-112.

Morin, J.A., Sinclair, W.D., Craig, D.B., and Marchand, M.

1977: Mineral Industry Report, 1976, Yukon Territory; Dep. Indian and Northern Affairs, EGS 1977-1.

Muller, J.E.

1967: Kluane Lake map-area, Yukon Territory; Geol. Surv. Can., Mem. 340, 137 p.

Mulligan, R.

1963: Geology of Teslin map-area, Yukon Territory; Geol. Surv. Can., Mem. 326, 96 p.

Pilcher, S.H. and McDougall, J.J.

1976: Characteristics of some Canadian Cordilleran porphyry prospects; **in** Porphyry Deposits of the Canadian Cordillera, Can. Inst. Min. Metal., Spec. Vol. 15, p. 79-84.

Poole, W.H., Roddick, J.A., and Green, L.H.

1960: Wolf Lake, Yukon Territory; Geol. Surv. Can., Map 10-1960.

Sawyer, J.P.B. and Dickinson, R.A.

1976: Mount Nansen; in Porphyry Deposits of the Canadian Cordillera; Can. Inst. Min. Metal., Spec. Vol. 15, p. 336-343.

Sinclair, W.D., Morin, J.A., Craig, D.B., and Marchand, M.

1976: Mineral Industry Report, 1975, Yukon Territory; Dep. Indian and Northern Affairs, EGS 1976-15.

Tempelman-Kluit, D.J.

1974: Reconnaissance geology of Aishihik Lake, Snag and part of Stewart River map-areas, west-central Yukon; Geol. Surv. Can., Paper 73-41, 97 p.

Tempelman-Kluit, D.J. and Wanless, R.K.

1975: Potassium-argon age determinations of metamorphic and plutonic rocks in the Yukon Crystalline Terrane; Can. J. Earth Sci., v. 12, p. 1895-1909.

55.

REGIONAL METALLOGENY OF THE NORTHERN CORDILLERA: TUNGSTEN AND BASE METAL-BEARING SKARNS IN SOUTHEASTERN YUKON AND SOUTHWESTERN MACKENZIE

Project 740098

K.M. Dawson and L.A. Dick[1]
Regional and Economic Geology Division, Vancouver

Abstract

Dawson, K.M. and Dick, L.A., Regional Metallogeny of the Northern Cordillera: Tungsten and base metal-bearing skarns in southeastern Yukon and southwestern Mackenzie; Current Research, Part A, Geol. Surv. Can., Paper 78-1A, p. 287-292, 1978.

In 1977, 25 tungsten and base metal-bearing skarns were examined in the first phase of a regional study. A four-fold classificaion is proposed, based mainly on ore element assemblages: I-W, Cu (Zn, Mo); II-W, Mo (Zn, Pb, Cu); III-Zn, Pb (W, Cu, Ag); and IV-Zn, Pb, Ag (Cu, Bi, Sn). The skarn groups show common silicate mineral assemblages, morphology, and regional distribution in relation to host and intrusive rocks.

Introduction

Twenty-five tungsten and base metal-bearing skarns were examined in 1977 as the first phase of a Ph.D. thesis study by the junior author, and as one aspect of a continuing study of the regional metallogeny of the northern Cordillera by the senior author. Skarn deposits and occurrences in southeastern Yukon and southwestern Mackenzie were selected for study primarily on the basis of their economic and geological significance, although access to the properties and availability of drill core and other data were also important considerations. Additional skarn deposits from elsewhere in the northern Cordillera will be studied in 1978, and, in company with related laboratory studies in progress, this will allow a more rigorous treatment of petrography, mineralogy, and genesis than is presented in this report.

Regional Setting

Skarn deposits were examined in the following areas: Macmillan Pass, South Nahanni-Flat River, Tillei Lake, Hyland River, Frances River, and Rancheria. Deposit locations are plotted on the accompanying map (Fig. 55.1), the base geology for which was excerpted from the preliminary Tectonostratigraphic Map of the Canadian Cordillera (Geological Survey of Canada, in preparation).

Most deposits studied are located within the Selwyn Fold Belt in southern Yukon and Mackenzie, but the deposits near Rancheria occur in the northern Omineca Crystalline Belt. Skarns in the former area are hosted by upper Proterozoic to Devono-Mississippian miogeoclinal sedimentary rocks – mainly interbedded shale and carbonate. These rocks may have been essentially contiguous with similar rocks in the latter area peripheral to the Cassiar batholith prior to large-scale dextral movements on several transcurrent faults in Cassiar and Omineca mountains (Gabrielse and Dodds, 1977; Gabrielse, pers. comm., 1977).

Plutons and associated skarn deposits in Selwyn Fold Belt lie to the west of a major tectonic hinge line defined by the westerly shaling out of Lower Paleozoic carbonate rocks (Gabrielse and Reesor, 1974, p. 130). As a group the plutons are: all Early to mid-Cretaceous age; notably discordant to regional structural trends, with steeply dipping contacts; predominantly quartz monzonites with biotite more abundant than hornblende; and emplaced into relatively unmetamorphosed rocks that show well-developed contact metamorphic aureoles.

Spatial relationships between pluton and skarn vary from proximal to distal. Skarns may occur as: xenoliths and screens within plutonic border phases; semi-concordant bodies developed in calcareous rocks immediately adjacent to the plutonic contact; essentially conformable units many tens to hundreds of metres away from the contact; and, discordant, fracture-controlled vein and replacement bodies that may be many kilometres removed from exposures of granitic rock. In granitized and migmatitic terrane skarns may develop in calcareous beds adjacent to conformable granitic bodies, without apparent spatial or temporal relationship to discordant plutonic or hypabyssal rocks.

In studying these skarn deposits in the field, we noted and compared their variable individual characteristics with the objective of defining inherent trends of possible regional metallogenic significance. An initial comparison of ore element assemblages only, readily showed that all but two deposits could be classified into four coherent groups, as illustrated in Table 55.1. Further comparisons on the basis of host rock age and lithology, degree of regional metamorphism, and hydrothermal alteration of associated plutons reinforced the initial groupings. As shown in Figure 55.1, 19 of the 22 deposits fall within definite zones related to the above classification and also to the regional geology. A degree of host rock and/or plutonic control on skarn mineralogy is evident in the regional distribution of these groups of deposits.

Group I – W, Cu (Zn, Mo) skarns

A. General characteristics

The group of deposits in which scheelite and chalcopyrite are the main ore minerals includes most of the economically significant deposits studied in 1977. These skarns are associated with an arcuate belt of small discordant plutons and are hosted by mainly Lower Cambrian and younger outer shelf carbonate-shale sequences. The Lower and mid-Cretaceous plutons are characteristically quartz monzonites, but granodiorite forms part of many of the larger bodies (Gabrielse and Reesor, 1974, Fig. 9). Plutons may be locally megacrystic, but extensive areas of even-textured medium grained rocks are common. Group I skarns tend to develop preferentially in the first thick and relatively pure limestone beds above the Proterozoic clastics. Host rocks are not regionally metamorphosed, but extensive thermal aureoles of pyritic and biotitic hornfels are developed in pelitic rocks peripheral to most stocks. The common morphology of a W, Cu skarn is a more or less concordant body localized some tens to hundreds of metres above a shallowly dipping intrusive contact. Dykes and intrusive aphophyses rarely cut up through the skarn/metasediment sequence.

[1] Queen's University, Kingston, Ontario

B. Ore mineralogy

With the exception of one ferberite occurrence at Mactung, scheelite is the only tungsten mineral present in Group I skarns. Scheelite commonly occurs as anhedral to subhedral grains with blue-white fluorescence, unevenly disseminated in dark green calc-silicate skarn. Skarn, hornfels, and intrusive rocks may be cut by scheelite-bearing veinlets of quartz, quartz-tourmaline, and quartz-calc-silicates. Fine grained disseminations of scheelite in biotite hornfels occur locally at Mactung.

Chalcopyrite occurs with scheelite in all deposits, in a less abundant and more erratic distribution. W:Cu ratios at Mactung and Cantung range from 6:1 to 7:1. In general, the Group I skarns contain greater amounts of copper than the other three groups.

Brown sphalerite is associated with some scheelite at Cantung and Clea, and in the former occurrence locally attains significant grade. Minor occurrences of sphalerite at Mactung are peripheral to tungsten-bearing skarn.

Small quartz-molybdenite veinlets at Mactung, Cantung, and Lened either cut skarn and pelitic hornfels or occupy greisened zones in adjacent intrusive rocks.

Pyrrhotite is abundant in all W, Cu skarns, and tends to increase with increasing tungsten content at Mactung and Cantung. Pyrite is subordinate to pyrrhotite in these two deposits, and at Mactung is localized in and near faults that cut pyrrhotite-bearing skarn (Dick, 1976).

C. Silicate mineralogy

Pyroxene (diopside-hedenbergite) and garnet are the main calc-silicate minerals accompanying scheelite-chalcopyrite. Actinolite, biotite, quartz, chlorite, epidote, vesuvianite, and wollastonite are subordinate but locally extensive. In addition anorthite, apatite, clinozoisite, and sphene are reported from Mactung skarn by Dick (1976), and from Cantung by Zaw (1976).

Biotite-actinolite skarns, which occur only with the Group I deposits, are well developed in the "E"-zone orebody at Cantung and less abundant at Mactung and Clea. Wollastonite occurs in the 'chert ore' at Cantung and locally at Mactung and Bailey, but not in association with sulphides, and only rarely with scheelite. Garnet-rich portions of skarns occur in association with calcite and vesuvianite. Garnet-rich skarns tend to be deficient in pyrrhotite, and vice-versa.

D. Mineral deposits

At Mactung, limestone-shale breccias of probable Cambrian age form a skarn zone that hosts the Lower Ore Zone and the lowest of three horizons of the Upper Ore Zone (Harris, 1977). Pelitic clasts have been altered to very fine grained calc-silicate hornfels devoid of W mineralization. Most scheelite occurs in hedenbergitic pyroxene-almandine-rich garnet skarns that may have undergone local retrograde alteration to actinolite-biotite and clinozoisite-plagioclase (Dick, 1976). Scheelite also occurs in quartz veinlets in hornfels and intrusive rocks and rarely as finely disseminated grains in biotite hornfels.

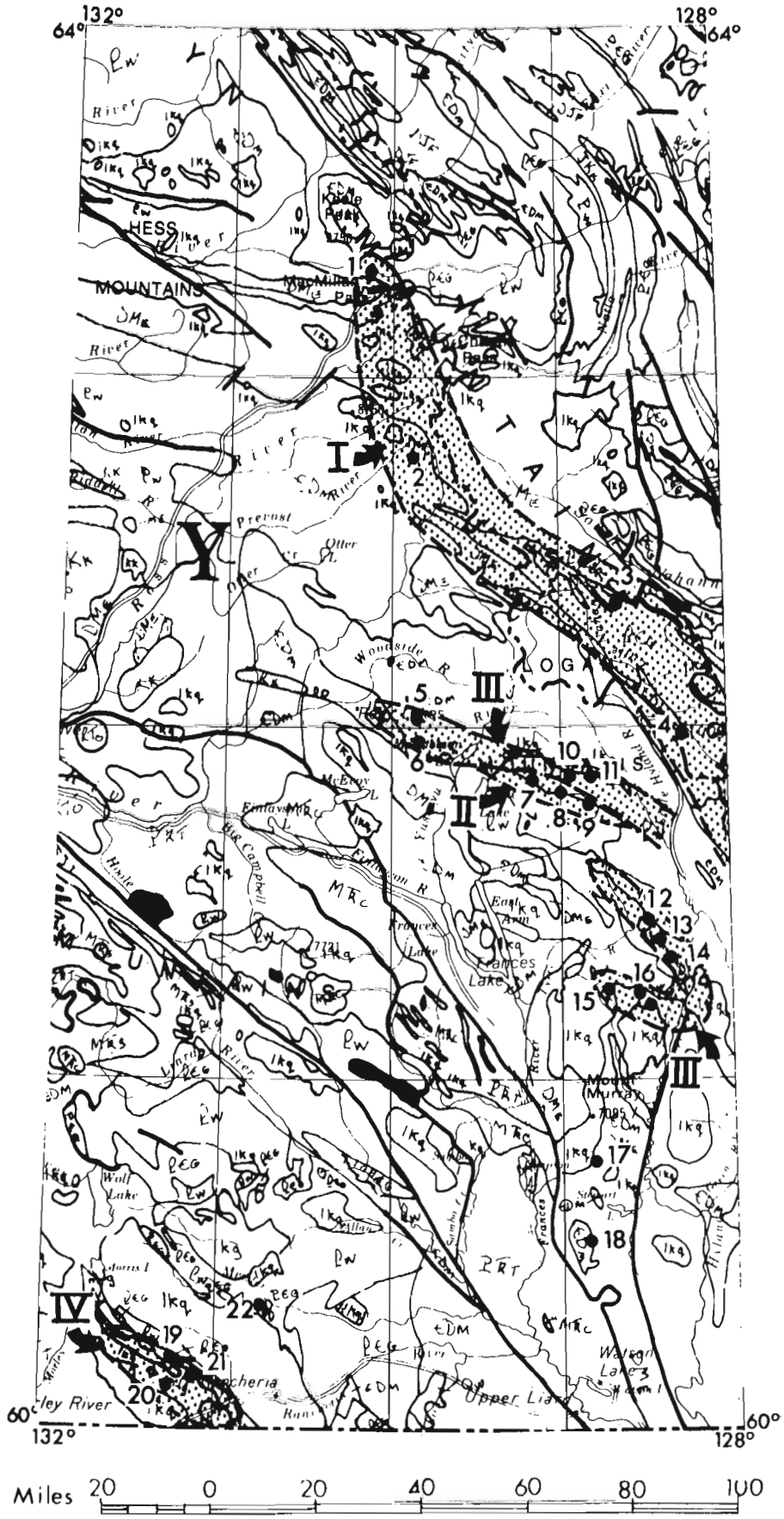

LEGEND

SEDIMENTARY AND VOLCANIC ROCKS

	ASSEMBLAGE	OMINECA CRYSTALLINE BELT & YUKON CRYSTALLINE TERRANE	NORTHERN AND EASTERN FOLD BELT
KJ, KK	Jackass Mountain, Kingsvale		South Fork
TR JT	Takla	Lewes River	
PTRT	Thompson	Englishman's, Kalzas, Klondike Schist	
MTRC	Cache Creek	Teslin, Kedahda, Horse Feed	
MTRS	Slide Mountain	Sylvester, Anvil Range	Anvil Range
DJF	Front Ranges		Besa River, Canol, Imperial
DME	Earn		Crystal Peak, Earn
CDM	Main Ranges	Kechika	Delorme, Nahanni, Headless, Landry, Funeral, Arnica, Grizzly Bear, Natla, Whittaker, Broken Skull, Rabbitkettle, Road River, Sombre, Camsell, Kechika, Harvey
PCG	Gog	Atan, Harvey	Backbone Ranges, Sekwi
PCW	Windermere		Rapitan, Keele, Sheepbed

PLUTONIC ROCKS

lKq	quartz monzonite	Glenlyon Batholith, Cassiar Batholith, Quiet Lake Batholith	O'Grady Stock, Anvil Batholith, Mount Billings Batholith
lKg	granodiorite		
mJg	granodiorite	Marker Lake Batholith	

SKARN DEPOSITS AND OCCURRENCES

No.	NAME(S)	METALS	COORD'S
1	MACTUNG	W, Cu (Zn, Mo)	63°17 130°09
2	CLEA (OMO)	W, Cu (Zn)	62°46 129°52
3	LENED (NIP)	W, Cu (Mo)	62°22 128°38
4	CANTUNG	W, Cu (Zn)	61°57 128°15
5	NAR	Zn, Pb, Cu, Ag (W)	62°01 129°53
6	NARCHILLA (Ptarmigan Creek)	Zn, Pb, (W, Cu)	61°57 129°52
7	WOAH	W (Mo, Zn)	61°51 129°11
8	TAI	W (Zn, Cu, Mo)	61°49 129°00
9	TANYA	W (Cu, Zn, Pb, Ag)	61°48 128°54
10	ZEUS (LOG)	Zn, Pb (W, Cu)	61°52 128°58
11	CHAP	Zn, Pb (W, Cu)	61°52 128°53
12	RON	Zn, Pb (Cu, Ag)	61°27 128°30
13	FIRTREE	Zn, Pb (W, Ag)	61°25 128°27
14	BLACKJACK	Zn, Pb (W, Ag)	61°22 128°23
15	MAX (BM)	W + Zn Pb Ag Cu	61°16 128°41
16	GLENNA-MIKO	Zn, Pb (W, Cu)	61°16, 128°35 (61°15 128°30)
17	BAILEY	W, Cu	60°46 128°51
18	HUNDERE (RITCO)	Pb, Zn (Ag)	60°31 128°53
19	ATOM	Zn, Pb (Cu, Ag, Bi)	60°11 131°13
20	BOM-MUNSON	Zn, Pb, Ag (Sn, Cu, W, Mo)	60°09 131°12 (60°09 131°15)
21	BAR (DAN)	Zn, Pb, Ag (Cu, Sn)	60°10 131°08
22	MID-NITE	W, Mo (Zn, Pb, Ag)	60°20 130°42 (60°20 130°41)

Figure 55.1

Location map of tungsten and base metal-bearing skarns examined in 1977. Geologic base from preliminary Tectonostratigraphic Map of the Canadian Cordillera (Geol. Surv. Can., in preparation).

At Cantung, mineralized skarn has formed in the massive, relatively pure Lower Cambrian 'Ore limestone', and in the underlying 'Swiss Cheese Limestone' (Blusson, 1968, p. 28). In the latter unit, 'chert ore' occurs in lenses and pods of skarn within siliceous hornfels. Scheelite-quartz veinlets that cut intrusive rock commonly are greisen-bordered. The open pit orebody, on the upper limb of an overturned anticline (Cummings and Bruce, 1977, Fig. 2) is mainly a garnet-pyroxene skarn with disseminated pyrrhotite-scheelite-chalcopyrite and many quartz-biotite veins. The 'E'-zone orebody, on the lower limb (Cummings and Bruce, 1977), is a garnet-pyroxene-massive pyrrhotite skarn that gives way locally to biotite-amphibole (actinolite/tremolite) skarn. Quartz veining in the 'E' zone is rare, pyrite is found only in fault zones, and sphalerite is locally abundant.

At the Bailey prospect of Canada Tungsten, two types of skarn are developed adjacent to a contact between Cretaceous granodiorite and Devono-Mississippian crystalline limestone (Unit 7, Gabrielse, 1967): a pyroxene-pyrrhotite-scheelite-chalcopyrite skarn close to the contact, and a garnet-pyroxene-scheelite-minor magnetite skarn several metres to tens of metres higher in the section. An underlying quartz-biotite schist unit contains abundant disseminated pyrrhotite. Both limestone and granodiorite are altered along their mutual contact.

The Lened prospect of Union Carbide is a conformable, mainly garnet-pyroxene-pyrrhotite skarn developed in Cambro-Ordovician 'Wavy banded' limestone at its contact with underlying Upper Proterozoic(?) phyllite (Blusson et al., 1968). The W, Cu-bearing skarn occurs in isoclinally folded beds adjacent to and shallowly underlain by a megacrystic quartz monzonite that is greisened locally and contains minor amounts of molybdenite. Higher in the section, silty limestone beds within graptolitic Road River shales are altered to garnet-pyroxene skarn adjacent to granitic apophyses.

Group II – W, Mo (Zn, Pb, Cu) skarns

A. General characteristics

This group of deposits in which scheelite predominates over molybdenite is typified by two contiguous prospects, the Woah and Tai, discovered in 1977 near Tillei Lake by Welcome North Mines Ltd. Including an older occurrence, the Tanya, these three skarns occupy a linear belt of screens and xenoliths that extends for 60 km along the northeastern margin of the Mount Billings Batholith. A fourth Group II skarn, the Mid-Nite occurrences owned by Rayrock Mines Limited, is neither a xenolith nor located in the Tillei Lake zone, but occurs at the northeastern contact of the Cassiar Batholith. It is however included in the group by virtue of similar mineralogy and host rocks.

The intrusive rock in the vicinity of the Tillei Lake skarns is mainly hornblende granodiorite, however major quartz monzonitic and minor quartz dioritic phases were noted. Adjacent to the contact, granodiorite is foliated, sheared, chloritized and contains abundant small mafic xenoliths. Intrusive contacts vary from sharp at Woah to more diffuse at Tai and Tanya, where a complex zone of lit-par-lit migmatites, sills and conformable granitic boudins borders the pluton. The quartz monzonite contact at Mid-Nite is sharp, but the border phase contains abundant angular xenoliths of hornfels.

The original composition of the mineralized screens in the Tillei Lake belt probably was limestone, several beds of which serve as markers in the folded, dominantly gritty phyllites of the Upper Proterozoic 'Grit Unit' in the area (Blusson, 1966). Regional

Table 55.1

A comparison of some characteristics of 22 skarn deposits

Group	Ore Element Assemblage	Host rock age, lithology	Regional Metamorphism	Alteration of pluton	Examples
I	W, Cu (Zn, Mo)	$\in$ to D carbonates, interbedded shale	Relatively unmetamorphosed terrane	Border phases argillized; locally greisened, tourmalinized	Mactung (1), Clea (2), Lened (3), Cantung (4), Bailey (17)
II	W, Mo (Zn, Pb, Cu)	Late P limestone xenoliths, screens	Relatively Metamorphosed terrane	Plutons Relatively Unaltered	Woah (7), Tai (8), Tanya (9), Mid-Nite (22)
III	Zn, Pb (W, Cu, Ag)	Late P limestone beds in quartz-biotite schist			Nar (5), Narchilla (6) Zeus (10), Chap (11), Ron (12), FirTree (13), Blackjack (14), Max (15) Glenna-Miko (16)
IV	Zn, Pb, Ag (Cu, Bi, Sn)	DM carbonates, interbedded shale			Atom (19), Bom-Munson (20), Bar (21)

metamorphic grade and intensity of migmatization in this schist-gneiss belt decrease northeastward away from the batholithic contact. Some marble and limy schist beds in contact with the Mount Billings Batholith developed no skarn, whereas others in contact with and up to several tens of metres above the contact host small base metal skarns notably devoid of tungsten (Fig. 55.2). A lithologically similar and probably equivalent sequence of Upper Proterozoic to Lower Cambrian quartz-biotite schist and interbedded marble hosts tungsten skarns at Mid-Nite (Poole et al., 1960).

Anomalous radioactivity of three to five times background was noted in two exposures of rusty-weathering grey andalusite schist separated by 37 km, on the Woah and Narchilla claims, within similar 'Grit Unit' sequences of grey micaceous phyllite, quartzite and marble.

B. Ore and silicate mineralogy

Skarns formed in screens and xenoliths in Tillei Lake belt are mainly coarse grained, brown-weathering, foliated assemblages of garnet-quartz-pyroxene-scheelite. Actinolite, epidote, wollastonite, and vesuvianite occur locally. Skarns are generally low in sulphides, although several occurrences of pyroxene-pyrrhotite-pyrite-chalcopyrite-sphalerite were noted. Skarn bodies may be cut by veins of coarse grained quartz-garnet-scheelite-molybdenite and/or quartz-magnetite-actinolite-chalcopyrite. At Woah, a southeasterly striking set of the latter assemblage shows anomalous radioactivity. Pronounced foliation in skarn may represent either relict textures that were developed in the host prior to engulfment by the intrusion, or syn- to postmineralization shearing and recrystallization in the border phase.

Small, essentially concordant skarns relatively rich in sulphides and base metals and deficient in tungsten are developed in folded calcareous interbeds in quartz-biotite schist adjacent to the batholithic contact. As shown in Figure 55.2, base metal skarn morphology includes concordant bodies adjacent to conformable granitic boudins and sills, semi-concordant skarns at or near plutonic contacts, and discordant skarns adjacent to dykes. Occurrences may contain varying proportions of pyrrhotite, sphalerite, galena, magnetite, and chalcopyrite in relatively fine grained pyroxene-garnet-amphibole-epidote skarn.

Skarns on Nite claims are a sulphide-deficient assemblage of garnet-pyroxene-quartz-wollastonite that are interbedded with quartz-biotite schist. Minor amounts of molybdenite accompany scheelite, which may fluoresce either blue-white or yellow. With the exception of late-stage sphalerite-pyrite-opaline silica veins, quartz veining is negligible. Minor scheelite was noted in local wollastonite-rich skarn although most tungsten occurs with pyroxene and quartz interstitial to coarse grained garnet. Similar garnet-pyroxene skarns on the nearby Mid claims contain disseminated scheelite and sphalerite.

Group III – Zn, Pb (W, Cu, Ag) skarns

A. General characteristics

Group III-Zn, Pb skarns are developed in calcareous beds within a belt of relatively high grade metamorphic and migmatitic rocks bordering the northern and eastern flanks of the Mount Billings Batholith. Nine occurrences examined in 1977 are included in this group, and numerous others are known in southeastern Yukon. The deposits are typically concordant bodies, a few metres thick and up to hundreds of metres long that are developed in relatively thin marble and calcareous schist beds of the Upper Proterozoic 'Grit Unit'. Like the concordant Zn, Pb(Cu) skarns of the Tillei Lake belt depicted in Figure 55.2, these deposits are commonly localized in beds draped around conformable leucogranite boudins and sills within a broad zone ranging from a few hundred metres to two or three kilometres from the batholithic contact. In addition, Zn, Pb skarns may be developed at the plutonic contact (e.g. the Chap occurrence) or at some distance from a contact in the apparent absence of conformable granitic bodies, as at the Nar and Narchilla skarns.

B. Ore and silicate mineralogy

Almost all Group III skarns are an assemblage of pyroxene, epidote, and pyrrhotite with only minor amounts of garnet, usually associated with calcite. Nar and Narchilla are the exceptions, having no epidote but abundant garnet. Magnetite forms an important constituent of half of the Zn, Pb skarns studied. Actinolite, wollastonite, and vesuvianite are either rare or absent. Brown sphalerite is more abundant than galena, the average Zn:Pb ratio being about 5:3. Values in silver up to 17 oz/ton have been reported from one of the deposits (Max), but average values for about half of the known Zn, Pb skarns are 1-2 oz/ton. Scheelite, usually associated with chalcopyrite, is a minor constituent of all but two (i.e. Ron and Max) of the Zn, Pb skarns examined.

Group III skarns in the Hyland River-Tyers River area display a notable similarity in morphology and mineralogy that apparently reflects the continuity of their host rocks. Epidote-rich, garnet-deficient skarns hosted by epidotized schist are characteristic of this group of deposits, and quite

distinct from skarn mineral assemblages of Groups I and II. Hyland River area skarns, each with considerable strike length, are aligned in an arcuate belt about 45 km long that extends from several small occurrences north of the Ron to the Max (Fig. 55.1). Skarns in the belt are hosted by calcareous beds within a 6 to 10 km-wide inlier of 'Grit Unit' schist, quartzite and phyllite which is enclosed by the Mount Billings Batholith. Most skarns are localized by adjacent conformable synmetamorphic leucogranite boudins, sills, and augen-shaped lenses, not by proximity to a batholithic contact that may be 3 km away, and not by discordant granitic dykes. A synmetamorphic pre-batholithic age of skarn development is indicated, however differences in age, if any, between the regional metamorphic event and the time of batholithic emplacement have not yet been determined.

Group IV – Zn, Pb, Ag (Cu, Bi, Sn) skarns

A. General characteristics

The four deposits that were examined in the Crescent Lake area 35 km northwest of Rancheria contain a characteristic Zn, Pb, Ag ore element assemblage in magnetite and tourmaline-rich skarns. Rocks hosting the skarns are a sequence of Devono-Mississippian chert, argillite, limestone and quartzite that is thermally metamorphosed to siliceous hornfels and laminated calc-silicate hornfels. The sequence is underlain by a thick Lower Paleozoic succession of carbonate and shale that forms an elongate, partly fault-bounded septum separating leucocratic granites of the Seagull Batholith from biotite quartz monzonites of the Cassiar Batholith to the northeast (Poole et al., 1960). Bar and Atom skarns occur at the northern contact of a dioritic and quartz dioritic phase of Cassiar Batholith, whereas the Bom and Munson occurrences, 5 km to the south, are associated with a miarolitic granite phase of Seagull Batholith. The age of the Seagull Batholith is Early Cretaceous (92-98 m.y., Wanless et al., 1972, p. 30) contemporaneous with the Cassiar Batholith (Poole et al., 1960).

B. Ore and silicate mineralogy

All Group IV skarns are an assemblage of garnet-epidote-actinolite-pyroxene generally rich in magnetite and deficient in pyrrhotite. Sphalerite, galena, chalcopyrite, and arsenopyrite are the most common metallic minerals, and only traces of scheelite were observed. The Bar and Atom are Zn-rich skarns that contain lesser amounts of Pb and Cu and reported minor values of Ag, Sn, and Bi, although no minerals of the latter group of elements were recognized in hand specimen. The host calc-silicate and quartz-biotite schists may be chloritized, epidotized and/or tourmalinized adjacent to skarn deposits, whereas diorite border phases are crowded with xenoliths but relatively unaltered. The Bom and Munson are characterized by equal proportions of galena and sphalerite in massive pyroxene-pyrrhotite-chalcopyrite-arsenopyrite skarn that may grade laterally to calcareous garnet-pyroxene skarn and contain sphalerite with traces of scheelite and molybdenite. In addition, Gower (1952) identified stannite, stanniferous ludwigite ($(Mg\ Fe)_2\ Fe\ BO_5$), pyrargyrite, and tetrahedrite, accounting for the reported assays of 5 to 6 oz/ton Ag and 0.1 to 0.3% Sn.

The Rancheria Zn, Pb, Ag skarns represent only one of many types of skarn, vein and replacement occurrences related to the Cassiar Batholith (Mulligan, 1975) and therefore cannot be considered representative. However, some aspects of the occurrences, particularly the Sn, Be, Bi, Mo and F-bearing mineral assemblages, may be characteristic of skarns associated with the Seagull Batholith (Mulligan, 1977, p. 77). Regional and local characteristics of additional skarns in the Cassiar Batholith region will be studied in 1978.

Other Occurrences

Two skarns that were examined in 1977 and do not correlate with any others in the classification scheme given in Table 55.1 are the Max W (vs. several Max Zn Pb occurrences) and Hundere. The Max, presently being mined by Turner Tungsten Corp., consists of two small, high grade W deposits in a zone of Group III base metal skarns (Fig. 55.1). Several discordant greisen-pegmatite zones are developed in Proterozoic biotite schist and marble adjacent to conformable coarse grained leucogranite bodies. Coarse grained scheelite is unevenly disseminated in a sulphide-free

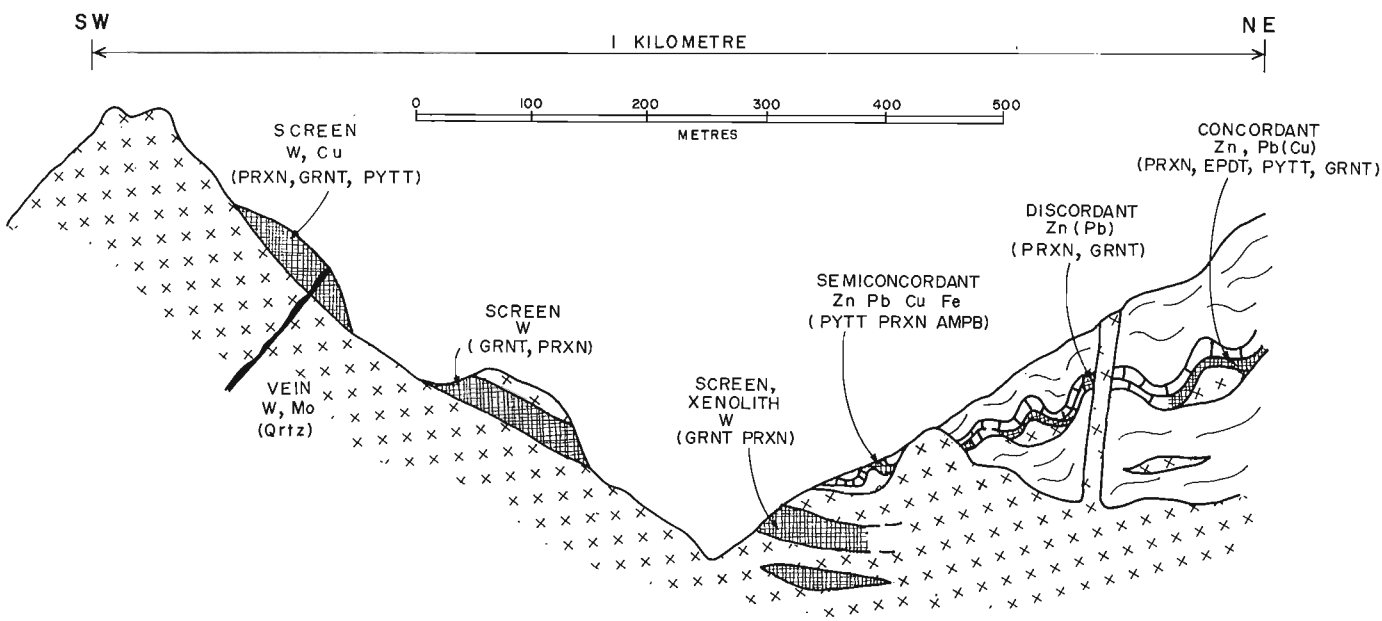

Figure 55.2. Idealized section showing several types of skarn deposits (i.e. WOAH, TAI, etc.) in the Tillei Lake area, Frances Lake sheet 105H/14.

greisen assemblage of quartz-muscovite-epidote-calcite-apatite-sphene. Located in the Frances River area (Fig. 55.1), the Hundere is three separate replacement-type skarns developed in contorted limestone beds adjacent to a north-south fault zone that cuts Lower Cambrian phyllite (Dawson, 1964). Small high-grade lenses of red-brown sphalerite and argentiferous galena occur within zones of actinolite-hedenbergite-garnet skarn that are cut by vuggy quartz-fluorite veins. Although a small aplite dyke is the only associated intrusive rock, Hundere skarns may be related to a shallowly buried pluton satellitic to the Mount Billings Batholith 20 km to the north.

Conclusions

In summary, the important regional characteristics of the four groups of skarns recognized in this study are:

Group I W, Cu skarns, the most significant economically, are associated with an arcuate belt of small Cretaceous plutons in southeastern Yukon and southwestern Mackenzie. Host rocks are the first thick limestone beds, usually Lower Cambrian, that occur above a relatively unmetamorphosed Upper Proterozoic clastic succession.

Group II W, Mo skarns, a recently recognized type, are developed mainly in Upper Proterozoic limestone screens in border phases of the Mount Billings Batholith. Scheelite and silicates display characteristic foliate textures in these garnet-rich, sulphide-deficient skarns.

Group III Zn, Pb(W) skarns, found only in relatively high grade metamorphic terrane, are localized in thin, continuous calcareous beds in Upper Proterozoic metasediments, adjacent to small, conformable leucogranite bodies. The stratiform morphology and distance from discordant intrusive contacts support a synmetamorphic age of mineralization.

Group IV Zn, Pb, Ag skarns that occur in Devono-Mississippian metasediments adjacent to the Cassiar Batholith are relatively rich in epidote, magnetite, and tourmaline and deficient in scheelite. The assemblage of minerals that contains Sn, Be, Bi, Mo and F may be characteristic of skarns associated with the Seagull phase of the Cassiar Batholith.

Some general observations on skarn mineral assemblages studied to date are:

a. Although the large W, Cu skarns contain pyrrhotite, the association of pyrrhotite with scheelite may not be essential for economic W concentrations.

b. Biotite-rich skarns occur only with W, Cu (Group I) mineral assemblages.

c. Scheelite occurs with many different calc-silicate and biotitic skarn mineral assemblages.

d. Garnet-rich skarns generally contain scheelite, whereas base metal skarns are low in garnet (as well as W) relative to W, Cu and W, Mo skarns.

e. Wollastonite-bearing skarns do not contain base metals, and only rarely contain scheelite.

f. Epidote-rich skarns are common only in regionally metamorphosed terrane.

References

Blusson, S.L.
1966: Frances Lake, Geology; Geol. Surv. Can., Map 6-1966.

1968: Geology and tungsten deposits near the headwaters of Flat River, Yukon Territory and southwestern District of Mackenzie, Canada; Geol. Surv. Can., Paper 67-22.

Blusson, S.L., Green, L.H., and Roddick, J.S.
1968: Nahanni, Geology; Geol. Surv. Can., Map 8-1967.

Cummings, W.W. and Bruce, D.E.
1977: Canada Tungsten-change to underground mining and description of mine-mill procedures; Can. Inst. Min. Metal. Bull., v. 70, no. 784, p. 94-101.

Dawson, K.M
1964: Geology of the Mount Hundere Lead-Zinc-Silver Deposit, Watson Lake, Yukon Territory; unpubl. B.Sc. thesis, Univ. of British Columbia.

Dick, L.A.
1976: Metamorphism and metasomatism at the Macmillan Pass tungsten deposit, Yukon and District of Mackenzie, Canada; unpubl. M.Sc. thesis, Queen's University.

Gabrielse, H.
1967: Watson Lake, Geology; Geol. Surv. Can., Map 19-1966.

Gabrielse, H. and Dodds, C.J.
1977: The structural significance of the northern Rocky Mountain Trench and related lineaments in north-central British Columbia; in GAC-MAC-SEG-CGU 1977 Annual Meeting Program with Abstracts, v. 2, p. 19.

Gabrielse, H. and Reesor, J.E.
1974: The nature and setting of granitic plutons in the central and eastern parts of the Canadian Cordillera; Pacific Geology 8, p. 109-138.

Gower, J.A.
1952: The Seagull Creek Batholith and its metamorphic aureole; unpubl. M.Sc. thesis, Univ. of British Columbia.

Harris, F.R.
1977: Geology of the Macmillan Tungsten deposits; 1976 Yukon Mineral Industry Report, Open File Edition, May 1977.

Mulligan, R.
1975: Geology of Canadian tin occurrences; Geol. Surv. Can.; Econ. Geol. Rep. 28.

Poole, W.H., Roddick, J.A., and Green, L.H.
1960: Wolf Lake, Geology; Geol. Surv. Can., Map 10-1960.

Wanless, R.K., Stevens, R.D., Lachance, G.R., and Delabio, R.N.
1972: Age determinations and geological studies; Geol. Surv. Can., Paper 71-2.

Zaw, U.K.
1976: The Cantung E-zone orebody, Tungsten, Northwest Territories; a major scheelite skarn deposit; unpubl. M.Sc. thesis, Queen's University.

OBSERVATIONS ON SOME LEAD-ZINC DEPOSITS OF NOVA SCOTIA

Project 770063

John W. Lydon
Regional and Economic Geology Division

Abstract

Lydon, John W., Observations on some lead-zinc deposits of Nova Scotia; Current Research, Part A, Geol. Surv. Can., Paper 78-1A, p. 293-298, 1978.

On the basis of selected criteria, several genetic types of lead/zinc mineralization can be recognized in Nova Scotia. Within Carboniferous rocks, dispersed lead and/or copper mineralization, most commonly occurring near the Windsor-Horton contact, is probably the result of fractional precipitation of metals by the local reduction of slowly circulating groundwaters. Mineralization in the lower part of the Windsor Group, characterized by a barium-iron association, probably represents deposition on the sea floor from reduced hydrothermal solutions mobilized by tectonic activity, whereas mineralization at about the same stratigraphic level characterized by a zinc-lead-low iron association probably represents early to late diagenetic deposition within carbonates from reduced solutions mobilized by the compaction of the sedimentary succession. Deposits in rocks of lower Paleozoic or greater age, include the deposit at Stirling which is of the volcanogenic massive sulphide type, and zinc-iron mineralization in highly metamorphosed carbonates of the George River Group which may represent original synsedimentary concentrations.

Introduction

During the 1977 field season, the author spent three weeks in Nova Scotia examining lead/zinc deposits. Some of these are used to illustrate how some of the criteria, outlined elsewhere in this volume (Lydon, 1978), can be used in a reconnaissance study to emphasize some genetically significant similarities and differences between ore deposits, and so provide a foundation for further work. The field work also gave the author the opportunity to make first-hand comparisons between the lead/zinc mineralization in Nova Scotia and similar mineralization in Western Europe.

The ten deposits (Fig. 56.1) selected for the purpose of illustration, probably cover the time span of metallogenic episodes in Nova Scotia (Zentilli, 1977). The observations noted here are selective, and are not offered as complete descriptions of the deposits. More attention is given to the Walton, Brookfield and Smithfield deposits, for which arguments are presented for a possible genetic model, whereas remarks on the other deposits are confined to some general observations. Although some of these observations or interpretations may not be new to those active in the area, most seem to have escaped mention in the literature. The terminology used is that defined or implied by Lydon (1978).

Walton – Brookfield – Smithfield Group

The Walton, Brookfield and Smithfield deposits all occur within a carbonate horizon below the evaporites in the lower part of the Windsor Group, and all are characterized by a barium-iron metal association with structures and textures suggesting rapid deposition on or near the surface of the lithosphere.

At Brookfield, cyclic sedimentation units consisting of barite and siderite are exposed over a vertical thickness of about 10 m. Each unit is composed of a basal, fine grained barite or interlaminated barite and siderite layer overlain by a layer consisting of prismatic barite in a siderite matrix. The barite prisms are usually smaller (1-5 cm) and the barite:siderite ratio usually greater at the top of the sedimentation unit than in the central part of the unit, where the barite prisms may attain lengths of over 20 cm (Figs. 56.3, 56.4). This vertical division is applicable to all the sedimentation units, although the relative development of each division may vary. Although prisms of barite extend downwards into the laminated layer of the same unit, they do not appear to extend upwards into the laminated layer of the overlying unit. A sedimentary unit may be between 10 cm and 1.5 m thick, each individual unit maintaining a constant thickness over the extent of the exposure. Within the 10-m vertical exposure of the mineralization, there are three horizons of argillaceous sediment which are parallel to the laminations of the basal divisions of the units and to the contacts between the units themselves, which adds support to the interpretation of the sedimentary nature of the barite/siderite mineralization.

The textures shown by this mineralization are interpreted as having resulted from the periodic discharage of hydrothermal solutions into a local topographic basin of the sea floor. The fine grained, laminated layer is regarded as the accumulated precipitate formed by the initial, rapid degeneration of the hydrothermal solution as it mixed with and displaced the ambient solution of the basin. The ambient solution may have been normal sea water or remnant hydrothermal brine from a previous discharge pulse, that may have been at any stage of degeneration i.e. possessed physico-chemical properties that were intermediate between those of the hydrothermal reservoir and those of the discharge environment – in this case that of normal sea water. The amount of precipitate produced by each discharge pulse was no doubt proportional not only to the quantity of discharge but also to the degree of disequilibrium between the discharging hydrothermal solution and the ambient solution.

The prismatic barite layer is interpreted as having crystallized within a dominantly sideritic mud that was deposited as a result of the progressive degeneration of the brine pool. The concentration of barite nucleation centres at the sediment-water interface, as reflected by the greater number of barite crystals at the top of the sedimentation units, suggests that the combined flux of barium and sulphate ions was greater at the surface than deeper within the sediment, a situation which could have arisen by downward diffusing sulphate ions meeting with barium ions being carried upwards by the dewatering of the underlying precipitates. At some horizons, a massive to nodular barite layer occurs between the prismatic division of one unit and the laminated division of the overlying unit, and may represent barite precipitated above the water-sediment interface from solutions discharged during the compaction of the underlying precipitates. The prismatic barite is reminiscent of the porphyroblastic selenite of some evaporite successions (Pettijohn, 1957, p. 479), and also, in a very general way, the textural relationships of the barite-siderite beds can be

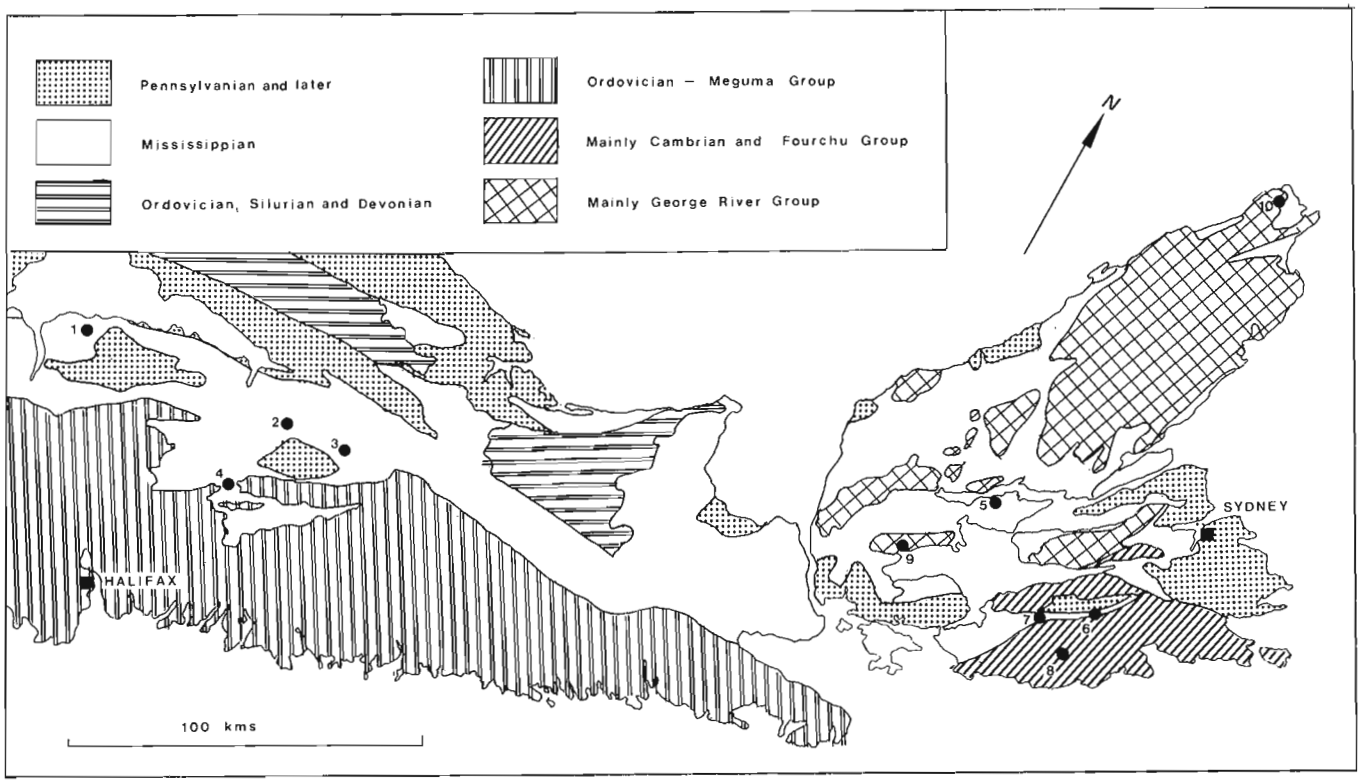

1. Walton
2. Brookfield
3. Smithfield
4. Gays River
5. Jubilee
6. Silvermine
7. Lake Enon
8. Stirling
9. Lime Hill
10. Meat Cove

Figure 56.1. Generalized geological map, exclusive of igneous rocks, of part of Nova Scotia showing the locations of mineral deposits mentioned in the text.

compared to those of some ultramafic rocks where spinifex texture overlies cumulate texture. However, at Brookfield the barite prisms/plates show a preferred orientation that is consistently inclined in the same direction with respect to the bedding, in contrast to the sub-perpendicular orientation of spinifex texture. This feature may in part be a compaction phenomenon.

The mineralization at Smithfield is not exposed at the surface. The bulk of the mineralization on the dumps from the underground workings consists of a mélange of fine grained pyrite, black calcareous/siliceous material, sphalerite, galena and fragments and small crystal clusters of barite. The mélange commonly has a planar fabric (Fig. 56.5a), especially where the rock consists only of pyrite and limestone. Colloform textures in the fine grained pyrite are also common (Fig. 56.5b). Pyrite, sphalerite, galena and barite infill fractures in all rock types and also apparent cavities on the convex side of some colloform structures in the pyrite. In the writer's experience, such textures are common in sulphide deposits which have been rapidly precipitated at the lithospheric surface, including those of volcanogenic affiliation, but in the absence of knowledge on the structure of the Smithfield deposit, it is not possible to determine whether the observed mineralization represents rapid deposition at the lithospheric surface or within large cavities near the surface.

The Walton deposit consists of juxtaposed barite, siderite and sulphide mineralization. The geology, geochemistry, mineralogy and textural features of this deposit have been described in detail by Boyle (1972), who concluded that the deposit formed by replacement and fracture-filling of sediments of the lower Windsor Group, probably during the Triassic. The complexity of the deposit, induced primarily by post-Windsor tectonic events and groundwater circulation (Boyle op. cit.), precludes any definite categorization of the deposit as a single type. However, it is noteworthy that the structure of the deposit on a gross scale is strikingly similar to that of other deposits for which there is more conclusive evidence for deposition at the lithosphere's surface and with which there are no spatially associated evaporites. Amongst these may be cited the Mogul "A" and "B" – Magcobar deposits at Silvermines, Ireland (Coomer and Robinson, 1976); the Meggen deposit, Germany (Gasser, 1974; Krebs, 1972); and the Fuenteheridos deposit, Spain (author's observations). In all cases, a barite deposit occurs laterally to and at a slightly different stratigraphic elevation from a dominantly pyritic sulphide body.

The Walton, Brookfield and Smithfield deposits lie on the same structural lineament, defined by the outcrop patterns of Carboniferous and older rocks (Fig. 56.1). Such a configuration suggests to the writer that the lineament indicates a zone of basement weakness with a prolonged history of structural instability, and may represent one of the fault systems, often with a strike-slip motion, that were active throughout the Lower Carboniferous both in Maritime Canada and the British Isles (Belt, 1968; Webb, 1968; Leeder, 1976). In this respect, these deposits may be comparable to the Silvermines and Tynagh deposits of Ireland, which appear to have been deposited in tectonically induced basinal structures along active fault zones, similar in nature and origin to those described by Kingma (1958) in New Zealand. It is presumed that the fault zones acted as channelways for movement of hydrothermal solutions.

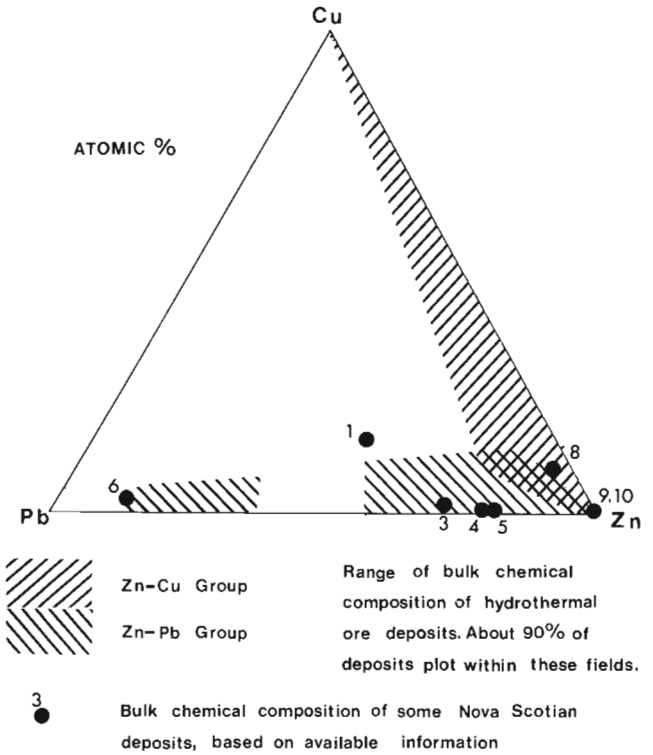

Figure 56.2. Comparison of the metal ratios of some Nova Scotian deposits with those of other deposits (Lydon, 1978). Numbers refer to those deposits indicated on Figure 56.1.

The chemistry of the sulphide body at Walton appears to be anomalous (Fig. 56.2) in that it contains relatively too much copper and possibly too much lead for a synsedimentary deposit of a low-medium temperature geothermal regime, based on the thermochemical calculations of Lydon (1977) and comparison with the bulk chemical compositions of other deposits of this type. Perhaps the copper, and possibly the lead, enrichment is a post main-ore event, and related to those processes which have produced a copper and/or lead enrichment at the Windsor-Horton contact throughout Nova Scotia (Binney and Kirkham, 1974, 1975). This late stage introduction of copper, and to some extent lead, would be consistent with the paragenetic relationships observed by Boyle (1972).

In summary, the similar fundamental characteristics of all three deposits suggest that they are of the same genetic type, having been deposited in similar discharge environments from hydrothermal solutions that were generated in mineralogically similar reservoirs of about the same temperature and mobilized at the same time by probably the same mechanism. If this is correct, then the absence of a sulphide deposit at Brookfield would be anomalous.

Gays River – Jubilee

Although texturally quite distinct (Fig. 56.5c, 56.5d), these two deposits have several characteristics in common. They appear to be chemically similar, having zinc-lead-low iron compositions, which indicates that the hydrothermal solutions from which they were deposited, based on thermochemical calculations, were probably more sulphur-rich, more oxidized, and probably slightly less acid and lower temperature than the hydrothermal solutions responsible for the mineralization of the Walton-Brookfield-Smithfield group. At both Gays River and at Jubilee the mineralization appears to have been relatively rapid within an aquifer, but at the same time slow enough to have allowed the fractional precipitation of sphalerite and galena. At Gays River, the depositional space seems to have been afforded by the primary and early diagenetic porosity of the host carbonate, which suggests deposition close to the surface of the lithosphere and possibly coeval with the overlying evaporites (MacLeod, 1975). In contrast to the deposits at Walton and Smithfield, the ores at Gays River do not appear to be associated with faults (Hannon and Scott, 1975). At Jubilee, the exposed mineralization appears to infill the spaces between and in part to replace, limestone fragments of a breccia. However, on such a small scale it cannot be determined whether the rock is an intralithosphere tectonic breccia associated with faulting or a sedimentary breccia, such as a talus breccia occurring at the foot of a fault-line scarp. The reasons for the localization of these two deposits is not known, but it may be significant that both Gays River (MacEachern and Hannon, 1974) and Jubilee (Greg Isenor, oral comm., 1977) occur on the flanks of antiform structures, which may have had some influence in directing the flow of the hydrothermal solutions in the Windsor Limestone aquifer contained between relatively impermeable clastic rocks below and evaporites above.

Dispersed Lead and Copper Mineralization in Carboniferous Rocks

There are numerous occurrences of lead and/or copper mineralization in Carboniferous rocks throughout Nova Scotia, particularly close to the Windsor-Horton contact (Binney and Kirkham, 1974, 1975; Binney, 1975a, b). A preliminary theoretical consideration of this lead-copper association suggests that it is probably a result of the reduction of initially metal-undersaturated, oxidized solutions (which contrasts with the initially reduced nature of most ore-forming hydrothermal solutions) leading to the fractional precipitation of the metals. The solutions responsible for mineralization of this type are probably "normal", slowly circulating groundwaters, albeit probably containing anomalous amounts of metal and already somewhat reduced relative to equilibrium with the atmosphere, from which the metals are fractionally precipitated by reaction with reducing agents, such as pyrite, natural gas or carbonaceous material, within or adjacent to the aquifer. Such a mechanism has been proposed by Kirkham (1973) for the origin of his "Kupferschiefer" and "Red Bed" types of deposits in general, and by Binney (1975a) for the Lake Enon mineralization, though this locality may be locally anomalous in that

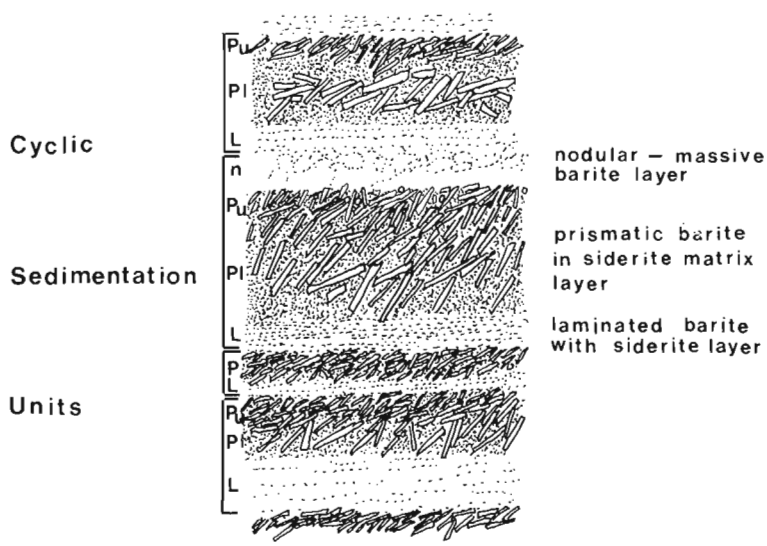

Figure 56.3. Illustration of the textural types and cyclic sedimentation of the Brookfield barite-siderite deposit. Note that the barite siderite ratio is usually higher in the upper part (Pu) of the prismatic barite layer (P) than in the lower part (Pl).

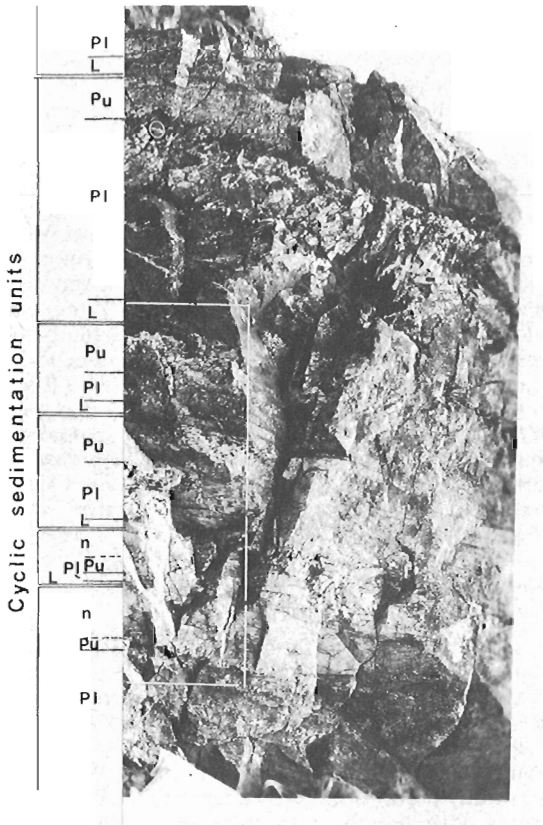

a

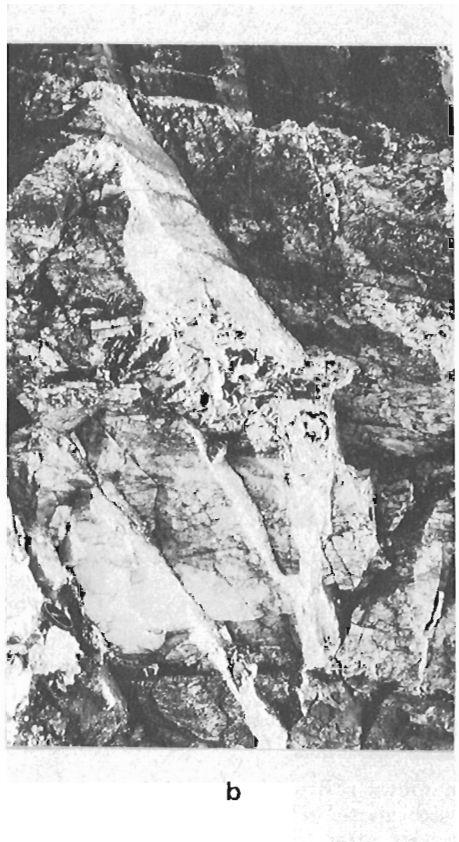

b

Figure 56.4

a) Photograph showing some cyclic sedimentation units of the Brookfield barite-siderite deposit. Symbols for textural types are the same as for Figure 56.3. Note the camera lens cap in the upper left for scale.

b) Close-up of the area indicated in 56.4a.

relatively significant quantities of zinc accompany the copper and lead mineralization. The Silvermine deposit, consisting mainly of galena, the bulk of which occurs in Pennsylvanian sandstone, may represent an unusually high concentration, both in terms of grade and tonnage (Northern Miner, March 1977), of sulphide mineralization of this type.

Stirling

Only dump material was available for inspection at the old Mindimar mine at Stirling. Two dominant types of sulphide mineralizaiton appear to exist. One consists of fine grained, massive, commonly laminated, pyrite, sphalerite, galena and chalcopyrite, and the other of quartz-carbonate vein(?) material, which in many specimens contains sulphides, and which appears to cut host rocks and the massive sulphides. The primary sphalerite-chalcopyrite association suggests deposition from a hydrothermal system of a higher temperature type than those discussed above, while the fine grained, laminated and massive nature of the ore suggests rapid deposition at the lithospere's surface. The deposit is hosted by the volcanic rocks of the Bourinot Group, assigned a Cambrian age by Weeks (1954), but considered possibly of Hadrynian age by Poole (1974).

The deposit has been described as a replacement and fracture filling in a shear zone (Watson, 1954; Keating, 1960), but its bulk chemical composition, ore textures and geological setting indicate that, consistent with the opinion of Poole (1974), it is a volcanogenic massive sulphide deposit.

Meat Cove – Lime Hill

The Meat Cove deposit has been described as a contact metasomatic replacement of limestones of the George River Group by sphalerite-pyrite-pyrrhotite mineralization (Keating, 1960). Chatterjee (1976) regards the sphalerite mineralization as resulting from the final stages of hydrothermal activity associated with a syenite intrusion. Although skarn mineralization is present, and sphalerite is commonly incorporated into this mineralization as well as being present as small, discordant, massive veins, most of the sphalerite appears to form an integral part of the crystal mosaic and foliation of the highly metamorphosed carbonate rock, and would appear to predate the metamorphism and foliation (see Fig. 56.5e). Judging from drillhole sections and other documents in the assessment files of the Nova Scotia Department of Mines, most of the zinc mineralization is in an elongate tabular mass parallel to the compositional layering in the host carbonate.

The author was struck by the similarity of the mineralization at Meat Cove to that of some small iron-zinc deposits in Cambrian carbonates of southern Spain and Portugal where the Cambrian is transgressed by Hercynian metamorphic zones that vary in grade from lower greenschist to upper amphibolite. In the lower grade metamorphic zones it is readily apparent that the stratiform iron-zinc (either pyrite-sphalerite or pyrite-magnetite-sphalerite) is a particular facies of more widespread iron-barium-zinc-lead-copper synsedimentary mineralization, though in high grade metamorphic zones, where they have been recrystallized and remobilized, their primary features are not easily recognizable. The geological setting of these Iberian deposits is a platform adjacent to the active rift system, within which volcanogenic massive sulphide deposits occur. If the mineralization at Meat Cove, and similar mineralization at Lime Hill, are indeed comparable to the Iberian mineralization, then not only "the possibility that there may have been a primary concentration in the limestones themselves" (Keating, 1960, p. 48), but also the possibility of a similar regional geological setting, should perhaps merit consideration.

Summary

All the zinc-lead deposits in rocks of Carboniferous age are the products of low temperature hydrothermal systems (< 200°C) that were active during the Carboniferous.

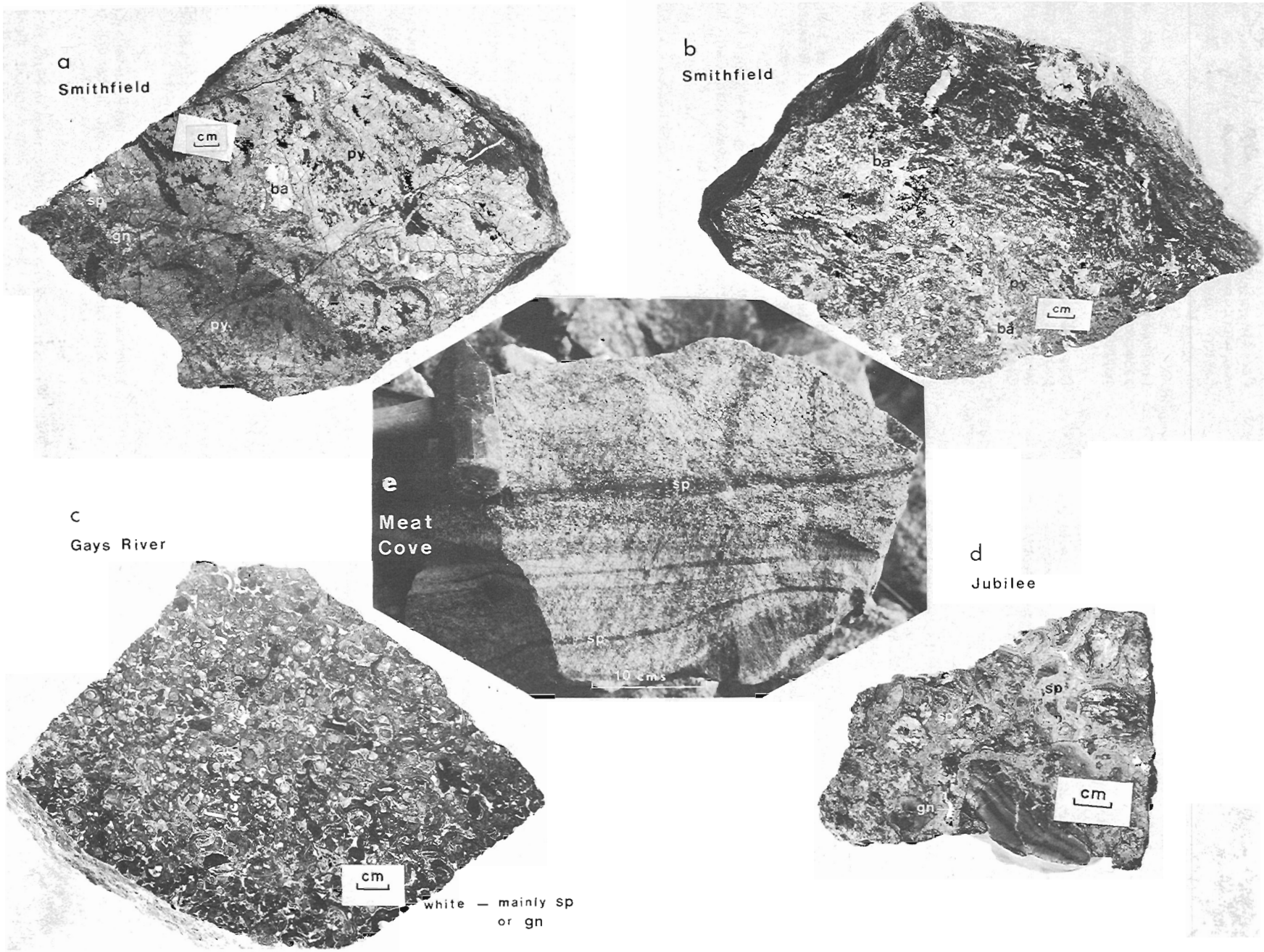

Figure 56.5. Some textural types of mineralization from Nova Scotian lead/zinc deposits.

The mobilization of the solutions in some cases was probably tectonically induced, possibly as true seismic pumping or by the fracture release of geopressured reservoirs (Walton, Brookfield, Smithfield); in other cases (Gays River, Jubilee), as suggested by Hannon and Scott (1975), solutions may have been mobilized by burial compaction of Lower Carboniferous or older sediments and the consequent lateral and upward migration of these expelled solutions was no doubt along convenient zones of relatively high hydraulic conductivity, such as the Windsor Limestone aquifer or a fracture zone.

The volcanogenic massive sulphide deposit at Stirling reflects the existence of a higher temperature geothermal regime in this area during the lower Paleozoic. If the Meat Cove and Lime Hill deposits are comparable to the iron-zinc deposits of the Cambrian in Spain and Portugal, they could represent the product of a lower temperature, platform type of hydrothermal system operative during the time of deposition of their George River host, which has been regarded as Helikian by Schenk (1971) and Wiebe (1972).

Acknowledgments

The author would like to acknowledge the co-operation of mining companies active in the area, particularly Imperial Oil Ltd. and Amax Explorations Ltd., and to thank them for their courtesies and help which allowed the field work.

References

Belt, E.S.
1968: Post-Acadian rifts and related facies, eastern Canada; in E.A. Zen, W.S. White and J.B. Hadley (editors), Studies of Appalachian geology: Northern and Maritime; Interscience, New York, p. 95-113.

Binney, W.P.
1975a: Lower Carboniferous stratigraphy and base-metal mineralization, Lake Enon, Nova Scotia; Unpubl. M.Sc. thesis, Queen's Univ., Kingston.

1975b: Copper occurrences in Lower Carboniferous sedimentary rocks of the Maritime Provinces; Geol. Surv. Can., Open File 281.

Binney, W.P. and Kirkham, R.V.
1974: A study of copper mineralization in Mississippian rocks of Nova Scotia; in Report of Activities, Part A, Geol. Surv. Can., Paper 74-1A, p. 129-130.

1975: A study of copper mineralization in Mississippian rocks of the Atlantic Provinces; in Report of Activities, Part A, Geol. Surv. Can., Paper 75-1A, p. 245-248.

Boyle, R.W.
1972: The geology, geochemistry, and origin of the barite, managanese and lead-zinc-copper-silver deposits of the Walton-Cheverie area, Nova Scotia; Geol. Surv. Can., Bull. 166, 181 p.

Coomer, P.G. and Robinson, B.W.
1976: Sulphur and sulphate-oxygen isotopes and the origin of the Silvermines deposits, Ireland; Mineral. Deposita, v. 11, p. 155-169.

Chatterjee, A.K.
1976: Geology of the Meta Cove zinc deposit, Cape Breton, Nova Scotia; Report of Activities, Nova Scotia Dep. Mines Rep. 76-2, p. 95.

Gasser, U.
1974: Zur Struktur und Geochemie der stratiformen Sulfidlagerstatte Meggen (Mitteldevon, Rheinisches Schiefergebirge); Geol. Rundschau, v. 63, p. 52-73.

Hannon, P. and Scott, F.
1975: Lead-zinc exploration in the Gays River district of Nova Scotia; Trans. A.I.M.E., v. 258, p. 209-212.

Keating, B.J.
1960: Massive sulphide deposits in Nova Scotia; Can. Inst. Min. Metall. Trans., v. 63, p. 43-49.

Kingma, J.T.
1958: Possible origin of piercement structures, local unconformities, and secondary basins in the Eastern Geosyncline, New Zealand; New Zealand J. Geol. Geophys., v. 1, p. 269-274.

Kirkham, R.V.
1973: Environments of formation of concordant and peneconcordant copper deposits in sedimentary sequences; (abstr.) Can. Mineral., v. 12, p. 145-146.

Krebs, W.
1972: Die paläogeographisch-faziellen Aussagen zur Position des Meggeners Lagers; Schr. Dtsch. Ges. Metallhütten-u. Bergleute, Schr. 24, p. 187-196. Clausthal-Zellerfeld.

Leeder, M.R.
1976: Sedimentary facies and the origin of basin subsidence along the northern margin of the supposed Hercynian ocean; Tectonophysics, v. 36, p. 167-179.

Lydon, J.W.
1977: The significance of metal ratios of hydrothermal ore deposits; Unpubl. Ph.D. thesis, Queen's Univ., Kingston.

1978: Some criteria for the categorization of hydrothermal base metal deposits; in Current Research, Part A, Geol. Surv. Can., Paper 78-1A, rep. 57.

MacEachern, S.B. and Hannon, P.
1974: The Gays River discovery — a Mississippi Valley Type lead-zinc deposit in Nova Scotia; Can. Min. Metall. Bull., v. 67, p. 61-66.

MacLeod, J.L.
1975: Diagenesis and sulphide mineralizaton at Gays River, Nova Scotia; Unpubl. B.Sc. thesis, Dalhousie Univ., Halifax.

Pettijohn, F.J.
1957: Sedimentary rocks; 2nd-edition Harper and Brothers, New York, 718 p.

Poole, W.H.
1974: Stratigraphic framework of volcanogenic massive sulphide deposits, Northern Appalachian orogen; in Report of Activities, Part B, Geol. Surv. Can. Paper 74-1B, p. 11-17.

Schenk, P.E.
1971: Southeastern Atlantic Canada, northwestern Africa, and continental drift; Can. J. Earth Sci., v. 8, p. 1218-1251.

Watson, K.D.
1954: Paragenesis of the zinc-lead-copper deposits at the Mindimar Mine, Nova Scotia; Econ. Geol., v. 49, p. 389-412.

Webb, G.W.
1968: Palinspastic restoration suggesting Late Paleozoic North Atlantic rifting; Science, v. 159, p. 875-878.

Weeks, L.J.
1954: Southeast Cape Breton Island, Nova Scotia; Geol. Surv. Can., Mem. 227.

Wiebe, R.A.
1972: Igneous and tectonic events in northeastern Cape Breton Island, Nova Scotia; Can. J. Earth. Sci., v. 9, p. 1262-1277.

Zentilli, M.
1977: Evolution of metallogenic domains in Nova Scotia; Abstr. Can. Inst. Min. 79th Annual General Meeting, Can. Min. Metall. Bull., v. 70, p. 69.

57.

SOME CRITERIA FOR CATEGORIZING HYDROTHERMAL BASE METAL DEPOSITS

Project 770063

John W. Lydon
Regional and Economic Geology Division

Abstract

Lydon, John W., Some criteria for categorizing hydrothermal base metal deposits; Current Research, Part A, Geol. Surv. Can., Paper 78-1A, p. 299-302, 1978.

Analogies with modern hydrothermal systems provide some criteria which may be useful for categorizing lead-zinc-copper ore deposits. The bulk chemical composition, particularly the ratio of the metals, reflects the temperature and mineralogy of the hydrothermal reservoir. The primary geometric and mineralogical structure of the ore deposit and the primary textures of the ores reflect the mechanism of mobilization of the hydrothermal solutions and the physical and chemical nature of the depositional environment. These criteria reflect the fundamental controls of the ore forming process and provide a basis for distinguishing between the basic genetic features of an ore deposit and those features which are only fortuitous associations.

Introduction

One of the concerns of the project is the investigation of the relationship between lead/zinc deposits and their geological environments. Most deposits of lead and zinc, with or without copper, have been precipitated from hydrothermal solutions. If anologies can be drawn between the hydrothermal systems of ancient ore-forming environments and those of modern geothermal areas, then several characteristics of the latter may be of importance in the understanding of the relationships between base metal deposits and their geological environments.

The purpose of this paper is to briefly point out what are considered to be these pertinent characteristics, and to summarize the rationale behind the approach being taken in current research, which focuses attention on the bulk chemistry and the structure of ore deposits, and the primary mineralogical/textural zonation of the ores.

Some Characteristics of Modern Hydrothermal Systems

The essential features of a hydrothermal system, considered either in terms of the rock units involved or in terms of the physico-chemical nature or changes of the solutions involved, are illustrated in Figure 57.1. The generation of a hydrothermal solution requires i) a heat source; ii) an aquifer unit which acts as a reservoir for the heated solutions; and iii) an overlying cap rock unit which prevents heat dissipation by mass transfer of the heated solutions from the aquifer unit, thus allowing the maintenance of elevated temperatures within the reservoir over an extended time period.

Temperature of Hydrothermal System

A vertical geothermal profile through the heated part of a hydrothermal system generally shows an increase in temperature with depth, which is usually close to the solution boiling curve through the cap rock unit, but is relatively constant through the aquifer unit (White, 1968). Typically, each separate hydrothermal system has its own characteristic reservoir temperature, which is dependent on its depth below surface and its tectonic environment (McNitt, 1970) - generally, hydrothermal systems in areas of active volcanism have the highest temperatures (>200°C), those associated with active faulting have intermediate temperatures, while those in a platform environment have the lowest temperatures (<120°C).

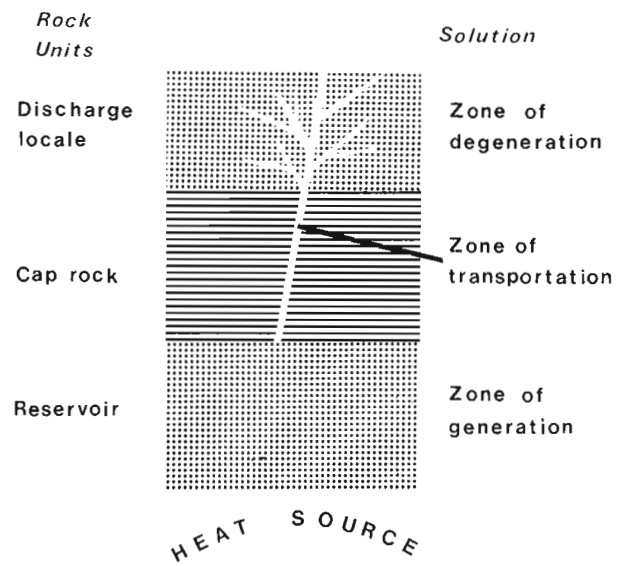

Figure 57.1 Schematic representation of a hydrothermal system.

Chemical Composition of Thermal Waters

The major cationic composition of thermal waters is determined by solution-mineral equilibria in the reservoir (Ellis and Mahon, 1964, 1967), this phenomenon being so consistent that the major cationic ratios of the solution can be used as geothermometers to indicate the reservoir temperature of the hydrothermal system up to about 350°C (White, 1970). It is also probable that the pH, pO_2, pCO_2, and pS_2 of the thermal water within the reservoir are also controlled by solution-mineral equilibria, while major anionic species, for example chloride, are probably dependent upon provenance, such as connate waters, availability of evaporites for dissolution, magmatic chloride etc.

Flow of Thermal Waters

The movement of thermal waters from the reservoir usually requires some form of cross-stratal permeability, which in most modern geothermal areas is provided by fracture zones (McNitt, 1970). The mechanism of movement may be thermal convection or conceivably artesian flow, both of which are essentially circulatory systems i.e. requiring a recharge of fluid displaced from the reservoir, or by a decrease in porosity of the aquifer zone, which does not necessarily require recharge and hence may be considered as

non-circulatory systems. A reduction in porosity may be achieved by compaction due to increase in burial depth or by tectonic stress. In this connection, the seismic pumping model (Sibson et al., 1975; also see Dandurand et al., 1972) in which pore solutions are expelled from the focus of shallow earthquakes by the collapse of a dilatant zone, merits emphasis. The rate of flow of the thermal waters is likely to be dependent on local conditions, but generally a mechanism such as seismic pumping would be expected to cause the most rapid flow, thermal convection an intermediate rate, and compaction due to burial the slowest migration of thermal waters. However, in all cases it is probable that flow within the channelways of transportation is very rapid compared to those in the reservoir zone, and therefore the residence time of the solution is too short and the effective water:rock ratio too large to allow any appreciable change in the solution as the result of interaction with the wall rocks. Thus, during the time of migration, the thermal solution maintains the chemical characteristics it acquired in the reservoir zone, a phenomenon which accounts for the successful use of chemical composition of surface discharge waters as an indicator of subsurface reservoir temperatures (White, 1970).

Discharge of Thermal Waters

Eventually, the thermal waters will be discharged from the restrictions of the channelways of transportation. This zone of discharge may be at the lithospheric surface or where the channelways of transportation intersect another aquifer unit. In the zone of discharge the nature of the thermal waters will change by progression towards physico-chemical equilibrium with the environment of discharge. These changes may be brought about by mixing with local solutions, reaction with wall rock, loss of some components as a gaseous phase, etc. In any specific discharge environment, although all processes of equilibriation are probably operative, only one process is likely to be dominant. The discharge locale, or the site where the hydrothermal solution degenerates from the initial physico-chemical character of its reservoir, is considered to be the site of deposition of hydrothermal ore deposits in ore forming systems.

Precipitation of Dissolved Constituents

Nucleation of crystals from an aqueous solution usually follows a rate law in which the number of nuclei formed per unit volume per unit time is highly dependent on the degree of supersaturation of the solution (Nielsen, 1964). At high degrees of supersaturation, which may be brought about by rapid physico-chemical changes in the discharge environment, the nucleation rates may be so great that most of the excess dissolved mass is precipitated as crystal nuclei, resulting in a very fine grained or gel-like precipitate. At lower degrees of supersaturation, crystal growth rates may exceed nucleation rates, resulting in a coarser grained precipitate. In a multicomponent system, particularly in the case where different cations are competing for a limited supply of the same anionic radical, the difference in nucleation and growth rates of the different crystalline phases may be great enough to allow a fractional precipitation, even though the solution is saturated with respect to all crystalline phases. Thus the path and rate of the degeneration of the hydrothermal solution through physico-chemical space may determine not only the texture, but also the chemistry and paragenetic relationships of the precipitate. Equating the degree of supersaturation of the solution with the degeneration rate, depositional phenomena may be analyzed in terms of the degeneration rates of a hydrothermal system and its flow rates through the discharge zone (see Fig. 57.3).

Ore Deposits and Hydrothermal Systems

Within the context outlined above, hydrothermal ore deposits could be genetically characterized in terms of i) the temperature and mineralogical nature of the hydrothermal reservoir; ii) the mechanism of mobilization of the hydrothermal solutions and the nature of the channelways of transportation; and iii) the nature and site of the degeneration of the hydrothermal solution. However, since these parameters cannot be directly observed when examining ore deposits, it is suggested that some insight into these fundamental controls of the process of mineralization can be obtained by consideration of the following parameters, which are observable or deducible from field work.

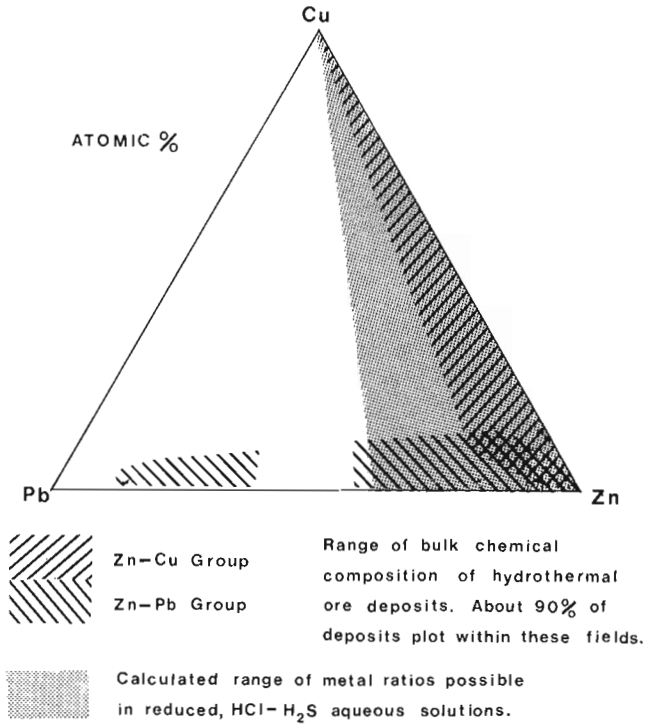

Figure 57.2 Comparison of the range of Cu-Zn-Pb ratios of hydrothermal ore deposits, based on 195 bulk compositions, with the range of calculated saturation ratios in HCl-H_2S aqueous solutions.

Bulk Chemical Composition of Ore Deposit

The range of Cu-Zn-Pb ratios shown by the bulk chemical composition of hydrothermal ore deposits corresponds very closely to the ranges, calculated from thermodynamic data, of these metal ratios that are likely in natural metal-saturated, reduced[1], aqueous solutions containing chlorine and sulphur species (Lydon, 1977). The consistency of the metal ratios of ore deposits formed in similar environments suggests that most hydrothermal ore deposits represent the total precipitation of the metal load of a hydrothermal system, and the correspondence of these ratios to those of saturated solutions suggests that the metal contents of ore-forming hydrothermal systems, like the major cationic constituents of modern hydrothermal systems, are determined by solution-mineral equilibria in the hydrothermal reservoir (Lydon, op. cit.). Thus the bulk chemistry of the ore deposit reflects the physico-chemical conditions of the hydrothermal reservoir which, as pointed out above, depends mainly on its tectonic environment (or geothermal regime) and the wall-rock mineralogy of the reservoir rocks. As shown in Figure 57.2 most hydrothermal ore deposits in this system can be classified as belonging to a zinc-copper group or a zinc-lead group, which in very general terms can be equated to higher temperature, feldspar-mica buffered hydrothermal

[1] 'Reduced solutions' as used here is defined as those solutions in which the activity of the dominant reduced sulphur aqueous species ($H_2S(aq)$, HS^- or S^{--}) is greater than the activity of the dominant oxidized sulphur aqueous species (HSO_4^- or SO_4^{--}).

reservoirs and lower temperature, clay buffered hydrothermal reservoirs respectively. The relatively lead-rich deposits probably incorporate a degree of fractional precipitation.

Timing and Location of Mineralization

Most hydrothermal systems do not contain sufficient metal to become ore-forming systems. The enrichment of metals in hydrothermal solutions seems to be favoured by a high effective rock:water ratio i.e. noncirculatory systems, which allows the attainment of high metal concentrations in the solutions, and by a concommitant metamorphism of the reservoir rocks during hydrothermal solution generation, which facilitates the leaching of the metals from their host minerals. The energy for the mobilization of the thermal solutions is most readily available in areas of steeply inclined geotherms for convective flow e.g. volcanic centres; along active fault zones for seismic pumping; or when a sedimentary pile reaches the requisite burial depth for compactional expulsion. A knowledge of the geological history of an area, with particular regard to thermal and tectonic events, is necessary to determine the most favourable sites and time periods of ore solution generation, migration, and deposition.

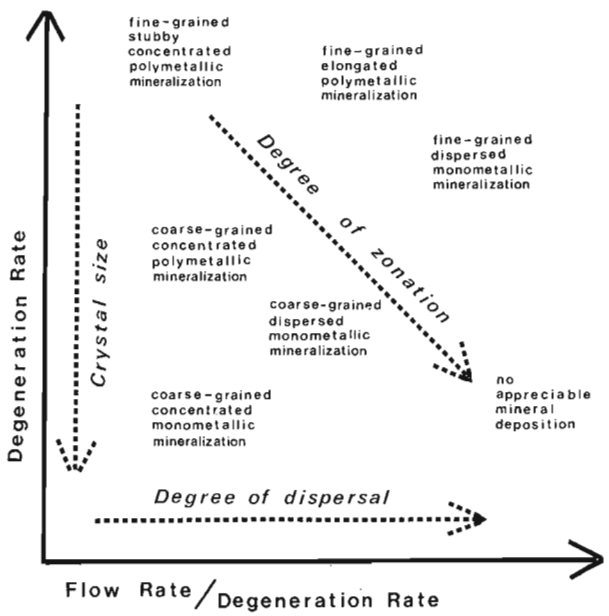

Figure 57.3 Possible effects of the degeneration rate and flow rate of a hydrothermal solution on the grain size, degree of chemical dispersal and degree of chemical zonation of the precipitate.

Structure of Deposit

'Structure' is used here in the sense of the architectural framework and would include not only the primary geometrical form of the volume of mineralization but also the chemical/mineralogical zonation of the deposit. The structure of the deposit reflects the nature of the discharge environment, which in turn largely determines the path and rate of degeneration of the hydrothermal solution through physico-chemical space, and also the types of depositional traps which are necessary for the containment and preservation of the mineral precipitates. Generally, deposition at the lithospheric surface gives rise to geometrically simple (e.g. tabular to cone-shaped), simply zoned deposits with well defined contacts with barren rocks, whereas deposition within the lithosphere gives rise to deposits which reflect the shape of the aquifer and the nature of its porosity (i.e. fracture intergranular etc.), and hence complex geometrical shapes, complicated zonation patterns, and gradational contacts with barren rocks can be expected.

Texture of Ores

Primary textures are small scale features which reflect the local depositional and later history of the mineralization. Textures can be expected to be variable within a single deposit reflecting the local variations both in degeneration rates of the hydrothermal solution and the local mechanism, rate and site of mineral precipitation. Thus it is best to consider deposits in terms of dominant textural types rather than the complete range of textural types.

Primary textures, like the structure of the deposit, reflect the nature of the discharge environment and therefore one would expect a correlation between the two. For example, degeneration of a hydrothermal solution is likely to be most rapid at the lithospheric surface, and hence fine grained, polyminerallic aggregates are more typical of the massive, well defined, structurally simple, synsedimentary deposits, whereas the coarsely crystalline, monominerallic, vug or fracture-filling ores, reflecting slower degeneration rates, are more typical of the structurally complex epigenetic deposits. Since primary textures are so susceptible to modification, often to the point of obliteration, by post-depositional processes such as metamorphism or later mineralizing episodes, it would be unwise to base a genetic model of a deposit solely on this small scale evidence.

Categorization of Hydrothermal Ore Deposits

The fundamental factors that produce differences among hydrothermal ore deposits are i) the temperature and mineralogy of the hydrothermal reservoir rocks, which determine the chemistry of the deposit, and ii) the physical nature and physico-chemical environment of the site of discharge, which determines the primary structure of the deposit and the primary textures of the ores. Two implications of this are that the major ore element association of a hydrothermal deposit is not related to the distribution of these elements in the source rocks, and the chemical characteristics of a deposit are not directly related to its host rocks.

The hydrothermal reservoir and discharge environment are not interdependent, and in theory, a complete spectrum of ore deposit types, with all possible combinations of the various features, should be possible. However, there is no doubt that certain types of deposits are more common than others e.g. few porphyry zinc deposits compared to many porphyry copper deposits. The prevalence of certain types appears to be the logical outcome of the interdependence of the major geological processes. For example, in the platform environment hydrothermal systems tend to be of the lower temperature type, reflecting the lower geothermal gradients of this tectonic domain. In this geological setting the dominant lithologies are clay, carbonate and sandstone, reflecting the tectonic stability of the area. Low temperature, clay-buffered, reduced, aqueous solutions can only give rise to a zinc/lead dominant association in metal-saturated, reduced solutions. In the platform environment, aquifers with the highest hydraulic conductivities are usually carbonate, and to some extent sandstone, lithological units. The combination of these factors thus explains why the Mississippi Valley type is the prevalent epigenetic base metal deposit in the platform environment.

It would be unwise to attempt a stringent classification of ore deposits on theoretical grounds alone because, from the practical point of view, inclusion of all possible types sheds no light on the relative probabilities of their occurrence and hence their priority as exploration targets, whereas classifications based on possibly erroneous interpretations of genesis, may lead to omission of a type and thus preclude its consideration as an exploration target. In this regard, descriptive classifications of ore deposits have great usefulness in providing standards for comparison, because it is probable that deposits with similar characteristics have been formed by similar processes.

In describing ore deposits it is desirable to distinguish between those features or characteristics which are directly related to the fundamental processes of ore formation from those features which may only be the fortuitous associations of a specific location, or of negligible consequence to an ore deposit type in general. Because the one characteristic that most ore deposits of lead, zinc and/or copper have in common is the fact that they were precipitated from hydrothermal solutions, it is suggested that criteria based on the characteristics of the hydrothermal system have the most fundamental significance. Based on the points outlined above, it is further suggested that the bulk chemical composition, particularly the metal ratios of the orebody, the primary structure of the ore deposit, and the primary textures of the ores are a direct consequence of the chemical and physical characteristics of the hydrothermal system, and are therefore important criteria for categorizing hydrothermal ore deposits.

References

Dandurand, J.L., Fortuné, J.P., Pérami, R., Schott, J., and Tollon, F.

1972: On the importance of mechanical action and thermal gradient in the formation of metal-bearing deposits; Mineral. Deposit, v. 7, p. 339-350.

Ellis, A.J. and Mahon, W.A.J.

1964: Natural hydrothermal systems and experimental hot-water/rock interactions; Geochim. Cosmochim Acta., v. 28, p. 1323-1357.

1967: Natural hydrothermal systems and experimental hot-water/rock interactions (Pt. II); Geochim. Cosmochim Acta., v. 31, p. 519-538.

Lydon, J.W.

1977: The significance of metal ratios of hydrothermal ore deposits; Unpubl. Ph.D. thesis, Queen's Univ., Kingston, Canada.

Neilsen, A.E.

1964: Kinetics of precipitation; MacMillan, New York, 151 p.

McNitt, J.R.

1970: The geological environment of geothermal fields as a guide to exploration; Geothermics, Spec. Issue 2, v. 1, p. 24-31.

Sibson, R.H., Moore, J.McM., and Rankin, A.H.

1975: Seismic pumping - a hydrothermal fluid transport mechanism; Geol. Soc. Lond. J., v. 131, p. 653-659.

White, D.E.

1968: Hydrology, activity and heat flow of the Steamboat Springs thermal system, Washoe County, Nevada; U.S. Geol. Surv. Prof. Paper 458-C. 109 p.

1970: Geochemistry applied to the discovery, evaluation and exploitation of geothermal energy resources; Geothermics, Spec. Issue 2, v. 1, p. 58-80.

58. LAYER SILICATES AND CLAYS IN THE RABBIT LAKE URANIUM DEPOSIT, SASKATCHEWAN

Project 750059

J. Rimsaite
Regional and Economic Geology Division

Abstract

Rimsaite, J., Layer Silicates and clays in the Rabbit Lake Uranium deposit, Saskatchewan; Current Research, Part A, Geol. Surv. Can., Paper 78-1A, p. 303-315, 1978.

In the Rabbit Lake uranium deposit, primary minerals are partly to completely altered to phyllosilicates, and locally replaced by secondary carbonates, oxides and borates. Brightly coloured, stained and bleached phyllosilicates determine the colour of host rocks, thereby producing red, green, black, grey and white alteration zones. The chemical, mineralogical and petrological studies of the phyllosilicates and their host rocks were made in an attempt to determine the relationship between different phyllosilicate groups associated with primary and secondary mineralizations, superimposed alterations, and the following geological events: retrograde metamorphism following Hudsonian orogeny; brecciation; faulting; uranium and sulphide-arsenide-selenide mineralization; and weathering. The most intensive alterations were observed along fractures and faults, and in breccias and surface alteration zones. It was found that phyllosilicates in high grade ore are poorly crystallized, with the degree of structural destruction being directly related to the uranium content of the ore.

Introduction

This paper describes methods and procedures used to study uranium mineralization in argillitized rocks containing poorly crystalline phases (phyllosilicates) in the Rabbit Lake uranium deposit, Saskatchewan. The mineralogical and chemical properties of phyllosilicates associated with pitchblende and secondary uranyl-bearing ore minerals at Rabbit Lake are described and attempts to correlate progressive alteration of the various phyllosilicate assemblages with the type and environment of alteration in the deposit vicinity are made.

This study is an extension of previous studies of mineral assemblages in the Rabbit Lake uranium deposit (Rimsaite, 1977b) and is partly based on a paper presented to the Clay Minerals Society in 1977 (Rimsaite, 1977a).

More detailed research into other aspects of this work, such as the temperatures and ages of successive alteration and mineralization are being conducted by J. Hoeve of the Saskatchewan Research Council with his work on stable and radiogenic isotopes, and fluid inclusions (Hoeve and Sibbald, 1976).

Phyllosilicate-rich Host Rocks of Uranium Deposits and Relationships to Local Petrology

Phyllosilicates are common hosts of some Australian and Canadian uranium deposits. The carnotite in the Murchinson district of Western Australia (Mann, 1974) occurs in smectite-lined cavities in calcrete. Vein type uranium deposits in the Alligator River area of Northern Australia are in chlorite and/or sericite-rich layers (Eupene, 1976; Mosher, 1976; Pedersen, 1976). In the Rabbit Lake uranium deposit, Saskatchewan, the high grade ore is in rocks altered to assemblages of chlorite, mica and montmorillonite-like aggregates derived from metasediments. Uranium mineralization is in brecciated zones where primary minerals are hydrated and altered to phyllosilicates. The recognition of original metasediments is possible only by rarely preserved textures and remnant apatite, coarse grained tourmaline, recrystallized titanium minerals and quartz. The tectonic and petrochemical evolution of the Hidden Bay area southwest of Wollaston Lake was studied by Wallis (1971) who distinguished three major tectonic episodes and six metamorphic events, followed by retrograde metamorphism at the close of the Hudsonian orogeny. Under high grade metamorphic and anatectic conditions, marine shales and limestones of Aphebian age were recrystallized to cordierite-diopside-tremolite-hornblende-biotite-microcline-plagioclase-scapolite-tourmaline schists and gneisses and diopside-bearing marbles that were altered to hydrous phyllosilicates during subsequent retrograde metamorphism. Diopside, dolomite and actinolite are major suppliers of magnesium, whereas disintegrating scapolite, microcline and plagioclase released silica, alumina, calcium and alkalis. Chloritized biotite and phlogopite supplied alkalis, iron, magnesium, silica and titanium. Feldspars are commonly replaced by a mosaic of fine grained quartz and mica-chlorite intergrowths. To study their progressive alteration and origin, the following five morphological types of phyllosilicates, PS-I to V, were distinguished on the basis of preserved textures of the original host:

Type PS-I – coarse grained chloritized biotite flakes > 50 μm in diameter (Figs. 58.1a, 58.2);

Types PS-II and III – flaky (PS-II) and fibrous (PS-III) aggregates pseudomorphously replacing and retaining the general habit of the host and generally <50 >10 μm in diameter (Figs. 58.1a to 58.1d);

Type PS-IV – groundmass phyllosilicates that have lost outlines of the original host mineral(s), (Figs. 58.1e, 58.1f);

Type PS-V – clays proper, having particle size of <2 μm (Fig. 58.4a).

Phyllosilicate aggregates usually consist of intergrowths of two or more morphological types and are seldom monomineralic. Transitions from type PS-I to PS-II and PS-III are illustrated in Figures 58.1a and 58.1c and chemical changes from metamorphic host through pseudomorphs PS-II to phyllosilicate groundmass PS-IV are given in Table 58.1.

Discussion of Mineralogy and Chemistry of Phyllosilicate Types PS-I to PS-V in Different Alteration Environments

Phyllosilicates type PS-I (Figs. 58.1, 58.2, Table 58.2, 1-I to 10-I)

These are biotites and phlogopites altered to chlorite during retrograde metamorphism (Table 58.2, Column 4; 1). They are bleached, or depleted in iron and stand out as "micaceous" patches in green, grey or beige altered rocks in the pit. At the first stages of retrograde alteration, the replacing chlorite contains remnants of the biotite host (Rimsaite, 1975, Example IVb). The same biotite flake may alter locally to muscovite and to Fe-, Mg-, or Al-rich chlorite, depending on adjacent mineral and micro-environmental differences (for example, in Table 58.2, 1-I to 5-I are all from the same flake). In drill core samples unaffected by surface weathering, chlorite replacing phlogopite is pale

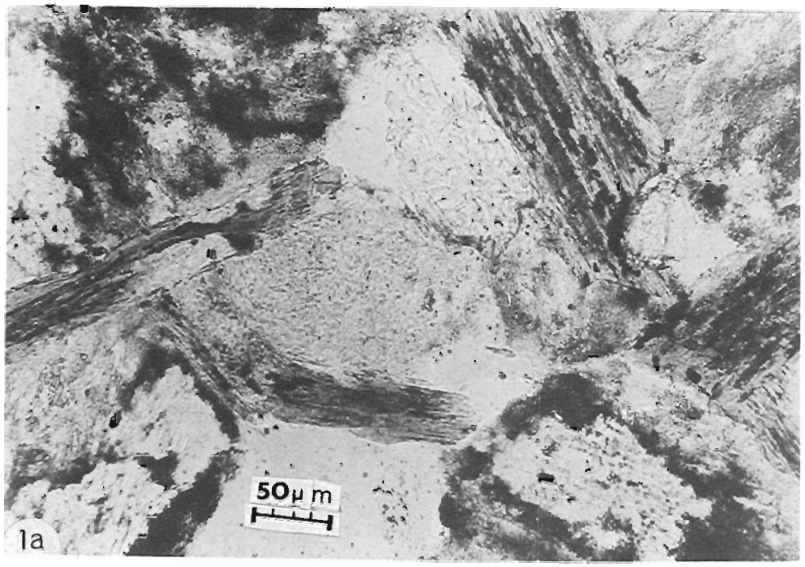
50µm
1a

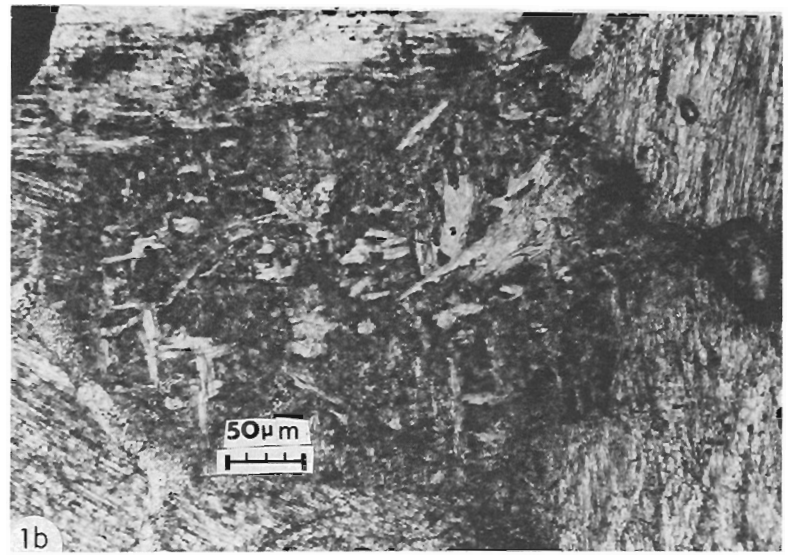
50µm
1b

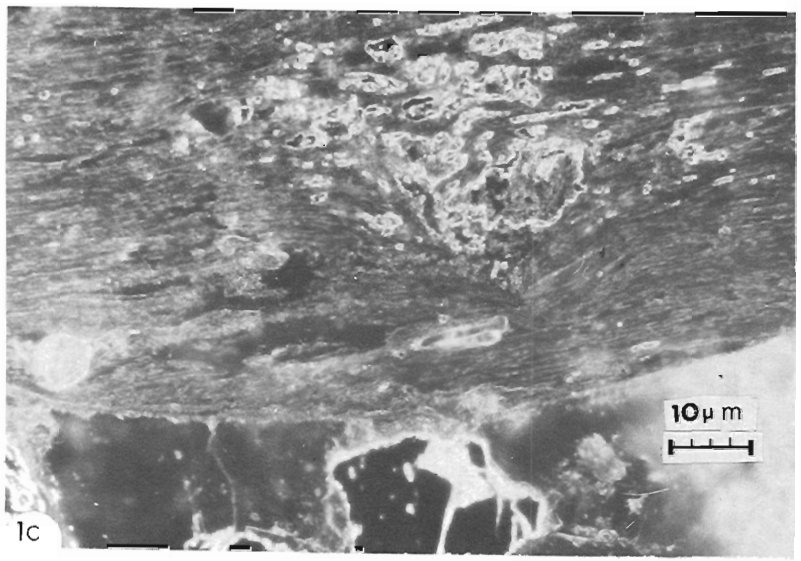
10µm
1c

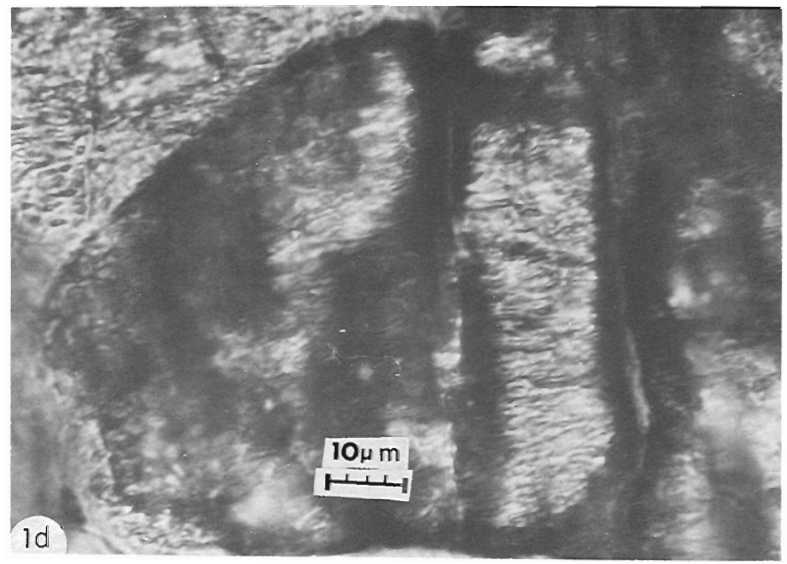
10µm
1d

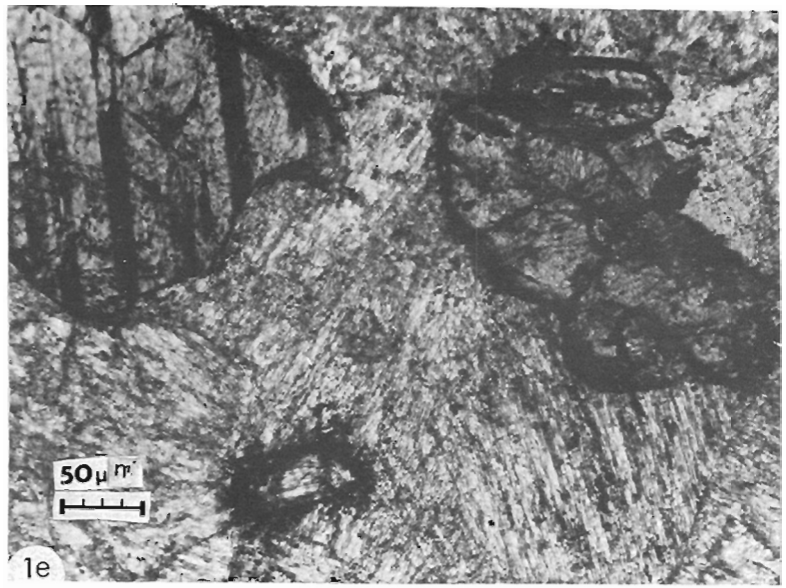

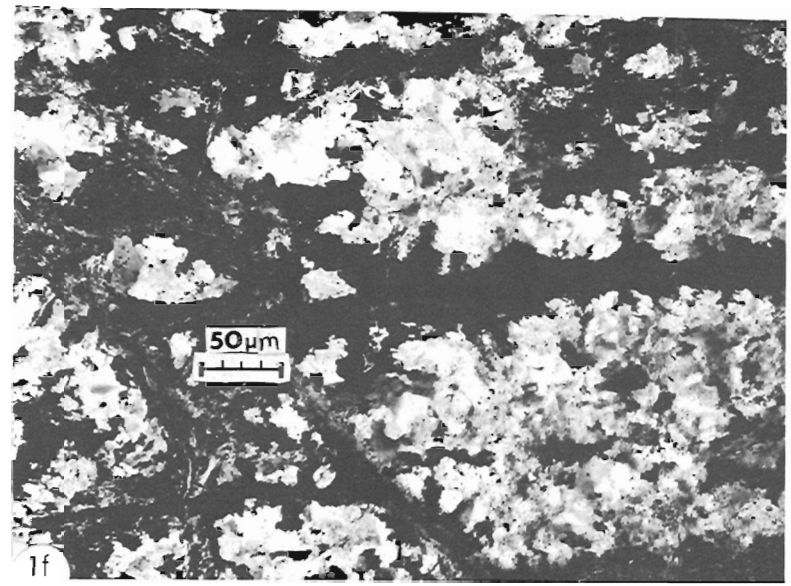

a. Coarse grained chloritized biotite "B" (PS-I) and feldspar "F" disintegrating into fine- to medium-grained flaky aggregates (PS-II) and minute clayey particles (PS-V). Gneiss from 38-foot depth. Transmitted light.

b. Microcline perthite altering to chlorite-sericite aggregates "S" that pseudomorphously replace the host and grade into flaky phyllosilicate type PS-II. Chemical changes accompanying this transformation are given in Table 58.1, 1-4. Upper gneiss from the pit. Transmitted light, +N30°.

c. Coarse grained altered biotite, grading into fibrous chlorite aggregate "C". These fibrous aggregates (PS-III) are impregnated with thin crusts of clausthalite, galena, carrollite (white) and rutile needles (Ti). Altered impure quartzite from the pit. Reflected light.

d. Pyroxene partly altered to fibrous talc-mica aggregates, phyllosilicate type PS-III. Upper gneiss from the pit, as in Figure 58.1b. Transmitted light.

e. Anatase and zircon in phyllosilicate aggregates that show a textural transition from flaky pseudomorphic type PS-II to the randomly oriented groundmass phyllosilicates of type IV. Upper gneiss as in Figure 58.1b. Transmitted light.

f. Groundmass mosaic of quartz and phyllosilicates type IV, transected by numerous fractures filled with iron oxides and banded serpentine-like aggregates (Table 58.2, 27-IV). Silicified gneiss from 250-foot depth. Transmitted light, +N30°.

Figure 58.1. Illustrations of five morphological types of phyllosilicates: PS-I to PS-V.

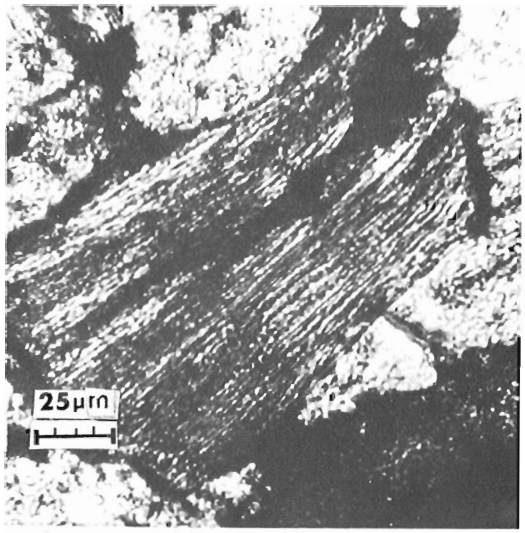

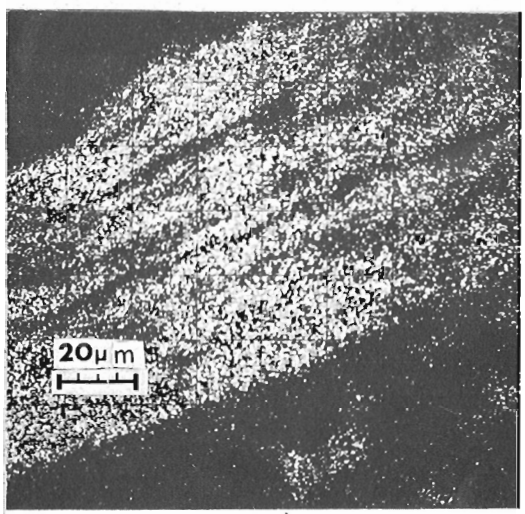

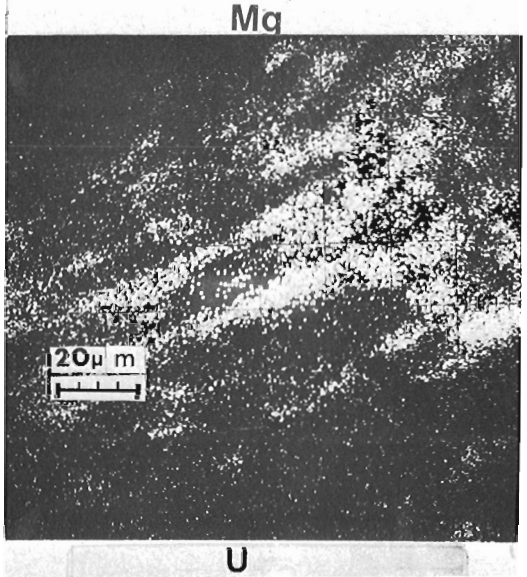

Figure 58.2

Photomicrograph (top) shows a coarse flake of chloritized biotite impregnated along (001) fractures with uraniferous compound containing ca. 70% U_3O_8, and X-ray scanning images showing distribution of Mg and U in the flake. Electron microprobe analysis by G.R. Lachance.

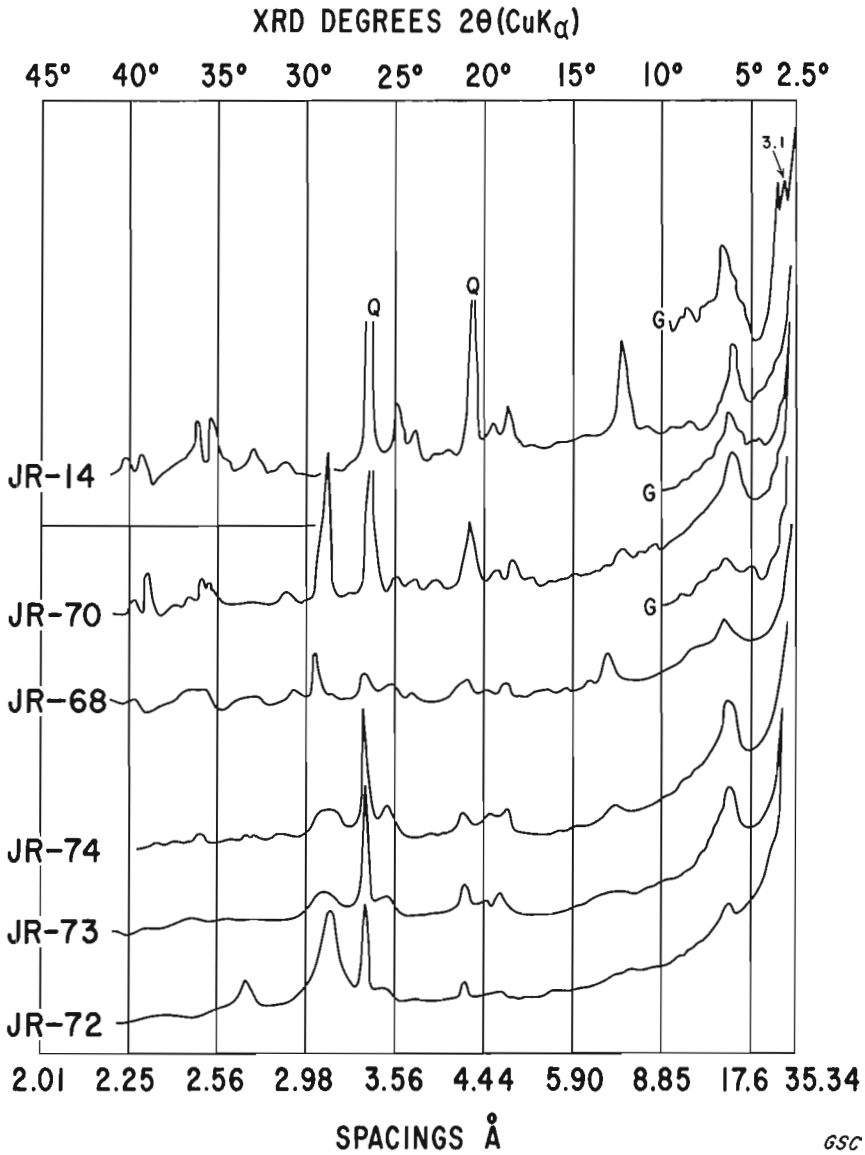

JR-14. Gneiss altered to quartzitic rock coated with red iron oxides (as that from the core in Fig. 58.5f).

JR-68. Radioactive bands composed of red stained mica-chlorite-tourmaline intergrowths from banded quartz-chlorite schist. XRD pattern is weak, indicating the presence of poorly crystalline chlorite, carbonate and traces of vermiculitic mica and pitchblende.

JR-70. Fracture contact between altered pitchblende and red fragments. The fracture is filled with quartz, calcite veinlets and poorly crystalline phyllosilicate type PS-IV.

JR-72. Altered and silicified pitchblende, minor quartz and "metamict" phyllosilicate.

JR-73 and 74. Poorly crystalline green-grey groundmass phyllosilicates type PS-IV separated from pitchblende JR-72.

Figure 58.3. X-ray diffractometer charts of radioactive breccias from oxidation zones: JR-14 is from the surface pit and five fractions: JR-68, 70, 72-74, concentrated from a drill core of red breccia at the contact with altered pitchblende, are from a depth of 187 feet (62 m), Table 58.3.

Table 58.1

Chemical changes* during alteration of feldspar and tourmaline to phyllosilicate pseudomorphs (PS-type II) and to groundmass aggregates (PS-type IV)

Specimen	Rock**	Type and Environment of alteration**	Weight per cent							
			SiO_2	Al_2O_3	TiO_2	FeO***	MgO	K_2O	Na_2O	CaO
1. Microcline	NM	Anatexis	63.7	18.0	0.00	0.0	0.0	15.8	0.7	0.2
2. Sericite, PS-II	"	I. Retrograde	48.9	36.2	0.01	0.3	0.3	9.3	0.3	0.2
3. Seric.-Chlor., PS-II	"	"	44.1	29.5	0.08	2.3	10.4	4.0	0.2	0.3
4. Seric.-Chlor., PS-IV	"	"	42.8	29.4	0.00	2.0	12.2	2.3	0.2	0.3
5. Tourmaline yellow	M, M^{IIb}	Boron metasomatism	35.2	28.2	1.3	4.9	10.9	0.02	1.8	2.2
6. Pseudomorphs, PS-II	"	I. Retrograde	42.5	31.4	0.1	3.2	3.4	1.8	0.5	1.4
7. Groundmass, PS-IV	"	"	38.4	19.1	0.02	10.8	13.0	2.5	0.6	0.8
8. Tourmaline white	M^{IIr}	VIII. Oxidation	35.8	36.4	0.0	0.3	9.8	0.0	1.0	0.0

* Electron microprobe analyses by M. Bonardi and A.G. Plant using an energy dispersive spectrometer (Lachance and Plant, 1973).

** Mineralization of host rocks: mineralized (M); secondary mineralization, "black ore" (M^{IIb}), "red ore" (M^{IIr}); unmineralized rocks (NM), for abbreviations and details see final section of text.

*** Total iron reported as FeO.

green in colour and shows the following chemical changes compared to the host: Al remains almost unchanged or slightly increases; Si and Fe slightly decrease; Ti, K and Na are totally removed and Mg oxide substantially increases from 21.5 wt. per cent in phlogopite to 32.5 wt. per cent in chlorite (Rimsaite, 1977b, Table 44.2, 21 to 24). In red rocks from an oxidizing environment chloritized micas are bright orange, red or deep green. They retain high iron and are commonly overgrown by red to opaque iron oxides and expanding clays PS-V (compare iron-rich chlorites in Table 58.2, 3-I, 7-I, 8-I and Fig. 58.3). In the weathering-bleaching environment the chlorite loses its green colour with decreasing iron content, whereas Al increases relatively, substituting for Fe, Mg and Si (Table 58.2, 9-I and 10-I). Coarse grained phyllosilicates of type PS-I are common at the contact of plagioclase-pyroxene gneisses and dolomite marbles. They also form pockets of chloritized mica aggregates and mica-chlorite patches in mica-rich layers in scapolite-microcline-bearing gneisses and in quartz-feldspar pegmatites. In mineralized rocks, coarse grained chloritized mica flakes are impregnated along (001) cleavage planes within uranium compounds and are thus important hosts for uranium (Fig. 58.2). Because the chloritization process involves liberation of silica, substantial silica is freed and under favourable conditions recrystallizes to form local silicified zones.

Phyllosilicate Types PS-II (Flaky, Figs. 58.1a, 58.1b, Tables 58.1 and 58.2, 11-II to 15-II) and PS-III (Fibrous, Figs. 58.1c and 58.1d, Table 58.2, 16-III to 18-III)

These form as a result of retrograde metamorphism and hydration and pseudomorphously replace coarse flakes of chloritized biotite type PS-I, scapolite, feldspar, pyroxene and amphibole (Figs. 58.1a to 58.1d). Two examples are given in Table 58.1 to illustrate the chemical changes involved in the alteration of feldspar and tourmaline to medium grained flaky aggregates PS-II. For the former, alteration of microcline to sericite-chlorite pseudomorphs of type PS-II in banded feldspar-diopside-mica gneisses involves substantial losses of Si, K and Na, and relative gains of Al, Ti, Fe, Mg and H_2O (Table 58.1, 1-3). The microcline is the supplier of Si, Al and K to sericite, but Ti, Fe and Mg are probably liberated from associated decomposed ferromagnesian minerals and adjacent dolomite bands.

Alteration of orange-yellow tourmaline to phyllosilicate in mineralized rock (Fig. 44.4 in Rimsaite, 1977b) involves losses of Ti, Mg, Na, K (B) and gains of Si and Al, indicating that some chemical components are derived from the host, while the others are introduced from the associated decomposing minerals. Phyllosilicate pseudomorphs of type PS-II (Table 58.2, 11-II to 15-II) are common in unmineralized, partly altered rocks that still retain their original textures. In the banded scapolite-microcline-diopside gneisses, scapolite and feldspar are partly altered to flaky sericite-chlorite intergrowths of type PS-II, whereas diopside, tremolite, actinolite and biotite bands have altered dominantly to fibrous talc, chlorite and sericite aggregates of type PS-III, some of which have high SiO_2 content (>50 wt. per cent), reflecting the composition of parent feldspar, scapolite and actinolite. The phyllosilicate pseudomorphs of type PS-II and PS-III have also been observed in altered marbles and carbonate veins replacing feldspar and diopside grains.

Alteration of coarse grained minerals to fine- or medium-grained aggregates of type PS-II and III involves a marked increase in surface area and a decrease in specific gravity with increasing hydration and hydroxyl content. In mineralized rocks these phyllosilicates are impregnated with minute specks of U, Ti, Co, Ni, Pb, U-C, and B compounds (Fig. 58.1c). As a result of increased surface area and porosity, they apparently acted as an absorbent for percolating aqueous solutions and caused precipitation of ore-forming ions. The secondary radiating tourmaline (Table 1,8 and Fig. 44.1i in Rimsaite, 1977b) also crystallizes in phyllosilicate aggregates of type PS-II from B-bearing solutions trapped in quartz interstices that were filled with altered micaceous minerals.

The colour of the phyllosilicate pseudomorphs is usually pale green because they are composed dominantly of silica, alumina and magnesia and have low to moderate iron and titanium content. Rarely, Fe-rich varieties replacing biotite, pyroxene and amphibole produce green layers and patches in altered gneisses, marbles and pegmatites. Phyllosilicate aggregates impregnated with minute specks of opaque sulphides, selenides, arsenides or U-C compounds give a black coloration to fracture surfaces and walls in the pit.

Table 58.2

Partial electron microprobe and chemical analyses* of five morphological types of secondary phyllosilicates in nine alteration environments from non-mineralized (NM) and mineralized (M) rocks at the Rabbit Lake uranium deposit, Saskatchewan

Analysis No. and phyllosilicate type	Dominant phyllosilicates	Mineralization of host rock	Alteration type and environment	Weight per cent							
				SiO_2	Al_2O_3	TiO_2	Total Fe as Fe_2O_3	MgO	CaO	K_2O	U_3O_8
1-I	Biotite alt.**	NM	1. Retrograde***	30.8	15.7	1.8	14.2	20.8	0.05	2.66	0.0
2-I	Mg-chlorite	NM	"	32.3	13.1	0.1	10.2	26.9	0.15	0.05	0.0
3-I	Fe-chlorite	NM	"	24.6	18.4	0.2	26.1	14.5	0.00	0.06	0.0
4-I	Al-chlorite	NM	"	32.1	27.0	0.03	1.8	17.9	0.00	0.26	0.0
5-I	Muscovite	NM	"	49.8	32.0	0.16	1.5	2.2	0.00	9.80	0.0
6-I	Chlorite	M	2. Brecciation	28.6	22.0	0.01	2.5	26.4	0.00	0.03	0.0
7-I	Chlorite green	M	8. Oxidation	29.5	17.4	0.06	20.5	20.4	0.01	0.01	0.0
8-I	Chlorite red	M	"	35.6	19.0	0.13	21.3	7.3	0.48	1.22	0.0
9-I	Chlorite green	NM	9. Weathering	34.0	17.0	0.20	3.0	34.0	0.10	0.10	0.0
10-I	Chlorite pale	M	"	30.0	22.0	0.40	2.0	32.0	0.14	0.10	0.5
11-II	Chlorite	NM	1. Retrograde	32.1	26.4	0.05	3.0	20.6	0.05	0.18	0.0
12-II	Eastonite-Chlor.	NM	"	40.2	16.2	0.00	8.9	22.1	0.14	3.24	0.0
13-II	Sericite	NM	"	48.9	36.2	0.01	0.3	0.3	0.2	9.34	0.0
14-II	Sericite-talc	NM	"	54.3	22.2	0.01	1.2	6.3	0.07	9.64	0.0
15-II	Chlorite	NM	8. Oxidation	34.8	23.2	0.01	3.9	20.6	0.22	0.55	0.0
16-III	Chlorite	NM	1. Retrograde	33.2	13.1	0.04	10.3	26.4	0.20	0.02	0.0
17-III	Talc-mica	NM	3. Carbonate veins	59.0	1.1	0.02	5.6	22.6	2.4	1.03	0.0
18-III	Chlorite	M	5. Co,Ni,As,Se,S	34.0	18.0	0.00	5.0	28.0	0.40	0.30	0.8
19-IV	Kaolinite-Chlor.	M	2. Brecciation	41.6	34.2	0.00	0.2	2.1	0.60	1.00	0.0
20-IV	Mica-chlorite	M	"	24.8	25.6	0.00	7.7	12.2	0.32	2.23	0.0
21-IV	Mica-chlorite	M	4. In pitchblende	41.6	15.6	0.07	5.8	7.1	0.29	3.41	0.0
22-IV	Eastonite-Chlor.	M	"	42.7	19.9	0.09	8.3	11.1	0.20	6.50	0.0
23-IV	Mica-chlorite	M	4. In coffinite	48.7	11.4	0.07	7.9	8.4	0.04	5.64	0.6
24-IV	Chlorite	M	5. Co,Ni,As,S	32.6	17.0	0.03	11.4	18.8	0.38	0.12	0.0
25-IV	U-phyllosilicate	M	6. Recryst, with U	37.5	21.7	0.10	6.1	6.1	1.20	1.1	21.3
26-IV	U-phyllosilicate	M	"	14.0	2.5	0.0	0.0	0.1	1.60	0.1	74.9
27-IV	Serpentine-like	M	7. Fractures	34.1	5.3	0.04	22.5	20.8	0.23	0.05	0.0
28-IV	Chlorite	NM	7. In faults	46.0	15.5	0.30	2.5	26.5	0.20	0.10	0.0
29-IV	Mica-Chlorite	MII	"	42.0	15.0	1.50	2.0	7.0	1.00	3.0	15.8
30-IV	Chlorite	NM	8. Oxidation	28.5	18.7	0.03	16.5	22.8	0.00	0.00	0.0
31-IV	Chlorite	NM	"	29.6	18.4	0.04	10.1	23.8	0.03	0.01	0.0
32-IV	Mica-Chlor, red	M	"	51.0	8.2	0.03	19.5	7.8	0.02	4.60	0.0
33-IV	Chlorite	MII	8. In Fe oxide	47.6	2.3	0.05	31.3	8.1	1.25	0.55	0.0
34-V	Montm.-Chlor.	MII	9. Regolith	39.0	21.0	0.15	3.0	19.0	1.20	0.20	2.2
35-V	U-Montm. green	MII	9. Weathering and Bleaching	33.7	25.9	0.15	0.7	2.3	1.14	1.71	6.6
36-V	U-Montm. beige	MII		35.2	25.6	0.08	0.4	2.5	2.10	2.10	2.0
37-V	Montm. green	MII	9. Weathering	43.5	21.2	0.13	4.8	3.7	1.00	4.13	0.0
38-V	Montm. white	MII	9. Bleaching	44.6	28.0	0.13	1.7	2.7	1.10	2.05	0.0

* Analysts: M. Bonardi, G.R. Lachance, A.G. Plant and Staff of the Analytical Chemistry Section.

** For abbreviations see final section of text.

*** Explanation of Table 58.2: types and environments of alteration are abbreviated as follows: 1, retrograde metamorphism following Hudsonian orogeny; 2, brecciation; 3, carbonate veins; 4, uranium ore; 5, sulphide, selenide, arsenide mineralization; 6, recrystallization in the ore and reactions between phyllosilicates and uranium; 7, fractures, faults, slickensided surfaces, gouge; 8, regolith and recent weathering, oxidation zones above groundwater table and in faults; 9, weathering zones, bleaching and removal of iron by percolating aqueous solutions. The columns from left to right indicate analyses numbers and types of phyllosilicate PS-I to PS-V, followed by the dominant mineral(s) in the aggregate, types of mineralization of the rock, various alteration environments, and chemical composition.

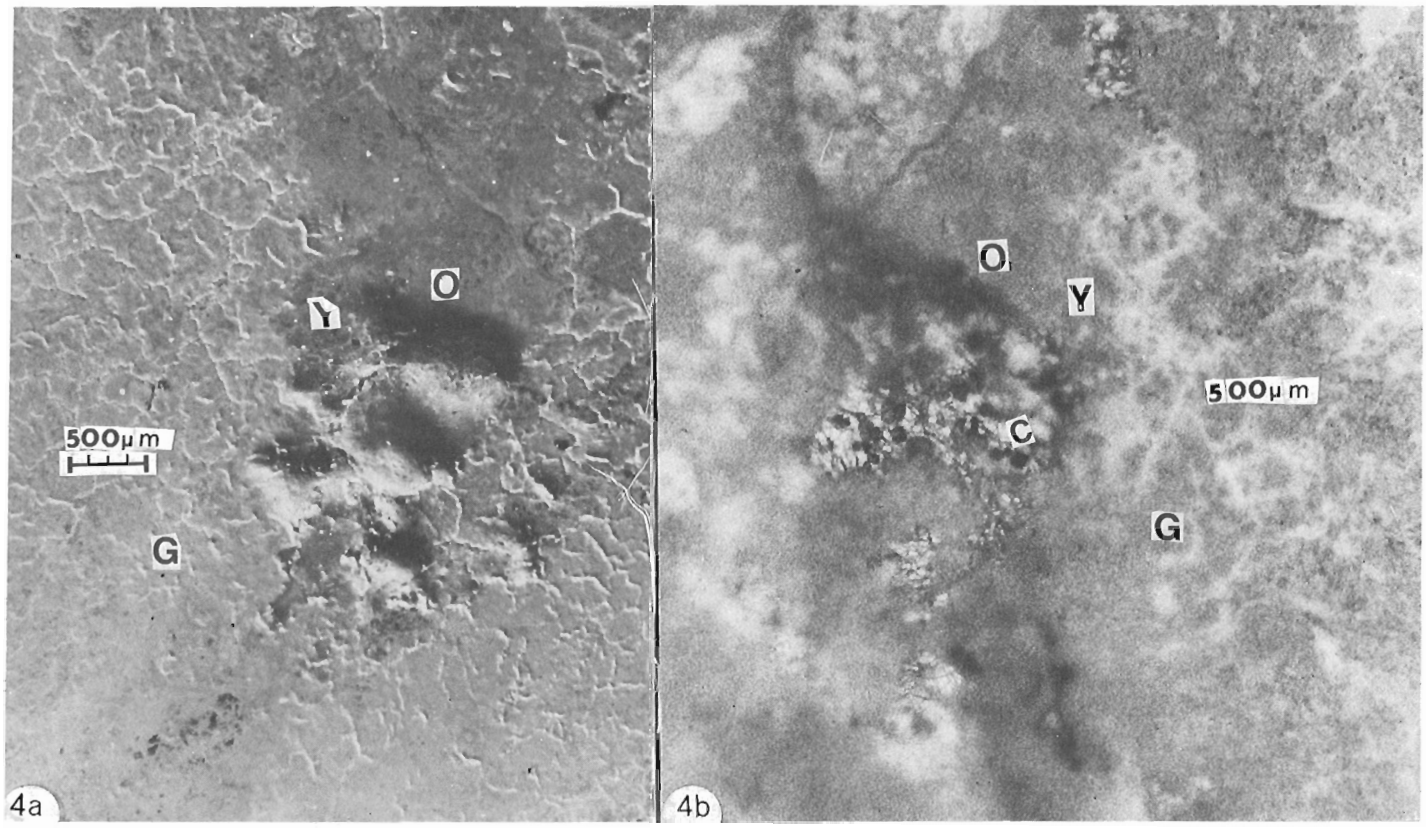

a. Photomicrograph showing replacement of radioactive compounds by white clay along fractures (white net), and blister-like swellings of montmorillonite in polished thin section. Secondary uranium ore from the pit (GSC 202203-L).

b. Autoradiograph of polished thin section in Figure 58.4a showing the relationship between various radioactive compounds and nonradioactive clay (white). The intensity of grey, or blackening of the autoradiograph, varies with uranium content in the aggregates (GSC 203226-F).

Figure 58.4. Fine grained intergrowths of orange "O", yellow "Y" and green "G" uranyl-bearing compounds with white montmorillonitic clays "C".

Groundmass Phyllosilicates, Type PS-IV (Figs. 58.1f and 58.6, Table 58.2, 19-IV to 33-IV)

The transition from pseudomorph aggregates to textureless groundmass is illustrated in Figure 58.1e. Chemical differences between the flaky pseudomorphs replacing microcline and tourmaline and their groundmass are shown in Tables 58.1, 4 and 7. With gradational loss of the original pseudomorphous textures, phyllosilicates of type PS-IV lose chemical integrity with their parent minerals. Depending on their origin and subsequent alteration, the phyllosilicates show varying mineralogical and chemical compositions. Chlorite is the main component in aggregates, followed by mica, serpentine and talc that locally grade to smectite and kaolinite-bearing clays. Much of the material is poorly crystalline or "metamict". Poorly crystalline, green grey phyllosilicates of type PS-IV are common hosts for "black uranium ore". They have a moderate iron and magnesium content, Al equal to the sum of Fe and Mg, and moderate silica which increases in more silicified samples. The phyllosilicates from the high grade ore zones are nearly amorphous to X-rays ("metamict") with structural destruction apparently being a factor bearing on uranium content of the ore (Figs. 58.3 and 58.6 and Table 58.3). Their X-ray patterns are usually dominated by well-crystallized quartz and carbonate impurities (Fig. 58.3), whereas weak and diffuse reflections of intergrowths resembling chlorite, glauconite, hydromica and montmorillonite are hardly distinguishable from the background. These X-ray patterns become slightly stronger after heat treatments of the aggregates (Fig. 58.6).

Slickensided surfaces and fracture fillings contain chlorite-like minerals with moderate to high iron content, and late fractures are filled with serpentine-like, low-alumina colloform aggregates that may possibly be related to late basic dykes in the area.

The colour of phyllosilicates of type PS-IV is similar to that of types PS-II and III but varies with the presence of uranophane, tourmaline and/or iron oxide crusts. Uranium-bearing phyllosilicates are brown, green, orange or yellow in ordinary daylight and greenish brown to opaque in transmitted light. The colour of irradiated phyllosilicates adjacent to strongly radioactive minerals is similar to that in discoloured pleochroic halos surrounding radioactive inclusions in micas.

Phyllosilicates of Type PS-V, or Clays (Figs. 58.4, 6, 7, 8; Table 58.2, 34-V to 38-V)

Clays are common constituents in fracture fillings, in gouge, and in weathering zones at the surface. They also form white cappings around secondary uranium ore. Clays crystallize as a result of further hydration and breakdown of groundmass phyllosilicates of type PS-IV with which they are commonly intergrown. Surface clays washed into the pit contain iron oxides and abundant chips of quartz and carbonate. These red mobile surface clays impregnate fractures in breccias thereby contaminating older rocks in the pit. Fine grained argillitized rocks host and ultimately replace secondary uranyl-bearing ore minerals (Fig. 58.4). The common clay minerals in specimens examined from the

Table 58.3

Selected chemical analyses* of altered and mineralized rocks from the Rabbit Lake Uranium Deposit

Analyses No.**	Specimens and major constituents ***	Type of alteration and mineralization***	Weight per cent											
			SiO_2	Al_2O_3	Fe_2O_3****	MgO	K_2O	Na_2O	CaO	H_2O	F	Cl	U_3O_8	PbO
JR-7	Paleoclay	$4,9;M^{IIb}$	42.	16.	3.	24.	0.2	0.5	1.0	12.4	0.22	0.06	0.3	0.0
RKp-10	"Black ore"	4,7;M	34.	7.	12.	12.	1.2	0.0	1.4	11.8	0.07	0.03	13.	1.
JR-14	Qtzite and Fe	8;NM	59.	13.	9.	11.	0.4	0.2	0.3	8.5	0.13	0.15	0.0	0.0
Replacement of "red U ore"***** by clay PS-V, surface weathering in the pit (Figs. 58.4 and 58.6)														
JR-23	Orange ore	$4,8;M^{IIr}_{IIr}$	6.	0.4	0.2	0.4	0.3	0.0	2.0	8.	0.02	0.01	59.	18.
JR-26	Yellow ore	$4,8;M^{IIr}_{IIr}$	3.	4.	0.3	1.0	1.0	0.0	3.0	11.3	0.03	0.01	7?.	2.5
JR-29	Green ore	$4,8;M^{IIr}_{IIr}$	7.	2.	0.3	1.0	0.4	0.0	4.0	12.	0.05	0.01	70.	1.5
JR-33	Montm. and Qtz.	$4,9;M^{IIr}_{IIr}$	47.	7.	1.	5.0	2.5	1.0	2.5	10.6	0.19	0.05	7.	9.
JR-34	Montm. and Qtz.	$4,9;M^{IIr}_{IIr}$	62.8	12.8	1.	5.2	2.4	0.3	0.8	10.5	0.23	0.03	?.	2.
Silicification and alteration of "black U ore" in clay PS-V, surface weathering in the pit (Fig. 58.7b)														
JR-38	Pitchblende on Qtz.	$4;M^{IIb}$	47.	2.	0.4	0.1	0.7	0.0	2.0	3.2	0.09	0.03	41.	1.5
JR-40	Pitchblende in PS-V	4,9;M	13.	4.	0.4	2.	1.0	0.0	2.0	4.2	0.14	0.04	69.	3.
JR-43	Pitchblende alt.	4,8;M	41.	5.5	1.5	4.	0.3	0.0	1.5	7.4	0.05	0.01	36.	0.8
JR-45	Pitchblende in Qtzite.	$8;M^{IIb}_{IIb}$	67.	7.5	2.	8.5	0.2	0.5	0.8	0.5	0.08	0.04	3.5	0.2
JR-53	Coffinite	$4,9;M^{IIb}$	10.	3.	0.7	2.	1.	0.0	1.6	8.4	0.03	0.01	60.	0.5
Fibrous chlorite PS-III grading into clay PS-V, impregnated with selenide and sulphides (Figs. 58.8 and 58.1c)														
JR-54	Clay fraction	$5,9;M^{II}$	38.	10.	10.	15.	0.1	0.0	0.5	21.2	0.07	0.04	4.5	0.1
JR-55	Fibrous PS-III	$1,5,9;M^{II}$	34.	18.	5.	28.	0.3	0.0	0.4	15.1	0.17	0.08	0.8	0.0
Fractions from a red banded quartz-phyllosilicate rock in contact with silicified pitchblende														
JR-68	Reddish PS-I	2,4,8;M	36.	7.	20.	7.	1.	0.0	8.	8.6	0.06	0.03	5.	0.5
JR-70	Contact-fracture	2,3,4;M	47.	10.	8.	7.	1.	0.2	10.	9.2	0.07	0.02	10.	0.3
JR-72	Pitchblende, alt.	2,4,8;M	10.	1.	5.	5.	0.	0.	0.	0.	0.15	0.01	60.	0.2
JR-74	Groundmass, PS-IV	4,8,9;M	35.	14.	3.	7.	0.	0.	2.	11.7	0.13	0.03	22.	0.1

* Analysts: G.R. Lachance and Staff of the Analytical Chemistry Section.
** Specimens and analyses numbers are the same as on X-ray diffractometer charts in Figures 58.3, 58.6 and 58.8.
*** For symbols and abbreviations see Table 58.2 and final section of text.
**** Total iron as Fe_2O_3. In U-bearing samples FeO values are not reliable.
***** The same samples as those analyzed for rare earths (Rimsaite, 1977a, Table 44.4, p. 245).

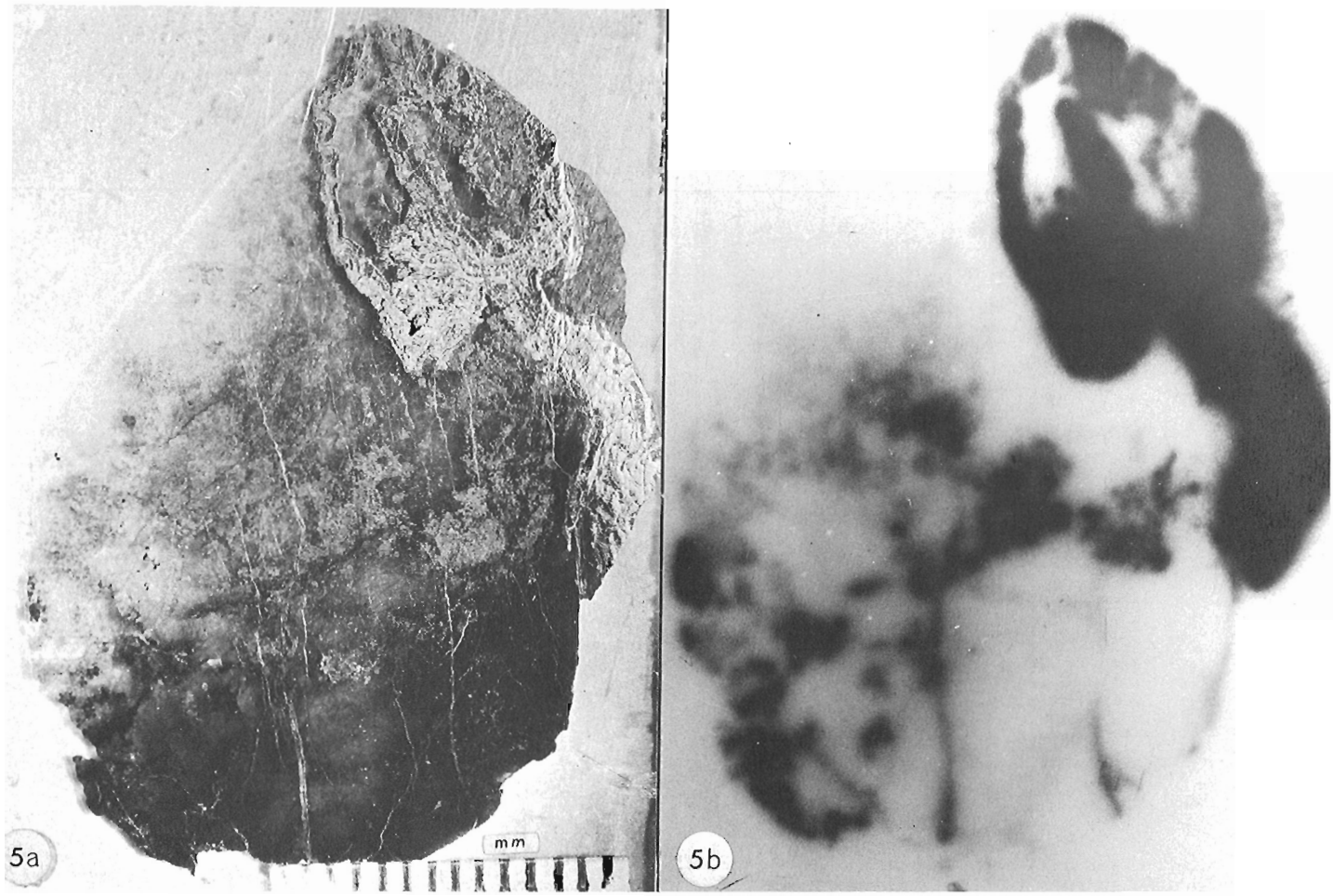

a. Photomicrograph taken in semi-transmitted/-reflected light showing light-grey reflecting pitchblende, in the upper field and fractures, in a groundmass of yellow and green phyllosilicates containing remnants of disintegrating orange tourmaline (Table 58.1) and quartz, and semi-transparent uraniferous phyllosilicate type PS-IV (Table 58.1). Details of pitchblende bands and of host rock are illustrated in a previous paper (Rimsaite, 1977a, Figs. 44.3a and b, p. 243, and 44.4f, p. 245).

b. An autoradiograph of the above section showing strongly radioactive pitchblende (black), disseminated uraniferous specks (grey) and moderately radioactive patches or uraniferous phyllosilicates (light grey) (GSC 203226-E).

Figure 58.5. Polished thin section of black uranium ore.

weathered zones in the pit and in drill cores are, in order of decreasing abundance: chlorite, glauconite, hydromica, montmorillonite and kaolinite. The main changes involved in argillitization are increases in surface area, hydration (to 30 wt. per cent H_2O), gradational losses of Mg, Fe, Ti and U, and, in late stages of alteration and bleaching, further losses of iron and potassium from montmorillonite interlayers.

In the early stages of alteration, greenish montmorillonite replacing orange and yellow uranyl-bearing ore minerals, contains 4 wt. per cent K_2O. After further hydration, the potassium decreases with decreasing iron content and the montmorillonite loses green colour (Table 58.2, 37-V and 38-V). In weathered and bleached rocks, clay consists mainly of hydrous silica and alumina compounds. Some iron, lead and uranium may be present in the structure of the clay minerals, probably in the interlayer, or as fracture coatings in secondary uranyl-bearing minerals, such as zippeite, bayleyite and uranophane. In some montmorillonitic clays the lead content exceeds or equals that of uranium (Table 58.3, JR-33 and JR-34). In such samples, lead is probably in secondary lead minerals associated with iron oxide crusts.

Depending on the abundance and distribution of iron, uranium-bearing minerals, anatase and tourmaline, the clays are varicoloured. All clays contain quartz fragments and remnants of coarser grained phyllosilicates. They are transected by numerous fractures filled with carbonate and goethite and locally contain quartz and carbonate minerals coated with hematite which produce white and red coloration of the rock. Depletion of iron and bleaching is probably caused by organic acids in percolating aqueous solutions, analogous to bleaching reactions observed in laterites and bauxite (Hill, 1977).

Fine grained grey clays in breccias are hard and consist mainly of chlorite. They possibly represent bleached and altered rocks of the regolith. The less compact clastic surface clays and fine grained fracture fillings exposed to surface weathering are more hydrated than the compact fragments and grade to montmorillonite. Radioactive minerals present in late fractures are mainly coffinite in carbonate and quartz veinlets and uranophane in carbonate and goethite filled veinlets. The coloform uranophane crystallizes along the walls whereas siliceous goethite fills

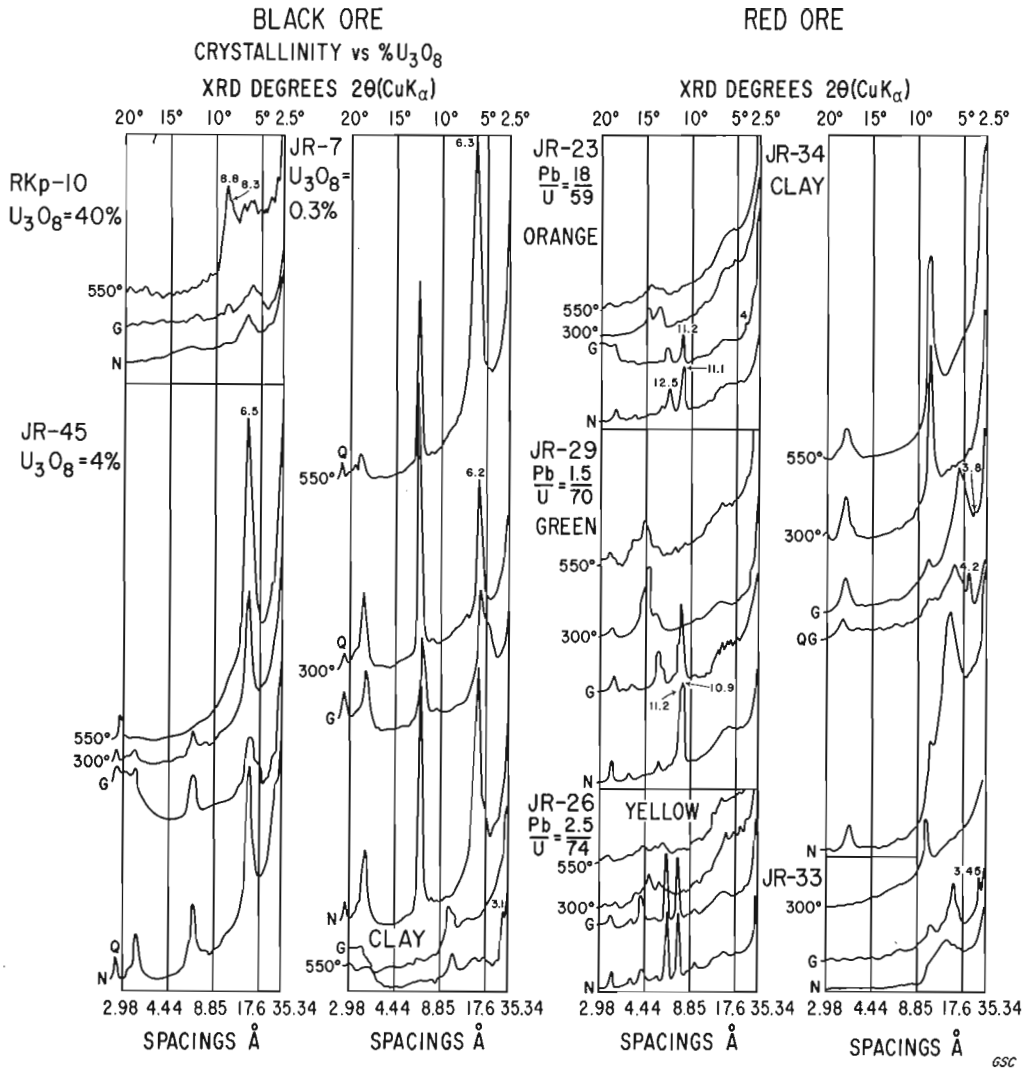

Figure 58.6. X-ray diffractometer patterns. The two columns at left show the relationship between crystallinity and uranium contents of the samples; RKp-10 (Fig. 58.5) is strongly radioactive and consists of poorly crystalline phyllosilicates, Type PS-IV that produce weak mica, chlorite and montmorillonite reflections. Samples JR-45 and JR-7 are less radioactive and better crystallized. Shown in the third column are uranyl-bearing compounds masuyite-uranophane with decreasing lead/uranium ratios from orange aggregate JR-23, through yellow JR-26 to green JR-29 (note shift of peaks and decreasing intensities in heated samples). In the fourth column at right, are associated white and pink montmorillonitic clays JR-33 and JR-34 that coat and replace the uranyl-bearing aggregates; all fractions were concentrated from the same specimen illustrated in Figure 58.4. Other data and symbols are as in Figure 58.8.

the central portion of the fracture. Goethite and kaolinite aggregates are commonly poorly crystallized or amorphous to X-rays. Chlorite and micaceous minerals have unusual compositions, the dominant varieties being enriched in silica, alumina and magnesia.

Summary and Conclusions

Distribution and properties of secondary phyllosilicates were studied in mineralized and unmineralized rocks from different alteration environments at the Rabbit Lake uranium deposit. Five morphological types are distinguished. Their chemical and mineralogical properties and distribution in nine alteration environments in mineralized and unmineralized rocks are summarized.

Based on samples examined during this work, the main results can be summarized as follows:

1. As a result of superimposed fracturing, hydration and redistribution of elements, metamorphic rocks and minerals have been altered to rocks resembling clays and sediments.

2. Coarse grained and medium grained phyllosilicate pseudomorphs of type PS-I, II and III retain the general outline and texture and in part chemical character of the host assemblages. They consist of chlorite, mica and talc intergrowths and in mineralized rocks are impregnated with U, As, Co, Ni, Pb, S, Se, C and Ti compounds. They are important carriers of ore

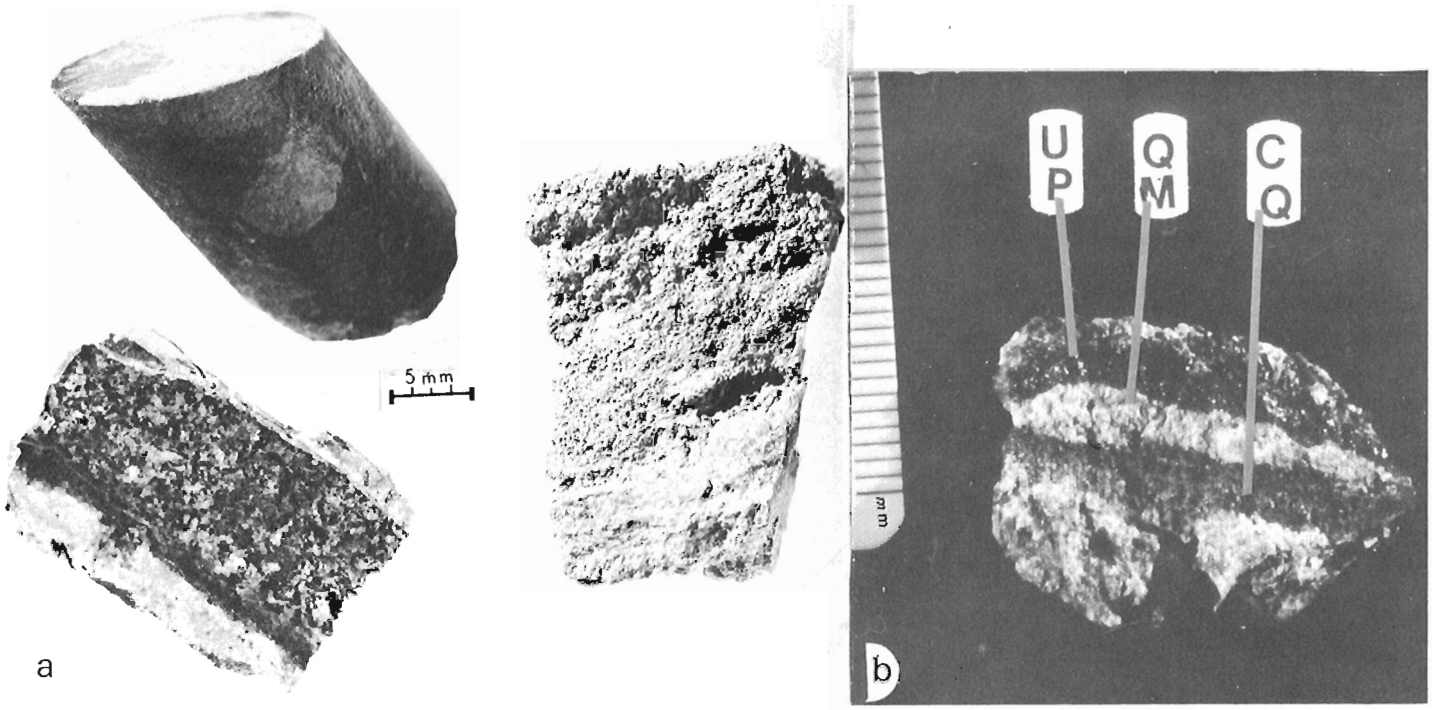

Figure 58.7a. Bleached rocks altered to hydrous phyllosilicates and in part replaced by secondary carbonates and silica. Partly bleached red core at top left; argillitized gneiss and white clay, phyllosilicate type PS-V, left; and porous altered rock formed in a surface stream as a result of picked out clay particles by streaming water, left.

Figure 58.7b. Black bands of speckled pitchblende (UP) and coffinite (CQ) in quartz-montmorillonite host (QM), Figure 58.8 and Table 58.3 JR-40 and JR-53.

minerals in low grade ore. Chemically the aggregates consist mainly of silica, alumina and magnesia, and contain moderate to low iron and potassium content.

3. Further disintegration and interactions between phyllosilicate pseudomorphs of types PS-I, II and III result in progressive disintegration of the original texture and the formation of textureless phyllosilicate groundmass (type PS-IV) that can be distinguished from a texturally similar assemblage of sedimentary origin by the presence of remnant apatite, tourmaline, quartz, recrystallized anatase pseudomorphs, and rare feldspar. The groundmass phyllosilicates of type PS-IV have similar chemical composition to that of pseudomorphs, but show less variation in individual samples. In high grade "black uranium ore" the phyllosilicates are poorly crystalline or "metamict" and are composed of intergrowths of chlorite, glauconite and hydromica having a prominent expanding component. Reactions between the phyllosilicate matrix and remobilized uranium following fracturing and brecciation, result in the formation of U-bearing phyllosilicates.

4. Clays of type PS-V form in fractures and breccias affected by weathering and radioactivity of adjacent uranium ore as a result of structural and chemical breakdown of metamorphic minerals and other secondary phyllosilicates. They consist of fine grained aggregates of chlorite, glauconite, hydromica, montmorillonite, kaolinite and allophane that usually contain remnants of the coarser grained hosts (PS-I, II, III and IV), quartz chips and Fe and Ti oxides. They host and gradationally replace uranyl-bearing secondary ore minerals, and in the advanced stages of hydration and alteration, they consist dominantly of silica, alumina and water.

5. In high grade ore, groundmass phyllosilicates of type PS-IV are poorly crystallized with structural destruction being a factor of uranium content in the ore. Montmorillonitic clays replacing secondary uranium mineral aggregates in the pit are relatively well crystallized, although some kaolinite-like phases are amorphous to X-rays.

6. Uranium-bearing and associated phyllosilicates in high grade ore may easily be overlooked on X-ray powder patterns because of their poor crystallinity and crystal structure destroyed by strong radiation. The amorphous or "metamict" U-bearing aggregates can be identified and studied by comparing autoradiographs with the optical properties of moderately radioactive aggregates removed from the rock and studied in oil immersion mounts. Their chemical compositions can be determined by electron microprobe and thermogravimetric analyses.

7. Red iron oxide coatings on quartz and phyllosilicate surfaces along fractures and in marbles are attributed to precipitation reactions similar to those in the formation of "terra rosa" in karst. This may involve precipitation of iron and other oxides from aqueous solutions as a result of differences in redox potential. Remobilization, bleaching of red rocks, and removal of iron following reduction of hematite to goethite, is probably due to increased activity of organic acids in percolating solutions. Uranium can be present in oxidation zones in uranyl-bearing compounds.

Analytical Methods and Procedures

Preparation of samples

Hand specimens from the Rabbit Lake pit and core samples were examined under a binocular microscope to study the relationship between altered and mineralized areas

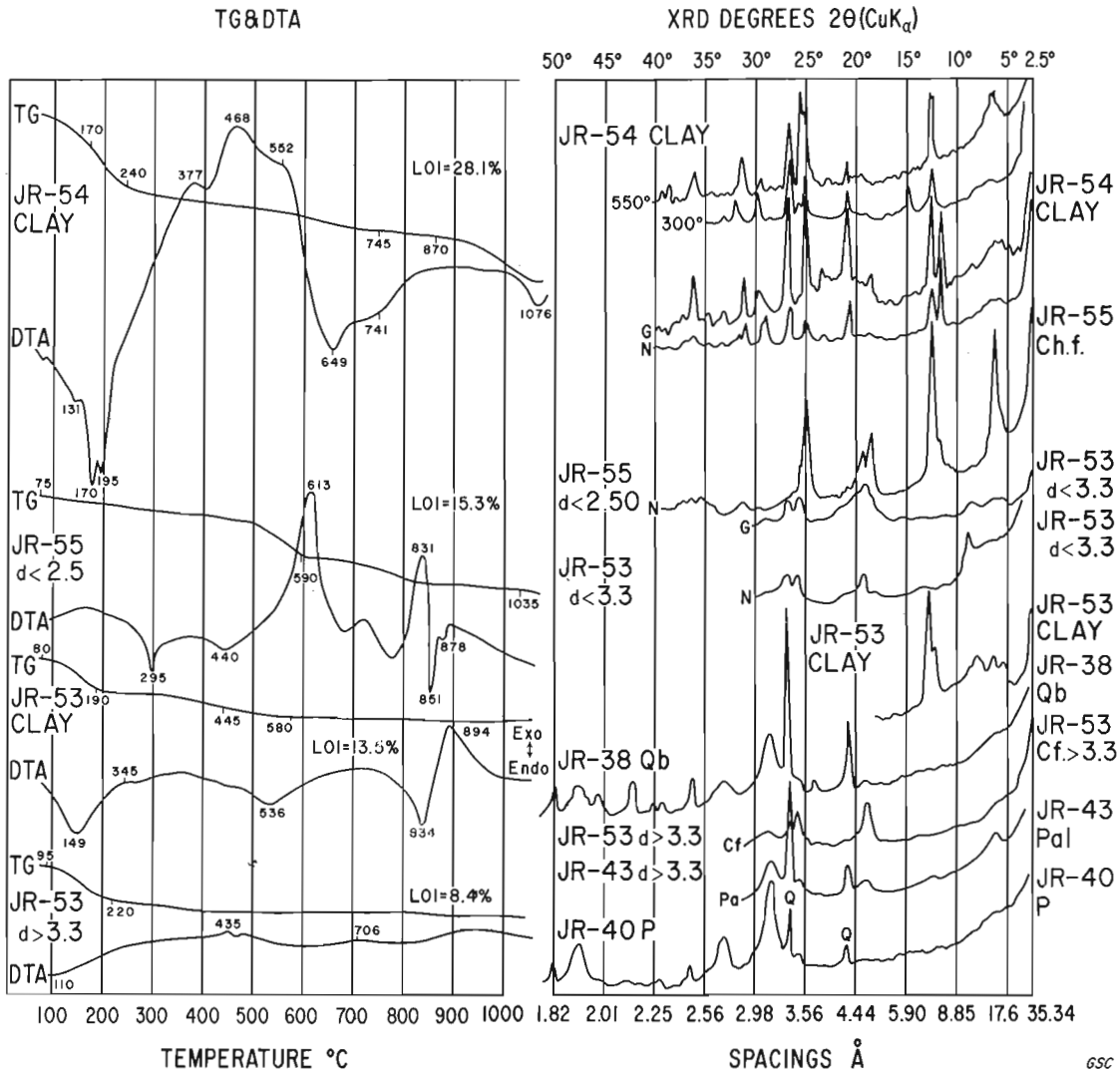

XRD, TG&DTA OF RADIOACTIVE AND ASSOCIATED MINERALS

XRD Samples

N = untreated

G = glycerated

300°C and 500°C = specimens heated at 300°C and 500°C one hour.

JR-38 = Black quartz coated with pitchblende.

JR-40 = Bands of shiny pitchblende, contaminated by quartz.

JR-43 = Corroded pitchblende partly replaced by quartz.

JR-53 Cf, d > 3.3 = Black-green coffinite in quartz and glauconite-like paleoclay from the pit.

JR-53, d < 3.3 = Poorly crystallized, glauconite-like paleoclay separated from the coffinite fraction, d > 3.3.

JR-53 "clay" = Clay fraction separated from the glauconite-like paleoclay containing expanding layers and kaolinite.

Figure58.8. Thermogravimetric (TG, 6°C/min), differential thermal (DTA, 10°C/min) and X-ray diffraction analyses (XRD, Ni-filtered Cu-radiation at 45kV and 16mA) of radioactive and associated minerals. LOI = weight loss on ignition.

(Figs. 58.7a and 58.7b). The mineralized and phyllosilicate-rich fragments were separated from less altered rock by hand picking, and further concentrated by heavy liquid, isodynamic separator, centrifuge and sedimentation procedures (Rimsaite, 1967). The settling time for the fine clay and colloidal particles, referred to here as "clay", was from two weeks to one month.

Mineral identification

The phyllosilicate intergrowths were examined in oil immersion mounts under the microscope in the refractive index range from 1.34 to 1.74. Fine grained fractions were analyzed by an X-ray diffractometer in natural condition ("N"), glycerated condition ("G"), and after heating at 300°C and 550°C for one hour (Figs. 58.3, 58.6, 58.8). Selected samples were studied by thermogravimetric (TG) and differential thermal analyses (DTA) at heating rates of 6°C/min and 10°C/min, from room temperature to 1200°C (Fig. 58.8). Optical studies in oil immersion mounts were useful for the detection of poorly crystalline or "metamict" phases which cannot be identified by the conventional XRD powder method, and were thus commonly overlooked in the past.

Polished thin sections and autoradiographs

The relict original textures and the relationships between phyllosilicate-rich groundmass and the ore minerals were determined in polished thin sections which allows simultaneous study of opaque ore minerals in reflected light and of transparent minerals in transmitted light (Fig. 58.5a). Special techniques, such as oblique illumination and partly crossed nicols, were used to study semi-transparent brightly coloured ores and amorphous aggregates.

The distribution of strongly, moderately, and weakly radioactive substances was studied in autoradiographs of the same polished thin sections (Figs. 58.4b and 58.5b), using a photographic film exposed to radiation from one hour to three weeks, depending on the uranium content of the samples.

Electron microprobe and chemical analyses

The relationship between phyllosilicates and uranium-bearing compounds was studied by an electron microprobe in X-ray scanning images (Fig. 58.2). Chemical compositions of fresh and altered minerals and chemical changes accompanying progressive hydration and alteration of minerals and rocks were determined by quantitative electron microprobe analyses (Lachance and Plant, 1973), and by rapid chemical and spectrographic analyses (Tables 58.1, 58.2, 58.3).

Abbreviations

The following abbreviations are used in Tables and Figures:

For minerals: alt. = altered; Chlor. = chlorite; Montm. = montmorillonite; Pitchbl. = pitchblende; PS = phyllosilicates; Q, Qtz, Qtzite = quartz, quartzite; U = uranium-bearing, uraniferous; Fe = iron, iron bearing, iron oxide.

For mineralization of host rocks: NM = unmineralized rock, U_3O_8 <0.14 wt. per cent; M = mineralized rock, U_3O_8 >0.14 wt. per cent; M^{II} = secondary mineralization; M^{IIb} = secondary "black uranium ore" (coffinite, pitchblende rims, type P-V, U-C compounds); M^{IIr} = secondary, coloured, uranyl-bearing ore (minerals bayleyite, masuyite, uranophane, zippeite).

Acknowledgments

This work was supported by DTA and TG analyses by W.S. Bowman of CANMET, X-ray identifications of minerals by A.C. Roberts, emission spectrographic analyses by P.G. Bélanger, G. Bender and K. Church, and rapid chemical analyses by G.R. Lachance and the staff of the Analytical Chemistry Section, Geological Survey of Canada. Electron microprobe analyses were provided by M. Bonardi, G.R. Lachance and A.G. Plant and preparation of photographic plates and autoradiographs was done by Jeanne White and the staff of the Photographic Section, Geological Survey. Drawings were prepared by the staff of the Cartography Section. The assistance of these persons is gratefully acknowledged. Gulf Minerals Canada Limited and Uranerz Canada Limited are thanked for their helpful co-operation and guidance at the minesite.

References

Eupene, G.S.
1976: The Ranger I uranium deposit; in Mining Centres of Northern Australia, Ed. Ryan, G.R., Excursion Guide No. 49AC, 25th Int. Geol. Congr., Sydney, Australia, p. 3-5.

Hill, V.G.
1977: Syngenetic and diagenetic changes in Jamaican bauxites; Joint CMS and ICSOBA Meeting, Kingston, Jamaica; Tech. Prog. Abstr., p. 15.

Hoeve, J. and Sibbald, T.I.I.
1976: Rabbit Lake uranium deposit; Proc. Symposium 10 Nov. 1976: "Uranium in Saskatchewan", Sask. Geol. Soc., Spec. Publ. No. 3, Ed. Dunn, C.E., p. 331-354.

Lachance, G.R. and Plant, A.G.
1973: Quantitative electron microprobe analysis using an energy dispersive spectrometer; in Report of Activities, Part B, Geol. Surv. Can., Paper 73-1B, p. 8-9.

Mann, A.W.
1974: Chemical ore genesis models for precipitation of carnotite in calcrete; CSIRO, Minerals Res. Lab., Div. Mineral., Rep. No. FP. 7, 18 p.

Mosher, D.V.
1976: The Jabiluka uranium deposit; in Mining Centres of Northern Australia, Ed. Ryan, G.R., Excursion Guide No. 49AC, 25th Int. Geol. Congr., Sydney, Australia, p. 5-9.

Pedersen, C.P.
1976: The Koongarra uranium deposit; in Mining Centres of Northern Australia, Ed. Ryan, G.R., Excursion Guide No. 49AC, 25th Int. Geol. Congr., Sydney, Australia, p. 9-13.

Rimsaite, J.
1967: Studies of rock-forming micas; Geol. Surv. Can., Bull. 149, p. 9-13, 23.

1975: Natural alteration of mica and reactions between released ions in mineral deposits; Clays Clay Miner., v. 23, p. 247-255.

1977a: Layer silicates (and clays) in the Rabbit Lake uranium deposit, Saskatchewan, Canada; Joint CMS and ICSOBA Meeting, Kingston, Jamaica, Tech. Prog. Abstr. p. 8-9.

1977b: Mineral assemblages at the Rabbit Lake uranium deposit, Saskatchewan; in Report of Activities, Part B, Geol. Surv. Can., Paper 77-1B, p. 235-246.

Wallis, R.H.
1971: The geology of the Hidden Bay area, Saskatchewan; Sask. Dep. Min. Resour., Rep. 137.

59. BRECCIAS AND URANIUM MINERALIZATION IN THE WERNECKE MOUNTAINS, YUKON TERRITORY – A PROGRESS REPORT

Project 750069

R.T. Bell
Regional and Economic Geology Division

Abstract

Bell, R.T., Breccias and uranium mineralization in the Wernecke Mountains, Yukon Territory – A progress report; Current Research, Part A, Geol. Surv. Can., Paper 78-1A, p. 317-322, 1978.

Uranium mineralization occurs associated with breccia columns and diatremes in Precambrian strata in Wernecke Mountains. These strata show weak uranium mineralization in black pelites. Breccias show general chemical enrichments in Fe, K, Ni, Co, Ti, Ba, Cu, and U. The breccias developed in a dilational tectonic regime and later were modified by reverse faulting. Development of the breccias probably coincided with deposition of the early Hadrynian Rapitan Group.

Introduction

In 1975 it was recognized that various breccias in the Wernecke Mountains were interrelated, widespread, and by the end of the summer of 1976, that these were exceptionally abundant and mainly discordant to the strata. Copper, cobalt, and iron mineralization have long been recognized in local breccias (Gross, 1965; Laznicka, 1977; Norris, 1975). Recognition of uranium mineralization in the breccias by Archer, Cathro and associates provided a stimulus for closer examination (Blusson, 1976; Bell and Delaney, 1977; Archer et al., 1977). Several conclusions require modification as a result of closer field examinations in 1977. This report summarizes these new data and presents a model for discussion. Continuing stratigraphic studies by G. Delaney, University of Western Ontario, with support of the Department of Indian Affairs and Northern Development and the Geological Survey of Canada and co-operation from industry, will provide, along with more detailed mapping, the necessary background for a more comprehensive understanding.

Stratigraphy

The breccias (Fig. 59.1) cut a sequence of drab, grey and black pelites and fine grained arenites (Units A and B, Bell and Delaney, 1977) and carbonates (Unit C, ibid.) previously thought to be 8000 m thick. Work during the past summer (Delaney, pers. comm., 1977) indicates these may be 14 000 m and perhaps as much as 18 000 m thick. Previously these rocks were referred to as the Wernecke succession (Archer et al., 1977).

Patches of an upper succession of carbonates, informally called the Mackenzie succession (Archer et al., 1977), were indicated to be unconformably on the Wernecke succession between locations 6a and 6b (Fig. 59.1). Work this summer indicated at least part of this, if not all, comprise overturned panels of unit C. Figure 59.2 illustrates this at location 6a. Earlier speculations that some of the breccias were related to unconformities are thus unfounded. This particular structural relationship (younger strata on the hanging wall of thrust faults) is due to reverse faulting reactivated on previously developed normal faults.

The supposed presence of volcanics in unit B (Bell and Delaney, 1977; Morin, 1976) and stratabound syndepositional breccias were found to be false. Felsite-like rocks were originally fine grained sediments variously altered by alkali and carbonate metasomation. Parenthetically most jasper and all hematite "iron formation" in the wall rocks adjacent to the breccias and in breccia fragments are probably due to hematite metasomatism. Greenstone fragments were traced to sills and dykes interfingering within the breccia complexes. In particular, those with a vesicular texture have been traced to intrusions just south of Fairchild Lake. These intrusions are heavily carbonatized and chloritized; the vesicular-like texture may in part be due to rapid degassing of the cooling intrusives.

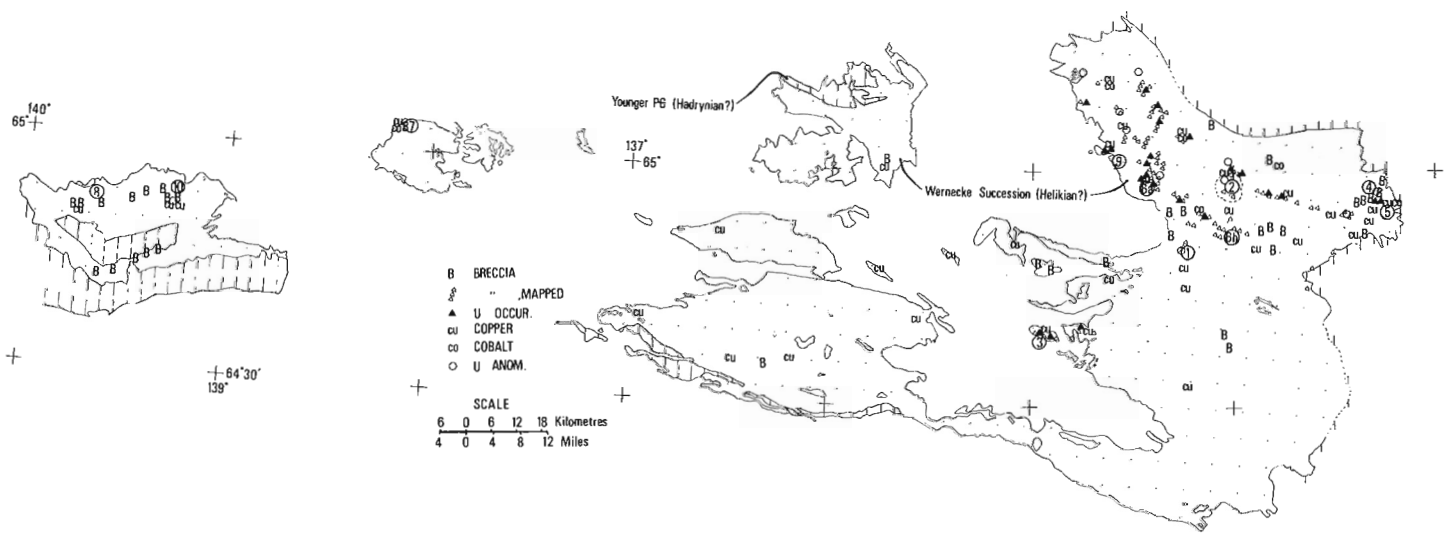

Figure 59.1 Location map, breccias and uranium mineralization in Wernecke and Ogilvie mountains. Single copper mineralization occurrences (CU) are indicated as a possible location of breccias.

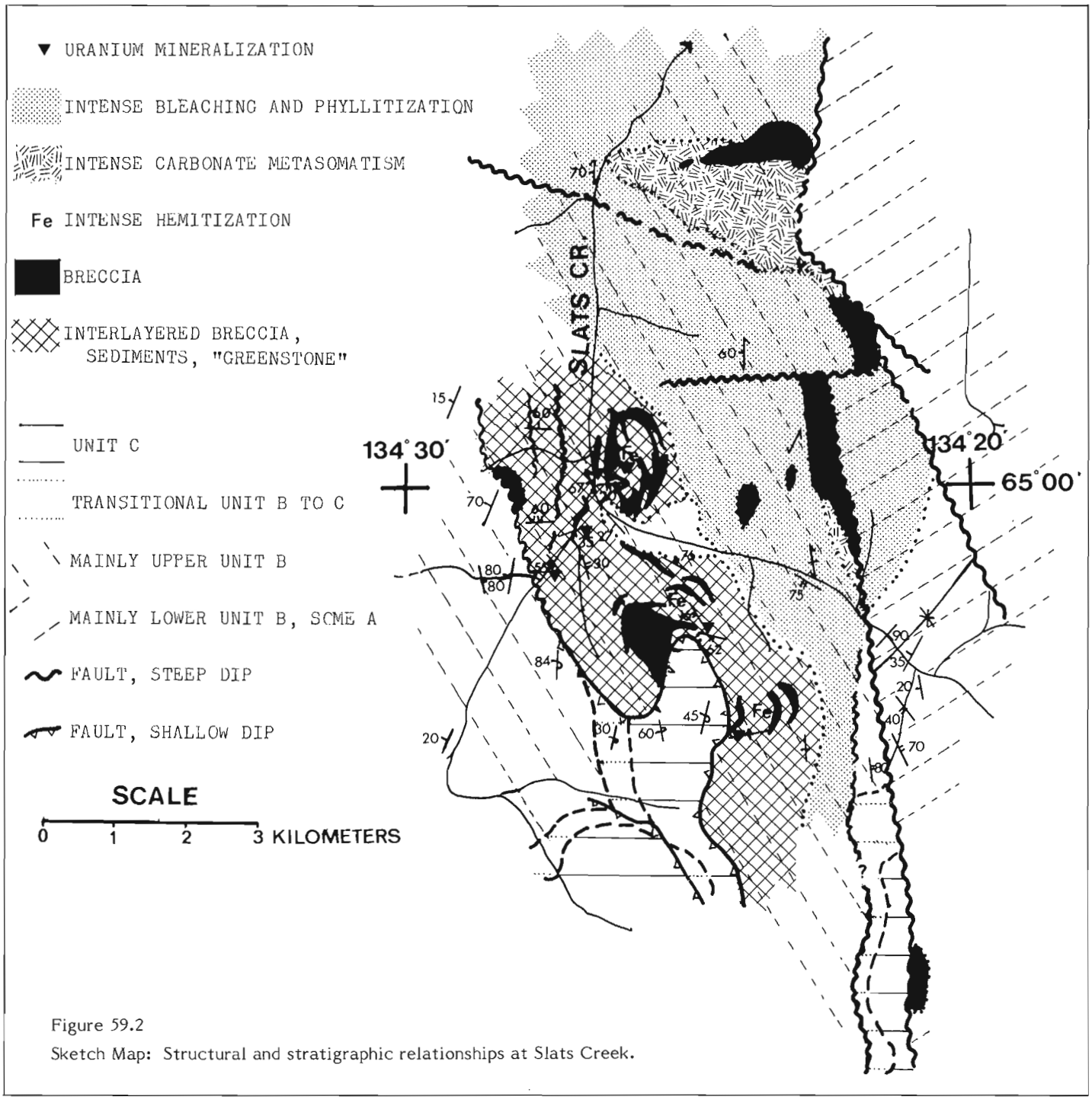

Figure 59.2
Sketch Map: Structural and stratigraphic relationships at Slats Creek.

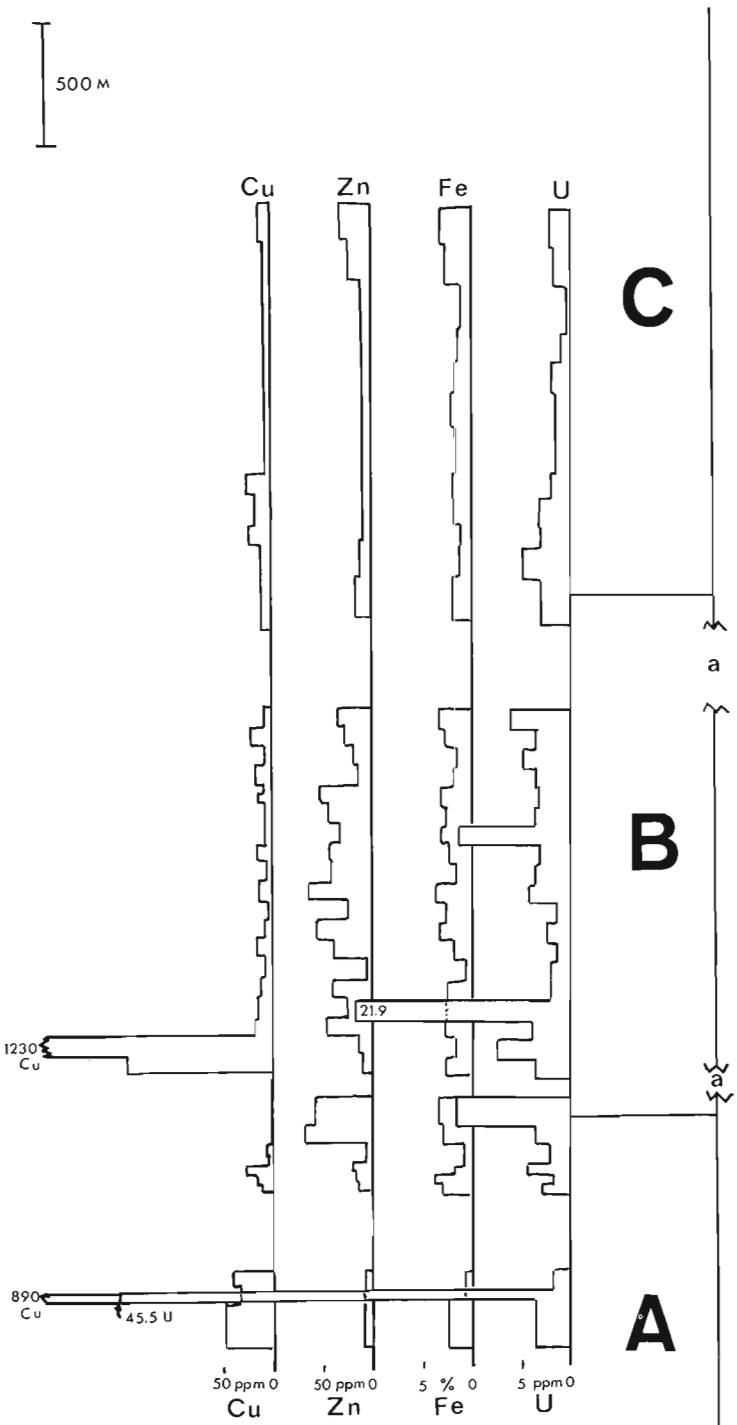

(a) Stratigraphic interval likely thicker than indicated

Units A and C thicker than indicated

Figure 59.3 Stratigraphy geochemistry of the Wernecke Succession. For lithostratigraphic detail see Bell and Delaney (1977).

Lustrous phyllites, resembling unit Ab (Bell and Delaney, 1977) occur just west of Fairchild Lake on the hanging wall of a shallow-angle (thrust?) fault. Accordingly this requires a reappraisal of the significance of unit Ab.

Finally, concordant breccias, almost always with a homolithic nature proved to be lateral concordant aphophyses of discordant homolithic breccia columns and heterolithic breccia pipes. Rarely concordant breccias may be purely tectonic and related to compressional faulting. However, detailed mapping is inconclusive and incomplete at the present time.

Geochemistry of Strata and Breccias

Preliminary stratigraphic geochemistry (Fig. 59.3) on samples collected in 1976 suggests that there is some stratabound uranium and copper enrichment of the black shale.

Comparison of the chemistry of this suite of rocks from the stratigraphic column with a suite systematically collected from the interlayered breccia-sediment-greenstone complex at Slats Creek (Fig. 59.2) shows significant chemical enrichments in Fe, K, Ni, Co, and Ba in order of decreasing intensity, and weak spotty enrichments in Ti, Cu, and U. Other analyses of 11 specimens from 7 separate breccia bodies show most have Ni, Co, U, and Cu enrichment. Molybdenum results are not yet available but it is expected they will show Mo enrichment in the breccias because soil geochemical sampling shows distinct Mo and Cu anomalies over breccias.

These data on the stratigraphic geochemistry are based on a single, incomplete composite section through the Wernecke succession. These results will be fully presented and discussed when specimens from more widespread sections with improved stratigraphic control are analyzed.

The greenstone sills and dykes within the breccias are considerably altered but a representative composition based on analysis of 5 samples is: SiO_2 - 50.60%, Al_2O_3 - 14.50%, Fe_2O_3 - 9.40%, FeO - 4.20%, MgO - 6.4%. CaO - 1.50%, Na_2O - 1.30%, K_2O - 5.80%, TiO_2 - 1.14%, P_2O_5 - 0.20%, MnO - 0.09%, S - 0.15%, CO_2 - 2.20%, H_2OT - 2.80%. Minor elements show ranges as follows: Zn - 17 to 58 ppm, Cu - 3 to 13 ppm, Pb - 2 to 4 ppm, Ni - 26 to 91 ppm, CO - 19 to 111 ppm, U -16 to 6.6 ppm. Some but not all greenstone shows a subophitic texture.

Model for Breccia Development

Figure 59.4 illustrates a proposed sequence of events for the development of breccia complexes in the Wernecke Mountains. Phases A to D represent a dilational tectonic regime.

Phase A depicts normal faulting with stratigraphic separations as much as 3000 m with local development of micro breccias. These faults are west-northwest dominantly and north to north-northwest with some evidence for left lateral movements on the latter. The drainage pattern in the core of the Wernecke Mountains is dominated by these trends and coincides with breccia and mineralization trends. In the Ogilvie Mountains north and east-northeast trends were identified.

Phases B and C depict the progressive development of shatter columns (Gilmour, 1977) likely produced by hydraulic stoping due to ascending fluids from a deep-seated, possibly upper mantle source accompanied by mafic to intermediate tholeiitic intrusive sheets. These shatter columns and intrusions would follow fractures established in Phase A. Softening and disintegration of country rocks by fluids and upwards thrusting of the breccias would produce the variety of plastic, semi-plastic, and brittle features observed in these rocks. Simultaneously during these stages the rising fluids would produce a variety of metasomatic effects (alkali, hematization, carbonatization) on both the developing shatter columns and on wall rocks. In addition these fluids could progressively leach some U, Cu, and perhaps Fe from units A and B, reducing them to bleached phyllites, and redeposit these metals higher in the wall rocks and the column. These breccias tend to be homolithic perhaps because the proposed

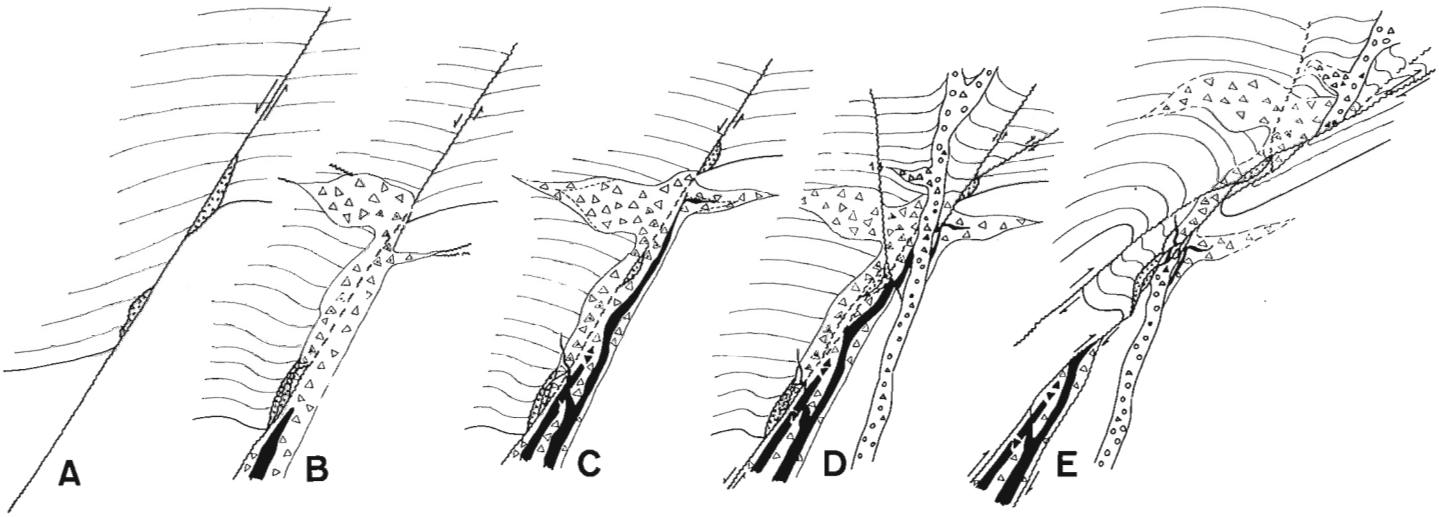

Figure 59.4 Sketches illustrating a model for development of breccia columns and diatremes in Wernecke Mountains.

process is non-explosive, the columns likely did not vent at the surface, and vertical movement of fragments was minimal. Large domains of uniform metasomatic effects would develop. Fluidization structures are evident in the most intensely hematized zones (Fig. 59.5d).

Phase D illustrates the development of explosive breccia pipes and dykes superimposed on fractures previously established. As noted by Gilmour (1977) rounded fragments present in such breccias suggests that they vented effectively at the surface. Many exotic-appearing fragments are of various previously metasomatized and bleached wall rock and breccia, mixed with pulverized shattered and abraded unaltered wall rock. Magnetite or siderite is commonly present and the breccias are commonly accompanied by barite-magnetite dykes. Some of these pipes may have undergone carbonate and/or hematite metasomatism although severe alteration tends to mask whether an individual phase is a shatter column or a breccia produced by explosive gas drilling. These explosive breccias have sharp, upwards-bent contacts (see Bell and Delaney, 1977, Figs. 8.3 and 8.5).

Phase E depicts the change to compressive tectonics and development of reverse faulting along zones of previously normal movements and explains the development of mechanically consistent thrust fault relationships with younger strata on the hanging wall such as near locations 6a, 6b, 8 and 10 in Figure 59.1 (see also Fig. 59.2).

Age

Earlier, Archer et al. (1977) suggested 1500 m.y. as the likely date for breccia formation. This is the result of a K/Ar date on biotite flakes in a breccia. However, the coincidence of moderate to extensive hematization in all breccia complexes and more impressively of completely hematized phases such as at Bear River (loc. 1, Fig. 59.1; Gross, 1965) and near Caribou River in the Richardson Mountains (Norris, 1975), with the nearby Rapitan (Hadrynian) iron-formation suggests an interdependence and hence similar age. Gross (1965) earlier drew this conclusion although in a different context. Eisbacher's (1977) picture of dilational tectonics for the Rapitan Group further adds to the case for an early Hadrynian age for the dilational phase in the development of these breccia complexes. In addition a case could be made for correlating part of Unit C (Bell and Delaney, 1977) which is cut by the breccias, with the Little Dal Formation in the Mackenzie Mountains. Perhaps the breccias developed at several ages.

Mineralization

Uranium mineralization of the brannerite type (BP style) occurs in the breccias throughout the Wernecke Mountains and at a site of hematitic breccias in the Richardson Mountains described by Norris (1975). The chemistry (anomalous Ti, Co, Ni, Fe, and reported rare earths) and accompanying hematite, alkali and carbonate metasomatism suggest a deep seated source. Coincidental with this, the dilational tectonic and diatreme environment suggests this area and style of mineralization (Miguta, 1976) to be ideal to test Gabelman's ideas (1977a, b) concerning taphrogenic uranium concentration.

Pitchblende or uraninite type mineralization occurs primarily at five localities, (eg. Fig. 59.1, locs. 3, 5, 9) four of which are demonstratably close to the sub-Phanerozoic unconformities and may be due at least in part to laterogene processes (surface leaching from the Wernecke succession and breccias and downward percolation of ground waters into porous breccia pipes). At two of these locations (Fig. 59.1: locs. 3 and 5; Fig. 59.6) disperse fragments of previously mineralized sediments were found indicating that significant mineralization may have occurred before that phase of brecciation. This lends credence to the earlier inference (Bell and Delaney, 1977) (Fig. 59.3, this report) that black shale mineralization is present in the Wernecke assemblage.

Acknowledgments

L. Jones and P. Ruck assisted the writer ably during the field season. The author is grateful for co-operation and courtesies extended by personnel from companies working in this area, particularly Archer, Cathro and Associates, Eldorado, Pamicon, and Cordilleran Engineering. Chemical analyses on specimens the author collected in 1976 were done under the auspices of W.D. Goodfellow's project in the Uranium Reconnaissance Program.

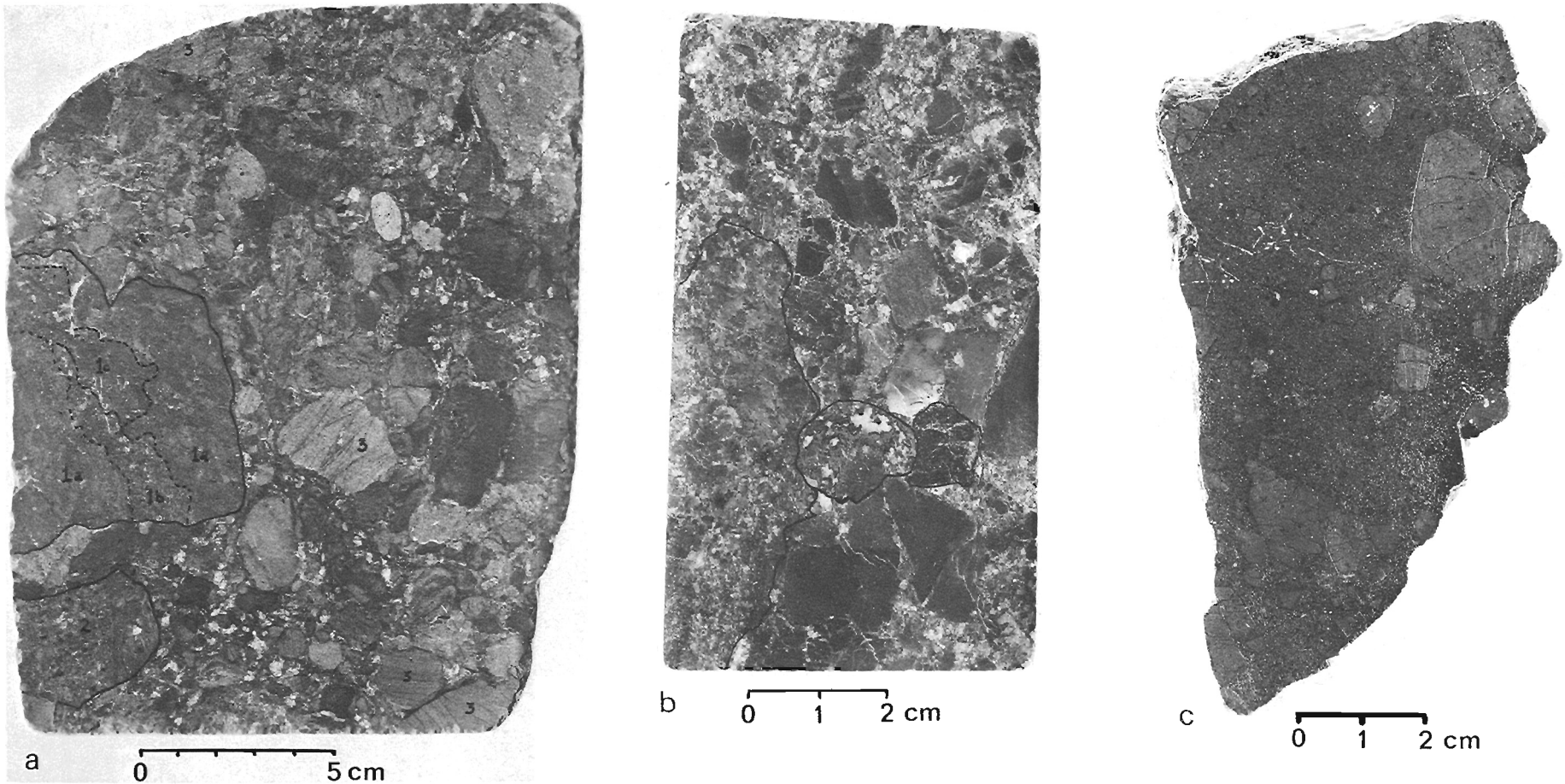

Figure 59.5

a Homolithic shatter breccia, pink hematitic argillaceous dolomitic fragments (protolith-grey to greenish grey argillite to fine-grained quartzite); 1a, b, c: compound fragment of 2 or 3 stages of brecciation; 2: breccia fragment; 3: cross-laminated fragments; Dempster Highway, Ogilvie map-area.

b Heterolithic shatter breccia, grey, red and pink jasper with siliceous dolomitic fragments; breccia fragments outlined; central outlined fragment largely of specularite; south of Bonnet Plume River, Nash map-area.

c Hematized (specularite) breccia. All fragments and matrix replaced almost entirely by specularite; Wind River map-area.

d Fluidization structure in hematized breccia; dark fragments weakly hematized (specularite) slate with matrix of finely crystalline quartz and K-feldspar; Trail River map-area, near Caribou River, Richardson Mountains.

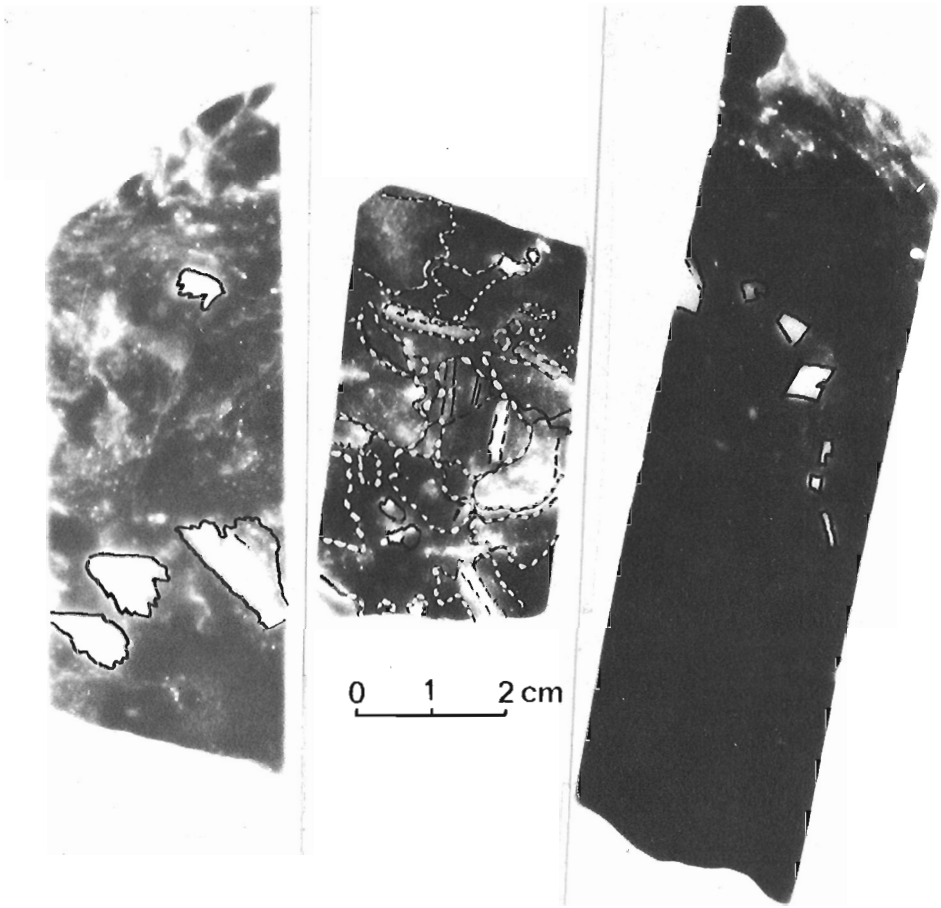

Figure 59.6 Autoradiographs of breccia from site 3, clasts outlined. Specimens courtesy of Eldorado Nuclear Limited.

References

Archer, A., Bell, R.T., Delaney, G.D., and Godwin, C.

1977: Mineralized Breccias of Wernecke Mountains, Yukon; G.A.C. Annual Meeting, April, 1977, Vancouver (abstract).

Bell, R.T. and Delaney, G.D.

1977: Geology of Some Uranium Occurrences in Yukon Territory; in Report of Activities, Part A, Geol. Surv. Can., Paper 77-1A, p. 33-37.

Blusson, S.L.

1976: Selwyn Basin, Yukon and District of Mackenzie; in Report of Activities, Part A, Geol. Surv. Can., Paper 76-1A, p. 131-132.

Eisbacher, G.H.

1977: Tectono-Stratigraphic Framework of the Redstone Copper Belt, District of Mackenzie; in Report of Activities, Part A, Geol. Surv. Can., Paper 77-1A, p. 229-234.

Gabelman, J.W.

1977a: Migration of Uranium and Thorium - Exploration Significance, A.A.P.G. Studies in Geology No. 3, 168 p.

1977b: Orogenic and Taphrogenic Uranium Concentration; in Recognition and Evaluation of Uraniferous Areas, International Atomic Energy Agency, Vienna, p. 109-121.

Gilmour, Paul

1977: Mineralized Intrusive Breccias as Guides to Concealed Porphyry Copper Systems; Econ. Geol., v. 72, p. 290-303.

Gross, G.A.

1965: Geology of Iron-ore Deposits and Iron-Formations in Canada; in Report of Activities: Field 1964, Geol. Surv. Can., Paper 65-1, p. 142-143.

Laznicka, P.

1977: Geology and Mineralization in the Delores Creek area, Bonnet Plume Range, Yukon; in Report of Activities, Part A, Geol. Surv. Can., Paper 77-1A, p. 435-439.

Miguta, A.K.

1976: Uranotianatovye rudnye formatsii (Uranium Titanium Ore Formations); Sovietskaya Geologiya, No. 12, p. 23-36.

Morin, J.A.

1976: Bond 1-96, Bozo 1-16, Pike 1-14, Otis, Wernecke Claims; in Mineral Industry Report 1975, Yukon Territory by Sinclair, W.D., Morin, J.A., Craig, D.B., and Marchand, M., EGS 1976-15, Indian and Northern Affairs, p. 61-65.

Norris, D.K.

1975: Structural and Stratigraphic Studies in the Northern Canadian Cordillera: in Report of Activities, Geol. Surv. Can., Paper 74-1A, p. 343-349.

60. THE GRAPHICAL REPRESENTATION OF MINERAL ASSEMBLAGES IN BIOTITE-BEARING GRANULITES

Project 740096

E. Froese
Regional and Economic Geology Division

Abstract

Froese, E., The graphical representation of mineral assemblages in biotite-bearing granulites; Current Research, Part A, Geol. Surv. Can., Paper 78-1A, p. 323-325, 1978.

At constant pressure, temperature, and chemical potential of water, and in the presence of quartz, magnetite, ilmenite, and plagioclase of fixed composition, phase relations in granulites may be represented in the AKFM tetrahedron, using components defined as follows: $A = Al_2O_3\ 3-(Na_2O + CaO + K_2O)$, $K = K_2O \cdot Al_2O_3$, $F = FeO - (Fe_2O_3 + TiO_2)$, $M = MgO$. In many granulites, biotite is a stable phase. In such rocks, a subdivision of the biotite composition surface, as plotted inside the AKFM tetrahedron, may be used to portray compatible mineral assemblages.

Orthopyroxene is the diagnostic mineral of the granulite facies or regional hypersthene zone (Winkler, 1976); it occurs in a variety of rocks ranging in composition from pelitic to basic. Phase relations in such rocks involve at least ten components: SiO_2, TiO_2, Al_2O_3, Fe_2O_3, FeO, MgO, CaO, Na_2O, K_2O, and H_2O. These may be rearranged as follows:

H_2O

SiO_2

$Na_2O \cdot Al_2O_3$

$CaO \cdot Al_2O_3$

$Fe_2O_3 \cdot FeO$

$TiO_2 \cdot FeO$

$A = Al_2O_3 - (Na_2O + CaO + K_2O)$

$K = K_2O \cdot Al_2O_3$

$F = FeO - (Fe_2O_3 + TiO_2)$

$M = MgO$

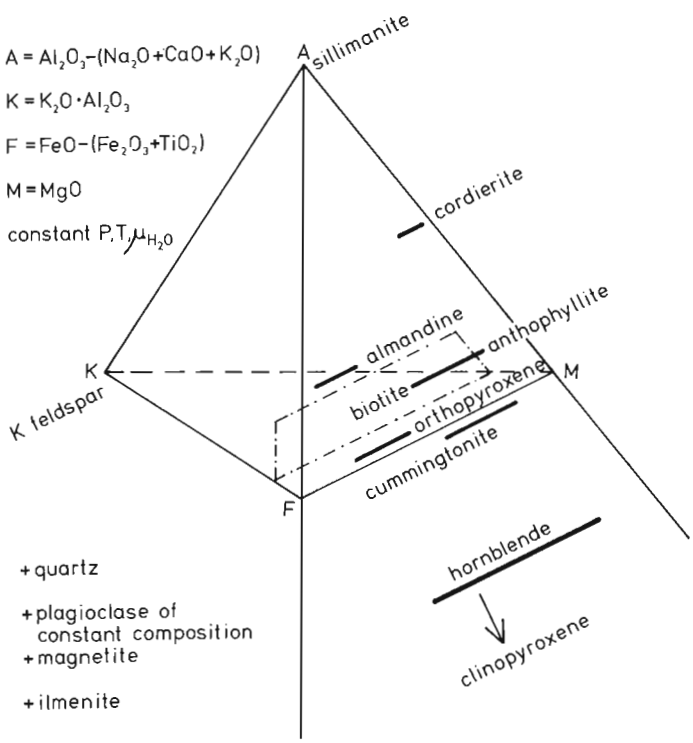

Figure 60.1. Some minerals of high-grade gneisses and granulites represented in the AKFM tetrahedron.

If the chemical potential of a component is fixed, the amount of this component does not affect the phase relations and it can be omitted in a graphical representation. Geometrically this corresponds to a projection from polydimensional space through this component. The presence of quartz, magnetite, and ilmenite determines the chemical potentials of SiO_2, $Fe_2O_3 \cdot FeO$, and $TiO_2 \cdot FeO$. The chemical potential may also be fixed by having the component present in a phase of constant composition. Therefore, plagioclase of a specified composition together with quartz determines the chemical potential of $Na_2O \cdot Al_2O_3$ and $CaO \cdot Al_2O_3$. Thus in rocks containing quartz, magnetite, ilmenite, and plagioclase of constant composition, phase relations may be represented in the tetrahedron AKFM at any given pressure, temperature, and chemical potential of H_2O (Fig. 60.1).

Eskola (1915) initiated the subsequently widespread use of graphical methods of representing mineral assemblages. He projected, in effect, through plagioclase of constant composition in the construction of his AKF diagram by defining $A = Al_2O_3 - (K_2O + Na_2O + CaO)$. The success of the AFM projection for muscovite-bearing rocks (Thompson, 1957) and Korzhinskii's (1959) treatment of mineral equilibria

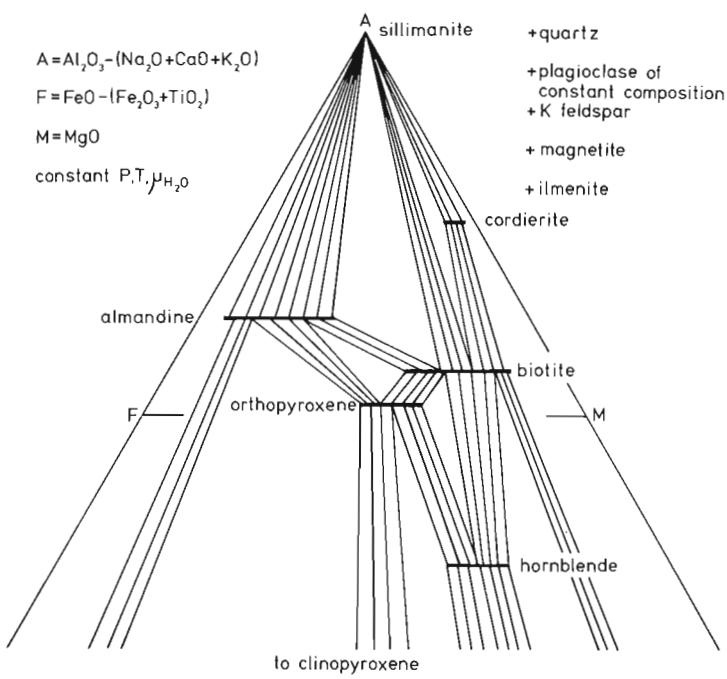

Figure 60.2. Mineral assemblages in gneisses and granulites from the Westport area, stable in the presence of K feldspar (Reinhardt and Skippen, 1970).

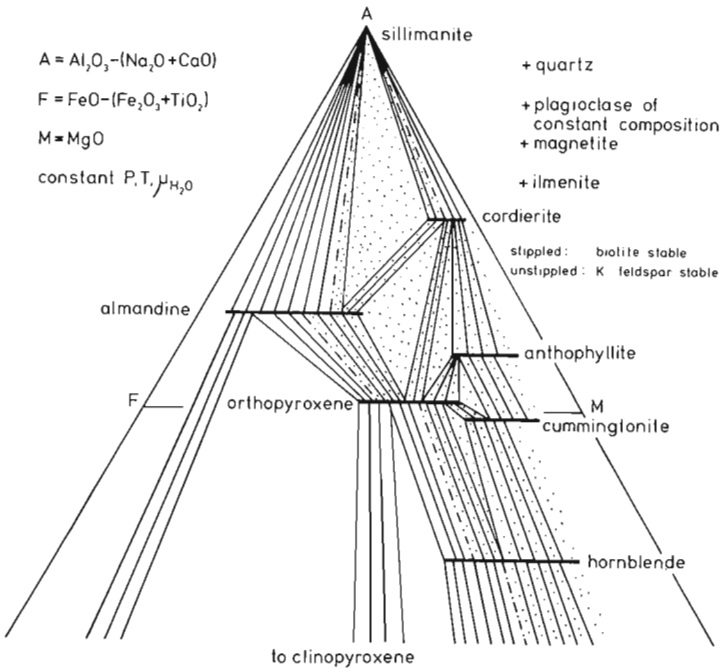

Figure 60.3. Postulated phase relations among minerals not containing K_2O at the grade of metamorphism indicated by mineral assemblages in Figure 60.2.

provided further incentives to the quest for suitable representations of mineral compatibilities. Thus the plagioclase projection became incorporated in a variety of diagrams (Green, 1960; Froese, 1963, 1969, and 1973; Reinhardt, 1968; Robinson and Jaffe, 1969; Reinhardt and Skippen, 1970; Stout, 1972). Several of these papers also make use of a projection through magnetite, or through both magnetite and ilmenite.

In rocks bearing K feldspar, phase relations may be projected through K feldspar onto a suitable projection plane, e.g. the AFM face of the AKFM tetrahedron. For example, Reinhardt and Skippen (1970) used this method to portray mineral assemblages in gneisses and granulites from the Westport area (Fig. 60.2). On the other hand, phase relations among minerals not containing K_2O may be conveniently shown on the AFM face of the AKFM tetrahedron (e.g. Froese, 1969; Robinson and Jaffe, 1969). At the grade of metamorphism reflected by the assemblages in Figure 60.2, the AFM face is expected to be as shown in Figure 60.3. This diagram includes anthophyllite and cummingtonite, minerals which cannot be seen in a projection from K feldspar. The F/M ratio is shown increasing in the order hornblende-cummingtonite-anthophyllite, consistent with the observations of Stout (1972). Phase relations involving biotite and K feldspar can be indicated in Figure 60.3 in the following manner. As noted by Albee (1965), the introduction of a new component, in this case $K_2O \cdot Al_2O_3$, will in general give rise to only one additional phase, in this case either biotite or K feldspar. This feature has been shown in Figure 60.3. Only along the boundary between assemblages with biotite and those with K feldspar, are both biotite and K feldspar present. This boundary must lie in two-phase fields so that the number of coexisting phases represented in the AKFM tetrahedron does not exceed four.

The appearance of orthopyroxene does not lead to the immediate elimination of hydrous minerals; instead granulites commonly contain biotite and hornblende (Winkler, 1976). In such rocks, another method of depicting phase equilibria, at least in a qualitative manner, may prove useful (Froese, 1969, 1972). Four-phase assemblages in the AKFM tetrahedron, which include biotite, are represented by subtetrahedra having one apex on the biotite composition surface.

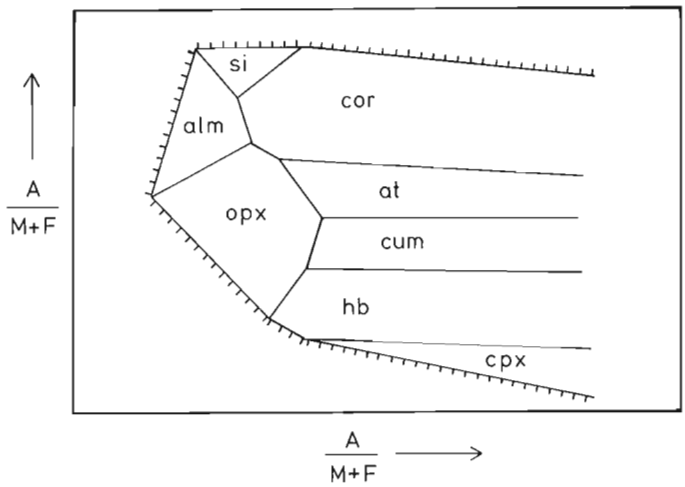

Figure 60.4. Mineral assemblages in biotite-bearing rocks from Figures 60.2 and 3 shown on the biotite composition surface.

Similarly, three-phase assemblages subtend a line and two-phase assemblages an area on the biotite composition surface. Consequently, a subdivision of the biotite composition surface, as seen from the AFM face of the AKFM tetrahedron, may be used to portray mineral compatibilities. The biotite composition surface is truncated along bevelled edges (see also Ushakova, 1972) from which tie lines extend towards K feldspar which, in this view, is hidden behind the biotite composition surface. Because the content of K component is nearly constant in biotites, the variation in composition is adequately given by the relative amounts of components A, F, and M. Due to the small amount of component A, it is best to choose co-ordinates M/(F+M) and A/(F+M); this allows an exaggeration of the A/(F+M) axis. Using this method, those mineral assemblages of Figures 60.2 and 60.3 which include biotite are shown in Figure 60.4.

It is hoped that graphical methods discussed in this note will be helpful in studying mineral compatibilities in granulites and deducing reactions which might constitute a petrogenetic grid. This in turn would provide a better understanding of the boundary between the granulite facies and rocks of lower metamorphic grade, which, at present, is based simply on the first appearance of orthopyroxene, regardless of rock type and specific reactions (Winkler, 1976).

References

Albee, A.L.
1965: Phase equilibria in three assemblages of kyanite-zone pelitic schists, Lincoln Mountain quadrangle, Central Vermont; J. Petrol., v. 6, p. 246-301.

Eskola, P.
1915: On the relations between the chemical and mineralogical composition in the metamorphic rocks of the Orijärvi region; Bull. Comm. Géol. Finlande, no. 44, 145 p.

Froese, E.
1963: A chemical study of garnets from the Stony Rapids area, Saskatchewan; Can. Mineral., v. 7, p. 698-712.

1969: Metamorphic rocks from the Coronation mine and surrounding area; Geol. Surv. Can., Paper 68-5, p. 55-77.

1972: The representation of mineral assemblages coexisting with biotite on the biotite composition surface (abstract); Can. Mineral., v. 11, p. 573.

Froese, E. (cont.)
1973: Metamorphism of basic rocks; Geol. Surv. Can., Open File 164, "Volcanism and volcanic rocks", p. 57-64.

Green, J.C.
1960: Geology of the Errol quadrangle, New Hampshire-Maine; unpubl. Ph.D. thesis, Harvard University.

Korzhinskii, D.S.
1959: Physicochemical basis of the analysis of the paragenesis of minerals; Consultants Bureau Inc., New York, 142 p.

Reinhardt, E.W.
1968: Phase relations in cordierite-bearing gneisses from the Gananoque area, Ontario; Can. J. Earth Sci., v. 5, p. 455-482.

Reinhardt, E.W. and Skippen, G.B.
1970: Petrochemical study of Grenville granulites; in Report of Activities, Part B, Geol. Surv. Can., Paper 70-1B, p. 48-54.

Robinson, P. and Jaffe, H.W.
1969: Chemographic exploration of amphibole assemblages from central Massachusetts and southwestern New Hampshire; Spec. Pap., Mineral. Soc. Am., v. 2, p. 251-274.

Stout, J.H.
1972: Phase petrology and mineral chemistry of coexisting amphiboles from Telemark, Norway; J. Petrol., v. 13, p. 99-145.

Thompson, J.B. Jr.
1957: The graphical analysis of mineral assemblages in pelitic schists; Am. Mineral., v. 42, p. 842-859.

Ushakova, E.N.
1972: The biotites; in: The facies of metamorphism, ed. by V.S. Sobolev; Australian National University, Dep. Geol. Publ. no. 214, p. 352-362.

Winkler, H.G.F.
1976: Petrogenesis of metamorphic rocks, 4th ed.; Springer-Verlag, New York, 334 p.

61. KITIMAT SUBMARINE SLUMP DEPOSIT(S): A PRELIMINARY REPORT

Project 740062

John L. Luternauer and Davis Swan
Regional and Economic Geology Division, Vancouver

Abstract

Luternauer, John L. and Swan, Davis, Kitmat Submarine Slump Deposit(s): A Preliminary Report; Current Research, Part A, Geol. Surv. Can., Paper 78-1A, p. 327-332, 1978.

Side-scan sonar records coupled with echo-sounding, sedimentologic and photographic evidence served as a basis for identifying submarine slump deposits on the floor of the northern Kitimat Arm, British Columbia. Preliminary examination of data suggests that at least two distinct submarine slides have coalesced to form a continuous deposit some 4-5 km in length and as much as 2 km wide.

Introduction

The Geological Survey of Canada conducted a survey in the northern Kitimat Arm of Douglas Channel (Fig. 61.1) August 12-17, 1977 to determine the areal extent and character of sea-floor deposits which have been generated by submarine slope failure. There is considerable demand for information on the behaviour of local submarine landslides because of the damage they can (or could) inflict directly or indirectly, on existing port facilities, on a proposed major oil port terminal, and on the sea-floor environment.

One such slide occurred on April 27, 1975. It appears to have started in the vicinity of Moon Bay (Figs. 61.2 and 61.3) and displaced an estimated 2.3 million m^3 of material (Golder Assoc., 1975; Bell and Kallman, 1976). Major factors contributing to failure were:

1. the presence of soft, moderately sensitive marine clay near shore, and beneath the sloping sea bottom,
2. excess pore pressure within the clay, and
3. an implied factor of safety only very slightly greater than 1.0 under normal conditions along this segment of the west shore of Kitimat Arm (Golder Assoc., 1975).

The slide generated a "seawave" described as being 8 m high, which caused an an estimated $600 000.00 damage to the Northland Navigation wharf (Fig. 61.3) and other coastal structures (Golder Assoc., 1975).

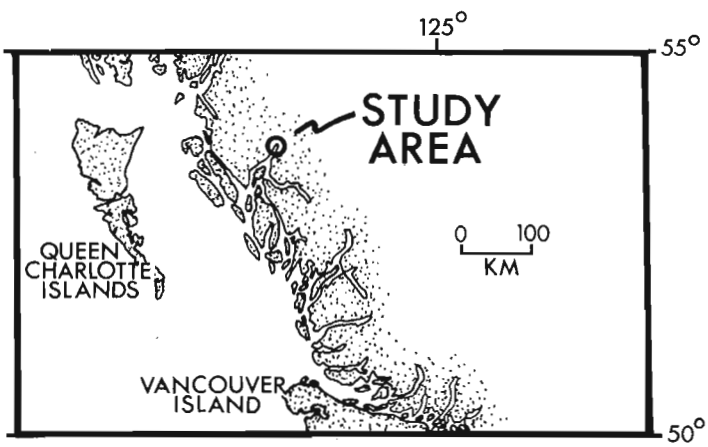

Figure 61.1. Index map.

Field Activities

Seventy-three bottom sediment samples and 15 short cores were recovered using a Dietz-Lafond grab and an Alpine dart corer, respectively (Fig. 61.2). Approximately 160 km of side scan sonar and echo-sounding trackline were obtained. These are concentrated within the heavily sampled zone shown in Figure 61.2 although two lines extend another 2-3 km to the south, parallel with the axis of the inlet. Navigation was accomplished with a Marconi Mini-Ranger. Most of the side scan lines were run along circular arcs centred at one of two shore transmitters. The error in position fixing is estimated to be less than 5 m in any direction. Bottom coverage by the side scan sonar was as great as 400 per cent in areas of complex morphology to ensure precise delineation of bottom features.

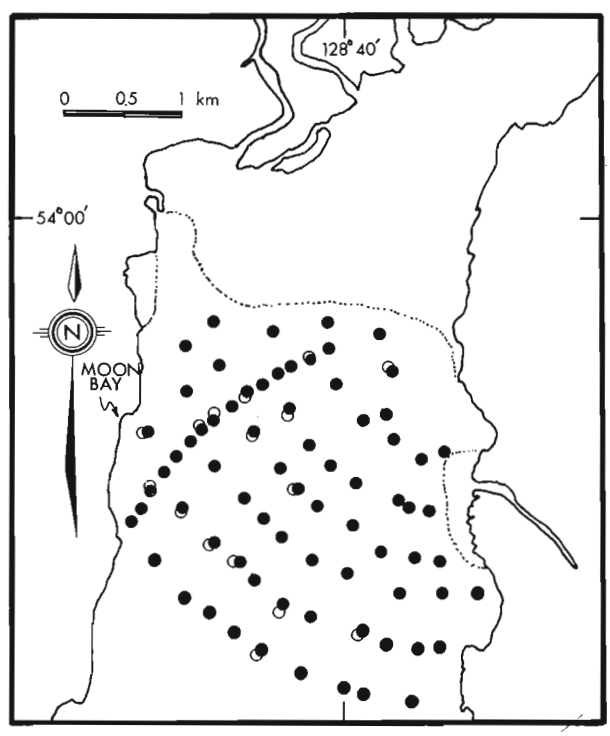

Figure 61.2. Bottom sediment sampling stations. Dots represent Dietz-Lafond grab sampling sites while open circles indicate Alpine gravity coring sites. The dotted line marks the seaward extent of tidal flats.

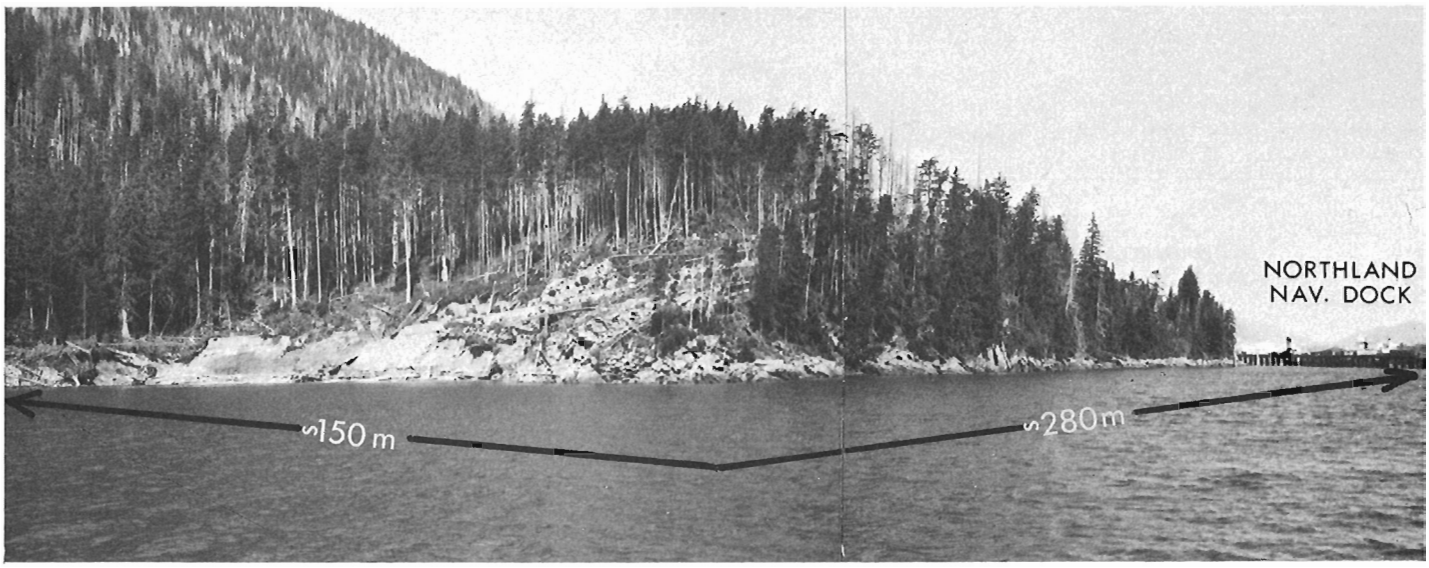

Figure 61.3. (above)

Composite photograph of the 1975 subaerial landslide site on the western shore of the northern Kitimat Arm (Fig. 61.2). Photograph faces north-northwest with Moon Bay (Fig. 61.2) left of centre.

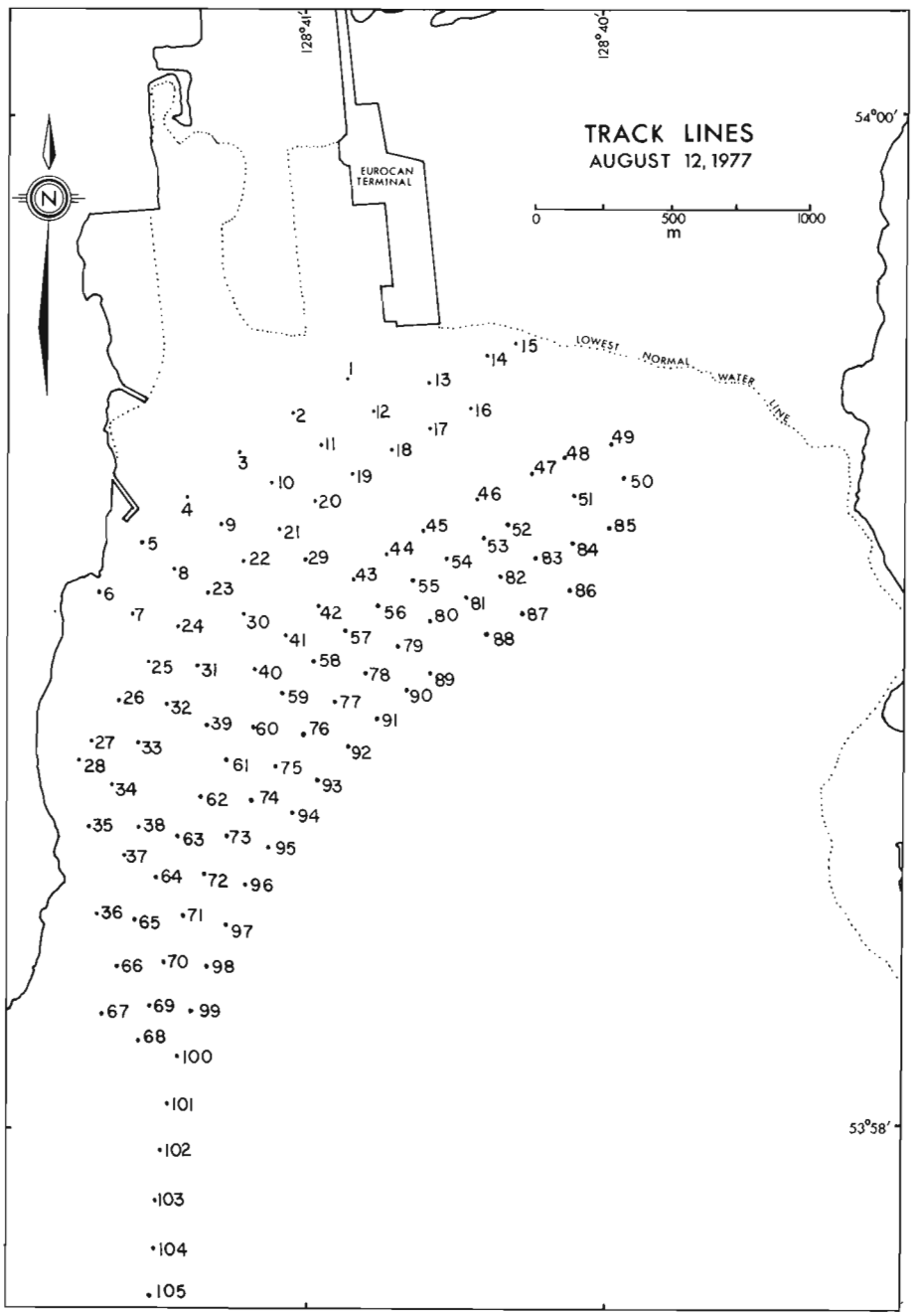

Figure 61.4

Side scan sonar and echo-sounding tracklines run August 12, 1977, in the northern Kitimat Arm. Numbers indicate sequential position fixes.

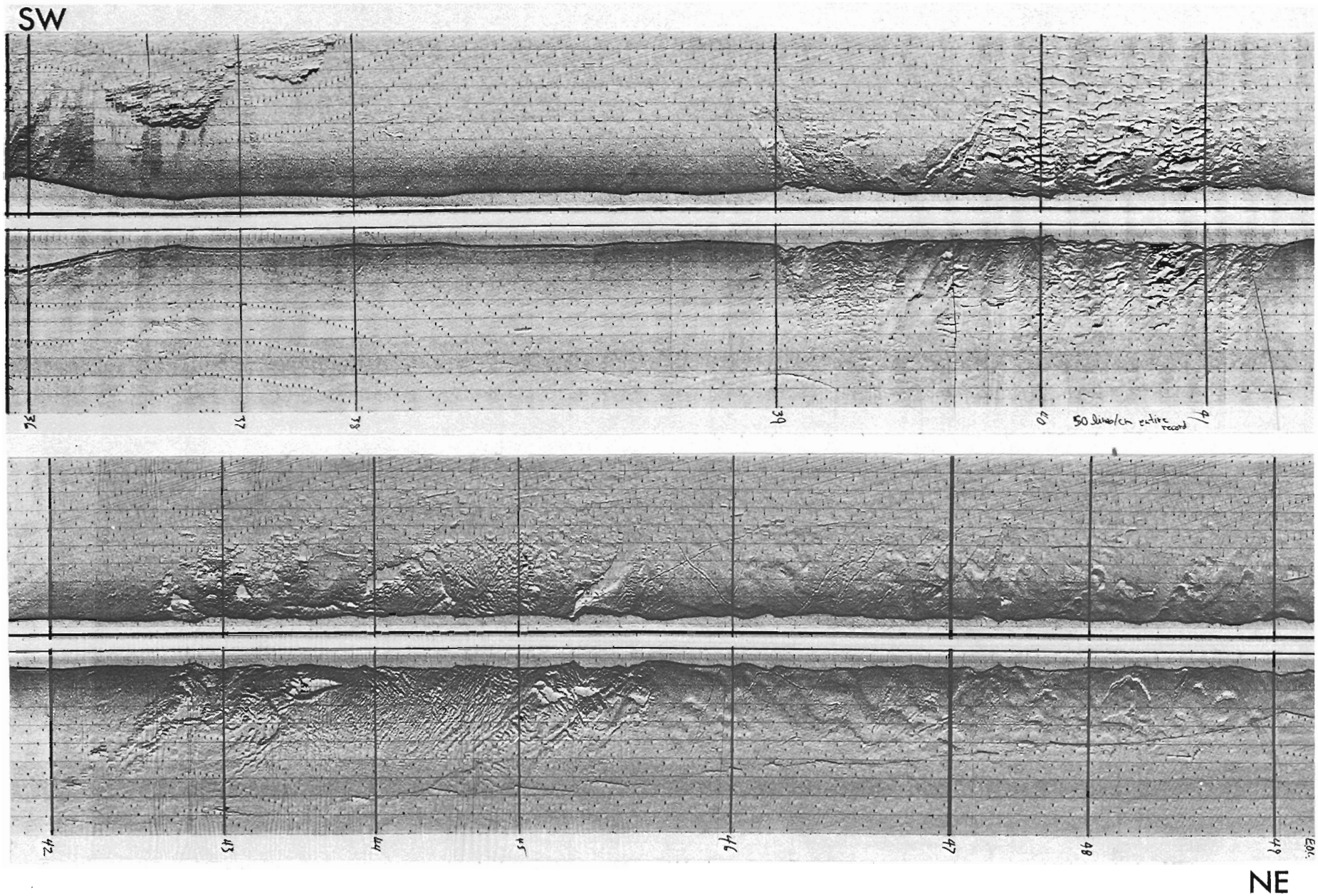

Figure 61.5. Side scan sonar record for August 12, 1977, fix numbers 36 to 49 (Fig. 61.4). Note that the fix marks on the record correspond to the times when the survey ship was at the position shown in Figure 61.4. Typically the side scan fish was actually about 100-200 m behind the ship, so that the plotted positions do not indicate the exact position of the side-scan records.

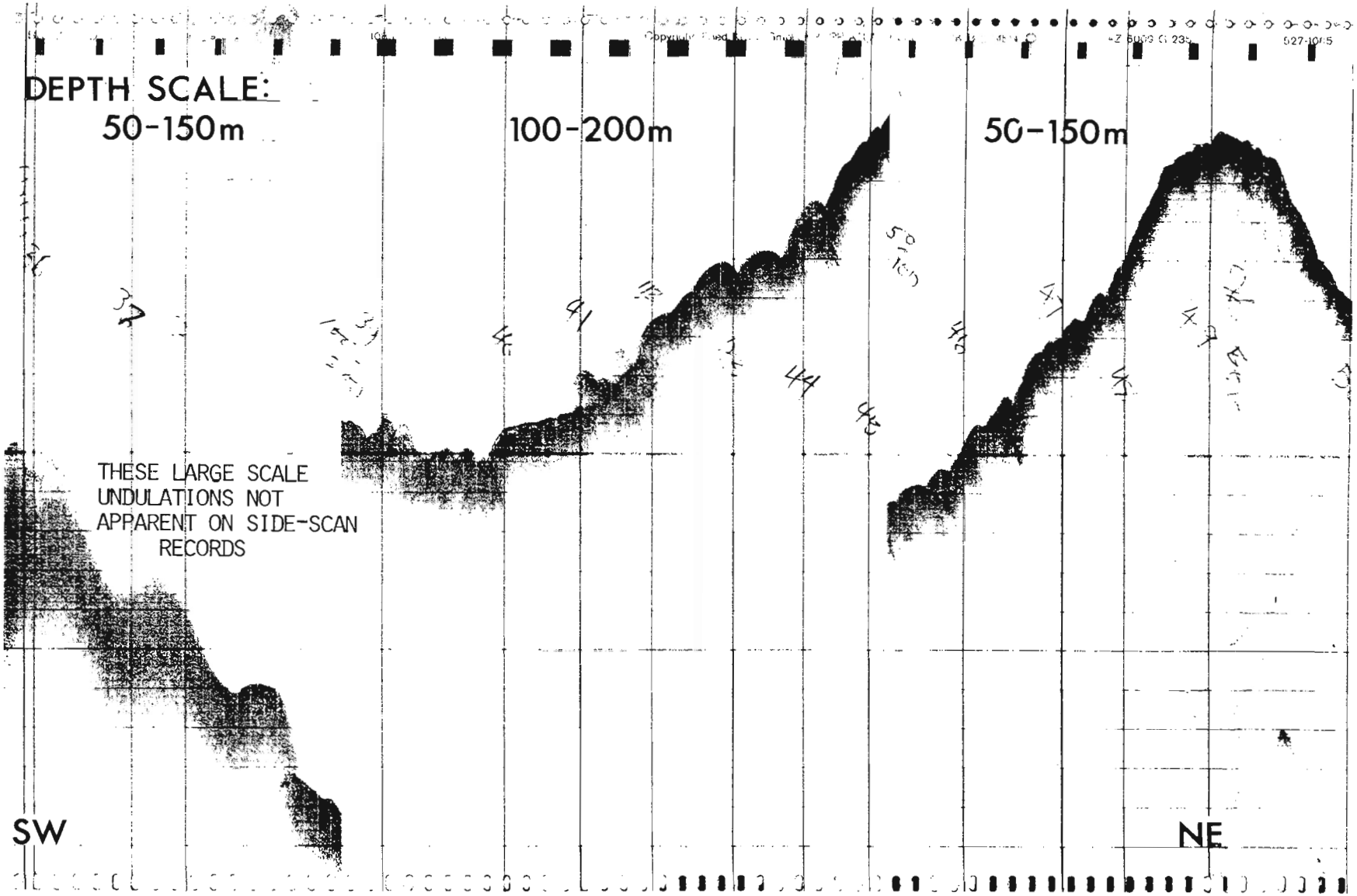

Figure 61.6. Echograms for August 12, 1977, fix numbers 36 to 49 (Fig. 61.4). Depths not corrected to common datum.

Figure 61.7

Bottom photograph showing relativley undisturbed sediment at the base of the inlet wall. Field of view is 1-2 m. Photograph by R. Hoos.

Preliminary Observations

The side scan sonar device very effectively distinguished the predominant submarine morphological features. These are evident on the illustrated records obtained along a trackline running approximately southwest-northeast across the head of the inlet (Fig. 61.4, Fixes 36-49, and Figs. 61.5 and 61.6).

A bedrock outcrop is recognizable along the mid-section of the slope (Fix 37, Fig. 61.5). From that point downslope to Fix 39 on the side scan record the sea floor appears to have subdued relief only. Sediment samples obtained on this slope consist of dense, plastic, fine grained material (probably Pleistocene marine muds). A photograph of this surface (Fig. 61.7) reveals the presence of numerous organisms, suggesting that this part of the sea bed may not have been affected by the 1975 slumping. At the base of the slope the sediment surface very abruptly becomes hummocky, and appears to be crossed by linear features generally aligned with the axis of the channel. Photographs of the surface here (Figs. 61.9A and B) reveal isolated blocks of material as well as sharply crested ridges. A section of relatively smooth sea-bed is evident just north-northeast of Moon Bay. Beyond this the floor of the inlet is again hummocky, indicating that at least two submarine slides may have occurred in this area; one originating in the vicinity of Moon Bay, and a second from the Kitimat River delta slope. Beyond the second hummocky patch and up the delta slope the sea floor again appears to be smoother. This section of record probably represents relatively undisturbed foreset deposits (scarred possibly by ships' anchors being dragged over the bottom).

A preliminary compilation of the side scan and echosounding records suggests that at least two distinct slump deposits have coalesced to form a continuous deposit some 4-5 km in length and as much as 2 km wide. Our findings confirm and complement those of Bornhold (1977) who defined the down-inlet limit of local slump deposits. Further processing of cores and surficial sediment samples and the preparation of a side scan sonar mosaic of the area will allow us to more precisely delineate the extent and character of the slump deposits. Further information on the thickness of slump deposits should be obtained from planned high resolution seismic surveys and deeper coring.

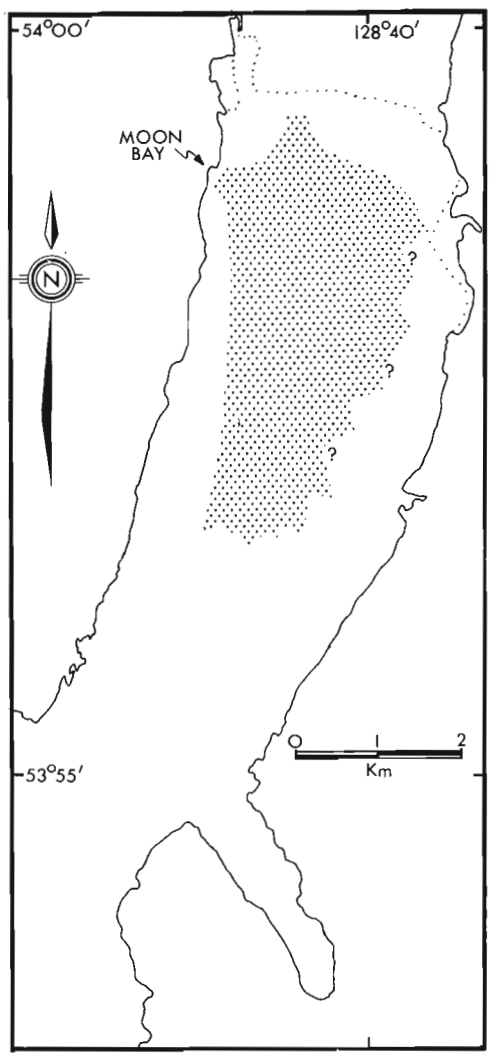

Figure 61.8

Generalized representation of the extent of slump deposits on the floor of northern Kitimat Arm, as determined from the side scan sonar and echogram records obtained August 12-17, 1977.

Figure 61.9. Bottom photographs showing typical surface character of what is considered to be a slump deposit. Field of view is 1-2 m. Photographs by R. Hoos.

Acknowledgments

The authors wish to thank Captain M.G. Wheeler and the crew of the **C.S.S. Richardson** for ably assisting us in our field activities. Mr. R. Hoos of the Environment Protection Service (Dep. of the Environment) kindly allowed us the use of bottom photographs he obtained in 1975 during a Pisces II submersible dive in the Kitimat Arm. Side scan sonar equipment was supplied by Canadian Hydrographic Services. A copy of the report prepared by Golder Associates was obtained with the permission of Mr. B. Marr, Deputy Minister of the Environment, Government of British Columbia, Victoria, British Columbia.

References

Bell, L.M. and Kallman, R.J.
1976: The Kitimat River estuary-status of environmental knowledge to 1976; Estuary Working Group, Environment Canada, Regional Board Pacific Region, Special Estuary Series No. 6, 296 p.

Bornhold, B.
1977: Echo-sounding and subbottom profiling in Douglas Channel and Kitimat Arm, British Columbia; in Report of Activities, Part B, Geol. Surv. Can., Paper 77-1B, p. 265-268.

Golder Associates
1975: Report to B.C. Water Resources Service on investigation of seawave at Kitimat, B.C., 9 p., 6 Figs., 1 Appendix.

62. RECONNAISSANCE OF THE MARINE GEOLOGY OF MAKKOVIK BAY, LABRADOR

David J.W. Piper[1] and R.J. Iuliucci[1]
Atlantic Geoscience Centre, Dartmouth

Abstract

Piper, David J.W. and Iuliucci, R.J., Reconnaissance of the marine geology of Makkovik Bay, Labrador; Current Research, Part A, Geol. Surv. Can., Paper 78-1A, p. 333-336, 1978.

The results of a reconnaissance study designed to develop a model of Holocene sedimentation in a typical Labrador fiord are presented. Six sediment types can be identified. These reflect the history of the bay from its inception during a mid-Quaternary glaciation to the present.

Introduction

Makkovik Bay is a 25-km-long inlet on the central Labrador coast at 55°N. It is a glacially excavated fiord cut into Precambrian metamorphic and igneous rocks. The geomorphology of the bay is illustrated in Figure 62.1, which shows bathymetric contours at 20-m intervals, compiled from Canadian Hydrographic Service field sheets. Rocky shoals and islands in the Approaches protect the bay from open ocean swell, and from large icebergs. Water depths in the Outer Bay reach 80 m; in the Inner Bay, there are several separate basins 40 to 60 m deep. Rivers drain into the head of the main bay, and also into the head of Makkovik Harbour. The bay is frozen over from December to June of each year.

The principal purpose of this study was to make a detailed reconnaissance of a typical coastal inlet in Labrador, in the hope that a generalized model of Holocene sedimentation could be developed, which could then be applied to other Labrador bays. The marine geology of Labrador coastal inlets is virtually unknown (Piper et al., 1975; Grant, 1975). A model has been developed in Nova Scotia applicable to a subsiding coastline where the principal sediment supply is from drumlins (Piper and Keen, 1976). In contrast, the Labrador coast is still isostatically rising, and glacial till is unimportant as a sediment source.

Methods

The survey was carried out in a way similar to previous small boat studies in Nova Scotia, using a rented 32-foot fishing boat. A Kelvin-Hughes, 14 kHz, model MS26G sounder was used to determine water depth and to obtain shallow seismic penetration in muddy sediments. A Varian M-50 magnetometer was used. Samples were obtained by Dietz-LaFond snapper and a 2" ID corer. Loss of the corer prevented a full coring program. Lack of a reverse gear on the boat limited our investigation of shallow water. Navigation was by sextant sights onto known points on land, and by comparison of bathymetry with the Hydrographic Service field sheets.

Bottom Reflector Types

Four types of bottom reflectors are recognized on MS26 profiles, and can be identified by sampling as follows:

(a) Rock. This gives a sharp reflection on MS26 records. It characteristically forms an irregular high relief sea floor.

(b) Sand and gravel. These also give a sharp reflection on MS26 records, but form a much smoother bottom than rock.

(c) Dark mud. This forms a smooth acoustically transparent bottom, with rare internal reflectors.

(d) Grey clay. This is also acoustically transparent, but generally appears internally stratified. The surface is generally irregular and erosional.

Rock

Most of the shoreline of Makkovik Bay is rocky, with small pocket beaches. The principal rock-free coastal areas are at the head of Fords Bight and Makkovik Bay, and along parts of the central and eastern Inner Bay. Shoal areas in the Approaches to the bay are of rock, with small patches of shelly sand or gravel in depressions. Most shoals in the Outer Bay have a core of rock, but are overlain, at least in part, by grey clay. Rock shoals are rarer in the Inner Bay, the most conspicuous being the line from North Head to Gull Island.

Differential glacial erosion of bedrock is probably responsible for some major physiographic features, such as the line of deep water basins extending north from Wild Bight.

Sediments

The results of detailed textural analysis, combined with the interpretation of MS26 profiles, allow 6 sediment types to be distinguished. Their distribution is shown in Figure 62.2.

1. Dark mud is found in ponded basins throughout the bay. The silt content of the mud is variable. It is rich in organic matter and well bioturbated. The minimum depth at which dark mud occurs in the approaches is about 60 m, but in the sheltered Inner Bay muds occur in waters as shoal as 20 m.

2. In places, the dark mud grades into silty sands in shallower water, but generally a zone of gravelly sandy mud lies between the basinal muds and nearshore sands. Short cores show that the gravel is frequently concentrated at the sediment surface, suggesting winnowing of finer sediment. In some cores, thin, gravel-rich beds are also found below the surface. The MS26 profiles suggest this is a zone of sediment bypassing, with little net deposition. The gravels are probably ice-rafted.

3. Well sorted sands are found in the nearshore zone. In the lower energy areas of the bay — in Inner Bay, Makkovik Bay and Fords Bight — the LWM is marked by a boulder barricade developed at the limit of shore-fast ice. Seaward of this, sediment is frequently of bimodal size distribution, with boulders and cobbles in a fine sand matrix. Seawards, the boulders and cobbles usually become less common, and the sand finer, passing into a coarse silt.

   In the Outer Bay and approaches, boulder barricades are less well developed. Nearshore sands are more unimodal, and in shallow water may be of coarse or medium grade. In deeper water, coarse silts occur.

4. In the Approaches of the bay, well sorted medium and coarse sands and pebble and cobble gravels, sometimes with much comminuted shell material, are common in small pockets and basins in the otherwise wave-swept, bare rock, shoals.

[1]Departments of Geology and Oceanography, Dalhousie University, Halifax, N.S.

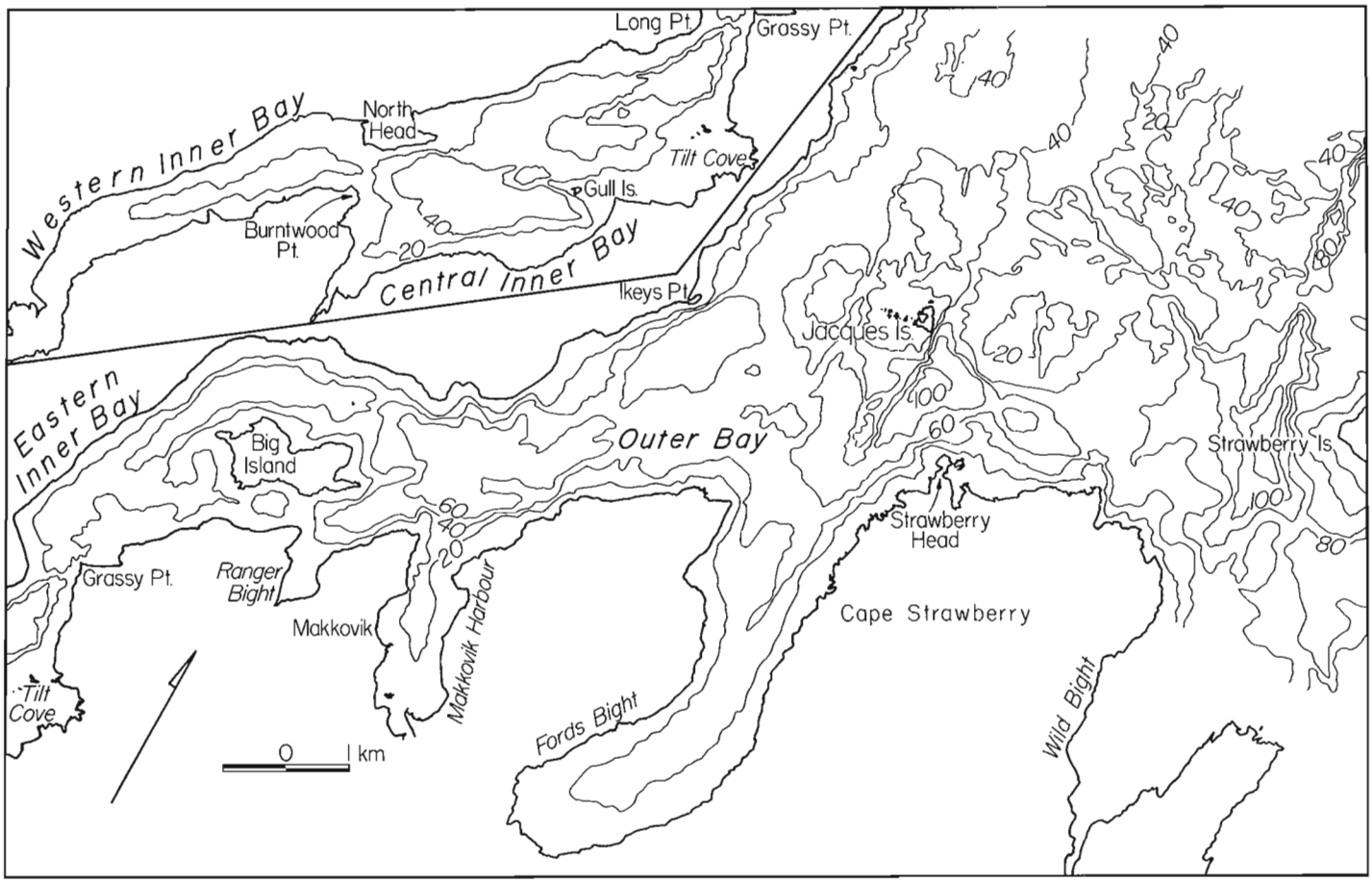

Figure 62.1. Bathymetry of Makkovik Bay. Contours at 20-m intervals based on Canadian Hydrographic Services field sheets.

5. Sands (often gravelly and rather poorly sorted) occur at the margins of the rocky shoals in the Approaches to the bay. They are generally thin enough to be penetrated by the MS26 profiler, and overlie the grey clay unit. They appear to be a lag concentrate.

6. The light grey clay found in many parts of Makkovik Bay is not a contemporary deposit. In many areas it is at present being eroded. MS26B profiles of the grey clay show prominent subbottom reflectors which are frequently truncated at the present sea floor.

In the shoals east of Jacques Island, in the Approaches, the grey clay forms a flat basin floor at a depth of about 50 m, through which rise the rocky shoals. In this area, there is no evidence that the unit is eroded; but in the deeper water farther south and in Wild Bight, the surface of the grey clay appears irregular and erosional. The surface of the grey clay also appears erosional throughout the rest of Makkovik Bay. The most spectacular example is the narrow 40-m-deep channel cut through a grey clay shoal between Gull Island and Long Point. Grey clay outcrops on the low tide terrace in southwestern Fords Bight, and at the mouth of Makkovik Brook. In many areas, a thin veneer of sandy sediment overlies the grey clay.

Only a few uncontaminated samples of the grey clay unit have been obtained. These suggest that this lithology consists of alternating thin beds of grey clay and silty mud with only small amounts of sand. The surface of the grey clay unit is generally bioturbated. Samples from the Approaches contain a normal marine foraminiferal assemblage.

Surficial Deposits on Land

Outcrops of surficial sediment are rare, being restricted to brooks, rare coastal bluffs, and artificial exposures close to Makkovik. Raised beaches are common on the exposed shoreline of the Outer Bay and Approaches. Generally they are only recognizable up to 10 m above present sea level; the highest raised beaches are less than 30 m above present sea level. Till has been seen in only one outcrop in Halibut Brook. It appears much less important than stratified drift as a source of sediment to the bay.

Stratified sands and gravels are well exposed at Burntwood Point, at the mouth of Makkovik Brook, and in a large pit between Ranger Bight and Makkovik. The former two outcrops comprise sands with rare gravels dipping at 20° to 30°. The Ranger Bight outcrop is more complex. The lower part of the sequence consists of gravels dipping 10° to 20°, and becoming finer and sandier upwards. Some higher gravels have a rather low dip, and the sequence is in places overlain by horizontally bedded sands and gravels. This gravelly succession is unconformably overlain by well sorted, fine sand with rare "floating" pebbles and some cross-bedding.

In all three outcrops the steeply dipping beds appear to be Gilbert-type deltas, built out into a body of probably fresh or brackish water. The foreset-topset transition seen at Ranger Bight, which occurs at about 35 m above present sea level, marks the approximate water level at the time the deltas formed. It seems most reasonable that these deltas developed during deglaciation at a time when sea level was 35 m above its present level, but more detailed work on land is needed to substantiate this suggestion.

The grey clay unit of Makkovik Bay may represent the bottomset unit of the Gilbert-type delta. Volumetrically, the foreset sands and gravels appear more important than either glacial till or modern delta deposits, and a corresponding importance of synchronous fine sediment can be expected. Grey clay appears to be overlain by foreset sand at the mouth

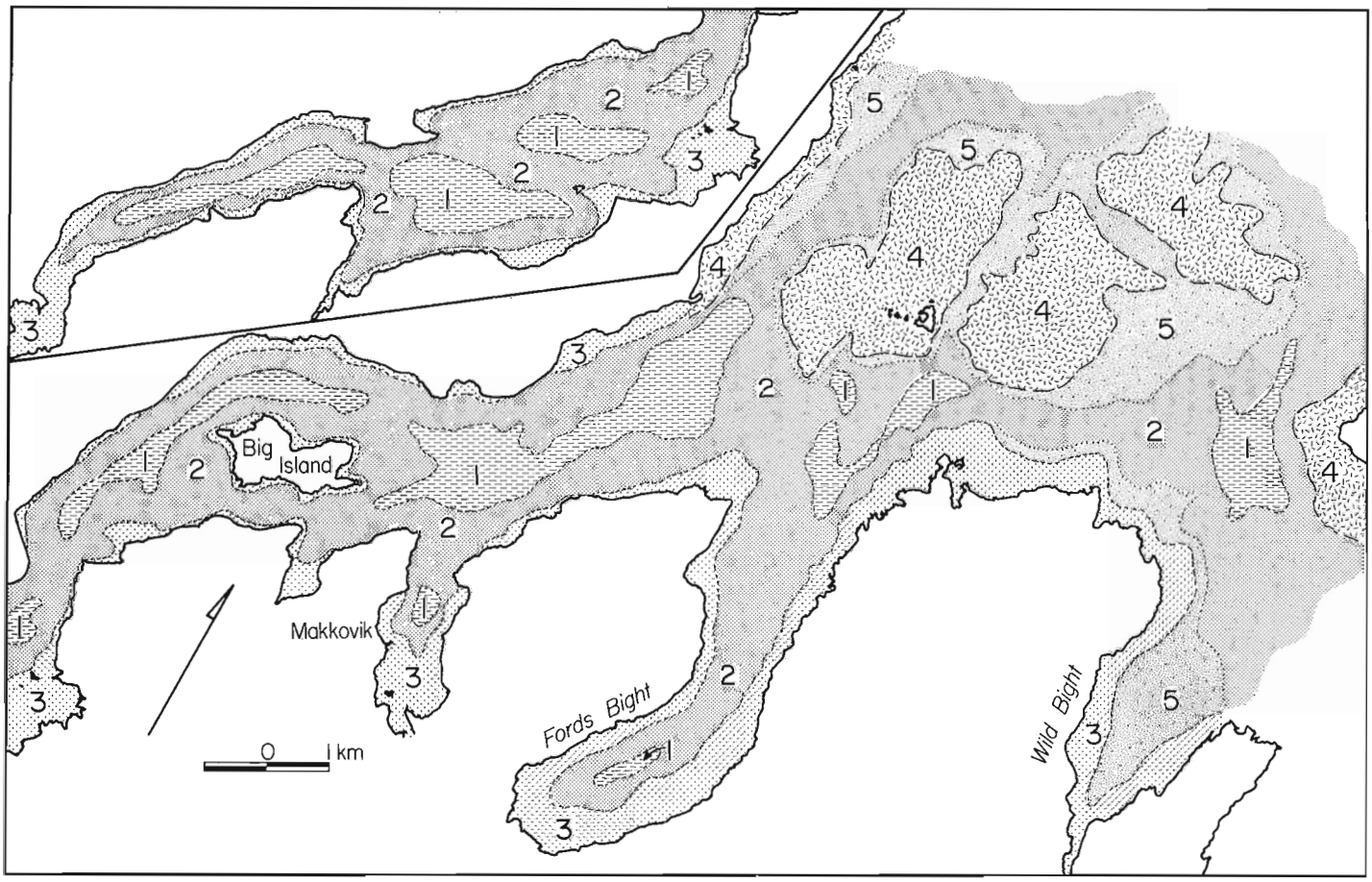

Figure 62.2. Surficial distribution of sediment types within Makkovik Bay. Full details in text 1: dark mud, 2: veneer of gravelly sandy mud; 3: nearshore sand prism; 4: coarse sands and gravels among rocky shoals; 5: veneer of sand and gravel.

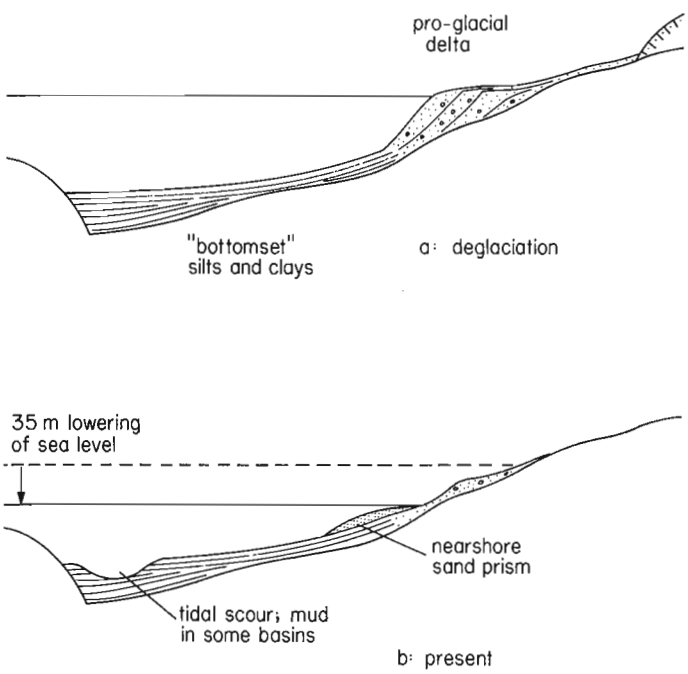

Figure 62.3. Model of postglacial development of Makkovik Bay.

of Makkovik Brook, in a manner similar to that found in late-Glacial Gilbert-type deltas on the north shore of the Minas Basin, Nova Scotia (Swift and Borns, 1967).

A Model of Development of the Bay

The basic erosional form of the bay probably dates from one of the extensive mid Quaternary glaciations. The last glaciation probably caused only minor erosion, and locally deposited very thin tills.

At the time of deglaciation, sea level stood 35 to 40 m higher than at present. The rapid supply of glacial detritus produced Gilbert-type deltas at the margin of the fiord, with gravelly topsets, steep sandy foresets, and grey clay bottomsets (Fig. 62.3). Ice-rafting deposited some coarser sediment in the bottomsets. In the Approaches to the bay, the bottomset clays filled topography to a level about 50 m below present sea level. In this open water area, there were normal marine salinities. In the more restricted waters of the Inner Bay, closer to the sediment source, conditions were probably brackish. Bottomset clays locally occur above present sea level.

Since this time, sea level has probably fallen continuously due to isostatic rebound. The rivers have not supplied large amounts of sediment to the bay, because of their irregular thalwegs, although small streams draining across deltaic sands and gravels have built up significant modern deltas. However, the bottomset grey clay unit has clearly been eroded, and this erosion has probably supplied most of the modern sediment to the bay. The mud has accumulated in the basins, while the small amounts of sand and gravel have been concentrated as a surface lag. Nearshore sands are, at least in part, derived from erosion of surficial deposits on land.

Erosion of the grey clay unit has been principally by tidal scours. Deep basin-like depressions are found close to bedrock constrictions. As sea level fell, the tidal prism became more and more restricted, and in consequence, erosion of the soft sediment occurred.

The contemporary distribution of sediment is similar to the model proposed by Swift (1976) for sediment-poor coastal zones. A thin nearshore sand prism passes offshore into a zone of no net sedimentation which is scoured clean by longshore currents during storms.

References

Grant, A.C.
1975: Seismic reconnaissance of Lake Melville, Labrador; Can. J. Earth Sci., v. 12, p. 2103-2110.

Piper, D.J.W., Wightman, D.M., Lewis, J.F., and Dwyer, G.J.T.
1975: Late Quaternary Geology of Nain Bay, Labrador; Marit. Sediments, v. 11, p. 53-54.

Piper, D.J.W. and Keen, M.J.
1976: Geological studies in St. Margaret's Bay, Nova Scotia; Geol. Surv. Can., Paper 76-18, 18 p.

Swift, D.J.P.
1976: Coastal sedimentation; in Marine Sediment Transport and Environmental Management (D.J. Stanley and D.J.P. Swift, eds.), p. 255-310.

Swift, D.J.P. and Borns, H.W.
1967: A raised fluviomarine outwash terrace, north shore of the Minas Basin, Nova Scotia; J. Geol., v. 75, p. 693-710.

63. DISSOLVED CHROMIUM SPECIES IN COASTAL WATERS

Project 750083

R.E. Cranston
Atlantic Geoscience Centre, Dartmouth

Abstract

Cranston, R.E., Dissolved chromium species in coastal waters; Current Research, Part A, Geol. Surv. Can., Paper 78-1A. p. 337-339, 1978.

A precise and accurate technique for determining the major species of chromium in natural waters has been developed. The results for samples from two fiords in British Columbia and from the northeast Pacific Ocean confirm general thermodynamic theory regarding the distribution of major species. Biological processes can alter the dissolved Cr distribution by reducing Cr (VI) to CR (III) and by taking up Cr from surface waters which is subsequently released at depth when the detritus decomposes.

Introduction

A challenging problem facing marine geochemists is that of identifying chemical speciation of elements. In order to study and to predict the fate of an element, the major species have to be identified and quantified. One element of interest is chromium (Cr) which is present in various forms in natural waters; these forms depend on the local concentrations of other ions, compounds and particles.

It is thought that Cr exists in two major oxidation states (III and VI) with the major species being $Cr(OH)_2 4H_2O^+$ and $CrO_4^=$ respectively (Elderfield, 1970). At natural seawater conditions (pE = 12.5, pH = 8.1) the thermodynamically stable form is $CrO_4^=$ (Fig. 63.1), however significant amounts of Cr (III) have been found in natural oxygenated waters (Brewer, 1975). This discrepancy may be partly due to peculiarities of the analytical techniques used by different workers. In addition, kinetics may be a significant factor since reactions involving the Cr (III) ligand are known to be slow (Mertz, 1969).

Biological activity can cause apparent nonequilibrium conditions that alter the relative abundance of the various forms of trace metals. Since Cr exists in the trivalent state in biochemical systems (Mertz, 1969), it is possible that localized Cr (III) anomalies could arise as a result of the excretion of body fluids. Biologic action can also concentrate many trace metals by physical and chemical uptake. The distribution of copper in ocean waters has been accounted for as surface depletion by biological processes and enrichment in bottom waters as the hard parts of the detritus dissolve on sinking to the sea floor (Boyle and Edmond, 1975).

Other natural parameters may control the species of Cr found; these include the nature and mixing of fresh water, the nature and concentration of suspended matter and dissolved organic matter. Results from investigations of these parameters will be discussed at a later date.

Analytical Method

Variation in analytical techniques account for a significant portion of the variance reported in the literature dealing with Cr speciation (Brewer, 1975). The shortcomings of these various methods has led to discrepancies and the absence of reliable deep-ocean profiles of chromium in published form. Solvent extraction techniques have been used to select Cr (III) (Chau et al., 1968) and Cr (VI) (Jan and Young, 1976), but in order to quantitatively extract each species, the pH of the sample had to be reduced to 6 and 3.5 respectively. From the pE-pH diagram (Fig. 63.1) it is apparent that such lowering of the pH changes the equilibrium of the system and may result in Cr (VI) being reduced to CR (III).

Because of the strong absorption characteristics for Cr (III), co-precipitation techniques have been used to remove Cr from large volumes of water (Chuecas and Riley, 1966). Pankow et al. (1976) used cation and anion exchange resins to differentiate between Cr (III) and Cr (VI) in river samples, but their lowest concentrations were much higher compared to those found in normal seawater. Differential pulse polarography has been used to determine Cr (VI) in fresh water with a detection limit about 100 times above seawater concentrations (Crosmun and Mueller, 1975).

In this work the co-precipitation method using $Fe(OH)_3$ to collect Cr (III) was chosen as the method after searching the literature and trying solvent extraction techniques. The major drawback seemed to be that nearly all iron sources used for the co-precipitation had large Cr background contamination. This was not the case for ferrous ammonium sulphate (Baker Chemical Co.). This ferrous salt could be converted to $Fe(OH)_3$ by adding NH_4OH and shaking the solution for a day to oxidize the ferrous iron. The resulting ferric iron recovered Cr (III) standard additions well.

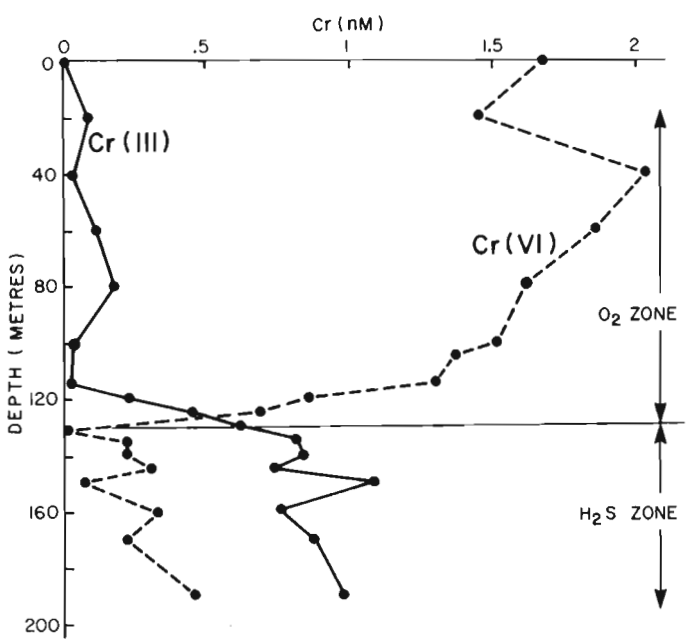

Figure 63.1. pE-pH Relationships for Cr species.

In further experiments, it was found that by adding NH_4OH to the $Fe(NH_4)_2(SO_4)_2$ and immediately adding this solution to a sample, both Cr (III) and Cr (VI) could be recovered quantitatively. It appears that the oxidation of Fe (II) to Fe (III) reduces the Cr (VI) to Cr (III) and results in quantitative total co-precipitation.

The final procedure adopted to obtain quantitative data on Cr (III) and Cr (VI) required selective co-precipitation of Cr (III) and then a co-precipitation of total Cr. This was accomplished by adding 1 ml of 0.01 M $Fe(OH)_3$ at pH 8 to 140 ml of aqueous sample in order to scavenge Cr (III). To recover both Cr species, 1 ml of 0.01 M $Fe(OH)_2$ at pH 8 and the required NH_4OH was added to 140 ml of sample. The samples were filtered through 0.4 ηm Nuclepore filters after shaking for 2 hours. The $Fe(OH)_3$ was dissolved from the filter with 6 M HCl and analyzed by atomic absorption spectroscopy using a heated graphite furnace.

Additions of Cr (III) and Cr (VI) have been made to seawater samples to test the accuracy and specificity of the method. The following table contains the recovery efficiencies for 10 additions.

		Recovery Efficiency (per cent ± Std. Dev.)	
Species Sought	Fe Type	Cr (III) added	Cr (VI) added
Cr (total)	$Fe(OH)_2$	93 ± 8	91 ± 8
Cr (III)	$Fe(OH)_3$	83 ± 7	1 ± 2
Cr (particulate)	none	8 ± 11	0 ± 0

Both Cr types were recovered by the $Fe(OH)_2$ addition. Only Cr (III) standard additions were recovered by the $Fe(OH)_3$. Particulate matter may collect some Cr (III) if enough particles are present. Efficiencies are less than 100 per cent due to adsorption to the walls of the containers and to the filtration equipment.

Triplicate seawater samples from a fiord and the northeast Pacific have been analyzed to determine the precision of the overall method. The average absolute precision (1 std. dev.) is ± 0.07 ηM. Results are included in the following table for 11 sets of triplicates.

Cr Type	Average Conc. (ηM)	Mean Std. Dev. (± std. dev. of mean for 11 sets, in ηm)
Cr (total)	2.60	0.12 ± 0.08
Cr (III)	0.17	0.05 ± 0.04
Cr (particulate)	0.12	0.05 ± 0.04

A detection limit of 0.02 ηM Cr in a 0.5 L sample, or 1 part per trillion was obtained.

Results

The Cr method was tested on two cruises during July, 1977 onboard the **R/V T.G. Thompson** of the University of Washington. The first cruise was designed to study the anoxic nature of Saanich Inlet, British Columbia and to compare it to Jervis Inlet, an oxidizing fiord. The second cruise was off the coast of Washington State, sampling the water column at shelf depths of 100 m to offshore depths exceeding 3000 m. The Saanich data (Fig. 63.2) indicate that Cr (VI) is the predominate species in oxgenated waters, while Cr (III) is dominant in reducing waters (i.e. the sulphide zone, Fig. 63.1) as is predicted thermodynamically. A linear regression analysis was applied to the chemical data from 3 stations in the region of redox cross-over. The resulting equation indicated that approximately 1 mole of Cr (III) is oxidized by 1 mole of oxygen ($r = 0.73$, $n = 17$, $p > 99.9\%$).

In Jervis Inlet, Cr (VI) was dominant, except for 2 samples in the top 50 m, where freshwater runoff, dissolved organic carbon, and biological activity may affect the redox couple. For the deep Pacific samples, Cr (VI) dominates, with a small Cr (III) peak at 75 m (Fig. 63.3). Cr (III) should be undetectable in oxygenated waters, however, out of 108 oxygenated fiord and open Pacific samples, 31 of the Cr (III) results were greater than 10 per cent of the total Cr. A majority of them occurred in the shallow water from the fiords or the continental shelf. It is suggested that some mechanisms related to shallow, near-shore waters are causing a reduction of a portion of the Cr (VI).

Correlation coefficients were obtained from supporting data in an attempt to describe this observation. A significant correlation ($p > 99.9\%$) for Cr (III) paired with nitrite has been obtained($r = 0.43$, $n = 82$). Surface anomalies of nitrite (NO_2^-) in oxygenated waters are attributed to zooplankton excretion of NH_4^+ which is oxidized initially to nitrite, then to nitrate (Riley and Chester, 1971). It is therefore suggested, by the correlation, that the anomalous Cr (III) is also related to the zooplankton excretion. Cr (VI) may be taken up by plankton, reduced to Cr (III) due to the reducing nature of the biochemical cycle and released as Cr (III) in excreted matter.

Another noteworthy result for the Pacific data is that the Cr (total) values appear to increase with depth. This distribution may be due in part to surface depletion by biological uptake and enrichment in bottom waters as the detritus dissolves. If this does occur, the data should correlate with depth and nutrient values, since the deep ocean contains the dissolved remains of many years of production and is greatly enriched in silicate, phosphate and nitrate. For 4 stations with depths greater than 2000 m, the following correlation coefficients were obtained.

	Depth	PO_4^{-3}	SiO_4^{-4}	NO_3^-
Cr (total)	0.78	0.52	0.74	0.51

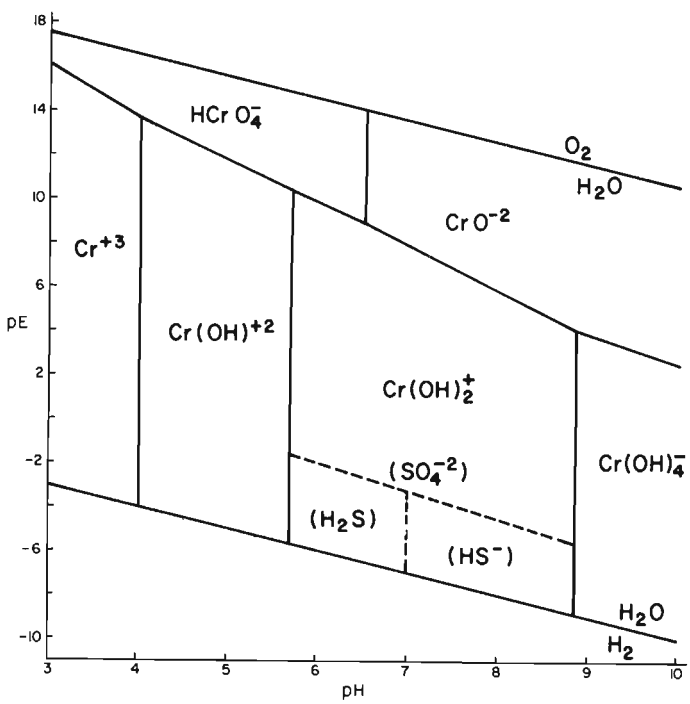

Figure 63.2. Cr species in Saanich Inlet, July, 1977.

All of the coefficients are highly significant ($p > 99.9\%$, $n = 42$). Cr correlates most strongly with depth and silica and somewhat less with phosphate and nitrate data. It is therefore suggested that a portion of the Cr variance can be explained by organism uptake at the surface and its subsequent release at depth as the detritus decomposes. The preference for the Cr-silica correlation suggests that the major type of biota involved may be silicious in nature.

Conclusion

A major drawback in chromium geochemistry for natural waters has been the lack of reliable methods. A precise and accurate method to analyze natural waters has been presented. The major advantage of the method over most others is that both forms of Cr are collected at their natural pH and analyzed by the same procedure, with a minimal problem due to blanks. A detection limit for 0.5 L of sample is 0.02 ηM (1 part per trillion). Average values for these ocean waters are 2.3 ηM for Cr (VI), 0.17 ηM for Cr (III), and 0.12 ηM for Cr (particulate).

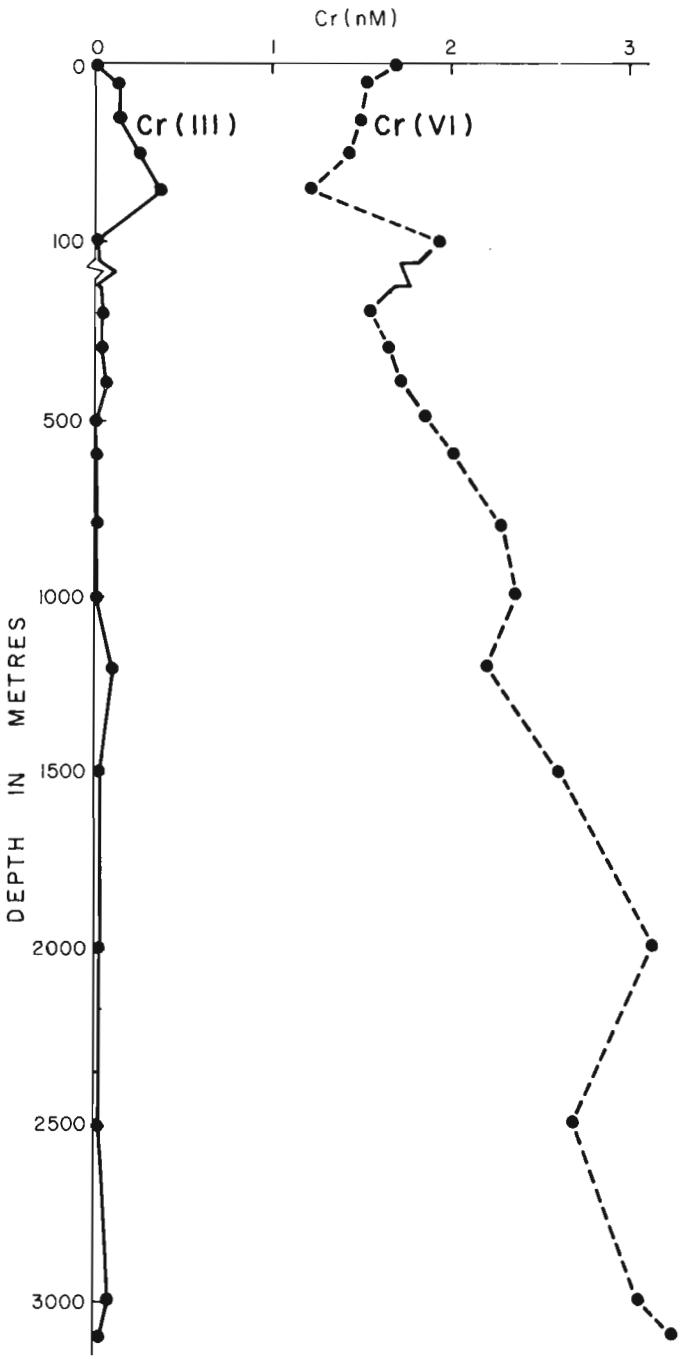

Figure 63.3. Cr species in northeast Pacific Ocean Waters (132.5°W, 47°N).

Natural distributions of Cr (III) are affected by reducing conditions such as those occurring in an anoxic fiord, with a majority of Cr (VI) being reduced to Cr (III) when H_2S is present. Biological activity appears to reduce some Cr (VI) and release it via excreted material. Elsewhere, the dominant form of Cr is Cr (VI), as is predicted by thermodynamic calculations. In addition to reducing some Cr (VI), biological processes appear to remove Cr from surface waters and release it in the deep ocean as the biomass decomposes.

Further work is currently being carried out to determine the form and migration pathways of Cr species in an estuary and in the eastern tropical Pacific, where an intense oxygen minimum may reduce Cr (VI). Laboratory experiments will also be carried out to study redox and adsorption kinetics, as well as the effect of dissolved organic matter on Cr speciation.

References

Boyle, E. and Edmond, J.M.
1975: Copper in surface waters south of New Zealand; Nature, v. 253, p. 107-109.

Brewer, P.G.
1975: Minor elements in seawater; Chemical Oceanography, (Riley and Skirrow, editors) 2nd edition, Volume 1, Chapter 7, Academic Press, London.

Chau, Y.K., Sim, S.S., and Wong, Y.H.
1968: Determination of chromium by atomic absorption – Spectrophotometry of chromium acetylacetonate; Anal. Chim. Acta., v. 43, p. 13-18.

Chuecas, L. and Riley, J.P.
1966: The spectrophotometric determination of chromium in seawater; Anal. Chim. Acta., v. 35, p. 240-246.

Crosmun, S.T. and Mueller, T.R.
1975: The determination of chromium (VI) in natural waters by differential pulse polarography; Anal. Chim. Acta., v. 75, p. 199-205.

Edlerfield, H.
1970: Chromium speciation in seawater; Earth Planet. Sci. Lett., v. 9, p. 10-16.

Jan, T.K. and Young, D.P.
1976: Southern California Coastal Water Research Program; Annual Report, El Segunda, California.

Mertz, W.
1969: Chromium occurrence and functions in biological systems; Physiologic Rev., v. 49, p. 163-230.

Pankow, J.F., Leta, D.P., Lin, J.W., Ohl, S.E., Shum, W.P., and Janauer, G.E.
1976: Analysis for Chromium Traces in the Aquatic Ecosystem: II. A study of Cr (III) and Cr (VI) in the Susquehanna River Basin of New York and Pennsylvania; Science of the Total Environment, v. 7, p. 17-26.

Riley, J.P. and Chester, R.
1971: Micronutrient Elements; in Introduction to Marine Chemistry, Chapter 7, Academic Press, London.

Project 770006

C.J. Yorath, R.G. Currie, D.L. Tiffin, and B.E. Cameron
Regional and Economic Geology Division, Vancouver

Abstract

Yorath, C.J., Currie, R.G., Tiffin, D.L., and Cameron, B.E., Submersible operations on the Canadian Pacific Continental Margin, Report II; Current Research, Part A, Geol. Surv. Can., Paper 78-1A, p. 341-349, 1978.

The primary purpose of this project was to evaluate the submersible ***Pisces IV*** *as a vehicle for conducting reconnaissance geological mapping on the Canadian Pacific continental shelf. Equipped with an improved sampling and communications system in addition to an underwater compass and acoustic navigation system, the submersible was used to conduct several traverses across a belt of stratigraphically and structurally complex terrain. Realizing its limitations, it is concluded that the vehicle can be used as an effective mapping tool.*

Introduction

In May and June 1977, the authors participated in geological mapping and stratigraphic studies on the continental shelf and slope adjacent to northern Vancouver Island (Fig. 64.1). The primary purpose of the project was to evaluate the **Pisces IV** submersible as a vehicle for conducting reconnaissance mapping on the continental shelf over areas where bedrock exposure was known. The testing of an underwater acoustic navigation system, underwater magnetic compasses, a new sampling system and improved underwater communication system were critical to the project.

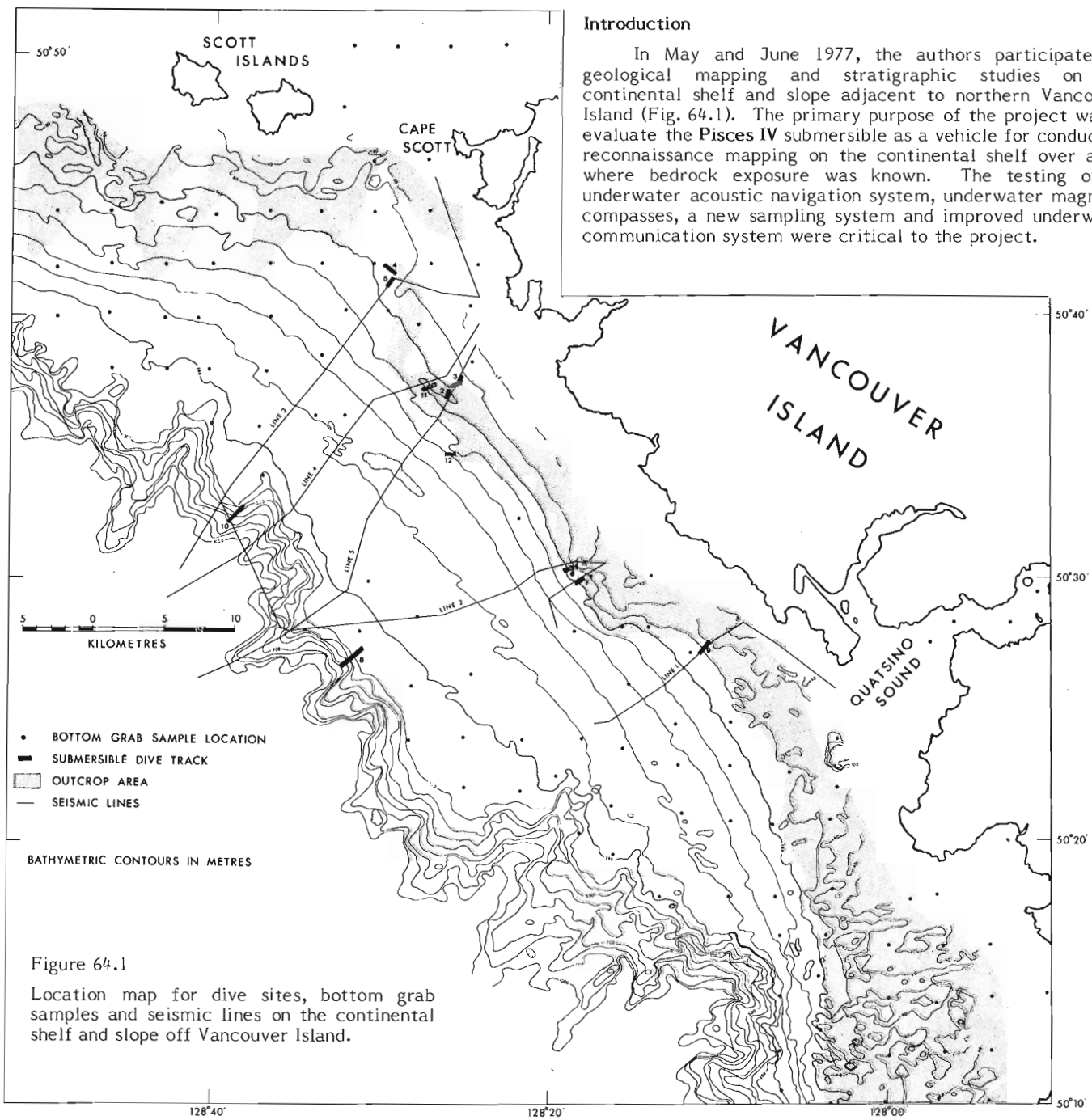

Figure 64.1

Location map for dive sites, bottom grab samples and seismic lines on the continental shelf and slope off Vancouver Island.

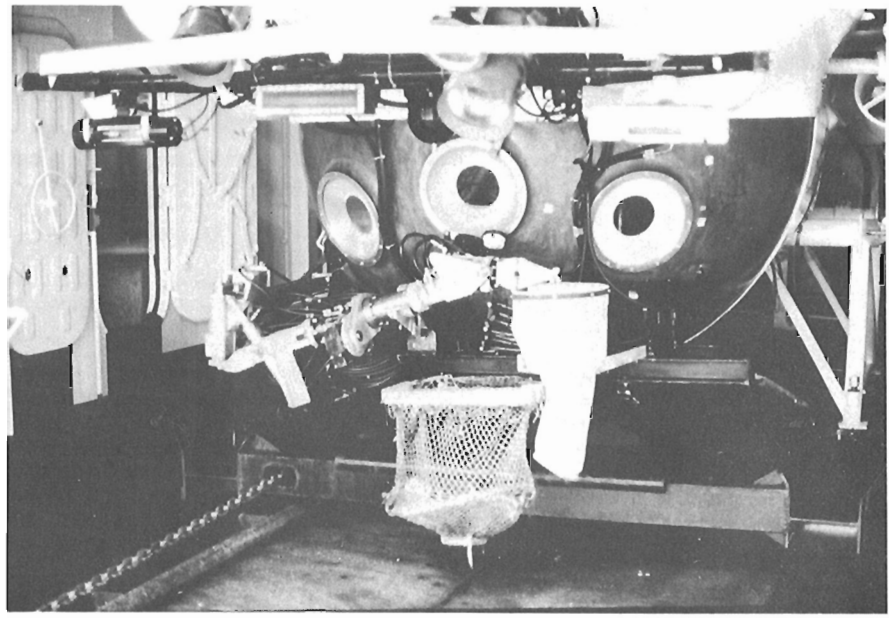

Figure 64.2

Submersible sampling system. The jaws of the mechanical arm are positioned above the stacked sample nets housed in a flexible container. The "T" handles for each net are below the wrist of the arm. The large sample storage net is mounted on a rigid metal frame below the centre viewport.

Survey Technique

Preliminary to the field season, maps were prepared illustrating regions of bedrock outcrop as deduced from the examination of echogram profiles obtained by the Canadian Hydrographic Service and seismic profiles recorded by the Geological Survey over the study area. Regions of complex topography, underlain by bedrock, occur as two broad belts. The first extends from the southern boundary of the map-area to off Cape Scott and is the area across which all the 1977 dives were conducted. The second region occurs as a series of broad arcs extending southward from Scott Islands (Fig. 64.1).

In addition to the echograms and seismic records, magnetic data were examined, which, in conjunction with the known geology of northern Vancouver Island (Muller et al., 1974) permitted a preliminary interpretation of the offshore geology. Field sheets of the region were constructed at a scale of 1:20 000 upon which was superimposed the Loran-C grid and bathymetry.

Based upon the previous year's experience (Yorath et al., 1977) the sample recovery and storage system was substantially modified. What was needed was a way of collecting an optimum number of samples and storing them on the submersible in such a way that following the dive, each sample could be positively identified and related by number to tape recorded and written notes. The system (Fig. 64.2) included a series of individually numbered, nested sample nets, each mounted on a metal right with a "T" handle, and stacked in a flexible container. Following the collection of a sample with the mechanical arm, the sample was dropped into the uppermost net inside the flexible container. The mechanical arm would then grab the "T" connection and lift the net containing the sample out of the container. The number of the net was recorded visually through the view ports and, for storage during the dive, the netted samples were dropped into a second larger net attached to a rigid metal frame which was positioned under the forward end of the submersible. Although minor problems such as fouling of the nets in the flexible container and tearing of the storage net on rough sea floor were encountered, the system worked satisfactorily and needs little further modification.

Submarine mapping with a submersible requires a reliable navigation system both for accurate mapping and safety. This was accomplished by installing an underwater magnetic compass and acoustic navigation system. The magnetic compass, obtained from Digicourse Inc. consists of a sensor, housed in a water-tight binnacle, and mounted on the "sail" of the submersible (Fig. 64.3), and a digital display mounted inside the personnel sphere. The compass was

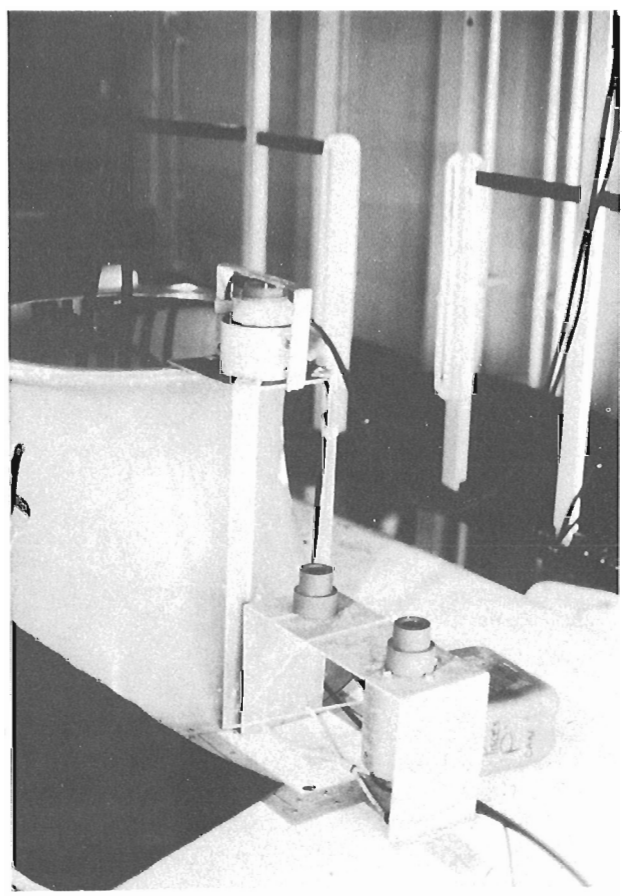

Figure 64.3. Underwater magnetic compass binnacle (top) and acoustic navigation transponder (below) mounted on the fiberglass cove of the submersible.

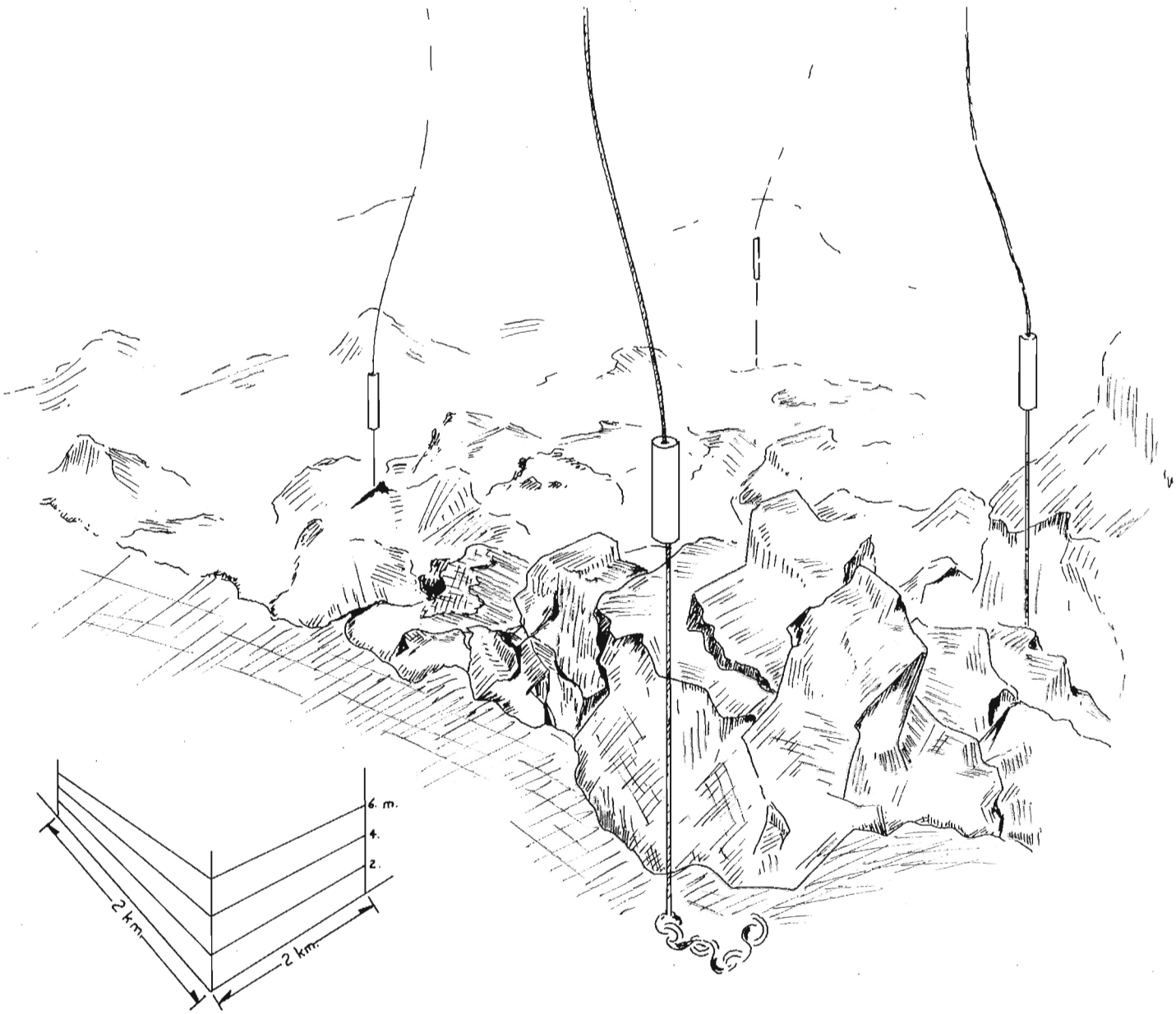

Figure 64.4. Compressed sketch of the seaward face of the outcrop belt illustrating geometry of the transponder arrow (metal floats not shown). The irregular rock masses represent the morphology of the belt at some of the dive locations.

corrected by a standard "swinging" method until a maximum variation of 2° was obtained using correcting magnets in the binnacle.

The success of the project greatly depended upon the underwater acoustic navigation system. This system, provided by Mesotech Systems Ltd. of Vancouver, consists of an array of four, bottom moored, 18 kHz transponders, and an interrogation and display console mounted inside the submersible. The position of the submersible within the transponder array, determined by the interrogator, was obtained by measuring the range (in metres) to each of the transponders within reception range of the submersible (maximum range approximately 3 km). The transponders were anchored by weights and suspended about 20 m above the sea bottom by spherical metal floats. This allowed the transponders to be positioned above the height of most predicted rock pinnacles, thus eliminating loss of signal under normal circumstances (Fig. 64.4). If the locations of the transponders were accurately determined, the measured ranges could be used to calculate the submersible's position within 10 m.

To determine the position of the transponders a survey method similar to that described by Heckman and Abbott (1973) was used. After placing the transponders at preselected positions, slant ranges to each were measured from a number of surface locations within the array. This was done by lowering the submersible's hull-mounted interrogation transducer (Fig. 64.3) into the water while **Pisces IV** was positioned on the launch deck of the mothership **Pandora II.** The resultant multiple slant ranges obtained permitted a number of equations to be written relating the ship's position to the transponder locations. The set of equations was then solved iteratively for the ship's locations in a manner that minimized the difference between calculated and observed ranges. This procedure was then inverted keeping the calculated ship's position fixed and adjusting the transponder locations, including depth, according to the same criteria. It took between 50 and 100 iterations and approximately 15 minutes using a Canon SX 100 programmable calculator to determine the relative transponder locations within ± 20 m. The geographic position of the transponder array was determined from Loran-C readings on the mothership.

Loran-C is a long-range (1500 km) radio aid to navigation that provides excellent repeatability and geographic accuracy. Although the Loran-C network on the west coast has yet to be fully calibrated, results from the east coast (Eaton, 1975) indicate that in the hyperbolic mode, a position repeatability of 250 m and a geographic accuracy of ± 1200 m or better may be expected. A limited amount of calibration was performed at Winter Harbour, Port Alice, and Port Harding during the project. At these locations the geographic accuracy was ± 200 m and the repeatability was ± 100 m.

The observed Loran-C readings were converted to latitude and longitude using an iterative algorithm similar to that of Grant (1973) as Loran-C navigation charts at suitable scales were not available at the time of the cruise. An estimate was made of the ship's position, the distance to the master and slave stations was determined and theoretical Loran-C readings were calculated. These values were compared with the observed readings and the ship's location was adjusted until the theoretical and observed readings agreed to within a specified degree of tolerance. The conversion from Loran-C to geographic co-ordinates took from 3 to 5 minutes depending upon the accuracy of the original estimate and the tolerance limits to the solution. To simplify the calculations in determining transponder locations the geographic co-ordinates were converted to UTM co-ordinates. The total error in submersible locations is thought to be ± 250 m.

Diving Operations

A total of eleven dives were carried out, nine of which were across the outcrop belt on the inner shelf and two were stratigraphic ascents of the continental slope (Fig. 64.1). An ancillary bottom sampling program was conducted following daily diving operations or when rough seas prevented diving.

The launch positions of many of the shelf dives were selected where the flat, gravel and sand covered sea floor intersected the seaward and landward faces of the outcrop belt. On a number of occasions, complete traverses across the outcrop belt were precluded by the rapid (4 hour) drawdown of the submersible's 28 volt instrument power system; this required an additional dive within the array, following battery charging, usually undertaken in the opposite direction.

During each dive, geological and other observations were recorded on a cassette tape recorder. At station stops ranges to each transponder, time and depth were recorded in written form. This information was passed to **Pandora II** by underwater telephone where the track and station positions were plotted on the 1:20 000 field sheets. Video tape recording with voice imprint was maintained throughout the length of each dive. One hundred and seventy-eight 70 mm colour photographs and thirty-six 35 mm colour photographs were taken. It is unfortunate that the photographs included in this report can not be shown in colour; a great deal of information is excluded as a result.

The operation is considered to have been very successful. Geological mapping can be done with a submersible given a reliable underwater and surface navigation system and effective sub-to-ship communications. Geological contacts can be observed, their local attitudes mapped and deformation structures including joints, faults and folds can be examined. Small scale geomorphic features and modern sedimentary processes including sand wave development can be observed and their important descriptive parameters recorded.

There are, however, a number of problems to be overcome.

1. Geological observations through the small view ports of a submersible under conditions of limited visability (Maximum 30 m) are necessarily very local in extent. The observer is unable to obtain a regional view of the terrain in the manner of many geological operations on land. One's concept of the regional geology therefore is obtained through the compilation of a large number of short traverses across areas of variable stratigraphic and structural complexity. As such it is not unlike geological mapping in the dense tree-covered terrain of the Canadian Shield.

Insofar as the aim of this project is to complete a reconnaissance geological map of the continental shelf and slope, the matter of scale is important. The field mapping scale has been chosen at 1:20 000 within the limits of which traverses will, on the average, be about 6 to 10 km apart. It is presently intended that the publication scale will be 1:250 000 to conform with present mapping on land. However, the geological accuracy of the product will more closely approximate a scale of 1:500 000.

2. Although the sampling system was successful in obtaining 24 bedrock samples during the 9 shelf dives, the sampling procedure is very time consuming (up to one half hour to obtain a single sample). In order to obtain in situ samples with a mechanical arm of limited strength and maneuverability, highly fractured exposures were sought. The rocks, commonly hard, dense volcanics, rarely break easily or into sizes convenient for the mechanical arm and

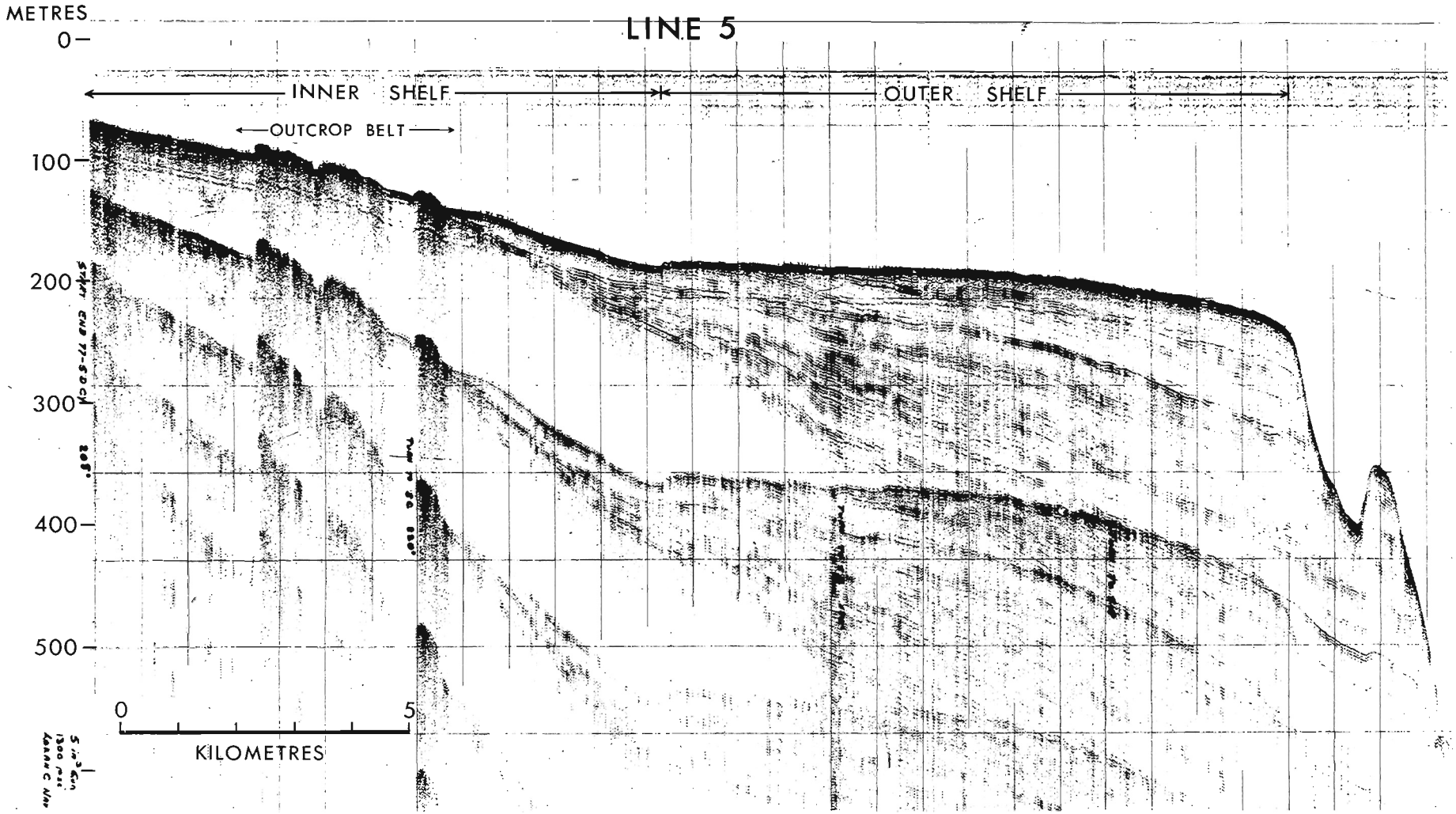

Figure 64.5. Seismic profile across the continental shelf and upper slope. For location of the line, see Figure 64.1.

the size of the nets. A considerable amount of searching was necessary at each station to obtain a recoverable sample. Furthermore, some difficulty in stabilizing the submersible was often encountered due to the presence of strong bottom currents that shifted the boat on the sea bottom. To overcome this, water had to be pumped into the submersible to increase its bottom weight, this adding to the sampling time.

3. Underwater, rocks of varying composition look much alike, particularly in the map-area where basic volcanics, greywackes and metamorphic rocks, all in complex structural juxtaposition, display the same dark colours and resistance to chemical and mechanical weathering. Although differences in internal structure are recognizable (bedded vs massive units), subtle differences in topographic expression were used in an empirical way to record different rock units. The surface colour of the rocks is the product of many factors, which in addition to composition, include the effect of chemical weathering and the amount and type of organic cover. Furthermore, a rock of given composition will have a substantially different surface colour for that part exposed to the sea compared to that portion in contact with a substrate, be it soft sandy bottom or bedrock. In the project area, all rocks examined and collected (including volcanic, metamorphic and sedimentary) possess a mottled dark brown and orange-brown colour where they were exposed to the sea. Their undersides exhibit a variety of colours but are mostly black. Considerable experience and close attention to subtle difference in topographic expression will play an important role in practical mapping. Moreover, a relationship may exist between rock composition and the amount and type of organic cover; if so, this could offer an additional and valuable empirical tool.

4. Selective verbal and written recording of geological and other observations is inadequate for the recovery of all the information needed to compile a geological map. Parameters such as time, course, depth, and position should be frequently recorded in digital form so as to free the observer to make as complete a description of the geological and morphological edifice as possible. To facilitate this the following is planned for future operations;

(a) Time and the digital display of the magnetic compass will be reproduced on the video tape.

(b) It is hoped that a microprocessor based, precision acoustic navigation system will be developed whereby all bottom navigational information will be recoverable both in real time on each vessel and following the dives. Such a system would provide maximum survey efficiency and safety.

(c) The newly acquired PHAS (Portable Hydrographic Acquisition System) hardware will be used to digitally record time, depth, course and position information as well as other data of value, from the navigation system.

Physiography and Geology

The compilation of geological observations for the 1977 diving operation is not yet complete, thus, an interpretive map is not included. Compilation will incorporate all navigation, seismic, magnetic, bathymetric and geological data pertaining to the area. During the 1977 cruise of **CFAV Endeavour** (see Tiffin et al., 1978) several carefully selected seismic profiles were obtained over the dive sites and outer continental shelf. These also will be incorporated into the interpretation. The final product for the initial phase of this project is not expected until following the 1978 season when it is hoped that much needed additional information on the geology of the region will be obtained. A few general observations may be of interest.

The continental shelf adjacent to northern Vancouver Island is approximately 20 km wide and is terminated by a steep continental slope. The shelf is divided into an inner and outer portion by a regionally persistent break in slope that trends in a locally sinuous manner parallel with the coast, about 11 km distant. The flexure occurs at an average depth of about 170 m throughout the map-area. The outer shelf slopes gently seaward at 0.75°, is generally flat, and intersects the continental slope at a sharp break that occurs at about 210 m. The outer part of the inner shelf slopes seaward at 1.20°, is flat to gently undulating and is interrupted on its landward side, approximately 5 km from shore, by a northwestward trending belt of irregular and rough topography. The belt, from Cape Scott to Quatsino Sound, is about 37 km long and continues southwards beyond the map-area. At its northern end its inner and outer limits are defined by steep cliffs which border flat, gently sloping area floor, however, to the south the belt is believed to expand almost to the coast of Vancouver Island. South of Quatsino Sound the belt further broadens as Brooks Peninsula is approached. The average depth of the belt is about 100 m with local internal relief of up to 50 m as expressed by irregular valleys and ridges.

Figure 64.5 illustrates a seismic profile that traverses the continental shelf and upper slope; its location is shown on Figure 64.1. The belt of irregular topography, included as part of the inner shelf, the shelf flexure, and outer shelf limits are shown. Beneath the outer shelf and outer part of the inner shelf is a seaward thickening wedge of Lower Miocene (Tiffin et al., 1972) to Upper Pliocene clastics, parts of which are volcanogenic (Yorath et al., 1977). This succession unconformably overlies Lower Cretaceous greywacke and feldspathic sandstone on the continental slope which probably are equivalents of the Longarm Formation-Queen Charlotte Group-Pacific Rim Complex interval of the west coast of Vancouver Island and Queen Charlotte Islands (Muller et al., 1974; Sutherland Brown, 1968). The Tertiary clastic succession appears to thin to a zero-edge at the seaward limit of the belt of irregular topography which is supported by outcropping volcanic, plutonic metamorphic and minor sedimentary rocks of presumed pre-Tertiary age. It is presently unknown if this thinning is due to stratigraphic condensation towards a depositional edge or whether the zero limit is erosional. Some seismic profiles tend to support the former because reflectors within the unit beneath the outer part of the inner shelf are parallel with the sea floor. However, it appears fortuitous that a depositional edge of Upper Tertiary rocks would coincide with the seaward limit of uplifted older rocks that underlie the belt of irregular topography. No information is available on the age and stratigraphy of the succession underlying the sea floor inshore of the northern end of the belt, however, south of Brooks Peninsula (south of the map-area), rocks of Late Eocene and younger age outcrop along the shores of Vancouver Island (Shouldice, 1971; Jeletzky, 1975; Cameron, 1971, 1972, 1973, 1975). Within the fault-bounded valleys and canyons of the outcrop belt, no strata similar to that exposed on the continental slope were observed.

The outcrop belt of irregular topography consists of extremely complex morphology comprising steep, narrow, V-shaped to commonly flat-bottomed valleys and canyons and irregular, anastomosing and hummocky ridges, pinnacle hills and mesas. Local relief is commonly in the order of 20 m but some hill tops stand 50 m above the nearby flat, gently sloping shelf.

The outer part of the inner shelf, adjacent to the outcrop belt is underlain by a variety of surficial materials including moderately well sorted gravels (Fig. 64.6), silt and fine sand, mixed comminuted, allochthonous carbonate shell hash, sand and boulders (Fig. 64.7) and boulders and erratics (Fig. 64.8) that increase in size and angularity towards the outcrop belt. The carbonate hash, sand and fine gravels are commonly moulded into linear to curvilinear, symmetrical sand waves (Figs. 64.9-64.11) that trend generally parallel

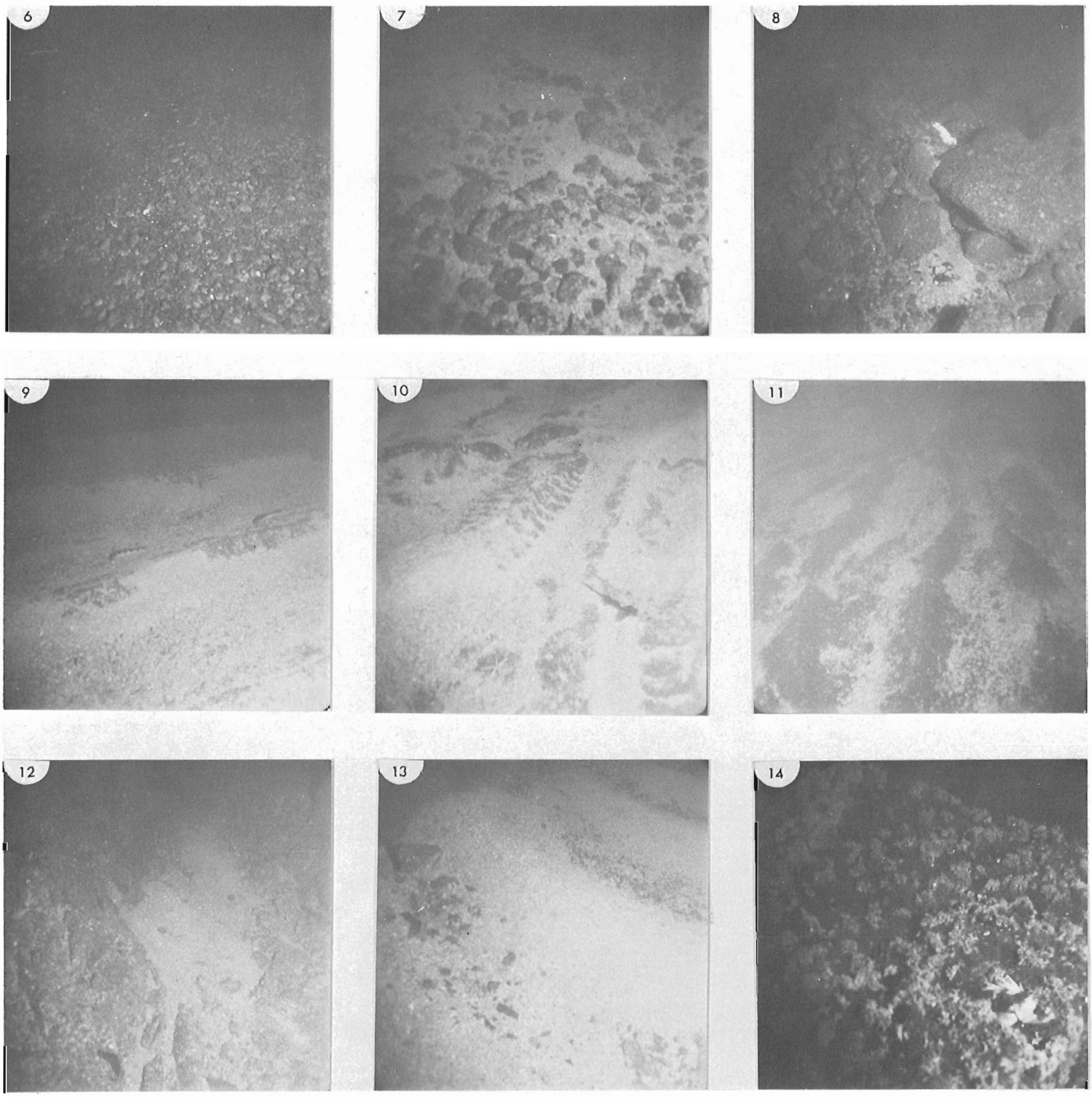

Figures 64.6 to 64.14

64.6. Well sorted sea-floor gravels adjacent to the seaward edge of the outcrop belt at dive site P-77-9.

64.7. Mixed carbonate shell hash, sand, and boulders at dive site P-77-5.

64.8. Boulders and erratics adjacent to the outcrop belt at dive site P-77-4. The octopus in the centre of the photo is about 2 m across.

64.9-64.11. Carbonate shell hash, sand, and fine gravel sand waves at dive site P-77-6.

64.12. Narrow, landward rising canyon at dive site P-77-9. Valley floor underlain by carbonate shell hash.

64.13. Carbonate shell hash wave, transverse to valley axis at dive site P-77-5. The sand wave sharply intersects the vertical valley wall in the upper left-hand corner.

64.14. Corals, bryozoa, molluscs, serpulid worms and echinoids covering massive volcanics at dive site P-77-6. Rock fish in lower right-hand corner.

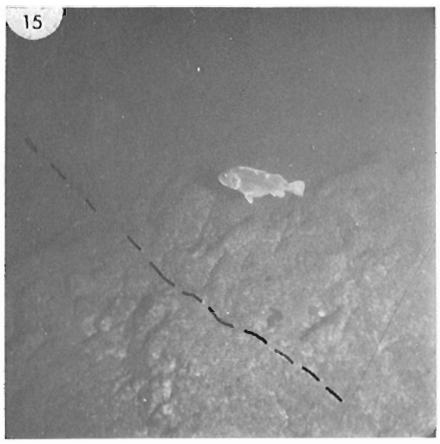

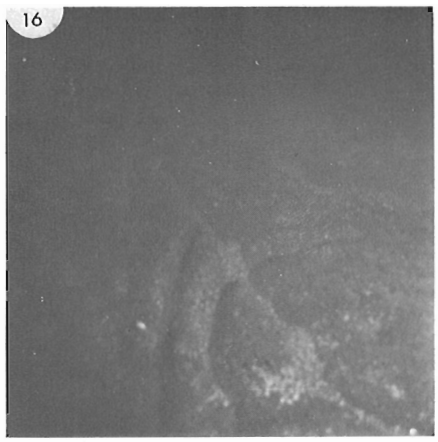

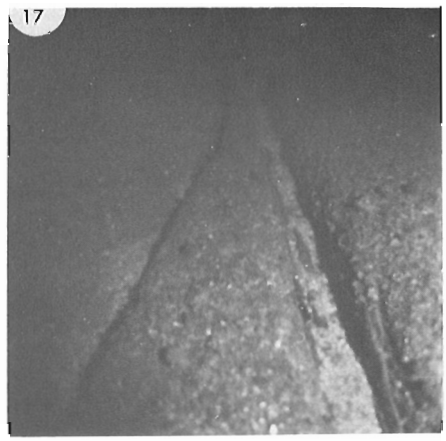

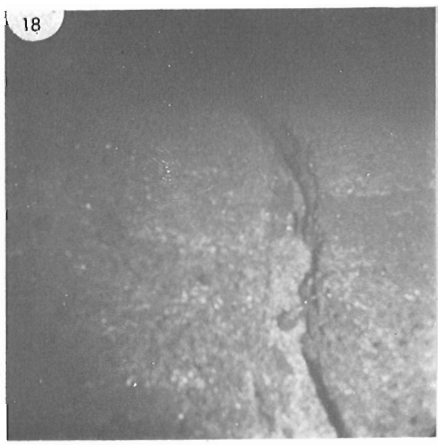

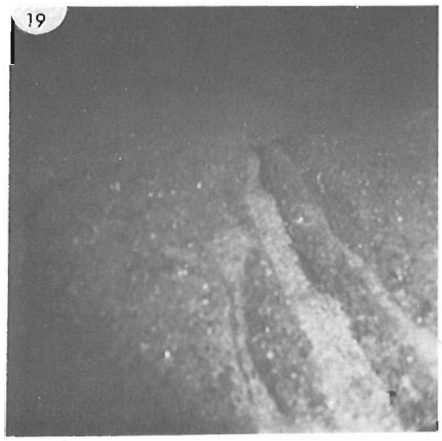

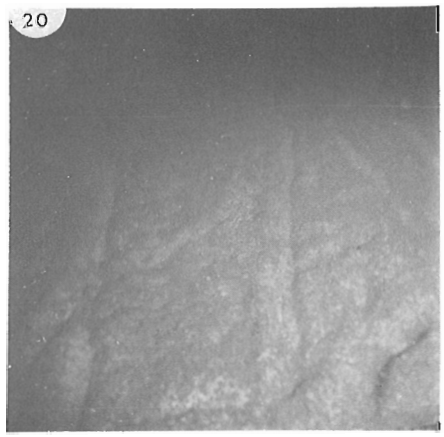

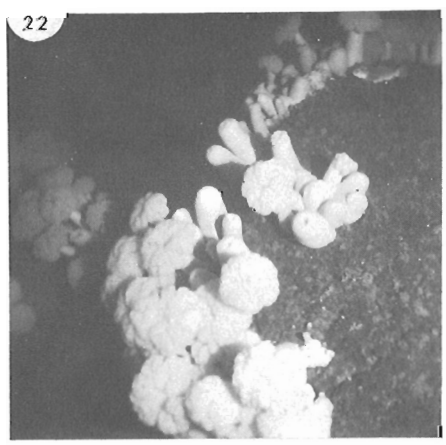

Figures 64.15 to 64.22

64.15. Rhyodacite flows overlying massive andesitic basalts (Bonanza volcanics) at dive site P-77-9.

64.16. Small fold interrupted by an axial plane fault at dive site P-77-11. The rocks are rhyodacites of the Bonanza Volcanics (Lower Jurassic).

64.17-64.20. Examples of narrow "grabens" on a mesa surface at dive site P-77-11.

64.21. Rock fish school at dive site P-77-11.

64.22. Sea anemones on massive andesitic basalt at dive site P-77-9.

with the coast of Vancouver Island and the trend of the outcrop belt. The outcrop belt rises steeply from the adjacent gently sloping sea floor. Access to its interior is locally provided by flat-bottomed, landward rising and narrowing valleys that are underlain by angular to rounded boulders, cobbles and carbonate shell hash (Fig. 64.12). The carbonate sediments in these valleys also are commonly moulded into sand waves, the trends of which remain parallel to the regional trend of the belt and traverse the axes of the valleys to sharply intersect the steep bounding valley walls (Fig. 64.13). The carbonate components are provided by corals, bryozoa, molluscs, serpulids, foraminifera and echinoids which abound on the irregular and scoriaceous rocks of the valley walls and pinnacles (Fig. 64.14).

The outcrop belt is composed of volcanic, plutonic, metamorphic and minor sedimentary rocks. The succession occurs closely offshore from an extensive terrain underlain by the Lower Jurassic Bonanza Volcanics, Lower Cretaceous Longarm Formation greywacke and pre-Cretaceous West Coast Crystalline Complex metamorphic rocks (Muller et al., 1974). Polished surfaces of samples collected in the belt appear macroscopically similar to some of the components that comprise these terrains. The bulk of the samples collected appear to be representative of the andesitic basalts and rhyodacites of the Bonanza Volcanics. The latter type locally display ilmenite mineralization in small stockwork type veinlets and irregularly distributed inclusions. Throughout most of the northern and central part of the dive area the andesitic basalts are massive, structureless and highly jointed. These are overlain by gently to steeply dipping rhyodacite flows (Fig. 64.15), samples from which reveal complex folds possibly induced during the time of emplacement. The succession is commonly broken by numerous fractures ranging from abundant minor vertical joints to faults with possible substantial displacements. The trends of the faults, some of which show slickensides, varied from parallel to the trend of the outcrop belt to those which traversed this trend at high angles. Folds, offset by faults, were observed in the rhyodacite sequence (Fig. 64.15).

At one locality on the flat surface of an extensive mesa which occurs at a constant depth of 100 m, long, mostly linear to locally curvilinear, steep sided, narrow, flat-bottomed grooves are impressed into rocks believed to be rhyodacite. Near the edge of the mesa the grooves are colinear with the strike of two sets of steeply dipping joints that were observed in the vertical cliffs bounding the mesa. Toward the centre of the mesa the grooves develop a variety of trends, their striking geometry becomes subdued, and their local relief diminishes. The central valleys of these small grabens are covered with a thin veneer of carbonate shell hash. Although their origin is uncertain they appear to be tectonic rather than erosional. Figures 64.17 to 64.20 illustrate the characteristics of some of these features.

The outcrop belt is the feeding area of many types of bottom feeding fish including ling cod and several types of rock fish (Fig. 64.21). Beyond the belt these fish were virtually absent; the only fish observed there were small rat fish. The higher (shallower) regions of the outcrop belt are commonly covered with several types of bottom attached organisms including brilliant pink corals and forests of sea anemones (Fig. 64.22). The corals and anemones tended to be most abundant on the massive, structureless andesitic basalts. Such relationships and others may prove to be valuable in future mapping.

Two deep dives to 700 m were conducted on the continental slope (Fig. 64.1). The purpose of these dives was to obtain additional stratigraphic and biostratigraphic information from the Upper Tertiary section examined in 1976 (Yorath et al., 1977). Uncompleted studies of one of the sections sampled tend to confirm the age of the upper part of the succession as Late Pliocene. One of the sections (Dive P-77-10) was very poorly exposed. Substantial quantities of particulate matter in the water in addition to downslope movement of sediment on the bottom suggest this area to be an active part of the continental slope.

References

Cameron, B.E.B.
1971: Tertiary stratigraphy and microfaunas from the Hesquiat-Nootka area, west coast, Vancouver Island (92E); in Report of Activities, Part B, Geol. Surv. Can., Paper 71-1B, p. 91-94.

1972: Tertiary foraminiferal succession of the western Cordillera and Pacific Margin; in Report of Activities, Part A, Geol. Surv. Can., Paper 72-1A, p. 198-201.

1973: Tertiary stratigraphy and microfaunas from the Pacific Margin, west coast, Vancouver Island; in Report of Activities, Part A, Geol. Surv. Can., Paper 73-1A, p. 19-20.

1975: Geology of the Tertiary rocks north of Latitude 49°, west coast of Vancouver Island; in Report of Activities, Part A, Geol. Surv. Can., Paper 75-1A, p. 17-19.

Eaton, R.M.
1975: Tests of Loran-C Performance; Can. Aeronaut. Space J., v. 21, no. 4, p. 129-132.

Grant, S.T.
1973: Rho-rho Loran-C combined with satellite navigation for offshore surveys; Int. Hydrog. Rev., v. 1, no. 2, p. 35-54.

Heckman, D.B. and Abbott, R.C.
1973: An acoustic navigation technique; Record of the Ocean 73 IEEE International Conference on Engineering in the Ocean Environment; IEEE Publication CHO77d-0 OCC, p. 591-595.

Jeletzky, J.A.
1975: Hesquiat Formation (New): A neritic channel and interchannel deposit of Oligocene age, western Vancouver Island, British Columbia; Geol. Surv. Can., Paper 75-32.

Muller, J.E.,Northcote, K.E., and Carlisle, D.
1974: Geology and mineral deposits of Alert – Cape Scott map-area, Vancouver Island, British Columbia; Geol. Surv. Can., Paper 74-8.

Shouldice, D.H.
1971: Geology of the western continental shelf; Can. Soc. Petrol. Geol., Bull., v. 19, no. 2, p. 405-436.

Sutherland Brown, A.
1968: Geology of the Queen Charlotte Islands, British Columbia; B.C. Dep. Mines Petrol. Resour., Bull. 54.

Tiffin, D.L., Bornhold, B.D., Yorath, C.J., Herzer, R.H., and Taylor, G.C.
1978: Bottom sediments – vicinity of Juan de Fuca and Explorer Ridges, northeast Pacific Ocean; in Current Research, Part A, Geol. Surv. Can., Paper 78-1A.

Tiffin, D.L., Cameron, B.E.B., and Murray, J.W.
1972: Tectonics and depositional history of the continental margin off Vancouver Island, British Columbia; Can. J. Earth Sci., v. 9, no. 3, p. 280-296.

Yorath, C.J., Tiffin, D.L., and Cameron, B.E.B.
1977: Submersible operation on the Pacific continental margin; in Report of Activities, Part A, Geol. Surv. Can., Paper 77-1A, p. 301-310.

65.

SAND WAVES ON THE SOUTHEASTERN SLOPE OF ROBERTS BANK, FRASER RIVER DELTA, BRITISH COLUMBIA

Project 740062

J.L. Luternauer, D. Swan, and R.H. Linden
Regional and Economic Geology Division, Vancouver

Abstract

Luternauer, J.L., Swan, D., and Linden, R.H., Sand Waves on the Southeastern Slope of Roberts Bank, Fraser River Delta, British Columbia; Current Research, Part A, Geol. Surv. Can., Paper 78-1A, p. 351-356, 1978.

The sand wave patch within a 4 km^2 segment of the Fraser Delta slope off a major port development was surveyed with side scan sonar and conventional echo sounder. A mosaic was prepared of the acquired side scan records. Local currents 3 m above the bottom were monitored for a period of 94 days. The sand waves generally have sinuous crests which become increasingly disjointed and lobate toward the east. The overall wave-crest orientation on the western part of the survey area is normal to the dominant tidal current flow direction. Maximum wave heights appear to increase from 2 to 3 m and wave lengths increase from approximately 15 to 30 or more metres west to east, respectively. On the basis of limited current observations, it is suggested that current velocities are high enough to permit general sediment motion at least 10 per cent of the time and that this contributes to a net westerly transport of sand.

Introduction

Since anomalous, hummocky zones on the Fraser Delta slope were first identified and mapped from echograms (Luternauer, 1976b), further studies have been undertaken to define their character in greater detail and explain their origin. Particular attention has been centred on the southernmost hummocky patch (Fig. 65.1): a) because of its proximity to existing port facilities and proposed new port developments, and b) because proposed Department of Public Works training of the main channel of the Fraser River may alter the sediment budget of this part of the slope. It became apparent from a single side scan sonar record, that the hummocks represent sand waves (Luternauer, 1977). The orientation of these waves strongly suggests that they are being generated by tidal currents. Additional investigations have been carried out to determine (a) the areal variation in sand wave morphology over the sand wave zone, (b) why sand waves are generated on only parts of the Roberts Bank delta slope when sediment mean grain-size is not significantly different in adjacent hummocky and essentially featureless parts of the slope (Luternauer, 1976a) and (c) what is the frequency of near-bottom current velocities high enough to transport local sediment?

Field Activities

In order to resolve these questions the following operations were carried out:

Current monitoring

At the request of the Geological Survey of Canada the Canadian Hydrographic Services placed two Aanderaa current meters on the sea-floor within the sand wave patch and to the west of it on a relatively smooth part of the slope. The device moored over the sand waves recorded 4 observations per hour for a total of 94 days, from January 28, 1977, to May 11, 1977. The meter was buoyed 3 m above its anchoring weight which was moored at a depth of 77 m (Fig. 65.1). Unfortunately, the second meter was not recovered and thus a comparison of the current regime over adjacent parts of the slope still cannot be made.

Side scan sonar and echo-sounding

A detailed side scan sonar and echo-sounding survey was made of the sand wave patch using the Canadian Hydrographic Services ship **Richardson** on January 20, 1977. Radar position fixes were taken every five minutes during the course of the survey. A rough estimate of the accuracy of these fixes was made by taking a range-bearing measurement for one target and a range for a second target. The mean difference in locations calculated using range-range and range-bearing was 143 m for 13 test locations. No determination could be made of the precise location of the side scan fish streaming behind the vessel, thus the fix marks on the side scan record indicate only approximately the part of the sea-floor being scanned.

Data Processing

Data acquired by the current meter was processed at the Institute of Ocean Sciences, Patricia Bay. Frequency per cent determinations of both current velocity and direction were calculated from the data summaries (Fig. 65.2).

Before the side scan record mosaic could be constructed an along-trace scale factor had to be calculated by simply dividing the recording paper advance speed by the ship speed. Since a mosaic consists of several tracklines, the average ship speed is used to calculate an average along-trace scale factor. All records are then cut at fix marks and arranged on a Northing-Easting grid which has been scaled appropriately. Although this procedure leads to overlapping of some records and gaps between the fix positions in others, the assembled mosaic (Fig. 65.4) does give a far clearer impression of the nature of the sand wave field than has been previously available. Echograms obtained along the second and eighth tracklines are also displayed to present a north-south profile view of the sand wave patch (Fig. 65.3).

Results and Discussion

The southeastern foreslope off Roberts Bank is blanketed by a continuous field of sand waves. The zone displaying highest relief (Fig. 65.1) is about 2 km wide and extends from 65-95 m depth. The largest features occur within the eastern half of this zone, most commonly at approximately 80-85 m depth. Echograms obtained during the side scan survey indicate that sand wave amplitudes increase from about 1-2 m in the western part of the surveyed area to about 3 m in the eastern section. Records obtained in 1974 suggested that the amplitude of these waves can be as great as 5 m (Luternauer, 1976a, b).

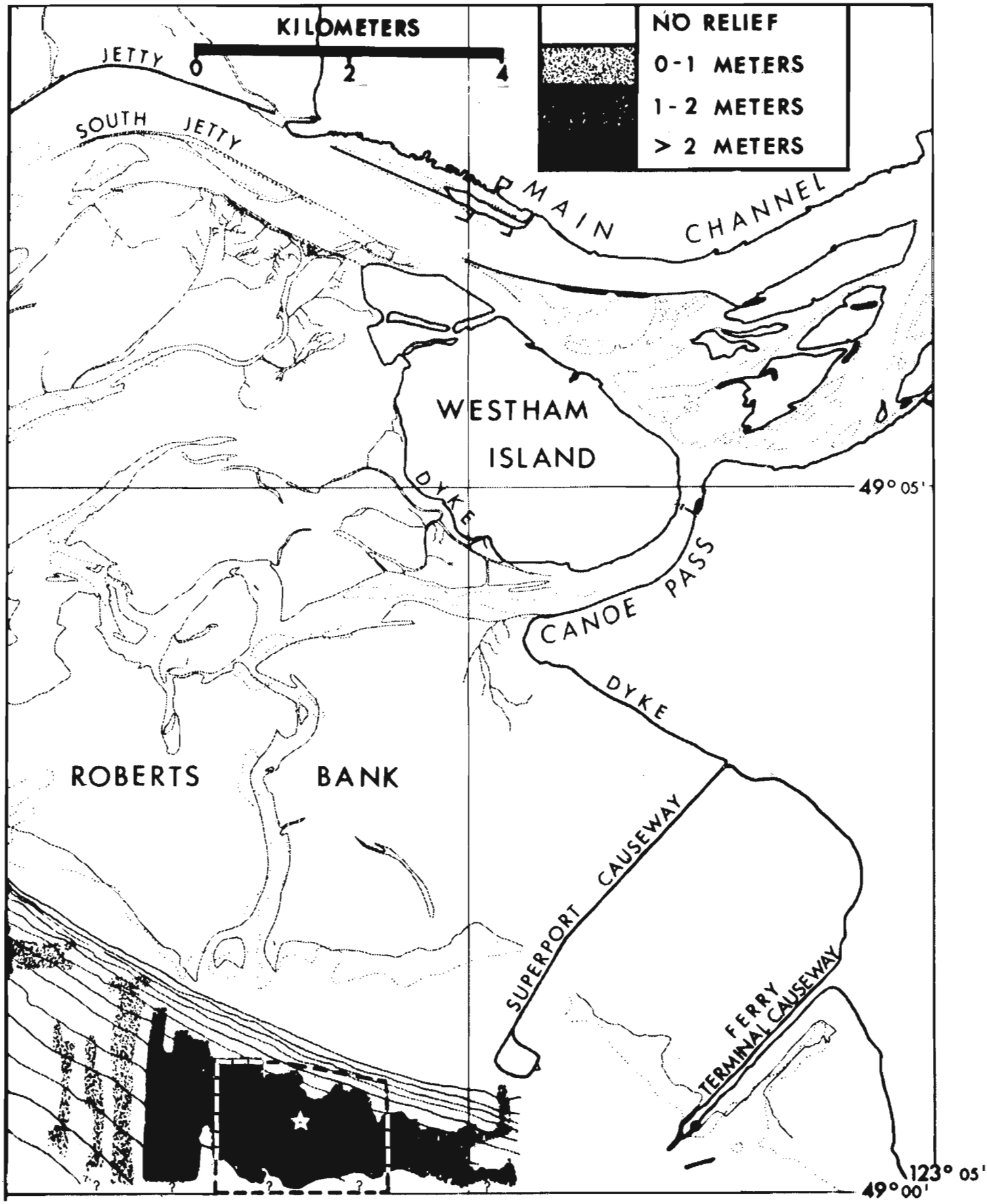

Figure 65.1. Index map. Area off Roberts Bank enclosed by dashed line represents segment of slope for which side scan sonar record mosaic compiled. Star indicates site where current meter was moored. Slope relief (exclusive of canyons) March-April 1974.

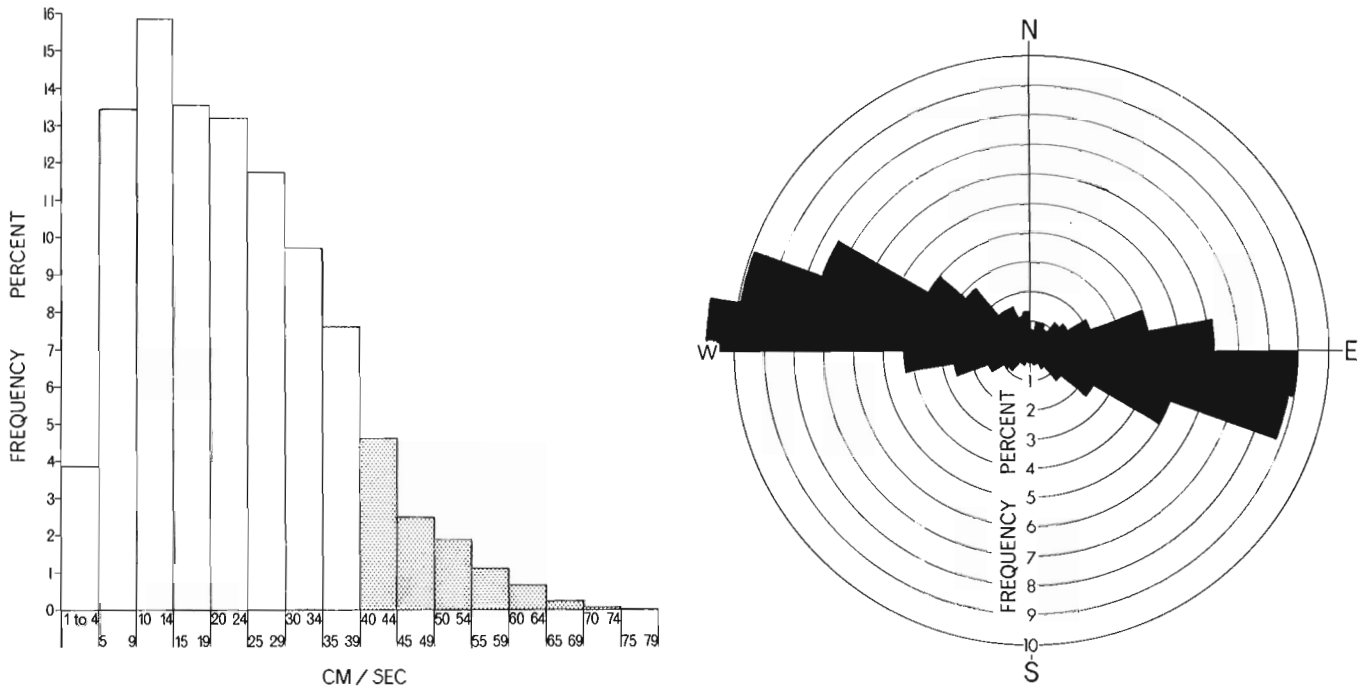

Figure 65.2. Velocity frequency-per cent histogram and current direction frequency-per cent rose compiled from data acquired during 94-day period by current meter moored at 77 m depth at location shown in Figure 65.1. Stippled bars on histogram indicate velocities probably capable of generating general sediment motion on the slope. Contour interval on slope is 10 m.

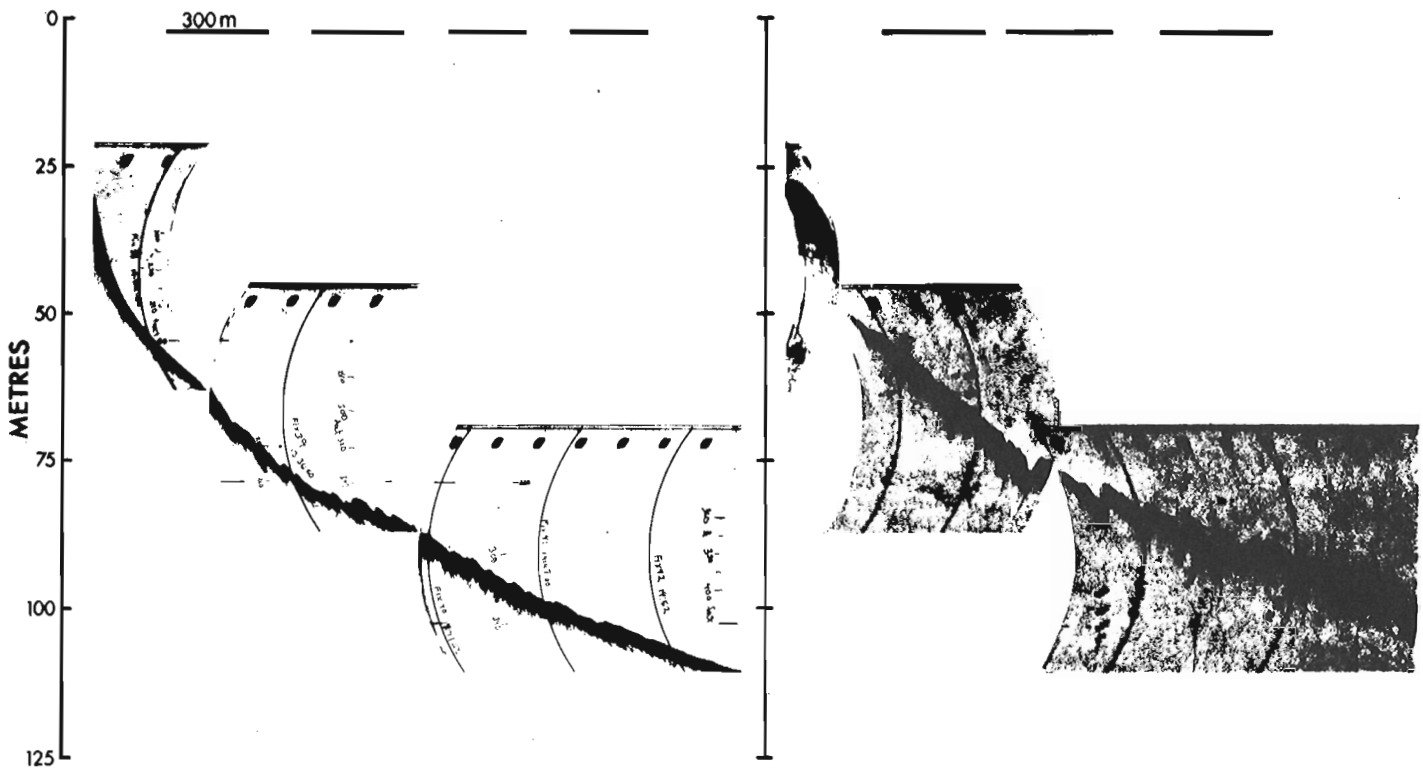

Figure 65.3. Representative echograms obtained along second and eighth tracklines of side scan mosaic (Fig. 65.3).

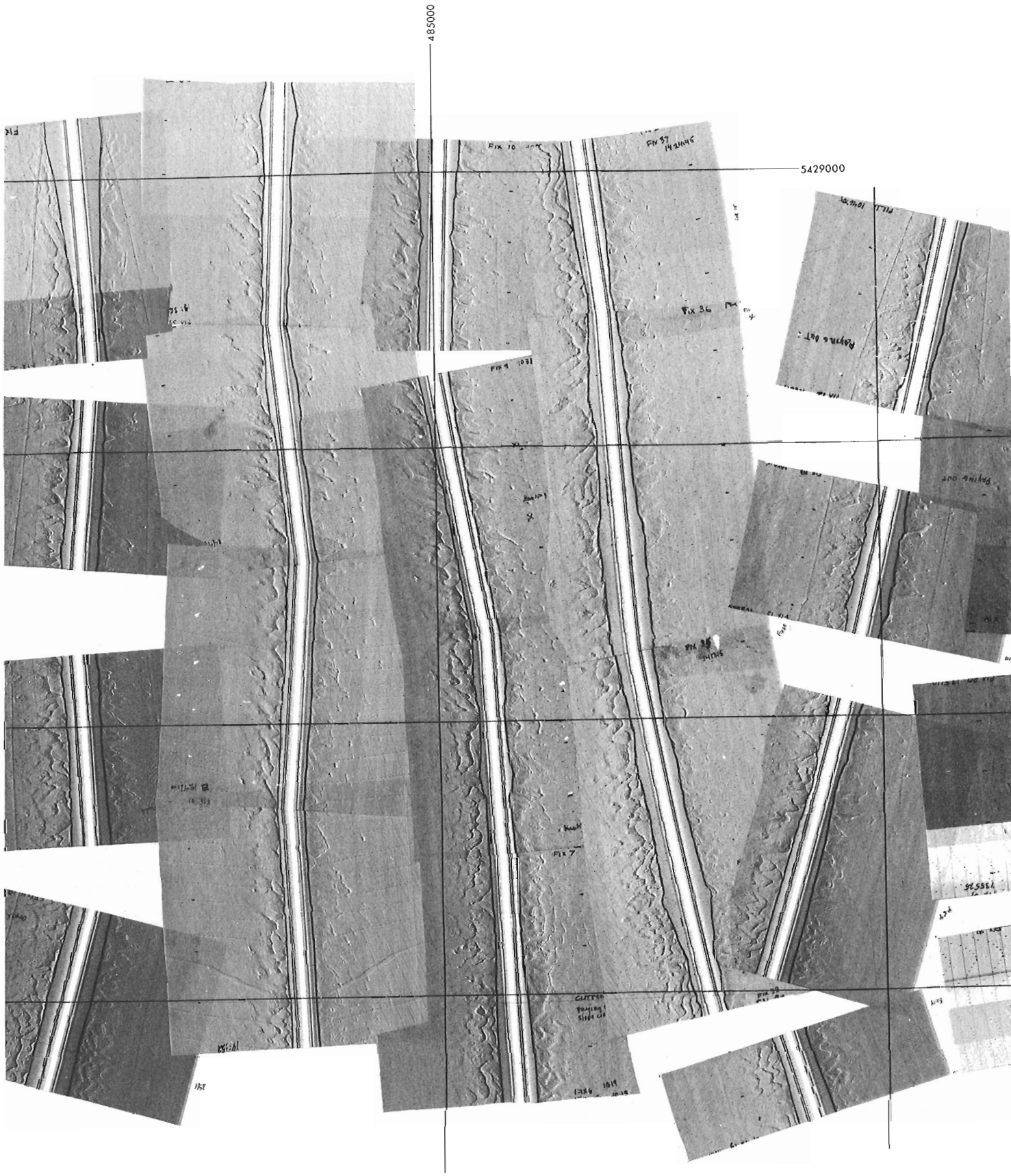
485000
5429000

Figure 65.4

Side scan sonar mosaic of area enclosed by dashed line on Figure 65.1.

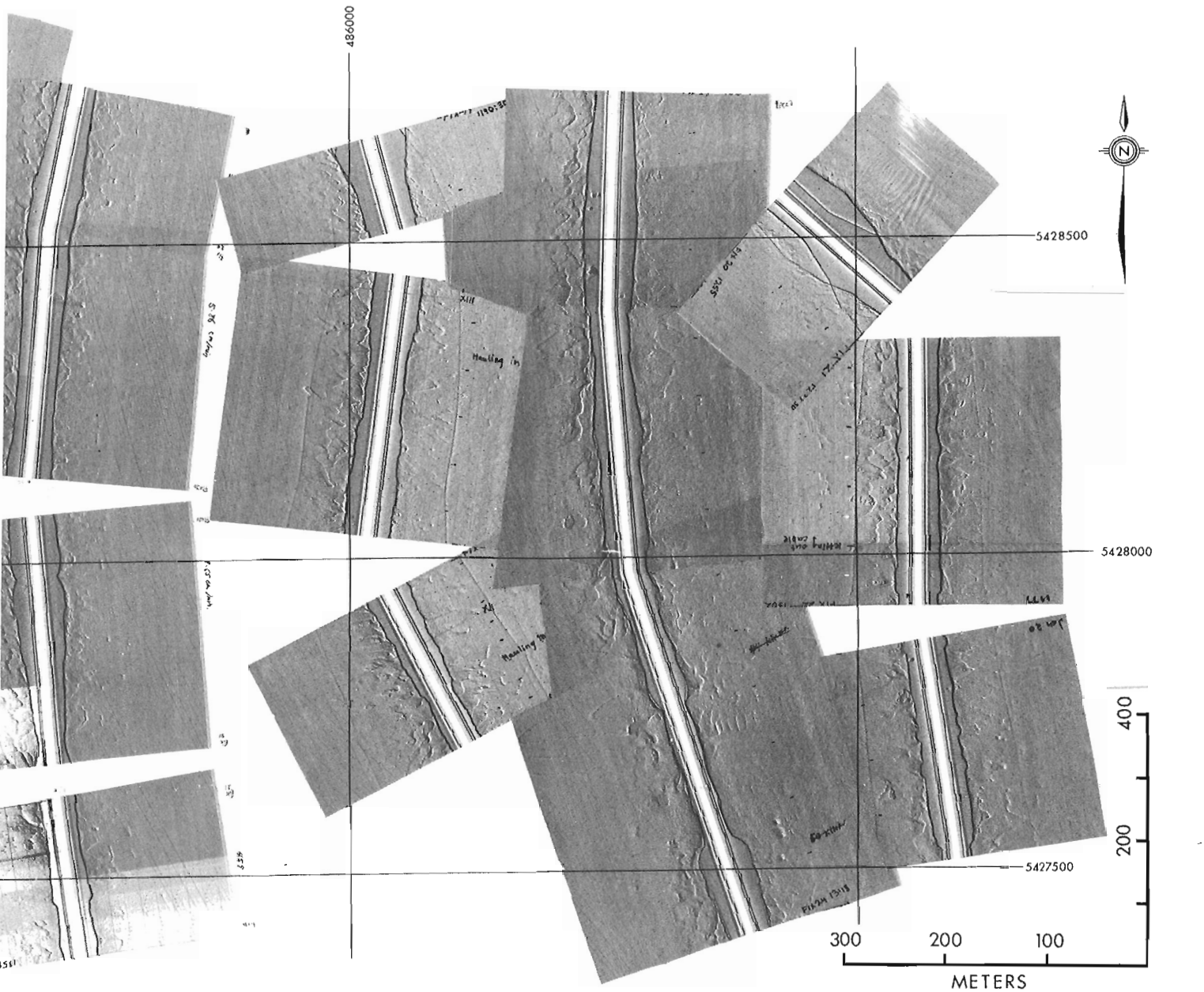

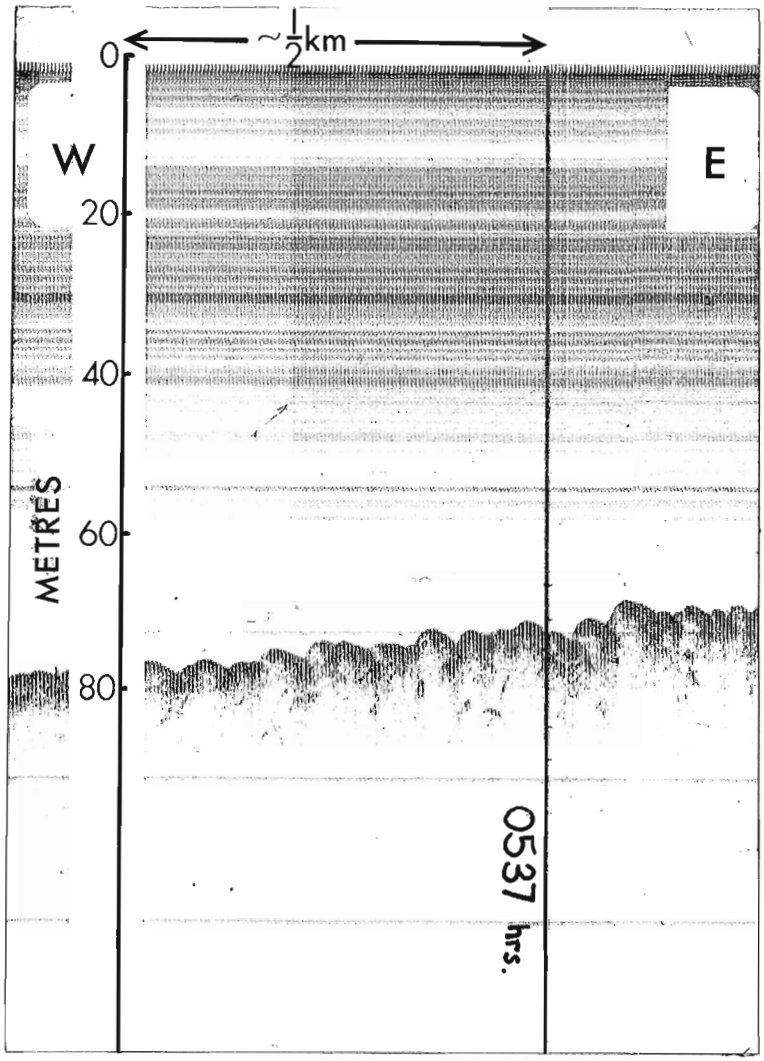

Figure 65.5. Segment of echogram obtained on July 22, 1976. Trackline is oriented west-east and lies on eastern portion of dashed area in Figure 65.1. Steep slopes on sand waves continued to face west in spite of the fact eastwardly ebbing tide had been running for 5 hours at time record acquired.

The side scan mosaic (Fig. 65.4) clearly reveals that the character of the sand waves changes from west to east. In the western section wavelengths are approximately 15 m and wave crests have a recognizable north-south orientation. The wave patterns become more irregular to the east, and wavelengths appear to be approximately twice those of waves in the western section (wavelengths are misrepresented on the echograms in Figure 65.3 which display depths across the width of sand lobes and not normal to the wave front).

The general north-south orientation of the wave crests clearly reflects the dominantly east-west direction of tidal current flow (Fig. 65.2). The slightly higher frequency of flows towards the west suggests that there is net transport of sediment in that direction. Studies in the North Sea have suggested (McCave, 1971) that asymmetric wave forms prevail where such net transport is occurring and that these features do not reform with a reversal of tidal flow. An echogram (Fig. 65.5) obtained on July 22, 1976 along a west-east trackline across the eastern half of the high relief zone in Figure 65.1 exhibited a series of asymmetric sand wave forms. Well-defined, west-facing, steep slopes of these waves still are evident after the tide had been running to the east for over 5 hours. Any continuous drift of sediment to the west can only lead to the retreat of the slope unless sediment is replenished by material supplied from the Fraser River.

The sands within the sand wave patch have mean sizes ranging from 1.6 to 2.2 phi and are relatively well sorted (0.5 to 0.7 phi) (samples collected in 1974 and 1977). Published modifications of the classic Sundborg sediment threshold velocity diagrams (Allan, 1965) and work carried out by Sternberg (1971) in tidal channels having sediment mean diameters equivalent to the coarsest sediments within the patch of sand waves suggests that general sediment motion probably occurs at least 10 per cent of the time when current velocities exceed 40 cm/s (Fig. 65.2). It must be stressed, however, that reasonably precise determinations of sediment threshold velocities will probably require that (a) current velocities be measured no higher than 1 m above the seafloor and (b) the effect of bed roughness and non-uniform flows on the transportive capacity of tidal flows be more reliably defined (Miller et al., 1977). Further studies may also require side scan sonar monitoring of specific sand waves so that changes in geometry accompanying variations in tidal currents can be recognized. In addition, determination of the nature of subsidiary high frequency wave forms associated with larger sand waves may help establish the relative importance of suspension and bedload transport in the genesis of the sand wave terrain (McCave, 1971).

Conclusions

The sand waves on the southeastern slope off Roberts Bank, Fraser Delta have generally sinuous wave crests which become increasingly disjointed and lobate towards the east. The overall wave crest orientation on the western part of the surveyed area is normal to the dominant tidal current flow direction. Maximum wave heights appear to increase from 2 to 3 m and wave lengths increase from approximately 15 to 30 or more metres west to east, respectively. On the basis of our limited current observations, it is suggested that current volocities are high enough to permit general sediment motion at least 10 per cent of the time and that this contributes to a net westerly transport of sand.

Acknowledgments

We wish to thank D. Tiffin and R. Herzer for suggesting several improvements to the text.

References

Allen, J.R.L.
1965: A review of the origin and characteristics of recent alluvial sediments; Sedimentology, v. 5, p. 89-191.

Luternauer, J.L.
1976a: Fraser Delta sedimentation, Vancouver, British Columbia; in Report of Activities, Part A, Geol. Surv. Can., Paper 76-1A, p. 213-219.

1976b: Fraser Delta sedimentation, Vancouver, British Columbia; in Report of Activities, Part B, Geol. Surv. Can., Paper 76-1B, p. 169-171.

1977: Fraser Delta sedimentation, Vancouver, British Columbia; in Report of Activities, Part A, Geol. Surv. Can., Paper 77-1A, p. 65-72.

Miller, M.C., McCave, I.N., and Komar, P.D.
1977: Threshold of sediment motion under unidirectional currents; Sedimentology, v. 24, p. 507-527.

McCave, I.N.
1971: Sand waves in the North Sea off the coast of Holland; Marine Geology, v. 10, p. 199-225.

Sternberg, R.W.
1971: Measurements of incipient motion of sediment particles in the marine environment; Marine Geology, v. 10, p. 113-119.

66.

SUBMARINE CANYONS AND SLUMPS ON THE CONTINENTAL SLOPE OFF SOUTHERN VANCOUVER ISLAND

Project 710048

Richard H. Herzer
Regional and Economic Geology Division, Vancouver

Abstract

Herzer, R.H., Submarine canyons and slumps on the continental slope off southern Vancouver Island; Current Research, Part A, Geol. Surv. Can., Paper 78-1A, p. 357-360, 1978.

Seismic profiles over part of the Continental slope off Vancouver Island indicate that submarine slides as well as submarine canyons have been instrumental in creating the present slope morphology. The canyons, which appear to have formed adjacent to Pleistocene ice fronts and structural lows near the shelf edge, follow courses on the slope which are at least partly controlled by major tectonic structures. Slump features, which may or may not be part of the same slide, can be traced continuously down-slope for 30 km from the shelf edge to a tectonically dammed sediment pond on the continental slope.

Introduction

The Continental slope is an environment where marine sedimentation and structural deformation commonly interact. In many cases the slope lies on a convergent plate boundary where compression and transcurrent faulting cause severe and rapid deformation. Growing folds, diapirs and steep, faulted scarps prevail (e.g. Lewis, 1971a; Barr, 1974). In other cases, where slopes lie within plate boundaries, the slope is gentle,

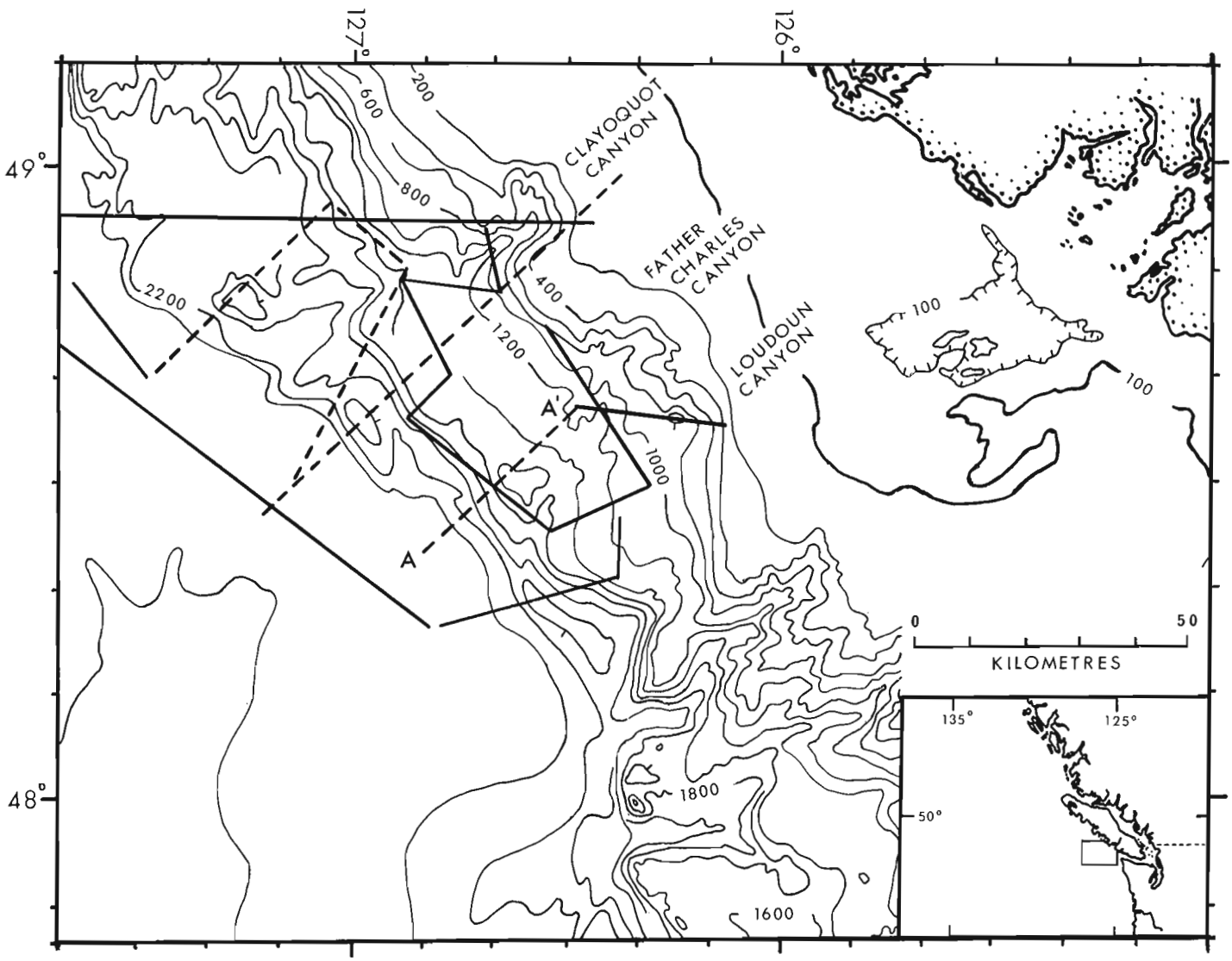

Figure 66.1. Locality map showing the tracks run in 1977. Solid lines — 3.5 kHz profiles. Dashed lines — air gun and 3.5 kHz profiles. Contour interval 200 m (100 m on the continental shelf).

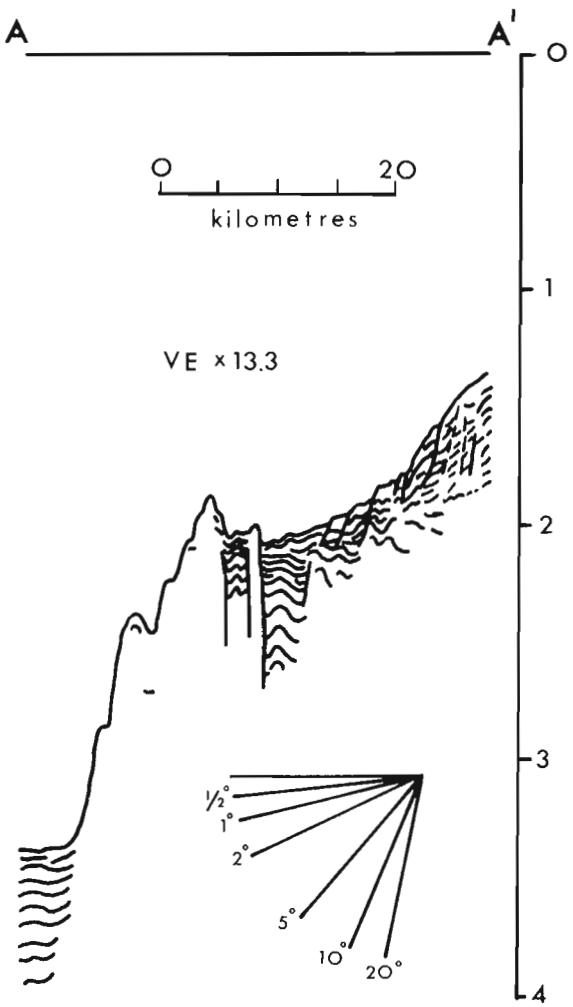

Figure 66.2. Air gun profile of the continental slope between Father Charles and Loudoun canyons showing the mid-slope plateau with ponded, deformed sediments. Slumping is evident on the continental slope above the plateau. The vertical scale is in seconds, two-way time.

depositional and structurally simple. Flexure is gentle and vertical and is due mainly to sediment or ice loading and to varying glacio-eustatic sea level pressure.

In both cases, however, the slope morphology is profoundly shaped by the down-slope transfer of sediments due to the force of gravity. Submarine canyons have long been known to be a common feature of continental slopes, and, with the advent of seismic reflection profiling, slope failure by slumping has been found to be a common phenomenon as well.

Most submarine canyons were formed by submarine processes. Such canyons are thought to form wherever coarse sediment is supplied in sufficient quantity to a submarine slope. Canyons have thus formed off river mouths (e.g. Heezen et al., 1964; Reimnitz and Gutierrez-Estrada, 1970), off beaches and headlands where coarse sediment of the littoral drift is directed offshore (e.g. Shepard and Dill, 1966; Dietz et al., 1968), and on the edge of the continental shelf where coarse sediment is carried over by strong tidal and other currents (Herzer, 1977). Many canyons that are isolated on the outer shelf, far from modern sources of mobile coarse sediment, have been related to fossil river and beach systems that operated during glacially lowered sea levels (e.g. Ewing et al., 1963; Herzer, 1977). The courses of many submarine canyons are controlled by geologic structures (e.g. Buffington, 1964; Martin and Emery, 1967).

Submarine slides have been reported less frequently in the literature. Most have been discovered on low-angle slopes such as delta fronts and prograding continental margins, where tectonic effects are minimal and the reflectors are sufficiently gently dipping to be seen on seismic reflection profiles (e.g. Heezen and Drake, 1964; Uchupi, 1967; Lewis, 1971b; Herzer, 1973 and 1977; Normark, 1974). These studies have shown that (a) sliding on the continental slope can take place on extremely gentle gradients – 1° or less (Lewis, 1971b; Herzer, 1973 and 1977); (b) a single slide can occupy an enormous area tens of kilometres across (Uchupi, 1967; Normark, 1974; Herzer, 1973 and 1977), (c) the slide terrain is frequently complicated by corrasional features – sea valleys and submarine canyons (e.g. Uchupi, 1967; Herzer, 1977), and (d) submarine sliding is an integral part of the process of progradation on some continental slopes (Herzer, 1977; King and Young, in press). On steep continental slopes, slides are not often detected because of the limitations of seismic reflection profiling, yet if the slope is composed of soft or partly consolidated sediment, sliding will undoubtedly have occurred.

In view of the present program of geological mapping of the western continental margin of Canada, utilizing submersibles as well as standard dredging and sampling techniques, it is desirable to know specifically where the section has been displaced by sliding, and to know the relative ages of such interacting geomorphic features as slides, down-cutting submarine canyons, growing folds or diapirs, and active faults. The present study is designed as a first attempt to examine the interaction of up-building forces (folding and faulting) and downgrading forces (submarine canyon erosion and submarine sliding) on a portion of the continental slope west of Vancouver Island.

During two cruises on **CFAV Endeavour** in the northeast Pacific Ocean (one conducted by the Geological Survey of Canada, and the other by Earth Physics Branch) 405 km of 3.5 kHz profiles and 224 km of air-gun seismic reflection profiles were run over an area of continental slope west of Barkley Sound (Fig. 66.1).

Setting

The structure of the continental slope has been described elsewhere (Tiffin et al., 1972; Barr, 1974). The slope is underlain by a series of apparent fault blocks which trend roughly parallel with the continental margin. They formed in response to oblique subduction of the Juan de Fuca Plate beneath the American Plate (Seely et al., 1974; Kulm and Fowler, 1974), and are thought to be composed largely of accreted Cascadia Basin sediments. Halfway down the slope, a plateau has been created where sediments have been ponded against a major uplifted block or en echelon series of blocks (Fig. 66.2). The ponded sediments are underlain by a series of smaller uplifted blocks and are themselves being deformed.

Three canyons lie within the area – Clayoquot Canyon, Father Charles Canyon and Loudoun Canyon (Fig. 66.1).

Observations

Submarine Canyons

The courses of the three submarine canyons are apparently affected by the plateau and the ridge that created it. The courses of Father Charles and Loudoun canyons are more or less straight down-slope, but are displaced laterally to a small degree by the uplift. Clayoquot Canyon is similarly displaced but appears to have two possible outlets from the mid-slope plateau. One is north of and the other south of a high on the ridge behind which the mid-slope sediments are ponded. It is not known which, if either, of the outlets is active.

The axes of the three canyons are generally V-shaped where their gradients on the continental slope are steep, indicating a lack of significant sediment fill. Where Clayoquot Canyon crosses the mid-slope plateau, the canyon cross-section appears to change to that of a leveed fan valley. This suggests that at least some of the sediments filling the basin are turbidites.

The origins of the submarine canyons are also being investigated. A buried extension of the glaciated troughs off Barkley Sound has been traced in seismic profiles to a terminus 9 km from the shelf edge. Father Charles and Loudoun canyons occur at the shelf edge adjacent to this terminus. Buried canyon heads underlie the shelf around the present head of Father Charles Canyon, indicating that it has had a history of changing loci of sediment input and that it is not therefore simply a young, modern canyon. These two canyons thus may have originated during the Pleistocene when debris-laden meltwater was supplied to the shelf edge and upper slope from shelf-wide ice lobes emanating from Barkley Sound.

Around the head of Clayoquot Canyon, no buried channels have been found, and seismic profiles show no evidence of glacial scouring of the Pleistocene sediment on the outer shelf. Instead, the sediments, including Pleistocene strata, are gently folded and the reflectors are smooth and apparently conformable. The head of the canyon is located where a large syncline intersects the shelf edge, suggesting that the position of this canyon is related mainly to tectonic rather than glacial factors. Coarse sediment, moving along the shelf or along a Pleistocene beach near the present shelf edge, would likely have spilled over the shelf edge where it is indented by a structural low. Likewise, a structural low would channel sediment-laden glacial meltwater from the ice front to the continental slope.

Submarine Slides

All available seismic profiles over the continental slope were scrutinized for evidence of sliding. Between Father Charles and Loudon canyons, a large slump was found to extend from the edge of the continental shelf, down the upper continental slope to the mid-slope plateau – a distance of 30 km. The slump, which is of unknown width, is composed of imbricated, down-dropped blocks (Fig. 66.2).

The mid-slope basin fill is thus also partly composed of slumped material shed directly from the slope. Because the basin is underlain by growing structures which may be fault blocks, tight folds or diapirs, the mid-slope sedimentary sequence, including turbidites, slumped material, ice-rafted and pelagic material will all be ultimately tectonically uplifted and deformed. A great deal of the accoustically opaque material underlying the slope may include such sediments, as well as accreted Cascadia Basin sediments.

In view of the great length of the slump and its location on a rather narrow ridge separating two canyons, there are three possible interpretations of its morphology and origin: a) It may be a long, thin slide that has developed independently of the canyons by progressive slumping of the continental slope, in which case its age would be unrelated to that of the canyons; b) It may be a series of small slumps that have slid laterally into the canyons due to erosional oversteepening of the canyon walls, in which case the slumping would post-date the formation of the canyons; c) It may be part of a huge slump with a width of the same order of magnitude as its length, in which case the vague, amphitheatre-like depression in which Father Charles and Loudoun canyons are found is a slump scar, and in which case also, the slump would probably predate the canyons and would perhaps have contributed to their origin.

Conclusions

Where grain-by-grain sedimentation, tectonic deformation and gravity sliding are taking place together, the stratigraphy, revealed on scarps and exposed submarine canyon walls, will be extremely complex. The interaction between tectonic deformation and large-scale gravity sliding reported on this part of the continental slope is probably not unique and may prove to be the rule rather than the exception for the rest of the continental slope off the West Coast of Canada. Further research may reveal the ages of the canyons and of the slump discussed in this paper, and the extent of large-scale slumping on other parts of the continental slope. This should help to lay some of the groundwork for later stratigraphic studies in this region.

Acknowledgments

The author is grateful to Drs. D.L. Tiffin and R.D. Hyndman who provided time on their cruises for these seismic lines to be run. The assistance of the officers and crew of **CFAV Endeavour** and of the scientific personnel on board is greatly appreciated.

References

Barr, S.M.
1974: Structure and tectonics of the continental slope west of southern Vancouver Island; Can. J. Earth Sci., v. 11, p. 1187-1199.

Buffington, E.C.
1964: Structural control and precision bathymetry of La Jolla Submarine Canyon; Marine Geol., v. 1, p. 44-58.

Dietz, R.S., Knebel, H.J., and Somers, L.H.
1968: Cayar Submarine Canyon; Bull. Geol. Soc. Am., v. 79, p. 1821-1828.

Ewing, J., LePichon, X., and Ewing, M.
1963: Upper stratification of Hudson Apron region; J. Geophys. Res., v. 68, p. 6303-6316.

Heezen, B.C., Menzies, R.J., Schneider, E.D., Ewing, M., and Granelli, N.C.L.
1964: Congo Submarine Canyon; Am. Assoc. Pet. Geol. Bull., v. 48, p. 1126-1149.

Heezen, B.C. and Drake, C.L.
1964: Grand Banks Slump; Am. Assoc. Pet. Geol. Bull., v. 48, p. 221-233.

Herzer, R.H.
1973: Uneven submarine topography south of Mernoo Gap – the result of volcanism and submarine sliding; New Zealand J. Geol. Geophys., v. 18, p. 183-188.

1977: Late Quaternary geology of the Canterbury continental terrace; unpubl. Ph.D. thesis, Victoria University of Wellington, New Zealand, 286 p.

King, L.H. and Young, I.F.
Paleocontinental slopes of East Coast Geosyncline (Canadian Atlantic Margin); Can. J. Earth Sci. (in press)

Kulm, L.D. and Fowler, G.A.
1974: Oregon continental margin structure and stratigraphy: a test of the imbricate thrust model; in The Geology of Continental Margins, C.A. Burke and C.L. Drake, eds.; Springer-Verlag, New York, p. 261-284.

Lewis, K.B.
1971a: Growth rate of folds using tilted wave-planed surfaces: coast and continental shelf, Hawke's Bay, New Zealand; in Recent Crustal Movements; Roy. Soc. New Zealand Bull., v. 9, p. 225-231.

Lewis, K.B. (cont'd.)
1971b: Slumping on a continental slope inclined at 1°-4°; Sedimentology, v. 16, p. 97-110.

Martin, B.D. and Emery, K.O.
1967: Geology of Monterey Canyon, California; Am. Assoc. Pet. Geol. Bull., v. 51, p. 2281-2304.

Normark, W.R.
1974: Ranger Submarine Slide, northern Sebastian Vizcaino Bay, Baja California, Mexico; Bull. Geol. Soc. Am., v. 85, p. 781-784.

Reimnitz, E. and Gutierrez-Estrada, M.
1970: Rapid changes in the head of the Rio Balsas Submarine Canyon System, Mexico; Marine Geol., v. 8, p. 245-258.

Seely, D.R., Vail, P.R., and Walton, G.G.
1974: Trench slope model; in The Geology of Continental Margins, C.A. Burke and C.L. Drake, eds.; Springer-Verlag, New York, p. 249-260.

Shepard, F.P. and Dill, R.F.
1966: Submarine Canyons and other Sea Valleys; Rand McNally, Chicago, 381 p.

Tiffin, D.L., Cameron, B.E.B., and Murray, J.W.
1972: Tectonics and depositional history of the continental margin off Vancouver Island, British Columbia; Can. J. Earth Sci., v. 9, p. 280-296.

Uchupi, E.
1967: Slumping on the continental margin southeast of Long Island, New York; Deep-Sea Res., v. 14, p. 635-639.

67. THE PRAIRIE CREEK EMBAYMENT AND ASSOCIATED SLOPE, SHELF AND BASIN DEPOSITS

Project 750085

D.W. Morrow
Institute of Sedimentary and Petroleum Geology, Calgary

Abstract

Morrow, D.W., The Prairie Creek Embayment and associated slope, shelf and basin deposits; Current Research, Part A, Geol. Surv. Can., Paper 78-1A, p. 361-370, 1978.

In Late Silurian to Early Devonian time a large north-trending re-entrant developed along the shelf-to-basin transition in the Virginia Falls map-area (NTS 95F). This embayment is filled with a distinctive suite of slope-deposited sediments in a sequence that is markedly thinner than the surrounding contemporaneous shallow water, shelf carbonates. The name Prairie Creek Embayment is applied to this feature because Prairie Creek traverses and drains most of the embayment area. Diagnostic slope deposits in the embayment include megabreccia sheets containing large blocks up to 5 m across, weakly graded polymictic conglomeratic debris flows 0.5 to 2.0 m thick and fine grained, graded allodapic carbonate sheets less than 0.5 m thick. Both the embayment and the surrounding shelf are underlain by an eastward-extending tongue of Road River shale.

The junction of the thin embayment slope facies and the surrounding shelf facies became the preferred site for faulting during Tertiary deformation in the Virginia Falls map-area.

Introduction

The study-area (Fig. 67.1) is in the southern Mackenzie Mountains and is contained entirely within the Virginia Falls map-area (95F), which is traversed by the South Nahanni River. This area was included in Operation Mackenzie, a Geological Survey of Canada reconnaissance mapping project conducted during the summer of 1957 and which resulted in the publication of several GSC papers with accompanying maps. One of these reports dealt specifically with the geology of the Virginia Falls map-area (Douglas and Norris, 1960). Douglas and Norris (1976) subsequently compiled a revised geologic map of the Virginia Falls map-area in which a predominantly carbonate Silurian-Devonian shelf sequence in the north and east passes south and west to a basinal shale sequence. A slight revision in this boundary between shelf and basinal deposits was presented by Cook (1977). The reader is referred to these publications, particularly Douglas and Norris (1960 and 1976), for a description of the existing formal stratigraphy of the Virginia Falls area.

This report describes and delineates a major north-trending embayment in the facies boundary between the Silurian-Devonian shelf and basin deposits of the Virginia Falls map-area (Fig. 67.1). This embayment, herein termed the Prairie Creek Embayment, is filled with a distinctive suite of slope-deposited sediments and is defined by the extent of these deposits. Previously, these deposits were referred to as basin deposits (Cook, 1977) and were not differentiated from the more typically basinal Silurian-Devonian shales in the southwest part of the Virginia Falls map-area (i.e., map-unit OSD of Douglas and Norris, 1976). The name Prairie Creek Embayment is applied because this large creek traverses and drains most of the embayment area.

Measured sections in and around the Prairie Creek Embayment are shown in Figure 67.1. Some of these measured sections have been projected to a restored east-west cross-section of Upper Silurian-Devonian sediments across the embayment (Fig. 67.2). Lithologically uniform facies are numbered (Fig. 67.2) to facilitate discussion of lithostratigraphic relationships. These facies correspond to formations and map-units or parts of the formations and map-units of Douglas and Norris (1976).

Basin and Slope Deposits

Facies 4 (Fig. 67.2) is composed of a uniform succession of very thin, smooth and planar bedded to laminated, light brownish grey weathering shaly calcilutite (Fig. 67.3). Typically, facies 4 is an almost varve-like uninterrupted succession of black to silvery grey, argillaceous laminae alternating with very thin, dark grey, slightly pyritic calcilutite beds. This suggests that facies 4 accumulated under anoxic conditions in quiet water, possibly below wave

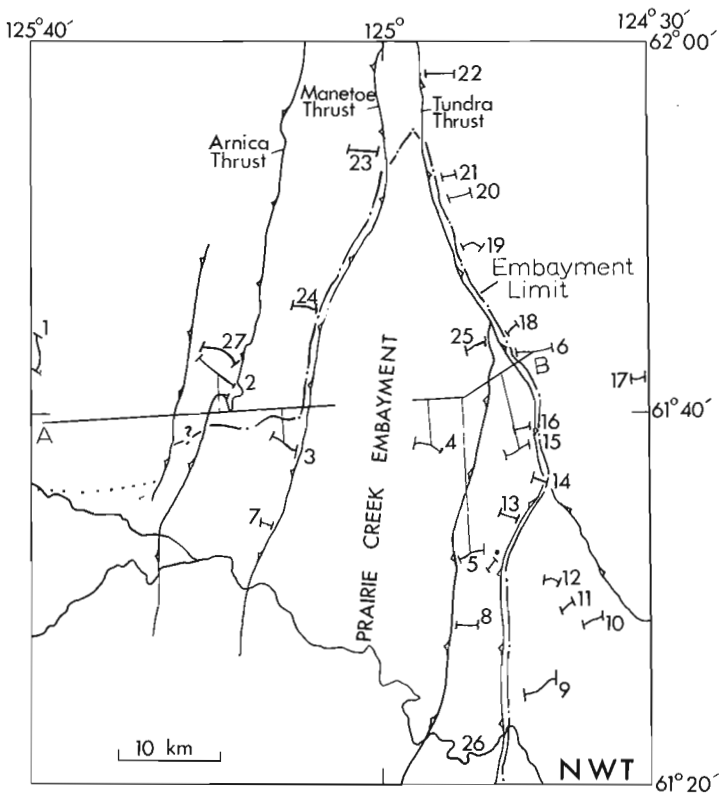

Figure 67.1. Map of report-area in the Virginia Falls area, Northwest Territories, with locations of measured sections. Boundary between Devonian shelf and slope sequences outlining the Prairie Creek Embayment is shown. Major faults also are shown (from Douglas and Norris, 1976). AB is the line of section for Figure 67.2.

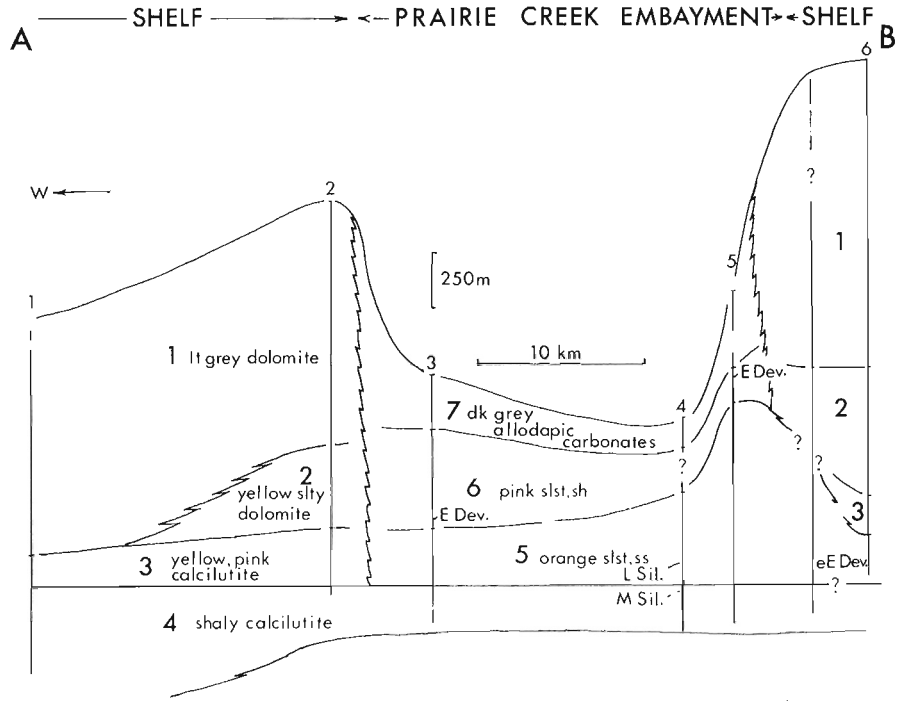

Figure 67.2. Stratigraphic cross-section across the Prairie Creek Embayment. Lithologically uniform facies are numbered, and the predominant lithologies are indicated on the cross-section. In the recent map (1378A) compiled by Douglas and Norris (1976), facies 1 and 2 are mapped as the Sombre and Camsell formations, respectively; the sequence of facies 3 and 4 is mapped as part of the Delorme Formation; the facies sequence 4, 5, and 6 is mapped as OSD undivided; and facies 7 is mapped as either a basinward extension of the Sombre Formation or of the Arnica Formation. Facies 5 contains abundant carbonate debris flow deposits formed of coarse fragments whereas facies 6 and 7 contain abundant fine grained mass flow deposits.

base. The top of facies 4 was used as a datum in constructing Figure 67.1 because this facies extends across the entire area and underlies both the predominantly shelf sequence of facies 1, 2, and 3 and the slope sequence of facies 5, 6, and 7. The upper part of facies 4 in several places contained the Middle Silurian graptolites **Monograptus spiralis** and **M. priodon** identified by B.S. Norford and A.C. Lenz.

The shaly calcilutite of facies 4 grades abruptly upward to the bright orange weathering, thin bedded, moderately recessive and dolomitic siltstones and sandstones of facies 5 (Figs. 67.4 and 67.5). The orange weathering colour is caused by small amounts of limonite that coats individual sand and silt grains. No cross-bedding was observed in these sediments which were commonly finely laminated and platy, although small ripple marks occurred on some bed surfaces. Conglomeratic carbonate debris flows are scattered throughout facies 5 (Fig. 67.4) in the thicker sections on the east side of the Prairie Creek Embayment (Fig. 67.2). These flows range in thickness from 0.5 m to at least 10 m thick.

Thinner debris flows are crudely graded with fragments that are strongly oriented parallel to bedding (Fig. 67.6). Abundant crinoid, coral and brachiopod fragments as well as elongate, slightly rounded, grey calcilutite fragments occur in thinner debris flows (Fig. 67.6). Beds underlying these flows are slightly contorted (Fig. 67.6).

Thicker debris flow breccias in facies 5 are very coarsely fragmental and display a chaotic internal fabric in which individual blocks have no preferential orientation (Fig. 67.7). The lack of colour contrast between fragments and matrix which causes difficulty in discerning the full outlines of fragments in these massive breccia bodies (Fig. 67.7) is unlike the strong contrast between fragments and matrix in thinner debris flows (Fig. 67.6). The lack of contrast between matrix and breccia in larger breccia masses may indicate that they have undergone a relatively short distance of transport.

SECTION 1

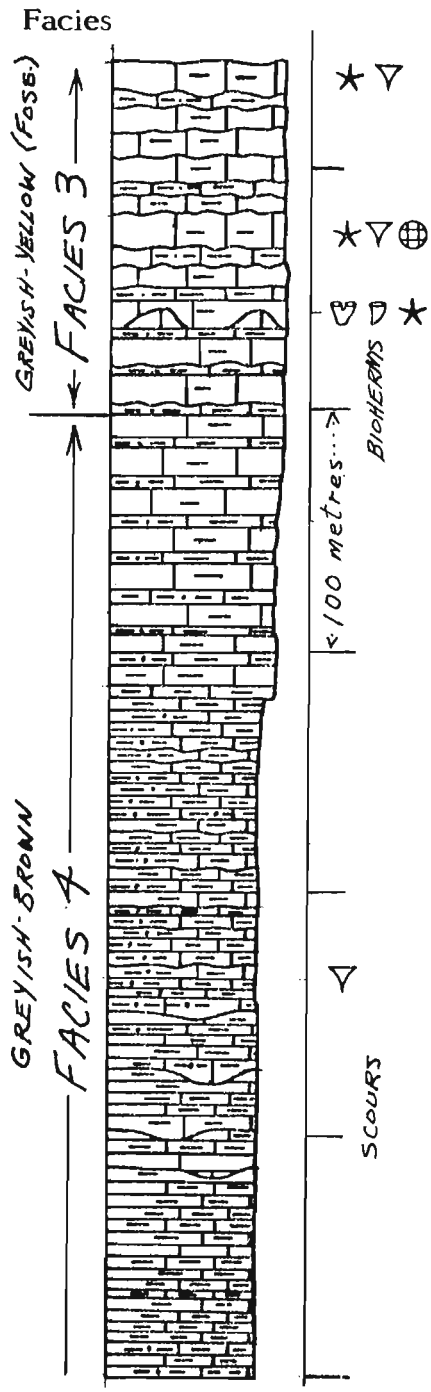

Figure 67.3

Columnar section 1 (at Cathedral Mountain) shown on Figures 67.1 and 67.2. Thin bedded to laminated, drab, grey and brown shale-calcilutite couplets constitute facies 4 in the lower part of the section. Facies 3 in the upper part of the section is formed of couplets of grey fossiliferous calcilutite and bright yellow or pink-weathering argillaceous material. Small coral-bearing bioherms occur near the top of facies 3 in this and some other sections.

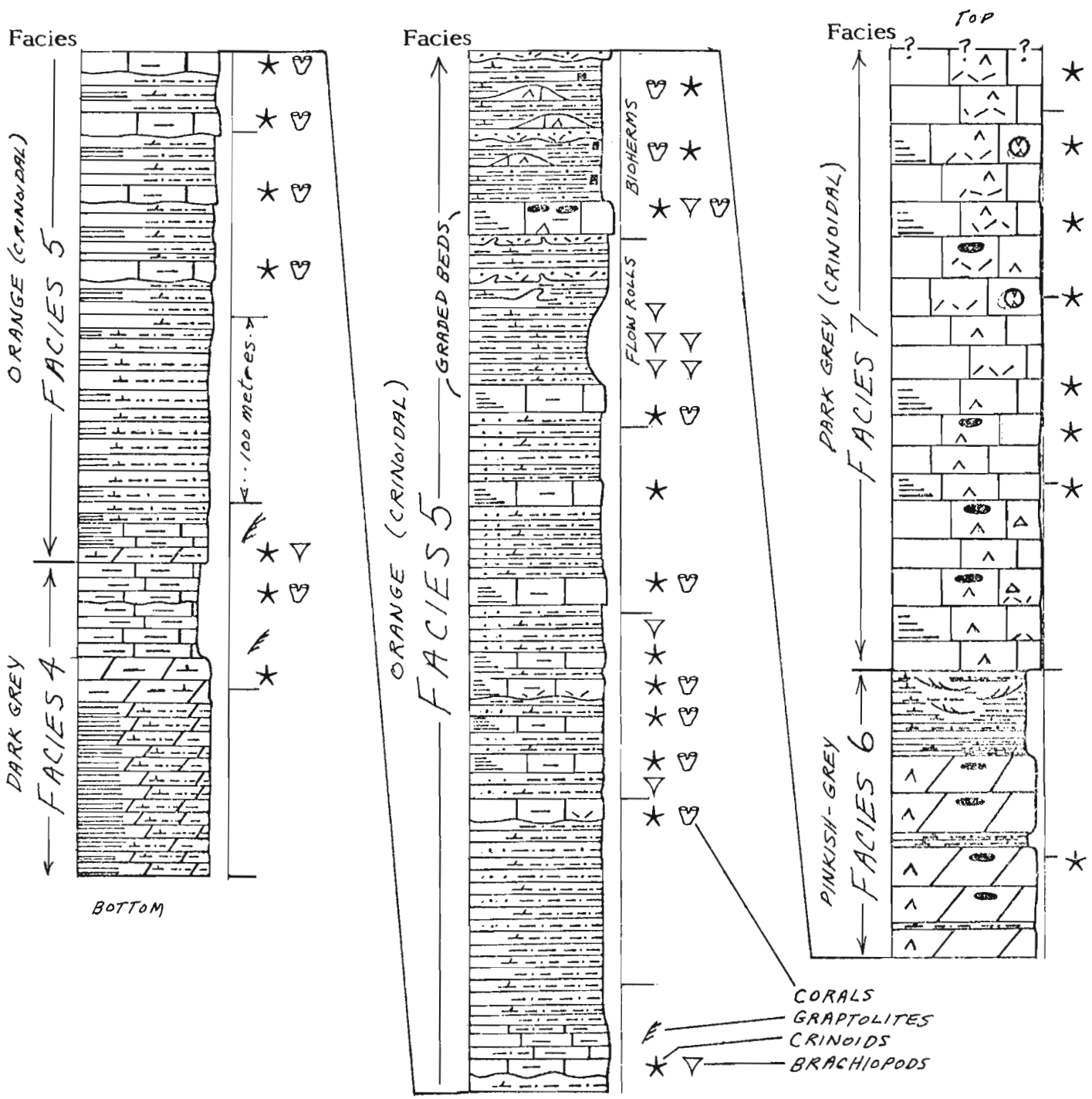

Figure 67.4. Columnar section 5 (near Prairie Creek) shown on Figures 67.1 and 67.2. This also shows the facies sequence 4, 5, 6, and 7 like that at locality 7. Facies 5 is very thick in this and other sections along the east side of the Prairie Creek Embayment.

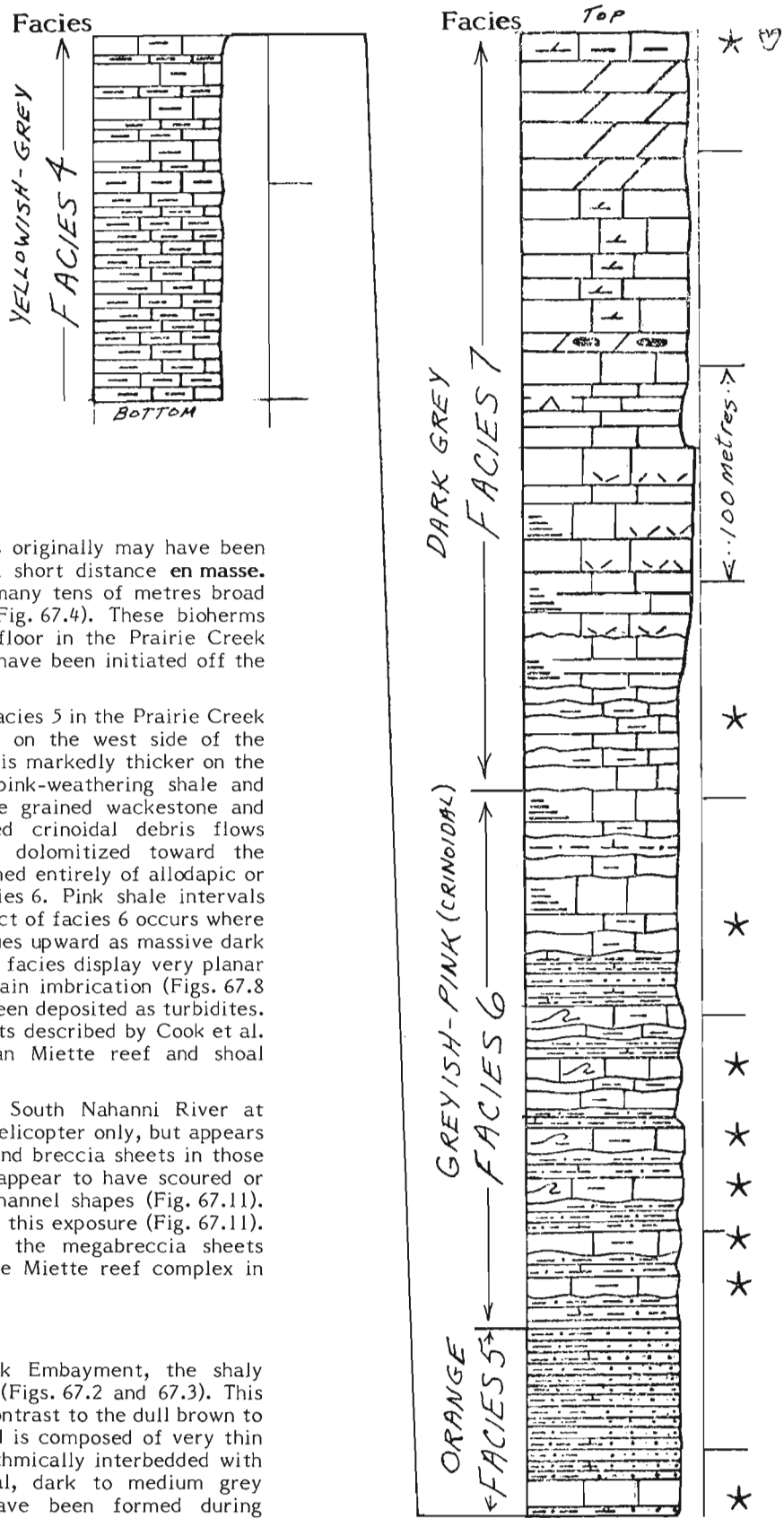

Figure 67.5

Columnar section 7 (south end of Manetoe Range) shown on Figure 67.1. This shows the complete sequence of facies 4, 5, 6, and 7 (Fig. 67.2) that is mapped as OSD undivided (shales, limestones and sandstones) by Douglas and Norris (1976). This section is similar to the one at locality 3 in the cross-section on Figure 67.2.

Some of these pod-shaped breccia masses originally may have been mud mounds or small bioherms that slumped a short distance **en masse.** Lenticular bioherms from 1 to 10 m thick and many tens of metres broad were observed in facies 5 in many sections (Fig. 67.4). These bioherms provided some local relief on the ancient sea floor in the Prairie Creek Embayment. Some of the thin debris flows may have been initiated off the flanks of these mounds.

Facies 6 and 7 occur in succession above facies 5 in the Prairie Creek Embayment. Both of these facies are thicker on the west side of the embayment unlike the underlying facies 5 which is markedly thicker on the east side. Facies 6 is formed of interbedded pink-weathering shale and siltstone and thin to thick bedded, graded, fine grained wackestone and grainstone turbidites and some coarse grained crinoidal debris flows (Fig. 67.5). These carbonates commonly are dolomitized toward the northern part of the embayment. Facies 7 is formed entirely of allodapic or transported carbonates similar to those in facies 6. Pink shale intervals become less abundant upward and the upper contact of facies 6 occurs where the pink shale disappears and the section continues upward as massive dark grey carbonate (Fig. 67.5). Graded beds in these facies display very planar contacts and a slight but noticeable uniform grain imbrication (Figs. 67.8 and 67.9), indicating that these strata may have been deposited as turbidites. They are similar to the allodapic carbonate sheets described by Cook et al. (1972) as turbidites derived from the Devonian Miette reef and shoal complex in Alberta.

A spectacular cliff exposure along the South Nahanni River at locality 26 (Fig. 67.1) has been observed from a helicopter only, but appears to show more proximal carbonate megabreccia and breccia sheets in those facies (Fig. 67.10). Some of the thicker sheets appear to have scoured or pushed soft sediments aside to form distinct channel shapes (Fig. 67.11). Large, apparently stranded blocks are common in this exposure (Fig. 67.11). These deposits are believed to be similar to the megabreccia sheets extending basinward several kilometres from the Miette reef complex in Alberta (Cook et al., 1972).

Shelf and Slope Deposits

On the west side of the Prairie Creek Embayment, the shaly limestones of facies 4 grade upward to facies 3 (Figs. 67.2 and 67.3). This facies weathers bright yellow, orange or pink in contrast to the dull brown to grey weathering of rocks underlying facies 4, and is composed of very thin beds of yellow or pink argillaceous material rhythmically interbedded with thin, slightly nodular beds of slightly crinoidal, dark to medium grey calcilutite (Fig. 67.12). Some nodules may have been formed during interstratal slip and shearing between beds (Fig. 67.12). However, there is

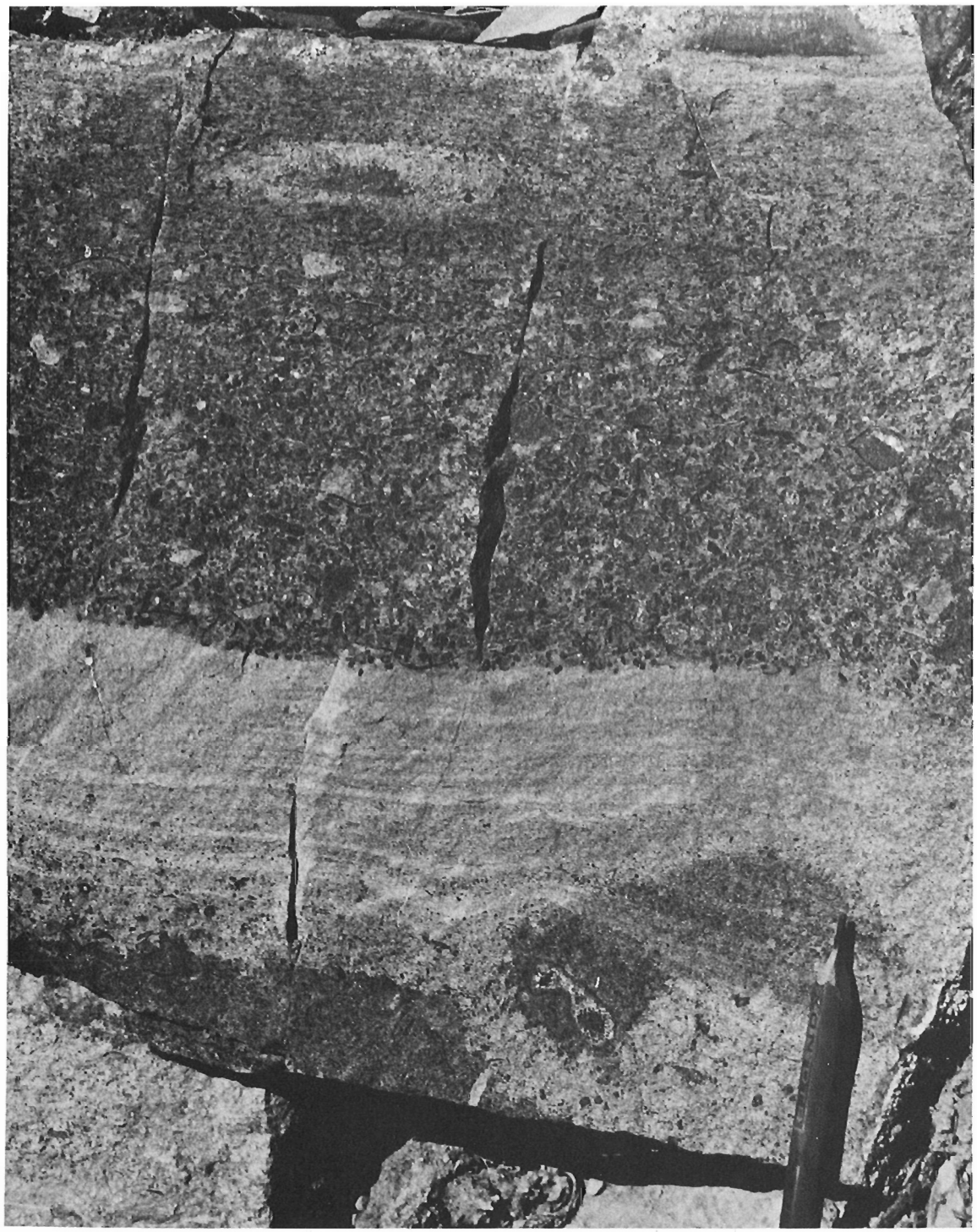

Figure 67.6. Coarsely conglomeratic limestone debris flow deposit that is characteristic of those that are interbedded with the orange siltstones and sandstone of facies 5. Lithified calcilutite clasts, coral, crinoid and brachiopod fragments constitute these crudely graded deposits. This bed occurs in section 5 (see Figs. 67.1, 67.2, 67.4), and is 465 m above the base of facies 5. GSC 199334.

little other evidence to indicate that these deposits accumulated on a pronounced slope. Possibly they may have formed below wave base on gentle slopes leading up to the edge of the Prairie Creek Embayment. Similar Devonian sediments in the Rhenohercynian Geosyncline of West Germany were interpreted to have accumulated on gentle slopes adjacent to submarine highs (Tucker, 1973).

In many areas beds near the top of facies 3 are very fossiliferous with a diverse fauna of brachiopods, corals, amphiporids, trilobites and gastropods, in some places small bioherms 1 to 5 m thick are common (Fig. 67.3). This probably indicates that facies 3 is an upward-shoaling sequence, an impression that is reinforced by the fact that the shallow water, shelf carbonates of facies 1 and 2 directly overlie facies 3. Facies 2 (Camsell Formation) is a light yellow, silty dolomite sequence of repetitive cycles of subtidal, dark grey, vuggy dolomite grading upward to intertidal light grey and yellow silty dolomite laminite displaying mudcracks and fenestral fabric whereas facies 1 (Sombre Formation) is a light to medium grey, shallow-water dolomite sequence.

Along the northern part of the Tundra Thrust on the west side of the Prairie Creek Embayment, facies 3 forms the base of the exposed section. But, in the southern part, this facies is underlain by facies 5 which, in turn, is underlain by facies 4 (Fig. 67.2).

Relationship of Lithofacies to Map-Units of Douglas and Norris (1976)

Facies 1 and 2 are identical to the Sombre and Camsell formations, although the Camsell Formation had not previously been recognized in the Arnica Thrust plate where it is shown at locality 2 on Figure 67.2. Facies 3 is mapped as the uppermost part of the OSD (Ordovician, Silurian and Devonian undivided) map-unit west of the Tundra Thrust Fault along the east side of the Prairie Creek Embayment. On the hanging wall of the Tundra Thrust itself this facies is mapped as part of the Delorme Formation. Facies 4, 5, and 6 also are mapped as part of the OSD map-unit everywhere west of the Tundra Thrust Fault. However, where facies 4 and 5 are present along the southern extension of the Tundra Thrust plate they have been mapped as part of the Delorme Formation. Facies 5 and 6 also have been mapped as Sombre Formation and facies 7 as Arnica or Sombre Formation.

These observations suggest that some reorganization of the stratigraphic nomenclature would be desirable to emphasize the contrast between the distinctive widespread and mappable slope deposits in the Prairie Creek Embayment and the surrounding shelf and basin deposits (Fig. 67.2). Possible facies 6 and 7 could be given separate formational names. However, facies 5 is not confined entirely to the Prairie Creek Embayment as it underlies the shelf sequence

Figure 67.7. Very coarsely fragmental debris flow breccia in facies 5 in section 13 (see Fig. 67.1). This chaotic breccia, which has a fabric that is only partly fragment-supported rests on laminated, slightly argillaceous calcilutite. Some fragments of the underlying limestone occur in breccia. GSC 199336.

on the east side of the embayment (Fig. 67.2). Also, this facies is similar to the orange-weathering siltstones and ridge-forming limestones of the Delorme Formation in the Whittaker Anticline (Douglas and Norris, 1961) only 40 km north of the tip of the Prairie Creek Embayment. This may indicate that facies 5 has a regional extent northward beyond the Prairie Creek Embayment although it is not known whether the "ridge-forming . . . dolomites and limestones" (Douglas and Norris, 1961, p. 10) in the orange siltstones of the Delorme Formation exposed on Whittaker Anticline are debris flows or not.

Facies 4 probably is best regarded as being a tongue of the Road River Formation. It is contiguous with the Upper Ordovician to Lower Devonian shale of the Road River Formation mapped by Gabrielse et al. (1973) in the adjoining Flat River map-area immediately west of the Virginia Falls map-area.

Development of the Prairie Creek Embayment and its Subsequent Structural History

A north-trending depression developed in the Virginia Falls map-area during Middle Silurian time and its axis coincided with the thickest part of facies 5. This depression or trough in which the sediments of facies 5 accumulated may have extended northward into the adjoining Root River map-area. In Early to Middle Devonian time, an expansion of the area of shallow shelf carbonate deposition defined the boundaries of the Prairie Creek Embayment and confined it to the Virginia Falls map-area. During this time, the axis of deposition moved slightly westward toward the centre of the Prairie Creek Embayment.

Following deposition of facies 1 and 7, shale of the Funeral Formation was deposited over sediments of the Prairie Creek Embayment and over much of the adjoining shelf and the Prairie Creek Embayment ceased to exist as a well-defined feature.

Tertiary faulting may have been localized along the junction of the carbonte shelf (facies 1, 2, and 3, Fig. 2) and the much thinner, silty and shaly slope deposits (facies 5, 6, and 7) to cause the coincidence of this facies transition with major thrust faults. The east-dipping Tundra Thrust appears to have been initiated along the eastern boundary whereas the west-dipping Manetoe Thrust appears to have formed along the western boundary of the Prairie Creek Embayment. The northward convergence of these faults probably reflects the original northward narrowing and termination of the Prairie Creek Embayment (Fig. 67.1). The thin sequence of slope sediments in the embayment probably has been overridden somewhat by both the Tundra and Manetoe Thrust faults so that the original breadth of the embayment may have been considerably greater than it now appears.

Figure 67.8. Medium to dark grey, mass flow deposits (turbidite?) with sharp planar contacts and formed of fine grained detrital carbonate fragments and crinoid ossicles, location 96 m above the base of facies 7 in section 7 (see Figs. 67.1, 67.5). GSC 199335.

Figure 67.9. A close-up view of the beds shown in Figure 67.8. Beds are noticeably graded and the grains display a gentle imbrication to the right or northeast. GSC 199331.

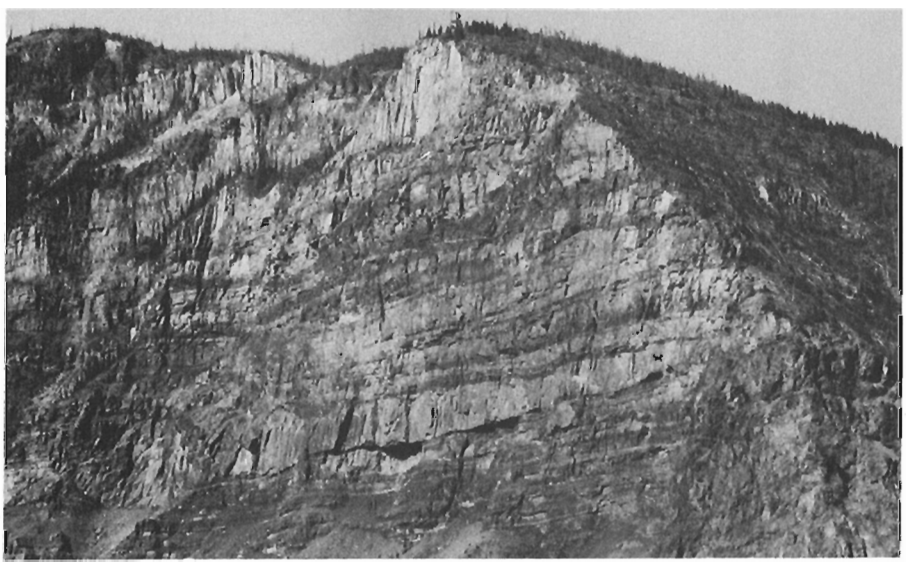

Figure 67.10.

View of the south-facing cliff on the South Nahanni River at locality 26 (Fig. 67.1). The cliff face shown is about 300 to 400 m high. The light beds appear to be debris slides or flows between dark grey shaly beds. This sequence is assigned tentatively to facies 7. GSC 199333.

Figure 67.11. A close-up of the debris slides and flows shown in Figure 67.10. Arrows point to large carbonate blocks that are more than a few metres across. GSC 199332.

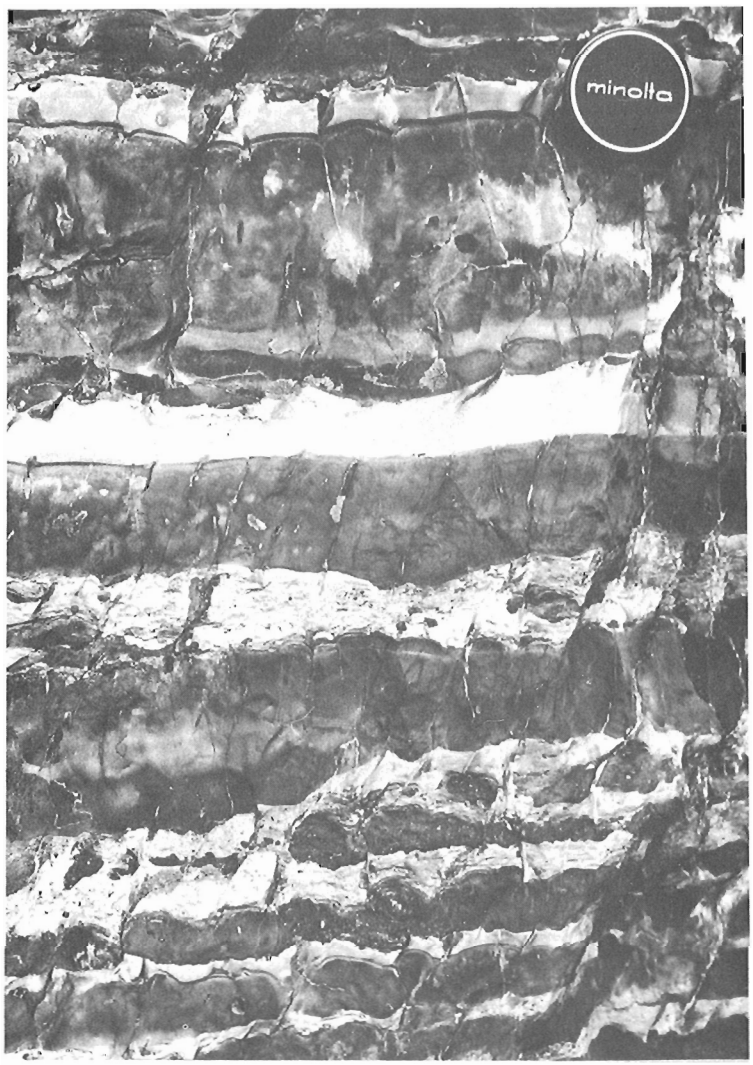

Figure 67.12. Bright yellow, silty, argillaceous bands interbedded with dark grey, slightly fossiliferous calcilutite in facies 3, 220 m below the top of facies 3 at section 2 (see Figs. 67.1, 67.2). Penecontemporaneous interstratal slip may have caused the fragmentation of parts of some calcilutite beds. GSC 199337.

Conclusions

1. The Prairie Creek Embayment is defined by a distinctive suite of Upper Silurian to Lower Devonian slope-deposited shales, siltstones and carbonates that form a sequence only half as thick (~1000 m) as the surrounding contemporaneous shelf sequence (>2000 m thick) in the Virginia Falls map-area.
2. Diagnostic slope deposits consist of conglomeratic, weakly graded, polymictic carbonate debris flows 0.5 to 2.0 m thick, thick (up to 15 m) carbonate megabreccia sheets that contain very large blocks (~5 m across), and fine grained, graded, allodapic (turbiditic) carbonate sheets.
3. A tongue of Middle Silurian Road River shale extends eastward into the northeast part of the Virginia Falls map-area and immediately underlies sediments in the Prairie Creek Embayment and in the surrounding contemporaneous shelf sequence.
4. Recognition of part or all of the Upper Silurian-Lower Devonian sequence as a separate formation in the Prairie Creek Embayment probably is desirable and may be named by Morrow and Cook (pers. comm.).
5. The junction of the thin, partly terrigenous Upper Silurian-Lower Devonian sequence in the Prairie Creek Embayment with the thicker, surrounding shelf carbonate succession provided a locus for stress concentration during Tertiary deformation with the result that the Manetoe and Tundra Thrust faults largely conform to the configuration of the embayment.

References

Cook, D.G.
1977: Two stages of faulting, Virginia Falls map-area, District of Mackenzie; in Report of Activities, Part A, Geol. Surv. Can., Paper 77-1A, p. 113-115.

Cook, H.E., McDaniel, P.N., Mountjoy, E.W., and Pray, L.C.
1972: Allochthonous carbonate debris flows at Devonian bank ('reef') margins, Alberta, Canada; Bull. Can. Petrol. Geol., v. 20, no. 3, p. 439-497.

Douglas, R.J.W. and Norris, D.K.
1960: Virginia Falls and Sibbeston Lake map-areas, Northwest Territories, 95F and 95G; Geol. Surv. Can., Paper 60-19.

1961: Camsel Bend and Root River map-areas, District of Mackenzie, Northwest Territories, 95J and K; Geol. Surv. Can., Paper 61-13.

1976: Geology — Virginia Falls, District of Mackenzie; Geol. Surv. Can., Map 1378A.

Gabrielse, H., Blusson, S.A., and Roddick, J.A.
1973: Geology of Flat River, Glacier Lake and Wrigley Lake map-areas, District of Mackenzie and Yukon Territory; Geol. Surv. Can., Mem. 366.

Tucker, M.E.
1973: Sedimentology and diagenesis of Devonian pelagic limestones (Cephalopodenkalk) and associated sediments of the Rhenohercynian Geosyncline, West Germany; N. Jahrb. Geol. U. Palaeontol., Abh. 142, p. 320-350.

68. REPORT ON ROAD RIVER STRATIGRAPHY AND THE MISTY CREEK EMBAYMENT, BONNET PLUME (106B), AND SURROUNDING MAP-AREAS, NORTHWEST TERRITORIES

Project 770044

M.P. Cecile
Institute of Sedimentary and Petroleum Geology, Calgary

Abstract

Cecile, M.P., Report on Road River stratigraphy and the Misty Creek Embayment, Bonnet Plume (106B), and surrounding map-areas, Northwest Territories; Current Research, Part A, Geol. Surv. Can., Paper 78-1A, p. 371-377, 1978.

In the Bonnet Plume map-area the Road River Formation is divided into four units ranging in age from Lower to Middle Cambrian to late Early Silurian. These units are correlated partly with adjacent lower Paleozoic shelf strata. Using the 'shale-out' line, thickness variations and paleocurrents, the Road River Formation is shown to have been deposited in a major embayment, which numerous anomalies suggest is fault controlled. Basic volcanic tuffs are interstratified with upper Road River units. Bedded barite occurs in three Road River units. Sphalerite and galena were found in association with transitional facies, volcanic tuffs and pyrobitumen.

Introduction

During the 1977 field season a stratigraphic-depositional study of the lower Paleozoic Road River Formation was initiated in the Mackenzie Mountains (Fig. 68.1). The main purpose of this study was: to define stratigraphic units within the Road River Formation; to relate these units to the adjacent homotaxial lower Paleozoic carbonate; to delineate the position of the carbonate-shelf to shale-basin transitions; to understand from these data the locus and nature of Road River deposition; and to correlate Road River stratigraphic units with other lower Paleozoic successions in the Canadian Cordillera.

Acknowledgments

J.D. Aitken organized logistic support and spent considerable time in introducing the author to Mackenzie Mountain geology. D.G. Cook gave critical guidance during discussions in the field. W.H. Fritz made tentative identification of some trilobite assemblages in the field. Exemplary assistance was given by Cathy Black (University of Alberta) and Kelly Kingsmith, Robin Sandau and Kevin Sharman (all from University of Calgary).

Previous Geological Work

The name Road River Formation was proposed by Jackson and Lenz (1962) for a succession of Siluro-Ordovician graptolitic shales and carbonates. The type section is located at the headwaters of the Road River in the Richardson Mountains 250 km northwest of the Bonnet Plume map-area. The name Road River Formation was introduced into the Bonnet Plume area by Aitken et al. (1973) and by Blusson (1974). Aitken et al. (ibid., p. 33) found Road River strata to range from Middle Cambrian to Early Ordovician in age. Blusson (ibid.) mapped as Road River Formation shales, argillaceous limestones, cherts and volcanic rocks that were underlain by the Lower Cambrian Sekwi Formation and overlain by Siluro-Devonian carbonates. Blusson (1974), and Aitken and Cook (1975) identified the carbonate-shelf to shale-basin transition trending along a northwest line through the northeastern Bonnet Plume map-area and the southwestern Mount Eduni map-area (106A).

Stratigraphy

Introduction

In the Bonnet Plume and surrounding map-areas the Road River Formation can be divided into four units ranging in age from Lower to Middle Cambrian to late Early Silurian or younger Silurian. These units are homotaxial with, and fall within the same time range of, in ascending stratigraphic order, the Mount Cap, Saline River, Franklin Mountain, and Mount Kindle formations, all units of the carbonate shelf; and with sub-Franklin Mountain, sub-Mount Kindle and sub-Saline River unconformities (see Aitken et al., 1973, and Norford and Macqueen, 1975). A Franklin Mount Formation 'transition to shale-basin facies', recognized by Aitken and Cook (1975) can be divided into two units.

The data presented here are based on 22 measured sections within the Bonnet Plume and surrounding map-areas, basinward from and along the southwestern part of the Mackenzie Arch (Fig. 68.1).

Road River Formation

The Road River Formation can be divided into four mappable units which, in ascending stratigraphic order, are: a lower shale unit (RRs); a yellowish weathering argillaceous limestone unit (RRal); a shale-chert unit (RRc) and an upper unit of sooty, grey, thin bedded limestones (RRl) (Fig. 68.2). Interstratified with the RRc unit at Sections 34, 36, 40, 46, 53, 55 (Fig. 68.1) and with the RRl unit at Sections 40, 49 are basic volcanic lapilli tuffs, fine grained tuffs, and volcanic breccias.

Shale unit (RRs)

In all but one section (36, Fig. 68.1) the base of the Road River Formation consists of 200 to 800 m of shale and argillaceous limestone, known as the RRs unit. This unit can be subdivided into a lower shale succession and an upper shale-argillaceous limestone succession (Fig. 68.2). In Section 45 only the basal sub-unit is present and is overlain by 1600 m of quartz sandstone-shale and quartz sandstone-siltstone flysch, followed by 600+ m of shale-argillaceous limestone rhythms. The RRs cannot be subdivided at Section 41.

The RRs is in sharp contact but conformable with the Lower Cambrian Sekwi Formation. The RRs unit contains Middle Cambrian trilobites in basin-edge sections (Sec. 31; W.H. Fritz, pers. comm.; see also Aitken et al., 1973, p. 77, Sec. U7) and Lower Cambrian trilobites (Olenellids) in deeper basin sections (Secs. 44, 45, Fig. 1). Fritz (1976) believed that the Sekwi-Road River boundary is diachronous and in the Bonnia-Olenellus zone.

Argillaceous limestone unit (RRal)

The RRs is conformably overlain gradationally by 400 to 800 m of very thin and thin bedded yellowish weathering argillaceous limestone. This unit, designated RRal, is

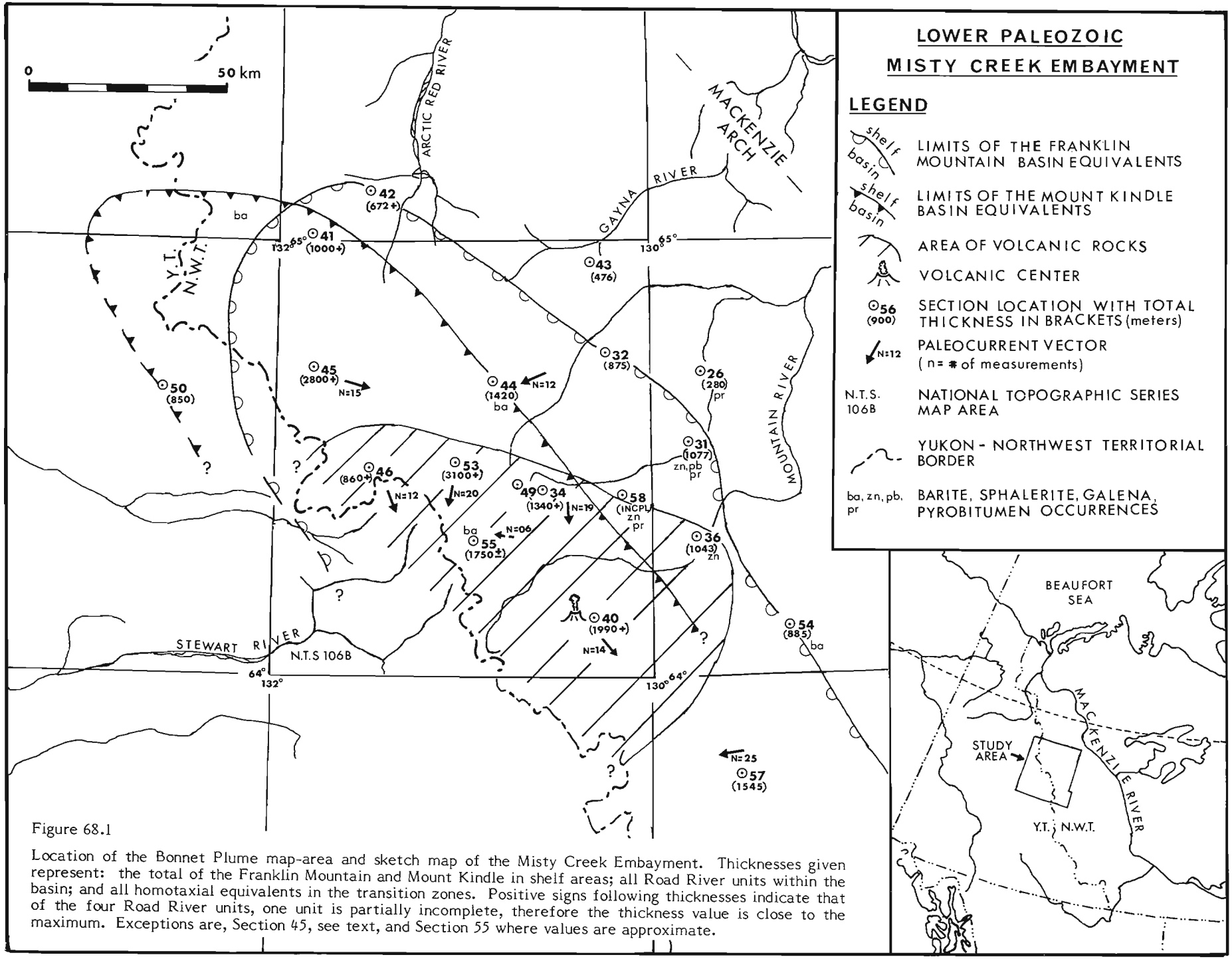

Figure 68.1

Location of the Bonnet Plume map-area and sketch map of the Misty Creek Embayment. Thicknesses given represent: the total of the Franklin Mountain and Mount Kindle in shelf areas; all Road River units within the basin; and all homotaxial equivalents in the transition zones. Positive signs following thicknesses indicate that of the four Road River units, one unit is partially incomplete, therefore the thickness value is close to the maximum. Exceptions are, Section 45, see text, and Section 55 where values are approximate.

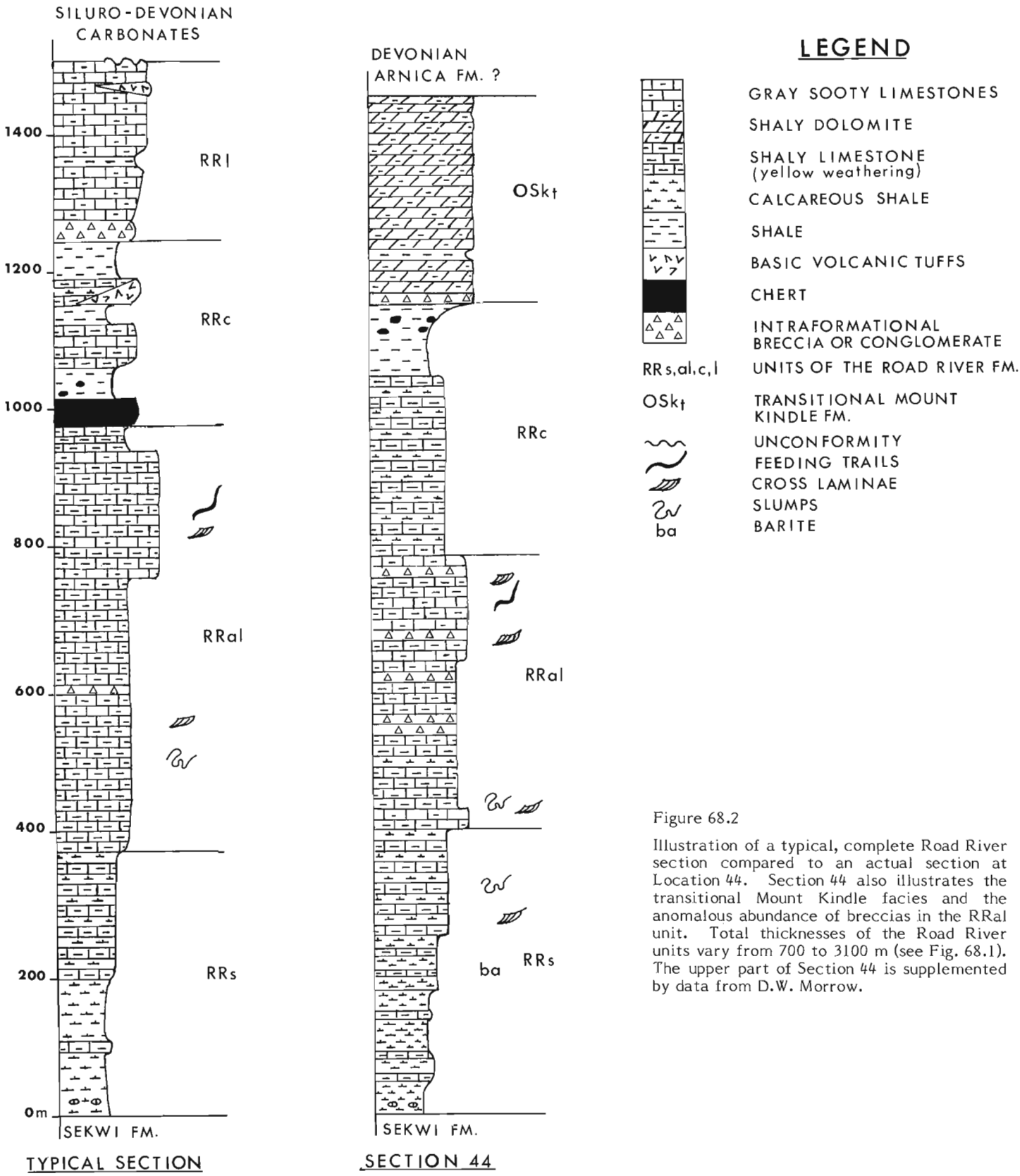

Figure 68.2

Illustration of a typical, complete Road River section compared to an actual section at Location 44. Section 44 also illustrates the transitional Mount Kindle facies and the anomalous abundance of breccias in the RRal unit. Total thicknesses of the Road River units vary from 700 to 3100 m (see Fig. 68.1). The upper part of Section 44 is supplemented by data from D.W. Morrow.

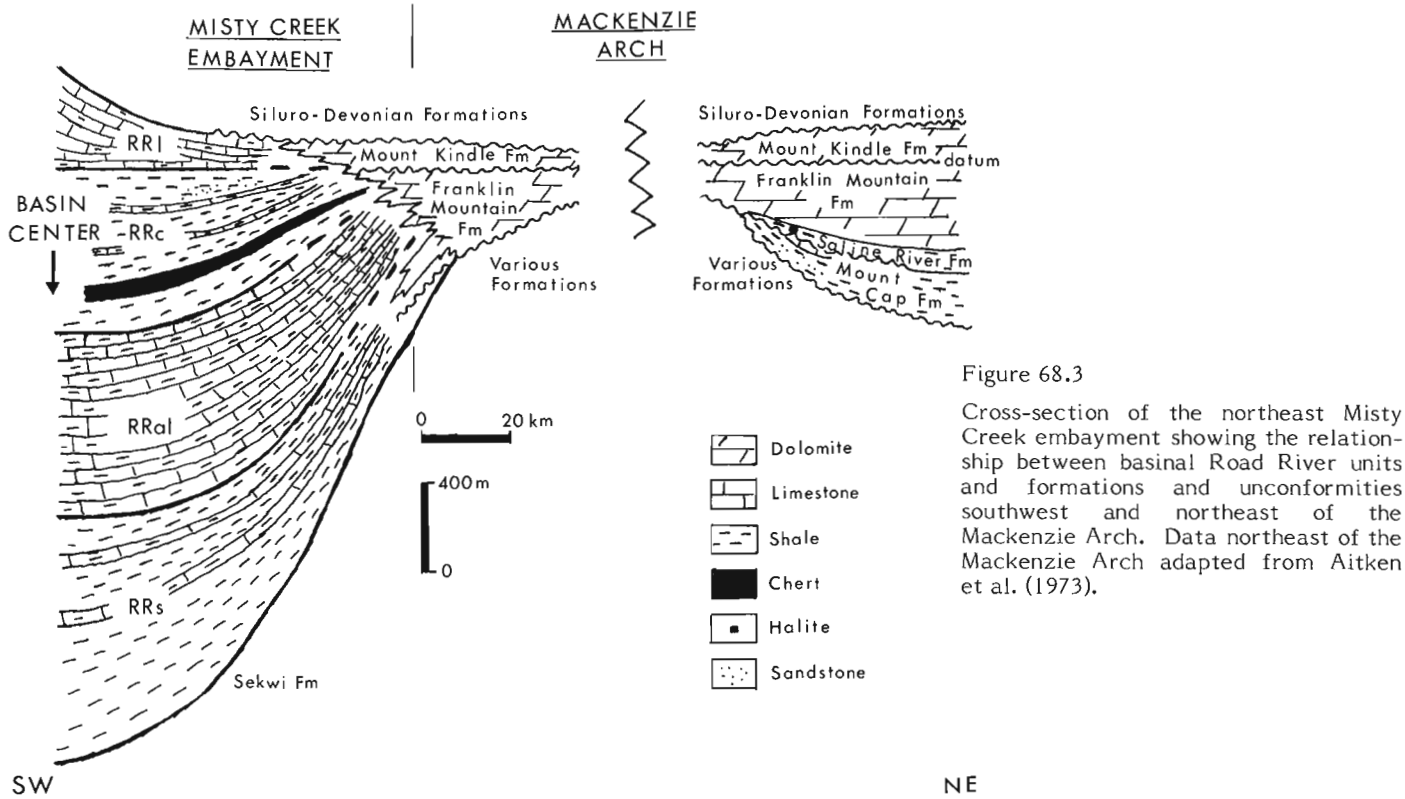

Figure 68.3

Cross-section of the northeast Misty Creek embayment showing the relationship between basinal Road River units and formations and unconformities southwest and northeast of the Mackenzie Arch. Data northeast of the Mackenzie Arch adapted from Aitken et al. (1973).

undivided although in some sections the presence of thin beds of clean limestone produces in places a prominent resistant interval (e.g. Fig. 68.2).

RRal rocks have all the characteristics of a slope facies: including slumps, in situ slump breccias, carbonate-clast conglomerates and breccias, trains of ripple-drift cross laminae, lensed and scoured bedding. Other characteristics of the RRal, that also may be slope features, are the presence of abundant feeding trails and beds of biosparite.

The RRal unit was identified in all basinal sections, except for Sections 36 and 45. The age of this unit presently is unassigned.

Chert-shale unit (RRc)

Conformably overlying the RRal unit are 200 to 500 m of interstratified black chert, siliceous shale, shale and argillaceous limestone rhythms, and thin bedded argillaceous limestone. Commonly interstratified with these rocks, but not restricted to this unit, are basic lapilli tuffs, tuffaceous sediments and, in Section 40, volcanic breccias. The lower contact of this unit, the RRc unit, is defined arbitrarily as the base of the first thick succession of shale, chert, or shale-argillaceous limestone rhythms, overlying the RRal succession. The contact may be sharp or broadly gradational. This unit is undivided.

Basal shale successions from the RRc unit are typically graptolitic. From the numerous graptolite assemblages collected the most common forms are tetragraptids, which indicate a Lower to early Middle Ordovician age for the shale.

Associated with the RRc unit in three sections (34, 49, 53) is a succession of quartz sandstone, arenaceous limestone, and carbonate-clast orthoconglomerate.

The RRc unit was identified in all basinal sections except 31 and 45. This probably is due to erosion of the upper part of Section 45 and the transitional nature of the upper part of Section 31.

Grey limestone unit (RRI)

The uppermost unit of the Road River Formation, designated RRI, is a 100- to 300-m succession of thin bedded, grey, sooty limestone with minor intercalations of black chert, shale and yellowish argillaceous limestone. In Sections 40 and 49 volcanic tuffs are interstratified with the RRI unit. The basal contact of the RRI rocks is defined arbitrarily as the first occurrence, in thick succession, of grey, thin bedded, sooty limestone above the RRc unit. The upper limit is a sharp contact with the Siluro-Devonian Delorme and Arnica formations.

The RRI unit was identified only in central and southwestern basinal sections. This unit was not found at Sections 31, 36, and 44, although a 300 m succession of thin bedded shaly dolomite at the top of Section 44 (Fig. 68.2) is considered a transitional equivalent to this unit (see following section).

In Sections 46 and 53 this unit is chaotically slump-folded over 100- to 250-m stratigraphic intervals. The unit contains, in Sections 41 and 55, a monomictic breccia that is as much as 60 m thick.

The RRI limestones commonly have interstratified biosparites and crinoidal biosparites, as well as both reworked and in situ favositid, halysitid and cup corals, and articulate brachiopods. Within a thin shale succession ≈200 m above the base of the RRI unit, Sections 34 and 49 contained **Monograptus spiralis** indicating that at least part of this unit is late Early Silurian in age.

Transitional Facies

Along the southwestern margin of the Mackenzie Arch, of all the lower Paleozoic strata homotaxial with the Road River Formation, only the Franklin Mountain and Mount Kindle formations, each overlying an unconformity, are present. Both formations have a zone of transitional facies where massive, thick bedded, shelf dolomite becomes thin bedded and shaly southwestward toward the basin.

Through the northeastern part of the study-area the Franklin Mountain Formation is the first to 'shale-out' whereas the Mount Kindle Formation continues as massive dolomite southwestward for another 20 to 30 km to where it rests directly on units of the Road River Formation (Figs. 68.1, 68.3). The extension of the Mount Kindle Formation basinward was recognized by Aitken et al. (1973). In the northwestern part of the study-area this trend is completely reversed with the Mount Kindle Formation 'shaling-out' before the Franklin Mountain Formation.

Part of the Franklin Mountain 'shale-out' involves a mixture of transitional Franklin Mountain and Road River units. Within this belt various combinations of the four Road River units are missing.

The Franklin Mountain Transition

The transitional Franklin Mountain rocks can be divided into two belts trending parallel to the basin edge. In the first basinward belt (Secs. 42 and 32) the Franklin Mountain Formation consists of two units. The lower unit is 150 m of thick bedded, grey, crystalline dolomite similar to rocks of the Franklin Mountain Formation on the Mackenzie Arch. The upper unit is 250 m of medium to thin bedded shaly dolomite with minor amounts of black chert and some slump folds. In the second belt the upper shaly dolomite of the Franklin Mountain Formation persists but overlies various combinations of the lower three Road River units, with thick intervals and biohermal-like mounds of massive dolomite.

The Mount Kindle Transition

Massive, thick bedded dolomites, with coral biostromes in places, continue basinward of the Franklin Mountain 'shale-out'. A sub-Mount Kindle unconformity with sharp boundary marked by ferruginous breccia can be traced across the two Franklin Mountain transitional belts, but not into the basin.

Transitional Mount Kindle sections were found at locations 44 and 58 (Fig. 68.1). At section 44 (Fig. 68.2) the Mount Kindle Formation is replaced by 300 m of brownish, thin bedded, shaly dolomite. This dolomite overlies the RRs, RRal and RRc units of the Road River Formation and is overlain by the Devonian Arnica Formation and is, therefore, homotaxial with the RRI unit. At Section 58, thick bedded Mount Kindle dolomite conformably overlies grey limestone of the RRI unit. This is the reverse situation to the Franklin Mountain transition where massive dolomite continues basinward, at the base of the transition unit, and is interstratified with Road River units in the second transition belt.

The Mount Kindle Formation does not extend basinward of Sections 44 and 58. Because the Mount Kindle Formation is homotaxial with the RRI unit, because both have similar coral assemblages (the Mount Kindle Formation has favositid, halysitid and cup corals (see Norford and Macqueen, 1975)), and because both are partly late Early Silurian in age (see Norford and Macqueen, 1975), it is probable that a large part of the RRI is the direct basin equivalent of the Mount Kindle Formation.

The Road River Transition

Units of the Road River Formation in the second Franklin Mountain transition belt show considerable stratigraphic variation. This variance will be discussed section by section from the northwest to the southeast.

At Section 41 (northwest) the RRs unit is present but undivided and interstratified with dolomite, the RRal unit is replaced by 100 m of massive crystalline dolomite, and the RRc and RRI units are present. At Section 31 the RRs unit is present but contains a sub-unit of massive dolomite and shaly dolomite between the lower shaly and upper rhythmic sub-units, the RRal unit is present, and shaly dolomite (Franklin Mountain transitional unit) occupies the same interval as the RRc unit, and the RRI is missing; the entire section is unconformably overlain by the Mount Kindle Formation. Section 36 is the most anomalous section in this belt. The base of this section has been dated by Fritz (1976, p. 2 and 20) as Early Ordovician and it rests directly on the Lower Cambrian Sekwi Formation. This section is similar to, and in part time equivalent with, the RRc unit. Rocks at this section are interstratified shale-argillaceous limestone rhythms, shaly dolomite with thin beds of black chert, argillaceous limestone, graptolitic shale (with tetragraptids), and volcanic tuff. The top of Section 36 comprises 60 m of grey, massive dolomite overlain unconformably by the Mount Kindle Formation. The RRs, RRal and RRI units are missing at this section. At Section 54, 300 m of thin bedded argillaceous limestone rests directly on the Sekwi Formation which is, in turn, overlain by 200 m of thin bedded shaly dolomite which is unconformably overlain by the Mount Kindle Formation. Section 54 may be an intertransition from the first to the second Franklin Mountain transition belt where the upper shaly dolomite persists but the basal massive dolomite changes laterally to limestone before becoming completely basinal.

Comparison of the Lower Paleozoic Shelf and Basinal Successions

Shelf sedimentary rocks homotaxial with the Road River Formation, northeast of the Mackenzie Arch, are the Mount Cap, Saline River, Franklin Mountain and Mount Kindle formations. These contain a sub-Mount Kindle unconformity and, near the Mackenzie Arch, a sub-Saline River unconformity (Fig. 68.3). These formations and unconformities are described by Aitken et al. (1973) and will be referred to only when comparisons are necessary.

On the southwest side of the Mackenzie Arch, within the study-area, the Road River Formation is homotaxial with the Franklin Mountain and Mount Kindle Formations and sub-Franklin Mountain and sub-Mount Kindle unconformities (Fig. 68.3).

On the southwest side of the Mackenzie Arch the Franklin Mountain Formation consists generally of 150 to 300 m of grey, massive, thick bedded, crystalline, vuggy dolomite. At a few locations the base of the Franklin Mountain Formation is a sub-unit comprising red quartz sandstone, shales, siltstone and dolomite; this sub-unit is known as the basal Franklin Mountain red beds (Aitken et al., 1973). On the southwest side of the Mackenzie Arch the Mount Kindle Formation consists of a single unit of dark grey, thick bedded, crystalline dolomite, containing, in places, coral biostromes. The coral biostromes are present at the top of Section 36, throughout Section 43, and are either rare or missing in other sections.

The Franklin Mountain Formation is dated as Late Cambrian to Early Ordovician and possibly younger; the Mount Kindle Formation is dated as Late Ordovician to Early Silurian and possibly younger (see Norford and Macqueen, 1975).

The first basin to shelf correlation, discussed in the section on 'Mount Kindle transition', is the equivalence of part of the RRI unit with the Mount Kindle Formation (Fig. 68.3). This provides an upper correlation limit. Below this the RRc unit which, in part is Lower to early-Middle Ordovician, must be equivalent to parts of the Franklin Mountain Formation. Quartz sandstone and carbonate-clast orthoconglomerate from the middle of the RRc unit at Sections 34, 49, 43 (these rocks are 10-30 m thick) are thought tentatively to be depositional equivalents of the sub-Mount Kindle unconformity. If this is so, rocks from the upper RRc would be equivalent to strata at the base of the Mount Kindle Formation. The RRal unit cannot be correlated until fossil collections from this unit are examined in the laboratory. The RRs unit, where dated, is older (Lower to

Middle Cambrian) than the Franklin Mountain Formation and is, therefore, a probable depositional correlative of the Mount Cap Formation, northeast of the Mackenzie Arch, and the sub-Franklin Mountain unconformity southwest of the Mackenzie Arch. The Mount Cap Formation, which is dated as Lower to Middle Cambrian, is similar to the RRs unit in that it consists of "dark grey to black pyritic shales, and thin bedded micritic limestones" and differs in that it contains glauconitic sandstones (Aitken et al., 1973, Table 1, p. 6). The 1600 m of alternating quartz sandstone and shale or siltstone and shale flysch at Section 45, which were deposited on Lower Cambrian shales, also may be depositional equivalents of the sub-Franklin Mountain unconformity.

Volcanism

Figure 68.1 illustrates the limits of basic volcanism within the Bonnet Plume study-area. Volcanic rocks are predominantly lapilli size or finer grained tuffs. These tuffs are poorly stratified, in places containing limestone, argillaceous limestone or shale clasts, and are of basic composition. In some sections these tuff beds are graded and are interbedded with typical Road River sedimentary rocks.

Volcanic rocks are interbedded with strata of Early to early Middle Ordovician and late Early Silurian age.

Section 40 shows evidence of the most extensive and continuous volcanism occurring through 900 m of strata. This includes about 60 m of coarse volcanic breccia. Section 40, therefore, must be located close to a volcanic centre. This hypothesis is supported by the distribution of volcanic tuffs in a semicircle around Section 40, and by the presence of a diabase dyke and numerous sills at the same section. In other sections dykes were not recognized, and only a few sills were observed. A few thin amygdaloidal flows? were interstratified with volcanic tuffs at Section 53.

Because of their basinal position, interstratification with Road River rocks, and their crude stratification, the volcanic tuffs appear to have been deposited in submarine environments. However, the predominance of fragmental materials of basic composition, suggests the probability of subaerial exposure, perhaps very close to the sea surface where basic lavas are likely to be quickly chilled and explosively fragmented.

The Misty Creek Embayment

The position of the Franklin Mountain and Mount Kindle 'shale-outs' and the tremendous thickening of equivalent or older Road River strata, outlines a northwest-trending lower Paleozoic depositional embayment, herein named the Misty Creek Embayment (Fig. 68.1). Misty Creek is a geographical feature in the southwestern Bonnet Plume map-area.

Initially the northeast side of the Misty Creek Embayment is fixed by the first belt of transitional Franklin Mountain Formation; this feature is extended by tracing map-units of Blusson (1971, 1974; map-areas 106B, 105P) and Aitken and Cook (1975; 106A, B). The early southwest margin of the embayment is positioned between massive, thick bedded Franklin Mount Formation dolomite, measured at Mount Macdonald (Sec. 50), and a thin Road River succession at Section 46. This margin is positioned along a northwest trend between a 60 km long belt of northwest trending lower Paleozoic carbonates mapped by Blusson (1974) around Mount Macdonald and outcrops of Road River Formation situated to the northeast of this belt. The northwestern margin of the Misty Creek embayment is defined by a thin succession of Road River strata at Section 41 and by a traverse section across the southern extremities of map-area 106F. This traverse established that typical Franklin Mountain Formation rocks replace the Road River Formation just northwest of Section 41. In map-area 106F the Franklin Mountain Formation consists of approximately 400 m of very vuggy, very crystalline, extensively silicified massive dolomite. The Franklin Mountain Formation has been mapped by Norris (1975) across the entire 106F map-area.

The trace of the Mount Kindle equivalent (RRl unit) basin area is defined by the 'shale-out' along the northeastern part of the study-area. In the southwest at Mount Macdonald, homotaxial with the Mount Kindle Formation, is a transitional facies consisting of 200 m of crackle-brecciated limestones overlain by 100 m of massive dolomite with halysitid and favositid corals. The trace of the Mount Kindle shale-out is placed through this section and assumed to trend northwest. The Mount Kindle 'shale-out' in the northwest is defined by map-units of Norris (1975, 106F). Norris mapped the Mount Kindle Formation through most of 106F map-area. In the southeastern 106F map-area Road River strata conformably overlie the Franklin Mountain Formation and are homotaxial with the Mount Kindle Formation. These Road River strata were found on a traverse section to be the RRl unit, basinal equivalent to the Mount Kindle Formation.

The area defined by Mount Kindle basinal equivalents shows a southwest and northwest shift in the position of the Misty Creek Embayment.

An important criterion in defining the embayment is the great changes in thickness of basinal sedimentary rocks. Variations in thickness are shown in Figure 68.1. Thicknesses range from 885 m in the transitional zones to in excess of 2800 m at Section 45 and 3100 m at Section 53, located at the basin centre (Fig. 68.3).

The geometric configuration of the Misty Creek Embayment is reflected by paleocurrents (Fig. 68.1). All paleocurrent measurements except those at Section 45, are from ripple-drift cross laminae within the RRal unit. Paleocurrent indicators at Section 45 are from ripple cross laminae within the flysch succession.

Structural deformation in the Misty Creek Embayment is predominantly open folding, with a few northeast-directed thrust faults, most occurring along the zone of transition. The effect of crustal shortening on the embayment is thought, therefore, to be minimal.

Fault control of the Misty Creek Embayment

A combination of several factors suggests that the Misty Creek Embayment was produced and controlled by extension faults. These factors are: 1) the geometry of the embayment; 2) rapid 'shale-out' of shelf carbonates on all sides; 3) rapid increase in Road River Formation thicknesses requiring sub-Road River Formation slopes of 6 to 8° (see Fig. 68.3); 4) stratigraphic anomalies in the Road River transition zone, where, for instance, the entire basal two units of the Road River Formation are missing at Section 36; 5) the confinement of 1600 m of Road River flysch to Section 45; 6) extensive slumping of, and presence of thick breccias within the RRl unit (Secs. 41, 46, 53, 55); 7) basic volcanism in the basin centre; 8) persistence of the Misty Creek Embayment during deposition of Mount Kindle basinal equivalents; and 9) presence of numerous slump folds, in situ slump breccias, and debris flows in the RRal unit at Section 44 proximal to the Franklin Mountain transitional belts (Fig. 68.2). However, further work will be needed, especially in transitional zones, to prove faulting is associated with deposition of rocks in the Misty Creek Embayment.

Economic Geology

Both secondary and primary bedded barite were identified at four localities. Megacrysts of barite were found scattered in sedimentary beds at the base of the RRl unit in the southeast part of map-area 106F. Megacrysts of barite forming sedimentary layers interstratified with argillaceous limestone were observed in the middle RRs unit at Section 44. Local accumulations of megacrystalline barite

nodules were found with the RRc unit at Section 55. Very coarse crystalline barite was found in a single vug within the Mount Kindle Formation at Section 54.

Bedded barite occurs within three of the four Road River units ranging in age from Lower to Middle Cambrian to late Early Silurian and is not confined, therefore, to a particular stratigraphic or time unit.

Galena and sphalerite

Small amounts of sphalerite were found in fracture fillings over a 10-m stratigraphic interval at the base of the Road River Formation, Section 36. One vug-filling of sphalerite was found in the Mount Kindle Formation at Section 58. A string of vugs lined with galena (≈ parallel to bedding) was observed in the Mount Kindle Formation at Section 31. The mineralization, at Section 31, is associated with more extensive galena-sphalerite occurrences in Siluro-Devonian carbonates at the same location (see Cecile and Morrow, 1978). Three areas of Silurian to Devonian carbonates, located within 40 km northwest of Section 31, have been staked by Welcome North for Zn-Pb mineralization (Dawson, 1975).

It is interesting that these mineral occurrences and associated occurrences of pyrobitumen are located in the area of the Franklin Mountain transition facies, and close to an area of volcanic rocks (Fig. 68.1).

Conclusions

The Road River Formation in the Bonnet Plume and surrounding map-areas can be divided into four units. In ascending stratigraphic order these units are: a shale-dominated succession (RRs); argillaceous limestone (RRal); interstratified chert, shale and argillaceous limestone (RRc); and a succession of sooty grey limestone (RRl). Some of the RRs unit rocks contain Lower to Middle or Middle Cambrian trilobites. The RRc unit includes shale with Lower to early Middle Ordovician graptolites, and the RRl unit includes a minor shale succession with late Early Silurian graptolites. With these partial ages, and because the Mount Kindle Formation extends basinward from the Franklin Mountain Formation 'shale-out', preliminary correlations with shelf strata can be made. The RRl unit is, entirely or in part, a basinal equivalent of the Mount Kindle Formation; the RRc unit is correlated with part of the Franklin Mountain Formation; the RRal is unassigned; and the RRs is correlated, entirely or in part, with the sub-Franklin Mountain unconformity and the Lower to Middle Cambrian Mount Cap Formation (northeast of the Mackenzie Arch).

The trace of the Franklin Mountain 'shale-out', Road River thicknesses, and paleocurrent trends outline a northwest-trending embayment, the Misty Creek Embayment. During deposition of basin equivalents to the Mount Kindle Formation, the position of the Misty Creek Embayment is shifted to the southwest and northwest.

Road River stratigraphy is complicated by associated basic volcanic rocks within the RRc and RRl units, 1600 m of flysch in a northwest section, and missing units in transitional belts. These and other factors such as basin geometry, extensive slumping and brecciation of the RRl unit suggest probable fault control of the Misty Creek Embayment.

A volcanic centre is situated in the southeastern part of the basin area.

Bedded barite deposits were found in three Road River units of different ages. Galena, sphalerite and pyrobitumen occurrences were observed in transitional sediments, at the edge of the area of basin volcanic rocks.

References

Aitken, J.D., Macqueen, R.W., and Usher, J.L.
1973: Reconnaissance studies of Proterozoic and Cambrian stratigraphy, lower Mackenzie River area (Operation Norman), District of Mackenzie; Geol. Surv. Can., Paper 73-9.

Aitken, J.D. and Cook, D.G.
1974: Geological maps showing bedrock geology of the northern parts of Mount Eduni and Bonnet Plume map-areas, District of Mackenzie, N.W.T.; Geol. Surv. Can., Open File 221.

Blusson, S.L.
1971: Sekwi Mountain map-area, Yukon Territory and District of Mackenzie; Geol. Surv. Can., Paper 71-22.

1974: Five geological maps of the northern Selwyn Basin (Operation Stewart), Yukon Territory and District of Mackenzie, N.W.T. (105N, O; 106A, B, C); Geol. Surv. Can., Open File 205.

Cecile, M.P. and Morrow, D.W.
1978: Note on Lead Zinc mineralization near Palmer Lake (64°28', 129°36'), Mackenzie Mountains, N.W.T.; in Current Research, Part A, Geol. Surv. Can., Paper 78-1A, "Notes".

Dawson, K.M.
1975: Carbonate-hosted zinc-lead deposits of the northern Canadian Cordillera; in Report of Activities, Part A, Geol. Surv. Can., Paper 75-1A, p. 239-243.

Fritz, W.H.
1976: Ten stratigraphic sections from the lower Cambrian Sekwi Formation, Mackenzie Mountains, northwestern Canada; Geol. Surv. Can., Paper 76-22.

Jackson, D.E. and Lenz, A.C.
1962: Zonation of Ordovician and Silurian graptolites of Northern Yukon, Canada; Am. Assoc. Pet. Geol. Bull., v. 46, p. 30-45.

Norford, B.S. and Macqueen, R.W.
1975: Lower Paleozoic Franklin Mountain and Mount Kindle formations, District of Mackenzie: their type sections and regional development; Geol. Surv. Can., Paper 74-34.

Norris, D.K., compiled by
1975: Geological maps of parts of Yukon and Northwest Territories: Hart River, Wind River and Snake River; Geol. Surv. Can., Open File 279.

69.

THE KOOTENAY-NIKANASSIN LITHOSTRATIGRAPHIC TRANSITION, ROCKY MOUNTAIN FOOTHILLS OF WEST-CENTRAL ALBERTA

Project 750018

D.W. Gibson
Institute of Sedimentary and Petroleum Geology, Calgary

Abstract

Gibson, D.W., The Kootenay-Nikanassin lithostratigraphic transition, Rocky Mountain Foothills of west-central Alberta; Current Research, Part A, Geol. Surv. Can., Paper 78-1A, p. 379-381, 1978.

Two poorly exposed but complete sections of the Kootenay and seven sections of the Nikanassin Formation (two complete and five partial) were examined and described in detail between Clearwater River and the Cadomin-Mountain Park area of west-central Alberta. Preliminary results indicate that in the vicinity of North Saskatchewan River, lithostratigraphic facies variations occur progressively from south to north between the two Kootenay Formation sections, and from south to north between the Kootenay sections and those of the Nikanassin Formation. The North Saskatchewan River would serve, therefore, as a distinct east-west geographical boundary in the Rocky Mountain Foothills and Front Ranges, for the nomenclatural transition between the two partly or wholly equivalent formations. Low volatile bituminous coal in seams up to 0.8 m thick was recorded in the Nikanassin Formation at Wapiabi Creek. Northward, in the vicinity of Cadomin and Mountain Park, coal seams are thinner and rarely exceed 0.1 m in thickness. Coal seams were not observed in the two Kootenay sections north of Red Deer River.

Introduction

During 1975 and 1976, a detailed stratigraphical and sedimentological study of the Jura-Cretaceous Kootenay Formation was undertaken by the writer, in the Foothills and Front Ranges of the southern Canadian Rocky Mountains of Alberta and British Columbia (Gibson, 1976a, b). The investigation demonstrated that the three lithostratigraphic units previously recognized by Newmarch (1953) and Jansa (1972) were valid, could be recognized at most localities, and were traced northward from the United States border at least as far as the Red Deer-Clearwater River area of Banff National Park (Fig. 69.1). The three units were informally named, in ascending order, Basal Sandstone member, Coal Bearing member, and Elk member. In 1977, part of the summer field season was spent in examining and describing in detail two complete sections of the Kootenay Formation as well as two complete and five partial sections of the Nikanassin Formation. The Nikanassin is a rock stratigraphic unit recognized in the Front Ranges and Foothills of west-central Alberta, and is considered equivalent or partly equivalent to the Kootenay Formation. The Nikanassin was studied in order to outline any similarities or differences in lithology, coal seam concentration and distribution, flora and fauna, and paleoenvironments between it and the Kootenay Formation. It was anticipated that the study would reveal also whether the three members of the Kootenay Formation could be recognized in the Nikanassin Formation and, accordingly, be extended northward beyond the Red Deer-Clearwater River area. In addition it was hoped that a convenient and practical geographic locality could be found, where the Kootenay nomenclature could be discontinued if necessary, in favour of the long-standing Nikanassin nomenclature used in the Rocky Mountain Foothills and Front Ranges of west-central Alberta. It is with these objectives that the following brief stratigraphic summary is presented. A more comprehensive report on the Kootenay and Nikanassin formations and the lithofacies transition, will be submitted at a later date.

Kootenay Formation

Two complete but poorly exposed sections of interbedded siltstone, sandstone, mudstone and shale of the Kootenay Formation were examined at Cutoff Creek (Sec. 1, Fig. 69.1), a tributary of Clearwater River, and Gap Lake (Sec. 2, Fig. 69.1), a locality south of North Saskatchewan River near Nordegg. The formation attained a thickness of 54 m and 40 m respectively, with only the lower Basal Sandstone, and the middle Coal Bearing members present. The upper Elk member may have been erosionally removed during development of the pre-Cadomin Formation unconformity, or the member may be absent due to a general west to east sedimentary thinning.

The field study revealed that lithostratigraphic facies differences were present between the two localities, particularly within the more resistant sandstone units. For example, at Cutoff Creek the Basal Sandstone member consists of a cliff-forming succession of medium light grey, fine- to coarse-grained, moderately well indurated, quartzose sandstone 22 m thick. At Gap Lake 42 km to the northwest (Fig. 69.1) the Basal Sandstone is still cliff-forming but is finer grained, lighter grey, more siliceous, and consequently better indurated. It is 24 m thick. The overlying Coal Bearing member, because of the high concentration of less well indurated siltstone, mudstone and shale, is poorly exposed at both localities. Very fine- to medium-grained sandstone which is characteristic of the member, protrudes above grass and partially talus covered slopes as resistant units. They follow a grain size and compositional trend similar to that noted in the underlying Basal Sandstone member, becoming finer grained, more siliceous and better indurated toward Nordegg and the North Saskatchewan River area.

Coal is a common and characteristic component of the Coal Bearing member in other areas of southwestern Alberta and southeastern British Columbia; however, it was not observed at either section locality. Because of the many covered intervals in the Coal Bearing member of these two Kootenay sections, one is not certain whether coal is present or not. At Limestone Mountain 14 km southeast of Cutoff Creek (Fig. 69.1) a completely exposed section of the Kootenay Coal Bearing member was examined in 1976. This section does not contain coal and, therefore, the sections along strike at Cutoff Creek and Gap Lake also may be barren of coal.

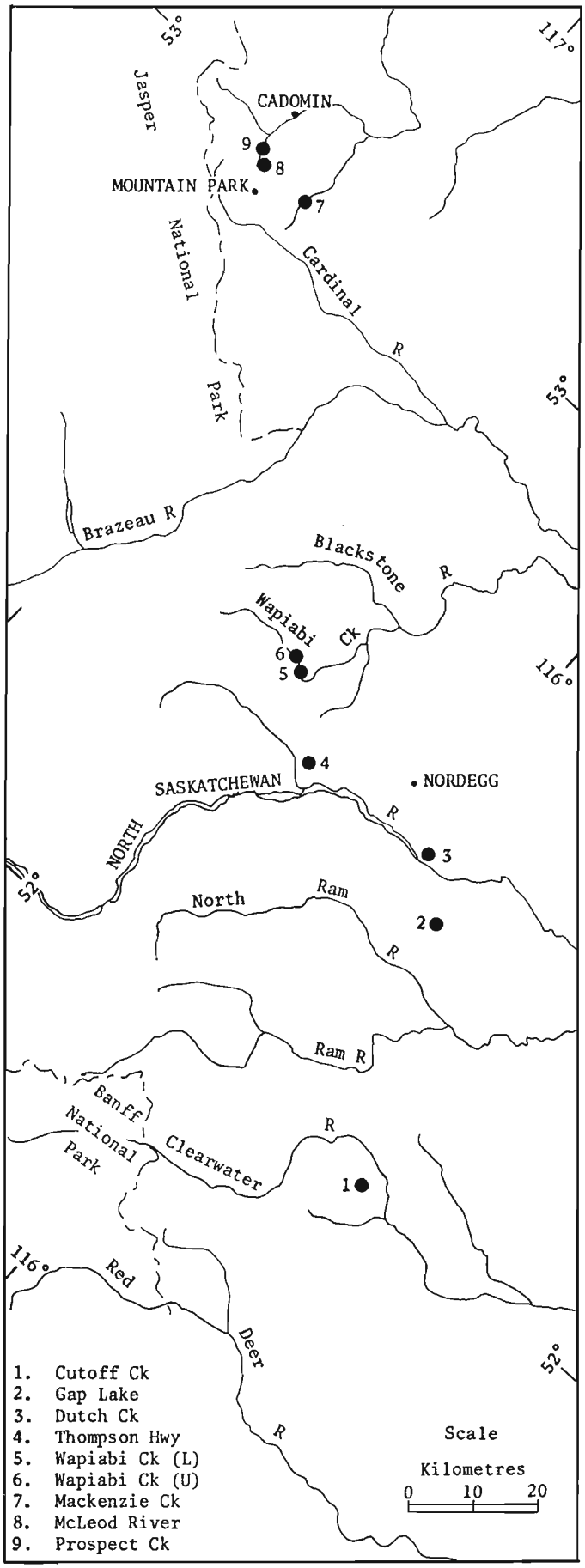

Figure 69.1 Location of measured sections.

The Kootenay Formation is conformably and abruptly underlain by interbedded siltstone, shale and minor sandstone of the "Passage Beds" of the Jurassic Fernie Formation. It is overlain unconformably by sandstone and conglomerate of the Cadomin Formation of the Blairmore Group.

Nikanassin Formation

The Nikanassin Formation in the Cadomin-Nordegg area (Fig. 69.1) comprises an interstratified sequence of medium to dark grey to yellow-brown weathering siltstone, sandstone, mudstone, shale and minor thin seams of coal in the thicker more westerly sections. The formation ranges in measured thickness from a minimum of approximately 53 m at Dutch Creek (section incomplete) near North Saskatchewan River (Sec. 3, Fig. 69.1), to a maximum of 488 m at Mackenzie Creek east of Mountain Park (Sec. 7, Fig. 69.1). The predominant lithology of the formation is the siltstone, which is dark grey, very sandy, carbonaceous-argillaceous, and commonly contains biogenic mottling and small sand-filled burrows. The mudstone and shale are dark grey, carbonaceous and contain a variable concentration of vegetal matter which is confined mainly to the upper half of the formation. Sandstone is common as individual beds and thick units; the former commonly associated with the siltstone as thin to medium beds, or as thin to thick lenticular to wavy laminations. The thicker, isolated sandstone units are of two main types, and in the Cadomin-Nordegg area can be used to subdivide the formation into two poorly defined units. The sandstone in the lower half and lower two thirds of the formation at Wapiabi and Mackenzie creeks respectively comprises fine to very fine grains of quartz and, accordingly, is well indurated. It is atypical of that in the Kootenay to the south of North Saskatchewan River and resembles that in the "Passage Beds" of the Fernie Formation between Nordegg and Cadomin. In contrast, the conspicuous sandstone units comprising the upper part of the Nikanassin are medium grey, commonly coarser grained (ranging from fine to medium grained) and, in places contain intraformational siltstone-shale clasts. These sandstone units closely resemble those of the Kootenay Formation in southwestern Alberta and southeastern British Columbia.

Coal is uncommon in the Nikanassin Formation of the study-area, and like the coarser grained sandstone is confined to the upper half to one third of the formation. For example, at Wapiabi Creek (Fig. 69.1) only two seams 0.8 and 0.7 m thick were encountered. The coal was hard, blocky, and classed as low volatile bituminous. At Mackenzie Creek to the north (Fig. 69.1), the thickest seam recorded was 0.1 m and occurred 178 m below the contact with the Cadomin Formation. Near Mountain Park in a river bank exposure along McLeod River, a thin lenticular seam of coal 0.4 m thick was recorded 9 m below the Cadomin contact.

Unlike the Kootenay Formation, cliff-forming sandstone generally does not form a conspicuous facies at the base of the Nikanassin Formation. It occurs only at localities near Nordegg in the vicinity of North Saskatchewan River. For example, in a highway exposure approximately 16 km west of Nordegg the lower 22 m of the Nikanassin consists of very fine to fine grained, argillaceous sandstone with thin recessive interbeds and partings of black shale and siltstone. The basal sandstone concentration does, however, decrease north and northwestward toward Cadomin and Mountain Park, with interbedded siltstone and shale becoming increasingly more common. At Mackenzie Creek and localities near Cadomin (Fig. 69.1) the base of the Nikanassin consists of a thick succession of interbedded sandstone, siltstone, and shale, similar in appearance to strata of the underlying "Passage Beds" of the Fernie Formation.

The contact of the Nikanassin Formation with the underlying "Passage Beds" of the Fernie Formation is conformable and distinct at some localities, and gradational at others. Where the contact is abrupt, near Nordegg and Wapiabi Creek (Fig. 69.1), it is placed at the first continuous occurrence of sandstone devoid of any interbedded siltstone or silty shale. Where the contact is gradational, as in the Cadomin, Mountain Park and Mackenzie Creek areas, the contact is placed at a point where sandstone forms more than half of the beds within the interbedded sequence of sandstone, siltstone and shale at the base of the Nikanassin and the top of the Fernie formations.

The Nikanassin is erosionally overlain at all observed sections by quartzitic sandstone and conglomerate of the Cadomin Formation.

Kootenay-Nikanassin Nomenclature Transition

From the foregoing brief discussion on lithostratigraphy and facies variations in the Kootenay and Nikanassin formations, it is apparent that, because of the northward change in grain size and composition of the sandstones, the general lack of or poor development of coal seams, and the general absence of the Basal Sandstone member in the Nikanassin Formation, strata of both formations differ from each other in the vicinity of North Saskatchewan River. The stratigraphic differences or facies changes are related probably to a difference in depositional environments. Most strata of the Kootenay Formation south of the river have been interpreted as characteristic of interdeltaic beach-barrier island, deltaic, and alluvial plain depositional environments (Gibson, 1976b). Strata of the Nikanassin Formation are tentatively interpreted as being more typical or characteristic of a lower delta plain or delta front depositional environment. It is evident, therefore, that the North Saskatchewan River could serve as a convenient east-west geographical boundary in the Rocky Mountain Foothills and Front Ranges for the nomenclatural transition between the two formations. Strata south of the river between the Cadomin and Fernie formations would be called the Kootenay Formation, whereas strata north of the river between the same formations would be called the Nikanassin Formation. Prior to the writer's study of the Kootenay and Nikanassin formations, no region or local area had ever been suggested or designated as appropriate for the nomenclatural transition.

References

Gibson, D.W.

1976a: The Kootenay Formation of Alberta and British Columbia - a stratigraphic summary; in Report of Activities, Part A, Geol. Surv. Can., Paper 77-1A, p. 95-97.

1976b: Sedimentary facies in the Jura-Cretaceous Kootenay Formation Crowsnest Pass area, southwestern Alberta and southeastern British Columbia; Bull. Can. Soc. Pet. Geol., v. 25, no. 4, p. 767-791.

Jansa, L.

1972: Depositional history of the coal bearing Upper Jurassic-Lower Cretaceous Kootenay Formation, southern Rocky Mountains, Canada; Geol. Soc. Am. Bull., v. 83, p. 3199-3222.

Newmarch, C.B.

1953: Geology of the Crowsnest coal basin, with special reference to the Fernie area; B.C. Dep. Mines, Bull. No. 38.

70. TWITYA UPLIFT: A PRE-DELORME PHASE OF THE MACKENZIE ARCH

Project 670068

Donald G. Cook and James D. Aitken
Institute of Sedimentary and Petroleum Geology, Calgary

Abstract

Cook, Donald G. and Aitken, James D., Twitya Uplift: A pre-Delorme phase of the Mackenzie Arch, Current Research, Part A, Geol. Surv. Can., Paper 78-1A, p. 383-388, 1978.

Pre-Delorme Formation (pre-Late Silurian) uplift and resultant erosion of Mount Kindle and Franklin Mountain formations occurred along a tectonic arch herein named the Twitya Uplift. The arch is marked by a pre-Delorme paleo-inlier of Precambrian and Lower Cambrian rocks surrounded by strata of the Franklin Mountain Formation. Within the inlier strata initially unconformably overlain by Upper Cambrian basal beds of the Franklin Mountain Formation are today unconformably overlain by the Upper Silurian to Lower Devonian Delorme Formation.

The arch is at least 100 km long and 40 km wide where it is defined in Mount Eduni map-area (106A). It may extend another 200 km to the southeast along the Plateau Thrust plate into Glacier Lake map-area (95M), but its actual extent southeast of Mount Eduni map-area cannot be determined because the Delorme and younger formations are missing in the critical area due to Pleistocene and Recent erosion.

Twitya Uplift can be considered a pre-Late Silurian phase of Mackenzie Arch.

Over most of the Mackenzie Mountains the Upper Silurian to Lower Devonian Delorme Formation overlies the Mount Kindle Formation or its equivalent the Whittaker Formation (see Aitken and Cook, 1974b; Aitken, Cook and Yorath, in press; Blusson, 1971, 1974; Gabrielse, Blusson and Roddick, 1973). In Mount Eduni map-area (106A), however, a pre-Delorme (pre-Late Silurian) arch, herein named the Twitya Uplift, can be delineated whereon Delorme Formation rocks unconformably overlie strata older than Mount Kindle Formation over an area that is at least 100 km long and 40 km wide. The writers (Cook and Aitken, 1971) first described the uplift as a pre-Devonian feature which they considered to be a northern extension of the Redstone Arch described by Gabrielse (1967). In a later paper on the geology of Carcajou Canyon map-area (96D) the writers (Aitken and Cook, 1976) again referred to the anomalous unconformable relationships in the adjacent Mount Eduni map-area. In a brief discussion they raised two possibilities: one, that abrupt changes in stratigraphic position of the base of the Delorme Formation from one side of a fault to another could be explained by tectonic juxtaposition of different parts of an erosional bevelled succession overlain by Delorme Formation, or two, that the abrupt changes across fault traces were due to pre-Delorme faulting and erosional truncation of the fault blocks. The analysis presented here strongly supports a model of gentle epeirogenic uplift and erosion across a belt which subsequently was severely compressed and horizontally shortened during Laramide deformation. The possibility of significant Pre-Delorme faulting is virtually eliminated.

The sub-Delorme (pre-Late Silurian) unconformity (see Fig. 70.1) cuts, in a short distance, from rocks as young as the Late Ordovician to Early Silurian Mount Kindle Formation to rocks as old as the Helikian(?) rusty shale subunit of Aitken (1977). Consequently, an erroneous first impression gained in the field is that great localized uplift accompanied by deep erosion occurred in pre-Delorme time. If, however, the sub-Delorme unconformity is considered in conjunction with the sub-Franklin Mountain Formation (pre-Late Cambrian) unconformity (Fig. 70.2) it becomes apparent that the "deep" erosion is, in fact, due simply to removal of Mount Kindle and Franklin Mountain formations with resultant exhumation of the sub-Franklin Mountain sequence in a paleo-inlier surrounded by Mount Kindle and Franklin Mountain formations.

Stratigraphy

Stratigraphy used here is summarized in Table 70.1, and is essentially that of Aitken and Cook (1974a) with additional subdivisions within map-unit H5 resulting from recent studies by Aitken (1977), and Aitken et al. (1978).

Some additional information on the Delorme Formation is perhaps justified. In Mount Eduni map-area a tripartite subdivision is recognized. Basal beds of thin and medium bedded sandy and silty dolomite locally grading to dolomitic sandstone and siltstone grade upward to a middle subdivision of pale grey, commonly laminated, medium and thick bedded micro-crystalline dolomite. This grades, in turn, to an upper subdivision which is sandy and silty dolomite much like the basal beds. The Delorme thins northeastward to where it has been included for mapping purposes in the Arnica and Bear Rock formations by Aitken and Cook (1974a).

At the present level of reconnaissance study, the Twitya Uplift does not appear to have affected sedimentary facies in the Delorme. This suggests that the uplift was almost completely peneplained so that essentially no topographic high existed at the time the Delorme was being deposited. Detailed studies of the Delorme and younger formations currently being carried out by D.W. Morrow of the Geological Survey of Canada should shed light on the facies effects, if any, resulting from the existence of the uplift.

Twitya Uplift

Twitya Uplift is illustrated best by a Delorme Formation subcrop map of Mount Eduni map-area (Fig. 70.1). In the area of the uplift both the Mount Kindle and the Franklin Mountain formations have been removed by erosion in pre-Delorme time to form a paleo-inlier of Precambrian and Lower Cambrian formations surrounded by Upper Cambrian Franklin Mountain Formation. Within the inlier the Delorme overlies a southwestward-dipping wedge of strata with formations as old as Helikian rusty shale subunit and as young as Lower Cambrian Sekwi Formation. Because the subcrop map (Fig. 70.1) has not been palinspastically corrected, stratigraphic contacts are closely spaced along the northeastern side of the uplift where they have been "telescoped" by displacement on the Plateau and related thrusts.

An understanding of the uplift is facilitated by considering another subcrop map, that of the Franklin Mountain Formation (Fig. 70.2). Because Mount Eduni map-area lies entirely on the southwest flank of Mackenzie Arch as it existed during the Early and Middle Cambrian (see Fig. 70.3); the Upper Cambrian basal Franklin Mountain Formation overlies successively younger strata southwestward (Fig. 70.2), from Helikian(?) upper part of the Katherine Group in the northeast corner of the map-area to the Lower Cambrian Sekwi Formation in the southwest part of the map-area. Again, because the map has not been palinspastically adjusted the contacts are spaced closely near Plateau Thrust due to "telescoping" by younger displacements.

In the area of the paleo-inlier along Twitya Uplift the pre-Franklin Mountain geology is unknown, and the pre-Delorme configuration is shown instead. Significantly, the pre-Franklin Mountain trends are not greatly different from the pre-Delorme trends. Clearly, the younger phase of erosion did not greatly modify the distribution of pre-Franklin Mountain stratigraphic units. This leads to the important conclusion that pre-Delorme erosion removed very little more than the Mount Kindle and the Franklin Mountain formations and essentially exhumed the old unconformity. Needless to say some erosion of the older units had to occur in the area of the inlier, and the localized erosion to the level of the rusty shale subunit may well have occurred at that time.

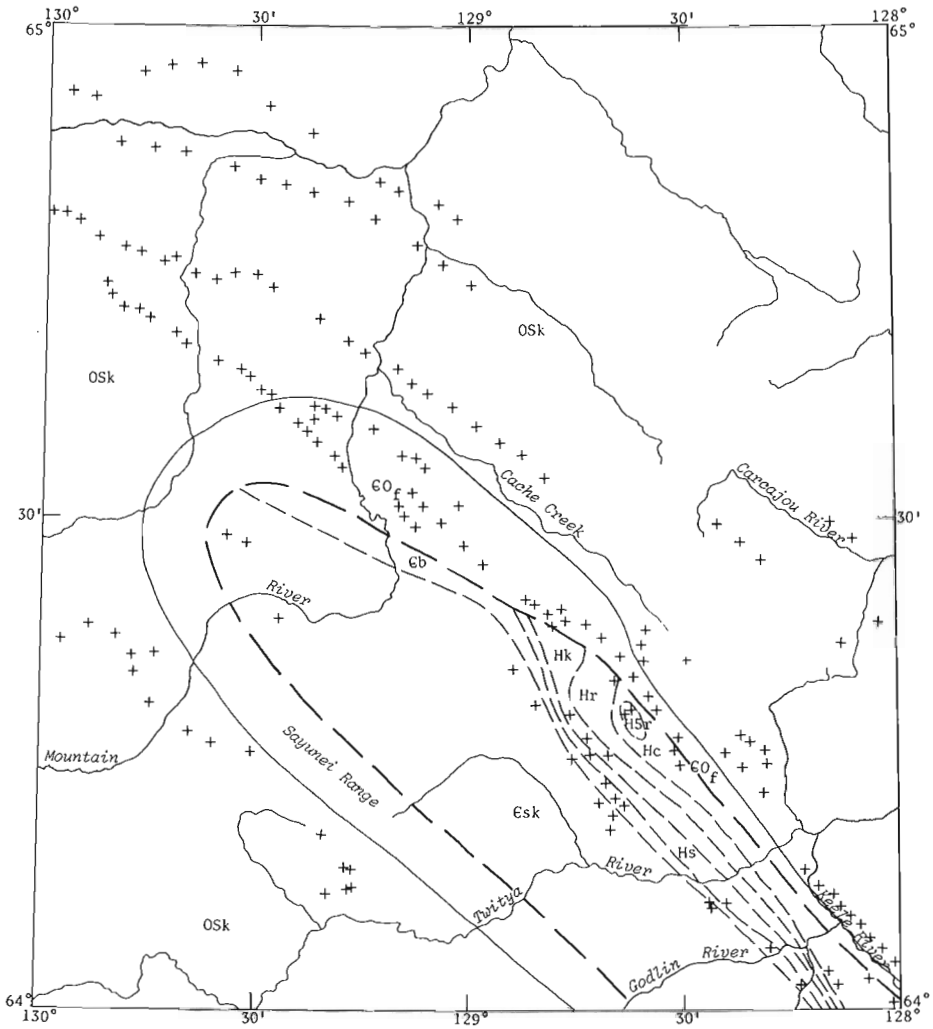

Figure 70.1. The Twitya Arch as outlined by Delorme Formation subcrop.

Southeastward Extent of Twitya Uplift

The uplift must extend to the southeast into Sekwi Mountain (105P) and Wrigley Lake (95L) map-areas, but cannot be outlined precisely there because Devonian rocks are missing due to Pleistocene and Recent erosion in the critical area (see maps of Blusson, 1971; Gabrielse et al., 1973). Where it occurs to the southeast, the Delorme Formation invariably overlies the Upper Ordovician and Lower Silurian Whittaker Formation (equivalent of Mount Kindle), but present-day distribution of Whittaker and Delorme (Fig. 70.3) permits extrapolation of Twitya Uplift for some 200 km southeastward from the south boundary of Mount Eduni map-area, and well into Glacier Lake map-area (95L). Present distribution of Lower, Middle, and Upper Cambrian strata, however, (Fig. 70.3) suggests that the uplift may not extend more than 100 km into Wrigley Lake map-area. It may be that the uplift did extend along the back of the Plateau Thrust Plate (see Fig. 70.3). If so, the presence of the epeirogenic arch may have localized the initiation of Plateau Thrust. Conversely, of course, the uplift could be interpreted to nose out abruptly, only a few kilometres south of Mount Eduni map-area.

Relationship of Twitya Uplift to Mackenzie Arch

Gabrielse (1967) outlined the Redstone Arch (see Fig. 70.3), a positive tectonic element which intermittently affected sedimentation from Late Proterozoic to Middle Devonian time. The name "Redstone Arch" appears to have been superseded by the name "Mackenzie Arch" used by Douglas et al. (1970) apparently as a blanket term for a broad, arcuate, generally positive belt, the axis of which was intermittently emergent and shifted basinward or shoreward and longitudinally along the belt from period to period. Mackenzie Arch, then, is a composite feature comprising a family of related but temporally separate uplifts including Redstone Arch. In that context Twitya Uplift marks the pre-Late Silurian axis of Mackenzie Arch (note the near coincidence of the uplift with Gabrielse's Redstone Arch on Fig. 70.3). However, because it is reasonably well defined geographically and temporally, the writers feel that the pre-Late Silurian uplift warrants an individual name, i.e. Twitya Uplift, rather than the more general name, Mackenzie Arch.

Pre-Franklin Mountain(?) Faults

The construction of the Franklin Mountain subcrop map (Fig. 70.2) contributes further to our understanding of a set of antecedent faults described by Aitken and Cook (1974c). The abrupt changes in Franklin Mountain stratigraphy across individual faults recognized by Aitken and Cook are more clearly documented in the subcrop map.

Laramide rejuvenation of these faults resulted in consistently right-lateral movements (see Aitken and Cook, 1974c), and no attempt has been made in Figure 70.2 to remove the effects of those displacements. In spite of that, or perhaps because of it the offsets of pre-Franklin Mountain markers is inconsistent in sense.

In this map, no clear pattern of fault displacement is apparent, however, the offsets mapped generally are consistent with an interpretation of the faults as normal faults.

Legend for
Figure 70.1 and Figure 70.2

ORDOVICIAN AND SILURIAN
UPPER ORDOVICIAN AND LOWER SILURIAN

OSk MOUNT KINDLE FORMATION

CAMBRIAN AND ORDOVICIAN
UPPER CAMBRIAN AND LOWER ORDOVICIAN

COf FRANKLIN MOUNTAIN FORMATION

CAMBRIAN
LOWER CAMBRIAN

Csk SEKWI FORMATION

Cb BACKBONE RANGES FORMATION

PROTEROZOIC
HADRYNIAN(?)

Hs SHEEPBED FORMATION

Hk KEELE FORMATION

Hr RAPITAN GROUP

HELIKIAN(?)

Hc UPPER CARBONATE (Note 1)

MAP-UNIT H5

H5r RUSTY SHALE SUBUNIT (Note 2)

H5g GYPSUM SUBUNIT (Note 2)

H5gr GRAINSTONE SUBUNIT (Note 2)

H5b MUD-CRACKED SUBUNIT and
BASINAL SEQUENCE undivided (Note 2)

Hku KATHERINE GROUP, upper division

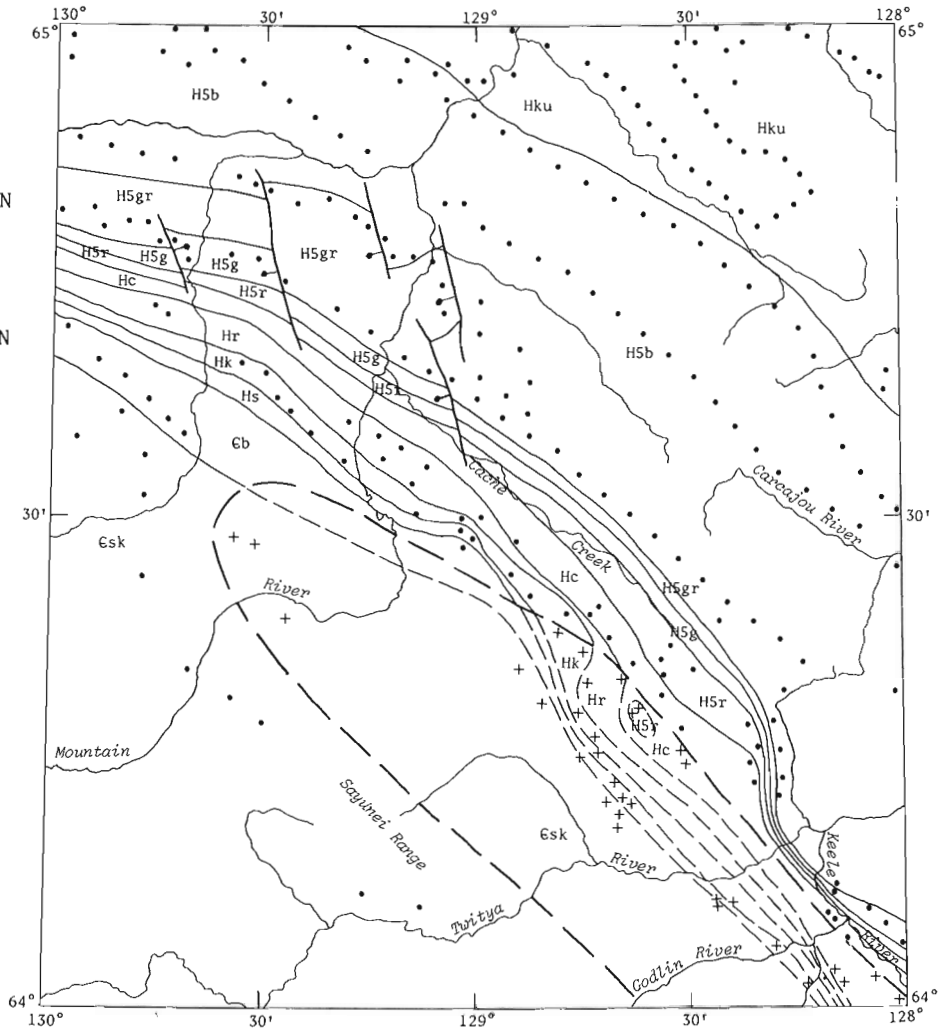

Figure 70.2. Franklin Mountain Formation subcrop map including Delorme Formation subcrop where Franklin Mountain Formation is absent.

LITTLE DAL GROUP
(see Aitken et al., this publication)

Note 1. Mapped as Little Dal Formation by Aitken and Cook, 1974, includes Redstone and Coppercap Formations.

Note 2. Subdivisions of map-unit H5 follow Aitken, 1977.

Sub-Franklin Mountain Formation geological contact

Sub-Delorme Formation geological contact

Pre-Franklin Mountain Fault (solid circle on apparent downthrown side)

Locality at which Franklin Mountain Formation overlies indicated older strata

Locality at which Delorme Formation overlies indicated older strata

Sub-Delorme zero-edge of Franklin Mountain Formation

Table 70.1. Table of Formations

ERA	PERIOD OR EPOCH		FORMATION AND MAXIMUM THICKNESS, in metres	LITHOLOGY
PALEOZOIC	SILURIAN	L	*DELORME FORMATION 270*	Dolomite, partly sandy, silty, argillaceous; marine
		U		
			Unconformity	
	ORDOVICIAN	L	*MOUNT KINDLE FM 310*	Dolomite, fossiliferous, siliceous; minor chert; marine
		U		
			Unconformity	
		LOWER	*FRANKLIN MOUNTAIN FORMATION AND ROAD RIVER FORMATION 460*	Basal red beds of sandstone, red shale, conglomerate overlain by very finely crystalline dolomite, finely- to medium crystalline dolomite, partly stromatolitic; marine Changes south westward to Road River Formation: black shale, limestone, dolomite, minor sandstone; marine; includes Middle Cambrian rocks to southwest
	CAMBRIAN	UPPER		
			Unconformity	
		LOWER	*SEKWI FORMATION 790*	Dolomite and limestone, partly argillaceous and sandy, minor shale and sandstone; marine
			Conformable Contact	
			BACKBONE RANGES FORMATION 800	Sandstone and quartzite, minor dolomite and shale; mainly marine
			Unconformity	
PROTEROZOIC	HADRYNIAN(?)		*SHEEPBED FORMATION 1010*	Shale, brown, dark grey; minor siltstone; dolomite local at top; marine
			KEELE FORMATION 510	Dolomite, limestone, quartzite, shale, conglomerate; marine (?)
			RAPITAN GROUP 1910	Upper Division: Argillite, siltstone, sandstone, minor conglomerate, pebbly mudstone, limestone at base Middle Division: Diamictite; dolomite-clast conglomerate; limestone; marine and(?) nonmarine Lower Division: Conglomerate, pebbly mudstone, red argillite, sandstone; marine and(?) nonmarine

Table 70.1 (cont'd)

ERA	PERIOD OR EPOCH	FORMATION AND MAXIMUM THICKNESS, in metres			LITHOLOGY
PROTEROZOIC		Unconformity			
	HELIKIAN (?)	*LITTLE DAL GROUP*		*Upper Carbonate* 700±	Dolomite and limestone, partly sandy, silty, and argillaceous; minor shale; marine
				Conformable Contact	
			Map-Unit H5	*Rusty shale subunit* 230	Shale, greenish grey, with purple intervals; dolomite; sandstone; rusty weathering overall; marine
				Conformable Contact	
				Gypsum subunit 530	Gypsum, white with red intervals minor gypsiferous shale
				Conformable Contact	
				Grainstone subunit 270	Dolomite, oolitic, cryptalgal, molar tooth, minor chert; platy to flaggy dolomite at top
				Conformable Contact	
				Basinal sequence 400	Shale, red, olive, grey, with limestone nodules, alternating with intervals of limestone-shale rhythmite; stromatolitic reefs
				Conformable Contact	
				Mudcracked subunit 60	Shale, dark-grey, red; sandstone, mainly thin-bedded; mudcracks, prominent ripple marks
		Conformable Contact			
		KATHERINE GROUP	*Upper division*	*Upper quartzite subunit* 430	Sandstone, quartzose, mostly thin-bedded
				Conformable Contact	
				Lower subunit 240	Shale, dark grey; minor quartzite; orange stromatolitic dolomite

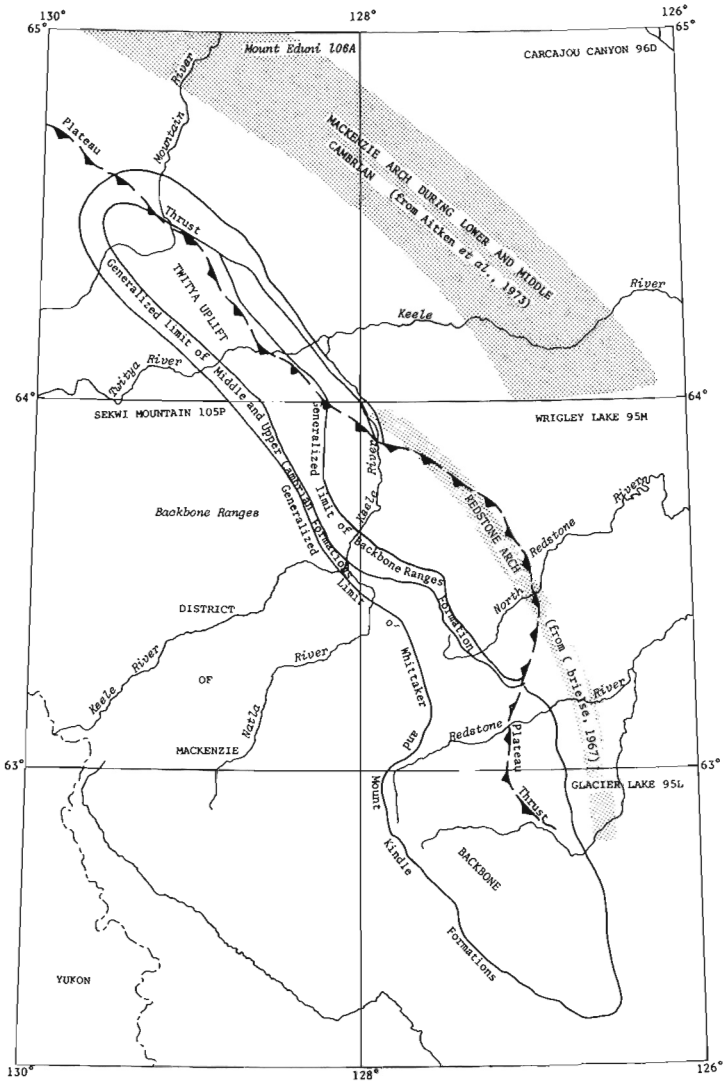

Figure 70.3. Potential limit of Twitya Uplift. The uplift is well defined in Mount Eduni map-area where Delorme Formation unconformably overlies older strata. To the southeast in the hanging wall of plateau thrust, Delorme and younger rocks have been eroded away by modern erosion. The generalized present-day zero-edges of selected units outline the potential area within which the arch could be extrapolated southeastward.

References

Aitken, J.D.
1977: New data on correlation of the Little Dal Formation and revision of Proterozoic map-unit H5; in Report of Activities, Part A, Geol. Surv. Can., Paper 77-1A, Rep. 26.

Aitken, J.D. and Cook, D.G.
1974a: Geology of parts of Mount Eduni (106A) and Bonnet Plume Lake map-areas, District of Mackenzie; Geol. Surv. Can., Open File 221.

1974b: Carcajou Canyon map-area (96D), District of Mackenzie, Northwest Territories; Geol. Surv. Can., Paper 74-13.

1974c: Effect of Antecedent faults on "Laramide" structure, Mackenzie Arc; in Report of Activities, Part B, Geol. Surv. Can., Paper 74-1B, Rep. 100.

Aitken, J.D., Cook, D.G., and Yorath, C.J.
Upper Ramparts River (106G) and Sans Sault Rapids (106H) map-areas, District of Mackenzie; Geol. Surv. Can., Mem. 388. (in press).

Aitken, J.D., Long, D.G.F., and Semikhatov, M.A.
1978: Progress in Helikian Stratigraphy, Mackenzie Mountains; in Current Research, Part A, Geol. Surv. Can., Paper 78-1A.

Aitken, J.D., Macqueen, R.W., and Usher, J.L.
1973: Reconnaissance studies of Proterozoic and Cambrian stratigraphy, lower Mackenzie River area (Operation Norman), District of Mackenzie; Geol. Surv. Can.,Paper 73-9.

Blusson, S.L.
1971: Sekwi Mountain map-area, Yukon Territory and District of Mackenzie; Geol. Surv. Can., Paper 71-22.

1974: Preliminary drafts of five geological maps, with legend, resulting from Operation Stewart (northern Selwyn Basin), Yukon Territory (106A, B, C; 105N, O); Geol. Surv. Can., Open File 205.

Cook, D.G. and Aitken, J.D.
1971: Operation Norman, District of Mackenzie; in Report of Activities, Part A, Geol. Surv. Can., Paper 71-1A, Rep. 119.

Douglas, R.J.W., Gabrielse, H., Wheeler, J.O., Stott, D.F., and Belyea, H.R.
1970: Geology of Western Canada; Geology and Economic Minerals of Canada, Ec. Geol. Rep. No. 1; Geol. Surv. Can., Chapter VIII, p. 365-488.

Gabrielse, H.
1967: Tectonic Evolution of the Northern Canadian Cordillera; Can. J. Earth Sci., v. 4, p. 271-298.

Gabrielse, H., Blusson, S.L., and Roddick, J.A.
1973: Flat River, Glacier Lake, and Wrigley Lake map-areas (95E, L, M), District of Mackenzie and Yukon Territory; Geol. Surv. Can., Mem. 366.

A NEW OSTRACODE GENUS FROM UPPER PERMIAN ROCKS IN ARCTIC CANADA

Project 680064

H. Kozur[1] and W.W. Nassichuk
Institute of Sedimentary and Petroleum Geology, Calgary

Abstract

Kozur, H. and Nassichuk, W.W., A new ostracode genus from Upper Permian Rocks in Arctic Canada; Current Research, Part A, Geol. Surv. Can., Paper 78-1A, p. 389-392, 1978.

***Boreokirkbya oertlii** n. gen., n. sp. from the Upper Permian Trold Fiord Formation in northern Ellesmere Island is the first Permian ostracode to be described from Arctic Canada. The Trold Fiord Formation on Ellesmere Island has been dated as early Kazanian (Wordian) mainly on the basis of boreal brachiopod assemblages. **Boreokirkbya oertlii** shows affinities with tethyan species and may refine currently ambiguous Upper Permian biostratigraphic relationships between Tethyan and Boreal realms. Mandibular and antennal muscle scars and shell morphology of **Boreokirkbya** indicate that the Kirkbyocopina belongs in the Podocopida.*

Introduction

Euryhaline ostracodes are distributed widely in all Permian stages in the Soviet Union and have been employed with particular success, along with certain groups of "small" foraminifers, to subdivide and correlate the Kungurian and Kazanian stages. The latter stages are characterized by lagoonal and marine sediments, evaporites and terrestrial-lagoonal beds; faunas indicative of "normal" marine environments are relatively rare. In North America, however, ostracodes have been employed only secondarily for marine biostratigraphy but hopefully their importance and the importance of other little studied groups such as calcareous foraminifers and conodonts will increase as Permian biostratigraphy becomes increasingly refined. Ostracodes are known to occur only sporadically in most marine Permian rock successions in Arctic Canada and none have been described previously. This paper describes the new kirkbyid genus **Boreokirkbya** which is associated with Boreal faunal elements in the Trold Fiord Formation on Ellesmere Island. The genus is important from a morphological point of view because it displays mandibular and antennal muscle scars which support the view that the suborder Kirkbyocopina does indeed belong in the Order Podocopida as was suggested by Kozur (1972a). Additionally, however, **Boreokirkbya** seems to be related to ostracodes of the Tethyan realm and may ultimately throw new light on currently ambiguous relationships between Upper Permian strata in 'tethyan' and 'boreal' regions.

Stratigraphy and Faunas

The Trold Fiord Formation was defined by Thorsteinsson (1974) as a succession of sandstone, conglomerate and minor limestone deposited rather widely in eastern, southern and northern parts of the Sverdup Basin. The type section (195 m thick) is on the north side of the Cañon Fiord, northern Ellesmere Island (Thorsteinsson and Tozer, 1971). The formation attains a maximum thickness of about 400 m in the "Sawtooth Mountains" of western Ellesmere Island, approximately 48 km southwest of the type section. The Trold Fiord Formation is equivalent to the Degerböls Formation, a succession of carbonate rocks in interior regions of the Sverdrup Basin. It is equivalent also to the Tahkandit Formation in Alaska and the Ogilvie Mountains area of the Yukon, and to an unnamed unit of clastic rocks in the Richardson Mountains farther north in the Yukon (Bamber and Waterhouse, 1971).

The ostracode described in this report, **Boreokirkbya oertlii,** was found near the middle of the Trold Fiord Formation, 0.2 km along strike to the north of the type section (Fig. 71.1). There, the formation is 102 m thick. It rests conformably on calcareous sandstones of the Roadian Assistance Formation and is, in turn, overlain by sandstones of the Lower Triassic Bjorne Formation. The Trold Fiord

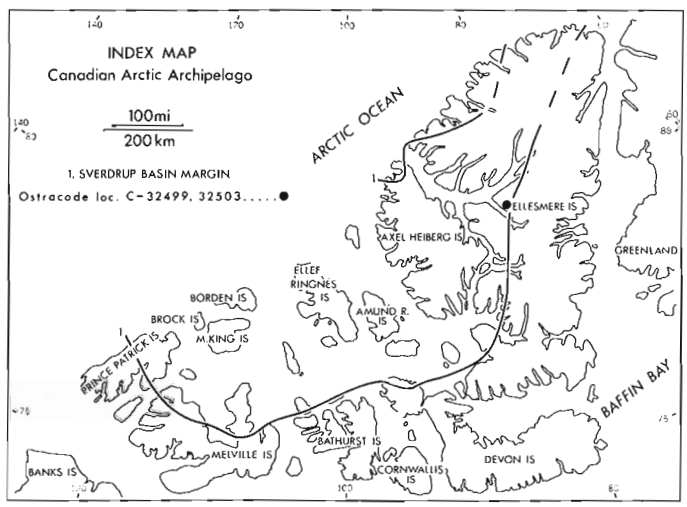

Figure 71.1 Index map showing ostracod occurrences at GSC localities C-32499 and C-32503 in the Upper Permian Trold Fiord Formation.

Formation forms a rather prominent cuesta in the type area and its greenish weathering character is in sharp contrast with yellow- and red-weathering, relatively more resistant sandstone of the overlying Bjorne Formation. The Trold Fiord is composed mainly of fine grained, glauconitic, calcareous sandstones that are thinly bedded with irregular, 'wavy' bedding planes; fine grained chert-pebble conglomerates occur at four levels and minor siltstone and sandy limestone beds occur throughout the formation. Near the middle of the formation, some sandstone beds, which probably are channel deposits, are lenticular, cross-bedded and extensively burrowed. On a regional scale, the Trold Fiord Formation clearly reflects an interval of transgression; progressively older beds are overstepped shoreward. Recurring conglomerates in the type area probably reflect episodes of more rapid transgression rather than local uplift. In terms of a biologically oriented depositional model proposed by Kozur (1972b), deposition probably occurred in water of fluctuating salinity between depths of 10 and 30 m with a moderate to high level of wave energy.

Brachiopods as well as fenestrate and ramose bryozoans occur abundantly throughout the Trold Fiord Formation in the type area; ammonoids, gastropods, pelecypods and solitary corals are relatively rare. Ostracodes described in this report were recovered from residues from glauconitic sandy limestones dissolved in acetic acid. Most specimens are preserved as fragmentary glauconitic steinkerns which are, for the most part, unidentifiable, but a few that are better preserved by

[1] Democratic Republic Germany, Meiningen, Staatliche Museen.

dolomitization and silicification are identified herein as a new kirkbyid, **Boreokirkbya oertlii** n. gen., n. sp. This, and other unidentified ostracode species are associated with a diverse fauna of calcareous and agglutinated foraminifers, bryozoans and minute, immature gastropods and brachiopods. Representatives of the latter three groups are silicified but foraminifers are preserved as steinkerns. Scales of bony fish and sharks are present also.

Fossils in the Assistance Formation beneath the Trold Fiord Formation north of Cañon Fiord indicate a Roadian age. The ammonoid **Daubichites fortieri** (Harker), which has its type locality in the type section of the Assistance Formation on Devon Island, was identified by Nassichuk (1975) from 43 m above the base of the Assistance directly beneath the type section of the Trold Fiord Formation. Conodonts recovered from this same horizon were identified by Kozur and Nassichuk (1977) as **Gondolella idahoensis** Youngquist, Hawley and Miller and an unnamed species intermediate between **G. idahoensis** and **G. nankingensis** Cheng. Kozur and Nassichuk (ibid.) indicated a late Roadian age; that is latest Chihsian to early Kubergandinian in the Tethyan scale.

The age of the Trold Fiord Formation in the Sverdrup Basin was summarized by Thorsteinsson (1974), who cited brachiopod data provided by R.E. Grant and J.B. Waterhouse, coral data by E.W. Bamber and ammonoid data from Nassichuk et al. (1966) to conclude that the formation is of Guadalupian (Wordian, Capitanian undiferrentiated) age. Waterhouse (1976) suggested that brachiopod data from the Trold Fiord throughout the basin indicated the presence of a single zone of early Kazanian (Wordian) age. Waterhouse (in Thorsteinsson, 1974) identified the following brachiopods collected between 18 and 30 m above the base of the type section:

Thamnosia (Thuleproductus) n. sp. A

Spiriferella sp.

?Kuvelousia sphiva Waterhouse

Neospirifer cf. **N. striatoparadoxus** (Toula)

The following, considerably more diversified brachiopod fauna was identified by Waterhouse (pers. comm., 1971) from near the base of the Trold Fiord Formation nearly 5 km north of the type section.

Streptorhynchus kempei Anderson

Waagenoconcha wimani Fredericks

Kuvelousia sphiva Waterhouse

Thamnosia sp.

Yakovlevia greenlandica (Dunbar)

Stenoscisma spitzbergiana (Stepanov)

Pterospirifer alatus (Sowerby)

Spiriferella keilhavii (von Buch)

Neospirifer striatoparadoxus (Toula)

The Trold Fiord ostracode fauna is clearly younger than Roadian ostracode faunas described from Texas by Sohn (1954). It resembles ostracode faunas from the upper Kazanian of the northern Russian Platform and from the lower Zechstein of Germany. Foraminifers in the Trold Fiord appear to indicate close affinities with post-Wordian that is, Capitanian or younger species in Tethyan regions of Germany, Hungary (Bükk Mountains), Yugoslavia and elsewhere. Thus, it is clear that additional studies of foraminifers, ostracodes and also conodonts are required to clarify relationships between the Trold Fiord Formation and sequences in the Urals established largely on the basis of boreal brachiopod assemblages.

Systematic paleontology

Subclass OSTRACODA Latreille, 1806

Superorder PODOCOPAMORPHES Kozur, 1972

Order PODOCOPIDA Sars, 1866

Suborder KIRKBYOCOPINA Gründel, 1969 emend. Kozur, 1972

Remarks

Kozur (1972a) tentatively assigned the Kirkbyocopina to the Podocopida. This assignment was made on the basis of muscle scars in **Scrobicula scrobiculata** Jones, Kirkby and Brady, 1884 as described by Gramm and Pösner (1972). Those scars, which include adductor muscle and numerous related secondary scars as well as antennal scars, showed that **Scrobicula** clearly is related to the Podocopida. **Scrobicula,** however, had only been assigned tentatively to the Kirkbyocopina and so relationships between the Kirkbyocopina and the Podocopida were known to be speculative. The presence of mandibular and antennal muscle scars and the shell morphology of **Boreokirkbya,** which has all the characteristics of a kirkbyacean ostracode, supports assignment of the Kirkbyocopina to the Podocopida.

Superfamily KIRKBYACEA Ulrich and Bassler, 1906

Family KIRKBYIDAE Ulrich and Bassler, 1906

Genus **Boreokirkbya** n. gen.

Type species

Boreokirkbya oertlii n. sp.

Diagnosis

Large. Carapace elongate rectangular. End margins almost equally round. One broad marginal rim; sometimes a second smaller marginal ridge is developed. Large smooth kirkbyan pit in the midlength. Reticulations of the lateral surface slight; small tubercles present. Rim and ventral surface smooth. Hinge consists of a terminal expanded groove in the left valve and a corresponding ridge and cardinal teeth in the right valve. Mandibular and antennal scars present.

Distribution

Trold Fiord Formation, Arctic Canada.

Included species

Boreokirkbya oertlii n. sp. and **Boreokirkbya** n. sp.

Discussion

Kirkbya Jones, 1859 has an acute posterior cardinal angle and a proportionately smaller kirkbyan pit. **Knightina** Kellett, 1933 has no terminal teeth. **Knightina? cuestaforma** Sohn, 1954, is similar to the new genus, but possesses 3 marginal ridges, the innermost of which consists of a row of hollow tubes.

Boreokirkbya oertlii n. sp.

Plate 71.1, figures 1-4

Derivatio nominis

In honour of Dr. H.J. Oertli, Pau.

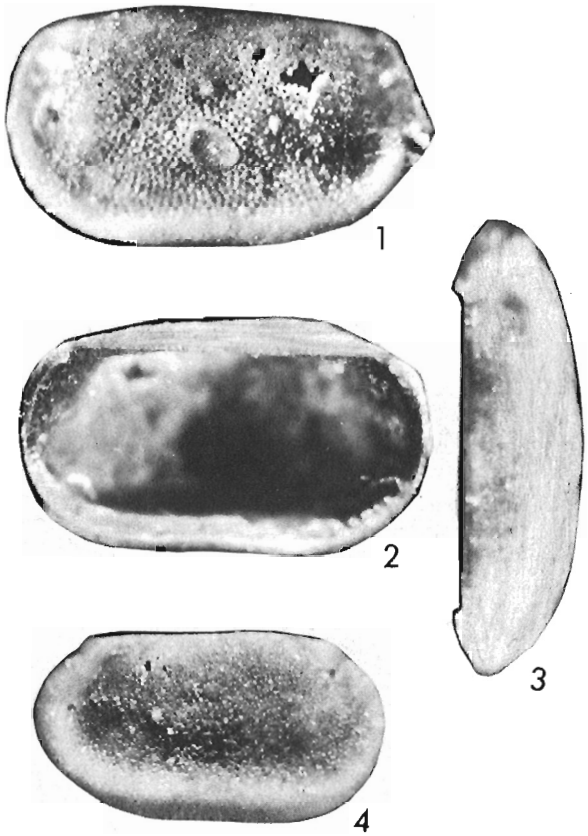

Figures

1. external view of right valve of holotype, GSC 53138, x20.
2. internal view of right valve of holotype, x20.
3. upper view of right valve of holotype, x20.
4. external view of left valve of paratype, GSC 53139, x20.

Plate 71.1 **Boreokirkbya oertlii** n. gen., n. sp. from the Trold Fiord Formation on northern Ellesmere Island (GSC loc. C-32499).

Description

Carapace large, elongate and rectangular in lateral view. Greatest length at mid-height. Dorsal margin straight. End margins almost equally rounded or anterior margin somewhat more broadly rounded. Ventral lateral view straight or slightly concave, ventral margin concave. Broad dorsal area. Posterior slope of shoulder rather steep. Anterior and ventral slopes of shoulder vary somewhat with individuals, but are always considerably less steep than the posterior slope. Lateral surface with small reticulations. Kirkbyan pit large, somewhat rimmed, shallow, reflected on inside of valve as smooth knob. Two small tubercles are situated anterior to the kirkbyan pit. Marginal rim broad and shallow, smooth. Ventral surface also smooth to very faintly pitted. Hinge as for the genus. Groove and corresponding ridge seem to be crenulated, but the state of preservation does not allow a precise description of this crenulation. At the adductor muscle scar, situated in the kirkbyan pit, as well as at the mandibular and antennal muscle scars, secondary scars cannot generally be observed clearly. The mandibular scar, however, probably consists of more than one secondary scar.

Comparisons

A second species, which we have not described because of the fragmentary nature of specimens but which we have designated **Boreokirkbya** n. sp., occurs in association with **Boreokirkbya oertlii**. **Boreokirkbya** n. sp. differs from **B. oertlii** in that the former has a smaller but higher marginal rim and a distinct second marginal ridge between the marginal rim and the margin.

Occurrence

The type locality of **Boreokirkbya oertlii**, GSC locality C-32499, is 43.5 m above the base of the Trold Fiord Formation, north of the Cañon Fiord, northern Ellesmere Island (Lat. 80°43'N, Long. 85°40'W; Textfig. 1). The species is also known to occur slightly higher in the same section in GSC locality C-32503, 49.5 m above the base of the Trold Fiord.

Type specimen

Holotype GSC 53138 and paratype GSC 53139.

References

Bamber, E.W. and Waterhouse, J.B.

1971: Carboniferous and Permian stratigraphy and paleontology, northern Yukon Territory; Bull. Can. Pet. Geol., v. 19, p. 29-250.

Gramm, M.N. and Posner, V.M.

1972: Morphology and ontogeny of the adductor scar in the Paleozoic ostracode **Scrobicula scrobiculata**; Paleontol. Zhurnal, no. 3, p. 370-375.

Kozur, H.

1972a: Einige Bemerkugen zur systematik der Ostracoden und Beschreibung neuer Platycopida aus der Tris Ungarns und der Slowakei; Geol. Paläont. Mitt. Innsbruck, v. 2, p. 1-27.

1972b: Die Bedeutung triassischer Ostracoden für stratigraphische und paläoözologische Unterschungen; Mitt. Ges. Geol. Gergbaustud 21, Symposium Innsbruck, p. 623-660.

Kozur, H. and Nassichuk, W.W.

1977: Permian conodonts in the Canadian Arctic Archipelago - biostratigraphic discussion in Report of Activities, Part A, Geol. Surv. Can., Paper 77-1A, p. 139-143.

Nassichuk, W.W.

1975: The stratigraphic significance of Permian ammonoids on Ellesmere Island; in Report of Activities, Part B, Geol. Surv. Can., Paper 75-1, p. 278-283.

Nassichuk, W.W., Furnish, W.M., and Glenister, Brian F.

1966: The Permian ammonoids of Arctic Canada; Geol. Surv. Can., Bull. 131 (1965).

Sohn, I.G.

1954: Ostracoda from the Permian of the Glass Mountains, Texas; U.S. Geol. Surv., Prof. Paper 264-A.

Thorsteinsson, R.

1974: Carboniferous and Permian stratigraphy of Axel Heiberg Island and western Ellesmere Island, Canadian Arctic Archipelago; Geol. Surv. Can., Bull. 224.

Thorsteinsson, R. and Tozer, E.T.

1971: Geology, Greely Fiord West, District of Franklin; Geol. Surv. Can., Map 1311A.

Waterhouse, J.B.

1976: World correlations for Permian marine faunas; Geology Papers, Univ. Queensland, v. 7, no. 2.

72. SUBSURFACE STRATIGRAPHY, CONODONT ZONATION, AND ORGANIC METAMORPHISM OF THE LOWER PALEOZOIC SUCCESSION, BJORNE PENINSULA, ELLESMERE ISLAND, DISTRICT OF FRANKLIN

Projects 750017 and 680101

Ulrich Mayr, T.T. Uyeno, and C.R. Barnes[1]
Institute of Sedimentary and Petroleum Geology, Calgary

Abstract

Ulrich Mayr, Uyeno, T.T., and Barnes, C.R., Subsurface stratigraphy, conodont zonation, and organic metamorphism of the Lower Paleozoic succession, Bjorne Peninsula, Ellesmere Island, District of Franklin; Current Research, Part A, Geol. Surv. Can., Paper 78-1A, p. 393-398, 1978.

Strata penetrated by two wells (Panarctic Tenneco et al. CSP Eids M-66 and Panarctic ARCO et al. Blue Fiord E-46), located at southern Bjorne Peninsula in southwestern Ellesmere Island, range in age from late Early Devonian to Early Ordovician (Eids to Copes Bay formations). In terms of conodont zonation, this span is from Faunas 7-8 of Klapper et al. (1971) to Fauna D of Ethington Clark (1971). An organic metamorphism study, based on conodonts, has been initiated only in the Canadian Arctic Islands, and no firm conclusions can be drawn at this time. The study does suggest, however, that in a rock that has been assessed as a mature hydrocarbon source by geochemical analyses, the values of the conodont colour alteration index (CAI) may be higher in terrigenous sediments than in carbonates.

Introduction

Two wells, Panarctic Tenneco et al. CSP Eids M-66 and Panarctic ARCO et al. Blue Fiord E-46, located in the southern part of Bjorne Peninsula in southwestern Ellesmere Island (Fig. 72.1), are under study. The rocks encountered in these wells were deposited in a marginal zone of a Siluro-Ordovician carbonate platform. The wells penetrated a sequence ranging from the Lower Devonian to Lower Ordovician, from the Eids to Copes Bay formations (Fig. 72.2).

In this account, description of formations and discussion of their stratigraphic relationships are by Mayr; biostratigraphic and colour alteration studies of the Siluro-Devonian conodonts are by Uyeno, and of the Ordovician conodonts by Barnes. The final part on organic metamorphism and source rock potential is a joint responsibility of the three authors.

We are grateful to Anita G. Harris of the U.S. Geological Survey, Washington, for providing a set of standards of conodonts of different CAI values. R. Thorsteinsson and T.G. Powell, both of I.S.P.G., provided us with graptolite identifications, and geochemical analyses, respectively. Three of the participants of the wells, Panarctic Oils Ltd., Petro-Canada Exploration Inc., and Tenneco Oil and Minerals, Ltd., provided us with bulk samples for conodont sudy.

Stratigraphy

Both wells were spudded in the Eids Formation, which consists of calcareous, dolomitic, and micaceous siltstone. A gradient in grain size appears to be present between the two wells, because the siltstone in the Eids M-66 well is interbedded with subordinate very fine grained sandstone, whereas the siltstone in the Blue Fiord E-46 well is generally argillaceous. The contact with the underlying Cape Phillips Formation is gradational and was drawn at a colour change from light to dark grey.

Only the Blue Fiord E-46 well [in the interval 60-1300 ft (18.3-396.2 m)] yielded stratigraphically useful conodonts from the Eids Formation; a form transitional between **Pandorinellina exigua philipi** (Klapper) and **P. exigua exigua** (Philip). Such a form was reported previously from the Road River Formation at Royal Creek, Yukon Territory (Klapper, 1969, p. 17, Pl. 5, figs. 1-7). The Royal Creek occurrence suggests an assignment of this form to Faunas 7 and 8 of Klapper et al. (1971, Fig. 1), or the **Polygnathus dehiscens** Fauna of Weddige and Ziegler (1977, p. 70), of late Early Devonian (Emsian) age. The informal faunal units of Klapper et al. (1971) are currently being given zonal terms (see Klapper and Johnson, 1977, p. 1051). This transitional form of **Pandorinellina exigua**, together with **P.** cf. **P. expansa** Uyeno and Mason, are present in a sample collected by R. Thorsteinsson from the Eids Formation at its type area (GSC loc. 57730; McLaren, 1963, p. 317; see Collins, 1969, p. 32, 33, 36 for locality details). **Pandorinellina exigua** (Philip) and **Polygnathus inversus** Klapper and Johnson were reported by Weyant (1975) from the lower member of the Blue Fiord Formation at its type area (McLaren, 1963, p. 319), and may be assigned to Fauna 9 of Klapper et al. (1971, Fig. 1) or the **Polygnathus latiscostatus** Fauna of Weddige and Ziegler (1977, p. 71).

At Sör Fiord, to the southeast of the study-area **Polygnathus dehiscens** was reported from the Eids Formation (Klapper and Johnson, 1975, Fig. 4) and, therefore, is of similar age to the Eids Formation in the E-46 well.

The stratigraphic relationship between the Eids and Cape Phillips formations is not known, but may be resolved by palynomorph identifications in progress.

The Cape Phillips Formation [top at 271 ft (82.6 m), M-66; 1576 ft (480.4 m), E-46] overlies and laterally replaces the Siluro-Ordovician carbonates of the Read Bay and Allen Bay formations. It is in the order of 500 m (1500 ft) thick and consists of calcareous and silty, very dark grey shale. Interbeds of dark brown lime mudstone and skeletal wackestone are present in the lower part of the formation in the Eids M-66 well.

Graptolites at a depth of 1720 feet (524.3 m) in the Eids M-66 well (?**Stromatograptus** sp. indet. and **Monograptus** sp. indet., R. Thorsteinsson, pers. comm., 1977) indicate a latest Llandoverian or earliest Wenlockian age for the lower part of the formation in the northern part of the study-area. The age assignment based on graptolites is corroborated by conodont dating. **Pterospathodus celloni** (Walliser) and **Astropentagnathus irregularis** Mostler in the 1740 to 1860 foot (530.4-566.9 m) interval indicate the **P. celloni** Zone of Walliser (1964) [=**Icriodella inconstans** Zone of Aldridge (1972)]. This zone correlates with the C_5 subdivision of the Upper Llandovery Series (Aldridge, 1972, p. 153, Tables 1-4; Klapper and Murphy, 1975, p. 7), and constitutes a part of the Telychian stage of Cocks et al. (1970). "**Neoprioniodus**" **planus** Walliser occurs in the interval from 1830 to 1980 feet (557.8-603.5 m) and suggests an early Silurian age (Fig. 72.2).

[1] Department of Earth Sciences, University of Waterloo, Ontario

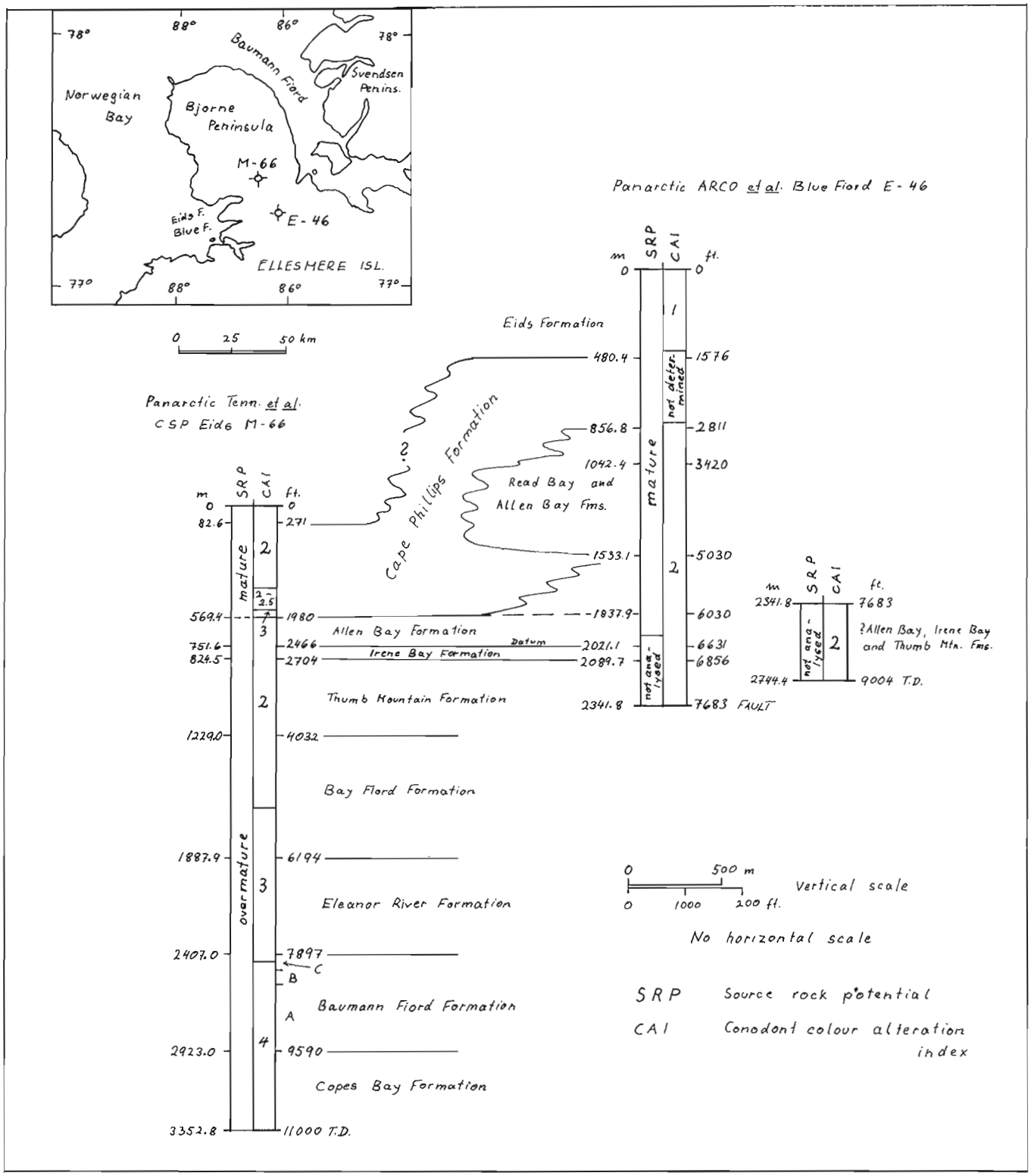

Figure 72.1. Correlation, conodont colour alteration index (CAI) values, and hydrocarbon maturity of Panarctic Tenneco et al. CSP Eids M-66 and Panarctic ARCO et a. Blue Fiord E-46 wells.

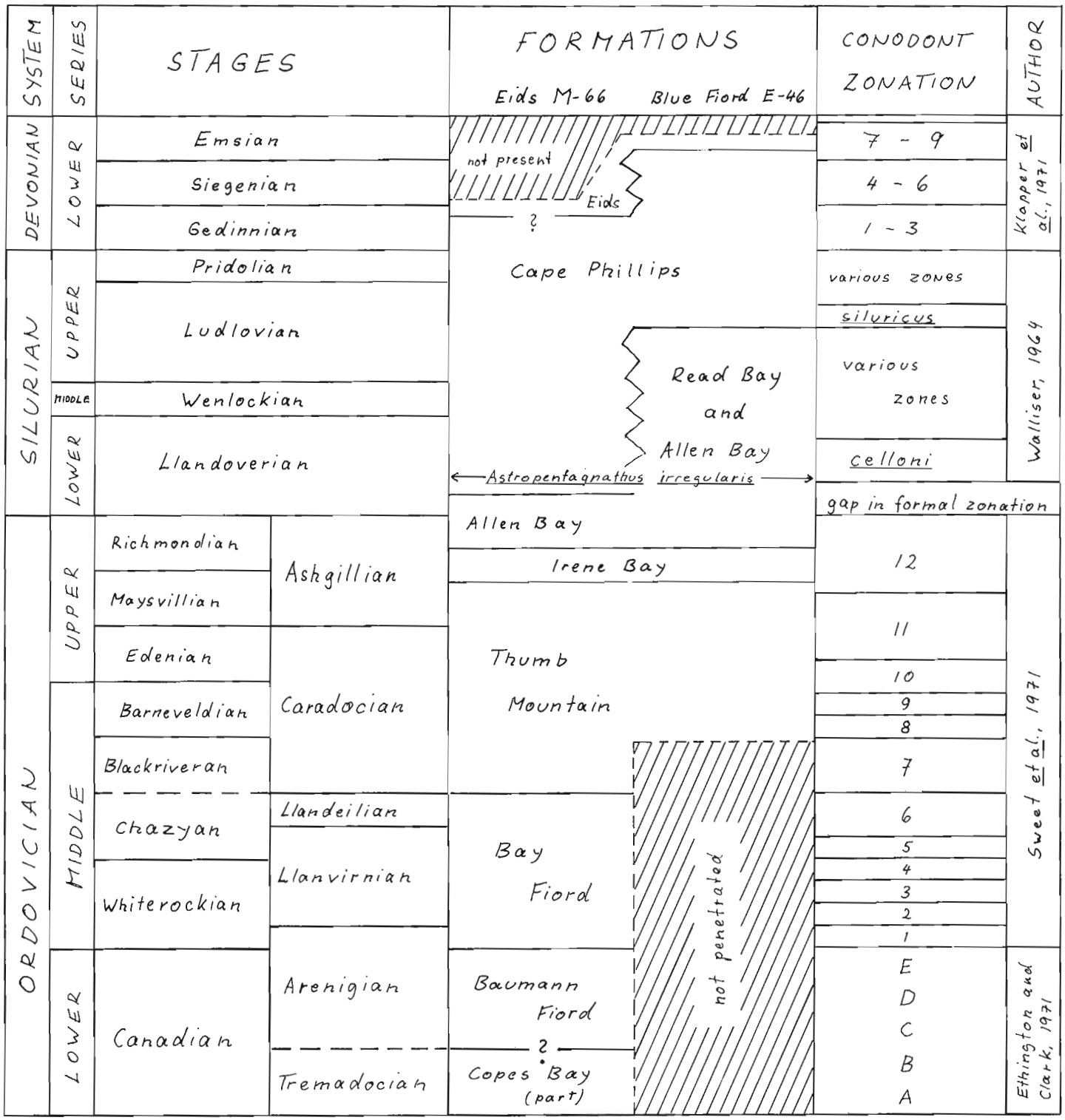

Figure 72.2. Conodont zonation of the strata encountered in the two wells studied herein.

A single conodont fragment was obtained from the Cape Phillips Formation in the Blue Fiord E-46 well, but was unidentifiable.

In the Eids M-66 well, the Allen Bay Formation is 148.1 m (486 ft) thick [top at 1980 ft (569.4 m)]. In the Blue Fiord E-46 well, the Siluro-Ordovician carbonates are 1164.3 m (3820 ft) thick [top at 2811 ft (856 m)] and include the Allen Bay and Read Bay formations. The Allen Bay Formation in the Eids M-66 well comprises carbonates of relatively deep water origin. They consist of dark brown-grey lime mudstone and very finely crystalline dolomite with abundant fragments of **Pseudogygites** sp. A similar very dark unit, although completely dolomitized and silicified, forms the lower part of the carbonates in the Blue Fiord E-46 well [top at 6030 ft (1837.9 m)]. This unit is overlain by carbonates, consisting of interbedded bioclastic limestone and dark coloured calcareous shale and argillaceous lime mudstone [top at 5030 ft (1533.1 m)]. These probable slope carbonates are overlain by 490.7 m (1610 ft) of very pale coloured, medium and finely crystalline dolomite [top at 3420 ft (1042.4 m)]. The extensive dolomitization of this unit hinders facies interpretation, but it is possible that the unit represents a reefoidal platform margin. Reefs are known from outcrops on Svendsen Peninsula (Mayr, 1974; McGill, 1975). The uppermost unit of the Silurian carbonates forms a transition zone to the overlying Cape Phillips Formation and consists of dolomitic, silty and argillaceous lime mudstone.

Ozarkodina excavata excavata (Branson and Mehl) in the Read Bay-Allen Bay unit of the Blue Fiord well [2700-2900 ft (823.0-883.9 m) interval] is a long-ranging form, extending from Middle Silurian (**Kockelella patula** Zone) through Lower Devonian (Klapper in Ziegler, 1973, p. 226). In the interval from 3300 to 3400 feet (1005.8-1036.3) is **Ozarkodina** cf. **O.** n. sp. B of Klapper (in Klapper and Murphy, 1975), a form identical to that illustrated by Uyeno (1977, p. 214, Pl. 41.1, figs. 7, 8) from the upper part of the Cape Storm Formation at eastern Cornwallis Island. There it cannot be dated precisely, but occurs just below an interval carrying conodonts of probable **Polygnathoides siluricus** Zone (about mid-Ludlow; Walliser, 1971, Text-fig. 1). **Astropentagnathus irregularis** occurs in the 5800 to 5900 foot (1767.8-1798.3 m) interval, indicating the **P. celloni** Zone (see discussion under Cape Phillips Formation), and is correlated with the 1740 to 1860 foot (530.4-566.9 m) interval of the Eids M-66 well (Fig. 72.2). **"Neoprioniodus" planus** ranges from 5600 to 6400 feet (1706.9-1950.7 m) in the E-46 well and suggests an early Silurian age.

Below the 2030-foot (618.7 m) level in the Eids M-66 well are conodonts assignable to Fauna 12 of Sweet et al. (1971) of Late Ordovician age [late Maysvillian to Richmondian; Barnes (1974)].

The Irene Bay Formation top at 2466 ft (751.6 m), M-66; 6631 ft (2021.1 m), E-46 is about 70 m (230 ft) thick and its lithology is variable. It is typical in the Eids M-66 well, where it consists of variably argillaceous lime mudstone and calcareous shale. In the Blue Fiord E-46 well, however, the formation consists of coarsely and medium crystalline, euhedral, white dolomite. The argillaceous material is preserved as green intercrystalline matrix. The upper boundary in the Blue Fiord well is based on a colour change from dark to light in the cuttings samples and a very small deflection in the gamma ray log.

Conodonts from the upper part of the formation in the Eids M-66 well [above 2570 ft (783.3 m)] are assignable to Fauna 12, as in the overlying Allen Bay Formation (Fig. 72.2).

The Thumb Mountain Formation [top at 2704 ft (824.5 m), M-66; 6856 ft (2089.7 m), E-46] is 404.5 m (1328 ft) thick in the Eids M-66 well. The lower part consists of lime mudstone with dolomitic mottling (Core 1 of Eids M-66 well), whereas the upper part consists of ?cryptalgal lime mudstone in the Eids well and of medium and coarsely crystalline dolomite in the Blue Fiord well.

Several intervals in the Eids M-66 well yielded conodonts. The interval from 3110 to 3430 feet (947.9-1045.5 m) contained conodonts belonging to Fauna 8 (Sweet et al., 1971), whereas in the lower part of the formation at 3910 feet (1191.8 m), the conodonts are assignable to Fauna 6 or 7. This faunal range is well within the age range of the Thumb Mountain Formation (Fig. 72.2) which is from Fauna 7 to 11, Blackriveran to early Maysvillian (Caradocian to early Ashgillian) according to Nowlan (1976).

Also assigned tentatively to the Thumb Mountain Formation, on the basis of similarity in lithology, is the upper part of the interval below 7683 feet (2341.8 m) in the Blue Fiord E-46 well. The interval between 8410 and 8900 feet (2563.4 and 2712.7 m), however, contains elements of Fauna 12 which suggest correlation of this interval with the Allen Bay and Irene Bay formations. At present, the true stratigraphic position of the sequence below the 7683-foot (2341.8 m) level in the E-46 well is not known. It probably is a complexly faulted and folded, perhaps even overturned, unit, which contains slices of Thumb Mountain, Irene Bay and, possibly, Allen Bay formations.

The Bay Fiord Formation [top at 4032 ft (1229.0 m), M-66] is 658.9 m (2162 ft) thick. The lower part comprises aphanocrystalline dolomite interbedded with shale and anhydrite. The thin middle part [4700-4845 ft (1432.6-1476.8 m)] contains dolomitic, probably mottled, lime mudstone with abundant fossil fragments. The upper part consists of dolomite and minor limestone and anhydrite.

Conodonts were obtained from several levels within the Bay Fiord Formation in the Eids M-66 well, ranging from 4540 feet (1383.8 m) at its highest part [with conodonts of Fauna 6 or 7 of Sweet et al. (1971)] to 6160 feet (1877.6 m) at the lowest (with Fauna 2 or 3). The lowest level is only a short distance above the lower formational boundary. The age of the formation, therefore, is from early Blackriveran (early Caradocian, late Middle Ordovician) to late Whiterockian (early Llanvirnian, early Middle Ordovician) (Fig. 72.2). This range is identical with that reported by Nowlan (1976) based on outcrop sections.

The Eleanor River Formation [top at 6195 ft (1887.9 m), M-66] is 519.1 m (1703 ft) thick and consists of dolomite and limestone. The middle part of the formation is argillaceous and contains subordinate interbedded shale and anhydrite.

In terms of conodonts, the formation has a slightly different age range than has been recorded from elsewhere in the Arctic Islands (Barnes, 1974; Nowlan, 1976) on Grinnell Peninsula and central eastern Ellesmere Island. In the Eids M-66 well, the range is from Fauna 2 or 3 [6210 ft (1892.8 m)] to Fauna E or 1 [(7900 ft (2407.9 m)] (Ethington and Clark, 1971; Sweet et al., 1971). This is a range from about late Whiterockian (early Llanvirnian, early Middle Ordovician) to late Canadian (late Arenigian) (Fig. 72.2).

On comparing the age span of the Eleanor River Formation in the Eids M-66 well with that reported from outcrops, it is noted that the upper limit is approximately the same. However, conodonts of Fauna D (Ethington and Clark, 1971) (about middle Arenigian or middle Early Ordovician) have been reported in the oldest part of the formation in outcrops (Nowlan, 1976).

The Baumann Fiord Formation [top at 7897 ft (2407.0 m), M-66] is 516.0 m (1693 ft) thick and its three members (Kerr, 1967) can be distinguished by the anhydrite content of the formation. Member A [top at 8402 ft (2560.9 m)] consists of very finely crystalline dolomite, interbedded with anhydrite and various types of limestone, including pelletoidal grainstone. Member B [top at 8146 ft (2482.9 m)] comprises lime mudstone, whereas member C is similar to member A, but appears to contain more argillaceous material.

Member B yielded conodonts belonging to Ethington and Clark's (1971) Fauna D which is of middle Arenigian (about middle Early Ordovician) age (Fig. 72.2).

The Copes Bay Formation is present below 9590 feet (2923.0 m) in the M-66 well and is more than 429.8 m (1410 ft) thick. The lower part consists of variable limestone with subordinate beds of calcareous sandstone and siltstone, whereas the upper part comprises finely crystalline or aphanocrystalline dolomite and lime mudstone. Cored intervals show ripple cross-beds, bioturbation and possibly mudcracks. No conodonts were found in the Copes Bay Formation.

Organic metamorphism study (conodont colour alteration)

Epstein et al. (1977) arranged the conodonts of different colours in an order of increasing darkness, grouped them according to similarity in darkness, and then assigned each set a value of colour alteration index (CAI). They demonstrated that the colour changes are time and temperature dependent, and that the different colours of conodonts, therefore, can be used as a tool to assess organic metamorphism. The conodont CAI values were correlated with vitrinite reflectance and fixed carbon ranges. Using the Appalachian basin as their test model, they found that a CAI value of 1.5 coincides with that level of organic metamorphism above which there is no known commercial oil and condensate production.

The relationship between the CAI and the degree of organic metamorphism may be related aside from being dependent on temperature, to variations in the host rock and the history of burial. For these reasons, Epstein et al. (1977, p. 15) limited their study to one rock type, namely limestone, in order to eliminate the unknown effect of host rock texture and composition on the colour alteration of conodonts.

It should be noted, also, that Epstein et al. (1977, p. 24) have stressed that the upper thermal limits, inferred from conodont CAI values, for oil production for different stratigraphic intervals, are not the same everywhere. This factor, in addition to the lack of information concerning the relationship between CAI and the source rock potential resulting from organic hydrocarbon analyses, have led the authors to a study, now in progress, to investigate what these relationships may be, if there are any, in the lower Paleozoic rocks of the Arctic Islands.

In the Eids M-66 well, the interval from 30 to 1410 feet (9.1-429.8 m) (Eids and the upper part of Cape Phillips formations) has yielded conodonts with a CAI value of 2 (Fig. 72.1). The interval from 1480 to 1860 feet (451.1-566.9 m) yielded conodonts with a CAI value of 2-2.5 and the interval from 1890 to 1980 feet (576.1-603.6 m), CAI value of 3. The change from terrigenous sediments to carbonates at 1980 feet (603.5 m) coincides approximately with a reversal of the CAI value to 2, but below that it increases gradually to 3 at 5300 feet (1615.4 m) and to 4 at 8000 feet (2438.4 m).

In the Blue Fiord E-46 well, conodonts from the Eids Formation [60-1300 ft (18.3-396.2 m) interval] have a CAI value of 1. Conodonts from the Cape Phillips Formation [2700-2800 ft (823.0-853.4 m)] and the Read Bay-Allen Bay formations [2800-6400 ft (853.4-1950.7 m)] have a CAI value of 2. From there the same CAI value continues downward through the Cornwallis Group to the bottom of the well (Fig. 72.1).

The organic source rock potential, based on the yield of liquid hydrocarbons as a percentage of the total organic carbon (T.G. Powell, pers. comm., 1977), has been plotted on Figure 72.1. One notes that there is no obvious direct relationship between the CAI and source rock potential. Differences in the characteristics of the host rock appear to affect, in varying amount, the degree of conodont colour alteration. In the terrigenous sediments of the Cape Phillips Formation, for example, the CAI value may go as high as 3 in the mature zone.

In carbonates, the correlation between the CAI and source rock potential is also variable. In the dominantly limestone sequence of the Eids M-66 well, a CAI value of 2 falls into the overmature zone, corroborating the conclusions of Epstein et al. (1977), but in the dolomite sequence of the Blue Biord E-46 well, a CAI value of 2 is present in an interval which has been assessed as mature.

In summary, an organic metamorphism study, based on conodont CAI values, has been initiated only in the Canadian Arctic Islands, so no firm conclusions can be drawn. It appears, however, that in a rock that has been assessed as a mature hydrocarbon source by geochemical analyses, the values of the conodont CAI may be higher in terrigenous sediments than in carbonates.

References

Aldridge, R.J.
1972: Llandovery conodonts from the Welsh Borderland; Bull. Brit. Mus. (Nat. Hist.), Geol., v. 22, no. 2, p. 127-231.

Barnes, C.R.
1974: Ordovician conodont biostratigraphy of the Canadian Arctic; Geol. Assoc. Can., Can. Soc. Pet. Geologists, Proc. Symp. Geology of the Canadian Arctic, p. 221-240 (1973).

Cocks, L.R.M., Toghill, P., and Ziegler, A.M.
1970: Stage names within the Llandovery Series; Geol. Mag., v. 107, p. 79-87.

Collins, D.H.
1969: Devonian nautiloids from northern Canada; Geol. Surv. Can., Bull. 182, p. 31-50.

Epstein, A.G., Epstein, J.B., and Harris, L.D.
1977: Conodont color alteration – an index to organic metamorphism; U.S. Geol. Surv., Prof. Paper 995.

Ethington, R.L. and Clark, D.L.
1971: Lower Ordovician conodonts in North America; Geol. Soc. Am., Mem. 127, p. 63-82.

Kerr, J. Wm.
1967: New nomenclature for Ordovician rock units of the eastern and southern Queen Elizabeth Islands, Arctic Canada; Bull. Can. Pet. Geol., v. 15, no. 1, p. 91-113.

Klapper, G.
1969: Lower Devonian conodont sequence, Royal Creek, Yukon Territory, and Devon Island, Canada, with a section on Devon Island stratigraphy by A.R. Ormiston; J. Paleontol., v. 43, p. 1-27.

Klapper, G. and Johnson, D.B.
1975: Sequence in conodont genus **Polygnathus** in Lower Devonian at Lone Mountain, Nevada; Geol. Palaeontol., v. 9, p. 65-83.

1977: Lower and Middle Devonian conodont sequence in central Nevada Abst.); Geol. Soc. Am., Abstr. v. 9, no. 7, p. 1051.

Klapper, G. and Murphy, M.A.
1975: Silurian-Lower Devonian conodont sequence in the Roberts Mountains Formation of central Nevada; Univ. Calif. Publ. Geol. Sci., v. 111 (1974).

Klapper, G., Sandberg, C.A., Collinson, C., Huddle, J.W., Orr, R.W., Rickard, L.V., Schumacher, D., Seddon, G., and Uyeno, T.T.
1971: North American Devonian conodont biostratigraphy; Geol. Soc. Am., Mem. 127, p. 285-316.

Mayr, U.
1974: Lithologies and depositional environments of the Allen Bay-Read Bay Formations (Ordovician-Silurian) on Svendsen Peninsula, central Ellesmere Island; Geol. Assoc. Can., Can. Soc. Pet. Geol., Proc. Symp. Geology of the Canadian Arctic, p. 143-157 (1973).

McGill, P.C.
1975: The stratigraphy and structure of the Vendom Fiord area; Bull. Can. Pet. Geol., v. 22, p. 361-386 (1974).

McLaren, D.J.
1963: Southwestern Ellesmere Island between Goose Fiord and Bjorne Peninsula **in** Geology of the north-central part of the Arctic Archipelago, Northwest Territories (Operation Franklin); Geol. Surv. Can., Mem. 320, p. 310-338.

Nowlan, G.S.
1976: Late Cambrian to Late Ordovician conodont evolution and biostratigraphy of the Franklinian Miogeosyncline, eastern Canadian Arctic Islands; unpubl. Ph.D. dissertation, Univ. Waterloo.

Sweet, W.C., Ethington, R.L., and Barnes, C.R.
1971: North American Middle and Upper Ordovician conodont faunas; Geol. Soc. Am., Mem. 127, p. 163-193.

Uyeno, T.T.
1977: Summary of conodont biostratigraphy of the Read Bay Formation at its type sections and adjacent areas, eastern Cornwallis Island, District of Franklin; in Report of Activities, Part B, Geol. Surv. Can., Paper 77-1B, p. 211-216.

Walliser, O.H.
1964: Conodonten des Silurs; Abh. Hess. Landesamtes Bodenforsch., v. 41.

1971: Conodont biostratigraphy of the Silurian of Europe; Geol. Soc. Am., Mem. 127, p. 195-206.

Weddige, K. and Ziegler, W.
1977: Correlation of Lower/Middle Devonian boundary beds; Newsl. Stratigr., v. 6, p. 67-84.

Weyant, M.
1975: Sur l'âge du membre inférieur de la formation Blue Fiord dans le sud-ouest de l'île Ellesmere (Archipel Arctique Canadien) d'après les conodontes; Newsl. Stratigr., v. 4, no. 2, p. 87-95.

Ziegler, W., ed.
1973: Catalogue of conodonts; E. Schweizerbart'sche Verlagsbuchhandlung, Stuttgart, v. I.

73. LIGNITE DEPOSITS IN THE BONNET PLUME FORMATION, YUKON TERRITORY

Project 770047

Darrel G.F. Long
Institute of Sedimentary and Petroleum Geology, Calgary

Abstract

Long, D.G.F., Lignite deposits in the Bonnet Plume Formation, Yukon Territory; Current Research, Part A, Geol. Surv. Can., Paper 78-1A, p. 399-401, 1978.

Lignite deposits occur in intimate association with conglomeratic rocks of alluvial fan and braided stream facies in both the upper (Paleocene) and lower (Albian) parts of the Bonnet Plume Formation. Conglomerate and associated coal in the upper (Paleocene) part of the formation may be correlated tentatively over 15 km, between the type section on Wind River and exposures on the south bank of the Peel River. Two previously unreported low grade coal seams in the (Albian) conglomerate sequence at the base of the formation may extend laterally more than 10 km along the strike with little to no surficial cover. The occurrence of these thick (4.5 and 9.0 m) seams in the lower part of the formation, and the possible extension of the Paleocene lignite seams in the upper part of the formation, suggest that the area underlain by coal in the Bonnet Plume Basin may be significantly greater than previously indicated.

Introduction

The Bonnet Plume Formation is a thick (1500 m+), predominantly clastic sequence, of Cretaceous and Tertiary ages, which occupies a structural depression known as the Bonnet Plume Basin (Norris and Hopkins, 1977), located in the Wind River map-area (106E) (Norris, 1975) of northern Yukon Territory. The structural framework and the prior history of investigation of this successor basin has been described in detail in a preliminary report by Norris and Hopkins (1977). Stratigraphic and paleontological data are given in papers by Mountjoy (1967) and Rouse and Srivastava (1972). Surficial geology is described by Hughes (1972).

Observations

Minor changes in the basin configuration, suggested by Norris (1975), are indicated in Figure 73.2. These changes include an extension of the Bonnet Plume Formation north of the Peel River, and a slight reduction in the area of outcrop of the formation east of Bonnet Plume River near its junction with the Peel River.

Norris and Hopkins (1977) recognized two mappable units within the Bonnet Plume Formation: a lower conglomeratic unit, with minor sandstone and shale (their unit 1 Kbp), and an upper unit of sandstone shale and conglomerate (their unit KTbp). The lower (conglomeratic) part of the formation is now recognized east of the Bonnet Plume River. Jurassic or Lower Cretaceous shales and sandstones, older than the Bonnet Plume Formation were recorded in the extreme southwest corner of the Bonnet Plume Basin. Accurate dating of these older rocks may lead to a better understanding of the timing of tectonic events which affected the Bonnet Plume Basin.

Paleocurrent observations in the Bonnet Plume Formation (Fig. 73.2) indicate a well defined basin configuration during deposition of the lowermost, conglomeratic facies, and may indicate that the northeastern margin of the basin was breached during deposition of the uppermost strata. Conglomeratic rocks in the lower part of the formation were deposited on wet alluvial fans, and in braided rivers. Sandstone and conglomerate in the upper part of the formation were deposited principally in high gradient braided streams, with the associated siltstones, mudstones and coals probably being deposited in adjacent lacustrine, paludal and overbank-floodplain environments. No evidence was found to support Norris and Hopkins' (1977) conjecture that the dip of the strata might possibly represent the initial dip of foreset beds; hence the thicknesses of strata reported by Mountjoy (1967) probably are valid.

Coal Seams

The thick (4-11 m) seams in the uppermost (Paleocene) strata of the Bonnet Plume Formation were sampled in detail, and will be reported on later. In both sections (106E17, 106E18) exposed along the south bank of Peel River, the coal-bearing strata are found in intimate association with pebble and cobble conglomerate and conglomeratic sandstone. As a similar association of coal seams with conglomeratic strata is seen in the uppermost part of the type section (106E16, exposed on the Wind River) a general correlation of strata can be made between these three sections, indicating the possibility of a more widespread distribution of coal deposits in the upper

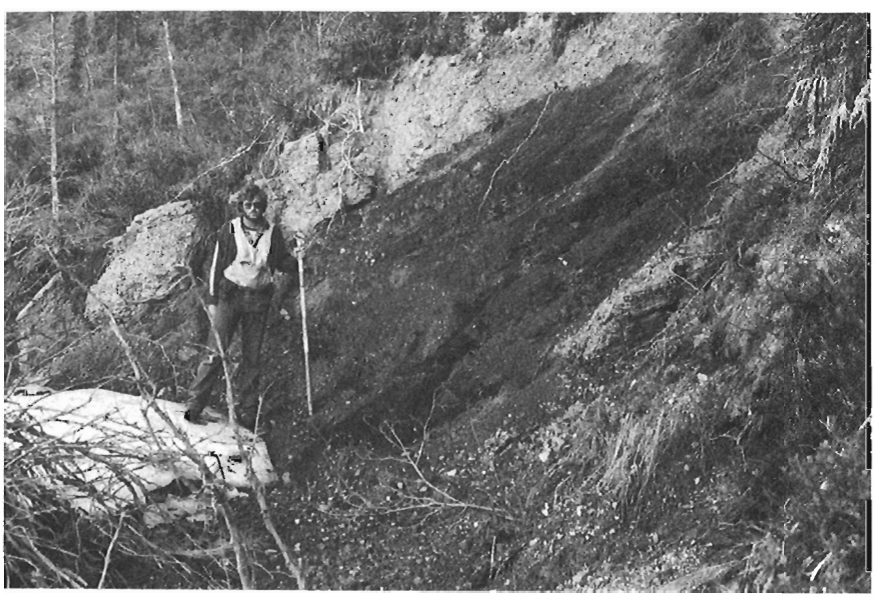

Figure 73.1

Lower of the two coal seams exposed on the small creel immediately south of section 106E9, showing sharp contact between the coal and overlying small pebble conglomerate (GSC photo 199330).

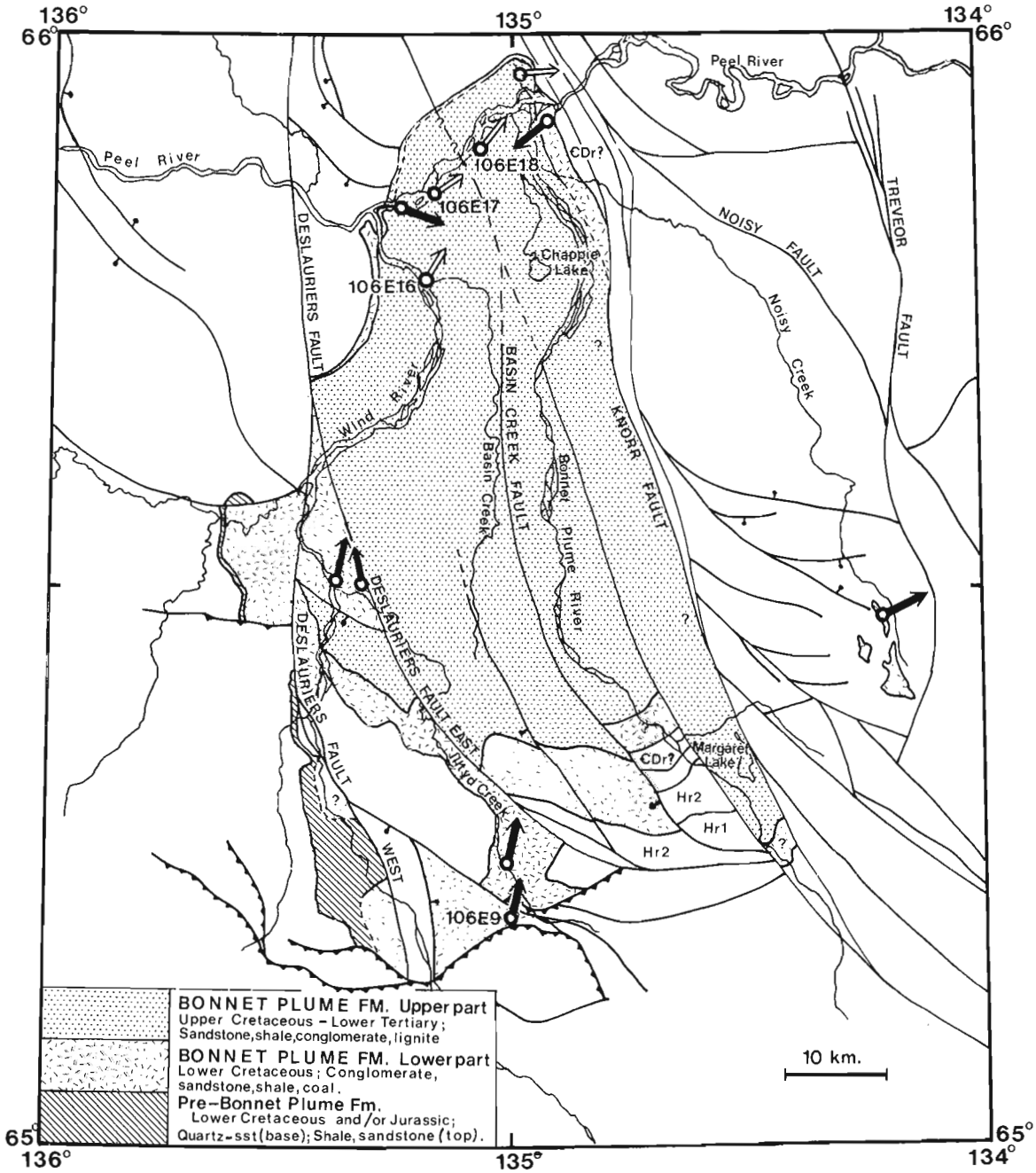

Figure 73.2. Geology (modified after Norris and Hopkins, 1977) and paleocurrents, of the Bonnet Plume Basin. For details of geology see Norris (1975), Norris and Hopkins (1977). Numbers are section locations mentioned in Norris and Hopkins (1977). Black arrows indicate inferred paleocurrents in the lower part of the Bonnet Plume Formation, and open arrows indicate paleocurrents in the upper part (Hrl = Rapitan Fm., diamictite: Hr2 = Rapitan Fm., mudstone dolomite; CDr = Road River Fm.). Paleocurrent observations, east of the Knorr fault zone based on only one observation, and are not considered significant.

Bonnet Plume Formation than has been indicated previously. Several thin coal seams (1-150 cm) of doubtful lateral continuity were recorded in the lower part of Norris and Hopkins' (1977) unit KTbp (Bonnet Plume Formation, upper part).

Coaly strata were recorded also in the lowermost (Albian) conglomerate part of the Bonnet Plume Formation, in a small creek, between Illtyd Creek and Wind River, immediately to the south of Norris and Hopkins' (1977) section 106E9. The seams at this location are 4.5 and 9.0 m thick, and correspond to units 9 and 14 respectively of section 106E9 (Norris and Hopkins, 1977, p. 17-18). Both seams form the upper part of fining upward cycles, which begin with conglomeratic material and are overlain abruptly by conglomerate of the overlying cycle (Fig. 73.1). A recessive interval, corresponding to the upper seam, can be traced along strike (northwest-southeast) on air photographs over 10 km of outcrop, with little or no surficial cover. The lateral continuity and concentration of coaly material within this recessive interval require testing by trenching or shallow boreholes. The upper seam may correlate with a 5m+ thick

seam exposed on Illtyd Creek 3 km to the north-northeast. Petrographic details of these coals and coaly strata will be reported at a later date.

Conclusions

Coal seams are conspicuous in both the upper and lower parts of the Bonnet Plume Formation, hence no part of the formation should be excluded in any future coal exploration program. The coal seams were deposited in small lakes or swamps, and owe their preservation to rapid progradation of conglomeratic fluvial sequences which may have occurred in response to contemporary tectonic activity (cf. Eisbacher, 1977; Heward, 1977; Steel et al., 1977).

References

Eisbacher, G.H.
1977: Vertical accretion during high-gradient progradation of fluvial systems; Can. Soc. Pet. Geol., The First International Symposium on Fluvial Sedimentology; Program and Abstracts, p. 9.

Heward, A.P.
1977: Stephanian A and B alluvial fan and lacustrine sediments from the La Matallana and Sabero Coalfields, Northern Spain; Can. Soc. Petrol. Geologists, The First International Symposium on Fluvial Sedimentology, Program with Abstracts, p. 12.

Hughes, O.L.
1972: Surficial geology of northern Yukon Territory and northwestern District of Mackenzie, Northwest Territories; Geol. Surv. Can., Paper 69-36, Map 1319A.

Mountjoy, E.W.
1967: Upper Cretaceous and Tertiary stratigraphy, northern Yukon Territory and northwestern District of Mackenzie; Geol. Surv. Can., Paper 66-16.

Norris, D.K.
1975: Geological maps of parts of Yukon and Northwest Territories; Geol. Surv. Can., Open File 279.

Norris, D.K. and Hopkins, W.S., Jr.
1977: The geology of the Bonnet Plume Basin, Yukon Territory; Geol. Surv. Can., Paper 76-8.

Rouse, G.E. and Srivastava, S.K.
1972: Palynological zonation of Cretaceous and Early Tertiary rocks of the Bonnet Plume Formation, northeastern Yukon, Canada; Can. J. Earth Sci., v. 9, p. 1163-1179.

Steel, R.J., Mæhle, S., Nilsen, H., Røe, S.L., and Spinnangar, Å.
1977: Coarsening-upward cycles in the alluvium of Hornelen Basin (Devonian) Norway: Sedimentary response to tectonic events; Geol. Soc. Am. Bull., v. 88, p. 1124-1134.

POSTGLACIAL DIATOM STRATIGRAPHY OF A LAKE BASIN OF THE EASTERN ARCTIC SHIELD

Project 770066

T.W.D. Edwards[1]
Terrain Sciences Division

Abstract

Edwards, T.W.D., Postglacial diatom stratigraphy of a lake basin of the Eastern Arctic Shield; Current Research, Part A, Geol. Surv. Can., Paper 78-1A, p. 403-407, 1978.

The diatom stratigraphy of a sediment core from a lake in southeastern Keewatin records a succession of environments of deposition from estuarine to lagoonal and finally to lacustrine conditions. This is believed to represent the emergence of the lake from Hudson Bay due to isostatic uplift in the last 5000 years. Micropaleontological evidence of marine origin of much of the sediment fill of the lake basin supports conclusions drawn by earlier researchers.

The dominant taxa of the modern oligotrophic lake diatom assemblage are ***Fragilaria construens****, F.* ***pinnata****, and species of* ***Melosira****.*

Introduction

Preliminary investigations of the diatom stratigraphy of Yandle Lake, District of Keewatin, Northwest Territories (61°53'N, 96°30'W) (Fig. 74.1) have been carried out (Edwards, 1977). The lake basin was the focus of an intensive program of subbottom profiling, grab sampling, and Livingston coring in 1975 (Shilts et al., 1976). Samples for the present study were obtained from a 194-cm core collected by R.A. Klassen during the 1976 field season.

During the 1977 field season operations were carried out by the author in association and co-ordination with J.D. Adshead from a base camp on an unnamed lake south of

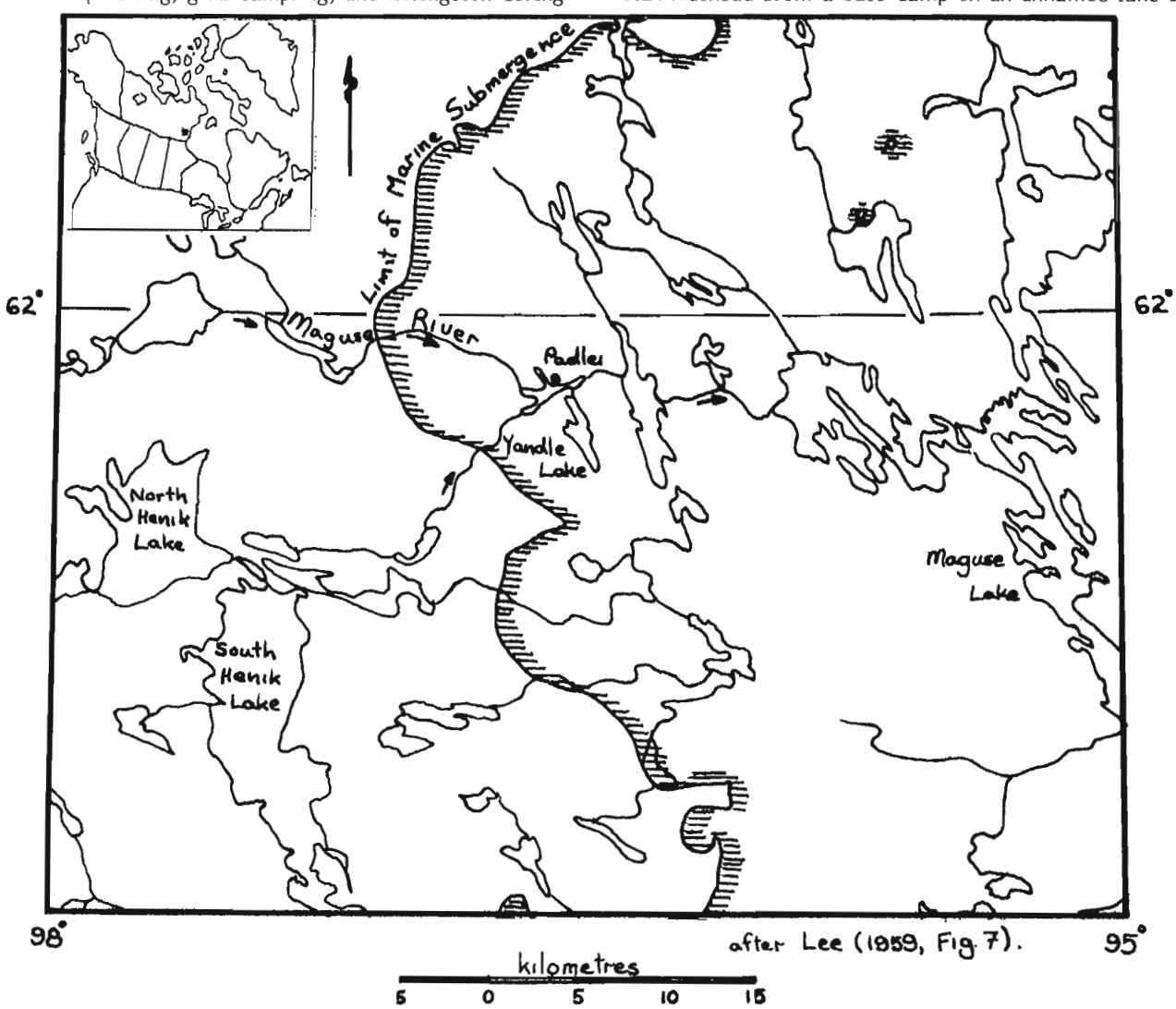

Figure 74.1. Location of Yandle Lake, District of Keewatin, N.W.T.

[1] Department of Geological Sciences, Queen's University, Kingston.

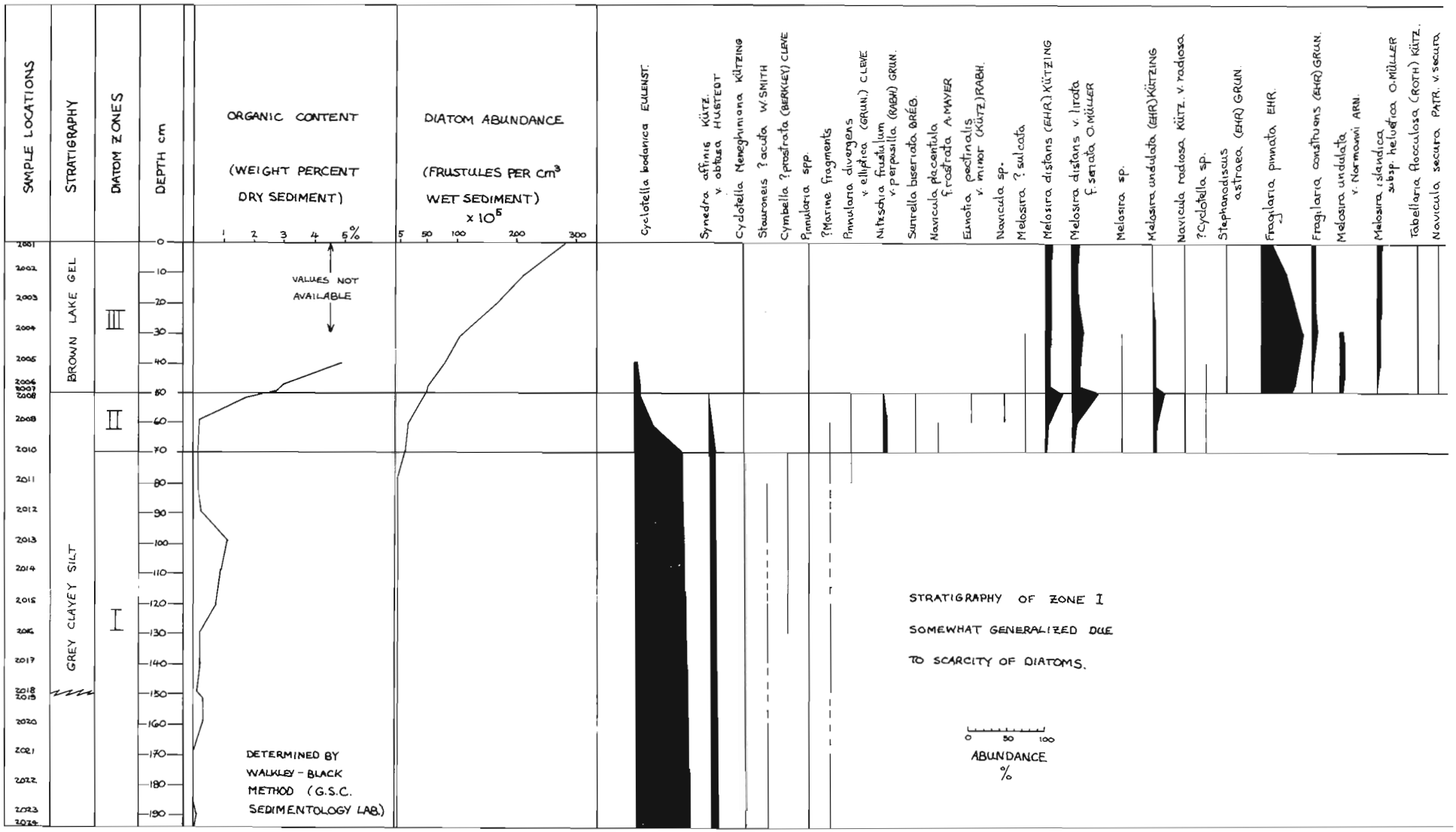

Figure 74.2. Diatom stratigraphy of Yandle Lake core. Jagged line at 148-cm depth indicates a break in the core tube which was incurred in transit.

Figure 74.2 (cont.)

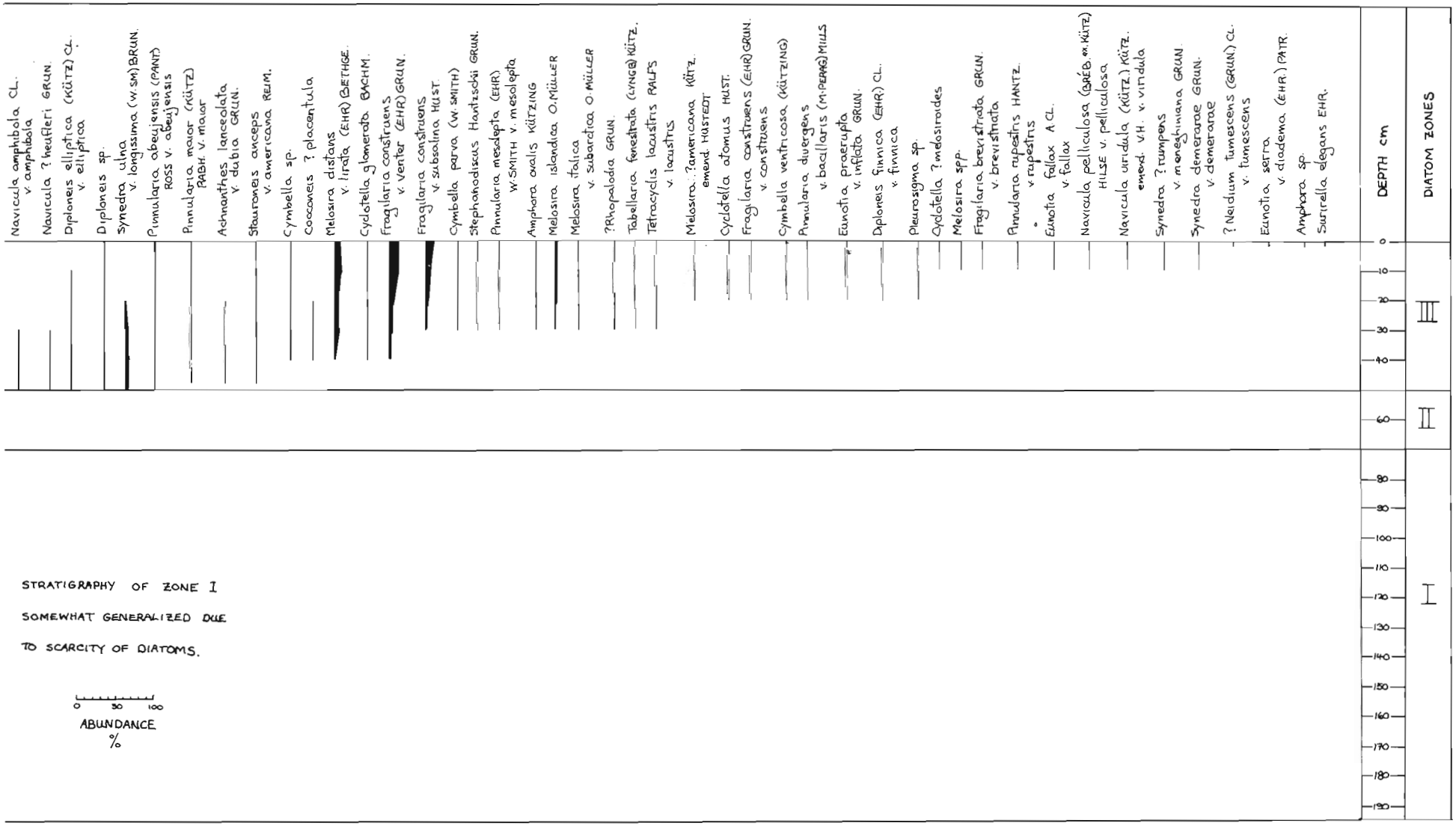

Ferguson Lake (62°40'N, 97°00'W). Scuba diving techniques were used extensively to allow observation and photography of underwater features and to collect samples and sediment cores. This material is to be utilized in a study of siltation and siltation processes in lakes of Keewatin as part of Integrated Environmental Impact Study, Arctic Islands Pipeline Project (AIPP-8), Department of Fisheries and Environment. The project constitutes a major segment of the author's Master of Science research program at Queen's University, Kingston.

Yandle Lake is situated east of the Keewatin Ice Divide at an elevation of ~110 m above sea level. The limit of most recent marine submergence passes approximately 10 km to the southwest of the lake at an altitude of about 170 m (Lee, 1959). Re-emergence of Yandle Lake is estimated to have occurred approximately 5000 years B.P. (W.W. Shilts, 1977, pers. comm.). Three sediment types of glacial, marine, and lacustrine origin have been recognized in the basin (Shilts et al., 1976). Their distribution was mapped using subbottom profiling and data based on the examination of more than 100 grab samples.

Till apparently underlies most of the lake basin and covers much of the surrounding terrain. Till is overlain by material described as massive (marine?) silty clay. In the deep basins within the lake (8 to 16 m depth) both of these sediments may have a thick cover of laminated (marine?) silty clay. In shallow areas (less than 4 m) and in the shore zone the bottom consists of sand or sand and boulders derived from wave washing of the till, or till and/or marine silty clay with frost heaved stones and well developed rib and trough patterns (Shilts and Dean, 1975). Lake sediment of gel-like consistency covers most areas; it ranges in thickness from less than 1 cm nearshore to greater than 1 m in offshore basins. The gel is a stiff to watery, flocculant material which is believed to be the 'modern' (postmarine phase) lake sediment. The core was collected from the central basin of the lake in water depth of 8 m. It penetrated two sediment units – a lower, mottled, grey clayey silt and an overlying thickness of brown gel. The silt unit shows faint banding in x-radiographs, and it is apparently equivalent to the laminated marine silty clay. (See Shilts et al. (1976) and Adshead (1978) for further discussion of sediment composition.)

Diatom Stratigraphy

Figure 74.2 illustrates the diatom stratigraphy of the core and the zonation drawn on this basis. Zone I consists of the lower 124 cm of the clayey silt unit. The sediment in this zone has extensive worm burrows, especially in the interval from 90 to 130 cm. The diatom assemblage is sparse, dominated by **Cyclotella bondanica** Eulenst. with **Synedra affinis** Kütz v. **obtusa** Hustedt subdominant. Fragments bearing coarse costae reminiscent of **Stephanopyxis** spp. or other marine diatoms are present. The zone is believed to represent sedimentation in an estuarine environment. This conclusion is supported by: 1) the predominance of the cool freshwater taxon **C. bodanica** in association with 2) the marine or brackish water taxon **S. affinis** v. **obtusa** and 3) the physiographic situation of the lake basin immediately prior to the emergence of Yandle Lake at which time the basin formed part of a bay into which Maguse River drained.

The upper 20 cm of the clayey silt unit, Zone II, is characterized by the decline of the major taxa of Zone I and the appearance and rise to dominance of species of **Melosira**, notably **M. undulata** (Ehr.) Kütz., **M. distans** (Ehr.) Kütz., and **M. distans** v. **lirata** f. **seriata** O. Müller. The characteristic brackish water diatom **Nitzschia frustulum** v. **perpusilla** (Rabh.) Grun. also marks this interval. **Cyclotella bodanica** declines upwards relative to the other taxa. The sediment within the upper 10 cm of Zone II is transitional in diatom composition to the overlying gel, although it resembles Zone I in texture, and the distinct sedimentological break is at the top of the zone. It is proposed that this interval represents a lagoonal period during which Yandle Lake basin was separating from Hudson Bay and the marine connection with the Maguse River estuary was becoming ever more restricted. The introduction of a richer flora containing both a freshwater and a distinct brackish water component suggests the stabilization of the water body and the beginnings of a lacustrine environment.

Zone III includes the entire lake gel sediment unit of the uppermost 50 cm of the core. A total of 62 taxa were recorded, of which 13 were found to be continuous throughout the interval. The lower boundary of the zone is marked by the introduction of 13 new taxa. The dominant taxa are species and varieties of **Fragilaria** and **Melosira, F. pinnata** Ehr., **F. construens** v. **venter** (Ehr.) Grun., **F. construens** v. **subsalina** Hustedt, and **M. distans** v. **lirata** f. **seriata** O. Müller. The diatom stratigraphy suggests that productivity has been increasing steadily since cessation of marine influence although the lake is still highly oligotrophic.

Summary

Three distinct depositional environments have been recognized from the Yandle Lake core with the aid of diatom stratigraphy. In chronological order these (and their sediments) are 1) estuarine (clayey silt), 2) lagoonal (clayey silt), and 3) lacustrine (diatomaceous lake gel). These form a prograding sequence of facies recording the change in sedimentation within a lake basin that emerged from Hudson Bay approximately 5000 years ago. As reported by Shilts et al. (1976), the thickness of the true lacustrine sediment is variable, and the estuarine or lagoonal sediments from the bottom of large parts of the lake.

Major taxonomic references used in the study were Hustedt (1930), Huber-Pestalozzi (1942), and Patrick and Reimer (1966). Also of considerable value were Rawson (1956), Lund (1962), Bradbury (1974), Remane (1971), Hutchinson (1967), and Sheath and Munawar (1974).

References

Adshead, J.D.
1978: Diatomaceous arctic lake sediment; in Current Research, Part A, Geol. Surv. Can., Paper 78-1A, "Notes".

Bradbury, J.P.
1974: Ecology of freshwater diatoms; edited transcription of a symposium held at Cedar Creek National History area, Univ. Minnesota, October 16-18, 1970, Contribution 108, Limnol. Res. Cen., Univ. Minnesota; Nova Hedwigia, v. 24, p. 145-168.

Edwards, T.W.D.
1977: Diatom stratigraphy of Yandle Lake, District of Keewatin, Northwest Territories; unpubl. B.Sc. thesis, Queen's University, Kingston, 41 p.

Huber-Pestalozzi, G.
1942: Das Phytoplankton des Süsswasser, 2. Teil, 2. Halfte; in Die Binnengawässer; 549 p., 645 figs.

Hutchinson, G.E.
1967: A Treatise on Limnology, Volume 2; John Wiley and Sons, Inc., New York, London and Sydney, p. 306-489.

Hustedt, F.
1930: Bacillariophyta (Diatomeae); in Die Süsswasser – Flora Mitteleuropas Heft 10, ed. A. Paschner; Jena, Verlag von Gustav Fisher, Prague, 466 p., 875 figs.

Lee, H.A.
1959: Surficial geology of southern District of Keewatin and the Keewatin Ice Divide, Northwest Territories; Geol. Surv. Can., Bull. 51, 42 p.

Lund, J.W.G.
1962: Phytoplankton from some lakes in northern Saskatchewan and from Great Slave Lake; Can. J. Bot., v. 40, p. 1499-1506.

Patrick, R. and Reimer, C.W.
1966: The Diatoms of the United States, Volume 1; Acad. Nat. Sci. Philadelphia, Mono. 13, Philadelphia, Penn., 688 p.

Rawson, D.S.
1956: Algal indicators of trophic lake types; Limnol. Oceanogr., v. 1, p. 18-25.

Remane, A.
1971: Biology of Brackish Water, Part I, Ecology of Brackish Water; John Wiley and Sons, Inc., New York, Toronto, Sydney, 210 p., 81 figs.

Sheath, R. and Munawar, M.
1974: Phytoplankton composition of a small subarctic lake in the Northwest Territories, Canada; Phycologia, v. 13, no. 2, p. 149-161.

Shilts, W.W. and Dean, W.E.
1975: Permafrost features under arctic lakes, District of Keewatin, Northwest Territories; Can. J. Earth Sci., v. 12, no. 4, p. 649-662.

Shilts, W.W., Dean, W.E., and Klassen, R.A.
1976: Physical, chemical, and stratigraphic aspects of sedimentation in lake basins of the eastern arctic shield; in Report of Activities, Part A, Geol. Surv. Can., Paper 76-1A, p. 245-254.

75.

QUELQUES INTERPRÉTATIONS DE L'INVENTAIRE DES DÉPÔTS DE SURFACE, PÉNINSULE NORD-EST DU NOUVEAU BRUNSWICK

Projet 760008

R.C. Gauthier[1]
Division de la science des terrains

Résumé

Gauthier, R.C., Quelques interprétations de l'inventaire des dépôts de surface, péninsule nord-est du Nouveau Brunswick; Current Research, Part A, Geol. Surv. Can., Paper 78-1A,p. 409-412, 1978

Un glacier avec un écoulement régional vers l'est a occupé la région étudiée, tel que le montrent la configuration de la dispersion des erratiques, les orientations des stries glaciaires et les trames de till. Par la suite, la morphologie du secteur ouest, les Hautes-Terres, a été modifiée par le passage d'un lobe glaciaire dont l'écoulement s'effectuait vers le nord-nord-est. Dans les Basses-Terres, l'événement équivalent serait une progression des glaces vers le nord-nord-ouest. Cette hypothèse explique la présence de sédiments rythmiques lacustres dans la vallée de la Sévogle, résultant du blocus de la vallée de la Miramichi Nord-Ouest. L'altitude de la submersion marine dans la région varie entre 125 et 250 pieds. L'ampleur de la déformation glacio-isostatique place l'altitude relative de la phase lacustre de la vallée de la Sévogle à 235 pieds, avec un exutoire vers le nord à 260 pieds.

Introduction

Au cours de l'été 1977, les travaux de cartographie à l'intérieur des limites de la carte N.T.S. 21P ont permis de compléter le levé des dépôts glaciaires et post-glaciaires de la région de Bathurst. Ces travaux ont été entrepris au début de l'été 1976; l'ensemble des régions accessibles de la feuille topographique 21P (échelle 1:250 000) a été visité. Quelques-uns des aspects de l'histoire glaciaire de la région ont été décrits dans un rapport antérieur (Gauthier et Cormier, 1977); on complète ici cette discussion par l'apport d'éléments nouveaux et en suggérant quelques hypothèses de travail.

Pendant les étés 1976 et 1977, une évaluation des ressources granulaires a été menée par le ministère des Ressources naturelles du Nouveau-Brunswick (Barnett et al., 1977). Les cartes N.T.S. suivantes à l'échelle 1:25 000 ont été publiées: 21P/13 (Brinsmead, 1977) et 12P/12 (Finamore, 1977). Des travaux similaires sont en cours de rédaction pour les régions des feuilles topographiques 21P/5, 21P/4 et 210/16. Une évaluation de la qualité des tourbes et de la dimension des tourbières est également supportée par le même Ministère, dans la région côtière de la carte 21P (Korpijaakko et al., 1977).

Direction de l'écoulement glaciaire

Étude de la dispersion des erratiques

Trois sources de roches de lithologies distinctives ont été utilisées pour baser les études de dispersion des erratiques glaciaires. Ces sources sont localisées à la figure 75.1. Les comptages d'erratiques ont été réalisés au cours des travaux de cartographie et complétés au besoin par des comptages subséquents, localisés dans des régions clefs.

Le stock granitique du lac Antinouri (21P/13) montre une dispersion des erratiques de granite vers l'est, conformément à la direction des stries glaciaires dans le même secteur. Cette dispersion présente des valeurs de concentration de 5% de matériel granitique à l'intérieur des tills de fond et d'ablation et des dépôts de contact glaciaire, à une distance de 8 km de la source. Aucun transport vers le nord et vers l'ouest n'a été observé.

Les granodiorites de stock du lac Nigadoo (21P/12) fournissent un système de dispersion plus difficile à interpréter. Des proportions importantes de granodiorites (>5%) sont présentes au nord et à l'ouest du lac Nigadoo. Ces observations sont contradictoires à celles du lac Antinouri, où le transport se fait préférentiellement vers l'est. Elles sont également en opposition avec le registre des stries glaciaires de ce secteur, qui indique un écoulement glaciaire vers l'est. Ces anomalies semblent refléter la présence d'intrusions inconnues autour du secteur du lac Nigadoo. Il est possible cependant qu'un mouvement vers l'ouest antérieur au mouvement vers l'est (Gauthier et al., 1977, tableau 76.1) soit responsable de cette dispersion. Les évidences d'un écoulement vers l'ouest sont préservées localement dans le registre des stries des régions environnantes. Il n'en demeure pas moins que la dispersion principale des erratiques s'est effectuée vers l'est.

Le dyke de diabase de Caraquet (carte 21P/11) représente une source d'erratiques distinctive dont la dispersion par l'action glaciaire s'est faite tant vers l'ouest que vers l'est. Cette dualité de la dispersion reflète la complexité de l'activité glaciaire dans la région des Basse-Terres et suggère l'existence de deux directions opposées de l'écoulement glaciaire.

Compilation des stries glaciaires

À l'intérieur de la région des Basses-Terres, à cause de la faible résistance à l'érosion des grès, très peu de surfaces de polis glaciaires ont pu être observées. Les sites de polis glaciaires sont rares pour deux raisons. D'une part, la faible résistance mécanique du grès ne permet pas toujours au glacier de développer une surface d'érosion unique, mais forme plutôt une zone de roche fracturée entre la roche saine et le till. D'autre part, la météorisation physique détruit rapidement par écaillement les affleurements de grès polis qui sont exposés en surface. Chaque site à l'intérieur des Basses-Terres est indiqué à la figure 75.1. Quatre sites de polis glaciaires ont des stries orientées vers l'est; les autres sites striés (six) de cette région indiquent un écoulement glaciaire vers le nord et le nord-ouest. Cette direction d'écoulement glaciaire semble être reliée au dernier glacier dans la région, car les trames de till et les dépôts morainiques frontaux suggèrent une même direction d'écoulement. Ce mouvement glaciaire, associé au dernier glacier, est distinct de celui observé à l'intérieur des Hautes-Terres. Ce contraste sera souligné plus loin, à la lumière d'une hypothèse de mécanisme glaciaire.

[1] Département de Géologie, University of Western Ontario N6A 5B8

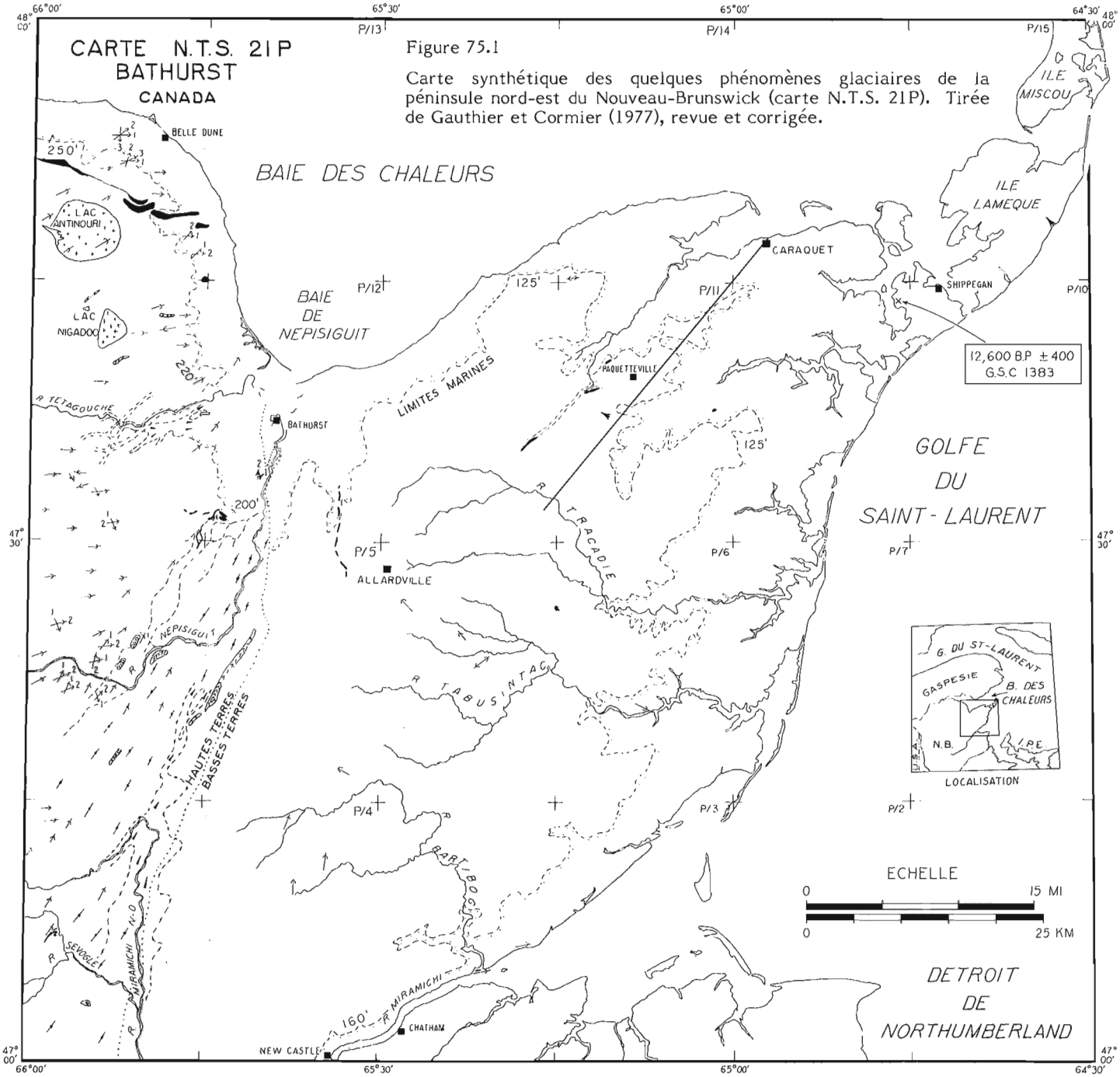

Figure 75.1

Carte synthétique des quelques phénomènes glaciaires de la péninsule nord-est du Nouveau-Brunswick (carte N.T.S. 21P). Tirée de Gauthier et Cormier (1977), revue et corrigée.

- Sédiments de contact glaciaire: moraines frontales, terrasses de kame, dépôts glacio-marins
- Sédiments fluvio-glaciaires
  - eskers, sens de l'écoulement inféré
  - plaine d'épandage de contact glaciaire, épandage sous-glaciaire
- Chenaux d'eau de fonte glaciaire, chenaux proglaciaires
- Limite de l'extension du lac proglaciaire
- Sens de l'écoulement des eaux de fonte
- Chenaux préglaciaires
- Surfaces fuselées (linéations et drumlins)
- × Localisation d'une datation au radiocarbone
- Synthèse des stries glaciaires d'un secteur; 1, 2: chronologie relative perçue
- Trame de till, direction modale de l'orientation des cailloux
- Limite de submersion marine 200', 125': altitudes maximales perçues, en pieds
- Division physiographique majeure: Hautes-Terres et Basses-Terres
- Dyke de diabase: dyke de Caraquet
- Stocks de granite et granodiorite, sources d'erratiques
- Limites des cartes topographiques N.T.S. au 1:50 000
- P/5 Numéro de la carte N.T.S. au 1:50 000

Trames de till

Une étude de la trame de till d'une section exposée le long de la côte est de l'île Lamèque suggère clairement que l'écoulement glaciaire s'est fait vers le nord-ouest. L'imbrication des cailloux est particulièrement bien développée à l'intérieur du till étudié et permet de déterminer avec sûreté le sens de l'écoulement glaciaire. Une autre compilation dont les résultats sont moins clairs, dans la région de Paquetteville, corrobore la compilation de l'île Lamèque. Ces observations sont comparables au relevé de la direction des stries glaciaires orientées vers le nord-ouest, dans la même région.

Sédimentation glaciaire

Dans les Hautes-Terres, le retrait du dernier glacier a laissé des évidences morphologiques abondantes de l'activité glaciaire. Une gamme variée d'évidences, telles les formes fuselées, les chenaux d'eau de fonte, les complexes morainiques frontaux, suggèrent le retrait d'un glacier actif dans cette région. Dans plusieurs secteurs de la région des Basses-Terres on rencontre des sédiments glaciaires qui témoignent de la présence d'un glacier non actif à son stade final. Ces dépôts ont généralement une apparence morphologique indéfinie; la présence de kettles, de kames, de zones mal drainées et marécageuses représentent les éléments les plus caractéristiques de ces unités. À l'intérieur des Basses-Terres, les dépôts glaciaires demeurent abondants, mais les formes de contact glaciaire sont plus rares et fragmentaires; les formes d'érosion macroscopiques sont absentes. Le bilan glaciaire de la région des Basses-Terres était plus faible, provoquant localement l'apparition de zones de stagnation glaciaire, au cours de la période du retrait des glaces. L'expression, glaciaire des Basses-Terres, reflète l'influence d'une région topographique uniforme et elle contraste avec la sédimentation glaciaire dynamique des régions accidentées des Hautes-Terres.

Les sédiments d'origine glaciaire sont présents sur l'ensemble de la péninsule. Les îles Miscou et Lamèque sont marquées par la présence d'un till de fond compact, silteux et rougeâtre. Le long de la côte, en autant que les dépôts glaciaires sont accessibles, on retrouve un till de fond reflétant les caractéristiques du grès des Basses-Terres. Il n'y a pas de doute pour l'auteur que l'ensemble de la péninsule a été recouvert par les glaciers, contrairement aux interprétations de Chalmers (1895, p. 97). La présence d'un till de fond compact sur les îles Miscou et Lamèque (île Shippegan de Chalmers) est commune. Le long des côtes érodées par par la mer et dans les excavations récentes, ce till apparaît au sommet du roc fragmenté, duquel il se dissocie par le caractère silteux de la matrice et la compaction du dépôt. La diversité lithologique des particules dans le till est un autre caractère qui supporte l'idée d'une origine allochtone du dépôt. Le till est généralement recouvert d'une couverture de dépôts marins sableux.

Submersion marine post-glaciaire

Les évidences de la submersion marine post-glaciaire sont perceptibles sur l'ensemble des régions côtières étudiées, quoique les sédiments reliés à cet événement soient souvent présents en quantité restreinte. Il est généralement difficile de déterminer la limite maximale de submersion marine pour la région. Les évidences proviennent d'observations morphologiques associées à un changement textural des dépôts glaciaires. Un bris de pente continu relié à l'apparition d'un till de fond remanié (changement de structure et de texture) constitue l'association décisive d'éléments la plus fréquente pour déterminer l'altitude maximale de la submersion marine d'un secteur. De telles observations sont rares, mais elles permettent néanmoins de définir la position de la mer post-glaciaire pour l'ensemble de la péninsule étudiée. Les sites caractéristiques sont localisés à la figure 75.1

La limite maximale de submersion marine est tracée sur la figure 75.1. À partir de cette compilation, une synthèse des données est présentée à la figure 75.2. On trace sur cette carte les isobases de l'amplitude de l'émergence à partir des indications locales de l'altitude maximale de l'invasion marine post-glaciaire. Cette interpolation permet de définir l'ampleur relative du déséquilibre glacio-isostatique post-glaciaire.

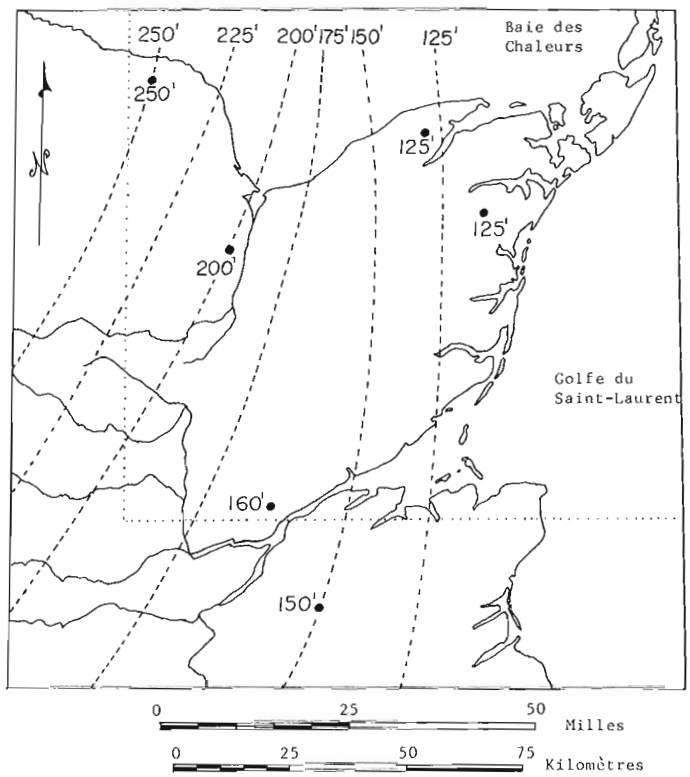

Figure 75.2 Isobases de la déformation glacio-isostatique tracées à partir de l'évaluation de l'amplitude de la submersion marine post-glaciaire de la région étudiée. Lignes pointillées: limite de la région étudiée; lignes en tirets: isobases de la déformation isostatique, valeurs exprimées en pieds; points: valeurs (en pieds) de la submersion post-glaciaire marine maximale.

Lac proglaciaire de la Miramichi Nord-Ouest

Dans la région des Hautes-Terres, un lobe tardiglaciaire est responsable de la majorité des formes sédimentaires glaciaires (eskers et complexes morainiques) et des formes d'érosion glaciaire présentes. La largeur du lobe est d'environ 30 m. Du côté ouest, son extension maximale semble s'associer avec une série de chenaux d'eau de fonte parallèles à la direction de l'écoulement glaciaire; du côté est, le lobe occupe les régions inférieures à une altitude de 500 pieds (la ligne de niveau de 500 pieds est orientée nord-sud et passe du côté ouest d'Allardville). Ce lobe a occupé la vallée de la Népisiguit (Gauthier et Cormier, 1977) et son front a régressé graduellement vers le sud, à l'intérieur du bassin de drainage de la Miramichi Nord-Ouest. Le retrait dans la vallée de la Miramichi Nord-Ouest est à l'origine d'un mécanisme de déglaciation intéressant. Une séquence de sédiments rythmiques à l'intérieur de la vallée de la Sévogle (à 1.8 m de son embouchure), découverte par Shaw (1936), est associée au retrait du lobe précité. La séquence de sédiments rythmiques, d'une hauteur exposée de 4.3 m, est composée d'une quantité minimale de 370 couplets silteux-argileux et silteux-sableux; chaque couplet a une épaisseur moyenne de 1.1 cm. Ces sédiments lacustres grano-classés sont des varves. La séquence est d'origine lacustre et nécessite pour sa mise en place le blocus de la section d'aval de la Miramichi Nord-

Ouest. Au moment où ce lac proglaciaire existait, son seul exutoire logique se trouvait dans la projection vers le nord du coude de la Miramichi Nord-Ouest, à une altitude d'environ 260 pieds. Ce coude est une relique morphologique qui reflète l'inversion du drainage, à la fin de la période du blocus glaciaire. Les évidences morphologiques du déversoir vers le nord sont perceptibles sur les photographies aériennes car les reliques de ce système de drainage contrôlent la position du drainage actuel. Le drainage actuel de la Miramichi Nord-Ouest se fait vers le sud, en conformité avec la pente régionale.

Des sédiments de contact glaciaire, fluvio-glaciaires et glacio-lacustres sont présents à l'intérieur du bassin de la Miramichi Nord-Ouest, au nord de la Sévogle. Les structures sédimentaires observées montrent un écoulement fluvial vers le nord. Des terrasses partiellement préservées reflètent l'environnement sédimentaire, au moment où le retrait graduel du lobe glaciaire formait une plaine alluviale proglaciaire.

Définies à partir des valeurs de l'amplitude de la submersion marine post-glaciaire, les isobases de l'amplitude relative de la déformation glacio-isostatique de la figure 75.2 permettent de déterminer l'altitude relative du plan d'eau dans la région de la rivière Sévogle par rapport à l'altitude de l'exutoire. Cette différence est de l'ordre de 25 pieds, ce qui reporte le niveau lacustre au moment de son existence à une altitude relative de 235 pieds, dans la région de la rivière Sévogle, avec un exutoire plus au nord à une altitude relative de 260 pieds. L'étendue du lac proglaciaire et la position de son exutoire vers le nord sont montrées à la figure 75.1.

Déglaciation de la péninsule

À la lumière de l'interprétation du mode de déglaciation suggéré, un problème important reste à résoudre. Il s'agit de la possibilité de l'influence de deux masses glaciaires distinctes à l'époque de la déglaciation à l'intérieur de chacune des unités morphologiques de la région, les Hautes-Terres et les Basses-Terres. À l'intérieur de la région des Hautes-Terres, deux directions d'écoulement glaciaire indépendantes dominent: l'écoulement régional vers l'est, suivi d'un mouvement vers le nord, contrôlé par la topographie régionale. Dans les Basses-Terres, des évidences diffuses suggèrent la présence d'une direction de l'écoulement glaciaire vers l'est également, alors que la majorité des observations indiquent la présence de glaces s'écoulant vers le nord-nord-ouest. Le mouvement régional vers l'est est présent sur l'ensemble de la région étudiée; il représente la phase glaciaire principale du Wisconsin supérieur dans la région nord-est du Nouveau-Brunswick. Ce mouvement est précédé d'autres dont les évidences sont partiellement préservées (Gauthier et al., 1977, tableau 76.1). Les mouvements glaciaires vers le nord-nord-est dans les Hautes-Terres et vers le nord-nord-ouest dans les Basses-Terres seraient corrélatifs, et marquent le stade terminal de l'histoire glaciaire de la péninsule. L'interrelation entre ces deux directions d'écoulement glaciaire est la question qui a engendré la présente discussion.

À l'intérieur des Basses-Terres, il existe la possibilité de la présence d'un masse de glace dont l'écoulement serait indépendant de celui des glaces des Hautes-Terres. Cette situation demeure hypothétique; le principal problème confronté ici consiste à définir l'extension vers le sud d'un glacier des Basses-Terres. Les évidences connues plus au sud (esker de Després, décrit par Kingston et Brinsmead (1974); Prest (1972), région de Kouchibouguac; observations de stries par l'auteur, région de Rogersville) indiquent un écoulement glaciaire vers l'est. Contrairement aux évidences à l'intérieur de la région étudiée, le front morainique de Paquetteville, la dispersion des erratiques de diabase, les trames de till et la majorité des stries glaciaires suggèrent la présence d'une masse glaciaire dans les Basses-Terres dont la direction d'écoulement est conflictuelle avec celle dans les Hautes-Terres. Du reste, l'hypothèse de cette masse glaciaire indépendante fournit une base intéressante pour expliquer le blocus du drainage de la Miramichi Nord-Ouest et la formation du lac glaciaire. Ce problème demeure en suspens; la solution qu'on y apportera aura un impact important sur le modèle de déglaciation de la région de la péninsule nord-est du Nouveau-Brunswick.

Bibliographie

Barnett, D.E., Brinsmead, R.A., and Finamore, P.F.

1977: Granular aggregate resources on the Belledune Planning District, Gloucester and Restigouche counties; Dep. Nat. Resour. New Brunswick, Mineral Resour. Br., Topical Rep. 77-5, 124 p.

Brinsmead, R.A.

1977: Granular aggregate resources, Maps 1 and 2 (21P/13); from: Barnett et al., 1977.

Chalmers, R.

1895: Surface geology of eastern New Brunswick, north-western Nova Scotia and a portion of Prince Edward Island; Geol. Surv. Can., Ann. Rep. v. VII, pt. M, 143 p.

Finamore, P.F.

1977: Granular aggregate resources, Maps 3 and 4 (21P/12); from: Barnett et al., 1977.

Gauthier, R.C. et Cormier, V.

1977: Cartographie des dépôts superficiels, péninsule nord-est du Nouveau-Brunswick; Geol. Surv. Can., Paper 77-1A, p. 371-378.

Kingston, P.W. and Brinsmead, R.A.

1974: Surficial Geology and Granular Resources of Blackville East (21I/12E); Dep. Nat. Resour. New Brunswich, Mineral Resour. Br., map 1:50 000, plate 74-130.

Korpijaakko, E. and Pheeney, P.

1977: Peatland resources of New Brunswick, Pt. I; Dep. Nat. Resour. New Brunswick, Mineral Resour. Br., Topical Rep. 77-3, 73 p.

Prest, V.K.

1972: Kouchibouguac National Park, eastern New Brunswick, geology; Dep. Indian Affairs and Northern Devel., Unpublished report, 15 p.

Shaw, E.W.

1936: Little Southwest Miramichi-Sevogle rivers area, New Brunswick; Geol. Surv. Can., Mem. 197, 15 p.

76. PORTIONS OF THE NATASHQUAN, MUSQUARO AND HARRINGTON HARBOUR MAP-SHEETS, EASTERN GRENVILLE PROVINCE, QUEBEC – A PRELIMINARY REPORT

Project 760020

J.H. Bourne, K.E. Ashton[1], N. Goulet[2], H. Helmstaedt[3], A. Lalonde[4], and P. Newman[5]
Regional and Economic Geology Division

Abstract

Bourne, J.H., Ashton, K.E., Goulet, N., Helmstaedt, H., Lalonde, A., amd Newman, P., Portions of the Natashquan, Musquaro and Harrington Harbour map-sheets eastern Grenville Province, Quebec – A preliminary report; Current Research, Part A, Geol. Surv. Can., Paper 78-1A, p. 413-418

Twenty thousand km² in the Grenville Province of eastern Quebec were mapped during the summer of 1977. Four main groups of rocks were recognized: (1) basement gneiss complex; (2) metasedimentary rocks (possibly correlative with the Wakeham Group to the west); (3) anorthosite suite; (4) late intrusive rocks. The metamorphic grade of the first three groups is upper amphibolite to granulite. Four sets of folds were mapped within the region; the last two are late and are not fabric forming. No showings of economic interest were found.

Introduction

During the summer of 1977 the eastern halves of sheets 12N (Natashquan River), 12K (Musquaro) and most of the western half of 12J (Harrington Harbour) were investigated on a reconnaissance scale. The centre of the area (Fig. 76.1) is approximately 235 km east-northeast of the town of Havre St-Pierre, Quebec.

In eastern Quebec and adjacent Labrador, the width of the Grenville Province, measured perpendicular to the Grenville Front, is about 450 km. The width of the area mapped, measured in the same manner, is about 200 km. This area thus provides an excellent opportunity to study a cross-section through the entire southern half of the Grenville Province.

The amount and quality of exposures vary widely within the region. Excellent exposures are present along the coast and up to roughly 20 km inland. The zone between 20 and 40 km inland is characterized by low scrub and good outcrop (about 10 per cent of total area). At greater distances the area is treed and outcrop quickly drops off to less than 1 per cent. Exposure is particularly poor in the northern and central portions of sheet 12N, where glacial sand coverage is extensive.

Description of the units

Twenty-one units are described in the section that follows. Some occupy too small an area to be shown on the accompanying sketch map (Fig. 76.2). These have been indicated with an asterisk on Figure 76.2 (legend).

Unit 1 – Granitic gneiss

A large part of the central portion of the map-area comprises a very complex unit of migmatitic gneissic rocks. The composition of these rocks is variable and while no one area can be taken as a type locality, the rocks exposed at lac Rouvel (60°27'W, 50°52'N) are representative of the unit as a whole.

The rocks at lac Rouvel are very complex lithologically. At least five phases are easily discerned in outcrop. The most abundant phase is a light grey foliated quartzofeldspathic gneiss poor in mafic minerals (about 5 to 10 per cent) which makes up about 65 per cent of the unit. The remainder consists of 10 per cent amphibolite, 5 per cent quartz pods, and 20 per cent pink and white pegmatite of variable composition and grain size. The composition of the main unit is itself variable; angular fragments of a more mafic bulk composition are commonly included in the predominant light grey phase.

The light grey unit has what has been called a "porphyroclastic" texture. This results from the presence of pale pink aggregates of potash feldspar which define ovoid-shaped lenses up to 30 mm x 10 mm in size. Their general appearance suggests that they were originally potash feldspar porphyroblasts which have subsequently been deformed.

Unit 2 – Grey gneiss

The grey gneiss complex extends from lac Musquaro to east of lac Cauchy and includes numerous phases. The essential constituent of the complex is a medium grained, grey biotite-plagioclase gneiss which forms approximately half of the unit. The gneiss is generally homogeneous and equigranular; however, potash feldspar porphyroblasts are locally present. Pegmatite and aplite dykes are common in the gneiss, with pegmatites usually more abundant than aplites. Nebulous schlieren of fine grained granitic material were also observed in the grey gneiss. Unit 2 locally contains as much as 20 per cent amphibolite or foliated biotite schist, present as elongated layers or schlieren.

Unit 3 – lac Macé complex

A complex of granitoid rocks of syenitic composition was encountered across the northern portions of sheet 12N. This unit is characterized by distinctive rusty pink weathering feldspars, a homogeneous nature (no quartz veins, amphibolite inclusions, compositional layering), and large grain size. Feldspar phenocrysts of up to 10 cm x 7 cm are present.

[1] Department of Geological Sciences, University of Saskatchewan, Saskatoon, Sask.

[2] Département des Sciences de la Terre, Université du Québec à Montréal, Montréal, Qué.

[3] Department of Geological Sciences, Queen's University, Kingston, Ont.

[4] Department of Geology, University of Ottawa, Ottawa, Ont.

[5] Department of Geology, Dalhousie University, Halifax, N.S.

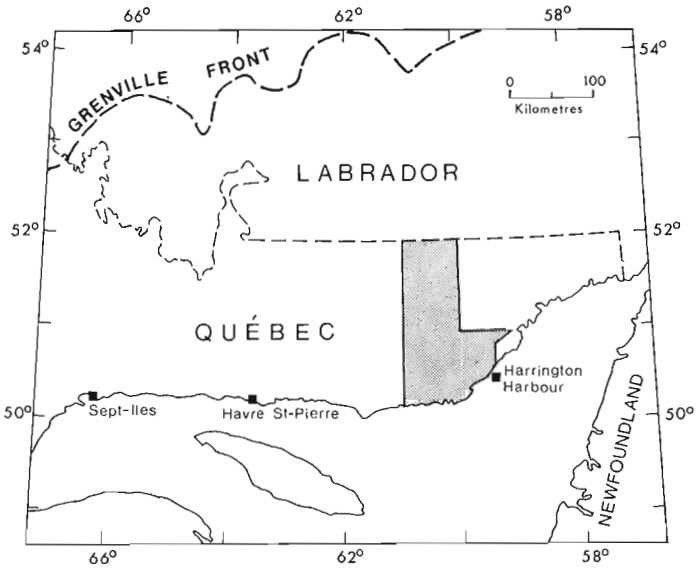

Figure 76.1. Location of the field area.

The homogeneous nature of this unit over considerable areas, coarse grain size, and lack of compositional layering, suggests an igneous parentage.

Unit 4 – Goyelle quartz monzonite

A homogeneous quartz monzonite unit is exposed on the shores of lac Goyelle.

Among the features distinguishing this from other granitoids in the area is the presence of aggregates with a maximum diameter of 40 mm, composed essentially of fine grained potash feldspar crystals with some quartz. Another characteristic feature of the Goyelle quartz monzonite is the presence of large amounts (5 per cent) of euhedral magnetite crystals up to 5 mm in diameter randomly distributed throughout the rock.

As a whole, the unit is quite homogeneous, and contains only minor pink pegmatite dykes up to 20 cm thick and quartz veins. Very small mafic schlieren, composed either of biotite or hornblende, are also present. These are generally less than 15 cm in length and represent less than 1 per cent of the outcrop.

The Goyelle quartz monzonite shows a complete gradation from massive to well foliated varieties. In most cases the foliation is expressed by an elongation of the potash feldspar aggregates.

The origin of the Goyelle quartz monzonite is unknown. The feldspar aggregates may be deformed igneous phenocrysts.

Unit 5 – Charnockitic gneisses

The dominant rock type of the coastal areas of map-sheet 12J from Mécatina Island to Etamamiou is a massive to foliated, homogeneous granitic rock, averaging 15 to 20 per cent quartz and approximately 5 per cent mafics. It usually weathers buff to yellow pink. Fresh surfaces are either pink or a pale to medium green. Green colours are believed to be related to the local attainment of granulite facies metamorphic conditions, although no orthopyroxene was positively recognized in the field.

The rocks range from a homogeneous granitic material through those containing a few mafic xenoliths and/or schlieren to those containing > 20 per cent mafic rocks as layers and xenoliths. Several outcrops were either wholly amphibolite or contained amphibolite bands from 4 to 7 m wide. These are well-foliated rocks showing clear layering, caused by variations in grain size, mafic content and texture of the weathered surface.

No definite conclusions can be made as to the origin of this unit. The presence of quartzites interlayered with the rocks of this unit suggests a metasedimentary origin.

The mineralogy and bulk composition of these rocks suggests a correlation between this unit and the meta-arkoses and impure meta-quartzites of unit 6. The major difference between the two units appears to be the superposed metamorphism. Rocks of unit 6 are upper amphibolite facies, whereas the green colour of unit 5 suggests exposure to granulite facies conditions.

Unit 6 – Pink meta-arkose/impure meta-quartzite

A very thick sequence of meta-arkose and impure (feldspathic) meta-quartzite is exposed along the coast between Wapitagun Sound and Washicoutai Bay. These rocks extend a considerable distance inland, being particularly well exposed in the vicinity of lac Coacoachou. The coastal exposures can be subdivided into two sub-units, namely:

1) a very clean feldspathic meta-quartzite. This sub-unit is almost devoid of mafic minerals. The weathered and fresh surfaces are both pink. The weathered surface, in particular, has a well indurated appearance. The essential minerals are quartz and potash feldspar, with lesser amounts of plagioclase.

2) a "granitic gneiss" which has been interpreted as a meta-arkose. The mafic mineral is biotite, present in amounts of approximately 5 per cent. Quartz is about 30 per cent and potash feldspar predominates over plagioclase. Inland, the hilltop exposures of this sub-unit have rusty streaks resulting from weathering of the biotite so that even though the mafic content is small the foliation direction is easily seen.

Both sub-units have a faint compositional layering. They grade into one another over a distance of 3 m, so there is no doubt that they are closely related.

The relationship of the rocks of this unit to the other units of the area is problematical. To the east the rocks are apparently intruded by the Wapitagun Pluton. The contact between the two is not exposed. The two units lie on opposite sides of a heavily wooded valley. Foliation measurements in both groups of rocks suggest that a "conformable" contact would be observed. To the west these rocks appear to be the lowest exposed unit of the paragneiss suite exposed along the shores of lac Washicoutai and lac d'Aune, underlying a distinctive garnet-sillimanite-bearing marker horizon and occupying the core of a domal structure. The basement to this unit has not been definitively recognized.

The coastal exposures described above apparently grade into more argillaceous rocks to the north and northeast. A typical example of the latter suite is exposed along the shores of lac Triquet. Here the rocks are more mafic-rich, and commonly contain amphibolite horizons. Amphibolite horizons are rare in coastal exposures, although one unit, from 10 to 30 m thick, was traced for over 30 km. In addition, the lac Triquet rocks contain quartzite and rare garnet-sillimanite horizons. In summary, the lac Triquet rocks are lithologically more variable and on the average more mafic-rich than the coastal rocks. Traverses in between the two areas show transitional rock types. It is possible that they reflect an original variation in sedimentary facies. The possible relationship between this unit and unit 5 has already been discussed.

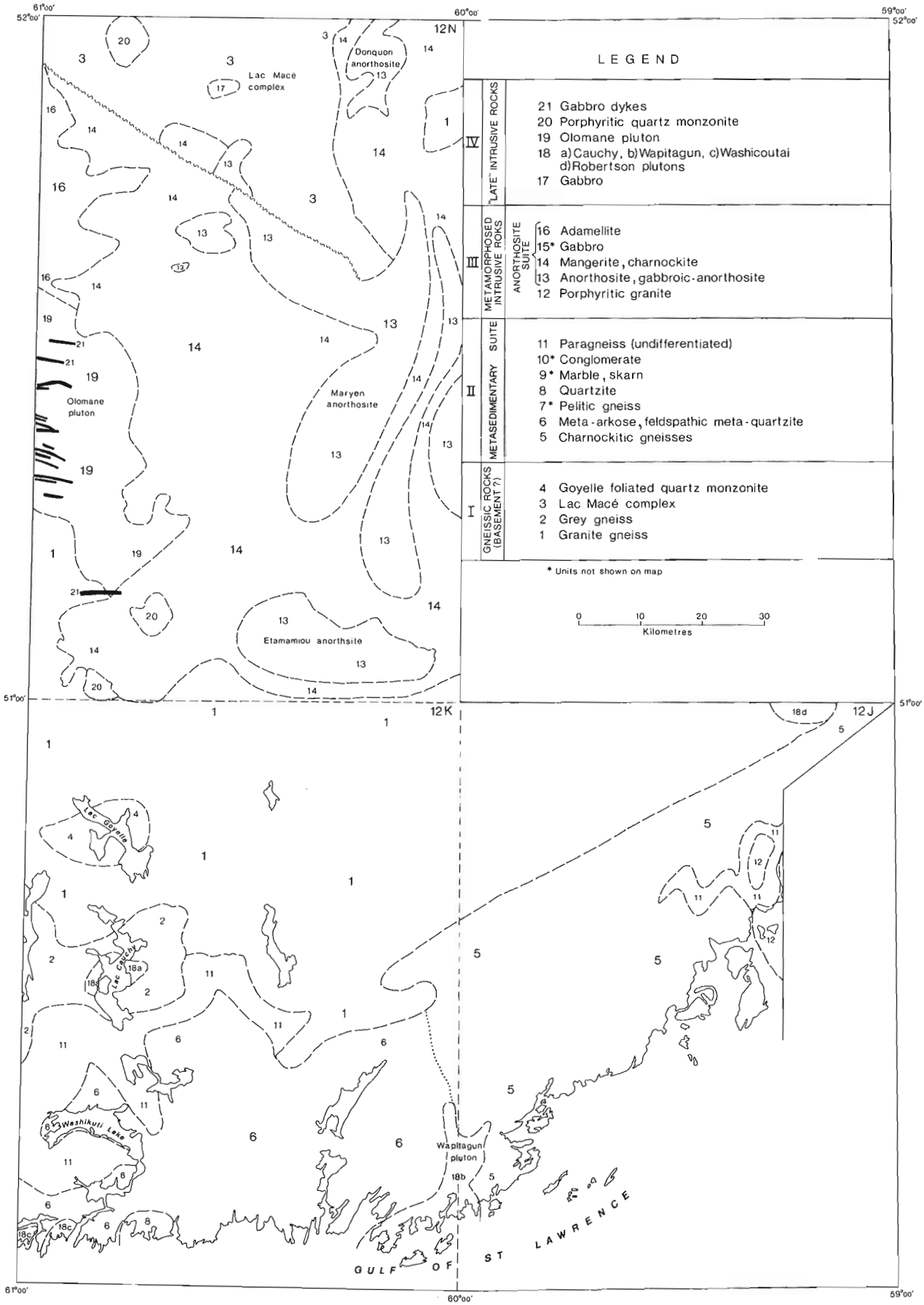

Figure 76.2. Simplified geological sketch map of the region. Units indicated with an asterisk are too small to be shown. Scale 1:1 000 000.

The thickness of the meta-arkose/feldspathic meta-quartzite unit is unknown, since the structural pattern of the area is very complex. It is unlikely to exceed 1500 m.

Unit 7 – Pelitic gneiss

Outcrops of garnet-sillimanite-biotite gneiss are scattered throughout the area studied. In most localities the unit is thin and occurs as layers or lenses in quartzofeldspathic gneisses of uncertain but presumably metasedimentary origin. The best exposures are along the south shore of lac Washicoutai where it lies immediately above unit 6. Megascopic examination strongly suggests the presence of cordierite in the lac Washicoutai area. In the lac Noirclair area, cordierite has been confirmed by X-ray diffraction. Garnet-cordierite-potash feldspar-biotite-quartz is the diagnostic metamorphic mineral assemblage of this unit.

Unit 8 – Quartzite

Orthoquartzite is exposed in the extreme southwestern corner of the map-area, along the sea coast between Coacoachou Bay and lac Washicoutai. It is interlayered with the meta-arkose and impure meta-quartzites of unit 6 and is of variable thickness. In this area, the weathered surface is white to light grey. On the fresh surface it is usually light grey. It constitutes an insignificant proportion of the metasedimentary rocks exposed along the coast.

Unit 9 – Marble/skarn

Marble is best exposed between the towns of Gethsémani and Bluff Harbour, as well as on the shores of lac Robertson and lac Plamendon, the last two being located in the extreme northeastern corner of the area mapped. It comprises only a very small part of the metasedimentary rocks of the map-area and is associated with quartzite, garnet-sillimanite-biotite gneiss and meta-arkose, and amphibolite. The estimated thickness of the marble unit in the lac Robertson area is 50 m and in the Gethsémani area, 30 m.

Unit 10 – Conglomerate

Polymictic conglomerate was encountered in two outcrops, one on the coast in the Gethsémani area, the other on lac Musquaro. Both are thought to represent only minor unconformities. In both outcrops rounded boulders of granitic material exhibit a planar foliation which is at an angle to the foliation seen in the matrix. This suggests that the foliation of the boulders is older than that of the conglomerate, and is therefore evidence of an earlier period of deformation.

Unit 11– Paragneiss (undifferentiated)

Outcrops of highly deformed, inhomogeneous, fine grained granitic material were found at many localities. The association of this unit with rocks of known metasedimentary origin suggests that these rocks may also have a sedimentary parentage. The largest area of this unit is exposed south of lac Washicoutai between this lake and the north shore of lac Couillard. It forms the uppermost part of the stratigraphic sequence of the lac Washicoutai area. In this region the undifferentiated paragneisses are granitic in composition and are garnetiferous throughout. Unit 11 contains numerous schlieren of amphibolitic material parallel to its foliation. In one locality, which consists of a migmatite composed of medium pink granitic material and a white leucosome, the leucosome is cordierite-bearing. Garnet is also found in the same outcrop.

Unit 12 – Porphyritic granite

Porphyritic pink to green granitic rock is well exposed in and northwest of the Tête-à-la-Baleine archipelago. It is foliated and ranges from granite to quartz-syenite. The foliation is the result of the subparallel orientation of 4 x 5 cm deformed pink phenocrysts of potassium feldspar. The green parts of this unit have resulted from local metamorphism to granulite facies. The contact with the surrounding units is conformable and sharp.

Units 13-16 – Anorthosite suite

The anorthosite suite of rocks is the most poorly exposed of the major units. It outcrops in the southern and central portions of sheet 12N where it is largely covered by an extensive sand plain and end moraine. Outcrops of units 14 and 15 are generally highly weathered.

The four main masses of anorthosite (unit 13) encountered are all identical in appearance. They are white to light grey rocks containing less than 10 per cent mafic minerals, typically an altered green pyroxene, and have been deformed to varying degrees. The deformation appears most intense near the margins of the massifs and decreases towards their cores. This deformation is manifested by fine, hair-like white streaks in the plagioclase grains, which often are parallel to the cleavage directions in the plagioclase. Where the deformation is most intense, the rock is white.

The anorthosite massifs, prior to the deformational event, were apparently finer grained near their margins than in their cores. The average diameter of the plagioclase grains near the margin is about 2 cm. However, even here very large, dark grey plagioclase crystals are scattered throughout the rock. These are up to 10 cm across and may originally have been even larger. The actual margin of the anorthosite is gneissic.

The term "charnockite" (unit 14) is used here in a general sense to refer to granitoid rocks and gneissic equivalents which are spatially related to the anorthosite masses, and which contain green feldspars and orthopyroxene. Members of this unit which surround the lac Hakluyt anorthosite mass are medium grained, equigranular (non-porphyritic) greenish coloured rocks. In some outcrops they are homogeneous, but exhibit a strong foliation defined by the preferred orientation of streaked out aggregates of mafic minerals. In other outcrops a distinct compositional layering is present.

The main area of the charnockitic rocks is in the west-central portion of sheet 12N, where they are associated with the distinctive "mottled" aeromagnetic pattern. The rock types range from a pink quartz syenite augen gneiss to greenish rocks of quartz monzonite to quartz dioritic composition.

The anorthositic gabbro unit (unit 15) consists of rocks of gabbroic composition, usually 30 to 40 per cent mafic minerals, which are spatially related to the anorthosite. They are found within the anorthosite massifs as well as around the margins of these massifs.

The gabbroic mass at lac Montcevelles (60°37'W, 51°08'N) is irregular in shape and is separated from the anorthosite to the east by both granite and mangerite. Because the gabbro and the anorthosite are not demonstrably associated at this particular locality, there is some doubt as to whether this particular gabbro should be considered a member of the anorthosite suite.

The foliated, pink weathering, augen-bearing adamellite of unit 16 represents the easterly continuation of a mass described by Bourne et al. (1977). In this area the mass is not spatially related to anorthosite, and no foliated diorite was encountered.

An attempt was made to correlate rock types of units 13-16 with aeromagnetic data, with the following results.

In areas where magnetic intensity is low (56 000 gammas or less) the rock is anorthosite sensu stricto (less than 10 per cent mafic minerals), or syenitic granitoids of unit 3. The major lows are:

a) the lac Hakluyt low along the eastern border of the map-area,

b) the lac Maryen low, southwest of the lac Hakluyt low,

c) the Etamamiou River low located east of lac Montcevelles in the southern part of sheet 12N.

Lows (a) and (c) are associated with anorthosite. No outcrops were found in the area of (b).

Immediately adjacent to the lac Hakluyt low and enveloping it on all sides is a strong linear aeromagnetic high whose associated outcrops are gabbroic (unit 15).

Some distance from the anorthosite lows there is a zone which contains anorthositic rocks but is predominantly green feldspar-bearing "charnockitic" rock. This zone is characterized by the mottled aeromagnetic pattern.

Late intrusive rocks

Unit 17 – Gabbro

One small intrusive mass of gabbro/diorite was encountered in the northern part of sheet 12N, where it is associated with an aeromagnetic high. Although it forms a roughly circular, high hill, it is poorly exposed. It is a massive rock in which blades of plagioclase up to 20 x 3 mm are set in a matrix of greenish, altered mafic minerals and pinkish altered plagioclase. The colour index of the outcrop varies slightly from place to place, but averages about 50 per cent.

In thin section, successive alteration rims of green hornblende, pale blue-green hornblende and finally chlorite, have developed about the primary pyroxenes.

Unit 18a – Cauchy quartz monzonite

The Cauchy quartz monzonite is well exposed on the shore of lac Cauchy. The intrusion is ovoid-shaped with a long axis of approximately 10 km; it consists of a massive to very poorly foliated potash feldsparphyric quartz monzonite. The unit lies completely within the grey gneiss complex. At the contact, the grey gneiss appears somewhat different from elsewhere, probably because of local metamorphic or metasomatic effects related to the intrusion. The unit, although rather homogeneous, contains a few other phases. Among these are pink pegmatite dykes 5 cm to 1 m thick, alaskite dykes up to 2 m thick, and very minor hornblende-rich schlieren or xenoliths up to 10 cm in length.

Unit 18b – Wapitagun Pluton

The Wapitagun Pluton is exposed along both the northern and southern shores of Wapitagun Sound, which is on the coast in the southeastern corner of sheet 12K/1E. The rock consists of two distinct phases: a) a porphyritic, foliated, pink quartz monzonite and b) a porphyritic, foliated grey and white quartz diorite. In the first the phenocrysts are pink potash feldspar up to 5 x 2 cm, but most commonly about 2 x 1 cm. They are set in a groundmass of coarse grained pink material. In the second phase the groundmass is medium grained and the phenocrysts of plagioclase are usually round, as opposed to rectangular, and are commonly 4 cm in diameter.

The shape of the pluton resembles a pear, with the axis of the pear north-south. The grey phase is apparently a marginal phase which envelops the pink phase on the southern, eastern and western margins of the pluton. The pink phase occupies the core of the southern, bulbous part of the complex, as well as all of the more narrow northern portion.

Unit 18c – Musquanousse granite

This mass outcrops in the extreme southwest corner of the map-sheet. Claveau (1950, p. 23-24) named it the Musquanousse mass and described it as a microperthite granite.

Unit 18d – Robertson granite

The Robertson granite is exposed along the shores of lac Robertson in the extreme northeast corner of the map-area. It correlates well with an aeromagnetic high. The field data indicate that this mass is not related to the Mutton Bay syenite (Davies, 1965) in spite of the similarity of their aeromagnetic expressions and geographic proximity. The term "granite" is used here in the broad sense.

Unit 19 – Olomane Pluton

The Olomane Pluton is a porphyritic adamellite extending along the western boundary of the northern half of the area. In the extreme north, it is bounded by a major fault zone and elsewhere it abuts against anorthosite-related mangerite. Its grain size varies from medium to coarse, but large (up to 15 mm) pink and grey feldspar phenocrysts are common. Both plagioclase and potash feldspars make up the phenocrysts. The rock was described by Bourne, et al. (1977) as "hornblende adamellite".

Accessory minerals include fluorite and metamict (allanite?) minerals. Opalescent blue quartz is also present in many of the samples.

Inclusions of quartzofeldspathic gneiss (unit 1?) were found in the pluton.

Unit 20 – Magnetic quartz monzonite

Two small plutons of quartz monzonite with a strong magnetic signature were encountered. These rocks are massive and apparently post-tectonic. Contacts with the surrounding rock types are not exposed. The field appearance of these rocks suggests that they are related to intrusive rock units mapped in the adjacent area to the west (Bourne, et al., 1977), of which the lac la Galissonière pluton is the type example. Similar small circular magnetic anomalies of the type associated with these plutons are seen on the aeromagnetic maps of sheet 13C to the immediate north of sheet 12N. The rock types associated with these anomalies were mapped by Stevenson (1967) as "granite".

Unit 21 – Diabase

An east-west trending swarm of diabase dykes crosses the west-central portion of sheet 12N and is continuous with a swarm of similar trend to the west of the map-area. They post-date all other rock types present in the area.

Metamorphism

With the exception of later intrusive rocks (units 17 to 21) all rocks encountered in the area have been metamorphosed to upper amphibolite or granulite facies conditions. The grade is highest in the extreme southeast portion of the area in the vicinity of Harrington Harbour and along the coast

between Etamamiou and Mécatina. Many of the quartzofeldspathic rocks within this area have the distinctive green colour commonly associated with granulite facies metamorphism although no orthopyroxene was positively recognized in the field. Throughout the remainder of the area the metamorphic grade appears to be no lower than upper amphibolite facies. Primary muscovite was not encountered in quartzofeldspathic gneisses. Migmatites are common in the quartzofeldspathic rocks. In the extreme southwestern portion of the map-area near lac Washicoutai, and farther northeast in the vicinity of lac Noirclair, garnet-cordierite-sillimanite assemblages are present.

Structural geology

The complex deformation shown by most rocks of the area resulted from superposition of at least three and locally, of four sets of structures. Bedding (S_0) in supracrustal rocks is generally obliterated. Marker horizons are scarce, and could not be traced across areas of significant size on this scale of mapping. Early folds of bedding (F_1) have been recognized locally on the mesoscopic scale. A planar fabric (S_1) is related to these F_1 folds and can also be seen as early schistosity in mafic layers which are folded by generally isoclinal F_2 folds. Axial planar to the mesoscopic and microscopic F_2 folds is the major planar anisotropy of the area (S_2), a foliation defined mainly by platy quartzofeldspathic minerals and biotites, but locally also developed in the gneissosity. This planar fabric pervades supracrustal as well as many of the plutonic rocks. The earlier planar fabrics, as well as remnant bedding, are generally transposed parallel to S_2. In pelitic rocks of the lac Triquet area the S_2 fabric deforms garnet porphyroblasts which had overgrown the S_1 fabric. Sillimanite is present in small inclusions parallel to S_1 within the garnets, but occurs also as larger porphyroblasts parallel to S_2, indicating that it was stable during the formation of both S_2 and S_2. S_2 is deformed by two later sets of folds, F_3 and F_4. The relatively tight F_3 folds have shallow plunges and upright axial surfaces which strike east to northeast. F_4 folds are more open, have shallow plunges to the north, and crudely northwest-trending axial surfaces. Those sets of main folds, F_3 and F_4, impinge upon one another to generate spectacular interference patterns which are recognizable on many airphotos of the southern part of the area. Many of these interference patterns are domes or basins of the type 1 pattern of Ramsay (1967); others are mushroom patterns (type 2 of Ramsay, 1967). Both patterns are complicated by interference with the earlier F_2 folds. Neither F_3 nor F_4 folds are associated with a penetrative planar fabric. The only fabrics observed in the field are a weak cataclastic fabric or fracture cleavage; both are localized in the hinge areas of these folds.

Interpretation

The following preliminary interpretation is based exclusively on the field work.

The first four units are considered collectively to comprise the "basement" to the remaining units. The one piece of evidence supporting this assertion consists of a boulder of what is interpreted as part of the Goyelle foliated quartz-monzonite (unit 4) which is found as a cobble in the conglomerate of the metasedimentary suite (unit 10). The cobble itself is foliated and this planar foliation is at a considerable angle to the later foliation formed in the surrounding conglomerate.

Units 1 to 16 inclusive have been affected by an upper amphibolite to granulite facies metamorphic event. The structures observed in the field postdate this metamorphic episode, since in all cases the highest grade minerals observed in the outcrop (sillimanite + K-spar, garnet + cordierite, etc.) have been affected by every phase of folding in the area. Evidence for all earlier structures has been completely eradicated by the F_1 and/or F_2 fold events which, as mentioned above, postdate the granulite facies mineralogy.

Units 17 to 21 are all post-granulite facies intrusive rocks. Unit 17 appears to have been metamorphosed to the greenschist facies conditions, whereas units 19 to 21 inclusive have completely escaped any metamorphic event. No data are presently available for the rocks of unit 18 in this regard. The porphyritic quartz-monzonite (unit 20) is identical to the rocks of unit 8 mapped by Bourne, et al. (1977).

The relationship between the metasedimentary rocks mapped this summer and the Wakeham Group rocks immediately to the west, remains unclear. The rocks exposed on lac Durocher immediately northwest of lac Goyelle are very similar to those of unit 6 in the lac Washicoutai area. Stable muscovite + quartz and the presence of fibrolitic sillimanite on lac Durocher, as opposed to garnet + cordierite + prismatic sillimanite on lac Washicoutai, suggests that the metamorphic grade falls off to the northwest. The Wakeham Group rhyolites and quartzites are located northwest of lac Durocher. It is therefore possible that the metasedimentary rocks mapped here are the higher grade equivalents of the Wakeham Group. However, the Wakeham rocks have been intruded by a large volume of gabbroic material, and these gabbros are not found outside the Wakeham outcrop area (Bourne, et al., 1977). The complete lack of gabbroic material in the metasedimentary rocks suggests that the two are not equivalent. The problem with the former hypothesis is to explain the lack of gabbro in the metasedimentary suite. The problem with the latter is that a boundary between the two supposedly different groups has so far not been recognized.

References

Bassaget, J.P.
1972: Geologie de la région du Lac Musquaro, Comte de Duplessis; Min. Rich. Nat. Qué., open file rep. no. QM-27564, 18 p.

Bourne, J.H., Stott, G., Borduas, B., and Lalonde, A.
1977: Lac de Morhiban and Natashquan River map-areas, Quebec; in Report of Activities, Part A, Geol. Surv. Can., Paper 77-1A, p. 199-204.

Claveau, J.
1950: North shore of the Saint-Lawrence from Aguanish to Washicoutai Bay, Saguenay County; Qué. Dep. Mines, Geol. Rep. 43, 40 p.

Davies, R.
1965: Baie-des-Moutons area, Duplessis County; Min. Rich. Nat. Qué., prelim. rep. no. 543, 13 p.

Ramsay, J.G.
1967: Folding and fracturing of rocks; McGraw-Hill, New York, 568 p.

Stevenson, I.M.
1967: Minipi Lake, Labrador; Geol. Surv. Can., Map 6-1967.

77.

URANIUM MINERALIZATION AT THE BASE OF THE WINDSOR GROUP, SOUTH MAITLAND, NOVA SCOTIA

Project 760045

B.W. Charbonneau and K.L. Ford
Resource Geophysics and Geochemistry Division

Abstract

Charbonneau, B.W. and Ford, K.L., Uranium mineralization at the base of the Windsor Group, South Maitland, Nova Scotia; Current Research, Part A, Geol. Surv. Can., Paper 78-1A, p. 419-425

Field investigations of airborne gamma-ray spectrometric anomalies were carried out in the Windsor-Truro area of Nova Scotia during the summer of 1977. One anomaly, near South Maitland was found to relate to uranium concentrations in Pembroke Formation limestone conglomerate (breccia). Results of this work indicate or suggest the favourability of the base of the Windsor Group for uranium mineralization.

Introduction

During 1976 gamma-ray spectrometry surveys were flown over southern Nova Scotia (Geol. Surv. Can., Geophysical Series Map 35121G; Open Files 466, 467, 468). The survey covering the Kennetcook 1:50 000 scale map sheet over the Windsor basin just west of Truro, Nova Scotia, and extending as far north as Minas basin, is shown by outline A on Figure 77.1 which is a compilation of the geology in the area as published in 1965 by the Nova Scotia Department of Mines. This airborne gamma-ray spectrometry survey was published by the Geological Survey of Canada in September 1977 as Open File 467 and contained in the release were initial results of a ground study made during the summer of 1977 (Charbonneau and Ford, 1977).

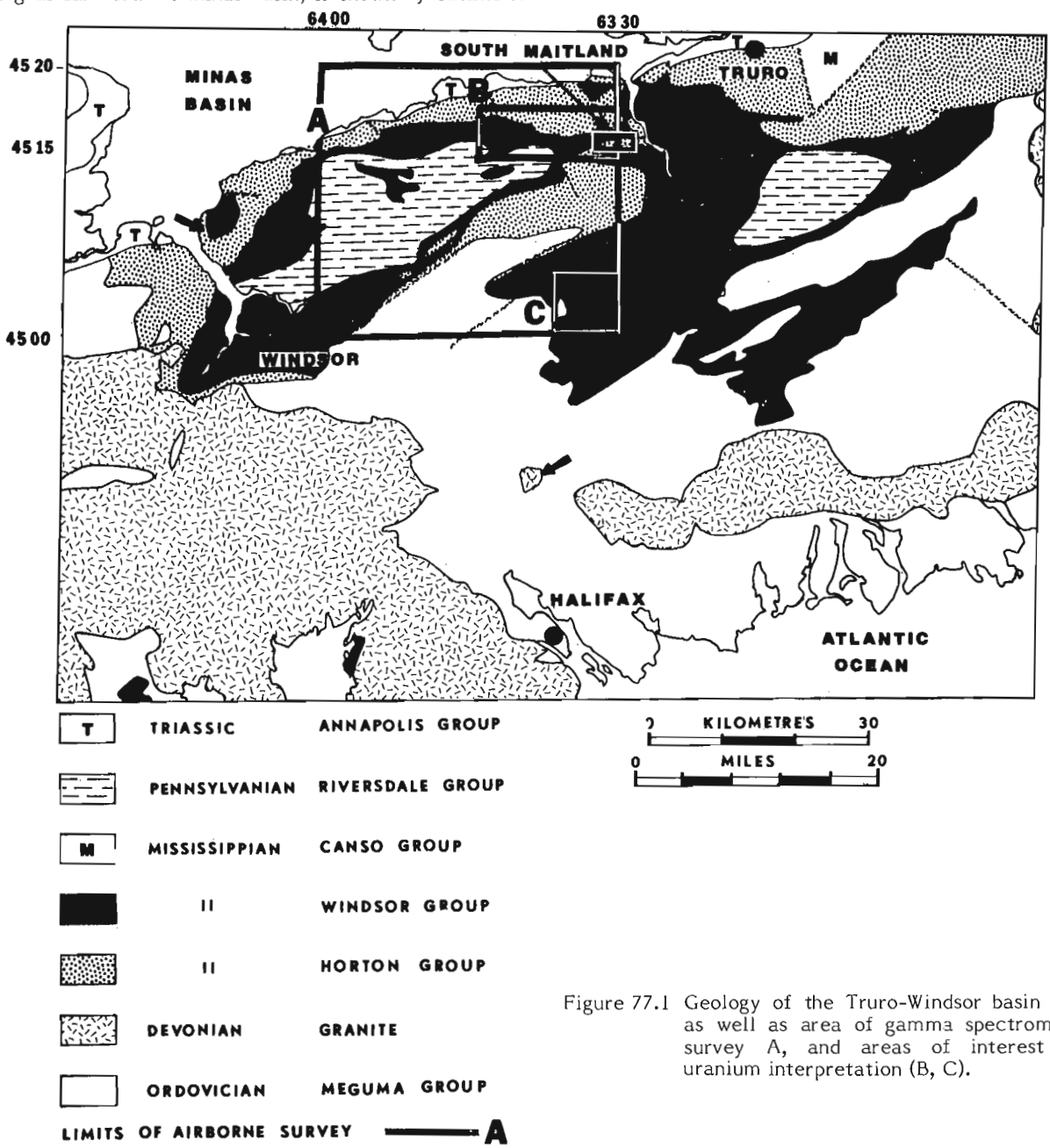

Figure 77.1 Geology of the Truro-Windsor basin area as well as area of gamma spectrometry survey A, and areas of interest for uranium interpretation (B, C).

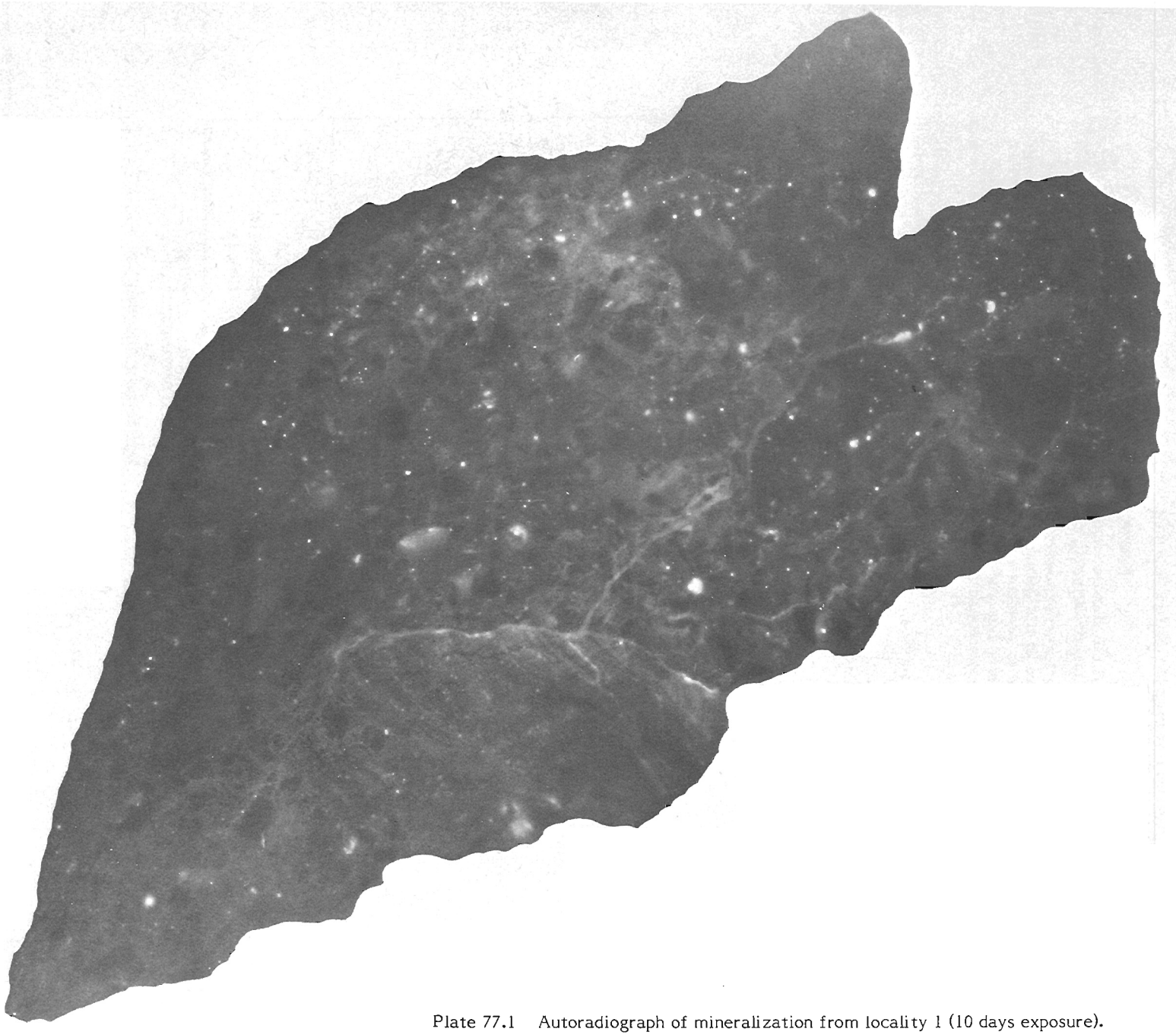

Plate 77.1 Autoradiograph of mineralization from locality 1 (10 days exposure).

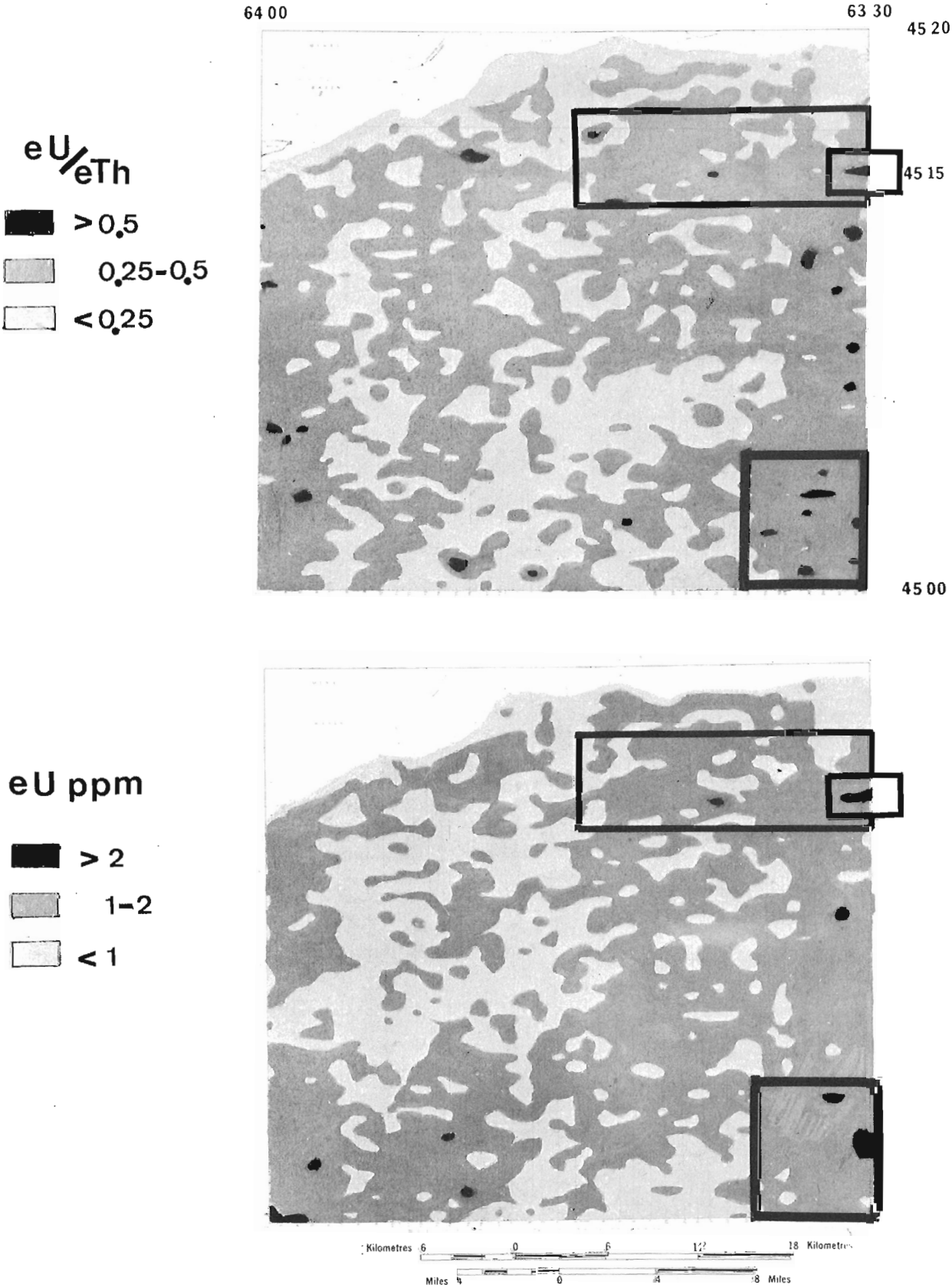

Figure 77.2 Airborne gamma-ray spectrometry survey Kennetcook area eU/eTh ratio and eU ppm.

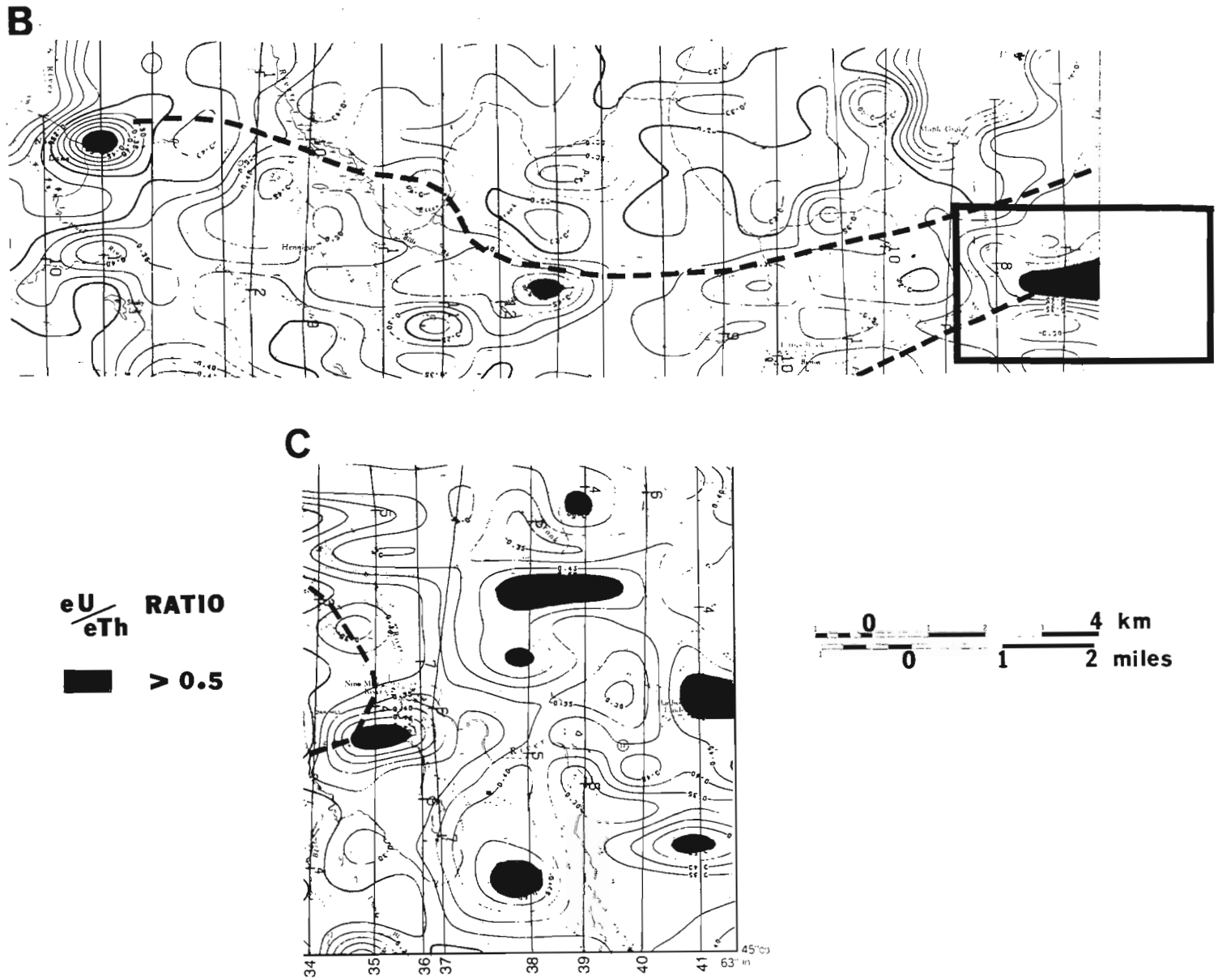

Figure 77.3 Relationship of eU/eTh ratio anomalies >0.5 to the Windsor Horton contact. The Windsor rocks lie with the dashed line.

General Discussion

Examination of the Kennetcook airborne spectrometer survey results (Fig. 77.2) revealed the presence of several areas exceeding 2 ppm equivalent uranium. Ratios greater than 0.5, i.e. more than twice the average crustal eU/eTh ratio, are evident. Such an increase in equivalent uranium along with the increase in eU/eTh ratio may suggest a zone of uranium mineralization. Three of these anomalies correlate with the base of the marine Mississippian Windsor Group which overlies continental Horton Group sandstone and shale as mapped in the area (Weeks, 1948; Stevenson, 1959). Area B on Figure 77.1 locates this area. This correlation was particularly evident between Five Mile River and Noel Lake and the relationship of eU/eTh ratio anomalies to the Windsor-Horton contact can be seen more clearly in Area B on Figure 77.3.

In order to understand the significance of these features, an anomaly was investigated in the Five Mile River area just west of South Maitland, where access was reasonable, the surface relatively undisturbed, and some outcrop was exposed along the river and adjacent slopes. The location of this anomaly, which is on the south limb of a syncline, can be seen on Figure 77.1 as the small rectangle inside Area B and just west of South Maitland. Profile anomalies over the mineralization (Fig. 77.4) are not particularly strong, because of relatively poor exposure.

Figure 77.5 shows the location of ground gamma-ray spectrometry and scintillometry traverses (50 m station spacing) which were made in August, 1977. The approximate location of the 2 ppm equivalent uranium contour from the airborne survey is also drawn on Figure 77.2. The uraniferous rocks were restricted to a relatively thin horizon, composed of the Pembroke Formation limestone conglomerate and brecciated Macumber Formation laminated carbonate (Weeks, 1948; Stevenson, 1959). Since no consensus exists as to the absolute criteria for separating brecciated Macumber Formation from Pembroke conglomerate (pers. comm., P. Giles, N.S. Dep. Mines) the two units have been grouped as basal Windsor on Figure 77.5. In this area it would appear that the mineralized rocks lie between the Horton sandstone and shales (which had uniformly low uranium content in this area) and the evaporitic sequences above the Pembroke-Macumber which are again uniformly low. The mineralized horizon appeared in all exposures to be grey to grey brown. Characteristically a fetid smell was noticed when the rocks were struck with a hammer.

Radioactive spots with scintillometer readings exceeding 200 ur, or approximately 10 times the average regional surface values of about 20 ur (units of radioelement concentration; IAEA, 1976), were noted at eight localities in a zone about 100 m wide and about two km long. The nature of the uranium concentrations is spotty but the distribution of the (U) symbols on Figure 77.5 shows the enrichments are stratigraphically restricted to the basal Windsor. All of the (U) symbols indicated are on bedrock. Equivalent uranium values determined by in situ gamma-ray spectrometry were above 100 ppm at two localities near the western extremity of the anomaly at (U) 1 and (U) 2. The uranium mineralization is best exposed at locality (U) 1 in a cross-section cut by a creek flowing into Five Mile River. More highly radioactive material than the above can be found in float slabs near locality (U) 1. Sample material from (U) 1, gave a laboratory gamma-ray spectrometric analysis of 150 ppm equivalent uranium and sample material from locality (U) 2 gave a result of 425 ppm equivalent uranium. The average of four uranium determinations by neutron activation for samples from locality (U) 1 was 32 ppm and for locality (U) 2 the average was 135 ppm (also four analyses). The difference between the radiometric and elemental uranium values indicates significant disequilibrium in the uranium decay series in this uranium occurrence.

Table 77.1

SAMPLE U 2

Element	PPM
Mn	690
Fe	6629
Co	18
Ni	23
Cu	115
Zn	18
Ag	--
Pb	171
U	135 (Neutron Activation)
U	425 (Radiometric)

Table 77.1 is a typical analysis of metals from the mineralized zone. Only uranium and lead probably of radiogenic origin are present in anomalous concentrations. In addition a phosphate analysis was <0.04% suggesting that the uranium was not present in phosphate minerals.

Minor radioactive increases to about 60 ur were noted in overburden near Hardwood Lands in the southeast corner of the Kennetcook map-area (C on Figure 77.1). Anomalies with eU/eTh ratios >0.5 are shown on Figure 77.3. The area is underlain by rocks of Middle-Upper Windsor age. This suggests that uranium concentrations may exist higher in the section than the basal Windsor. Airborne anomalies similar in appearance to the basal Windsor anomalies are also found over the Ordovician Meguma Group (Fig. 77.1) as can be seen by comparing Figures 77.1 and 77.2.

Large airborne anomalies which exist in the Uniacke sheet to the south (Geol. Surv. Can., Open File 468) appear to relate to the presence of muscovite-biotite bearing (two mica) granitoids. This type of lithology in other parts of Canada often has a high radioactivity and a high eU/eTh ratio – for example north of Yellowknife, Northwest Territories. The Uniacke granitoids could be source material for uranium concentrations in the basal Windsor Group or the source could be in overlying evaporite sequences (Dunsmore, 1977). A traverse of thirteen stations across the small granitoid body to the south marked with an arrow indicated uranium contents of 6 ppm with uranium/thorium of approximately 2.

Mineralogy

An autoradiograph of the mineralization using a ten-day exposure can be seen on Plate 77.1. The conglomerate clasts are rimmed by increased radioactivity (light). As well certain clouded areas suggest dispersed uranium enrichment. Uranium mineral species were not identified by electron microprobe and scanning electron microscope analyses. Furthermore, microprobe investigation of highly radioactive spots indicated by the autoradiograph showed no appreciable uranium concentration. Presumbly these spots represent concentrations of uranium daughter nuclides, and the uranium is dispersed in the rock.

Summary

Only exhaustive examination of the basal Windsor and Upper Horton Group rocks will permit an assessment of uranium potential of this horizon.

However, the importance of rather small anomalies in uranium and uranium/thorium ratio must be emphasized in interpreting airborne gamma-ray spectrometric maps in sedimentary environments. For example, potentially significant U-Cu mineralization has already been reported in Paleozoic rocks of the March Formation in the Ottawa-St. Lawrence Lowlands (Charbonneau et al., 1975a, b).

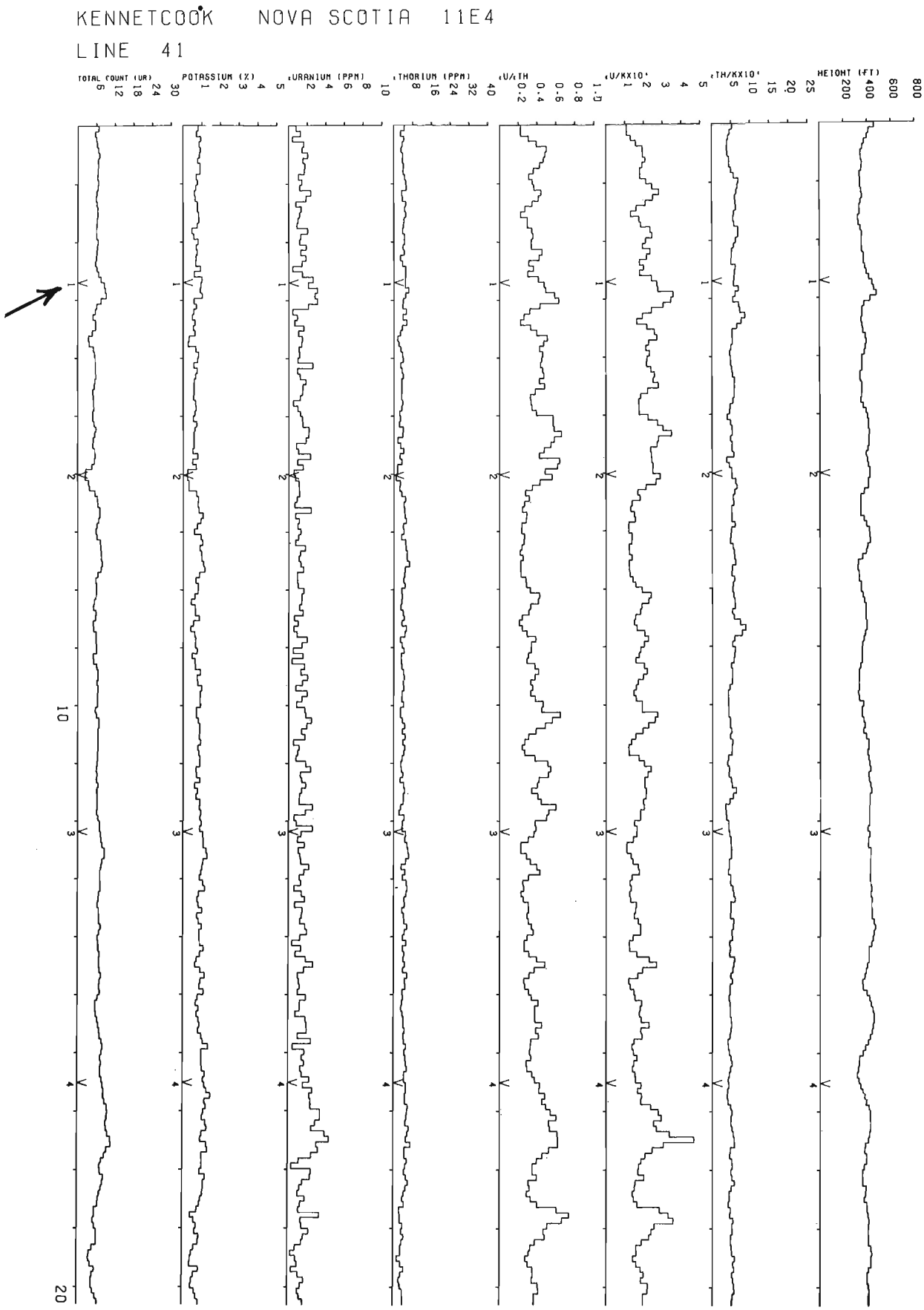

Figure 77.4 Airborne radiometric profile over the South Maitland anomaly.

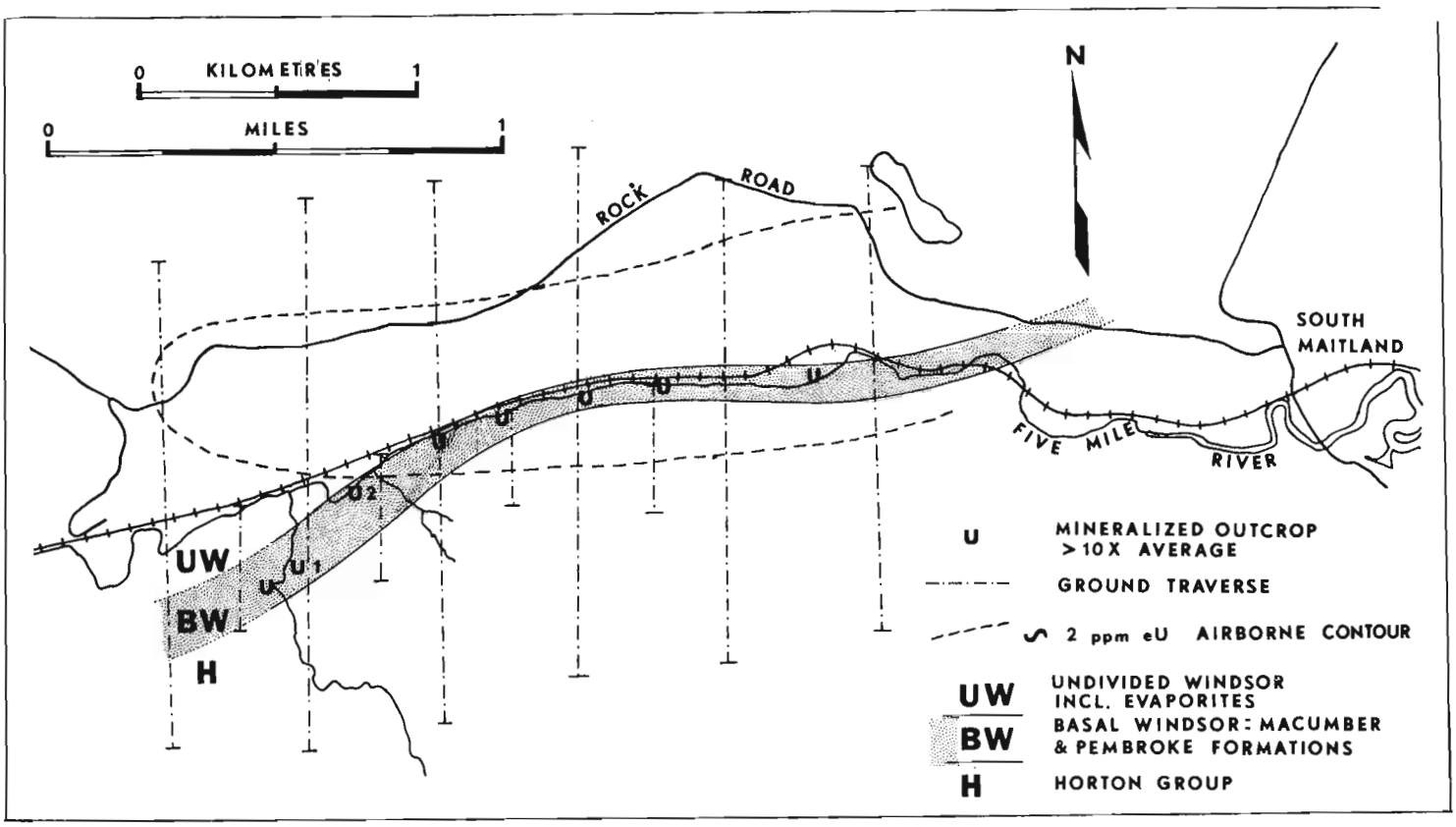

Figure 77.5 Location of ground gamma ray spectrometry and scintillometry traverses made with 50 m station spacing plotted on geology map. Location of the 2 ppm eU airborne contour and the uranium enrichment locations are also indicated.

References

Charbonneau, B.W. and Ford, K.L.

1977: Ground radiometric investigations Kennetcook area, Nova Scotia; in Geol. Surv. Can., Open File 467.

Charbonneau, B.W., Jonasson, I.R., and Ford, K.L.

1975a: Cu-U mineralization in the March Formation Paleozoic rocks of the Ottawa St. Lawrence Lowlands; in Report of Activities, Part A, Geol. Surv.Can., Paper 75-1A, p. 229-233.

Charbonneau, B.W., Jonasson, I.R., Holman, P.B., and Ford, K.L.

1975b: Regional airborne gamma-ray spectrometry and stream sediment geochemistry, detailed ground gamma-ray spectrometry and soil geochemistry in an environment of stratabound Paleozoic U-Cu mineralization in the Ottawa-Arnprior area; Geol. Surv. Can., Open File 264.

Dunsmore, H.E.

1977: A new genetic model for uranium-copper mineralization, Permo-Carboniferous Basin, Northern Nova Scotia; in Report of Activities, Part B, Geol. Surv. Can., Paper 77-1B, p. 247-253.

International Atomic Energy Agency

1976: "Radiometric reporting methods and calibration on uranium exploration"; International Atomic Energy Agency Technical Report Series No. 174, IAEA Vienna, Austria.

Stevenson, I.M.

1959: Shubenacadie and Kennetcook map-areas, Colchester, Hants and Halifax Counties, Nova Scotia; Geol. Surv. Can., Mem 302.

Weeks, L.J.

1948: Londonberry and Bass River map-areas, Colchester and Hants Counties, Nova Scotia; Geol. Surv. Can., Mem. 245.

78.

URANIUM SUBPROVINCES AND TYPES OF URANIUM DEPOSITS IN THE PRECAMBRIAN ROCKS OF SASKATCHEWAN

Project 750058

L.P. Tremblay
Regional and Economic Geology Division

Abstract

Tremblay, L.P., Uranium subprovinces and types of uranium deposits in the Precambrian rocks of Saskatchewan; Current Research, Part A, Geol. Surv. Can., Paper 78-1A, p. 427-435, 1978.

This paper defines three uranium subprovinces in Saskatchewan and describes the main types of deposits that characterize each. Vein deposits of the Beaverlodge-type characterize the Beaverlodge subprovince, disseminated mineralization in sediments the Wollaston uranium subprovince, and vein deposits of the unconformity-type the Athabasca subprovince. Two other types of uranium deposits in Saskatchewan, pegmatite and sandstone, are also described.

Introduction

The area of Saskatchewan underlain by Precambrian rocks is a uranium-bearing province surpassed in importance in Canada only by the area of the Huronian Supergroup in Ontario. This province, for convenience termed the Saskatchewan Uranium Province, is not here considered to include the area east of the Needle Falls Shear Zone because this area, although containing several radioactive pegmatites (Fig. 78.5), is regarded as being outside the main uranium geochemical area of Saskatchewan.

The Saskatchewan Uranium Province comprises three uranium subprovinces, several smaller and less important uranium-bearing districts and large barren areas. The subprovinces are referred to as the Beaverlodge Uranium Subprovince, the Wollaston Uranium Subprovince and the Athabasca Uranium Subprovince (Fig. 78.1). Each subprovince is characterized by several widely distributed uranium occurrences, some of which are economic, and by the predominance of mainly one type of uranium deposit. The smaller districts are represented mainly by pegmatite deposits and, in general, are less well known. The pegmatites of Charlebois Lake area are in such a district.

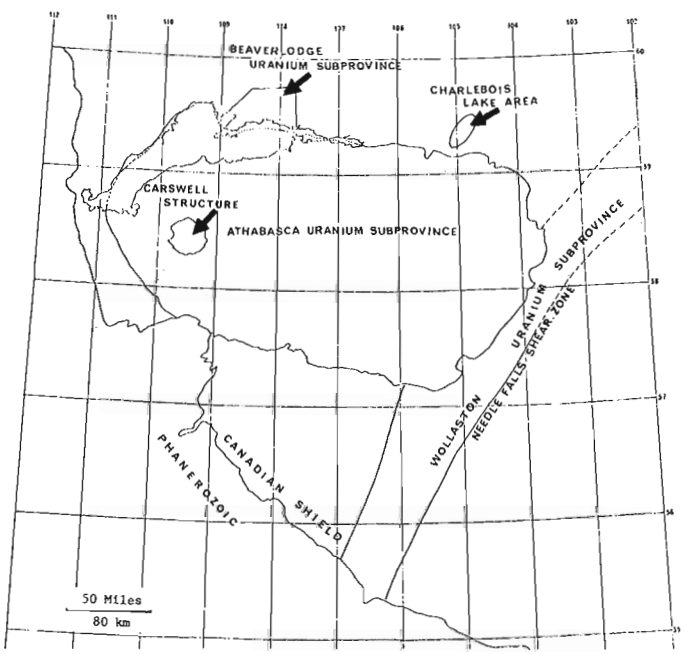

Figure 78.1. Subdivisions of the Saskatchewan Uranium Province. Three subprovinces and a district are shown.

This paper defines the uranium subprovinces named above and gives the characteristics of the main uranium deposit types of Saskatchewan.

Uranium Subprovinces of Saskatchewan

Beaverlodge Subprovince

The Beaverlodge Uranium Subprovince is essentially the Beaverlodge (Uranium City) Mining area (Tremblay, 1972). It is an area of granitized, mylonitized and altered metasediments (Fig. 78.2), and extends to the south to the Gunnar Mine area, to the east to Oldman River area, to the west to Black Bay region and to the north to the area of Hab and Virgin lakes. It is the classic region for vein uranium deposits herein called the Beaverlodge-type. These deposits are generally mineralogically simple (Tremblay, 1958, p. 494) and are characterized by pitchblende fracture fillings. These epigenetic deposits have grades averaging between 0.03 and 0.4% U_3O_8. The minerals commonly present with pitchblende are hematite, chlorite, and calcite, along with minor pyrite, chalcopyrite, galena, quartz and feldspar. A crude metal zoning is suggested locally, particularly by titanium, vanadium, copper and selenium (Robinson, 1955, p. 78). Some deposits have a more complex mineralogy (Robinson, 1955) and carry arsenides and selenides of copper, cobalt and nickel.

The Beaverlodge Subprovince also contains local syngenetic uranium accumulations, mainly uraninite and monazite, in uneconomic concentrations in granitized remnants of country rocks and in granite and pegmatitic areas (Robinson, 1955). These accumulations, are regarded as the source of the uranium of the vein deposits (Tremblay, 1970). The uranium of the veins is assumed to have been mobilized several times and to have been transported in hydrothermal solutions (Tremblay, 1972, p. 221; Beck, 1977). These solutions are regarded as the end product of granitization associated with the metamorphism of the Hudsonian Orogeny. There was a further uranium concentration probably during the Grenville Orogeny when the mylonitized granitized rocks along the major fault zones were intensely shattered.

Wollaston Subprovince

Wollaston uranium subprovince comprises the part of the Wollaston Lake Belt that adjoins the Needle Falls Shear Zone on the east (Fig. 78.1). At Key Lake it is 60 km wide. Northeast of Key Lake it is made up almost entirely of Aphebian metasediments whereas at its southern end the metasediments are intermixed with granitic material and represent less than half of the belt (Fig. 78.3). Uranium mineralization occurs mainly as disseminations in the metasediments and is probably syngenetic. Deposits in this subprovince are mainly uraninite and pitchblende

Figure 78.2

Geology of most of the Beaverlodge uranium subprovince. The localization of the main deposits is also given. Rocks interpreted to correlate with the Fay Complex are shown in the Gunnar area and in the area southwest of Boom Lake fault.

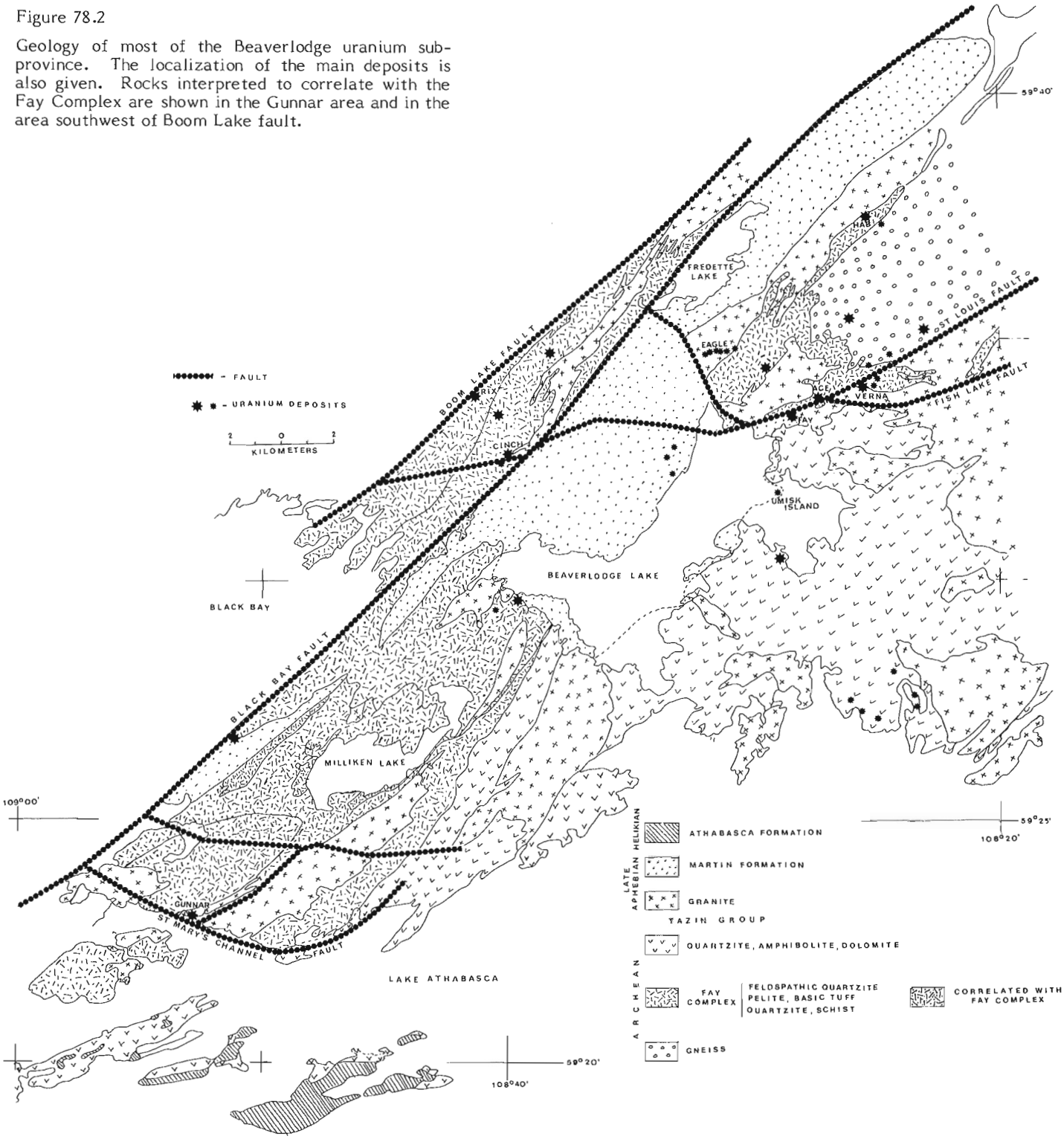

disseminations but also include minor pitchblende veins. The disseminations comprise uranium that was deposited with the sediments and recrystallized when the rocks were deformed and metamorphosed. The uranium in veins came from the disseminations in the metasediments and was deposited when the rocks were metamorphosed. The uranium content of the disseminations is generally less than one pound per ton. Most deposits are small. In addition to uraninite and pitchblende they have minor or trace amounts of pyrite, chalcopyrite graphite, carbon, molybdenite and arsenopyrite. A few deposits are phosphoritic. The disseminations are within the source area of the Helikian Athabasca Formation and are the likely source of the uranium of the deposits related to the Athabasca sandstone unconformity. In addition to the disseminated deposits the Wollaston Subprovince contains local radioactive pegmatites.

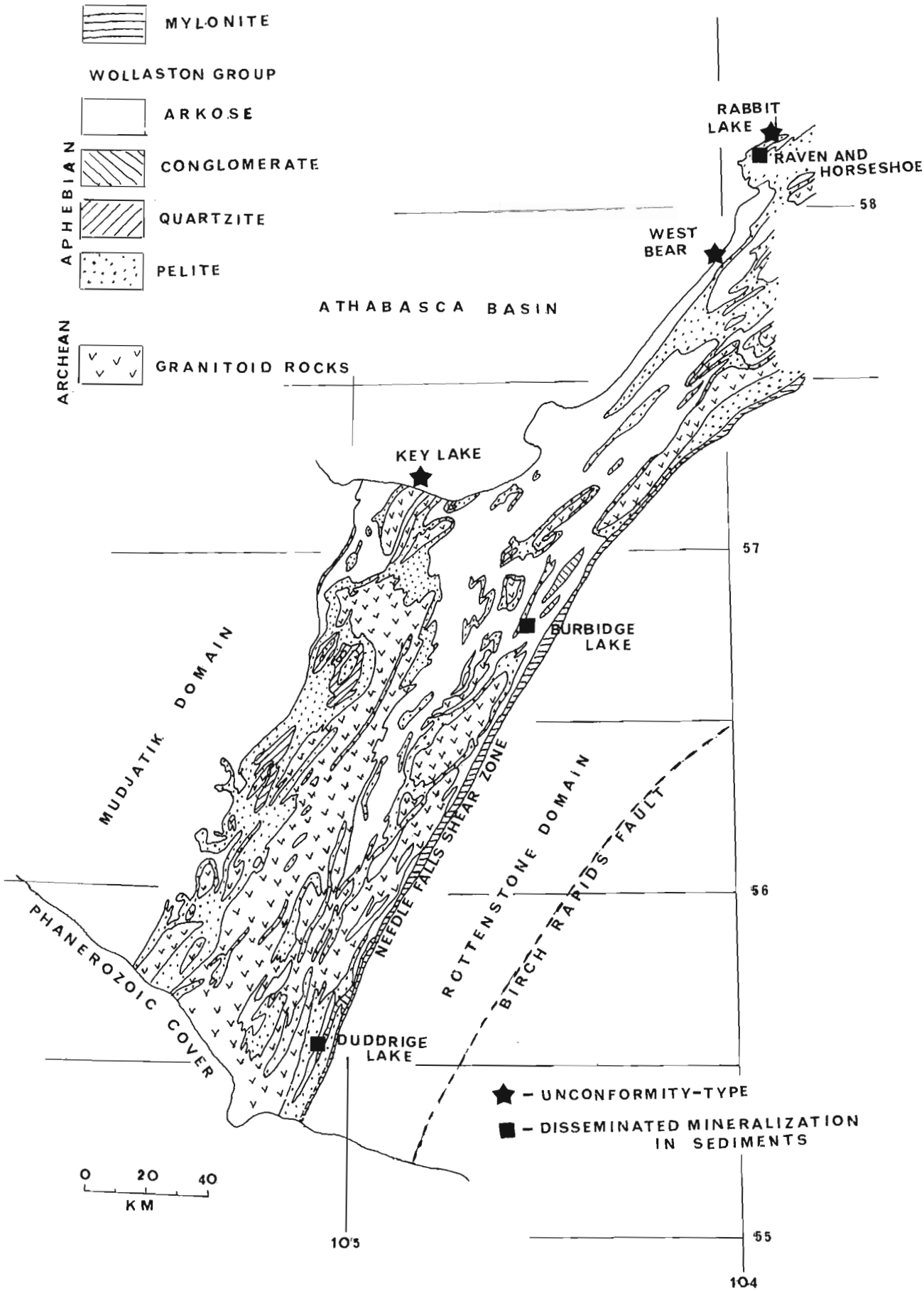

Figure 78.3. Geology of the Wollaston uranium subprovince south of the Athabasca Basin in Saskatchewan. The Wollaston Lake Belt extends to the northeast in Manitoba and probably to the southwest underneath the Phanerozoic cover.

Athabasca Subprovince

The Athabasca Uranium Subprovince comprises essentially the area underlain by the Athabasca sandstone (Fig. 78.1). However, because of the great local thickness (up to 1500 m) of the Athabasca Sandstone this subprovince should probably be limited for practical purposes to a narrow zone at the periphery of the Athabasca Formation and to any areas of thin sandstone within the Athabasca Basin. This subprovince is characterized by vein-type uranium deposits that are termed here 'unconformity-type' to distinguish them from the veins of the Beaverlodge. In the former, the uranium mineralization appears to be localized by the position of the unconformity at the base of the Athabasca sandstone and not by major faults like the veins of the Beaverlodge-type.

The uranium deposits of the Athabasca Subprovince range from small to large and show low to high grade mineralization. Pitchblende and coffinite are the main uranium minerals. Their origin is controversial but it is assumed that the uranium removed from the source rock and taken into solution, was transported and precipitated in the weathered zone probably after the deposition of the Athabasca Formation. This interpretation is supported by the fact that some uranium is found also in the overlying Athabasca Sandstone. However it is possible that the uranium in the overlying sandstone is remobilized from an old deposit along the Athabasca unconformity. Alteration along the unconformity appears to be of two types. The first is characterized by regolithic clay deposits probably formed by weathering under low temperature conditions prior to the deposition of the Athabasca Sandstone. The second is characterized by a mineral association (mainly chlorite and sericite) formed at somewhat higher temperature and superimposed on the low temperature clay alteration. This second alteration also affects the Athabasca sandstone. Dating of the mineralization (Knipping, 1974; Tapaninen, 1975) and of rocks strongly affected by the second alteration (Geol. Surv. Can., Geochronology Laboratory) in company with studies of liquid inclusions (Little, 1974; Pagel, 1975) suggest that the uranium mineralization may be related mainly to the higher temperature alteration.

As shown on Figure 78.5, there are several radioactive pegmatites to the east of the eastern limits of the Saskatchewan Uranium Province. These occur in the area extending from Lac La Ronge in the south to Reindeer Lake in the north and east of the Needle Falls Shear zone. These pegmatites are probably related to the pegmatites of Group A described below, but because the variety of uranium deposits found northwest of the Needle Falls shear zone does not appear to be present in this area, it is not included in the Saskatchewan Uranium Province.

Types of Uranium Deposits

A. Beaverlodge-Type

Type examples of vein deposits of the Beaverlodge subprovince (Figs. 78.2, 78.4) particularly those in the immediate area of Uranium City and the Eldorado mine are those of the Fay-Ace-Verna mines of Eldorado Nuclear Ltd. at Beaverlodge, Saskatchewan (Tremblay, 1972). These deposits have the following characteristics:

1. They are related to faults of crustal dimension, such as the St. Louis, Boom Lake and St. Mary's channel faults. In general these faults extend to great depth, cut areas of granitized rocks and are represented by wide zones of mylonitized and brecciated rocks that commonly have been closely fractured over wide areas, suggesting that the faults were active at intervals over a long time.

2. The uranium is found along subsidiary fractures within the major fault zones. Uranium also occurs over narrow zones in the rocks adjacent to the fractures, particularly in the brecciated parts of the fault zones where uranium also replaces part of the brecciated matrix near fractures and extends as disseminations into the fragments of the breccia. The mechanism of precipitation of uranium along fractures and in openings in the breccia is interpreted as vein filling of open spaces (Robinson, 1955, p. 49). Commonly there is accompanying evidence of retrograde metamorphism.

3. The deposits occur within or near specific lithologies best exemplified by the Fay Complex succession. This succession has been mapped (surface and underground) at the Eldorado Mine as a thinly bedded mixture of white to pink feldspathic metaquartzite, black to grey metapelites and dark green basic tuffs. Similar assemblages are believed to be present near other deposits such as the Rix, Gunnar and Lake Cinch but since the rocks are granitized, strongly cataclastically deformed, and altered, the lithologies are not easily recognized. An apparent preference of uranium for feldspathic quartzite and other highly altered rocks of the assemblage may be due to the tendency for these rocks to fracture more readily than the pelites and tuffs and it is apparent that fracturing in the rocks of this complex was the main mechanism for localization of the uranium minerals. Although some members of the Fay Complex succession are possible source rocks (Tremblay, 1970) these uranium deposits are considered epigenetic and not stratabound (Sassano, 1972) since they occur mainly along fractures.

4. The uranium occurs where red hematitic and dark green chloritic alterations accompanied by white carbonate, are present in the rocks. This alteration is locally so intense as to obliterate the original nature of the rocks. Feldspathization and silicification are also common but are not as diagnostic of uranium mineralization as chloritization, hematitization and carbonatization. The white clay argillic alteration, which is so characteristic of the vein deposits of the unconformity-type described below, is absent in the Beaverlodge-type deposits or is present only in very local areas such as along the Crackingstone River fault southwest of Lake Cinch and along the Donaldson Lake Fault (Trueman and Fortuna, 1976, p. 380). Alteration is assumed to be related to retrogression associated with the deformation and the action of hydrothermal solutions accompanying the uranium mineralization.

5. It is possible that vein deposits of the Beaverlodge-type are related to the Tazin-Martin unconformity at the base of the Martin Formation since most of the vein deposits occur at or near the trace of the unconformity (Langford, 1977, p. 30). Furthermore, many of the deposits do not extend more than a few feet or a few hundreds of feet below the present surface which is locally the unconformity plane itself. However, although the unconformity may be a contributing element, the St. Louis and other major faults are regarded as the main controlling factor in the localization of these deposits. The few deposits in the Beaverlodge area that exhibit a spatial relationship to the unconformity are those in the Eagle Shaft area, on Umisk Island in Beaverlodge Lake and in the West Fay area of the Eldorado mine workings. However, these deposits are small and represent only a minor part of the total uranium mineralization of the Beaverlodge area. The Tazin-Martin unconformity is a secondary channelway along which the uranium-bearing solutions could have circulated (Tremblay, 1972, p. 197). This structural relationship suggests that some of the deposits are later than the unconformity and possibly later than the deposition of most of the Martin Formation. This suggests also that the 1140 m.y. date (Tremblay, 1972; Koeppel, 1968) is possibly the main period of uranium mobilization in the Beaverlodge subprovince. Major ore zones extend to 1500 m depth.

The layer of detritus found locally at the base of the Martin Formation in the Beaverlodge area is the result of mainly mechanical action. Thus, this detritus layer is not of the same type of 'paleosol' (Langford, 1977, p. 29) as that

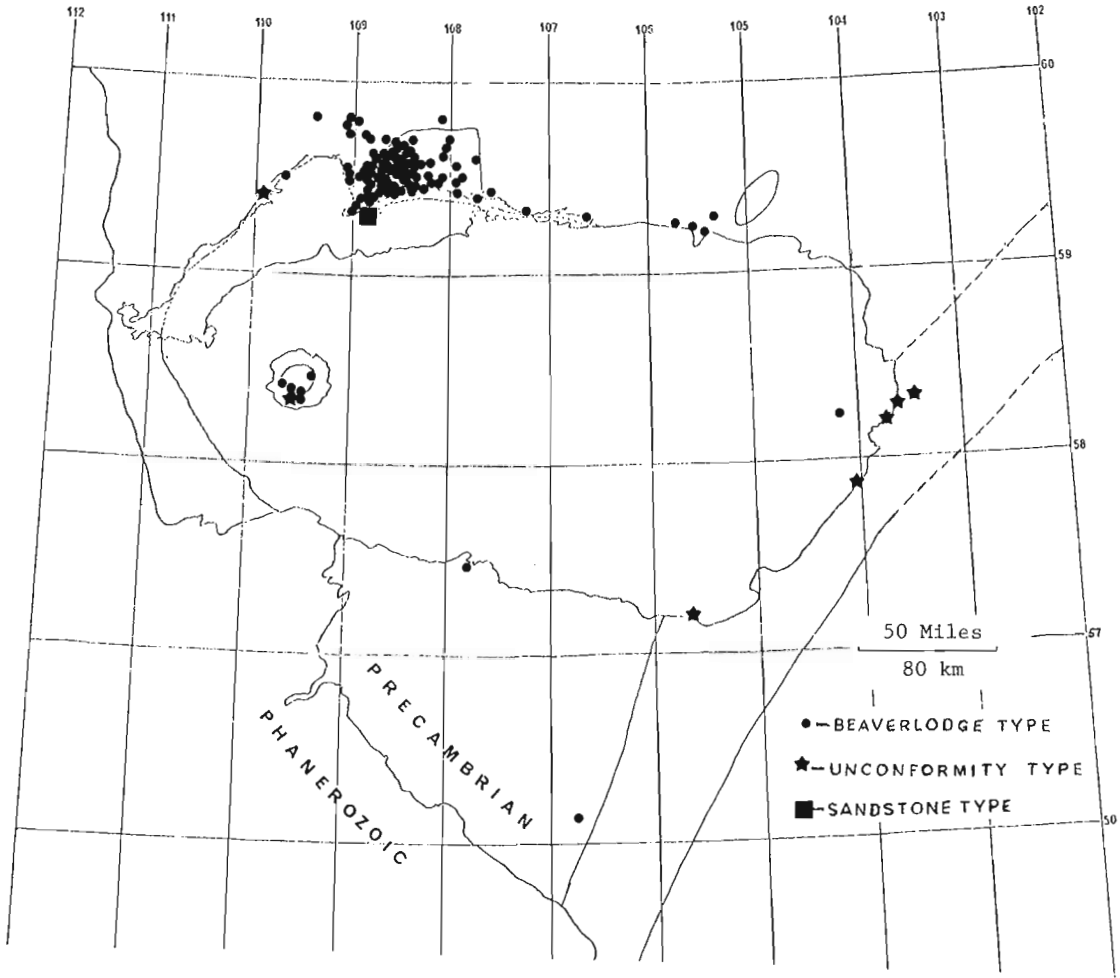

Figure 78.4. Map showing the localization of vein deposits of the Beaverlodge type and their concentration in the Beaverlodge subprovince. The vein deposits of the unconformity-type and a sandstone deposit are also shown.

found at the base of the Athabasca Formation. Accordingly, this feature cannot be used to establish a genetic relationship to the Tazin-Martin unconformity in the same manner as the deposits of the unconformity-type are related to the unconformity at the base of the Athabasca Formation.

The presence of Martin rocks at or near the St. Louis Fault within the workings of the Fay-Ace-Verna mine of the Eldorado property at Beaverlodge was suggested by Sassano (1972), Smith (1974) and Little et al. (1972). These areas of assumed Martin rocks are at a depth of 1000 to 2000 feet and the rocks were described as conglomerate and conglomeratic arkose and a basic volcanic rock. These rocks were assumed to represent remnants of Martin rocks along the plane of the Tazin-Martin unconformity, suggesting that the present plane of the St. Louis fault corresponds in position almost to the plane of the Tazin-Martin unconformity. This assumption led Smith (1974) to state that the mineralization in the Beaverlodge area was always found within 200 m of the unconformity. A study of six thin sections of these rocks by the present writer suggests that they are cataclastic and not clastic and that the volcanic rock is probably a late gabbro dyke and not a flow. This view is also supported by the observation that the assumed remnants of Martin rocks are always related to the plane of the St. Louis fault which dips consistently at 55 degrees to the southeast in this area, and that along the St. Louis fault as along all the other major faults in the Beaverlodge area there are wide zones of mylonitized and brecciated rocks.

6. Pitchblende is the main uranium mineral in the Beaverlodge-type deposits. Secondary yellow uranium minerals are rare but were noted at several places near the surface outcrops of the deposits. Only in the Gunnar mine were they reported at greater depths (about 300 m). Brannerite occurs rarely. Copper, vanadium, selenium and titanium occur in minor or trace amounts. A crude zoning is suspected from the distribution of the above elements in ore zones that have large horizontal and vertical extensions. However, a definite general zoning pattern has not yet been established for the area.

7. The deposits are of two main ages 1780 ± 20 m.y. and 1140 ± 50 m.y. (Koeppel, 1968; Tremblay, 1972). The 1780 m.y. age is regarded as the main age of mineralization in the Beaverlodge subprovince (Tremblay, 1972). However, dates obtained on the unconformity-type deposits in the Athabasca Subprovince suggest that the 1140 m.y. age may have been also an important period of mobilization. This may be true for the entire Saskatchewan Uranium Province.

8. Based on liquid inclusion, stable isotope and petrographic studies, emplacement temperatures of the Fay-Ace-Verna pitchblende were reported by Sassano (1972) as varying from a maximum of 440° ± 30°C to a minimum of 80° ± 10°C. This confirms results previously published by Robinson (1955, p. 100).

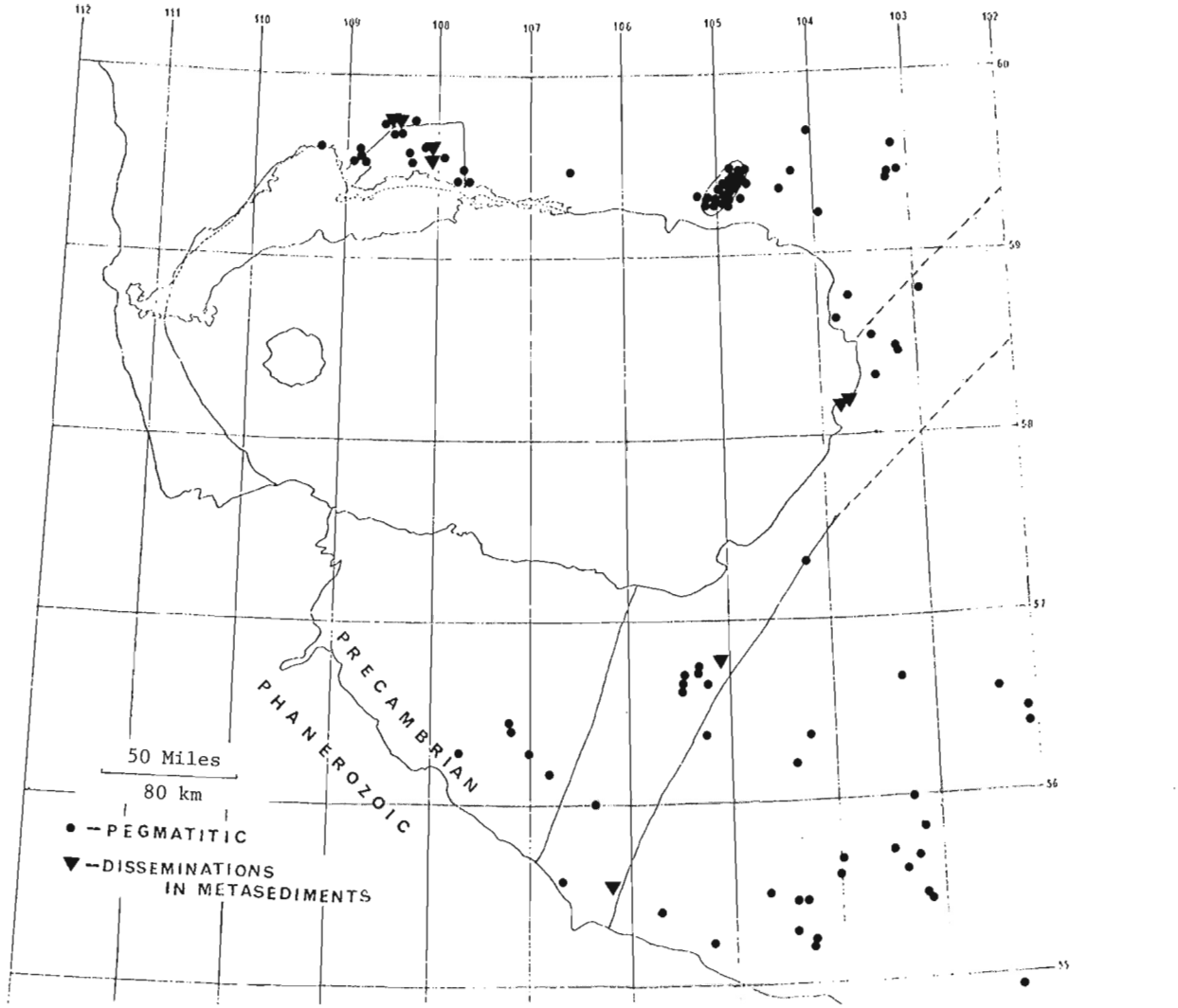

Figure 78.5. Map showing the localization of radioactive pegmatites and of the deposits defined here as disseminated mineralization in sediments.

9. The rocks in the vicinity of the deposits have undergone retrograde metamorphism to the greenschist facies and this is also regarded as an important consideration in the development of the uranium deposits of the Beaverlodge-type. As noted earlier, retrogression is believed to be related to cataclastic deformation and to the action of hydrothermal solutions that accompanied the formation of the deposits.

B. Disseminated Mineralization in Sediments

This type of deposit characterizes uranium mineralization of the Wollaston Subprovince. The uranium is regarded as having been deposited with the sediments that contain it and thus the deposits are considered syngenetic. However, it is assumed that after deposition much of the uranium was taken into solution, and redeposited elsewhere in the section. This is suggested by the presence of minor veins and seams of uranium mineralization and by seemingly enriched areas in an otherwise slightly mineralized horizon.

Examples of disseminated deposits include the Duddridge showing in the Sandfly Lake area at the south end of the Wollaston Subprovince, the Raven and Horseshoe deposits south of Rabbit Lake toward the north end of the subprovince, the Burbridge showing (Beck, 1977) and several other minor occurrences. Figures 78.3 and 78.5 show the location of the known uranium deposits of this type.

The following features are diagnostic of these deposits.

1. The uranium occurs in well layered metamorphosed rocks that were originally probably mainly arkoses, sandstones, feldspathic sandstones and limestones. The latter are now mainly calcsilicate rocks and marbles but their original sedimentary nature is still recognizable.

2. The uranium is generally restricted to a specific horizon or to a few beds within a succession or to a particular facies of these horizons and beds. The uranium concentrations of economic interest are similarly restricted to specific horizons and sections of the succession. In general, uranium concentrations are erratically distributed but most are in conformable lenses, or less commonly in irregular bodies and blebs of various sizes within the mineralized horizons. The uranium-bearing rocks are normally black to dark grey carbonaceous facies of quartzite or quartz feldspar rocks. Less commonly they are light green, calc-silicate-bearing quartzites, calc-silicate rocks of various compositions or phosphorous-bearing beds. Locally they also appear as lenticular bodies of quartzofeldspathic rocks in pelitic horizons or in carbonate rocks. The latter grade locally into the conformable pegmatite type deposits found in metapelites (see later discussion of pegmatites). There are also a few beds of radioactive quartz-pebble conglomerates that are generally high in thorium and low in uranium (Money et al., 1970). The radioactive parts of these conglomerates are small and lenticular.

3. The uranium occurs as uraninite, as finely disseminated sooty pitchblende and as veins of yellow secondary uranium minerals. The uraninite is distributed interstitially amongst the other rock-forming minerals. Pitchblende appears to have formed contemporaneously with uraninite but some may be slightly later as elongated grains resembling hair-line fracture-fillings are present locally. The yellow mineral is much later and occurs mainly along cleavage and schistosity planes. It may be, in part, a phosphate as tyuyamunite has been identified from the same deposits. The uraninite and pitchblende are believed to have formed from uranium derived from the rocks that contain them. Since most of the uranium has remained in its source rock, the uranium concentrations are regarded as syngenetic. In a general way these deposits resemble the stratabound Colorado Plateau type. Their grade is generally less than one pound U_3O_8 per ton but locally reaches five pounds per ton.

4. Other minerals occurring in the deposits include pyrite, chalcopyrite, galena, and locally bornite and molybdenite. Like the uranium minerals these appear to have formed when the rocks were metamorphosed but since they also occur as disseminations along schistosity planes, they may have been in part remobilized with later-stage mineralization.

C. Unconformity-type

The unconformity-type deposits that are characteristic of the Athabasca Uranium Subprovince occur at or near the unconformity at the base of the Athabasca Formation and are held to be genetically related to this unconformity and to the alteration processes that operated along it (Derry, 1976). They are a variant of the general vein type of deposit but they differ from those of the Beaverlodge-type mainly by their close relation in space to the Athabasca unconformity and by the presence of the ubiquitous clay-white alteration. Included in this group are the Maurice Bay deposit, some of the deposits at Cluff Lake, the Key Lake deposits and some of the deposits in the general Rabbit Lake area. The type deposits are those at Cluff Lake and Key Lake. Figure 78.3 and 78.4 show their distribution. The following is characteristic of this deposit type.

1. The uranium occurs at the unconformity between basement rocks and the overlying Helikian Athabasca sandstone. The mineralization is generally confined, in stratigraphic distribution, to within a few tens of metres to a few hundred metres of the unconformity. However, it may show fairly extensive horizontal distribution. Thus, the overall horizontal extent of the Gärtner and Deilmann orebodies at Key Lake reaches about 2.7 km in a northeast-southwest direction but their maximum width is less than 110 m (Dahlkamp and Tan, 1977).

2. The deposits are associated with well defined faults that are present in basement rocks and have affected the overlying sandstone through brecciation and mylonitization and have caused vertical offset of the unconformity plane. The faults are more pronounced in basement rocks than in the Athabasca Sandstone and probably they first developed in the basement and were later reactivated after the deposition of the sandstone. In some instances it seems that the last movement on the fault was later than the mineralization because the ore zones are locally brecciated.

3. The unconformity-type deposits are found both in basement rocks and in the Athabasca Sandstone but the bulk of the mineralization is in the former and in some deposits it is entirely in basement rocks. In rare cases the reverse is true and the mineralization is entirely within the Athabasca Formation. It seems possible that mineralization in the sandstone is in part due to remobilization of uranium from basement deposits.

4. Where deposits occur in the basement the host rocks at the unconformity are generally strongly altered to form a clay white regolithic zone (Hoeve and Sibbald, 1976). The alteration appears to be strongest at the unconformity and is also locally intense along faults in basement rocks where it decreases gradually with depth. However, mineralization is not always present where the alteration is strongest and most extensive.

5. In the vicinity of the deposits the Athabasca Sandstone is also locally intensely altered to a white clay-like mass of chlorites and micas for a few centimetres to a few metres above the unconformity. Thus it seems that some alteration is later than the Athabasca Formation. However, since the alteration does not always show its strongest development at the unconformity it may be of a different origin from the earlier weathering alteration noted in item 4 above. The late alteration also locally affects the basement rocks to great depth and is superimposed on the regolithic alteration in the basement. It also extends locally into the Athabasca Sandstone for a few hundred metres above the unconformity. The cause of the late alteration is still not known but its mineral association suggests a temperature of formation higher than that of the early alteration. Based on fluid inclusions studies on Athabasca Sandstone samples from Cluff Lake and Rumple Lake, the temperature of formation was probably in the range of 60°C to 260°C (Pagel, 1975). The chlorite and the micas representing this alteration are light greenish white and magnesium rich (Rimsaite, 1977).

6. The uranium does not seem to be everywhere restricted in location and distribution to any specific horizon or lithology within a particular stratigraphic succession. However, commonly the basement rocks that are mineralized are graphitic or lie stratigraphically near a graphitic horizon. Such graphitic rocks represent zones where faulting could have developed more readily than elsewhere as any movement would be more readily accommodated by graphitic rocks than by the other commonly associated arkoses and granitoid rocks. It is possible that where only carbonate or calc silicate rocks were present they were the controlling factors of uranium localization. The presence of amphibolite was suggested as possibly important in localizing uranium at Key Lake (Dahlkamp and Tan, 1977) and is suggested for some of the Cluff Lake deposits. It is possible also that the clay of the alteration zone was an added catalytic attraction for uranium mineralization in these deposit-types.

7. The mineralogy of the known deposits ranges from complex to simple, and the distribution of constituent elements is variable and erratic. Pitchblende and coffinite are the main uranium minerals, but secondary yellow, red and green uranium minerals are present locally. Copper, selenium, nickel, gold, silver, arsenic and tellurium may be locally present in significant concentrations but generally they occur in trace amounts only.

8. On the evidence available to date, all of the deposits are about the same age, that is, around 1100 m.y. (Tapaninen, 1975; Little, 1974; and Knipping, 1974).

D. Uraniferous Pegmatites

Uraniferous pegmatites of Saskatchewan (Fig. 78.5) are normally medium- to coarse-grained and granitic to pegmatitic in character. They may be either conformable or discordant. Included in this category of deposits are some of the mineralized pegmatites or quartz feldspar rocks mapped with mineralized calc-silicate rocks in some areas. The uranium in these rocks is partly in veins suggesting that it is in part remobilized uranium. Radioactive pegmatites occur at several places in the Precambrian of Saskatchewan but the largest concentration is in the Charlebois Lake area east of Lake Athabasca. Other occurrences are known in the Lac La Ronge area and in the Mudjatik River area south of the Athabasca basin. The grade of uraniferous pegmatites is generally low and averages less than one pound per ton and

mineralized areas are of irregular size and shape and show erratic distribution. The uraniferous pegmatites of Saskatchewan have been classified in two main groups by Sibbald (1975): Group A, coarse pegmatites related to the Archean basement rocks; and the younger Group B pegmatites related to the zones of pelitic rocks in the Aphebian succession. The pegmatites of Charlebois Lake, Middle Foster Lake and Frazer Lake areas belong to the Group B category (Sibbald, 1975, p. 128).

The pegmatite deposits of Group A (Sibbald, 1975) are most widespread and they account for most of the airborne radioactive anomalies. Uranium occurs in massive to faintly foliated granite as well as in pegmatites that form part of the Archean basement gneiss complex. The uraniferous pegmatites are of various dimensions and their distribution in basement rocks is erratic. The pegmatitic parts of the uraniferous granites form layers, lenses and patches and they are generally more strongly radioactive than the granite hosts (Sibbald, 1975). Since the pegmatites occur only in basement granites and granitic gneisses to which they are closely related in composition, they are regarded as the anatectic fractions of the basement granitic rocks. It is assumed that uranium was concentrated first in fractions of the granitic gneisses and subsequently further concentrated in the pegmatitic phase. In general the pegmatites of Group A are typically coarse grained and are not as a group related to a single large intrusive granite body. However a few of the radioactive pegmatites within this group are much coarser grained, show some differentiation, and have a more complex mineralogy than typical Group A pegmatites. They are also transgressive and they may represent a different group related to an intrusive Hudsonian granite not recognized yet.

The pegmatite deposits of Group B are restricted to areas of Aphebian rocks and are particularly common near the base of the Aphebian succession such as at Charlebois Lake. They generally form concordant layers and lenses but local examples are discordant with the country rocks. These pegmatites are generally much more variable in grain size and composition than the pegmatites of Group A. They are usually interlayered with metapelites and locally resemble meta-arkoses and metaquartzites of the Aphebian succession. They are believed to be metasediments, possibly feldspathic metaquartzites transformed by metamorphism into medium- to coarse-grained granite and pegmatitic granite. The pegmatitic facies normally occur as irregular bodies within the granite. The uranium content of these pegmatites is generally low and is probably due to original syngenetic accumulations of uranium in the metasediments remobilized and concentrated in the pegmatitic phases during recrystallization. In the areas of uraniferous Group B pegmatites marble or other carbonate rocks are usually present in the Aphebian succession in addition to pelite and quartzite (Mawdsley, 1958). The pegmatites are apparently not mineralized where the carbonate rocks are missing. Some mineralized pegmatites associated with mineralized carbonate rocks have been mapped as remobilized basement rocks (Sibbald, 1975). Uraninite is the main uranium mineral of both Group A and Group B pegmatites and in general uraninite is found mainly in the part of the pegmatites or pegmatitic granite bodies that are high in biotite and grey to black quartz (Mawdsley, op. cit.). Other accessory minerals present include muscovite, molybdenite, pyrite and pyrrhotite.

E. Sandstone-Type

These deposits are known only in the unmetamorphosed basal sandstones of the Athabasca Formation. Although they may possibly occur also at higher stratigraphic localities within the Athabasca Formation this has not yet been demonstrated. The known deposits show similarities to the Colorado Plateau type and are represented on Stewart and Johnston islands by pitchblende cement in grey to black glassy orthoquartzite (Beck, 1969). The occurrences are small, discontinuous and lenticular. Tiny pitchblende veins are also present in the immediate vicinity of the pitchblende-cemented quartzite occurrences. The veins probably represent remobilized uranium deposited subsequent to the uraniferous cement. The veins and cementing pitchblende may represent material transported through the unconformity and deposited in an environment of heavy metal concentrations as suggested by the presence of magnetite. If so, this type of occurrence could be near-surface evidence of much larger uranium deposits existing in the basement below. Conversely, it is possible that the uranium was not deposited at the unconformity merely because the conditions there were not suitable for uranium concentrations. The group of deposits described previously as disseminated mineralization in sediments are probably in part related to this type of deposit but because they occur in older metamorphosed rocks they have been considered as a separate deposit type.

Acknowledgments

Much assistance was given the writer by companies and government agencies operating in the area during this study. This assistance was much appreciated. Sincere thanks are extended to all of them, particularly to Eldorado Nuclear Ltd., Gulf Minerals (Canada) Ltd., Aurole Ltd., Uranerz Explorations and Mining Ltd., and the Saskatchewan Department of Natural Resources.

References

Beck, L.S.
1969: Uranium deposits of the Athabasca Region, Saskatchewan; Sask. Dep. Mineral Resour., Rep. 126, p. 139.

1977: Changing ideas on metallogenesis of Saskatchewan's uranium deposits; Can. Min. J., v. 98, p. 49-51.

Dahlkamp, Franz, J. and Tan, B.
1977: Geology and mineralogy of the Key Lake U-Ni deposits, northern Saskatchewan, Canada; Inst. Min. Met. Trans. Sec. B, Applied Sci., London, January.

Derry, D.R.
1976: Future supplies of Uranium; Geol. Assoc. Can., Volume of Abstracts.

Hoeve, J. and Sibbald, T.I.T.
1976: The Rabbit Lake Uranium Mine; in Uranium in Saskatchewan, Symp. Proc. Sask. Geol. Soc., Spec. Publ. No. 3, p. 331.

Knipping, H.D.
1974: The concepts of supergene versus hypogene emplacement of uranium at Rabbit Lake, Saskatchewan, Canada; in Formation of Uranium Deposits, Int. Atomic Energy Agency, Vienna.

Koeppel, V.
1968: Age and history of uranium mineralization of the Beaverlodge area, Saskatchewan; Geol. Surv. Can., Paper 67-31.

Langford, F.F.
1977: Surficial origin of North American pitchblende and related uranium deposits; Am. Assoc. Pet. Geol., Bull., v. 61, no. 1, p. 28-42.

Little, H.W.
1974: Uranium in Canada; in Report of Activities, Part A, Geol. Surv. Can., Paper 74-1A, p. 137-139.

Little, H.W., Smith, E.E.N., and Barnes, F.Q.
1972: Uranium deposits of Canada; Int. Geol. Congr., Guideb. Field Excursion C67.

Mawdsley, J.B.
1958: The radioactive pegmatites of Saskatchewan; United Nations Proc. 2nd Int. Conf. Peaceful Uses of Atomic Energy, Geneva, v. 2, p. 484-490.

Money, P.L., Baer, A.J., Scott, B.P., and Wallis, R.H.
1970: The Wollaston Lake Belt, Saskatchewan, Manitoba, Northwest Territories; in Symposium on Basins and Geosynclines of the Canadian Shield, Geol. Surv. Can., Paper 70-40, p. 171-200.

Pagel, Maurice
1975: Determination des conditions physico-chimiques de la silicification diagénêtique des grés Athabasca (Canada) au moyen des inclusions fluides; C.R. Acad. Sc., Paris, T. 280, Mai.

Ray, G.E.
1976: Foster Lake (NW) – Geikie River (SW) area; Sask. Dep. Mineral Resour., Summary of Investigations 1976, Geol. Surv. Sask., p. 18-23.

Rimsaite, J.
1977: Mineral assemblage at the Rabbit Lake Uranium deposit, Saskatchewan; a preliminary report; in Report of Activities, Part B, Geol. Surv. Can., Paper 77-1B, p. 235-246.

Robinson, S.C.
1955: Mineralogy of uranium deposits, Goldfields, Saskatchewan; Geol. Surv. Can., Bull. 31, p. 1-128.

Sassano, G.
1972: The nature and origin of the uranium mineralization at the Fay Mine, Eldorado, Saskatchewan, Canada; unpubl. Ph.D. thesis, Univ. Alberta, Edmonton, Canada.

Sibbald, T.I.T.
1975: Investigation of certain radiometric anomalies in Crown Reserve 621; Sask. Dep. Mineral Resour.; Summary of Investigations 1975; Geol. Surv. Sask.

Sibbald, T.I.T., Munday, R.J.C., and Lewry, J.F.
1976: Setting of uranium mineralization in northern Saskatchewan; Sask. Geol. Soc., Sp. Publ. no. 3, p. 51-98.

Smith, E.E.N.
1974: Review of current concepts regarding vein deposits of uranium; Inter. Atomic Energy Agency, Vienna, Paper SM-183/45.

Tapaninen, K.
1975: Geology and metallogenesis of the Carswell area uranium deposits; Can. Inst. Min. Met., Annual Meeting, Edmonton.

Tremblay, L.P.
1958: Geology and uranium deposits of Beaverlodge region, Saskatchewan; United Nations 2nd Int. Conf. Peaceful Uses of Atomic Energy, Geneva, v. 2, p. 491-497.

1970: The significance of uranium in quartzite in the Beaverlodge area, Saskatchewan; Can. J. Earth Sci., v. 7, p. 280-305.

1972: Geology of the Beaverlodge Mining Area, Saskatchewan; Geol. Surv. Can., Mem. 367, p. 1-265.

Trueman, T. and Fortuna, P.A.
1976: Dubyna Lake Uranium Deposit, (31 Zone), Eldorado, Saskatchewan; Sask. Geol. Soc., Sp. Publ. no. 3, p. 380.

79. NOTES ON POSSIBILITIES FOR ADDITIONAL URANIUM DEPOSITS IN SASKATCHEWAN

Project 750058

L.P. Tremblay
Regional and Economic Geology Division

Abstract

Tremblay, L.P., Notes on possibilities for additional uranium deposits in Saskatchewan; Current Research, Part A, Geol. Surv. Can., Paper 78-1A, p. 437-439, 1978.

Uranium potential in Saskatchewan is mainly associated with the St. Louis fault and other major faults north of Lake Athabasca, the Athabasca unconformity below the Athabasca sandstone, and, areas of metasediments and cover rocks where because of reducing conditions at the time of deposition sandstone-type deposits or disseminations in sediments could have formed.

This report considers briefly the possibilities for undiscovered deposits in Saskatchewan in the light of the distribution, geological characteristics and assumed mode of origin of the known uranium deposits. The uranium subprovinces of the Precambrian rocks of Saskatchewan are defined and the features that are diagnostic of the types of uranium deposits of the various subprovinces are described in Tremblay (1978).

Deposits associated with major faults (Beaverlodge-type)

Possibilities for additional vein deposits of the Beaverlodge type appear good north of Lake Athabasca, particularly in the Beaverlodge and Stony Rapids linear belts as defined by Beck (1969) and in proximity to their possible extensions for short distances to the south and southwest beneath the Athabasca sandstone toward the Carswell structure. These belts are within the Tazin Belt, north of Lake Athabasca (Fig. 79.1). Others occur west of the lake in the Chipewyan belt. All the linear belts are characterized by wide mylonite and brecciated zones which probably represent faults of crustal dimension. Figure 79.2 shows the location of known major faults in the area north and west of Lake Athabasca. These faults serve to outline some of the tectonic elements of Figure 79.1. The St. Louis fault is an example of such a major fault zone and is the main control of mineralization in the Beaverlodge-Uranium City area. It seems likely that other similar zones north and west of Lake Athabasca to the west of the Black Lake fault could also be important ore controls. Thus, it is suggested that they should be investigated to determine relationships similar to those along the St. Louis fault with respect to late, closely-spaced fracturing, alteration, type and degree of metamorphism, position relative to source rock, rock associations and stratigraphic position in the Tazin succession. The possibilities for Beaverlodge-type deposits in other parts of Saskatchewan, particularly south of Lake Athabasca and in the Wollaston uranium subprovince are not considered good because of different tectonic settings. This area is characterized by a ductile type of deformation (Sibbald et al., 1976) in contrast to the area north of Lake Athabasca where uranium mineralization appears to have been associated with brittle deformation (Tremblay, 1972).

Deposits associated with unconformity (Unconformity-type, Beaverlodge-type)

If a genetic relation exists between the unconformity at the base of the Athabasca Formation and the unconformity-type uranium deposits along it, the possibilities of finding other similar deposits in Saskatchewan seem excellent within the area overlain by the Athabasca sandstone. This is the area of the Athabasca basin of Figure 79.1. Logical places to prospect for this type of deposit in the Athabasca Uranium Subprovince are in areas where the unconformity is still recognizable in outcrop, is exposed in section and is likely preserved in the subsurface. In general, this target embraces the 107 000 km^2 that the Athabasca sandstone covers.

It is known that the unconformity was developed under strong chemical weathering conditions, as deep weathered zones accompanied by thick regoliths are present locally along the unconformity. If the regolith is preserved along the unconformity it must have been buried shortly after its formation and this situation has been identified in a number of places. Most of the known deposits along the unconformity are associated with these regolithic zones, so the first target in prospecting for additional deposits of this type is to determine the distribution and thickness of these alteration zones along the unconformity. However, since the thickness of the sandstone is more than 1500 m in the centre of the Athabasca basin, possible targets in the interior areas are inaccessible. Therefore reasonably accessible targets for unconformity-type deposits are limited to areas where the sandstone cover is less than about 200 m, or areas within the sandstone where major fault zones are present. If these fault zones are found to carry minor uranium mineralization it may suggest that they could extend to mineralized basement and that the uranium represents the surface indication of uranium at depth.

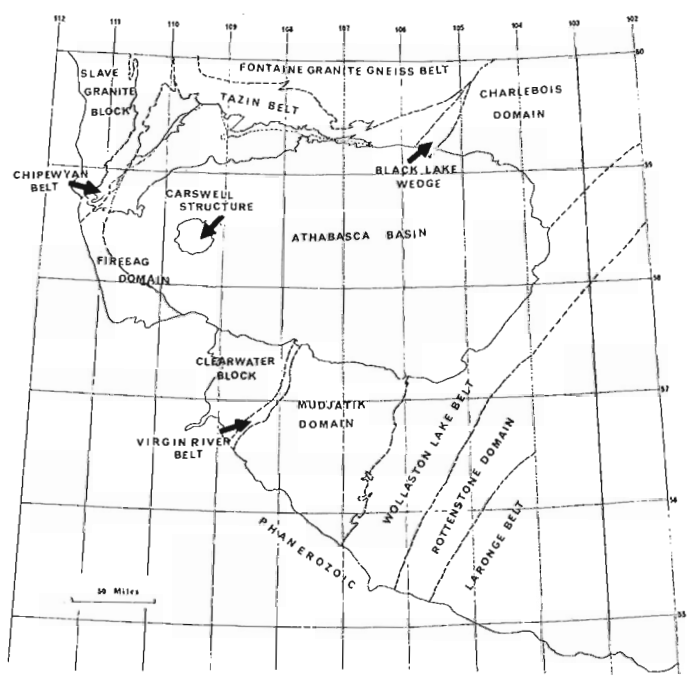

Figure 79.1. Tectonic subdivisions of Precambrian rocks in Saskatchewan and Alberta west of longitude 104°W.

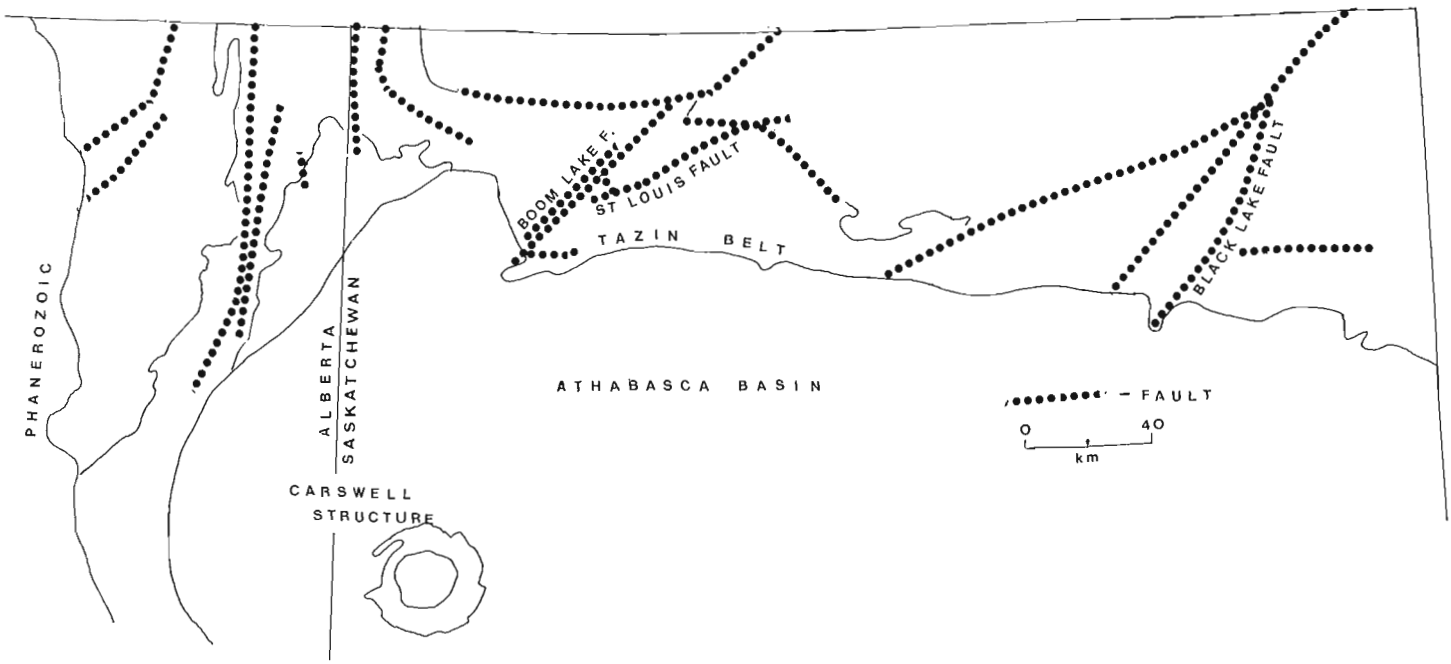

Figure 79.2. Major known faults north and west of Lake Athabasca.

If the genetic relation supposed above between the Athabasca unconformity and unconformity-type uranium deposits is valid it would appear that, by analogy, other unconformities could be likely places to look for similar uranium deposits even if they formed at different times. Two other unconformities are known in Saskatchewan that may warrant investigation on this basis. These are: the Archean-Aphebian unconformity at the base of Aphebian rocks in the Wollaston Subprovince; and the Tazin-Martin unconformity at the base of Martin rocks in the Beaverlodge Subprovince. The trace of the Tazin-Martin unconformity is outlined on Figure 78.2 and that of the Archean-Aphebian unconformity on Figure 78.3. The Archean-Aphebian unconformity is marked by a thin unit of graphitic metapelite at the base of the Aphebian succession lying above Archean granitic gneisses and the Tazin-Martin zone is marked locally by a thin layer of angular, little displaced basement detritus. Where these two unconformities are observed some distance away from the Athabasca sandstone they do not show the typical white alteration associated with the mineralized zones of the Athabasca unconformity. This suggests that the alteration conditions were not the same along the three unconformities, and thus conditions for the formation of uranium deposits of the type found along the Athabasca unconformity may not have been present along the other two unconformities. However, since it is known that some of the vein type deposits in the Beaverlodge Subprovince are structurally related to the Tazin-Martin unconformity, additional deposits of this type may possibly be found in association with all three unconformities.

Other metapelite units higher in the Aphebian succession behave in the same way as the basal graphitic unit when they lie along the Athabasca unconformity. They might thus have been involved in the development of the regolith and its accompanying mineralization in the same way as the basal graphitic unit. On this basis other graphitic units of the Aphebian succession might warrant investigation.

Sandstone-type deposits

The possibilities for sandstone-type deposits seem better in rocks of the Athabasca Formation and in those of the Martin Formation than in rocks of the Tazin Group and other Archean supercrustal rocks. Sandstone-type deposits can be of two types: those of the roll-front Wyoming type where uranium was introduced after deposition of the sediments; and, those of the Colorado Plateau type where the uranium was deposited penecontemporaneously with the sediments within a closed system. The roll front type is not likely to be present in the Archean rocks because of the climatic conditions in Archean time nor is it likely in the Aphebian rocks because of the restricted reducing environments. This type of deposit may however, occur in the more porous Martin and Athabasca formations if reducing conditions were present. Reducing environments are suggested by green beds interbedded with red beds in the upper siltstone unit of the Martin Formation. Based on available evidence, reducing conditions appear to have been scarce in the Athabasca Formation. Thus it is risky to estimate the potential of these two formations to contain sandstone-type deposits analogous to the Wyoming type.

Colorado Plateau type deposits could be expected in areas of Archean rocks and in rocks of the Martin and Athabasca formations only if the rocks in their respective source areas are in part uranium-bearing, and provided that the conditions for the concentration of uranium in these formations existed locally. These features are not known for the Archean rocks and in general the hypothesis is not regarded as promising for these rocks because of their antiquity. The hypothesis however holds more promise for the Martin and Athabasca formations. In the latter case the source area for the Martin Formation includes the Beaverlodge uranium-bearing area to the northeast and that for the Athabasca Formation is the Wollaston Lake belt to the southeast which contains disseminated uranium in Aphebian metasediments. As examples, the Stewart Island occurrence and those on Johnston Island in Athabasca sandstone on Lake Athabasca have been regarded as sandstone deposits of this type (Tremblay, 1978). The Stewart Island occurrence is of interest as values up to 1.05% U_3O_8 over 2 1/2 m have been reported (Beck, 1969). Deposits of this type probably occur also in Aphebian rocks along the Wollaston Lake belt but because they are metamorphosed they have been described as disseminated mineralization in sediments (Tremblay, 1978) and their potential is further discussed below.

Disseminated uranium mineralization

Disseminated mineralization in sediments is known in several areas in Saskatchewan and the possibilities for additional deposits of this type seem generally good, particularly in the Wollaston Uranium Subprovince where subeconomic deposits are already known. However, from the available information it seems likely that such deposits will be small and of low grade. Typically they occur in carbonaceous, black, glassy quartzite, carbonaceous grey to black feldspathic gneiss, calc silicate rocks of various composition, or arkoses and impure quartzites. It seems probable that most deposits of this type will be found in Aphebian successions and in stratigraphically high successions in Archean rocks such as the Tazin Group.

References

Beck, L.S.
1969: Uranium deposits of the Athabasca region, Saskatchewan; Sask. Dep. Mineral Resour., Rep. 126, p. 139.

Sibbald, T.I.T., Munday, R.J.C., and Lewry, J.F.
1976: Setting of uranium mineralization in northern Saskatchewan; Sask. Geol. Soc., Sp. Pub. no. 3, p. 51-98.

Tremblay, L.P.
1972: Geology of the Beaverlodge mining area, Saskatchewan; Geol. Surv. Can., Mem. 367, p. 1-265.

1978: Uranium subprovinces and types of uranium deposits in the Precambrian rocks of Saskatchewan; in Current Research, Part A, Geol. Surv. Can., Paper 78-1A, rep. 78.

80. AN EXPERIMENTAL FLUME STUDY ON THE FORMATION OF TRANSVERSE RIBS

Project 710070

B.C. McDonald[1] and T.J. Day
Terrain Sciences Division

Abstract

McDonald, B.C., and Day, T.J., An experimental flume study on the formation of transverse ribs; Current Research, Part A, Geol. Surv. Can., Paper 78-1A, p. 441-451, 1978.

Transverse ribs constitute a distinctive bed form occupying the riffle portion of shallow streams with coarse alluvial beds. Ribs occur in a series of regularly spaced pebble, cobble, or boulder ridges extending across the channel and oriented transversely to current direction. They are widespread on braided alluvial plains and in high gradient, single channel streams where they result in a stair-step arrangement forcing water to flow through a series of regularly spaced cascades.

Similar bed forms have been formed experimentally with pebbles in a laboratory flume. The pebbles are transported by supercritical flow and accumulate in a transition zone containing a hydraulic jump where the flow reverts to subcritical. Water waves in the transition zone are deformed by pebbles accumulating under them, until the waves collapse in an upstream direction and restabilize at a discrete distance upstream. Bed form spacing is a function of slope and Froude number of the supercritical flow upstream from the jump. Individual "ribs" form in seconds and subsequently are rendered inactive in a subcritical flow field as the hydraulic jump steps farther upstream.

It is possible that transverse ribs may be useful to geologists as an indication of paleoflow conditions.

Introduction

The occurrence of this peculiar but distinctive bed form, occurring as a series of regularly spaced pebble, cobble, or boulder ridges oriented transversely to the current direction and occupying the riffle portions of channels (Fig. 80.1), appears to be widespread. These features have been named "transverse ribs" by McDonald and Banerjee (1970, 1971). At about the same time they were reported by Boothroyd (1970) on the Scott Glacier outwash plain in south-central Alaska and have been discussed recently in greater detail by Boothroyd and Ashley (1975).

Transverse ribs are not restricted to outwash plains but are a common feature of many stream beds characterized by coarse gravelly alluvium. They have been observed in numerous locations in the Canadian and Colorado Rockies. I. Banerjee (written comm., 1971) reports their widespread occurrence in streams in the Himalayas; W.A. Van Wie (written comm., 1971) reports their presence on alluvial fans in southern Nevada; and numerous colleagues have reported their presence in small streams. Transverse ribs form stony ridges across the channel which result in a stair-step arrangement forcing water to flow through a series of regularly spaced cascades (Figs. 80.2a, 80.2b). In all cases where transverse ribs were observed, the largest clasts in the stream bed seemed to occur in the rib itself.

Intrigued by the potential of transverse ribs to exert a strong influence on channel development and sedimentation pattern, and also by the possibility of identifying them in the geologic record as a useful environmental indicator, it was decided to investigate experimentally the mechanics of their formation. Field study had provided documentation of their configurations, but the formative process was obscure.

This paper summarizes field characteristics of transverse ribs and presents experimental evidence that transverse ribs can be formed under a "stepping" hydraulic jump.

Field Characteristics of Transverse Ribs

This portion of the paper is presented to facilitate direct comparison of field data with experimental results.

Figure 80.1

Transverse ribs on Peyto outwash plain. Ribs bifurcate near pebbly channel bank, on which 50-cm shovel rests. Flow was from right to left (GSC 201959-A).

[1] Program Branch, Treasury Board, Place Bell Canada, Ottawa, Ontario, K1A 0R5.

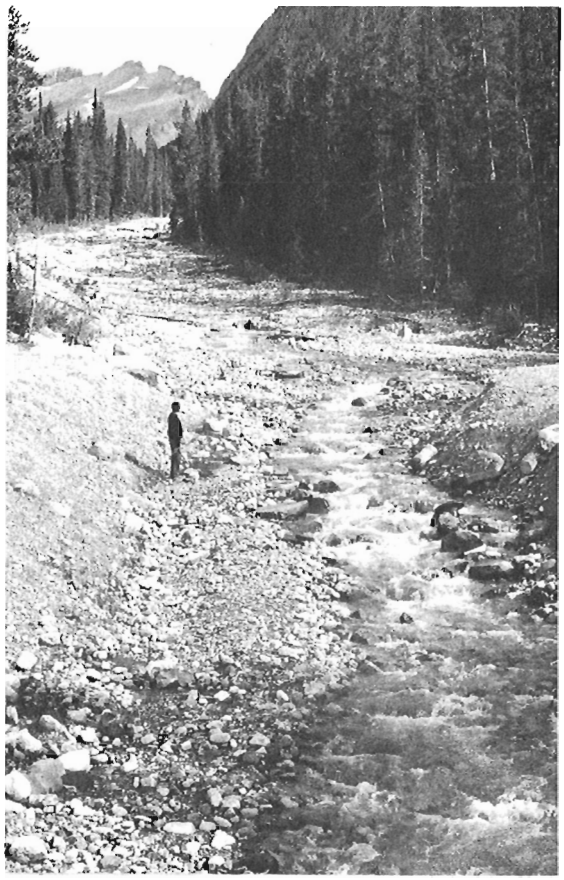

Figure 80.2a. Transverse ribs marked by regularly spaced cascades along No-See-Um Creek, Alberta. Slope of reach = 0.0712 (GSC 157709).

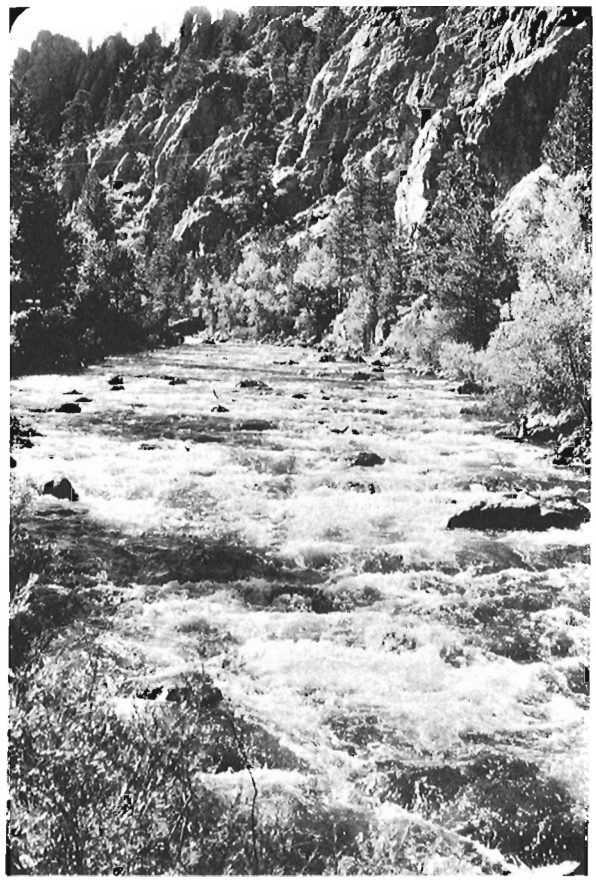

Figure 80.2b. Transverse ribs marked by regularly spaced cascades along Cache la Poudre River in the Rocky Mountains west of Fort Collins, Colorado.

Field measurements of transverse ribs were made in the Canadian Rockies (1) on the braided outwash plain about 2 km below Peyto Glacier, (2) on the braided North Saskatchewan River about 30 km downstream from Saskatchewan Glacier, and (3) on No-See-Um Creek – a high gradient, single channel, mountain stream near the Peyto outwash plain. Other data and observations were abstracted from Boothroyd and Ashley's (1975) studies of the Scott and Yana outwash plains in Alaska and from Judd and Peterson's (1969) study of rough, high gradient streams in Colorado, Utah, and New Mexico.

Field characteristics of transverse ribs that must be explained satisfactorily by any proposal of origin are:

(1) ribs occur as regularly spaced ridges of coarse clasts and commonly comprise the coarsest clasts in the channel;

(2) ribs are oriented transversely to current flow in riffle portions of channels;

(3) rib crests are generally straight, although a tendency was noted for gentle convexity downchannel at points of channel expansion;

(4) crests are continuous over long distances relative to rib width, and there is a tendency for the crest to bifurcate near channel edges where pebbly bars form the banks;

(5) commonly a marked grain size sorting has occurred with coarser clasts concentrated in the ribs, and silty laminae, on which the stones rest, being exposed in the inter-rib zones. Less commonly, however, ribs occur as stony ridges with no obvious grain size difference between rib and inter-rib zones;

(6) clasts in the ribs have their a-axes oriented transversely to the flow, i.e., parallel with the rib trend, and the a-b planes dip upstream;

(7) width and spacing of ribs increase with increasing stone size;

(8) maximum channel depth in the ribbed reaches is only about twice as large as the largest b-axes of stones in the ribs; and

(9) slope and size of bed material are primary factors in spacing.

In addition, it was noted that interrelationships between parameters are defined more clearly where data from different localities are considered separately (Fig. 80.3). The two No-See-Um Creek measurements lie on the extended regression line for the data from the nearby Peyto outwash plain, whereas the North Saskatchewan River data fall on a different, though well defined, line. Not only does this encourage the view that the larger scale, stair-step cascades on No-See-Um Creek represent the same phenomenon as transverse ribs on the Peyto outwash plain, but the difference between these sites and the North Saskatchewan River sites suggests that some other variable, perhaps pebble shape, also influences rib development.

Possible Formative Process

The formation of transverse ribs has never been observed in the field because these features are formed during high flows. Boothroyd (1970) first suggested that ribs were relict antidunes. Although this mechanism remains the favoured one (e.g. Boothroyd and Ashley, 1975; Church and Gilbert, 1975; Judd and Peterson, 1969), definitive

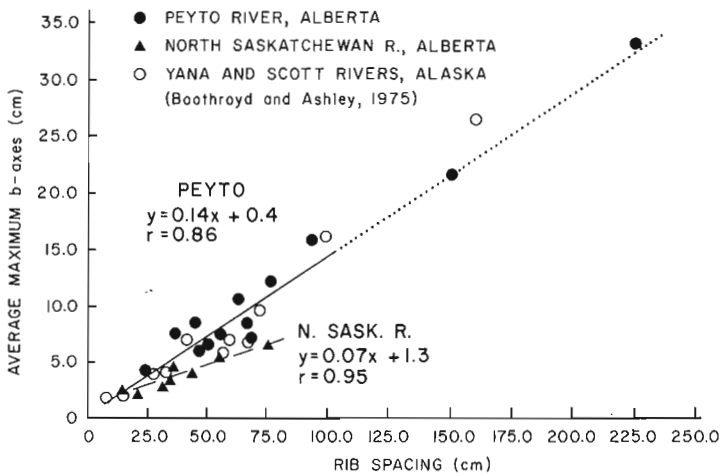

Figure 80.3. Transverse rib spacing vs. average maximum b-axes of pebbles for field sites studied in Alberta and Alaska.

experimental work has yet to be done. Day (1976) observed that rib-like features forming as antidunes in coarse gravel (2-90 mm) were degraded under steady flows. Also, Koster (1976) observed in-phase pebble accumulation under a train of standing waves; Judd and Peterson (1969) suggested this as a possible mechanism of transverse rib formation.

The experimental study reported herein was undertaken by the senior author during 1971, well before explanation was directed towards antidune formation in the upper flow regime, a mechanism that has yet to be proven. It is difficult to transfer the formative mechanism described herein (moving hydraulic jump) to natural channels; however, this mechanism can result in ribs with properties very similar to those found in the field, and therefore the results may be an important example of different processes resulting in similar sedimentary features.

Laboratory Experiments

Apparatus

Experiments were performed in the tiltable, open channel, recirculating, sedimentation flume of the Geological Survey of Canada, described by McDonald (1972). The main channel, not including the headbox, is 18.3 m long, 0.76 m wide, and 0.6 m deep. The channel floor is made of aluminum plate, but the walls are plate glass, permitting observation of processes in the channel. Rails mounted on the channel walls support an instrument carriage on which is clamped a point gauge for measuring features in the channel. Water slope is determined using a combination of the point gauge measurements and a conventional level. Discharge, Q, is measured by manometers connected to orifice plates mounted in each of the two return pipes. Precision of the measurements is indicated with the parameter in the table of experimental data.

Pebbles used in these experiments were naturally worn rock fragments occurring in a local glaciofluvial deposit. Two size ranges of pebbles were used throughout; their grain size distributions, sorting, and shape factors are summarized in Figure 80.4. In order to spare the pump impellers from unnecessary wear, pebbles were fed in at the upstream end of the open channel and were trapped in a screen basket at the downstream end.

Description of Experiments

After several unsuccessful attempts to produce rib features similar to field observations (e.g., placing pebbles across sand beds; and flow over a gravel bed), suitable bed forms finally were generated from the following procedure. Channel slopes were set sufficiently high that "shooting", or supercritical, flow existed in the channel and resulted in relatively high pebble transport rates. At a point downstream, the supercritical flow reverted to subcritical flow by passing through a transition zone containing a hydraulic jump. (A brief discussion of the hydraulics is presented in a subsequent section.) Pebbles transported by the flow were deposited in well defined transverse concentrations when they encountered the deeper and slower subcritical flow. Successive transverse ribs (Fig. 80.5), strikingly similar to the well defined bed forms observed in riffle reaches in the field, were deposited by the hydraulic jump "stepping" rapidly upstream in an episodic fashion, described in detail in the following section. Pebbles in the bed forms had an evident upstream dip of their a-b planes, with a-axes parallel to the crests of the ribs, although these details were not measured.

Initially, pebbles transported down the channel were supplied by erosion from the pebble bed artificially placed near the headbox. Subsequently it was found more convenient to establish supercritical flow in the pebble-free channel, force a hydraulic jump near the downstream end, and then trigger the formation of the ribs by manually feeding pebbles into the flow near the upstream end of the channel.

Crests of the ribs were oriented at right angles to the flow direction as long as the pebble supply rate was roughly uniform across the channel. In cases where the pebble feed was uneven, the transition zone from supercritical to subcritical flow was oriented obliquely to the channel axis and was located farthest upstream in the zone of highest pebble supply rate. This resulted in pebbles shifting obliquely downstream along the front of the transition zone. The ribbed pebble bed that eventually accumulated tended to be thicker on the side towards which the pebbles migrated, i.e., on the side that initially had the lower pebble supply rate.

The numerical data on which this report is based were obtained during 16 runs each for the large and small pebbles by pre-setting channel slope (S_o) to 0.0100, 0.0124, 0.0145, and 0.0200, and for each channel slope running discharges of 9.9, 15.9, 21.2, and 28.3 litres/s. Measurements in the transition zone were taken during formation of the ribs, and measurements on the pebble bed that was deposited behind the stepping jump were taken after the run had been stopped.

Experimental Results

A Process of Transverse Rib Formation

The hydraulic jump and transition zone. Hydraulic jumps have received much attention from engineers because of their use as dissipators of energy in flow-control structures such as dam spillways. The subject is adequately treated, for purposes of the present discussion, in standard texts (cf. Chow, 1959; Henderson, 1966).

Supercritical flow is defined as flow in which Froude number ($F = \frac{V}{\sqrt{gy}}$, where V is the mean velocity, g is acceleration due to gravity, and y is the mean flow depth) exceeds unity. This is a direct function of water velocity and water depth, but these parameters are dependent on channel slope and roughness, channel dimensions, and discharge. Transition from supercritical flow (F>1) to subcritical flow (F<1) usually is accompanied by the formation of a hydraulic jump. This is a turbulent stationary surge, or abrupt shock-wave front, on the water surface downstream from where the abruptly increased water depth exceeds critical depth and the velocity is subcritical. Much energy is dissipated in turbulence in a hydraulic jump, and form of the jump, length of the jump, and ratio of downstream to upstream water depths all can be related to the Froude number of the supercritical flow entering the jump.

The supercritical-subcritical transition zone, typical of one in which pebbles are accumulating to form transverse ribs, is shown in Figure 80.6a, and a definition sketch is given in Figure 80.6b. The position of the critical depth line (C.D.L.) is shown, i.e. the depth that will give F = 1 for the particular discharge illustrated. Supercritical flow exists where the water surface is below this line, and subcritical flow exists where the water surface lies above this line.

Supercritical flow entering the transition zone is deflected upward by the pebbles on the bed. The pebble accumulation functions as a broad-crested weir that offers resistance to the flow and locally decreases the bed slope. At the same time, however, because the pebble accumulation is permeable and because it increases in height at a relatively low angle (angle of repose for the pebbles), the velocity change is gradual. This permits supercritical flow to pass smoothly into subcritical flow in a standing wave, without passing through a hydraulic jump. Froude numbers as low as 0.45 have been calculated under the crest of the standing wave. On the downstream side of the pebble accumulation, the bed slope is effectively increased. The accelerating flow passes smoothly back to supercritical. Soon after flow depth becomes less than critical depth, the flow passes through a hydraulic jump with energy dissipated in intense turbulence at the breaking front. Flow in the reach downstream from the jump remains subcritical.

Formation of transverse ribs. The sequence of formation of transverse ribs is detailed in six successive stages (Fig. 80.7). The illustration is based on actual measurements in the flume during run 20-6 (V_1 = 93.0 cm/s; y_1 = 2.2 cm; F_1 = 2.0). The sequence begins with a hydraulic jump in the channel, positioned by setting the tailgate to create a pool at the downstream end of the channel. Pebbles are transported downstream by uniform supercritical flow where water slope equals bed slope.

The pebbles stop moving (stage 1) just downstream from the jump because the subcritical water velocity there does not provide adequate tractive force for transportation. As the pebbles accumulate and form a ridge under the jump (stage 2), two things happen: (1) the simple hydraulic jump configuration is deformed into a transition zone consisting of a standing wave followed by a hydraulic jump, the hydraulics of which have been discussed briefly in connection with Figure 80.6a, b; and (2) pebbles continue to accumulate under the standing wave in a zone of flow separation behind the initial accumulation. Pebbles roll across the initial ridge and are packed against its downstream edge by a back eddy in the zone of flow separation. The standing wave grows in amplitude as pebbles accumulate under it (e.g. stage 3). The standing wave is higher than the crest of the associated hydraulic jump by an amount approximately equal to the height of the pebble accumulation. The crest of the standing wave is located slightly downstream of the pebble accumulation. As pebbles accumulate beneath the front wave, the crest of this wave and the crest of the jump are displaced slightly downcurrent. The maximum amplitude that can be sustained by a stable wave on the water surface limits the upward growth of the standing wave. The steepness of the standing wave upstream from its crest at point of breaking is seen from Figure 80.7, stage 4, to be about 0.29 (wave height/wave length). Descending flow downstream from the crest pinches off the zone of flow separation on the downstream side of the pebble ridge. When the zone of flow separation is full of pebbles (stage 4), all pebbles being fed into the standing wave roll over the pebble ridge and on downstream. By this time the crest of the wave is located directly above the mid-point, and high-point, of the ridge. Pebbles moving through the standing wave cause the downstream side of the wave to flatten, forcing the wave to break upstream as a turbulent hydraulic jump. The jump "steps" rapidly upstream and restabilizes (stage 5) a distance approximately equal to $\frac{\lambda}{2}$ upstream of its position in stage 1, and the cycle begins again. In stage 6 the hydraulic jump has been deformed again into a transition zone with a standing wave followed by a hydraulic jump. As a new trough with supercritical flow develops over the former pebble accumulation, the pebbles are rolled back a distance of $\frac{\lambda}{2}$ to a subcritical position under the new jump. The accumulation here is a true transverse rib. Since the pebbles remain in subcritical flow, they are not subjected again to a tractive force capable of their wholesale transportation.

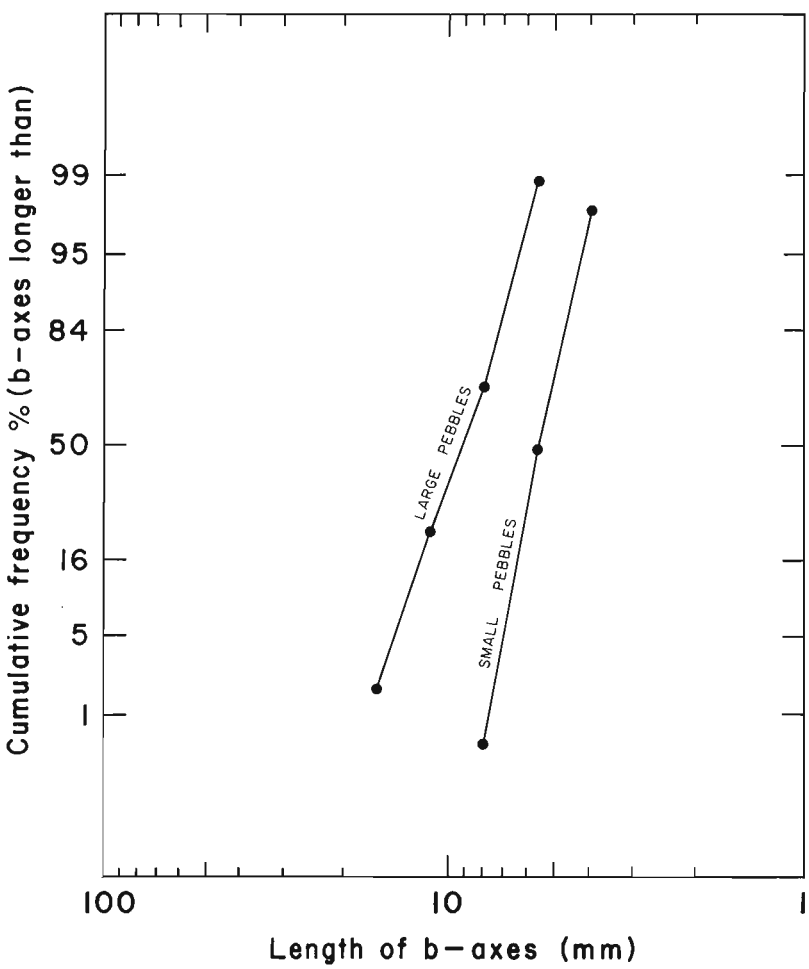

PARAMETER \ PEBBLES	LARGE	SMALL
MEDIAN SIZE d_{50}	9.2 mm	5.6 mm
ϕ DEVIATION = $\frac{\phi_{84} - \phi_{16}}{2}$	0.37	0.25
COREY SHAPE FACTOR = $\frac{c}{\sqrt{ab}}$	0.61	0.55

Figure 80.4. Grain-size distributions, sorting, and shape factors of pebbles used in experiments.

Figure 80.5a

Transverse ribs generated in the sedimentation flume channel, looking upstream; small pebbles used; Q = 13.9 l/s; S_o = 0.0124 (GSC 201910-A).

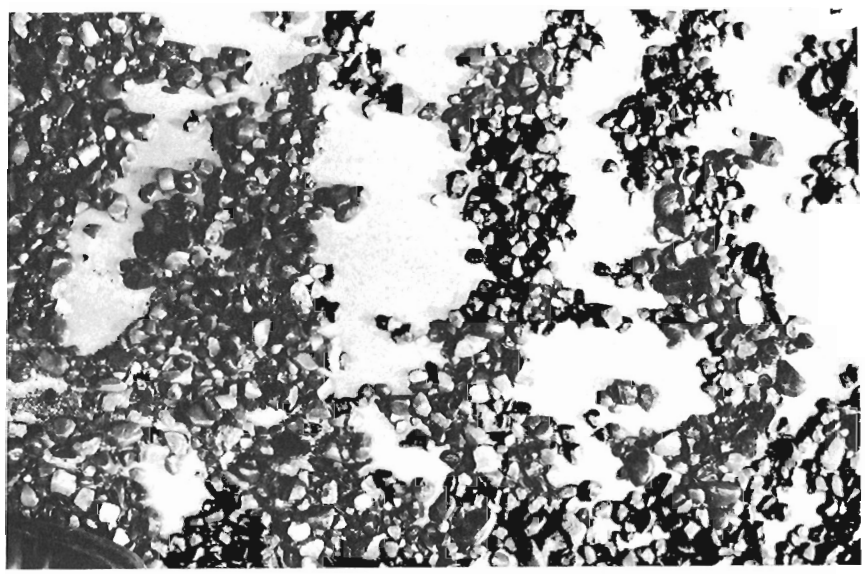

Figure 80.5b

Transverse ribs formed in run 21-9; flow from right to left (GSC 201910-D).

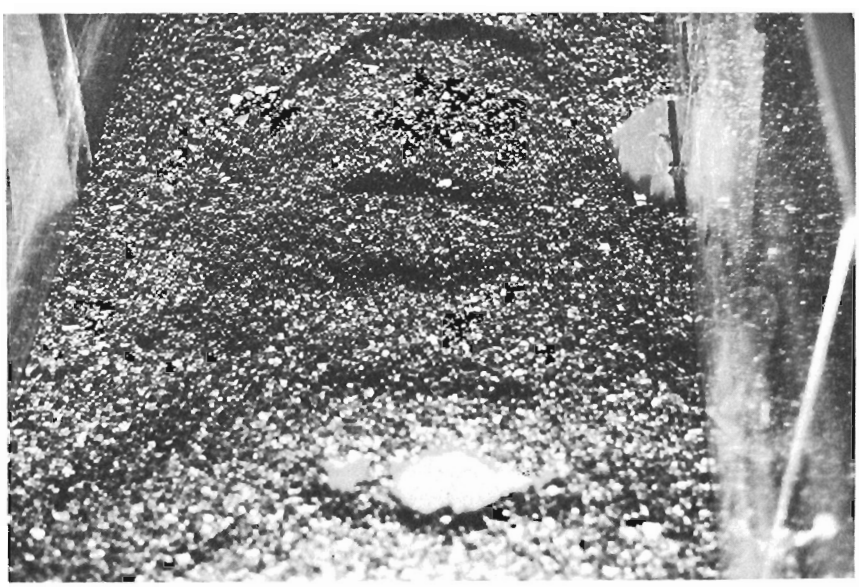

Figure 80.5c

Transverse ribs preserved as ridges on a pebble bed; dark areas are troughs between ridges; looking upstream after run 20-13 (GSC 201910-C).

The process of pebble accumulation followed by the hydraulic jump stepping upstream to a new location takes place in seconds. Cycles measured during a typical run in the laboratory averaged 23 s per rib, but ranged from 14 to 30 s. Thus ribs do not represent an equilibrium bed form as formerly suspected (McDonald and Banerjee, 1971), but rather they result from unsteady, rapidly varied flow and become progressively younger in an upstream direction. Successive stepping of the hydraulic jump in an upstream direction leaves the reach mantled by transverse ribs (Fig. 80.8). Passive surface-water waves are in phase with the transverse ribs and tend to be about twice the amplitude of the ribs.

Importance of pebble supply rate. Formation of transverse ribs, and the distinctiveness of the individual ribs, is dependent to a degree on the rate that pebbles are supplied to the standing wave. The relationship is summarized qualitatively in Figure 80.9. For the hydraulic jump to step upstream more pebbles must enter the standing wave from the upstream side than leave it on the downstream side, otherwise the pebble budget in the wave is negative, and the wave shifts gradually downstream. As long as the pebble budget under the front wave is positive, ribs can form, but they become increasingly indistinct as the budget becomes more highly positive. If the pebble budget is very high, upstream migration of the standing wave is a continuous process, and a uniform bed of pebbles is deposited in its wake.

This points out the dual importance of sediment feed and flow conditions to the formation of transverse ribs. The depth and velocity of the incoming supercritical flow determines the depth and velocity of the subsequent subcritical flow. But in order for transverse ribs to form and be preserved, the critical tractive force required for entrainment and transportation of pebbles in the ribs must be intermediate between the tractive forces provided by the two flow conditions, and rate of pebble supply to the jump must be sufficient for the jump to step upstream.

Interrelationship of Variables

Parameters that can be measured in a natural reach containing transverse ribs are rib spacing, rib width, rib height, bed slope, and pebble size and shape. If bank height can be measured, it will provide an upper limit for y_2. The objective here is to examine interrelationships of these parameters, as measured in the laboratory, with the flow parameters that prevailed during transverse rib formation, in order to permit estimation of the paleoflow conditions.

Details of the process (Fig. 80.7) indicate that height and width of the pebble accumulation under the standing wave at stage 4 might be related to the dimensions of the standing wave and incoming flow. It is these measurements of height and width that are reported in the table of

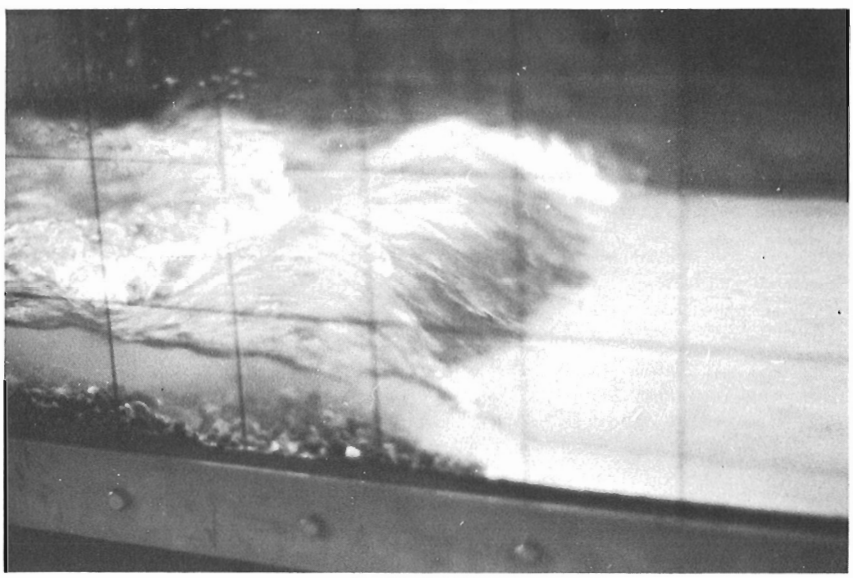

Figure 80.6a

Supercritical flow leading into the transition zone with a front standing wave, under which pebbles are accumulating, and a trailing hydraulic jump; flow is right to left; run 21-16; 10-cm grid on glass panel (GSC 201910-E).

Figure 80.6b (below)

Definition sketch of transition zone where pebbles accumulate. See text for discussion.

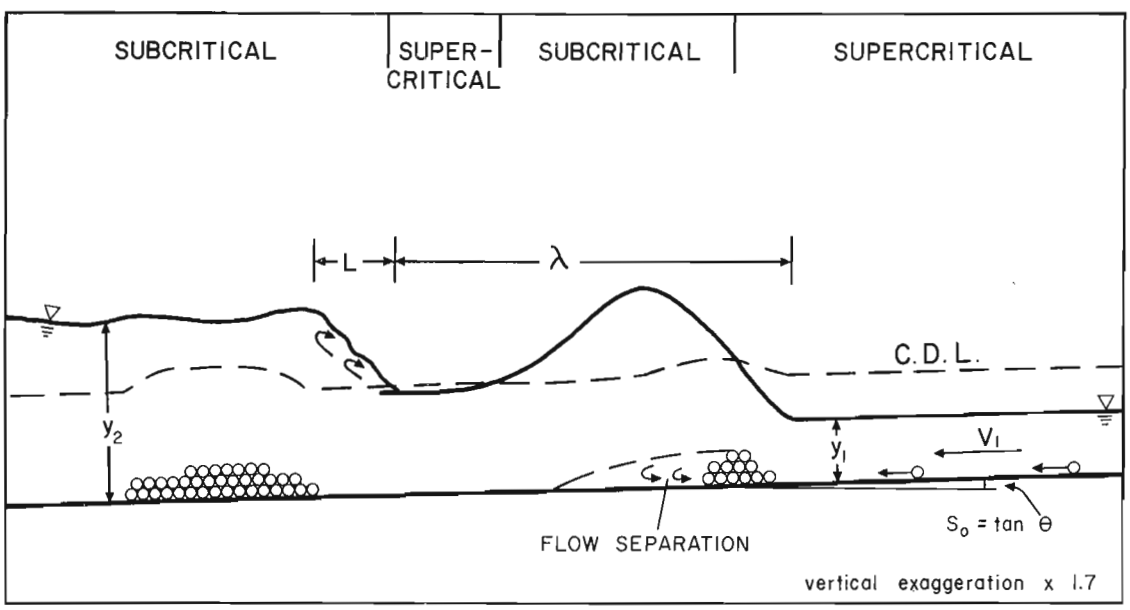

Key:

C.D.L.	=critical depth line
y_1, V_1	=water depth and velocity, respectively, in upstream supercritical section
y_2	=water depth in downstream subcritical section
S_o	=bed slope
L	=length of hydraulic jump
λ	=length of standing wave

experimental data (Table 80.1). Because the pebbles are re-entrained during stage 5, however, rib height as measured in the field will be related more to pebble size than to flow conditions during rib formations. To a lesser extent this also will be true of rib width measured in the field, although rib width would still be related to the volume of pebbles that accumulated beneath the standing wave before it collapsed upstream. Only in the most clearly defined ribs, however, can rib width be measured in the field with any precision.

Rib spacing appears from the process to be a useful field measure, insofar as it is determined by the dimensions of the water surface waves in the transition zone. It was found that, over the conditions tested, rib spacing is most directly related to the full width ($L + \lambda$) of the transition zone (Fig. 80.10), where

$$\text{rib spacing} = 0.60\ (L + \lambda) + 3.3.$$

Rib spacing is also strongly related individually to L, λ, and the spacing of wave crests in the transition zone. Because the dimensions of the standing wave are closely related to ($L + \lambda$), width of the pebble accumulation beneath the standing wave just as the wave breaks also is related to the width of the transition zone (Fig. 80.11) by

$$\text{width of pebble accumulation} = 0.34\ (L + \lambda) + 2.0.$$

Neither bed slope nor pebble size affects the relationships shown in Figure 80.11.

Presently no satisfactory theory exists for calculating the length, L, of a hydraulic jump. However, consistent relationships are found if L is incorporated in a dimensionless quantity by dividing it by a related water depth, and then this quantity is plotted against the Froude number, F_1, of the incoming supercritical flow (cf. Chow, 1959, p. 428). The relationships are increasingly dependent on bed slope as values of F_1 increase. Rib spacing, divided by y_1 to form a

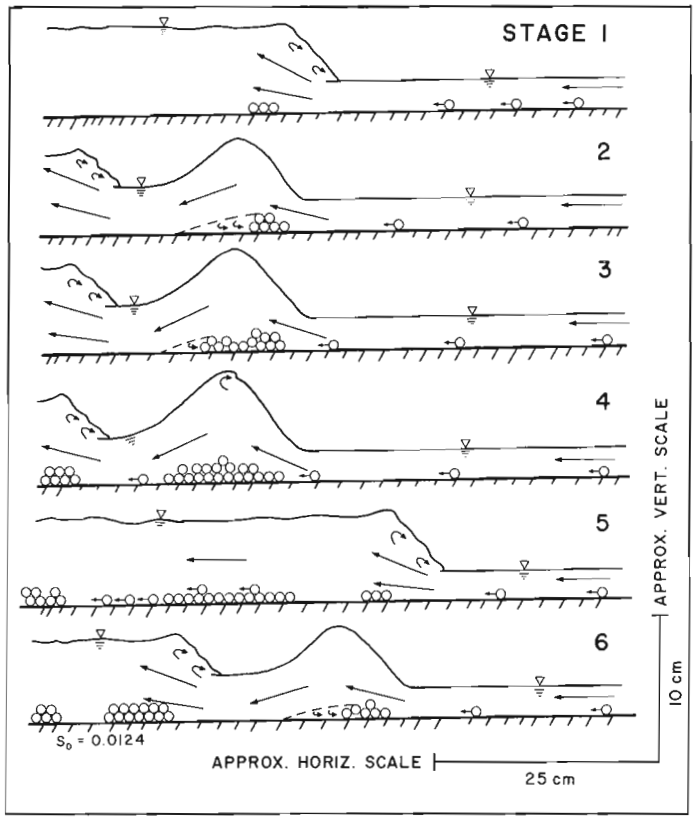

Figure 80.7. Process of transverse rib formation by stepping hydraulic jump. See text for discussion of the various

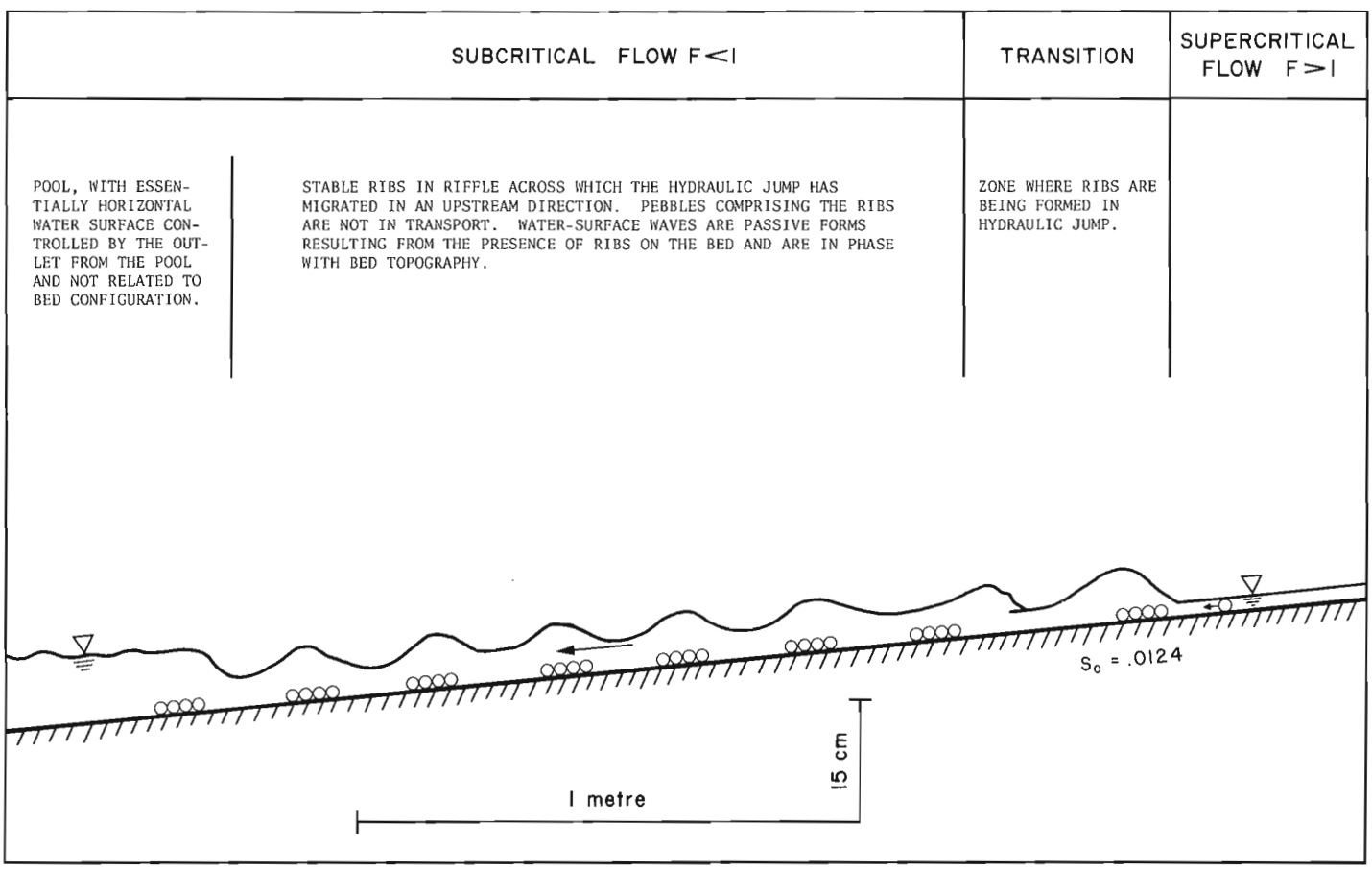

Figure 80.8. Series of ribs "fossilized" in subcritical flow field as hydraulic jump migrates upstream.

Table 80.1

Experimental data

Run[1]	S_o	Q litres/s	y_1[2] cm	V_1 cm/s	F_1	y_2[2] cm	L cm	λ cm	height of pebble accumulation[3] cm	width of pebble accumulation[3] cm	Rib spacing[4] cm	Max. number distinct ribs in single series
Estimated Precision		±1.0	±.05			±0.1	±2	±1	±10%	±10%	±0.5	
I. Small pebbles												
20-1	0.0100	9.9	1.85	69.8	1.64	4.5	5	13.5	2.1	10	14.4	9
20-2	0.0100	15.9	2.39	86.8	1.79	6.0	6	21	2.2	12	18.8	12
20-3	0.0100	21.2	2.83	97.7	1.86	8.2	9	26	2.5	13	27.3	8
20-4	0.0100	28.3	3.41	108.2	1.87	9.5	9	29	2.9	13	28.8	8
20-5	0.0124	9.9	1.70	75.9	1.86	n.m.[5]	5	10	2.6	8.5	16.9	11
20-6	0.0124	15.9	2.23	93.0	1.99	n.m.	7	19	2.7	11	18.0	8
20-7	0.0124	21.2	2.58	107.2	2.13	n.m.	11	25	3.2	12	24.2	8
20-8	0.0124	28.3	3.07	120.2	2.19	n.m.	13	29	3.5	15	35.3	8
20-9	0.0145	9.9	1.53	84.4	2.18	4.7	8	18.5	n.m.	10	17.1	14
20-10	0.0145	15.9	2.02	102.7	2.31	6.8	11	23	n.m.	14.5	24.4	4
20-11	0.0145	21.2	2.31	119.7	2.52	8.0	15	29	n.m.	18	32.0	3
20-12	0.0145	28.3	2.79	132.3	2.53	n.m.	18	34	n.m.	22	33.0	3
20-13	0.0200	9.9	1.51	85.5	2.22	4.6	12	n.m.	2.9	11	17.6	13
20-14	0.0200	15.9	1.96	105.8	2.41	n.m.	14.5	n.m.	3.8	14	20.4	8
20-15	0.0200	21.2	2.16	128.0	2.78	n.m.	16	n.m.	4.1	13.5	27.0	3
20-16	0.0200	28.3	2.67	138.2	2.70	n.m.	21	23	4.6	20.5	33.0	2
II. Large pebbles												
21-1	0.0100	9.9	1.92	67.2	1.55	4.0	5	17	2.5	9	14.6	8
21-2	0.0100	15.9	2.38	87.1	1.80	5.2	5	15	2.8	11	19.3	8
21-3	0.0100	21.2	2.85	97.0	1.84	6.9	7	22	2.8	15	19.9	8
21-4	0.0100	28.3	3.34	110.5	1.93	9.5	9	31	3.0	16	25.1	7
21-5	0.0124	9.9	1.59	81.2	2.06	3.6	4	13	2.8	7	12.7	7
21-6	0.0124	15.9	2.21	93.8	2.02	6.2	9	21	2.9	13	18.5	10
21-7	0.0124	21.2	2.65	104.3	2.05	6.3	10	22	3.1	12.5	23.6	10
21-8	0.0124	28.3	3.10	119.1	2.16	9.5	15	32	3.3	14.5	30.6	5
21-9	0.0145	9.9	1.77	72.9	1.75	4.6	9	13	1.8	7	15.3	21
21-10	0.0145	15.9	2.24	92.6	1.98	6.7	11	22	1.8	13	17.0	9
21-11	0.0145	21.2	2.47	111.9	2.28	8.6	15	27	3.0	17	22.6	7
21-12	0.0145	28.3	2.92	126.4	2.36	9.5	18	32	3.2	19	26.0	5
21-13	0.0200	9.9	1.56	82.8	2.12	4.9	9	14	3.1	8	13.4	18
21-14	0.0200	15.9	1.91	108.6	2.51	7.1	15	19	3.4	11	26.2	10
21-15	0.0200	21.2	2.33	118.7	2.48	9.4	15	28	4.1	16	27.7	8
21-16	0.0200	28.3	2.73	135.2	2.61	9.5	18	28	4.7	20	42.1	5

[1] All runs carried out at water temperature = 21 ± 1°C.
[2] y_1 and y_2 represent averages of 2-4 measurements.
[3] As measured beneath standing wave at stage 4 (see Fig. 80.9).
[4] Rib spacing is average value from as many ribs as could be measured (as many as 21) after the run was stopped.
[5] n.m. – not measured.

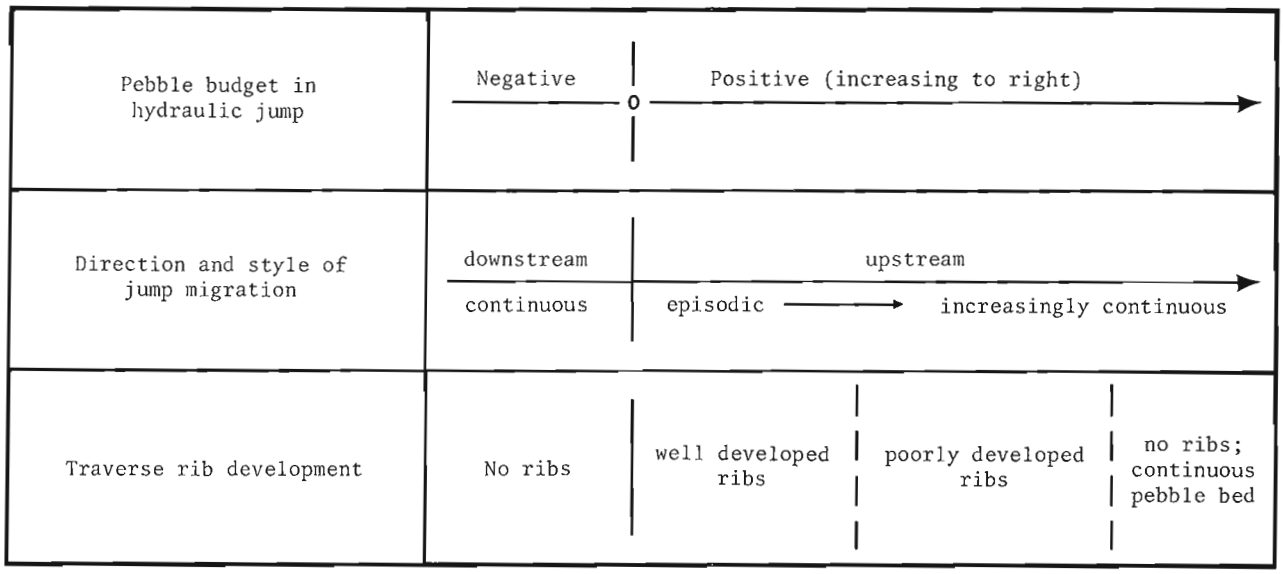

Figure 80.9. Qualitative relationship of pebble supply rate to transverse rib development.

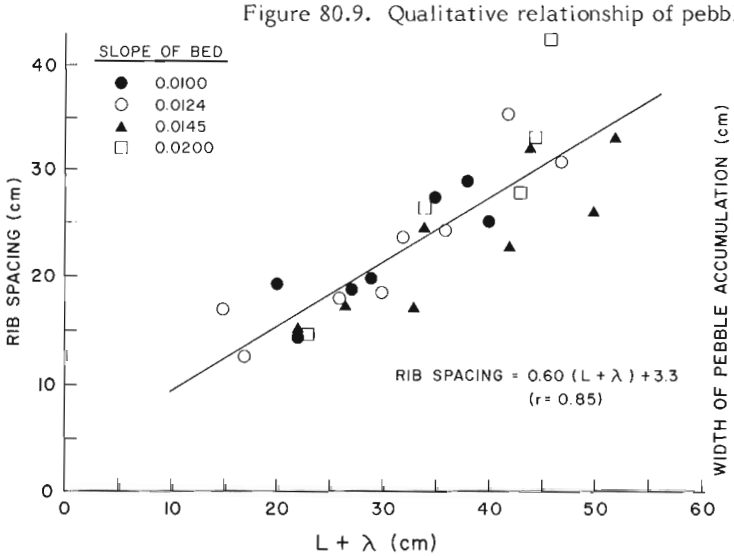

Figure 80.10. Transverse-rib spacing vs. width of transition zone.

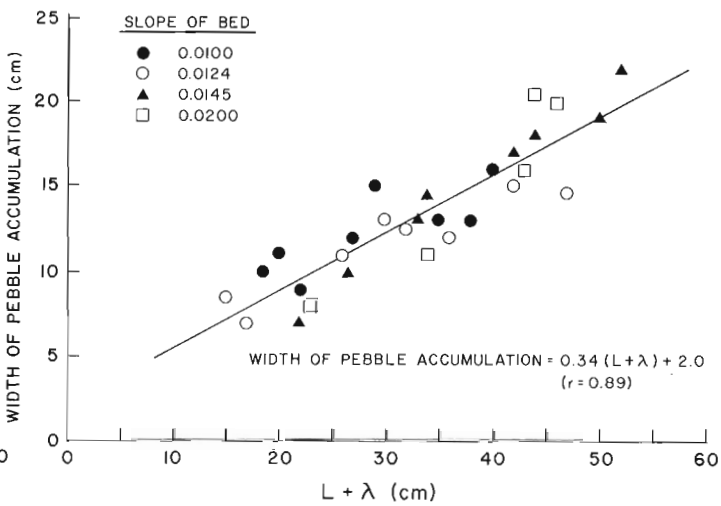

Figure 80.11. Maximum width of pebble accumulation under standing wave vs. width of transition zone.

dimensionless number, which is related to $(L + \lambda)$ as shown in Figure 80.10, is related to the Froude number as follows:

$$\frac{\text{rib spacing}}{y_1} = 5.7\ F_1 - 2.2$$

for the range of conditions examined. It is not affected by pebble size. Greater slopes have resulted in higher Froude numbers, but the data for different slopes cluster evenly about the general trend, suggesting that slope is not a significant variable at these relatively low Froude numbers.

Rib spacing, through its dependence on $(L + \lambda)$, can be related to y_1. The relationship (Fig. 80.12) is strongly slope dependent. Rib spacing and y_1 values measured at a given discharge and channel slope for each of the two pebble sizes were averaged to produce the points on which Figure 80.12 is based. The slope of the lines indicates that rib spacing increases more rapidly with y_1 as the bed slope becomes greater.

For bed roughness values other than those for aluminum plate used in this experiment, the location of the curves in Figure 80.12 would change. However, the roughness values of aluminum plate and of silty-clay laminations commonly observed underlying transverse ribs in the field are probably similar (Manning's n=0.013 according to tables in Chow, 1959).

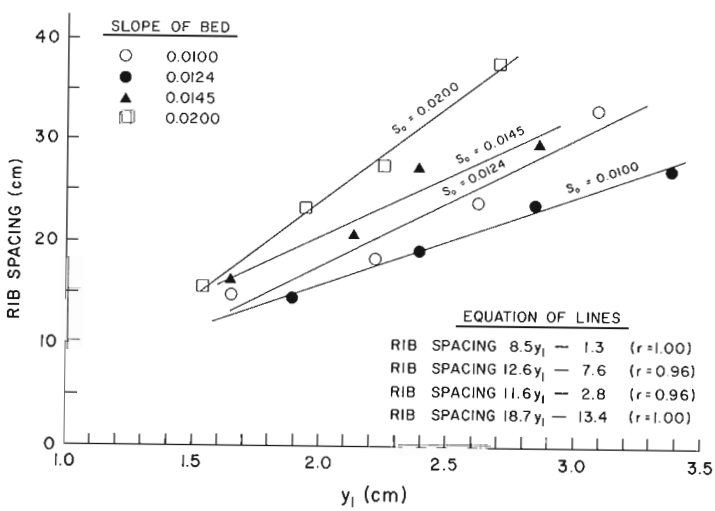

Figure 80.12. Transverse rib spacing vs. upstream depth at particular slopes.

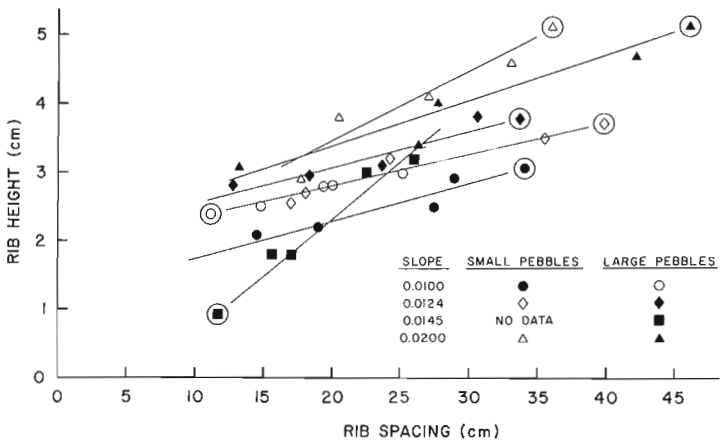

Figure 80.13. Transverse rib spacing vs. rib height at particular slopes.

The relationships among rib spacing, rib height, and channel slope are shown in Figure 80.13. The main observation is that for a constant grain size distribution, larger slopes are associated with higher and more closely spaced ribs. Judd and Peterson (1969) observed a similar relationship in high gradient streams.

Other general relationships for the range of conditions examined in the experiment can be summarized as follows:

(1) rib spacing averages about 7.25 (varies from 5 to 10) times the height of the pebble accumulation under the standing wave as the wave breaks;

(2) the pebble accumulation beneath the standing wave at the breaking point of the wave is 3 to 7 times wider than it is high;

(3) the height of the pebble accumulation as the standing wave breaks is 1 to 2 times y_1; and

(4) transverse ribs formed easily at F_1 values between 1.6 and 2.5, but distinct ribs were difficult to preserve in the few runs where F_1 exceeded about 2.5.

In the case of uneven pebble supply causing the jump to be oriented obliquely to the flow, with pebbles tending to "pile up" on one side of the channel, y_2 varies from one side of the channel to the other. This does not influence rib spacing, but rib heights preserved in the subcritical flow field are lowest where y_2 is lowest, presumably in response to a relatively high bed shear stress there.

The experiments indicate conclusively that transverse ribs can form in association with a hydraulic jump where supercritical flow reverts to subcritical flow. The ribs formed by step-wise upstream migration of the jump do not represent an equilibrium bed form, but rather the ribs become younger upstream. The process satisfactorily explains characteristics of ribs observed in the field.

Conclusions and Summary

Transverse ribs are bed forms that are common in shallow streams carrying coarse alluvium. Experiments in a laboratory sedimentary flume indicate that ribs may form in the transition zone where supercritical flow reverts to subcritical flow. Ribs were formed in the laboratory sequentially by a step-wise upstream migration of a hydraulic jump. Formation of individual ribs takes place in seconds, after which the ribs are "fossilized" in a subcritical flow field. The process would be observed only fortuitously in the field, during a short lived and transitory supercritical flow event. As observed in a reach, they do not represent an equilibrium bed form, but rather they were formed quickly under former conditions of rapidly varied flow. Development of distinct ribs at given bed slope and flow conditions is partially dependent on the calibre of sediment fed into the hydraulic jump and on the rate of sediment transport. Spacing of transverse ribs is dependent on the dimensions of the water waves in the transition zone; these dimensions are related in turn through bed slope to depth and velocity of the incoming supercritical flow and to depth of the succeeding subcritical flow. Formation of transverse ribs in a stream increases bed roughness in that reach and exerts an influence on eddy generation and local turbulence.

More data need to be gathered, from both field and laboratory, regarding the following: (1) the effect, if any, of pebble shape on rib dimensions; (2) the effect of various particle size mixes, that are supplied to the hydraulic jump, on characteristics of the deposit; (3) the distribution of transverse ribs in active streams both on beds that have been subjected to exceptionally large discharges and in the geologic record; (4) the frequency and controls of supercritical flow events in natural channels; and (5) the importance of supercritical flow for transport of the larger particles in a given stream.

Acknowledgments

Capable laboratory assistance was provided by D.M. Morel and J-S. Vincent. Drs. A.V. Jopling and H.J. McPherson furnished pebble measurements from North Saskatchewan River for comparison with measurements from the Peyto outwash plain. The comments by R. Kellerhals, G. Middleton, and N. Smith on an earlier draft of this paper are acknowledged by adoption wherever appropriate.

References

Boothroyd, J.C.
1970: Recent braided-stream sedimentation, south-central Alaska (Abstr.); Am. Assoc. Pet. Geol., Bull., v. 54, p. 836.

Boothroyd, J.C. and Ashley, G.M.
1975: Processes, bar morphology, and sedimentary structures on braided outwash fans, Northeastern Gulf of Alaska; in Glaciofluvial and glaciolacustrine sedimentation, eds. A.V. Jopling and B.C. McDonald; Spec. Pub. No. 23, Soc. Econ. Paleontol. Mineral., p. 193-220.

Chow, V.T.
1959: Open-channel Hydraulics; McGraw-Hill Book Co., Inc., 680 p.

Church, M.A. and Gilbert, R.
1975: Proglacial fluvial and lacustrine environments; in Glaciofluvial and glaciolacustrine sedimentation, eds. A.V. Jopling and B.C. McDonald; Spec. Pub. No. 23, Soc. Econ. Paleontol. Mineral., p. 22-100.

Day, T.J.
1976: Preliminary results of flume studies into the armouring of a coarse sediment mixture; in Report of Activities, Part C; Geol. Surv. Can., Paper 76-1C, p. 277-287.

Henderson, F.M.
1966: Open Channel Flow; Macmillan Co., 522 p.

Jopling, A.V. and Richardson, E.V.
1966: Backset bedding developed in shooting flow in laboratory experiments; J. Sediment. Petrol., v. 36, p. 821-825.

Judd, H.E. and Peterson, D.F.
1969: Hydraulics of large bed element channels; Utah Water Res. Lab., Rep. PRWG 17-6, Utah St. Univ., Logan, 115 p.

Koster, E.H.
1976: Experimental studies of coarse-grained sedimentation; unpubl. Ph.D. dissert., Univ. Ottawa, Ottawa, 253 p.

McDonald, B.C.
1972: The Geological Survey of Canada sedimentation flume; Geol. Surv. Can., Paper 71-46, 12 p.

McDonald, B.C. and Banerjee, I.
1970: Sedimentology studies on the outwash plain below Peyto Glacier, Alberta; in Report of Activities, Part A, Geol. Surv. Can., Paper 70-1A, p. 199.

1971: Sediments and bed forms on a braided outwash plain; Can. J. Earth Sci., v. 8, p. 1282-1301.

81. SPATIAL ASYMMETRY OF A DISPERSING TRACER MASS

Project 750081

Terry J. Day
Terrain Sciences Division

Abstract

Day, Terry J., Spatial asymmetry of a dispersing tracer mass; Current Research, Part A, Geol Surv. Can., Paper 78-1A, p. 453-458, 1978.

During the course of a longitudinal dispersion experiment in a meandering gravel channel (Banks Island, Northwest Territories), twelve partial or complete descriptions of a distance-concentration distribution were determined. These data indicate that for large times, the distance-concentration curve is distinctly asymmetric, with a tail of tracer concentration extending upstream. This asymmetry is considered to be consistent with the theory that tracer material is retained in, then subsequently slowly released from, fluid traps distributed along the flow boundary.

Introduction

The field experiment was undertaken with the purpose of assessing the longitudinal dispersion of tracer particles in a meandering stream. These measurements are part of a series required to determine relationships between channel and flow parameters and dispersion characteristics. As theoretical approaches are limited in application to natural channels, field measurements are required.

The mean longitudinal motion of an initially concentrated mass of tracer (or contaminant), and its determining mechanisms, has been the focus of considerable scientific study. The common theoretical approach has been based on Taylor's (1954) analysis for dispersion in pipe flow. For sufficiently large times, Taylor showed that

$$C = Bt^{-1/2} \exp \quad -(x-ut)^2/4K_x t \qquad (1)$$

where C is the mean cross-sectional concentration, B is a constant proportional to the amount of dispersing material, t is time from initiation, x is distance downstream, K_x is the longitudinal dispersion coefficient, and u is the mean cross-sectional velocity. At a fixed time the concentration distribution along the channel described by equation (1) is Gaussian. The assumption made for this Gaussian distribution and for the necessary constant value of K_x is uniform, steady flow with a constant mass balance of tracer material. Under these conditions, and after sufficiently large time, the velocity of a particle becomes a stationary random function because the statistical properties of the flow are the same at any longitudinal position, and a particle contained within a uniform cross-section samples all parts of the cross-section. The time required for this Gaussian shape to develop is termed the convective period (Fischer, 1966). When the fluid particles have entered the second, or final, period the advection of the dispersing cloud proceeds at a rate equal to the velocity of the flow (i.e. linear advection), while the symmetric spreading of the cloud about the mean position proceeds as the square root of time or distance.

The duration of the convective period in open channel flows can be compared by computing Fischer's (1966) dimensionless time parameter, t, where

$$t' = t\ 0.23du_*/\ell^2 \qquad (2)$$

d is flow depth, u_* is shear velocity, and ℓ is a characteristic length (taken as one half the flow width for centre injection). Fischer stated that t' = 0.4 is a reasonable practical criterion for the end of the convective period. Chatwin's (1972) criterion of t' > 1.0 is much more stringent. He had shown earlier that Fischer's laboratory work had not extended over sufficiently large times, as the measured time-concentration

Table 81.1

Summary of test data

Sampling Site	Downstream Distance (km)	Flow Width (m)	Flow Area (m^2)	Mean Velocity (m/s)	Shear Velocity (m/s)	Tracer Variance (min^2)
1	2.95	39.0	23.4	0.22	0.083	577.7
a	5.80					
2	6.55	33.2	16.0	0.34	0.074	2118.2
b	7.00					
c	7.85					
d	8.64					
e	9.09					
3	9.75	51.8	24.4	0.17	0.080	3366.6
f	10.41					
g	10.90					
h	11.60					
4	12.09	54.6	36.8	0.12	0.089	6870.0
5	14.80	35.1	21.2	0.21	0.084	7476.1

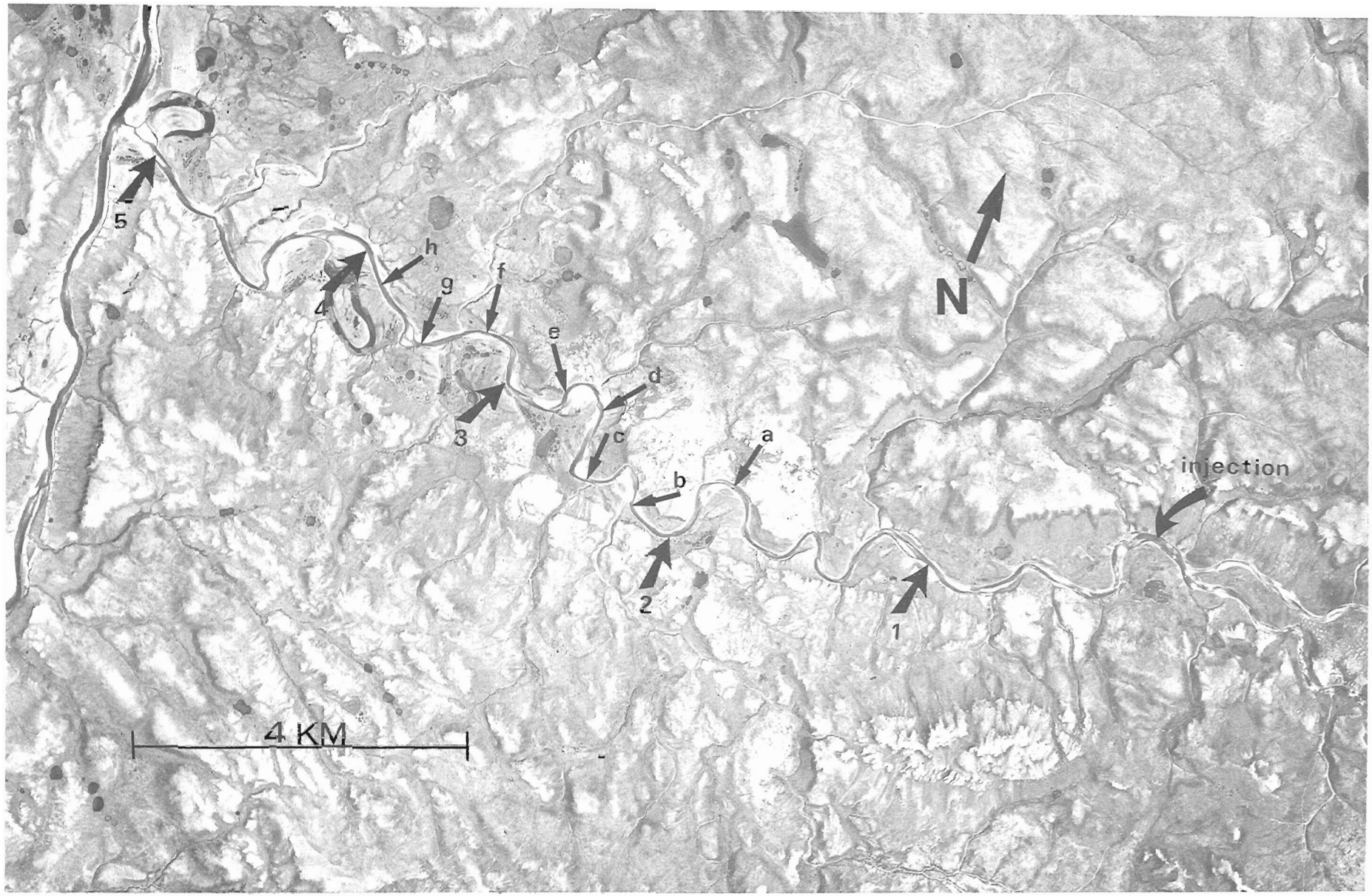

Figure 81.1. Enlarged portion of an aerial photograph (A17379-40) showing the spatial sampling sites on the north bank (a to h) and the time sampling sites on the south bank (1 to 5).

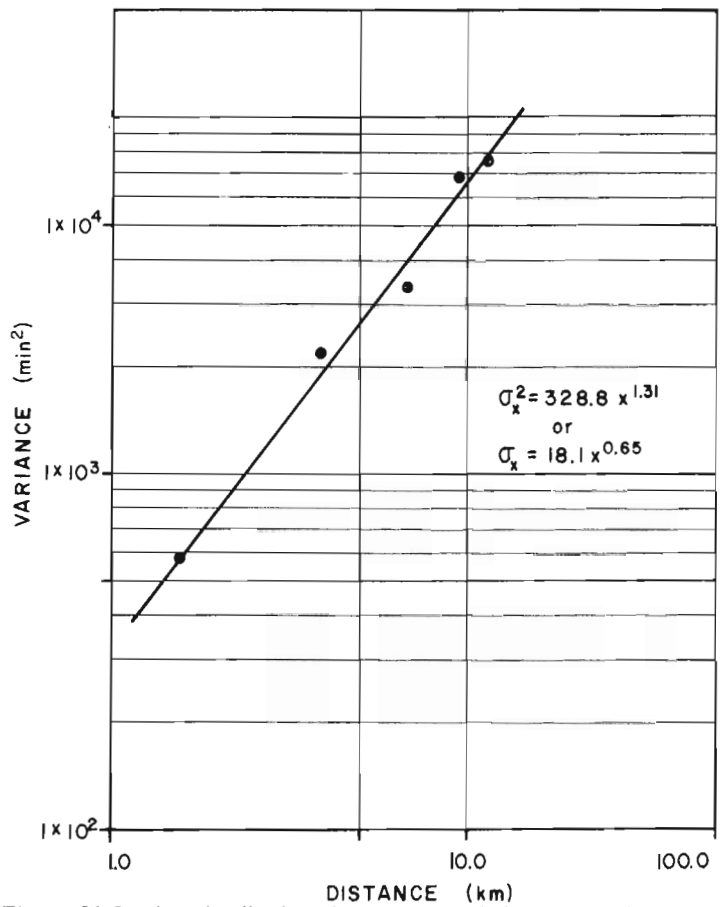

Figure 81.2 Longitudinal variance trend of the tracer cloud. Downstream distance is measured from point of injection.

curves were not Gaussian (Chatwin, 1971). Chatwin also showed that the results of Taylor's pipe flow experiments produced a Gassian curve. Sayre (1968) numerically solved Aris' (1956) moment equations to show that although the approach to a Gaussian distribution was relatively slow, the variance rapidly satisfied the Taylor predictions that the increase of variance and distance was proportional to time.

The asymmetric concentration distributions measured in Fischer's open channel experiments are common to open channel studies. Many explanations for this shape have been advanced. Both Elder (1959) and Sullivan (1971) considered the laminar sublayer to play a role in producing skewness. Hays (1966) and Thackston and Schnelle, (1970) showed how trapping the tracer material in dead zones can affect the shape of the concentration distribution. Fischer (1966) dismissed both the laminar sublayer and the dead zone concepts in preference for the view that skewness develops during the convective period when the tracer particles adopt the form of the velocity profile. Day (1975) showed that a tracer cloud dispersing along rough channels maintains a persistent asymmetry when measured over time at a fixed distance. Nordin and Sabol (1974) presented similar data for a wide variety of rivers. Day and Wood (1976) showed that a persistent asymmetry is characteristic of the self-similarity (linear spreading and a constant dimensionless shape of the time-concentration curve) of dispersion in some natural channels. Valentine and Wood (1977) showed that these deviations could be explained in terms of a Stationary eddy structure adjacent to the bed and that the presence of these fluid traps could delay arrival of the final period.

A problem in determining the shape of concentration distributions in natural channels results from using the technique of placing one or more probes at a fixed cross-section and measuring particle concentration as a function of time (t) as the cloud passes the probe. From equation (1) it can be seen that the graph of C against t is not symmetric about the peak because of the factor t^{-1} in the exponential and $t^{-1/2}$ multiplying the exponential. Portions of the cloud passing the probe first are younger than those that pass later.

Table 81.2

Time and concentration data for spatial concentration pattern

Sampling Site	Downstream Distance (km)	Time and Concentration Data*											
		6.25	6.50	6.75	7.00	7.25	7.50	7.75	8.00	8.25	8.50	8.65	9.00
a	5.80	**	4.77	4.22	3.55	3.25	2.45	2.73	2.18	2.05	**	**	**
2	6.55	12.55	11.05	8.60	6.28	5.19	3.28	**	**	**	**	**	**
b	7.00	21.56	19.10	16.37	12.69	10.37	8.59	6.68	5.45	4.64	3.82	3.55	2.73
c	7.85	29.96	29.22	27.72	20.88	17.74	13.37	10.37	9.82	7.64	4.55	5.45	4.09
d	8.64	4.90	10.64	18.83	25.11	25.79	24.29	24.83	25.79	18.83	16.51	15.01	12.69
e	9.09	0.34	1.16	3.21	6.88	13.58	19.98	22.68	26.27	26.27	23.82	22.72	19.43
3	9.75	0.0	0.0	0.0	0.68	0.27	5.32	5.44	10.64	16.92	21.15	19.38	21.83
f	10.41	0.0	0.34	0.48	0.34	1.17	1.03	1.03	1.43	3.76	8.26	10.44	16.58
g	10.90	1.36	1.08	0.41	1.23	0.55	0.82	1.23	1.37	1.64	2.59	4.91	7.37
h	11.60	**	**	**	0.96	0.68	0.96	1.23	0.41	0.96	0.41	1.23	0.96

* Time refers to that elapsed from injection in hours, and concentration is in ppb.
** No samples taken.

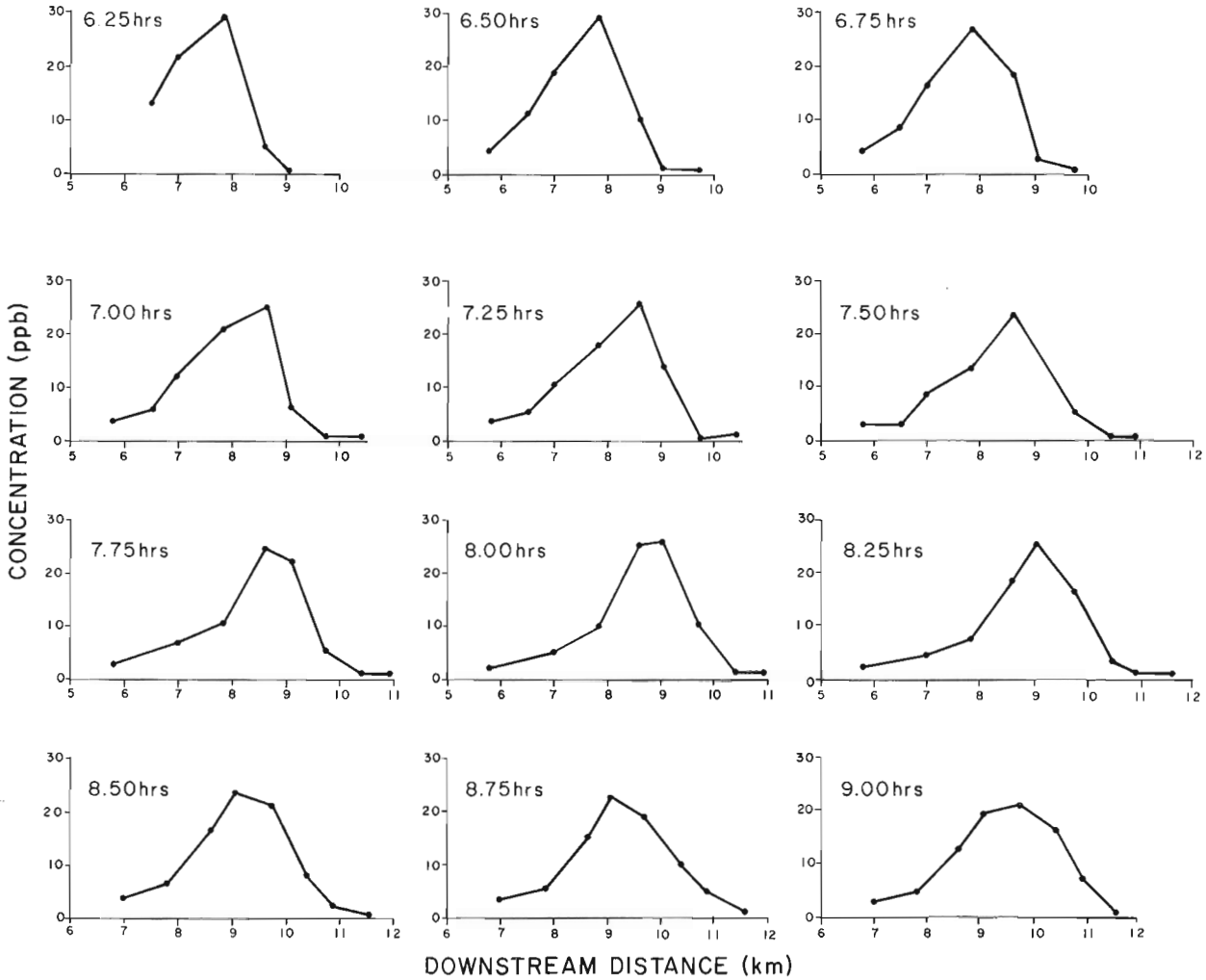

Figure 81.3. Distance concentration data for the twelve spatial sampling sites.

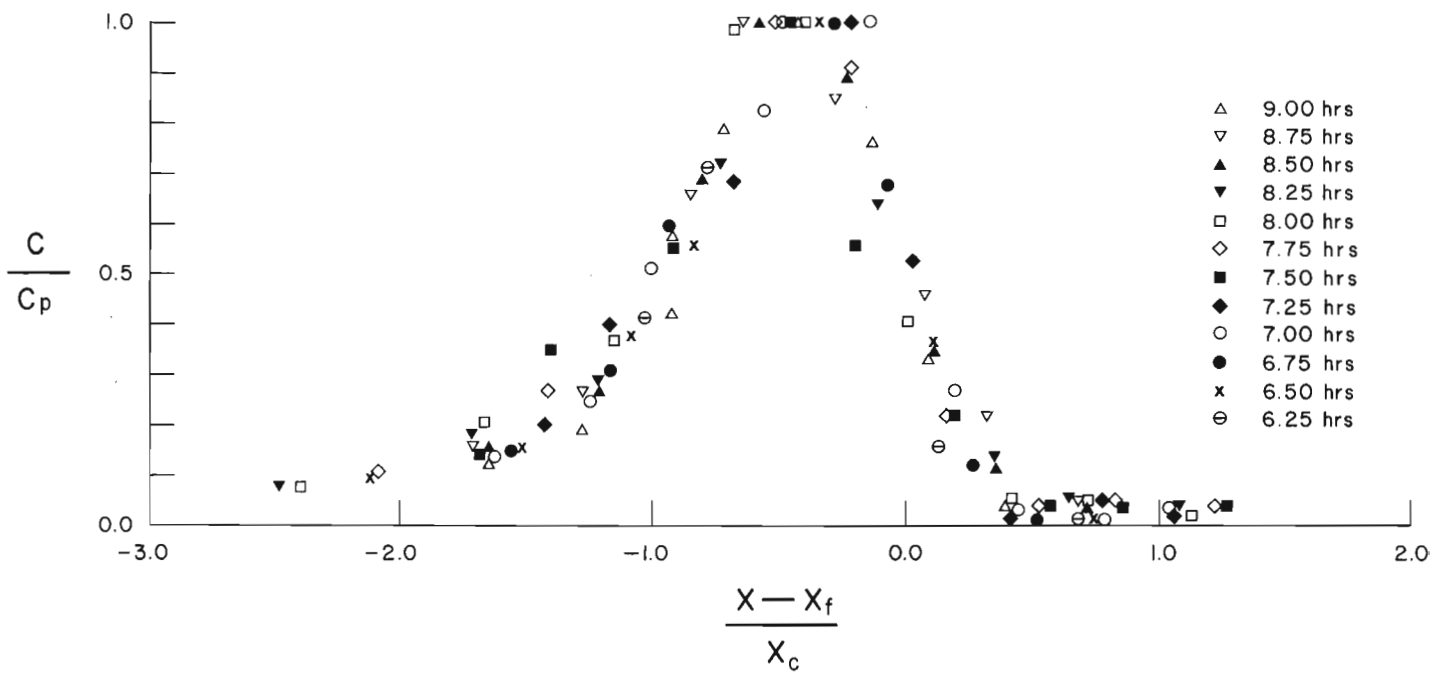

Figure 81.4. Composite nondimensional plot of the twelve spatial samples.

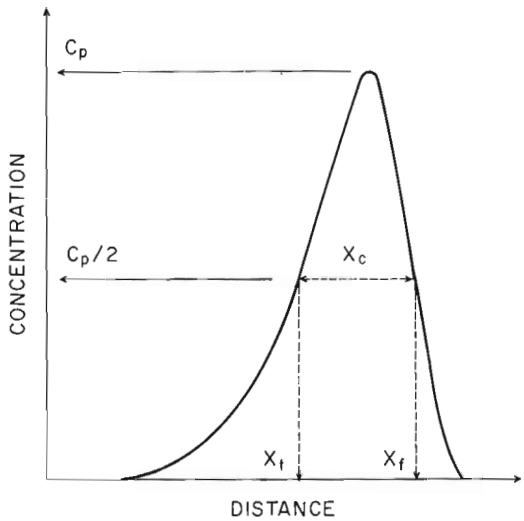

Figure 81.5

Definition sketch for nondimensionalizing the tracer dimensions. C_p is the peak concentration, X_f is the midpoint ($C_p/2$) on the leading or downstream edge of the tracer, X_t is the midpoint on the trailing or upstream edge, and X_c is the distance between the two points. To nondimensionalize a distance-concentration curve, all concentration values can be divided by C_p and all distance co-ordinates by a time parameter representing the dimensions (X_c) and the position of the tracer from injection (say X_f).

Experimental data

The tracer test was undertaken on July 19, 1975 in an unnamed river on Banks Island, Canadian Arctic Archipelago. The location of the river is approximately 73°12'N, 119°29'W (mid reach). Four litres of Rhodamine WT 20% were injected into the river, and the resultant path of the tracer cloud was followed over 14.8 km. An aerial photograph of the test reach and sampling sites is shown in Figure 81.1. The river has a well developed meander pattern, a gravel bed, and a distinct pool and riffle sequence. The longitudinal slope is approximately 0.0012. Discharge during the 18.5 hour sampling period was about 4 m^3/s (determined from five current metering sites, one at each main sampling site (1-5) over a nine hour period).

At sites 1 to 5 (Fig. 81.1) the passing tracer cloud was sampled over time. The distances and hydraulic measurements (based on current metering) for these sites are listed in Table 81.1. Sites a to h were positioned for spatial sampling (Table 81.1) which began at 6.25 hours after injection and continued at quarter hour intervals for 2.75 hours (12 samples) until 9 hours after injection. All samples were taken just below the surface in what was considered to be the centre of flow.

Discussion of results

The longitudinal spreading of the tracer cloud through the test reach is shown in Figure 81.2 where the tracer variance (measured over time at a fixed distance) is plotted against distance. These data, listed in Table 81.1 are best fitted with an equation of

$$\sigma_t^2 = 324x^{1.31} \quad (3)$$

or

$$\sigma_t = 18x^{0.65} \quad (4)$$

where σ_t^2 is the variance, and σ_t the standard deviation, measured over time for a fixed distance. Equations (3) and (4) explain 98% of the variance. The exponent in equation (4) indicates that the rate of spreading is near to that rate required for Taylor's analysis. This exponent is also considerably lower than the mean value of 1.0 determined by Day (1975) for a wide range of natural channels. The mean travel time of the tracer cloud was 0.20 m/s, similar to the mean cross-sectional velocity (mean of column 5, Table 81.1) of 0.21 m/s.

Concentration data for the ten spatial sampling sites are listed in Table 81.2 and are plotted in Figure 81.3. Location of the peak concentration at 7.85 km (site c) for the first three sampling periods is due to the wide spacing of the sites and not to a stationary or slowly advecting tracer cloud. As dispersion continued the dimension of the cloud increased so that the widely spaced sampling sites produced a better description. By 7.0 hours; definition of the tracer had improved and the asymmetric shape emerged and was maintained at all subsequent sample times. The downstream or leading edge of the tracer cloud rises steeply to the peak. Along the upstream or trailing limb, concentrations decline more gradually, forming a long tail. This tail is best defined in the waves sampled at 7.75, 8.0, and 8.25 hours but also is evident in all but the first wave.

A nondimensional comparison of the asymmetric shape among the twelve spatial samples, based on parameters defined in Figure 81.5, is given in Figure 81.4. Even with the scatter it is evident that the asymmetric shape of the tracer cloud maintained a consistent form over the 2.75 hour sampling period. Some of this scatter results from poor definition of the peak concentration.

These spatial descriptions were measured within the usual criteria of the final period. Calculation of Fisher's convective length equation (2) indicates a distance about 3.9 km (t' = 0.4)

It is unfortunate that these data are insufficient to assess the spatial dynamics of the tracer cloud as it travels through the test reach. The limited results, however, are important because they appear to be the first spatial descriptions in natural channels, and the tracer cloud is shown to maintain a distinct asymmetry downstream from where conventional methods estimate that a Gaussian shape should develop. The most likely cause of this persistent asymmetry is the trapping and subsequent slow release of tagged particles from dead or slowly moving zones along the flow boundary. Although dead zones appear to delay the attainment of the Gaussian shape, they do not, in this case, appear to increase the dispersion rate as much as found by Day (1975) for rough, high gradient natural channels or by Beltaos and Day (1977) for a large meandering river.

Acknowledgments

The author would like to thank numerous field personnel, particularly J-S. Vincent, and also S. Miller for his assistance in the analysis of tracer samples.

References

Aris, R.
1956: On the dispersion of a solute flowing through a tube; R. Soc.Lond., Ser. A., v. 235, p. 67-77.

Beltaos, S. and Day, T.J.
1977: Longitudinal dispersion in a natural stream: Lesser Slave River, Alberta; Alberta Res. Coun., 30 p.

Chatwin, P.C.
1971: On the interpretation of some longitudinal dispersion experiments; J. Fluid Mech., v. 48, no. 4, p. 689-702.

1972: The cumulants of the distribution of concentration on a solute dispersing in solvent flowing through a pipe; J. Fluid Mech., v. 51, no. 1, p. 63-67.

Day, T.J.
1975: Longitudinal dispersion in natural channels; Water Resour. Res., v. 11, no. 6, p. 909-918.

Day, T.J. and Wood, I.R.
1976: Similarity of the mean motion of fluid particles dispersing in a natural channel; Water Resour. Res., v. 12, no. 4, p. 655-666.

Elder, J.W.
1959: The dispersion of marked fluid in turbulent shear flow; J. Fluid Mech., v. 5, no. 4, p. 544-560.

Fischer, H.B.
1966: Longitudinal dispersion in laboratory and natural channels; unpubl. Ph.D. thesis, Rep. KH-R-12, Calif. Inst. Technol., Pasadena, 250 p.

Hays, J.R.
1966: Mass transport phenomena in open channel flow; unpubl. Ph.D. thesis, Vanderbilt Univ., Tennessee, 138 p.

Nordin, C.F. and Sabol, G.V.
1974: Empirical data on longitudinal dispersion in rivers; U.S. Geol. Surv., Water Resour.-Invest., 20-74, p. 331.

Sayre, W.W.
1968: Dispersion of mass in open channel flow; Colo. State Univ., Hydrol. Boulder, Pap. 13, 3 p.

Sullivan, P.J.
1971: Longitudinal dispersion within a two-dimensional turbulent shear flow; J. Fluid Mech., v. 149, no. 3, p. 551-576.

Taylor, G.I.
1954: The dispersion of matter in turbulent flow through a pipe; R. Soc. Lond., Proc., Ser. A, v. 233, p. 446-468.

Thackston, E.L. and Schnelle, K.B.
1970: Predicting effects of dead zones of stream mixing; Am. Soc. Civ. Eng., J. San. Eng. Div., v. 96(SAZ) p. 319-331.

Valentine, E.M. and Wood, I.R.
1977: Longitudinal dispersion with dead zones; Am. Soc. Civ. Eng., J. Hydraul. Div., v. 103, no. 9, p. 975.

82.

SOME PHYSICAL AND CHEMICAL PROPERTIES OF TILL DERIVED FROM THE MEGUMA GROUP, SOUTHEAST NOVA SCOTIA

Project 690095

W.E. Podolak and W.W. Shilts
Terrain Sciences Division

Abstract

Podolak, W.E. and Shilts, W.W., Some physical and chemical properties of till derived from the Meguma Group, southeast Nova Scotia, Current Research, Part A, Geol. Surv. Can., Paper 78-1A, p. 459-464

Samples were collected from selected stratigraphic sections and other exposures of Quaternary sediments in southeastern Nova Scotia in order to make a preliminary assessment of the value of till sampling to enhance interpretation of results of a proposed lake sediment sampling project. Analyses of the samples indicated weathering of economically important indicator minerals to depths of more than 2 m. Trace element concentrations showed significant regional variations both within a till type and among some of the major till types. These results confirm the premise that the extensive sampling program carried out by Nova Scotia Department of Mines should provide data essential to the proper interpretation of the results of regional lake sediment sampling.

A till sampling program was begun by the Nova Scotia Department of Mines in 1977 in order to enhance interpretation of results of a planned regional geochemical lake sediment sampling program. Modern lake sediments were collected in 1977 over folded Paleozoic sedimentary rocks and granitic intrusions of the Meguma Group in southern Nova Scotia, east of Halifax.

At the beginning of the program, the authors visited the study area briefly to sample selected till exposures and to offer suggestions based on drift sampling work elsewhere in the Appalachians (Shilts, 1973a, b, 1975, 1976; Shilts and McDonald, 1975; Grant and Tucker, 1976). Profile samples were collected through sections at Hartlen Point (near Halifax), at Ecum Secum, along Musquodoboit River, and at Cooks Cove; several individual samples were collected elsewhere (Fig. 82.1). A number of geochemical and geotechnical tests were performed on these samples in order 1) to illuminate the differences in physical and chemical properties

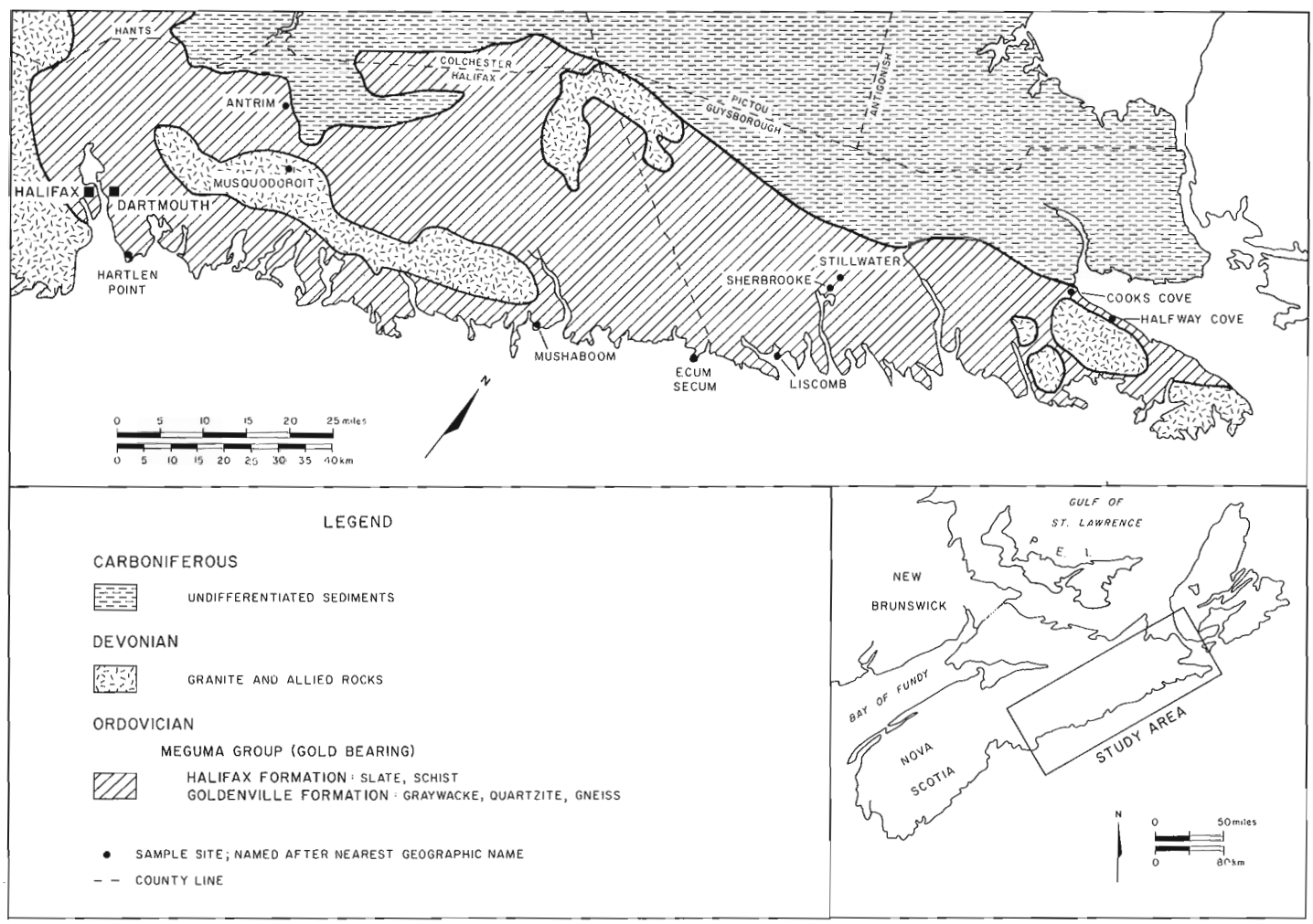

Figure 82.1. Location of samples and generalized bedrock geology modified from Weeks (1965).

among the various lithological types of till described by Grant (1963) and Prest et al. (1972); 2) to define primary vertical sedimentological and stratigraphic variations in properties in sections through one or more till sheets; and 3) to define the depth and intensity of weathering of the more labile components of the various types of till. This latter study is particularly important in the extensive areas of red till where the primary hematitic colour tends to mask the secondary iron oxide/hydroxide deposits that usually indicate weathering.

Techniques

The trace element content of the clay (< 2 μ) fractions and the fine sand-sized heavy mineral (specific gravity, s.g. > 3.3) fractions were analyzed for all till samples. Analyses were carried out by Bondar-Clegg and Co., Ltd. using hot, mixed acid leach and atomic absorption and fluorescence techniques. In addition to the chemical tests, weight percentages of the fine sand-sized heavy mineral and magnetic fractions were measured, and complete grain size distributions (< 2 mm >2 μ) and Atterberg limits were calculated.

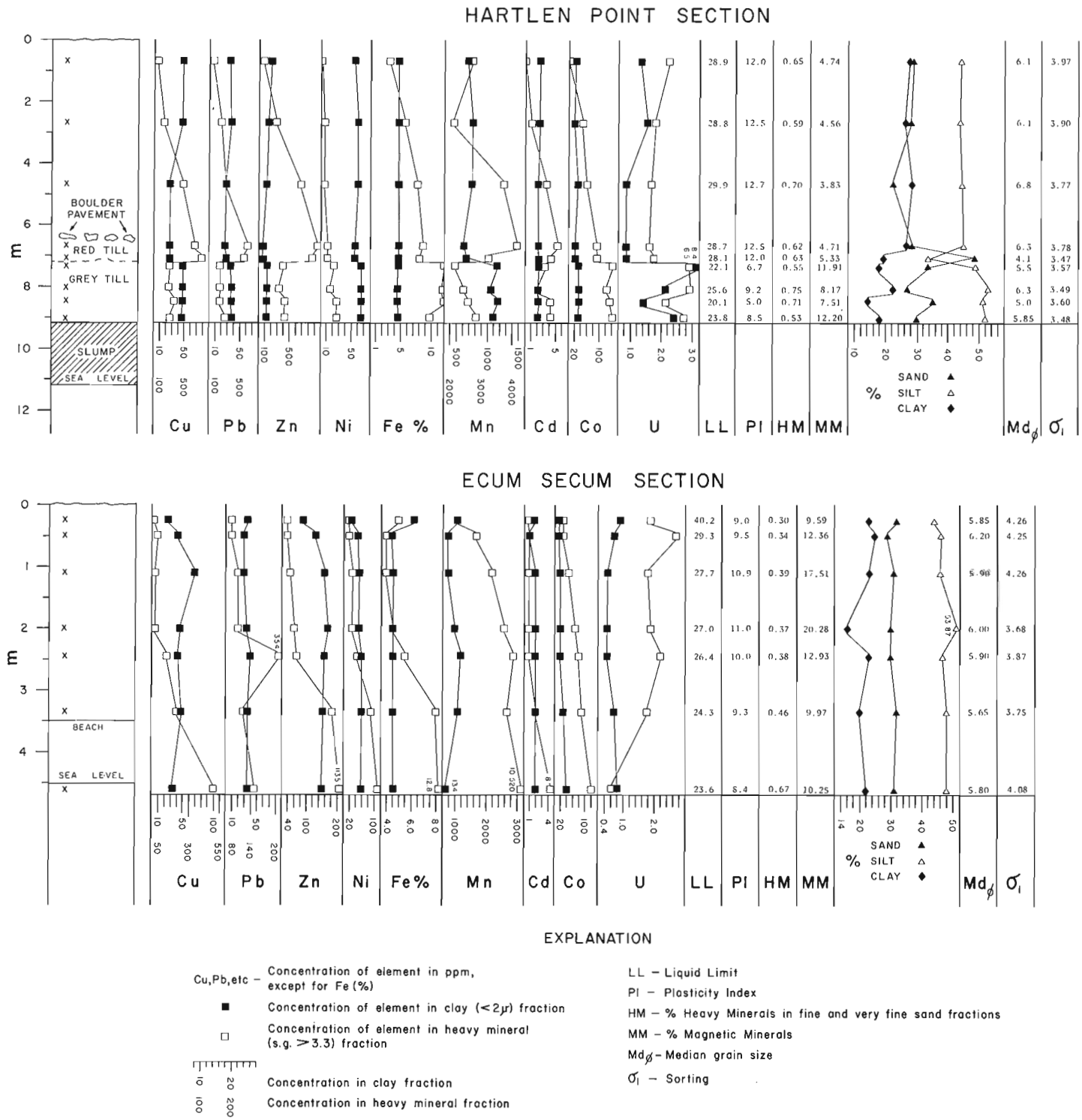

Figure 82.2. Vertical variations of selected chemical and physical parameters, Hartlen Point and Ecum Secum sections.

Previous work

The tills of Nova Scotia were first seriously studied by Grant (1963) who found that several types of till or related sediments could be found at the surface in southern Nova Scotia. In areas underlain by slates, quartzites, and granitic rocks of the Meguma Group, Grant noted the occurrence of several significant and distinct types of till among which he described 1) quartzite till; 2) granite till; 3) slate till; 4) red (clay) till; 5) compact grey till underlying red till; and 6) Bridgewater conglomerate. Grant noted that the first three types contained clasts eroded predominantly from quartzite, granite, or slate of the Meguma Group with very little exotic detritus from outside its outcrop area; furthermore, the distribution of these local till types was confined largely to outcrop areas of the rock that provided the dominant lithology with little, but predictable, overlap onto rock types down ice. The red till was found to replace, overlie, or underlie the first three types of till in many areas and occurred particularly commonly as drumlins in fields. The compact grey till was found to underlie red till in some exposures and was interpreted to have been deposited during an earlier glacial stade than the surface tills. Grant described the Bridgewater conglomerate as a till-like to stratified, iron and manganese cemented gravel, containing abundant slate fragments and erratics from outside the slate terrane. It was described as a glaciofluvial unit that was older than any of the tills because it always was found directly on slate bedrock and/or under till. However, because of the presence of erratics that could only have been transported by glacier, Grant ruled out earlier interpretations that described the Bridgewater conglomerate as a preglacial fluvial deposit.

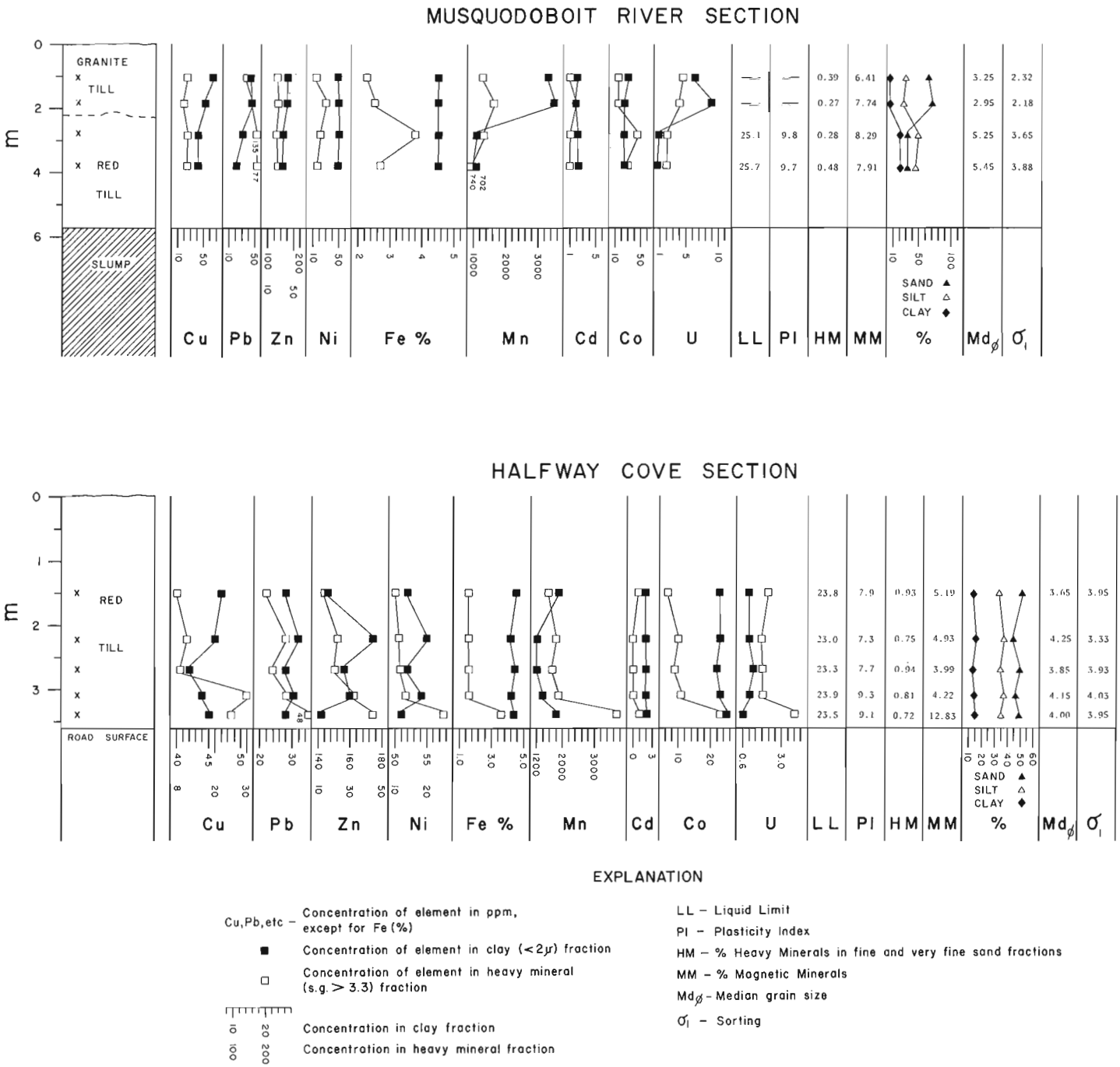

Figure 82.3. Vertical variations of selected chemical and physical parameters, Musquodoboit River and Halfway Cove sections.

In the brief reconnaissance, most of the till types that Grant (1963) described were noted, both in sections that he studied and in new exposures. The authors noted, as did Grant, that some of the loose, coarse textured tills are difficult to place in either the lodgment or ablation classifications.

Two exposures of iron cemented slate till that overlies loose quartzite till and, possibly, red till were found near and east of Halfway Cove on the south shore of Chedabucto Bay. In cementation, texture, and clast composition, this material closely resembles the sediment that Grant described as Bridgewater conglomerate. The occurrence of the cemented till may be due to the presence of a permeable till with abundant pyritiferous slate fragments in a topographic situation where presently undefined local groundwater conditions lead to the characteristic cementation.

At Hartlen Point, south of Dartmouth, a section described by Grant (1963) as red till overlying grey compact till was examined. A boulder layer, which Grant described as a possible lag deposit separating two tills of different glacial stades, was found not to be confined to the contact, but to occur considerably above the base of the red till in some places (Fig. 82.4).

Results

Although the sampling was designed to provide preliminary trace element data on various types of till, some other parameters, such as texture, Atterberg limits, and magnetic mineral content, have been determined. These latter mineralogical and physical properties help give an impression of the variations of properties evident in the field. In addition, they can support the interpretation that compositional differences implied by trace element variations are related to till provenance rather than to local hydromorphic factors. The trace elements reported here were selected because they might reasonably be expected to be associated with various types of base metal or radioactive mineral occurrences thought likely to be present in the area. Figures 82.2 and 82.3 show the variations in selected trace element concentrations and in some other properties for four vertical sections through one or more till sheets.

Trace elements

Copper Copper concentrations range from 40-60 ppm and show little variation in the clay fraction of most samples, with the exception of two samples of quartzite till from a borrow pit in Mushaboom (138-188 ppm), quartzite till samples from Liscomb (176 ppm) and Sherbrooke (136 ppm), and the only sample of iron cemented till from Halfway Cove (206 ppm).

In the heavy mineral fraction copper contents are generally low (6-50 ppm) in all but the samples collected from depths greater than 3 m below the surface. At depths of more than 2 m at Hartlen Point the lower grey till contains 228-296 ppm Cu, and the upper till contains 444-726 ppm (Fig. 82.4). In a wave cut cliff of red till at Ecum Secum, Cu in the heavy minerals in the top 2 m of the section ranges from 12-40 ppm but the lowermost samples, near and below sea level, contain 213-502 ppm.

Lead Lead in the clay fraction ranges from 20-40 ppm in all samples except for the quartzite tills at Liscomb (74 ppm) and Sherbrooke (51 ppm), red till over Triassic bedrock at Cooks Cove (56 ppm) and iron cemented till at Halfway Cove (211 ppm).

In the heavy mineral fraction lead is more variable, attaining levels at Hartlen Point of 260-536 ppm in the upper till and 228-296 ppm in the lower till; at Ecum Secum lead concentrations are as high as 354 ppm in a sample about 2 m below the surface. Samples of red till from Musquodoboit River (77-135 ppm) and a sample of quartzite till from Stillwater (122 ppm) have elevated lead values. Other samples generally have lead concentrations of 12-50 ppm in the heavy mineral fraction.

Zinc Zinc in the clay fraction of most till samples ranges from 120-170 ppm except for a sample of red till from over Triassic bedrock at Cooks Cove (91 ppm), the iron cemented till at Halfway Cove (68 ppm), two samples of quartzite till from Mushaboom (65-92 ppm), and the upper sample at Ecum Secum (91 ppm). The higher background values of zinc are similar to those for tills from the slate-granite-quartzite terranes of the Quebec Appalachians.

In heavy minerals, zinc concentrations are uniformly low (7-67 ppm) except for the lowest two samples at Ecum Secum (184-1135 ppm) and the lower (291-382 ppm) and upper (265-1070 ppm) till at Hartlen Point

Cobalt Cobalt shows little variation in clay fractions (20-40 ppm) except in the iron cemented till, which has 85 ppm Co. In the heavy mineral fraction, cobalt is enriched in the lowermost sample at Ecum Secum (119 ppm) and in the lower grey till at Hartlen Point (121-141 ppm).

Nickel There is little variation in nickel in the clay fraction of all samples collected (33-69 ppm). In the heavy mineral fraction, Ni is enriched in the lower Ecum Secum samples (69-133 ppm), in the lower till at Hartlen Point (198-233 ppm), and in the lower part of the upper till at Hartlen Point (70-115); all other samples have a low content of Ni (10-46 ppm).

Chromium Chromium is uniformly low (10-22 ppm) in the heavy mineral fraction from which magnetic minerals were removed.

Molybdenum Molybdenum is uniformly low (1-4 ppm) in clay fractions of most tills except for the iron cemented till at Halfway Cove (20 ppm) and one sample at Mushaboom (12 ppm).

Manganese Manganese in the clay fraction of these tills commonly occurs in the 1000-3000 ppm range, a relatively high concentration for till that has not been intensely weathered. Exceptionally high values of 11 220 and 5790 ppm were recorded for the red till on Triassic rocks at Cooks Cove and in the iron cemented till, respectively. An exceptionally low Mn concentration (134 ppm) was found in the clay fraction of the lowest Ecum Secum sample. In contrast, a concentration of 10 520 ppm Mn was found in the heavy mineral fraction of the lowest Ecum Secum sample, whereas most other heavy mineral separates ranged from 1000-4000 ppm.

Cadmium All but four samples (three at 1 ppm, one at 3 ppm) have concentrations of 2 ppm Cd in the clay fraction. In heavy mineral fractions, Cd is not detectable in many samples and varies from 1-4 ppm in the rest, with two exceptions – lowermost Ecum Secum sample (8 ppm) and lowermost red till at Hartlen Point (6 ppm).

Uranium In the Clay fractions uranium is less than 3 ppm except in the quartzite till samples at Mushaboom (4.2-8.5 ppm), in the upper granite till samples on Musquodoboit River (6.4-9.0 ppm), and in the uppermost part of the lower grey till at Hartlen Point.

In the heavy mineral fraction, uranium is less than 3 ppm except for the two upper Musquodoboit River samples (4.3-4.5 ppm), the upper part of the lower till at Hartlen Point (6.5 ppm), and the Mushaboom samples (5.6-13.0 ppm).

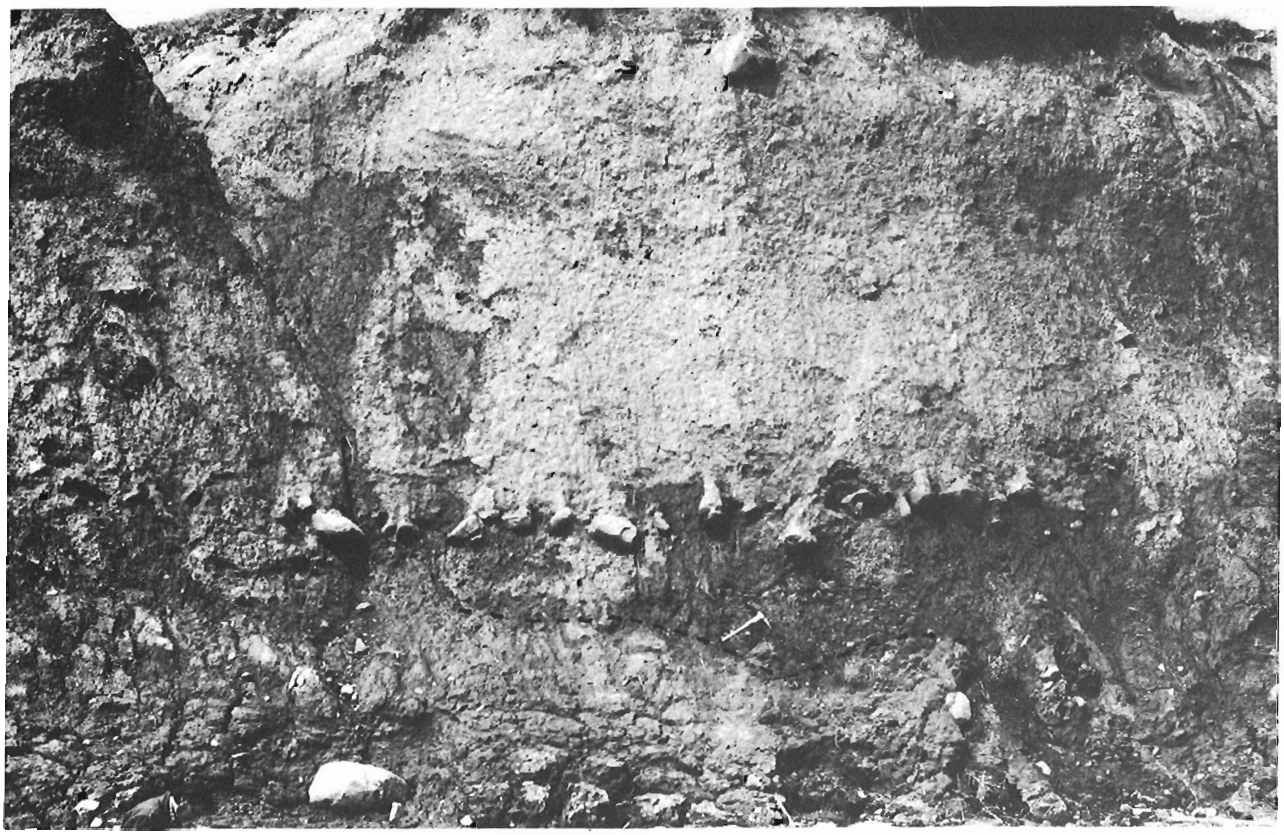

Figure 82.4. Hartlen Point section. Dashed line marks contact of upper red till and lower grey till. Note boulder pavement above contact within red till. (GSC photo 203215-C)

Iron Iron contents in the clay fraction are mostly between 4 and 5% the red tills containing no more iron than others. The iron cemented till contains 12.6% iron, and two of the three Mushaboom samples contain only 3% iron.

In the heavy mineral fraction, iron concentrations are less than 5% except in the Ecum Secum section (5-12%, top to bottom), in the lower till at Hartlen Point (9.4-12.4%), and the lower part of the upper till at the same site (6.8-8%).

Texture, Atterberg limits, magnetic mineral per cent, and heavy mineral per cent These parameters are summarized for the sections in Figures 82.2 and 82.3, and are mostly self-explanatory. Magnetic minerals are present in far greater amounts (7-12%) in the heavy mineral fraction of the lower till at Hartlen Point than in the upper till (4-5%). At Ecum Secum they comprise up to 20% of the heavy fraction. Atterberg limits are fairly typical for Appalachian lodgment tills; they are distinctly different in the two tills at Hartlen Point, and the uppermost sample in the solum at Ecum Secum has a high liquid limit.

Heavy minerals were examined briefly under a binocular microscope. Compared to tills from the western Appalachians and in other areas of Laurentide glaciation, the variety of heavy minerals in any given sample is very limited, one, two, or three species predominating. Very few heavy mineral species were observed other than those expected to occur in the local bedrock. In tills containing high amounts of Cu, Pb, Zn, Co, and Fe in heavy mineral separates at Hartlen Point and at Ecum Secum, abundant unoxidized fragments of pyrite and, possibly, other sulphides were observed. Evidence of sulphides was not observed in other samples except for rare pseudomorphs of limonite after pyrite.

Discussion

While there are several potentially interesting aspects to the mineralogical and trace element distributions of these few samples, it is expected that the extensive till sampling program undertaken by Nova Scotia Department of Mines will provide many answers based on far more data. However, a few preliminary observations regarding stratigraphy, areal variations of parameters, provenance, and weathering can be made here, bearing in mind that they are based on very few samples.

Areal variation

Areal variations of parameters are related closely to the various types of till, which in turn are related to bedrock characteristics. The red till, however, which derives its colour and many other components from outside the Meguma basin, shows considerable variation from site to site. This variation is thought to be related to local components added to the till during its transport. The high levels of cadmium and zinc in the lowermost Ecum Secum till sample may indicate a nearby source of sphalerite, for example. Quartzite till appears to be enriched in copper and lead, probably reflecting a homogenization of zones in the Goldenville (quartzite) Formation that are rich in these elements. The Mushaboom quartzite till samples and the Musquodoboit granite till samples are enriched in uranium, suggesting that tills and derived postglacial sediments on or down ice from areas underlain by granite might have elevated uranium contents (granite comprises 23-30% of the coarse clasts in the Mushaboom samples). The areal variations suggested by these few samples seem to be potentially

significant and when more accurately outlined by the till sampling program, should be used rigorously in evaluating other types of geochemical anomalies.

Stratigraphic variations

Variations of parameters that may occur where two types of till are exposed at one site are well illustrated by the Hartlen Point and Musquodoboit River sites. At these sites nearly all parameters measured vary significantly between tills (Figs. 82.2 and 82.3). It should be emphasized that these data do not indicate that these sites record two episodes of glaciation but may merely reflect two facies (i.e., subglacial and englacial) or shifts in ice flow direction during the same glaciation. Although there are no known outcrops of mafic rocks near or up ice from Hartlen Point, the relatively high ratio of Co-Ni-Fe to other trace elements sometimes is associated with tills with mafic rocks in their source areas. This element association stands in contrast to the Cu-Pb-Zn association in heavy minerals in the upper till, an association more typical of sedimentary sulphide mineralization.

As in the Appalachians of southeastern Quebec (Shilts, 1975, 1976), destruction of the more labile components (sulphides, carbonates, etc.) takes place to considerable depths and is reflected most sensitively by radical trace element decreases and by the disappearance of sulphide fragments upward in the sand-sized heavy mineral fractions. The transition from unweathered till upward into progressively more weathered till is well demonstrated in the profiles of heavy mineral chemistry of the red till at Hartlen Point and at Ecum Secum. The upward decreases of Cu, Pb, Zn, Co, Fe, Mn, and Cd in heavy minerals correspond with the disappearance of the abundant sulphide fragments found in the deeper, unweathered till samples. At all other sections and sample sites the heavy mineral fraction appears to have been stripped of labile components by weathering.

These observations confirm observations made elsewhere in the Appalachians (Shilts, 1976) – that labile components, which include many important indicators of mineralization, are destroyed to depths of several metres below the surface. Also, as observed elsewhere, the clay-sized portion of the tills fixes a portion of the cations released by weathering, with the result that concentrations of certain cations increase slightly in the clay fractions of tills that have been weathered. The compositional changes caused by the effects of weathering are superimposed on compositional variations related to varying bedrock sources.

Summary

Weathering of tills in Nova Scotia has destroyed many labile components (sulphides) to depths of 2 m or more below the surface. The clay-sized fraction of the tills probably is best to analyze for comparative purposes because 1) it is not affected by textural variations in the matrix of the widely varying types of till; 2) it is the fraction most likely to become part of lake sediments or to react with organic and other components that contribute to lake sediment, and 3) it probably scavenges cations released by weathering of labile components, as has been found elsewhere (Shilts, 1975). The effects of weathering are superimposed on stratigraphic, sedimentological, and areal variations and must be understood in order to understand regional and vertical compositional data.

Mapping of the distribution of types of till and their trace element geochemistry is essential to the interpretation of data obtained on sediments derived from the various types of till terrain. It is particularly important to map the distribution of the iron cemented till because of its high content of several cations scavenged by its iron-manganese rich matrix.

Maps of areal variations of chemical and mineralogical parameters and variations of those parameters in profile sampling of stratigraphic columns, along with soils maps and maps and information supplied by Grant (1963), should be carefully integrated into the regional lake sediment sampling program.

Acknowledgments

The authors would like to thank John Fowler of Nova Scotia Department of Mines and Ralph Stea and John Dickie, who carried out the till sampling program, for guiding us to the numerous exposures from which these samples were collected. Their hospitality and insights into local geology were much appreciated. This paper has been reviewed by R.N.W. DiLabio, J.S. Scott, and R.A. Klassen.

References

Grant, D.
1963: Pebble lithology of the tills of southeast Nova Scotia; unpubl. M.Sc. thesis, Dalhousie Univ., Halifax, 235 p.

Grant, D.R. and Tucker, C.M.
1976: Preliminary results of terrain mapping and base metal analysis of till in the red Indian Lake and Gander Lake map-areas of central Newfoundland; in Report of Activities, Part A, Geol. Surv. Can., Paper 76-1A, p. 283-285.

Prest, V.K., Grant, D.R., Borns, H.W., Brookes, I.A., MacNeill, R.H., and Ogden, J.G.
1972: Quaternary geology, geomorphology and hydrogeology of the Atlantic Provinces; 24th Int. Geol. Congr., Guideb., Excursion A61-C61, 79 p.

Shilts, W.W.
1973a: Glacial dispersal of rocks, minerals, and trace elements in Wisconsinan till, southeastern Quebec, Canada; Geol. Soc. Am., Mem. 136, p. 189-219.

1973b: Till indicator train formed by glacial transport of nickel and other ultrabasic components: a model for drift prospecting; in Report of Activities, Part A, Geol. Surv. Can., Paper 73-1A, p. 213-218.

1975: Principles of geochemical exploration for sulphide deposits using shallow samples of glacial drift; Can. Inst. Min. Metall., Bull., v. 68, no. 757, p. 73-80.

1976: Glacial till and mineral exploration; in Glacial Till, ed. R.F. Legget; R. Soc. Can., Spec. Pub. 12, p. 205-224.

Shilts, W.W. and McDonald, B.C.
1975: Dispersal of clasts and trace elements in the Windsor esker, southern Quebec; in Report of Activities, Part A, Geol. Surv. Can., Paper 75-1A, p. 495-499.

Weeks, L.V. (consulting geologist)
1965: Geological map of the Province of Nova Scotia; N.S. Dep. Mines, Halifax.

II: SCIENTIFIC AND TECHNICAL NOTES

SURFICIAL GEOLOGY AND TERRAIN EVALUATION, SOUTHERN YUKON

R.W. Klassen, E. Thorsteinsson, and O.L. Hughes
Terrain Sciences Division, Calgary

The purpose of this project is to prepare a surficial geology inventory to be available as background data for pipeline, hydroelectric, and highway engineering construction, mining exploration, land use planning, and terrain sensitivity rating.

A preliminary classification of surficial materials and landforms of parts of the Whitehorse (105D), Teslin (105C), Wolf Lake (105B), and Watson Lake(105A) map-areas was prepared from aerial photographs. Data resulting from field reconnaissance during the 1977 field season will be used for modification of the preliminary classification and for characterization of the surficial materials. Surficial geology maps, at a scale of 1:100 000 for areas bordering Alaska Highway and a scale of 1:250 000 for the remainder of the studied area, are currently in preparation.

The area covered is divisible into two parts: (1) an area of mountainous uplands and glaciated valleys comprising parts of the Boundary Ranges, Yukon Plateau, and Cassiar Mountains glaciated during late Wisconsin time by ice that flowed generally to the northwest and (2) an intermontane lowland, the Liard Plain, that was glaciated by southwesterly flowing ice.

In the former area, there is a broadly consistent pattern of distribution of surficial deposits according to topographic position. Glaciolacustrine and glaciofluvial deposits are widespread on the floors of the largest valleys. Steep, light-coloured bluffs, which stand out sharply along Yukon, Takhini, and Teslin rivers, are mostly in glaciolacustrine silt, although glaciofluvial sand and gravel are closely associated with silt in the pitted areas and predominate within the scattered kame, esker, and meltwater channel complexes somewhat higher up the valley sides. Morainic, glaciofluvial, and colluvial deposits and landforms commonly veneer the valley sides up to some 150 to 300 m above the valley bottoms, except for thick blankets of till and/or coarse, poorly sorted, glaciofluvial sand and gravel that form channel dissected benches along parts of the sides of large valleys and around the confluences with their tributary valleys. The smaller tributary and alpine valleys generally are bottomed by morainic debris and scattered patches of glaciofluvial deposits. In places lacustrine silt and clay veneer the bottoms. The valley sides typically are veneered with colluvium and morainic debris. The highest surfaces are glacially sculptured bedrock with a thin mantle of soliflucted glacial deposits and frost riven bedrock.

The Liard Plain is mostly a till plain marked by southeast trending drumlinoids. Parts of the plain are underlain by glaciolacustrine and glaciofluvial deposits that are most extensive in the southeast, bordering Liard River.

The most visible evidence of postglacial processes in this region are the channels of the major rivers deeply incised in glacial drift. Scattered fields of postglacial dunes, now stabilized by vegetation, occur in sandy glaciolacustrine and glaciofluvial deposits in the large valleys. Thermokarst depressions occur as roughly circular or oval ponds rimmed by banks 2 to 5 m high in parts of low relief glaciolacustrine silts in the large valleys. The presence of freshly collapsed banks bordering some depressions indicates that melting of ground ice continues today. Solifluction terraces and lobes in colluvium and morainic debris are common along slopes in the alpine areas above the treeline as are alluvial fans where small V-shaped gulleys meet glaciated valleys. At lower elevations soil creep is active on moderately steep bedrock slopes veneered with colluvium and/or morainic debris. Slumping occurs in sections of the lower Liard Valley bottom where the river banks are in glaciolacustrine silt and clay.

Evidence for multiple glaciation was found along stretches of Liard River and its tributaries. Two tills, overlying and separated by stratified sediments, were seen in several sections. The best section measured was along Tom Creek several miles upstream from the confluence with Liard River (60°13'45"N, 129°00'25"W). Here the olive grey surface till, about 5 m thick, is separated from an older, dark grey till of about the same thickness by stratified sediments including a bed of fossiliferous, organic clay about 1.5 m thick. A wood bearing sand underlies the older till. Samples have been submitted for radiocarbon dating and identification of fossils. A similar, but less accessible, stratigraphic succession was measured along Liard River about 40 km to the northwest. Wood collected by W.H. Poole in 1952 (GS-412) from a lower sand (now covered) yielded a radiocarbon age of greater than 40 100 years B.P. (Dyck et al., 1966). Further study will provide information on the nature of the two nonglacial intervals recorded by these strata, particularly the last one which previously was not recognized in this part of the Cordilleran Region.

Reference

Dyck, W., Lowdon, J.A., Fyles, J.G., and Blake, W., Jr.
1966: Geological Survey of Canada radiocarbon dates V; Geol. Surv. Can., Paper 66-48, 32 p.

From: Scientific and Technical Notes in Current Research, Part A; Geol. Surv. Can., Paper 78-1A.

THE TIDAL REGIME AND SEDIMENTATION PATTERNS IN JOHNSTONE STRAIT, BRITISH COLUMBIA - A PRELIMINARY REPORT

R.E. Thomson[1] and J.L. Luternauer
Regional and Economic Geology Division, Vancouver

Introduction

A joint project was initiated during the summer of 1977 by personnel of the Ocean Physics Division and Canadian Hydrographic Services based at the Institute of Ocean Sciences and the Marine Geology Group at the Vancouver office of the Geological Survey. The object of the project is to determine the extent to which the distinctive oceanographic processes in Johnstone Strait are reflected in the local sediment distribution. The results of this study also will contribute to the on-going offshore resource mapping program of the Geological Survey.

Johnstone Strait is a long, constricted part of the Inland Waterway between northeastern Vancouver Island and the mainland of British Columbia through which vigorous tidal currents flow. Along the axis of the area examined (Fig. 1) water is shallowest (68 m) over the sill-like feature off western Hardwicke Island. The sea floor slopes gradually from the base of this feature to the deepest part of the strait (512 m) off the western end of West Cracroft Island. From there the basin gradually shoals to 155 m at the westernmost sampling site.

Prior to this investigation the most detailed study of the sediment distribution in this area consisted of the examination of 10 core and/or grab samples collected along the length of the strait (Cockbain, 1963) who found that: "sand occurs at the eastern and western ends of Johnstone Strait; in the central portion the sediment is varied but sandy material predominates". Intensive oceanographic studies of the area which were initiated in 1976 have consisted of current monitoring and measurement of water properties (Huggett et al., 1976; Thomson, 1976, 1977).

Field Procedures

Field activities for this joint project were performed during the period 21 through 25 July, 1977 when 110 surficial sediment sampling stations were occupied. Where no sample was obtained on the first drop with the Shipek sampler at least one other attempt at recovery was made. Oceanographic information was acquired from STD and Niskin bottle surveys and from moored current meters. The entire survey was performed with the **CSS Parizeau**.

Preliminary Geological Observations

Cockbain (1963) correctly described the Johnstone Strait sediments as being sand-rich in general and muddy along the central part of the study area. Current investigations have further established that gravels abound at the eastern reaches of the sampled area and shell debris constitutes a major part of many of the sediments, especially along the western part of the study area. On the whole, the character of the sediments suggests that the basin has been sediment-starved since the retreat of the last lobes of Pleistocene glaciers. This is probably due to the relatively low discharge of Vancouver Island rivers draining into the strait and to the fact that sediment discharged from mainland rivers has largely been ponded within the inlets or bays fringing the strait.

Detailed grain size analysis of the coarser sediments on the floor of Johnstone Strait will identify areas most likely being reworked by oceanographic processes, and what, if any, is the principal direction of sediment transport. Side-scan sonar surveys may be required to determine the composition of the sea floor at sites where no sample was recovered (boulder patches, rock surfaces swept clean of sediment) or to bring to light any sediment wave forms that may have developed.

References

Cockbain, A.E.

1963: Distribution of sediments on the continental shelf off the southern British Columbia coast; Univ. Brit. Columbia, Inst. Oceanogr., Ms. Rep. 15, 7 p.

Huggett, W.S., Bath, J.F., and Douglas, A.

1976: Data record of current observations, v. XIV, Johnstone Strait 1973; Institute of Ocean Sciences, Patricia Bay, 155 p.

Thomson, R.E.

1976: Tidal currents and estuarine type circulation in Johnstone Strait; B.C. J. Fish. Res. Bd. Can., v. 33, no. 10, p. 2242-2264.

1977: Currents in Johnstone Strait, B.C. - supplemental data on the Vancouver Island side; J. Fish. Res. Bd. Can., v. 34, no. 5, p. 697-703.

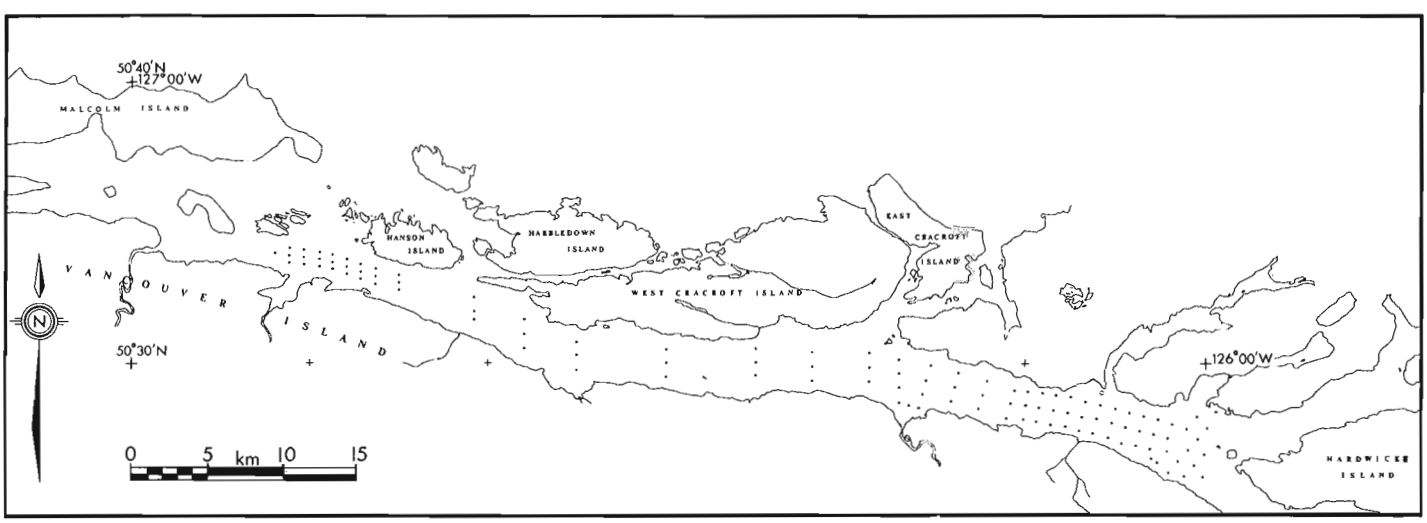

Figure 1. Index map. Dots represent sediment sampling sites.

[1] Institute of Ocean Sciences, Patricia Bay, B.C.

From: Scientific and Technical Notes in Current Research, Part A; Geol. Surv. Can., Paper 78-1A.

SOME ORIENTATION SURVEYS FOR URANIUM MINERALIZATION IN PARTS OF THE ATLIN AREA, BRITISH COLUMBIA

S.B. Ballantyne, D.R. Boyle, W.D. Goodfellow, I.R. Jonasson, and B.W. Smee
Resource Geophysics and Geochemistry Division

Introduction

In August 1976 selected test sites in the Atlin, British Columbia (104N) area were visited on two occasions with a view to assessing the geochemical response in rocks and surficial materials, viz., stream waters and sediments, to known U, Mo, W, and Pb-Zn occurrences (Fig. 1). These studies were designed to assist in the development of a Federal-Provincial reconnaissance geochemical survey to be carried out in July 1977. At the time of writing, this Uranium Reconnaissance Program survey has been completed and covers NTS map sheet 104N at an average density of one stream sediment and water sample per 12.5 km^2. Further detailed geochemical studies were carried out concurrent with the regional survey by D.R. Boyle and S.B. Ballantyne.

Figure 2 shows the geology of part of the Atlin map-area (Map 1082A, Aitken, 1959), together with mineralization occurrences and sample location sites at which geochemical samples were collected in the study area. The main geological features of interest to this work were the Jurassic granites (Coast Intrusions), the Surprise Lake alaskites of Cretaceous age and the basal sediments underlying Tertiary olivine basalts near Ruby Mountain. Because of the presence of a minor uranium showing in volcanics of the Cache Creek Group near Deep Bay (Atlin Lake) some attention was given to these rocks elsewhere in the area where they are also known to host Pb-Zn sulphide occurrences.

A number of W occurrences (Fig. 2) are known in the Coast Intrusives and Surprise Lake alaskites and in skarns near alaskites; some of these occurrences also contain molybdenite. Mo occurrences (Fig. 2) are present in the same host rocks, the Adanac deposit being the best known of these in the headwaters of the Ruby Creek drainage system (Aitken, 1959).

Some Pb-Zn showings (Fig. 3) occur in greenstones of the Cache Creek Group. A small productive operation for Pb and Ag is presently being worked by Atlin Silver Mines northeast of MacDonald Lake.

Uranium mineralization near Deep Bay (Hussellbee Property) is characterized by high radioactivity in an amphibolized skarn zone adjacent to a granitic body (Holland, 1953). Red jasper, pyrite, fluorite and galena are also present and two representative samples reported assays of 0.014% and 0.07% U_3O_8; 0.16% and 0.17% ThO_2 (Holland, 1953).

Uranium mineralization, in the form of the copper uranylarsenate, (zeunerite) and lead uranylsilicate, (kasolite), occurs within the Surprise Lake alaskite body, in silicified shear zones containing primary and secondary sulphides of Cu, Pb, and Mo. A selected assay from these occurrences (Cracker Creek – Purple Rose) from Holland (1955) reported 0.088% U_3O_8 and 0.11% ThO_2.

Results

Table 1 gives the analyses of water samples for Zn, U, and F; pH was also determined. Table 2 is presented in two parts because essentially different methods of analyses were used. The 3000 series samples were analyzed mainly by atomic absorption methods (a.a.s.), whereas the 1000 series samples were analyzed mainly by emission spectrography. Only results for U are directly comparable for samples from the same stream sites. Spectrographic data give total anlayses compared with strong acid partial attacks for a.a.s. methods. Differences are particularly obvious for Zn, Cu, and Pb data. The 1000 series samples only were analyzed for K, As, Sb, and total F and the 3000 series only were analyzed for W.

Table 3 presents mainly spectrographic data for some rock samples collected in the Deep Bay area (9000 series) and near radioactive zones at Surprise Lake (5000 series). Data for K have been added to this table because of the contribution K makes to the total radioactivity measured at these sample sites.

Discussion

The highest levels of uranium in both sediments and waters were observed over the same areas of the Surprise Lake alaskite. Uranium values in waters draining this intrusion are not particularly high, but compared with a normal background for the area of 0.02 ppb they are commonly 10 to 20 times (or more) greater. pH values measured in waters draining the alaskite bodies were typical of those observed in granitic terrane (around 7.2 to 7.5). In contrast, pH of waters draining the granites of the Jurassic Coast Intrusions were commonly around 8.2, values more typical of pH controlled by the leaching of carbonate-bearing rocks than granites. Elevated levels of carbonate, and also fluoride, may perhaps explain the presence of some high U in these waters in the absence of matching stream sediment anomalies. Waters from a small stream draining granites and alaskites just north of Surprise Lake (location 3006) showed low absolute levels of dissolved U in spite of the fact that the underlying rocks were found to contain up to 33 ppm U (Table 3). The water is, however, anomalous for U at about 15 times background, as well as for dissolved F at around 3 times background.

Fluorine may prove to be very useful in delineating uraniferous areas because of the apparent association of fluorite with U, Mo, and W mineralizations in alaskitic bodies. Inspection of data from Table 1 indicates that F is highest in areas where U is highest. Reference to Tables 2 and 3 shows that F is abundant in the alaskite and in stream sediments derived mechanically from it. Similar observations have been made for Cretaceous alkaline intrusive bodies of the Tombstone Mountains, Yukon, by Goodfellow and Jonasson (1977) and in the granitic and syenitic terrane of the Okanagan region of British Columbia by S.B. Ballantyne and D.R. Boyle.

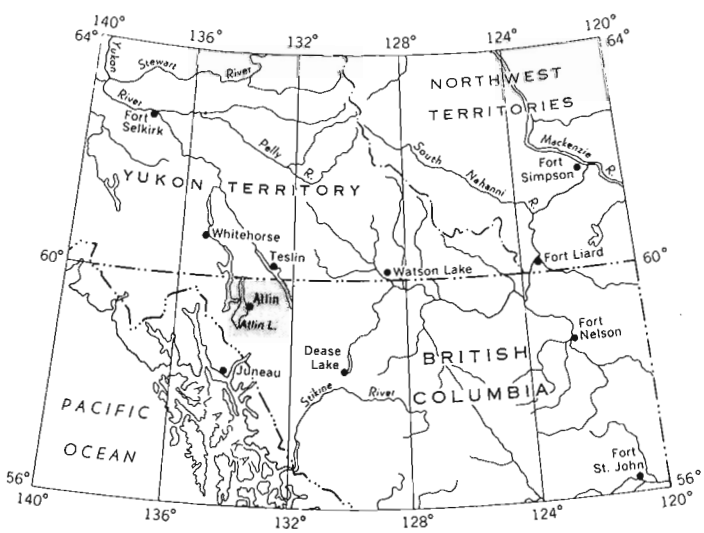

Figure 1. Index map.

From: Scientific and Technical Notes in Current Research, Part A; Geol. Surv. Can., Paper 78-1A

Data in Tables 2a and 2b demonstrate a consistent clustering of elevated values of U, Mo, W, and Pb; As and F also appear to group with these elements. These relationships are reflected in the mineralogy of known uraniferous showings.

An interesting U anomaly in both waters and sediments was found in streams draining the vicinity of the Atlin Silver Mines property where Ag-rich galena and sulphosalts are the important ore minerals. These deposits lie in rocks of the Cache Creek Group (Fig. 2) which also host the Hussellbee showing at Deep Bay. Further attention should be paid to these rocks as possible hosts of uranium mineralization.

Of the other trace and minor elements studied, Pb, Zn, and Cu indicated the proximity of base metal sulphides near MacDonald Lake but the contribution of contamination in the drainage due to mining activity has not been gauged. These same metals were also anomalous in the headwaters of Ruby Creek and are likely associated with Mo-W rich skarns in the area.

Ni anomalies appear to have originated from peridotite and gabbroic rocks in the Boulder and Ruby Creek areas. Values up to 400 ppm Ni were recorded in stream sediments in association with persistent Cr levels in excess of 125 ppm, the upper limit of the spectrographic method used in this work. It is interesting to note that the ferruginous precipitate from the carbonated spring in Atlin village is also enriched in Ni. This spring is located in gabbros of the Atlin Intrusions.

Table 1

Analytical data: Waters

Sample Location		Zn	U	F	pH	Comments
Atlin spring strm.	3002	0.3	0.02	144	7.0	
Ruby Ck. trib.	3003	0.7	0.10	320	7.5	dupl. 1005
Ruby Ck. trib.	3004	2.8	0.04	280	7.7	
Ruby Ck. trib.	3005	5.2	0.14	420	7.6	
minor stream	3006	7.7	0.34	800	8.0	
minor stream	3007	0.7	0.02	240	8.0	
Boulder Ck.	3008	0.0	0.16	800	7.8	dupl. 1008
Boulder Ck. trib.	3009	4.2	0.02	46	8.1	
Boulder Ck. trib.	3010	7.1	0.02	60	8.2	dupl. 1007
Boulder Ck. trib.	3011	1.0	0.04	156	8.0	dupl. 1006
Boulder Ck. hdw.	3012	7.1	0.18	800	7.3	
Boulder Ck. hdw.	3013	15.8	0.10	620	7.4	
Boulder Ck. hdw.	3014	13.9	0.16	800	7.2	
Atlin spring	3015	4.9	0.02	180	7.3	
Blackbear Run Ck.	3017	5.7	0.16	64	8.3	
4 July Ck.	3018	3.7	0.24	150	8.1	
Burnt Ck.	3019	3.8	0.32	220	8.2	dupl. 1014
Telegraph Ck.	3020	2.0	0.20	132	8.4	dupl. 1015
Indian Ck.	3022	1.1	1.76	340	8.2	
Glacier Ck.	3023	0.0	0.32	280	8.2	
Basecamp Ck.	2024	2.0	0.18	200	8.2	dupl. 1016
Hitchcock Ck.	3025	2.0	0.96	200	8.3	dupl. 1017
Ruby Ck. hdw.	1001	-	0.06	340	6.5	
Ruby Ck. hdw.	1002	-	0.12	300	6.8	
Ruby Ck. hdw.	1003	-	0.04	980	7.0	
Ruby Ck. trib.	1004	-	0.14	360	7.3	
Ruby Ck. trib.	1005	-	0.06	320	7.6	dupl. 3003
Boulder Ck. trib.	1006	-	0.02	80	8.2	dupl. 3011
Boulder Ck. trib.	1007	-	0.02	50	8.1	dupl. 3010
Boulder Cr.	1008	-	0.24	500	8.0	dupl. 3008
Otter Ck.	1009	-	0.02	90	8.1	
Atlin Silver	1010	-	0.52	210	7.5	
Crater Ck.	1011	-	0.24	210	7.4	
4 July Ck. trib.	1012	-	0.12	54	7.6	
4 July Ck.	1013	-	0.20	140	7.7	
Burnt Ck.	1014	-	0.12	200	8.1	dupl. 3019
Telegraph Ck.	1015	-	0.38	120	8.3	dupl. 3020
Basecamp Ck.	1016	-	0.58	180	8.3	dupl. 3024
Hitchcock	1017	-	0.76	192	8.1	dupl. 3025

Zn was determined by atomic absorption spectrometry following its extraction by APDC into methylisobutylketore.

U was determined by a fluorometric method.

F was determined by ion-specific electrode.

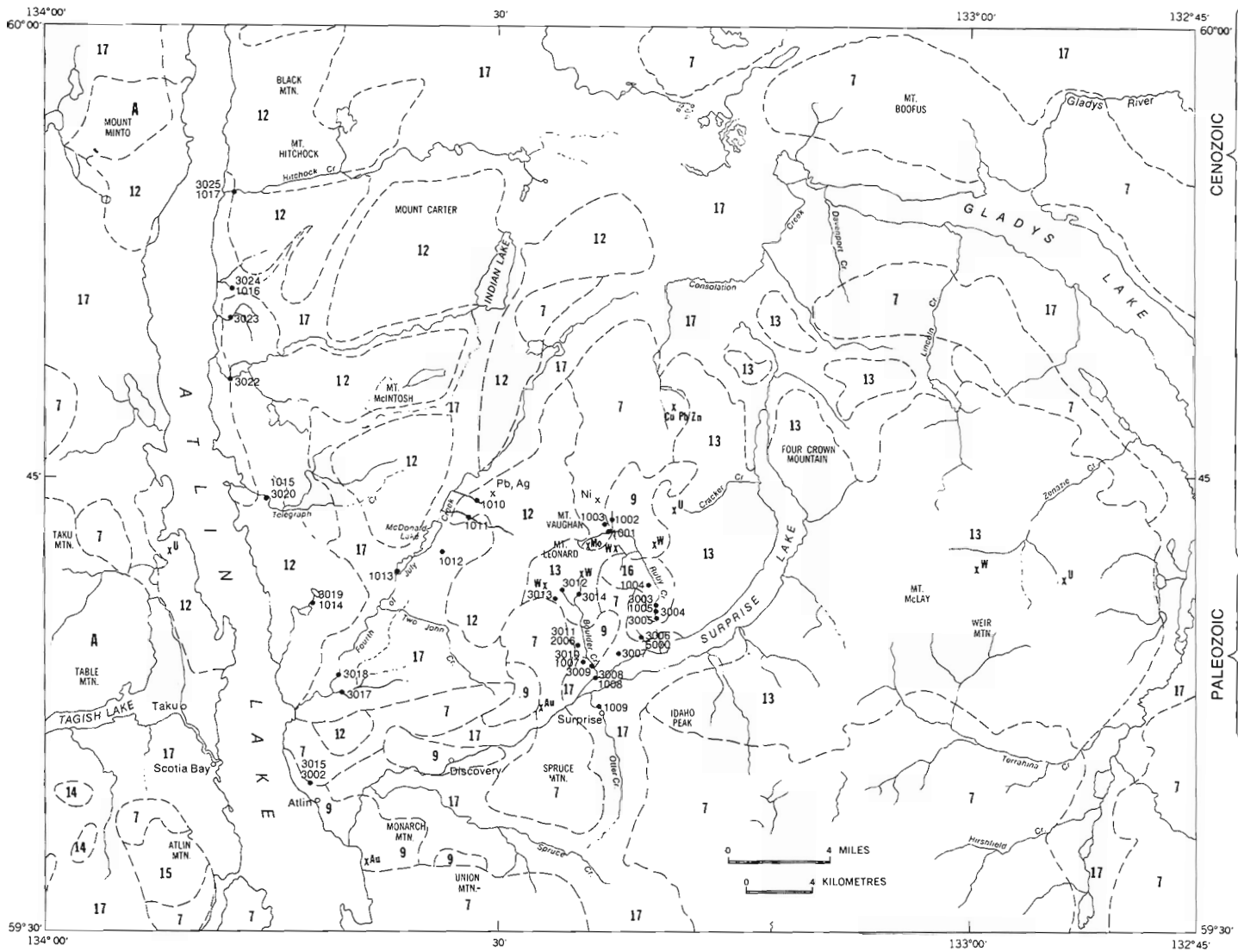

LEGEND

CENOZOIC

QUATERNARY
PLEISTOCENE AND RECENT

17 — *Glacial drift, alluvium.*

TERTIARY AND QUATERNARY

16 — *Olivine basalt and scoria.*

TERTIARY (?)

15 — *Quartz monzonite; granophyre; gabbro and diorite.*

CRETACEOUS OR TERTIARY
SLOKO GROUP

14 — *Andesite, basalt; rhyolite, conglomerate, sandstone.*

CRETACEOUS

13 — *Alaskite, quartz monzonite*

JURASSIC *(May be in part older and younger)*
COAST INTRUSIONS

12 — *Undifferentiated granitic rocks.*

PALEOZOIC

PENNSYLVANIAN AND PERMIAN
ATLIN INTRUSIONS

9 — *Peridotite; meta-diorite and meta-gabbro; serpentinite*

CACHE CREEK GROUP

7 — *Chert, argillite, chert-pebble conglomerate; greenstone and volcanic greywacke; limestone and limestone breccia*

A — *Undifferentiated, mainly volcanic rocks of uncertain, possibly several, ages, perhaps Triassic.*

Figure 2

Sample location map, Atlin, B.C.

Table 2

(a) Analytical data: Stream Sediments (ppm)

Sample Location		Zn	Cu	Pb	Ni	Ag	%Fe	Ba	Mo	W	U	Comments
Atlin Spring stream	3002	82	15	10	16	0.1	1.0	1700	2	4	5.7	downstream from carbonated spring
Ruby Ck. trib.	3003	40	38	10	62	0.1	1.2	340	2	4	3.4	minor stream in alaskite
Ruby Ck. trib.	3004	78	30	15	260	0.1	2.6	730	1	8	5.8	minor stream in alaskite
Ruby Ck. trib.	3005	70	23	7	170	0.1	2.3	820	1	7	6.5	minor stream in alaskite
minor stream	3006	88	138	16	380	0.1	2.1	700	3	7	3.1	draining alaskite, gabbro. High radioactivity.
minor stream	3007	34	56	5	200	0.1	1.1	380	5	5	5.1	draining gabbro
Boulder Ck.	3008	510	43	99	44	1.0	1.8	720	2	75	21.4	draining alaskite and gabbro known W shows.
Boulder Ck. trib.	3009	66	29	8	245	0.1	2.2	760	1	2	1.9	draining gabbro
Boulder Ck. trib.	3010	77	160	5	420	0.1	2.0	710	1	6	3.2	draining greenstone, gabbro
Boulder Ck. trib.	3011	108	60	6	310	0.6	3.0	740	3	5	4.5	draining alaskite
Boulder Ck. hdw.	3012	53	25	9	225	0.1	2.3	860	2	15	3.5	draining alaskite, W shows nearby
Boulder Ck. hdw.	3013	430	30	86	34	0.4	2.0	820	3	40	29.4	draining alaskite, Mo-W shows nearby
Boulder Ck. hdw.	3014	150	42	47	19	0.1	1.8	780	2	25	16.0	draining alaskite, W shows nearby
Atlin spring ppte.	3015	24	10	1	445	0.1	19.0	3450	1	2	0.4	ferruginous ppte at spring source
Blackbear Run Ck.	3017	36	14	3	104	0.1	1.8	1200	2	5	2.5	drains Coast granites.
4 July Ck.	3018	38	17	3	82	0.1	2.1	1200	3	15	3.9	drains Coast granites, considerable glacial deposits.
Burnt Ck.	3019	37	18	2	56	0.1	1.6	1320	1	6	5.0	drains Coast granites
Telegraph Ck.	3020	31	11	3	31	0.1	1.6	1660	1	2	3.4	drains Coast granites
Indian Ck.	3022	43	17	1	48	0.1	3.9	1400	4	2	5.3	drains Coast granites
Glacier Ck.	3023	26	8	2	19	0.1	1.3	1400	1	4	3.6	drains Coast granites
Basecamp Ck.	3024	39	15	64	32	0.1	2.2	1650	2	4	3.3	drains Coast granites
Hitchcock Ck.	3025	28	11	1	19	0.1	1.4	1440	2	2	7.1	drains Coast granites

U was determined by a delayed neutron activation method.

W was determined by a colorimetric method following sample fusion.

Other elements were determined by atomic absorption spectrometric methods following sample digestion in a strong hot HNO_3 - HCl solution.

(b) Analytical data: Stream Sediments (ppm)

Sample Location		Zn	Cu	Pb	Ni	Ag	%Fe	Ba	Mo	%K	U	As	Sb	F	Comments
Ruby Ck. hdw.	1001	215	127	95	15	0.5	3.2	421	>20	2.6	35.9	113	6	325	near Adanac Mo
Ruby Ck. hdw.	1002	122	28	49	15	0.1	2.6	595	>20	2.6	19.6	24	2	325	near Adanac Mo
Ruby Ck. hdw.	1003	601	200	69	>125	0.6	4.8	441	4	1.9	21.2	132	13	1200	drains Cache Creek volcs, Tert. olivine basalt.
Ruby Ck. trib	1004	217	62	46	>125	0.8	6.9	874	8	2.1	9.1	28	2	493	drains Tert. olivine basalt
Ruby Ck. trib.	1005	126	48	28	>125	0.1	4.5	669	2	1.2	5.4	18	1	241	draining alaskite; c.f. 3003
Boulder Ck. trib	1007	117	39	13	>125	0.5	4.1	804	3	0.9	2.1	22	0	123	draining gabbro; c.f. 3010
Boulder Ck.	1008	100	37	13	>125	0.1	4.1	893	2	1.2	2.1	14	1	100	draining gabbro and alaskite; c.f. 3008
Otter Ck.	1009	112	59	12	>125	0.1	4.1	1168	2	0.9	1.6	17	1	130	glacial material, drains Au placers
Crater Ck.	1011	323	40	>100	30	2.8	4.8	>1500	3	1.7	15.4	217	4	300	drains granites, Atlin Silver Mine area
4 July Ck. trib.	1012	115	23	15	53	0.6	4.3	1321	3	1.2	17.4	15	0	352	draining Coast granites
4 July Ck.	1013	101	27	10	>125	0.1	4.4	1230	3	1.0	3.4	6	0	114	draining Coast granites;
Burnt Ck.	1014	91	44	9	>125	0.1	3.4	1368	2	1.2	7.7	9	0	130	draining Coast granites; c.f. 3019
Telegraph Ck.	1015	69	24	9	85	0.1	3.3	1423	2	1.3	4.8	7	0	141	draining Coast granites; c.f. 3020
Basecamp Ck.	1016	83	23	71	41	0.1	4.1	>1500	3	1.4	3.4	17	1	205	draining Coast granites; c.f. 3024
Hitchcock Ck.	1017	68	18	7	27	0.1	3.6	>1500	2	1.2	8.9	18	0	173	draining Coast granites; c.f. 3025

U was determined by a delayed neutron activation method.

As and Sb were determined by flameless atomic absorption spectrometry.

F was determined by ion specific electrode following fusion of sample.

Other elements were determined by quantitative emission spectrography (D.C. arc). Upper limits of the method for Ni, Pb, Mo, and Ba were 125, 100, 20, and 1500 ppm respectively.

A number of other elements were sought in these samples including Cr, V, Be, La, Y, K, Mn. However data proved to be featureless except for Cr which exceeded 150 ppm in all but samples 1001 and 1002, Be which reached 16 ppm in samples near Adanac. Analyses were by D.C. arc spectrography.

Table 3

Analytical data: rocks (ppm)

Sample Number	Zn	Cu	Pb	Ni	Ag	%Fe	Ba	Mo	U	As	Sb	F	%K	Comments
a) Location 3006 near Surprise Lake														
5001	71	6	20	2	0.1	1.3	118	0.5	12.0	12	1	2470	2.6	Cretaceous porph. granite; Fe stained
5002	53	4	6	4	0.1	1.6	579	0.5	10.5	1	0	1120	2.9	Cretaceous fine gr. granite
5003	58	4	1	2	0.1	1.3	205	0.5	25.4	1	1	1270	3.7	Cretaceous green alaskite; smoky qtz.
5004	122	6	100	2	1.6	1.3	274	0.5	33.4	1	0	806	2.9	Cretaceous green alaskite; smoky qtz.
b) Location near U showing, Deep Bay														
9001	55	96	1	11	0.1	1.2	>1500	1.2	1.9	0	0	189	0.7	chert, Cache Creek group (Penn.)
9002	120	19	44	39	0.1	5.1	>1500	3.5	1.9	7	0	189	1.9	amphibolite, Cache Creek group
9005	48	2	10	5	0.1	2.3	>1500	1.1	4.0	4	0	222	2.7	granite, Coast Intrusives (Jur.)

U was determined by a delayed neutron activation method.

As and Sb were determined by flameless atomic absorption spectrometry.

F was determined by ion-specific electrode following fusion of sample.

Other elements were determined by quantitative emission spectrography (D.C. arc)

Finally, the Ba levels in stream sediments clearly distinguish between sediments derived from Coast Range granites and Cretaceous alaskites (Tables 2a and 3); values are approximately twice as high in the latter. Similarly, the K contents of sediments derived from alaskite are high compared with those from Coast Range granites. These factors suggest an increased alkalinity for the Cretaceous alaskite body over that of the Jurassic granites.

Conclusions

The geochemical response in the Atlin area to mineralization containing any of F, U, Mo, W, Pb, Ag, Zn, and Ni is positive. Stream sediments are useful for delineating occurrences of these elements. Water samples are effective in locating uraniferous zones when using both U and associated F. For future work Pb and Mo could be added to the list of elements to be analyzed.

References

Aitken, J.D.
1959: Atlin Map Area, B.C. (104N); Geol. Surv. Can., Memoir 307, 89 p.

Goodfellow, W.B. and Jonasson, I.R.
1977: Geochemical distribution of uranium, tungsten and molybdenum in the Tombstone Mountains batholith, Yukon; in Report of Activities, Part B; Geol. Surv. Can., Paper 77-1B, p. 37-45.

Holland, S.S.
1953: Hussellbee Uranium Report of Minister of Mines, B.C.; p. 79-81.

1955: Purple Rose and Fisher Report of Minister of Mines, B.C.; p. 7-9.

GALENA-SPHALERITE MINERALIZATION NEAR PALMER LAKE, NORTHWEST TERRITORIES

M.P. Cecile and D.W. Morrow
Institute of Sedimentary and Petroleum Geology, Calgary

Introduction

Significant sphalerite and galena mineralization was discovered in Ordovician to Devonian carbonates at one locality near Palmer Lake during stratigraphic and sedimentological field studies (1977) of Paleozoic strata in the Mackenzie Mountains, Northwest Territories. This mineralization is located within 40 km of three other occurrences in carbonates of the same age. Sphalerite was also discovered in the Road River Formation 25 km south-southeast of this mineralization.

Stratigraphy and Location

The mineralization is located at 64°32' and 129°53' (7156000N; 455500E in U.T.M. co-ordinates), 5 km north of the Mountain River, and will herein be referred to as the Mountain River occurrence (Fig. 1). Coarsely crystalline sphalerite and galena occur sporadically in vugs that are scattered in Ordovician to Devonian dolomites of the Mount Kindle, Delorme, and Arnica formations; and as massive sphalerite and minor galena in veins cutting the Delorme Formation (Figs. 2-5). All three formations overlie the Cambrian to Ordovician Road River and transitional (to basin) Franklin Mountain Formations, on the northeastern edge of the lower Paleozoic Misty Creek Embayment, just north of an area of Ordovician and Silurian volcanic tuffs (Cecile, 1978). Within 4 km of Mountain River three claim groups with Zn-Pb mineralization in Silurian to Devonian carbonates have been staked by Welcome North (Dawson, 1975). The Mountain River mineralization occurs adjacent to outcrops of the lower Cambrian Sekwi Formation that have been staked, in the past, for zinc and sphalerite mineralization.

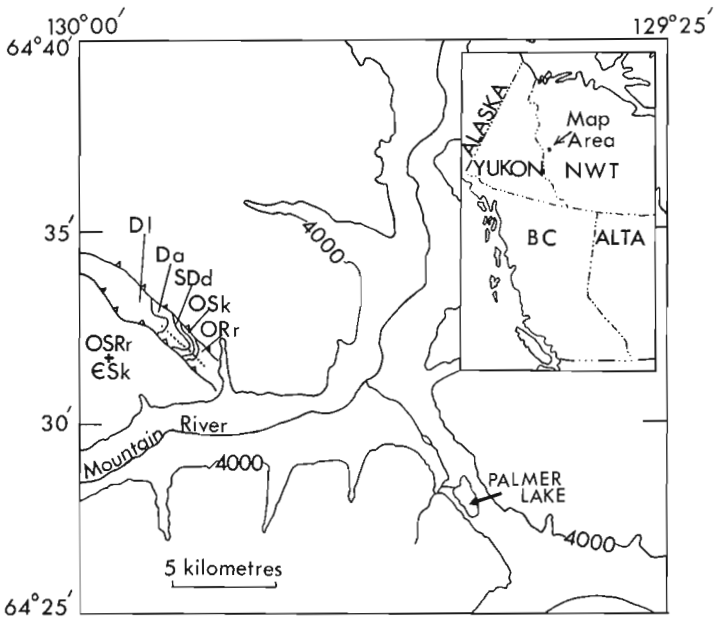

Dl = Landry
Da = Arnica
SDd = Delorme
OSk = Mount Kindle
€SK = Sekwi
ORr and OSRr = Road River

Figure 1. Location of the Mountain River occurrence with sketch showing distribution of mineralized units between two east-dipping thrust faults. The dotted line is the line of section for Figure 2. Geology adapted from Aitken and Cook (1974).

In ascending stratigraphic order the stratigraphy of the Mountain River occurrence is: 75 m of vuggy, medium crystalline, thick bedded, dark and light grey dolomites of the Mount Kindle Formation which rest unconformably on transitional shaly dolomites of the Franklin Mountain Formation; 150 m of vuggy thick bedded, massive, light grey, biostromal dolomite, and 50 m of yellow and orange silty dolomite and sandstone which rest unconformably on the Mount Kindle Formation and together constitute the Delorme Formation; 125 m of thick bedded petroliferous brown-grey dolomite interbedded with medium light grey beds of the Arnica Formation which lie conformably on the Delorme Formation (Fig. 2).

Description of the Mountain River Mineralization

The Mountain River mineralization occurs as secondary sphalerite and galena in vugs or veins. Most vug mineralization is in the lower biostromal Delorme Formation (Fig. 3). Regionally, biostromal dolomites are atypical within strata of the Delorme Formation. In the Arnica Formation mineralization is also associated with vuggy biostromal beds (Fig. 4) but is widely scattered. Some Arnica biostromes are mineralized exclusively with galena whereas others are mineralized exclusively with sphalerite. In the Mount Kindle Formation galena fillings occur in a set of vugs trending subparallel to the bedding.

Vein mineralization was only observed cutting rocks of the Delorme Formation (Fig 5). Mineralized veins are filled with 10 to 100 cm of coarsely crystalline dolomite in sharp planar contact with 5 to 10 cm of reddish yellow, massive sphalerite both surrounded by discontinuous pods and veins of galena.

Veins trend west-northwest—east-southeast and appear to be en echelon. Trends are perpendicular to the depositional slope of the older Misty Creek Embayment (Cecile, 1978). Because veins occur over transitional facies of the embayment this trend may relate to dilational fracturing caused by differential compaction of thick basinal shaly strata and adjacent thin shelf carbonate strata. However this trend is also subparallel to thrust faults in the transition zone and may instead relate to post-thrusting stress relaxation.

Small amounts of pyrobitumen were found in the Road River Formation near the Mountain River occurrence, and in the Mount Kindle and Franklin Mountain formations 10 km southwest and north of the Mountain River occurrence, respectively. Calcite fractures filled with sphalerite were found at the base of the Road River Formation 25 km south-southeast of the Mountain River occurrence (64°20'N and 129°40'W).

The Mountain River occurrence has many of the features of other Rocky Mountain Zn-Pb showings, according to the characteristics of Rocky Mountain Zn-Pb deposits listed by Macqueen (1976, p. 72-73). Features in common are: the mineralization is hosted in porous dolomites; bitumen occurs in associated rocks; mineralization occurs as open-space fillings, mineralization occurs with a platform carbonate to basinal shale facies change; and the host rocks are unmetamorphosed. The Mountain River occurrence differs with the typical Rocky Mountain showing in that: it occurs over a large stratigraphic range (Fig. 2); it has vein mineralization; and it is at least spatially associated with basic volcanic tuffs.

From: Scientific and Technical Notes in Current Research, Part A; Geol. Surv. Can., Paper 78-1A.

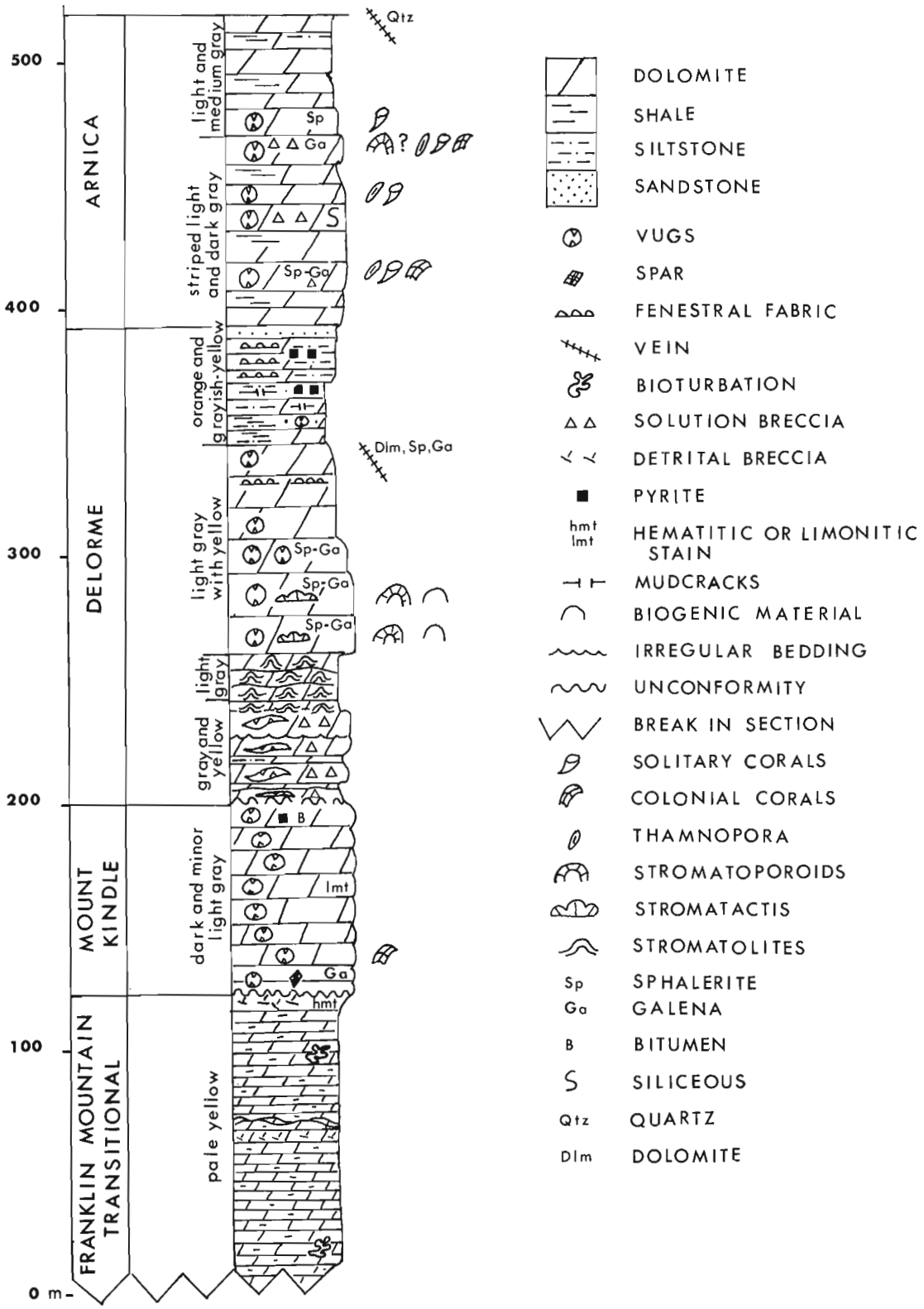

Figure 2. Measured section from the Mountain River occurrence showing mineralized parts of the section.

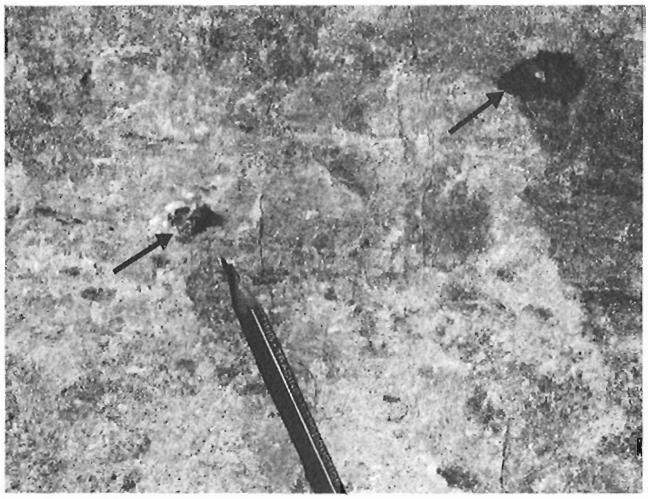

Figure 3. Galena-filled vugs (arrows) in sucrosic white biostromal Delorme dolomite, 64 m above the base of the Delorme Formation. GSC 199327.

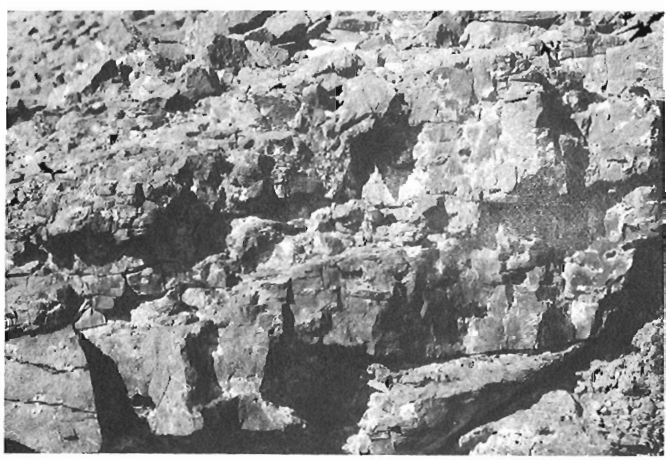

Figure 4. Vuggy mineralized Arnica biostrome, 16 m above the base of the Arnica Formation. GSC 199329.

Figure 5. Dolomite-sphalerite-galena vein cutting the Delorme Formation, 135 m above the base of the Delorme. Scale: the vein has a total width of 15 to 20 cm. GSC 199328.

Origin

An assessment of presently available data favours a Mississippi Valley type origin, that is, defluidization of adjacent shaly Road River rocks, with fluid migration into the overlying porous carbonates directed through compaction produced fractures over the Road River transitional zone. Data supporting this hypothesis are: 1) the Misty Creek Embayment is filled with black, organic-rich, pyritiferous shales and basic volcanic rocks, providing an excellent source of metals; 2) the Road River Formation has sphalerite mineralization in the same area; 3) mineralization occurs above transitional sediments of the Misty Creek Embayment and has vein fillings that are compatible in trend with those expected from fracturing due to differential compaction; 4) mineralization occurs in vugs and veins and must have been moved by secondary fluids; 5) the presence of pyrobitumen in associated carbonates suggests accumulation of organic matter in the same rocks.

Some other origins that must be considered but for which hard data are lacking, are hydrothermal fluids of Columbian or Laramide age and sub-Cretaceous karstification.

References

Aitken, J.D. and Cook, D.G.
1974: Geological maps showing bedrock geology of the northern parts of Mount Eduni and Bonnet Plume map-areas, District of Mackenzie, N.W.T.; Geol. Surv. Can., Open File Report 221.

Cecile, M.P.
1978: Report on the Road River stratigraphy and the Misty Creek Embayment, Bonnet Plume (106B) and surrounding map-areas, N.W.T.; in Current Research, Part A, Geol. Surv. Can., Paper 78-1A, rep. 68.

Dawson, K.M.
1975: Carbonate-hosted zinc-lead deposits of the northern Canadian Cordillera; in Report of Activities, Part A, Geol. Surv. Can., Paper 75-1A, p. 239-241.

Macqueen, R.W.
1976: Sediments, zinc and lead, Rocky Mountain Belt, Canadian Cordillera; Geosci. Can. v. 3, no. 2, p. 71-81.

DIATOMACEOUS ARCTIC LAKE SEDIMENTS

J.D. Adshead
Terrain Sciences Division

Introduction

A study was undertaken to examine by electron microscopy the fine fractions (clay and silt) of sediments from an eastern Arctic lake. The composition and properties of the fine fractions are of interest in relation to the distribution of trace metals among the various particle size fractions of weathered tills (Shilts, 1975) and in relation to lake deposits derived from glacial sediments. This work is part of a program designed to provide a framework of mineralogical and compositional data on sediments from arctic lakes and watersheds, most particularly (1) to produce baseline information for potential construction activities and (2) to develop data in support of environmental geochemistry studies or geochemical prospecting programs. This report describes electron microscope observations made on selected glacial and nonglacial sediments collected from the Yandle Lake basin (Fig. 1).

Previous studies of the lake water chemistry and bottom sediment parameters of Yandle Lake and other lakes in the same area have been reported by Shilts and Dean (1975), Klassen (1975), Klassen et al. (1975), and Shilts et al. (1976). Gelatinous muds or gels cover a large part of the floor of Yandle Lake, although these sediments rarely exceed 1 m in thickness and appear to be absent or very thin over shallow areas and along the margins of the lake (Shilts et al., 1976). Lake gel is underlain by clayey silt of probable marine origin (Shilts et al., 1976). The mechanical properties of the gel and marine clayey silt (MCS) are distinctive; in particular, the MCS is less watery and more dense and compact (plastic) than the gel.

Electron micrographs from the present study have revealed that the gels contain moderate to high amounts of amorphous silica in the form of diatom frustules and fragments of frustules. In contrast, electron micrographs of the MCS samples show an absence of diatom material, except for extremely rare fragments which may be due to contamination during laboratory processing or due to admixing of small amounts of gel with underlying MCS during sampling. In a core from a central basin in Yandle Lake, Edwards (1978) reports that frustules are rare, but are present, in the coarser fractions of sediment thought to correlate with MCS.

Samples and Methods

Seven samples from the Yandle Lake basin, including five bottom sediments (three gels and two marine clayey silts) and two land samples (tills from near the edge of the lake), were selected for a pilot study of sediment properties. Bulk samples and selected particle size fractions isolated from the bulk samples were prepared for various analyses, including: electron microscopy, X-ray diffraction, major and minor element determinations, and isotope and rare earth analyses. The results of the electron microscopy are reported herein for four of the samples (Table 1). Preliminary X-ray studies have been completed and will be reported separately; chemical determinations are in progress. Details of the sample preparation are outlined in this report because of the problems that have been encountered by laboratory personnel in dispersing lake gels for routine fractionation and geochemical analysis.

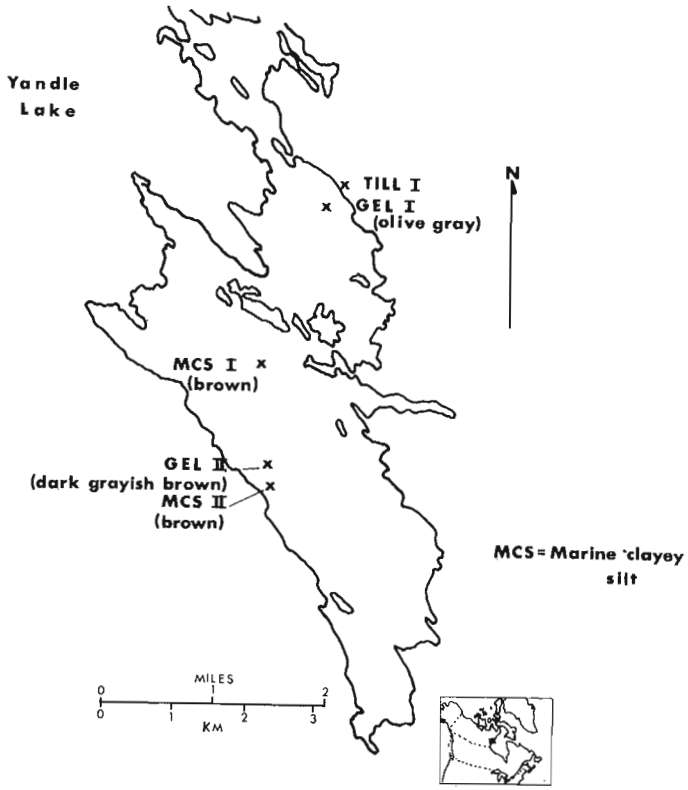

Figure 1. Location of samples, Yandle Lake.

Bulk sediment was gently agitated in deionized water for one hour, followed by centrifugation to remove soluble salts. Several ten-second ultrasonic treatments were then employed to disaggregate the centrifuge cake. Fractionation was effected by three or more separations at the boundary of each particle size class of interest. Fractions included <0.1, 0.1-2, 2-20, 20-62, and 62-2000 μm fractions.

Specimens for transmission electron microscopy (TEM) were prepared on Formvar coated grids onto which a light film of carbon was evaporated prior to deposition of clay suspension. Specimens were examined on a PHILIPS 300 transmission electron microscope operated at 100 KV. Silt particle size fractions were prepared for scanning electron microscopy (SEM): dried sediments were subjected to very light grinding after which powders were pressed onto double stick tape. A very light film of carbon was then evaporated on the specimen surface, followed by gold. Specimens were examined on a CAMECA MEB/07 electron microscope operated at 20 KV.

Results and Discussion

Descriptions of the gels and marine clayey silts are given in Figures 2 to 13. Diatom frustules and fragments of diatom tests ranging downwards from about 10 μm to particles <1 μm are abundant in GEL I (olive grey), and amorphous silica may account for more than half of the < 2 μm equivalent spherical diameter (e.s.d.) fraction. Diatom debris is less abundant in GEL II (brown), and combined clay and nonclay minerals may comprise half of the 0.1-2 μm (e.s.d.) fraction and appear to account for more than half of the finest fraction (<0.1 μm). Estimation of amorphous silica by a selective dissolution procedure is in progress.

From: Scientific and Technical Notes in Current Research, Part A; Geol. Surv. Can., Paper 78-1A.

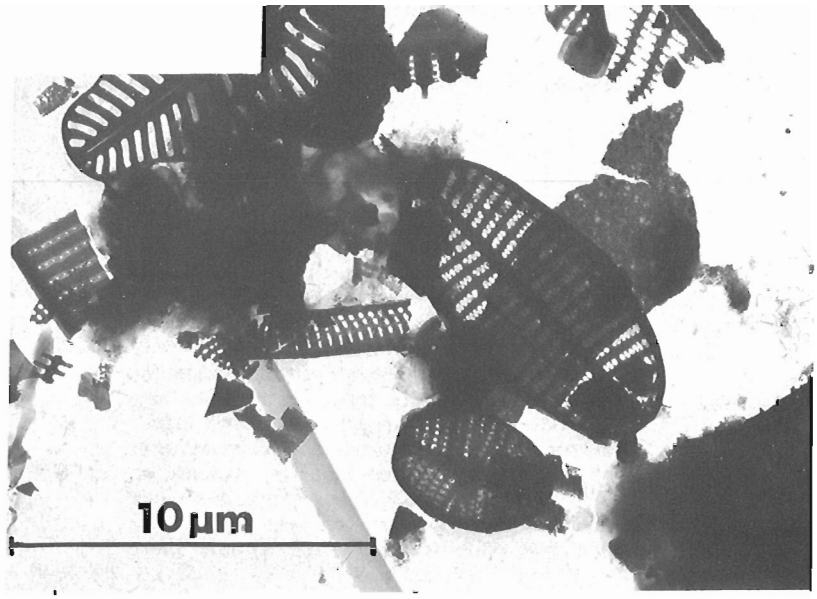

Figure 2

Gel I, olive grey, Transmission Electron Micrograph of the <2 µm (e.s.d.) fraction. Pennate diatom frustules and fragments of diatom tests are the dominant constituents of the <2 µm (e.s.d.) fraction.

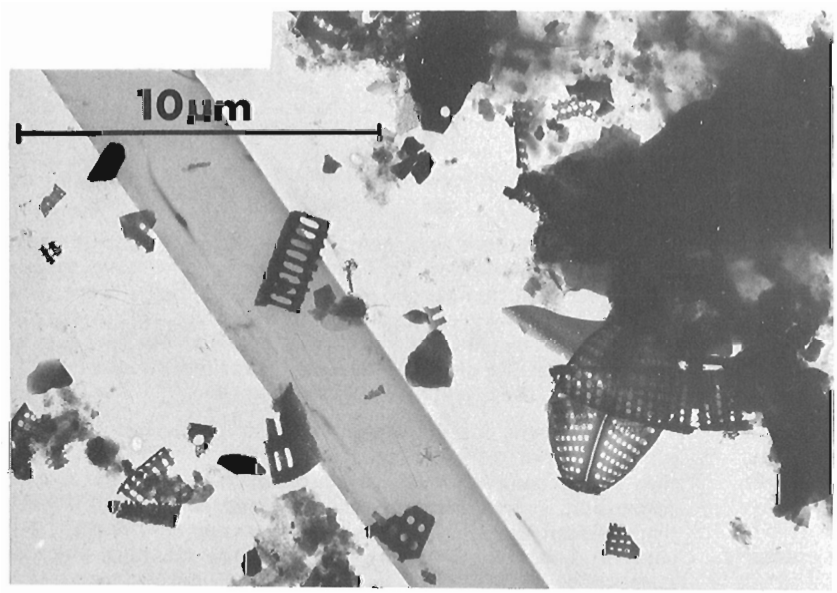

Figure 3

Gel I, olive grey, Transmission Electron Micrograph of the <2 µm(e.s.d.) fraction showing clay-size fragments of diatom frustules.

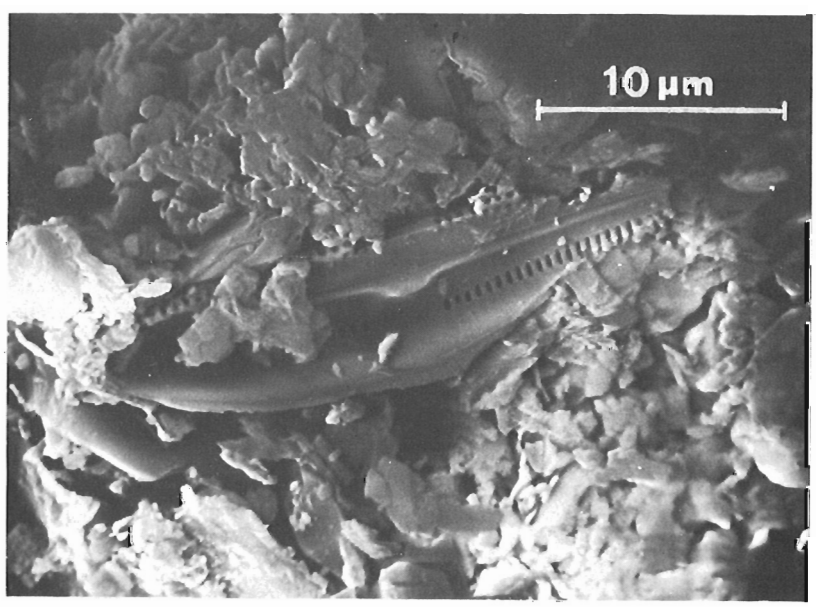

Figure 4

Gel I, olive grey, Scanning Electron Micrograph of the 2-20 µm (e.s.d.) fraction. A pennate diatom is shown. Diatom debris detectable by SEM was extremely rare in the 2-20 and 20-62 µm (e.s.d.) fractions. No centric diatoms were observed by SEM in the silt fractions of this sample. Air dried sediment was subjected to light grinding prior to examination.

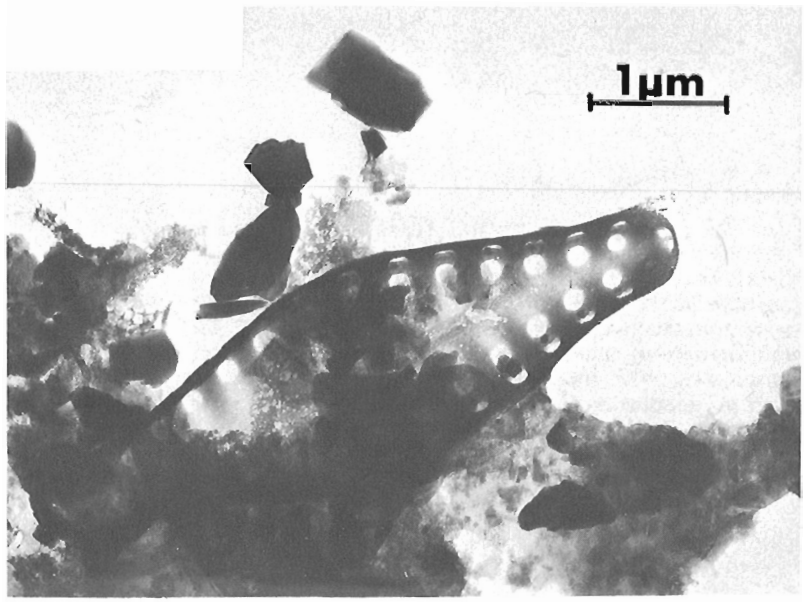

Figure 5

Gel II, dark greyish brown, Transmission Electron Micrograph of the 0.1-1 µm (e.s.d.) fraction. Pennate diatom frustules and fragments of diatom tests are common. Diatom debris is noticeably less abundant in the <2 µm (e.s.d.) fraction of this brown gel (II) than in the olive grey gel (I). The <0.1 µm (e.s.d.) fraction of gel II appears to have a lower content of diatom debris than the 0.1-1 and 1-2 µm fractions.

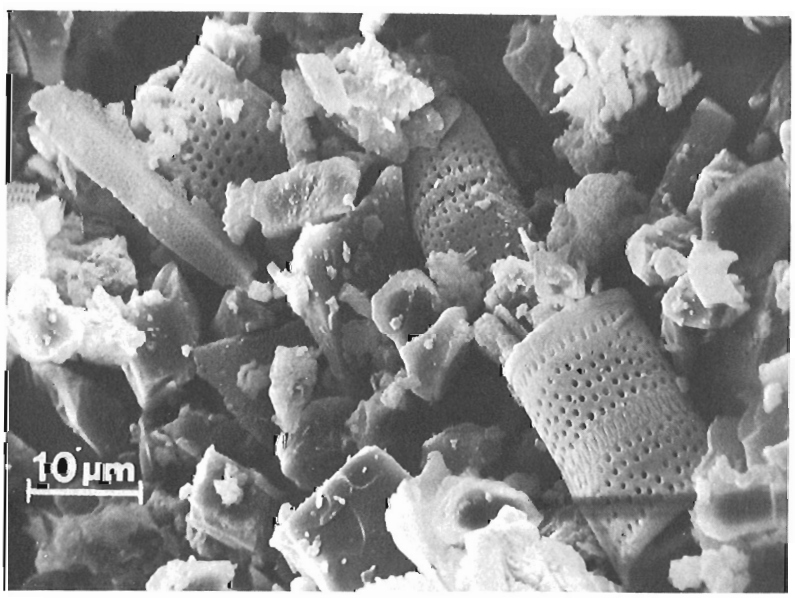

Figure 6.

Gel II, dark greyish brown, Scanning Electron Micrograph of the 5-20 µm (e.s.d.) fraction. Centric diatoms are a common constituent of the silt fractions of this sample. The sediment has been subjected to light grinding.

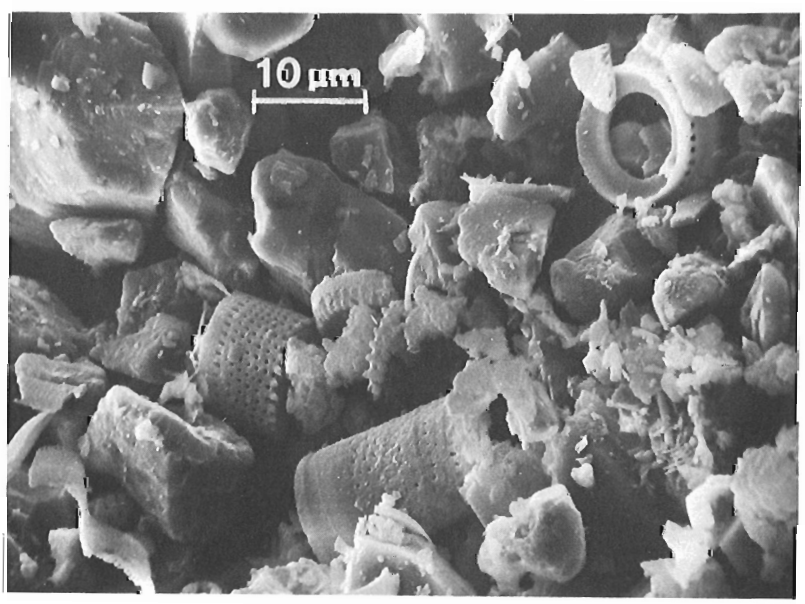

Figure 7

Gel II, dark greyish brown, Scanning Electron Micrograph of the 5-20 µm (e.s.d.) fraction showing fragments of centric diatoms.

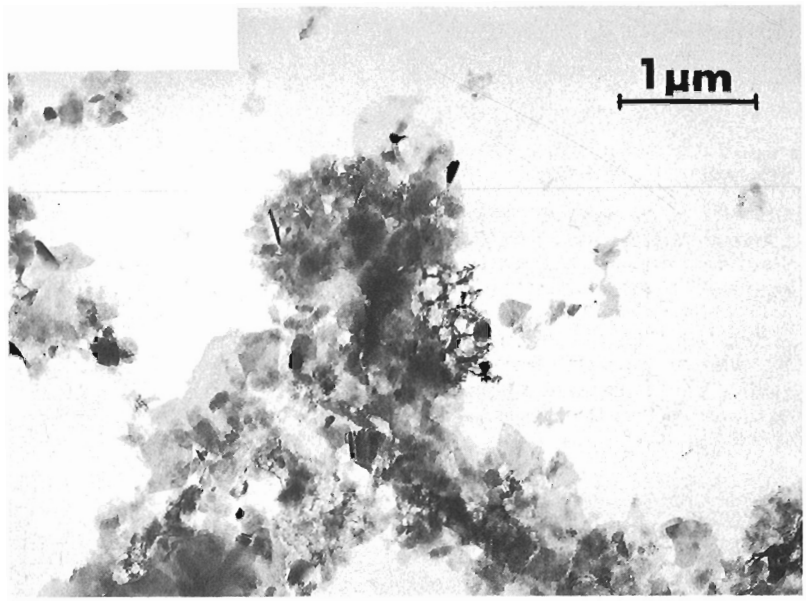

Figure 8

Gel II, dark greyish brown, Transmission Electron Micrograph of the <0.1 µm(e.s.d.) fraction. Diatom debris is only a minor component of this fraction. The particle in the centre of the micrograph may represent a diatom fragment (see Crawford, 1977, Fig. 22 for micrograph of immature valve which shows similar structure). The fragment appears to have undergone partial dissolution either prior to collection of the sample or during processing.

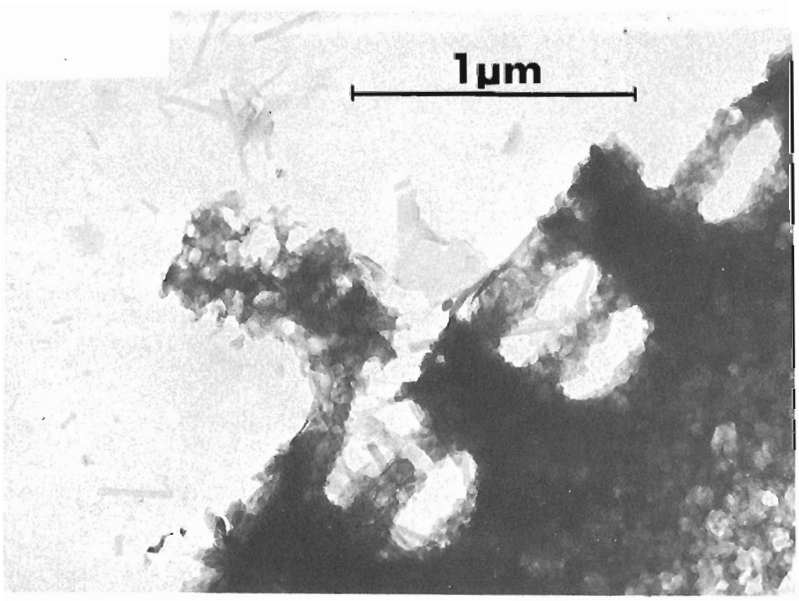

Figure 9

Gel I, olive grey, Transmission Electron Micrograph of the 0.1-2 µm (e.s.d.) fraction. High magnification of the broken surface of a diatom fragment. Small lath-shaped particles of uncertain composition, generally less than 0.5 µm in length, are a trace component of this sample.

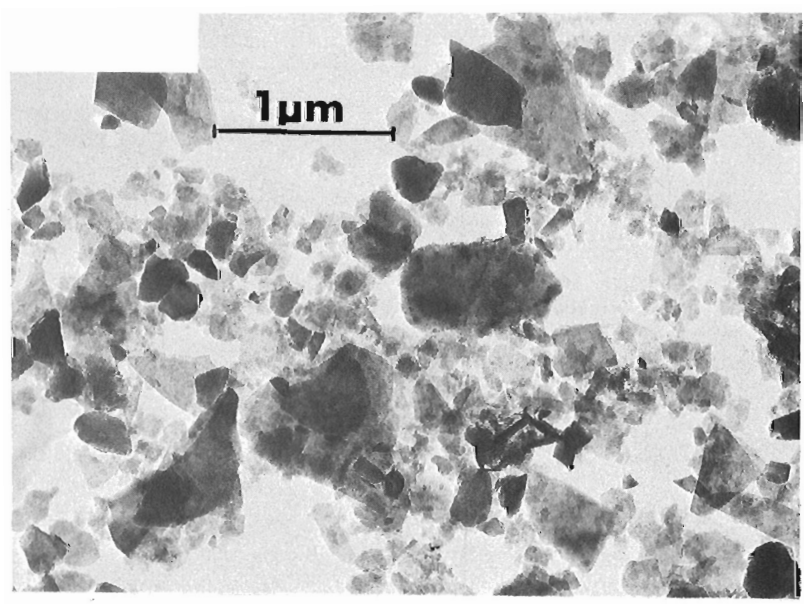

Figure 10

Marine Clayey Silt I, brown, Transmission Electron Micrograph of the 0.1-2 µm (e.s.d.) fraction. Diatom debris is absent. The only diatom material observed in this sample by either transmission or scanning electron microscopy was a fragment of a centric diatom in the 2-20 µm(e.s.d.) fraction.

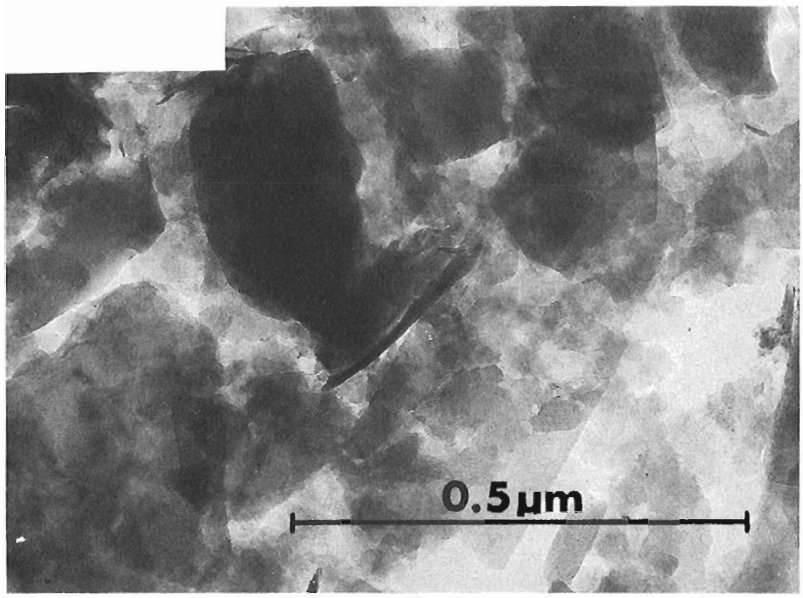

Figure 11

Marine Clayey Silt I, brown, Transmission Electron Micrograph of the 0.1-2 µm (e.s.d.) fraction. High magnification micrograph showing apparent scroll structure, possibly due to expansible clay, which is a common component of the clay mineral suite of the marine clayey silt samples (unpublished data).

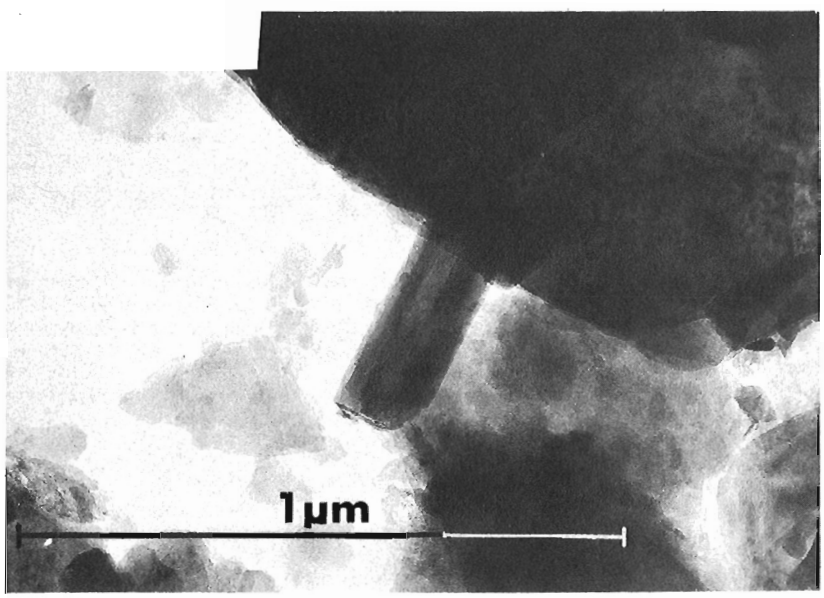

Figure 12

Marine Clayey Silt I, brown, Transmission Electron Micrograph of the 0.1-2 µm (e.s.d.) fraction. Lath-shaped particles, similar in appearance to the one shown, are very sparsely distributed through the sample. The particle shown appears to be a serpentine mineral, based on its electron diffraction pattern.

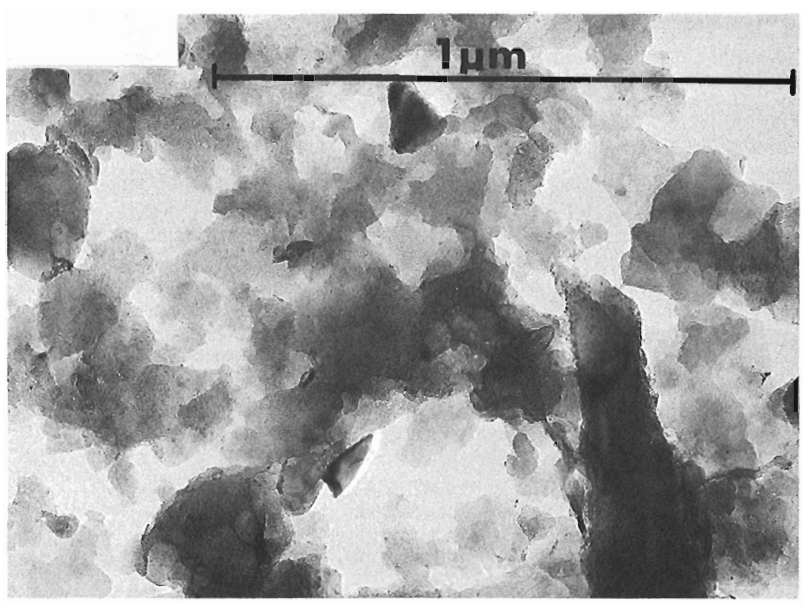

Figure 13

Marine Clayey Silt II, brown, Transmission Electron Micrograph of the <2 µm (e.s.d.) fraction. This micrograph illustrates the absence of diatom debris in the second MCS sediment examined.

Table 1

Description of samples

Sample	Sample Colour (Wet)	Per cent Sand:Silt:Clay*	Water Depth	Comments
GEL I (199)	Olive grey 4/2 5Y (Munsell Charts, 1975 ed.)	11:76:13	6.0 m	Very thin oxidation layer on surface.
GEL II (77)	Dark greyish brown 4/2 10YR	5:79:16	7.0 m	At time of collection, gel was olive in colour and overlain by 2 to 3 cm orange layer which was subsequently mixed with the olive material in the sample bag.
MCS I (87A2)	Brown 5/3 10YR	7:56:37	6.6 m	MCS was overlain by 1 cm orange layer which was removed.
MCS II (75)	Brown 5/3 10YR	2:64:34	–	Surface pebbles and organic film removed.
TILL I (122)		52:43:5		

*63-2000 μm: 2-63 μm: <2 μm

Conclusions

Electron microscope observations on several gels and marine clayey silts from Yandle Lake indicate:

1. Diatom debris is absent in the marine clayey silt samples examined, except for extremely rare fragments which dould have resulted either from very low concentrations of diatoms or from sample contamination at the time of sediment collection or during subsequent processing of the samples.

2. Lake gels, which overlie the marine clayey silts, have a moderate to high content of amorphous silica in the form of diatom frustules and fragments of diatom tests in the < 2 μm (e.s.d.) fraction. Diatom debris in this fraction consists of pennate diatom frustules, generally less than 10 μm maximum dimension, and fragments of diatom frustules which range downward in size to less than 1 μm.

3. Centric diatom fragments are a common constituent of the fine silt fraction of the brown gel from the southern part of Yandle Lake but were not observed by SEM in the olive grey gel from the northeast arm of the lake. Details of the diatom stratigraphy of the lake gel deposits in different parts of the lake basin might clarify these preliminary observations.

Acknowledgments

I thank Professors G. Millot, J. Lucas, and G. Dunoyer de Segonzac of the Institut de Géologie, Université Louis Pasteur and the Centre de Sédimentologie et Géochimie de la Surface, Strasbourg, France, and Professor J-P. Eberhart of the Laboratoire de Minéralogie, Strasbourg, for kindly allowing me laboratory space and use of analytical facilities. I appreciate the technical assistance of D. Trauth (CSGS), and I. Peterschmitt, Laboratoire de Minéralogie, Université Louis Pasteur. W.W. Shilts provided the samples used in this study and gave helpful comments on field and laboratory observations relevant to sedimentation in Yandle Lake. I thank W. Podolak for particle size analyses.

References

Crawford, R.M.
1977: The taxonomy and classification of the diatom genus Melosira C. Ag. II. M. moniliformis (Müll.) C. Ag.; Phycologia, v. 16, p. 277-285.

Edwards, T.W.D.
1978: Postglacial diatom stratigraphy of a lake basin of the eastern arctic shield; in Current Research, Part A; Geol. Surv. Can., Paper 78-1A, report 74.

Klassen, R.A.
1975: Geochemistry of lakes and lake sediments in the Kaminak Lake area, District of Keewatin, N.W.T.; unpubl. M.Sc. thesis, Queen's University, Kingston, 205 p.

Klassen, R.A., Nichol, I., and Shilts, W.W.
1975: Lake geochemistry in the Kaminak Lake area, District of Keewatin, N.W.T.; Verh. Internat., Verin-Limnol., v. 19, p. 340-348.

Shilts, W.W.
1975: Principles of geochemical exploration for sulphide deposits using shallow samples of glacial drift; Can. Inst. Min. Met., Bull., v. 68, no. 757, p. 73-80.

Shilts, W.W. and Dean, W.E.
1975: Permafrost features under arctic lakes, District of Keewatin, Northwest Territories; Can. J. Earth Sci., v. 12, no. 4, p. 648-662.

Shilts, W.W., Dean, W.E., and Klassen, R.A.
1976: Physical, chemical, and stratigraphic aspects of sedimentation in lake basins of the eastern arctic shield; in Report of Activities, Part A; Geol. Surv. Can., Paper 76-1A, p. 245-254.

PROGRESS IN HELIKIAN STRATIGRAPHY, MACKENZIE MOUNTAINS

J.D. Aitken, D.G.F. Long, and M.A. Semikhatov[1]
Institute of Sedimentary and Petroleum Geology, Calgary

Fieldwork

Fieldwork devoted to Precambrian stratigraphy in Mackenzie Mountains in 1977 was for the following periods: Aitken – 10 weeks; Long – 7 weeks; Semikhatov – 3 weeks.

Results

Map-unit H1

Two sections of map-unit H1 (Aitken et al., 1973) were measured and described. The more complete of these will serve as a type section when the unit is given formational status. At the type section (lat. 62°12'30", long. 130°42'00"), map-unit H1 is 410 m thick, and consists of three distinct members. The basal member, with base covered, is recessive and poorly exposed. It consists of flaggy to platy, laminated, very finely crystalline dolomite, in part silty and sandy, that weathers brownish orange, with interbeds of dolomitic shale. The second member of massive, resistant, grey weathering dolomite is dominated by stromatolite biostromes and bioherms up to 5 m high. The third, or upper member is well bedded and resistant, and consists of grey weathering dolomite that is mainly thick bedded cryptagal laminite, alternating with subordinate beds of quartz sandstone and minor shale. In this member, silicification of dolomite to pale grey to black chert increases upward, and chert is very conspicuous near the top. The contact with the overlying Tsezotene Formation is exposed at a single locality, and appears conformable.

The stromatolite assemblage of map-unit H1 has not previously been reported elsewhere in Mackenzie Mountains. The second member contains **Canophyton, Jacutophyton, Baicalia** and extraordinary bioherms consisting of **Stratifera** forming roof-shaped ridges of high relief. The upper member contains **Svetliella.**

Tsezotene Formation and Katherine Group

Fieldwork for a publication on the stratigraphy and sedimentology of this mainly clastic succession was completed. A twofold subdivision of the Tsezotene Formation was found to be applicable on a regional scale (from Cranswick River to Coates Lake), (Fig. 1). The lower member is dominated by grey argillaceous rocks and the upper member by varicoloured argillite, sandstone, and minor carbonate. A locally developed stromatolitic carbonate member is present between these two members in the vicinity of Mount Eduni. Collectively the Tsezotene Formation is a coarsening upward sequence, representing gradual basin filling, or shallowing, on which is imposed a large number of smaller-scale cycles reflecting local shoaling in the form of tidal flat, lagoonal and barrier island and biohermal development.

The predominantly arenaceous Katherine Group is divisible regionally into three units of formational rank (Fig. 2) which can be traced into the type section of the Tigonankweine Formation (Gabrielse et al., 1973). As the term "Katherine Group" is now in common use for these rocks in the area north of the Wrigley Lake map-area, it is preferable to retain this name for the group, rather than raise "Tigonankweine" to group status. North of Wrigley Lake the

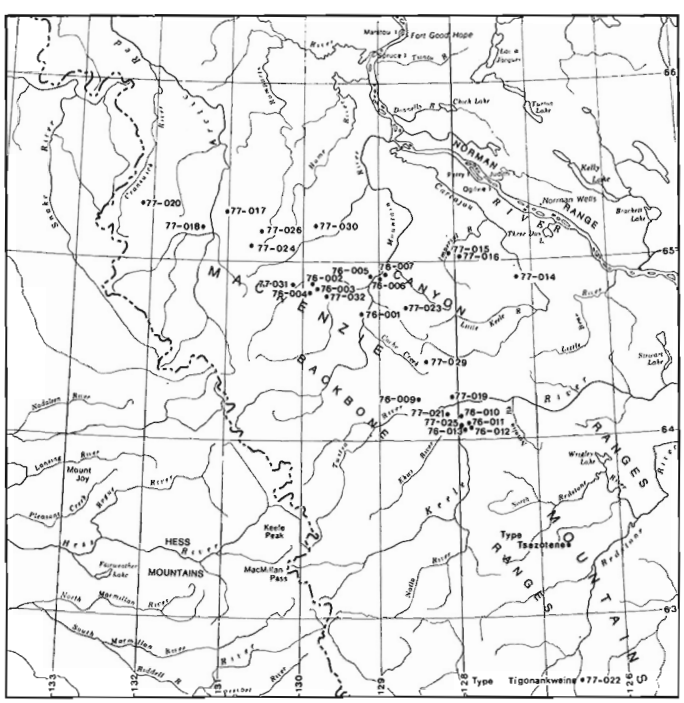

Figure 1. Location map, measured sections of Tsezotene Formation and Katherine Group.

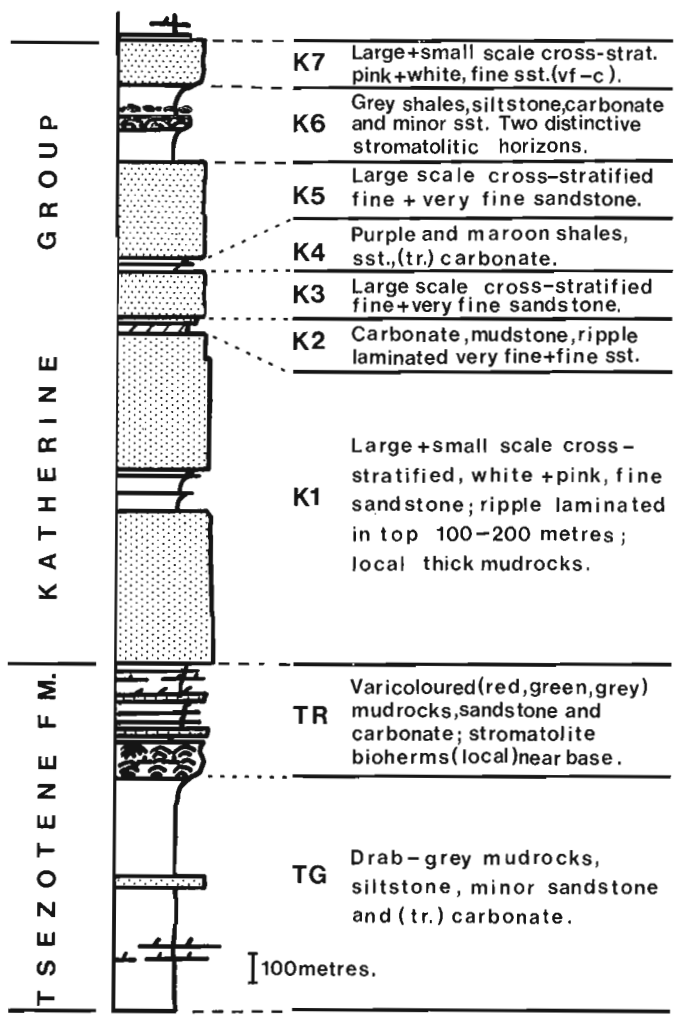

Figure 2. Subdivision of Tsezotene Formation and Katherine Group.

[1]Geological Institute of the Academy of Sciences of the USSR, Moscow.

From: Scientific and Technical Notes in Current Research, Part A; Geol. Surv. Can., Paper 78-1A.

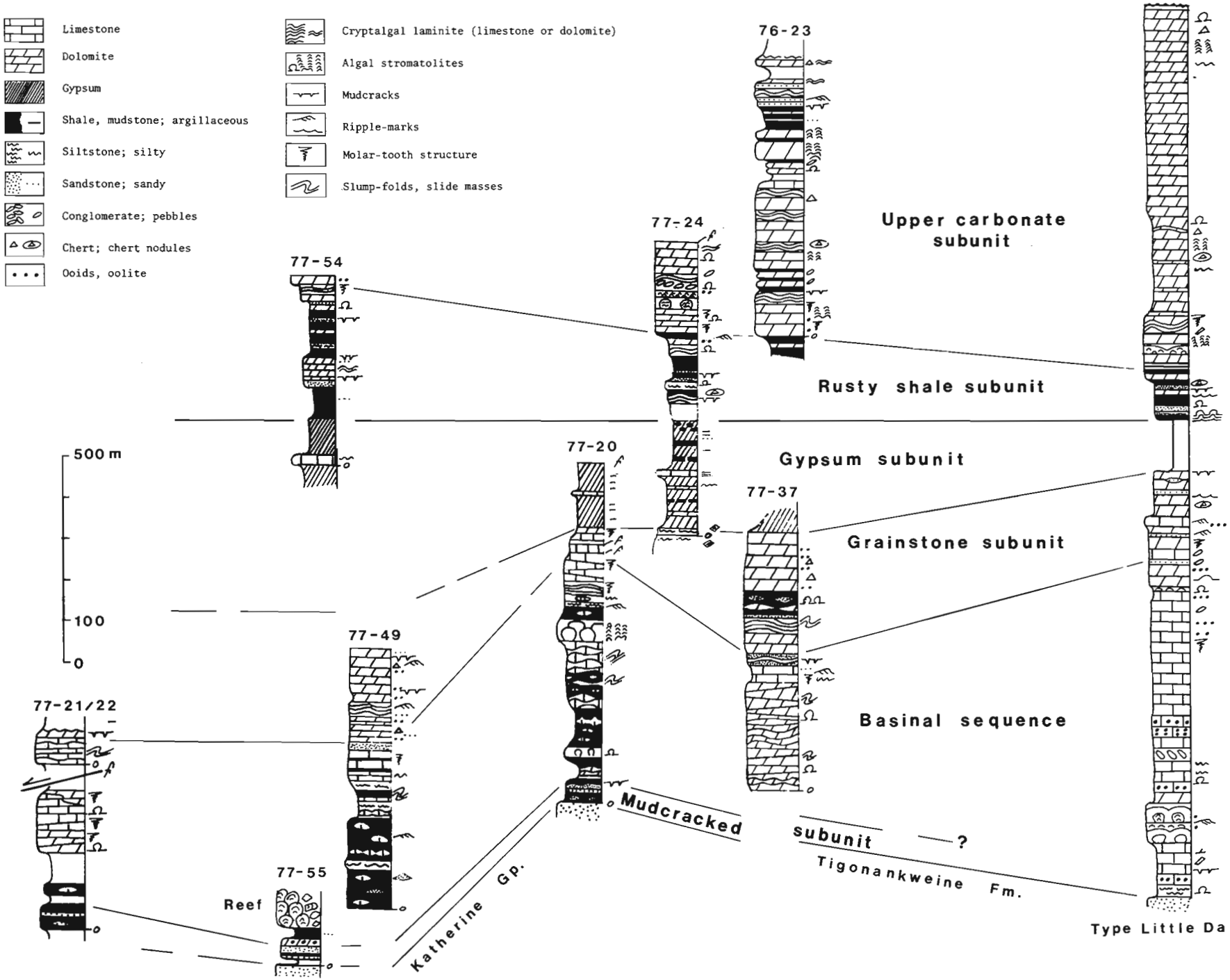

Figure 3. Northwest to southeast correlation of sub-units of Little Dal Group from Cranswick River (left) to Coates (Little Dal) Lake (right) (see Fig. 3). "Type Little Dal" after Gabrielse et al. (1973), modified and amended.

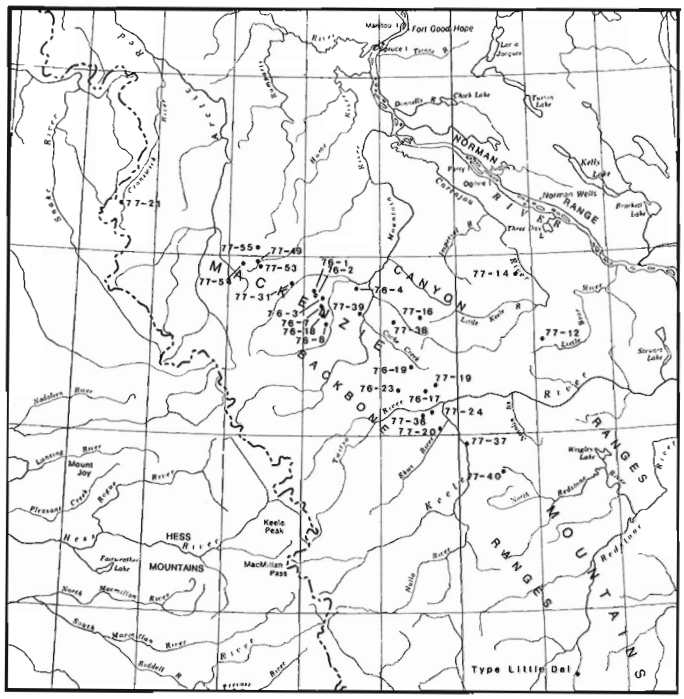

Figure 4. Location map, measured sections of Little Dal Group.

lower formation of the Katherine Group is divisible into five distinctive members. Of these, only the upper two can be traced into the type section of the Tigonankweine with any certainty. The group is interpreted to have originated as a result of a complex interaction of marine and fluvial processes, with sandstone members representing, in part, the deposits of rapidly prograding fluvial-deltaic complexes, which advanced at least four times over shallow marine sands, shales and carbonates. The destructive phase of each of these major progradations is marked by extensive ripple laminated sandstones or large scale cross-stratified marine sand sheets, which are, in turn, overlain by argillaceous rocks with or without carbonates.

Little Dal Group and Map-unit H5

The regional validity (from Cranswick River to Coates Lake) of informal, mappable subdivisions suggested in 1976 (Aitken, 1977a) was confirmed (Figs. 3, 4). Clearly, it is desirable now to recognize the entire post-Katherine/ Tigonankweine, pre-Redstone River succession as the Little Dal Group.

Aitken (ibid.) was mistaken in his conjecture that the type section of the Little Dal Formation (Gabrielse et al., ibid.) contained only the Plateau Thrust Sheet assemblages described below. In fact, it contains, in stratigraphic continuity above the type Tigonankweine (Katherine) Formation, the following sub-units established as subdivisions of map-unit H5 but equally appropriate as subdivisions of a Little Dal Group (Fig. 4): "Basinal sequence", "Grainstone sub-unit", "Gypsum sub-unit", and "Rusty shale sub-unit". The "Gypsum sub-unit" is covered along the line of the type section, but is exposed both north and south of the line.

At the type section, the unit overlying the "Rusty shale" is the unit inappropriately referred to as "Little Dal, sensu stricto" by Aitken (1977a). This unit is better referred to as the "Upper carbonate sub-unit", pending a formal revision of nomenclature.

The original partition of the type Little Dal Formation into lower and upper members (Gabrielse et al., 1973, Part II, Sec. 2) was done at a level that, although it approximates the base of the "Grainstone sub-unit" is by no means as obvious a contact as, for instance, the base or top of either the gypsum or the rusty shales. Furthermore the basis for partition, mainly weathering colour, is not one that can be successfully applied regionally. Therefore it is understandable that "Upper" and "Lower" Little Dal have been mapped wrongly over wide areas in Wrigley Lake and Glacier Lake map-areas. For instance, the prominent carbonate unit above the Plateau Fault is the "Upper carbonate sub-unit" of this report, but is mapped as "Lower Little Dal", whereas in other localities to the northeast, "Upper Little Dal" is mapped where only the lower part of the formation is preserved (ibid.).

"Flying-out" the Plateau Fault in Wrigley Lake and Glacier Lake map-areas (Gabrielse et al., 1973) confirms that, as in Mount Eduni and Bonnet Plume Lake map-areas (Aitken and Cook, 1974), the fault follows the "Gypsum sub-unit", seen to outcrop intermittently at the base of the Plateau Thrust Sheet until the thrust begins to die out southward between Redstone and South Redstone rivers. The dark brown weathering, mainly clastic formation near the base of the thrust sheet, mapped as Tigonankweine Formation by Gabrielse et al. (ibid.), is in fact the "Rusty shale sub-unit", some 1200 m stratigraphically higher. Thus, the Plateau thrust sheet contains no formation older than the "Gypsum sub-unit" of map-unit H5 (Aitken, 1977a).

Further examination of stromatolite reefs in the "Basinal sequence" yielded evidence of the following:

a. The reefs, during their period of active growth, had relief of at least several tens of metres up to, possibly, one hundred metres above the floor of the basin.

b. The constituent stromatolites grew in large part subtidally, in a "low-energy" environment. Minimum water depth of 15 m is established locally for sheets of **Stratifera**; the small, wall-less, irregularly active-branching columnar stromatolites that dominate in the reef cores probably grew at greater depths.

c. Wherever the depositional tops of reefs are preserved, they are flat or stepped. These flat surfaces appear to have developed in an agitated and probably shallow subtidal environment.

d. The reefs have no genetic connection with contemporaneous, regionally persistent stromatolite biostromes in the southeastern extent of the "Basinal sequence". These biostromes, whose northwestern termination may be taken to separate "basin" from "platform" environments, are fully developed in the type section of the Little Dal Formation.

Undoubted fossil metaphytes, in association with **Chuaria**, were collected at four widely separated localities, from the upper part of the "Basinal sequence" of map-unit H5.

Redstone River and Coppercap Formations

The Redstone River and Coppercap formations were found (contrary to a previous report by Aitken (1977b)) to be present over wide areas in front of Plateau Fault, in structural panels between Hay Creek and Cache Creek, from Twitya River to about 129°40' west longitude.

A panel of strata occurring immediately east of Keele River and north of latitude 63°55', in Wrigley Lake map-area, mapped as "Upper Little Dal – Redstone River – Coppercap (?)" by Gabrielse et al. (1973), was found to consist instead of the following sequence of sub-units of map-unit H5 (i.e. equivalents of the type Little Dal): "Basinal sequence", "Grainstone sub-unit", "Gypsum sub-unit", and locally, "Rusty shale sub-unit" (Aitken, 1977a), overlain by the Cambro-Ordovician Franklin Mountain Formation.

Stromatolite Biostratigraphy

The effectiveness of intrabasinal correlation on the basis of stromatolites was demonstrated, as follows (all taxonomic determinations are on a preliminary, i.e., field, basis):

The stromatolite assemblage of map-unit H1 (see above) is unique within the region.

The stromatolite assemblages of all units from the upper division of the Katherine (Tigonankweine) Group to the lower part of the "Upper carbonate sub-unit" of the type Little Dal (see above) are dominated consistently by **Baicalia.** Above the lower third, more or less, of the "Upper carbonate sub-unit" ("Little Dal s.s." of Aitken, 1977a), the first **Boxonia** and **Gymnosolen** consistently appear. These, with **Parmites, Jurusania,** cf. **Minjaria** and some **Baicalia,** characterize the upper two thirds of the sub-unit. Correlation lines based on this change in stromatolite assemblages parallel lithologic correlations based on such unmistakable formations as the "Gypsum sub-unit", and are confirmed by geological maps published and in manuscript.

The changes in stromatolite assemblages described above are recognized in Riphaean (Upper Proterozoic) strata of the Soviet Union, where they are considered to be significant with regard to geological age. Thus, the presence of **Svetliella** in map-unit H1 suggests a basal Middle Riphaean age (1350 ± 50 m.y.; see Semikhatov, 1974, Fig. 14). Similarly, the appearance of **Boxonia** and **Gymnosolen** above **Baicalia**-dominated assemblages is taken by many Soviet geologists to mark the base of the Upper Riphaean (950 ± 50 m.y., ibid.).

References

Aitken, J.D.
1977a: New data on correlation of the Little Dal Formation and a revision of Proterozoic map-unit 'H5'; in Report of Activities, Part A, Geol. Surv. Can., Paper 77-1A, p. 131-135.

1977b: Redstone River Formation (Upper Proterozoic) in Mount Eduni and Bonnet Plume Lake map-areas, District of Mackenzie; in Report of Activities, Part A, Geol. Surv. Can., Paper 77-1A, p. 137-138.

Aitken, J.D. and Cook, D.G.
1974: Geology of parts of Mount Eduni (106A) and Bonnet Plume Lake (106B) map-areas, District of Mackenzie; Geol. Surv. Can., Open File 221.

Aitken, J.D., Macqueen, R.W., and Usher, J.L.
1973: Reconnaissance studies of Proterozoic and Cambrian stratigraphy, lower Mackenzie River area (Operation Norman), District of Mackenzie; Geol. Surv. Can., Paper 73-9.

Gabrielse, H., Blusson, S.L., and Roddick, J.A.
1973: Flat River, Glacier Lake and Wrigley Lake map-areas (95E, L, M), District of Mackenzie and Yukon Territory; Geol. Surv. Can., Mem. 366.

Semikhatov, M.A.
1974: Stratigrafia i geokhronologia Proterozoia; Acad. Sci. USSR, Trudy, No. 256; "Nauka", Moscow.

CORRELATION OF HELIKIAN STRATA, MACKENZIE MOUNTAINS – BROCK INLIER – VICTORIA ISLAND

J.D. Aitken, D.G.F. Long and M.A. Semikhatov[1]
Institute of Sedimentary and Petroleum Geology, Calgary

Field and Laboratory Investigations

Aitken and Long spent the first week of June re-examining the Precambrian succession of Brock Inlier, before continuing their investigations in Mackenzie Mountains (Fig. 1). John Park (Earth Physics Branch) accompanied them for the first three weeks, to sample the succession for paleomagnetic investigations.

Semikhatov spent the period from July 25 to August 13 with the party in Mackenzie Mountains (see preceding note "Progress in Helikian Stratigraphy, Mackenzie Mountains"), where he familiarized himself with the Precambrian succession and sampled the stromatolite assemblages.

On return to Calgary, Semikhatov made a preliminary examination of stromatolites collected this year from Brock Inlier, and those collected by Aitken from Victoria Island in 1975.

Results

A consistent succession of stromatolite assemblages in the three regions (Fig. 1) suggests correlations differing in part from those proposed by Jefferson and Young (1977) and Young (1977a, b).

Mackenzie Mountains

The oldest formation exposed in the frontal Mackenzie Mountains, map-unit H1 (Aitken et al., 1973) contains the stromatolites **Conophyton, Jacutophyton, Svetliella, Baicalia** and a distinctive development of **Stratifera** with roof-like ridges (Table 1). This assemblage is unknown at Brock Inlier and Victoria Island. On the basis of studies in the USSR, the presence of **Svetliella** suggests a basal Middle Riphaean age, 1350 ± 50 m.y.

Stromatolites of the Tsezotene Formation, known from one member only, were not examined.

Stromatolite assemblages from the upper division of the Katherine Group and map-unit H5 (Aitken, 1977) are dominated by **Baicalia** and similar but unbranched stromatolites (Table 1). A possible **Inzeria** occurs in unit K6 of the Upper Katherine (Aitken et al., 1978) and passively branching wall-less forms in the "Basinal sequence" of map-unit H5. Stromatolite reefs in this "Basinal sequence" (ibid.) are dominated by small, irregularly active-branching, wall-less forms.

The dominance of **Baicalia** persists upward through about the lower third of the "Upper carbonate sub-unit" (Aitken et al., 1978; inappropriately referred to as "Little Dal Formation, sensu stricto" by Aitken, 1977). Higher in the sub-unit, **Boxonia** and **Gymnosolen** appear. These two groups, with **Jurusania**, cf. **Minjaria, Parmites** and some **Baicalia** characterize the upper two thirds of the sub-unit. The overlying Redstone River and Coppercap formations lack well organized columnar stromatolites.

Table 1

Correlation of Helikian formations between Mackenzie Mountains and Victoria Island

STROMATOLITE ASSEMBLAGE	REGION		
	MACKENZIE MOUNTAINS	BROCK INLIER	VICTORIA ISLAND
Gymnosolen, Boxonia	Coppercap Fm. (carbonates)		not present
	Redstone River Fm. (red beds, conglomerate, evaporites)	not present	Kilian Fm. (red beds, evaporites, minor carbonates)
Baicalia and others	Type Little Dal Formation (Gabrielse *et al.*, 1973): Upper carbonate subunit ("Little Dal s.s.") (mainly carbonates)	not present	Wynniatt Fm. (mainly carbonates)
	Map-unit H5 (Aitken, 1977a): Rusty shale subunit (mainly clastics); Gypsum subunit	Map-unit P5 (Cook and Aitken, 1969) (evaporites, clastics)	Minto Inlet Fm. (evaporites, fine clastics)
	Map-unit H5 (Aitken, 1977a): Grainstone subunit (mainly carbonates); Basinal sequence (carbonates, fine clastics)	Map-unit P4 (*ibid.*) (mainly carbonates)	Reynolds Point Fm. (except basal clastics)
	Map-unit H5 (Aitken, 1977a): Mud-cracked subunit (sandstone, shale)	Map-unit P3 (*ibid.*) (sandstone, quartzite)	Reynolds Point Fm. (basal sandstones only)
	Katherine Group (mainly sandstone)		Glenelg Fm. (upper sandstones only)
		Correlation of lower formations unresolved	
Conophyton, Jacutophyton, Svetliella	Tsezotene Fm. (mainly clastics)	Map-unit P2 (*ibid.*) (carbonates)	Glenelg Fm. (cherty dolomites)
	Map-unit H1 (mainly carbonates)	Map-unit P1 (*ibid.*) (mainly shale)	

[1] Geological Institute of the Academy of Sciences of the USSR, Moscow.

From: Scientific and Technical Notes in Current Research, Part A; Geol. Surv. Can., Paper 78-1A.

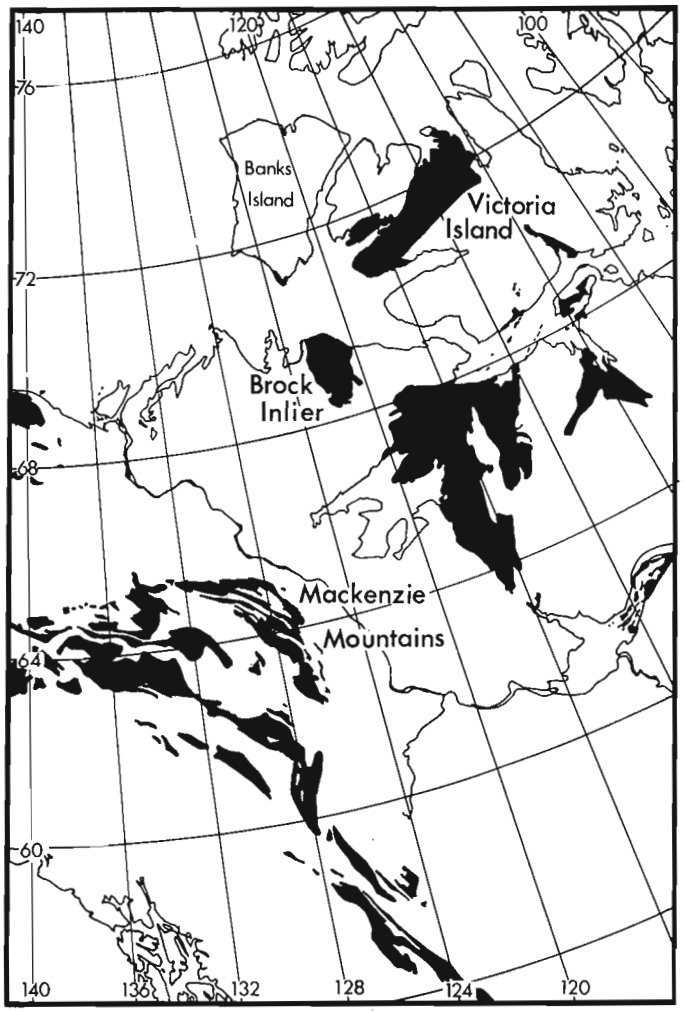

Figure 1. Index map. Exposures of Precambrian rocks shown in black.

The appearance of **Boxonia** and **Gymnosolen** is taken by many Soviet geologists to mark the base of the Upper Riphaean (950 ± 50 m.y.; see Semikhatov, 1974, Fig. 14).

Brock Inlier

The Brock Inlier contains two carbonate-dominated formations, designated "P2" and "P4" by Cook and Aitken (1969). The lower "P2" is characterized by **Colonella** and **Baicalia.** The upper "P4" is extremely stromatolitic and characterized throughout by **Baicalia** and similar but unbranched columns, comparable to those that occur in biostromes present as tongues in the "Basinal sequence" of map-unit H5 in Mackenzie Mountains (Aitken, 1977).

Victoria Island

The lowest stromatolites reported from the Shaler Group are **Basisphaera** and **Inzeria,** from a unit of cherty dolomite within the Glenelg Formation (Young and Jefferson, 1975). **Conophyton** also occurs in the Glenelg Formation (C.W. Jefferson, pers. comm., 1977).

At the top of the Glenelg, **Inzeria** appears with **Baicalia** in a regional biostrome.

The Reynolds Point Formation is dominated by **Baicalia.** Here also occurs a small, irregularly active-branching wall-less form similar to the principal reef-builders of the "Basinal sequence" of map-unit H5. This is the "finger stromatolite" of Young and Jefferson (ibid.).

The Wynniatt Formation contains **Baicalia** in its lower part, but **Boxonia** occurs in the formation as low as 300 m above the base.

Stromatolites collected from the Kilian Formation have not yet been identified.

Summary

Three distinct stromatolite assemblages can be recognized through preliminary field studies. The lowest, characterized by **Conophyton, Jacutophyton,** and **Svetliella,** is known only from the base of the Mackenzie Mountains succession. It is succeeded by an assemblage, characterized by the dominance of **Baicalia** and passively branching, wall-less forms, that occurs in Mackenzie Mountains, Brock Inlier and Victoria Island. The third assemblage, found near the top of the Mackenzie Mountains and Victoria Island successions, is characterized by **Boxonia** and **Gymnosolen.**

Correlation of the boundary between the **Baicalia**-dominated and the **Boxonia-Gymnosolen** assemblages supports a straightforward correlation, based on gross lithology, for the top of the principal sandstone formation in each region and the succeeding formations (Table 1). Correlation of lower formations is not yet clear.

References

Aitken, J.D.
1977: New data on correlation of the Little Dal Formation and a revision of Proterozoic map-unit 'H5'; in Report of Activities, Part A, Geol. Surv. Can., Paper 77-1A, p. 131-135.

Aitken, J.D., Macqueen, R.W., and Usher, J.L.
1973: Reconnaissance studies of Proterozoic and Cambrian stratigraphy, lower Mackenzie River area (Operation Norman), District of Mackenzie; Geol. Surv. Can., Paper 73-9.

Aitken, J.D., Long, D.G.F., and Semikhatov, M.A.
1978: Progress in Helikian stratigraphy; Note in Current Research, Part A, Geol. Surv. Can., Paper 78-1A.

Cook, D.G. and Aitken, J.D.
1969: Geology, Erly Lake, District of Mackenzie; Geol. Surv. Can., Map 5-1969 (with descriptive notes).

Gabrielse, H., Blusson, S.L., and Roddick, J.A.
1973: Flat River, Glacier Lake and Wrigley Lake map-areas (95E,L,M), District of Mackenzie and Yukon Territory; Geol. Surv. Can., Mem. 366.

Jefferson, C.W. and Young, G.M.
1977: Use of stromatolites in regional lithological correlations of Upper Proterozoic successions of the Amundsen Basin and Mackenzie Mountains, Canada (Abstract); Geol. Assoc. Can., Program with Abstracts, v. 2, p. 26.

Semikhatov, M.A.
1974: Stratigrafia i geokhronologia Proterozoia; Acad. Sci. USSR, Trudy, No. 256; "Nauka", Moscow.

Young, G.M.
1977a: Stratigraphic correlation and provenance of Upper Proterozoic rocks of Brock Inlier, District of Mackenzie, N.W.T. (Abstract); Geol. Assoc. Can., Program with Abstracts, v. 2, p. 57.

1977b: Stratigraphic correlation of upper Proterozoic rocks of northwestern Canada; Can. J. Earth Sci., v. 14, p. 1771-1787.

Young, G.M. and Jefferson, C.W.
1975: Late Precambrian shallow water deposits, Banks and Victoria Islands, Arctic Archipelago; Can. J. Earth Sci., v. 12, p. 1734-1748.

CHARACTERISTIC MAGNETIZATION OF SOME MIDDLE PLEISTOCENE SEDIMENTS FROM THE MEDICINE HAT AREA OF SOUTHERN ALBERTA

R.W. Barendregt[1] and A. MacS. Stalker
Terrain Sciences Division

Introduction

This paper reports on the results of an exploratory study of the paleomagnetic characteristics of some river and lake deposits found in southeastern Alberta. The study was conducted at Mitchell Bluff (Stalker, 1969, p. 20-23), which lies along the southeast bank of South Saskatchewan River about 8 km north-northeast of Medicine Hat, Alberta. Samples were collected from the lower part of the bluff at its east end, in NW1/4 sec. 33, tp. 13, rge. 5, W 4th mer. (58°8'N, 110°37'30"W). Barendregt collected and analyzed the samples, and Stalker studied the stratigraphy and chronology.

Laboratory facilities were provided by Woodward-Clyde Consultants of San Francisco, California. The authors express their thanks to Dr. D. Packer of the Paleomagnetics Laboratory at Woodward-Clyde Consultants, San Francisco, and to Dr. J.H. Foster, Geological Survey of Canada, for providing much useful discussion about interpretation of the results and for critically reading the manuscript.

Stratigraphy

The sequence of deposits sampled for the paleomagnetic studies is indicated in Figure 1. They included units MBC and MBD of Stalker (1969) and units E, F, and G of Stalker and Churcher (1972).

The lowest 7 m of the exposure consists largely of greyish blue, fine silt and clay, which is finely laminated and interbedded. The top metre consists of buff, fine sand. These materials were deposited in a lake that may have formed when glaciers advancing from the northeast blocked the ancestral South Saskatchewan River. The laminae show remarkably little disturbance, and if they represent yearly deposition along the lines of varves, as is probably the case, the deposits were laid down at a rate of almost 1.5 mm per year near the base and 1 mm per year near the top. The main body of silt and clay gives no indications of any interruptions in deposition or of erosional intervals, although these cannot be ruled out. If such are absent, deposition of these beds probably took about 5000 years. There likely are hiatuses in the sandy, top metre of the unit, particularly about 0.5 m from the top where a thin gravel band probably represents a lag deposit developed through erosion and sorting of some of the silt and clay by a slow stream.

The lower deposits are overlain by 11 m of sand, for the most part strongly cross and channel bedded (Fig. 1). Most of this sand is coarse and contains grit and pebble bands, and so it is not suitable for paleomagnetic studies. However, two bands of finer, horizontally bedded material, about 7 and 9 m above the base of the unit, were sampled (samples S and T).

The coarse sand is overlain by 6 m of buff silt and fine sand. This unit, which forms a near-vertical cliff face, contains scattered pieces of wood and near its centre is crossed by a 1 m thick peaty band. Sample U came from the top metre of this unit, which consists mostly of finely laminated, brown silt and clay, and which also probably represents varves. This fine material is covered by about 0.5 m of lag gravel, the remnant of fluvial erosion of till and outwash from the first Laurentide glacier to overrun the region. This lag material contains the first stones from the Canadian Shield brought into the area by that glacier.

Much of the section, and particularly its lower part, contains scattered bones. These were studied in detail by Dr. C.S. Churcher, Department of Zoology, University of Toronto, who concluded that most of the deposits were of Early Yarmouth age, or perhaps late Kansan for the lowest part of the section (Stalker and Churcher, 1972, p. 112).

Paleomagnetic results

Altogether 125 drive core samples were collected from a 24 m thick section at the horizons indicated in Figure 1. As the samples were taken manually, only those deposits that are above the level of South Saskatchewan River could be sampled; the section and sample sites are referred to by height above river. At the time of investigation river level was about 4 m below the irrigation pump on the Mitchell homestead, a short distance farther downstream.

Declination, inclination, and remanent intensity (moment) were measured at the sites indicated in Figure 1. The results given in Figure 1 are the averages of (the number) N specimens from separately oriented drive cores at each of the lettered horizons. Where N is less than 5 the results of

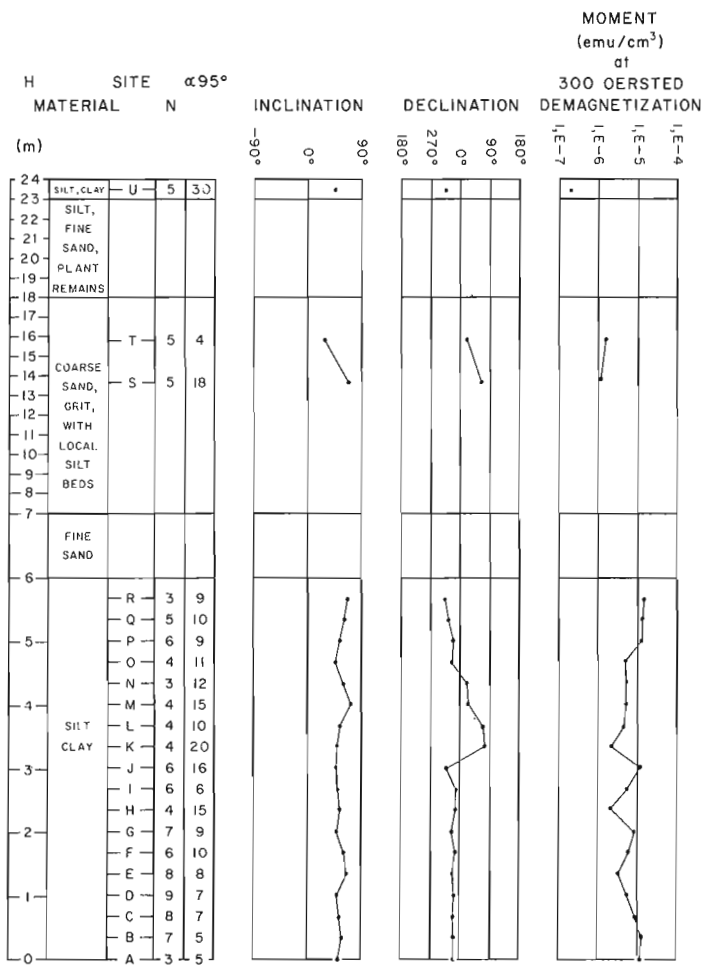

H = height in metres above level of South Saskatchewan River (note change of scale at 7 m);

Site A = sampling horizon reference letter;

N = number of separately oriented drive core specimens;

α95° = radius (in degrees) of 95% zone of confidence.

Figure 1. Inclination, declination, and moment (remanent intensity) of the lower part of Mitchell Bluff East.

[1]San Francisco State University, California

From: Scientific and Technical Notes in Current Research, Part A; Geol. Surv. Can., Paper 78-1A.

certain specimens were rejected because they were strongly divergent from the cluster of results at that horizon. The radius (in degrees) of the 95% zone of confidence ($\alpha 95$) also is given for each horizon. Pilot specimens first were measured for natural remanent magnetism (N.R.M.) and were remeasured after demagnetizaitons of 25, 50, 100, 200, 300, 400, 500, 600, 800 and 1000 oersteds. The characteristic magnetization was found to be of a single component and well represented by the direction of the remanent magnetization after 300 oersted demagnetization. The remaining samples were measured for N.R.M. and were remeasured after demagnetizations of 100, 300, and 600 oersteds. Cluster statistics for each of these steps confirmed the choice of 300 oersteds as best representative of the characteristic direction. Abrupt directional changes do not occur in the inclination profile; however, there is a shift in the declination profile at point J. Negative inclinations were not found.

Remanent intensity (moment) fluctuates in a somewhat cyclic fashion between sample locations C and L and then remains rather stable. This may reflect a change in the strength of the geomagnetic field but more likely is a change in the magnetic mineral constituents, corresponding to a change in particle size distribution and orientation.

Only a few exploratory samples were collected and analyzed at points S, T, and U. The top part of the section (points R to U) will be sampled more thoroughly at a later date.

Interpretation and discussion

Most of these mid-Pleistocene sediments consist of fine material deposited under quiet water conditions, and they proved to be very suitable for the study. Such sediments offer much promise for further work towards paleomagnetic correlation. The major problem lies in the difficulty of determining the positions of any interruptions in deposition or erosion intervals that may be present.

The 24 m section examined was considered to have been deposited before any Laurentide glacier had reached the area and so was considered to consist solely of material picked up from the local Cretaceous bedrock or else brought by east flowing rivers from the Rocky Mountains or the Foothills. Such material generally has a weak natural remanent magnetic intensity; thus the strength of the intensity found in samples A to R was a surprise. It may result from a large, but previously unrecognized, component of shield material introduced as outwash from a Laurentide glacier that blocked South Saskatchewan River to form the proglacial lake in which the sediment was deposited. On the other hand, it may represent a large content of fresh volcanic ash that fell or was washed into the lake during deposition of the sediment. A third possibility is that preglacial streams brought in material from an area containing much magnetic material, such as the Sweet Grass Buttes area near the Montana-Alberta border. None of these explanations, however, is wholly satisfactory. Evidently the supply of strongly magnetic material had much lessened during deposition of the beds that supplied samples S and T; those beds consist chiefly of material from the local Cretaceous beds and from the foothills and Rocky Mountains farther west.

Conclusion

These mid-Pleistocene sediments have a strong, single component characteristic magnetization. This implies that a more extensive paleomagnetic sampling program might provide detailed lateral correlations for this section. Such detailed stratigraphic work is important to resolve a large number of faunal relationships in the area.

References

Stalker, A. MacS.
1969: Quaternary stratigraphy in southern Alberta, Report II: Sections near Medicine Hat; Geol. Surv. Can., Paper 69-26, 28 p.

Stalker, A. MacS. and Churcher, C.S.
1972: Glacial stratigraphy of the southwestern Canadian Prairies, the Laurentide record; 24th Int. Geol. Congr. (Montreal), Sect. 12, p. 110-119.

URANIUM IN THE HELIKIAN OF THE NORTHERN CANADIAN CORDILLERA – A PRELIMINARY ASSESSMENT

R.T. Bell
Regional and Economic Geology Division

Fraser et al. (1970) demonstrated a very general correlation of Helikian successions in the Cordillera with the Helikian basins, largely dominated by continental red beds, of the Canadian Shield and suggested they were once coextensive but now are separated by post-Helikian epiorogeny features such as the Slave Arch and Peace River Arch. Their suggestion that the Cordilleran Helikian rocks are eugeosynclinal does not appear to be valid. Figure 1, based in part on their paper, illustrates the distribution of Helikian and probable Helikian rocks and pertinent paleocurrent data[1].

Fairly direct correlation and tracing through the Mackenzie Mountains could be made, but broader, more elegant correlations are now becoming possible because of the detailed stratigraphic studies by Aitken (1975, 1977), Aitken et al. (1978), and Eisbacher (1976) of the Geological Survey, and by Delaney, Jefferson, and Young of the University of Western Ontario.

An important barrier to correlation is the Knorr fault system separating the Mackenzie Mountains in the east, and the Wernecke, Ogilvie, and British mountains in the west, in that there is a distinct break in pre-Hadrynian lithologies. The past two summers field experience leads the author to believe that a correlation of Little Dal Formation with Unit 2 of Green (1972; see also Bell and Delaney, 1977) in the Wernecke and Ogilvie mountains may be possible. Young's (1977, see Figure 18, columns 1 and 2) correlation further suggests to the author that unit 1 of Green (1972) includes the lateral pelitic equivalent of the Tsezotene and

Figure 1.

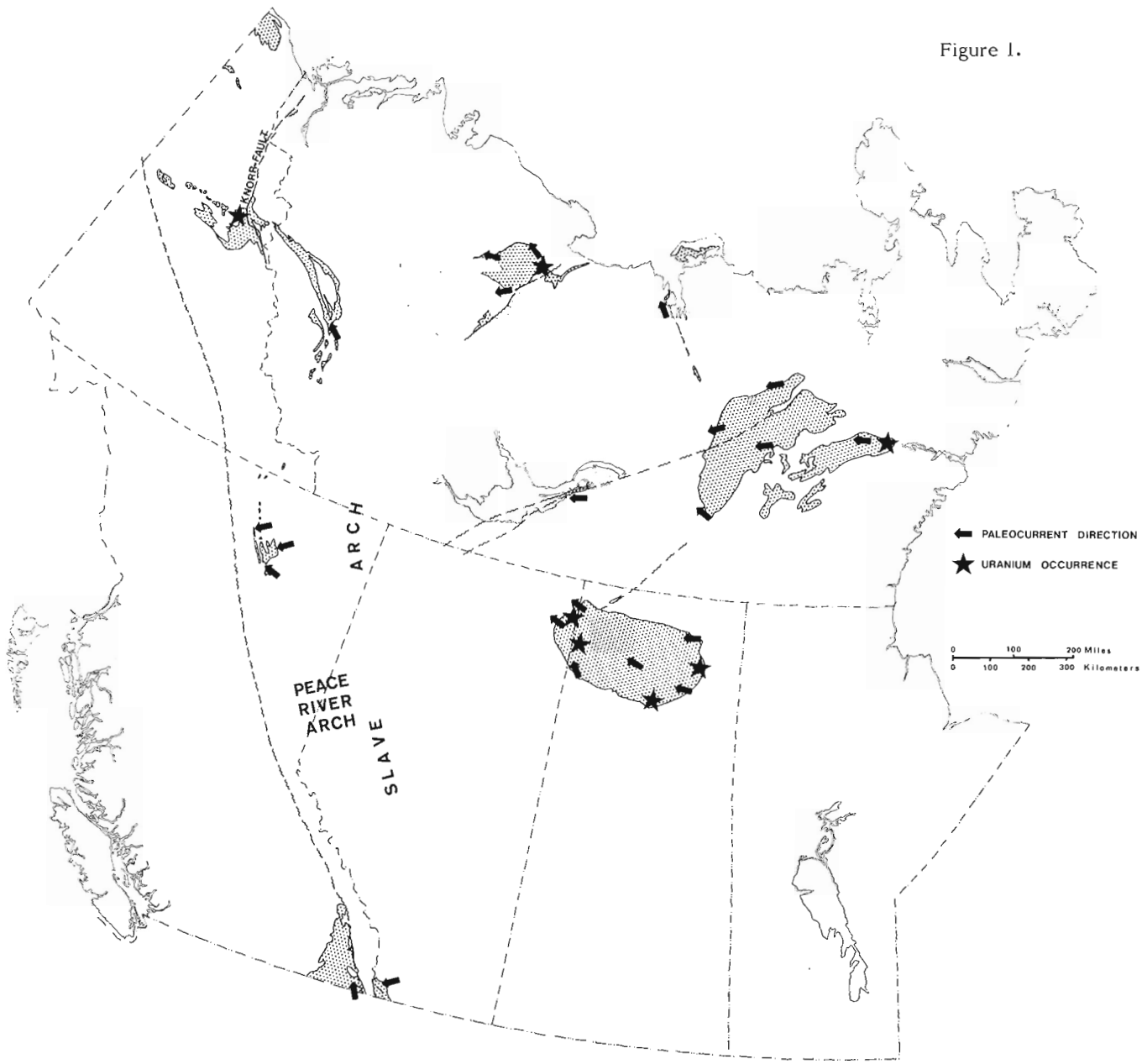

[1] Paleocurrent direction in Mackenzie Mountains by D.G.F. Long (pers. comm.).

From: Scientific and Technical Notes in Current Research, Part A; Geol. Surv. Can., Paper 78-1A.

Tigonankweine-Katherine units. Shaley strata in the British Mountains in northernmost Yukon resemble those of the Ogilvie and Wernecke mountains but that is all that may be stated on that matter.

Correlation from the Mackenzie Mountains to the Rocky Mountains is tenuous. Strikingly similar lithologies and environments of deposition occur in pre-Aida rocks of northeastern British Columbia and in the Helikian of the Mackenzie Mountains. The same can be said (Bell, 1968) regarding correlation from northeastern to southeastern British Columbia and the Belt or Purcell succession there.

Implications

Uranium mineralization (Fig. 1) is present within sandstones, pelites, volcanics and at unconformities related to Helikian basins of the Canadian Shield. Uranium mineralization along with copper is reported from the Belt-Purcell sequence (R. Morton, pers. comm.). Uranium mineralization is present in dark shales of the Wernecke and Ogilvie mountains (Bell, 1978). It is therefore concluded that the Helikian rocks in the Cordillera provide a fertile ground for exploration of this commodity. Three stratigraphic targets are suggested:

1) Texas style uranium sandstone mineralization in sandstones in environments above marine wave base (beach, bar, lagoon deltaic) with parts of the Tigonankweine, Tsezotene, Katherine, Tuchodi and Chischa formations being favourable;

2) Black shale uranium mineralization with parts of Green's unit 1 Tsezotene, lower Aida and Tetsa formations being favourable;

3) Copper-bearing shale (Kuperschiefer) with parts of Green's unit 2, Little Dal, Coppercap, Tuchodi, George and Chischa formations perhaps being favourable.

References

Aitken, J.D.
1975: Proterozoic stratigraphy and sedimentology, Tuchodi Lakes map-area, B.C.; in Report of Activities, Part A, Geol. Surv. Can., Paper 75-1A, p. 511.

Aitken, J.D. (cont'd.)
1977: New data on correlation of the Little Dal Formation and a Revision of Proterozoic map-unit 'H-5'; in Report of Activities, Part A, Geol. Surv. Can., Paper 77-1A, p. 131-135.

Aitken, J.D., Long, D.G.F., and Semikhov, M.A.
1978: Progress in Helikian stratigraphy, Mackenzie Mountains; in Current Research, Part A, Geol. Surv. Can., Paper 78-1A; a note.

Bell, R.T.
1968: Proterozoic stratigraphy of northeastern British Columbia; Geol. Surv. Can., Paper 67-68.

1978: Breccias and uranium mineralization in the Wernecke Mountains – A progress report; in Current Research, Part A, Geol. Surv. Can., Paper 78-1A, rep. 59.

Bell, R.T. and Delaney, G.D.
1977: Geology of some uranium occurrences in Yukon Territory; in Report of Activities, Part A, Geol. Surv. Can., Paper 77-1A, p. 33-37.

Eisbacher, G.H.
1976: Proterozoic Rapitan Group and related rocks, Redstone River area, District of Mackenzie; in Report of Activities, Part A, Geol. Surv. Can., Paper 76-1A, p. 117-125.

Frazer, J.A., Donaldson, J.A., Fahrig, W.F., and Tremblay, L.P.
1970: Helikian basins and geosynclines of the northwestern Canadian Shield; in Symposium on basins and geosynclines of the Canadian Shield, Baer, A.J. (ed.), Geol. Surv. Can., Paper 70-40.

Green, L.H.
1972: Geology of Nash Creek, Larson Creek, and Dawson map-areas, Yukon Territory; Geol. Surv. Can., Mem. 364.

Young, G.M.
1977: Stratigraphic correlation of Upper Proterozoic rocks of northwestern Canada; Can. J. Earth Sci., v. 14, p. 1771-1787.

PRELIMINARY SUBDIVISIONS OF THE MALTON GNEISS COMPLEX, BRITISH COLUMBIA

V.E. Chamberlain[1], R. St. J. Lambert[1] and J.G. Holland[2]
Regional and Economic Geology Division

The Malton Gneiss was mapped and defined by Campbell (1968) as a 1000 km^2 mass of amphibolite facies gneiss cropping out in the mountains southeast of Valemount, B.C. (centred on 52°35'N and 119°W). As mapped by Campbell (op. cit.), the bulk of the Gneiss lies to the west of the Rocky Mountain Trench (Fig. 1). Two outcrops however, are shown east of the Trench: one in the Bulldog Creek area (approx. 4 km^2) and one at The Cherries (approx. 80 km^2). The present studies were initiated in part to determine how far the gneiss east of the Trench can truly be equated with that on the west, and so to place some limits on movement along the Trench.

Reconnaissance of the most accessible parts of the Malton Gneiss (in the Canoe Mountain area to the west of the Trench) has revealed at least four geochemically and petrologically distinct units – all of igneous character. These units (labelled 1 to 4), are shown in Figure 2 where yttrium versus niobium contents of the rocks are plotted. These particular trace elements were chosen as parameters because they are relatively inert during metamorphism and because they appear to be diagnostic of each unit. Group 1 consists of "mafic" hornblende and hornblende-biotite tonalite and diorite gneiss with high potassium contents. These rocks occur near the top of Canoe Mountain, and again near the foot, where they have been intruded by the leucocratic alkaline gneissic sheets of group 3. Gneiss of group 4 forms a subset of alkaline granite gneiss with higher yttrium contents than that of group 3. Group 4 gneiss also occurs as intrusive sheets into mafic gneiss of group 1 and reconnaissance of the remainder of the Complex shows that it also occurs elsewhere. Gneiss of group 2 occurs as isolated outcrops on Canoe Mountain. It appears to underlie upper group 1 gneiss conformably and form part of the same structural sequence. Group 2 gneiss is non-alkaline granitic and tonalitic often garnetiferous, with characteristically low yttrium and niobium contents and with Y/Nb ratios of about 2.

Rb-Sr isotopic analyses of these suites of rocks suggest late Proterozoic ages for gneiss of groups 1, 3 and 4 and an Archean age for some group 2 gneiss; however there is considerable scatter of the data, and interpretation is beyond the scope of this note although preliminary U-Pb isotopic and petrographic studies on bulk zircons from group 2 gneiss roughly confirms the Rb-Sr age.

Preliminary geochemical and petrographic work on a further 200 samples of gneiss from less accessible parts of the Malton Gneiss, including those outcrops on the eastern side of the Rocky Mountain Trench, has revealed that the area may be divided into four geographical regions, which appear to have a geological basis.

1. The Malton Range, extending from Canoe Mountain in the north to Clemina in the south. Over this region, the fourfold division of gneiss established on Canoe Mountain seems to hold, with group 1 occupying most of the higher ground.

2. Northern Monashee Mountains, immediately south of the Malton Range and extending from Clemina in the north to Lempriere in the south. Over this region the rocks are rather varied. Some are similar to those found on Canoe Mountain but K-feldspar porphyritic gneiss of granodioritic and granitic nature are prominent near Mount Albreda.

3. The Bulldog Creek area, east of the trench, is comparatively poorly exposed, but a limited number of samples show considerable geochemical and petrological similarity to units 1 and 2 of the Canoe Mountain area, although strongly sheared. Felsic gneiss of types 3 and 4 has not yet been identified. Identity with the Canoe Mountain block seems to be the most likely solution.

4. The gneissic rocks on The Cherries, separated from a massive muscovite psammite unit of Miette Group schist by

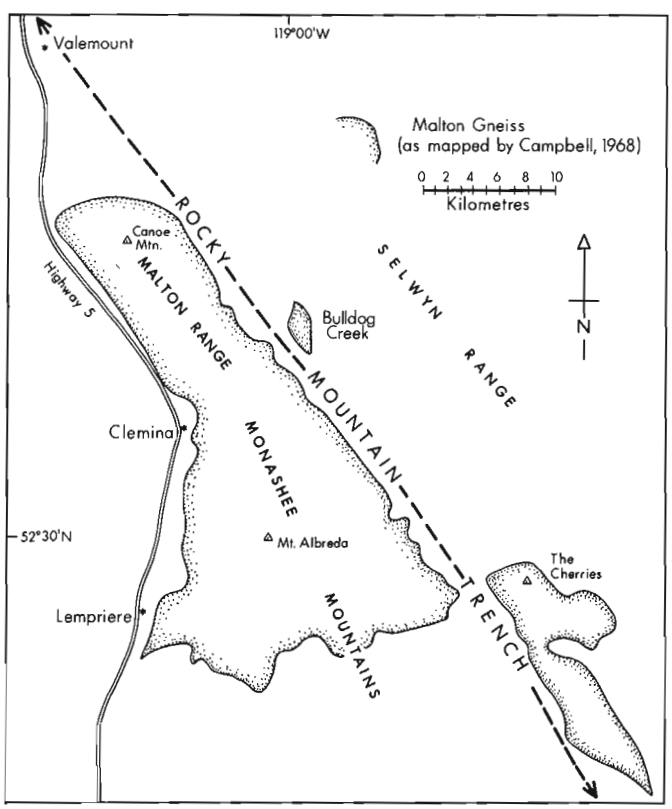

Figure 1. Map showing location and outcrop of Malton Gneiss.

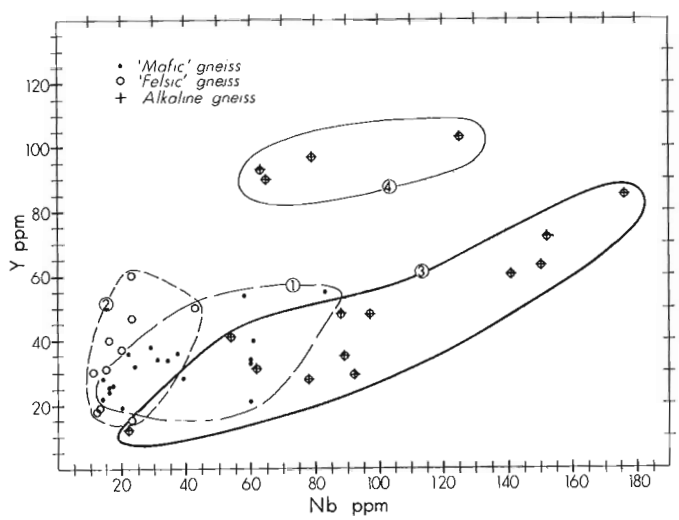

Figure 2. Yttrium and niobium contents of Malton Gneiss.

[1] Department of Geology, University of Alberta, Edmonton, Alberta, Canada, T6G 2E3.

[2] Department of Geological Sciences, Science Laboratories, South Road, Durham, England.

From: Scientific and Technical Notes in Current Research, Part A; Geol. Surv. Can., Paper 78-1A.

mylonitic schist, do not contain any units which can be correlated petrologically or geochemically with those west of the Trench. A general similarity of appearance is caused by the occurrence of mafic hornblende-gneiss sheets in both areas, but the average felsic gneiss of The Cherries appears to be metasedimentary in origin with a petrography and chemistry related to arkose or arkosic quartzite, not very dissimilar from those in the Miette Group. Preliminary Rb-Sr work also suggests lack of identity with the Malton Gneiss. Indications are, therefore, that The Cherries gneiss and Malton Gneiss proper are not true correlatives.

In conclusion, the Malton Gneiss appears to be a meta-igneous shield-type rock. Correlatives are probably best sought to the south and southeast rather than to the north and northeast.

References

Campbell, R.B.
1968: Canoe River, British Columbia; Geol. Surv. Can., Map 15-1967.

Wheeler, J.O., Campbell, R.B., Reesor, J.E., and Mountjoy, E.W.
1972: Structural style of the southern Canadian Cordillera; Field Excursion X01-A01, XXIV Int. Geol. Cong., Montreal, 1972.

THE EFFECT OF BOTTOM-FAST ICE ON THE STAGE-DISCHARGE RELATIONSHIP

P.A. Egginton
Terrain Sciences Division

Introduction

As part of an environmental monitoring program of bridge crossing sites along Mackenzie Highway, observations have been made on breakup, highwater, and backwater events, and stream stability on rivers in the Fort Norman-Wrigley area, Northwest Territories (Egginton, 1976; Egginton and Day, 1976, 1977).

The rivers in this area have a nival regime. The precipitation accumulated over the seven winter months is released in the spring in a period of a few weeks. The balance of the flow is sustained throughout the season by melt from areas of high elevation and by summer storms. In the study area it is suspected that the highest discharges (i.e., design floods) on the rivers are reached as the result of a combination snowmelt-precipitation event; these floods likely occur in the early spring (Jasper and Anderson, 1977). Flood stage is an important design consideration as it is used to calculate flood discharge, flood velocity, and expected scour. The spring flood is dominant, and, as such, the effect of bottom-fast ice on the stage-discharge relationship is of considerable interest.

Ice and Stage

In the study area pre-freezeup discharge in stream basins of less than 1000 km^2 characteristically drops to less than 1 m^3/s, and except for deep pools, the rivers commonly freeze to the bottom. Bottom-fast ice therefore is limited to low flow channels and is at maximum thickness in pool sequences where ice depths may exceed 1.5 m.

Figure 3 shows a pool section of Little Smith Creek (Profile 1) as it was viewed on April 18, 1976. Much of the snow had melted from the flood plain and only the low flow channel remained snow and ice covered when flow commenced. Using a bench mark system installed along the river it was possible to survey several cross-sections during breakup. Two transects were run across Profile 1 in late April, revealing the presence of a degrading sheet of bottom-fast ice (Fig. 1). Bottom-fast ice was found in all pools sampled in late April 1976 in the lower Little Smith Creek basin.

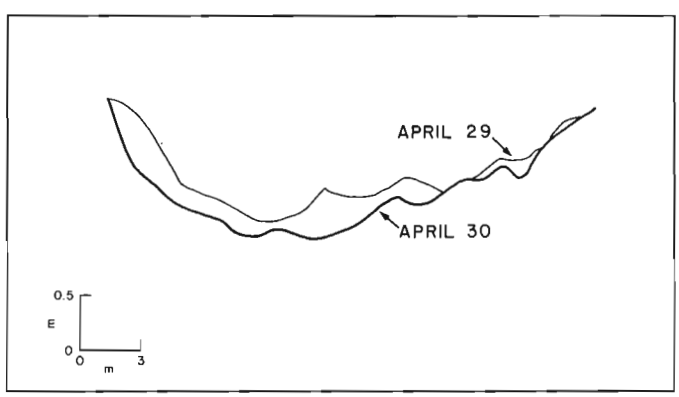

Figure 1. Transects, Profile 1, Little Smith Creek, April 29 and 30, 1976. During both transects the bed was ice covered. The profile change over time results from the degradation of bottom-fast ice.

The effect of bottom-fast ice on the stage-discharge relationship is illustrated by two profiles on Little Smith Creek (Fig. 2). In both cases the lower and later discharges (i.e., discharges occurring after May 10) plot as a straight line on semi-logarithmic paper. The larger, earlier flows occurred at higher stage elevations than might be expected purely on the basis of an extension of the low flow relationship, as the ice effectively elevated the bed. It is possible at higher discharge values, for the sections studied, that stage does not vary as a simple semi-logarithmic function of discharge. It is impossible, however, to discern the effect of (non-ice) channel shape on the relationship because of the overriding influence of the bottom-fast ice.

A portion of the stage record, Profile 1, Little Smith Creek, is shown in Figure 4. According to this record, river stage and presumably discharge decreased from April 29 onward. It was determined from stage data at other 'non-ice' stations, however, that peak annual stream discharge was reached on the night of May 2, 1976 (cf. Fig. 4). The recorded stage decline at Profile 1 merely reflects the degradation of anchor ice through time which effectively lowers the stream bed.

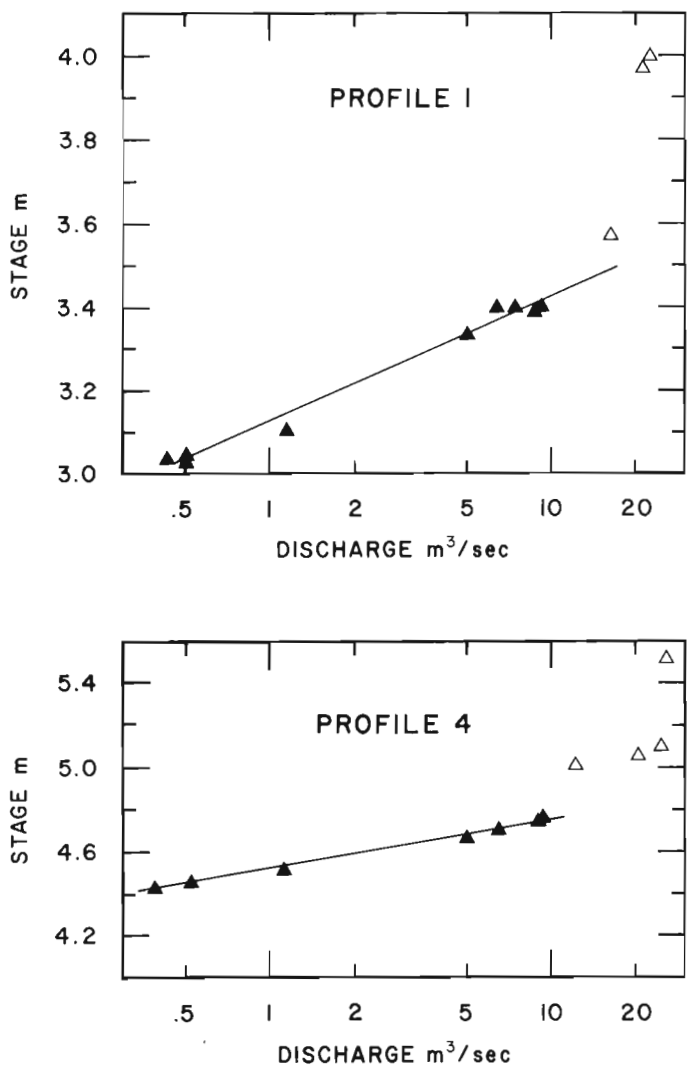

Figure 2. Stage-discharge relationships for two profiles on Little Smith Creek, 1976. The higher stage discharge readings (open triangles) were taken when bottom-fast ice was visible on the bed. The lower stage-discharge readings (solid triangles) were taken under 'non-ice' conditions.

From: Scientific and Technical Notes in Current Research, Part A; Geol. Surv. Can., Paper 78-1A.

Figure 3. Ice conditions at Profile 1 on Little Smith Creek, April 18, 1976. The line positions the surveyed transects shown in Figure 2. GSC 203165-C.

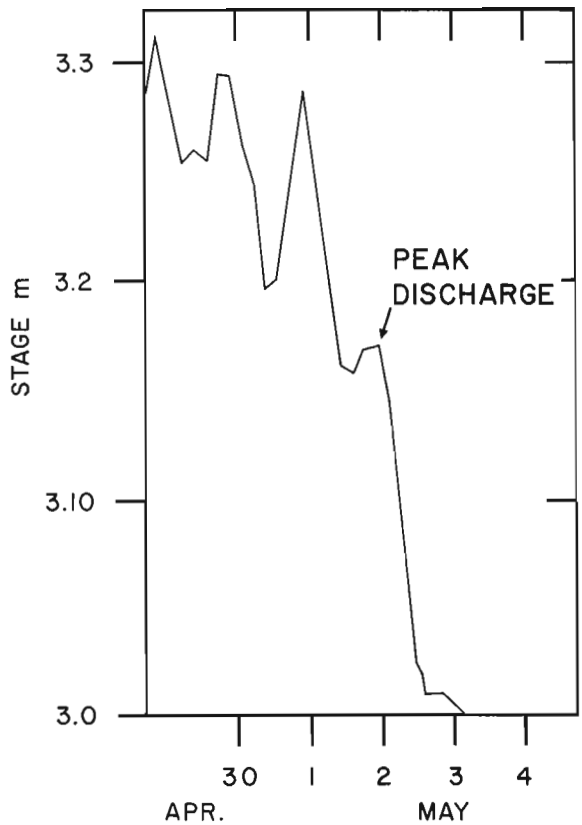

Figure 4. Stage record for Profile 1, Little Smith Creek, 1976. The maximum yearly discharge was reached on the night of May 2 in spite of a declining stage record from April 29 onwards. This irregularity results from river flow over a degrading bed of bottom-fast ice.

On a larger scale, the entire flood plains of the study streams commonly are snow covered in early spring, and the initial flow may be over the snow. Figure 5 shows a portion of the Little Smith Creek flood plain that remained covered with an ice-crusted snow layer throughout the 1977 spring flood. The effect of the snow on the stage-discharge relationship can be expected to be similar to that of bottom-fast ice; however, the snow usually does not persist throughout the entire flood period.

The time distribution of the spring flood may limit the extent to which snow and bottom-fast ice modify the stage, discharge, and hydraulic relationships of a stream. It is expected that those streams with peaked spring flood hydrographs (i.e., the spring flood passes quickly) are influenced by snow and bottom-fast ice to a greater degree than streams with less peaked floods because snow and bottom-fast ice do not persit through long duration floods.

The presence of bottom-fast ice in a section, through breakup, has several implications:

(1) The stream may be competent to transport large material entering the reach because of the low frictional resistance of the ice to material moving over it.

(2) The bed may be protected from the high erosive velocities associated with higher discharges.

(3) A stream flowing over a layer of bottom-fast ice maintains a higher stage than at similar discharge under non-ice conditions. Thus, in certain reaches, and under certain ice conditions, a flood may occur at higher elevations than expected on the basis of flood magnitude alone.

(4) The extension of the stage records derived under non-ice conditions in such sections, or the use of the slope area method (using highwater marks), to determine peak discharge, may lead to erroneously high results. For example, the 1976 peak discharge calculated using the slope area method and the highwater marks at Profile 1, Little Smith Creek, was 56.5 m^3/s, whereas the actual peak flow was 25.2 m^3/s.

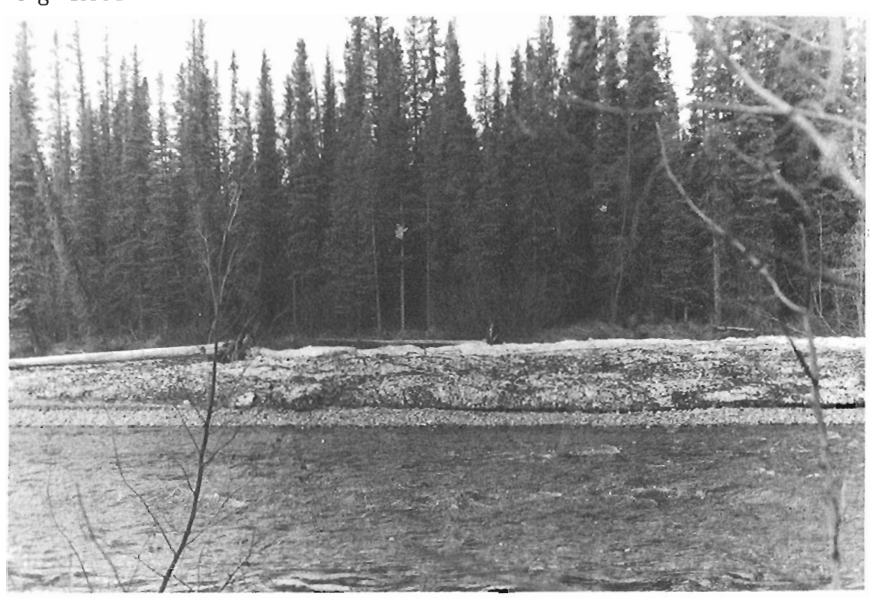

Figure 5. Snow and remnant debris remaining on the flood plain of Little Smith Creek after the passage of the 1977 spring flood. The snow here is approximately 0.6 m deep and covers 50 per cent of the active flood plain. GSC 2-27-77.

Acknowledgments

The field assistance of R. McKercher, S. Miller, and M. Monteith is gratefully acknowledged. Thanks are extended to T.J. Day and L.A. Dredge for their comments on the paper.

References

Egginton, P.A.
1976: Hydraulic and morphologic studies of selected bridge crossing sites along the proposed Mackenzie Highway; in Report of Activities, Part A; Geol. Surv. Can., Paper 76-1A, p. 229-231.

Egginton, P.A. and Day, T.J.
1976: Channel instability studies, District of Mackenzie, Northwest Territories; in Report of Activities, Part C; Geol. Surv. Can., Paper 76-1C, p. 207-213.

Egginton, P.A. and Day, T.J. (cont.)
1977: Dendrochronologic investigations of Hodgson Creek highwater events, District of Mackenzie; in Report of Activities, Part A; Geol. Surv. Can., Paper 77-1A, p. 381-384.

Jasper, J. and Anderson J.
1977: An assessment of hydraulic design at stream crossings on Mackenzie Highway; rep. to Hydraulic Design Assessment Committee, Environ. Working Group, Mackenzie Highway, Dep. Indian Affairs Nor. Der., 75 p.

AN APPARATUS FOR THE MEASUREMENT OF RIVER STAGE

P.A. Egginton
Terrain Sciences Division

To facilitate stream gauging in remote areas where air or general transportation is limited, several low cost (less than $30 each), light weight, portable plexiglass stage recorders, suitable for carrying in back packs, were constructed.

Each stage recorder consists of a plexiglass stilling well, floats, two float runners, an input tube, and a plywood base (Fig. 1). The basic frame is a 0.5 cm thick, 7.5 cm I.D. plexiglass tube, 1.25 m in length. Each float consists of two lengths of thin walled plexiglass tubing, one 2.5 cm in diameter and the other 1.25 cm in diameter. They are sealed at both ends, one inside the other.

The floats and float runners are critical to the operation of the apparatus. A sketch enlargement of the minimum water level recorder (Fig. 1) shows that the float slides on an aluminum rod cut with a buttress thread (15.7 threads to the centimetre). The stainless steel spring permits the float to slide freely down the rod in response to water level decline; however, when the water level rises, the spring jams against the thread and the minimum stage is recorded. The maximum water level recorder differs from the minimum recorder only in that the float runner and float are inverted in the stilling well. Stage is read relative to a scale mounted on the outside of the well.

Installation and Operation

The upstream end of the input tube is covered by a porous cloth and is buried by boulders in a small depression in the stream bed less than 10 m from the instrument (Fig. 2). The distance is not critical, but it should be small enough to prevent the formation of air bubbles within the tube and should be large enough to ensure adequate head and water levels in the recorder. Higher water levels are read more easily and comfortably. Rocks are placed on the plywood base to support the recorder and small guy ropes may be used. In certain cases it may be desirable to set up the recorder outside of the stream bed.

Evaluation

Stage readings are accurate to the nearest 0.6 mm (the thread spacing on the float runner). The recorder functions well even when stream depth is less than 3 cm. The recorder proved very useful on streams where only maximum and minimum stage records were required. The major benefits of the apparatus are its portability, accuracy, and low cost. Its major drawback is that the instrument is not automatic and requires manual resetting of the maximum and minimum floats.

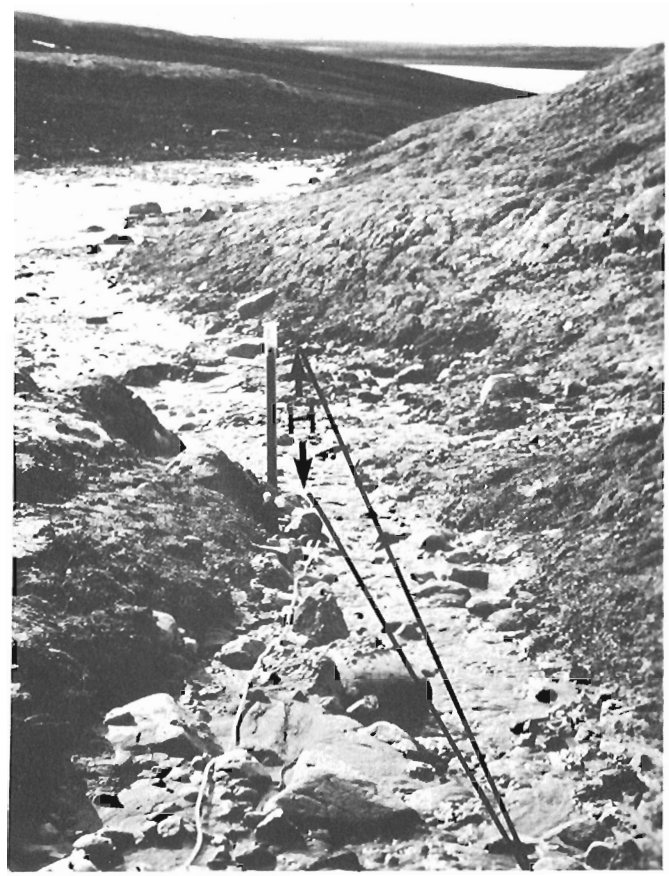

Figure 2. The maximum-minimum water level recorder installed on a steep stream. Note the location of the open end of the input tube some 7 m upstream from the recorder. The input tube is positioned to ensure adequate head (H) in the well. GSC 203165-F.

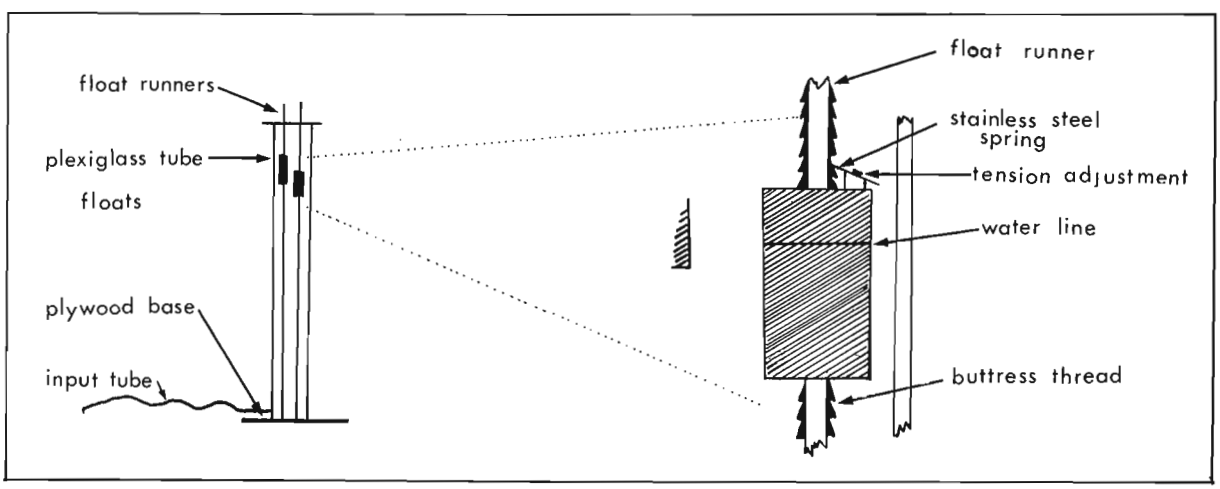

Figure 1. Line diagram illustrating the maximum-minimum stage recorder. The enlargement shows the minimum water lever recorder.

From: Scientific and Technical Notes in Current Research, Part A; Geol. Surv. Can., Paper 78-1A.

RECONNAISSANCE PALEOMAGNETISM OF THE ORDOVICIAN ROBERTS ARM GROUP VOLCANICS, NEWFOUNDLAND

E.J. Schwarz and H.H. Bostock
Regional and Economic Geology Division

Introduction

Oriented drill cores (5 or 6) were collected at each of 29 sites in the Roberts Arm Group basic volcanics, and used for paleomagnetic investigation. The Roberts Arm Group occurs essentially in two steeply dipping fault blocks (Bostock, 1976). The objectives of this study were to correlate between the blocks using magnetostratigraphy and to derive a pole position for comparison with pole positions obtained by others (e.g. Deutsch and Rao, 1977) for lower Paleozoic rocks from eastern Canada.

The southern fault block consists of a northwest-facing homocline of basic pillow lavas, large lenses of pillow breccia, some chert and greywacke interbeds, and small, probably synvolcanic intrusive gabbroic bodies (Fig. 1). It is separated from the northern block by a northeast-trending fault of unknown displacement. The northern block is of similar lithology and structure but also includes a granitic pluton, the Sunday Cove granite, which is intrusive into pillow lavas and is thought to have been the source of felsic lavas and breccias which form volcanic centres in the upper part of this block. Opaque grains in these volcanics are commonly altered to leucoxene-like material but scattered magnetite grains are also observed (up to 0.2 mm). The general geology and location of most sampling sites are indicated on Figure 1.

Remanent Magnetization

Two cylindrical specimens were cut from each of the 5 or 6 cores collected at each site. Determination of the Natural Remanent Magnetization (NRM) showed that the within-core and within-site agreement in intensity is good but varies greatly from site to site (10^{-3} to 10^{-7} emu/g). Within-core directions, however, differ by an average of 20°, and the within-site scatter was large for all but a few sites.

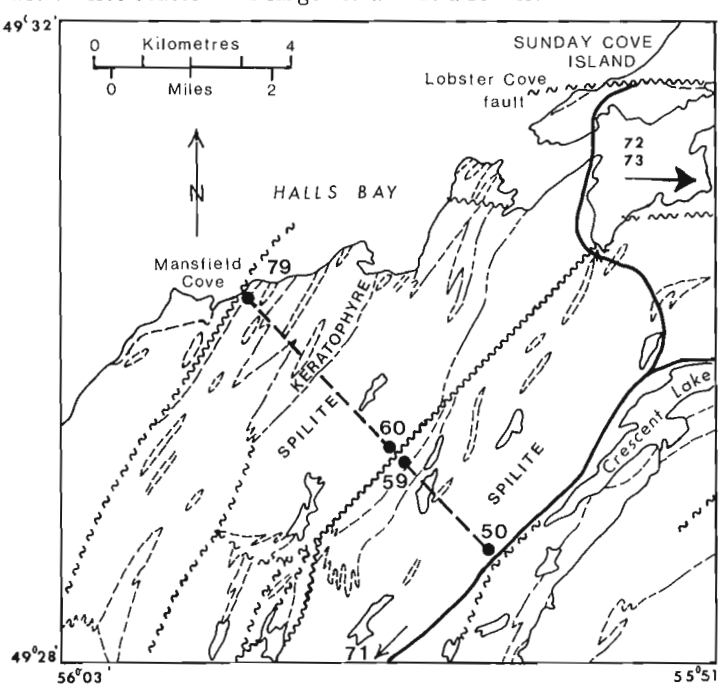

Figure 1. Geological map showing the section sampled within the Roberts Arm Group (modified from Bostock, 1976). Sample sites are indicated.

The stability of the NRM was tested by partially demagnetizing two specimens from each site in alternating magnetic fields (AF) of stepwise increasing intensity up to 500 oe. The intensity decay curves (Fig. 2A) suggest good stability for some samples over the whole coercivity range affected by the treatment (e.g. 72-2, 68-2) while others (e.g. 59-2, 55-2) showed the presence of large low coercivity components. The direction of many specimens turned away from the present local field direction indicating the removal of a recently acquired component (e.g. 77-2, 63-6 on Fig. 2B). However, a substantial number of specimens were not significantly affected by the AF treatment, and the angle between the two

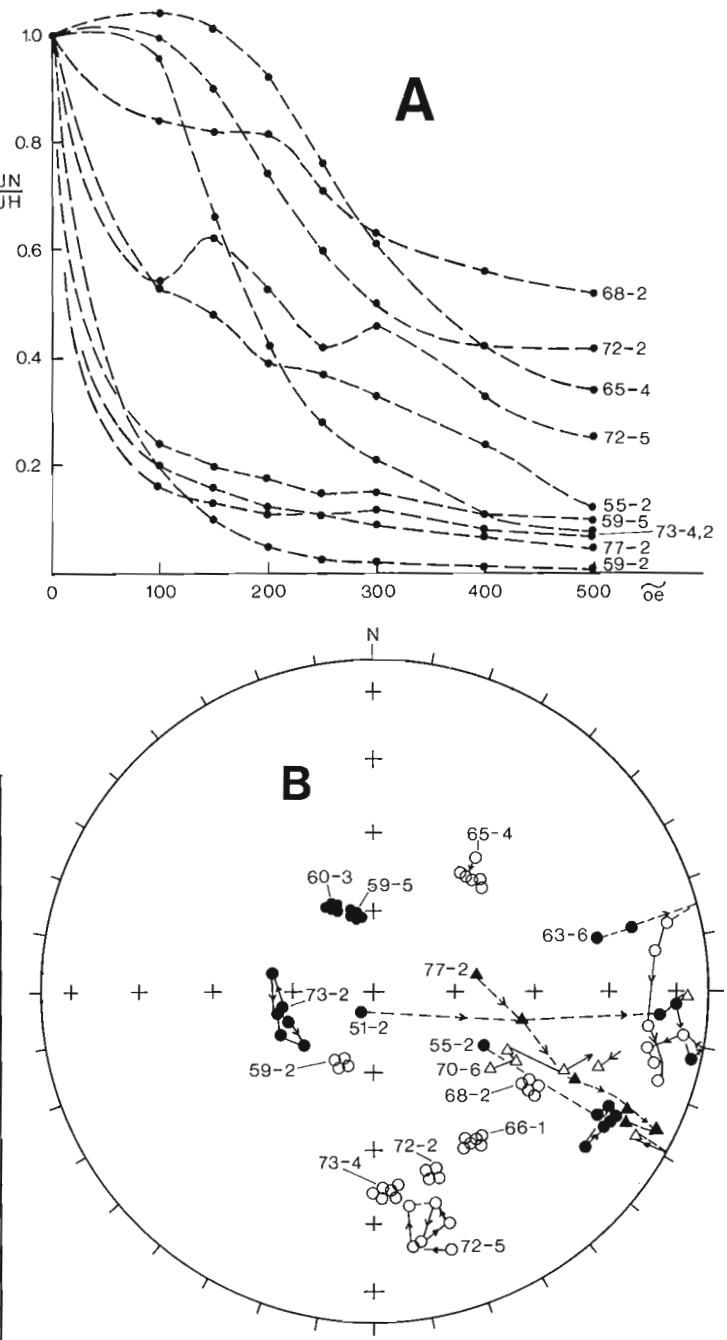

Figure 2. Effect of AF treatment up to 500 oe (100, 150, 200, 250, 300, 400, 500) on intensity (A) and direction (B) of magnetization of test specimens. The numbers indicate site followed by core number. Open circles and dots indicate respectively upward and downward north-seeking directions. Equal area stereographic projection.

From: Scientific and Technical Notes in Current Research, Part A; Geol. Surv. Can., Paper 78-1A.

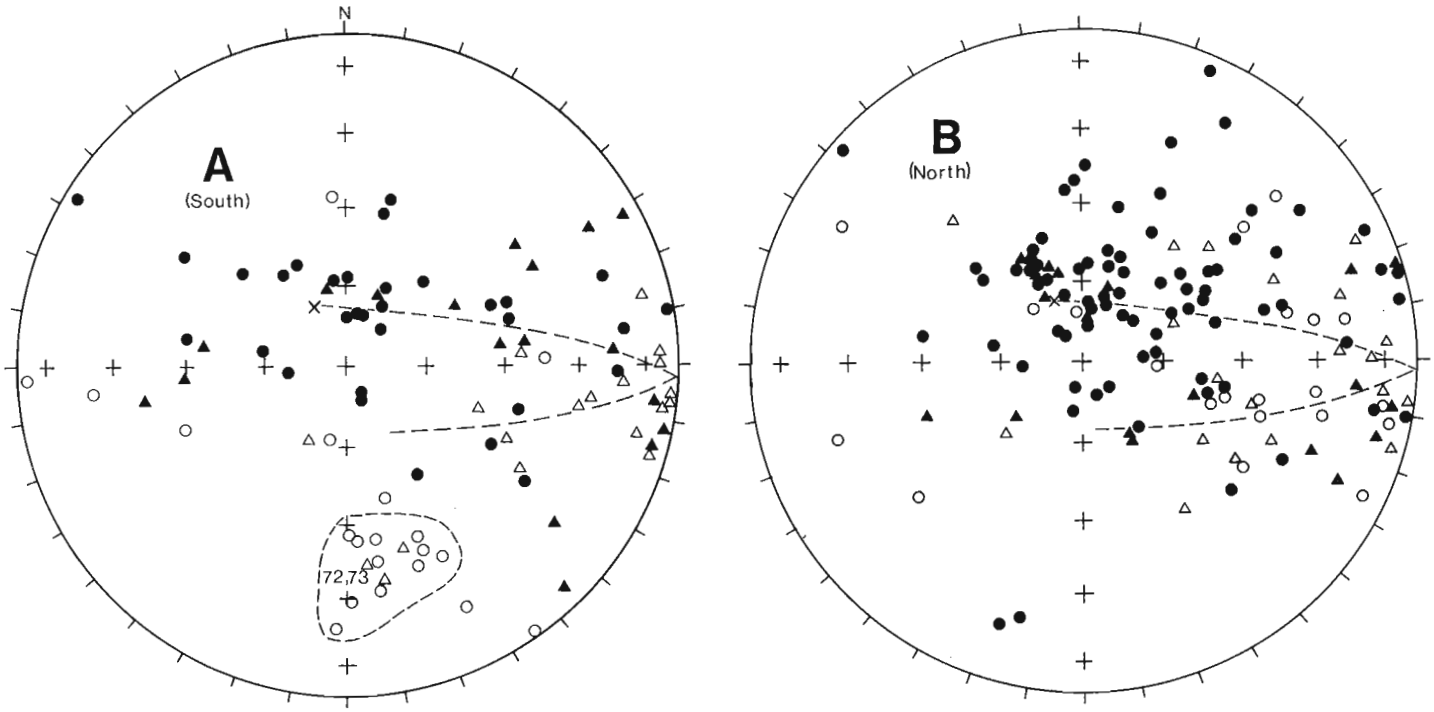

Figure 3. Specimen directions for the South block (A) and the North block (B). Triangles and circles indicate respectively directions after 200 and 300 oe demagnetization. Open and closed symbols indicate respectively north-seeking directions in the upper and lower hemispheres. The dashed line indicates the approximate great circle path along which magnetic directions tend to rotate away from the present local geomagnetic field direction indicated by x.

test specimens did not decrease (e.g. 59-2, 59-5, 72-2, 73-4 on Fig. 2B). This observation and the very high within-core and within-site scatter render the results (with possible exception of 59 and 72) unacceptable for detailed paleomagnetic analysis. For this reason, all other specimens were treated in fields of 200, 250, and 300 oe, and the individual specimen directions were plotted in Figure 3A and B to see if the data allowed a qualitative interpretation.

The data for both the South fault block (Fig. 3A) and the North block (Fig. 3B) suggest the presence of two components (1) North-down in the approximate direction of the local field, and (2) east-southeast-up. In addition the relatively coherent sites, 72 and 73, collected in the village of Roberts Arm (2 miles east of the map-area, Fig. 1) show a concentration of directions toward south-southeast and up. Flows at these sites strike 090 and dip 85 degrees south whereas those along the sample section strike 045 and dip mostly about 75 degrees southeast through both fault blocks. Consequently, this south-southeast-up direction can be brought into coincidence with the east-southeast direction by unfolding (rotation around strike). This implies that the east-southeast-up direction is older than the folding (probably Acadian). Correction for the tilt of the blocks yields a general east-southeast-down (~30°) direction if the low inclinations are regarded as hybrids containing an appreciable young component directed north-downwards, resulting in a markedly streaked distribution. The general east-southeast-down direction is similar to the well-defined directions listed by Deutsch and Rao (1977) for nearby volcanics and sediments of early Paleozoic age.

References

Bostock, H.H.

1976: Volcanic rocks of the Appalachian Province: Roberts Arm Group, Newfoundland (2E and 12H); in Report of Activities, Part A, Geol. Surv. Can., Paper 76-1A, p. 173-175.

Deutsch, E.R. and Rao, K.V.

1977: New paleomagnetic evidence fails to support rotation of western Newfoundland; Nature v. 266, p. 314-318.

OCCURRENCES OF DISRUPTED BEDROCK ON THE GOULBURN GROUP, EASTERN DISTRICT OF MACKENZIE

R.N.W. DiLabio
Terrain Sciences Division

Reconnaissance flights in a fixed-wing aircraft were made in late July 1977 to observe the surficial geology of NTS map-areas 76 E, F, G, J, K, L, 86 H, and I. Areas of highly disrupted bedrock were noted in the southwestern part of the Tinney Hills map-area (Fig. 1). Such disruptions have been noted elsewhere on the perennially frozen parts of the Canadian Shield and constitute one style of bedrock heaving that could be a hazard to general or pipeline construction.

The most common types of disruptions are crater-like depressions, 1 to 6 m in diameter, with elevated rubble rims (Fig. 3). Most craters occur on glacial erratic-littered bedrock surfaces, but a few occur on bedrock surfaces in the shallows of small lakes. Pervasively fractured bedrock (Fig. 4) is an associated feature in places. The fractures resemble frost cracks, but they may mimic jointing.

The disruptions observed in 1977 occur on gently dipping beds of the Burnside River and Quadyuk formations of the Goulburn Group (Fig. 1). The rock types that could be involved are quartzite, subarkose, quartz-pebble conglomerate, arenaceous dolostone, doloarenite, stromatolitic carbonates, and clastic carbonates (Campbell and Cecile, 1976), but it is not known if the disruptions are restricted to certain of the rock types. Similar occurrences of craters have been observed in the District of Keewatin by Shilts et al. (1976) on vertically dipping quartzites of the Hurwitz Group near Carr Lake (Fig. 5). F.W. Chandler (pers. comm., 1977) observed conical heaves of horizontally sheeted granitic rocks (Fig. 6) near McQuoid Lake, District of Keewatin.

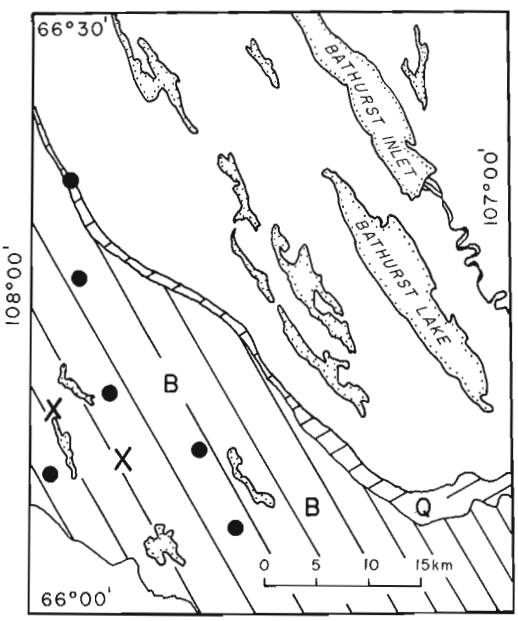

Figure 1.
Location map showing areas of disrupted bedrock in the southwestern part of the Tinney Hills map-area (76 J). Black circle = area of craters, X = area of fractured bedrock. Areas B and Q are underlain by Burnside River and Quadyuk formations (Campbell and Cecile, 1976).

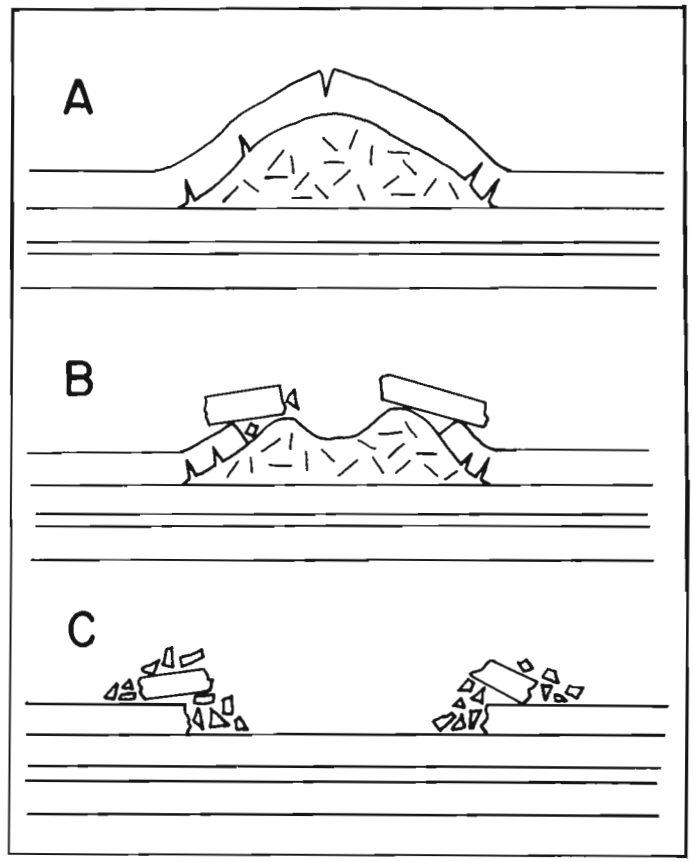

Figure 2. Schematic diagram of the development and collapse of a heave in bedrock. Diagram A shows heaving and fracturing of a bedrock slab pushed up by an ice lens. Diagram B shows melting of the ice lens after fracturing and sliding of the heaved slab. Diagram C shows central crater surrounded by a rim of rubble produced by sliding and subsidence of the broken rock.

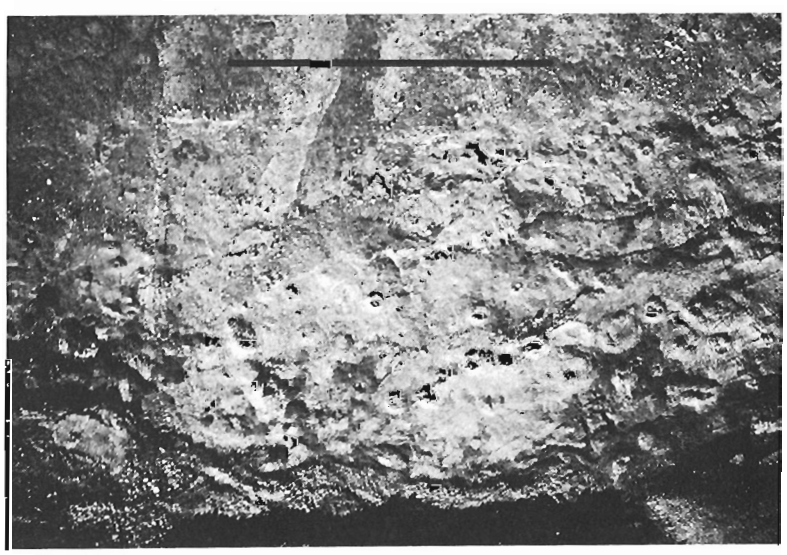

Figure 3. High-angle aerial view of craters on Burnside River Formation rocks. Most have collapsed to form rimmed craters, but a few show conical shapes. Scale bar is about 50 m long. (GSC 203266-B)

From: Scientific and Technical Notes in Current Research, Part A; Geol. Surv. Can., Paper 78-1A.

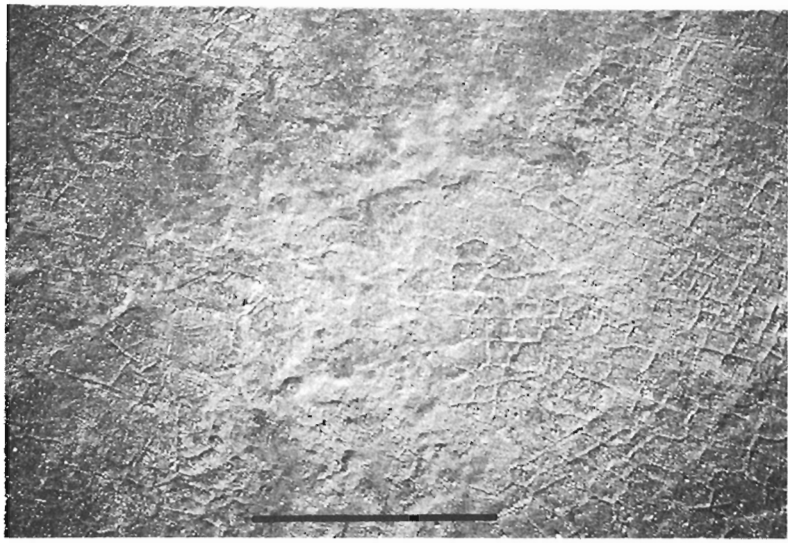

Figure 4. High-angle aerial view of fractured Burnside River Formation rocks. Scale bar is about 50 m long. (GSC 203266)

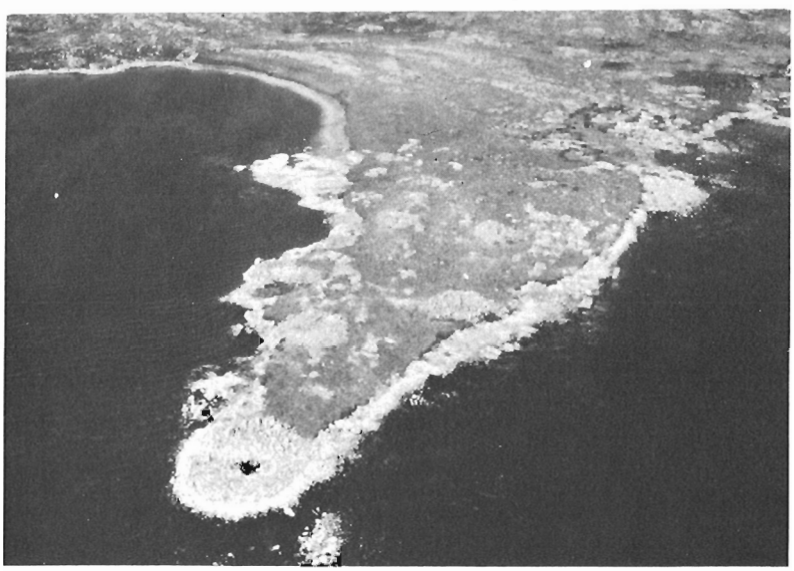

Figure 5. Low-angle aerial view of craters on Hurwitz Group quartzites near Carr Lake, eastern District of Keewatin. Field of view in centre of photo is about 100 m wide. (GSC 203266-D) Photo by W.W. Shilts.

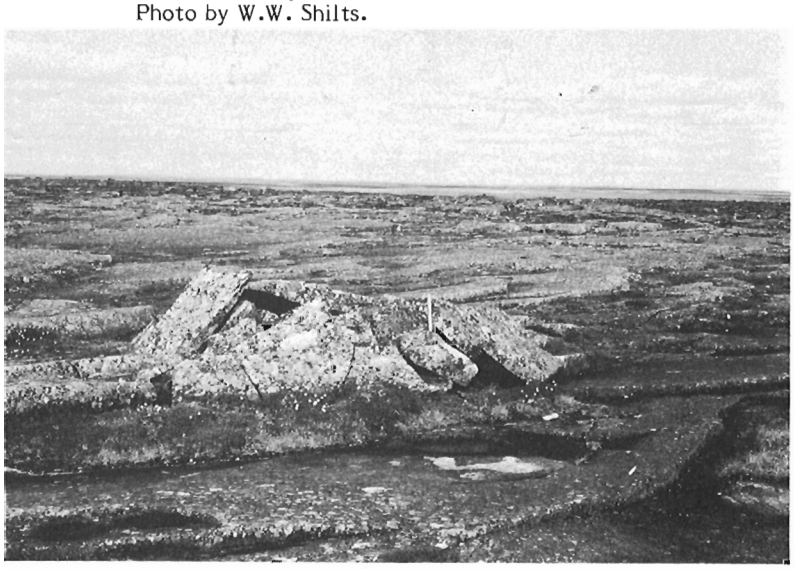

Figure 6. Conical heave of horizontally sheeted granitic rock near McQuoid Lake, eastern District of Keewatin. Hammer is 40 cm long. (GSC 203266-E) Photo by F.W. Chandler.

The craters in bedrock appear to occur preferentially on relatively thickly bedded or sheeted hard rocks, but it is not known why only small parts of the outcrop areas of bedded, hard rock units are susceptible to this type of failure. It is hypothesized that a crater develops by the formation of a conical heave of bedrock over an ice lens. Fracturing of the overlying rock creates slabs that slip to the base of the cone. Ultimately the ice lens is exposed and melts, forming a crater with an elevated rim of rubble heaved from the centre of the cone (Fig. 2). Such features are tentatively considered to be analogous to the open system type of pingos (Müller, 1959). The craters form as a result of frost heave caused by the development of ice lenses on bedding or sheeting planes. It is possible that local thermal and/or groundwater conditions govern their distribution.

References

Campbell, F.H.A. and Cecile, M.P.

1976: Geology of the Kilohigok Basin, Bathurst Inlet, N.W.T.; Geol. Surv. Can., Open File 332.

Müller, F.

1959: Observations on pingos; Nat. Res. Coun. Can., Tech. Transl. 1073, 117 p.

Shilts, W.W., Arsenault, L., and Kettles, I.M.

1976: Surficial geology, southeast Keewatin (NTS map-areas 55 E, F, L, 65 H); Geol. Surv. Can., Open File 356, expanded legend.

QUALITATIVE RATES OF FROST HEAVING IN GNEISSIC BEDROCK ON SOUTHEASTERN BAFFIN ISLAND, DISTRICT OF FRANKLIN

A.S. Dyke
Terrain Sciences Division

There are at least two approaches to the problem of establishing rates of frost heaving: (1) the study of active processes – e.g., detailed levelling and relevelling of a number of small study sites to measure short term rates of movement of bedrock blocks, and (2) the morphostratigraphic approach, by which a statistical study is made of the amounts of block displacement on a number of morphologic units of known age. Both are probably necessary and fruitful. The purpose of this note is to point out the potential of using the stratigraphic method, to suggest a rough research design, and to warn against possible misinterpretations of data collected from areas (such as the Arctic Islands pipeline route) where the stratigraphic framework has not been deciphered.

Table 1

Summary of the weathering properties of the morphostratigraphic units in the Clearwater Fiord/western Penny Ice Cap area

Morphostratigraphic Unit	Age (years)	Weathering
Inner Penny moraine	400	Glacial polish and striae well preserved. Surface of boulders and bedrock incompletely oxidized.
Outer Penny moraine	4500	Glacial polish and striae well preserved. Minor frost heaving. Complete oxidation and vegetation cover.
Ranger moraine	8700	Minor frost heaving. Glacial grooves common but most polish and striae destroyed.
Pre-Ranger terrain	20 000 40 000	Felsenmeer. Few macropits ≤10 cm deep. Glacial polish and striae destroyed. Few grooves remaining.

Rupturing and dislocation of bedrock masses by frost heaving is a type of weathering. Quaternary stratigraphers have used data on differential surface rock weathering as a means of relative age-dating morphostratigraphic units in many areas of the world. The writer has used this technique in studying the surficial geology and glacial chronology of southwestern Cumberland Peninsula, Baffin Island (Dyke, 1977). The rationale is as follows: degree of weathering, just as degree of soil development, is a function of climate, parent material (structure, lithology), topography (drainage), organisms, and time. If sites are selected in such a way that the first four variables are held roughly constant, then degree of weathering is a function of the length of time that the parent material, be it a bedrock outcrop or till clast, has been exposed to the weathering processes.

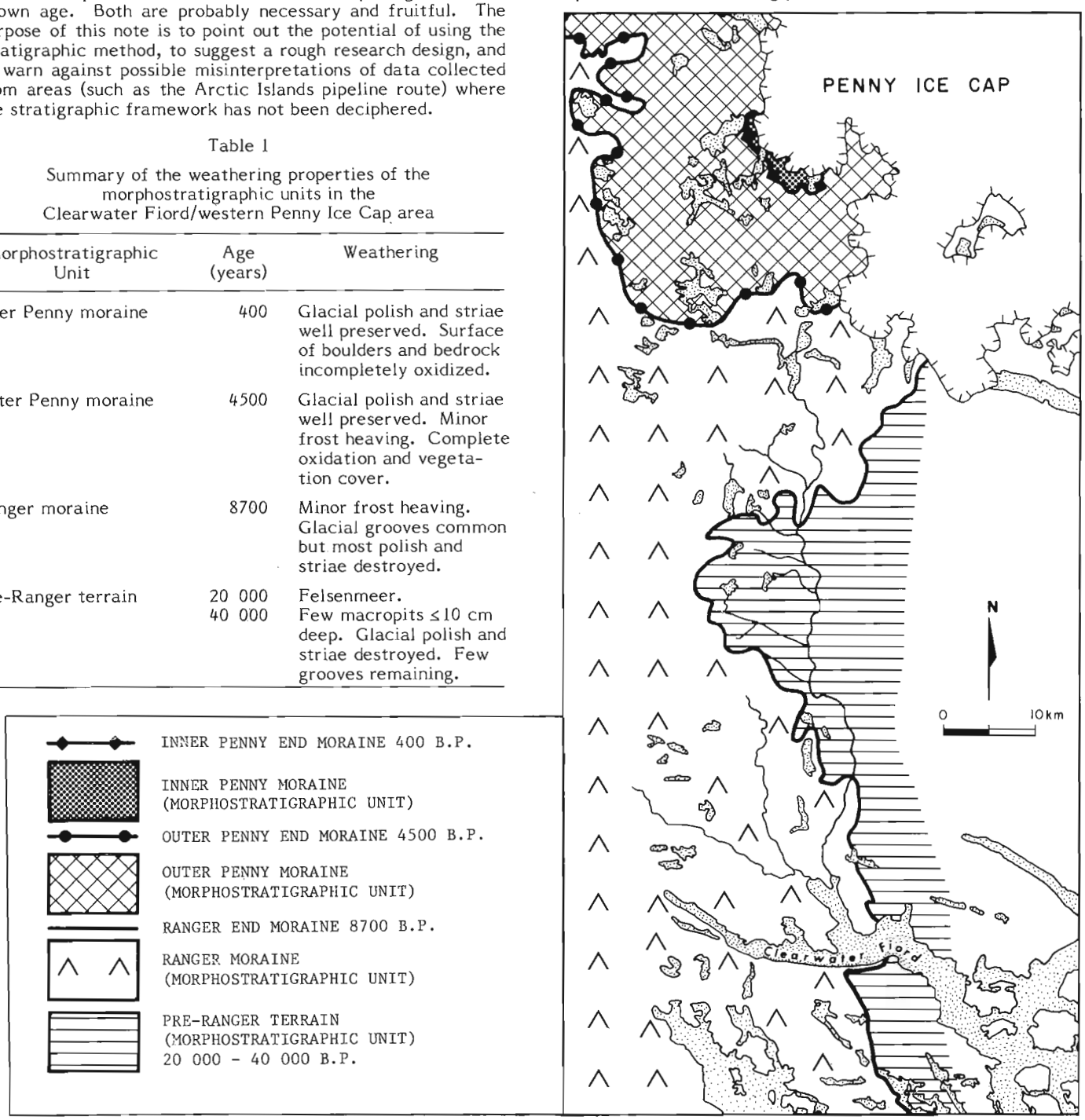

Figure 1. A map of morphostratigraphic units and the major end moraines marking their boundaries in the Clearwater Fiord/western Penny Ice Cap area, Baffin Island, Northwest Territories. Ages and weathering properties of the units are given in Table 2.

From: Scientific and Technical Notes in Current Research, Part A; Geol. Surv. Can., Paper 78-1A.

Table 2

Qualitative granitic gneiss weathering rates on southwestern Cumberland Peninsula
(B, A5, etc. are weathering zone designations)

Weathering Zone and Duration of Weathering	Amount of Weathering Accomplished
A1 — 500 y	Partial surface oxidation.
A2 — 4-5000 y	Complete surface oxidation.
A3 — 8-9000 y	Minor surface crystal removal as indicated by destruction of striae and polish. Minor disruption by frost heaving.
A4 — 20-40 000 y	Sufficient crystal removal to destroy almost all striae and grooves. Either major disruption by frost heaving or felsenmeer cover. First appearance of macropits and surface grusification of bedrock.
A5 — 60 000 y	Increased frequency of macropits and more common surface grusification of bedrock.
B — >100 000 y	Sufficient denudation to produce tors. Extensive grusification of bedrock and boulders. Frequent occurrence of macropits.

One of the most conspicuous differences between juxtaposed morphostratigraphic units on Baffin Island lies in the varying degrees of frost rupturing and dislocation of bedrock. Figure 1 shows four morphostratigraphic units in the area between the western lobe of the Penny Ice Cap and the head of Cumberland Sound. Contacts between the units are defined by major end moraines, and units are named after the moraines that form their boundaries.

Table 1 summarizes the weathering properties of each unit shown on the map, and they are discussed below in order of age. Methods of assigning absolute ages are discussed in Dyke (1977). The Inner Penny end moraine lies only 3 km from the active margin of the ice cap. Ice retreated from the moraine about 400 years ago, so bedrock behind it has been exposed to subaerial weathering for less than 400 years. Most outcrops are glacially polished and finely striated and show no sign of dislocation due to frost heaving.

Ice retreated from the Outer Penny end moraine about 4500 years ago. Polish and striae are well preserved on most outcrops. Most outcrops have not been disturbed by frost heaving; those that have, show dislocations of only a few centimetres.

Ice recession from the Ranger end moraine commenced 8700 years ago. There is a striking increase in the amount of bedrock disruption behind this moraine as compared to the younger unit mentioned above, but the glacially moulded surface, displaying grooves and more rarely striae, is still easily recognized.

Terrain beyond the Ranger end moraine has been exposed to subaerial weathering for some 20 000 to 40 000 years. There the original glacially moulded bedrock surface rarely is preserved. On the contrary, bedrock blocks commonly exhibit 1 m or more of dislocation by frost heaving, or the whole bedrock surface is mantled by felsenmeer.

Similar differences in weathering between morphostratigraphic units were observed in other parts of the study area. These observations are summarized in Table 2 which gives qualitative rates of weathering of granitic gneiss. It is concluded that 5000 to 10 000 years are required to produce minor disruption of gneissic bedrock terrain, and 20 000 years or more are required to produce felsenmeer in this area.

The purpose of the work described above was merely to determine whether weathering differences existed between the various morphostratigraphic units. Hence, little effort was made to collect quantitative data. It is obvious, however, that areas that have a variety of ages of terrain are well suited to the study of weathering rates. The quantification of frost heaving simply requires study sites within each morphostratigraphic unit where various parameters can be measured (e.g. amount of upthrust of blocks relative to adjacent in situ glacially planed surfaces, percentage of joint blocks exhibiting displacement, etc.). As the duration of weathering is relatively well known, the time control is provided.

Whereas, regional stratigraphies can provide the basic framework for design of field research, studies that are done without knowledge of the local Quaternary stratigraphy or in areas where the stratigraphic framework has not been deciphered, may lead to erroneous interpretations. The most obvious danger is that of interpreting older terrains (those much disturbed by frost heaving) as being relatively more sensitive to the process than adjacent younger terrains.

Reference

Dyke, A.S.
1977: Quaternary geomorphology, glacial chronology, and climatic and sea-level history of southwestern Cumberland Peninsula, Baffin Island, Northwest Territories, Canada; unpubl. Ph.D. thesis, University of Colorado, Boulder, 184 p.

BEDFORM MOVEMENT STUDIES BY REMOTE SENSING BALLOON TECHNIQUE IN MINAS BASIN, BAY OF FUNDY

Bernard F. Long and J.R. Belanger[1]
Atlantic Geoscience Centre, Dartmouth

Introduction

Studies to determine the sediment transport rates in the intertidal and subtidal zones are in progress in the Minas Basin, Nova Scotia (Fig. 1). The hydrodynamic, morphologic, and sedimentary factors are being evaluated in this macrotidal environment. Long (1977) attempted to determine sand transport rates and directions using a radioactive tracer. His results, however, indicated that it is necessary to distinguish between bedload transport and bedform movement. These two movements are largely due to two different hydrodynamic parameters: waves and tidal currents (Long, in prep.). This interaction of processes produces a rapid variation of sand bar topography which is illustrated by the burying of a current meter stand by 40 cm of sediment between October 27 and November 12, 1976 (Figs. 2a, b). The sand bar morphology evolved from a planar surface, with no ripples in October 1976 (Fig. 3a) to small megaripples in April 1977 (Fig. 3b) and finally, to very high megaripples (amplitude = 1 m, wavelength = 3 m) in June 1977 (Figs. 3c, d).

The aim of the present project is to test a new method of relating bedform movement and hydrodynamic conditions. The method consists of correlating measured tidal currents with daily air photo coverage of bedform movements obtained from a camera suspended under a tethered tropospheric balloon. In the next phase of the program (October and November 1977), a systematic daily air photograph survey of the sand bar is planned to obtain quantitative estimates on the bedform movement.

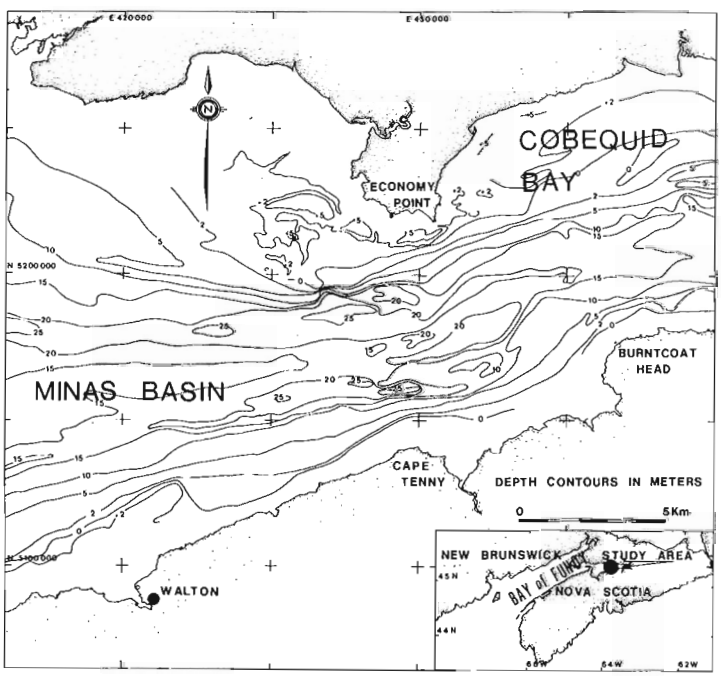

Figure 1. Bathymetry of study area in Minas Basin. The experiment site is located adjacent to Economy Point in the intertidal area.

Study Area

The study area is the intertidal flats south of Economy Point (Fig. 1), at the juncture of the Minas Basin and the Cobequid Bay. In this area the tidal range of the Bay of Fundy is amplified by resonance. The maximum spring range is 17.7 m (Canadian Hydrographic Service, 1966). The Minas Basin is 77 km long and up to 31 km wide (Pelletier and McMullen, 1972). However, the marine passage between Minas Basin and Cobequid Bay to the south of Economy Point is only 8.25 km wide. The intertidal zone in this area is 1.25 km wide on the north shore (Economy Point) and 0.75 km on the south shore (Cape Tenny). The perimeter is bordered by friable Triassic sandstone cliffs which are eroding at a rate of 0.5 m/year (Amos and Joice, 1977).

Along the south shore the thickness of sediment in the intertidal zone is minimal (Atlantic Tidal Power Programming Board, written comm., 1969), but on the north shore a large sand bar complex up to 5 m thick is present between the cliff and the 10 m isobath. Three different generations of bedforms are developed on the surface of this sand bar complex: ripples, dunes or megaripples, and sand waves (Klein, 1970). Klein (1970) measured mean bedform movement rates of 0.25 m/tidal day, and Dalrymple (1977) measured rates of 0.2 m/tidal cycle (0.4 m/tidal day) during neap tide and 1.2 m/tidal cycle (2.4 m/tidal day) during spring tide. Each of these measurements are at only one location. The major goal of this study is to consider changes over the entire Economy Point sand bar system by using a remote sensing balloon.

Equipment

The equipment is composed of two major parts:

- the camera and accessories
- the balloon and logistic equipment

The camera is a motorized 70 mm Hasselbad type 500 EL/M. A 50 mm wide angle lens covers a ground area of 90 000 m^2 from an altitude of 300 m. For the best resolution with precision to 10 cm on the sand bar, a balloon altitude of 150 m is recommended. KODAK Plus X (ASA 125) Black and White film was used. The camera is centred above fixed marks and a radio-linked remote system controlled the shutter. The camera is placed inside a protective box and suspended 15 m below the tropospheric balloon. The balloon, which has a volume of 12 m^3, is manufactured by ZODIAC ESPACE and is inflated with helium gas (Fig. 4) to a pressure suitable to the wind conditions. If the connection line breaks, a security valve, fixed on the front part of the balloon (Fig. 5b) automatically opens. The 1000 m connecting line is made of high strength (330 kgf), low density (2 g/m) "Kevlar" cable. The cable is fixed to a winch mounted on an all terrain vehicle, type A.T.V. ARGO (Figs. 5a and b) which moves the system on the sand bar.

It is possible to photograph a 1200 m by 600 m area with this equipment in one hour. Each of the 36 square frames covers an area of 1300 m^2. There is a 50 per cent overlap between images. If the overlap were only 30 per cent, the area photographed can be increased to 1900 m with a ground resolution of 0.2 m. A movable ground scale consisting of two black and white planks (0.5 m on side) connected by 5 m of cable (one scale of 6 m) provides ground control for each image.

For a better resolution during the next phase of the project, KODAK AERO Color Negative No. 2445 will be used.

[1] Atlantic Oceanographic Laboratory, Department of Fisheries and the Environment, Dartmouth.

From: Scientific and Technical Notes in Current Research, Part A; Geol. Surv. Can., Paper 78-1A.

Figure 2a.

Figure 2b.

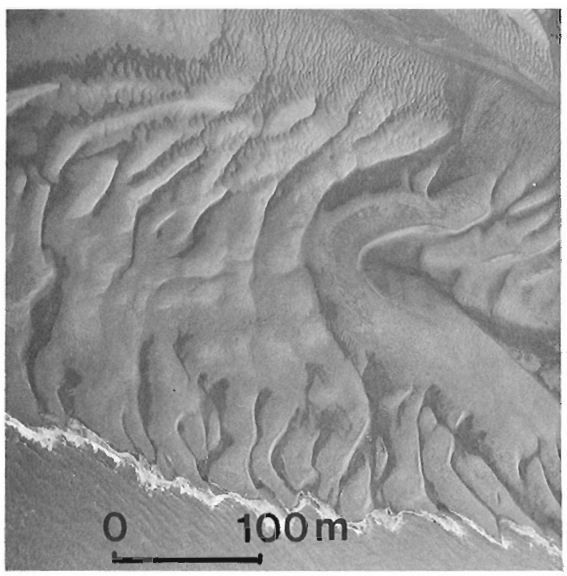

Figure 3a.

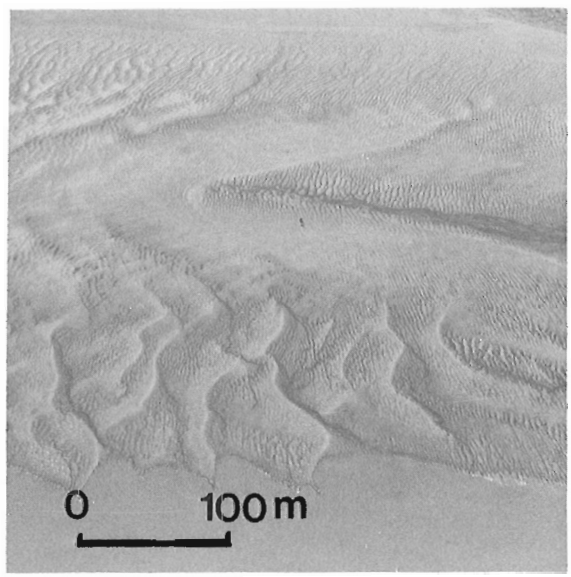

Figure 3b.

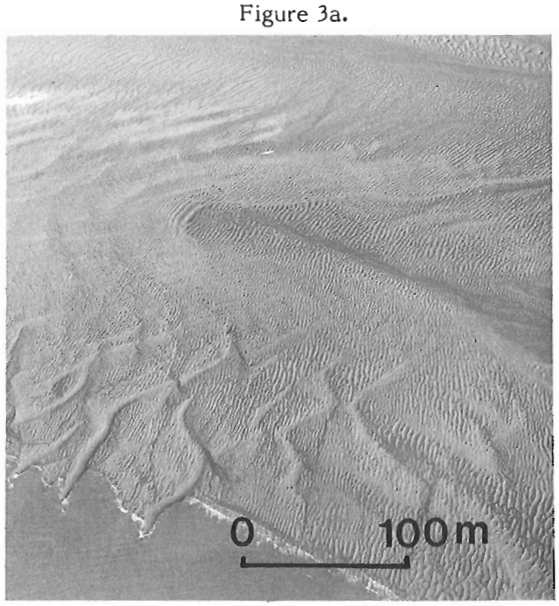

Figure 3c.

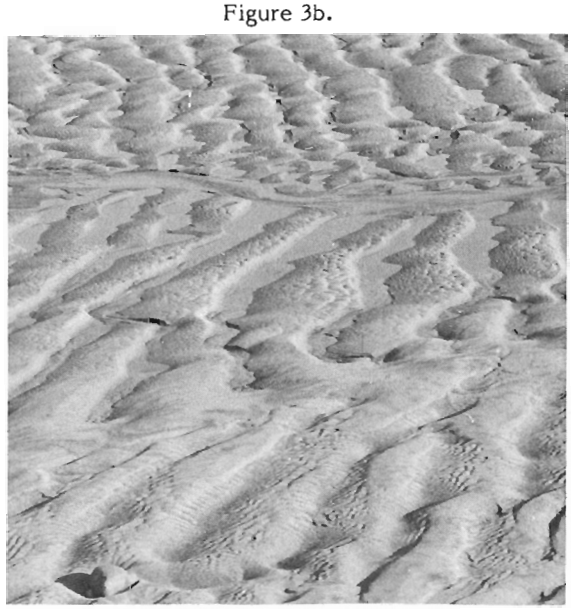

Figure 3d.

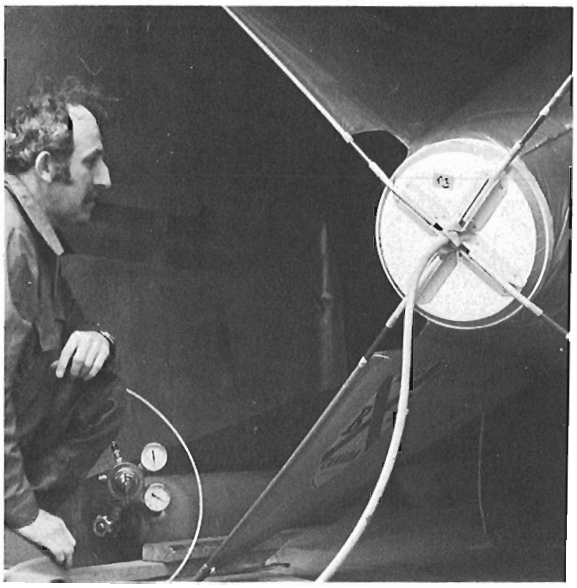

Figure 4. The tropospheric balloon is inflated with helium gas. The operator controls the helium pressure in the balloon (BIO 4421-02).

Figure 5a. Remote sensing balloon before the operation. The camera, supported by an operator, (1) is fixed on the tropospheric balloon. A winch (2) is on the ATV (BIO 4421-08).

Figures 2a and b (top left)

Variation of the topography and the morphology of the sand bar between October 27 (Fig. 2a, BIO 4129-02) and November 12, 1976 (Fig. 2b, BIO 415039). During this period 40 cm of sediment were deposited.

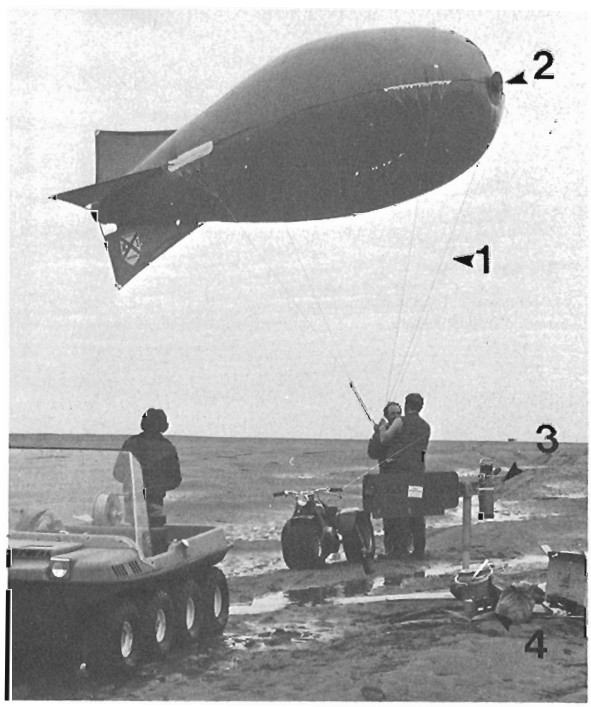

Figure 5b. Remote sensing balloon after the survey. The operators disconnect a security line (1). The security valve is on the front part of the balloon (2). In the foreground an Anderra current meter is fixed on a support (3). The camera (4) is in the protection box (BIO 4421-27).

Figures 3a to d (lower left)

a. October 27, 1976 – A system of large sand waves covers the sand bar (BIO 415021).

b. April 15, 1977 – A system of small megaripples is superimposed on a system of large sand waves (BIO 4386-03).

c. June 1, 1977 – A system of large megaripples is superimposed on a system of small sand waves (BIO 4444-03).

d. June 1, 1977 – Detail of megaripples. A boulder situated at the left and bottom part of the photo is 1 m wide (BIO 4444-24).

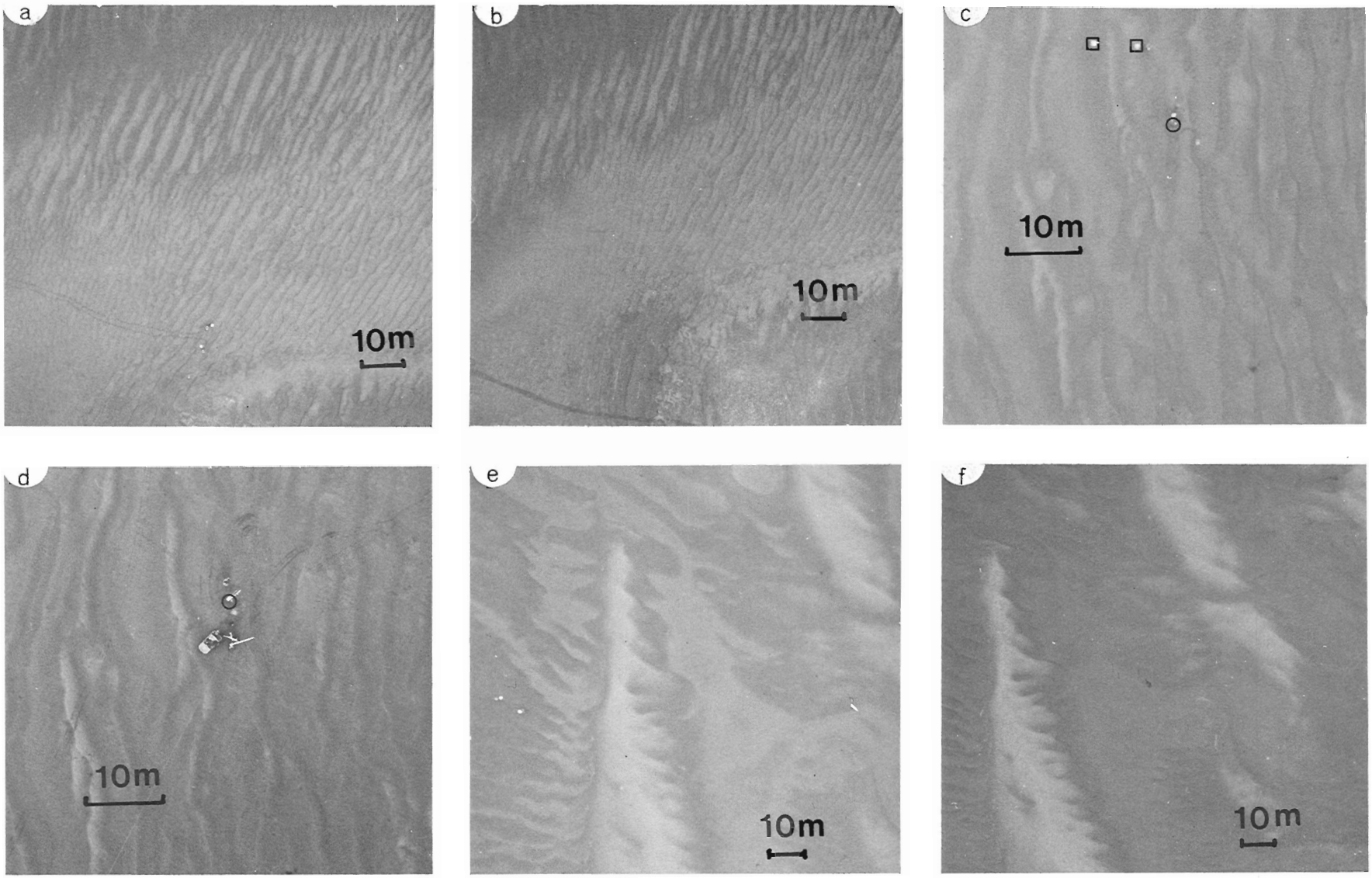

a. Site A, May 15 (BIO 4419-09).

b. Site A, May 16 (BIO 4420-18).

c. Site B, May 15. The current meter support is in the circle; the scale is given by the two white squares (BIO 4419-22).

d. Site B, May 16. The current meter support in the circle (BIO 4420-53).

e. Site C, May 15 (BIO 4419-02).

f. Site C, May 16 (BIO 4420-22).

Figure 6. Results of remote sensing balloon test — for all photos the north is at the top.

Table 1

Wavelength measurements between peak amplitudes at Station A

	May 15, 1977		May 16, 1977	
Location	Crest of sand bar (metres)	North of Crest (metres)	Crest of sand bar (metres)	North of Crest (metres)
bed-form	2.6	4.3	4.3	5.8
wavelengths	2.0	4.3	3.5	5.8
	2.0	4.6	4.7	5.8
	2.0	4.6	4.7	5.8
	2.6	5.3	3.5	7.0
	2.0	5.0	2.3	5.8
	1.3	3.0	2.3	6.5
	2.6	5.0	2.3	5.8
	2.0	5.0	1.9	7.0
	2.6	4.6	2.3	8.2
Wavelength Average	2.17m	4.57m	3.1m	6.35m

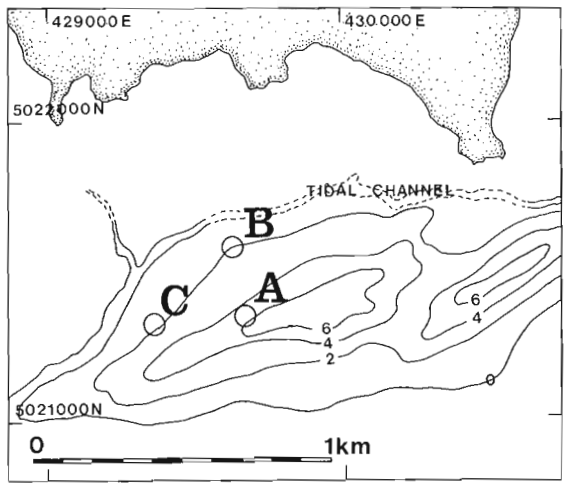

Figure 7. Location of the measurement sites on East Sand Bar of Economy Point. 0 is the low tide line. The contours above low tide are in metres (after Klein, 1970).

Table 2

Measurement of megaripple wavelengths and bedform migration rates at Station B. An error of ±0.2 mm of reading on the image is equal to ±0.15 m in the field. The reference point used for the determination of the bedform movement is the support of the current meter (Fig. 7c)

May 15, 1977		May 16, 1977		
Distance from Reference Point to Crest of Megaripples (metres)	Wavelength of Megaripples (metres)	Distance from Reference Point to Crest of Megaripples (metres)	Wavelength of Megaripples (metres)	Bedform Migration Rate (metres/day)
13.0 W		13.2 W		0.2
32.5 W	19.5	31.5 W	18.3	1.0
46.8 W	14.3	45.8 W	14.3	1.0
58.5 W	11.7	58.0 W	12.2	0.5
03.9 W	16.9	06.7 W	19.9	2.8
11.7 E	07.8	12.8 E	06.1	1.1
19.5 E	07.8	21.0 E	08.2	1.4
24.7 E	05.8	25.7 E	04.7	1.0
29.9 E	05.2	32.3 E	06.6	2.4
37.7 E	07.8	40.3 E	08.0	2.6
42.9 E	05.2	44.0 E	03.7	1.1
48.9 E	05.2	52.8 E	08.8	4.7
56.6 E	08.5	61.1 E	08.3	4.5
62.4 E	05.8			
68.9 E	06.5	69.3 E	08.2	0.4
75.4 E	06.5	77.0 E	07.7	1.6
80.6 E	05.2	82.5 E	05.5	1.9
85.8 E	05.2	88.0 E	05.5	2.2
91.0 E	05.2	93.5 E	05.5	2.5
	8.3±0.15		8.9±1.5	1.9±0.3 m/d

Table 3

Wavelength measurements at Station C

May 15, 1977		May 16, 1977	
Sand Wave	Megaripple	Sand Wave	Megaripple
116 m	4.6 m 5.4 m	117 m	4.5 m 7.6 m
121 m	6.6 m 5.0 m	120 m	6.0 m 3.0 m
	4.15 m 4.6 m		4.5 m 5.3 m
	4.6 m 4.15 m		3.8 m 3.8 m
	4.6 m 5.4 m		3.8 m 3.8 m
	4.15 m 4.6 m		3.0 m 3.8 m
	3.7 m 4.15 m		3.8 m 3.8 m
	5.0 m 3.3 m		3.8 m 4.0 m
	4.14 m 3.7 m		3.0 m 3.8 m
	5.4 m 4.7 m		3.6 m 3.8 m
Mean...118 m	.....4.5±0.15 m	.....118 m	.....4.1±0.15 m

Results

During the first study, two photo-surveys of the sand bar were obtained on May 15th and 16th. Three different sites were selected for analysis (Fig. 7) corresponding to three different levels of hydrodynamic energy. On each site the mean wavelength of the different bedforms was determined.

Site A (Figs. 6a, b and 7) is located on the crest of a sand bar in an area where the flood-tidal currents are dominant (Klein, 1970; Dalrymple, 1977). Two series of wavelength measurements were obtained from the photographs. The first was on the crest of the sand bar and the second at 100 m to the north of the crest on the slope. The results are tabulated in Table 1.

Site B (Figs. 6c,d and 7) is located on the north part of the sand bar near a tidal channel 300 m from site A. At this location, the resultant current vector is 5 km/d to the west (Long, in prep.) and the maximum current speed is 1 m/s during spring tide and 0.65 m/s during neap tide. Klein (1970) and Dalrymple (1977) show the dominance of ebb flow for this site. In this area an average measurement of bedform movement was determined to be 1.9 ± 0.3 m/d (see Table 2).

The third site, C (Figs. 6e, f and 7) is located on the west part of East Sand Bar. In this area, a parallel sand wave system (118 m mean wavelength) is superimposed on megaripples with a mean wavelength of 4 m (Figs. 6e, f). Table 3 contains the results of the wavelength measurements. No measurements of bedform migration rate are available from this site because the fixed points used during the survey were not detectable on the images.

Conclusion

In scientific terms, the experiment was not a complete success because bedform migration could be calculated only on one site. However, in technical terms the experiment was successful by demonstrating the feasibility of a remote-sensing balloon application for the study of bedform migration. In October-November 1977, the remote sensing experiment will be conducted in conjunction with radioactive tracer experiments and continuous recording current and meteorological meters. This multiparameter survey will provide complete documentation of the sediment movement on Economy Point sand bar.

References

Amos, C.L. and Joice, G.H.
1977: The sediment budget of the Minas Basin, Bay of Fundy, N.S.; Bedford Institute of Oceanography, Data Series Bi-D-77-3/June 1977.

Canadian Hydrographic Service
1966: Bay of Fundy, data report on tidal and current survey, 1965; Bedford Institute of Oceanography, Report Series/66-2-D, August 1966.

Dalrymple, R.W.
1977: Sediment dynamics of macrotidal sand bars, Bay of Fundy; Unpublished Ph.D. thesis, McMaster University.

Klein, G. de V.
1970: Depositional and dispersal dynamics of intertidal sand bars; J. Sed. Petrol., v. 40, p. 1095-1127.

Long, B.F.
1977: Determination of sediment transport rate in the Minas Basin, Nova Scotia: Preliminary results of the first tracer experiment using radioisotopes; in Report of Activities, Part B, Geol. Surv. Can., Paper 77-1B, p. 85-92.

Long, B.F.
Sediment transport in the intertidal area. Correlations between bedload movement and hydrodynamic factors. (in prep.)

Pelletier, B.R. and McMullen, R.M.
1972: Sedimentation patterns in the Bay of Fundy and Minas Basin; in Tidal Power, Ed. Gray, T.J., Gashus, O.K., Plenum Publishing Company, p. 153-187.

COMPILATION TECHNIQUES EMPLOYED IN CONSTRUCTING THE MAGNETIC ANOMALY MAP OF CANADA

P.H. McGrath, E.L. Haley, D.A. Reveler,
and C.P. Letourneau[1]
Resource Geophysics and Geochemistry Division

The Magnetic Anomaly Map of Canada (1255A) is one of a series of regional compilation maps published at the scale of 1:5 000 000 by the Geological Survey of Canada. It was first presented by L.W. Morley, A.S. MacLaren and B.W. Charbonneau at the Canadian Centennial Conference on Mining and Groundwater Geophysics at Niagara Falls during October, 1967, published in 1968, and updated in 1971 and 1977.

Source of Data

From 1948 to 1962 the Geological Survey of Canada flew, compiled and published aeromagnetic surveys at the scale of one mile to one inch. Photographic reductions to the four-mile scale of two degree east-west and one degree north-south compilations of the one-mile map sheets were also published (16 one-mile sheets per four-mile sheet). In 1959 the first contract was let to Spartan Air Services for complete outside production of aeromagnetic surveys. To date approximately 8250 one-mile map sheets have been published under the auspices of the Federal Government, and the Federal/Provincial Aeromagnetic Cost-Sharing Agreement which came into effect in 1962. From time to time the Geological Survey has also acquired existing data which were brought to Survey cartographic standards and published. Many individuals, in particular E.E. Ready and P.J. Hood, have made major contributions toward the acquisition and production of this material. Data were also given by Atlantic Richfield Company, Bethlehem Steel Company, Dominion Gulf Company, Imperial Oil Ltd., Mobil Oil Ltd. and the Newmount Mining Company. Sea magnetometer data in the southeastern Gulf of St. Lawrence, the Grand Banks of Newfoundland and the Scotian Shelf were contributed by the Geological Survey's Atlantic Geoscience Centre, Dartmouth, Nova Scotia. The aeromagnetic survey contractors involved in the approximately 9 million kilometres of flying and data compilation were Aero Photo Inc., Canadian Aero Services Ltd., Geoterrex Ltd., Hunting Survey Corporation, Lockwood Survey Corporation, Spartan Air Services Ltd., Spartan Aero Ltd., Kenting Earth Science, and Survair Ltd. The various individual aeromagnetic surveys employed in the compilation are shown in Figures 2. 3. and 4.

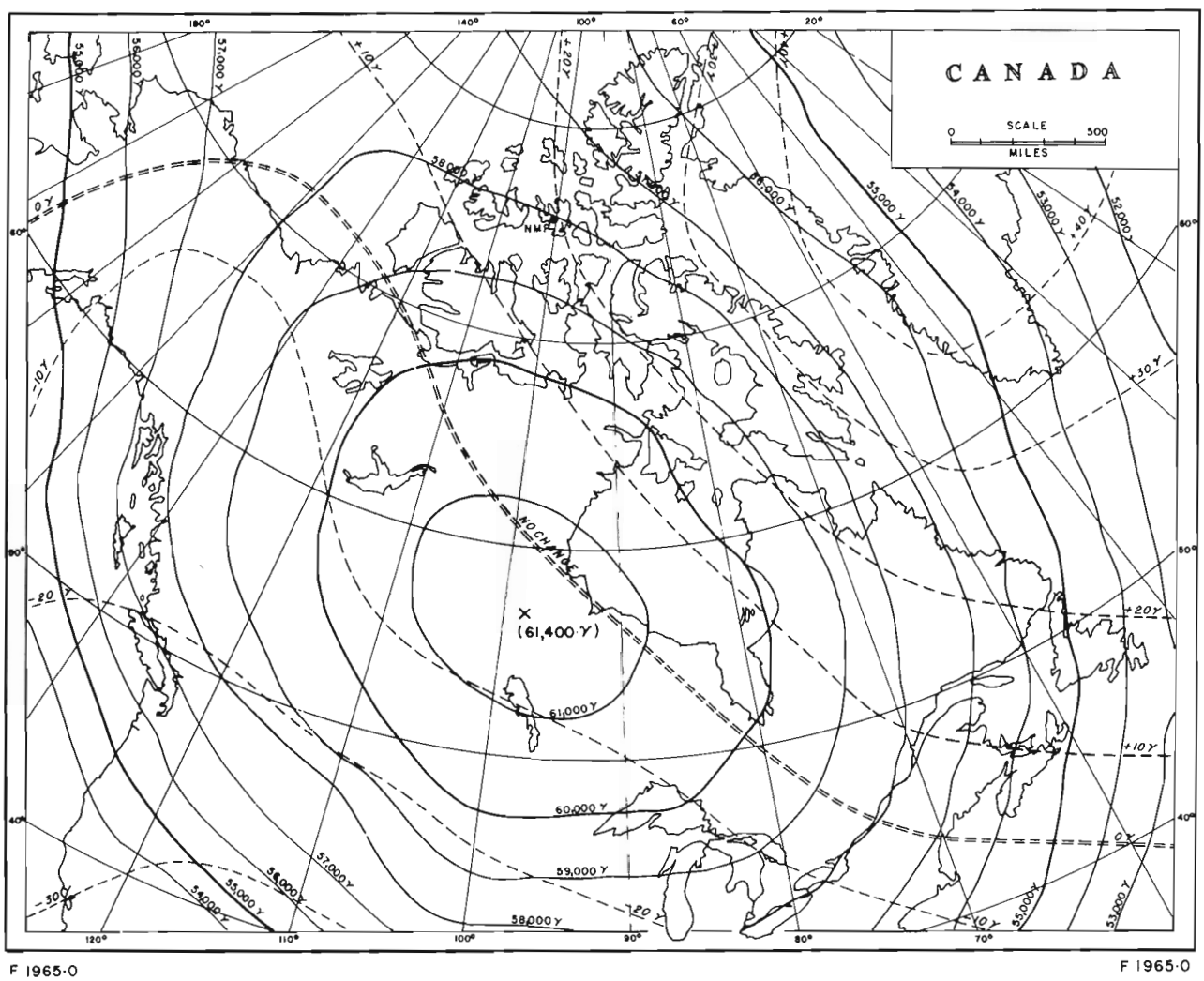

Figure 1. Total Intensity (F) Map of Canada for 1965.0. The dashed lines are the secular variation in the total geomagnetic field.

[1] Waterloo University, Waterloo, Ontario.

From: Scientific and Technical Notes in Current Research, Part A; Geol. Surv. Can., Paper 78-1A.

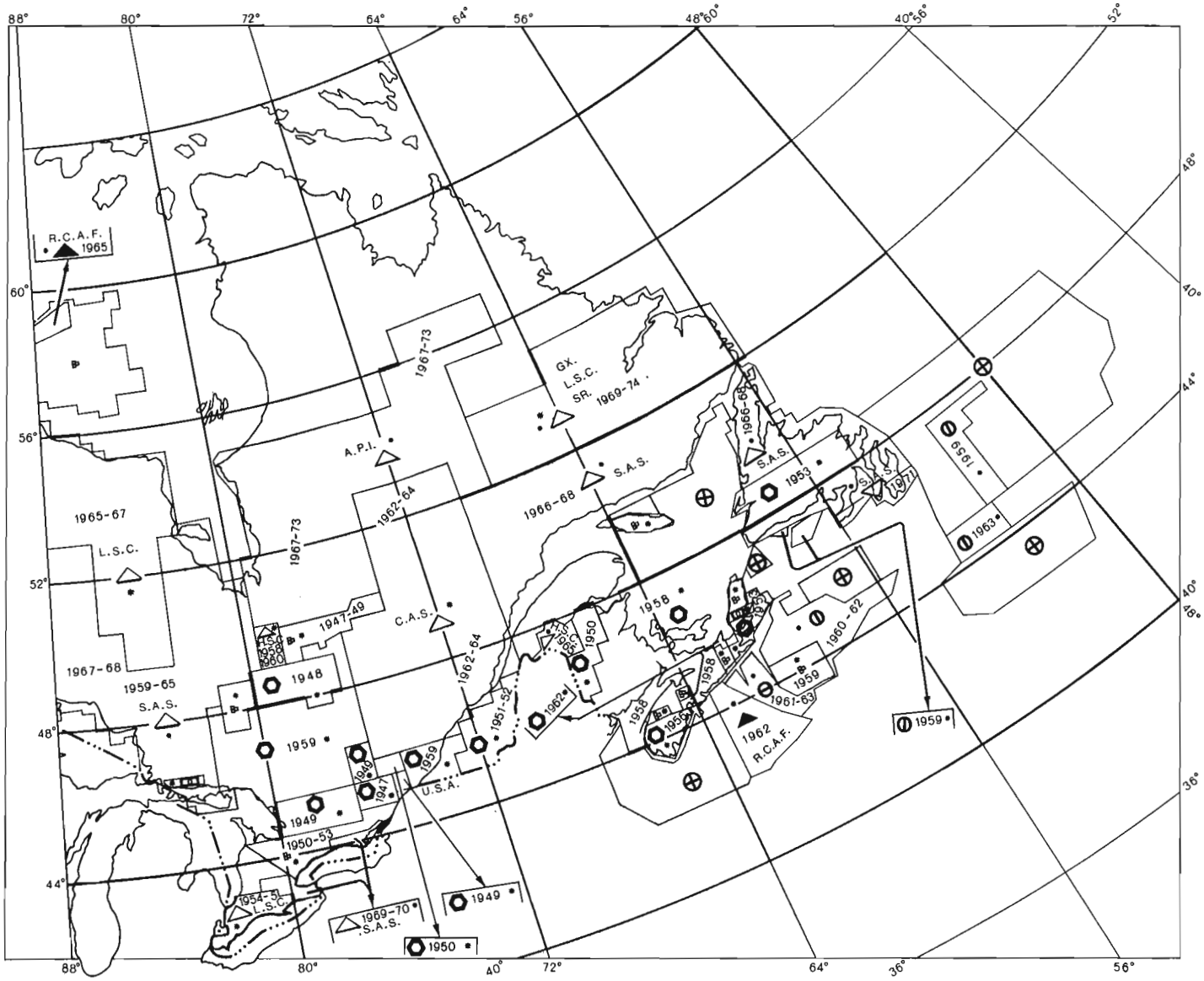

Figure 2. Aeromagnetic surveys in eastern Canada employed in the compilation of the Magnetic Anomaly Map of Canada.

Survey Area Boundaries

1977 Survey Years

Geological Survey of Canada

Federal Provincial Cost Sharing

Atlantic Geoscience Centre

Canadian Hydrographic Service

Relative Total Field Surveys

Absolute Total Field Surveys

National Aeronautical Establishment

Private Companies

Provincial Governments

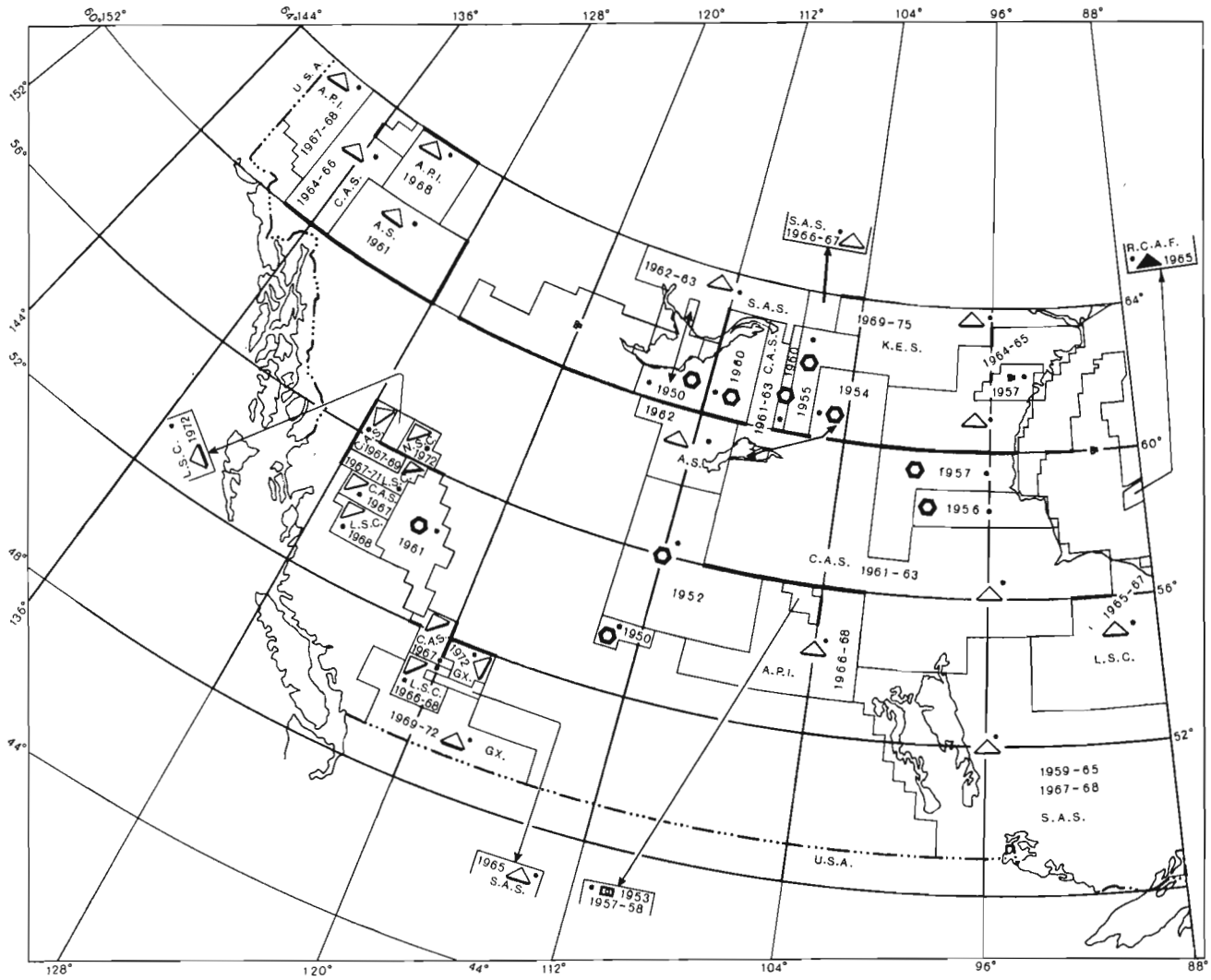

Figure 3. Aeromagnetic surveys in western Canada employed in the compilation of the Magnetic Anomaly Map of Canada.

A.P.I.	Aero Photo Inc.
A.S.	Aero Surveys Ltd.
C.A.S.	Canadian Aero Service Ltd.
GX.	Geoterrex Limited
H.S.C.	Hunting Survey Corporation Ltd.
K.E.S.	Kenting Earth Sciences Ltd.
L.S.C.	Lockwood Survey Corporation Ltd.
N.S.C.	Northway Survey Corporation Ltd.
R.C.A.F.	Royal Canadian Air Force
S.A.	Spartan Aero Ltd.
S.A.S.	Spartan Air Services Ltd.
SR.	Survair Ltd., Ottawa

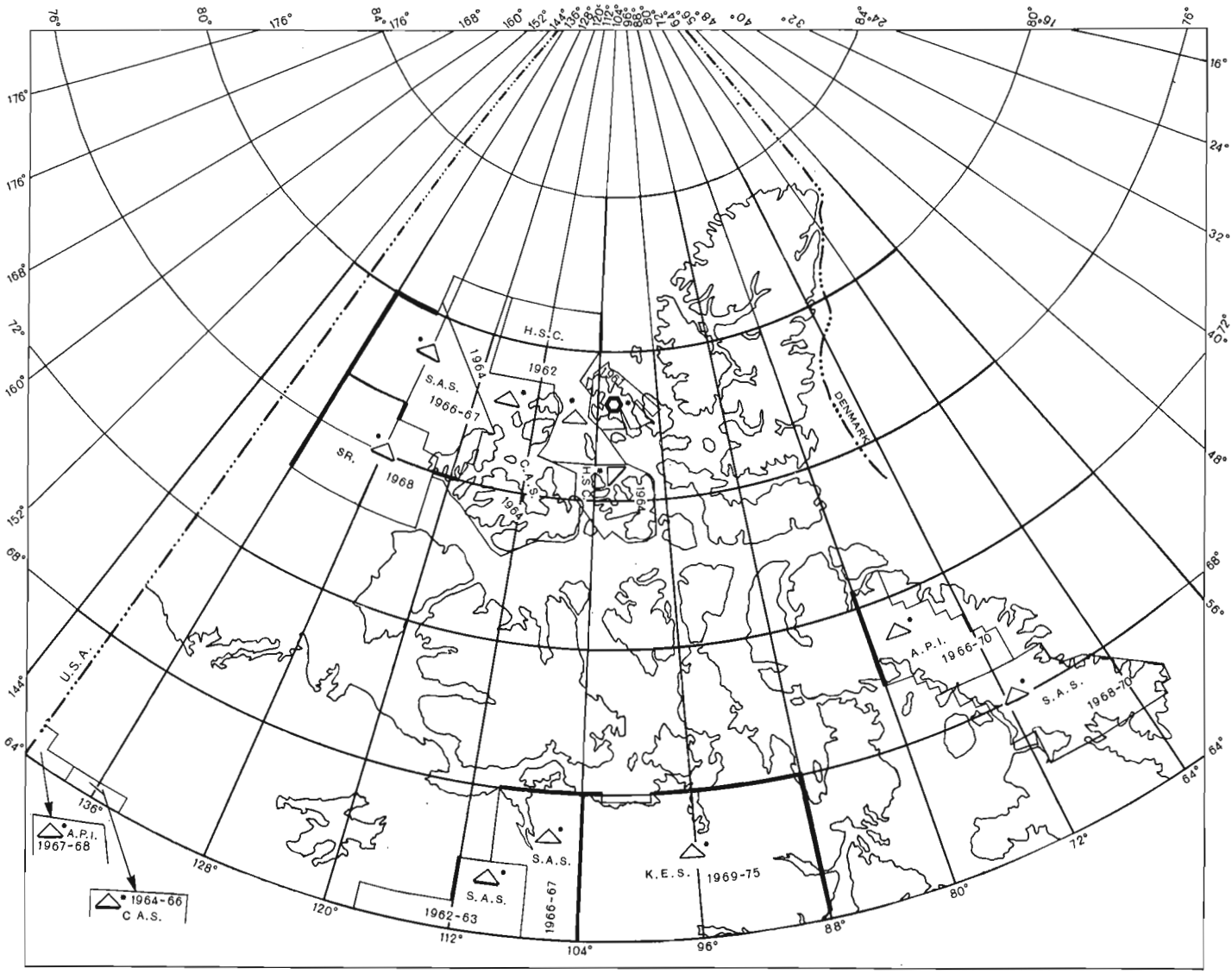

Figure 4. Aeromagnetic surveys in northern Canada employed in the compilation of the Magnetic Anomaly Map of Canada.

Compilation Procedures

The Magnetic Anomaly map was an outgrowth of the systematic colouring of the four-mile aeromagnetic maps. A distintive banding, apparent on the coloured maps, was caused by the dominating effect of the main geomagnetic field which has its origin in the earth's core. The general band pattern was similar to that shown by the contours found on the total field (F) map for 1965.0 (solid lines in Fig. 1) published by the Dominion Observatories Branch (now the Earth Physics Branch). It was decided to produce a 200 gamma magnetic anomaly map of Canada by subtracting the core-generated component of the geomagnetic field from the aeromagnetic data using values derived from the F map. This procedure avoids the production of a map which would have been dominated by a large beehive-like anomaly some 9000 gammas in amplitude, and which would have obscured the magnetic detail related to crustal geology.

Step 1

The initial activity in the compilation was to obtain the total magnetic field (F) map (Fig. 1) which was published at the one inch to 100 mile scale for epoch 1965.0. The 1000 gamma contours shown on the F map were subdivided into 100 gamma intervals, and the map was recontoured taking care to maintain smooth changes in magnetic gradient. Using the resultant map, total field values were interpolated for all of the four-mile aeromagnetic map sheet corners, each map being two by one degrees in extent in the east-west and north-south directions respectively. Secular variation values (dashed lines in Fig. 1) were also obtained at the same points, and all of these values were tabulated.

Step 2

All the relevant aeromagnetic maps at the one-inch to four mile scale were assembled. Initially the compilation commenced in northern Manitoba in the centre of the geomagnetic high (Fig. 1) using aeromagnetic map data obtained by Canadian Aero Service during the period 1961 to 1963 with a fluxgate magnetometer. The background map values are in the order of 2500 gammas, being relative to an arbitrarily assigned value at a base station within the survey area. Secularly corrected F values (in this case to 1962) were calculated from the tabulated data derived from the F map (Step 1), and recorded on the corners of the respective four-mile map sheets. The positions of the intersections of each 100 gamma F contour with the edges of each map were

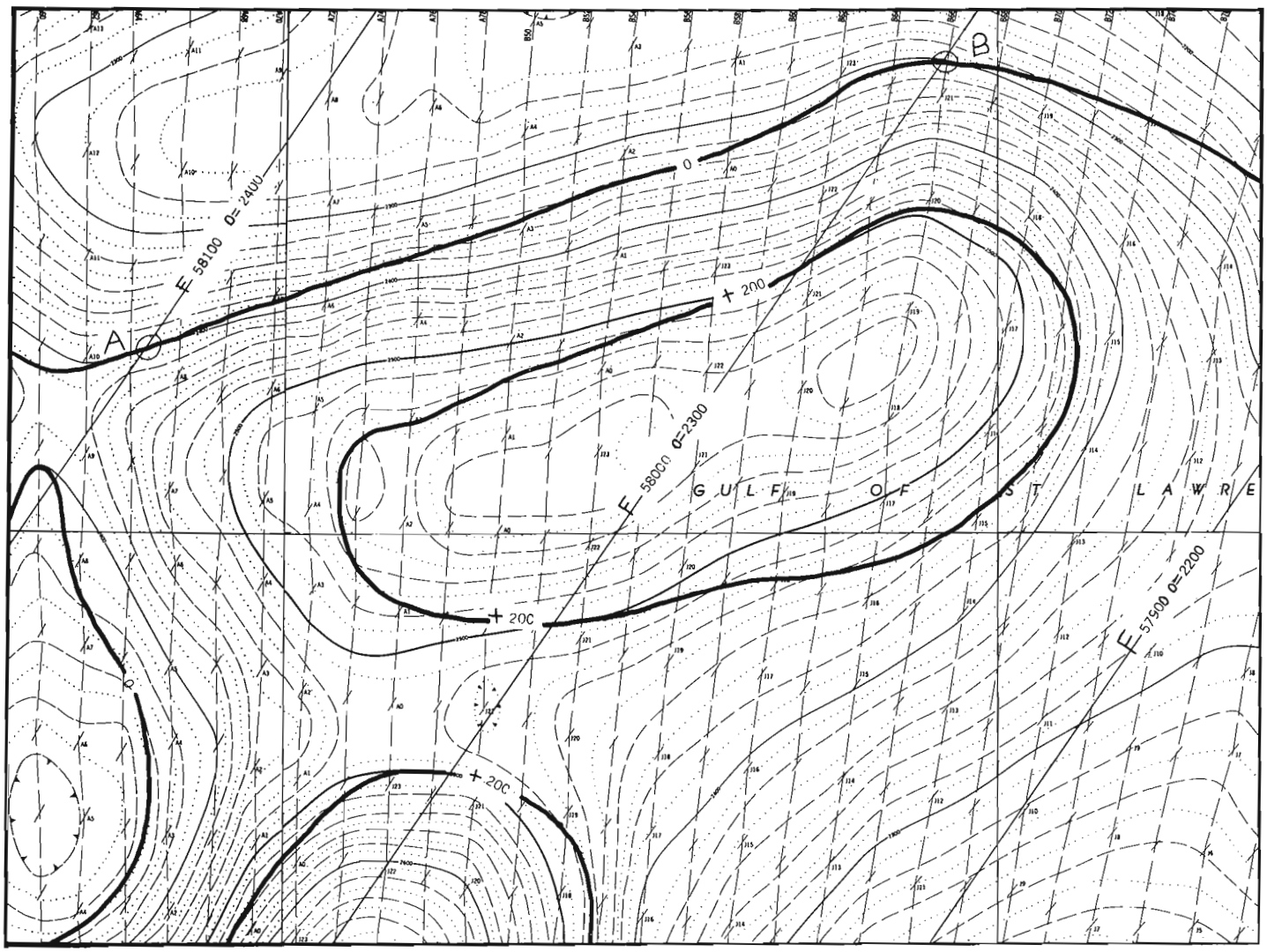

Figure 5. Map illustrating graphical separation procedure employed in deriving the -200, zero and +200 gamma contours displayed on the Magnetic Anomaly Map of Canada.

determined by linear interpolation along the various map edges using the F values obtained at the adjacent map corners. Then straight lines were drawn across each map sheet joining points of equal F value. In this manner 100 gamma F contours which represent the main geomagnetic field corrected to 1962.0 were represented on each four-mile aeromagnetic map sheet. The value of each F contour was written beside it on the map margins in black pencil.

Next it was necessary to determine the base level difference between the relative total field (fluxgate) aeromagnetic map data (≈2500 gammas) and the absolute total field F map (≈60 000 gammas). This difference was found by visually determining the average background level of the fluxgate data along one of the F field lines. This background represents the gamma value which the aeromagnetic anomalies seem to be placed in. It was assumed that the difference between the given F field line value and the background fluxgate value along this same line represented the change in base level between the two sets of contour map data. For convenience, the difference value obtained was subtracted from each of the F field lines and the result recorded in brown pencil beside the respective field lines on each four-mile aeromagnetic map. The same procedure would be followed had the original survey data been obtained using a proton precession magnetometer. In the latter case the survey would be an absolute one, and the difference between it and the F field would approach or be equal to zero. Finally values 200 gammas above and below those shown in brown on each map sheet were recorded in blue and red pencil respectively for every F contour.

Step 3

The next operation, a modification to the procedure described in Step 2, was only applied where the compilation was moving from one survey area (for example, the 1961-63 Canadian Aero Service survey in northern Manitoba – see Fig. 2) into an immediately adjacent survey area. Proceeding according to Step 2, the F field lines were transferred at 100 gamma intervals onto each four-mile map sheet in the adjacent survey area. Corresponding F lines may not join across the survey boundary because of differing secular corrections in the two survey areas. Next, instead of determining the base level difference between a given F line and the corresponding aeromagnetic survey data as in Step 2, the difference between the two adjacent surveys was obtained by performing an edge analysis along the common boundary. Level differences between the two surveys were obtained in areas of low magnetic gradient. If necessary a secular correction was determined by linear interpolation from the nearest map corners and applied to the respective differences. If the base level difference between the two surveys was zero, then the values shown in red, brown and

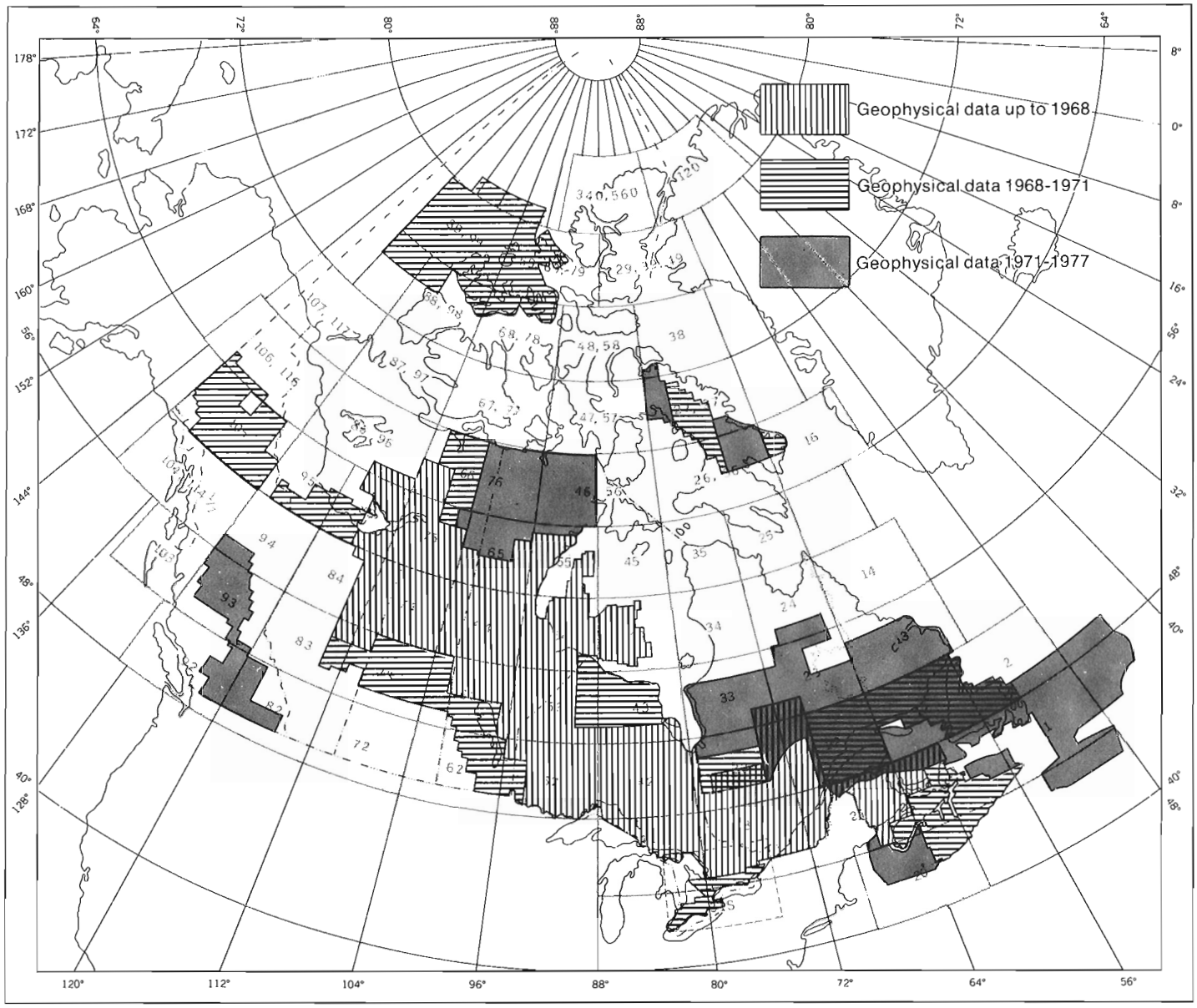

Figure 6. Aeromagnetic coverage of the three editions of the Magnetic Anomaly Map of Canada released in the years 1968, 1971, and 1977.

blue in the compiled survey area were carried directly over onto the corresponding F lines in the new survey area. However, if for example the base level in the new survey area was 50 gammas below that in the previously compiled area, then all of the values shown in red, brown and blue must have 50 gammas subtracted from each of them before they are transferred onto the corresponding F field contours in the new survey area. This modified procedure is considered to yield results superior to that described in Step 2 because of possible deviations of the F field model from the real core-generated magnetic field component. In addition, problems such as gradients or warps between the base levels along the common join of adjacent surveys may become apparent. In the latter case exotic modifications to the compilation procedures may be required. However unless one has access to independent magnetic data in the vicinity of such a troublesome boundary, it is impossible to determine which of the two surveys is in error.

Step 4

Four colours and three contours (-200, zero and +200 gammas) are displayed on the Magnetic Anomaly map. The following procedure was employed to separate these contours from the aeromagnetic map data. First, a point (A, Fig. 5) was located where aeromagnetic and F field contours of equal value intersected. On the four-mile compilation sheets the brown values on the F contours were used in compiling the zero contour; red and blue values for the -200 and +200 gamma contours respectively. In Figure 5, the F58 000 gamma contour represents the F field value derived from the 1965.0 map of Canada (Step 1). The equivalent value shown of 2300 gammas is the background value of the fluxgate magnetometer map data along the 58 000 gamma F line, and would be recorded in brown pencil on the four-mile compilation sheets. Starting at point A (Fig. 5) a line was drawn which initially followed the respective aeromagnetic survey contour away from the intersection point. As the aeromagnetic contour begins to deviate away from its corresponding

valued F line, for example towards an F line of lower value, then the drawn line gradually migrates towards lower aeromagnetic map contours until it approaches at point B an aeromagnetic contour of value 100 gammas less than that at point A. Point B is a second intersection point of aeromagnetic and F contours of equal value only in this case the value is 100 gammas less than at point A. The procedure continues until all contours have been separated. Keeping with our convention, the -200, zero and +200 gamma contours are traced on the four-mile compilation sheets in red, brown and blue.

Step 5

The resultant red, brown and blue contours on the four-mile aeromagnetic compilation sheets were traced onto a large overlay of cartographic material on which the map corners had previously been marked. The overlay was then reduced photographically to a scale of one inch to twenty miles, and a print of the reduction was coloured using four colours and the 200 gamma contour interval. Next a copy of the 1:5 000 000 Lambert Conformal Conic projection base map of Canada was obtained in four sections on stable material at the scale of one inch to twenty miles. When the base map was overlain on the coloured 20-mile magnetic reduction, slight differences were noted resulting from the Universal Transverse Mercator Projection used in the preparation of the aeromagnetic maps. Reference points from the base map were transferred onto a second stable base overlay, and using a best fit technique within each National Topographic System quadrangle, a second copy of the magnetic map at the 20-mile scale was prepared. During this tracing the complicated magnetic anomaly patterns on the coloured map were generalized taking into account legibility and the requirements of the photomechanical cartographic procedures that followed in the production of the colour publications. This second overlay was photographically reduced to the 1:5 000 000 scale and submitted to the Geological Information Division for preparation for publication. Information regarding this process may be obtained by contacting the Superintendent of Cartography, Geological Survey of Canada, Ottawa.

Figure 1 is an illustration showing the coverage of the three editions of the map which were released in the years 1968, 1971 and 1977. Note that some of the areas were recompiled for subsequent editions.

Utilization and Conclusions

There are three major applications for the Magnetic Anomaly map. First as an index, the map presents an overview of magnetic coverage in Canada. Second, it presents the major patterns produced by the continental rocks in the Canadian landmass. As such it enables a person to observe the regional magnetic patterns, and then go back to the larger scale aeromagnetic maps for the fine details, and in this sense does not in any way replace the original data. The map may be used both as an aid in the interpretation of regional geological features in the basement rocks (MacLaren and Charbonneau, 1968) as well as to help in planning more detailed investigations. Lastly and probably the greatest asset of the map is its use as a vehicle or medium to initially stimulate comparisons of magnetic data with other types of geoscientific information.

Finally a few comments concerning the method of production. The compilation of the map has been an ongoing if somewhat sporadic activity since its inception in 1967. Most of the magnetic data used in the compilation are available in map form only and as analog records. The digitization of these data would be a massive undertaking. Hence the production of the third edition of the map during 1977 was constrained to follow procedures defined ten years earlier when the first edition was compiled. Only limited access to the more recently developed rapid data handling and treatment techniques used by modern computers and related equipment was possible. However in spite of these constraints as well as the additional financial and manpower limitations imposed on the project, the resultant map is an entirely adequate end product with regard to the resources expended. However, it is certainly a desirable goal to produce a Magnetic Anomaly map by subtracting the International Geomagnetic Reference Field (IGRF) from the aeromagnetic map data rather than a model (Fig. 3) of the core-generated magnetic field which is restricted to the Canadian region. The IGRF was defined in October 1968, subsequent to the release of the first edition of the Magnetic Anomaly map. Also it would be useful to obtain aeromagnetic data from a series of cross country flights. These data would be a useful reference with which to facilitate a more reliable joining together of the numerous individuals magnetic surveys employed in the compilation of the Magnetic Anomaly Map of Canada.

The compilation for eastern Canada was based both on published and unpublished maps by R.T. Haworth of the Atlantic Geoscience Centre, and on a compilation map by P.J. Hood.

A significant contribution to the production of the present edition of the Magnetic Anomaly Map of Canada was made by the Cartographic section, especially J.G. Roberts, P. Debain, G.J.J. Barbary, E. Maahs, R.E. Saffin, T.L. Papps, J.A.Y. Pratt, and N. Buck and the entire photomechanical unit.

References

Anonymous

1966: F - Isodynamic Chart, Canada, 1965.0; Geomagnetic Division, Earth Physics Br., Dep. Energy, Mines and Resources.

Haworth, R.T.

1974: Magnetic Map of the Bay of Fundy to Gulf of St. Lawrence; Map 801-E, published by the Canadian Hydrographic Service, Dep. of the Environment, Ottawa.

Hood, P.J.

1977: Magnetic Anomaly Map of the Atlantic Provinces; Geol. Surv. Can., Open File 496.

MacLaren, A.S. and Charbonneau, B.W.

1968: Characteristics of Magnetic Data over Major Subdivisions of the Canadian Shield; Geol. Assoc. Can. Proc., v. 19, p. 57-65.

McGrath, P.H., Hood, P.J., and Darnley, A.G.

1977: Magnetic Anomaly Map of Canada; Geol. Surv. Can., Map 1255A, 3rd. ed.

Morley, L.W., MacLaren, A.S., and Charbonneau, B.W.

1968: Magnetic Anomaly Map of Canada; Geol. Surv. Can., Map 1255A, 1st. ed.

OBSERVATIONS ON SLOPEWASH PROCESSES IN AN ARCTIC TUNDRA ENVIRONMENT, BANKS ISLAND, DISTRICT OF FRANKLIN

A.G. Lewkowicz[1], T.J. Day, and H.M. French[1]
Terrain Sciences Division

A reconnaissance study, aimed at an understanding of the hydrologic and geomorphic importance of slopewash processes in an arctic permafrost region, was undertaken at Thomsen fly camp, north-central Banks Island (73°14'N; 119°32'W), between May 25 and July 28, 1977.

Slopewash embodies two sets of processes: (a) surface wash, the downslope transport of weathered material over the ground surface by running water and (b) subsurface wash, the group of processes associated with water moving within the regolith. Although slopewash processes have been reported for most climatic zones (e.g. Carson and Kirkby, 1972, p. 188-230; Young, 1972, p. 62-74), there is a lack of quantitative measurement from permafrost regions (French, 1976, p. 141). It is generally agreed, however, that due to the sparse vegetation cover, slopewash is potentially most important in semiarid regions. The few quantitative measurements available for permafrost regions support this assumption; values of sediment transport of up to 18 g/m^2/y were reported by Jahn (1961) from melting snow on Spitsbergen; Wilkinson and Bunting (1975) concluded that 0.03 metric tons/y of sediment was transported by 68 rills over a 450 m wide slope on Devon Island.

Field Methods

Three sites of varying slope, aspect, topographic position, and microrelief were selected in the immediate vicinity of Thomsen fly camp (Fig. 1). Site characteristics are presented in Table 1. At each site, a runoff plot was delimited, and a surface wash (overland flow) collector was installed at the downslope exit to the plot. The collector consisted of a copper trap box, open upslope, with an outlet pipe connected to a calibrated collecting pan by a length of flexible tubing. Subsurface wash (throughflow) was measured by the installation of a series of gutters placed horizontally within the active layer at depths varying between 5 and 50 cm. Each gutter was connected by flexible piping to collecting containers downslope. Suspended sediment in the runoff was analyzed by field filtration using an Ostrem filter pump and by the reweighing of filter papers in the laboratory. Solute concentrations in the overland flow were measured in the field using a portable conductivity meter, giving values in microhms/cm^3 which then were transformed into mg/L of $CaCO_3$.

A number of complementary supporting procedures also were undertaken. Measurements of snowpack densities enabled initial water equivalents of the snowpack to be calculated, and the depths, densities, and spatial extents of the snowpacks were recorded at intervals throughout the ablation period. Net radiation and air temperatures were monitored continuously throughout the study. Precipitation was recorded at site 1 by an automatic tipping bucket rain gauge, and four nonrecording rain gauges were installed at the other two sites. Evaposublimation from the snow and evapotranspiration from the ground surface were not recorded adequately.

Overland flow was monitored at site 1 between May 28 and June 5, at site 2 between June 5 and 19, and at site 3 between June 20 and July 27. Throughflow was monitored at site 1 between June 1 and July 17, and at site 3 between June 20 and July 27.

Results

Overland Flow

There was a clear correlation between net radiation, air temperature, and overland flow at site 1 (Fig. 2) for the period May 30 to June 2, during which time two hydrographs were obtained. Total overland flow was 0.974 m^3 which constituted only 9.4% of the original water equivalent of the snowpack on the plot (10.33 m^3). Thus, a significant amount of snow ablated without causing surface runoff. Furthermore, the response of overland flow to snowmelt was not of a simple linear nature since a lag period was apparent. The low runoff coefficient probably was related to the local weather conditions of May 25 to 31, when overcast conditions prevailed and amounts of incoming solar radiation were small; melt probably occurred as a result of turbulent heat transfers, mostly in the form of sublimation. The three consecutive days of sunshine, and high radiation and air temperature values, caused melting sufficient to exceed the evaporative and subsurface losses and for overland flow to occur. Regression of overland flow against net radiation using a number of lag times revealed a lag of 2.5 hours to be the most appropriate, explaining 66% of the variability.

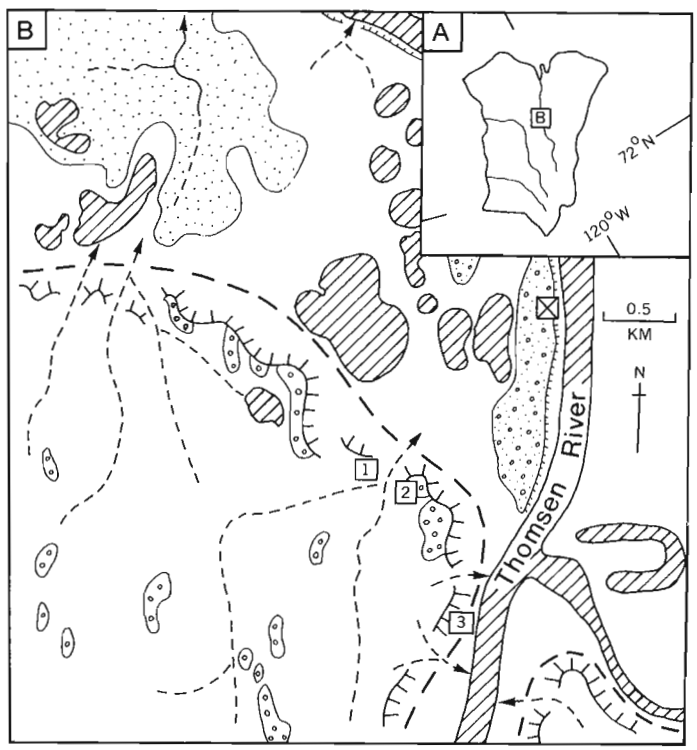

Figure 1. Location of slopewash sites, Thomsen fly camp, north-central Banks Island. A - General location. B - Detailed location.

[1] Department of Geography and Regional Planning, University of Ottawa, Ottawa, Ontario.

From: Scientific and Technical Notes in Current Research, Part A; Geol. Surv. Can., Paper 78-1A.

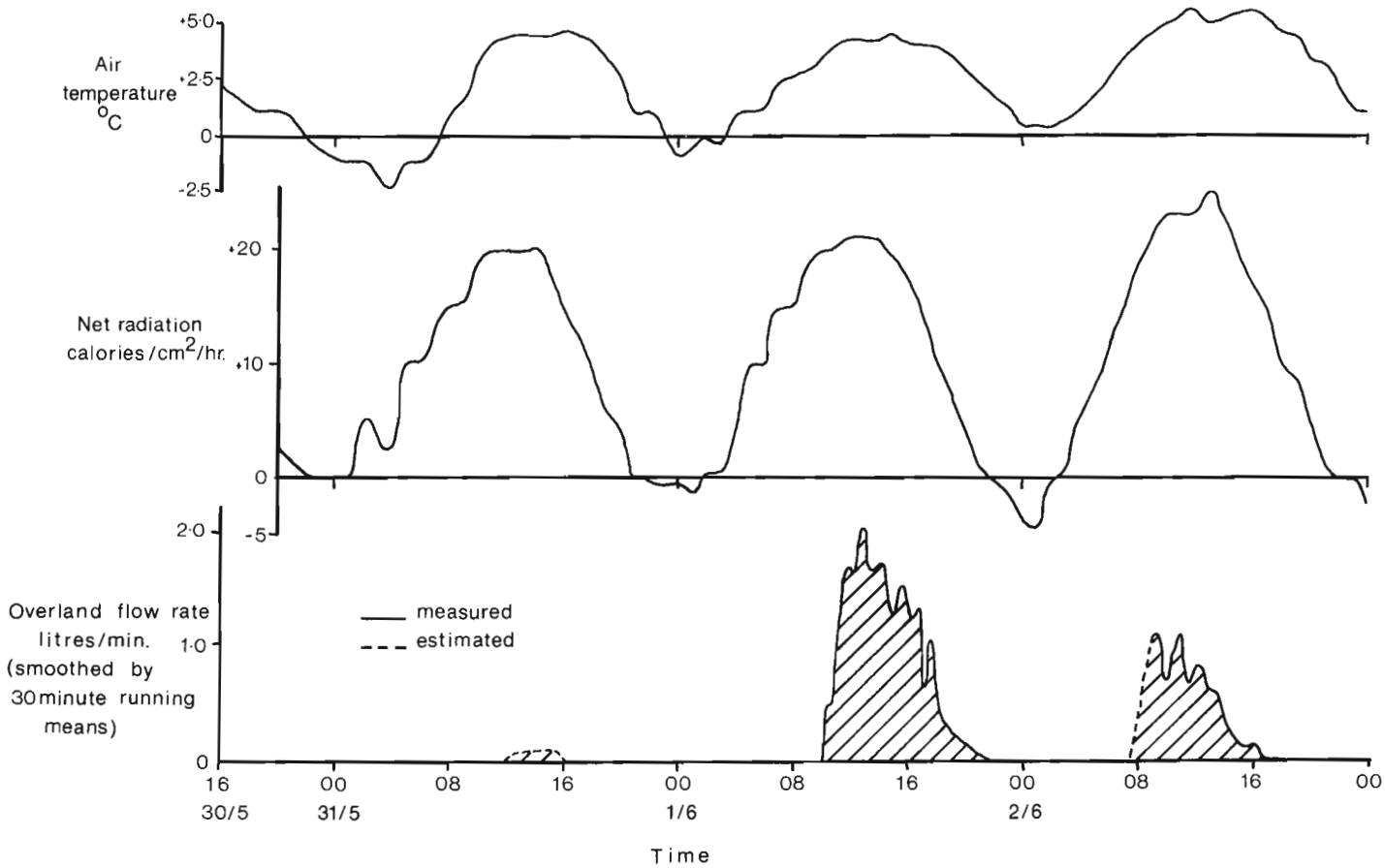

Figure 2. Overland flow, net radiation and air temperatures at site 1, May 30 - June 2, 1977.

At site 2 snowmelt already had occurred when measurement commenced, but the bulk of the snowbank (127 m^3) remained. In all, twelve hydrographs were obtained by June 17 when snowmelt-derived overland flow ceased. As at site 1, there was a clear correlation between overland flow, prevailing weather conditions, and the water supply present in the remaining snow. A typical day illustrating the influence of net radiation and air temperatures was June 11 (Fig. 3). A lag of three hours occurred between peak net radiation and air temperature values. Overland flow, however, commenced approximately two hours prior to peak net radiation and eventually peaked five hours later, reaching a maximum of 13.85 L/min (30 minute running mean). Overland flow represented 52.9% of the estimated changes in water equivalent that occurred on the plot during the day. The lag time between net radiation and overland flow was attributed to the vertical and horizontal movements of water in the snowbank combined with the flow of water over the ground surface of the collector. With the use of Rhodamine dye the average ground surface water velocity was estimated at 1.32 cm/s. Using this value, only fourteen minutes out of the three hour time lag on June 11 could be attributed to the time taken for water to pass over the ground surface from the snow front to the collector. Thus, the majority of the time lag was associated with the passage of water through the snowbank.

Although snowmelt is thought to be the major source of water for overland flow in the High Arctic, summer precipitation also may influence overland flow. Storm precipitation of 6.25 mm in five hours was recorded in the hydrograph obtained from site 2 on June 15 (Fig. 4). Analysis of this information enabled some assessment to be made of the hydrologic importance of such events as regards overland flow. The hydrograph (Fig. 4) was separated by regression against lagged net radiation into runoff thought to result from snowmelt (i.e. 'base flow') and that derived from the storm. The runoff due to the storm totalled 640 L, giving a storm runoff coefficient of 26.4%.

It might be assumed that the plot source area for surface runoff resulting from storm rainfall would consist of the snowbank itself and the saturated area between it and the overland flow collector. On June 15 these sections of the plot accounted for 85% of its area. As the runoff coefficient was less than one third this figure, it follows that rain falling on the snowbank failed to cause runoff and/or that the water was 'lost' either as evaporation or as increased throughflow. The rapid response time of runoff to precipitation at the beginning of the storm and the equally rapid fall-off at the end suggest that most water is stored in the snowbank rather than passing through, thus confirming earlier observations.

Throughflow

Throughflow was recorded at sites 1 and 3; however, interpretation is tentative in view of the considerable disturbance caused by the installation of the gutters. Furthermore, throughflow is more complex in nature because, in addition to supply factors, it is influenced by permeability and hydraulic gradients. Another complicating factor is the seepage of water directly beneath the surface organic mat which tends to blur the distinction between overland flow and throughflow.

At site 1, throughflow at an average depth of 5 cm was recorded contemporaneously with overland flow. Maximum throughflow values ranged between 150 to 250 cm^3/min and were of the same order of magnitude as overland flow per unit width of slope. Throughflow ceased one day after the cessation of overland flow. This suggests that the input to throughflow from active layer melt was negligible and that on well drained upland sites both overland and throughflow are of limited occurrence and duration.

Table 1
Characteristics and dimensions of slopewash sites, Thomsen fly camp

	Topographic Position	Aspect	Length (m)	Average Width (m)	Area (m^2)	Slope (degrees)	Material	Vegetation Cover (%)
Site 1	Interfluve	SE	28.7	5.2	149.6	5	Sandy Gravels	10-20
Site 2	Valleyside Slope	NW	54.1	7.2	387.5	5	Silty Colluvium	60-80
Site 3	Valleyslope Slope	SE	18.8	1.4	26.6	14	Silty Colluvium	100

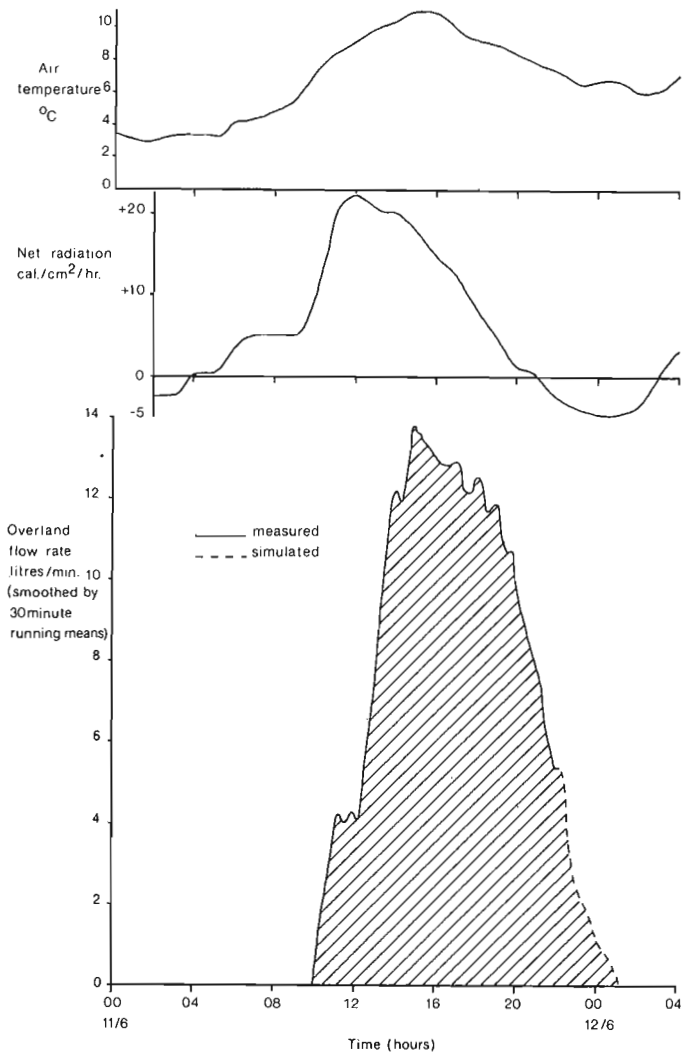

Figure 3. Response of overland flow to net radiation and air temperatures at site 2, June 11-12, 1977. To simulate overland flow the following formula was used: overland flow = $0.573R_n + 1.815$, where R_n is lagged 3 hours, N = 76, and $r^2 = +0.89$.

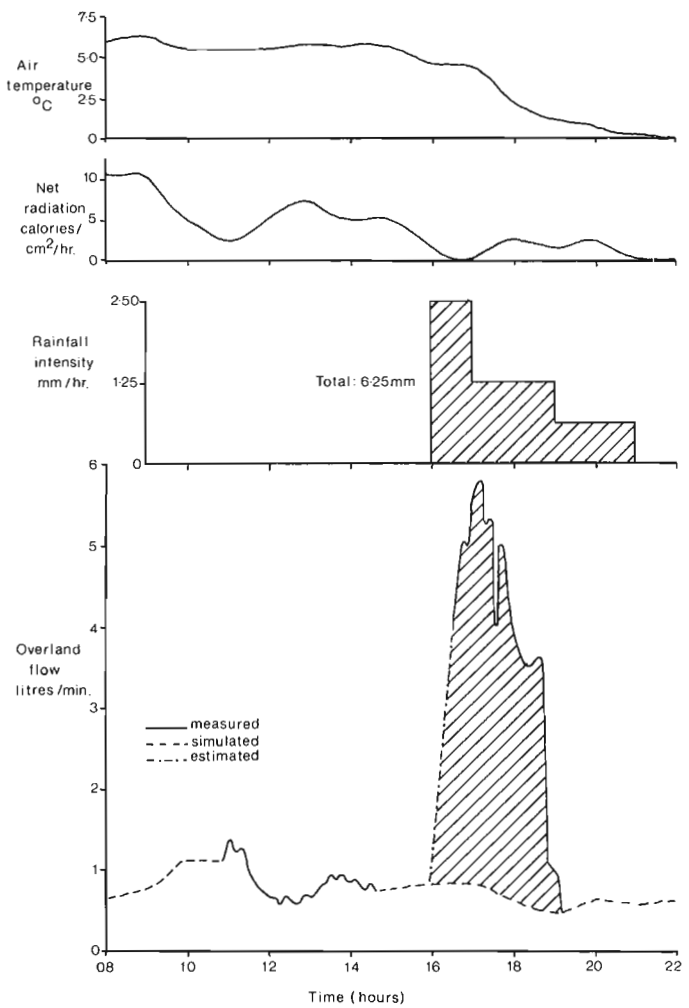

Figure 4. Relationship between storm rainfall and overland flow at site 2, June 15, 1977. To simulate overland flow the following formula was used: overland flow = $0.06R_n + 0.48$, where R_n is lagged 2 hours, N = 25, and $r^2 = +0.55$.

Table 2
Amounts of suspended solids in overland flow and denudation estimates

	Time Period	Mean Concentration (ppm)	Standard Deviation	Total Flow Volume* (litres)	Denudation Estimate**
Site 1	May 28 - June 5	130	15.4	964	0.92 g/m^2/y
Site 2	June 5 - June 19	110	6.1	35,000	10.04 g/m^2/y
Site 3	June 20 - July 27	111	11.5	---	--

* Include simulated values where actual data are missing.
** Denudation Estimate = (Total Flow Volume x Mean Concentration (ppm)/Plot Area).

At site 3, throughflow measurements were made approximately 150 m downslope from the runoff plot. Continuous throughflow at an average depth of 6 cm was recorded between June 22 and June 30 (Fig. 5). A steeply falling hydrograph pattern emerged with a maximum flow of 94 cm^3/min recorded on June 22. The decline in the hydrograph was attributed to a reduction in the supply of water derived from the snowbank as it progressively ablated. By June 27 the snowbank had disappeared. The rise after June 27 presumably was related to 6.5 mm of precipitation. An earlier precipitation event of 8.25 mm on June 23, however, did not significantly affect the hydrograph. This probably was a result of the very different magnitudes of throughflow being measured on the two occasions.

Throughflow was monitored at site 3 at a depth of 31 cm between June 23 and July 27. Amounts were small, however, with a maximum flow of 0.41 cm^3/min recorded. The hydrograph patterns did not appear to be diurnal, in contrast to over and flow and throughflow at shallower depths; instead, a rise over several days was followed by a slow decline. This may be related either to the progressive downward movement of the frost table and its associated active layer water table or to the slow downslope movement of snowmelt-derived water.

Sediment Transport

Sixty-six samples of overland flow obtained from all three plots were analyzed for suspended solids; values ranged from 98 to 175 ppm (mean values are given in Table 2). Estimates of overall slope denudation were computed for sites 1 and 2. At site 3 it was not thought valid to undertake similar computations because the majority of snowmelt had occurred prior to instrumentation. The value of 10.04 g/m^2/y obtained for site 2 is similar to that recorded by Jahn (1961). The lower value for site 1 reflects the greatly reduced slopewash activity at that site. It is assumed at both sites that the annual slopewash activity was confined to the period of measurement. These values, however, do not necessarily represent total denudation since no account is made of other sediment inputs and outputs to the slope, notably of an eolian nature.

Throughflow samples were not analyzed for suspended solids because it was felt that the degree of disturbance associated with the installation of the equipment would have significantly affected results.

Solute concentrations were determined for sixty of the overland flow samples. At site 1 an average equivalent value of 127 ppm of $CaCO_3$ gave a denudation estimate of 0.82 g/m^2. At site 2, although an average equivalent value of only 26 ppm of $CaCO_3$ was obtained, the greater flow at that site gave a denudation estimate of 2.38 g/m^2.

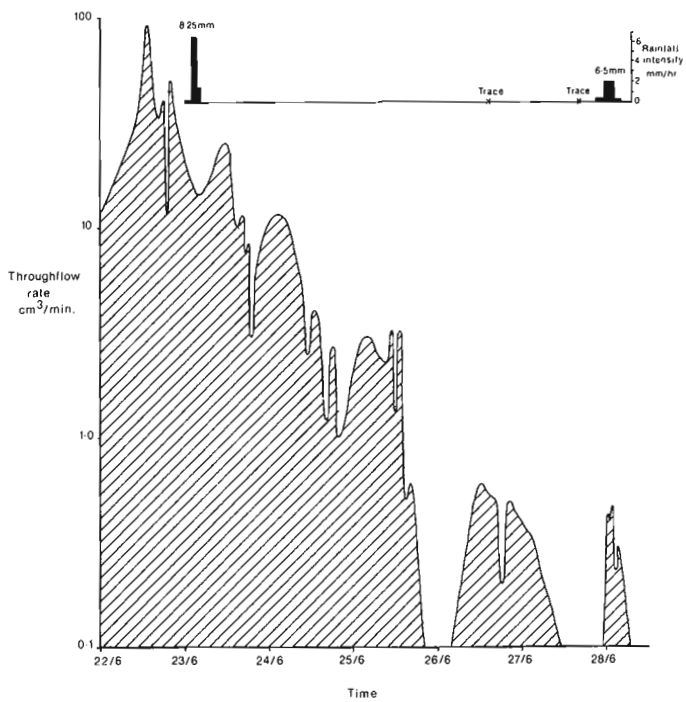

Figure 5. Throughflow hydrograph obtained at site 3, June 22-28, 1977.

Conclusions

In general, the amount of slopewash recorded was small compared to the total amount of moisture originally available on the runoff plots. Therefore, attention must be focused upon the other means of moisture removal from the plots, notably evaporation and sublimation.

The overland flow data for June 15 at site 2 indicates, by the low runoff coefficient, that Hortonian overland flow, where infiltration capacity is exceeded, as a result of rainfall did not occur. Furthermore, at site 1 no flow whatsoever was recorded at that time. These observations support the concept of partial area contribution to runoff in permafrost areas.

Finally, the study reinforces the belief that slopewash processes in arctic tundra environments may be of considerable geomorphic importance, particularly at snowbank locations where nivation processes traditionally have been regarded as being very potent.

Acknowledgments

Research was supported in part by National Research Council of Canada grant A-8367 (H.M. French), the University of Ottawa Northern Research Group, and the Polar Continental Shelf Project (Projects 34-73 and 54-77).

References

Carson, M.A. and Kirkby, M.J.

1972: Hillslope Form and Process; Cambridge University Press, England, 475 p.

French, H.M.

1976: The Periglacial Environment; Longman Group Limited, London, New York, 309 p.

Jahn, A.

1961: Quantitative analysis of some periglacial processes in Spitsbergen; Nauka o Ziemi II, Seria B, Nr 5, Warsaw, p. 3-34.

Wilkinson, T.J. and Bunting, B.T.

1975: Overland transport of sediment by rill water in a periglacial environment in the Canadian High Arctic; Geogr. Ann., Ser. A, v. 57, p. 105-116.

Young, A.

1972: Slopes; Oliver and Boyd, Edinburgh, 288 p.

THE SURFACE TEMPERATURE OF AN ICE-RICH MELTING PERMAFROST EXPOSURE, GARRY ISLAND, NORTHWEST TERRITORIES

J. Ross Mackay[1]
Terrain Sciences Division

Permafrost may be exposed to summer melting in many arctic areas as a result of a natural or artificial disturbance. If the terrain is steep and permafrost ice-rich, scarp retreat typically produces an amphitheatre-shaped depression with a steep headwall and mudflows downslope from the headwall. Such features are variously referred to as retrogressive thaw flow slides, thaw slumping, ground-ice slumps, thermocirque, and so forth. The headwall retreats upslope from active layer slumping, ablation of the exposed permafrost surface, and water erosion. The processes involved are of practical concern to northern construction and a knowledge of the surface temperature is relevant to remote thermal sensing of the environment. The purpose of this note is to discuss results of radiometer surface temperature measurements of a thawing headwall developed in ice-rich permafrost as measured on a typical bright sunny day at Garry Island, Northwest Territories. Although data for only one day are given, other measurements have shown similar results.

Field Site

The thawing permafrost headwall, where surface temperature was measured, is shown in Figure 1. The headwall retreated actively from 1963 to 1971 at a rate of about 6 m/y but has been inactive since (Kerfoot and Mackay, 1972, Fig. 3; Mackay, 1966, Figs. 5 and 6). As the ice content of the main scarp averaged nearly 300 per cent (weight of water to dry soil), the 6 m/y of retreat involved the melting of about 5 m/y of ice.

Surface Temperatures

The surface temperature measurements were made with a Stoll-Hardy HL4 radiometer (Williams Development Company, West Concord, Mass.: radiometer head aperature of 1.5 cm; 20° field of view; response time about 0.1 s; accuracy of about 0.1°C; a silver sulphide filter with a 3 micron cutoff was attached to the radiometer head; Stoll and Hardy, 1952). The surface temperatures (Table 1 and Fig. 2) were taken from a distance of 3 cm with the melting permafrost surface in bright sunshine. Other readings were made from a greater distance (e.g. 1 to 5 m) and also in the shade. It should be noted that a radiometer measures the surface radiation temperature, which in the case of water originates in the upper 20 to 30 microns (Gates, 1961). Attempts to measure the subsurface temperature with a thermistor probe were unsuccessful, because when the probe was inserted into a small hole drilled below the frozen surface, entry of meltwater made the reading unreliable. Subsurface temperatures were taken, however, at those sites where a few centimetres of thawed material allowed subsurface measurements.

Table 1

Surface temperatures, as measured with a radiometer, for a thawing, ice rich permafrost surface exposed to bright sunshine

Material	Temperature Range (0°C)		
Clear ice; clear ice with scattered mud pellets	2.5	to	5.5
Film of water over ice or muddy ice	4.5	to	6.0
Film of mud over ice or muddy ice	5.0	to	10.0
Muddy water, flowing	6.0	to	17.0
Muddy ice face, little water	12.0	to	14.0
Mudflow, moving	17.0	to	20.0
Organic matter, frozen a few mm below surface	19.0	to	28.0
Several mm mud over ice	24.0	to	27.0

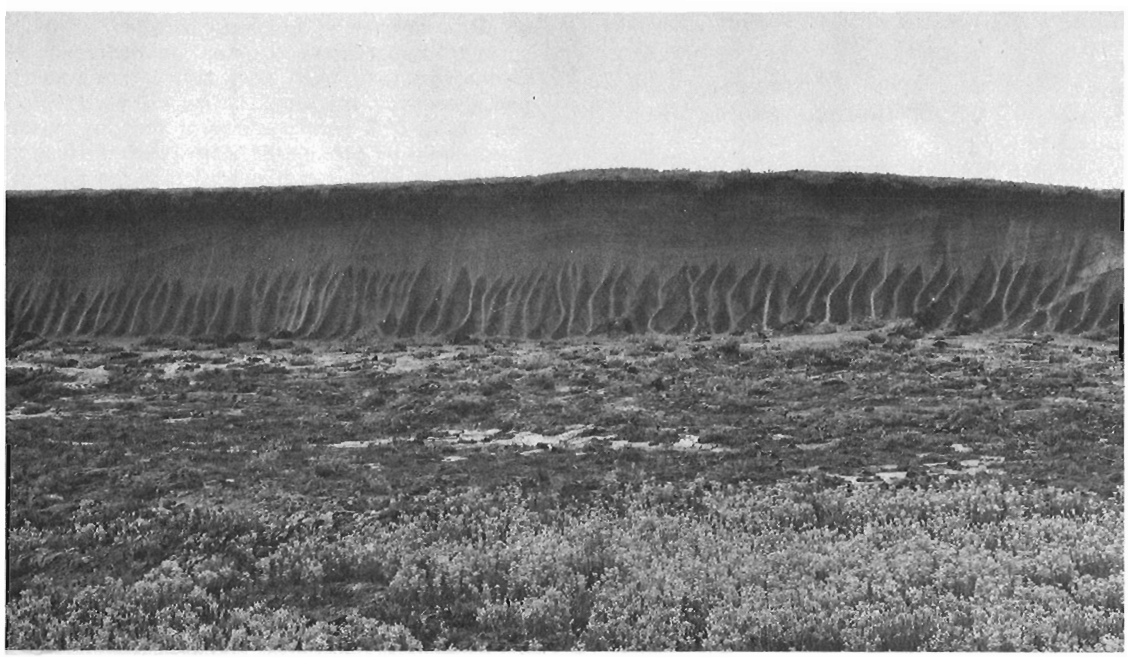

Figure 1. Thawing headwall of ice rich permafrost at Garry Island, Northwest Territories.

[1] Department of Geography, University of British Columbia, Vancouver, British Columbia, V6T 1W5.

From: Scientific and Technical Notes in Current Research, Part A; Geol. Surv. Can., Paper 78-1A.

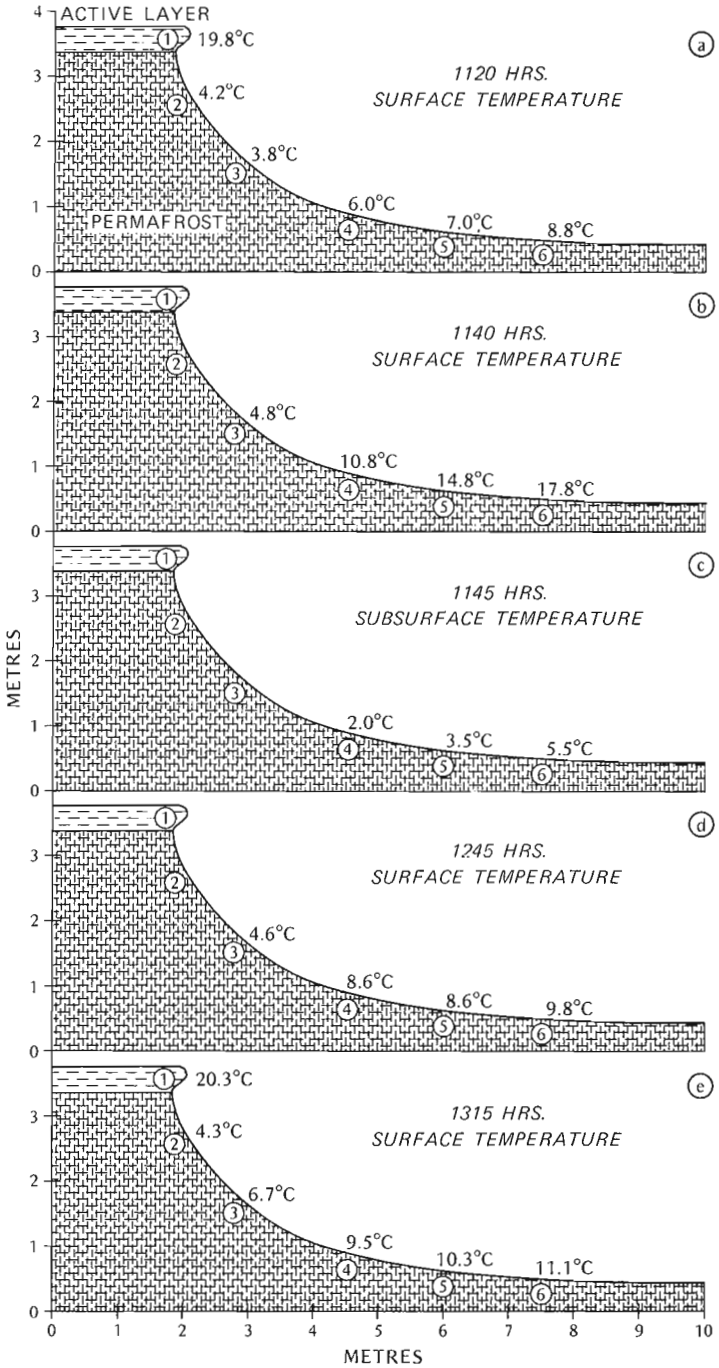

Figure 2. Radiometer surface temperatures for the thawing headwall shown in Figure 1 as measured on a bright, calm day, August 15, 1965. The subsurface measurements were with a thermistor probe.

Data for August 15, 1965 are shown in Figure 2 and in Table 1 for the 1000 h to 1530 h period when the headwall was in bright sunshine, the air temperature ranged from 16°C to 23°C, and there was no wind. All surface temperatures were well above 0°C. The lowest temperatures (Table 1) were for clear ice lenses, usually with little included soil. The ice lenses were covered, at the most, with a thin film of water. When the water film grew sufficiently thick to flow down the scarp face, warmer mud quickly was incorporated into the water and then the temperature increased rapidly. Ice with many mud pellets and soil inclusions registered a much higher temperature than clear ice. The temperatures of organic matter and of viscous mudflow debris often exceeded the ambient air temperature.

Figure 2 shows that the surface temperature increased rapidly as muddy water flowed downslope. The amount of water flowing from site 2 to 3 (Fig. 2) was so slight that a velocity estimate was usually impractical. The time taken for flow from site 3 to 5 was usually less than 15 s and from site 5 to 6 less than 30 s. Therefore, a surface temperature warming of 5°C or more often occurred in less than a minute as muddy water flowed from site 3 to 6. Subsurface measurements at sites 4, 5, and 6, however, showed that the warming usually was confined to a thin surface skin, because at a depth of 1 cm the temperature was as much as 10°C colder than at the surface (Figs. 2b and 2c).

Conclusions

The radiometer surface temperature measurements of a thawing headwall in high ice-content permafrost on a bright August day show that all temperatures were well above 0°C including that of lens ice covered by only a thin film of water. The surface temperature rose with an increase in the soil content. As water flowed downslope and entrained mud en route, surface temperatures increased rapidly: a rise of 5° to 10°C often occurred in less than one minute. When the flow was thick enough (e.g. 1 cm or more) so that subsurface temperatures could be measured, however, a difference of up to 12°C existed between surface and subsurface temperatures. The implication of the preceding for the modelling of ablation studies is evident, because of 0°C or near 0°C surface temperature cannot be inferred for a thawing permafrost face, even when only a thin water film is present, and, moreover, the temperature will vary from top to bottom. The above 0°C temperatures of thawing permafrost surfaces also should be considered in evaluating some remote sensing techniques which have been used in the past in an attempt to map thawing permafrost exposures.

References

Gates, D.M.
1961: Winter thermal radiation studies in Yellowstone Park; Science, v. 134, no. 3471, p. 32-35.

Kerfoot, D.E. and Mackay, J.R.
1972: Geomorphological process studies, Garry Island, N.W.T.; in Mackenzie Delta Area Monograph, ed. D.E. Kerfoot; 22nd Int. Geogr. Cong. (Montreal), p. 115-130.

Mackay, J.R.
1966: Segregated epigenetic ice and slumps in permafrost, Mackenzie Delta area, N.W.T.; Geogr. Bull., Ottawa, v. 8, p. 59-80.

Stoll, A.M. and Hardy, J.D.
1952: A method of measuring radiant temperatures of the environment; J. Appl. Physiol., v. 5, p. 117-124.

THE USE OF SNOW FENCES TO REDUCE ICE-WEDGE CRACKING, GARRY ISLAND, NORTHWEST TERRITORIES

J. Ross Mackay[1]
Terrain Sciences Division

Ice wedges are widespread in Arctic Canada. Ice-wedge cracking can cause problems in northern construction. In the U.S.S.R. ice-wedge cracking has created excessive deformations of buildings and has ruptured underground communication cables. Ice-wedge cracks belong to the category of thermal contraction cracks which result from low winter ground temperatures. At Garry Island, Northwest Territories, ice-wedge cracking has been studied since 1967 at three sites with a natural snow cover (Mackay, 1974), and it has become evident that crack frequency is inversely related to snow depth (Fig. 1). Consequently, in 1974 two snow fences were installed at Garry Island to see if excess snow would reduce or prevent ice-wedge cracking. This note summarizes the results of the snow fence experiment for the period 1974-1977.

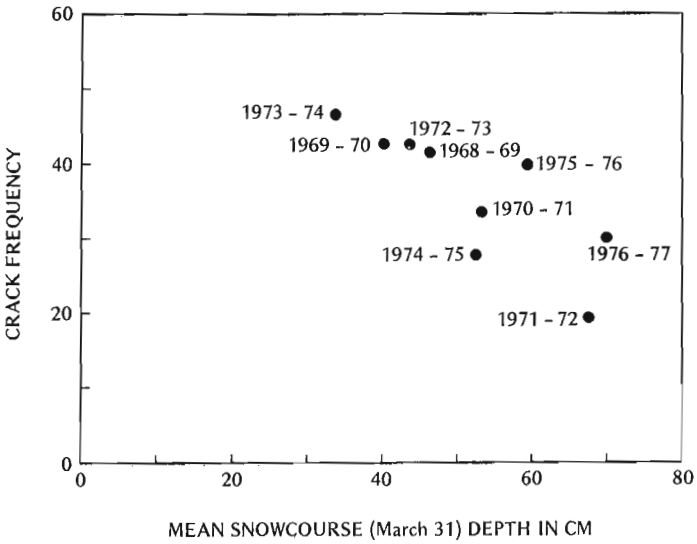

Figure 1. The relationship between mean snow cover for a snowcourse (Mackay and MacKay, 1974) and crack frequency for 100 ice-wedge cross-sections at Garry Island, N.W.T.

Field Experiment

In the summer of 1974, two wooden slatted, 30 m-long snow fences, 1.2 m high, were installed near an ice-wedge experimental site on Garry Island (Mackay, 1974, his Fig. 3, Site C) where data on ice-wedge cracking were available since 1967. The fences were supported by steel pipes anchored in holes drilled into permafrost. Where possible, the bottoms of the fences were raised about 20 cm off the ground, but locally, the fences touched the ground because of topographic irregularities. The snow fences were placed about 20 m apart and oriented northeast-southwest, at right angles to the prevailing winter winds (Fig. 3). Twenty-four snowpoles also were driven into the ground. In order to determine where ice-wedge cracking occurred, 25 "breaking cables" of fine copper wire were buried in the active layer of the ice-wedge troughs (Fig. 3; Mackay, 1974, p. 1367-1370). Previous experience had shown that such fine wires usually broke if an ice wedge cracked and did not break if the ice wedge did not crack.

Results

In the winters of 1974 to 1977, the additional snow depths in mid-December in the central part of the snow fence area reached about 50 to 80 cm. By mid-March, the snow depths along the fences ranged from about 1.2 to 1.5 m, and snow depths midway between the fences averaged about 1 m (Fig. 2). The snow was windblown and hard packed, with a density of 0.35 to 0.45 g/cm^3. In 1974-75 none of the 25 breaking cables broke; in 1975-76 cables 31, 32, 40, and 50 broke; and in 1976-77 cables 31 and 32 broke.

Figure 2. View looking across the snow fence site on March 19, 1975. Note that only the tops of the 1.2 m-high snow fences protrude, and some parts are completely under the snow. No ice wedges within the field of view of the photograph cracked.

[1]Department of Geography, University of British Columbia, Vancouver, British Columbia, V6T 1W5

From: Scientific and Technical Notes in Current Research, Part A; Geol. Surv. Can., Paper 78-1A.

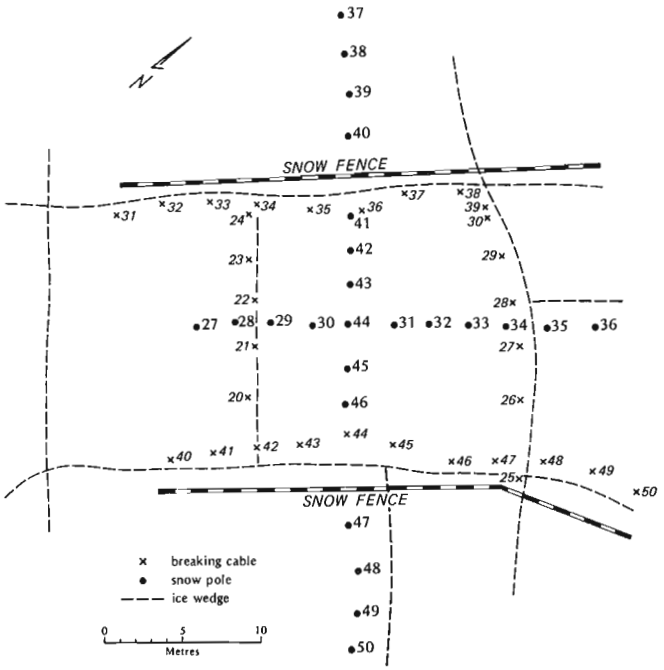

Figure 3. Diagram of the snow fence site showing the locations of the ice wedges, breaking cables, and snowpoles.

Discussion

In the three year period 1974-1977, the only signs of ice-wedge cracking, along some 80 linear metres of ice wedges, was at the periphery of the snow fence accumulation area (breaking cables 31, 32, 40, and 50) where snow depths were far less than in the centre. Thus, the snow fences effectively prevented ice-wedge cracking except for the sparser snow depth areas at the ends of the fences. The prevention or reduction of cracking can be attributed to the insulation effect of snow, which reduced the amplitude of the ground temperature and keeps it warmer than the undisturbed site would otherwise be.

Conclusion

The frequency of ice-wedge cracking at Garry Island, Northwest Territories, and presumably in other arctic areas is dependent, to a considerable extent, on the snow cover. At Garry Island when the snow cover on the ground approaches 1 m, ice wedges rarely crack. Snow fences or other means of insulation may be used to prevent ice-wedge cracking. By inference, sheltered areas of deep snow probably have few or no active ice wedges. The cracking of ice wedges cannot be forecast solely from a knowledge of winter air temperatures.

References

Mackay, J.R.
1974: Ice-wedge cracks, Garry Island, Northwest Territories; Can. J. Earth Sci., v. 11, p. 1366-1383.

Mackay, J.R. and MacKay, D.K.
1974: Snow cover and ground temperatures at Garry Island, N.W.T.; Arctic, v. 27, p. 287-296.

AN ACTIVE RETROGRESSIVE THAW FLOW SLIDE ON EASTERN MELVILLE ISLAND, DISTRICT OF FRANKLIN

J.A. Heginbottom
Terrain Sciences Division

During field work on eastern Melville Island in July 1977, two active retrogressive thaw flow slides were noted in the lower valley of the stream draining Tingmisut Lake (75°56'N, 107°54'W). The slides were on either side of the stream valley, in slumped and frost riven material of the Canyon Fiord Formation, about 1.5 km from the lake and an equal distance from the sea at Weatherall Bay. Figure 1 shows the slide area on the southwest side of the valley. Figures 2 and 3 and Table 1 all relate to the slide on the northeast side of the valley, which was examined in some detail.

The slide was first visited on the morning of July 17, 1977, and a set of marker pegs was installed around the uphill edge of the slide area. The pegs were 30 cm lengths of 2 cm diameter birch dowel. Distances between pegs and from the pegs to the edge of the slide area were measured to the nearest centimetre using a steel tape. The bowl or basin of the slide was roughly circular in shape, with a diameter of approximately 45 m. The side and backwalls were 50 to 250 cm high. Exposed in the backwall was a layer of thawed soil, 75 to 100 cm thick, overlying massive ice with dirt bands at least 2 m thick. The headwall was retreating actively. Near the foot of the headwall the floor of the basin was a mass of liquid mud with free water on the surface. This mud was moving slowly downhill, draining and drying as it did so. Farther out from the headwall the water was flowing in the central part of the slide zone, with bands of dried mud on either side.

Headwall retreat was mainly by melting of the exposed massive ground ice and the continual falling away of the thawed soil above as individual crumbs to clods of soil, rather than as coherent blocks. Clods of soil falling onto the icy glacis slid down it and dissolved into the liquid mud of the basin floor.

Along the sides of the basin, there were several cracks in the ground surface several decimetres from the edge. As these walls were not retreating actively, it was not clear when, how, or why these cracks had developed.

Table 1
Headwall retreat of retrogressive thaw flow slide, Tingmisut Lake, Melville Island, Northwest Territories

Date and time of survey	Line and distances (m) P	Q	R	S	T
17 July 1977, 1210h	18.67	16.61	15.00	13.59	14.12
21 July 1977, 1615h	17.94	16.13	14.22	13.18	13.69
Differences (m/100 h)	0.73	0.48	0.78	0.41	0.43
Mean rate of headwall retreat (m/100 h)			0.57		

The absolute age of the two slides is not known. They are not visible as discrete features on the 1959, 1:60 000 scale aerial photographs. Examination of these photographs (A16763-54 and -55) shows that the valley of this stream is marked by numerous landslide scars of various ages.

Similar features to these slides have been described from the Mackenzie Delta area (Mackay, 1963; Kerfoot and Mackay, 1972), from Banks Island (French and Egginton, 1973), and from Ellef Ringnes Island (Lamothe and St-Onge, 1961).

The slide was examined again on the afternoon of July 21, 1977, and the distances from the pegs to the headwall were remeasured. From these two sets of measurements (Table 1) the amount of headwall retreat was determined. In the 100 hours between the two sets of measurements, the amount of retreat was between 40 and 80 cm. During this time, the air temperature, measured at the camp at Tingmisut Lake, ranged from +1 to +13°C with an average of +6.5°C. There was only a trace of precipitation.

The mean rate of retreat of 0.57 m/100 h compares well with values reported by Kerfoot and Mackay (1972) for "mud slumps" on Garry Island in the Mackenzie Delta and by French (1974) from eastern Banks Island. Kerfoot and Mackay surveyed a large mud slump on Garry Island nine times between June 1964 and August 1971. In 1964, 1965, and 1971 they visited it twice each summer, and retreat rates in metres/100 hours can be derived from the data they present. The mean rate was 0.28 m/100 h, whereas the maximum rate was 0.46 m/100 h. French surveyed two "slumps" in the Thomsen River-Johnson Point area of Banks Island in 1972

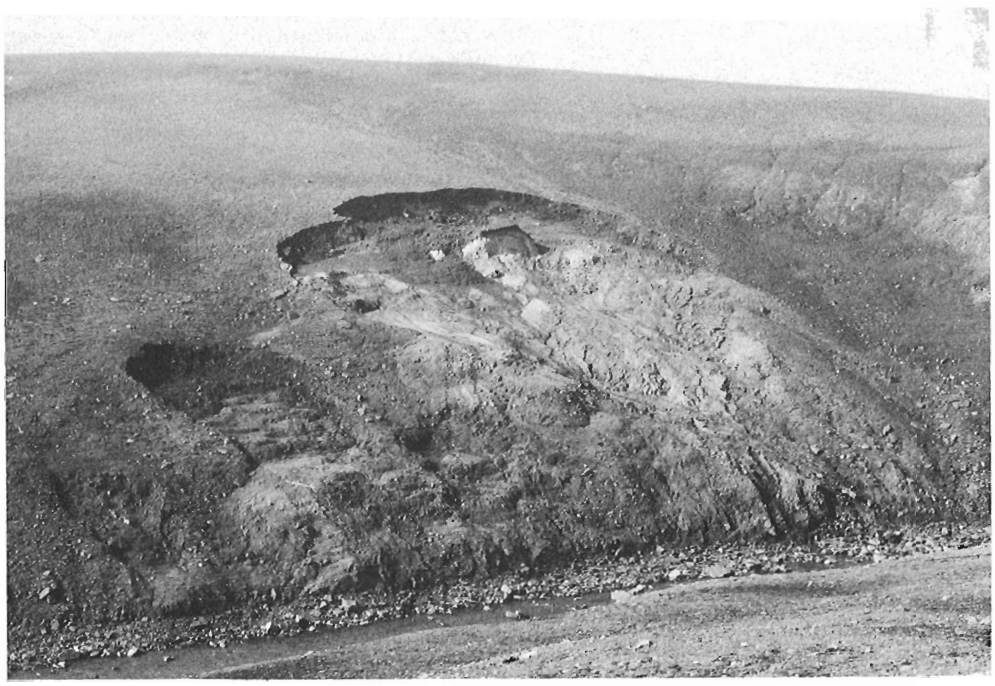

Figure 1

Retrogressive thaw flow slide on the southwest side of a valley (July 17, 1977).

From: Scientific and Technical Notes in Current Research, Part A; Geol. Surv. Can., Paper 78-1A.

Figure 2

Detail of headwall of a slide on the northeast side of a valley. See Figure 3 for the location of the area shown (July 17, 1977).

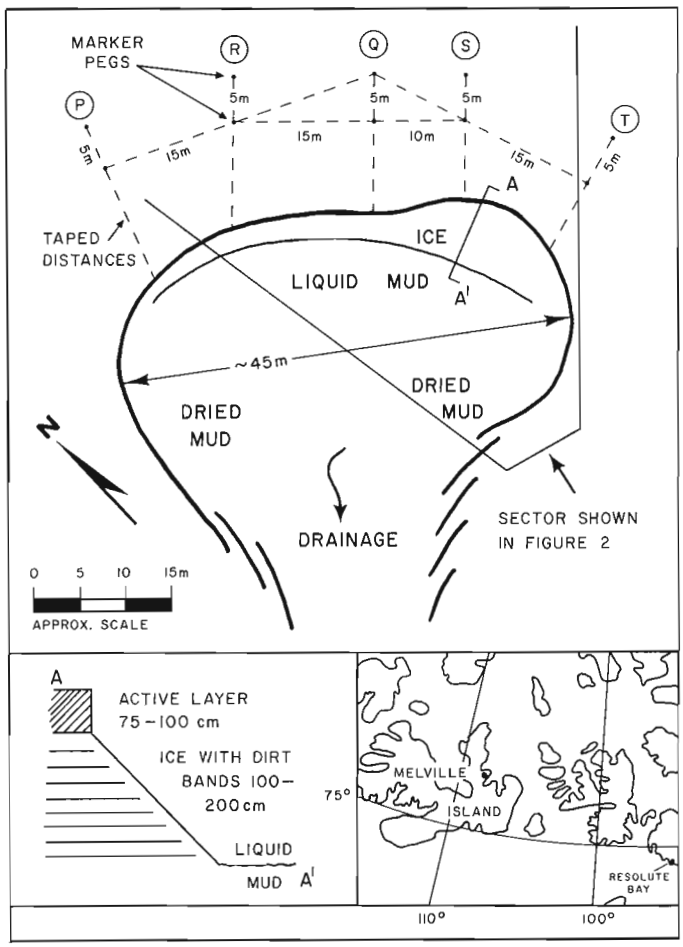

Figure 3. Sketch plan of retrogressive thaw flow slide near Tingmisut Lake, Melville Island, N.W.T.

and 1973. Mean retreat rates calculated from his data are 0.43 m/100 h for 1972 and 0.56 m/100 h for 1973. The minimum rate was 0.22 and the maximum 1.08 m/100 h.

It is hoped to revisit these features in the future and to make further measurements on their rate of development.

References

French, H.M.

1974: Geomorphological processes and terrain sensitivity, Banks Island, District of Franklin; in Report of Activities, Part A; Geol. Surv. Can., Paper 74-1A, p. 263-266.

French, H.M. and Egginton, P.A.

1973: Thermokarst development, Banks Island, Western Canadian Arctic; in Permafrost: North American Contribution, 2nd Int. Conf. Permafrost (Yakutsk, U.S.S.R.); Nat. Acad. Sci. Publ., Washington, p. 203-212.

Kerfoot, D.E. and J.R. Mackay

1972: Geomorphological process studies, Garry Island, N.W.T.; in Mackenzie Delta Area Monograph, ed. D.E. Kerfoot; Brock Univ. for 22nd Int. Geogr. Cong. (Montreal), p. 115-130.

Lamothe, C. and St-Onge, D.A.

1961: A note on a periglacial erosional process in the Isachsen area, N.W.T.; Geogr. Bull., no. 16, p. 104-113.

Mackay, J.R.

1963: The Mackenzie Delta area, N.W.T.; Dep. of Mines and Tech. Surveys, Geogr. Branch, Mem. 8.

AN EXAMPLE OF COMPUTER SOLUTIONS TO GROUNDWATER FLOW AND SLOPE STABILITY PROBLEMS

D.A. Proudfoot and P.B. Fransham
Terrain Sciences Division

Introduction

The natural heterogeneity of soil and rock lithologies renders the manual solution of groundwater flow and slope stability problems both time consuming and tedious. Computer solutions are, in most cases, efficient and generally more accurate. For the purpose of groundwater studies and slope stability analysis, four computer programs have been obtained. The groundwater flow program (UNSAT2) was developed by Neuman et al. (1974) and is capable of solving for both saturated and unsaturated flow. The other three programs, dealing with slope stability analysis, were compiled by Fredlund (1976). The main analysis program (SLOPE), used for calculating factors of safety, has many options making it versatile yet maintains a simple data input. Two supplementary programs (SLOPE1 and SLOPE2) are used for description and graphical presentation of the slope geometry and results of the stability calculations.

An integral part of a slope stability calculation is the estimation of pore pressures along the potential failure surface. Pore pressures can be obtained through field monitoring of piezometers or by mathematically simulating the groundwater flow. Either method can be used independently; however, a combination of field measurements and numerical simulation is by far the best approach. Where it is necessary to perform many stability calculations over a variety of geological sites, it may not be practical to instrument every potentially unstable slope with piezometers. An alternative is to use a numerical approach and to input the calculated pore pressures directly into the stability calculations. For this purpose UNSAT2 has been modified so that the pore pressures are output in a format compatible with the input to the program SLOPE. To illustrate the potential of the four programs, an example of a slope stability analysis using UNSAT2 and SLOPE is presented. The results of the stability calculations have been plotted using SLOPE1 and SLOPE2 and have been included in this report.

Description of hypothetical slope

To show the interaction of the four programs (Fig. 1) in analyzing a slope stability problem, a hypothetical slope was used. The slope is 20 m high and is at an angle of 30°. The stratigraphy consists of a basal layer of fractured bedrock, overlain by fissured sensitive clay, and capped by a layer of fine, well sorted sand. Normally there would be a vegetation cover; however, for the purposes of this example it has not been included. An external body of water (i.e., a river or lake) covers the slope to a depth of 5 m above the toe. Values of the hydraulic conductivity, porosity, and specific storage were assumed for each stratigraphic unit (Table 1).

The program UNSAT2 is capable of simulating actual climatic conditions; for the purpose of this example mean monthly precipitation values were used. Evapotranspiration is the volume of water which can be extracted from the soil by the combined effect of transpiration of vegetation and evaporation from the soil. This value has been calculated and subtracted from the monthly precipitation to give an approximate value of the potential flux of water across the infiltration-evaporation boundary. In some cases the potential infiltration will exceed the infiltration capacity of the soil. Water that does not enter the dynamic groundwater regime will be lost through runoff. The pore pressures in the

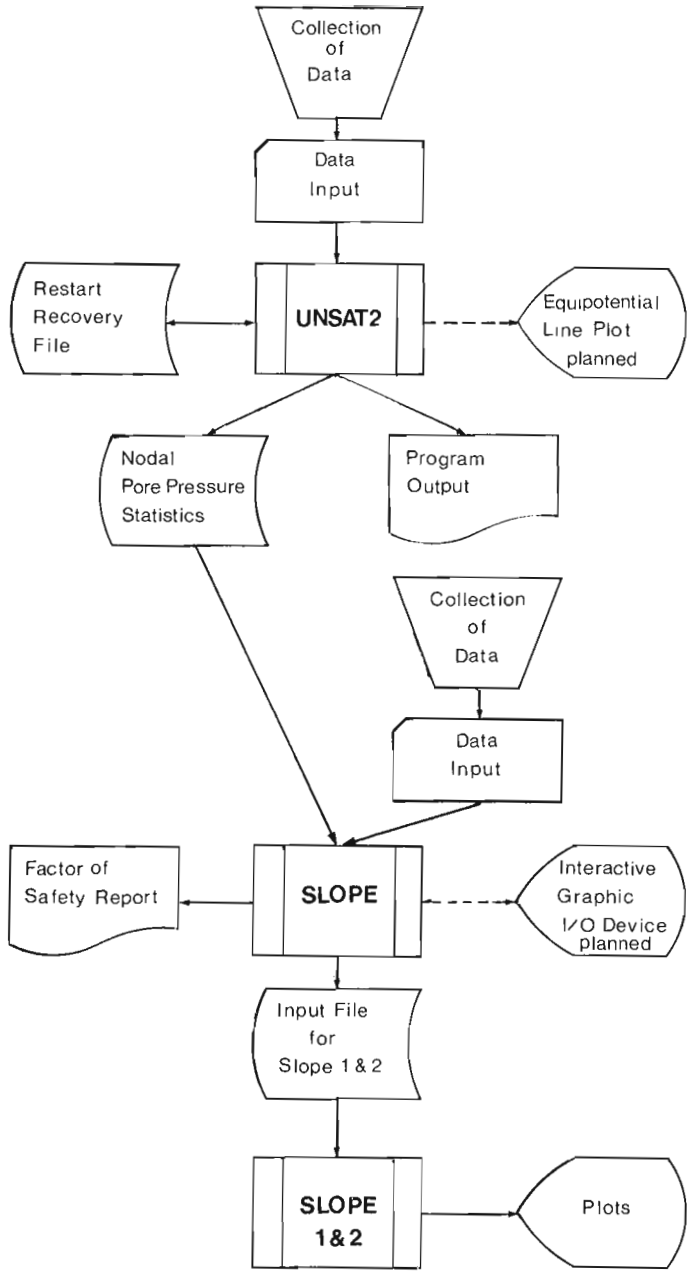

Figure 1. System flow diagram (dotted lines indicate planned enhancements).

Table 1

Hydraulic properties of the soil layers

Soil	Vertical Conductivity m/day	Horizontal Conductivity m/day	Porosity %	Specific Storage
Fractured Bedrock	8.46×10^{-2}	8.46×10^{-1}	45	0.0
Fissured Clay	8.46×10^{-6}	8.46×10^{-5}	50	0.0
Well Sorted Sand	8.46×10^{-2}	8.46×10^{-1}	35	0.0

From: Scientific and Technical Notes in Current Research, Part A; Geol. Surv. Can., Paper 78-1A.

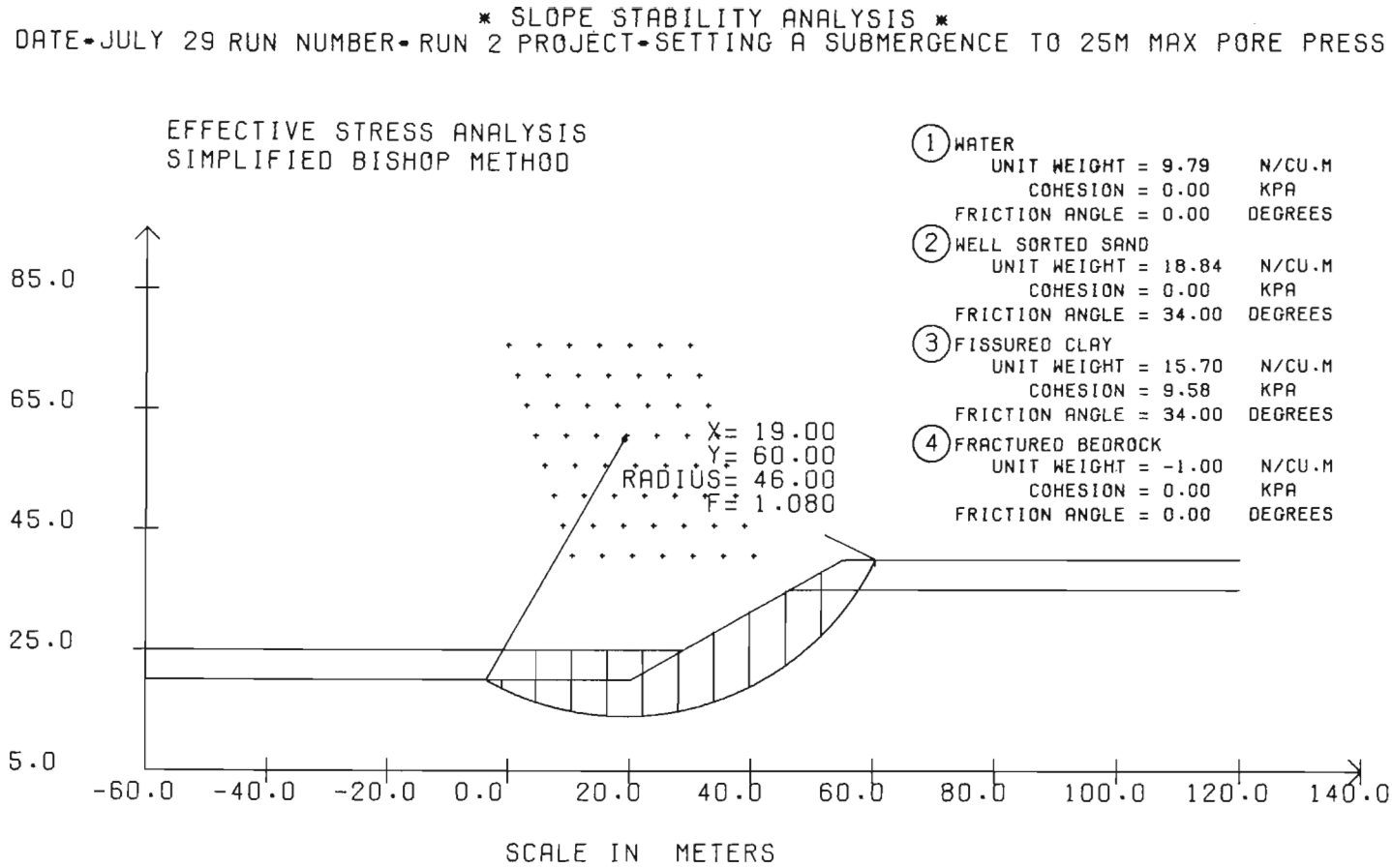

Figure 2. SLOPE1 plot of the problem geometry, critical failure circle, trial centre locations, and soil descriptions.

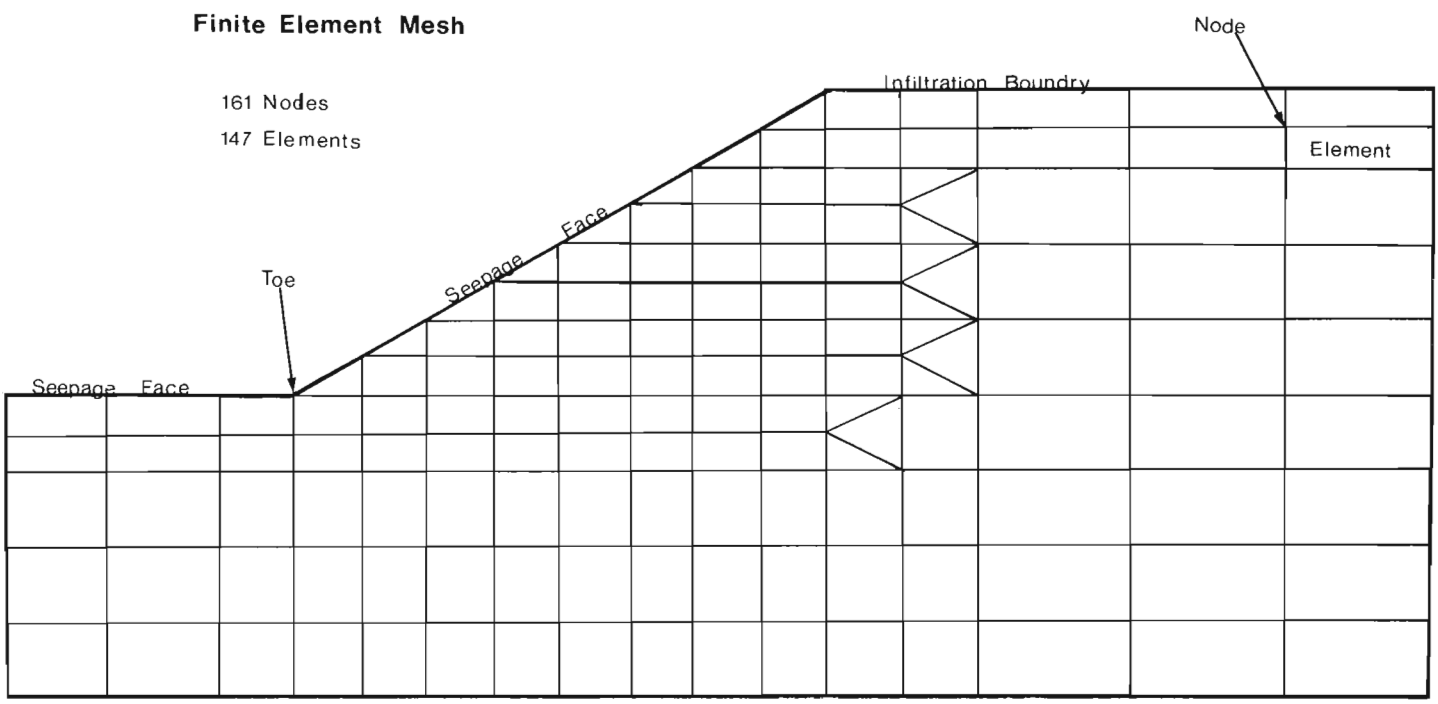

Figure 3. Finite element mesh used for the problem slope analysis example.

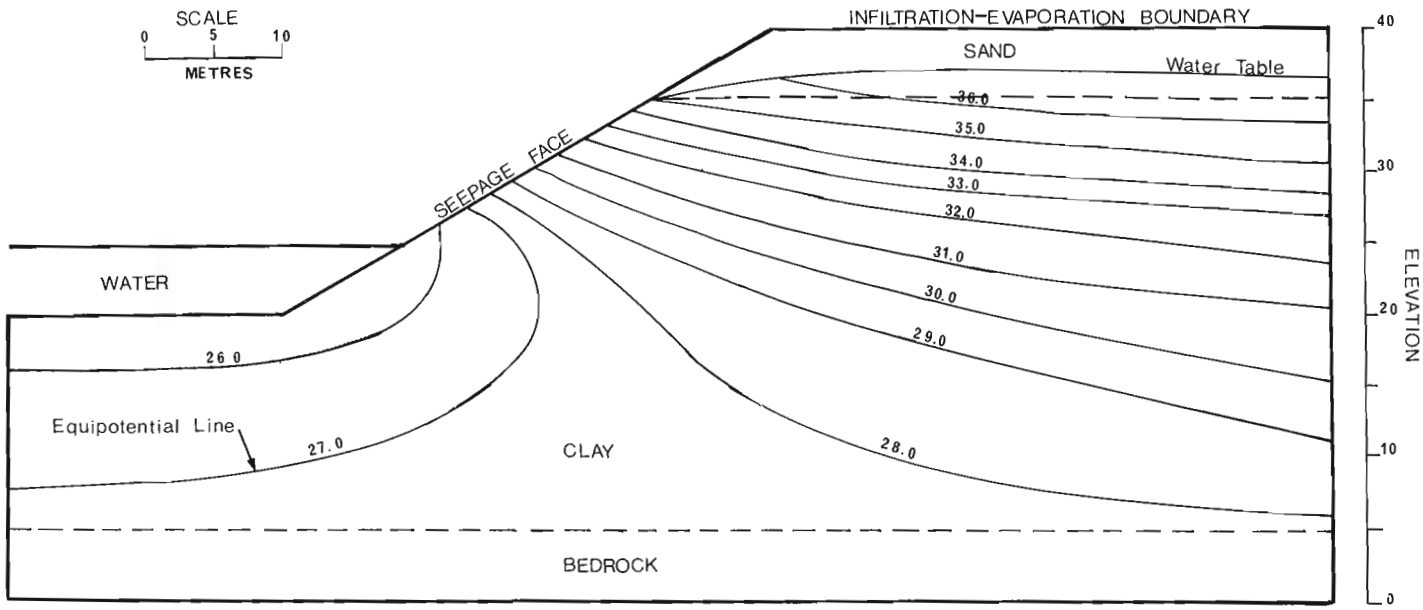

Figure 4. Plot of the equipotential lines for the problem slope analysis example using mean pore pressure values.

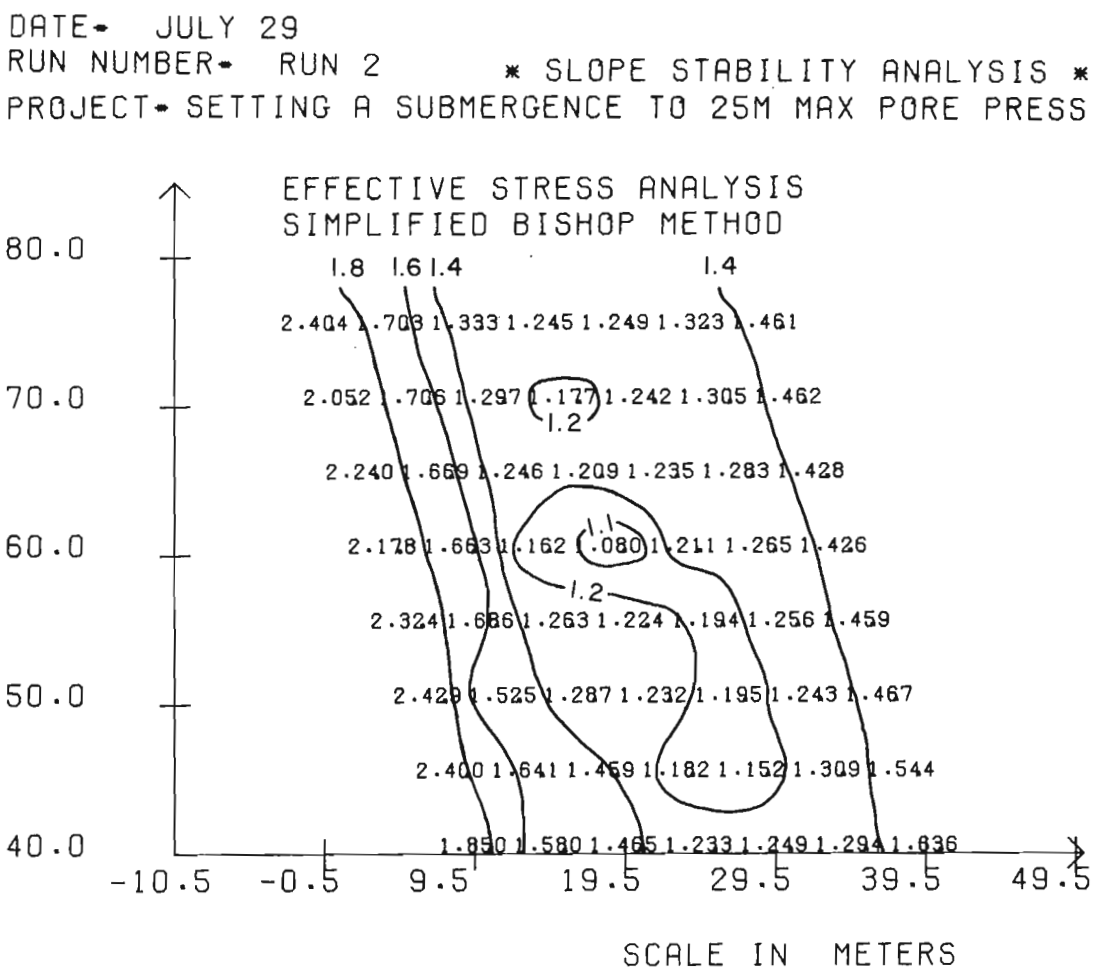

Figure 5. SLOPE2 plot of the trial centre locations with the minimum factor of safety recorded for each centre. Contoured by hand.

example were modelled for a period corresponding to one year. Mean, maximum, and minimum pore pressures were calculated for each node of the finite element mesh (Fig. 3). The mean pore pressure values were used in contouring equipotential lines (Fig. 4) and also are used as input to the stability analysis. Correlation of pore pressures measured in the field with those that were calculated indicates that the finite element method is a useful tool for obtaining estimates of pore pressures where field data is lacking. The results of the correlation and an indepth study of the groundwater regime in the Ottawa Valley are part of the second author's Ph.D. thesis.

The search for a minimum factor of safety was made using a grid of points as centres for trial failure arcs. At each of the trial centres, a series of different radii was used so that factors of safety were calculated for essentially all potential failure surfaces. Figure 2 shows the problem geometry, the trial centre locations, and the critical failure arc, together with some engineering properties corresponding to the different soil layers. The bedrock is assigned a unit weight of -1.0, which indicates that the layer is sufficiently strong that a trial failure circle will not pass through the bedrock. Figure 5 gives the minimum factor of safety for each trial centre. Contouring of Figure 5 was done manually and shows that the minimum factor of safety for the slope has a x-co-ordinate of 19.0 m and a y-co-ordinate of 60.0 m. The minimum factor of safety of 1.080 indicates that the slope is only marginally stable under the groundwater conditions simulated by UNSAT2 and the strength parameters assumed for the different soil layers.

Program Description

This section describes some of the options available in the programs and also the modifications which were made to optimize the programs for the computer available at Energy, Mines and Resources.

UNSAT2

UNSAT2 solves the problem of nonsteady flow of water in saturated-unsaturated porous media by a Galerkin type finite element approach. The program is capable of handling: 1) irregular boundaries; 2) varying degrees of local anisotropy; 3) uptake of water from the soil by plant roots, allowing for different species of plants to simulate more closely actual field conditions; and 4) axisymmetric flow to a partially or fully penetrating well.

In this example a finite element mesh consisting of 147 elements and 161 nodal points was used (Fig. 3). Both quadrilateral and triangular elements can be used. The mesh is drawn so as to give the maximum density of nodal points in the critical areas close to the crest of the slope and a lower concentration of nodes in areas where the likelihood of a slope failure occurring is remote. It is not necessary to input all node and element descriptions as data. The program will generate all the intervening nodes and elements within a soil type. It is necessary to input only boundary nodes and elements and also those elements that are triangular. A criterion of the mesh design is that the vertical lines are continuous from one side of the problem to the other. The maximum number of nodes along any one vertical line is directly related to the size of the computer memory needed to solve the problem. Therefore, in order for the program to run efficiently, the number of nodes in the vertical direction should be kept to a minimum.

UNSAT2 initially was written for use on an IBM 370-165 computer. Modifications to the original program have been made to convert the program to run on a CDC CYBER 70 Model 74 computer and to allow true dynamic field length modification. This eliminates the need to recompile the main program when running problems of different sizes and allows the program to run with minimum central memory storage. Provision also has been made to store the nodal point co-ordinates, the nodal number, and the mean, maximum, minimum, and standard deviation of the pressure head for each nodal point. These statistics may be generated for any desired time span. The file in which the statistics are saved can be catalogued and used as input to other programs requiring pore pressure data.

A planned future enhancement to the program is a subroutine which will plot the problem geometry, including soil boundaries and properties, and the pore pressures at the nodal points. Provisions also will be made to contour equipotential lines from the pore pressure grid.

SLOPE

The computer program SLOPE offers six different methods of slope stability analysis. Each method employs slightly different statistics in deriving the factor of safety as well as different assumptions which render the problem determinant (Fredlund, 1974). Because the factor of safety obtained is dependent on the method of analysis, this program affords the user the option of calculating the factor of safety by several different methods, allowing comparisons of the various results.

One option allows the generation of the information necessary to plot the slope geometry, critical circle, and grid of radius centres (SLOPE1, Fredlund, 1976). Also the grid circle centres can be requested and plotted with the corresponding factors of safety and/or slip circle radii (SLOPE2, Fredlund, 1976).

Local enhancements and modifications have been made to the SLOPE program to facilitate its implementation and operation on the CDC CYBER 70 Model 74 computer. Modifications to the SLOPE program have drastically reduced the central memory requirements. Further debugging output was added at critical points in the program to aide with program verification and error detection and now is controlled by an input parameter. Options to have the output in either English or SI units and to have soil descriptions plotted through SLOPE1 along with the soil parameters have been included. Programs SLOPE1 and SLOPE2 have been combined to allow intermixed SLOPE1 and SLOPE2 data to be plotted in one run.

A planned enhancement to the slope analysis system is the ability to plot and contour the POR5 (pore pressure) grid from the SLOPE program; this subroutine will be the same routine to be implemented with UNSAT2. The program will be converted locally for use with the CDC SEGLOAD utility, allowing further central memory reduction. In conjunction with core reduction, an interactive graphics input-output option is planned whereby a user can sketch his problem geometry directly on a CRT (cathode ray tube) and have the critical slip circle plotted immediately.

References

Fredlund, D.G.

1974: Slope stability analysis – user's manual; Dep. Civ. Eng., Univ. Saskatchewan, Saskatoon.

1976: CALCOMP Plotting of geometry and factor of safety for slope stability analysis – user's manual; Dep. Civ. Eng., Univ. Saskatchewan, Saskatoon.

Neuman, S.P., Freddes, R.D., and Bresler, E.

1974: Finite element simulation of flow in saturated-unsaturated soils considering water uptake by plants; Israel Inst. Technol. 3rd Ann. Rep., Part 1, Haifa.

AN EFFICIENT, LOW COST, AEOLIAN SAMPLING SYSTEM

P.S. Rosen
Atlantic Geoscience Centre, Dartmouth

Introduction

A system for monitoring the total aeolian transport in a coastal sand dune environment was developed and field tested. An aeolian trap was modified and enlarged from a device described by Leatherman (1976). This sampler proved effective for both unidirectional and multidirectional sampling over either short- or long-term intervals. Concurrently, small diameter pins set in arrays around the samplers give an accurate measurement of dune or beach deflation and accretion.

Specifications

The body of each sampler unit (Fig. 2) consists of a 106 cm length of Schedule 40 PVC sewer pipe (10 cm I.D.). Two slits, 6.3 cm and 9.8 cm wide, extend 45 cm down from the top of the tube. The larger slit is covered with 60 micron screening, while the other serves as an entry for sediment. The base is covered with window screening. A 60 cm liner (9.5 cm O.D.) of clear plastic is capped at one end with 60 micron screening. The liner fits into the base of the sampler loosely, to inhibit jamming by sand. An O-ring (Precision No. 153) forms a seal at the top. A string was glued to the top of the liner to facilitate removal. Small fins may be glued at the base of the unit to prevent shifting when in place. The cost of materials for each unit is less than $14.

The aluminum pins are 1 m long, and .32 cm wide (1/8"). A washer (1/4" opening) loosely slides on this shaft.

Discussion

The sampler unit is buried to the level of the slits. The narrow slit is oriented in the direction to be sampled. The screening provides maximum possible flow-through of wind, while trapping all sand-sized material in the liner. The screening on the liner allows rain water to drain, and prevents bouyancy from ground water. The units may be placed in sets of four to provide multidirectional sampling. The large slits leave a small solid surface in the direction of sampling. Resistance and scour are thus minimized. Wind scour around the sampler is reduced further by tamping the sand around the unit when it is buried.

Figure 1

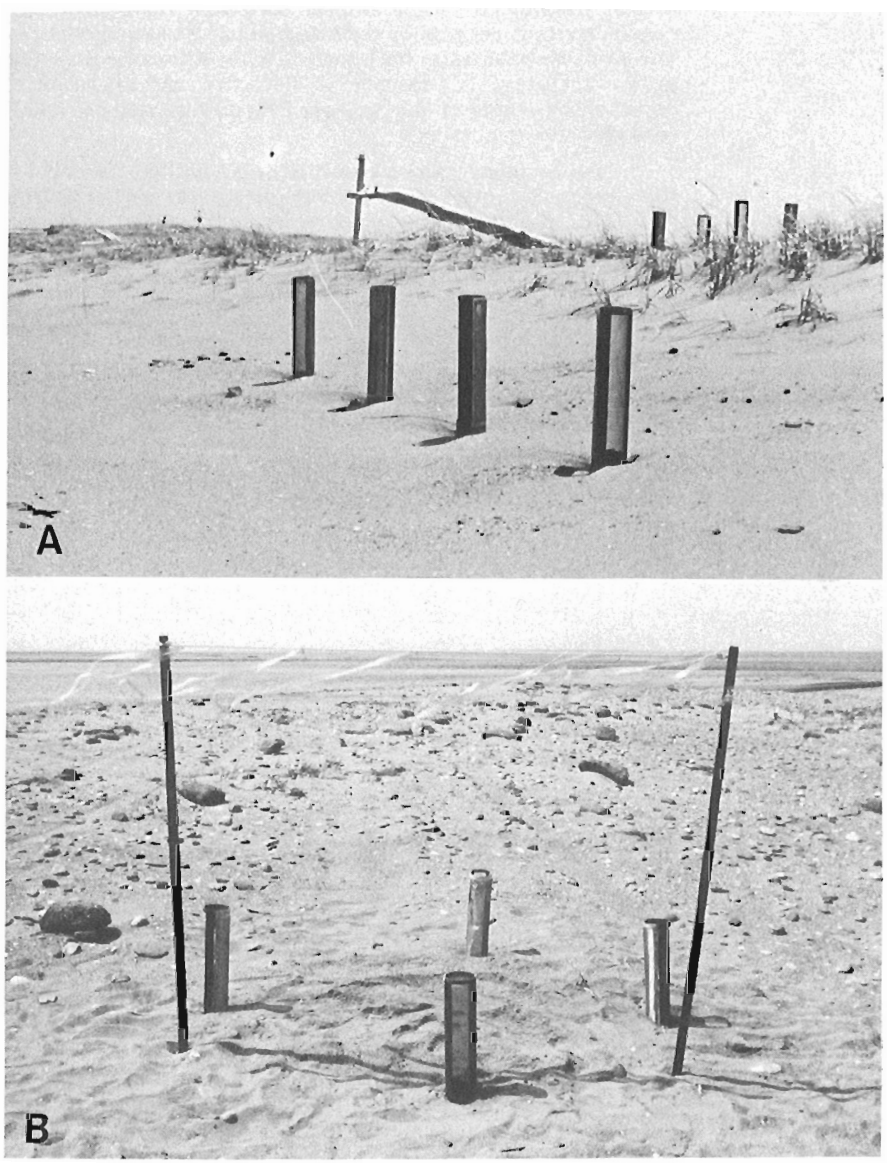

A. Sets of sampling units arranged linearly at the base and crest of a sand dune. This arrangement provides measurements of offshore-onshore, and longshore transport in both environments.

B. A set of sampling units arranged in a square pattern on an overwash area. The scarecrow prevents interference by seagulls.

From: Scientific and Technical Notes in Current Research, Part A; Geol. Surv. Can., Paper 78-1A.

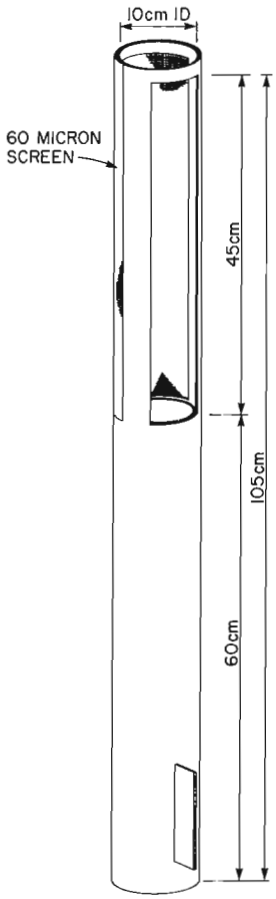

Figure 2. The aeolian transport sampler.

The liner provides two advantages:

- A 'stratigraphic' record of the variations in transport is preserved in the liner.
- Emptying the unit is efficient, as the liner can be pulled up, and replaced with another without disturbing the sampler. Detailed sampling can also be made by measuring the distance down the liner to the sediment surface. In this way, the position of sedimentation units in the liner is known, and can be correlated with precise wind and weather data.

The total capacity of the trap is .075 m^3/linear metre of beach. Although a single storm can move this much material, the units never were completely filled in non-storm intervals up to one month.

The samplers often accumulated significant volumes of amphipods and other fauna. Hence, seagulls repeatedly damaged the units in the spring nesting season. They only attacked units in unvegetated areas. This problem was circumvented with scarecrows of flagging tape. The use of similar units for biologic sampling should be considered.

The sampler sets were placed in a linear pattern on linear features, such as dune crests and dune bases. In open areas, they were placed in a square pattern (Fig. 1A, 1B).

The aluminum pins were placed in transects and arrays in the vicinity of each set of samplers. The pins gave concommittant records of dune and beach elevation changes. The pins were initially half buried, with the washers resting at the surface. A sequence of deflation and accretion is recorded by burial of the washer. The pins caused no visible resistance to wind flow.

An accurate measurement of total aeólian transport in the longshore, and shore-normal directions and resulting elevation changes can be obtained efficiently with this sampling system.

Reference

Leatherman, S.P.
1976: Quantification of overwash processes: unpubl. Ph.D. thesis, University of Virginia, 245 p.

BOTTOM SEDIMENTS – VICINITY OF JUAN DE FUCA AND EXPLORER RIDGES, NORTHEAST PACIFIC OCEAN

D.L. Tiffin, B.D. Bornhold, C.J. Yorath, R.H. Herzer, and G.C. Taylor[1]
Regional and Economic Geology Division, Vancouver

Introduction

During August 1977, the authors undertook a sediment coring cruise on **CFAV Endeavour** to the region traversed by Explorer and Juan de Fuca ridges in the northeast Pacific Ocean (Fig. 1). The purpose of the cruise was to obtain regional information on sediment types within deep water basins associated with these ridges, and to examine the sediments for possible mineralization through hydrothermal enrichment.

Table 1

List of core locations, lengths and water depths

Core No.	Water Depth metres	Core Length centimetres	Latitude	Longitude
1	3015	16	50° 12.01	131° 26.14
2	3030	42	50° 10.56	131° 10.58
3	2650	60.5	50° 05.64	130° 44.96
4	2540	152	50° 05.65	130° 36.74
5	2690	59	50° 05.25	130° 19.07
6	1805	155	50° 04.24	130° 09.31
7	2070	283	50° 03.99	129° 59.20
8	2550	190	50° 04.67	129° 54.22
9	2350	133	49° 57.16	129° 43.74
10	2465	152	49° 49.50	129° 43.86
11	No Recovery			
12	3240	167	49° 38.97	132° 04.04
13	3260	166	49° 40.45	131° 56.24
14	3170	193	49° 40.11	131° 38.20
15	2760	121	49° 42.40	130° 56.03
16	2855	85	48° 37.51	130° 14.81
17	2845	146	48° 41.04	130° 21.77
18	2830	130	48° 44.34	130° 27.21
19	3405	218	48° 52.03	130° 45.07
20	3225	182	49° 21.55	132° 21.90
21A	No Recovery			
21B	3215	165	49° 19.26	132° 14.21
22	3260	300	49° 13.59	131° 54.19
23	3235	300	49° 11.30	131° 48.47
24	3245	300	49° 09.70	131° 42.04
25	3480	287	48° 55.83	133° 23.12
26	3280	209	49° 04.29	133° 09.27
27	3165	240	49° 22.48	132° 39.13
28	3725	238	48° 15.60	134° 30.27
29	3695	589.5	48° 34.24	133° 56.69
30	No Recovery			
31	3230	107	49° 04.75	131° 27.14
32	3290	115	49° 00.07	131° 15.92
33	2775	169	49° 43.43	130° 38.87
34	2445	115	49° 18.14	130° 12.76
35	2500	62	49° 20.25	130° 14.14
36	2605	91	48° 00.54	128° 48.50
37	2540	188	48° 03.15	128° 53.56
38	2565	225	48° 07.34	129° 10.47
39	2700	115	48° 11.14	129° 23.50
40	2680	102	48° 14.54	129° 30.98
41	2820	281	48° 17.16	129° 36.49
42	2475	53	48° 27.15	128° 39.41
43	2440	101	48° 27.77	128° 36.83
44	2425	134	48° 28.42	128° 32.56

[1] Institute of Sedimentary and Petroleum Geology, Calgary.

In 1976, R.D. Hyndman measured very high values on heat flow profiles made in the vicinity of northeast Juan de Fuca Ridge (Hyndman et al., in press). High resolution subbottom profiles taken concurrently over the heat flow drift profiles by Geological Survey of Canada and University of Washington indicated that in at least one area peaks in heat flow (17.6 h.f.u.) coincided with sediment mounds apparently formed above normal faults in the oceanic basement, comparable to hydrothermal sediment mounds found near the Galapagos rift zone and other oceanic areas (Williams et al., 1974; Craig, 1966; Bischoff, 1969; Backer and Schoell, 1972; Bostrom and Peterson, 1966; Dymond et al., 1973; Piper et al., 1975; Cronan, 1976; Bischoff and Rosenbaur, 1977; Corliss et al., in press). Under conditions of active oceanic crust generation, hydrothermal circulation of sea water within the crust (Lister, 1972) brings dissolved minerals to the sea floor which are precipitated in both the oceanic basalts and in the supra-adjacent sediments (Andrews and Fyfe, 1976; Fryer and Hutchison, 1976).

To evaluate the mineral potential of sediments adjacent to plate sutures of the northeast Pacific Ocean, two coring cruises were made in 1977. The first, conducted by the Department of Geology at the University of British Columbia, concentrated its efforts in three small basins, one close to the northeastern end of Juan de Fuca Ridge where the highest heat flux values were obtained and two others at the northeastern end of Explorer Ridge. The second cruise, conducted by the Geological Survey was more regional in scope and was designed to evaluate several basins over a broader area of the ridges and to obtain background sediment information.

Navigation for the Geological Survey of Canada cruise was accomplished by the use of Loran-C, the land based stations which began transmitting earlier in 1977. Loran-C readings were recorded every five minutes during data recording periods, corresponding to each 2/3 mile at the reduced ship's speed. Navigational precision was excellent (estimated to be within 30 m repeatability) which allowed for precise repositioning over core sites.

A 3.5 kHz high resolution subbottom profiling system was used to obtain shallow seismic profiles along predetermined tracks across the region (Fig. 1). Magnetic data were also collected concurrently. Following completion of each overnight line segment, favourable core locations were selected on the flanks of, and within, narrow and broad basins of sedimentary areas bounded by ridges and seamounts (Fig. 2). Loran-C co-ordinates for each core site selected were recovered from the navigation.

Upon recovery, each core was split, subsampled for geochemical analysis, described with the aid of binocular microscope, and photographed on board ship. After examination and since cruise completion the cores have been placed in cool storage (4°C) while subsamples collected for geochemical analysis were frozen.

From: Scientific and Technical Notes in Current Research, Part A; Geol. Surv. Can., Paper 78-1A.

The most striking aspect of the sediments of the region is their degree of uniformity across a very broad area. With the exception of the westernmost cores (28 and 29) the stratigraphy is generally represented by four units: an uppermost grey unit, followed by a dark brown layer, a transition unit, and a bottom medium to dark grey unit. Table 1 lists core number, location, water depth and length for each core and Table 2 lists the thicknesses of each unit for the cores obtained.

The uppermost unit comprises medium grey, water saturated, soft, silty lutite that varies in thickness from zero to 27 cm thick (Table 2). Other components of this unit include finely disseminated opaque minerals, diatoms, and foraminifera. This layer has rarely been reported in cores collected in deep water from other areas of the eastern Pacific Ocean.

Underlying the "upper grey unit" with commonly sharp but locally convoluted and interdigitated contact is the "dark

Table 2

Thickness of core units in centimetres

Core No. Type	1.	2.	3.	4.	3+4	Remarks
1(A)	NR	1	NR	16		
2(A)	4	4.5			33.5	
3(A)	2	9	6	43.5		
4(A)	9	7	69	66		
5(A)	NR	3	56	NR		Obsidian sand in Cutter
6(A)	8	6	54	87		
7(A)	22	5.5			255.5	
8(A)	6	12			172	
9(A)	NR	6			127	
10(A)	NR	5			147	
11(A)	–	–	–	–	0	No recovery
12(A)	12	24	NR	131		
13(A)	NR	2	NR	164		Basalt pebbles in 4
14(A)	3	8	9	173		
15(A)	NR	2	6	113		
16(A)	NR	4	5	76		
17(A)	4.5	8.5			133	
18(A)	NR	12.5			117.5	
19(A)	3	10	16	189		
20(A)	6	29	NR	147		
21A(A)	–	–	–	–	0	No recovery
21B(A)	12	7	14.5		131.5	
22(A)	27	22	NR	251		
23(A)	9	17	NR	274		
24(A)	NR	17	NR	183		
25(A)	9	19	14	245		
26(A)	NR	46	26	137		
27(A)	3	18	9	210		
28(A)	3	6	5	224		Foraminiferal ooze unit 4
29(A)	NR	2	NR	532.5		Foram lutite and ooze unit 4
30(A)	–	–	–	–	0	No recovery
31(B)	NR	3	13	91		
32(B)	NR	10	2	103		
33(A)	14	3	2	150		
34(A)	1.5	2.5	8	107		
35(A)						Units not measured
36(A)	8	6	8	69		
37(A)	16	6	1	165		
38(A)	2.5	6.5			216	
39(B)	NR	19	7	89		
40(B)	NR	13	8	81		
41(A)	47	11	3	220		Double penetration
42(B)	NR	3	NR	50		
43(B)	NR	0.5	11	89.5		
44(A)	1 + 2 = 6		NR	134		

1 = Upper grey unit
2 = Dark brown unit
3 = Transitional unit
4 = Medium and dark grey unit
NR = Not represented.

A = 1200 lb. Alpine corer

B = Boomerang cover

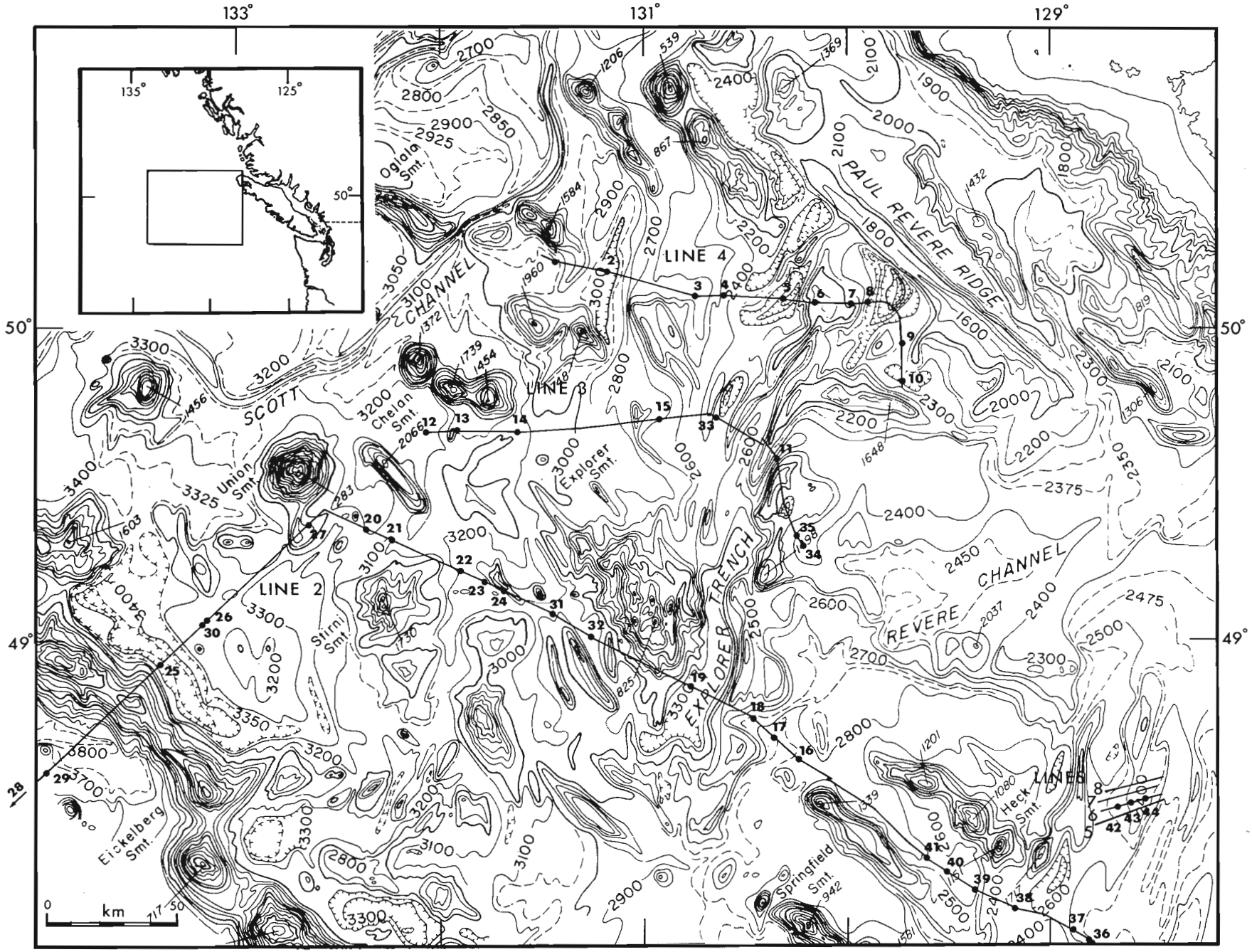

Figure 1. Location of ship's tracks and core sites over Explorer and Juan de Fuca ridges in the northeast Pacific Ocean west of Vancouver Island. Inset: The area of bathymetry is shown in the rectangle outlined.

Figure 2.

A 3.5 kHz high resolution profile over a portion of line 2 extending from approximately 129°40'W to 129°05'W. The profile shows obvious differences with the known bathymetry. After obtaining the profile, core locations were chosen and relocated using Loran-C. Vertical twoway travel time of 0.2 s corresponds to approximately 150 m in water depth. West is to the right hand side.

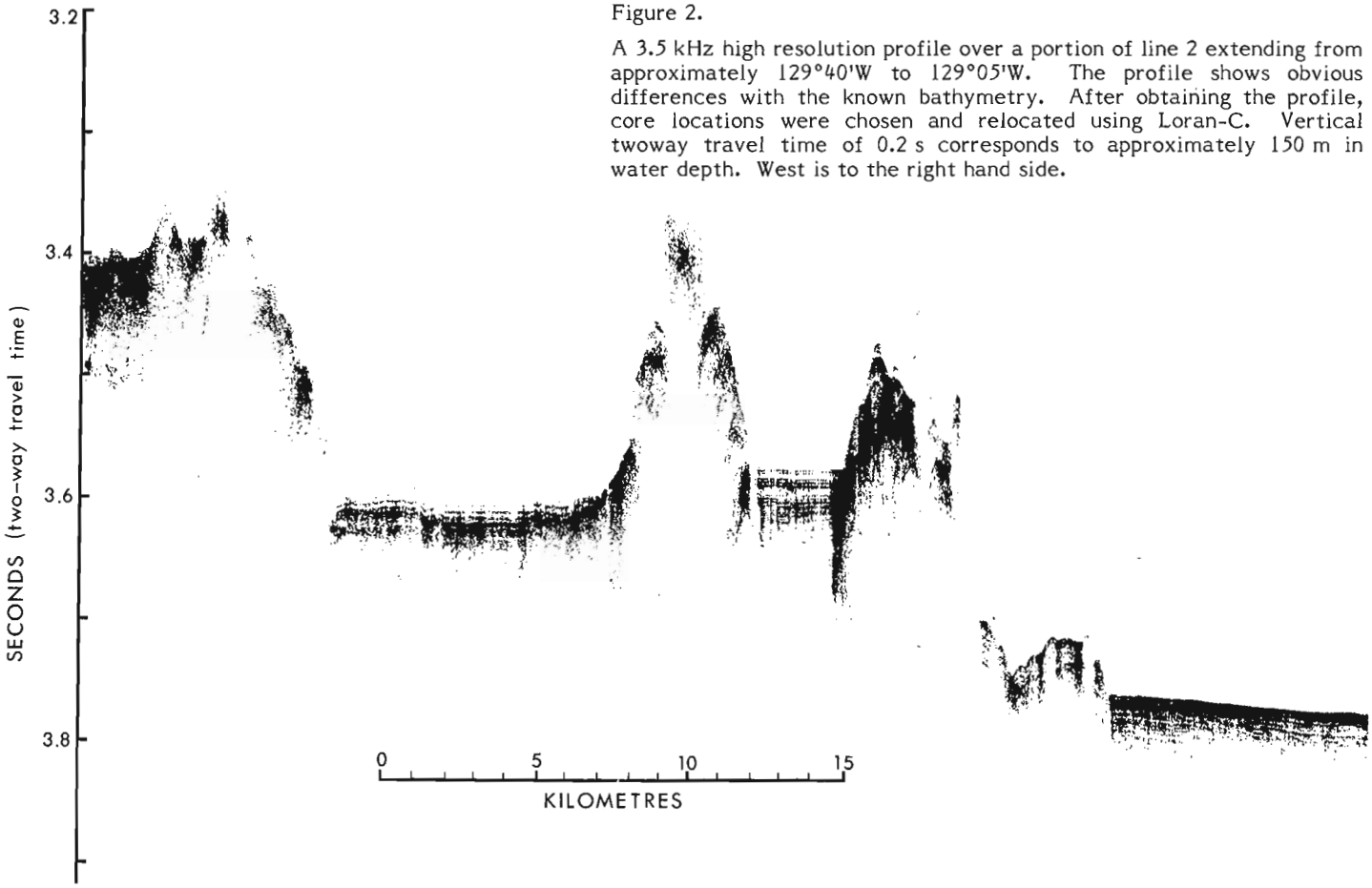

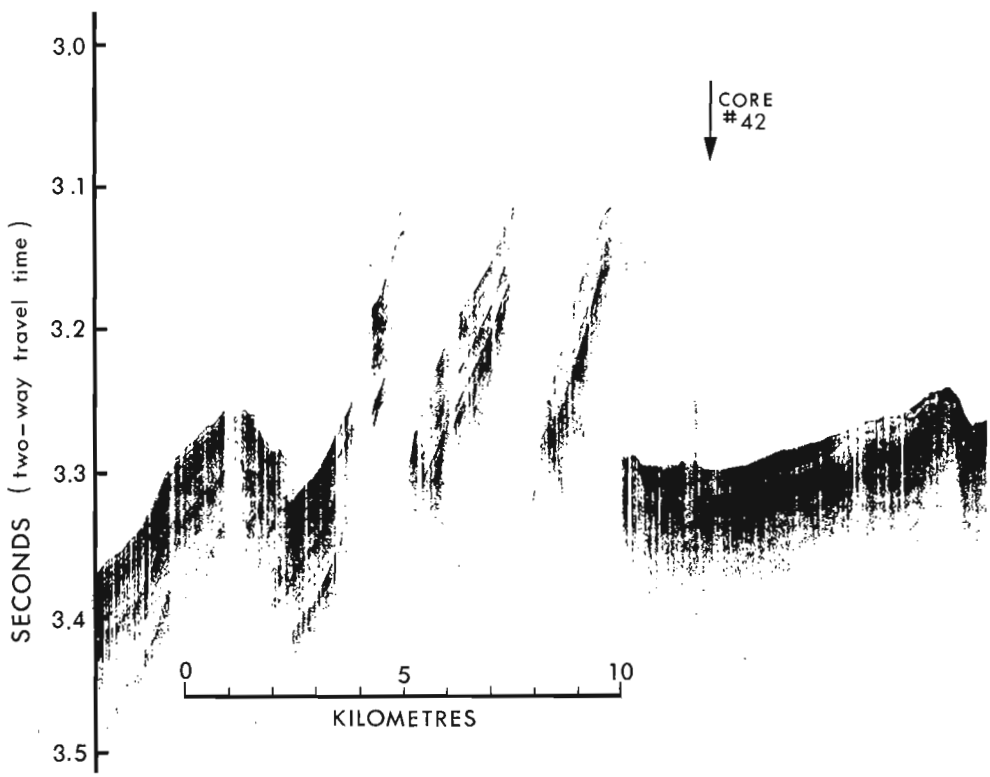

Figure 3. A 3.5 kHz high resolution seismic profile over line 6, Juan de Fuca Ridge. Several faults are obvious in the profile. Core number 42 was obtained on the small sediment mound over which high heat flow was measured in 1976. West is the right hand side.

brown unit". This layer consists of commonly very dark reddish brown, relatively soft, grain to locally matrix supported, fine grained, well sorted, clear, angular quartz silt, finely disseminated opaque minerals and rare foraminifera. The dark colour is seen in the matrix and stained silt. The unit varies in thickness from 0.5 to 46 cm (Table 2).

Beneath the "dark brown unit" and in commonly sharp but locally gradational contact with it is the "transitional unit". The interval, ranging in thickness from zero to 69 cm, comprises commonly banded olive green and olive brown, moderately firm, matrix supported, flocculated, silty lutite. The colour and macrolithology appear to be transitional with the overlying "dark brown unit".

The lowermost "medium to dark grey unit" underlies the "transitional unit" with gradational contact. It comprises medium to dark grey, firm to stiff, matrix supported, commonly intensely flocculated (in discreet zones) silt and silty lutite. Disseminated foraminifera occur throughout and are commonly abundant in local thin layers. The unit is generally banded dark and light grey. Some of the layering is due to the flocculated zones but some is caused by the presence of fine to medium graded sand and silt. The sand layers appear to be composed of terrigenous arenites and opaque minerals. The nature and composition of the remaining silt-sized components in this and the overlying units is unknown but its clarity and angularity are suggestive of a volcanic source. A thick (415 m) unit of Late Miocene to Late Pliocene clastics, part of which is volcanogenic, is present beneath the outer continental shelf and slope adjacent to northern Vancouver Island (Yorath et al.,1977).

The westernmost cores (28 and 29) contained substantial amounts of foraminiferal ooze in their lower sections.

The cores did not contain any obvious macroscopic indications of hydrothermal mineralization. Very finely crystalline pyrite may be present in the dark brown and transitional units of some cores. A botryoidal mineral that may be an oxide is present in the lower medium to dark brown unit of cores 13 and 38 and clusters of what appear to be metallic grains are widely scattered throughout the transitional and underlying unit of core 42. The latter core was of the Boomerang type and was collected in an area across which the 3.5 kHz record indicated the presence of a possible thermal vent (Fig. 3). Geochemical studies of samples from all cores will provide useful information pertinent to the realization of the mineral potential of the region.

The writers express their thanks to the Geological Survey of Canada technical personnel I.I. Frydecky, D.A. Seemann, and L. Simpson, and student assistants G. Beland, G.E. Myrfield, and J.P.T. Davis for their competent support both prior to and during the cruise. We also thank E.P. Fleischer, the captain and crew of **CFAV Endeavour** for their assistance and enthusiasm in completing the ship board work.

References

Andrews, A.J. and Fyfe, W.S.
1976: Metamorphism and massive sulphide generation in oceanic crust; Geosc. Can., v. 3, no. 2, p. 84-94.

Backer, H. and Schoell, M.
1972: New deeps with brines and metalliferous sediments in the Red Sea; Nature, v. 240, p. 153-158.

Bischoff, J.L.
1969: Red Sea geothermal brine deposits; their mineralogy, chemistry and genesis; in Hot brines and Recent heavy Metal Deposits in the Red Sea; Heidelbert New York, Springer-Verlag, p. 368-401.

Bischoff, J.L. and Rosenbauer, R.J.
1977: Recent metalliferous sediment in the north Pacific manganese nodule area; Earth Planet. Sci. Lett., v. 33, p. 379-388.

Bostrom, K. and Peterson, M.N.A.
1966: Precipitates from hydrothermal exhalations on the East Pacific Rise; Econ. Geol., v. 61, p. 1258-1265.

Corliss, J.B., Lyle, M., Dymond, J., and Crane, K.
Sediment Mounds: Hydrothermal Ferromanganese Deposits near the Galapagos Rift; Earth, Planet., Sci., Lett. (in press)

Craig, H.
1966: Isotopic composition and origin of the Red Sea and Salton Sea geothermal brines; Science, v. 154, p. 1544-1548.

Cronan, D.S.
1976: Basal metalliferous sediments from the eastern Pacific; Geol. Soc. Amer., Bull., v. 87, p. 928-934.

Dymond, J., Corliss, J.B., Heath, G.R., Field, C.W., Dasch, E.J. and Veeh, H.H.
1973: Origin of metalliferous sediments from the Pacific Ocean; Geol. Soc. Am., Bull., v. 84, p. 3355-3372.

Fryer, B.J. and Hutchison, R.W.
1976: Generation of metal deposits on the sea floor; Can. J. Earth Sci., v. 13, p. 126-135.

Hyndman, R.D., Rogers, G.C., Bone, M.N., Lister, C.R.B., Wade, U.S., Barrett, D.L., Davis, E.E., Lewis, T., Lynch, S., and Seemann, D.
Geophysical Measurements in the Region of the Explorer Ridge off Western Canada; Can. J. Earth Sci., (in press)

Lister, C.R.B.
1972: On the Thermal Balance of a mid-Ocean Ridge; Geophys. J. v. 26, p. 515-535.

Piper, D.Z., Veeh, H.H., Bertrand, W.G., and Chase, R.L.
1975: An iron-rich deposit from the northeast Pacific; Earth Planet. Sci. Lett., v. 26, p. 114-120.

Williams, D.L., Von Herzer, R.P., Slater, J.C., and Anderson, R.N.
1974: The Galapagos Spreading Center: Lithospheric cooling and hydrothermal circulation; Geophys. J., v. 38, p. 587-608.

Yorath, C.J., Tiffin, D.L., and Cameron, B.E.B.
1977: Submersible operation on the Pacific continental margin; in Report of Activities, Part A, Geol. Surv. Can., Paper 77-1A, p. 301-310.

THE TYPE SECTION OF THE LOWER JURASSIC BORDEN ISLAND FORMATION, BORDEN ISLAND, ARCTIC ARCHIPELAGO, CANADA

R.A. Rahmani and J.T. Tan[1]
Institute of Sedimentary and Petroleum Geology, Calgary

Introduction

The writers, in the summer of 1977, measured and described the type section of the Lower Jurassic Borden Island Formation at the Oyster Creek area of southern Borden Island, Arctic Archipelago (Fig. 1). Rocks assigned to the Borden Island Formation are natural gas reservoirs in the southwestern part of Sverdrup Basin, but the relationship of the rocks there to the type locality of the formation is problematical.

H.R. Balkwill, A. Embry, and L.V. Hills made constructive comments on the report, and their suggestions are gratefully acknowledged.

The name Borden Island Formation was given by Tozer and Thorsteinsson (1964, p. 121), to "... about 200 feet of glauconitic sand with hard red ferruginous bands and grey phosphatic nodules", exposed in the Oyster Creek area of southern Borden Island. It was dated as Sinemurian (early Early Jurassic) on the basis of the ammonite **Arietites sensu lato** sp. indet. (GSC loc. 35322) collected form loose fragments near Oyster Creek. Tozer and Thorsteinsson (1964) also recognized a thinner Borden Island Formation in northwestern Melville Island and suggested that the formation is overstepped by younger rocks on parts of Prince Patrick Island and the Sabine Peninsula of Melville Island. The formation has been mapped also along the eastern margin of Sverdrup Basin in Axel Heiberg Island (Tozer in Thorsteinsson and Tozer, 1970, p. 579). Frebold (1975) reported late Sinemurian to late Pliensbachian ammonites from beds mapped as the Borden Island Formation on Prince Patrick Island, Melville Island, and Axel Heiberg Island.

The Borden Island Formation is considered a basin-marginal sandy facies because it has not been recognized in the axial parts of the Sverdrup Basin. Tozer (in Thorsteinsson and Tozer, 1970, p. 579) suggested the possibility that the lower beds of the Savik Formation are of Sinemurian age and are the basinal equivalents of the Borden Island sandy beds. More recent lithological and biostratigraphical evidence lends support to Tozer's suggestion.

Location and quality of exposures

In the Oyster Creek area (Fig. 1, Sec. A), the Borden Island Formation measured approximately 75 m thick (Fig. 2, Sec. A). A second incomplete section was measured also on the eastern side of Piper Bay, approximately 5 km west of the Oyster Creek section (Figs. 1, 2, Sec. B). Exposures of the Borden Island Formation throughout Borden Island are relatively poor except for a few ferruginous sandstone beds that cap the hills. The near horizontal dips (normally less than two degrees), the softness of the rocks and the very low, rolling topography made the task of measuring and describing the formation difficult.

Lower and upper contacts

At Oyster Creek, the Borden Island Formation lies disconformably on the Schei Point Formation (Karnian). At Section A (Fig. 2), the contact was chosen at an abrupt lithological change between a brown (weathering light grey), fine grained sandstone bed containing animal burrows, and medium to light brown sandy mudstone that is covered with a lag of fragments of dusky red sandy ironstone and ferruginous animal burrows.

The upper contact of the Borden Island Formation is conformable probably with the lower part of the Savik Formation, and was picked at the abrupt lithological transition between brown glauconitic sandstone beds and the overlying brown to light brown plastic clay and mud bed (Fig. 2, Sec. A).

Description

From field observations the type Borden Island Formation consists of 75 m of interbedded mud (about 31%), silt (about 19%), sand and sandstone (about 50%) (Fig. 2). The

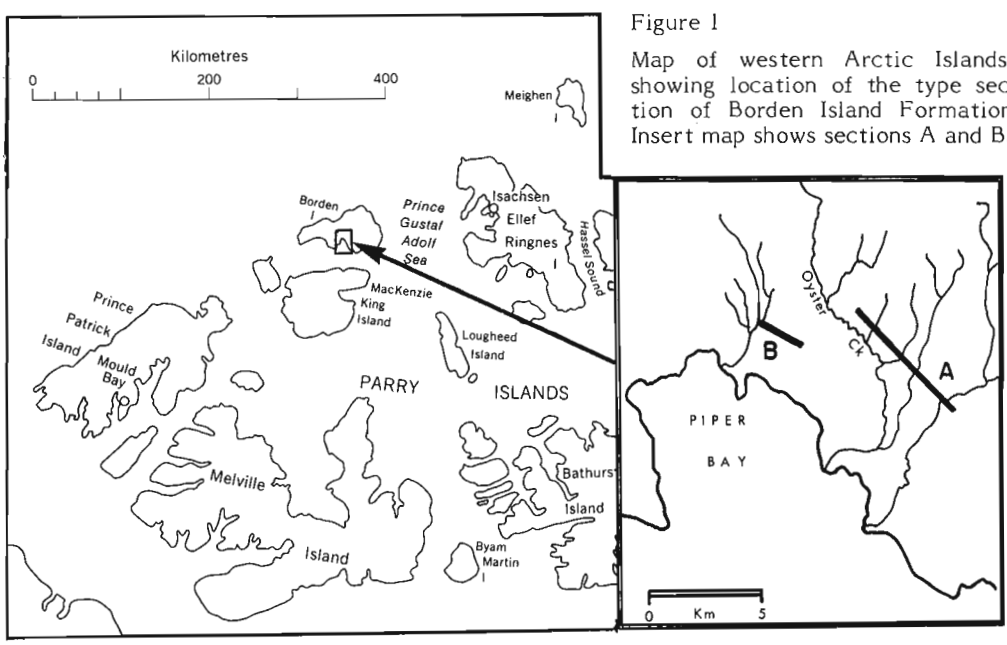

Figure 1

Map of western Arctic Islands showing location of the type section of Borden Island Formation. Insert map shows sections A and B.

[1]Department of Geology, University of Calgary, Calgary.

From: Scientific and Technical Notes in Current Research, Part A; Geol. Surv. Can., Paper 78-1A.

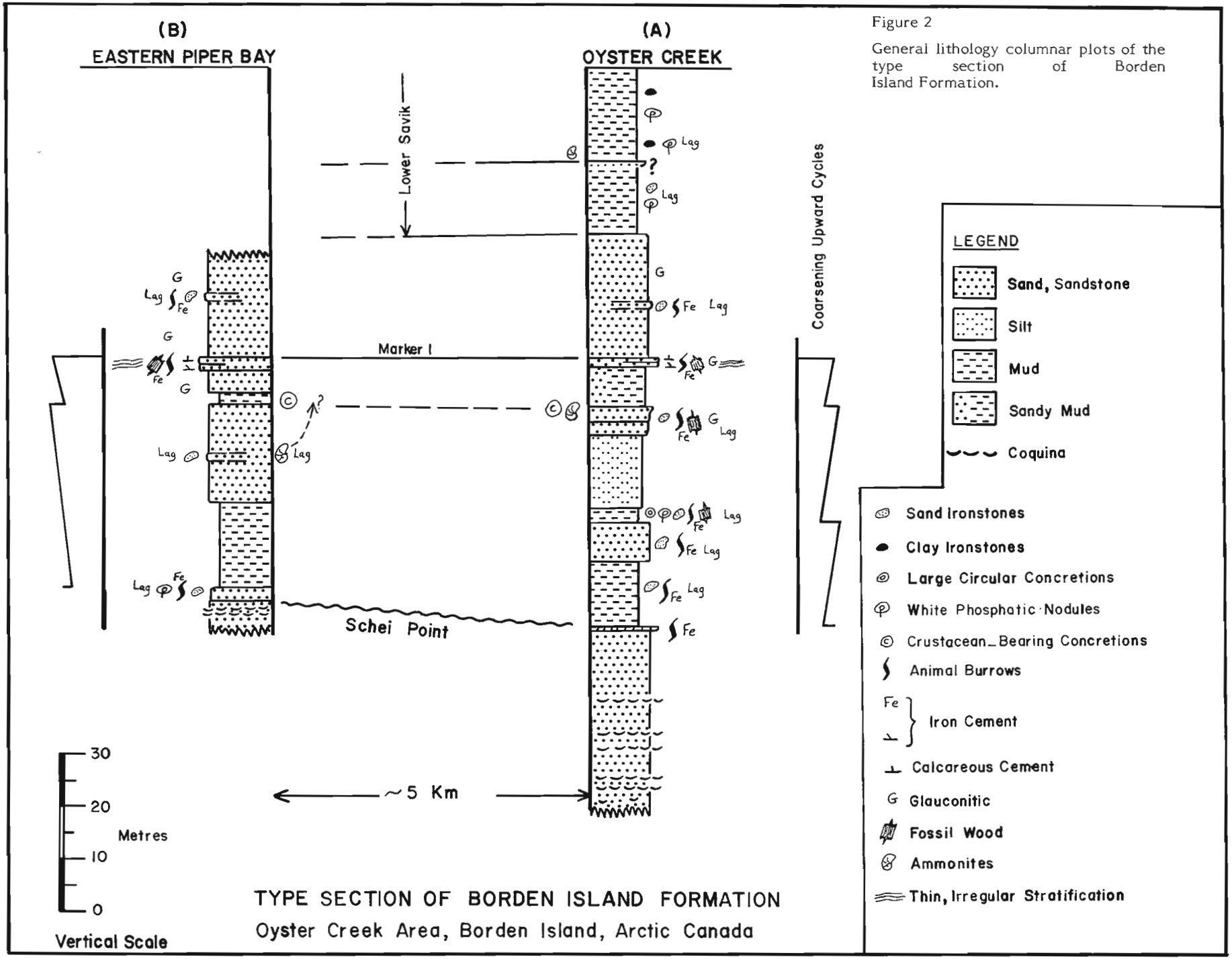

TYPE SECTION OF BORDEN ISLAND FORMATION
Oyster Creek Area, Borden Island, Arctic Canada

Figure 2

General lithology columnar plots of the type section of Borden Island Formation.

mud weathers brown to light grey and is brown-grey to medium brown in wet, fresh cuts. In places it is occasionally sandy and covered with a lag of dusky red fragments of sandy ironstone and ferruginous animal burrows. Fragments of whitish phosphatic nodules were found on one sandy mud bed 20 m above the base of the Borden Island Formation. A silt bed, 14 m thick and 22 m above the base, weathers brown-grey and is medium brown in fresh cuts. The sand of the Borden Island Formation is quartzose, weathers brown- to light grey and is light brown to yellow-brown in fresh cuts. The sand ranges from very fine to fine grained, is variably argillaceous, commonly glauconitic and usually is covered with abundant fragments of dusky red sandy ironstone and ferruginous animal burrows and wood remains. A distinctive 2.5 m thick sand bed, 40 m above the base of the Borden Island Formation, of the Oyster Creek section (Fig. 2, Sec. A), yielded ammonoid and crustacean remains in greyish brown phosphatic concretions. Similar ammonoid and crustacean specimens were found as float in nearby creeks and their source is believed to be this sand bed. This bed weathers brown and is yellowish brown in fresh cuts. It is quartzose, very fine to fine grained and glauconitic. The top of this bed is covered with a veneer of dusky red fragments of sandy ironstone that may represent the remnant of a hard ferruginous sandstone bed. In the eastern Piper Bay section (Fig. 2, Sec. B), this fossiliferous sand bed was not found. However, at approximately the same stratigraphic level, a lag of crustacean-bearing concretions was found and, down-slope from this (down section), a lag of ammonoid-bearing concretions also was found. Perhaps these fossiliferous concretions have been weathered out from a sand bed stratigraphically at the same level as the fossiliferous sand bed of Section A (Fig. 2). A ledge-forming marker unit, in both sections, comprises 2 to 3 m of sandstone, about 45 to 50 m above the base of the formation (Fig. 2, bed labelled Marker 1). This unit is composed of two sandstone beds. The lower of these two beds is massive, dusky red, ferruginous, very fine to fine grained quartzose and probably glauconitic sandstone containing ferruginous wood remains. The upper bed weathers buff yellow and is light grey to light yellowish brown on fresh surfaces, calcareous and is very fine to fine grained. It is thinly stratified, glauconitic and contains in-place animal burrows (e.g. **Ophiomorpha, Teichichnus** and horizontal grazing traces) and wood remains.

The lag of dusky red sandy ironstone and ferruginous animal burrows that forms a veneer on the Borden Island Formation is likely derived from lenticular hard bands of dusky red, ferruginous sandstone, some of which is still exposed.

Some of the ammonite specimens found in the Oyster Creek section are identical to specimens collected previously from the same area by Elf Oil Exploration and Production Canada Ltd., and dated by Frebold (1975, p. 3, Pl. 3, figs. 1a-c) as late Sinemurian (T. Poulton, pers. comm.).

Depositional environment

Interpretation of the environment of depositon of the Borden Island Formation sediments in the type area is hampered by the poor exposure and paucity of sedimentary structures. The overall arrangement of lithologies (Fig. 2) suggests a cyclicity of depositional environments. At least three such cycles were observed in the Oyster Creek section and two cycles in the eastern Piper Bay section. The cycles have an overall coarsening-upward trend of grain size from mud at the lower part of each cycle to sand/sandstone at the top.

The presence of ammonites, crustaceans, animal burrows (**Ophiomorpha, Teichichnus** and horizontal grazing traces) and glauconite in the sand and sandstone attest to depositon under shallow-marine environments, most probably in the middle to lower shoreface (sublittoral, subtidal, shelf) realms of Howard (1972, Fig. 4, p. 221) and closely corresponding to a transition between the Skolithos and Cruziana Ichnofacies of Seilacher (1967, Figs. 2, 3). The muds probably were deposited in deeper offshore conditions. The coarsening-upward cycles indicate upward shoaling of depositonal surface due to migration of the sand bars (or sand waves). Indicators of subaerial deposition were not found, except perhaps for the presence of ironstone bands, if this at all constitutes evidence for syndepositional and not postdepositonal emergence.

We suggest that the Borden Island Formation of the western Arctic Islands passes eastward into basinal Lower Savik shale and the latter grades into the eastern part of Sverdrup Basin to upper Heiberg Formation/Borden Island Formation deltaic and marine sands (Pliensbachian and older). Early Jurassic paleogeography thus featured a delta in the eastern Arctic Islands (uppermost Heiberg/Borden Island sands), and a normal marine shelf in the central islands (lower Savik argillaceous sediments), and a shallow regime in the western islands where the Borden Island sandwaves were formed. Source of the Borden Island sand may have been the re-working of local underlying sand and/or sand dispersed laterally along basin margin by longshore currents. The shoals where these sandwaves were deposited may have been a manifestation of the Sverdrup Basin northwest rim of Meneley et al. (1975).

References

Frebold, H.
1975: The Jurassic faunas of the Canadian Arctic; Lower Jurassic ammonites, biostratigraphy and correlations; Geol. Surv. Can., Bull. 243.

Howard, J.D.
1972: Trace fossils as criteria for recognizing shorelines in stratigraphic record; in Recognition of ancient sedimentary environments, J.K. Rigby and W.K. Hamblin, eds.; Soc. Econ. Paleontol. Mineral., Spec. Publ. 16, p. 215-225.

Meneley, R.A., Henao, D., and Merritt, R.K.
1975: The northwest margin of the Sverdrup Basin in Canada's continental margin, C.J. Yorath, E.R. Parker and D.J. Glass, eds.; Can. Soc. Petrol. Geol., Mem. 4, p. 531-544.

Seilacher, A.
1967: Bathymetry of trace fossils; Marine Geol., v. 5, p. 413-428.

Thorsteinsson, R. and Tozer, E.T.
1970: Chapter X, the Arctic Archipelago in Geology and economic minerals of Canada, R.J.W. Douglas, ed.; Geol. Surv. Can., Econ. Geol. Rep. 1, 5th ed., p. 547-590.

Tozer, E.T. and Thorsteinsson, R.
1964: Western Queen Elizabeth Islands, Arctic Archipelago; Geol. Surv. Can., Mem. 332.

PERMIAN STRATIGRAPHY AT PIPER PASS, NORTHERN ELLESMERE ISLAND, DISTRICT OF FRANKLIN

Andrew D. Miall
Institute of Sedimentary and Petroleum Geology, Calgary

Introduction

For two days in June, 1977 the writer studied the Permian rocks exposed at the southern end of Piper Pass (Fig. 1) as a contribution toward the regional mapping project led by H.P. Trettin and U. Mayr (Mayr, 1976).

These rocks were included originally in map-unit 13 of Christie (1964) as "Permian to Jura-Cretaceous". Mapping during 1977 indicated that map-unit 13 occurs in three areas:

1. North of the main Hazen Thrust Fault, Permian strata rest unconformably on the Grant Land Formation (Cambrian and/or Ordovician, according to Trettin, 1971) and are the youngest rocks present in the area.

2. A second thrust fault has been mapped south of the main Hazen Thrust. Between the two faults is an area 1 to 8 km wide underlain by a steeply dipping to overturned Permian to Lower Cretaceous section, including the unit described in this report (also including map-unit 10G of Christie, 1964).

3. South of the two faults map-unit 13 includes an area of Mesozoic outcrop, not shown on Figure 1.

The detailed structural geology of the thrust belt in this area will be reported on elsewhere.

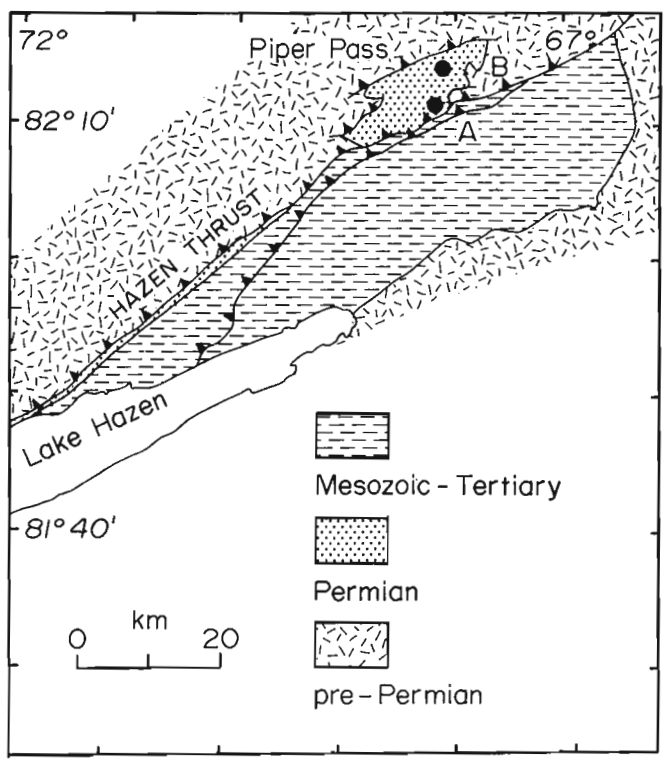

Figure 1. Report-area, showing location of stratigraphic sections A and B.

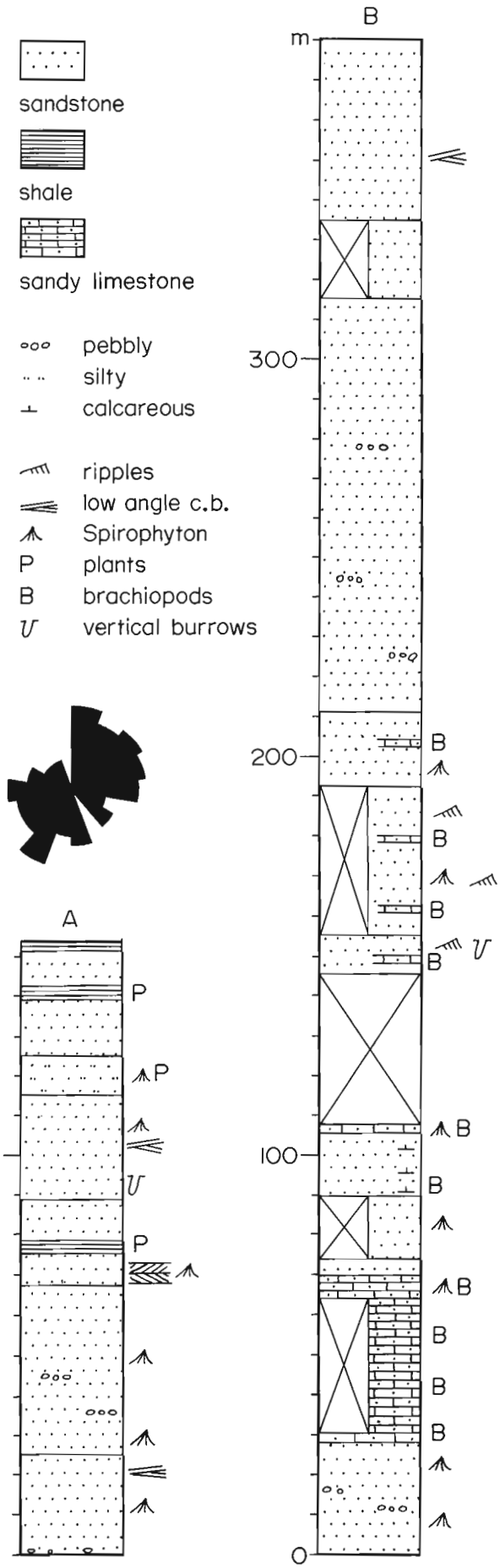

Figure 2. (right) Stratigraphic sections A and B through the Permian rocks at Piper Pass. Both sections commence at the base of the Permian. The rose diagram at left-centre represents 55 cross-bed orientation measurements made on herringbone cross-stratification in the 67-75 m interval of section A.

From: Scientific and Technical Notes in Current Research, Part A; Geol. Surv. Can., Paper 78-1A.

Thickness and Lithology

Two sections through the Permian rocks exposed north of the main Hazen Thrust were described and measured in detail (Fig. 2). Both sections commenced at the unconformable contact of the Permian with the Grant Land Formation. The thicker of the two sections totals 380 m, with an estimated 100 m of poorly exposed section present, but not measured, above the highest stratigraphic level reached.

The dominant lithology throughout is sandstone, which generally is fine to medium grained, white to pale grey, cream to pale buff or brown weathering. Small pyrite nodules and small pebbles of white vein quartz and black chert are common locally. Spirophyton traces are abundant, and some units contain numerous trace fossils (Fig. 3). Trace fossil types include simple vertical tubes up to 18 cm long (Asterosoma-type), "knobbly"-walled tubes (Ophiomorpha-type) and meniscus-filled burrows (Diplocraterion-type). Most of the sandstone is massive, bedding being very faint. However, in section A the interval between 67 and 75 m contains abundant high-angle herringbone cross-stratification (Fig. 4). Low-angle (<5°) cross-bed sets rarely are present elsewhere in this section, and ripple marks and small trough sets were recorded at a few levels in section B.

In section B brachiopod debris is common, in some places forming a sandy brachiopod coquina. Several intervals of dark grey fissile claystone containing coaly plant fragments are present in section A.

Correlation

Lithologically these rocks are similar both to the Sabine Bay Formation (Lower Permian) and to the Trold Fiord Formation (Upper Permian). Regional mapping indicates that they probably should be assigned to the Trold Fiord, but formal designation must await a detailed examination of the brachiopod collection. Differences between the Piper Pass rocks and the type Trold Fiord described by Thorsteinsson (1974) include a much greater thickness in the report-area and an absence of the distinctive green weathering common in areas farther south.

Depositional Environment and Paleogeography

The presence of abundant brachiopods in section B and of herringbone and low-angle cross-bedding in section A indicate a marine origin for the Piper Pass rocks. Herringbone cross-bedding is found in areas characterized by bimodal or polymodal current directions such as those influenced by waves or tides. There are various causes of low-angle cross-bedding, but a common one is the slow progradation of beach surfaces under the influence of waves in a foreshore or inner shoreface environment (intertidal to shallow subtidal). Trace fossils of the type shown in Figure 3 are common in marine (intertidal toshallow subtidal) environments. Coquina deposits are typically shallow subtidal in origin.

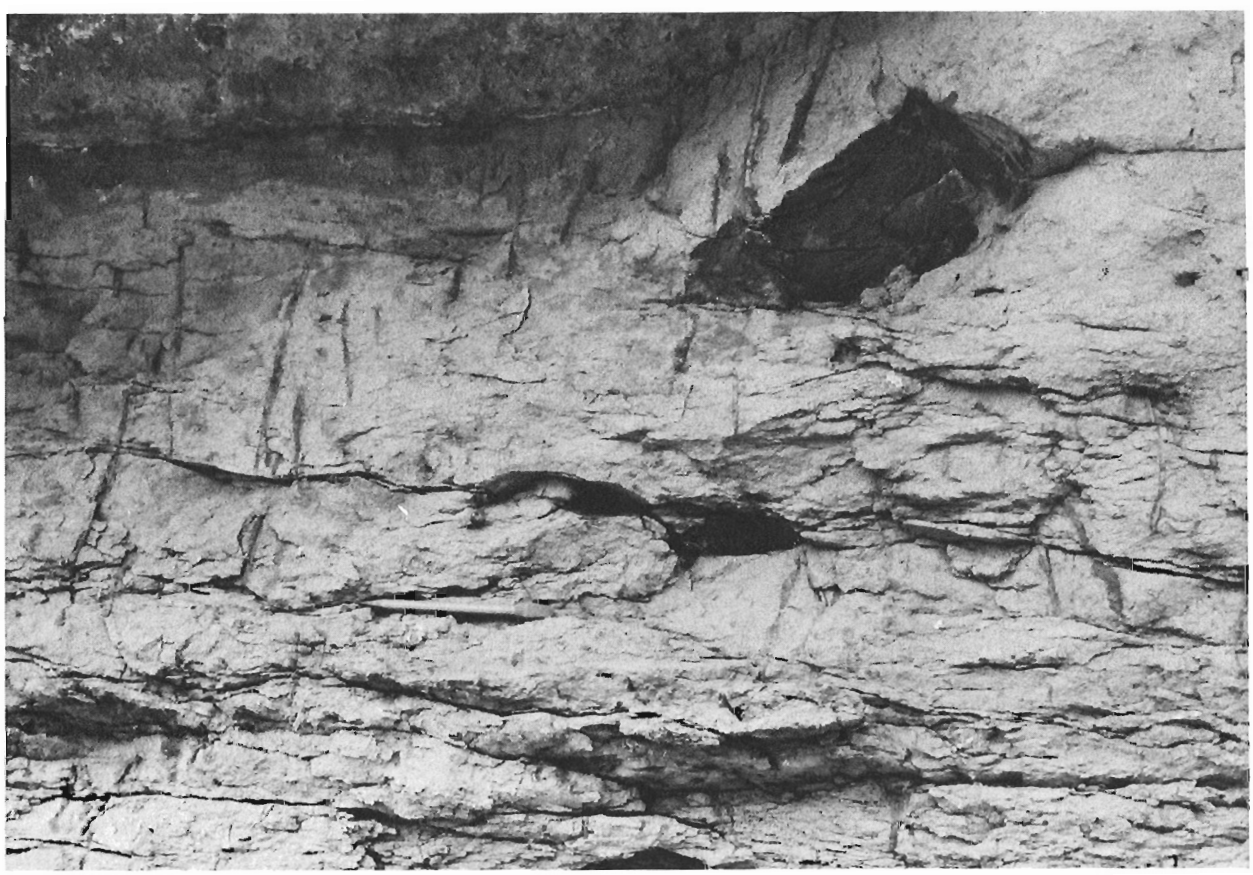

Figure 3. Trace fossils, 146-156 m interval of section B. Visible are **Spirophyton** and numerous vertical tubes. Note pencil for scale. GSC 199326.

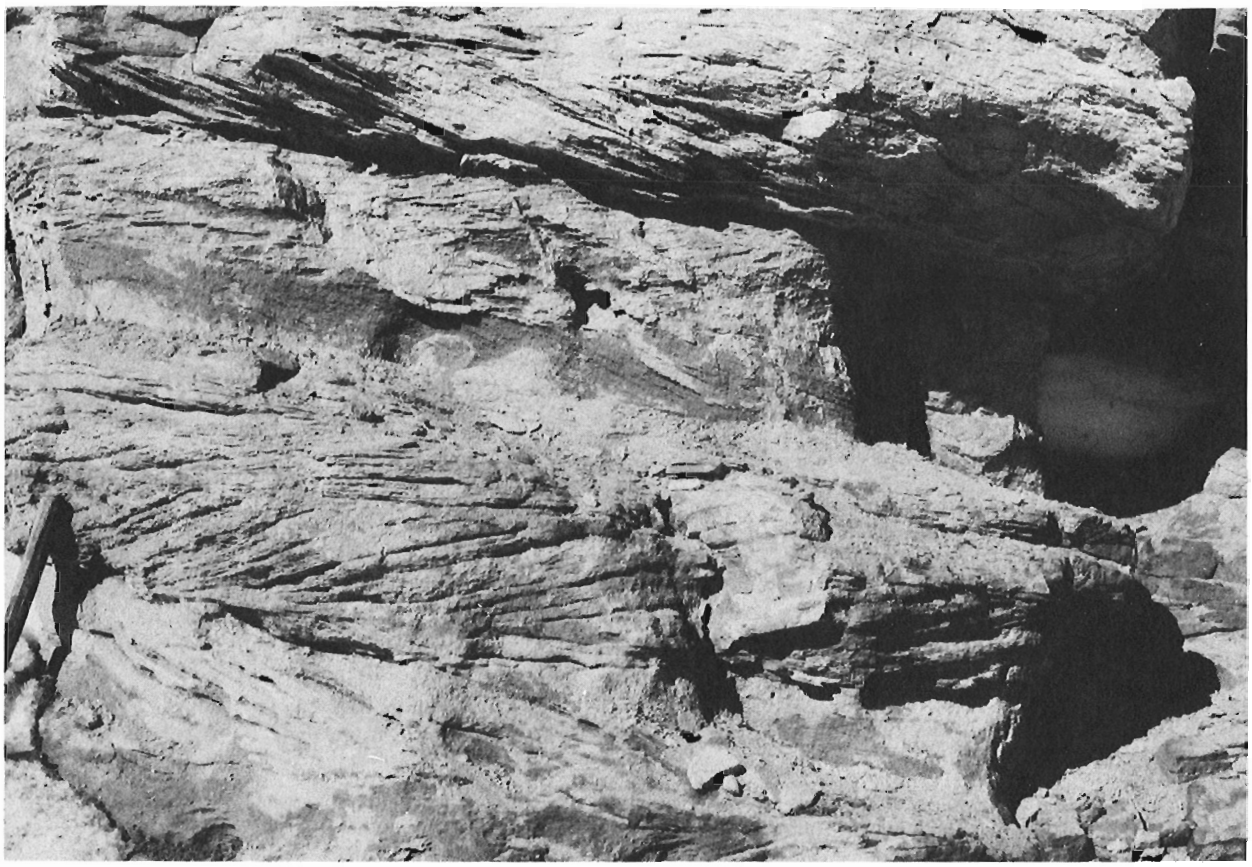

Figure 4. Herringbone cross-stratification, 67-75 m interval of section A. Five sets are present, showing alternate southwesterly and northeasterly orientations (set next to top of hammer handle is 20 cm thick). GSC 199325.

Detailed environmental interpretations are hindered by the lack of obvious cyclicity or repeated facies associations in these rocks, and by the marked contrast between the sequences present in the two sections. There are general similarities with the shallow shelf sandstone deposits described by Goldring and Bridges (1973) and Brenner and Davies (1974). Shoreline and barrier environments commonly generate coarsening-upward sequences (Davies et al., 1971), and these are absent in Piper Pass, with the possible exception of the 75 to 115 m interval in section A. In this interpretation the thin shale unit at 75 to 77 m would be interpreted as an offshore deposit, containing transported plant material. However, it could represent a lagoonal deposit originally formed landward from a coastal barrier island. The underlying sandstone unit contains abundant herringbone cross-stratification which could represent a foreshore, inner shoreface, or tidal delta environment within a barrier system.

Fifty-five cross-bed orientation measurements were made on the herringbone cross-stratification (Fig. 2). The distribution of readings is strongly bimodal about a northeast-southwest axis, which is parallel to the present-day structural grain, and also parallels the interpreted axis of the Sverdrup Basin during Carboniferous-Permian time (Throsteinsson, 1974). Two possible interpretations of the data are offered:

1. The cross-bedded sandstone represents the deposits of a tidal delta formed during ebb and flood through an inlet in a barrier system. In this case the current modes likely would be oriented perpendicular to the local coastline. In view of regional paleogeographic considerations, this interpretation does not seem very plausible.

2. Cross-bed orientations were caused by strong, offshore, reversing tidal currents such as occur at the present day in narrow seaways, for example the English Channel and the Malacca Strait. The relatively narrow (less than 100 km) outcrop belt of the Carboniferous-Permian rocks that extends northeastward through northern Ellesmere Island may reflect an original paleogeography consisting of a narrow linear seaway, in which case evidence of strong reversing tidal currents might well be expected. Based on this hypothesis, the lithologic contrasts between sections A and B could reflect narrow facies belts parallel to a shoreline that deepened toward the northwest (sandier in shallow coastal environments and more calcareous in the open sea).

References

Brenner, R.L. and Davies, D.K.

1974: Oxfordian sedimentation in western interior United States; Am. Assoc. Pet. Geol. Bull., v. 58, p. 407-428.

Christie, R.L.

1964: Geological reconnaissance of northeastern Ellesmere Island, District of Franklin (120, 340, parts of); Geol. Surv. Can., Mem. 331.

Davies, D.K., Ethridge, F.G., and Berg, R.R.

1971: Recognition of barrier environments; Am. Assoc. Pet. Geol. Bull., v. 55, p. 550-565.

Goldring, R. and Bridges, P.

1973: Sublittoral sheet sands; J. Sediment. Petrol., v. 43, p. 736-747.

Mayr, U.

1976: Upper Paleozoic succession in the Yelverton area, northern Ellesmere Island, District of Franklin; in Report of Activities, Part A, Geol. Surv. Can., Paper 76-1A, p. 445-448.

Thorsteinsson, R.

1974: Carboniferous and Permian stratigraphy of Axel Heiberg Island and western Ellesmere Island, Canadian Arctic Archipelago; Geol. Surv. Can., Bull. 224.

Trettin, H.P.

1971: Geology of lower Paleozoic formations, Hazen Plateau and southern Grant Land Mountains, Ellesmere Island, Arctic Archipelago; Geol. Surv. Can., Bull. 203.

AN UPDATE OF SUBSURFACE INFORMATION, CRETACEOUS ROCKS, TROUT LAKE AREA, SOUTHERN NORTHWEST TERRITORIES

G.K. Williams
Institute of Sedimentary and Petroleum Geology, Calgary

Introduction

In the past two decades, about sixty-five wells have been drilled through Cretaceous rocks in the vicinity of Trout Lake, southern Northwest Territories (Fig. 1). The near-surface samples of most of these wells have been examined recently by the writer. Reasons for undertaking this project were: 1) to provide more information on drift thickness, Cretaceous facies changes, pre-Cretaceous geology and geography, etc., and 2) to standardize the nomenclature.

Revised markers are presented in Table 1. The main change is the abandonment of any attempt to subdivide the Fort St. John Group into formations, as can be done in outcrop to the west; rather a set of markers within the group is identified and correlated, with as much consistency as possible, across the map-area (Figs. 2, 3). A series of maps based on the revised markers illustrates some aspects of Cretaceous history (Figs. 4-8).

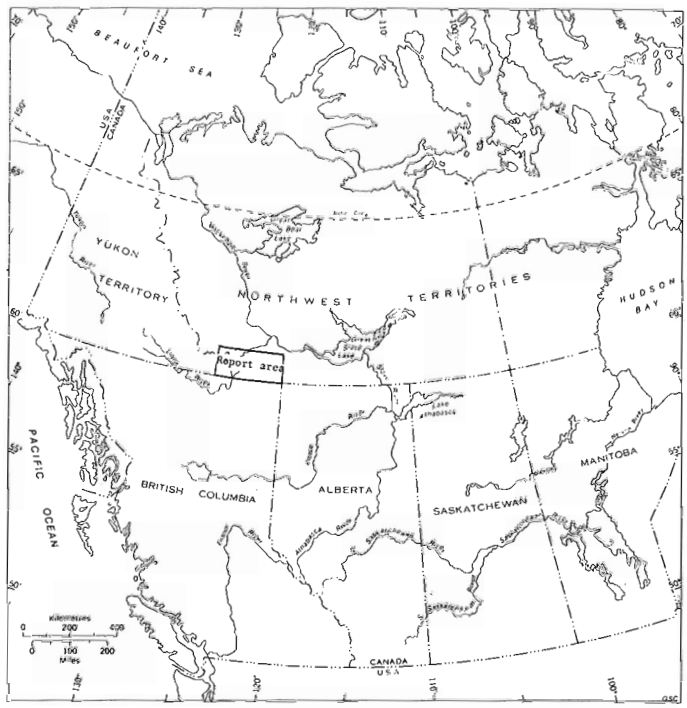

Figure 1. Index map.

Discussion of lithology, formations, markers

Basal Cretaceous and/or upper Paleozoic sandstone

A sandstone, up to 50 m thick, occurs in five wells in the central part of the map-area (Fig. 4). It lies on the eroded surface of the Mississippian Flett Formation; it is overlain by the Fort St. John shale.

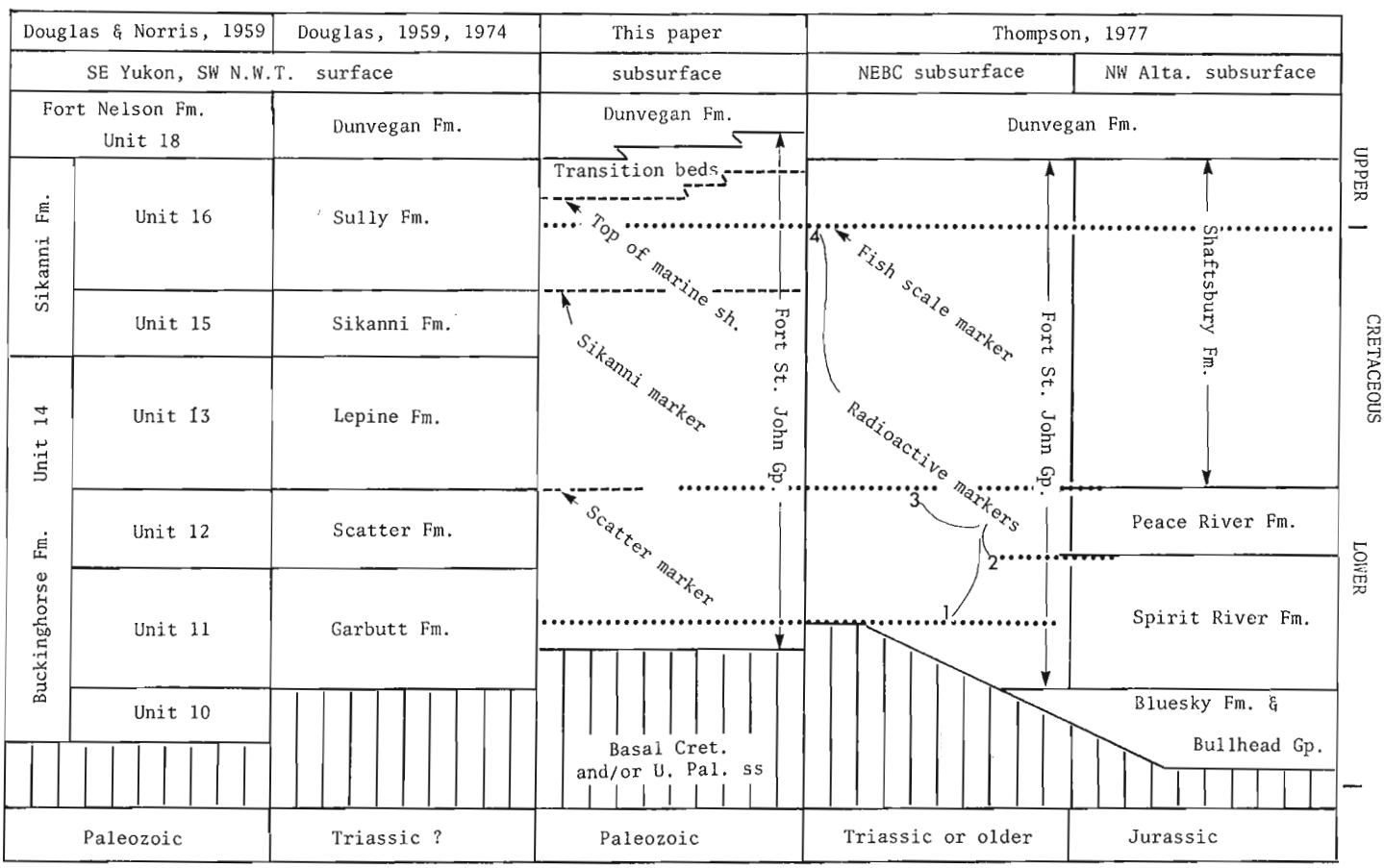

Figure 2. Nomenclature and approximate surface to subsurface correlation, Trout Lake and adjoining areas.

From: Scientific and Technical Notes in Current Research, Part A; Geol. Surv. Can., Paper 78-1A.

Table 1

Revised Cretaceous markers

Wells are listed geographically according to the Y.T. and N.W.T. Grid Survey System. Wells drilled before this system was introduced have been given a section-unit designator, e.g. Briggs Tetcho Lake No. 1 is identified as L-26; on the maps these older wells are differentiated by heavier type.

Grid	Well Name	Location	Casing depth	Samples from	Top of mech. log
60°10'	Atkinson et al. Island R. J-44	60°03' 120°23'	727	0	720
	Union Pan Am Trainor K-70	60°09' 120°27'	1505	6040	1505
	Union Pan Am Trainor K-30	60°09' 121°04'	885	890	850
	Pan Am A-1 Island R. D-29	60°08' 121°05'	1283	100	1283
	Imperial Island R. No.1	60°09' 121°08'	592	50	400
	H.B. Pan Am S. Island R. M-41	60°00' 121°09'	828	50	740
	H.B. Amoco S. Island R. M-52	60°01' 121°11'	912	1000	830
	H.B. Petitot C-60	60°09' 121°25'	795	910	740
	Shell Trout L. O-41	60°00' 121°38'	870	870	870
	Banner et al. Little Growl N-11	60°00' 121°48'	810	20	590
	Home Signal C.S.P. Celibeta No. 6	60°09' 122°10'	846	170	40
	Home Signal C.S.P. Celibeta No. 5	60°05' 122°11'	895	140	120
	Home Signal C.S.P. Celibeta No. 2	60°07' 122°13'	327	300	170
	Dome et al. Celibeta C-77	60°06' 122°14'	300	300	300
	U. Gas. C.S.P. et al. S. Celibeta J-13	60°02' 122°17'	626	630	630
	Home Signal C.S.P. Celibeta No. 1	60°03' 122°22'	833	0	160
	Canada Southern Celibeta N-39	60°08' 122'36'	755	240	720
	Home Signal C.S.P. Celibeta No. 7	60°09' 122°37'	775	90	770
	Texaco N.F.A. Bovie L. No. 1	60°02' 122°58'	263	40	--
	Can S'thn. et al. N. Beaver R. YT I-27	60°06' 124°03	1027	120	950
	Pan Am Beaver R. YT G-01	60°00' 124°15'	1201	400	1190
60°20'	Union Pan Am Trainor O-72	60°11' 120°13'	768	770	720
	Union Pan Am Trainor E-35	60°14' 120°22'	808	30	770
	Union Pan Am Trainor H-28	60°17' 120°34'	710	1800	710
	Union Pan Am Trainor L. C-39	60°18' 120°34'	270	0	80
	Atkinson Union Island R. G-42	60°11' 121°08'	742	800	720
	Dome et al. Island R. E-56	60°15' 121°11'	915	920	915
	I.O.E. Amoco Bovie M-05	60°14' 122°46'	630	0	10
	Texaco Bovie L. J-72	60°11' 122°58'	1160	30	90
60°30'	Atkinson et al. Trainor L. F-48	60°27' 120°23'	1356	980	1270
	Union Pan Am Trainor L-59	60°28' 120°40'	207	207	1090
	Pan Am et al. A-1 Island R. O-12	60°21' 121°02'	1190	40	1060
	Atkinson C.S.P. Trout L. M-51	60°20' 121°10'	755	305	755
	Atkinson et al. Trout L. H-57	60°26' 121°24'	1003	2000	910
	McDermott et al. Trout L. A-45	60°24' 121°52'	845	890	845
	Gobles et al. Celibeta K-01	60°20' 122°16'	905	560	900
	Gobles et al. Celibeta D-66	60°25' 122°27'	918	1000	890
	I.O.E. Chevron Celibeta D-31	60°20' 122°37'	465	0	50
	I.O.E. et al. Arrowhead L-49	60°28' 122°39'	472	40	160
	B.A. Tex. Arrowhead B-76	60°25' 122°59'	955	40	100
	Amoco Pointed Mountain P-24	60°23' 123°48'	600	0	600
60°40'	Briggs Tetcho L. No. 1	60°35' 120°35'	588	10	10
	Atkinson et al. Island R. I-63	60°32' 120°56'	666	670	590
	Dome et al. Trout L. M-73	60°32' 121°29'	922	0	870
	Imperial Sun Arrowhead Aurora M-47	60°36' 122°38'	869	200	870
	B.A. Texaco Arrowhead N-02	60°31' 123°01'	966	690	40
	Amoco B-1 East Flett H-13	60°32' 123°17'	597	370	580
60°50'	U.O.H.L. Trout R. O-80	60°49' 120°28'	467	490	440
	Shell Union Pan Am Tetcho J-12	60°41' 121°02'	736	30	720
	Dome et al. Trout L. H-45	60°44' 121°22'	918	0	920
	Murphy B.O.C. Muskeg R. No. 1	60°43' 122°03'	600	0	530
	Imperial Sun Arrowhead I-46	60°45' 122°22'	979	0	20
	Imperial Sun Netla Raven F-73	60°42' 122°44'	857	0	830
	Imperial Sun Netla C-07	60°46' 122°46'	964	80	960
61°00'	Briggs Trout R. No. 3	60°58' 120°01'	349	70	20
	Briggs Trout R. No. 4	60°59' 120°15'	289	100	15
	Briggs Trout R. No. 6	60°57' 120°17'	279	20	30
	Briggs Trout R. No. 2	60°57' 120°18'	452	30	70
	Briggs Trout R. No. 5	60°55' 120°31'	416	0	20
	Briggs Trout R. No. 1	60°52' 120°36'	506	0	290
	Scurry et al. Corm L. I-49	60°58' 121°52'	849	40	800
	Murphy B.O.C. Arrowhead R. No. 1	60°50' 122°05'	995	0	980
	Horn River et al. Cormack C-65A	60°54 122°27'	685	50	630
	Amoco Murphy Cormack N-33	60°52' 122°36'	720	600	650
	Murphy et al. Netla M-31	60°50' 123°07'	574	0	10
61°10'	Amoco Decalta A-1 Poplar R. G-32	61°01' 121°21'	733	150	700

< means at a shallower depth than. All depths are in feet.

Table 1 (cont.)

map symbol	Base of drift	Dunvegan Fm.	Transition beds	Marine shale	Fish scale marker	Sikanni marker	Scatter marker	RA marker 3	RA marker 1	Basal Cret. and/or U. Pal. ss	Base of Cret.	Underlying beds
J-44	290			290	690	835		1410	1680		1718	Banff
K-70	?							1740	2035		2054	Banff
K-30	?			<890	1010	1170		1833	2090		2127	Flett
D-29	280		280	760	970			1775	2050		2075	Flett
G-50	70	70	200	840	1020	1180		1860	2110		2110	Flett
M-41	520		520	650	860	1030		1750	1960		1998	Flett
M-52	?				930	1100		1845	2055	2100	2145	Flett
C-60	?							1370	1580		1602	Flett
O-41	?							1070	1254		1254	Flett
N-11	30							?870	1035		1058	Flett
F-60	640											Banff
E-56	545											Banff
H-78	410											Banff
C-77	<300											Banff
J-13	<630											Banff
I-44	825											Banff
N-39	<240								790		790	Flett
H-50	130								945		945	Fantasque
B-73	40											Fantasque
I-27	<120						<120				1180	Triassic
G-01	<400										<400	Triassic
O-72	?				850	1010		1490	1790		1826	Banff
E-35	370	370	420	1050	1200	1370		1860	2150		2168	Banff
H-28	?			860	1020	1170		1660	1950		1975	Banff
C-39	120	120	270	840	980	1125		1570	1850		1876	Banff
G-42	?			<720	965	1120		1775	2020		2033	Flett
E-56	?				960	1110		1780	2040		2040	Flett
M-05	40					110	1100		1565	1565	1710	Flett
J-72	670						<670		1120		1120	Fantasque
F-48	1090							1325	1620		1650	Banff
L-59	500				600			1160	1425		1456	Banff
O-12	310			310	400			1150	1440		1455	Banff
M-51	330		330	360	660	800		1400	1670		1685	Flett
H-57	<1000							1460	1720		1741	Flett
A-45	?							1252	1500		1500	Flett
K-01	<560								1175	1175	1300	Flett
D-66	?								1237	1237	1266	Flett
D-31	20			20	110	300	1195		1600		1600	Flett
L-49	110			110	355	545	1380		1843	1843	1970	Flett
B-76	170						1070		1610		1610	Flett
P-24	120						250				1395	Fantasque
L-26	700							1125	1415		1415	Banff
I-63	?							945	1220		1248	Banff
M-73	130			130	250			1020	1300		1300	Banff
M-47	530						1500				2006	Banff
N-02	?				?400	?580	1550		2050	2070	2250	Flett
H-13	<370						690		1200		1212	Flett
O-80	<490								560	560	613	Exshaw
J-12	500								890		932	Banff
H-45	470										920	Banff
L-14	530			530	660	765	1380		1780		1780	Banff
I-46	220			220	403	530	1210		1620		1637	Banff
F-73	280		280	470	750	925	1690		2095		2095	Banff
C-07	<80	<80	130	440	700	890	1620		2020		2020	Banff
I-19	50											Kotcho
A-10	30								65		65	Kotcho
K-18	100								115	160	200	Kotcho
D-18	90								160		160	Kotcho
D-06	400											Kotcho
K-33	427											Kotcho
I-49	480							?530	840		840	Kotcho
H-31	480						1115		1525		1550	Banff
C-65A	450			450	500	630	1280		1675		1712	Kotcho
N-33	650						1235		1650		1670	Kotcho
M-31	90					<90					410	Kotcho
G-32	420										620	Kotcho

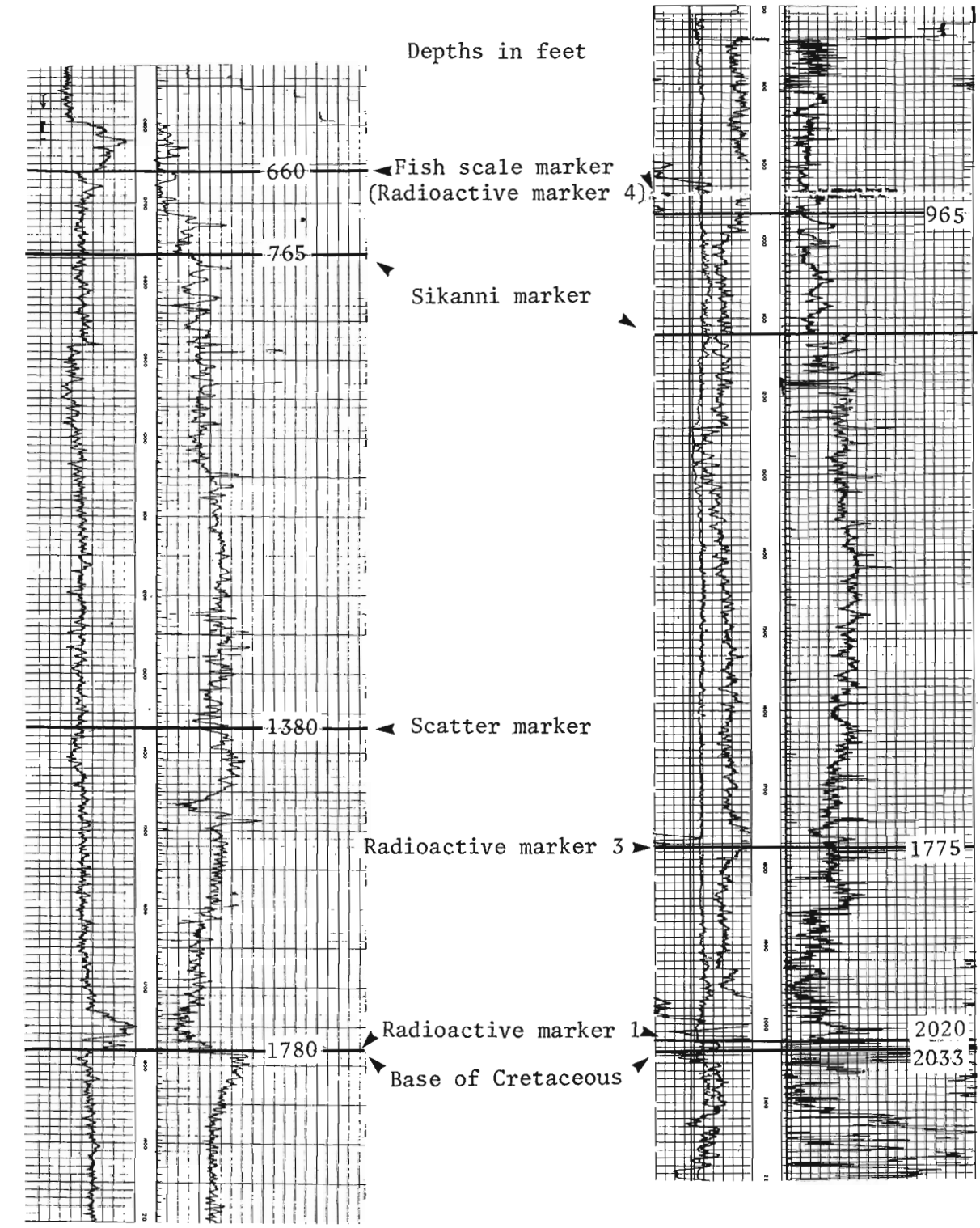

Figure 3. Typical well logs, Cretaceous markers.

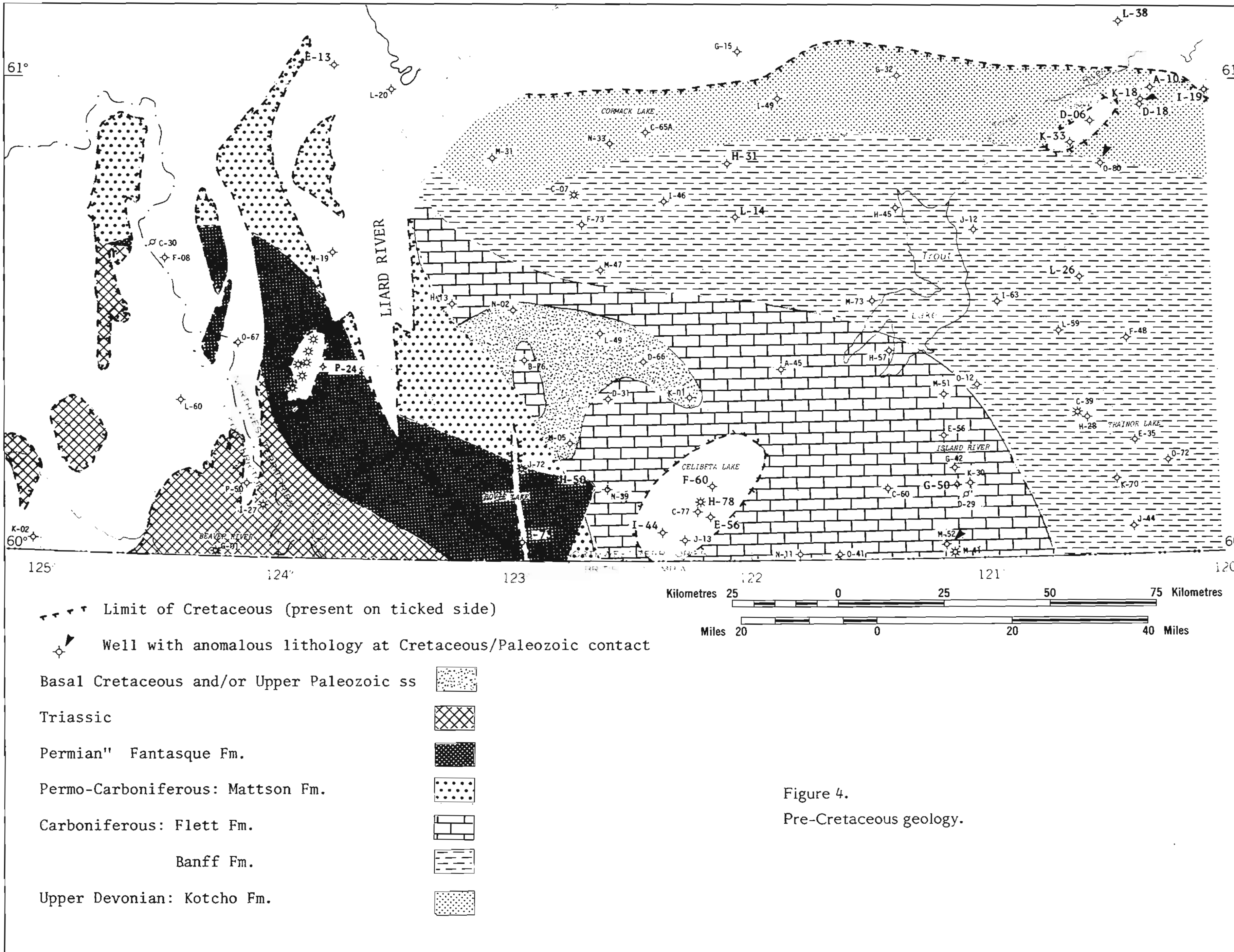

Figure 4.
Pre-Cretaceous geology.

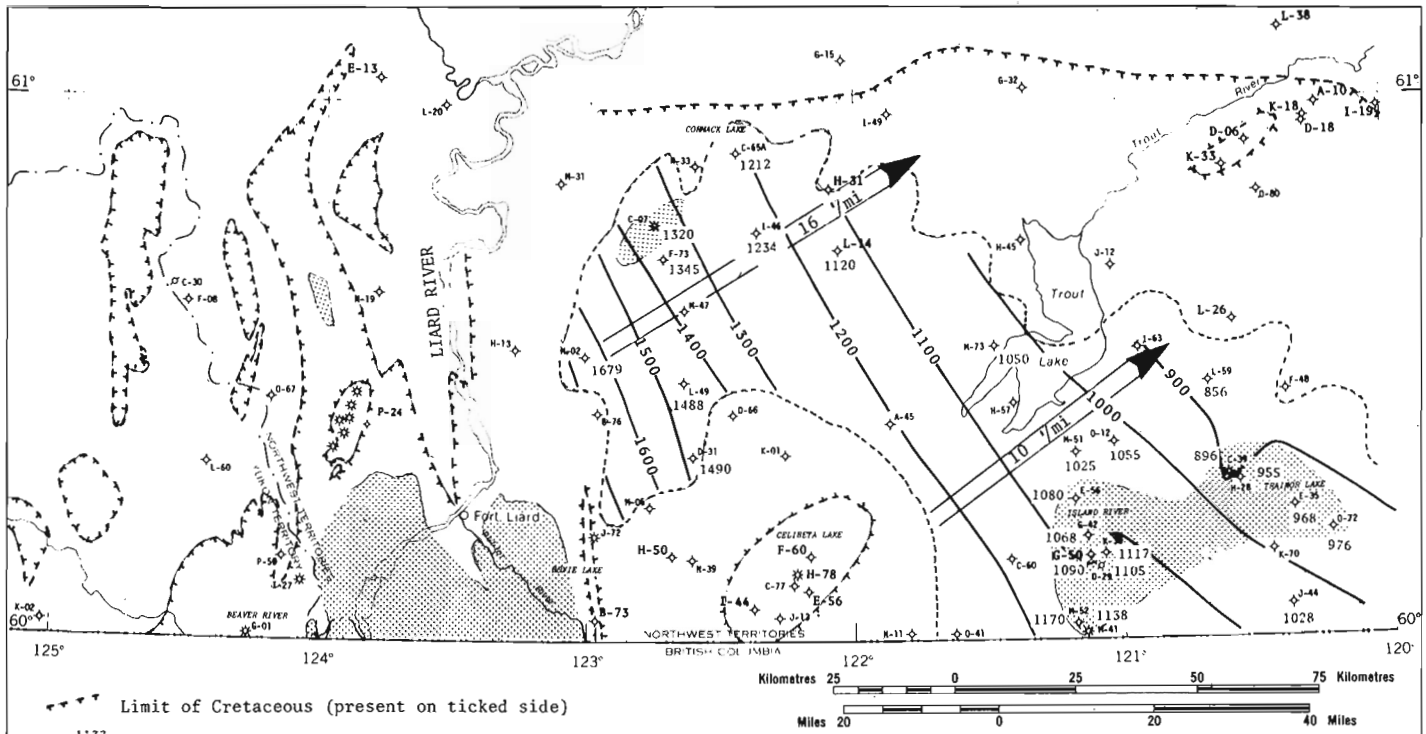

Limit of Cretaceous (present on ticked side)

1137 Well location, thickness of isopached interval in feet

Distribution of Dunvegan Fm.

Thinning rate of isopached interval in feet per mile

Trace of Fish scale marker, outcrop or pre-Drift subcrop

1000 Isopach, in feet

Figure 5

Isopachs, Fish Scale marker to base of Cretaceous (excluding basal Cretaceous and/or upper Paleozoic sandstone).

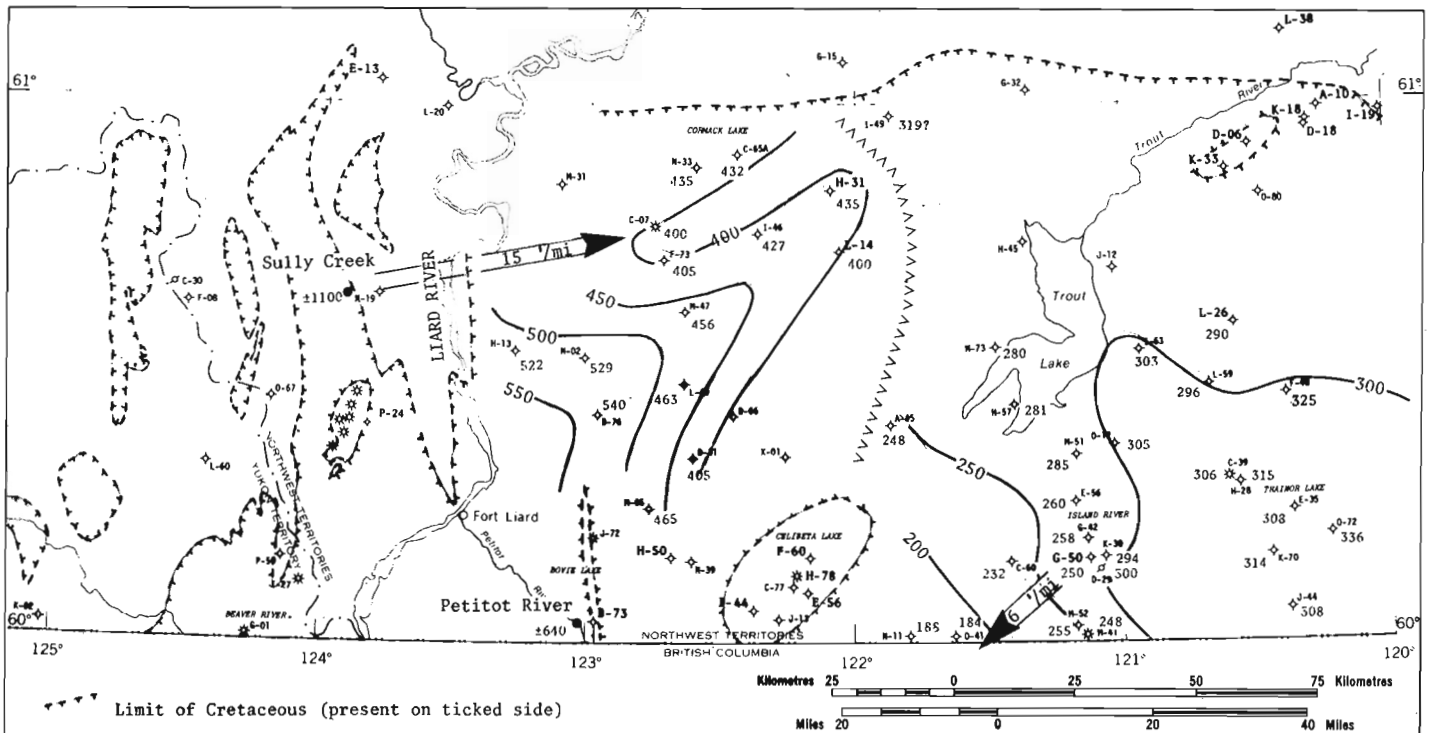

Limit of Cretaceous (present on ticked side)

300 Well location, thickness of isopached interval, in feet

Outcrop sections, Stott, 1960

Eastern depositional limit of Scatter sand

Thinning rate of isopached interval in feet per mile

300 Isopach, in feet

Figure 6

Isopachs, Scatter marker (west) or Radioactive marker 3 (east) to base of Cretaceous (excluding basal Cretaceous and/or upper Paleozoic sandstone).

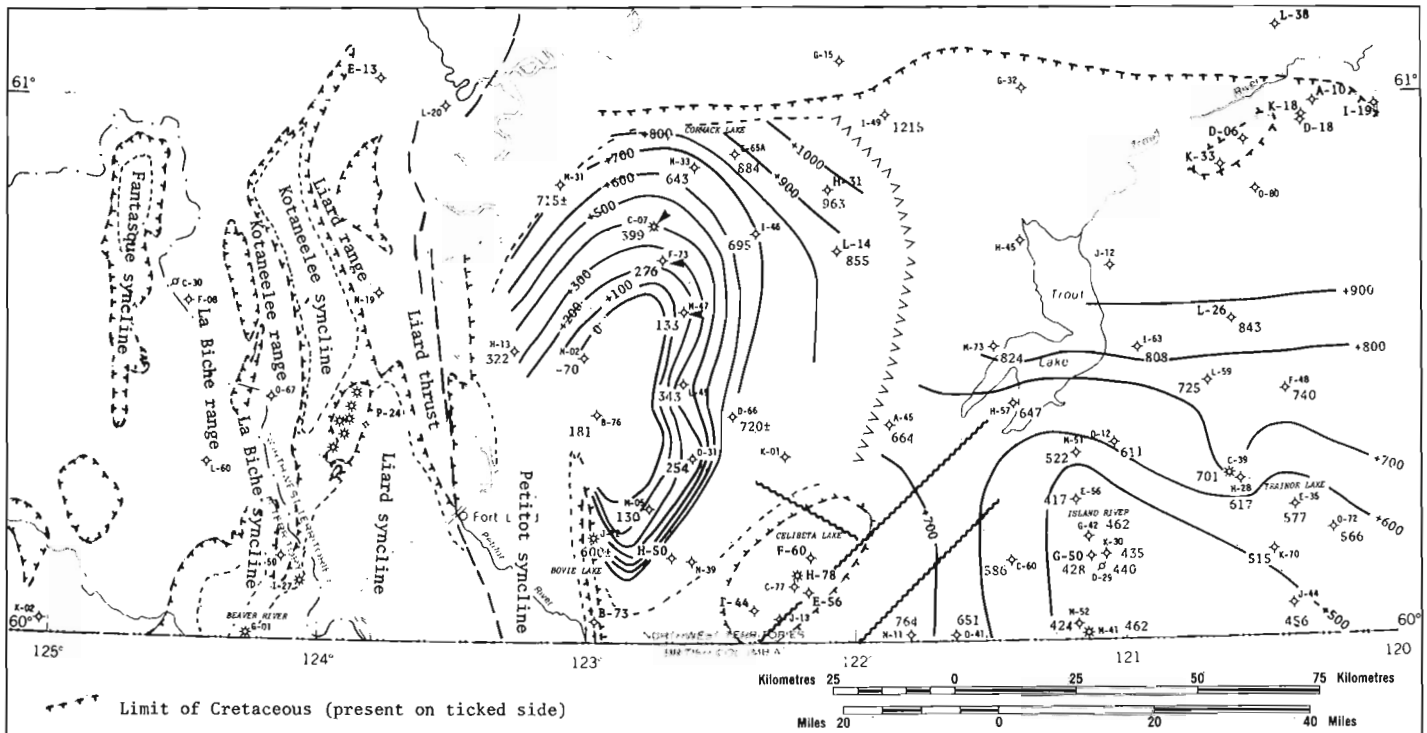

Limit of Cretaceous (present on ticked side)

Well location, marker elevation relative to sea level, in feet

Eastern depositional limit of Scatter sand

Inferred basement faults

Main faults, eastern part of disturbed belt

Trace of Scatter marker, outcrop or pre-Drift subcrop (Top of Scatter Fm. west of 123°)

Oil stain in Scatter ss

Structure contour, in feet, datum sea level

Figure 7

Structure contours on Scatter marker (west) or Radioactive marker 3 (east) and occurrence of oil stain in Scatter sandstone.

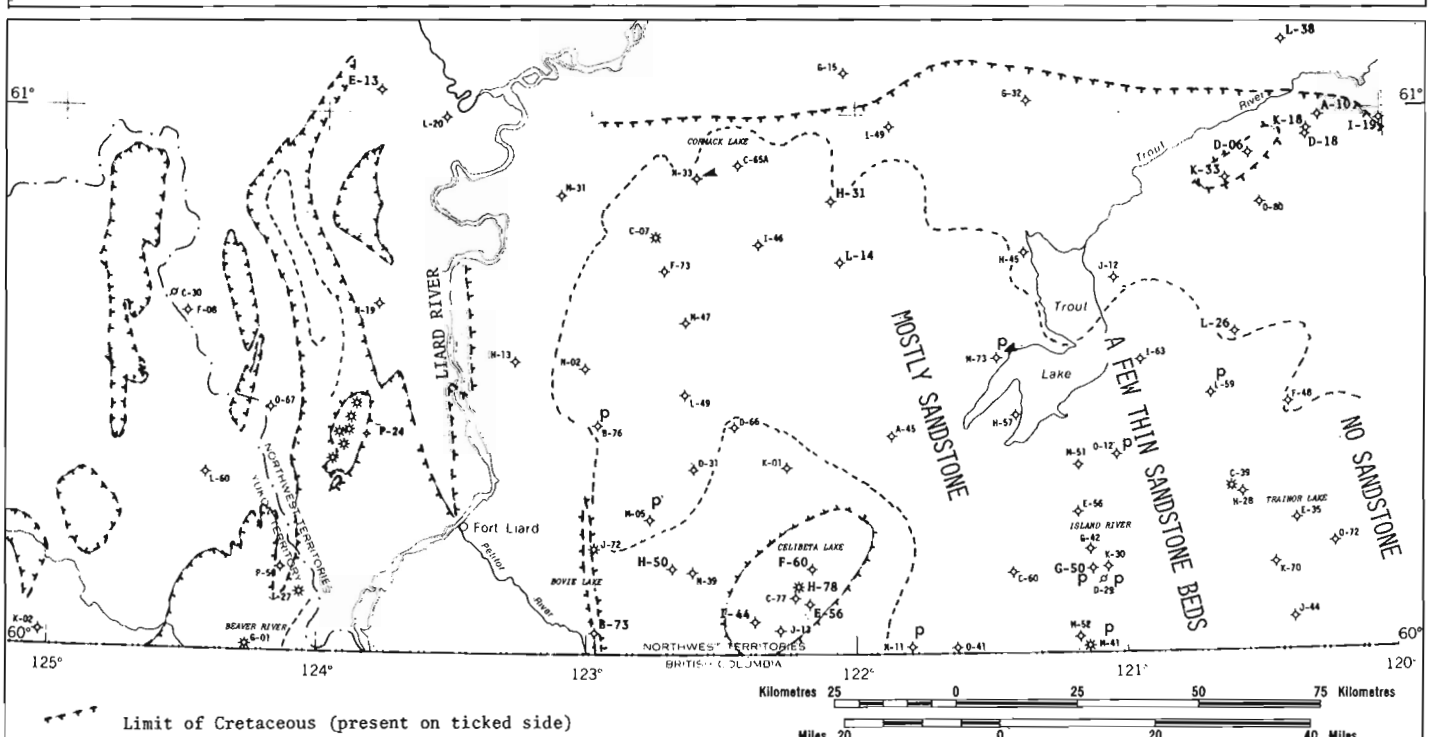

Limit of Cretaceous (present on ticked side)

Well location

Trace of Sikanni marker, outcrop or pre-Drift subcrop (Top of Sikanni Fm. west of 123°)

P Oil stain, porosity, in Sikanni ss

Figure 8

Rough indication of sandstone/siltstone or shale ratio of a 200-foot interval below the Sikanni marker; and porosity or oil stain in Sikanni sandstone.

Where seen in cores, this unit consists of poorly sorted quartz sandstone and medium grey, sandy shale. Coal occurs as grains, as large detrital chunks, and as veinlets. From well samples there are indications that chert pebbles occur at the top of the unit. Glauconite grains occur, but are rare. In one well (M-05), carbonate occurs in the well samples, whether from pebbles or from beds cannot be determined.

Three other wells have anomalous lithologies at the base of the Cretaceous (Fig. 4): chert pebbles in shale in K-18; very fine grained, calcareous sandstone in 0-80 (both wells lie northeast of Trout Lake); and pebbly sandstone in M-52 south of Trout Lake.

Fort St. John Group

Figure 2 shows the relationship of this group to formations mapped in outcrops west of the Liard River.

Except for the transition beds (described separately), the Fort St. John Group consists of marine shale, mostly silty or sandy, and marine sandstone, mostly shaly and silty. From west to east across the map-area, there is a gradual decrease in the sand plus silt to shale ratio; Figure 8 illustrates the pattern.

Sandstones of the Fort St. John Group are medium to light grey, depending on the amount of clay matrix, very fine to fine grained, quartzose, and commonly glauconitic. Only rarely are the sandstones clean; usually they have some silt and clay matrix. Although sandstone layers are most common at or below the Sikanni and Scatter markers, they also occur elsewhere throughout the group.

The shale of the Fort St. John Group (except that of the transition beds) is medium to dark grey, usually silty; in the west it is commonly sandy and glauconitic. Fissile clay-shale is rare, usually found only toward the base of the section.

Throughout the Fort St. John Group, the following occur: ironstone, **Inoceramus** prisms, bentonite, fish debris, carbonaceous debris, and a substance that looks like coal but (as it is most common in the radioactive shales) may be a form of bitumen. Except for ironstone, the above occur only in trace amounts. Fish debris is more common in the radioactive shales which are otherwise not noticeably different from nonradioactive shale.

The Sikanni and Scatter markers correspond approximately (determined from intervals) with the tops of those formations in outcrop. Both of these are mechanical log markers (Fig. 3) but, in western wells, they also can be detected in samples: a change downward from silty or sandy shale to fairly clean sandstone. Unlike the tops, the bases of these sandy units are gradational to more shaly beds, no consistent marker can be traced between wells, hence the futility of attempting to apply formation names.

The Sikanni marker can be traced, with reasonable certainty, across the map-area; in the east, however, it is detectable only on the sonic log (Fig. 3) as a change to a more silty shale. The Scatter marker cannot be traced across the map (Fig. 6), because west of Trout Lake it disappears.

In northeastern British Columbia, there are four widespread radioactive markers (Thompson, 1977). The upper, or No. 4 marker, is the widespread Fish Scale horizon which marks the Lower/Upper Cretaceous boundary (Gleddie, 1954). Three of the four radioactive markers can be followed into the Northwest Territories (Fig. 2). Nos. 1 and 4 can be traced throughout the map-area; No. 3 can be followed only a short distance west of Trout Lake (Fig. 6). Radioactive marker No. 3 and the Scatter marker occur at approximately the same stratigraphic level; the western limit of the former and the eastern limit of the latter appear to coincide.

Radioactive marker No. 1 occurs near but usually not at the base of the Fort St. John Group; there is usually a thin layer of nonradioactive shale between this marker and the eroded Paleozoic surface. Samples near the basal contact commonly show scattered quartz grains, up to coarse grained, in the shale; in many wells this interval contains traces of a siliceous, gritty rock which appears to be composed of corroded radiolaria (J.H. Wall, pers. comm., 1976).

Transition beds

This interval, at the top of the Fort St. John Group, is characterized by very poor samples. In most instances, the cuttings resemble balls of dried drilling mud – possibly an indication that the rock is highly bentonitic. The original sediment appears to have been a mixture of clay, silt and sand. The dominant lithology is a poorly consolidated claystone-siltstone mixture, usually dull grey in colour but ranging through shades of brown, red, grey to sooty-black; the latter is carbonaceous. Sandstone beds are usually very fine to fine grained, quartzose, and shaly but traces of coarser sandstone, of the Dunvegan type, also occur in the upper part of the transition beds. The following occur as traces: ironstone, cone-in-cone limestone, coal, sorted quartzose sandstone, glauconite.

The transition beds are up to 200 m thick. They probably are nonmarine in part. The basal contact apparently is gradational and is picked at the change, downward, to medium grey shale. The basal contact does not occur at a consistent stratigraphic level.

The designation of these transition beds in the Schedule of Wells, 1921-1971 (DIAND, 1973a) has not been consistent; all or part have been reported variously as Fort St. John Group, the Sully Formation or as the Dunvegan Formation. These beds have more in common with the Fort St. John Group than with the Dunvegan Formation.

Three small outcrops were found on the hills southwest of Trout Lake by Hage (1945); they have not been revisited, at least by Geological Survey geologists. Judging from their elevations relative to nearby wells, these outcrops lie within the transition beds. Hage (pers. comm., 1976) recalled that these outcrops were fairly dark shale and shaly sandstone with a marine aspect.

Dunvegan Formation

The characteristic lithology is an immature sandstone. The colour is usually light grey with a salt and pepper appearance, but may be various shades of red. The sorting is poor, grains range from silt to coarse sand, with rare granules. Rounded grains are scarce. Up to 30 per cent of the grains are non-quartz: feldspar, chert, shale, siltstone (commonly red) and coal. The matrix is a calcareous clay-silt mixture. Interbedded shales are varicoloured, from red to black; the latter are carbonaceous.

Drift thickness

In the highlands around Trout Lake, the drift is in the order of 150 ± 60 m thick; in one well east of the lake there are 335 m of drift. Like the Horn Plateau (Williams, 1977a), the pre-glacial Trout Lake highlands may have been capped by sandstone, but glaciation has destroyed most of the cap-rock.

Significance of marker changes

The age of the Celibeta structure
(near Lat. 60°00'N, Long. 122°00'W; Figs. 4-8)

In some wells on the crest of the Celibeta structure, markers in the Schedule of Wells 1921-1971 (DIAND, 1973a) indicate that Cretaceous rocks overlie the Banff shale. This implies that much of the structural growth predated the sub-Cretaceous unconformity. The author found no Cretaceous

rocks in any of these wells; in all wells drilled on the crest of the structure, the Banff shale is overlain by thick drift. Cretaceous and Paleozoic rocks are folded in close structural concordance (Williams, 1977b). The main folding was post-Early Cretaceous, probably during Laramide deformation.

Extent of the Dunvegan Formation

By defining the lower contact of the Dunvegan Formation as the base of a sequence composed predominantly of lithic sandstone, the areal extent of this formation is reduced to a patch southeast of Trout Lake and a smaller patch northwest of the lake (Fig. 5). Most of the high land around Trout Lake is composed of glacial drift. The area shown as Dunvegan Formation by Douglas (1958, 1973) and Douglas and Norris (1959, 1974) coincides approximately with the extent of the transition beds of the Fort St. John Group.

Some observations on Cretaceous depositional history

Figure 4 is a pre-Cretaceous geological map. This erosion surface must have been a nearly featureless plain on a south-dipping homocline. Surface rocks ranged from Upper Devonian in the north to Triassic in the southwest. Although not indicated by Figure 4, this homocline is actually the southern flank of a structural high whose axis lies along the Liard River. North of latitude 61°00'N, the pre-Cretaceous subcrop trend of Paleozoic formations is north-south.

The rather insignificant layer of shale below radioactive marker No. 1 contains the surviving record of a large part of Early Cretaceous history. As indicated on Figure 2, this interval expands to include the thick Bullhead Group to the south and west (Thompson, 1977). Not far east of the map-area, radioactive marker No. 1 overlies a basal Cretaceous quartz sandstone, similar to and possibly an extension of the McMurray Formation. North of the map-area in the Horn Plateau, Martin Hills and Ebbutt Hills, there are up to 75 m of shale below the lowest radioactive marker.

The above can be interpreted as simple onlap onto a pre-Cretaceous topographic high. An alternative hypothesis, perhaps more in accord with the lithology and facies, is as follows. The Trout Lake area was part of a much larger tectonically stable area which, although flooded by the Early Cretaceous sea, remained a starved basin. To the west, rapid subsidence coincided with rapid clastic deposition. Throughout the Early Cretaceous, the sea bottom sloped to the east. In this hypothesis, the eastern Trout Lake area was always under relatively deep water.

Isopachs of that part of the Fort St. John Group below the Fish Scale marker (Fig. 5) show a regular pattern of west to east thinning. Although no quantitative facies analysis was attempted, it is obvious that the facies strike was about north-south, and that the sand source was in the west. A crude facies map (Fig. 8) illustrates the pattern. The lower Fort St. John sandstone units shale out first, for example sandstones below the Scatter marker shale out west of Trout Lake (Fig. 6) whereas the Sikanni marker extends across the map-area. Although this part of the sequence is entirely marine, the pattern is of west to east regression.

Although there is not sufficient control to construct an isopach map, the upper part of the Fort St. John Group does not appear to thin eastward to the same extent. This is probably because the transition beds, in part at least, are the time equivalent of the lower part of the Dunvegan Formation – the prodeltaic facies of the Dunvegan conglomerates and sandstone. Thus, the Fort St. John Group includes progressively younger beds from west to east. The transition beds-Dunvegan Formation are a continuation of the west to east regression.

There are some features illustrated by the maps which may or may not be fortuitous. Note the coincidence of isopach thicks (Fig. 6) with synclines (Fig. 7). Note also that the distribution of the basal Cretaceous and/or upper Paleozoic sandstone (Fig. 4) coincides roughly with a syncline (Fig. 7). These coincidences suggest (although they do not establish) that the present structure is partly inherited from ancient structural trends, and that these exerted a very mild influence on Cretaceous sedimentation.

References

Department of Indian Affairs and Northern Development
1973a: Schedule of wells, 1921-1971; IAND Publication No. QS-1214-000-EE-A-1.

1973b: Schedule of wells, 1970-1972; IAND Publication No. QS-1509-000-EE-A-1.

1974: Schedule of wells, 1971-1973; IAND Publication No. QS-1509-00-EE-A-2.

Douglas, R.J.W.
1958, 1973: Geology, Trout River, District of Mackenzie; Geol. Surv. Can., Map 1371A.

1959, 1974: Geology, La Biche River, District of Mackenzie; Geol. Surv. Can., Map 1380A.

Douglas, R.J.W. and Norris, D.K.
1959: Fort Liard and La Biche map-areas, Northwest Territories and Yukon; Geol. Surv. Can., Paper 59-6.

1959, 1974: Geology, Fort Liard, District of Mackenzie; Geol. Surv. Can., Map 1379A.

Gleddie, J.
1954: Upper Cretacous in western Peace River Plains, Alberta in Western Canada Sedimentary Basin – a Symposium, L.M. Clark, ed.; Am. Assoc. Pet. Geol., Ralph Leslie Rutherford Memorial Volume, p. 486-507.

Hage, C.O.
1954: Geological reconnaissance along lower Liard River, British Columbia, Yukon and Northwest Territories; Geol. Surv. Can., Paper 45-22.

Stott, D.F.
1960: Cretaceous rocks in the region of Liard and Mackenzie Rivers, Northwest Territories; Geol. Surv. Can., Bull. 63.

Thompson, R.I.
1977: Geology of Beatton River, Fontas River and Petitot River map-areas, northeastern British Columbia; Geol. Surv. Can., Paper 75-11.

Williams, G.K.
1977a: Some observations on the Horn Plateau, District of Mackenzie; in Report of Activities, Part B, Geol. Surv. Can., Paper 77-1B, p. 191-196.

1977b: The Celibeta structure compared with other basement structures on the flanks of the Tathlina High, District of Mackenzie; in Report of Activities, Part B, Geol. Surv. Can., Paper 77-1B, p. 301-310.

NOTE TO CONTRIBUTORS

Submissions to the *Discussion* section of *Current Research* are welcome from both the staff of the Geological Survey and from the public. Discussions are limited to 6 double-spaced typewritten pages (about 1500 words) and are subject to review by the Chief Scientific Editor. Discussions are restricted to the scientific content of Geological Survey reports. General discussions concerning branch or government policy will not be accepted. Illustrations will be accepted only if, in the opinion of the editor, they are considered essential. In any case no redrafting will be undertaken and reproducible copy must accompany the original submissions. Discussion is limited to recent reports (not more than 2 years old) and may be in either English or French. Every effort is made to include both *Discussion* and *Reply* in the same issue. *Current Research* is published in January, June and November. Submissions for these issues should be received not later than November 1, April 1, and September 1 respectively. Submissions should be sent to the Chief Scientific Editor, Geological Survey of Canada, 601 Booth St., Ottawa, Canada, K1A 0E8.

III: DISCUSSIONS AND COMMUNICATIONS

URANIUM IN NISLING RANGE ALASKITE AND RELATED ROCKS OF YUKON CRYSTALLINE TERRANE: DISCUSSION

W.D. Goodfellow, I.R. Jonasson, and B.W. Smee
Resource Geophysics and Geochemistry Division
Geological Survey of Canada, 601 Booth St., Ottawa K1A 0E8

Manuscript received November 22, 1977

Introduction

A very interesting paper by Tempelman-Kluit and Currie (1977) provides considerable basic geochemical data on abundance of uranium in the Nisling Range alaskite and related rocks. By way of comment, we offer some further geochemical data on uranium and certain accessory or indicator elements in these same rocks and from similar suites elsewhere. Certain aspects of the paper require clarification. We shall point out these and discuss them in turn because the conclusions drawn by Tempelman-Kluit and Currie may be affected significantly by them.

Discussion

The first omission we note is the absence of any description of analytical methods, particularly for uranium. It is quite important to know whether analyses followed partial attacks by hot acid or total dissolutions, or whether some other total determination such as neutron activation analysis was employed. Depending on the chemistry and especially the mineralogy of uranium (and other metals) in these samples, the abundances measured may change considerably according to method employed.

Table 1 presents some trace analytical data for granitoid rocks similar to those studied by Tempelman-Kluit and Currie. Analyses were made by the following methods.

Zn, Cu, Pb, Mo and Ba: quantitative DC arc spectrography

W,F: colorimetry and ion electrode, respectively, following total decomposition of sample by fusion

Th: X-ray fluorescence (powder)

U_1: strong nitric acid attack, fluorometric finish

U_2: total U by delayed neutron activation analysis.

It is clear that U values found are quite dependent on the analytical method employed. It is difficult to compare the data of Table 1 with those of the authors because we do not know how U was determined. Moreover, comparisons with data provided by one of us (B.W.S.) are also in doubt because most of the North American data quoted derive from a few samples of unknown weathering history, with U determined by neutron activation. Those from Japan were analyzed by methods unknown.

Table 1. Trace element data for some granitoid rocks. (ppm)

Sample	Number	Rock unit	Zone	Easting	Northing	Zn	Cu	Pb	Mo	W	F	Th	U_1	U_2	Ba	Location
104N	765001	GRNT	8	594100	6614700	71	6	20	0.5	-	-	-	-	12.0	118	Surprise Lake, Atlin.
104N	765002	GRNT	8	594100	6614700	53	4	6	0.5	-	-	-	-	10.5	579	Surprise Lake, Atlin.
104N	765003	ALSK	8	594100	6614700	58	4	1	0.5	-	-	-	-	25.4	205	Surprise Lake, Atlin.
104N	765004	ALSK	8	594100	6614700	122	6	100	0.5	-	-	-	-	33.4	274	Surprise Lake, Atlin.
104N	769005	GRNT	8	563800	6619800	48	2	10	1.1	-	-	-	-	4.0	1500	Deep Bay, Atlin.
105F	752022	QZFP	8	635000	6819500	137	12	30	16	6	1730	72	4.4	13.9	950	McConnell Ck. Pelly Mts.
105F	752023	SYNT	8	635000	6819600	550	9	100	10	0	6100	109	8.0	19.5	890	McConnell Ck., Pelly Mts.
105F	752024	SYNT	8	635000	6819700	625	11	43	6	4	5650	75	12.5	22.6	996	McConnell Ck., Pelly Mts.
105F	752025	SYNT	8	635000	6819800	155	4	27	22	0	22000	35	16.1	25.7	563	McConnell Ck., Pelly Mts.
105K	752014	GRNT	8	589200	6907000	25	2	17	1	0	1320	39	2.1	9.4	1597	Mt. Mye
105F	752019	GRNT	8	635000	6819100	345	8	79	5	5	900	5	0.1	7.1	418	Mt. Mye
115P	752089	GRNT	8	373400	7074800	18	1	16	0	0	770	11	6.4	7.8	467	Ura, Clear Creek
115P	752091	GRNT	8	372900	7074200	32	2	14	1	0	550	34	4.8	8.8	604	Ura, Clear Creek
115P	761001	GRNT	8	372900	7074200	59	7	23	0.5	-	108	-	-	10.8	1142	Ura, Clear Creek
115P	761002	GRNT	8	372900	7074200	150	3	19	3.1	-	340	-	-	58.3	342	Ura, Clear Creek
115P	761003	GRNT	8	372900	7074200	122	5	24	2.7	-	370	-	-	28.8	345	Ura, Clear Creek
115P	761004	GRNT	8	372900	7074200	95	9	32	1.2	-	455	-	-	25.3	655	Ura, Clear Creek
115P	761005	GRNT	8	372900	7074200	102	12	38	2.6	-	148	-	-	12.3	1500	Ura, Clear Creek
115J	752095	ALSK	7	611100	6915500	69	0	11	2	0	280	18	3.0	5.6	385	Klotassin River
115J	752096	ALSK	7	611200	6915500	74	2	12	2	0	550	22	2.8	6.0	628	Klotassin River
115J	752097	ALSK	7	611300	6915500	60	2	11	2	0	1700	33	4.4	8.5	566	Klotassin River
115J	752098	ALSK	7	610900	6915500	67	2	11	2	0	115	20	2.0	5.7	559	Klotassin River
115J	752099	ALSK	7	610800	6915600	52	1	10	2	0	1060	25	4.6	7.7	229	Klotassin River
115J	761001	MNZN	7	628000	6950800	35	194	25	5.0	6	680	-	12.0	15.6	825	drill core, 266 feet
115J	761003	MNZN	7	628000	6950800	25	22	18	1.0	1	680	-	3.8	5.6	1398	drill core, 984 feet
116B	765002	MNZN	7	617850	7150000	16	9	40	7.9	2	415	-	9.4	16.4	540	Tombstone Mts.
116B	765003	MNZN	7	617850	7149120	68	2	40	3.8	2	3900	-	13.6	22.2	330	Tombstone Mts.
116B	765004	MNZN	7	617460	7149088	36	3	17	2.5	2	700	-	34.0	60.0	210	Tombstone Mts.
116B	765005	MNZN	7	616950	7147140	47	4	32	2.5	4	586	-	3.6	5.1	1880	Tombstone Mts.
116B	765006	SYNT	7	616620	7146760	16	4	17	3.8	4	610	-	2.4	3.0	1860	Tombstone Mts.
116B	765007	SYNT	7	614750	7144910	68	5	48	7.2	4	760	-	5.2	10.0	1840	Tombstone Mts.
116B	765008	SYNT	7	614752	7142900	54	4	64	11.6	4	2350	-	20.0	31.3	470	Tombstone Mts.
116B	765009	SYNT	7	614752	7142900	88	3	80	3.8	2	1280	-	16.8	26.1	1560	Tombstone Mts.
116B	765010	TNGT	7	614752	7142900	91	4	48	4.4	2	785	-	14.4	24.7	230	Tombstone Mts.
116B	765014	TNGT	7	616180	7141900	18	1	20	3.8	2	785	-	2.8	3.9	200	Tombstone Mts.

From: Discussions and Communications in Current Research, Part A; Geol. Surv. Can., Paper 78-1A.

A second consideration not discussed by the authors concerns the weathering history of the "surface rock samples" studied. Much of the area from which these samples came is underlain by unglaciated terrain. Our own observations made in the Klotassin River area confirm that deep leaching of the alaskitic rocks therein has taken place. The effect on all trace metal levels is quite pronounced.

Table 1 includes a few examples of leached alaskite (115J). U levels are low and there is little difference between partial and total determinations indicating that much of the easily leached U, e.g., perhaps that associated with fluorite, micas or sulphides, has been removed as the host minerals were destroyed by weathering.

The usefulness of subtle comparisons of mean U levels for plutonic rocks and volcanic rocks is also in question since small differences measured in weathered rocks may merely reflect differences in mineralogy and leachability. Thus there is some doubt that U levels measured in any surface rock samples from unglaciated terrain reflect original composition no matter what analytical method might be employed.

Analyses of two samples of unweathered quartz monzonite from drill core have been added to Table 1. It is of interest to note that the ratio of total U to extractable U is not all that different from other examples in the Table. However, there are too few samples here to be of real use in interpretation.

We have presented data for a number of other alaskites, granites and syenites from glaciated terrain for comparison. It is probable that these specimens are considerably "fresher" than those from the Nisling Range. Certainly samples from the Tombstone Mountains and Atlin were observed to be quite fresh. We make no comment here on the effects of weathering on other metals, however comparison with data published by Jonasson and Goodfellow (1976) will yield some interesting relationships.

Finally we would point out that attempts to assess a given rock unit in terms of its potential as a host for U mineralization must be made with caution given the doubts which can be cast on the value of geochemical data at hand. We agree with Tempelman-Kluit and Currie that the Nisling Range alaskite should be regarded as a source of U which could be redeposited elsewhere. Moreover we would add that there is also a good chance of forming zones of supergene enrichment within the body of the intrusive itself. The fact that U continues to be mobile is reflected in anomalous levels in stream and spring waters percolating through the alaskite body (Jonasson and Gleeson, 1976). We consider that the combined use of water, sediment and rock sampling may lead to the detection of easily leached supergene U mineralization.

References

Jonasson, I.R. and Gleeson, C.F.
1976: On the usefulness of water samples in reconnaissance surveys for uranium in Yukon Territory; Report of Activities, Part C, Geol. Surv. Can., Paper 76-1C, p. 241-244.

Jonasson, I.R. and Goodfellow, W.D.
1976: Uranium reconnaissance program: orientation studies in uranium exploration in the Yukon; Geol. Surv. Can., Open File 388, 97 p.

Tempelman-Kluit, D.J. and Currie, R.G.
1977: Uranium in Nisling Range alaskite and related rocks of Yukon Crystalline Terrane; Report of Activities, Part C, Geol. Surv. Can., Paper 77-1C, p. 89-94.

From: Discussions and Communications in Current Research, Part A; Geol. Surv. Can., Paper 78-1A.

URANIUM IN NISLING RANGE ALASKITE AND RELATED ROCKS OF YUKON CRYSTALLINE TERRANE: REPLY

D.J. Tempelman-Kluit and R.G. Currie
Regional and Economic Geology Division
Geological Survey of Canada, 100 West Pender St.,
Vancouver, B.C. V6B 1R8

Manuscript received November 28, 1977

We welcome the discussion of Goodfellow, Jonasson and Smee and are gratified they agree with our conclusion concerning the uranium possibilities of the Nisling Range alaskite. Our failure to specify the analytical technique used for our uranium determinations was a serious oversight as their discussion demonstrates. Our uranium analyses were by neutron activation with delayed neutron counting and were done at the laboratory of the Atomic Energy Commission in Ottawa. Our results should therefore be compared with the "U2" analytical values quoted by Goodfellow, et al. and give similar values to the samples they analyzed. Comparison of our results with the North American data was therefore valid.

Goodfellow, Jonasson and Smee observe that we did not discuss the weathering history of the rocks of the rocks and point out that the unglaciated and weathered nature of the rocks of the Klotassin River region implies deep leaching and removal of a large proportion of the original uranium. We refrained from discussing the weathering history because its relationship to the degree of uranium leaching is not understood and because the glacial history and physiographic development is detailed elsewhere (Tempelman-Kluit, 1974). We caution Goodfellow et al. in equating deep weathering with deep leaching. The "freshness" of a rock sample is no guarantee that its uranium has escaped leaching. Similarly derivation of samples from glaciated or unglaciated regions bears no simple relationship to the completeness or depth to which the rocks are leached of uranium. This is illustrated by their own data using one of their criteria, namely the ratio of total uranium to partial uranium. For their 9 samples from the unglaciated part of Yukon this ratio is 1.8 ± 0.5 and for their 15 samples from the glaciated part 2.0 ± 0.8 (we neglect the outlier from Mt. Mye); statistically indistinguishable.

We do not necessarily disagree with the conclusion that rocks in Klotassin River area are deeply leached of uranium, but we do disagree that their "own observations confirm the deep leaching of the alaskitic rocks...". Their analyses of 5 surface specimens and 2 of drill core from depths of 266 and 984 feet in the alaskite have similar U concentration excepting the sample from 266 feet. This suggests only that the rocks are either all leached equally to a depth of 984 feet or that all have escaped leaching equally.

Goodfellow, Jonasson and Smee also state that in the "few examples of leached alaskite (115 J). U levels are low and there is little difference between partial and total determinations...". In rocks from which uranium is naturally leached the ratio total to partial uranium should increase progressively, not decrease as they imply, and the difference should also increase. This suggests for example that sample 752019 from Mt. Mye has been more effectively leached than the samples from the Klotassin River.

We consider the differences in mean uranium levels of the various rock units significant for the very reasons Goodfellow et al. distrust them. Namely, they reflect differences in mineralogy and leachability in the rocks.

This discussion emphasizes the problems in interpreting uranium geochemical data and that more effort must be focussed on interpreting the results rather than on acquiring more data.

Reference

Tempelman-Kluit, D.J.
1974: Reconnaissance geology of Aishihik Lake, Snag and part of Stewart River map-areas, west-central Yukon; Geol. Surv. Can., Paper 73-41, 97 p.

AUTHOR INDEX

NOTES

NOTES

NOTES

NOTES

NOTES